Solvent Extraction for the 21st Century

Proceedings of ISEC'99

volume two

edited by
Michael Cox
Manuela Hidalgo
Manuel Valiente



SCI
where science meets business

SOLVENT EXTRACTION FOR THE 21ST CENTURY

(Proceedings of ISEC '99)

Volume 2

SOLVENT EXTRACTION FOR THE 21ST CENTURY

(Proceedings of ISEC '99)

Volume 2

Edited by

Michael Cox
Department of Physical Sciences, University of Hertfordshire, UK

Manuela Hidalgo
Departamento de Química, Universitat de Girona, Spain

and

Manuel Valiente
Departamento de Química, Universitat Autònoma de Barcelona, Spain

sci
where science meets business

ISEC'99

SOLVENT EXTRACTION FOR THE 21ST CENTURY
Proceedings of ISEC '99

© 2001 Society of Chemical Industry (SCI)
All rights reserved. No part of this publication may be reproduced, stored in a retrieval system, or transmitted in any form or by any means, electronic, mechanical, photocopying, recording, or otherwise, without the prior written permission of the copyright owners, Society of Chemical Industry.

Volume 2

ISBN: 0-901001-83-8

First published in 2001 by

Society of Chemical Industry (SCI)
14/15 Belgrave Square
London SW1X 8PS
UK
T: +44 (0)20 7598 1500
F: +44 (0)20 7235 0887
W: www.soci.org

British Library Cataloguing-in-Publication Data
A catalogue record for this book is available from the British Library.

Note. No responsibility is assumed by either the Society of Chemical Industry, ISEC or the Editors for any injury and/or damage to persons or property as a matter of products liability, negligence or otherwise, or from any use or operation of any methods, products, instructions or ideas contained in the material herein.

The material is produced from the authors' electronic manuscripts.

This book is only available as part of a two-volume set and is not available separately.
ISBN Volume 1: 0-901001-83-X
ISBN Volume 2: 0-901001-84-8

Orders should be sent to:
Accounts Department
SCI, 14/15 Belgrave Square
London SW1X 8PS, UK

Printed on acid-free paper in Great Britain by Page Bros Ltd (Norwich)

FOREWORD

The property of a chemical species to move between immiscible liquid phases has revolutionised the science of separations in the millennium that finishes soon. During the present century, the most significant event has been the growth and development of the field of Solvent Extraction. This technique has lead to hundreds of separation methods and thousands of systems that have been described, investigated and several of which have successfully been applied to solve, in a unique manner, complicated problems in the industrial fields of hydrometallurgy, petrochemical, food, pharmaceutical, environmental, waste treatment and analytical chemistry. Scientific and technologically the most important contribution of liquid-liquid distribution studies has been to the acquisition of basic knowledge in co-ordination chemistry, chemical thermodynamics, interfacial phenomena, hydrodynamics of two phases and mechanisms of chemical reactions, as well as process development, equipment design and process control. It must be emphasised that such knowledge has been applied not only to process separations but also to other important aspects of the areas mentioned above, i.e., development of chemical sensors, controlled release devices, etc.

Because of this record of achievement, Solvent Extraction can be considered as a mature technique and thus further innovation becomes more difficult. This is always a challenge to practitioners in the technique, but it never will be a final barrier in itself, unless we confuse the creation of scientific knowledge with the opportunity of obtaining funds for research. In addition, at this moment, when environmental concern has reached a significantly high social and scientific consideration, the name of Solvent Extraction is sometimes interpreted as a negative factor that has been reflected in some political decisions. We know well that again, this is a consequence of ignorance, but still, we must consider this fact and include it in the real scientific and technological challenges.

The area of Solvent Extraction has several well-identified areas and topics with specific demands for scientific and technological research. Some of these areas are related to the *chemistry* of Solvent Extraction and include: the need for speciation studies of the compounds formed both in the aqueous and organic phases during the operation of the process; understanding the interrelation between chemical thermodynamics vs. real operation; the role of the diluent in relation to its chemical nature; degradation of reagents as an important chemical factor that influences system performance. In addition, there are the new methods for Solvent Extraction which include: non-dispersed extraction; microemulsions; extraction chromatography; etc.

Yet another area is concerned with the engineering aspects of Solvent Extraction and here a proper understanding of modelling of both the chemistry and system design is important. Also here there is a lack of data on thermodynamics in concentrated solutions which is the typical situation in plant operations. Monitoring and control of the process is an area which needs specific attention. Monitoring of the two phase process is a system dependent problem which possesses several weak points that are key factors to the advance of the appropriate knowledge to predict the behaviour of solvent extraction systems. Therefore it is important that both specific on-line analytical equipment and robust monitoring techniques should be implemented in the Solvent Extraction process.

Concerning the environmental aspects, the real impact of the Solvent Extraction process must be characterised in several areas: the health effects of solvents and solutions; toxicity of new hazardous reagents; fire hazards; treatment of wastes. In addition design of equipment must also address safety i.e., minimising venting, use of columns, entrainment. These are all considered in an overall risk assessment analysis.

These are just a few aspects of the challenge to be faced by future practitioners in the subject.

So, the International Solvent Extraction Conference has come to Barcelona, the capital city of Catalunya (Spain), in July 1999. Most of the above mentioned areas in need of research and development have been the subject of excellent contributions from the participants and will be presented and discussed during the Conference sessions.

We understand that such an international meeting to discuss Solvent Extraction has to provide the facilities to make the transmission of knowledge easier, to stimulate the will to meet the exciting challenges we are now facing and to make Solvent Extraction attractive to newcomers. To accomplish this, we have organised the International Solvent Extraction School to take place simultaneously with the Conference, and invited international experts to provide tutorials in their fields of expertise and thus to increase our knowledge of Solvent Extraction.

During preparations for the Conference the idea presiding over all the discussions and plans was the question:

> *Will this way of thinking, studying, developing and applying the optimum give the answers to the actual needs and competitiveness that may arise in the next century?*

The Organising Committee has been working to try to answer this question, and we believe that ISEC'99 will be able to provide an appropriate answer. For all their work and dedication which has gone to make ISEC'99 possible, I would like to thank all members of the Organising Committee because without them this Conference would not have been possible.

The Organising Committee in turn wish to express their warm appreciation to all the authors for their contribution and to all those who will be attending ISEC'99 and thus contributing to a most exciting and enjoyable Conference. We thank you for accepting our invitation to meet on the Mediterranean and we hope you will have happy memories of this meeting.

These Proceedings have been compiled from electronic versions of papers submitted by the authors after refereeing and have not been submitted to full textual editing by the editors. We hope that they will provide a valuable resource for the future.

Manuel Valiente
Chairman, Organising Committee

TABLE OF CONTENTS

PLENARY AND KEYNOTE LECTURES 1

Molecular Dynamics of Liquid Surfaces and Interfaces 3
I Benjamin

Solvent Extraction and Materials Science 9
M Muhammed and AA Zagorodni

One Phase Micellar Extraction as a New Separation Technique 19
J Szymanowski

Physico-chemical Modelling of Liquid–Liquid Extraction Systems of Highly Concentrated Electrolytes 25
P Dannus

State of the Art and Future Directions in Solvent Extraction 37
GM Ritcey

ANALYTICAL CHEMISTRY 45

Liquid-supported Membranes as Sample Interfaces in a Flow Probe Optosensor for Chromium(VI) Analysis 47
E Castillo, M Granados, MD Prat, AM Sastre, A Kumar and JL Cortina

Recent Advances in the Development of Extraction Chromatographic Materials for the Isolation of Radionuclides from Biological and Environmental Samples 53
ML Dietz, EP Horwitz and R Chiarizia

Ion–paired Extraction of Copper into Chloroform and its Application in Practical Analyses 59
I Kojima, M Ito and T Mizuno

Determination of Arsenic in Biological Matrices by Anodic Stripping Voltammetry Coupled with a Two-step Extraction Process 65
J-M Lo, J-D Lee and C-M Tseng

Solvent Extraction Separation Studies of Some Metal Ions with 2-Ethylhexylphosphonic Acid Mono-2-Ethylhexyl Ester 71
SV Bandekar and PM Dhadke

Bis(ethanedithioamido)-2,4-dioxo-3-oxyminopentane as a New Analytical Reagent for the Extractive Radiochemical-spectrophotometric Determination of Selenium(IV) and its Separation from other Elements 77
A Varadarajan and SP Malve

BIOTECHNOLOGY 81

A Novel Protein Refolding Technique Utilizing Reversed Micellar Extraction 83
M Goto, S Furusaki and TA Hatton

Effect of Interaction between Protein and Surfactant in Aqueous Phase on Extraction Rate of Protein into Reversed Micellar Solution 89
T Kinugasa, K Sanagi, K Watanabe and H Takeuchi

Reverse Micellar Extraction of Proteins Using pH Responsible Mixed Micellar Systems 95
K Shiomori, T Honbu, Y Kawano, R Kuboi and I Komasawa

Extraction of Proteins using Reversed Micelles in a Graesser "Raining Bucket" Contactor 101
LH Poppenborg, S Jarudilokkul and DC Stuckey

Tailoring of Reverse Micellar System for Selective Separation of Proteins Using Protein–Protein Affinity Interactions 107
M Adachi, M Harada, A Shioi and S Katoh

Selective Separation of α-Amylase, Bovine Serum Albumin and Trypsin Inhibitor using Reverse Micelles 113
S Jarudilokkul, LH Poppenborg and DC Stuckey

Strategies for Extraction Methods in the Extractive Fermentation Process of Carboxylic Acid 119
W Qin and ST Yang

Recovery of Carboxylic Acids from Fermentation Broths using Reactive Sorption 125
M Traving and H-J Bart

Extraction and Interactions in Two-phase, Multi-acid, Multi-base Systems 131
N Cohn-Syzov and AM Eyal

Extractive Synthesis of Peptides with Catalytically Active Enzymes in Organic Media 137
Y Murakami, H Kawakita and A Hirata

Protease-catalyzed Synthesis of Peptides Utilizing an Extractive Reaction in an Aqueous/ Organic Biphasic System 143
Y Murakami, T Oda, A Takehara and A Hirata

Extractive Hydrolysis of Proteins with Enzymes in an Aqueous Two-phase System 149
Y Murakami and A Hirata

The Effect of Surfactants during Solvent Extraction of Erythromycin-A from Buffer and Filtered Fermentation Broth 155
MR Pursell, MA Mendes-Tatsis and DC Stuckey

Recovery of Ethanol from Aqueous Solution by Extraction with 1-Dodecanol 161
F Ruiz, V Gomis, N Boluda and H Bailador

ENVIRONMENTAL IMPACT 165

Soil Remediation by Supercritical Extraction with Solvent Recirculation under Quasiisobaric Operation Conditions. Application to Soil Polluted by Hydrocarbons 167
E Alonso, JJ Alonso and MJ Cocero

Organic Solvent-free Extraction of Phenol Through Liquid-Coacervate Systems 171
EL de Barros Neto, JP Canselier and C Gourdon

Removal of VOCs from Wastewater with Membrane Extraction 177
Y Wang, S Zhu and Y_Dai

Removal of Dyestuffs From Dilute Solution with Electro-extraction 183
GS Luo, YC Lu, WB Jiang and YY Dai

Recovery of Pickling Liquors from the Steel-making Industry 189
CE Da Silva, JS Benedetto and EB Tambourgi

The Chromium Recovery Process from Tanning Effluents by Microemulsion in the Morris Extractor 195
TN de C Dantas, AA Dantas Neto and MCPA Moura

A New Zinc Solvent Extraction Application: Spent Domestic Batteries Treatment Plant 201
D Martín, MA García, G Diaz and J Falgueras

Micellar Extraction versus Solvent Extraction: Advantages and Drawbacks 207
M Hebrant and C Tondre

Interaction of Thorium with Gray Humic Acid 213
A-A A Helal

Extractive Recovery of Boron in Wastewater from a Coal Thermal Power Plant 219
M Hirata, H Takanashi, S Kokubu, M Matsumoto, T Takada and T Hano

Reactive Liquid–Liquid Extraction of Heavy Metals from Landfill Leachate 225
W Mickler, A Reich and E Uhlemann

A Comparative Study of the Treatment of Chromium Electroplating Wastewater using Two Extractants, Alamine 336 and Aliquat 336 231
YKP Sze, CSW Lam, WK Long and JMY Ho

EXTRACTANTS AND DILUENTS 237

Tailor-made Aromatic Cage Compounds as Tools for Selective Solvent Extraction of Metal Ions 239
K Gloe, C Chartroux, T Rambusch, F Ahuis, S Ibach and F Vögtle

Solvent Extraction Separation of some Transition Elements with Hexaacetato-calix(6)arene 245
DD Malkhede, PM Dhadke and SM Khopkar

Lanthanide and Actinide Extraction with Calix[4]- and Calix[6]-arenes Bearing Amide Groups 249
NTK Dunga, K Kunogi, and R Ludwig

Coextraction of Various Metal Ions with Calix[4]arene Carboxylate Complexed with Sodium Ion 255
K Ohto, H Ishibashi, S Kuwata and K Inoue

Extraction of Europium(III) and Americium(III) with Diamide Compounds from Nitric Acid Solution 259
W-J Chen, L Zhu, S-D Ding, Z-Q Liu, S-J Chen, C Xia, Z Huang and Y-D Jing

Application of Diazapolyoxabicyclic Ligands to the Quantitative Extraction Separation of Alkali and Alkaline Earth Metal Ions as the Ion-size Selective Masking Reagents 265
S Tsuruboi, S Umetani and Y Komatsu

Solvent Extraction of Base Metal Cations such as Iron(III) from Hydrochloric Acid Solutions using N,N'-Substituted Malonamides 271
MC Costa, CE Fernandes, MJ Hudson and PB Iveson

Recent Advances in Structure–Reactivity Studies of Solvent Extractants in Metal Extraction 277
CY Yuan, SS Li, SG Yuan and HL Ma

Extraction Studies and *ab initio* Calculations of some Substituted Malonamides 281
L Spjuth, JO Liljenzin, MJ Hudson, MGB Drew, PB Iveson and C Madic

Photostability of Hydroxyoxime Commercial Copper Extractants: Acorga P5100 and SME529 287
E Krzyanowska and A Olszanowski

Photodegradation of Oximes of 2-hydroxy-5-*t*-octylbenzophenone, 2-Hydroxy-5-*t*-octyl-benzaldehyde as Models of Hydroxyoxime Extractants of Metals 293
E Krzyanowska and A Olszanowski

Synergistic Effects in the Extraction of Metal Ions by Mixtures of Dialkylphosphoric Acids and Substituted Crown Ethers 299
R Chiarizia, ML Dietz, AH Bond, VJ Huber, AW Herlinger and BP Hay

Solvent Extraction of Calcium and Some Divalent Transition Metals by Mixtures of Organophosphorus Acids and Bifunctional Phosphonates 305
JS Preston and AC du Preez

The Effect of Reagent Structure on the Extraction and Separation of Nickel and Cobalt by Mixtures of Carboxylic Acids and Pyridine Derivatives 311
JS Preston and AC du Preez

Synergistic Systems for the Selective Extraction of Trivalent Actinides from Mixtures of Trivalent Actinides and Lanthanides. 317
PY Cordier, N François, N Boubals, C Madic, MJ Hudson and JO Liljenzin

Separation of Trivalent Americium and Europium with some Substituted Oligopyridines and Triazines in Synergy with 2-Bromodecanoic Acid 323
Å Enarsson, L Spjuth, JO Liljenzin, G Källvenius, MJ Hudson, PB Iveson, ML Russell, C Madic and PY Cordier

Synergetic Solvent Effects in the Kinetics of the Extraction of Chromium(III) 329
C Mack and MJ Hampe

Micellar Extraction of Complexes of Lanthanides with Humic Acids 335
J Reitmeir, JI Kim and P Plucinski

Solvent Extraction of Transition Metals by an *in situ* Extractant Formation Method. VI. Utilization of an Easily-solidifying Solvent 341
K Fujinaga, Y Seike, and M Okumura

A New Hydroxamic Acid Derivative Extractant for the Extraction of Cobalt(II) and Uranium(VI) from Nitrate Medium 347
FA Shehata, S El-Afifi and HF Aly

Solvent Extraction of UO_2^{2+} and Th^{4+} with Petroleum Sulfoxide 353
S-N Yu, Z-P Fan, L Ma, Y-Z Yang and B-R Bao

Palladium(II) Extraction with Alkyl Derivatives of Nicotinamide 359
M Wiœniewski, I Szczepanska and A Borowiak-Resterna

Cloud Point Extraction of Gallium(III) with Nonionic Surfactants from Hydrochloric Acid Media 363
S Akita, N Hyodo, N Kobayashi, S Nii, K Takahashi and H Takeuchi

Additive Tailoring in Biphasic Systems for an Enzymatic Condensation Reaction 369
R Dunowicz and AM Eyal

LIX®-7800 Series: a New Reagent Family for Reversibly Extracting Anions from Alkaline Solutions 375
P Mattison and M Virnig

Advances in Gold(III)-Chloride Solvent Extraction Using Neutral Organo-phosphorous Derivatives. Estimation of $AuCl_4^-$–H^+ Interaction Coefficients 381
AM Sastre and FJ Alguacil

Solvent Extraction of Gallium(III) with Nonionic Surfactants from Hydrochloric Acid Media 387
N Kobayashi, N Hyodo, S Nii, K Takahashi, H Takeuchi and S Akita

Solvent Extraction of Gold from Hydrochloric Acid Solutions Using Bis(dialkylphosphonate)s 393
S Kamata, S Fukunaga and DA Chowdhury

Sulphur–Nitrogen Ligands in the Solvent Extraction of Silver from Chloride Solutions 399
AP Paiva

Foam Separation of Tributyl Phosphate from Aqueous Solution by Sodium Dodecylsulfate 405
Z-D Chang, H-H Liu, N Yao and J-Y Chen

Extraction Equilibria of Nicotinic Acid using Alamine 300/Diluent and Conventional Solvent Systems 411
A Senol

Separation of Phenol from Aqueous Solution by Predispersed Solvent Extraction 419
Y-D Wang, M Chen, L Xu and Y-Y Dai

EXTRACTION EQUIPMENT AND DESIGN 425

The AP Column – Development of a High Capacity Extraction Column 427
RW Cusack, DJ Glatz and TL Holmes

Development of a Multistage Mixer–Settler Column with a Novel Impeller 433
M Yamaguchi, H Yamashita, M Kaneda and H Noda

Drop Size and Phase Distribution in Extraction Columns 439
J Koch and A Vogelpohl

The Application of Electrical Capacitance Tomography to Liquid–Liquid Extraction Columns 445
GT Bolton, WJ Korchinsky, RC Waterfall and PD Martin

Study on Characteristics of Pulsed Packed Columns using Super-Mini-Rings (SMR) 451
J Yu and W Fei

Impacts of Packing on Mass Transfer of High Viscosity Solvents Drop Swarms 457
J Yu and W Fei

Flow Structure and Turbulent Flow Energy in Stagewise Extraction Columns: Influence of Stage Configuration 463
G Angelov and C Gourdon

Hydrodynamic and Mass Transfer Characteristics of Super-Mini-Ring (SMR), Raschig Ring and Pulsed Perforated Plate Columns 469
D Chen, W Fei, HRC Pratt and GW Stevens

Axial Mixing in a Large-scale Packed Extractor 475
O Becker, C Lewis, R Hardy and F Seibert

Performance of a Vibrating Perforated Plate Extractor – Hold-up and Characteristic Velocity 481
LMN Góis, EB Tambourgi, JAFR Pereira and JJ Marques

The Importance of Drop Coalescence in a Stirred Liquid–Liquid Extraction (Kühni) Column 487
MLACN Gomes, MML Guimarães, G Zamponi, J Stichlmair, PFR Regueiras and JJC Cruz-Pinto

Stage Efficiencies and Mass Transfer Coefficients in a Mixer–Settler Extraction Column 493
K Takahashi, T Ban, K Tani, S Nii and F Kawaizumi

Effect of Phase Entrainment on the Process in Centrifugal Extractors 499
GI Kuznetsov, AV Kosogorov, AA Pushkov and VS Skachkov

The Effect of Air Sparging on the Electrical Resolution of a Water-in-Oil Emulsion 503
PJ Bailes and PK Kuipa

Use of a Video Camera for the Development, Monitoring and Documentation of SX Processes 509
B Grinbaum

Multicomponent Kinetics in Liquid–Liquid Systems: an Experimental Study 513
MJ Brodkorb and MJ Slater

In-line Mixers for the Extraction of Uranium by a Tertiary Amine from Ore Leach Sulphuric Acid Solutions 519
GM Ritcey

Fast Pre-neutralisation and Extraction in a Tubular Reactor using an Acidic Extractant 525
E Jääskeläinen and E Paatero

Comparison between Different Extractors for a High Viscosity Extraction Application 531
D Kirschneck, H Schmitt and R Marr

Extraction Behavior of Pd(II) with Tri-*n*-octylamine in a Vibro-mixer Type Extractor 537
Y Kawano, K Shiomori, S Yamada, H Yoshizawa and Y Hatate

Comparison of Membrane-assisted Solvent Extraction Technologies for the Separation of Cd–Ni Mixtures 543
I Ortiz, F San Román, B Galán and AM Urtiaga

Reactive Extraction using a Karr Column for the Production of Dioxolane from an Aldehyde 549
B Grinbaum, M Adda and Ch Eidelman

FUNDAMENTAL STUDIES 553

Studies of the Extraction Thermodynamics of f-Elements 555
KL Nash

Synergistic Solvent Extraction of Aluminium(III), Gallium(III), and Indium(III) with 2-Thenoyltrifluoroacetone and TOPO 561
J Noro, A Hokura, I Tanaka, M Yamada and T Sekine

The Influence of 1-Octanol on Metal Extraction into HDEHP 567
OA Sinegribova, V Kim, NV Bukar, OV Sviridenkova and OO Olenicheva

Extracting Emulsions — Theoretical Review and Practical Usage 573
EV Yurtov and M Yu Koroleva

Gel-like DEHPA Salt Systems in Organic Solutions and on the Interface 579
EV Yurtov and NM Murashova

Extraction Behaviour of Alkali Metals under the Control of pH in Crown Ether–β-Diketone Extraction and Crown Ether–Substituted Phenol Extraction Systems 585
T Shimosato, N Hirayama and T Honjo

A Mechanistic Study on Ion Association Extraction with Quaternary Ammonium Ions 591
S Motomizu, T Takayanagi and E Wada

pH Dependence of Dicarboxylic Acid Extraction by a Strong Amine Based Extractant 597
R Canari and AM Eyal

A Spectral Study of the Relative Basicity of Long Chain Water-immiscible Organic Amines 603
L Poulad-Meyer and AM Eyal

A Study of the Motion of a Single Drop under the Influence of a Pulsed DC Electric Field 609
PJ Bailes, JGM Lee and AR Parsons

Single Drop Coalescence – Experiment and Simulation 615
A Eckstein and A Vogelpohl

Diffusivities for Multicomponent Mass Transfer Calculations 619
AR Uribe-Ramírez and WJ Korchinsky

Characterization of Polymeric Reversed Micelles 625
Y-D Wang, Z Li, H Huang and YY Dai

Membrane Coalescence as a Novel Phase Separation Stage for Extraction Processes 631
S Hoffmann and W Nitsch

Third Phase Formation: a New Predictive Approach 637
L Lefrancois, F Belnet, D Noel and Ch Tondre

Salt Effect in the Quaternary System Water + Ethanol + 1-Pentanol + Sodium Chloride at 25°C 643
MM Olaya, A Botella and A Marcilla

Study of Inclusion Complex Formation of Substituted Cyclodextrins with Xylene Isomers 651
I Uemasu

Modelling TBP/Diluent Mixtures and Water Extraction by these Mixtures Using the UNIQUAC Equation and Taking Account of Complex Formation 655
B Rat, B Dinh and C Poitrenaud

GUEST–HOST BINDING 661

A Novel Strategy for the Design of Organic Ligands of High Selectivity 663
S Umetani and QTH Le

The Ligand-thickness Effect Leads to Enhanced Preference for Large Anions in Alkali Metal Extraction by Crown Ethers 669
BA Moyer, TJ Haverlock and RA Sachleben

Liquid–Liquid Extraction of Metal Ions with a Monoazatetrathiacrown Ether and its Acyclic Analogues 675
K Chayama, C Kurihara, H Tsuji and E Sekido

Solvent Extraction of Rare Earth Nitrates by Phosphorylated Calix[4]arenes 681
M Burgard, B Ernst, MR Yaftian, CB Dieleman, C Wieser-Jeunesse and D Matt

QSPR of Extractability Trends of the Lanthanoid Series Using Novel Molecular Mechanics Calculations 687
K Yoshizuka, K Inoue, K Ohto, K Gloe, H Stephan, T Rambusch and P Comba

Extraction Behavior for Trivalent Lanthanides with Amides and EXAFS Study of their Complexes 693
H Narita, T Yaita and S Tachimori

Extraction of Uranium(VI) and Plutonium(IV) from Nitric Acid Solutions by Substituted Cyclic Amides 697
S Suzuki, K Tamura, S Tachimori and Y Usui

Oxidation of Cyanex 302 and Cyanex 301 by FT-Raman and UV-V Spectroscopy 703
A Almela, B Menoyo, MP Elizalde and F Mijangos

HYDROMETALLURGY 709

Indium Recovery from Industrial Zinc Residues 711
JS Benedetto, EB Tambourgi and RM Mingote

Indium Recovery by Solvent Extraction with D2EHPA using a Statistical Approach to the Experimental Design 717
MCB Fortes, AH Martins and JS Benedetto

A Separation and Recovery Process of Gallium and Indium from Zinc Refinery Residue 723
S Nishihama, T Hirai and I Komasawa

A Highly Efficient Process to Strip Iron from a New Organophosphorus Extractant 729
F Delmas and CA Nogueira

Solvent Extraction Studies for Cobalt and Nickel Separation from the Processing of Ammonium Carbonate Mixed Sulfides 735
E Garcia Liranza, AM Moreno Daudinot, R Viera Martínez and B Rosales Barazaga

Application of Solvent Extraction in Metal Recovery from Spent Nickel-Metal Hydride Batteries 741
P Zhang, T Yokoyama, O Itabashi, Y Wakui, TM Suzuki and K Inoue

Hydrometallurgical Process for Ni and Cd Recovery from Batteries: Preliminary Data. 747
Loris Pietrelli, Gianni Ponzo and Laura Ranieri

Cation Separation in Sulphate Medium using Solvent Extraction 753
AM Moreno Daudinot and E García Liranza

Extraction of Copper Contained in Ammonia Solutions from the Electronics Industry with LIX84 759
JM Chimenos, MA Fernández, M Segarra, AI Fernández, A Esparducer and F Espiell

Recovery Process of Ni with EHO from a Waste Etching Solution of Lead Frame Material 765
J Shibata, S Matsumoto, M Sano and S Nishimura

Strategies for Platinum Group Metal (PGM) Separation using Impregnated Resins 771
M Rovira, JL Cortina and AM Sastre

Solvent Extraction of Gold from Chloride Copper Anode Slime Liquors 777
K Soldenhoff and D Wilkins

Study of a Microemulsion System for Application in the Extraction of Gold 783
TN de C Dantas, AA Dantas Neto and WF de La Salles

Production of High Purity Tantalum Oxide by Solvent Extraction 789
A Feather, P Clark and G Boshoff

Recovery and Purification of Cerium(IV) and Thorium(IV) from Bastnasite Ore 795
J Lu, D Li, J Tang and T Zheng

Precipitation Stripping of Samarium Hydroxide from Tri-*n*-Butyl Phosphate with Aqueous NaOH Solutions 801
K Koyama and M Tanaka

New Extraction Technologies for the Treatment of Rare Metal Raw Materials Using Mechanochemical Methods 805
SV Chizhevskaya, AM Chekmarev, MV Povetkina, VL Shafirov and M Cox

Author index I

Keyword index IX

VOLUME 2

KINETICS AND INTERFACIAL PHENOMENA 811

A Study of Metal Ion Extraction at the Oil/Water Interface Using Evanescent Wave Spectroscopy 813
P Deljouie, JM Perera, GW Stevens and F Grieser

External Reflection Spectra at the Liquid–Liquid Interface of Extraction Systems Containing Porphyrins 819
N Ogawa, Y Moriya and H Watarai

Some Ideas on the Nature of Interfacial Processes in HDEHPA Extraction of Metals 825
VV Tarasov, OA Sinegribova and OV Sviridenkova

Mechanism of Interfacial Reactions in the Extraction of Iron by D2EHPA 829
T Kanki, H Kim, A Tomita, T Asano and N Sano

Mass Transfer of Organic Acids at Charged Liquid Interfaces 835
C Czapla and H-J Bart

The Coupling of Diffusion Coefficients in Continuous Phases at Liquid–Liquid Interfaces 841
A Tokarz, M Millies and D Mewes

Mass Transfer and Fluorescence Tracer Technique in Solvent Extraction 847
M Mörters and H-J Bart

Kinetics of Mass Transfer and the Different Effects of Surfactants 853
M Weigl and W Nitsch

Mass Transfer Characterization in Forward and Back Extractions of an Amino Acid by Reverse Micelles across a Flat Liquid–Liquid Interface 859
T Nishiki, K Nakamura and D Kato

Effect of Applied Voltage on the Extractive Separation of Rare Earth Metals by D2EHPA in the Presence of an Oil-soluble Complexing Agent 865
M Yamaguchi, D Kojima, M Goto, F Nakashio and S Nagao

Effect of Global Salt Concentration on the Rate of Extraction of Copper(II) by Acorga® CLX-50 and Germanium(IV) by Kelex® 100S 871
G Cote and C Bouvier

A Rotating Membrane Cell Technique for the Study of LLX Kinetics. Application to the Study of Salt Effects 877
JP Simonin, H Hendrawan and J Weill

Kinetic Studies and Molecular Dynamics Simulations of Interfacial Complexation in Solvent Extraction Systems 883
H Watarai and Y Onoe

Mass Transfer Kinetics of Rare Earth Elements with Hollow Fibre Membrane Based Extraction 889
Yujie Wang and D Li

Solvent Extraction Kinetics through Hollow Fibre and Flat Membranes. Investigation with Nitroxide Radicals 893
NM Kocherginsky, AN Osipov and AB Grishchenko

Kinetics and Mechanism of Synergistic Extraction of Gallium(III) with an Acidic Organophosphorus Compound in the Presence of Oxine Derivatives 899
K Kondo, M Matsumoto, K Yano and T Okubo

Extraction Kinetics in the Er(III) 2-Ethylhexyl-2-ethylhexylphosphonic acid (HEH/EHP) Heptane System 905
J Lu, Z Zheng, D Li and G Ma

The Rule of Transition of Extraction Kinetic Behaviour of Rare Earth Elements with DMHMP 911
D Sun, S Le and D Li

Extraction of Iron(III) from Aqueous Sulphuric Acid Solution Using a Packed Column 915
M Rosinda, C Ismael and JMR Carvalho

A Mass Transfer Model for the Extraction of Te(IV) in the Presence of Se(IV) using Tri-*n*-Butylphosphate as Extractant 921
M Bandyopadhyay, S Datta and SK Sanyal

Extraction–Chromatography: Equilibria and Kinetics 927
A Schöneberger, H-J Bart, A Nanoti and A Wildberger

Computer Simulation of Interfacial Behaviour of N-8-Quinolylsulfonamide for the Extraction Kinetics of Copper 933
F Nakashio, A Sakoguchi, E Zushi, R Ueoka and K Yoshizuka

The *LAP*-Model – a New Approach for Modeling the Kinetics of Reactive Extraction 939
M Roos and H-J Bart

LIQUID MEMBRANES 945

Comparing Cyanex 301 with D2EHPA for the Extraction of Nickel through Emulsion Liquid Membranes 947
A Hoffmann, M Verhaege and RF De Ketelaere

Effects of some Parameters on Cobalt/Nickel Separation and on Cobalt Permeation by a Liquid Surfactant Membrane Process 953
A Salum, GL da Silva, MB Mansur, TLS Miranda and VST Ciminelli

Liquid Membrane Permeation of Zinc in a Continuous Countercurrent Column 959
MTA Reis, H-J Bart and JMR Carvalho

Purification of a Radioactive Liquid Effluent: Elimination of Caesium by Liquid Surfactant Membrane Extraction 965
D Pareau, P Kaplan, M Stambouli and G Durand

Mechanism of Transmembrane Water Transfer and Emulsion Swelling 971
MYu Koroleva, NV Bakastova and EV Yurtov

Recovery of 4-Hydroxybenzoic Acid from Aqueous Solutions by Emulsion Liquid Membranes 977
PFMM Correia and JMR Carvalho

Purification and Concentration of Lactic Acid by Emulsion Liquid Membrane Extraction 983
T Berrama, D Pareau, M Stambouli and G Durand

Preparation of Metal–Silicate Microballoons with Liquid Surfactant Membrane 989
T Hano, M Hirata, H Takanashi and Y Nakahara

Selective Recuperation of Copper by Supported Liquid Membrane (SLM) Extraction 995
RF De Ketelaere and J Van der Linden

Uphill Transport of Silver(I) from Nitric Acid Media using Binary Extractants as Potential Liquid Membrane Carriers 1001
A Kumar, PK Gautam, JP Shukla, RK Singh and AM Sastre

Chromium(VI) and Chromium(III) Separation by Supported Liquid Membranes and Polymeric Inclusion Membranes 1007
J Gega, C Kozlowski and W Walkowiak

Dispersion-free Membrane Based Extraction and Stripping of Pb(II) and Cd(II) with Kelex 100 as Carrier 1013
J de Gyves, JC Aguilar and E Rodríguez de San Miguel

Membrane-based Solvent Extraction for Indium(III)–Iron(III) Separation using a Hollow Fibre Contactor 1019
E Rodríguez de San Miguel and J de Gyves

Pertraction of Neodymium and Holmium in a Hollow Fibre Contactor 1023
G Cara, Š Schlosser, M Muñoz and M Valiente

Characterisation of the Stability and Efficiency of a Hollow Fibre Supported Liquid Membrane Containing Aliquat 336 as Carrier for Rhodium(III) Transport 1029
C Fontàs, C Palet, V Salvadó and M Hidalgo

Separation of Amine and Amino Acid Enantiomers Using Supported Liquid Membranes with Chiral Phosphoric and Phosphonic Acid Esters 1035
P Wieczorek, P Dzygiel and P Kafarski

Pertraction and Membrane Based Extraction of Carboxylic Acids in Hollow Fibre Contactors 1041
Š Schlosser, E Sabolová and J Marták

Transport Properties of Activated Composite Membranes Containing Di-(2-Ethylhexyl)-Dithiophosphoric Acid as a Carrier Towards Polyvalent Metal Ions 1047
M Oleinikova, J Macanas, M Muñoz and M Valiente

Use of a PVC-based Aliquat 336 Membrane to Extract Cd(II) and Cu(II) from Chloride Solutions 1053
L Wang, R Paimin, RW Cattrall and SD Kolev

Separation of Esters of Polyunsaturated Fatty Acids by Bulk Liquid Membrane with a Porous Partition 1059
S Nii, R Yokosawa and K Takahashi

Transport of Phenol through Bulk Liquid Membranes 1065
W Cichy, Š Schlosser and J Szymanowski

Recovery of Silver Traces from Electronic Wastes 1071
G Durand, D Pareau and K Ennassef

METAL AND NON-METAL EXTRACTION 1079

Rare Earths Separation Study 1081
D Li

Solvent Extraction Separations of Trivalent Lanthanide and Actinide Ions using an Aqueous Aminomethanediphosphonic Acid 1089
MP Jensen and KL Nash

Extraction and Separation of Lanthanides and Actinides in Aqueous Nitric Acid by 'CMPO-like' Calixarenes 1095
A García-Carrera, H Rouquette, JF Dozol, V Böhmer and AM Sastre

Solvent Extraction of Rare Earth Elements(III) with a Bifunctional Phosphinic acid 1103
Y Wakui, T Yokoyama and K Akiba

Solvent Extraction of Lanthanides and Yttrium from Nitrate Solutions with Cyanex 923 1109
D Chu, G Ma and D Li

Separation of Yttrium and Neodymium from Nitrate Solutions by Di-(2-Ethylhexyl)-phosphoric Acid Impregnated on Amberlite XAD-2 Resin 1115
M Iglesias, E Anticó and V Salvadó

Distribution of Neodymium(III) between Acidic Aqueous Nitrate Solutions and Organic Solutions of Di-(2-Ethylhexyl)phosphoric Acid in Kerosene at Low Metal Concentration 1121
JM Sánchez, M Hidalgo, M Valiente and V Salvadó

Solvent Extraction Studies of Erbium(III) by 2-Ethylhexylphosphonic Acid Mono-2-Ethylhexyl Ester (Ionquest 801) from Hydrochloric Acid Solutions 1127
IO Masson, PSM Soares, M Aguilar and JL Cortina

Synergistic and Antagonistic Behaviour in the Stripping of Heavy Rare Earth Elements from Solvent Mixtures Containing Phosphonic and Phosphinic Acids and Trialkylphosphine Oxides 1133
D Nucciarone, CD Pagnucco, B Jakovljevic and WA Rickelton

Extraction of Chloro Complex Acids of Platinum Group Metals with Binary Extractants 1139
VV Belova, AI Kholkin and TI Jidkova

Thermodynamic and Kinetic Studies of Palladium(II) Extraction by LIX 63–Aliquat 336 Mixtures 1143
C Foulon, S Pareau, M Stambouli and G Durand

Extraction Behaviour of Platinum(IV) in Chloroform with a Crown Ether from Acidic Media 1149
KZ Hossain and T Honjo

Comparative Studies of Solvent Extraction and Liquid Membrane Permeation of Gold(III) from Chloride Media 1155
R Haddad, A Kumar, FJ Alguacil and AM Sastre

Extraction of Pentachloroaquaosmate(IV) Ion from Sulphuric Acid Solutions 1161
AB Maiboroda, ID Troshkina and AM Chekmarev

Solvent Extraction of Ruthenium(III) as a Thiocyanate Complex 1167
B Tamhina, V Vojkovic and N Brajenovic

Extraction of Iron(III) from Hydrochloric Acid Solutions by an α-Hydroxyoxime 1173
T Sato, M Ito and M Hotta

Third Phase Appearance in Cobalt(II) and Nickel(II) Extraction with Mono-(2-Ethylhexyl)-phosphonic Acid 2-Ethylhexyl Ester (MOOP) 1177
Da Maljkovic, Z Lenhard and Du Maljkovic

Extraction Equilibria of Nickel with LIX860 and DEHPA 1181
T Sana, K Shiomori, Y Kawano and K Nagayoshi

Stoichiometry of the Extraction of Nickel with Organophosphorus Acids 1187
CC Bourget, M Cox and DS Flett

Copper Extraction from Ammoniacal Solutions with Commercial Chelating Extractants and their Mixtures 1193
G Kyuchoukov, MB Bogacki and J Szymanowski

Extraction of Copper from Chloride Media with a New Alkyl Derivatives of Pyridine-3,5-Dicarboxamide 1197
A Borowiak-Resterna, G Cote and J Szymanowski

Extraction of Copper and Zinc from Chloride Solutions by an Hydrophobic Alkyl Derivative of 8-Hydroxyquinoline 1203
G Kyuchoukov, A Jakubiak and J Szymanowski

Liquid–Liquid Extraction of Zinc(II) by Solvating Extractants from HCl/H_2SO_4 Mixed Media 1209
JA Barron Zambrano, M Avila-Rodríguez, TI Saucedo Medina, R Navarro Mendoza and AM Sastre

Solvent Extraction of Divalent Zinc and Cadmium from Hydrochloric Acid Solutions by Dihexylsulphoxide 1215
T Sato, I Ishikawa and K Sato

Solvent Extraction of Divalent Zinc and Lead from Sodium Hydroxide Solutions by an Alkylated Hydroxyquinoline 1221
T Sato, K Sato and F Tahiani

Extraction of Lead(II) by Cyanex 302 and Cyanex 301 from 2.19 mol/dm^3 Phosphoric Acid Medium 1227
B Menoyo and MP Elizalde

Solvent Extraction of Scandium(III) with Cyanex 302 and H[BTMPTP] 1233
D Li , C Wang and Z Wei

Solvent Extraction of Scandium(III) by Cyanex 272 and H[BTMPP] 1239
C Wang and D Li

Solvent Extraction of Tin(IV) from Hydrochloric Acid Solutions by High Molecular Weight Amines 1245
T Sato, K Sato and Y Noguchi

Separation of Cesium and Strontium from s-Block Metal Ions by Double and Triple Phase Systems 1249
Y Komatsu, S Umetani and S Tsurubou

The Stoichiometric Modelling of the Exchange Extraction of Mg, Ca and Na with Potassium Di-2-Ethylhexylphosphate from Concentrated Brines 1255
NM Rice and MA Tomlinson

Extraction of Arsenic(III) and Arsenic(V) from Sulphuric Acid Solutions with Trialkylphosphine Oxides and Hydroxamic Acids 1261
M Wisniewski, L Iberhan and J Szymanowski

New Developments in Solvent Impregnated Resins. An Overview 1267
A Warshawsky, JL Cortina, M Aguilar and K Jerabek

Influence of Polymeric Support on Selectivity of Extractant in Solvent Impregnated Resins 1273
A Gonzalo, D Muraviev and M Valiente

Extraction of Heavy Metal Ions using Encapsulated Extractant-impregnated Resin 1279
S Nii, M Masutani and H Takeuchi

Design of a Truly Continuous Fluidized Bed System for Metal Recovery using Impregnated Resins 1285
M Rovira, J Herranz, JL Cortina, N Miralles, J Arnaldos and AM Sastre

Extraction of Non-extractable Ionic Species in Aqua Impregnated Resin Systems 1291
D Muraviev, A Torrado and M Valiente

Extraction of Rare Earth Metals with PC-88A by a Hollow Fibre Membrane System 1297
F Kubota, M Goto, S Furusaki, K Yoshizuka, F Nakashio and T Hano

Hollow Fibre non-Dispersive Solvent Extraction: a Promising Approach to Environmental and Hydrometallurgical Applications 1303
A Kumar and AM Sastre

Hydration of Metal Perchlorates Extracted with Trioctylphosphine Oxide in Hexane 1309
S Kusakabe

Solvent and Solid Extraction of Metal Ions with 4-*n*-Dodecyl-6-(2-thiazolylazo)resorcinol 1313
H Matsunaga

The Separation of Phenol from Neutral Oils by Liquid–Liquid Extraction 1319
DL Venter and I Nieuwoudt

Extraction of Acetic and Propionic Acids from Aqueous NaCl Solutions by Trioctylphosphine Oxide 1325
HF Al-Mudhaf, AI Abu-Shady, SA Amer and MF Hegazi

NUCLEAR APPLICATIONS 1331

Extraction of Lanthanides(III) and Actinides(III) by N,N′-Substituted Malonamides: Thermodynamic and Kinetic Data 1333
MC Charbonnel, M Daldon, C Berthon, MT Presson, C Madic and C Moulin

The Solvent Extraction Behaviour of Tetravalent Actinides in the Presence of Simple Hydroxamic Acids 1339
RJ Taylor, I May and NJ Hill

Development of a Universal Cobalt Dicarbollide Solvent for the Removal of Actinides, Cesium and Strontium from Acidic Wastes 1345
TA Todd, KN Brewer, JD Law, RS Herbst, DJ Wood, VN Romanovskiy, V Esimantovskiy, IV Smirnov, VA Babain and B Zaitsev

Extraction of Tetravalent Uranium from Phosphate Medium by HDEHP and OPAP 1351
JA Daoud, MM Zeid and HF Aly

Synergistic Extraction of U(VI) and Th(IV) from Nitric Acid with HBMPPT and TOPO in Toluene 1357
S-N Yu, L Ma and B-R Bao

Study on the Solvent Extraction of U(VI) and Th(IV) from Nitric Acid with HBMPPT 1361
S-N Yu, T-J Wang and B-R Bao

Solvent Extraction of Tc and Cs from Alkaline Nitrate Wastes 1365
BA Moyer, PV Bonnesen, LH Delmau, TJ Haverlock, RA Sachleben, RA Leonard, C Conner and GJ Lumetta

Extraction of Strontium and Cesium Using a Synergistic Solvent Mixture 1371
TA Todd, DJ Wood, MA Afonin and VV Romanovski

Use of Binary Extractants for Recovery of Silver(I) from Waste: a Novel Concept in Solvent Extraction 1375
A Kumar, PK Gautam, JP Shukla, RK Singh and AM Sastre

New Reducing Agents for Neptunium(VI) and Plutonium(IV) 1381
RJ Taylor, I May, IS Denniss, VS Koltunov, SM Baranov, VI Marchenko, EA Mezhov, VG Pastuschak, GI Zhuravleva and OA Savilova

Thermodynamics of Extraction Behavior of Eu(III) And Tm(III) by Thenoyl-trifluoroacetone and Crown Ethers in Organic Solvents from Nitrate Medium 1387
FA Shehata, N El-Hefny and HF Aly

PETROLEUM APPLICATIONS 1395

A Deep Desulfurization Process for Light Oil by Photochemical Reaction in an Organic Two–Phase Liquid–Liquid Extraction System 1397
Y Shiraishi, T Hirai and I Komasawa

Hydrogen Sulfide Removal from Hydrocarbon C_3–C_4 Fraction 1403
S Costic, F Oprea and F Enachescu

PHARMACEUTICAL APPLICATIONS 1409

Extraction of Citric Acid in Hollow Fibre Modules 1411
I Miesiac, P Kirschling and J Szymanowski

Solvent Extraction of Phthalic Acid with Basic Extractants, and the Structure of the Complexes Formed 1417
S Rambocus, N Kelly, BG Reuben and A Drake

Specific Inhibitory Effects of Hybrid Membranes on the Growth of Tumors *in vitro* and *in vivo* 1423
R Ueoka, Y Matsumoto, T Kato, A Kanno, M Tsuchiya, K Tsuzaki and Y Murakami

PLANT EXPERIENCE 1429

The Thermal Oxide Reprocessing Plant at Sellafield: Four Years of Active Operation of the Solvent Extraction Plant 1431
C Phillips

Mini-plant Trials on the Recovery of Nickel by Solvent Extraction 1437
VM Nagel, BM Davies and PM Cole

Pilot-plant Evaluation of Manganese Removal and Cobalt Purification by Solvent Extraction 1443
A Feather, KC Sole, and DB Dreisinger

Updated Available Solvent Extraction Technologies 1449
G Díaz, D Martín, C Frías and O Pérez

Comparison of the Performance of Full Scale Pulsed Columns *vs* Mixer–Settlers for Uranium Solvent Extraction 1455
RL Movsowitz, R Kleinberger, EM Buchalier, B Grinbaum and S Hall

PROCESS DEVELOPMENT 1461

The Development of Chemical Flowsheets for an Advanced Purex Process 1463
AL Wallwork, P Bothwell, JE Birkett, IS Denniss, RJ Taylor and I May

Distribution behaviour of Uranium, Plutonium, Neptunium and Technetium in an Advanced PUREX Process (PARC process) 1469
G Uchiyama, T Kihara, H Mineo, T Asakura, S Hotoku, M Watanabe, K Kamei, Y Nakano, S Kimura, M Goto and S Fujine

Development of Fission Product (artificial) Palladium Liquid–Liquid Extractive Recovery and Refining Operations 1475
Ed V Renard, VG Torgov, VV Tatarchuk, TM Korda and IA Druzhinina

A New Process Producing Phosphoric Acid from Phosphate Rock and Hydrochloric Acid via Ferric Phosphate 1481
J Mizrahi

Selection of Extractants for the Removal of Cadmium from Industrial Grade Phosphoric Acid 1487
I Ortiz, S Zamacona and AM Urtiaga

Production of WO_3 from Scheelite Concentrates by Extraction Technology 1493
SI Stepanov, VG Giganov, GP Giganov and AM Chekmarev

Separation and Concentration of l-Phenylalanine in Hollow Fibre Modules: Decrease of the Extraction Rate 1499
H Escalante and A Irabien

Process Development, Design and Scale-up Using a Large Scheibel Extraction Column 1503
TC Lo

SIMULATION AND MODELLING 1509

Modelling of the Separation of Cadmium from Phosphoric Acid using Emulsion Liquid Membranes 1511
T Gallego Lizon and ES Pérez de Ortiz

Hollow Fibre Modules as Novel Phase Contactors for the Separation of Multi-cation Mixtures by Chemical Extraction 1517
A Geist, JI Kim, P Plucinski and W Nitsch

Modelling of Continuous Reactive Extraction and Stripping of Zinc in Hollow Fibre Modules 1523
P Schöner, W Nitsch, P Plucinski and A Fedorov

Mathematical Modelling of Metal Permeation across Supported Liquid Membranes Considering Membrane Rate Controlling Parameters 1529
G Benzal, A Kumar, A Delshams and AM Sastre

Modelling Phase Equilibria in the Industrial Caprolactam Recovery from Aqueous Ammonium Sulphate Solutions with Benzene 1537
AB de Haan and SH Niemann

Modelling and Optimization of Sulfolane Extraction: a Neural Network Approach 1543
G Su, X Wen, and W Fei

A New Method for the Simulation of Multistage Metal Extraction Processes Based on the Steady-State Local Linearization 1549
M Tanaka, K Koyama and J Shibata

DISTREC: a New Computer Program for Solvent Extraction Equilibrium Calculations, Modelling and Simulation 1555
M Aguilar, JL Beltran and JL Cortina

Soft Modelling Techniques: a Tool for Studying Solvent Extraction Processes 1561
JL Cortina, M Aguilar, M El-Gharbi and R Tauler

Co-current Extraction: Design of Industrial Equipment by Scaling-up Laboratory Tests 1567
V Alessi, A Franzoni, C Gradella, R Penzo and MJ Slater

Influence of Continuous Phase Flow Field and Compartment Geometry on Droplet Breakage in Rotating Disc Contactors 1573
G Modes and H-J Bart

Mass Transfer Performance in a Pulsed Sieve Plate Extraction Column 1579
GS Luo, HB Li, W Fei and JD Wang

Prediction of Flooding in Random and Structured Packed Columns using a Drift Flux Methodology 1585
LS Hutahaean, DM Schaefer, JS Kanel and V Van Brunt

Supercritical Extraction 1593

A Mechanically Agitated Supercritical Extraction Column 1595
A Laitinen and J Kaunisto

Separation of Enantiomeric Acids and Bases by Supercritical Fluid Extraction 1601
B Simándi, S Keszei, E Fogassy, E Székely, A Prechl, V Varga, S Kemény and J Sawinsky

Supercritical Fluid Extraction of Tocopherols from Olive Tree Leaves 1607
A de Lucas, E Martínez de la Ossa, J Rincón, MA Blanco and I Gracia

Supercritical Fluid Extraction of Borage Oil 1611
A Delgado, A Molero and E Martínez de la Ossa

Supercritical Fluid Extraction of Anthocyanins from Grape Pomace 1615
C Mantell, E Martínez de la Ossa and M Rodríguez

Acetic Acid Extraction by Supercritical Carbon Dioxide: Pressure Effect 1619
C Pereyra, G Di Giacomo and E Martínez de la Ossa

Regeneration of ß-Cyclodextrin with Supercritical Carbon Dioxide 1623
G Del Re, G Di Giacomo and M Cinti

Tocopherol Extraction by Liquid and Supercritical Carbon Dioxide 1629
MA Blanco, A Molero and E Martínez de la Ossa

Extraction of Wheat Germ Oil by Liquid and Supercritical Carbon Dioxide 1633
A Molero and E Martínez de la Ossa

Extraction of the Antibiotic Pleuromutilin from Fermentation Broth using Compressed Carbon Dioxide 1639
T Walford, T Lu, R Santos, MB King, AJ Biddlestone and A Stefanska

Direct Supercritical Fluid Extraction of Organic Compounds from Aqueous Solutions 1645
Yu A Zolotov, IA Revelsky and IN Glazkov

Supercritical Fluid Extraction of PCBs from Real World St. Lawrence River Sediments 1651
Z Wu and LL Tavlarides

Ligand-assisted Supercritical Fluid Extraction and Environmental Management needs for Removal of Metals 1657
RV Fox, RD McMurtrey and JD Navratil

Supercritical Fluid Extraction in Gold Hydrometallurgy 1663
EO Otu

Modelling of Supercritical Fluid Extraction from Natural Materials with Interaction between Solutes and Solid 1669
M Goto, A Kodama and T Hirose

Modelling of the Fluid–Solid Equilibria of the Antibiotic Penicillin G in Supercritical Carbon Dioxide 1675
MD Gordillo, A Molero and E Martínez de la Ossa

Author index I

Keyword index IX



Kinetics and Interfacial Phenomena

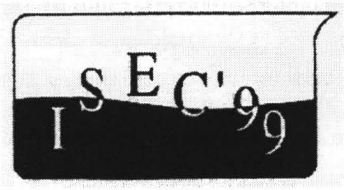

A STUDY OF METAL ION EXTRACTION AT THE OIL/WATER INTERFACE USING EVANESCENT WAVE SPECTROSCOPY

Parisa Deljouie[2], Jilska M Perera[1], Geoffrey W Stevens[1] and Franz Grieser[2]

Advanced Minerals Products Special Research Centre (AMPC)
[1]Department of Chemical Engineering, [2]School of Chemistry, University of Melbourne, Parkville, Victoria 3052, Australia.

ABSTRACT

An optical technique using Variable Angle Evanescent Wave Spectroscopy has been developed to study the kinetics of extraction of Copper (II) by Kelex 100 at the oil/water interface. The Attenuated Total internal Reflectance (ATR) signal which is a result of coupling of the evanescent wave with the Cu/Kelex 100 complex in the vicinity of interface has been measured by means of UV-visible absorption spectroscopy. These results have been used to calculate the interfacial area occupied by the complex and compared with the area per molecule calculated by means of interfacial tension measurements.

Keywords: copper(II), Kelex 100, interfacial kinetics, ATR spectroscopy

INTRODUCTION

Solvent extraction processes involving chelating extractants are widely used in the hydrometallurgical industry as a technique for the separation and purification of metals, and also the removal of heavy metals from waste-water streams. Commercially available ligands are generally insoluble or sparingly soluble in water, therefore, the complexation reaction occurs at the interface between the oil and aqueous solution. Despite considerable research, using techniques involving the stirred cell,[1-3] the single drop,[4,5] the rotating diffusion cell (RDC) [6,7] and the liquid jet recycle reactor (LJRR),[8,9] which are designed to measure reactions at the liquid-liquid interfaces, the methods are still limited in comparison with the techniques measuring reactions at the air-liquid and solid-liquid interfaces. Recent reviews [10-12] have highlighted drawbacks in many current techniques and concluded that for many studies "there are no generally established criteria for proper interfacial kinetics measurements". In recent years there have also been studies on measuring the interfacial kinetics of metal complex formation at liquid-liquid interfaces using electrochemical methods which had previously been used at solid-liquid interfaces, such as the Scanning Electrochemical Microscopy (SECM) technique.[13,14]

The technique of ATR spectroscopy widely used with solid-liquid interfaces[15,16] and recently applied to liquid-hydrocarbon gel interfaces,[17] has also been applied to liquid-liquid interfaces for the measurement of interfacial ion adsorption.[18-20] In the present work UV-visible ATR spectroscopy have been used to measure the interfacial concentration of a metal-ligand complex during extraction of Cu^{2+} from an aqueous phase into n-heptane using Kelex 100 as the extractant ligand. A static cell previously used [21,22] for measurement of total organic phase complex concentration has been modified and a model interfacial system has been developed which enables us to measure the interfacial concentration directly.

EXPERIMENTAL

Chemicals

7[4-ethyl-1-methyloctyl]-8-hydroxyquinoline (Kelex100) was kindly provided by Schering Industrial Chemical Company. Kelex 100 was shaken with H_2O (W/O=10) at reduced pH (1.3-1.5) to remove 8-hydroxyquinoline (8HQ). Spectrophotometric absorbance measurements indicated that more than 90% of

© 2000 Society of Chemical Industry

8HQ was removed in this way. Analytical reagent grade n-heptane, and sulfuric acid (BDH chemicals), copper sulfate, sodium hydroxide and sucrose (Ajax chemicals) were used as received.

ATR apparatus

A schematic diagram of the ATR cell is presented in Figure 1. This cell is a modified version of the static cell previously used by Perera et al.[21] and McCulloch et al.[22]

Figure 1- Schematic diagram of the ATR cell (in all our ATR experiments there are two reflections at the interface, only one is shown here for simplicity). Insert (a) displays depth of penetration as a function of angle of incidence for our particular system.

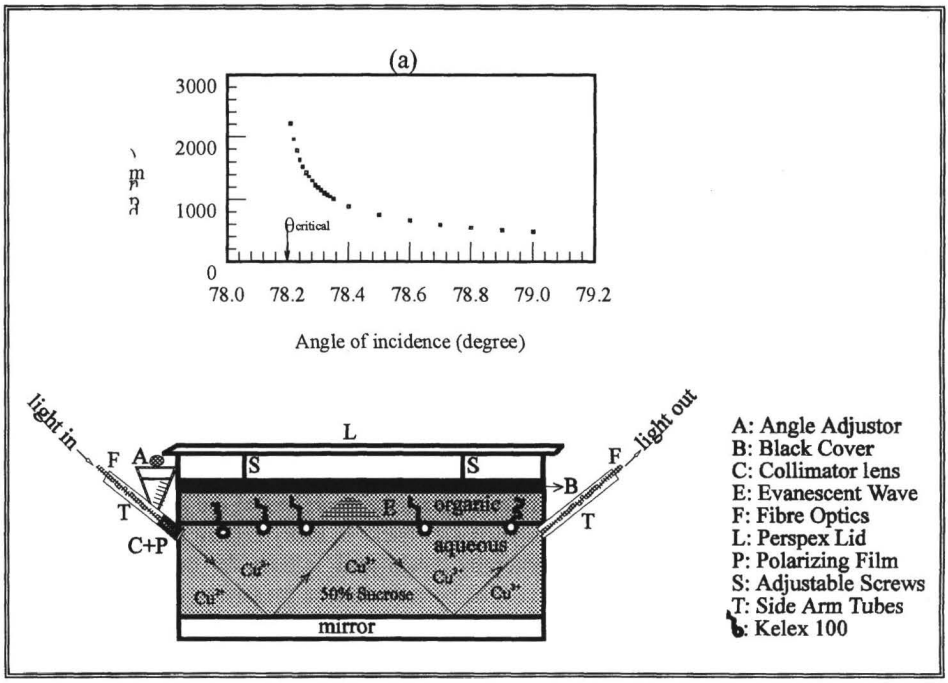

The incident light beam from an Oriel 150-W Xenon arc lamp is passed through a 10 cm path length water filter (to remove IR radiation) down a 3mm diameter quartz fibre optic (Dolan Jenner), F, fitted with a beam collimator (C) (Dolan Jenner-RFQ), a polarizing film, P, (Polaroid-HN42), and into the ATR cell (dimensions- length x width x height = 40cm x 6cm x 5cm). The angle of the incident beam is adjusted higher than the critical angle by the angle adjustor (A) screwed to the left hand side arm quartz window tube, T. A mirror is attached to a Teflon base at the bottom of the cell. 50% by weight sucrose has been dissolved in the aqueous phase in order to make the refractive index higher than that of the oil phase (n-heptane). In this situation an incident beam with an angle higher than the critical angle hits the mirror and reflects off the aqueous-oil interface, being totally reflected within the aqueous phase. The evanescent wave (E) penetrates into the organic phase, to a depth which can be adjusted by the angle of incidence beam. This evanescent beam is capable of coupling with an absorbing chromophore (in this case the Cu^{2+}/Kelex 100 complex) in the vicinity of interface causing an attenuation of the total internal reflected beam. A black acrylic cover (B) is suspended from the perspex lid (L) of the cell via adjustable screws (S) covering the organic phase, ensuring all the stray light is absorbed. The reflected light is then collected by a second fibre optic bundle into an Oriel Multispec 1/8 m monochromator, the output from which is spread onto an Oriel Instaspec (II) photodiode array detector and the absorbance information is processed by a PC using Instaspec II software.

ATR experiments

In ATR experiments the conditions were chosen so that the copper ion was always in excess (aqueous and organic phase volumes were 500 mL and 100 mL respectively). Two total internal reflections of the incident light at the interface with an angle of incidence (θ=79°) were used in all experiments; the refractive indices of the two phases were measured in a Bellingham & Stanley Ltd refractometer before being introduced into the cell.

a) Static measurements. The aqueous phase at an appropriate pH was contacted with the organic phase (n-heptane) in the ATR cell and a reference scan then taken and stored. Known volumes of concentrated Cu/Kelex 100 complex were injected into the organic phase and the increase in the absorbance peak measured spectrophotometrically.

b) Kinetic measurements. The aqueous phase containing 50% sucrose by wt. and sufficient amount of Cu^{2+} (at appropriate pH) was contacted with n-heptane in the ATR cell and a reference scan taken and stored. The n-heptane was then removed and the organic phase containing Kelex 100 was introduced into the cell and the rate of formation of the complex spectrophotometrically measured at known time intervals.

Interfacial tension measurements

The interfacial tension of the Cu/Kelex100 complex in n-heptane was measured using image analysis of a pendant drop of the aqueous phase in the organic phase in an FTÅ 200 device. The two phases were first equilibrated for 10 min, the phases separated and the pH values measured. A droplet of the aqueous phase was then formed in the organic phase at constant temperature (20°C) and the interfacial tension was measured.

RESULTS AND DISCUSSION

The results of a typical static ATR experiment are displayed in Figure 2. Each spectrum is an evanescent wave absorbance spectrum at different concentrations of Cu^{2+}/Kelex 100 complex in the vicinity of interface.

The depth of penetration (dp) of an evanescent wave, the distance required for the electric field amplitude to fall to 1/e of its value at the interface, is defined by Equation (1),[23]

$$dp = \lambda / 2\pi(\sin^2\theta - n_{21}^2)^{1/2} \quad (1)$$

where $n_{21} = n_2/n_1$ is the ratio of the refractive index of the oil phase (n-heptane) divided by the refractive index of the aqueous phase (water containing 50% sucrose by wt.). It is clear from Equation (1) that the depth of penetration of evanescent wave at a certain wavelength (λ) can be controlled by the angle of incidence (θ) of the light beam, thus enabling the monitoring of complex concentration at various depths from the interface.

The absorbance of an ATR reflection at the interface can be predicted by a Beer-Lambert type equation,[24]

$$A(\theta,\lambda) = N\,\varepsilon(\lambda)\,[c]\,\frac{1}{\cos\theta}\int_{z=0}^{\infty} I(z)\,dz \quad (2)$$

where $A(\theta,\lambda)$ is the absorbance measured by the spectrophotometer at a wavelength of λ and an angle of incidence θ, N is the number of reflections at the interface, $\varepsilon(\lambda)$ is the extinction coefficient ($M^{-1}cm^{-1}$) at a wavelength of λ, [c] is the concentration of the light absorbing complex (M) and I(z) is the intensity of the evanescent wave at a distance z from the interface, namely, $I(z) = I_0\,e^{-2z/dp}$.

Equation (2) can be rewritten for p-polarized light as:

$$A(\theta,\lambda) = N\,\varepsilon(\lambda)\,[c]\,\frac{dpI_{op}}{2\cos\theta} \quad (3)$$

where $I_{op} = \frac{4n_{21}\cos^2\theta(2\sin^2\theta - n_{21}^2)}{(1-n_{21}^2)\{(1+n_{21}^2)\sin^2\theta - n_{21}^2\}}$ and dp (cm) is as defined earlier in Equation (1).

The interfacial concentration (Γ_{ATR}) and the interfacial area of the complex (α_{ATR}) for the static ATR experiments have been calculated as per Equation (3) and are listed in Table 1. In order to obtain an independent measure of the area occupied by the complex at the interface the interfacial tension of the same liquid phase pair, using an image analysis pendant drop method for a series of Cu^{2+}/Kelex 100 complex concentrations was measured. Using the Gibbs adsorption isotherm the surface excess (Γ_{ATR}) and the interfacial area of the complex (α_{ATR}) were estimated. These results have been listed in Table 1.

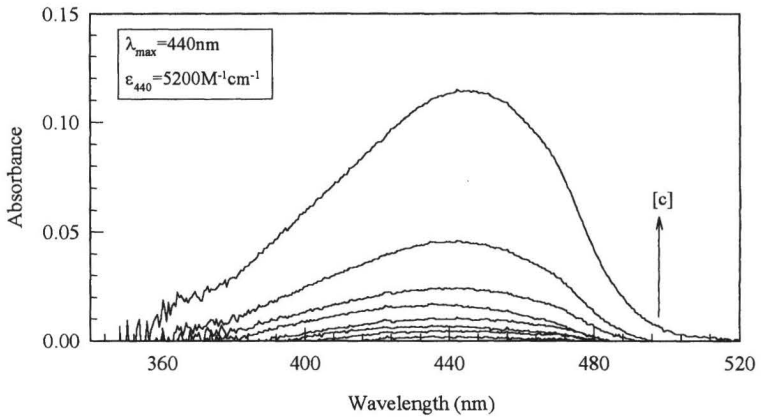

Figure 2- Absorbance spectra of Cu^{2+}/Kelex 100 complex as a function of concentration. Conditions: angle of incidence (θ)=79°, aqueous phase- 50% sucrose (w/w), pH=6.20, organic phase- 0.37, 0.95, 1.31, 2.13, 3.10, 5.68, 8.52, 17.05 (10^{-3}M) Cu^{2+}/Kelex 100 complex.

[Cu^{2+}/Kelex 100] (10^{-3}M)	Γ_{IT} (mol/cm^2)	α_{IT} (Å/molecule)	Γ_{ATR} (mol/cm^2)	α_{ATR} (Å/molecule)
0.10	4.1×10^{-11}	341	6.7×10^{-11}	246
1.00	8.4×10^{-11}	197	1.2×10^{-10}	131
10.00	1.2×10^{-10}	139	1.9×10^{-10}	85
51.80	1.4×10^{-10}	114	5.4×10^{-10}	30
95.30	1.5×10^{-10}	107	-	-

Table 1 Interfacial concentration (Γ) and area/molecule (α) for the Cu^{2+}/Kelex 100 complex at the heptane/water (containing 50% by wt. sucrose) interface from interfacial tension (IT) and ATR measurements. Conditions: pH=6.30, T=20°C.

As can be seen from Table 1, the α_{ATR} values are lower than the α_{IT} values which suggests that the evanescent wave in the ATR cell may have a higher depth of penetration than expected from the angle of incidence beam used. It is likely that this is as a result of the light not being completely collimated and therefore giving a range of angles of incidences reflecting off the interface. It can be seen in Figure 1 (insert a) this will lead to light at angles less than 79° penetrating deeper into the solution and consequently the amount of complex will be overestimated in the calculations using Equation (3).

A typical set of Cu^{2+}/Kelex 100 complex formation kinetics in the ATR cell observed by absorbance increase at 440 nm as a function of time, is represented in Figure 3.
The results show that there is a rapid increase in absorbance at short times (<10 s) followed by a slower growth occurring over hundreds of seconds. The short time absorbance corresponds to more than monolayer coverage of the interface, indicating that significant complex formation occurs during the mixing time of the two overlaying phases. The longer time kinetics reflects the diffusional approach to saturation of the complex in the organic phase. We are currently investigating the complex formation between Kelex 100 and other transition metals with slower kinetics. Addition of surfactant modifiers to the Cu^{2+}/Kelex 100 system is also under investigation to examine if they can retard Kelex 100 adsorption at the interface, thereby, slowing down the formation of the complex at the interface.

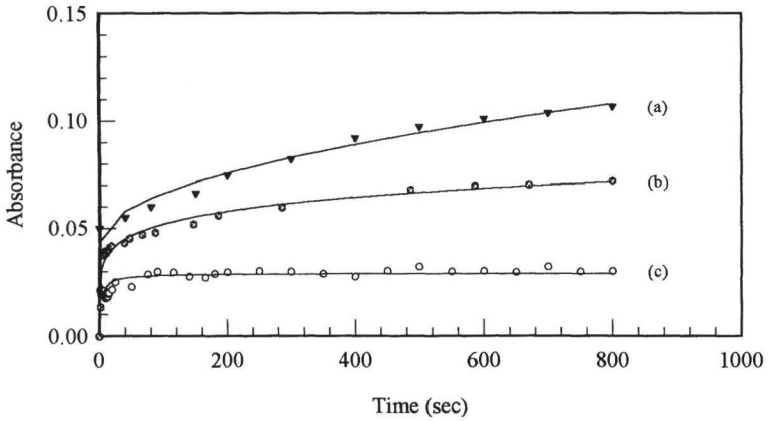

Figure 3- Absorbance versus time for extraction of Cu^{2+} by Kelex 100 as observed by ATR experiments. Conditions: angle of incidence (θ)=79°, aqueous phase- Cu^{2+}/50% sucrose (w/w), organic phase- Kelex 100/n-heptane. (a) 0.08M Kelex 100, 0.04M Cu^{2+}, pH=3.30, (b) 0.08M Kelex 100, 0.04M Cu^{2+}, pH=2.45, (c) 0.04M Kelex 100, 0.02M Cu^{2+}, pH=2.00.

CONCLUSION

Results from the ATR experiments indicate that with slight improvements this technique can be applied as an effective tool to directly measure the interfacial concentration during the metal extraction processes.

REFERENCES

1. Lewis JB *Chem. Eng. Sci.*, **3**, 218, (1954)
2. Flett D, Okuhara D and Spink DR, *J. Inorg. Nucl. Chem.*, **35**, 2471, (1973)
3. Freiser H, *Bull. Chem. Soc. Jpn.*, **61**, 39, (1988)
4. Komasawa I, Otake T and Muraoka T, *J. Chem. Eng. Jpn.*, **13(3)**, 204, (1980)
5. Preston JS and Luklinska Z, *J. Inorg. Nucl. Chem.*, **42**, 431, (1980)
6. Albery JW and Fisk PR, *Proc. Hydrometallurgy 81*, F5, 15, (1981)
7. Dreisinger DB and Cooper CW, *Solv. Ext. Ion Exch.*, **4(1),** 135, (1986)
8. Freeman RW and Tavlarides LL, *Chem. Eng. Sci.*, **35**, 559, (1980)
9. Tavlarides LL, Freeman RW and Hsia AM, *U.S. Patent 4294800*, (1981)
10. Hanna GJ and Noble RD, *Chem. Rev.*, **85**, 583, (1985)
11. Atherton JH, *Res. Chem. Kinet.*, **2**, 193, (1994)
12. Stevens GW and Perera JM, *Min. Pro. Ext. Met. Rev.*, **17**, 205, (1997)
13. Slevin CJ, Umbers JA, Atherton JH and Unwin PR, *J.Chem.Soc., Faraday Trans.*, **92**, 5177, (1996)

14. Barker AL, Macpherson JV, Slevin CJ and Unwin PR, *J. Phys. Chem. B*, **102**, 1586, (1998)
15. Harrick NJ, *J. Phys. Chem.*, **64**, 1110, (1960)
16. Trau M, Grieser F, Healy TW and White LR, *J. Chem. Soc. Faraday Trans.*, **90**, 1251, (1994)
17. Sperline RP and Freiser H, *Langmuir*, **6**, 344, (1990)
18. Watarai H and Saitoh Y, *Chem. Lett.*, **1995**, 283
19. Watarai H and Funaki F, *Langmuir*, **12**, 6717, (1996)
20. Saitoh Y and Watarai H, *Bull. Chem. Soc. Japan*, **70**, 351, (1997)
21. Perera JM, McCulloch JK, Murray BS, Grieser F and Stevens GW, *Langmuir*, **8**, 366, (1992)
22. McCulloch JK, Perera JM, Kelly ED, White LR, Stevens GW and Grieser F, *J. Colloid Interface Sci.*, **184**, 406, (1996)
23. Harrick NJ, *Internal Reflection Spectroscopy*, John Wiley & Sons, Inc., NY, (1967)
24. Born M and Wolf E, *Principles of Optics*, Pergamon, New York, (1983)

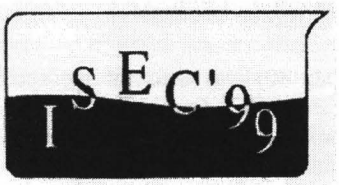

EXTERNAL REFLECTION SPECTRA AT THE LIQUID–LIQUID INTERFACE OF EXTRACTION SYSTEMS CONTAINING PORPHYRINS

Nobuaki Ogawa, Yoshio Moriya and Hitoshi Watarai[1]
Department of Materials-Process Engineering and Applied Chemistry for Environments, Faculty of Engineering and Resource Science, Akita University, 1-1, Tegata Gakuencho, Akita 010-8502, Japan.
[1]Department of Chemistry, Graduate School of Science, Osaka University, Machikaneyama, Toyonaka, Osaka 560-0043, Japan.

ABSTRACT
External reflection (ER) UV-vis spectra of the interfacially adsorbed species of protonated porphyrins at toluene/aqueous sulphuric acid interfaces were successfully observed with clear negative absorption bands and without overlapping by the spectrum of the organic bulk phase. The ER spectrum had three peaks (412, 475 and 722 nm) for the adsorbed species of protonated and aggregated tetraphenylporphyrin. Among the three bands of ER spectrum, the band of 412 nm was hardly detected by using the corresponding total internal reflection spectroscopy.

Keywords: external reflection spectra, liquid-liquid interface, porphyrin

INTRODUCTION

Chemical properties of liquid-liquid interfaces are one of the attractive subjects in some fields, especially in that of solvent extraction. In recent years, therefore, several direct spectroscopic methods have been employed to recognise the interfacial species. Among the approaches, an optical stirred cell method and a Teflon capillary plate method have been devised[1] to identify the interfacial species in high specific interface area. In addition, the total internal reflection (TIR) spectroscopy is one of the most informative methods.[2,3] This method is very useful for the ion-association adsorption of water-soluble extractants as that investigated in the TIR fluorescence spectroscopy.[4,5] However, an organic phase often contains strongly light-absorbing ligands and complexes in solvent extraction, hence the application of TIR spectroscopy to such systems is limited. In the research field, therefore, a more effective method which enables the detection of only the interfacial species is strongly desired.

In our research group, a successful application of an external reflection (ER) spectroscopy for the *in situ* measurements of the interfacial species of hydrophobic porphyrin (tetraphenylporphyrin [TPP]) at toluene/water interface have been reported. [6] The previous paper is the first experimental research for the application of ER spectroscopy to liquid-liquid interface system, as far as we know. In the present study, An improvement is reported of the cell arrangement together with the spectra of ER, TIR, organic and aqueous bulk phases for some hydrophobic porphyrins. The interfacial quasi-equilibrium and the polarised spectra of TPP is also discussed.

EXPERIMENTAL

Reagents

The porphyrins used in this work are 5,10,15,20-tetraphenyl-21*H*,23*H*-porphine (tetraphenylporphyrin) (TPP), 2,3,7,8,12,13,17,18-octaethyl-21*H*,23*H*-porphine (OEP) and 5,10,15.20-tetrakis(2,6-dichlorophenyl)porphine (TDCP) purchased from Dojindo Laboratories (figure 1). Several concentrations of porphyrin in toluene (Wako, GR) as the organic phase and a constant aqueous concentration 4 mol/dm^3 of sulphuric acid as the aqueous phase are adopted in these experiments for comparison with other reports.[1,6] All other chemicals were of analytical reagent grade and were used without further purification.

© 2000 Society of Chemical Industry

Cell arrangements and procedure of measurements

A Perkin Elmer double beam spectrophotometer (Lambda 40) was used for the spectral measurements. The optical arrangements for the measurements of ER, TIR, organic and aqueous bulk spectra are schematically illustrated in figure 2, which is an improvement on our previous work for obtaining these four spectra at the same interfacial and bulk conditions. [6] On both sides of the 2.0 cm quartz cell, a pair of right-angle prisms were set in appropriate positions so that the incident beam struck the centre of the interface with an incident angle 74.4° for TIR or 72.5° for ER. The former angle in the arrangement of TIR was larger enough than the critical angle 63.3° for the toluene/4 mol/dm^3 sulphuric acid interface.

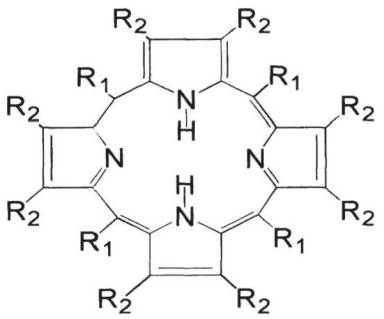

Figure 1. Porphyrins used in this work. TPP: R_1= phenyl, R_2=H, OEP: R_1=H, R_2= -CH_2CH_3, TDCP: R_1=2,6-dichlorophenyl, R_2= -CH_2CH_3

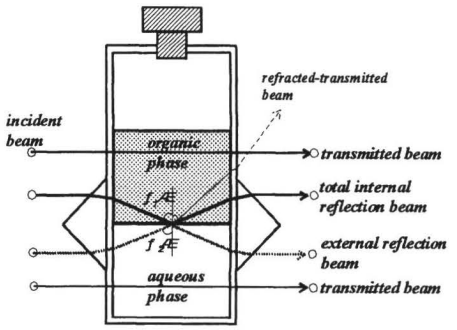

Figure 2. Schematic drawing of the optical cell arrangement

In the ER spectroscopy, however, the incident beam is separated into an externally reflected beam and a transmitted-refracted beam (with a refraction angle 58.4° in this system). The upper inside of the cell was treated with dichlorodimethylsilane in toluene as an hydrophobic coating, so as to make a flat toluene/water interface.[4,5] At first for the spectral measurements, a reference scan of the toluene, (not including porphyrin)/4 mol/dm^3 sulphuric acid interface, or the organic or aqueous bulk phase, was taken and stored as a blank, then 15 to 40 μL portions of porphyrin solution (4.0×10^{-5} mol/dm^3) were added stepwise to the organic phase. As a result, four spectra could be obtained at the same interfacial and bulk condition by changing the height of the adjuster. The temperature of the inner sample solutions was kept at 298 ± 0.5 K by a thermostatic circulator. The interfacial adsorption quasi-equilibration was achieved within 1 hour. The four spectra data at quasi-equilibration were mainly used for analysis, but the spectral change after the quasi-equilibration was also obtained and is discussed later.

RESULTS AND DISCUSSION

Spectra of TPP

Figure 3 shows the spectra under the total TPP concentration $[TPP]_{T,org}$ of 1.6×10^{-6} M. The spectrum a for the organic bulk phase after adsorption equilibration has at least five absorption maximums at the wavelengths (λ_{max}): 419, 515, 548, 592 and 648 nm within the region 350-800 nm. In the TIR spectrum b in figure 3, however, two new peaks were observed at 475 and 722 nm in addition to the peaks observed for the spectrum a. Therefore, the two new peaks could belong to the interfacial species. The peak at 475 nm agreed in general to the corresponding peak at 472 nm of the transmission absorption spectrum measured by the Teflon capillary plate method.[1] The peak can be

ascribed to a coagulated or aggregated species, $(H_2TPP^{2+})_n$.[7] In contrast to the TIR spectrum b, the ER spectrum c, which was focused in this study was clearly observed as a negative absorption spectrum with three absorption minimums at λ_{min} = 412, 475 and 722 nm. The λ_{min} for the latter two peaks agreed to the corresponding λ_{max} observed in the TIR spectrum b. Moreover, the band around 412 nm, which may be hidden by the strong Soret band in the case of TIR spectrum, could also belong to the interfacial species as mentioned later. The absorption spectrum d for the aqueous bulk phase under the quasi-equilibration had only a weak band around 436 nm assigned to a monomeric H_2TP which scarcely affected the ER spectrum (which may if necessary, be corrected in the ER spectrum c by using a certain factor of the absorbance of d). Thus, a UV-vis spectrum for only the interfacial species without any interference of bulk species is obtained by the ER method.

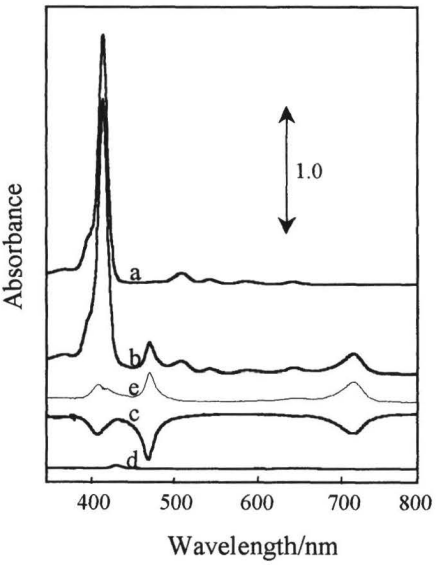

Figure 3. Spectra of TPP at toluene/H_2SO_4 4M interface. a: absorption spectrum of organic bulk, b: TIR spectrum, c: ER spectrum, d: absorption spectrum of aqueous bulk, e: a-b $\mathrm{cosec}\theta_1$.

Concentration dependence of ER spectral peak

It is convenient, hereinafter, to use the term of reflection difference, ΔR_T for TIR or ΔR_E for ER spectrum defined by the absorbance difference from the blank spectrum, instead of the term 'absorbance'. The bands at 412, 475 and 722 nm were measured under the concentration region 1.0×10^{-7} mol/dm^3 < $[TPP]_{T,org}$ < 2.0×10^{-6} mol/dm^3 (figure 4) and plotted for the quasi-equilibrated TPP concentration in the organic bulk phase, $[TPP]_{eq,org}$ as shown in figure 5. The value of ΔR_E at each of the three wavelengths increased steeply with the increase of $[TPP]_{eq,org}$ and then reached a plateau above *ca.* 1.3×10^{-6} mol/dm^3 in a similar pattern. The similarity means that the band around 412 nm is not influenced by the organic bulk species within experimental errors. It was supported by the ER spectra for the TPP/(1 mol/dm^3 Na_2SO_4 neutral aqueous solution) interface, where it was not possible to observe any band in

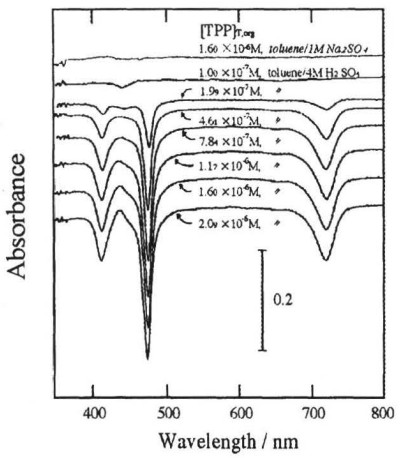

Figure 4. Concentration dependence of ER spectra for TPP

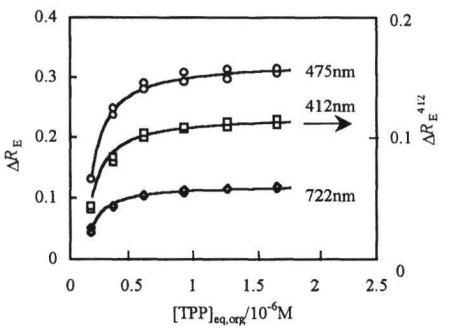

Figure 5. Plots of external reflection difference (ΔR_E) vs. $[TPP]_{eq,org}$

figure 4. It is clear that all of the three ER bands belong to only one species, because a constant ratio of $\Delta R_E^{412}/\Delta R_E^{475}/\Delta R_E^{722} \cong 1.0/2.7/1.0$ was obtained for the variation of $[TPP]_{eq,org}$. It is one of the attractive results obtained in this work that the intensity of ER spectral band around 412 nm (which may be a Soret band) is relatively smaller than that of the strongest band (419 nm) of TPP in bulk as compared with that of the other bands. Consequently, figure 5 shows that the saturated curve shape of the three solid lines are due to an interfacial adsorption phenomenon.

Spectra of OEP and TDCP

The four spectra under the total OEP concentration $[OEP]_{T,org}$ of $1.6x10^{-6}$ mol/dm^3 are shown in figure 6. The intensity of four spectra for OEP was lower than that for the TPP system. The difference spectrum (e) between the TIR spectrum (b) and the organic bulk one (a) showed that there was an adsorbed species at the interface (band near 400 nm) under quasi-equilibration. The ER spectrum has a strange shape band around 400 nm, because the OEP distribute in aqueous bulk phase more than in the case of TPP. However, the difference spectrum (f) between the ER spectrum (c) and the aqueous one (d) was similar to the difference spectrum (e) for TIR. Figure 7 shows the four spectra for the TDCP. In this system, there are no bands of adsorbed species at the interface in the ER, TIR nor those difference spectra. We recognise that three examples could be demonstrated: 1. the TPP system was a most typical example for observing much adsorbed species at the interface; 2. the TDCP system showed an example for non-adsorbed species, and 3. the OEP system showed a small amount of adsorbed species, which showed the intermediate characteristic between the TPP and TDCP systems.

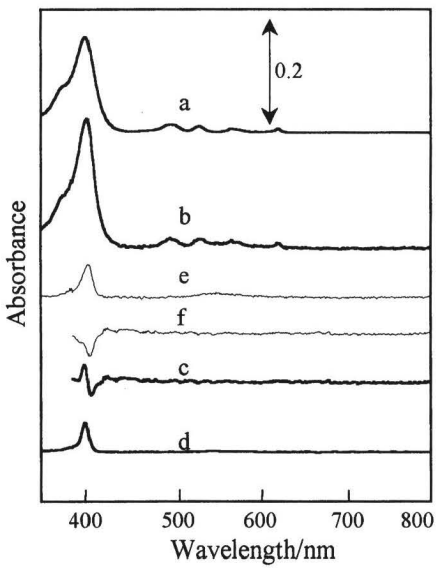

Figure 6. Spectra for OEP. $[OEP]_{T,org}$: $1.6x10^{-6}$ mol/dm^3, a: spectrum of organic bulk, b: TIR spectrum, c: ER spectrum, d: spectrum of aqueous bulk, e: b-a $\mathrm{cosec}\theta_1$, f: c-d

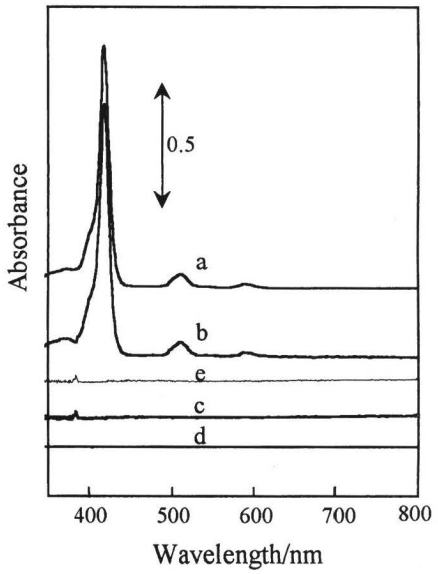

Figure 7. Spectra for TDCP. $[TDCP]_{T,org}$: $1.6x10^{-6}$ mol/dm^3, a: spectrum of organic bulk, b: TIR spectrum, c: ER spectrum, d: spectrum of aqueous bulk, e: b-a $\mathrm{cosec}\theta_1$

Sensitivity of ER spectroscopy

In the case of partial adsorption at an interface as shown in figure 5, the ΔR_E should be in proportion to the interfacial concentration of TPP. When the interfacial concentration (mol cm^{-2}) of the aggregated species $(H_2TPP^{2+})_n$ is shown as $[(H_2TPP^{2+})_n]_i$, an equation:

$$\Delta R_E = \rho(\lambda) n[(H_2TPP^{2+})_n]_i \, (S_i/V_o) \qquad (1)$$

should be valid, where $\rho(\lambda)$is a coefficient (M^{-1}) at a λ, S_i is an interface surface area (cm^2) and V_o is an organic bulk volume (dm^3). The ρ is a function of reflection coefficient at normal incidence which varies with the incident angle. Therefore, the ρ is only a function of λ, since the incident angle is constant in our optical cell arrangements. The concentration $n[(H_2TPP^{2+})_n]_i$ (S_i/V_o) in equation 1 is written as follows:

$$n[(H_2TPP^{2+})_n]_i \, (Si/Vo) = [TPP]_{T,org} - [TPP]_{eq,org} \, . \qquad (2)$$

When the value $\Delta R_E^{475} = 0.237$ is used for $[TPP]_{eq,org} = 3.5 \times 10^{-7}$ mol/dm^3 with a 23.6% reduction of $[TPP]_{T,org} = 4.6 \times 10^{-7}$ mol/dm^3 by the interfacial adsorption, the value of $n[(H_2TPP^{2+})_n]_i$ (S_i/V_o) is 1.1×10^{-7} mol/dm^3 from the equations 1 and 2. Then, the value obtained for ρ^{475} is 2.2×10^6 M^{-1}. The numerical value is much higher than that of the molar extinction coefficient times 1 cm (light-path length), $\varepsilon^{472} \times 1 = 3.4 \times 10^5$ M^{-1} in the transmission absorption spectroscopy.[1] The value of $\rho^{412}(\cong\rho^{722})$ can also be calculated out from the spectrum to be 8.1×10^5 M^{-1}.

Time dependence of ER spectra for absorbed TPP

The ER spectral time change of TPP system was measured from 0 up to 22 hours. The absorbance at several spectral peaks for the ER, TIR, aqueous and organic bulk phase was plotted versus the elapsed time, where the time zero is at the time when TPP solution was added to the organic phase. From these results, we can recognise first the quasi-equilibration at 1 hour, but after the quasi-equilibration the spectra changed, especially for the band around 475 and 722 nm which were broadened. The peak height of 419 nm in organic bulk phase decreased with the elapsed time, nevertheless the peak for adsorbed species (475 nm/ER) was saturated at about seven hours. These results mean that after the quasi-equilibration, the multi-layer of the aggregated TPP species could be produced at the interface.

Polarised ER spectra

From the polarised ER spectra of TPP, was also obtained the results that the bands at 475 nm and 722 nm of the ER spectra were coupled and contributed to the partial porphyrin structure of adsorbed species, but that of 412 nm contributed to a different structure from the former two bands.

CONCLUSIONS

We suggest that the ER spectroscopy using a pair of right-angle prisms is easily applicable to analyse the adsorbed species at liquid-liquid interfaces for extraction systems with high sensitivity, without overlapping of the spectrum of the organic bulk phase.

REFERENCES

1 Watarai H and Chida Y. *Anal. Sci.*, **10**, 105, (1994).
2 Mishima K, Watanabe K, Kanki T and Iuchi S. *Kagaku Kogaku Ronbunshu*, **12**, 393, (1986).
3 Perera JM, McCulloch JK, Murray BS, Grieser F and Stevens GW. *Langmuir*, **8**, 366, (1992).
4 Watarai H and Saito Y. *Chem. Lett.*, 283, (1995).
5 Okumura R, Hinoue T and Watarai H. *Anal. Sci.*, **12**, 393, (1996).
6 Moriya Y, Ogawa N, Kumabe T and Watarai H. *Chem. Lett.*, 221, (1998).

7 Akins DL, Zhu H-R and Guo C. *J. Phys. Chem.*, **100**, 5420, (1996).

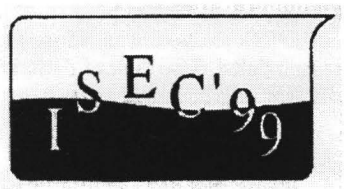

SOME IDEAS ON THE NATURE OF INTERFACIAL PROCESSES IN HDEHPA EXTRACTION OF METALS

VV Tarasov, OA Sinegribova and OV Sviridenkova
D. Mendeleyev University of Chemical Technology of Russia, Moscow, Russia

ABSTRACT
A horizontal rotating cell (HRC) was used for the examination of interfacial process in metal ion extraction. Three interfacial phenomena explain the peculiarities of mass transfer rate behaviour in the extraction of Ca, Sr, Ba and La, Ce (III), Pr, and Zr with HDEHPA solutions in toluene. The first feature is the dispersed zones (DZ) formation inside the diffusion layer. Second is the coagulation of dispersed particles inside the layer to form condensed interfacial films (CIF), and the third is the spontaneous interfacial convection (SIC) taking place mainly at the initial stage of the DZ formation. The first and the third phenomena accelerate mass transfer rate, whereas the second one decreases the intensity of mass transfer. A very high acceleration was obtained in the presence of typical surfactants, as diethanolamides and carboxylic acids of alkylsulphoethoxylates. The mass transfer Ca and La with particles of DZ in the conditions of the SIC is one of the most appropriate reason for the effect. Low molecular alcohols increase mass transfer rate because of their dispersing role. Higher intensity of mass transfer as well as low specific surface area in HRC could be used for the design in new type of environmentally friendly extraction equipment.

Keywords: mass transfer, interfacial films, horizontal rotating cell, D2EHPA, alkaline earths, lanthanoids, zirconium

INTRODUCTION

It has been shown that solid bodies moving normally to the interface cause a dramatic growth of the mass transfer coefficients even at very slow body displacements in the case of condensed interfacial film (CF) formation.[1,2] The main reason of the phenomenon is mechanical impulse transfer (momentum transfer) from the body to the interface.[2] The horizontal rotating cell (HRC) is the simplest device for the examination of the momentum transfer to the interface.[1] The HRC is a cylindrical flask with a cork. When the flask is placed in horizontal position the interface becomes parallel to the axis of symmetry of the cylinder. Thus three phases brought in contact at the cylinder wall and the perimeter of the contact slips over the cylinder surface during the rotation of the HRC. As a result of the slipping interfacial perturbations arise and enlarge over the interface cause the acceleration of mass transfer. This effect was also successfully used for dispersed zones (DZ) detection.[2,3] DZ are considered[4] as a first stage of the condensed film formation and are described as common phenomena in solvent extraction with chemical reaction. The most essential effects of DZ could be expected in the extraction across the flat interface of the Lewis cell (LC), which is the main device for the study of the kinetics and mechanism of interfacial reactions. Unfortunately, the phenomenon has not yet been studied systematically. The comparative study of the extraction kinetics of Ca^{2+}, Sr^{2+},Ba^{2+} as well La^{3+}, Ce^{3+}, Pr^{3+} and Zr^{4+} with HDEHPA in toluene has been carried out using both the LC and the HRC.

EXPERIMENTAL

Water solutions of salts above metals were prepared using compound with the purity about 98%. "Merck - Schuchardt" grade diethylhexylphosphoric acid (HDEHPA)was diluted with toluene. Low molecular alcohols were 98% grade. Metal concentration changes were measured by titration of samples taken from aqueous phase with solutions of Na-EDTA. The metal accumulation in interfacial condensed film was calculated fom the mass conservation law. Kinetic experiments were carried out under conditions of pH change as a result of H^+ evolution in the process. The LC as well as the HRC was used in a comparative conditions to examine some features of extraction kinetics and the role of the mechanical perturbation of the interface. By the analogy with [3] it is proposed that the momentum transfer into interfacial region increases the interfaces covered with CIF and DZ. In the absence of CIF, DZ and surfactants the interface as a whole almost has not to dissipate mechanical

© 2000 Society of Chemical Industry

energy. Effects of low molecular weight alcohol and surface active compounds have also been studied. The intensity of stirrer rotation in LC was 100 rpm. The intensity of HRC rotation was 15 rpm.

Three types of mass transfer coefficients K_0, K_t and K_{int} were calculated. Two first of these are differential, third is integral one K. The initial mass transfer coefficient is calculated according to expression:

$$K_0 = (dC / dt)_{t=0} / C_{eq} \cdot a \qquad (1)$$

where a is thespecific interfacial area.

K value at time $t = \tau$ was calculated as:

$$K_\tau = (dC /dt)_{t=\tau} / (C_{eq} - C_\tau) \cdot a \qquad (2)$$

Integral value K_{int} was obtained from the slope of function, $-\ln (1 - E_t) = f(t)$ if it is a straight line:

$$K_{int} = - \ln (1 - E_t) / a \cdot t \qquad (3)$$

where $E = C_\tau / C_{eq}$.

If the straight line occurs in the interval $t = 0$ and $t = \tau$, the mass transfer coefficients $K_0 = K_\tau = K_{int}$. Interfacial processes like CIF or DZ formation change the shape of the function $-\ln(1 - E_t) = f(t)$, to decrease the slope with time. When the SIC takes place K_0 and K_τ values are the higher the more intensive SIC.

RESULTS AND DISCUSSION

The mass transfer kinetics in systems studied exhibit the following properties and features:

1) mass transfer coefficients K_{int} do not correlate with the distribution coefficients;
2) K_τ and K_{int} values for Zr^{4+} are much higher for the HRC than those for the LC;
3) K_τ and K_{int} values are very sensitive to interfacial perturbations especially in Zr extraction;
4) interfacial perturbation enhances the rate of mass transfer of Zr^{4+} much more then La^{3+}, Ce^{3+}, Pr^{3+} and Ca^{2+}, Sr^{2+}, Ba^{2+};
5) the rate of metal extraction depends strongly on the low molecular alcohol concentration, whereas rate of alcohol transfer across the interface does not depend on the metal flow in the system: HDEHPA- alcohol- diluent // Me^{n+} - H_2O;
6) the concentration of low molecular alcohol (e.g. octanol) exceeds the value of its solubility in water phase almost immediately after the beginning of the mass transfer in the system: HDEHPA- alcohol- diluent // Me^{n+} - H_2O;
7) the rate of the extraction of some metals, e.g. Ca^{2+} and La^{3+} grows dramatically in the presence of Aminol KDE (diethanolamide C_{12}-C_{18}) and Texapon N70 (carboxylic acids of alkylsulphoethoxylates C_{10}-C_{14}).

The first property is rather common. K values have to be independent of distribution coefficients as it has been shown.[4] The second and the third features were also found by Semina,[1] who studied extraction kinetics of HCl with tri-n-octylamine solutions; $Th(NO_3)_4$, UO_2SO_4 and $Zr(SO_4)_2$ with HDEHPA solutions using the HRC and five similar devices, which allow disturbance of the interface by moving solid bodies. The HRC and its analogues were much more effective than the LC, and higher values of K were obtained for the same energy input into the system. The highest effect was observed for the systems addicted to the interfacial film formation.[1,2] The fourth feature has ben previously observed [1] and was proved in this work.

New principal results obtained in this work consist of features 5 - 7. It has been shown that low molecular alcohols when added to the organic phase causes a maximum in $D = f(U)$ functions in all systems under study, where D is the distribution coefficients, U the molar ratio of alcohol to HDEHPA, (U=[octanol-1]/[HDEHPA]). At the same time K_τ and K_{int} values show a monotonous increase or independence of the U value. The accumulation of intermediates and by-products of the

reaction of extracted compound formation accompany extraction of rare earth elements and zirconium. This was proved from mass balance. Alcohols decrease the accumulation and lead to the intensification of interfacial mass transfer (figures 1-3).

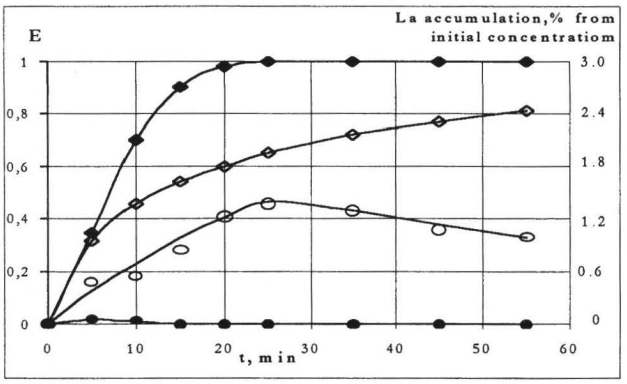

Figure 1. The influence of octanol-1 on kinetics of lanthanum extraction and on kinetics of lanthanum accumulation in the interfacial field, in HRC. $[La(NO_3)_3]$ = 0.36 mol/dm^3, pH=1.7, [HDEHPA]=0.7 mol/dm^3 in toluene.
E: -◊- U=0.0; -♦- U=0.8
La accumulation, % (mass) from initial concentration:
-o- U=0.0; -□- U=0.8.

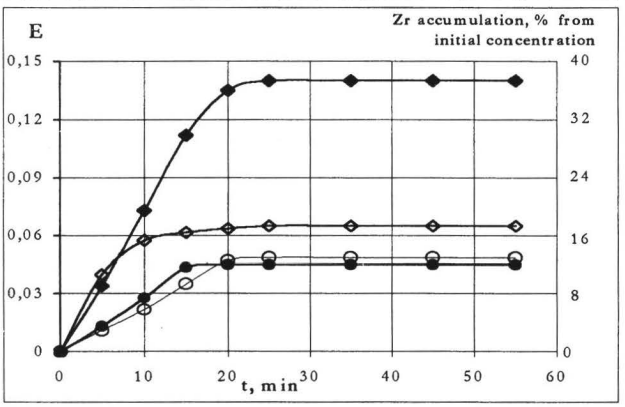

Figure 2. The influence of octanol-1 on kinetics of zirconium extraction and on kinetics of zirconium accumulation in the interfacial field, in LC. $[Zr(SO_4)_2]$ = 0.05 mol/dm^3, pH=1.1, [HDEHPA]=0.7 mol/dm^3 in toluene.
E: -◊- U=0.0; -♦- U=0.15
Zr accumulation, % (mass) from initial concentration:
-o- U=0.0; -□- U=0.15.

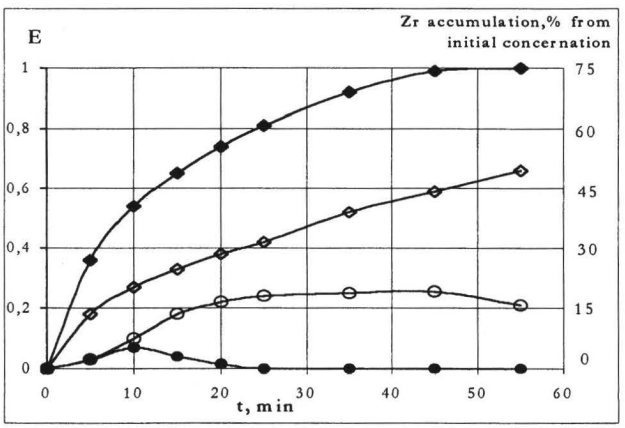

Figure 3. The influence of octanol-1 on kinetics of zirconium extraction and on kinetics of zirconium accumulation in the interfacial field, in HRC. $[Zr(SO_4)_2]$ = 0.05 mol/dm^3, pH=1.1, [HDEHPA]=0.7 mol/dm^3 in toluene.
E: -◊- U=0.0; -♦- U=0.15
Zr accumulation, % (mass) from initial concentration:
-o- U=0.0; -□- U=0.15.

The fact the accumulation passes through a maximum (figures 1 and 3) shows that the condensed interfacial film consists of slowly dissolved intermediates. On the other hand the comparison of figure 2 and figure 3 shows that the accumulation process depends sufficiently on the hydrodynamic conditions at the interface. Moreover the permeability of the CIF arising for the LC is much lower than that for the HRC despite the fact that the mass of the CIF for the LC less than that for the HRC. It means that the CIF for the HRC is more porous than for the LC.

The influence of alcohol addition on the extraction rate is explained by the dispersing role of the alcohol. The latter causes a decrease of the coagulation rate and leads to the increase of the amount of smaller particles inside the diffusion layer. These are then most effective in the transfer of the extracted complexes with the dispersed matter. The extraction rate increases by a factor of 3 - 5 because of the mechanism proposed by Sharma,[6] and Mehra and Sharma.[7] Moreover alcohols increase the solubility of intermediates in organic phase. This causes the dissolution of the CIF and the increase of its diffusion permeability.

Although the rate of metal transfer into the organic phase depends strongly on the low molecular alcohol concentration the rate of alcohol transfer into the aqueous phase does not depend on the intensity of metal transfer. So, the interfacial flows of metal and alcohol are coupled only in the processes of the metal transfer. It has been stated that the concentration of low molecular alcohol (e.g. octanol) exceeds its solubility in the water phase almost immediately after the beginning of the mass transfer in the system: HDEHPA-alcohol-diluent // Me^{n+} -H_2O. After two minutes of mass transfer the octanol concentration exceed the solubility by two orders of the value. This proves the suggestion that mass transfer accompanies DZ formation and explains the acceleration of mass transfer at least at the initial stage of the process. Moreover this shows that the aqueous solutions of micelles arise during the mass transfer and the process of micelles formation begins from the interface.

Figure 4 shows the role of surfactants (octanol-1, Aminol KDE and Texapon N70) in extraction of Zr^{4+} in HRC. The action of Aminol KDE and Texapon N70 was found to be similar.

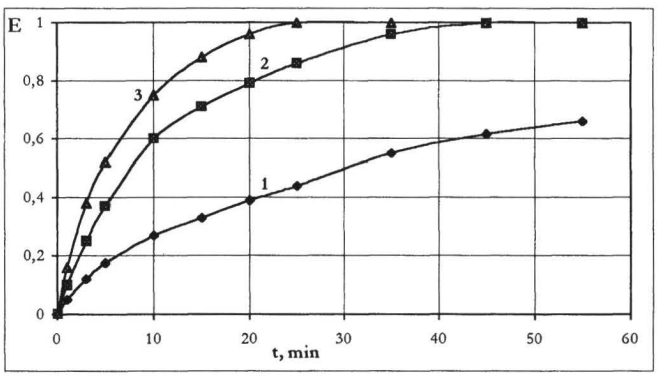

Figure 4. Zirconium extraction kinetics in HDEHPA without surfactant (1), in the presence of octanol-1(2) and Aminol KDE (3), in HRC. $[Zr(SO_4)_2]$ = 0.05 mol/dm^3, pH=0.95; [HDEHP]=0.25 mol/dm^3 in toluene. U = 0.05 (2); concentration of Aminol KDE = 0.5%(mass) (3).

The rate of mass transfer in classic LC almost in the order of value less than one (curve 1) (figure 4), which shows the process for HRC in the absence of any admixtures. Curve 2 corresponds that octanol increases the rate almost twice. A higher acceleration takes place in the presence of such SAC as Aminol KDE and Texapon N70 (curve 3).

The same surfactants cause much more growth in the mass transfer rate of Ca^{2+} and La^{3+}. Values K_τ and K_{int} increase in one order of the value (till 7 ~ $9 \cdot 10^{-4}$ m·s^{-1}). These values are the highest ones obtained for diffusion cells. We believe that higher intensity of mass transfer as well as low specific surface area in HRC could be used for the design in a new type of environmentally friendly extraction equipment.

REFERENCES

1. Semina Yu M *Intensification of the mass transfer in solvent extraction by means of a weak mechanic interfacial perturbations.* Thesis of C of Chem Sci. Mendeleyev Institute of Chem. Technol., Moscow, (1992).
2. Tarasov V and Xiang ZD, *Dokl. RAN*, **350**, 647, (1996).
3. Tarasov V, Xiang ZD and Larin G, (to be published)
4. Tarasov V and Yagodin G, *Solvent Extr. Ion Exch.*, **10**, 141, (1988).
5. Yurtov E and Koroleva M, *Uspehi himii*, (Rus.), **60**, 2422, (1991).
6. Janakiraman B and Sharma MM, *Chem. Eng. Sci.*, **37**, 1497, (1982).
7. Mehra A, Sharma MM, *Chem. Eng. Sci.*, **43**, 1071, (1988).

MECHANISM OF INTERFACIAL REACTIONS IN THE EXTRACTION OF IRON BY D2EHPA

Tatsuo Kanki, Hiroyoshi Kim, Akihoro Tomita, Tsuyoshi Asano and Noriaki Sano
Department of Chemical Engineering, Himeji Institute of Technology, 2167 shosha, Himeji 671-2201, Japan

ABSTRACT
In extraction of iron by D2EHPA, the mechanism of interfacial reaction was investigated focusing on surface-active chemical species identified from practical behaviour of interfacial tension and rates of extraction that were determined by measuring local concentrations of ferric iron near the interface. Consequently it was shown that there are two different reaction zones depending on pH and extractant concentration and new rate equations in these respective zones are proposed. At currently operated higher concentrations, surface-active dimer extractants and/or their anions react with ferric ions, as a rate determining step, to form 1:2 intermediate complexes and the resulting complexes instantaneously agglomerate together with dimer extractants to form micro-emulsions.

Keywords: mass transfer, interfacial reaction, interfacial tension, D2EHPA, iron(III)

INTRODUCTION

The rate of extraction of iron by D2EHPA, di-(2-ethylhexyl)phosphoric acid is known to be much slower when compared with those of copper, nickel, cobalt and other metals. Despite the intensive research on reaction mechanism, the existing models proposed up to the present are still diverse.[1-3] Most of the models have been deduced on the basis of the extraction rates which were determined in experiment using stirred cells; such data cannot be free from effects of hydrodynamic fluctuation of the interface, numerous droplets generated in both phases, and errors in estimating boundary layer resistances. In addition in explaining the extraction rates, some intermediate complexes are assumed to be surface-active without any experimental evidence.

If a static cell is used instead a stirred cell, the rates of extraction can be determined much more precisely by measuring local concentrations of metallic ions near the interface in the aqueous phase and/or the stable complexes in the organic phase. Measurements will also be carried out under desired conditions free from such hydrodynamic effects. In this research, extraction of iron by D2EHPA was investigated using a cell in which organic phase is contacted statically with aqueous phase. Interfacial tensions of D2EHPA in benzene/aqueous solution systems were measured to identify surface-active species by the Wilhelmy plate method and partly by laser-light scattering method for the systems with and without the addition of metallic ions. Local concentrations of ferric ion and the complex near the interface were also measured by a position-scanning spectrophotometer and the dependency of extraction rate on concentrations of ferric ion, extractant and hydrogen ion were determined.

The reaction mechanism is discussed on the basis of the practical relations of interfacial tension and of extraction rates against concentrations of related chemical species and a new kinetic model is proposed.

EXPERIMENTAL

Reagents

The organic phase was prepared by diluting D2EHPA in benzene with concentration of dimer extractant ranging from 10^{-9} to 10^{-1} mol/dm^3. The aqueous phase was prepared by diluting iron (III) perchlorate in distilled water. Concentration of Fe (III) was set at 1 x10^{-4} to 3 x10^{-3} mol/dm^3. The pH of the aqueous phase was adjusted by perchloric acid ranging from 10^{-1} to 10^{-2} mol/dm^3 and ion strength was adjusted to 1 mol/dm^3 by sodium perchlorate.

© 2000 Society of Chemical Sciences

Measurement of Interfacial Tension

Interfacial tensions were measured by the Wilhelmy plate method using a platinum plate (Kyowa Int. Sci.) 24 mm wide by 10 mm high with thickness 0.15 mm. Vertical motion of the plate was controlled by microcomputer, with one step being 1.7 x 10^{-2} mm in 3 seconds. In each run, the weights were detected every step by a microbalance (AEL200; Shimazu) and the maximum value was recorded for the interfacial tension. To confirm reproducibility of the data, a laser light scattering technique was also used.[4]

Measurements of local concentrations

Organic solutions (10 cm^3) of the desired extractant concentration were contacted very calmly with the same amount of aqueous solution with the desired ferric ion concentration in a quartz optical cell 20 x 30mm^2 base by 40 mm high. Local concentrations of ferric ion in the aqueous phase and stable complexes in the organic phase were measured by a position scanning spectrophotometer using a deuterium lump as a light source. The light was filtered by an optical element (MG03FIM018; Melesgrio) whose wavelength is 280 nm with half-peak-width 10 nm and used as an incident beam for photometry. The light is adjusted further by a convex lens to provide a parallel beam which is led into the cell through a 400μm slit. The intensity of the light beam penetrating the cell was detected by a photomultiplier (R955; Hamamatsu Photonics). The light beam can be scanned by traversing the total optical system including the light source vertically through the photo-detector which is free from the stand carrying the optical cell, with the full scale being 10 mm. The scanning speed was controlled at 5.88 x 10^{-1} mm/sec by microcomputer. Measurements in each run were made at appropriate time intervals, for instance at 120, 240, 360, 960 and 1440 minutes.

RESULTS AND DISCUSSION

Formation of Micro Emulsion

Local concentrations were measured by changing the initial ion concentration $[Fe]_0$ from 1 x 10^{-4} to 3 x 10^{-3} mol/dm^3, extractant concentration $[(HR)_2]_0$ from 1.34 x 10^{-2} to 2.48 x 10^{-1} mol/dm^3, hydrogen ion concentration $[H]_0$ from 5 x 10^{-2} to 5 x 10^{-1}. Measurements were not allowed in organic phase at all settled concentrations for formation of emulsion. In the aqueous phase there exists a measurable zone, EL, and non-measurable zone, EE, according to pH and extractant concentration. In zone EE, emulsions appear even in the aqueous phase. The respective zones are shown in figure 1.. LL is the zone where no emulsions form in either organic or aqueous phases. In this zone the extraction rate is too slow to detect changes in local concentrations.

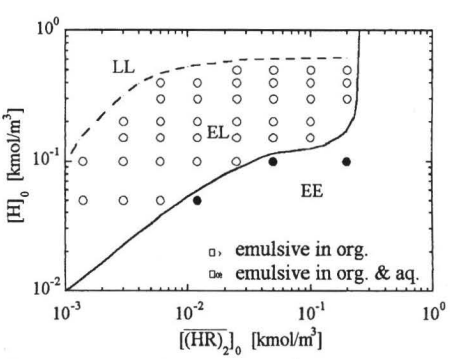

Fig.1 Concentration zone where emulsion is formed, $[Fe]_0$=1x10^{-3}, I=1 kmol/m^3.

Rate of Extraction Rates

As an illustration, changes in concentration profiles of ferric ion in the aqueous phase for several extractant concentrations are shown in figure 2. From a series of data, it can be shown that the extraction rate in zone EL is proportional to the product of $[Fe]_0$ and $[(HR)_2]_0$, and inversely proportional to $[H]_0$ at lower extractant concentrations but becomes zeroth order with $[(HR)_2]_0$ at higher concentrations. This implies that when the extractant concentration is in zone EL the extraction rate should be determined by reaction of ferric ion with dimer extractant. At much lower concentrations in zone LL, the extraction rate is extremely slow, and the reaction mechanism is

thought to be quite different from that in zone EL.

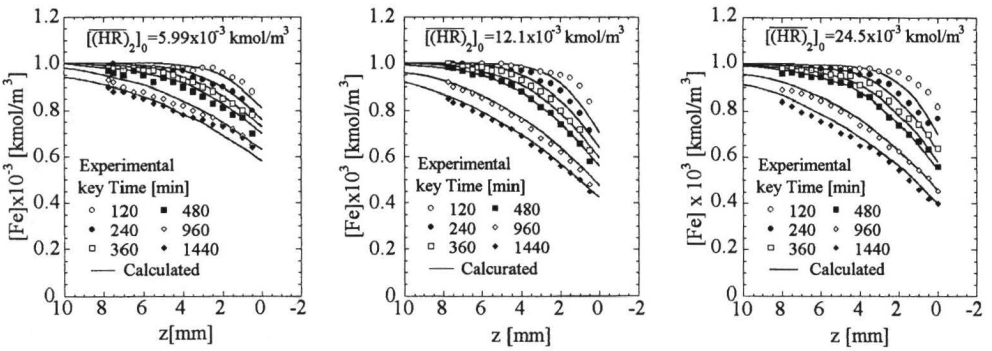

Figure 2 Changes with time in concentration profiles of ferric iron in aqueous phase, effect of dimer concentration, $[Fe]_o = 1 \times 10^{-3}$ kmol/m^3, $-\log[H]_o = 1$, I = 1 kmol/m^3

Surface-Active Species and Adsorption Scheme

The reagent D2EHPA is known to exist as a dimer in the organic phase[5,6]. However, according to the practical behaviour of the interfacial tension of D2EHPA in a benzene/aqueous solution system free of ferric ion, the reagent is confirmed as adsorbing as a monomer and its dehydrogenized anion at the interface. The dependency of the interfacial tension on pH and extractant concentration can be well explained by the monotonously decreasing curve specified by Gibbs-Langmuir (GL) equation with the assumption that monomer extractant and its dehydrogenized anion should adsorb at the interface.[7]

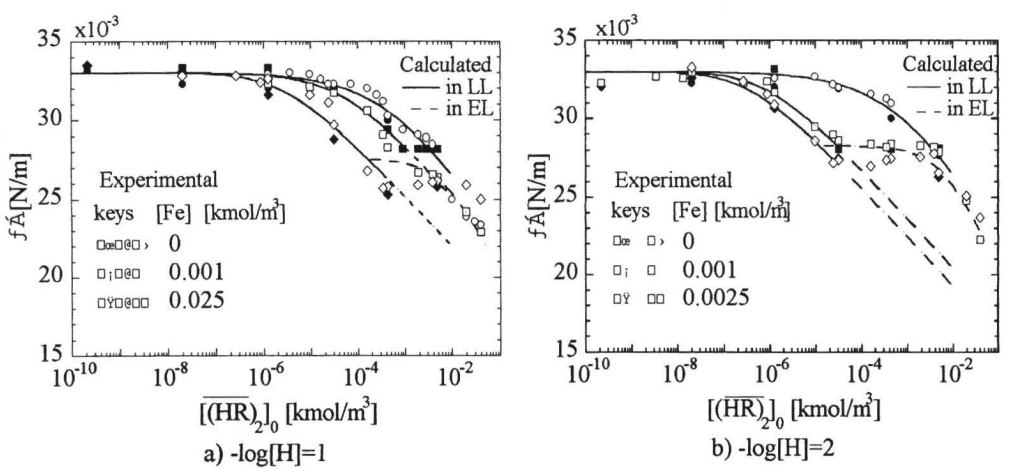

Figure 3 Relation between interfacial tension and dimer extractant concentration by laser light scattering (open key), by Wilhemy plate (solid key)

When Fe(III) perchloride is added to the aqueous phase, drastic change in interfacial tension are found as shown in figure 3. The interfacial tension against extractant concentration curve shifts appreciably to lower concentrations; the shift becomes greater as ferric ion concentration or pH

becomes higher. And the curve has an inflection at a specific concentration $[(HR)_2]_c$, showing a plateau at $[(HR)_2]>[(HR)_2]_c$ where the interfacial tension becomes almost constant and decreases again at much higher concentrations.[8] The $[(HR)_2]_c$ at a given pH lies nearly on the dashed line in figure 1 which discriminates the zones LL and EL and corresponds to the critical micelle concentration (CMC). Though not illustrated here for clarity, changes in interfacial tension with time after contacting the two phases is unexpectedly small, which shows that the reactions between the adsorbed species should be very fast.

At lower concentrations of extractant, in zone LL, the dependency on the related species concentration of the interfacial tension can be successfully explained by assuming that a couple of monomer extractants or their anions (or monomer and its anion) react with ferric ions to form surface-active 1:2 intermediate complex.[7] The dependency cannot be explained if the formation of a 1:1 complex is assumed. If this were the case, the interfacial tension expressed in terms of the concentration ratio [Fe]/[H], for instance, the interfacial tensions when $[Fe]=2.5 \times 10^{-3}$ mol/dm^3 and pH = 2 should have the same value as those when $[Fe]=2.5 \times 10^{-2}$ mol/dm^3 and pH = 1, which is inconsistent with the practical behaviour. The physical scheme for adsorption of related species can now be deduced as shown in figure 4a. The solid lines show the interfacial tensions predicted by the GL equation based on this adsorption scheme.

At higher concentrations, in zone EL, as stated above, micro-emulsions are generated in the organic phase. These are formed from a certain amount of 1:2 intermediate complexes together with dimer extractants at the interface and dissolve easily in the organic phase. Taking this into consideration with the rate of extraction being proportional to dimer extractant concentration, it can be safely presumed that in zone EL dimer extractants in the organic phase should adsorb directly in that form or its anion on the remaining unoccupied area at the interface.[9] The dashed lines show the GL equation which is derived by assuming dimer extractant molecules should adsorb at the interface according to the physical scheme as shown in figure 4b.

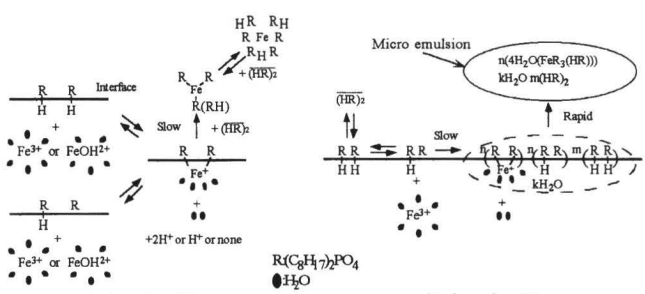

Fig. 4 Adsorption schemes at the interface.

Rate Equations of Interfacial Reaction

In zone LL, as described above, surface-active equilibrium species of HR, R^- and FeR^{2+} exist at the interface. This means that the proton exchange reaction of Fe^{3+} with HR and/or R^- is very rapid. Reaction of FeR^{2+} with $(HR)_2$ to form $FeR_3(HR)$ can be assumed to be rate determining. The rate equation is then given by

$$R = k(\Gamma_{HR}^{\infty} K_{ad})^2 \frac{K_1}{K_{dm}} \theta_v^2 \left(\frac{[Fe]_i [(HR)_2]_i^2}{[H]_i^2 (1 + K_{OH}/[H]_i)} - \frac{[H]_i [FeR_3(HR)_3]}{K_{ex}[(HR)_2]} \right) \quad (1)$$

$$\theta_v = \left[-(1 + c[HR]_i) + \sqrt{(1 + c[HR]_i)^2 + 4a[HR]_i^2} \right] / 2a[HR]_i^2$$

where θ_v is the unoccupied area. The monomer concentration [HR] is related to dimer concentration as $[HR]^2 = [(HR)_2]/K_{dm}$.

In zone EL, at currently operated higher concentrations, the reaction of Fe^{3+} with surface-

active $(HR)_2$ and HR_2^- to form 1:2 intermediate complex is rate determining. Resulting complexes instantaneously agglomerate at the interface together with dimer extractants to form non-surface-active micro-emulsions. The rate equation is given by,[9]

$$R = k' K_a' \Gamma^{\infty}_{(HR)2} \theta_v' \left(\frac{[Fe]_i [(HR)_2]_i}{[H]_i (1 + K_{OH} / [H]_i)} - \frac{[H]_i^2 [FeR_3(HR)_3]}{K_{ex} [(HR)_2]_i^2} \right) \quad (2)$$

where θv' is the unoccupied area for dimer extractant molecules.

$$\theta_v' = 1 / \left(1 + K_{ad}' (1 + K_a' / [H]_i)[(HR)_2]_i\right)$$

The physicochemical constants in these equations are presented elsewhere.[5,7] The extraction rates predicted by equation 2 are closely related to the experimental data as shown in figure 5.

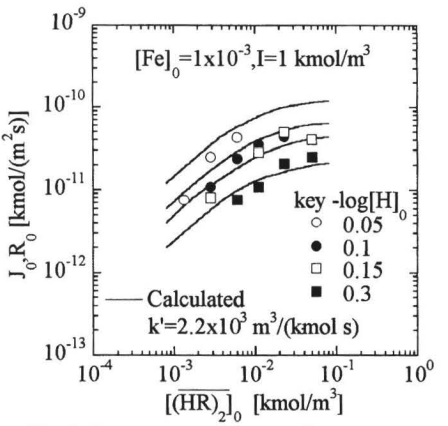

Fig.5 Relation between rate of extraction and dimer extractant concentration

CONCLUSIONS

Based on the discussions above, the following conclusions can be made remarks:

1) There are two different extraction reaction zones LL (emulsion free) and EL (with formation of emulsion in organic phase) depending on pH and extractant concentration.

2) D2EHPA adsorbs as a monomer HR or its anion R^- at the interface when the aqueous phase is free of ferric ions. When ferric ions are added, the adsorption scheme is drastically changed. In zone LL, exist HR, R^- and the 1:2 intermediate complex FeR^{2+} at the interface as equilibrium adsorbed species. In zone EL, dimer extractant molecules and their anions, in addition of these three species, can adsorb at the interface.

3) In zone LL, the monomer extractant molecules first react rapidly with ferric ions to form surface active 1:2 intermediate complexes, the resulting complexes secondly react rather slowly with dimer extractant molecules to form 1:4 complexes, and the 1:4 complexes finally react instantaneously with dimer extractant molecules to form stable complexes.

4) At currently operated extractant concentrations, in zone EL, micro- emulsions are generated near the interface in the organic phase. The rate of extraction is proportional to ferric ion concentration and the inverse of hydrogen ion concentration, and is of first order of dimer extractant concentration at lower concentrations and zeroth order at higher concentrations. The rate of extraction can be explained by the kinetic model in which ferric ions first react with dimer extractant

molecules or their anions to form 1:2 intermediate complexes and a certain number of intermediate complexes secondly agglomerate together with dimer extractant molecules to form micro-emulsions, with the first step being rate determining.

REFERENCES

1 Roddy JW, Coleman CF and and Arai S: *J.Inorg.Nucl.Chem.*, **33**, 1099, (1968)
2 Harada M, Yamazaki F, Shiomi N, Adachi M and Eguchi W: *J.Chem.Eng., Jpn.*, **17**, 521, (1984)
3 Matsuyama H., Miyake Y and Teramoto M: *Hydrometallurgy*, **24**, 37, (1990)
4 Kanki T, Asano T and Yoshikawa K: *Kagaku Kogaku Ronbunshu*, **22**, 1055, (1991)
5 Komazawa T, Otaka T and Higaki Y: *J.Inorg. Nucl.Chem.*,**43**, 3351, (1981)
6 Miyake Y, Matsuyama H and Teramoto T: *Hydrometallurgy*, **24**, 19, (1990)
7 Kim H, Kanki T and Asano T: *Kagaku Kogaku Ronbunshu*, **22**, 837, (1996)
8 Kanki T, Asano T, Yamashita H, Uetani S and Kim H: *Kagaku Kogaku Ronbunshu*, **23**, 296, (1997)
9 Kim H, Kanki T and Asano T: *Kagaku Kogaku Ronbunshu*, **23**, 95, (1997)

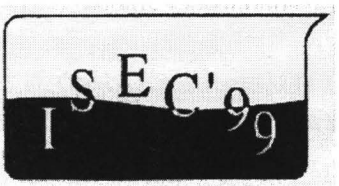

MASS TRANSFER OF ORGANIC ACIDS AT CHARGED LIQUID INTERFACES

C Czapla and H-J Bart
Universität Kaiserslautern, Lehrstuhl für Thermische Verfahrenstechnik, Gottlieb-Daimler-Straße, D-67653 Kaiserslautern, Germany

ABSTRACT
The mass transfer rate of acetic acid from the aqueous to the organic phase with tri-n-octylamine and toluene as solvent has been studied in a constant interfacial cell area as function of the stirring speed, concentrations of the transfer species and the influence of chemical adsorption layers. The interfacial charges of systems with different surfactants have been observed by electrophoresis. A kinetic model and its electrostatical extension are introduced to describe the interfacial reactions and mechanism, when using a thermodynamic consistent activity coefficient model.

Keywords: mass transfer, interfacial covering, electrophoretic mobility, acetic acid, tri-n-octylamine

INTRODUCTION

A lot of information is available on extraction equilibria in amine systems. Very little information is given on the kinetics of organic acid extraction, on the reaction mechanism and on the rate determining steps of the extraction process.[10, 11] The mass transfer can be limited generally by diffusion or by reactions, when the interface is defined as the place of reaction. So the basic problem concerning the kinetic investigations of liquid-liquid reactions, is the identification of the rate controlling step. The rate equation for an interfacial reaction demands an analysis of the plateau rates.[6] The present work is a systematic investigation of the mechanism of acetic acid extraction from an aqueous to a toluene diluted organic phase with tri-n-octylamine as anion exchanger. The equilibria of the system acetic acid / water // tri-n-octylamine / toluene have been investigated and described with an activity coefficient model.[12] The enhancement and reduction of the initial mass transfer rate, when using neutral, cationic and anionic surfactants have been investigated in detail and modelled considering the electrophoretic mobility and the zeta potential.

EXPERIMENTAL AND MODELING

Chemicals

For the surfactant-free-system the following chemicals were used: acetic acid (HA, Rotipuran, >99.7%) was used to prepare the acid solutions of various concentrations in the aqueous phase. Tri-n-octylamine (TOA, Alamine®300, Henkel, >95%) was used as anion exchanger, toluene (TOL, Riedel de Haen, >99.7%) as solvent. The investigated adsorption layers were obtained by a hygroscopic-nonhygroscopic orientated covering of sodium-dodecylsulfate (NaDdS, Merck, >99 %, anionic), 1-dodecanesulfonic acid sodium salt (NaLS, Fluka, >98 %, anionic), dodecyltrimethylammonium chloride (DTACl, Fluka, >98 %, cationic) and Triton X-100 (TX 100, Boehringer, >99 %, nonionic). Tri-n-octylamine purified by washing with a 0.005 mol/dm^3 NaOH solution (Riedel de Haen). All other reagents were standard chemicals of analytical grade and were used without any further purification.

Interfacial Covering and Charge Determination

The interfacial tension γ of the pre-saturated phases was observed by the volume drop method with a tensiometer TVT1 (Lauda). The covering and therefore the amount of surfactant per unit area adsorbed at the interface at a given temperature can be calculated on the basis of the Gibbs equation of adsorption:

© 2000 Society of Chemical Industry

$$\Gamma = -\frac{1}{m \Re T}\frac{d\gamma}{d \ln c} \tag{1}$$

where c is the bulk aqueous concentration of the surfactants and m the surfactant specific parameter which is 1 for neutral adsorbates and 2 for salt free solutions of ionic surfactants.

Equilibrium and Kinetics Experiments

For the experiments concerning the phase equilibrium, 40 cm^3 of the aqueous and the organic solutions were mixed intensively in a 100 cm^3 vessel for a minimum of 10 hours in a thermostatic bath at 25°C using a magnetic stirrer.

The kinetic experiments were carried out in a modified Nitsch cell[1,5] at 25°C. The concentration-time curves were measured by taking samples of the organic phase with syringes. At the end of every experiment, samples were taken from the aqueous and from the organic phase for controlling the mass balance. The aqueous and organic samples were weighed with a Sartorius R300S (0.1 mg) and analysed for the acetic acid concentration using an autotitrator (Orion 940/960) with NaOH. The transfer rates are calculated by correlating the concentrations of the organic phase obtained with a function developed by Kamenski and Dimitrov:[3]

$$f(t) = C_1 \cdot \frac{t + C_2}{t + C_3} \tag{2}$$

The transfer rate R_0 at the beginning of the experiment (t = 0 min)

$$R_0 = \left.\frac{\partial f(t)}{\partial t}\right|_{t=0} \cdot \frac{w_s}{A} \tag{3}$$

is very important for the discussion concerning the limitation of the flux as a cause of reaction or transport limitation. According the values of R_0, the reaction order can be determined and directly calculated.

Interfacial Reactions and Mechanism

The equilibrium studies and the slope analysis[1] at different acetic acid concentrations in the aqueous phase and tri-n-octylamine concentrations in the organic phase have shown that the reaction stoichiometry can be represented by the following general equation for the concentration area of the significant plateau regions:

$$HA + \overline{TOA} \rightleftharpoons \overline{TOAHA} \tag{4}$$

(bar indicates organic phase). The reaction and therefore the general equation can be described through following reaction steps:

$$H^+ + TOA_{ad} \rightleftharpoons TOAH^+_{ad} \qquad rds: k_1; k_{-1} \tag{4a}$$

This step represents the protonation of the adsorbed TOA-molecule at the interface.

$$TOAH^+_{ad} + A^- \rightleftharpoons TOAHA_{ad} \qquad qss: K_2 \tag{4b}$$

In this step an adsorbed ion-pair molecule is formed at the interface .

$$TOAHA_{ad} + \overline{TOA} \rightleftharpoons TOA_{ad} + \overline{TOAHA} \qquad rds: k_3; k_{-3} \tag{4c}$$

In this case the ion-pair-molecule at the interface is replaced by a fresh TOA-molecule of the organic bulk phase. The combination of the rate laws for equation 4a and 4c and the assumption of a saturated interface with adsorbed TOA-molecules leads to the following expression for the reaction kinetics:

$$R = \frac{C_1 [H^+][A^-][\overline{TOA}]}{C_3 [A^-][\overline{TOA}] + 1} - \frac{C_2 [\overline{TOAHA}]}{C_3 [A^-][\overline{TOA}] + 1} \tag{5}$$

Electrophoretic Mobility EM and Zeta Potential ζ

The electrophoretic mobility of oil-in-water-droplets was measured with a ZETA-sizer (ELS-800, Otsuka Electronics Co.). Electrophoresis measures the migration of charged particles under the influence of an external electrical field.[3,9] The electrophoretic mobility EM can be related to the zeta potential ζ , which is the potential at the plane of shear, by the Henry equation that describes the general case:

$$EM = \frac{2\,\varepsilon\,\zeta}{3\,\eta}\, f(\chi\, a) \tag{6}$$

where ε and η are the dielectric constant and the viscosity of the continuous phase, a is the particle radius and χ is the Debye-Hückel-Parameter. The electric double layer is described by the Stern model which combines the Helmholtz rigid and the Gouy Chapman diffused double layers. The extension of the kinetic model (equation 5) is a fully developed mass transfer model which also includes the zeta-potential effects. The changed interfacial concentration of the aqueous species which is caused by the induced electrical potential is described according to the Boltzmann equation: [3,7]

$$c_i = c_{i,B} \exp\left(\frac{-z_i e \Psi_o}{kT}\right) \tag{7}$$

where z_i is the valence of the ion i and Ψ_0 is the interfacial potential, which is calculated in accordance to the electric double layer theory and by the measured electrophoretic mobility.

RESULTS AND DISCUSSION

For a relative low acetic acid concentration a transport limitation by a heterogeneous reaction at the interface could be found for an aqueous impeller speed range of 120 to 180 rpm. Above 180 rpm the liquid-liquid interface becomes unstable and organic droplets move in the aqueous phase. Below 120 rpm the transfer rate is dominated by diffusion or even a mixed regime, which is also recognised for the flux at higher acetic acid concentrations.

Figure 1 shows the significant plateau regions for the calculated initial mass transfer of the surfactant-free system in comparison to the used amphiphiles. The induced charge at the interface, which is caused by a hygroscopic-nonhygroscopic orientated covering of surfactants at the interface, has a strong influence on the flux.

The anionic active layers decrease the flux while,at an equal covering and charge density, the flux is improved by cationic surfactants and independent of non-ionic surfactants. Furthermore, there is no difference in flux between the two anionic surfactants NaDdS and NaLS, which means that the flux is determined by the induced charge and not by the adsorbed substance.

By comparison of different charged adsorption media it could be shown that electrostatic interactions have to be taken into account. The presence of surfactants in the aqueous phase affects the EM of oil drops through interfacial adsorption of the surfactant molecules at the interface. Figure 2 shows the influence of the surfactants on the EM of oil drops at the same charge density as in the stirred cell. Concerning DTACl, the EM is positive over the whole pH-range, in the case of the anionic NaDdS and NaLS the EM becomes negative in about the same way. The non-ionic surfactant does not affect the EM over the pH-range.

These results are in a very good agreement with those of the stirred cell and they are comparable to the other chemical systems of Osseo-Asare and Lin.[7] Reaction inhibition is to be expected at the presence of an interface with the same charge as the extractable species and an increase in extraction rate is to be expected when the aqueous transfer species and the interface are oppositely charged.

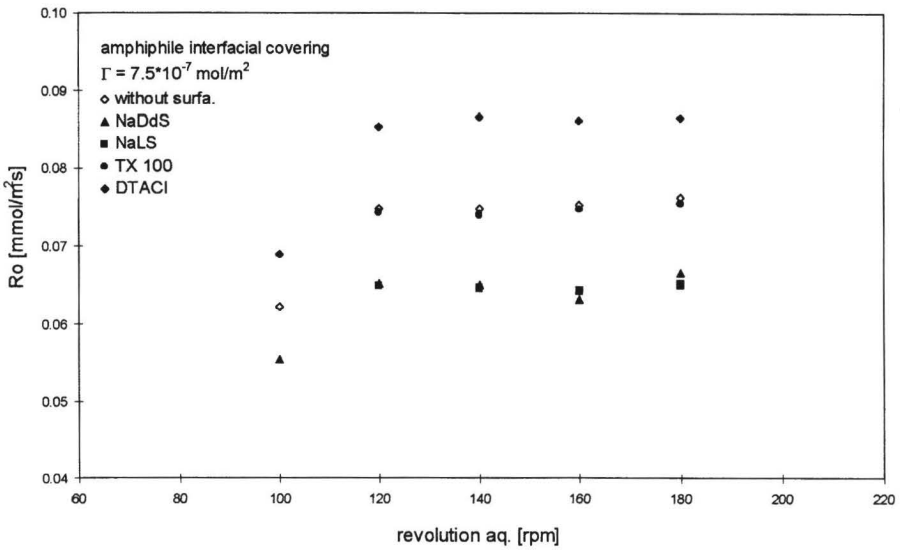

Figure 1. Influence of surfactants on the reaction limited regime, 0.2 w-% HA/H_2O//10 w-% TOA/TOL

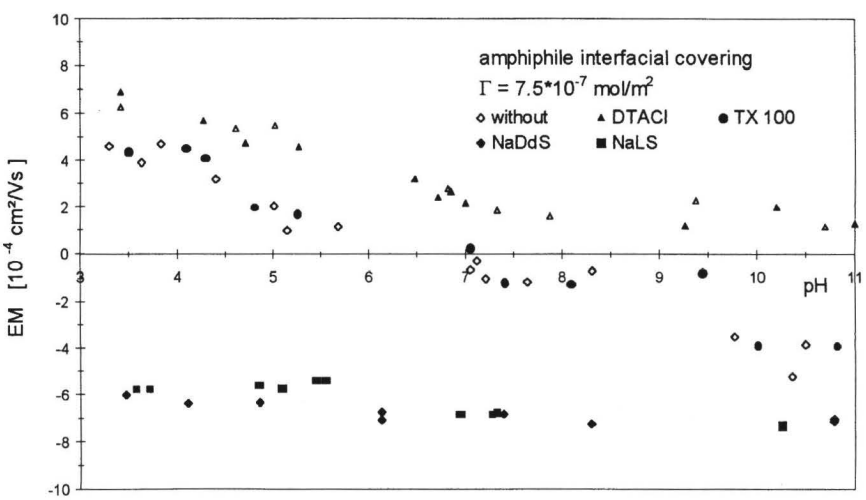

Figure 2: EM-pH-curves for 10 w-% TOA/TOL//H2O emulsions in the absence and presence of surfactants, 4-5*10^{-3} M Na($OCOCH_3$)

In Figure 3, four reactive mass transfer regimes with different concentrations of acetic acid and tri-n-octylamine are plotted over time. Simulated values are indicated by lines and the experimental data are shown as points. The introduced model can describe the measured values quite well. The kinetic parameter C_2, which describes the ratio between forward and backward reaction, is obtained by the calculation of the equilibrium constant K_{EX}. The parameters C_1 and C_3 are estimated simultaneously. Equilibria and mass transfer were formulated on the basis of the chemical potential. An extended

Hildebrand theory[2] for the calculation of the organic activity coefficients is used and the aqueous activity coefficients were calculated by the Pitzer theory.[8]

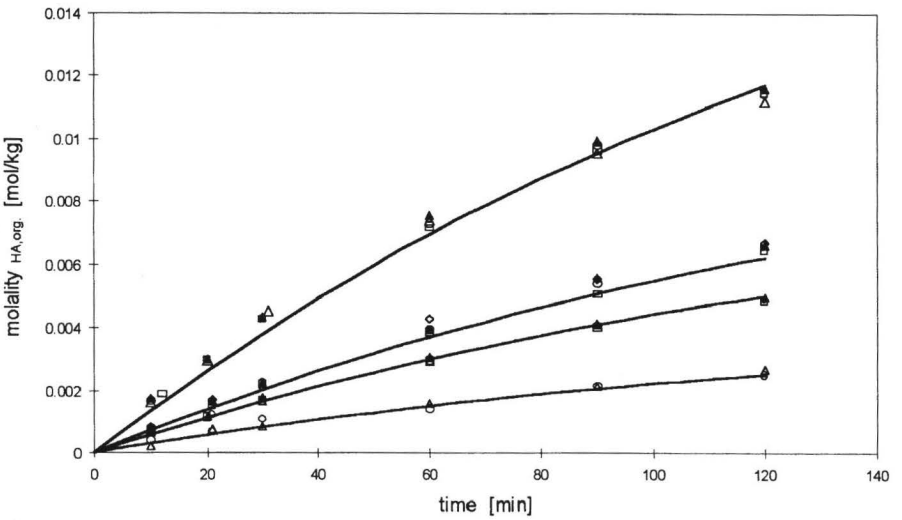

Figure 3: Calculated concentration-time-curves for the measured systems, X w-% HA/H_2O//X w-% TOA/TOL

CONCLUSIONS

A rate law for the reaction kinetics and its electrostatical extension, which describes the measured data quite well, has been proposed. The charge at the interface has a strong influence on the initial mass transfer in the reaction dominated regime. In general, those influences are not caused by a shifting of the corresponding extraction equilibria but by the charged interface, which changes the amount of extractable aqueous species. The measurements concerning the electrophoretic mobility of neutral, anionic and cationic surfactants loaded liquid surfaces underline this fact.

ACKNOWLEDGEMENTS

The authors thank Henkel KGaA for the donation of Alamine®300 and the „Stiftung Rheinland-Pfalz für Innovation, Mainz“ for financial support.

REFERENCES

1 Czapla C and Bart H-J, *Acetic Acid Extraction under the Influence of Chemical Adsorption Layers*, CHISA 98, Prague,(1998)
2 Hildebrand JH and Scott RL, *The solubility of Nonelectrolytes*, Dover Pub, London, (1950)
3 Hunter RJ, *Zeta Potential in Colloid Science*, Academic Press , London, (1981)
4 Kamenski DI and Dimitrov SD. *Computers Chemical Eng.* **17**, 643, (1993).
5 Nitsch W and Hillecamp K, *Chem. Ztg.* **96**, 254, (1972).
6 Nitsch W, *Faraday Discuss. Chem. Soc.* **77**, 85, (1984).
7 Osseo-Asare K and Lin KL, *Recent Developments in Separation Science* (Li NN and Calo JM, eds.), CRC Press, Boca Raton(1986)
8 Pitzer KS, *Activity Coefficients in Electrolyte Solutions*, CRC Press, Boca Raton, (1991)
9 Shaw DJ, *Electrophoresis*, Academic Press, New York, 1. (1963)
10 Siebenhofer M, *Dissertation*, Techn. Universität Graz. (1983)
11 Tamada JA, Kertes AS and King CJ. *Ind. Eng. Chem. Res.* **29**,1319, (1990).
12 Ziegenfuß H, *Dissertation*, Universität Kaiserslautern. (1993)

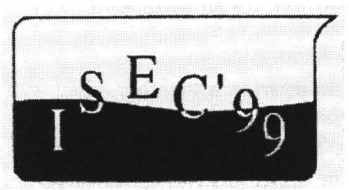

THE COUPLING OF DIFFUSION COEFFICIENTS IN CONTINUOUS PHASES AT LIQUID–LIQUID INTERFACES

A Tokarz, M Millies and D Mewes
Institute for Process Engineering, University of Hannover,
Callinstrasse 36, 30167 Hannover, Germany

ABSTRACT
The mass flux across a liquid/liquid-interface is dependent on the diffusion in both continuous phases as well as in the interface. To date, all three transport processes are calculated using separate transport coefficients and equations. The diffusion coefficients in both continuous phases are generally assumed to be independent of each other. However, the transport from one continuous phase through the interface into the other continuous phase ought to be described by a single transport equation. It is shown theoretically, that assuming the existence of this single transport equation, the diffusion coefficients in both continuous phases are coupled. The relation between the diffusion coefficients can be calculated from thermodynamic equilibrium data of the liquid/liquid system. Experimental investigations are being planned to validate the assumptions.

Keywords: diffusion coefficient, liquid/liquid interface, thermodynamic equilibrium, mass transfer

INTRODUCTION

Interfaces play a significant role for virtually all mass transfer processes in the nature as well as in industry. The transfer of components across an interface can be subdivided into three steps. Initially the transferring components are transported to the interface. Successively they cross the interface and are finally transported away from the interface. In addition, chemical reactions at the interface as well as in the boundary layers adjacent to the interface may occur.

The interface is generally regarded as a two-dimensional dividing surface at which all phases are in thermodynamic equilibrium and which moves with the mean velocity of the adjacent continuous phases. For the design of mass transfer equipment in the industrial practice, the mass transport processes at interfaces are most commonly modelled using either the film theory or the surface renewal theory. The former is originally developed by Whitman and Lewis,[1] the latter by Higbie,[2] however, based on these two models, a large variety of modified equations has been published ever since – see for instance Godfrey and Slater.[3] Both theories have in common, that only the concentration boundary layers adjacent to the interface are modelled while at the actual interface, thermodynamic equilibrium is assumed.

Numerous investigations have been carried out on the diffusion in multicomponent liquid phases at binodal states - such as those existing at interfaces.[4-7] The results show that the diffusion at binodal states takes place in a different manner as compared to the diffusion in a continuous phase far away from the binodal state. While in the latter case, cross effects between the transport fluxes of different components can be quite strong (Maxwell-Stefan diffusion), at binodal states the cross coefficients of the diffusion matrix vanish.[6] It has been supposed that the entire process of mass transport in liquids at binodal states is not governed by the equations for diffusion at all but by other transport phenomena such as a structure transport.[8-10] However, it has yet neither been confirmed nor proved wrong that such a structure transport exists.

In the present investigation, a new theoretical concept is outlined. The theory is based on the existence of a single equation - similar to Fick's law of diffusion for continuous phases - which describes the mass transfer from one continuous phase through the interface into the second continuous phase. Assuming the existence and validity of such an equation, a possible formulation is shown. Also the consequences with respect to the diffusion coefficients in the immediate vicinity of the interface on both sides are described.

© 2000 Society of Chemical Industry

Theory

Hampe [8] and Millies et al.[9], introduced the concept of structure to provide a variable which can be used to describe the properties of a multiphase and multicomponent system in the immediate vicinity of the interface as well as in the interfacial region. The structure a_i of a component i is generally a function of the concentration c_i as well as of the derivatives of the concentration with respect to the coordinate z perpendicular to the interface:

$$a_i = f\left(c_i, \frac{\partial^2 c_i}{\partial z^2}, \left[\frac{\partial c_i}{\partial z}\right]^2, \ldots\right), \text{ with } i=1,\ldots,n. \tag{1}$$

Note that only even derivatives of the concentration and the square of derivatives determine the structure. This is necessary to assure the invariance of the structure to the choice of the coordinate system. Within the bulk phase where the concentration gradients are relatively small, the structure becomes identical with the concentration and the well-known transport equations apply.
Equation (1) may be written as a vector equation for all n components

$$\underline{a} = f\left(\underline{c}, \frac{\partial^2 \underline{c}}{\partial z^2}, \left[\frac{\partial \underline{c}}{\partial z}\right]^2, \ldots\right). \tag{2}$$

Here the elements of the vectors do not denote fractions belonging to a certain coordinate in space but the n components of the multicomponent system.
At thermodynamic equilibrium, the structure is defined to be constant across the interface, i.e.

$$\underline{a}(z) = \text{const.} \tag{3}$$

In a two-phase system it is:

$$\underline{a}' = \underline{a}'' = \underline{a}. \tag{4}$$

where the indices ' and '' denote the two phases.
For the transport of structure, an equation similar to Fick's equation of diffusion can be defined

$$\Lambda_j^{zz} = -\sum_{i,j\neq n} T_{i,j} \frac{\partial a_i}{\partial z}, \tag{5}$$

where Λ_j^{zz} is the structure flux of the component j in the z-direction and $T_{i,j}$ is the transport coefficient for the structure comparable to the diffusion coefficient in a continuous phase.
In a distance far away from the interface, the structure is identical to the concentration and hence the structure flux is identical to the molar flux $\dot{n}_j$

$$\dot{n}_j = \Lambda_j^{zz} = -\sum_{i,j\neq n} T_{i,j} \frac{\partial a_i}{\partial z}. \tag{5a}$$

Equation (5) can be formulated for all components in a vectorial way

$$\underline{\dot{n}} = -\underline{\underline{T}} \frac{\partial}{\partial z} \underline{a}. \tag{6}$$

Again, the individual elements of the vectors in Equation (6) do not denote a fraction belonging to a certain coordinate in space but the individual components. In a system with n components, the vector of the molar flux and of the structure have the dimension n. The transport coefficient is an n x n matrix.

Thermodynamic Equilibrium at the Interface

In a two-phase liquid/liquid-system the relation between the concentrations of any component on either side of the interface can be determined by equilibrium thermodynamics

$$\underline{c'_{\mathrm{Int,Eq}}} = f\left(\underline{c''_{\mathrm{Int,Eq}}}\right). \tag{7}$$

Here $\underline{c'_{\mathrm{Int,Eq}}}$ and $\underline{c''_{\mathrm{Int,Eq}}}$, respectively, are the interfacial concentration vectors of the *n* components in both phases being in thermodynamic equilibrium. The function on the right hand side of Equation (7) – Nernst's distribution function – can either be calculated using appropriate models or experimentally determined.

If the concentrations of the components in phase I are varied by an infinitesimal small value, the concentrations of the components in phase II change accordingly once thermodynamic equilibrium is
attained again. It is:

$$\mathrm{d}\underline{c'_{\mathrm{Int,Eq}}} = \frac{\partial \underline{c'_{\mathrm{Int,Eq}}}}{\partial \underline{c''_{\mathrm{Int,Eq}}}}\,\mathrm{d}\underline{c''_{\mathrm{Int,Eq}}}\,. \tag{8}$$

The partial differential $\dfrac{\partial \underline{c'_{\mathrm{Int,Eq}}}}{\partial \underline{c''_{\mathrm{Int,Eq}}}}$ can also be calculated from equilibrium thermodynamics.

One disadvantage for the use of Equation (8) is the fact, that all elements of the vectors $\mathrm{d}\underline{c'_{\mathrm{Int,Eq}}}$ and $\mathrm{d}\underline{c''_{\mathrm{Int,Eq}}}$ are different from zero. The individual elements are a function of the position along the binodal curve. To overcome this, a new vector of concentrations $\underline{\zeta}$ is introduced as a function of the concentration vector $\underline{c}$

$$\underline{\zeta} = f(\underline{c}). \tag{9}$$

The characteristics of the vector $\underline{\zeta}$ are illustrated in Figure 1 showing the miscibility diagram of a ternary system with two phases. For an infinitesimal small change $\mathrm{d}\underline{\zeta'}$ in phase I the change $\mathrm{d}\underline{\zeta''}$ in phase II can be calculated similarly to Equation (8)

$$\mathrm{d}\underline{\zeta'} = \frac{\partial \underline{\zeta'}}{\partial \underline{\zeta''}}\,\mathrm{d}\underline{\zeta''}\,. \tag{10}$$

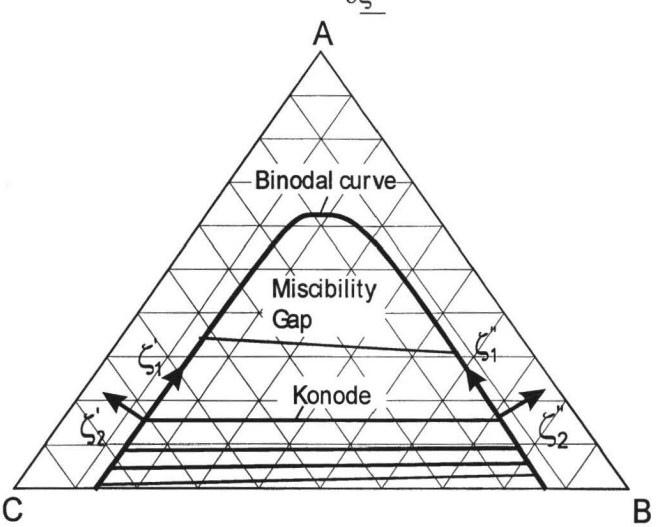

Figure 1: Phase diagram with co-ordinates $\underline{\zeta'}$ and $\underline{\zeta''}$

For all concentration variations along the binodal curve, the vectors $d\underline{\zeta}$ have only one element $d\zeta_1$ which is non-vanishing. All other elements have the value zero. This simplifies the upcoming calculations. The functional dependence according to Equation (9) can be derived from equilibrium thermodynamics similar to a coordinate transformation.

On the assumption of Equation (4) the structure can be partially differentiated by $\underline{\zeta}$ to yield

$$\frac{\partial \underline{a}}{\partial \underline{\zeta}''} = \frac{\partial \underline{a}}{\partial \underline{\zeta}'} \frac{\partial \underline{\zeta}'}{\partial \underline{\zeta}''}. \tag{11}$$

Thermodynamic Non-Equilibrium at the Interface

The following equations can be derived from Equation (6) for the molar transfer across an interface:

$$\begin{aligned} \dot{\underline{n}} &= -\underline{\underline{T}} \frac{\partial \underline{a}}{\partial \underline{\zeta}'} \frac{\partial \underline{\zeta}'}{\partial \underline{c}'} \left(\frac{\partial}{\partial z} \underline{c}' \right) \\ &= -\underline{\underline{T}} \frac{\partial \underline{a}}{\partial \underline{\zeta}''} \frac{\partial \underline{\zeta}''}{\partial \underline{c}''} \left(\frac{\partial}{\partial z} \underline{c}'' \right). \end{aligned} \tag{12}$$

At a considerable distance to the interface these equations change into Fick's law of diffusion

$$\begin{aligned} \dot{\underline{n}} &= -\underline{\underline{D}}' \left(\frac{\partial}{\partial z} \underline{c}' \right) \\ &= -\underline{\underline{D}}'' \left(\frac{\partial}{\partial z} \underline{c}'' \right). \end{aligned} \tag{13}$$

Here, $\underline{\underline{D}}'$ and $\underline{\underline{D}}''$ are the matrices of the diffusion coefficients in phase I and II, respectively. Instead of Fick's law of diffusion, the Maxwell-Stefan formulation of the law of diffusion could be used. However, since experimental investigations have shown that the cross diffusional effects along the binodal curve are negligible,[6] Fick's law appears to be the rational choice. Comparing the coefficients of Equations (12) and (13), the following yields

$$\underline{\underline{D}}' = \underline{\underline{T}} \frac{\partial \underline{a}}{\partial \underline{\zeta}'} \frac{\partial \underline{\zeta}'}{\partial \underline{c}'} \tag{14}$$

and

$$\underline{\underline{D}}'' = \underline{\underline{T}} \frac{\partial \underline{a}}{\partial \underline{\zeta}''} \frac{\partial \underline{\zeta}''}{\partial \underline{c}''}. \tag{15}$$

Expanding Equation (11) with the transport coefficient $\underline{\underline{T}}$ and the partial derivative $\frac{\partial \underline{\zeta}''}{\partial \underline{c}''}$ yields

$$\underline{\underline{T}} \frac{\partial \underline{a}}{\partial \underline{\zeta}''} \frac{\partial \underline{\zeta}''}{\partial \underline{c}''} = \underline{\underline{T}} \frac{\partial \underline{a}}{\partial \underline{\zeta}'} \frac{\partial \underline{\zeta}'}{\partial \underline{\zeta}''} \frac{\partial \underline{\zeta}''}{\partial \underline{c}''}. \tag{16}$$

Combining Equation (16) with the Equations (14) and (15) yields

$$\underline{\underline{D}}'' = \underline{\underline{D}}' \left(\frac{\partial \underline{\zeta}'}{\partial \underline{c}'} \right)^{-1} \frac{\partial \underline{\zeta}'}{\partial \underline{\zeta}''} \frac{\partial \underline{\zeta}''}{\partial \underline{c}''}. \tag{17}$$

Using the following definitions

$$\underline{\underline{Z}} \equiv \frac{\partial \underline{\zeta}'}{\partial \underline{\zeta}''} \tag{18}$$

and

$$\underline{\underline{F}} \equiv \frac{\partial \underline{\zeta}}{\partial \underline{c}}, \tag{19}$$

Equation (17) can be rewritten

$$\underline{\underline{D''}} = \underline{\underline{D'}}\ \underline{\underline{F'}}^{-1}\ \underline{\underline{Z}}\ \underline{\underline{F''}}. \tag{20}$$

From Equation (20) an important conclusion can be drawn: the matrices of the diffusion coefficients at the interface in two immiscible phases are dependent on one another. The functional dependence can be calculated from equilibrium thermodynamics using the matrices $\underline{\underline{Z}}$ and $\underline{\underline{F}}$.

CONCLUSION

It has been shown theoretically that in multicomponent, multiphase systems, the diffusion coefficients for any component on both sides of the interface are not independent of one another. This is the case if a mathematical expression in form of a structure exists which at thermodynamic equilibrium is constant across the interface, see Equations (2) and (3). Also a transport equation for the structure (Equation (6)) must exist which is defined in the interface in such a way that the molar transport across the interface can be calculated from phase I through the interface into phase II with a single transport coefficient. The coupling between the diffusion coefficients only occurs for small deviations from the thermodynamic equilibrium in a multiphase system consisting of three or more components. Hence, the phases must be present in a composition very close to the binodal curve. The derived coupling effects can be validated by measuring the diffusion coefficients under the outlined boundary conditions. These measurements are presently being carried out. The results will be presented in due time.

ACKNOWLEDGEMENTS

We would like to thank the German Research Foundation (DFG) for the financial support of this project in one of its priority programs.

REFERENCES

1 Whitman WG and Lewis WK, *Ind. Eng. Chem.*, **16**, 1215, (1924)
2 Higbie R, *Trans. Amer. Inst. Chem. Engnrs.* **31**, 365, (1935)
3 Godfrey JC and Slater MJ, '*Liquid-Liquid Extraction Equipment*', Wiley and Sons, New York, (1994)
4 Cussler EL, *AIChE J.*, **26**, 43, (1980)
5 Hampe MJ, Schermuly W and Blaß E, *Chem. Eng. Techn.*, **14**, 219, (1991)
6 Pertler M, Stevens GW and Blaß E, *AIChE J.*, **42**, 910, (1996)
7 Pertler M and Blaß E, *Proceedings of ISEC '96*, Melbourne, (1996)
8 Hampe MJ, *Ber. Bunsenges. Phys. Chem.*, **85**, 834, (1981)
9 Millies M, v. Bose St, Tokarz A and Mewes D, *Wärme- und Stoffübertragung*, **30**, 17, (1994)
10 Tokarz A, Millies M and Mewes D, *Proceedings of ISEC '96,* Melbourne, (1996)

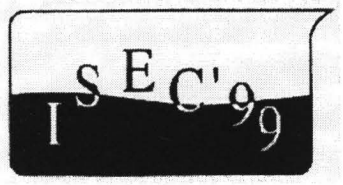

MASS TRANSFER AND FLUORESCENCE TRACER TECHNIQUE IN SOLVENT EXTRACTION

M Mörters and H-J Bart
Universität Kaiserslautern, Lehrstuhl für Thermische Verfahrenstechnik, 67653 Kaiserslautern, Germany.

ABSTRACT
The reactive multi-component mass transfer is investigated in the system $ZnSO_4$–Na_2SO_4–H_2SO_4/di-(2-ethylhexyl)phosphoric acid in isododecane in stirred cell and droplet swarm experiments. Additionally, an optical method for measuring concentration gradients near the interface using fluorescence tracers is developed.

Keywords: multi-component, mass transfer, droplet swarm, stirred cell, interfacial reaction, zinc, D2EHPA, fluorescence tracers

INTRODUCTION

The aim of this work is a fundamental description of the reactive multi-component mass transfer at droplets in the system $ZnSO_4$–Na_2SO_4–H_2SO_4 / di-(2-ethylhexyl)phosphoric acid (D2EHPA) in isododecane, which is proposed as a test system for the reactive extraction by the European Federation of Chemical Engineering (EFCE).[1] Test systems are widely used in extraction technique not only to characterise and discriminate between different types of extraction apparatus, but also to give a basis to fundamental extraction studies.

Former works published about this[2] and comparable systems[3,4] give information other than about physical properties and the chemistry of the system based on equilibrium and stirred cell experiments. Slope analyses lead to the stoichiometry:

$$Zn^{2+} + 1.5\overline{R_2H_2} \rightleftharpoons \overline{ZnR_2RH} + 2H^+$$

confirmed by independent IR-spectroscopic investigations.[3] The equilibrium model uses the Pitzer equation for aqueous and Hildebrand-Scott theory for organic non-ideality and is in good accord with experimental data.

Experiments in a stirred cell have been carried out to discriminate between kinetic, mixed or diffusion controlled regime. For low concentrations a kinetic model with two rate determining reaction steps was developed, leading to the following rate law:

$$-\frac{d[c(Zn^{2+})]}{dt} = \frac{\kappa_f \cdot [c(\overline{R_2H_2})]^{1.5} \cdot [c(Zn^{2+})] - \kappa_r \cdot [c(H^+)]^2 \cdot [c(\overline{ZnR_2(RH)})]}{[c(\overline{R_2H_2})]^{1.5} + C_1 \cdot [c(H^+)]^2} \cdot \left(\frac{\sqrt{[c(\overline{R_2H_2})]}}{C_2 + \sqrt{[c(\overline{R_2H_2})]}} \right)^2$$

It is formulated in activities with $\kappa_f / \kappa_b = K_{1,3}$ as equilibrium constant and gives a good description of the experimental concentration-time curves. For higher concentrations, diffusional effects have to be taken into account. Here, the Maxwell-Stefan diffusion equations based on the two-film theory were used to describe the mass transfer of the reactants to the interface and of the products into the bulk.[4]

Effects found during the mass transfer into or out of droplets in a flowing continuous phase (as summarised[5]) have not been part of this model. Whereas very small drops behave as rigid spheres with molecular diffusion controlling the mass transfer, circulation within the drop starts with rising drop diameter. For internally well-mixed large drops, molecular diffusion is not of any importance for the dispersed phase. Surface active components like the ion exchanger D2EHPA have an influence on the internal circulation of the droplets thus on mass transfer. In order to get more information about the described effects on mass transfer, experiments in a venturi tube with varied droplet size and concentration have been performed. Also an optical measuring system using fluorescence tracers has been developed to visualise concentration profiles especially near the interface on aqueous and

© 2000 Society of Chemical Industry

organic side. However, effects during drop formation and coalescence can also be sensed with this tracer technique.

EXPERIMENTAL

Kinetics at droplets and droplet swarms

The laboratory equipment used to measure the mass transfer kinetics with droplets is based on a principle which has been published in 1986 by Schügerl.[6] A mono-dispersed droplet swarm is produced with a metering pump and a double-flow valve. The droplet size can either be determined by counting the droplets via a video system or with the capillary method.[7] The vertically rising swarm is detained floating in a venturi tube by the countercurrent continuous phase flow. The continuous phase is temperature controlled at 25 ±0.5 °C. If the velocity of the continuous phase is reduced by about 10 %, the droplets keep rising and finally coalesce in a collecting funnel where they are withdrawn for analysis. Afterwards, the organic zinc concentration is determined with atomic absorption spectroscopy. By repeating this experiment with varied residence time (possible between 15 seconds and several hours), kinetic information is obtained. These experiments have been carried out under variation of the starting concentrations of zinc, sulphuric acid and extractant and with different droplet sizes. The derived concentration – time curves have been fitted by:

with the two fitting parameters: t_0 representing the effects during drop formation and coalescence, and K_{OC} representing all resistances during mass transfer.

$$c(Zn)_d = c(Zn)_d^* \cdot \left(1 - \exp\left[-K_{OC} \cdot a \cdot (t - t_0)\right]\right)$$

Fluorescence tracer technique

Additionally, a new method for measuring concentration gradients of several components has been developed. Thus, fluorescence tracers are added to one of the phases and used as indicators. The tracers are detected with an optical probe, which is connected via fibre optics to a laser spectroscopic fluorescence detector. This gives the possibility to obtain local and time-dependent concentrations near the interface.

Optical probe

The fluorescence intensity is measured with a laser spectroscopic fluorescence detector (model MD 33710, Laserlabor Adlershof). To indicate fluorescence in small volumes, a confocal probe was developed (figure 1).

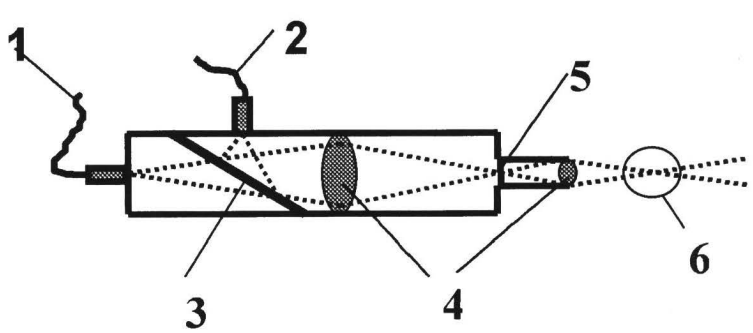

Figure 1: Confocal probe

A laser beam is focused onto an optical fibre. The beam enters the probe (2) and is focused with a pair of positive lenses (4) into the volume (6). Parts of the fluorescence light is reflected and, having now a different wavelength, are passed through the dichroitic mirror (3) and are focused onto a second fibre (1) leading to a photomultiplier. The size of the investigated volume depends on the lens system, the fibre core diameter and the diameter of the pinhole (5), thus a resolution is between 30 and 200 μm with a position shift in a range of 5 nm to several mm.

Fluorescence tracers

Fluorescence dyes are obtainable in a broad variety of properties. These properties are not only the absorption and emission wavelength but also depend on the concentration of a certain ionic component. As most of the dyes are surface active, they have to be used in very dilute concentrations. Measuring the surface tension with varied dye and ion exchanger concentration proved, that the tracer influence can be neglected at concentrations $< 10^{-6}$ mol/dm^3.

Observing the aqueous diffusion is possible with two different kinds of dye. During the reactive extraction, the pH-value decreases due to the ionic exchange of Zn^{2+} and H^+. The rising aqueous concentration of protons can be measured with pH dependant dyes. This phenomenon has been traced with Eosine Yellow, a derivative of fluorescein (Aldrich, dye content ~94%). The fluorescence changes approximately linearly from maximum to almost zero between pH 3 and 1.5. Calceine (Molecular Probes, high purity) is a polyanionic fluorescein derivative. Its fluorescence intensity rises with the zinc concentration, giving the possibility of measuring metal ion concentration gradients in the aqueous phase. As it is also H^+-dependent, it can only be used in buffered systems.

By replacing one component in the system with a fluorescent tracer, the basic behaviour especially in the organic phase can be investigated. Besides using a fluorescent ion exchanger, the transferred component can also be a dye. Rhodamine 6G (Aldrich, dye content ~95%), a dye that is transferred by ion exchange was used to get basic information about diffusion limited mass transfer.

Measuring Systems

To evaluate the measuring system and to investigate a diffusion controlled regime, experiments in a capillary were carried out. Between two vessels containing the phases, a capillary containing the liquid-liquid interface was installed. Because convection is prevented, diffusion takes place over the whole length of the capillary. The probe was moved away from the interface along the capillary. The result is a time-dependent concentration gradient of the investigated component.

In a second step, fluorescence was investigated at single droplets, diameter between 1 and 4 mm. These droplets were produced with a syringe and are fixed on the cannular hanging in the continuous phase. By moving the optical focus of the probe through the droplet and the region around it, the fluorescence is scanned. Organic droplets in the aqueous phase or aqueous droplets in the organic phase can be obtained with this system. First, experiments have been carried out with a stagnant continuous phase. To measure diffusion at droplets under conditions comparable to these found in technical apparatus, further experiments have been carried out with a flowing continuous phase.

Finally it is possible to investigate the effects during droplet formation. A droplet is formed into a non-reactive continuous phase. After the inner circulation of the droplet has calmed down, reactive continuous phase starts flowing around it and mass transfer is measured. Comparing these measurements with the mass transfer into a droplet, which has been formed directly into reactive continuous phase gives the effects during droplet formation.

RESULTS AND DISCUSSION

Basically the transfer rate coefficient rises with rising starting concentrations. Figure 2 shows examples of overall rate coefficients K_{OC} depending on the droplet size, received from venturi tube experiments and fitted with the described equation. The derived constant or falling curves indicate rigid spheres. The

adsorption of the surface active ion exchanger D2EHPA, that has also been determined within interfacial tension experiments, reduces or prevents the internal circulation of droplets. For higher starting concentrations than the depicted ones, the equilibrium state is reached after less then 20 seconds.

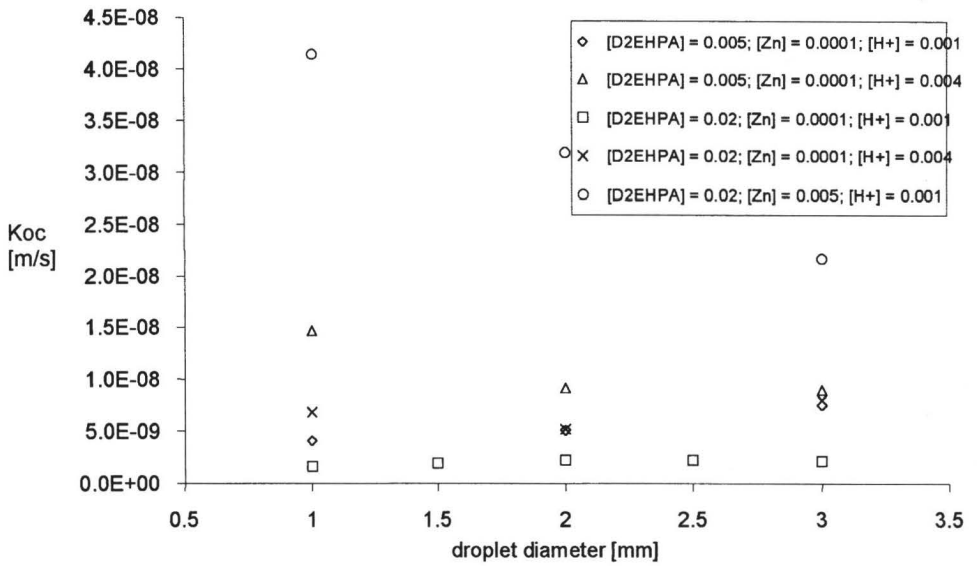

Figure 2: Droplet size dependent rate coefficients

Diffusion controlled fluorescence experiments within the capillary using the pH- dependent dye eosine gave pH–gradients in the aqueous phase over the whole length of the capillary. For infinite time, the profile would become a constant at equilibrium pH.

Observing the aqueous phase in the same concentration range at single droplets gave constant profiles with changing pH values from starting pH to equilibrium. Even in the region close to the interface (< 25 µm), no gradient could be measured. This leads to the conclusion, that diffusion on the aqueous side is negligible. Due to the larger molecules and the higher viscosity, the diffusion on the organic side is the rate-determining step. Simulations confirmed this result, with concentration gradients and the size of the diffusion film the calculated parameters.

Analysing the organic side with the fluorescence method using the dye rhodamine as the transferred component leads to time dependent concentration profiles within the organic droplet. Figure 3 shows an example (starting concentrations: [Rhodamine] = 0.0001 M, $[H^+]$ = 0.001 mol/dm^3, [D2EHPA] = 0.1 mol/dm^3; droplet diameter 2 mm). The diffusion film contains a concentration gradient and becomes larger during the extraction. The gradient ends again as a constant in equilibrium state. This is in contrast to the two-film-theory that assumes diffusion films of constant size during the extraction on each side of the interface.

Further experiments have been carried out with $ZnCl_2$ and HCl as aqueous components. Differences in equilibrium and mass transfer between the sulphate and the chloride system are thus predictable with the same model.

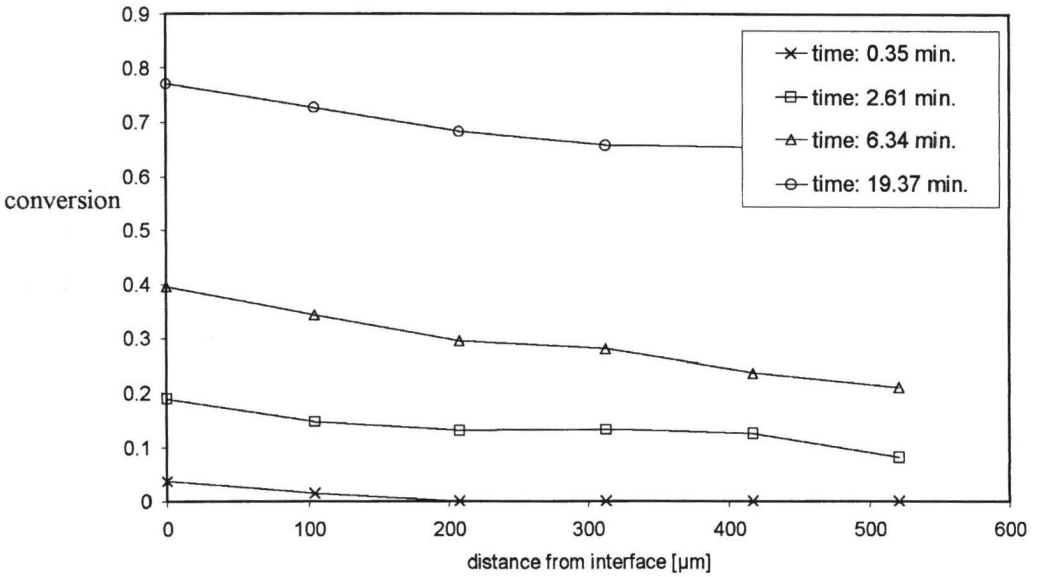

Figure 3: Concentration gradients in an organic droplet

REFERENCES

1 Bart H-J, Berger R, Misek T, Slater MJ, Schröter J and Wachter B: *Liquid-Liquid Extraction Equipment*, Ed. Godfrey and Slater, John Wiley.(1994)

2 Bart H-J and Rousselle H-P: *Hydrometallurgy*, submitted (1998)

3 Sainz-Diaz CI, Klocker H, Marr R and Bart H-J: *Hydrometallurgy* **42**, 1, (1996)

4 Klocker H, Bart H-J, Marr R and Müller H: *AIChE J*, **43(10)**, 2479, (1997)

5 Slater MJ : *Liquid-Liquid Extraction Equipment*, Ed. Godfrey and Slater, John Wiley (1994)

6 Haensel R, Halwachs W and Schügerl K: *Chem. Eng. Sci.* **41(3)**, 555, (1986)

7 Pilhofer T and Miller H-D: *Chemie-Ing.-Techn.* **44(5)**, 295, (1972)

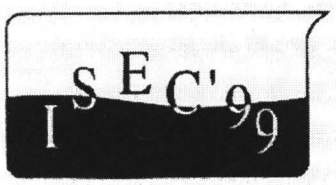

KINETICS OF MASS TRANSFER AND THE DIFFERENT EFFECTS OF SURFACTANTS

Michael Weigl and Walter Nitsch
Technische Universität München, Institut für Technische Chemie, Lichtenbergstrasse 4, 85748 Garching, Germany

ABSTRACT
The presented contribution is directed to the possibility of identifying the two different actions of surfactants on the mass transfer between two liquid phases. From regarding measurements of physical or chemical mass transfer in dependence from convection (special stirred cell) a very characteristic "fingerprint" appears for the case that transport processes are rate limiting. Due to the fact that the typical flow dependency of the fluxes (fingerprint) has shown to be independent from the mass transfer system as well as from the added anionic, cationic or nonionic surfactant, transport limitation can be unequivocally identified. Special experiments show that convection induced macroscopic gradients of the interfacial tension are responsible for the change of the interfacial flow, causing the inhibition of the transport processes. The alternative case concerns the influence of adsorption layers on the rate of a chemical interfacial reaction, being rate determining. This kinetic borderline case is characterized by independence of the flux from the state of convection (plateau rate) in the stirred cell. A systematic analysis of the interfacial kinetics (zinc ion complexation with dithizone) in either absence or presence of surfactants shows not only a distinct acceleration and inhibition of fluxes, caused by different anionic adsorption layers, but also a change of the kinetics of the interfacial reaction. In comparison with the surfactant free system, the upper case thus is characterized by pronounced saturation kinetics, the disappearance of the proton sensitivity and the appearance of a strong influence of added electrolytes. These kinetic effects in the studied example of metal extraction takes place only when the interface has been given a negative charge (anionic surfactant). Besides bearing these new inside views of interfacial kinetics, the applied method (special stirred cell) is demonstrated to be suitable to resolve the different influences of surfactants on mass transfer between liquid phases.

Keywords: interfacial kinetics, surfactants, AOT, dodecyltrimethylammonium bromide stirred cell, zinc, dithizone

INTRODUCTION

Mass transfer between two liquid phases is distinguished by coupling of transport and reaction processes. Hence the effect of surface active substances can be subdivided into two fundamental different domains:

- effect on transport processes
- influences on the chemical interfacial reaction.

At examinations of surfactant action this classification requires a experimental techniques, which easily and beyond any doubt allow to discriminate the cases of mass transfer limited by transport processes or the interfacial reaction. This is excellently possible by means of our special flow calibrated stirred cell. Here transport limitation turns out as an linear dependence of transfer rate from stirring speed, while processes limited by the chemical reaction show transfer rates which are independent from the stirring speed.[1]

Comparatively detailed knowledge could be collected concerning the influence of surfactants on transport processes. In this case it is only possible, that surfactants act on the liquid flow adjacent to the interface. This consequently hydrodynamic inhibition is caused by gradient of interfacial tensions reducing the crucial flow near the interface.[2] Through measurements in the stirred cell it was possible to obtain the typical phenomena's of hydrodynamic surfactant action (Figure 1). This characteristic influence could be demonstrated using different kind of surfactants with heat transfer measurements, physical mass transfer and as well transport limited metal extraction.[3,4]

Of fundamental different character the surfactant effectson mass transfer processes are limited by chemical reactions. Few publications exist about micellar system, concerning reactions between metal ions (aqueous phase) and solubilized compounds.[5,6,7] But such micellar systems exist

© 2000 Society of Chemical Industry

inherently only in presence of surfactants, which means that there is no way to detect the influence of surfactants on the base mechanism of an interfacial reaction.

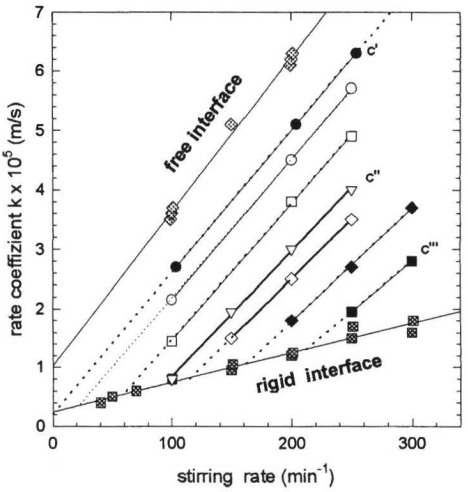

Figure 1. The effect of surfactants on transport limited mass transfer: toluene transfer from toluene to water at different surfactant concentrations (c'''> c''> 'c').

EXPERIMENTAL

All the measurements of mass transfer were performed in our prototype of a stirred cell, which has been previously described.[8] The convection was varied by the stirring speed N (min^{-1}), keeping constant the stirring ratio N_{aq}/N_o = 1.39 of the aqueous (N_{aq}) and the organic phase (N_o). The mass transfer between the already stirred phases was started with the injection of a concentrated solution of zinc sulfate into the water phase. The course of mass transfer was followed time-resolved by photometric measurement (λ = 533 nm) of the zinc dithizonate concentration ($\overline{ZnX_2}$) in the toluene phase. In the presence of surfactants, the selected concentrations are always distinctly below the critical micelle concentration (cmc), proved by corresponding measurements of the interfacial tension. That the surfactants are exclusively distributed in favor of the aqueous phase was shown by ICP-AES (inductively coupled plasma atomic emission spectroscopy). All surfactants were applied in pA quality as delivered by Fluka or Merck. Only SDS (pA Merck) was purified by charcoal adsorption followed by freeze-drying. Dithizone (1,5-diphenylthiocarbazone) was used in pA quality (Merck). The surface activity of dithizone proved with interfacial tension was always negligible.

RESULTS and DISCUSSION

Because we focused on the interaction of surfactants with the interfacial reactions, only cases of mass transfer being independent on convection are taken into consideration. The applied stirred cell technique allows to guarantee, that the interfacial reaction controls the mass transfer, recognizable by the independency of the mass transfer from the convection. To obtain a clear picture of the effects of the surfactants, we used as a model system the reaction of zinc from buffer-free water solution to toluene with dithizone (1,5-diphenylthiocarbazone) according to the stoichiometric equation (overscore means species in the organic phase).

$$Zn^{2+} + 2\,\overline{HX} \rightarrow \overline{ZnX_2} + 2\,H^+ \qquad (1)$$

We cleared up the kinetic of this interfacial reaction. Through that examination a comparison of the kinetics of the surfactant free-system (the so-called base system) and the kinetics in presence of different surfactants is possible and the effects of surfactants on the reaction can be discussed.

Base System

Analogous to the former reported successful procedure,[9] chemical mass transfer was measured for fixed initial H^+ and $\overline{HX}$ concentrations with different levels of zinc ion concentration, in order to realize the kinetic regime of chemical control. The plots of the initial fluxes (Figure 2) characterize the kinetic behavior of the base reaction. At low zinc concentrations ($Zn \leq 2 \times 10^{-4}$ kmol/m³) the interfacial reaction is rate determing, indicated by the flow independent fluxes. In the case of high zinc concentrations ($Zn \geq 10^{-1}$ kmol/m³) the observed linear relationship between flux and stirring speed indicates fluxes being limited by transport processes. The curve ($Zn = 5 \times 10^{-3}$ kmol/m³) between both kinetic borderline cases represents an example of a so-called mixed kinetic. Analogous behavior is published for dithizone systems at different liquid/liquid phase systems for different cations, but always which the application of buffer systems.[1,9]

For the discussion of surfactant effects later on, the mechanism of the base reaction is necessary. Therefore the influence of the participating species (H^+, $\overline{HX}$, Zn^{2+}) on the rates must be studied to derive the rate equation of the interfacial reaction. The corresponding results are summarized through the kinetic equation, which shows that the concentration dependencies for the interfacial reaction are of first order for the zinc ions (see plateau rates in Figure 2) and dithizone[10] and of a reciprocal first order for the proton concentration (Figure 4).

$$j = k \cdot \frac{[Zn^{2+}]^{\bullet}[\overline{HX}]^{\bullet}}{[H^+]^{\bullet}} \qquad (2)$$

The overall rate constant k is calculated with eq. 2 to be 8×10^{-5} cm/s.

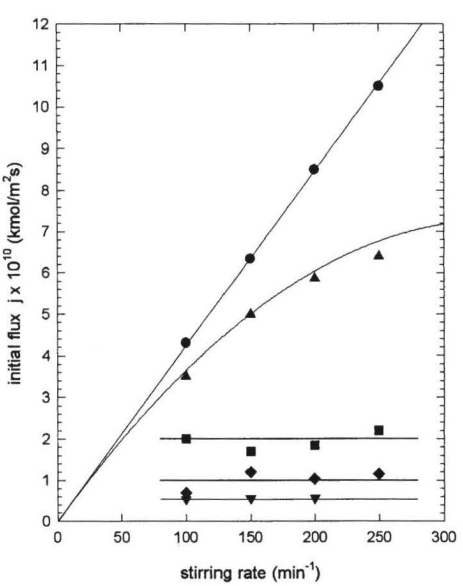

Figure 2. Dependency of initial fluxes from stirring rate for different zinc ion concentrations: $[\overline{HX}] = 1.25 \times 10^{-4}$ mol/l, pH 4. Zinc concentrations were as follows: ł 0.1 kmol/m³; ş 5×10^{-3} kmol/m³; ⁿ 2×10^{-4} kmol/m³; □ 1×10^{-4} kmol/m³; ţ 5×10^{-5} kmol/m³.

Concerning the mechanism of the interfacial base reaction, the simplest consecutive scheme of reaction steps in agreement with the measured concentration dependency is characterized by

$$\overline{HX} \underset{}{\overset{K_{Diss}}{\rightleftharpoons}} H^+ + X^- \qquad \text{(fast)}$$

$$Zn^{2+} + X^- \xrightarrow{k_R} ZnX^+ \qquad \text{(slow)}$$

$$ZnX^+ + X^- \longrightarrow \overline{ZnX_2} \qquad \text{(fast)}$$

The three steps are localized at the interface. Corresponding to these consecutive reactions the overall constant in eq. 2 is given $k = k_r K_{diss}$.

Kinetics in Presence of Surfactants

Instead of measuring mass transfer in presence of different surfactants for constant concentrations for all educts,[11] in frame of this contribution we decided to vary all concentration in order to study the action of surfactants related to the mechanism of the controlling interfacial reaction.

A. Anionic Surfactants

The chemical mass transfer in presence of AOT(bis(2-ethyl-hexyl)sulfosuccinate sodium salt) was the first example for the action of a negatively charged interface. Compared with the base reaction, the striking "layer effect" is the dependency on the zinc ion concentration. Caused by the AOT layer the increase of the measured flux with zinc ion concentration shows the behavior of a pronounced saturation kinetic (Figure 3), instead of the first-order dependency of the base reaction. Additionally the AOT-layer causes a strong acceleration of the interfacial-controlled fluxes in the range of low zinc ion concentrations. Both effects are plausible with the assumption of a fast zinc ion adsorption at the negatively charged AOT-layer at the interface, followed by the slow interfacial complexation.

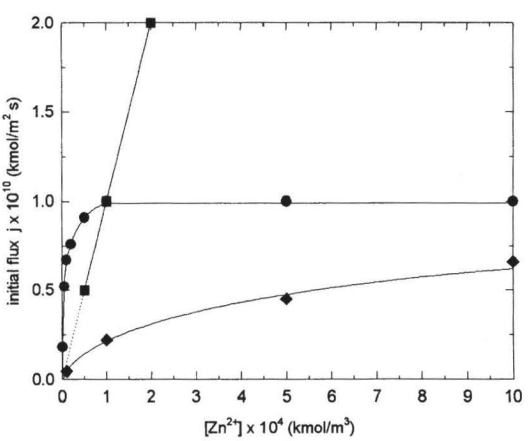

Figure 3. Dependency of initial fluxes from zinc ion concentration for the base reaction and the reaction in presence of AOT and inhibition by calcium ions: pH 4, $[\overline{HX}] = 1.25 \times 10^{-4}$ mol/l, $N_{aq} = 200\ min^{-1}$; n base system; ł $[AOT] = 1 \times 10^{-4}$ kmol/m³; □ $[AOT] = 1 \times 10^{-4}$ kmol/m³ and $[Ca^{2+}] = 5 \times 10^{-4}$ kmol/m³.

Further, for the complexing agent dithizone measured in the zinc regime of saturation kinetics a first order dependency was found, analogous to the base reaction. Rather unexpected is the result concerning the proton concentration. While the flux of the base reaction is proportional to the reciprocal proton concentration, in the presence of AOT layers, the influence of the pH is almost nearly completely diminished (Figure 4).

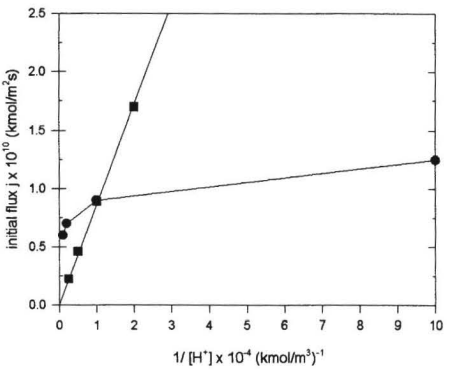

Figure 4. Influence of the reciprocal proton concentration for presence and absence of AOT: $[Zn^{2+}] = 1 \times 10^{-4}$ kmol/m³, $[\overline{HX}] = 1.25 \times 10^{-4}$ kmol/m³; ł [AOT] = 2×10^{-4} kmol/m³; ⁿ base reaction.

Mechanism and Rate Equation

Concerning the comparison between base reaction and "layer reaction" apart from the saturation kinetics, the AOT caused decrease of the pH sensitivity is the most striking result. The attempt for an explanation has to consider the three step mechanism of the base reaction (eq. 2), which shows the necessity of a HX dissociation, since from kinetic reasons the dithizone anion is the educt for the limiting first step of complexation at the interface. Therefore one have to conclude that the complexation reaction in the interfacial AOT layer is introduced not by the anion but the dithizone molecule itself.

The postulate of the zinc adsorption as the reason of the saturation behavior is supported by the strong inhibition by added electrolytes (e.g. calcium ions), which compete with the zinc ions for the negative sites at the AOT-interface (Figure 3). Regarding the measured concentration dependencies, the rate equation for the interfacial reaction at the AOT layer can be formulated with

$$j = k' \left[Zn^{2+}_{ad}\right]\left[\overline{HX}\right] \qquad (3)$$

Related to this equation and the kinetic interpretations given above, the interfacial reaction in the AOT layer should follow the three step scheme

$$2AOT^-_{ad} + Zn^{2+} \longrightarrow Zn(AOT)_{2_{ad}} \text{ (fast)}$$

$$Zn(AOT)_{2ad} + HX \xrightarrow{k'} ZnAOTX_{ad} + HAOT \text{ (slow)}$$

$$ZnAOTX_{ad} + HX \longrightarrow ZnX_2 + HAOT \text{ (fast)}$$

Though in Equation (3) the explicit isotherm for the adsorbed Zn species (Zn^{2+}_{ad}) is not involved, the comparison with the corresponding rate Equation (2) for the base reaction shows, that two different mechanisms are responsible for the interfacial complexation in the absence and the presence of the anionic surfactant. It is demonstrated here for the first time, that surfactants change not only the rate constant but also the mechanism of an interfacial reaction. Further measurements with SDS (Figure 5) and OBS (octylbenzol-sulfonate sodium salt) show analogous results.[9] This suggest, that this kind of influence on the kinetic of an interfacial reaction is a general feature for anionic surfactants.

B. Cationic Surfactants

The results for the anionic surfactants show, that the interfacial reaction is very sensitive to a negative charge of the interface. Therefore it is interesting, how a positively charged interface influences

the interfacial complexation of cations. We used the cationic surfactant DTAB (dodecyltrimethylammonium bromide) for our experiments. The comparison of the base reaction with the reaction in the presence of anionic or cationic surfactants shows a clear result (Figure 5).

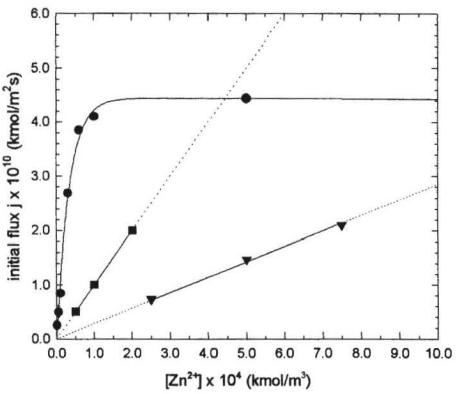

Figure 5. Dependency of the initial fluxes from the zinc ion concentration for the presence of anionic (SDS) or cationic (DTAB) surfactant compared with the base reaction: $[\overline{HX}] = 1.25 \times 10^{-4}$ kmol/m³, pH 4, $N_{aq} = 200$ min^{-1};ł [SDS] = 1.1×10^{-4} kmol/m³;ţ [DTAB] = 1×10^{-4} kmol/m³; ^{n} base reaction.

Instead of the strong acceleration of the fluxes caused by the anionic layer, in the case of a positive charge of the interface the fluxes are always inhibited. This effect is simple to explain as a potential effect. If the interface is positively charged, the zinc ions are repulsed, and this means a decrease of both the interfacial zinc ion concentration and therefore the interfacial reaction. Further measurements proved[12] that the rate equitation in the case of cationic surfactants corresponds to the mechanism of the base reaction.

CONCLUSION

Summarizing the presented results the methodical procedure is demonstrated directed to the interaction of surfactants with interfacial reactions. Moreover examples are given for the pronounced different action of anionic and cationic surfactants on interfacial reactions at liquid/liquid interfaces. Until now, this field of interfacial science and extraction is rather underdeveloped, in spite of perspectives in separation technology, molecular catalysis and biological transport.

REFERENCES

1. Nitsch N, *Faraday Discuss. Chem. Soc.*, 77, 85, (1984).
2. Davies JT, *"Turbulence Phenomena"*, 2nd ed.; Academic Press, New York, (1972).
3. Nitsch W and Kniep P, *Chem.-Ing.-Tech.*, **46**, 726, (1974).
4. Nitsch W, Raab M and Wiedholz R, *Chem.-Ing.-Tech.*, **46,** 726 (1974).
5. Ruxiu C, Freiser H and Muralidharan S, *Langmuir*, **11**, 2926, (1995).
6. Tondre C, Claude-Montigny B and Ismael M, *Polyhedron*, 1991, **10**, 1791, (1991)
7. Cierpiszewski R, Hebrant M, Szymanowski J and Tondre C, *J. Chem. Soc., Faraday Trans.*, **92**, 249, (1996).
8. Nitsch W and Kähni J, *J. Ger.-Chem.-Eng.*, **3**, 96, (1980).
9. Nitsch W and Kruis B, *J. Inorg. Nucl. Chem.*, **40**, 857, (1978).
10. Nitsch W and Weigl M, *Langmuir*, **14**, 6709, (1998).
11. Michel T and Nitsch W, *Chem.-Ing.-Tech.*, **62**, 738, (1990).
12. Weigl M, running thesis, TU München.

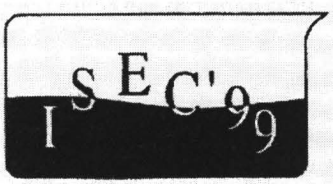

MASS TRANSFER CHARACTERIZATION IN FORWARD AND BACK EXTRACTIONS OF AN AMINO ACID BY REVERSE MICELLES ACROSS A FLAT LIQUID–LIQUID INTERFACE

Tadaaki Nishiki[1], Kiyohiko Nakamura[1] and Daisaburo Kato
[1]Department of Chemical Engineering, Osaka Prefecture University,1-1 Gakuen-cho, Sakai, Osaka 599-8531, Japan
[2]Department of Industrial Chemistry, Osaka Prefectural Technical College, 26-12 Saiwai-cho, Neyagawa, Osaka 572-8572, Japan

ABSTRACT
The mass transfer characterization in reversed micellar extraction of the amino acid phenylalanine (Phe) is presented. The mass transfer rates in forward extraction of Phe from aqueous KCl solutions (pH 1.4~2.3) to AOT/isooctane reversed micellar solutions and in back extraction from the organic phase to $KHCO_3$/KOH buffer solutions (pH 9.0~11.0) were investigated using a stirred cell with a flat liquid-liquid interface. Both the forward and the back extraction rates are controlled by the interfacial rate processes, i.e., the solubilization and the release processes. The effects of pH, initial AOT and Phe concentrations, ionic strength and alcohol addition on their rates are demonstrated. The back extraction rates are fairly slow compared to the forward extraction rates, and are extremely accelerated by the addition of 2-methyl-2-propanol as well as the extraction of protein lysozyme.

Keywords: reversed micellar extraction, interfacial reactions, phenylalanine, AOT.

INTRODUCTION

Reversed micellar extraction has been noted as an attractive and promising method for protein and amino acid recovery. In the practical application of this separation method, it is important to elucidate the transport mechanism of amino acids and proteins between a bulk aqueous and a reversed micellar organic phase. Several papers have been presented on the interfacial transport processes of proteins, but different results have been reported by the researchers.[1-6]

The purpose of this study is to describe the mass transfer characterization in the reversed micellar extraction of an amino acid, which has a clear and simple molecular structure and is a constituent molecule of protein. The mass transfer rates in forward extraction of L-phenylalanine (Phe) from aqueous KCl solutions to AOT/isooctane reversed micellar solutions and in back extraction from the organic phase to $KHCO_3$/KOH buffer solutions were measured using a stirred cell with a flat liquid-liquid interface. The effects of stirring speed, pH, initial AOT and Phe concentrations, ionic strength and alcohol addition on the extraction rates have been investigated. On the basis of these results, the solubilization and release rates of Phe at the liquid-liquid interface are evaluated and compared with our previous results for the protein lysozyme (Lys).[6,7]

EXPERIMENTAL

The experimental apparatus and procedure for measuring the forward and back extraction rates of Phe (MW 165.2, pI 5.48) are the same as described in elsewhere.[6] The anionic surfactant used in this study was bis(2-ethylhexyl) sodium sulfosuccinate (AOT). The experimental conditions for forward and back extraction rates are shown in table 1. For back extraction experiments, AOT/isooctane solutions of presolubilized Phe were used as the reversed micellar organic phase. The pH of aqueous phase was adjusted in the region being favorable for forward and back extractions, respectively. Phe concentration in each phase was determined from UV absorption at 257 nm.

© 2000 Society of Chemical Industry

RESULTS AND DISCUSSION

Forward extraction

Forward extraction experiments were performed at the conditions shown in table 1. From the results of time-dependent concentrations of Phe, the overall mass transfer coefficients, K_{fO}, in the forward extraction across a liquid-liquid interface were obtained by using the following equations.

$$\ln\{1-(1+1/m_f)(Corg/Caq^0)\}=-(A/V)(1+1/m_f)K_{fO}t \quad (1)$$

$$1/K_{fO}=1/k_{fS}+\{1/kaq+(1/m_fkorg)\} \quad (2)$$

These equations are derived when amino acids are transferred from an aqueous to an organic phase through the same processes as in the transport of protein proposed in the previous study.[6]

Forward extraction rate
Organic phase: AOT(0.05~0.2 kmol/m^3)-isooctane
Aqueous phase: Phe(0.0025~0.01 kmol/m^3)-KCl(0.1 kmol/m^3) pH=1.4~2.3
Back extraction rate
Organic phase: Phe(0.005 kmol/m^3)-AOT(0.01~0.2 kmol/m^3)-isooctane
Aqueous phase: $KHCO_3$/KOH buffer(0.1, 1.0 kmol/m^3)-2-methyl-2-propanol(0~10 vol%) pH=9.0, 11.0
Stirring speed (N): 1.00, 1.67 s^{-1}
Temperature: 298K

Table 1 Experimental conditions for forward and back extractions

The values of K_{fO} are plotted against the stirring speed, N, as a parameter of initial AOT concentration in figure 1. The results for Lys [6] are also shown in the figure. It is seen that the K_{fO} values for Phe extraction were not influenced by N and became nearly constant at each AOT concentration. This result suggests that the transport of Phe from the aqueous to the organic phase is not influenced by the diffusional resistances in the phases and is controlled by the solubilization resistance at the interface. Therefore, as can be seen from Eq.(2), the K_{fO} value is assumed to be equal to the solubilizing rate constant, k_{fS}.

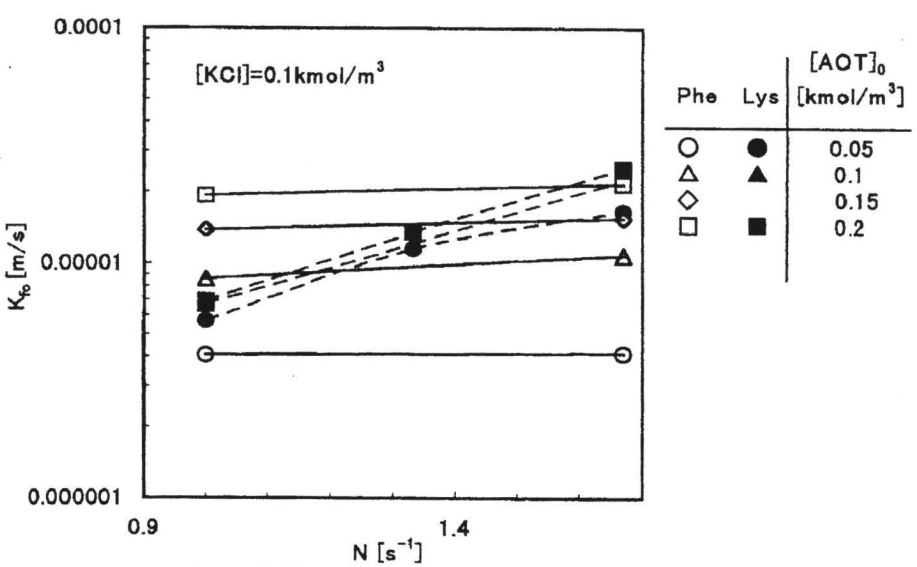

Figure 1. Effect of N on K_{fo} in foward extraction

Phe: Caq^0=0.005kmol/m^3 (pH=1.4) Lys: $Caq^0=7\times10^{-5}$kmol/m^3 (pH=5.5)

The relation between the value of k_{fs} and initial AOT concentration at pH 1.4 and 1.9, respectively, is shown in figure 2. The k_{fs} value increases linearly with increasing AOT concentration at both pH values. This is due to an acceleration of the solubilization by enhancing an interaction at the interface, because the number of AOT molecules per Phe molecule at near the interface increases by an increase of AOT concentration. The k_{fs} value for Lys extraction [6] shown in the figure also increases linearly with increasing initial AOT concentration, but is seven to ten times larger than that of Phe.

Figure 3 shows the values of k_{fs} that were obtained by changing initial Phe concentration. The k_{fs} value decreases gradually with an increase in Phe concentration. This is presumed to be due to the analogous interaction for the dependence of initial AOT concentration described above.

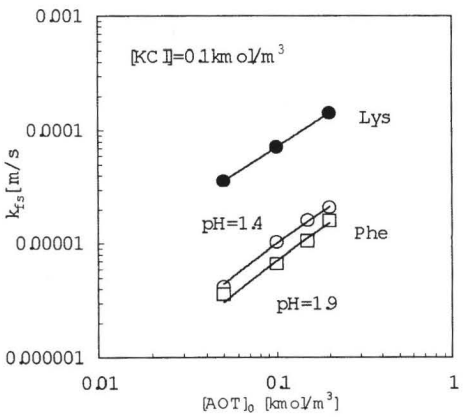

Figure 2. Relation between k_{fs} and $[AOT]_0$

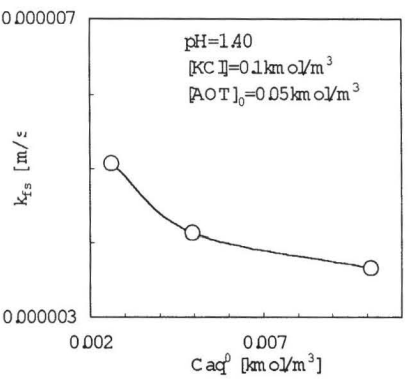

Figure 3. Relation between k_{fs} and Caq^0

Phe: Caq^0=0.005 kmol/m^3
Lys: Caq^0=7□ 10^{-5} kmol/m^3 (pH=5.5)

Fig.2 Relation between k_{fs} and $[AOT]_o$

Phe: C^0_{aq} = 0.005 kmol/m3
Lys: C^0_{aq} = 7* 10^{-5} kmol/m3 (pH=5.5)

Back extraction

Back extraction rates of Phe from the organic to the aqueous phase were measured at the conditions shown in table 1. From the results and the following equations, which are derived for the back extraction,[6]

$$\ln\{1-(1+m_b)(Caq/Corg^0)\}=-(A/V)(1+m_b)K_{bO}t \quad (3)$$

$$1/K_{bO}=1/k_{bd}+\{1/korg+(m_b/kaq)\} \quad (4)$$

the overall mass transfer coefficients, K_{bO}, in the back extraction of Phe were evaluated. Figure 4 shows a dependence of K_{bO} on the stirring speed, N. The values of K_{bO} for each AOT concentration were little influenced by N. It is found that the back extraction rate of Phe was controlled only by the release process at the interface as well as Lys back extraction.[6] Therefore, it is regarded that the K_{bO} value becomes equal to the releasing rate constant, k_{bd}.

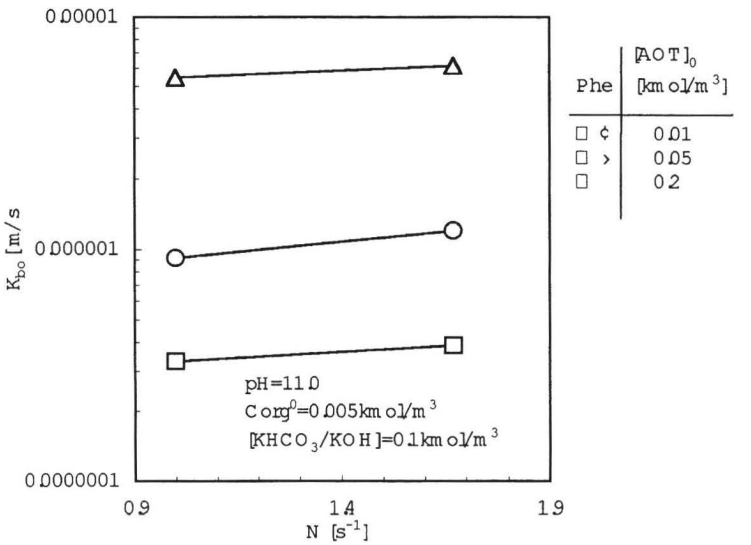

Figure 4. Effect of N on K_{bo} in back extraction

The effects of pH and ionic strength on the value of k_{bd} are shown in figure 5 as a relation between k_{bd} and initial AOT concentration. The result for Lys back extraction [6] is also shown in the figure. The value of k_{bd} for Phe increases with decreasing AOT concentration and with increasing ionic strength, but is not influenced by pH. The k_{bd} values of Phe are a little larger than those of Lys over the region of measuring AOT concentrations. This tendency is opposite from the result of the solubilizing rate constant for the forward extraction represented above.

The overall mass transfer coefficients, K_{bO} and K_{fO}, are respectively plotted against initial AOT concentration in figure 6 to compare the back extraction rates of Phe with the forward extraction rates. The values of K_{bO} decrease with increasing initial AOT concentration, which is an opposite tendency from the dependence of K_{fO} on AOT concentration. The K_{bO} value is a quarter and one-fiftyfifth of K_{fO} at initial AOT concentration of 0.05 and 0.2 kmol/m^3, respectively.

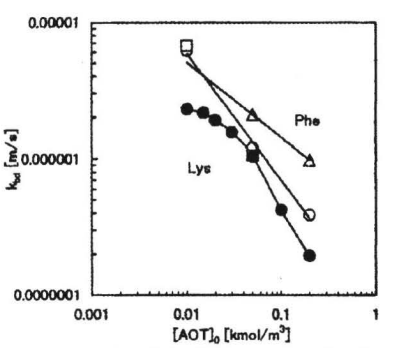

Figure 5. Relation between k_{bd} and [AOT]$_0$

Phe: Corg^0=0.005 kmol/m^3

[KHCO$_3$/KOH] [kmol/m^3]	pH 9.0	pH 11.0
0.1	□	○
1.0		△

Lys:
Corg^0=7 × 10^{-5} kmol/m^3
[KCl]=1 kmol/m^3
pH=11.5

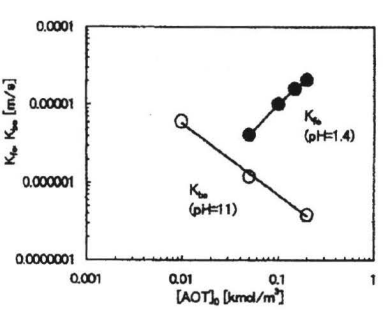

Figure 6. Effect of [AOT]$_0$ on K_{fo} and K_{bo}

Ceq^0=Corg^0=0.005 kmol/m^3
[KCl]=[KHCO$_3$/KOH]=0.1 kmol/m^3
N=1.67s^{-1}

The back extraction rates of Phe are fairly slow compared to the forward extraction rates as well as Lys extraction.[6] The effect of the addition of 2-methyl-2-propanol (t-Bu), by which Lys back extraction was extremely accelerated,[7] on the back extraction rate of Phe was examined. The result is shown in figure 7 as a relation between the value of K_{bO} and the added volume of t-Bu. The K_{bO} value increases linearly with an increase in the added volume of t-Bu and at 10 vol% is about 17 times of that for no addition. This acceleration effect is about two times of that for Lys back extraction as represented in the figure.

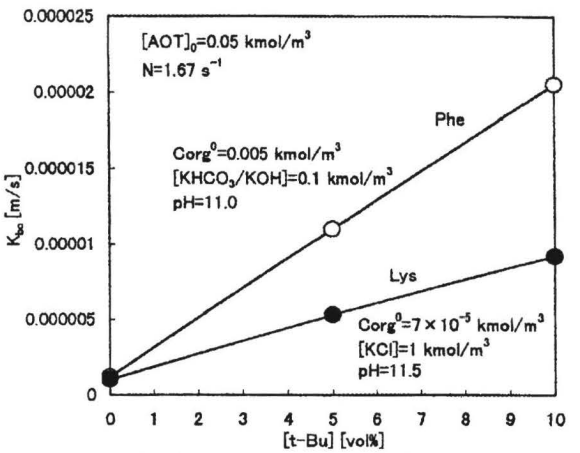

Figure 7. Effect of t-Bu addition on K_{bo}

NOMENCLATURE

A interfacial area (m^2)
C concentration of amino acid ($kmol/m^3$)
k mass transfer coefficient in the film (m/s)
m_f, m_b partitioning equilibrium constant of amino acid for forward and back extraction, respectively
V volume (m^3)
<Superscript>
0 initial
<Subscripts>
aq aqueous phase
org reversed micellar organic phase

REFERENCES

1. Plucinski P and Nitsch W, *Bunsen B, Phys. Chem.*, **93**, 994, (1989).
2. Dekker M, Van't Riet K, Bijsterbosch BH, Fijneman P and Hilhorst R, *Chem. Eng. Sci.*, **45**, 2949, (1990).
3. Dungan SR, Bausch T, Hatton TA, Plucinski P and Nitsch W, *J. Colloid Interf. Sci.*, **145**, 33, (1991).
4. Kinugasa T, Tanahashi S and Takeuchi H, *Ind. Eng. Chem. Res.*, **30**, 2470, (1991).
5. Lye GL, Asenjo JA and Pyle DL, *Chem. Eng. Sci.*, **49**, 3195, (1994).
6. Nishiki T, Sato I, Muto A and KataokaT, *Biochem. Eng. J.*, **1**, 91, (1998).
7. Nishiki T, Muto A and Kataoka T, *Kagaku Kogaku Ronbunshu*, **23**, 286, (1997).

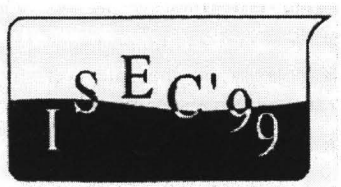

EFFECT OF APPLIED VOLTAGE ON THE EXTRACTIVE SEPARATION OF RARE EARTH METALS BY D2EHPA IN THE PRESENCE OF AN OIL-SOLUBLE COMPLEXING AGENT

Manabu Yamaguchi, Dai Kojima[1], Masahiro Goto[2], Fumiyuki Nakashio[3] and Shigemitsu Nagao[4]

Department of Mechanical Engineering Himeji Institute of Technology Himeji 671-22, Japan

[1]Shinko Pantec, Co. Ltd.,

[2]Kyusyu University,

[3]Kumamoto Institute of Technology,

[4]Mitsui Cytec, Ltd

ABSTRACT

As a series of fundamental studies for application of an electric field to solvent extraction, and the effect of the applied voltage on the selective separation of rare earth metals was investigated using a modified Lewis cell in which the DC voltage was applied across the plane interface between organic and aqueous solutions. In this experiment of selective separation, the system of Pr and Nd in the aqueous nitrate solution and ISOPAR M containing an oil-soluble complexing agent, EDTA - DOA, and an extraction agent, D2EHPA, was used. The thermodynamic characteristics of the adsorption equilibrium of both agents at the interface between the organic and aqueous solutions, in the absence of the electric field, were also investigated by measurement of the interfacial tension. The experimental rates of Pr extraction, in the absence of the electric field, were measured by varying the stirring speed and EDTA-DOA concentration under given concentrations of Pr and D2EHPA and the rates were in good agreement with the calculated values using the extraction model proposed by Goto et al. Under the experimental conditions of hydrodynamic and mass transfer obtained in this experiment, the effects of the applied voltage, its polarity and EDTA-DOA concentration on the extraction rate of Pr and separation factor of Nd and Pr were examined.

Keywords: applied voltage, Lewis cell, rare earth metal, D2EHPA, EDTA-DOA

INTRODUCTION

As novel extraction equipment based on a new concept, some electrostatic extractors have been proposed; application of electric fields to solvent extraction are well known to cause interfacial turbulence, and improve the hydrodynamics around the drops involving the breakage /coalescence balance and enhance mass transfer due to interfacial flow on the drop.[1-4,6,7] In a previous study,[7] the selective separation of Pr and Nd in the presence of water-soluble complexing agents by D2EHPA in the electric field, and the effect of applied voltage on the separation were reported.[7] However, these system have some problems concerning the low solubilities of these complexing agents in an aqueous solution and the recovery of these agents from a residual solution. If new oil-soluble complexing having a high selectivity and high interfacial activity can be developed, the process of solvent extraction of rare earth metals, etc., will be effectively improved and provide a cost savings. In the present study, the effects of the oil-soluble complexing agent coexisting with D2EHPA, and applied voltages on the extraction mechanism of Pr were investigated using a modified Lewis cell with well known hydrodynamic properties.

In a preliminary experiment, the thermodynamic characteristics of the adsorption equilibrium of both agents, EDTA-DOA and D2EHPA, were investigated in the absence of the electric field by measurement of the interfacial tension. The adsorption equilibrium constants and the interfacial area occupied by each agent were obtained. The adsorption structure of both agents was also discussed. Using the extraction experiment with rare earth metals, the initial rate of Pr extraction by D2EHPA was measured using the Lewis cell under different stirrer speeds in the absence of an applied voltage and EDTA-DOA. The contribution of diffusional resistance to the observed rate was estimated and

© 2000 Society of Chemical Industry

the hydrodynamic conditions under which the chemical reaction might be occurring were identified. Simultaneously, the effect of EDTA-DOA concentration on the Pr rate was examined using 25 mM dimeric D2EHPA. Also, the effects of applied voltage and its polarity on the rate were newly investigated. Finally, the influence of the different operations on the selective separation between Pr and Nd was discussed.

EXPERIMENTAL STUDIES

Experimental apparatus

A schematic diagram of the experimental apparatus is shown in Figure 1. The modified "Lewis cell" ,1, a transparent acrylic resin vessel with two electrode has a 100 mm inner diameter and a 130 mm height. A lower electrode of copper wire, 8, was fixed, and grounded to the bottom of cell and an upper electrode, 7, was a stainless steel plate and fixed on the baffle plates. An arrangement of the electrodes was devised such that the applied electric field was effectively applied perpendicular to the plane interface between the organic and aqueous solutions and not disturbed by any obstruction like the impeller in the organic phase. Four baffle plates, 5 mm wide and 2 mm thick were installed vertically to get satisfactorily mixing of both phases along the inner wall of the cell and were spaced at equal intervals. The plane interface between the organic and aqueous solutions was formed at the stator opening, 4, having a 50 mm diameter.

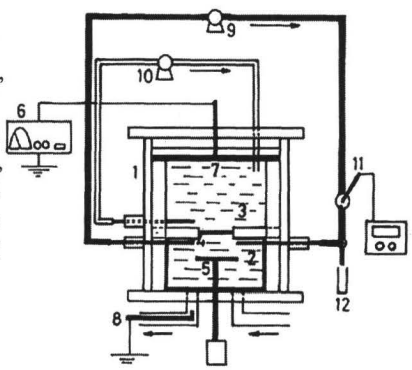

1: Lewiscell 2: Aqueous Phase 3: Organic phase 4: Stator ring 5: Rotating disc 6: High voltage generator 7: Plate electrode 8: Earth electrode 9,10: Liquid circulating pump 11: pHmeter 12: Sampling port

Figure 1 Experimental apparatus

Liquid test system

The extractant, D2EHPA, provided by Daihachi Chemicals, was used without further purification. ISOPAR M, Exxon Chemicals, was used as the organic diluent. Pr and Nd, Wako Pure Chemicals, were used as the rare earth metals. The complexing agent used in the present study was a new oil-soluble complexing agent, ethylenediamine-diacetic acid-N N'dioleyamide (abbreviated as EDTA-DOA; Mitsui Cytec, Ltd.) which was synthesized by Goto et al.[5] (see Figure 2). The organic solution was prepared with a given concentration by dissolving the extractant, $C_{(HR)2}$=25 mM, and with different concentrations of the complexing agent in ISOPAR M. The aqueous solution was prepared at a concentration of 0.5 mM by dissolving ones Pr nitrate, or Pr nitrate and Nd nitrate in deionized water. A buffer solution was not used during the experiment in order to avoid mixing multi- ionic species in the aqueous solution.

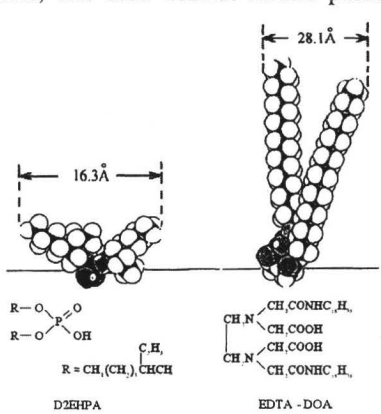

Figure 2 Extraction agent and complexing agent

Experimental procedure

The nitrate aqueous solution containing Pr, or Pr and Nd, was fed to the middle position of the stator opening, 4, and the organic solution containing D2EHPA and EDTA-DOA was carefully fed into the cell in order to minimize any disturbance at the interface. The aqueous solution, 2, was agitated by a disc impeller, 5, and the circulating flow, 9, of the aqueous solution. On the other hand, the organic phase, 3, was agitated by only the circulating flow,10, of the organic solution as shown in the Fig. 1. This is because the electric field was effectively applied perpendicular to the interface of the aqueous/organic solutions where the impeller could not disturb the electric field. Both solutions around the interface of the aqueous/organic solutions were sucked and circulated by roller pumps, 9 and 10. The aqueous solution was sampled at a constant time interval from the circulation path, 12, and the concentrations of the sampled rare earth metals were measured using ICP atomic emission spectroscopy. The hydrogen concentration in the solution was monitored by the pH meter, 11.
Three kinds of experiments were carried out under the following conditions. 1) The effects of stirring speed and EDTA-DOA concentration on the extraction rate of Pr were examined in the absence of an applied voltage. 2) Conditions of stirring speed during the rate controlling step of the chemical reaction between Pr and D2EHPA were determined for each EDTA-DOA concentration in the first experiment, and under these conditions, the effects of the applied voltage, its polarity and complexing agent concentrations on the extraction rate were investigated. 3) Under the conditions determined in the second experiment and using the binary components of Pr and Nd, the effects of the applied voltage, its polarity and complexing agent concentration on the degree of selective separation of Pr and Nd were investigated.

RESULTS AND DISCUSSION

Thermodynamic characteristics of the adsorption equilibrium of EDTA-DOA and D2EHPA

Interfacial tension was measured by the drop weight method. The tested liquid-liquid systems were distilled water and ISOPAR M containing D2EHPA, and D2EHPA and EDTA-DOA. The relations between between interfacial tension, and D2EHPA and EDTA -DOA concentrations were determined. The interfcail activity of EDTA-DOA was much high than that of D2EHPA. The adsorption equilibrium constant, K_i, and interfacial area, S_i, occupied by the agent molecules are listed in Table 1. Their values are calculated from the Gibbs equation for adsorption assuming the Langmuir adsorption isotherm. The adsorption constant of EDTA-DOA at the interface is several times larger than that of D2EHPA. In addition to this, EDTA-DOA can closely align at the oil-water interface based on its S value.

Table 1 Adsorption equilibrium constant and interfacial area occupied by unit mole

$K(HR)_2$,ad	$S(HR)_2$	KH_2S,ad	SH_2S
[m^3/mol]	[m^2/mol]	[m^3/mol]	[m^2/mol]
3.75	6.29Ç10^5	861	2.22Ç10^5
3.28*	10.7Ç10^5	201	2.31Ç10^5 *

*Literature value (Goto, et al.:1992)

Influence of stirring speed on extraction rate of Pr during coexistence of extractant and complexing agent

As a typical experimental result under constant concentrations of Pr and D2EHPA as shown in the figure, the relation between extraction rate of Pr, RPr, and stirring speed, N, is shown in Figure 3 together with concentration of the complexing agent as a parameter. The rates decrease with an

increase in the complexing agent concentrations, this showing similar tendencies. This occurs because the D2EHPA molecule adsorbed at the interface is removed and the number of molecule decreases with an increase in the concentration of EDTA-DOA having a high interfacial activity; the collision frequency for the reaction between Pr ions and D2EHPA molecules decreases. As a result, the increasing

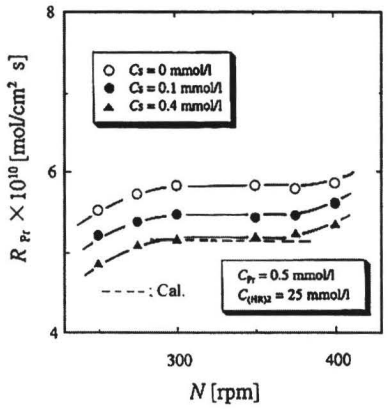

Figure 3 Effect of stirring speed on extraction rate of Pr (Ep=0 kV)

complexing agent concentration decreases the chemical reaction frequency between Pr ions and D2EHPA molecules. The constant range of the rates in the figure suggests that the resistance of diffusion can be ignored in comparison with that of the chemical reactions; the rate-controlling step of the chemical reaction. Accordingly, a constant stirring speed of 350 rpm was used for all the experiments. The solid line in the Figure 3 is the value calculated by Goto's model;[5] a k_f value was obtained using the RPr data with CH2S=0 mM, and the kH2S value was obtained using the RPr data with CH2S=0.1 mM, and finally RPr in the case of CH2S=0.4 mM was calculated using k_f and kH2S values obtained in the above procedure, and furthermore the K(HR)2,ad and KH2S,ad values in Table 1 are used. Consequently, the RPr,exp. value was 5.20×10^{-6} mol/(m^{2}s) and RPr,cal value was 5.17×10^{-6} mol/(m^{2}s). The experimental values were in good agreement with values calculated by the model. The RPr values shown in the figure were determined by the following equation and slope analysis using a graphical plot of Pr concentration in the organic phase, CPr, vs. contact time, t, where the results in the absence of the complexing agent at a 350 rpm stirring speed are shown in Figure 4 together with and without an applied voltage.

$$R_{pr} = \frac{V}{A} \text{Ç} \frac{\mathrm{d}\overline{C_{pr}}}{\mathrm{d}t}$$

where V is the volume of the organic phase, A is the interface area of $19.6 \times 10^{--4}$ m^2, Cpr is the concentration of Pr in the organic phase, and t value is the contact time. The values of RPr change depending on N as shown in Figure 3. It is understood that RPr increases with an increase in N up to 300 rpm, but the rate becomes independent of the stirrer speed in the range of 300 to 375 rpm. Furthermore, the rate further increases as the stirring speed exceeds 400 rpm; this means that the interface was disturbed.

Effect of applied voltage on the extraction rate

The extraction rates show significant differences with and without a positive applied voltage and its magnitude as shown in Figure 4.; for a negative voltage, the slope was almost the same as that for the positive voltage. The effects of applied voltage on the rate under the condition of the rate-controlling step, N=350 rpm, are shown in Figure 5 together with the rates in the absence of an applied

voltage.

The rates in the applied electric field enhanced with increasing applied voltage irrespective of its polarity. This reason is not clear, but the following facts may be useful to consider their causes. When the applied voltage exceeds positive or negative 5 kV, the interface began to move with small fluctuations due to the field-induce stress. The fluctuation formed wave and water drops were ejected

from the tip of the waves and the experiments were not possible. Taking into account the formation of the drops at a higher applied voltage than positive or negative 5 kV and the RPr values nearly correspond to the interfacial turbulence at N=500 rpm, it is considered that the increasing rate with applied voltage resulted from the interfacial turbulence due to the field-induced stress. The effect of

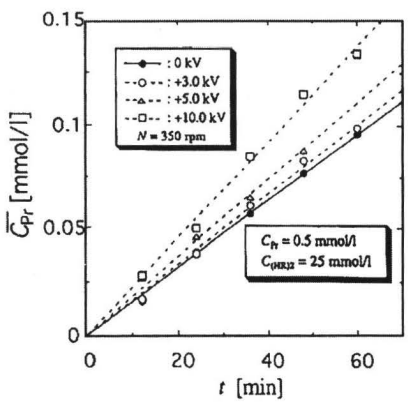

Figure 4 Effect of applied positive voltage on Pr extraction without complexing agent

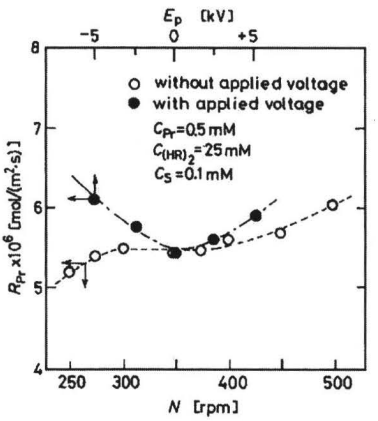

Figure 5 Effect of stirring speed and applied voltage on extraction rate of Pr

applied voltage on the extractive separation of Pr and Nd was investigated and their results are shown in Figure 6. The effect of applied voltage on the separation was not significant, but the separation degree increased with the applied voltage.

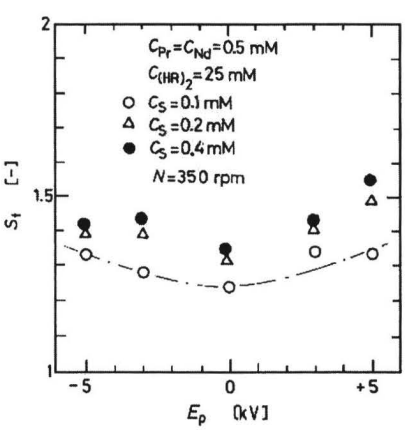

Figure 6 Effect of applied voltage and complexiмg agent on separation factor

CONCLUSIONS

1) EDTA-DOA and D2EHPA showed a strong interfacial activity together, but in the case of co-adsorption, the interfacial activity of EDTA-DOA was several times larger than that of D2EHPA.
2) EDTA-DOA molecules adsorbed at the interface between the organic and aqueous solutions showed a significant mass transfer resistance.
3) The extraction rate of Pr increased about 10% in the presence of an electric field of 1 kV/cm, and was independent of its polarity.
4) The effect of EDTA-DOA in the oil-soluble complexing agent on the separation factor was almost 1.3 and the effect of applied voltage on the factor was about 1.5.

REFERENCES

1. Austin LJ, Banczyk L and Sawistowski H, *Chem.Eng.Sci.*, **26**, 2120, (1971)
2. Bailes PJ and Mani IA, *Proc.ISEC'96*, 1143, (1996)
3. Chang LS and Berg JC. *Int. Heat and Mass Transfer*, **26**, 823, (1983)
4. Hund M and Lancelot F, ISEC'86, **I**, 511, (1986)
5. Goto M, Kubota F, Miyata T and Nakashio F, *J. Membrane Sci.*, **74**, 215, (1992)
6. Yamaguchi M, Sugaya H and Katayama T, *J. Chem.Eng. Japan*, **22**, 25, (1989)
7. Yamaguchi M. *Trans IChemE.*, **75A**, 447, (1997)

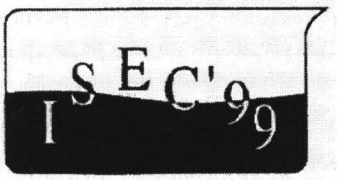

EFFECT OF GLOBAL SALT CONCENTRATION ON THE RATE OF EXTRACTION OF COPPER(II) BY ACORGA® CLX-50 AND GERMANIUM(IV) BY KELEX® 100S

Gerard Cote and Celine Bouvier
Laboratoire d'Electrochimie et de Chimie Analytique (UMR CNRS No 7575), Ecole Nationale Superieure de Chimie de Paris, France

ABSTRACT
This paper gives a rapid overview of the works dedicated to the influence of the "medium effect" upon the kinetics of metal extraction. Then, it discusses the varied origin of such an influence with kinetic data concerning the extraction of copper (II) by ACORGA® CLX-50 (diffusional regime) and germanium (IV) by KELEX® 100S (kinetic regime).

Keywords: extraction kinetics, medium effect, Lewis cell, copper, germanium, Acorga® CLX-50, Kelex® 100.

INTRODUCTION

The aqueous solutions involved in hydrometallurgical processes and effluent treatments are often complex (i.e., they contain many species) and are highly loaded with salts and/or acids. As a result, thermodynamic activities should be considered instead of concentrations in the mass action laws. From a physico-chemical standpoint, this means that, for any species participating in a given chemical reaction, the progress of the latter depends not only on the concentration of the considered species but also on its interactions with its surrounding environment. Schematically one can consider that a "medium effect" is superimposed to the "mass effect".

In liquid-liquid extraction many examples including the extraction of copper (II) and zinc (II) from chloride media by neutral extractants[1,2] show that the "effect of medium" can dramatically influence the distribution equilibrium of a given solute. Such a phenomenon has been extensively investigated from a thermodynamic point of view and its effects upon extraction equilibria can be successfully modelled by various physico-chemical models developed for predicting the activity coefficient values.[3-8]

Conversely, the influence of the "medium effect" upon the kinetics of mass transfer in liquid-liquid systems has been poorly investigated. However, such a question attracts increasing interest because of the recent tendency to prefer short time contactors (especially in the nuclear field), the efficiency of which obviously depends on the kinetic characteristics of the considered systems. The present paper gives both a rapid overview of the works dedicated to the influence of the "medium effect" upon the kinetics of metal extraction and discusses kinetic data concerning the extraction of copper (II) by ACORGA® CLX-50 and germanium (IV) by KELEX® 100S.

EXPERIMENTAL

ACORGA® CLX-50 (containing 1 mol/dm^3 di-isodecylpyridine 3,5-dicarboxylate in a high flash point kerosene) and KELEX® 100S (containing about 90% of 7-(4-ethyl-1-methyloctyl)-8-hydroxyquinoline)[9]) were kindly supplied by ZENECA Specialties and WITCO, respectively. They were carefully washed with 1 mol/dm^3 HCl and rinsed with water before use. All the other reagents were of analytical reagent grade. The kinetics of extraction were investigated with a constant interfacial-area Lewis-type cell, at a controlled temperature.

STATE OF THE ART

Various authors have shown that the addition of electrolytes such as NaCl, LiCl, $NaClO_4$, $NaNO_3$, etc., to a given extraction system, may significantly influence the rate of mass transfer.[10-19] It is interesting that there is no general trend, but that the rate of extraction may increase or decrease, or

© 2000 Society of Chemical Industry

even does not change, as the electrolyte concentration is increased. The magnitude of the phenomenon as quantified by the ratio r_{MAX}/r_{MIN} (r = extraction rate) ranges between 1 (no effect) and 5, with an average value close to 3, for an increase of ionic strength (ΔI) typically varying between 0.2 and 5 mol/dm^3. It should be pointed out that there is no general development in the literature for explaining this type of phenomenon, but only some limited and often tentative explanations. Four types of phenomena were typically invoked to explain the kinetic changes arising from electrolyte addition : the involvement of activities instead of concentrations in the kinetic laws and a change in the chemical resistance,[18-21] a change in the diffusional resistance,[19] the appearance of more labile species in the bulk of the aqueous phase due to the formation of metal complexes[13,14,17] and finally the modification of the interfacial properties.[22] To further illustrate the "medium effect" upon the extraction kinetics two examples are considered below.

RESULTS AND DISCUSSION

Copper(II) extraction with ACORGA® CLX-50

The extraction of copper (II) from chloride media by ACORGA® CLX-50 (denoted hereafter EXT) is thermodynamically controlled by equations 1 and 2:[1]

$$Cu^{2+} + 2Cl^- + 2\overline{EXT} \Leftrightarrow \overline{CuCl_2(EXT)_2} \qquad \text{(extraction constant : } K_{ex}) \qquad (1)$$

$$Cu^{2+} + jCl^- \Leftrightarrow CuCl_j^{(2-j)} \qquad \text{with } j = 1 \text{ to } 4 \qquad \text{(formation constant : } \beta_j) \qquad (2)$$

where overbars refer to the species in the organic phase, H_2O molecules have been omitted for clarity. Examination of figure 1 shows that the influence of the "medium effect" upon the rate of copper(II) extraction by ACORGA® CLX-50 is rather strong. Indeed, the initial flux of copper (II) is multiplied by more than 10 when 3.5 mol/dm^3 $NaClO_4$ is added to the aqueous phase, all the other conditions being kept constant.

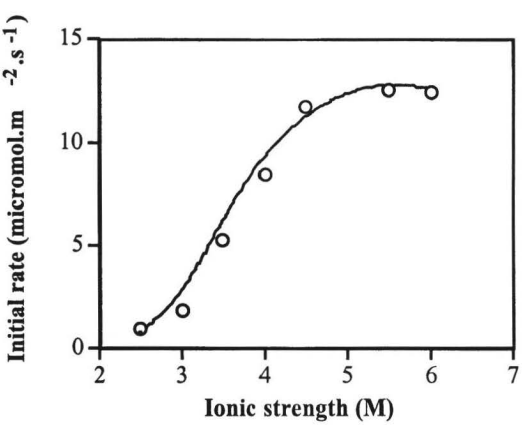

Figure 1. Experimental (o) and theoretical (dashed lines) plots of J_o versus ionic strength (I) for the extraction of copper (II) (initially 10^{-2} mol/dm^3) from 2.5 mol/dm^3 NaCl + x mol/dm^3 $NaClO_4$ with x ranging between 0 (i.e., I = 2.5 mol/dm^3) and 3.5 (i.e., I = 6 mol/dm^3), by 0.24 mol/dm^3 ACORGA® CLX-50 in *n*-decane, at pH = 3 and 274 K. The theoretical curve derives from equation 3 with Δ_{aq} varying between 5.8 x 10^5 (I = 2.5 mol/dm^3) and 7.6 x 10^5 m^{-1}s (I = 6.0 mol/dm^3) and Δ_{org} = 1.5 x 10^6 m^{-1}s.

This phenomenon is a result of two antagonistic effects as briefly explained below. A full kinetic study showed that the extraction of copper (II) was under total diffusional control in the Lewis cell used, which therefore leads to equation 3 for J_0:

$$J_o = [Cu(II)]_o \Big/ [\Delta_{aq} + \frac{\Delta_{org}}{(\frac{K_{ex}}{1+\sum_j \beta_j [Cl^-]^j})[Cl^-]^2 [\overline{EXT}]_o^2}] \quad (3)$$

where Δ_{aq} and Δ_{org} denote the diffusional terms ($\Delta = \delta/D$ with δ = thickness of the diffusional films and D = diffusion coefficient), K_{ex} and β_j refer to the concentration extraction constant and the concentration formation constants of copper chlorocomplexes [see equations 1 and 2], respectively, and $[Cu(II)]_o$ and $[\overline{EXT}]_o$ represent the initial concentration of copper(II) in the aqueous phase and that of ACORGA® CLX-50 in the organic phase, respectively.

The addition of $NaClO_4$ to the aqueous phase increases the viscosity of the latter and therefore increases the term Δ_{aq}, which has the tendency to decrease the value of J_o. However, in parallel, the addition of $NaClO_4$ provokes a strong salting-out effect which causes a sharp increase of K_{ex}, which itself has the opposite tendency to increase the value of J_o. Experimentally, it is observed that the latter phenomenon is prevalent. Furthermore, a good fit is obtained between the theoretical curve derived from equation 3, using the values of $K_{ex}/(1+\sum_j \beta_j [Cl^-]^j)$ determined in a previous thermodynamic study and realistic values of Δ, and the experimental points, which strengthens the validity of the above given interpretation.

Germanium (IV) extraction with KELEX® 100S

The extraction of germanium (IV) from weakly acidic media (pH = 3 to 7) by KELEX® 100S (denoted hereafter HL) is thermodynamically controlled by equation 4:[23]

$$Ge(OH)_4 + 2\overline{HL} \Leftrightarrow \overline{GeL_2(OH)_2} + 2H_2O \quad (4)$$

The extraction of germanium (IV) by KELEX® 100S is slow and occurs entirely in a chemical regime. From the experimental data obtained in the present work, the following kinetic law was established:

$$J_o \approx k[Ge(IV)]_o [\overline{HL}]_o^{0.5} \quad (5)$$

where k is a constant and $[Ge(IV)]_o$ and $[\overline{HL}]_o$ denote the initial concentrations of germanium (IV) and KELEX® 100S, respectively. To interpret Eq. (5), two limiting steps should be assumed in the mechanism of extraction as reported below:

$$Ge(OH)_4 + (HL)_{ads} \overset{k_1}{\underset{k_{-1}}{\Leftrightarrow}} (Ge(OH)_3 L)_{ads} + H_2O \quad (6)$$

$$(Ge(OH)_3 L)_{ads} + \overline{HL} \xrightarrow{k_2} \overline{Ge(OH)_2 L_2} + H_2O \quad (7)$$

These two equations lead to the theoretical equation 8 which can reasonably be simulated by equation 5 within an appropriate restricted range of HL concentration :

$$J_o = \frac{k_1 k_2 [Ge(IV)]_o \Gamma_{HL}^{max} [\overline{HL}]_o}{k_{-1}[H_2O] + k_2 [\overline{HL}]_o} \quad (8)$$

where Γ_{HL}^{max} denotes the interfacial concentration of HL at saturation.

The influence of the "medium effect" upon the rate of germanium (IV) extraction by KELEX® 100S is shown in table 1. It appears that the variation of J_o as $NaClO_4$ is added is weak (less than a factor 2 for ΔI = 3 M) compared to what is observed in figure 1 in the case of copper (II) extraction by ACORGA® CLX-50.

To interpret the phenomenon reported in table 1, an attempt was made to rewrite the kinetic constants appearing in equation 8 by using Brönsted-Bjerrum equation 9 stated for the reaction between two reagents A and B: [24]

$$k=k_o \frac{\gamma_A \gamma_B}{\gamma_{AB^*}} \quad (9)$$

where k and k_o denote the kinetic constant at a given ionic strength I and zero ionic strength, respectively, γ refers to the activity coefficients and AB^* represents the activated complex. Thus, equation 10 was finally obtained :

$$J_o = \frac{k_1^\circ k_2^\circ \alpha \gamma_{Ge(OH)_4} \gamma_{\overline{HL}} [Ge(IV)]_o \Gamma_{HL}^{max} [\overline{HL}]_o}{k_{-1}^\circ \beta a_{H_2O} + k_2^\circ \theta \gamma_{\overline{HL}} [\overline{HL}]_o} \quad (10)$$

where α,β and θ denote appropriate ratios of activity coefficients for species adsorbed at the interface or dissolved in the bulk of the organic phase (e.g., $\theta=\gamma_{Ge(OH)_3L_{ads}}/\gamma_{Ge(OH)_3L.HL_{ads}}$ where $Ge(OH)_3L.HL_{ads}$ is assumed to be the activated complex associated with equation 7). It is of interest that the theoretical values of J_o derived from equation 10 simulate rather well the experimental data when one uses the values of $\gamma_{Ge(OH)_4}$ obtained in a previous thermodynamic study and one assumes that α,β,θ $\gamma_{\overline{HL}}$ and Γ_{HL}^{max} do not significantly vary with the ionic strength. Thus, the preceding observation suggests that the influence of the "medium effect" upon the extraction kinetics of germanium (IV) by KELEX® 100S occurs mainly through a change of the activity coefficient of $Ge(OH)_4$ in the aqueous phase.

$[NaClO_4]]$ (mol/dm^3)	1.0	2.0	2.7	3.3	3.7	4.0
Ionic strength (mol/dm^3)	1.0	2.0	2.7	3.3	3.7	4.0
J_o (mol.m^{2}s^{-1}) x 10^8 expt.	1.43	1.62	1.88	2.23	2.40	2.63
J_o (mol.m^{2}s^{-1}) x 10^8 (eq.10)	1.16	1.54	1.87	2.22	2.40	2.63

Table 1 Experimental and theoretical values of J_o versus ionic strength (I) for the extraction of germanium(IV) (initially 10^{-2}mol/dm^3) from x mol/dm^3 $NaClO_4$ by 0.13 mol/dm^3 KELEX® 100S in *n*-decane + 10 % (v/v) *n*-decanol, at pH = 5.5 and 313 K.

ACKNOWLEDGEMENTS

The authors greatly acknowledge PRACTIS GDR (Gdr No 1115) for financial support.

REFERENCES

1 Cote G, Jakubiak A, Bauer D, Szymanowski J, Mokili B and Poitrenaud C, *Solvent Extr. Ion Exch.* **12**, 99, (1994).
2 Cote G and Jakubiak A. *Hydrometallurgy,* **43**, 277, (1996).
3 Baes CF, Moyer BA, Case GN and Case FI. *Sep. Sci. Techn.*, **25**, 1675, (1990).
4 Zhou L, Chang-Ming y, Yao SG and Hang L. in : *Value Adding Through Solvent Extraction (ISEC'96).* Shallcross DC, Paimin R and Prvcic LM, eds.,The University of Melbourne, **1**, 159 (1996)
5 Klocker H, Sainz-Diaz CI, Wachter B, Bart HJ and Marr R, in: *Value Adding Through Solvent Extraction (ISEC'96).* Shallcross DC, Paimin R and Prvcic LM. eds.The University of Melbourne, **1**, 617, (1996).
6 Mokili B and Poitrenaud C. *Solvent Extr. Ion Exch.* **13**, 731, (1995).
7 Mokili B and Poitrenaud C. *Solvent Extr. Ion Exch.* **14**, 617, (1996).
8 Mokili B and Poitrenaud C. *Solvent Extr. Ion Exch.* **15**, 455, (1997).
9 Dziwinski E, Cote G, Bauer D and Szymanowski J. *Hydrometallurgy*, **37**, 243, (1995).
10 Roddy JW, Coleman CF and Sumio A. *J. Inorg. Nucl. Chem.* **33**, 1099, (1971).
11 Sekine T, Yumikura J and Komatsu Y. *Bull. Chem. Soc. Japan*, **46**, 2356, (1973).
12 Sato T, Nakamura T and Ikeno M. *Hydrometallurgy*, **15**, 209, (1985).
13 McClellan BE and Menis O. *Anal. Chem.* **43**, 436, (1971).
14 Sun D, Yue S and Li D. in *Solvent Extraction in the Process Industries (ISEC'93),* Logsdail DH and Slater MJ, Eds., SCI/Elsevier, London, **1**, 391, (1993).

15 Ellender PS and Lawson GJ. *J. Appl. Chem. Biotechnol.*, **28**, 435, (1978).
16 Eccles H, Lawson GJ and Rawlence DJ. in *Proc. ISEC'77*, CIM Special volume 21, Can.Inst.Min.Metal., Montreal, , **1**, 203, (1979).
17 Li Z, Fürst W and Renon H. *Hydrometallurgy*, **21**, 213, (1988).
18 Ajawin LA, Perez de Ortiz ES and Sawistowski H. *Chem. Eng. Res. Des.*, **61**, 62, (1983).
19 Aparicio J, Valiente M and Muhammed M. *Solv. Extr. Ion Exch.*, **3**, 485, (1985).
20 Danesi PR and Chiarizia R, in *Proc. ISEC'77*, CIM Special volume 21, Can.Inst.Min.Metal., Montreal, , **1**, 219, (1979).
21 Tochiyama O, Nakamura Y, Hirota M and Inoue Y. *J. Nucl. Sci. Tech.*, **32**, 118, (1995).
22 Perez de Ortiz ES, *J. Appl. Chem. Biotechnol.* **28**, 149, (1978).
23 Marchon B, Cote G and Bauer D. *J. Inorg. Nucl. Chem.*, **41**, 1353, (1979).
24 Brönsted JN. *Z. physik. Chem.*, **102**, 169, (1922).

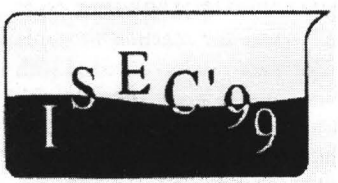

ROTATING MEMBRANE CELL TECHNIQUE FOR THE STUDY OF LLX KINETICS: APPLICATION TO THE STUDY OF SALT EFFECTS

JP Simonin, H Hendrawan and J Weill
Laboratoire Liquides Ioniques et Interfaces Chargées (LI2C), UMR 7612, Université P.M. Curie, Boîte no. 51, 4 Place Jussieu, 75252 Paris Cedex 05, France.

ABSTRACT
The rotating membrane cell (RMC) technique is based on the principles of the short-time phase-contacting method and the rotating disk of Levich. The cell consists of a membrane, containing one of the phases, that is glued on the base of a cylinder and that is rotated in the other phase at a definite speed. The set-up has been used with two types of systems: acetic acid extracted by isopropylmyristate (true first-order reaction), and nickel and zinc ions by an extractant: di(2-ethylhexyl)phosphoric acid (D2EHPA). The results for acetic acid are in accordance with an interfacial reaction mechanism. In contrast, the results for the metal cations may be explained by a transfer of extractant to the aqueous phase. The influence of the addition of a salt on the partitioning and kinetics of acetic acid extraction has been considered.

Keywords: kinetics, acetic acid, isopropylmyristate, nickel, zinc, D2EHPA, salt effect, rotating membrane cell

INTRODUCTION

A large body of experimental data has been gathered in the field of kinetics of solute transfer at free liquid/liquid (LL) boundaries.[1,2] However, the determination of the mechanisms of extraction processes still seems to be the subject of controversy.[3] In particular, the location of the complexation reaction for transfers involving an extractant is either taken at the interface or in a thin aqueous layer close to the interface.

Moreover, because of the development of new methods of investigation, this classic[4] subject of debate will certainly be supplemented soon with new questions, arising particularly from studies in two area: numerical simulation and optical probing. So, recent simulations have suggested unexpected phenomena[5] and optical second harmonic and sum frequency generation[6,7] are now able to study liquid interfaces. Both methods give information on a molecular scale.

At the same time experiments performed on macroscopic scale with classic methods can provide valuable information, provided that some conditions be fulfilled: in particular control of the hydrodynamics is a crucial point. The short-time phase-contacting method[9] and the rotating diffusion cell (RDC)[8] satisfy this requirement. Another such technique is the rotating stabilized cell (RSC)[10] that has features in common with the last two techniques: it operates in non-stationary regime and the hydrodynamics are those of the rotating disk as described by Levich.[11]

However, the presence of a gel in the RSC constitutes a drawback and for this reason the gel has been replaced now with a membrane.[12] This version has been called the rotating membrane cell (RMC). As with the RSC, the RMC method is used in a transient regime that highlights the effect of chemical reaction kinetics because, for short contact times, diffusion is not the limiting factor and mass transfer is limited by chemical reactions. The RMC technique is simple to implement and does not require any special machinery.

This paper reports on experiments carried out with the RMC. The technique has been tested on two types of system: acetic acid extracted by isopropylmyristate (IPM) and two divalent metal cations, Ni^{2+} and Zn^{2+}, by di(2-ethylhexyl)phosphoric acid (D2EHPA). The interest of the first system is that transfer is most likely to occur purely at the interface between the two liquids and to consist of desolvation-resolvation of the acid. Therefore it is expected that interfacial transport be described by true first-order kinetic rate law. Extraction of acetic acid thus provides a good benchmark system to test the validity of the method. The extraction of cations such as nickel and zinc is of interest for metal separation and recovery, and D2EHPA is a widely used industrial

© 2000 Society of Chemical Industry

extractant. Besides, as mentionned above,the mechanism of extraction in such systems is not clear: some workers have postulated,[13] or have arrived at the conclusion[14,15] that the reaction proceeds mainly at the aqueous-organic interface. In contrast, others[16] found that their results, obtained with the RDC, could not be described by an interfacial mechanism. They used a mass transfer with chemical reaction (MTWCR) model,[17] with however unequal success. Therefore further results on these systems are still needed to better understand their mechanisms of extraction.

Lastly, the effect of a salt on liquid-liquid extraction (LLX) partitioning and kinetics is considered through the description of experiments on acetic acid at the interface water+LiCl/IPM. To the author's knowledge, salt effects on this type of ('simple') system have not been studied previously.

THEORY

The case of a purely interfacial extraction process obeying a true first-order kinetic rate law constitutes a reference that is useful to consider in the first place.

Consider a porous membrane, of thickness L and geometric area S. It contains phase A and the species to be transferred. It is glued on the base of a cylinder. The cell is set into rotation at a definite speed and, at time zero, it is put in contact with the other phase B of kinematic viscosity ν. Let us denote by S' the available contact area between the liquids ($S' < S$), and define $\sigma = S'/S$.
Fickian diffusion is assumed within the membrane pores, with diffusion coefficient D_A.
Continuity of the flux at the interface can be written

$$-S' D_A \partial C/\partial x\ (x=0^-,t) = S' [k_f C_-(t) - k_r C_+(t)] = - S D_B \partial C/\partial x\ (x=0^+,t)$$

with $C_-(t)$ and $C_+(t)$ the concentrations in phase A and B, respectively, in the vicinity of the interface ($x=0^-$ and $x=0^+$), D_B the diffusion coefficient in B, and k_f and k_r the forward and reverse interfacial reaction rate constants.

The average-reaction-time approach has been used: here it can be stated as

$$P(t) \approx 1 - \exp(-t / \tau)$$

in which τ is the mean-passage time of the species being transferred from A to B and, using the latter relation, this time is given by :

$$\tau = \int_0^\infty [\ 1 - P(t)\ ]\ dt$$

It has been shown [12b] that a rigorous expression for this average time is

$$\tau = \tau_f + \tau_A + \tau_B$$

with

$$\tau_f = L / k_f$$
$$\tau_A = L^2 / (3 D_A)$$
$$\tau_B = \tau_f\ (\sigma k_r) / (D_B / \delta)$$

Here τ_f is the characteristic time for the interfacial forward reaction, τ_A represents the mean diffusion time in the membrane and τ_B is the mean residence time of the species in the diffusion layer, that results from the competition between reextraction (or stripping, at a rate σk_r) and removal by dilution in B (at a rate D_B/δ). The parameter δ represents the diffusion layer thickness whose expression[12] was given by Levich.[11]

In the case that the interfacial kinetics are very fast the above equation for τ reduces to

$$\tau_\infty = \tau_A + \tau_B$$

which gives the diffusive limit for the extracted rate of matter, $P_\infty(t)$.

EXPERIMENTAL

The cell, sketched in figure 1, consists of a thin Millipore membrane, *ca.* 120 microns thick, that is glued on the base of a cylinder made of perspex with the use of a polyurethanne mastic (Scotch-Seal 5300). This mastic was chosen for its excellent chemical resistance to organic solvents.The diameter of the membrane was about 0.8 cm.

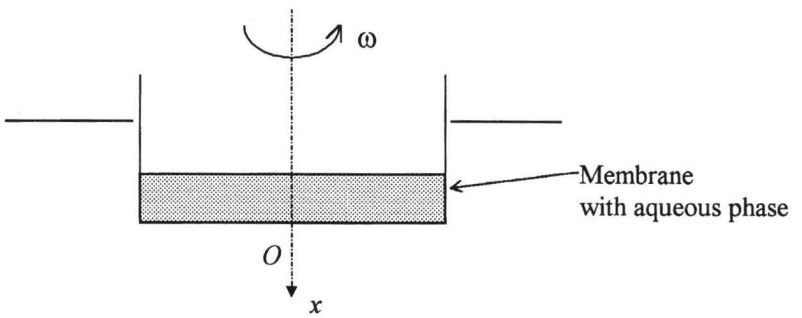

Figure 1: Sketch of the RMC. Membrane: thickness= 120 microns, diameter= 8 mm.

In this work, the membrane contained the aqueous phase. It was set into rotation at a known speed and, at t=0, it was immersed into the organic phase. Analysis of the extracted amount of matter has been performed by using radiolabelled species.

The membrane was purchased from Millipore™. The membrane used in this study was a hydrophilic PVDF membrane (HVLP type). It was chosen for its good chemical compatibility with acid solutions and aliphatic solvents. Its thickness, 118 +/- 1 microns, was measured using a micrometer and its average pore size was 0.45 microns (manufacturer's value). The void porosity σ was measured by impregnating a membrane sample with a solution of known specific activity and measuring the absorbed activity. By using the known characteristics of the sample, it was found that σ= 0.685 +/- 0.015 compared to the manufacturer's value of 0.70.

All chemicals used were purchased commercially and aqueous solutions were prepared with deionized water. The D2EHPA (BDH) was used as received. According to the manufacturer its purity was better than 96 %. The n-dodecane and the IPM were purchased from Merck (purity > 99 % and 98 %, respectively).

The D2EHPA was not further purified because, in a previous study using the same BDH product,[18] it was found that this untreated extractant led to kinetics of zinc extraction that were the same as with a copper-purified D2EHPA. Moreover, a similar conclusion has been obtained in another work,[19] although with a D2EHPA of higher purity.

When the cells were ready a small volume of aqueous solution was placed on the membrane, which absorbed it instantaneously. Then the solution excess was wiped thoroughly and the cell was immersed rapidly into the organic phase. To avoid evaporation a drop of dodecane was put on the membrane immediately after wiping the surface. Then, after a measured lapse of time, the cell was taken out. A sample was taken from phase B and its activity together with that remaining in the membrane were determined. These measurements yielded the relative amount of matter, $P(t)$, that had been transferred. One experiment gave one percentage for one time.

The composition of the aqueous solutions were as follows. The solution containing acetic acid was composed of 0.01 mol/L HCl+10^{-3} mol/dm^3 acetic acid and it was spiked with tracer amounts of radiolabelled ^{14}C-acetic acid. For the extraction with D2EHPA, the solutions need be buffered: the solutions consisted of 0.1 mol/dm^3 acetate buffer (acetic acid + KOH, pH = 4), 10^{-3} mol/dm^3 $NiCl_2$ or $ZnCl_2$ and tracer amounts of ^{63}Ni or ^{65}Zn. For acetic acid the organic phase was

pure IPM. It was composed of 0.1 mol/dm^3 and 0.02 mol/dm^3 D2EHPA in n-dodecane (monomer concentration) for nickel and zinc, respectively.

Diffusion in the membrane was studied by impedance spectroscopy, conducted with a membrane impregnated with 0.1 mol/dm^3 NaCl solution and mercury electrodes. The diffusion coefficient of Ni(II) in the bulk aqueous buffer solution was measured by using the open-end capillary technique.

Extraction experiments were conducted at 22 °C.

Lastly, the effect of adding increasing amounts of LiCl to the aqueous phase has been studied in the case of acetic acid. The salt LiCl has been chosen for its high solubility in water. The organic-to-aqueous partition coefficient has been determined for each LiCl concentration. Then, the first-order kinetic rates k_f and k_r have been estimated as a function of this concentration.

RESULTS AND DISCUSSION

Impedance spectroscopy experiments led to the result that the conductibility of a 0.1 mol/dm^3 NaCl solution was decreased by a factor of 1.85 within the pores of the membrane. Thus it was assumed that diffusion in the membrane was slowed down by the same (tortuosity) factor.
The organic-to-aqueous partition coefficients K were measured experimentally with radioactive tracers by sampling each phase.

Acetic Acid Extraction:

An important result was that the experiments at various rotation speeds can be assigned a common value for k_f. This result is compatible with the expectation of a strictly interfacial transfer process involving only a change of solvation, which must not be influenced by the motion of the nearby liquids.

The final value for the rate constant is $k_f = (5.7 \pm 0.3)\ 10^{-5}$ cm s^{-1} is appreciably different from previously published[12] values. Discrepancy with results from other studies, in particular those using the RDC[8] and the RSC,[12] may deserve further examination.

Nickel (II) and Zinc (II) Ions Extraction

The main result is that these systems are not amenable to the same description as acetic acid. No common value for k_f could be determined. Instead, the apparent rate parameter k_f was found to increase strongly with stirring.

These results may be explained by a transport of extractant from the organic to the aqueous phase, which is the basis of the MTWCR model.[3] The extractant may react with the metal in the aqueous phase and the resulting complex may then be transferred to the organic. Increasing the rotation speed of the cell would result in a larger flux of extractant into the membrane, which would accelerate the rate of extraction.

However, the possibility that impurities such as M2EHPA are transferred to the aqueous cannot be ruled out. This issue will have to be examined more carefully in the future.

Salt effect on the LLX of acetic acid:

This subject is in course of being investigated. Results will be presented at the conference.

ACKNOWLEDGEMENT

The help of N. Prulière is gratefully acknowledged.

REFERENCES

1. *'Principles and Practices of Solvent Extraction'*, Eds. Rydberg J, Musikas C and Choppin GR, Dekker, New York, (1992).
2. Danesi PR and Chiarizia R, *CRC Crit. Rev.Anal. Chem.*, **10,** 1, (1980).
3. Blum L, Durand-Vidal S, Simonin JP and Turq P, *'Electrolytes at Interfaces'*, Kluwer, to be published.
4. Hanson C, Hughes MA and Marsland JG, *Proceedings of ISEC'74*, SCI, London, **3**, 2401, (1974).
5. Benjamin I, *Science*, **261,** 1558, (1993).
6. Shen YR, *Nature*, **337,** 519, (1989).
7. Eisenthal KB, *Chem. Rev.*, **96,** 1343, (1996).
8. Albery WJ, Burke JF, Leffler EB and Hadgraft J, *J. Chem. Soc. Faraday Trans.*, **72,** 1618, (1976).
9. Tarasov VV, Kizim NF and Yagodin GA, *Russ. J. Phys.Chem.*, **45,** 1425, (1971).
10. Simonin JP, Turq P and Musikas C, *J. Chem.Soc. Faraday Trans.*, **87,** 2715, (1991).
11. Levich VG, *'Physicochemical Hydrodynamics'*, Prentice Hall, Englewood Cliffs, NJ (1962).
12. Simonin JP, *Solvent Extr. Ion Exch.*, **14,** 889, (1996); (b) Simonin JP and Weill J, *Solvent Extr. Ion Exch.*, **6**, (1998) to be published.
13. Cianetti C and Danesi PR, *Solvent Extr. Ion Exch.*, **1,** 9, (1983).
14. Komasawa I and Otake T, *Ind. Eng. Chem. Fund.*, **22,** 367, (1983).
15. Miyake Y, Matsuyama H, Nishida M, Nakai M, Nagase N and Teramoto M, *Hydrometallurgy*, **23,** 19, (1990).
16. Dreisinger DB and Cooper WC, *Solvent Extr. Ion Exch.*, **7,** 335, (1989).
17. Hughes MA and Rod V, *Faraday Discuss. Chem. Soc.*, **77,** 75, (1984).
18. Hancil V, Slater MJ and Yu W, *Hydrometallurgy*, **25,** 375, (1990).
19. Cianetti C and Danesi PR, *Solvent Extr.Ion Exch.*, **1,** 9, (1983).
20. Simonin JP, *Solvent Extr. Ion Exch.*, **13,** 941, (1995).

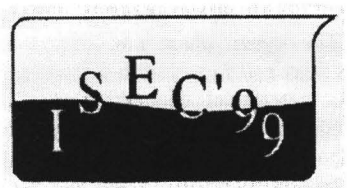

KINETIC STUDIES AND MOLECULAR DYNAMICS SIMULATIONS OF INTERFACIAL COMPLEXATION IN SOLVENT EXTRACTION SYSTEMS

Hitoshi Watarai and Yuki Onoe

Department of Chemistry, Graduate School of Science, Osaka University, Toyonaka, Osaka 560-0043, Japan

ABSTRACT

A new approach to elucidate what happened at the interface of chelate extraction systems is proposed by the combination of experimental kinetic measurements and computer simulations using high-speed stirring spectrometry or centrifugal liquid membrane spectrometry and molecular mechanics (MM) and molecular dynamics (MD) simulations. The molecular mechanisms of the interfacial reactions in the extraction kinetics of Ni(II) or Pd(II) with 2-hydroxyoxime or pyridylazo-ligands are studied by this new approach.

Keywords: interfacial complexation, extraction kinetics, new methods of studying extraction kinetics, molecular dynamics simulations, 2-hydroxyoxime and pyridylazo extractants, nickel, palladium

INTRODUCTION

The adsorption of extractants at liquid-liquid interfaces and resulting reactions with metal ions at the interface are primarily important processes which determine solvent extraction rates, especially in highly dispersed or agitated systems. However, the molecular mechanisms of such interfacial reactions are still less well understood than those in bulk solutions. This situation is a consequence of the fact that only limited experimental methods and theoretical approaches have so far been developed.

In the present study, we propose a new approach which includes both the strategies of experimental and computational methods. In this approach, at first, the relationship between extraction rate of a metal ion and interfacial concentration of extractant is determined by the experimental methods such as high-speed stirring spectrometry[1] or centrifugal liquid membrane spectrometry.[2] Then, the interfacial mechanism involved in the solvent extraction kinetics is elucidated This kind of experimental measurement afford us various stoichiometric parameters such as the composition of an interfacially adsorbed complex and formation rate constants of the complex at the interface. However, it is impossible to see experimentally at the present stage how the solvent molecules construct the liquid-liquid interface and where the extractant molecule is located in the interfacial region. Therefore, we adopted molecular mechanics (MM) and molecular dynamics (MD) simulations to explain or predict the interfacial adsorptivity of extractants or complexes and their reactivity at the liquid-liquid interfaces.[3]

The potential of this approach is demonstrated in the present study for various chelate extraction systems which include the extraction kinetics of Ni(II) with 2-hydroxyoximes,[4] the solvent effect on the interfacial reaction of 2-(5-bromo-2-pyridylazo)-5 diethylaminophenol (5-Br-PADAP) with Ni(II),[3] the catalytic effect of 4-(2-pyridylazo)-N,N-dimethylaniline (PADA) on the extraction of Ni(II) with 1-(2-pyridylazo)-2 naphthol (Hpan)[5] and the acid-catalyzed interfacial complexation in the extraction kinetics of Pd(II) with 5-Br-PADAP.[6] The present study also indicates that the interfacial reaction can effectively be used to control or accelerate solvent extraction rates of metal ions.

EXPERIMENTAL

Extraction kinetic measurements

The solvent extraction rate of Ni(II) or Pd(II) ions and the interfacial concentration of extractant and the complex were measured by the high-speed stirring method. Briefly, a heptane or toluene phase (45ml) and the same volume of an aqueous phase were stirred at the rate of 4700-5000 rpm in a vessel

© 2000 Society of Chemical Industry

thermostatted at 25±0.1°C, 5 ml of ligand solution was added, and then 5 ml of metal solution was spiked into the mixture to initiate the extraction of the metal ion. The organic phase was continuously separated by means of a Teflon phase separator, introduced into a flow cell mounted in a diode array spectrophotometer and returned to the vessel by a pump. The interfacial concentration of the extractant or complex was determined from the absorbance change resulting from alternate stirring between 200 rpm and 5000 rpm. The high-speed stirring of the two-phase system increases the interfacial area about 500 times. From the continuous decrease of the extractant or the increase of metal complex in the organic phase, the extraction rate can be determined. The interfacial reaction was also directly observed by means of the centrifugal liquid membrane method combined with spectrophotometry. All experiments were carried out at 25 °C.

MM and MD simulations

The liquid-liquid interfaces of heptane/water and toluene/water were simulated by the use of the DREIDING force field on the Minimizer and Dynamics modules of Cerius2 version 3.5 (MSI, San Diego) on a SG Indigo II or O_2 work-station. The position and the orientation for 500 molecules of water and 62 molecules of heptane or 100 molecules of toluene were optimized in a quadratic prism cell (ca. 25 Å × 25 Å × 52 Å) at 300 K. Each bulk phase was optimized for 500 ps at 300 K under (NPT) ensemble in advance. The periodic boundary conditions were applied along all three directions. The calculations of the two-phase system were run under (NVT) ensemble. The density vs. distance profile showed a clear interface with a thickness of ca. 7 – 8 Å in both systems. In the simulation of the adsorptivity of extractant, one molecule of the extractant was introduced into the two-phase system and the calculation was carried out at the time step of 1fs over the period of 100-800ps. The charge distribution of the extractant was optimized by MOPAC PM3. Before the start of MD simulations of the system including the solute molecule, the whole system was optimized by the MM calculation.

MD simulation was further applied for the estimation of the stabilization energy at the interface. First, a MD simulation was carried out to obtain an equilibrated configuration of the extractant and solvent molecules. Secondly, a spherical region with the radius of 8.5 Å around the center of mass of the extractant molecule was defined, then the internal energy of the spherical region (E_1) was calculated by MM calculation. The surroundings of the spherical region were fixed during the MM calculation. Thirdly, after removing the extractant molecule from the spherical region, the energy of the residual solvent molecules in the spherical region (E_2) and the energy of the removed extractant molecule in a vacuum (E_0') were calculated. Finally, by the relationships:

$$\Delta E_i = E_1 - E_2 - E_0' \qquad (1)$$

$$\Delta\Delta E_i = \Delta E_i\,(\text{int}) - \Delta E_i\,(\text{org}) \qquad (2)$$

the solute-solvent interaction energy, ΔE_i , and the adsorption energy from a bulk phase to the interface, $\Delta\Delta E_i$, were calculated.

RESULTS AND DISCUSSION

Interfacial mechanism in the extraction of Ni(II) with 2-hydroxyoxime

The extraction rates of Ni(II) with 2-hydroxyoximes which include 5-nonylsalicylaldoxime (P50), 2-hydroxy-5-nonylacetophenone oxime (SME529) and 2-hydroxy-5 nonylbenzophenone oxime (LIX65N) in heptane were measured by means of the high speed stirring method. The interfacial concentration of the 2-hydroxyoxime during the extraction was also measured simultaneously. Experimental results showed that the rate determining step is the formation of a 1:1 complex at the interface and the observed interfacial rate constants showed the explainable order from the Eigen mechanism as listed in Table 1.[4] The key process in the interfacial mechanism was the interfacial adsorption of the extractant which showed about 20% adsorptivity even in its neutral form. The

adsorptivity of the three oximes were not very different as they have the same polar functional groups =N-OH and -OH. We tried to estimate their adsorption energy, or the transfer energy from heptane phase to the interface, from the difference between the solvation energies in the two circumstances. A 2-hydroxyoxime molecule after 400 ps simulations was located at the interface where the polar group was almost immersed in the aqueous phase and the nonyl group was in the organic phase. The polar group was expected easily to react with Ni(II) ion in aqueous phase. This is the reason why the extractants could react with Ni(II) ion at the interface with similar rate constants to those in aqueous solution. Table 1 shows the calculated results of the interfacial adsorption energy. The adsorption energy may reflect mainly the interaction energy of the polar group of the 2-hydroxyoxime with water molecules.

2-Hydroxyoxime	pK_a	log K_D	log K'^{a} (cm)	log k_i^{b} (1/Ms)	$\Delta\Delta E_i^{c}$ (kcal/mol)
5-Nonylsalicylaldoxime (P50)	9.00	3.36	-3.34	4.57	-9.3
2-Hydroxy-5-nonylaceto-phenone oxime (SME529)	9.79	3.99	-3.29	5.11	-12.1
2-Hydroxy-5-nonylbenzo-phenone oxime (LIX65N)	8.70	5.69	-2.97	5.14	-6.6

a) Adsorption constant from organic phase to interface
b) Rate constant for the interfacial complexation
c) Adsorption energy from organic phase to interface

Table 1 Kinetics and Adsorption Parameters in the Extraction of Ni(II) with 2-Hydroxyoxime in Heptane/0.1M(H,Na)ClO_4 at 25°C

Solvent effect on the interfacial reaction of 5-Br-PADAP with Ni(II)

5-Br-PADAP showed significant adsorption at the heptane/water interface under high-speed stirring conditions (5000rpm). In the toluene/water system, the adsorptivity was significantly reduced. Hpan and PADA did not adsorb at all at the heptane/water and toluene/water interfaces. Using the Langmuir isotherm, the adsorption parameters, $K'A_i$, of 5-Br-PADAP (HL) at the heptane/water and toluene/water interfaces were obtained as 4.4×10^{-2} dm^3 and 4.3×10^{-4} dm^3, respectively, where A_i is the total interfacial area under the high-speed stirring (ca.$2\times10^4 cm^2$). The smaller adsorption constant in toluene/water system seems to correspond to the larger distribution constant; log K_D(toluene/water) = 4.78 and log K_D(heptane/water) = 3.22.

When a heptane solution of 5-Br-PADAP and an aqueous solution of Ni^{2+} were stirred, the ligand in the organic phase was continuously consumed according to the complexation reaction. The complex formed was completely adsorbed at the interface. In the toluene system, the complex was extracted very slowly. From the initial rate of consumption of HL_o, the rate-determining reactions were elucidated as:

$$HL_o \quad HL_i \quad \underset{k'}{K'=[HL]_i/[HL]_o} \quad \text{Interfacial adsorption (Langmuir isotherm)} \qquad (3)$$

$$Ni^{2+} + HL_i \underset{k}{\rightarrow} NiL^+_i + H^+ \quad \text{Interfacial reaction} \qquad (4)$$

$$Ni^{2+} + HL \rightarrow NiL^+ + H^+ \quad \text{Aqueous phase reaction} \qquad (5)$$

where k and k' are the 1:1 formation rate constants in the bulk aqueous phase and at the interface, respectively. The value of $k = 5.3 \times 10^2$ $M^{-1}s^{-1}$ was determined in aqueous solution by stopped-flow spectrometry under conditions where the formation rate was independent of pH. The values of $k' = 3.8 \times 10^2$ $M^{-1}s^{-1}$ for heptane/water and $k' = 1.8 \times 10$ $M^{-1}s^{-1}$ for toluene/water were also determined. These results meant that the percentage of the interfacial reaction over the total reaction was 99.9% in

heptane/water and 94.5% in toluene/water, respectively. The interfacial rate constant in heptane system was comparable with that in aqueous phase, however, the large retardation effect of toluene on the k' was not explained by the experimentally obtainable parameters. Here we found that the molecular dynamics (MD) simulations were significantly useful. The MD simulations suggested that the location of the extractant adsorbed at the interface depended on the nature of the organic solvent; in heptane system, the extractant is in contact with the aqueous phase, while the extractant at the toluene/water interface is highly surrounded by the toluene molecules which may lower the probability of the reaction with Ni^{2+} ion in aqueous phase.[3] (see Figure 1)

Catalytic effect of PADA on the extraction of Ni(II) with Hpan

The extraction rate of $Ni(pan)_2$ into toluene is very slow even under a high-speed stirring regime and at high pH. Whereas, the addition of PADA even as dilute as 10^{-5} M accelerated the extraction rate about ten times. It was noted that there was no change in the extracted species and no consumption of PADA after the extraction. However, a significant decrease in the organic phase concentration of PADA was observed during stirring. Analyses of the experimental results suggested the interfacial adsorption of $Ni(pada)^{2+}$ complex which was rapidly formed in the aqueous phase. Thus, the catalytic effect of PADA could be explained by the rate-determining reaction between $Ni(pada)^{2+}{}_i$ and Hpano, followed by an interfacial ligand-exchange reaction,

$$Ni(pada)^{2+}{}_i + Hpan_o \xrightarrow{k'} Ni(pan)(pada)^{+}{}_i + H^+ \quad (6)$$

$$Ni(pan)(pada)^{+}{}_i + Hpan_o \rightarrow Ni(pan)_{2,o} + pada_o + H^+ \quad (7)$$

The value of k' was obtained as 90 $M^{-1}s^{-1}$.

The key processes in this extraction mechanism were no adsorptivity of PADA and strong adsorptivity of $Ni(pada)^{2+}$. MD simulations could explain these difference in the adsorptivity satisfactorily; $\Delta\Delta E_i$ for the transfer of PADA from toluene to interface was 0.5 kcal/mol and $\Delta\Delta E_i$ for the transfer of $Ni(pada)^{2+}$ from aqueous phase to interface was -7.4 kcal/mol.

Acid-catalysis in the extraction of Pd(II) with 5-Br-PADAP

Extraction rate of PdLCl from acidic solution of Pd(II) with 5-Br-PADAP (HL) in toluene was increased with the lowering of pH. The acid concentration was controlled by perchloric acid under the constant concentration of chloride ion (0.1M). The rate determining step under the condition of pH < 3 was found to be the complexation of $PdCl_n^{(n-2)-}$ (n=2,3,4) and the protonated 5-Br-PADAP adsorbed at the interface whose concentration was increased at the lower pH. The key step of the catalytic effect of the acid was the interfacial accumulation of 5-Br-PADAP by the protonation at the diethylamino group. The protonation of this group did not interfere with the complexation of the metal ion. The MD simulation showed that the protonated 5-Br PADAP was adsorbed at the interface in contact with the aqueous phase, keeping its orientation which therefore easily reacts with the hydrated metal ion (Figure 1).

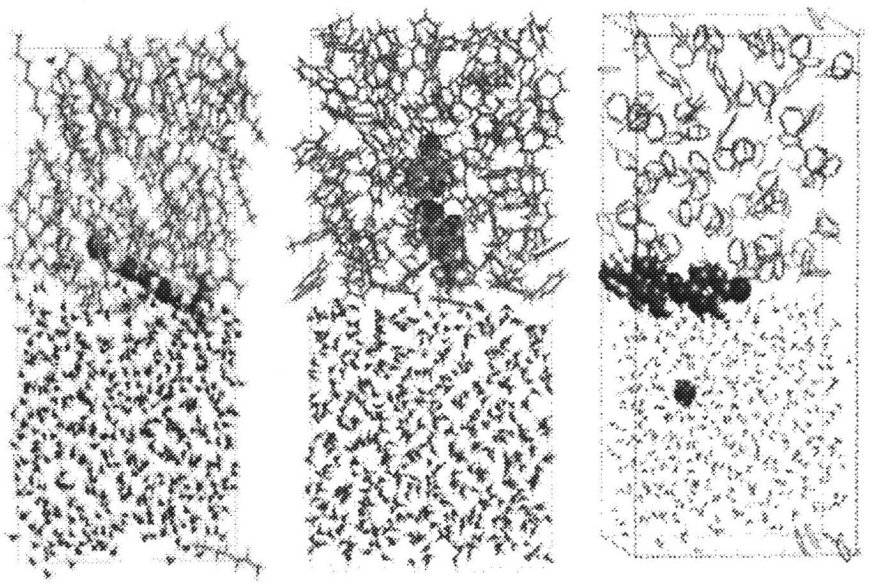

(a) (b) (c)

Figure 1. MD simulations of 5-Br-PADAP; (a) 100ps in heptane/water system, (b) 100ps in toluene/water system, and (c) 400ps in toluene/acid (pH=1.1) system which includes a protonated 5-Br-PADAP and a chloride ion.

REFERENCES

1. Watarai H, *Trends in Analytical Chemistry*, **12**, 313, (1993).
2. Nagatani H and Watarai H, *Anal. Chem.*, **70**, 2860, (1998).
3. Watarai H, Gotoh M and Gotoh N, *Bull. Chem. Soc. Jpn.*, **70**, 957, (1997).
4. Watarai H and Satoh K, *Langmuir*, **10**, 3913, (1994).
5. Onoe Y, Tsukahara S and Watarai H, *Bull. Chem. Soc. Jpn.*, **71**, 603, (1998).
6. Ohashi A, Tsukahara S and Watarai H, *Anal. Chim. Acta*, **364**, 53, (1998).
7. Onoe Y and Watarai H, *Anal. Sci.*, **14**, 237, (1998).

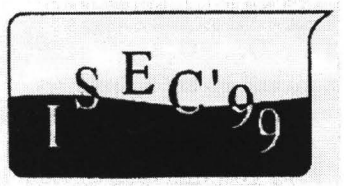

MASS TRANSFER KINETICS OF RARE EARTH ELEMENTS WITH HOLLOW FIBRE MEMBRANE BASED EXTRACTION

Yujie Wang and Deqian Li
Laboratory of Rare Earth Chemistry and Physics, Changchun Institute of Applied Chemistry, Chinese Academy of Sciences, Changchun, 130022, China

ABSTRACT
The solvent extraction of Ce^{4+}, Ce^{3+} and trivalent lanthanides was studied by the method of microporous hollow fibre (MHF) extraction. The results showed that the mass transfer coefficient of Ce^{4+} was about 10 times larger than those of Ce^{3+} and La^{3+}. The mass transfer rate of Ce^{4+} was controlled by its dispersion in the critical layer of the water phase. That of the other trivalent rare earths (RE^{3+}) was controlled by its dispersion in the membrane. Therefore Ce^{4+} could be effectively separated from the rare earth solution.

Keywords: cerium, rare earths, hollow fibre membrane, extraction kinetics, amine N1923

INTRODUCTION

Microporous hollow fibre (MHF) extraction, as a novel separation technology, has been studied since the 1980's. It is possible that this technology will be applied to the separation of some solutes in industrial scale because of many successful works on separation systems,[1-3] membrane materials,[4] controlling emulsification,[1-4] mass transfer kinetics and certain designs,[5] etc. These systems involve a large number of solutes such as biologically active substances, organic solutions and inorganic ions. Which solute will be first separated on an industrial scale will depend on the work on these separation systems. Such MHF extractions depend on solutes that can be extracted completely by a extractant by having a larger partition coefficient or more rapidly by their mass transfer coefficient. It is well known that the partition coefficient of Ce^{4+} in N1923 is very large,[6] but its mass transfer rate had not been studied. In this paper, its mass transfer coefficient has been measured and its possibility of separation from RE^{3+} tested.

EXPERIMENTAL

The MHF device consisted of a MHF module and necessary pumps and tube for flow of water and oil phase, as shown in previous paper.[1] The MHF was a single polysulfone fibre (provided by Tokyo University, Jpn.) that was installed in a glass shell with a thermostatic water flow. The effective length and inner and outer diameter were 305.5mm, 1.220mm and 1.648mm respectively. The inlets and outlets for the aqueous and organic phases were enlarged to slow down the variation in flow rate and pressure of the solutions caused by the change of tube diameter at the connection. The aqueous phase was driven by an electric pump and the organic phase by a tube pump(JLB2).

The water phase flowed in the lumen-side and the organic phase ran counter-currently in the shell-side. Thus an interfacial contact area was established on the side of the inner surface. The micropores of the MHF was filled with the organic phase that wetted the polysulfone membrane. It was found that it was not necessary to maintain a higher pressure on the aqueous side of the membrane to avoid unwanted solvent breakthrough and mixing reported by others.

RESULTS AND DISCUSSIONS

For the anti-current extraction with MHF, it is well known that a mass transfer equation could be induced from the Fick's First Law:[5]

© 2000 Society of Chemical Industry

$$\frac{1/Q_W + 1/(Q_S K_D)}{1/V_W + 1/(Q_S K_D)} \ln\left(\frac{\Delta C_A}{\Delta C_A^0}\right) = -t\{1 - \exp[-\frac{4K_W V_M}{d}(\frac{1}{Q_W} + \frac{1}{Q_S K_D})]\} \quad (1)$$

where Q_W and Q_S are the flows of the aqueous and organic phase; V_W and V_M are the volumes of the aqueous and organic phase reservoirs, always 50ml in our experiments; V_S and d are the volume and diameter of the fibre; $\ln[\Delta C_A/\Delta C_A{}^0]$ was indicated as equation 2; K_D is the partition coefficient; K_W denotes the mass transfer coefficient based on the water phase. It was possible to test whether or not cerium was separated from rare earths by comparison of the K_W values with each other under a variety of experimental conditions or a variety of ions.

$$\ln[\frac{\Delta C_A}{\Delta C_A^0}] = \ln\{\frac{C_A[1 + V_W/(V_S K_D)] - C_A^0 V_W/(V_S K_D) - C_A^{S,0}/K_D}{C_A^0 - C_A^{S,0}/K_D}\} \quad (2)$$

where $C_A{}^0$ and $C_A{}^{S,0}$ denote the solute concentrations in the water and organic phase at the beginning of the experiment.

In equations (1) and (2), the only variable with time is C_A and the other parameters concerning the device or its operation are constants for every experiment. The total mass transfer coefficient based on water could be obtained by the slope of the curve of $\ln[\Delta C_A/\Delta C_A{}^0]$ with time, $\ln[\Delta C_A/\Delta C_A{}^0]$ being calculated according to equation (2).

According to equations (1) and (2), K_W will increase with the increase of K_D under the same experimental conditions. Ce^{3+} and La^{3+} with larger K_D values were representative of rare earths when the separation of Ce^{4+} was studied in the experiment.

It has been suggested in many previous papers that the process of MHF extraction consists of three successive steps: the first being the dispersion of solute to the oil/water interface; the second one is the dispersion of solute in the pores of the membrane; the last one is the dispersion of solute from the outer surface to the oil bulk phase. The resistance of every step is connected as follows:[7]

$$1/K_W = 1/k_w + 1/k_m K_D + 1/k_s K_D \quad (3)$$

where k_w is the mass transfer coefficient in water phase, and $1/k_w$ is the mass transfer resistance; k_m is the mass transfer coefficient in the membrane, and $1/k_m K_D$ is the mass transfer resistance; k_s is the mass transfer coefficient in the bulk organic phase, and $1/k_s K_D$ is the mass transfer resistance. In the last two terms of the above equation, K_D is present because the membrane can be wetted by organic phase. From this equation, the main steps controlling the total mass transfer resistance can be tested by the change of the total mass transfer coefficient with the flow rate of water phase or oil phase.

Figure 1 shows the curves of the solute concentrations in aqueous phase with respect to time for the extraction of each ion. The results show that the concentration of Ce^{4+} was approximately zero after 7 hours, but the extraction of Ce^{3+} and La^{3+} reached about 50% and 30% at 10 hours. According to equations (1) and (2), the total mass transfer coefficient can be obtained from these curves. Figure 2 showed the total mass transfer coefficients of Ce^{4+} and Ce^{3+}. The mass transfer coefficients of Ce^{4+} hardly changed with the flow rate of organic phase and changed even less with the flow rate of water phase. The mass transfer coefficients of Ce^{3+} were about 10 times less than these of Ce^{4+} and increased with the flow rate of the organic phase but hardly changed with the aqueous flow rate. Therefore, the results suggest different mass transfer processes for Ce^{4+} and Ce^{3+}. The mass transfer rate of Ce^{4+} was mainly controlled by its dispersion in the critical layer of the water phase. This conclusion was reasonable because of the lower dispersion resistance term, as shown in eqn.(3), with a large partition coefficient. The mass transfer rate was controlled by the dispersion in the membrane. There were identical experimental results for La^{3+} ion. The special interest was in the separation of Ce^{4+} from the trivalent lanthanide, as shown in figure 3. The decrease of La^{3+} concentration was much slower in figure 3 than in figure 1. The reason for this might be the competition between the interfacial reactions of Ce^{4+} and RE^{3+} with N1923. The result shows the possibility of extraction of Ce^{4+} from trivalent lanthanide with immobilized interface in a MHF.

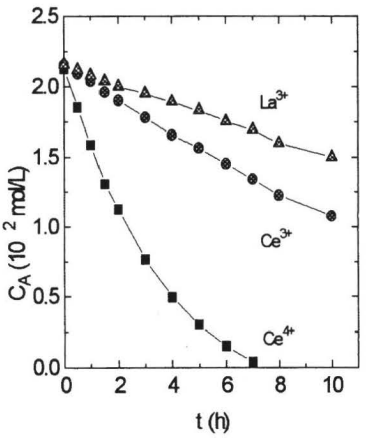

Fig.1 Curves of the solute concentrations in aqueous phase to time.

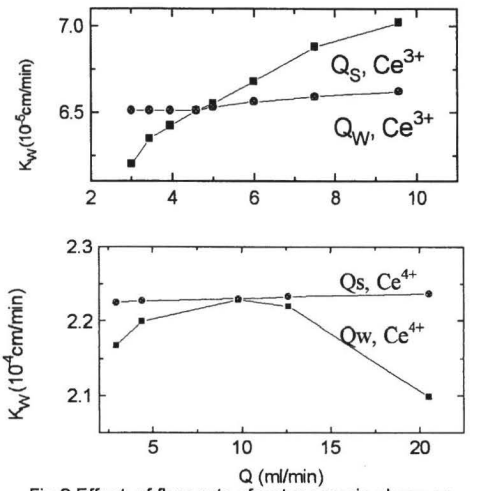

Fig.2 Effect of flow rate of water organic phase on mass transfer coefficient of Ce^{3+} and Ce^{4+}.

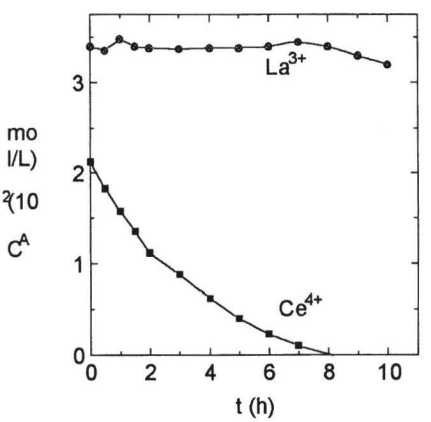

Fig.3 Separation of Ce^{4+} and La^{3+} with MHF extraction.

REFERENCES

1 Kubota F, Goto M and Nakashio F, *Sep. Sci. Tech.*, **30**(5), 777, (1995).
2 Coony DO and Poufos MG ,*Chem. Eng. Comm.*, **61**, 159, (1987).
3 Frank GT and Sirkar KK , *Biotechnology and Bioengineering Symp.*, **17**, 303, (1986).
4 Kim BM *J. Membr. Sci.*, **21**, 5, (1984).
5 D'Ella NA, Dahurone L and Cussler EL , *J. Membr. Sci.*, **29**, 309, (1986).
6 Li D, Wang Z and Zeng G, *J.Nuclear and Radiochem.*, **6**(3), 153, (1984).
7 Prasad R and.Sirkar KK , *J. Membr. Sci.*, **50**, 153, (1990).

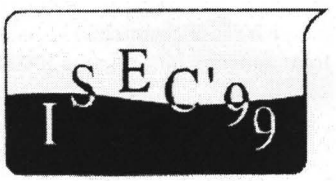

SOLVENT EXTRACTION KINETICS THROUGH HOLLOW FIBRE AND FLAT MEMBRANES: INVESTIGATION WITH NITROXIDE RADICALS

NM Kocherginsky, AN Osipov and AB Grishchenko
Chem. & Env. Eng. Department, National University of Singapore, Singapore

ABSTRACT
Kinetics of extraction of stable nitroxide radicals ("spin probes") from organic solvents into water through hollow fibres and flat membranes was investigated. It was demonstrated that Mass Transfer Coefficients based on organic phase (MTCo) for exit through hollow fibres with mineral oil practically do not correlate with the hydrophobicity of low molecular weight radicals and are determined by diffusion through the organic solvent. In the experiments with a less viscous octane organic phase does not play a dominant role, but still the process cannot be explained simply by the influence of aqueous layer. Ascorbic acid reduced nitroxides in water and enhanced the rate of nitroxide exit from octane due to the decrease of transport resistance of unstirred aqueous layers. Addition of ascorbic acid up to 1 mol/dm^3 resulted only in the four-fold increase of MTCo for Tempo, which is less than the value predicted by the model of parallel diffusion and reaction in water. Low effect of ascorbic acid can be explained by addition of an interface resistance, which is usually neglected.

Keywords: nitroxide radical, hollow fibre membranes, extraction kinetics, two-film theory, interface resistance, interfacial kinetics.

INTRODUCTION

The initial purpose of this research was the investigation of kinetics of a low molecular weight organic substance removal from oil phase into water. Stable nitroxide radicals, known as spin probes due to the sensitivity of their EPR spectra to the properties of microenvironment, were used as model substances. Results on hollow fibres and flat membranes demonstrated that the kinetics of nitroxide transport from a liquid organic phase into water through the porous support cannot be described by the classical two-film theory, according to which the mass transfer resistance of extraction is determined by the total resistances of the organic and aqueous unstirred layers.[1] Also the mass transfer resistance of the liquid/liquid interface, which usually is assumed to be negligible, is considered.

EXPERIMENTAL

Experiments were conducted in a hollow fibre contactor module with microporous polypropylene fibres (Celgard 5PCM-102, Hoechst-Celanese). Another group of experiments was conducted in the experimental cell with a vertical flat membrane, separating the octane and aqueous phases. In this case it was a Millipore nitrocellulose membrane, thickness about 150 μm. Both phases were mechanically stirred with a rotating mechanical stirrer. Initial concentration of nitroxides in organic solvent was 10^{-3}-10^{-4} mol/dm^3, and changes in concentration were measured periodically by EPR spectrophotometry.
Mass transfer coefficients (MTCo and MTCa) for nitroxide transport from organic solvent into aqueous buffer were calculated based on equations 1 and 2:

$$\ln A(t) = \ln\left[1 - \frac{(K_d + 1)C_a}{C_o^o}\right] = -(MTCo + MTCa)\frac{S}{V}t \qquad (1)$$

where V is the volumes of the organic and aqueous phases, C_o° initial concentration of nitroxide in organic phase, C_a current concentration of nitroxide in aqueous phase, K_d distribution coeficient oil/water, S surface area of the membrane, MTCo and MTCa mass transfer coefficients calculated for the organic and aqueous phases respectively.

© 2000 Society of Chemical Industry

$$MTCa = MTCo \times K_d \qquad (2)$$

In experiments with ascorbic acid, after nitroxide leaves the organic phase it is chemically reduced in water and one can neglect the influence of backward transport from aqueous into organic phase. In this case $C_a = 0$ and:

$$\ln\left(\frac{C_o}{C_o^o}\right) = -\frac{MTC_o}{V} St \qquad (3)$$

Where C_o is the current concentration of the radical in organic phase.

RESULTS

The rate of radical concentration increase in the aqueous phase was used to characterise the mass transfer through hollow fibre. The linear representations of the kinetic curves based on equation 1 are presented in figure 1. Correlation coefficients in all cases were higher than 0.99 with the changes of ln A(t) by more than unity. Values of MTCo and MTCa calculated from the corresponding slopes, are given in table 1 together with the distribution coefficients K_d, measured at the end of experiments.

Radical	K_d	MTC_o 10^{-5} cm/s	MTC_a 10^{-5} cm/s
Tempo	15	0.3	4.5
Imidazolidine R*	0.5	0.9	0.5
Imidazoline R*	0.1	0.5	0.05

Table 1 Parameters of transport of nitroxides between mineral oil and phosphate buffer (pH = 4) through the hollow fibres.

Another method of MTC_o calculation was based on the values of initial rates of the kinetics, when the backward transfer from aqueous solutions can be neglected. The results were in good agreement with the data calculated from the linear representations.

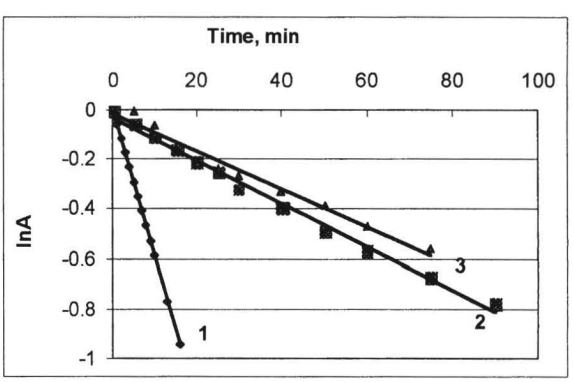

Figure 1. Linear representations for kinetics of free radical distribution between mineral oil and buffer in a hollow fibre module, pH = 4.
1: Tempo; 2: Substituted Imidazolidine; 3: Substituted Imidazoline.

MTCo and MTCa values usually are described based on the double-film theory as a function of resistance in aqueous and organic unstirred layers (equations 4 and 5):

$$MTCo = \frac{1}{\frac{L_o}{D_o} + \frac{K_d L_a}{D_a}} \quad (4)$$

$$MTCa = \frac{1}{\frac{L_o}{K_d D_o} + \frac{L_a}{D_a}} \quad (5)$$

where D_o and D_a are diffusion coefficients in organic and water phases, L_o and L_a the effective thickness of organic and aqueous unstirred layers respectively. In these experiments the membrane was impregnated by organic solution, so L_o was the sum of the effective thickness of unstirred organic layer near the membrane and the membrane itself. EPR spectra of the membrane after the experiment demonstrated that the nitroxide is still in liquid phase, filling the pores.

MTCo values of nitroxides are independent of K_d for different radicals (table 1). On the other hand values of MTCa are approximately proportional to K_d. Both K_d and MTCo change by 100-150 times from Tempo to the imidazoline radical. From equations 4 and 5 one can see that unstirred organic layer in the case of mineral oil plays a dominant role in mass transfer processes. The influence of the aqueous unstirred layer and the interface seems to be small for this viscous solvent. For the much more hydrophobic octyl-imidazoline radical (K_d ~ 200) MTCo was much lower (~10^{-7} cm/s). Aqueous concentration in this case is much lower and the resistance of unstirred aqueous layer plays an essential role.

If instead of mineral oil octane was used as a solvent, the rate of Tempo distribution through the hollow fibres in the two phase system was much higher and equilibrium was practically established in less than five minutes. K_d in this case was also near 15 and the estimated MTCo and MTCa are ~$2*10^{-5}$ cm/s and $3*10^{-4}$ cm/s, respectively.

Estimation of D_o for Tempo according to Wilke-Chang[2] gives 2.8 x 10^{-7} and 1.8 x 10^{-5} cm^2/s in mineral oil and octane, respectively. This difference is much bigger than that for the corresponding MTC_o values, which probably reflects the changes of the rate-limiting step.

To investigate transport from octane the cell with a vertical flat membrane was used. Mass transfer coefficients for the cell with the vertical membrane were in good agreement with the data found for hollow fibres. For example, MTCo in the case of one membrane is 1.8 x 10^{-5}cm/s for octane and 4.4 x 10^{-6} cm/s for mineral oil. In the separate experiment Tempo was added into the aqueous phase and kinetics of its entrance from water into octane also gave a straight line in the semi-log co-ordinates with similar mass transfer parameters.

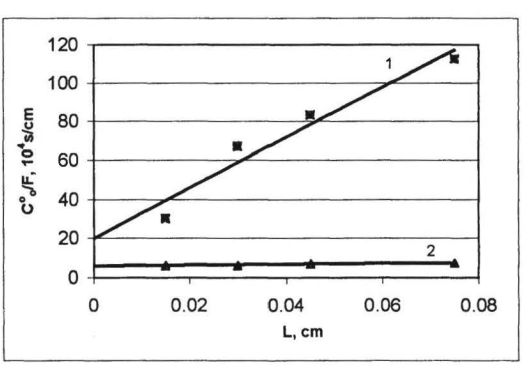

Figure 2. Transport resistance of flat membranes as a function of the membrane thickness:
1 – mineral oil, 2 – octane

Analysis of the flux dependence on the membrane thickness (different number of filters) allows determination of the effective diffusion coefficient (D_m) in the membrane (figure 2). Values of D_m were 7×10^{-8} and 5×10^{-6} cm^2/s for mineral oil and octane, respectively. One can see that the value of D_m are 3-4 times less then corresponding D_o values found from Wilke-Chang equation,[2] which could be the result of the influence of porosity and tortuosity of the membrane. Another possible explanation is partial immobilisation of the organic solvent in membrane pores, which is proved by comparison of the EPR spectra in a bulk organic solvent and the membrane after experiment.

The value of the intercept with the Y-axis, which corresponds to the extra resistance, determined by unstirred organic layer, interface organic solution /water and unstirred aqueous layer, was 2×10^5 and 6×10^4 s/cm for mineral oil and octane, respectively. In the case of mineral oil the extra resistance is comparable to the transport resistance of one membrane. In the case of octane the extra resistance plays a dominant role.

To further investigate this interface resistance the reaction of nitroxides in water with ascorbic acid was used. The reaction is first order with respect to each of the reactants and its rate constant is near 500 $M^{-1}min^{-1}$ at pH = 7.[3] In general case the acceleration factor due to the reaction in aqueous phase should be described by equation 6:[1]

$$f = \sqrt{\frac{D_a k C_{asc}}{MTC_a^2}} \coth \sqrt{\frac{D_a k C_{asc}}{MTC_a^2}} \qquad (6)$$

where C_{asc} is the concentration of ascorbic acid and k the rate constant for reaction between nitroxide and ascorbic acid. Based on this equation an acceleration factor equal to 20 should be expected in the presence of 1mol/dm^3 ascorbic acid, which is much bigger then the experimental value, equal to 4 (figure 3).

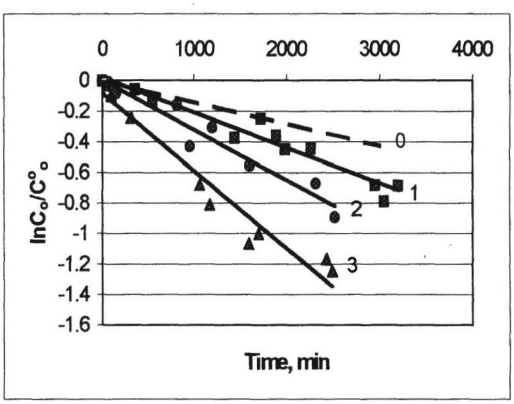

Figure 3. Tempo exit from octane through flat membrane in presence of ascorbic acid at pH 6:
0: 0 mM (calculated), 1: 10 mM, 2: 10^2 mM, 3: 10^3 mM

DISCUSSION

Usually it is assumed that penetration through the interface is a fast reversible process, described by distribution coefficient K_d. To explain these results at least one more step, which has non-zero mass transfer resistance for example resistance of the interface, has had to be added.

In this case MTCo and MTCa values are dependent on resistance of aqueous and organic unstirred layers, and also on the resistance of interface:

$$MTCo = \frac{1}{\frac{L_o}{D_o} + \frac{K_d L_a}{D_a} + \frac{1}{k_o}} \quad (7)$$

$$MTCa = \frac{1}{\frac{L_o}{K_d D_o} + \frac{L_a}{D_a} + \frac{1}{k_a}} \quad (8)$$

If $k_0 >> 0$ (usual assumptions), the expression gives usual equations 4 and 5. In the opposite situation, when k_o is small, we have:

$$MTCo = k_o \quad \text{and} \quad MTCa = k_a \quad (9)$$

The dependence of the flux on the concentrations in this case is similar to the one, based on the usual double-film theory, but the physical meaning of the MTC's is different. It means that only the concentration dependence of the flux cannot be used as the criteria to prove one or another mechanism.

In the experiments with octane due to its low viscosity it was possible to demonstrate the role of interface resistance directly in the case of Tempo penetration through one flat membrane. In the presence of 1mol/dm^3 ascorbic acid resistance of aqueous phase is negligibly small. Based on the diffusion coefficient of nitroxide in membrane, impregnated with octane half-life for its exit would be expected to be less then 5 hours. The experimental number was at least 10 times more, thus demonstrating the dominant role of interfacial resistance.

Kinetics of Tempo concentration decreases in presence of 1mol/dm^3 ascorbic acid (figure 3, curve 3) allowing the determination of k_0 (6.4 x 10^{-5} cm/s). Based on the K_d value k_a also equals 9.6 x 10^{-4} cm/s. These values can be qualitatively explained by the theory of the absolute rates with reasonable activation energies. For the interface transport extra activation energy has to be added to overcome the physical barrier existing due to the non-homogeneity of the media and the solvation / hydration of nitroxide. Thus the experimental k_a value for the interface transfer can be assumed to be described by equation:

$$k_a = k_l \exp(-E_{act}/RT)$$

Diffusion of a small molecule through the homogeneous layer with the thickness 10A (reasonable for the interface thickness) and diffusion coefficient as in water should give:

$$k_l = \frac{D_a}{L_i} = 50\ cm/s.$$

Using experimental k_a (~10^{-3} cm/s), the activation energy is equal to only 27 kJ/mol, and is probably determined by dehydration processes, when molecule moves from water through the interface. The activation energy for the exit from organic phase is bigger (34 kJ/mol) and can be easily explained by van der Waals interactions of the relatively big nitroxide molecule with the organic solvent.

REFERENCES

1. Cussler EL, *Diffusion*, 2nd ed., Cambridge University Press, (1997).
2. Wilke CR and Chang P, *A.I.Ch.E. J.*, **1**, 264, (1955).
3. Kocherginsky NM and Swartz HM, *Nitroxide Spin Labels*, CRC Press, (1995).

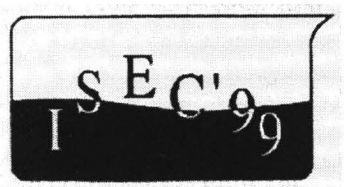

KINETICS AND MECHANISM OF SYNERGISTIC EXTRACTION OF GALLIUM(III) WITH AN ACIDIC ORGANOPHOSPHORUS COMPOUND IN THE PRESENCE OF OXINE DERIVATIVES

Kazuo Kondo, Michiaki Matsumoto, Kazuhiro Yano and Toyo Okubo

Department of Chemical Engineering and Materials Science, Doshisha University, Kyotanabe, Kyoto 610-0321 Japan

ABSTRACT

The large synergism in the extraction of gallium with the mixed extractant of 2-ethylhexylphosphonic acid mono-2-ethylhexyl ester (EHPNA) and 5-chloro-8-hydroxy-quinoline (HA) was found. The extraction reaction with the mixed extractant can be reasonably interpreted based on the formation of three gallium complexes. To clarify the synergistic extraction mechanism of gallium with the mixed extractant of EHPNA and HA, the initial extraction rates of gallium with EHPNA and/or HA were measured using a stirred transfer cell. First, the extraction mechanism with EHPNA as the main extractant was examined. The extraction mechanism consisted of three processes that are a mass transfer of metal ion to the interface, an extraction reaction at the interface, and a mass transfer of metal-complex to the bulk organic phase was proposed. Next, the extraction mechanism of gallium with HA as the synergist was examined. Because HA has relatively high hydrophilic property, the extraction mechanism of gallium with HA taking account of the complex formations in both the aqueous film and the interfacial zone, and the film diffusion was made clear. Finally, based on the information of the extraction mechanism of gallium with EHPNA or HA alone, the synergistic extraction mechanism of gallium with the mixed extractant of EHPNA and HA was clarified.

Keywords: synergism, extraction kinetics, mechanism of extraction, gallium, 2-ethylhexylphosphonic acid mono-2-ethylhexyl ester, 5-chloro-8-hydroxy-quinoline

INTRODUCTION

Gallium is present in extremely small amounts compared to common metals coexisting in all primary and most secondary sources. Solvent extraction is one of the promising techniques to recover gallium from dilute resources. Acidic organophosphorus compounds have been used as extractants for recovery of gallium from zinc refinery[1]. In the present paper, we studied the kinetics and mechanism of synergistic extraction of gallium with 2-ethylhexylphosphonic acid mono-2-ethylhexyl ester (EHPNA) and 5-chloro-8-hydroxyquinoline (HA). First the overall mechanism of synergistic extraction was examined from the viewpoint of equilibrium. Next, the extraction rates were measured in the stirred transfer cell to clarify the kinetic mechanism.

EXPERIMENTAL

Chemicals

2-Ethylhexylphosphonic acid mono-2-ethylhexyl ester (EHPNA) delivered from Daihachi Chem. Ind. Co. Ltd. Japan, was used as a main extractant without further purification. In a previous paper[2], because 5-chloro-8-hydroxyquinoline gave the highest synergism in the extraction of gallium with the mixed extractant, 5-chloro-8-hydroxy-quinoline was used as a synergist. Toluene was used as an organic diluent.

Extraction equilibrium

The organic solution was prepared by dissolving EHPNA and/or 5-chloro-8-hydroxyquinoline in toluene. Gallium chloride was dissolved in sodium sulfate and sulfuric acid solutions. The pH of the aqueous solution was adjusted by mixing sodium sulfate solution with sulfuric acid solution. The aqueous and organic solutions of equal volume (20 cm^3) were mixed in a flask and shaken at various temperatures to attain extraction equilibrium. Gallium concentration in the aqueous phase was

© 2000 Society of Chemical Industry

determined by an inductively coupled plasma spectrophotometry, Shimadzu ICPS-8000. The activity of hydrogen ion in the aqueous solution before and after equilibration was determined by a Horiba F-12 pH meter.

Extraction kinetics

The stirred transfer cell[3-6] was used to measure the rate of gallium extraction by EHPNA and/or HA at 303 K. The cell consists of two compartments with equal volume (about 140 cm^3), an upper compartment for the organic solution and a lower one for the aqueous solution. The interfacial area between both solutions is 1.3 x 10^{-3} m^2. The solutions in the cell were stirred in opposite directions by two flat-blade stirrers at 100 rpm in order not to disturb the interface. The concentration change of gallium in the aqueous solution with time was measured under various experimental conditions. The initial extraction rate of gallium, R_0, was obtained from the concentration change of gallium in the aqueous solution with time in the initial period.

RESULTS AND DISCUSSION

Extraction equilibrium

The result of the extraction of gallium(III) with mixed extractant of EHPNA and HA are shown in Figure 1, along with those of extraction with EHPNA or HA alone. In this figure, E represents the extent of the metal extracted, that is, the ratio of the metal concentration in the organic phase at equilibrium to that of the initial one in the aqueous phase. From the figure, the large synergism was confirmed. Experimental results were analyzed by the formation of following three gallium complexes. Where $K_{ex,HA}$, $K_{ex,HR}$ and $K_{ex,syn}$ are the extraction equilibrium constants of Equations (1) to (3), respectively. The values of these constants obtained are listed in Table 1.

$$Ga^{3+}_{aq} + 3HA_{org} \rightleftharpoons GaA_{3org} + 3H^{+}_{aq} \quad :K_{ex,HA} \quad (1)$$

$$Ga^{3+}_{aq} + 2(HR)_{2org} \rightleftharpoons GaR_3(HR)_{org} + 3H^{+}_{aq} \quad :K_{ex,HR} \quad (2)$$

$$Ga^{3+}_{aq} + (HR)_{2org} + HA_{org} \rightleftharpoons GaR_2A_{org} + 3H^{+}_{aq} \quad :K_{ex,syn} \quad (3)$$

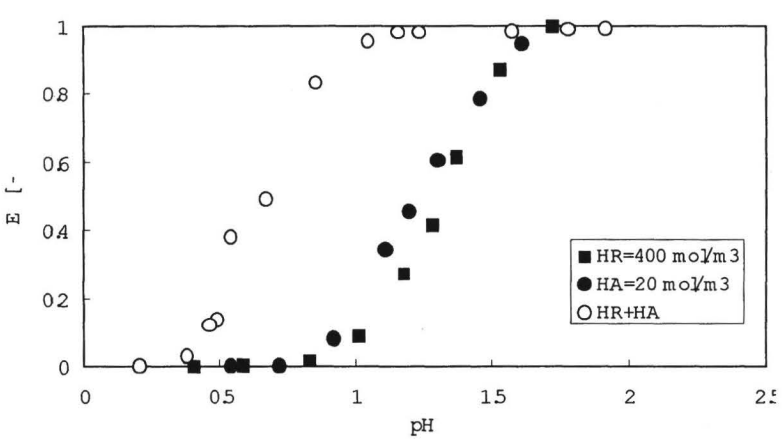

Table 1 Extraction equilibrium constants of gallium

Extracted species	GaA_3	GaR_3HR	GaR_2A
log K_{ex}	0.79	2.59	3.46

Extraction kinetics

Figure 2 shows the relations between the logarithm of R_0 and pH in the extractions of gallium with EHPNA and/or HA. In all cases, the slopes of this relation are about 1.0 in the low pH range and approach zero with increasing pH. Change of the dependency suggests the change of rate-determining step.

Figure 2 Effect of pH on initial extraction rates of gallium,$C_{Ga,0}$=4mol/m^3
BHR=500mol/m^3, JHA=20mol/m^3, EHR +HA, Solid lines are calculated ones.

Figure 1 Effect of pH on extent of gallium extracted ($C_{Ga,0}$=4mol/m^3)
Table 1 Extraction equilibrium constants of gallium

Extracted species	GaA_3	GaR_3HR	GaR_2A
log K_{ex}	0.79	2.59	3.46

Extraction kinetics

Figure 2 shows the relations between the logarithm of R_0 and pH in the extractions of gallium with EHPNA and/or HA. In all cases, the slopes of this relation are about 1.0 in the low pH range and approach zero with increasing pH. Change of the dependency suggests the change of rate-determining step.

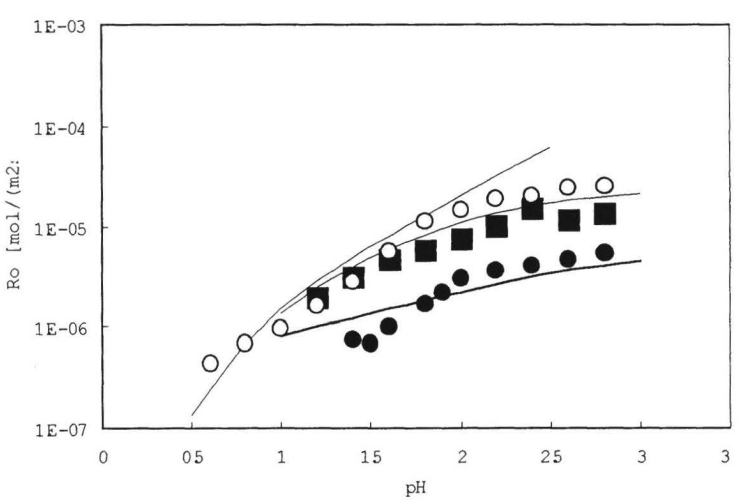

Figure 2 Effect of pH on initial extraction rates of gallium,$C_{Ga,0}$=4mol/m^3
BHR=500mol/m^3, JHA=20mol/m^3, EHR +HA, Solid lines are calculated ones.

Extraction mechanism of gallium with EHPNA

Considering that EHPNA is a surface-active molecule, the following reaction scheme is derived[7] (Scheme 1).

Scheme 1 Formation of gallium-EHPNA complex

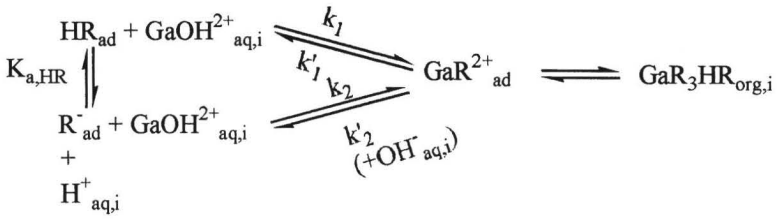

The rate equation taking account of diffusion of gallium in the aqueous film and the complex in the organic film was derived as Equation (4). It is not necessary to take account of the diffusion effects for the extractant and hydrogen ion because the extractant is present in large excess compared with the gallium ion and a buffer solution is used.

$$R_0 = 1/(R_{aq,HR}^{-1} + R_{i,HR}^{-1} + R_{org,HR}^{-1}) \qquad (4)$$

where $R_{aq,HR}$,$R_{i,HR}$ and $R_{org,HR}$ are the rate processes of the aqueous film, the interfacial reaction and the organic film, respectively and were derived as Equations (5) to (7).

$$R_{aq,HR} = k_{M,aq} C_{Ga,aq,total} \qquad (5)$$

$$R_{i,HR} = \frac{k_i \delta C_{HR,org,i} C_{Ga,aq,total}}{2(1 + \frac{C_{H,aq}}{K_{OH}})} \qquad (6)$$

$$R_{org,HR} = \frac{k_{com,org} K_{ex,HR} K_d C_{HR,org,i}^4 C_{Ga,aq,total}}{K_{OH}\left(1 + \frac{C_{H,aq}}{K_{OH}}\right) C_{H,aq}^2} \qquad (7)$$

The solid line in Figure 2 is the calculated results using by Equations (4) to (7) and explains well the experimental data.

Extraction mechanism of gallium with 5-chloro-8-hydroxyquinoline

Because 5-chloro-8-hydroxyquinoline (HA) has relatively high hydrophilic property, the extraction of gallium with HA occurs in both the aqueous film and the interfacial zone. Gallium is considered to be extracted by the following scheme.

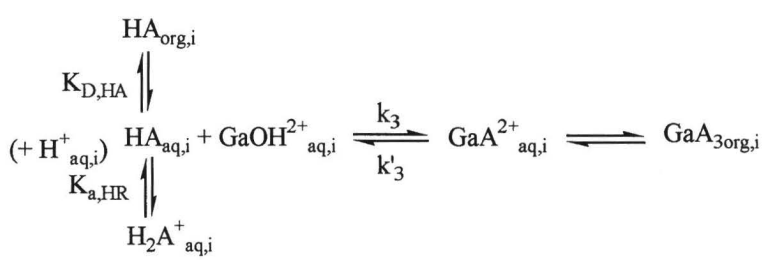

Scheme 2 Formation of gallium-5-chloro-8-hydroxyquinoline complex

Assuming that the rate-determining step is the 1:1 complex formation, the reaction rates in the aqueous film and interfacial zone, $R_{f,HA}$ and $R_{i,HA}$, and the mass transfer rates in the aqueous and organic films, $R_{aq,HA}$ and $R_{org,HA}$, are expressed as Equations (8) to (11).

$$R_{f,HA} = \sqrt{k_3 D_{HA,aq}} \cdot \sqrt{\frac{C_{Ga,aq,total}}{1 + C_{H,aq}/K_{OH}}} \cdot C_{HA,aq,i} \tag{8}$$

$$R_{i,HA} = \frac{k_3 \delta C_{HA,org,i} C_{Ga,aq,total}}{2\left(1 + \frac{C_{H,aq}}{K_{OH}}\right)} \tag{9}$$

$$R_{aq,HA} = k_{M,aq} C_{Ga,aq,total} + k_{HA,aq} C_{HA,aq,i} \tag{10}$$

$$R_{org,HA} = \frac{k_{com,org} K_{ex,HA} C^3_{HA,org,i} C_{Ga,aq,total}}{\left(1 + \frac{C_{H,aq}}{K_{OH}}\right) C^3_{H,aq}} \tag{11}$$

Therefore, the overall extraction rate is expressed as follows:

$$R_0 = \frac{R_{org,HA}\left(R_{f,HA} + R_{i,HA} + R_{aq,HA}\right)}{R_{f,HA} + R_{i,HA} + R_{aq,HA} + R_{org,HA}} \tag{12}$$

The solid line in Figure 2 was produced by non-linear least square method. Good agreement was obtained.

Extraction mechanism of gallium with mixed extractant

Based on the information of the extraction mechanism of gallium with EHPNA or HA alone, the synergistic extraction mechanism of gallium with the mixed extractant of EHPNA and HA is assumed to obey the following scheme (Scheme 3).

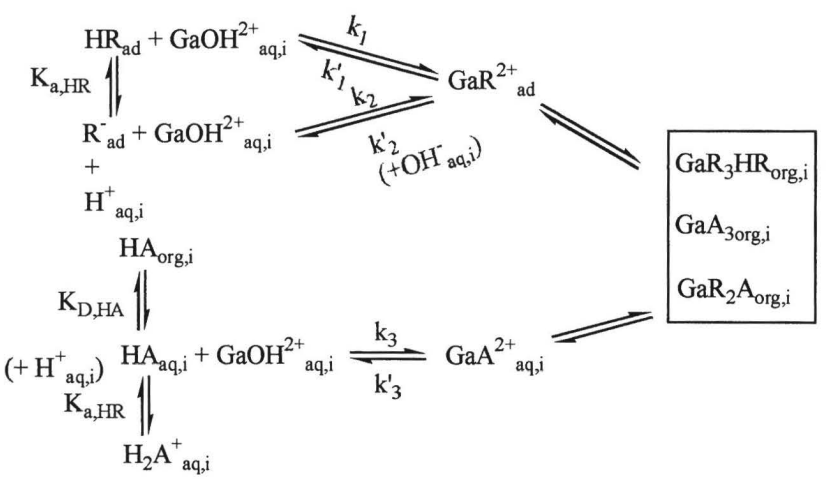

Scheme 3 Formation of gallium-mixed extractant complex

The reaction rates in the aqueous film and interfacial zone, $R_{f,syn}$ and $R_{i,syn}$, and the mass transfer rates in the aqueous and organic films, $R_{aq,syn}$ and $R_{org,syn}$, are expressed Equations (13) to (16).

$$R_{aq,syn} = R_{aq,HA} \tag{13}$$

$$R_{f,syn} = R_{f,HA} \tag{14}$$

$$R_{i,syn} = R_{i,HR} + R_{i,HA} \tag{15}$$

$$R_{org,syn} = R_{org,HA} + R_{org,HR} + \frac{k_{com,org} K_{ex,syn} K_d C^2_{HR,org,i} C_{HA,org,i} C_{Ga,aq,total}}{\left(1 + \frac{C_{H,aq}}{K_{OH}}\right) C^3_{H,aq}} \tag{16}$$

Therefore, the overall extraction rate is expressed as follows:

$$R_0 = \frac{R_{org,syn}\left(R_{f,syn} + R_{i,syn} + R_{aq,syn}\right)}{R_{f,syn} + R_{i,syn} + R_{aq,syn} + R_{org,syn}} \tag{17}$$

In Figure 2, the solid line is the calculated one and good agreement was obtained.

This is the first report that clarifies the extraction mechanism of synergistic extraction of a metal.

REFERENCES

1. Mihalov I and Distin PA, *Hydrometallurgy*, **28**, 13, (1992).
2. Kondo K, Yano K and Matsumoto M, *J. Chem. Eng. Japan*, **29**, 836, (1996).
3. Kondo K, Hashimoto T, Sumi H and Matsumoto M, *J. Chem. Eng. Japan*, **28**, 511, (1995).
4. Kondo K and Matsumoto M, *Separ. Sci. Technol.*, **31**, 557, (1996).
5. Kondo K, Tao LX and Matsumoto M, *Hydrometallurgy*, **44**, 321, (1997).
6. Kondo K, Matsumoto M and Okubo T, *Kagaku Kogaku Ronbunshu*, **23**, 555, (1997).
7. Kondo K and Matsumoto M, *Solv. Extr. Res. Develop., Japan*, **3**, 178, (1996).

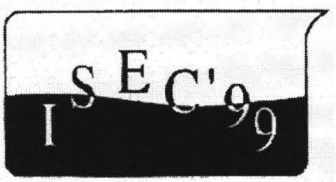

EXTRACTION KINETICS IN THE Er(III) 2-ETHYL-HEXYL-2-ETHYLHEXYLPHOSPHONIC ACID (HEH/EHP) HEPTANE SYSTEM

Jun Lu, Zhong Zheng, Deqian Li and Gengxiang Ma
Laboratory of Rare Earth Chemistry and Physics, Changchun Institute of Applied Chemistry, Chinese Academy of Sciences, Changchun, 130022, China

ABSTRACT

A simplified mass transfer equation $\ln[(1/\beta+1)C^a_b/C^a_{b,o}-1/\beta] = -S_i \cdot K(\beta+1)t/V^a$ has been proposed to determine the extraction regime. The conclusion was further verified by the study on the extraction kinetics of Er(III) by 2-ethylhexyl 2-ethylhexylphosphonic acid (HEH/EHP) at industrial concentration using a interfacial cell with laminar flow. The effect of the concentration of two mineral acid (nitric acid and hydrochloric acid) and Er(III) concentration on the extraction rate was investigated in Er(III)-HEH/EHP-heptane system. The extraction rate in nitric acid solution were higher than in hydrochloric acid solution. The extraction rate decreased with the increase of hydrochloric acid concentration, however, the extraction rate increased with the increase in the nitric acid concentration at the lower than 0.3 mol/L region and decreased at higher than 0.3mol/L region. With the increase of Er(III) concentration the extraction rate increased in the both mineral acid media. The existence of phase transfer agent quaternary amine $N263(R_3N^+CH_3Cl^-$, Aliquat 336) did not improve the mass transfer in hydrochloric acid solution but did in nitric acid medium.

Keywords: interfacial kinetics, Er(III), 2-ethylhexyl-2-ethylhexylphosphonic acid, Aliquat 336, Lewis cell

INTRODUCTION

2-ethylhexyl-2-ethylhexylphosphonic acid(HEH/EHP) has been widely used in the rare earth hydrometallurgy industry.[1,2] There were some reports on the low concentration rare earth(III) extraction kinetic with diluted HEH/EHP.[3-5] But little attention was paid on the rare earth(III) extraction kinetics and mass transfer in the industrial operation concentration system. The extraction kinetics of Er^{3+} by HEH/EHP has been investigated using novel interfacial cell with laminar flow in this paper. This constant interfacial cell with laminar flow has been proposed as a means to obtain extraction kinetics data in liquid-liquid systems.[6] A mass transfer equation $\ln[(1/\beta+1)C^a_b/C^a_{b,o}-1/\beta] = -S_i \cdot K(\beta+1)t/V^a$ has been proposed to determine whether the controlling step is diffusion or chemical reaction controlling process. The dependence of aqueous phase concentration on time is recommended to determine the extraction regime. The conclusion was further verified by the study on the extraction kinetics of Er(III) by HEH/EHP at industrial concentration.

EXPERIMENTAL

Apparatus and Reagent

Apparatus and procedure employed in this study were described previously[3,7] HEH/EHP was supplied by Shanghai Institute of Organic Chemistry, Chinese Academy of Sciences and purified according to the literature.[8] Stock solutions containing lanthanides(III) were prepared by dissolving rare earth oxide (>99.9%) in hydrochloric acid and standardized by EDTA titration using xylenol orange as an indicator. All other reagents were of analytical grade.

Analytical methods

A Model SA720 (Orion) pH meter calibrated daily with 4.01 and 6.86 standard buffer solution was employed for measuring pH value in aqueous phase. The concentration of the Er(III) in aqueous phase was analyzed by EDTA titration. Concentration of HEH/EHP was determined by titrating with standard sodium hydroxide in an ethanol-water mixture using phenolphthalein as an indicator.

© 2000 Society of Chemical Industry

RESULTS AND DISCUSSION

Effect of acidity on the extraction kinetics

In the rare earth separation process, the acidity of aqueous phase is changeable and it is necessary to study the effect of acidity on the extraction kinetics. Figure 1 showed the relationship of $\ln[(1/\beta+1)C^a_b/C^a_{b,o}-1/\beta]$ with extraction contacting time t at various acidity, where $\ln[(1/\beta+1)C^a_b/C^a_{b,o}-1/\beta]/-S¡¤K(\beta+1)t/V^a$ was defined as ln(f)/coeff. Good linear relationship between ln(f)/coeff and time can be obtained in both hydrochloric acid (Figure 1a) and nitric acid (Figure 1b) solution. It also indicated the extraction were governed by diffusion process in these conditions which was same as the regime in the diluted concentration.

Figure. 1 Relationship of $\ln[(1/\beta+1)C^a_b/C^a_{b,o}-1/\beta]$ with time at various acidity in HEH/EHP-mineral acid- heptane system

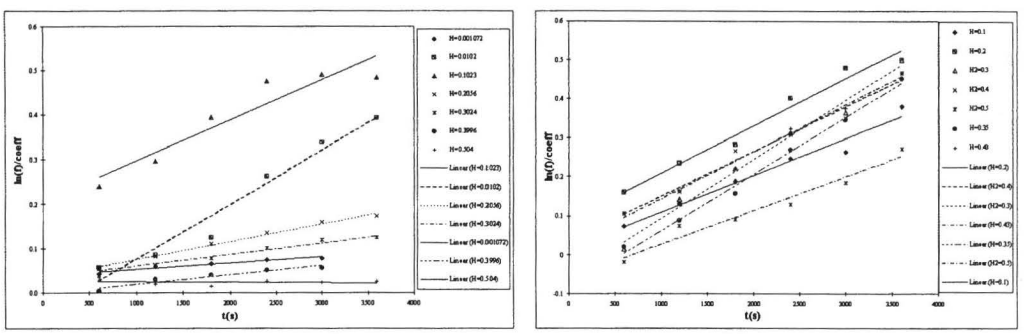

$C_{HEH/EHP}$=1.5M, $C_{Er(III)}$=0.4M, T=30°C, U^a=3.3cm/s, U^0=3.3cm/s, S=3.5×6cm^2

Figure 2 shows the effect of acidity on the Er(III) extraction rate by HEH/EHP. The extraction rate decrease in the region of pH 3.0 to $[H^+]$=0.5 mol/L HCl, however the extraction rate increase with the increase in the acidity in the region of 0.1-0.3 mol/L HNO_3 and decrease above 0.3 mol/L HNO_3. It shows that the extraction rate in nitric acid medium (Figure 2b) is greater than that in hydrochloric acid medium (Figure 2a) and the existence of NO_3^- benefit the mass transfer, this maybe due to there is another extraction reaction(equation 2) besides the ion exchange reaction of Er(III) and HEH/EHP.

$$Er^{3+} + 3(HL)_2 \rightleftharpoons Er(HL_2)_3 + 3H^+ \quad (1)$$

$$Er^{3+} + 3NO_3^- + n(HL)_2 \rightleftharpoons Er(NO_3)\cdot 2nHL \quad (2)$$

The extraction was accelerated because NO_3^- involved in the extraction reaction, with the increase of nitric acid, the free nitrate ion increase and the solvent reaction became the important and it make the extraction rate increase. On other hand with the increase of acidity the distribution ratio decrease which would lead the decrease of extraction rate.

Effect of concentration of Er(III) on the extraction kinetics

Figure 3 shows the relationship of $\ln[(1/\beta+1)C^a_b/C^a_{b,o}-1/\beta]$ with time at various concentration of Er(III) in HEH/EHP-HNO3-heptane system. A good linear fit between ln(f)/coeff and time was obtained. It shows the concentration of Er(III) did not change the control step of extraction. Figure 4 shows the extraction rate increase a little with the increase in the concentration of Er(III).

Figure 2 Effect of acidity on extraction rate in HEH/EHP-mineral acid- heptane system

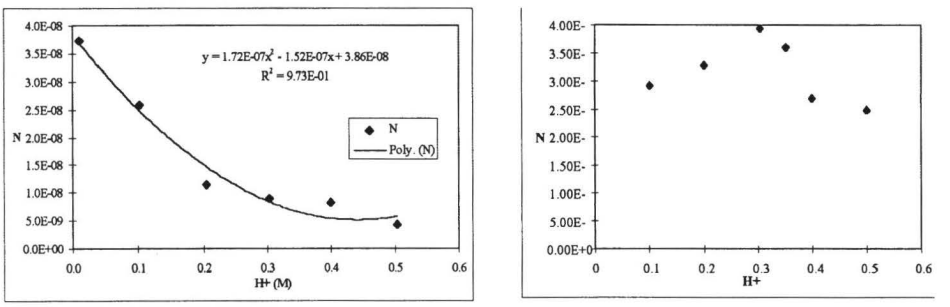

$C_{HEH/EHP}$=1.5M, C_{ErCl3}=0.4M, T=30°C, U^a=3.3cm/s, U^0=3.3cm/s, S=3.5×6cm^2

Figure 3 Relationship of $\ln[(1/\beta+1)C^a_b/C^a_{b,o}-1/\beta]$ with time at various concentration of Er(III) in HEH/EHP-HNO_3- heptane system

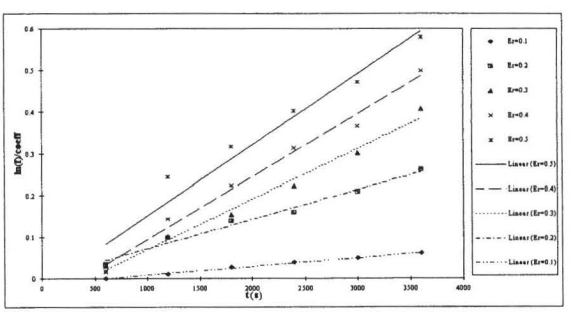

$C_{HEH/EHP}$=1.5M, C_{HNO3}=0.3M, T=30°C,U^a=3.3cm/s, U^0=3.3cm/s, S=3.5×6cm^2

Figure 4 Effect of concentration of Er(III) on extraction rate in HEH/EHP-mineral acid- heptane system

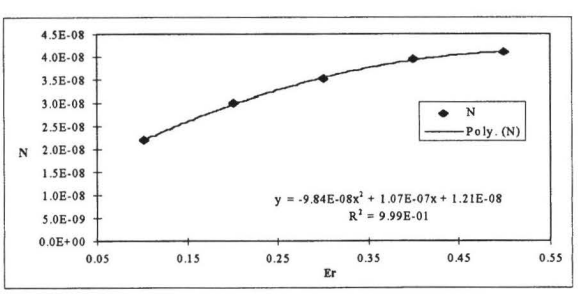

$C_{HEH/EHP}$=1.5M, C_{HNO3}=0.3M, T=30°C, U^a=3.3cm/s, U^0=3.3cm/s, S=3.5×6cm^2

Effect of additive N263 on the extraction kinetics

Figure 5 shows the relationship of ln(f)/coeff with time at various concentration of N263 in HEH/EHP-HNO_3- heptane system. Linear fit between ln(f)/coeff and time was obtained. It shows the addition of N263 did not change extraction regime. Figure 6 shows the extraction rate increase with the increase in the concentration of N263, however with respect to hydrochloric acid medium the extraction rate is lower than without additive, with respect to nitric acid medium the addition of N263 benefit the extraction.

Figure 5 Relationship of $\ln[(1/\beta+1)C^a_b/C^a_{b,o}-1/\beta]$ with time at various concentration of N263 in HEH/EHP-HNO_3- heptane system

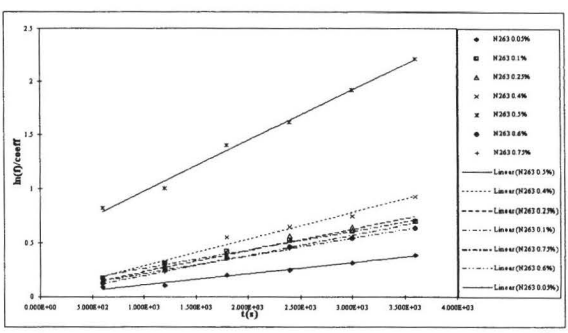

$C_{HEH/EHP}$=1.5M, $C_{Er(NO3)3}$=0.4M, C_{HNO3}=0.3M, T=30°C U^a=3.3cm/s, U^0=3.3cm/s, S=3.5×6cm^2

Figure 6 Effect of concentration of N263 on extraction rate in HEH/EHP-mineral acid- heptane system

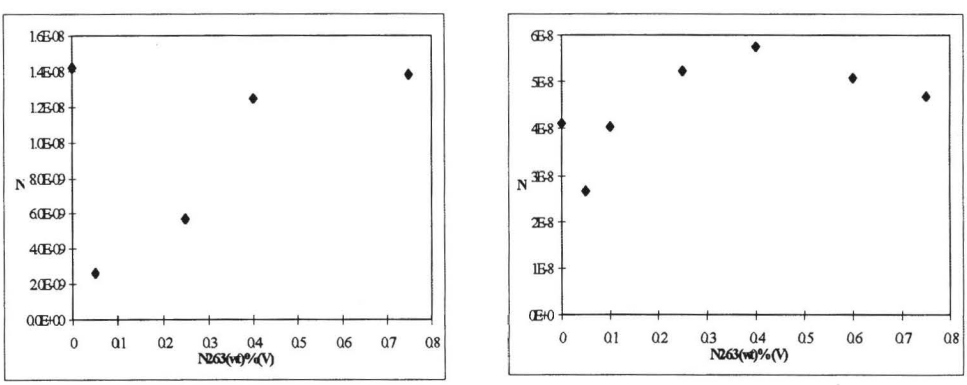

$C_{HEH/EHP}$=1.5M, C_{Er}=0.4M, C_{H+}=0.3M, T=30°C V^a=3.3cm/s, U^0=3.3cm/s, S=3.5×6cm^2

NOTATION

C^a_b	concentration of component in aqueous phase	U^a	fluid's velocity of the aqueous phase
$C^a_{b,o}$	initial concentration of component in aqueous phase	V	volume of phase
K	mass transfer coefficient	β	distribution coefficient
N	mean molar rate of mass transfer	b	bulk phase
S	area of the interface	0	start state
T	Temperature	o	organic phase
t	time	a	aqueous phase
U^o	fluid's velocity of the organic phase		

ACKNOWLEDGEMENT

The authors gratefully acknowledge the support provided for this work by the National Science Committee on "The Basic Research of Rare Earth Science" and National Natural Science Foundation.

REFERENCES

1. Li DQ, Wan X, Lin DZ, Xie YF, Lin SX, Wang ZH, Li H and Ji EY, *Proc. ISEC'80*, Liege, Belgium, **3**, 80, (1980)
2. Sato T, *Hydrometallurgy*, **22**, 121 (1989)
3. Li DQ and Zheng Z, *Value Adding Through Solvent Extraction (ISEC'96)*, edited by D. C. Shallcross et al., Melbourne, 237, (1996)
4. Sun D, Yue S and Li DQ, *Solvent Extraction in the Process Industry(ISEC'93)*, edited by D. H. Logsdail and M J Slater. 391, (1993)
5. Yue ST and Li DQ, *Solvent Extraction 1990*, Edited by T. Sekine, 811, (1992)
6. Zheng Z, Lu J, Li DQ and Ma GX, *Chem. Engng Sci.*, **53(13)**, 2327, (1998)
7. Zhong Z and Li DQ, *Acta Metallurgica Sinca*, **8(1)**, 52, (1995)
8. Komatsu Y and Freiser H, *Anal. Chim. Acta*, **227**, 397, (1989)

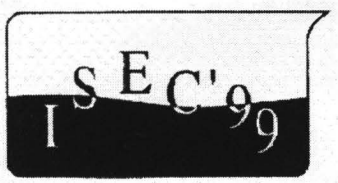

THE RULE OF TRANSITION OF EXTRACTION KINETICS BEHAVIOUR OF RARE EARTH ELEMENTS WITH DMHMP

Ducheng Sun [1], Shantang Le [2] and Deqian Li [3]

[1]Department of Chemistry, Xinjiang University, Urumuqi, 830046, China

[2]Department of Chemistry, Huboi Teachers College, Huangshi, 435002, China

[3]Changehun Institute of Applied Chemistry, Chinese Academy of Sciences, Changchun, 130022, China

ABSTRACT

On the basic theory of extraction kinetics, the rule of transition of extraction kinetics behaviour of rare earth elements with di-(1-methylheptyl)methyl phosphate (DMHKP, P350) has been studied using a stirred Lewis cell in this paper. The transitional rules of distribution ratio and separation factor of rare earth elements with time are discussed. The forward rate constant (kf) and the backward rate constant (kb) are measured. The 'tetrad effect', the 'oblique W effect', the 'Oddo-Harkins rule' and the 'gadolinium break ' phenomena of the rate constants have given for the first time in extraction kinetics of neutral extractants

Keywords: extraction kinetics, rare earth elements, di-(1-methylheptyl)methyl phosphate, Lewis cell

INTRODUCTION

Di-(1-methylheptyl)methylphosphate (DMHMP, P350) is an excellent extractant for the extraction separation of rare earths.[1] Recently the rule of transition of extraction kinetics behaviour of rare earth elements with 2-ethylhexylphosphonic acid [HEH(EHP)]was reported.[2] This work indicates that the 'tetrad effect', the 'oblique W effect', and the 'gadolinium break' phenomenon of the rate constants have given for the first time in extraction kinetics. However, the rule of transition of extraction kinetics behaviour of rare earth elements with DMHMP has not previously reported. The present work reports these studies on the rule of transition of extraction kinetics behaviour of rare earth elements with DMHMP.

EXPERIMENTAL

DMHMP was supplied by Shanghai Institute of Organic Chemistry, Chinese Academy of Sciences and was purified with $NaCO_3$. Sulphonating kerosene (fraction = 185-225°C) was employed as diluent. The stock solution of RE(III) was prepared by dissolving its oxide (purity>99.9%) in concentrated nitric acid. Other chemicals wore of analytical reagent grade.

The concentration of RE(III) in aqueous phase or organic phase (after stripping with a solution of 4 mol/dm^3 HNO_3) was determined volumetrically. The experimental apparatus and procedures for the studies of extraction kinetics of RE(III) by the constant interfacial area stirred cell have been described.[3] The extraction experiments were carried out at 25 ± 1°C.

RESULTS AND DISCUSSION

The rate of mass transfer of RE(III) from an aqueous phase into an organic phase can be described as a simple approach to equilibrium

$$RE\ (III) \underset{kb}{\overset{kf}{===}} RE\ (III)_{(o)} \qquad (1)$$

where subscript (o) represents organic phase and aqueous phase has no sign, , and kf and kb, represent the rate constant from aqueous to organic phase and the organic to aqueous phase respectively.

© 2000 Society of Chemical Industry

Assuming that the RE(III) is initially introduced into the aqueous phase, then the rate of change of RE(III) in the organic phase can be describes by the following equations:[4]

$$\frac{V}{A}\frac{dC_{RE(III)(o)}}{dt} = k_f C_{RE(III)} - k_b C_{RE(III)(o)} \qquad (2)$$

$$\frac{Ci - Ce}{Ci} \ln \frac{Ci - Ce}{Ct - Ce} = \frac{A}{V} k_f t \qquad (3)$$

$$\frac{Ce}{Ci} \ln \frac{Ci - Ce}{Ct - Ce} = \frac{A}{V} k_f t$$

where A is the area of the interface (cm^2), Y is the volume of the organic phase. Ci, Ce, Ct refer to $[RE(III)]_{(o)}$ at initial , equilibrium and t time, t represents the time (min)of the reaction.
From this equation it can be shown that plots of [(Ci-Ce)/Ci]/ln[(Ci-Ce)/(Ct-Ce)].or (Ci/Ce)ln[(Ci--Ce)/(Ct-Ce)] vs time have a slope to the rate constant kf or kb.

The verification of being first order reaction for RE(III)

This is confirmed by the plots shown in figure 1.

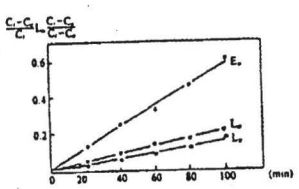

Figl. The verification of being first order reaction for RE(III)

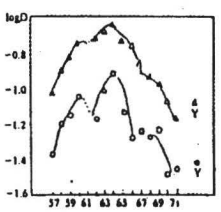

Fig2. Relationship between the distribution and the atomic number

△-the equilibrium stage of extraction process
O-the initial stage of extraction process

The rule of transition of distribution ratio (D)

The data of table 1 and figure 2 show: (1) the distribution ratios of RE(III) increase with increasing the time of extraction; (2) the time of extraction equilibrium of rare earth elements is similar and in the same unit time the increasing value of distribution ratio corresponds to increasing atomic number; (3) the 'tetrad effect' phenomenon exists not only in the equilibrium stage of extraction process,[1,5] but also in the initial stage of extraction process.

The kinetic property of separation factor (β)

The data of table 1 indicate that the most values of separation factors for most of rare earth elements have been obtained in the initial stage of extraction process and there is no marked change with time for all extraction processes.

Similar results were found previously for the extraction of RE(III) by HEH(EHP) from chloride solution.[2]

RE element		Time (minutes)						
		0	20	40	60	80	100	infinity
La	Ct	0.0418	0.0401	0.0396	0.0388	0.0387	0.0385	0.0382
	D	0	0.042	0.056	0.077	0.080	0.086	0.094
Ce	Ct	0.0421	0.0396	0.0390	0.0384	0.0382	0.0378	0.0373
	D	0	0.063	0.079	0.096	0.102	0.114	0.129
	β(Ce/La)	0	1.499	1.410	1.247	1.276	1.326	1.372
Pr	Ct	0.0395	0.370	0.361	0.0356	0.0352	0.0348	0.0344
	D	0	0.068	0.094	0.11	0.122	0.135	0.148
	β(Pr/Ce)	0	1.080	1.190	1.145	1.196	1.185	1.147
Nd	Ct	0.0426	0.0390	0.0384	0.0371	0.0369	0.0366	0.0360
	D	0	0.093	0.110	0.149	0.156	0.165	0.184
	β(Nd/Pr)	0	1.368	1.170	1.355	1.279	1.222	1.244
Sm	Ct	0.0406	0.0382	0.0361	0.0356	0.0350	0.0344	0.0341
	D	0	0.063	0.125	0.140	0.160	0.180	0.191
Eu	Ct	0.0411	0.0373	0.0356	0.0350	0.0344	0.0341	0.0339
	D	0	0.102	0.154	0.174	0.195	0.205	0.212
	β(Eu/Sm)	0	1.618	1.232	1.242	1.218	1.139	1.110
Gd	Ct	0.0401	0.0356	0.0344	0.0338	0.0332	0.0327	0.0325
	D	0	0.126	0.166	0.186	0.208	0.226	0.234
	β(Gd/Eu)	0	1.235	1.078	1.070	1.066	1.103	1.104
Tb	Ct	0.0412	0.0384	0.0376	0.0362	0.0360	0.0351	0.0348
	D	0	0.073	0.096	0.138	0.144	0.177	0.184
	β(Tb/Gd)	0	0.579	0.578	0.742	0.693	0.783	0.786
Dy	Ct	0.0413	0.0390	0.0378	0.0367	0.0361	0.0356	0.0350
	D	0	0.059	0.093	0.125	0.144	0.160	0.180
	β(Dy/Tb)	0	0.808	0.969	0.962	1.000	0.904	0.978
Ho	Ct	0.0418	0.0395	0.0384	0.0376	0.0373	0.0370	0.0367
	D	0	0.058	0.089	0.112	0.121	0.130	0.139
	β(Ho/Dy)	0	0.983	0.957	0.896	0.840	0.812	0.772
Er	Ct	0.0422	0.0401	0.0395	0.0390	0.0384	0.0382	0.0378
	D	23	0.055	0.071	0.085	0.102	0.107	0.119
	β(Er/Ho)	0	0.948	0.797	0.759	0.843	0.823	0.858
Tm	Ct	0.0401	0.0378	0.0373	0.0370	0.0367	0.0365	0.0362
	D	0	0.061	0.075	0.084	0.093	0.099	0.108
	β(Tm/Er)	0	1.109	1.056	0.988	0.912	0.925	0.907
Yb	Ct	0.0402	0.0390	0.0386	0.0380	0.0375	0.0373	0.0371
	D	0	0.031	0.041	0.058	0.072	0.078	0.084
	β(Yb/Tm)	0	0.508	0.547	0.691	0.774	0.788	0.778
Lu	Ct	0.0416	0.0401	0.0397	0.0394	0.0392	0/0391	0.0390
	D	0	0.037	0.048	0.056	0.061	0.064	0.067
	β(Lu/Yb)	0	1.193	1.171	0.956	0.847	0.820	0.797
Y	Ct	0.0412	0.0402	0.0396	0.0390	0.0387	0.0384	0.0382
	D	0	0.025	0.040	0.056	0.065	0.073	0.079

Table 1 The Experimental Data of Kinetics for the Extraction of RE(III) with DMHMP

The rule of transition kr and kb

The data of table 1 were calculated by the Least Square Method for the equation 3 with the result shown in figure 3. It indicates that the kf change from increase to decrease with the increasing value of atomic number and that kf has a periodic changing rule, which is similar to the 'Oddo-Harkins' rule.[6] There are also the 'tetrad effect' and the 'gadolinium break' phenomenon of kf in the figure 3.

Figure 4 is the relationship between the rate constant and the quantum number of orbital angular momentum of ground state. It shows the 'oblique W effect'.

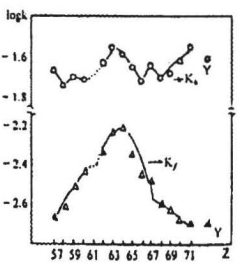

Fig3. Relationship between rate constants and the atomic number

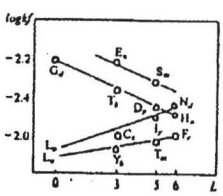

Fig3. Relationship between rate constants and L

In the above data, the position of yttrium is near to the position of holmium which suggests that the ionic radius of RE(III) has the important effect.[6] However, the 'gadolinium break' phenomenon indicates that the above rules are also under the influence of position hinder, hydration and valence of extraction complex.

REFERENCES

1. Wang Xin-tong et al, *Rare Earth*, **3**, 25, (1986).
2. Sun Du-cheng, *Acta Chimica Sinica*, **52**, 1095, (1994).
3. Shen Jing-lanetal, *Chem. J. Chinese Univ.*, 7(8). 657, (1986).
4. Flett DS, Cox M and Heels JD, *J.Inorg.Nucl.Chem.*, **37**, 2533, (1965).
5. Sinha SP, *Helv.Chem.Acta*, **58**, 1978, (1975).
6. ZHNG Ru-hua, *Rare Earth Chemistry* , Tianjin, Publishing House of Science and Technology, 207,(1987).

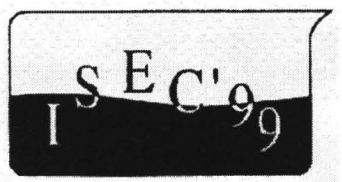

EXTRACTION OF IRON(III) FROM AQUEOUS SULPHURIC ACID SOLUTION USING A PACKED COLUMN

M Rosinda, C Ismael and Jorge MR Carvalho
Dep. Eng. Química, Instituto Superior Técnico, Av. Rovisco Pais, 1096 Lisboa Codex, Portugal

ABSTRACT
Iron recovery from an aqueous solution, using as solvent a mixture of an organophosphoric acid and a primary amine in ShellSol T, was carried out in a packed column. The influence of the pH on the efficiency of extraction was studied. Measured concentrations profiles were compared with those ones predicted by numerical simulation using the axial dispersion model. The axial mixing coefficient for continuous phase used in the model were determined experimentally, using the following expression for Peclet number (Pe_c):

$$\frac{V_c d_p}{E_c(1-\phi)e} = 0.022 + 0.03\frac{F_c}{F_d}$$

The size of the drops was measured by a photographic technique. It was also assumed that no coalescence occurs among drops.

Keywords: Iron, sulphuric acid, packed column, axial mixing, D2EHPA, Primene JMT

INTRODUCTION

A packed column was used for continuous extraction of iron from an acid aqueous sulphate solution by di(2-ethylhexyl)phosphoric acid and primary amine (JMT) in ShellSoll T. The packed column is more efficient than a spray tower and some other non-agitated columns because the packing elements increase the hold-up and decrease the axial mixing.
In this work the axial dispersion model:[1-4]

$$e(1-\phi)E_c\frac{d^2c_{Fe,c}}{dh^2} - V_c\frac{dc_{Fe,c}}{dh} - a(N_F - N_R) = 0 \qquad (1)$$

$$e\phi E_d\frac{d^2c_{Fe,d}}{dh^2} + V_d\frac{dc_{Fe,d}}{dh} + a(N_F - N_R) = 0 \qquad (2)$$

was used to predict the concentration profiles in the continuous (aqueous) and in the dispersed (organic) phases. The second derivative term in equations 1 and 2 takes into account the non-ideal phenomena of axial mixing. The boundary conditions at the bottom and at the top of column[1] are expressed by:

$$h=0 \qquad \frac{dc_{Fe,d}}{dh} = 0 \qquad -e(1-\phi)E_c\frac{dc_{Fe,c}}{dh} + V_c c_{Fe,c} = V_c c_{Fe,c,0}$$

$$h=L \qquad \frac{dc_{Fe,c}}{dh} = 0; \qquad e\phi E_d\frac{dc_{Fe,d}}{dh} + V_d c_{Fe,d} = V_d c_{Fe,d,0}$$

As published elsewhere[5,6] that expressions for the forward (N_F) and reverse (N_R) reaction rates are the following:

© 2000 Society of Chemical Industry

$$N_F = k_F^{o} \frac{\gamma_{Fe^{3+}} \alpha \, c_{Fe_{total,aq}} \, c_{B,org}}{\gamma_{H^+} c_{H^+_{aq}}} = k_F \frac{c_{Fe_{total,aq}} \, c_{B,org}}{c_{H^+_{aq}}} \quad (3)$$

$$N_R = k_R c_{Fe,org} c_{H^+_{aq}} \quad (4)$$

The composition of aqueous solution, Fe^{3+} and H^+ also the ionic strength, was defined by a set of mass balance and equilibrium equations related to the presence of Fe^{3+}, $FeSO_4^+$, $FeHSO_4^{2+}$, $Fe(SO_4)_2^-$, H^+, HSO_4^-, SO_4^{2-} in the ferric sulphate solution.[6,7] The fraction of free Fe^{3+} was determined from $\alpha = \frac{c_{Fe^{3+}}}{c_{Fe_{total}}}$. The activity coefficient (γ) for H^+ was determined by the Pitzer method [8] and for Fe^{3+} the extended Debye-Huckel law was used.[9,10]

EXPERIMENTAL

Reagents

The organic phase contains 20% (v/v) of DEHPA (di-(*2*-ethylhexyl)phosphoric acid) (Albright & Wilson), 10% (v/v) of Primene JMT (alkyl primary amines) (Rohm and Haas), 10% of 2-octanol (Riedel-de-Haen) and Shellsol T (Shell). The aqueous solutions were prepared using technical grade chemical reagents.

Equipment and procedure

The experiments were performed in a continuous scale pilot plant with a packed column. The active height was 5.9 m and the internal diameter was 0.08 m. The packing used was glass Raschig rings with d_p=1 cm, the porosity (e) of the packed bed was 0.761. The distributor for the dispersed phase had 14 holes of 3 mm diameter.

The experiments were always carried out with the aqueous phase as the continuous phase. The column was first filled with the aqueous phase and then the organic phase was introduced in the column. Under steady-state conditions, c_{out} constant, 14 samples of each aqueous and organic phase were taken from taps distributed along the column. The dispersed phase hold-up was determined from the measured volume of organic phase in the column after closing inlets and outlets of both phases. The drop diameters were measured at top and bottom of the column by photographically during the experiments.

The axial mixing studies for continuous phase were performed under transient-state conditions using tracer technique.[11] The tracer, copper sulphate solution, was introduced in the inlet of aqueous phase and samples at different time were taken at 3.46 m and 4.48 m.

The concentrations of iron (III) in both the organic and aqueous phases were directly analysed using atomic absorption spectrophotometry. The acid solutions were titrated with NaOH using Mg-EDTA as complexing agent for iron.[12]

RESULTS AND DISCUSSION

Axial mixing coefficients

The axial dispersion coefficients for the continuous phase were always determined under two-phase flow and some studies were also carried out in the presence of mass transfer. The experiments make use of tracer injection through a step-input perturbation. The E_c was calculated comparing the

transient-state concentration profiles with the theoretical ones predicted by the semi-infinite model[13] at different Peclet ($\frac{V_c d_p}{E_c(1-\phi)e}$) numbers. The experimental results are presented in figure 1.

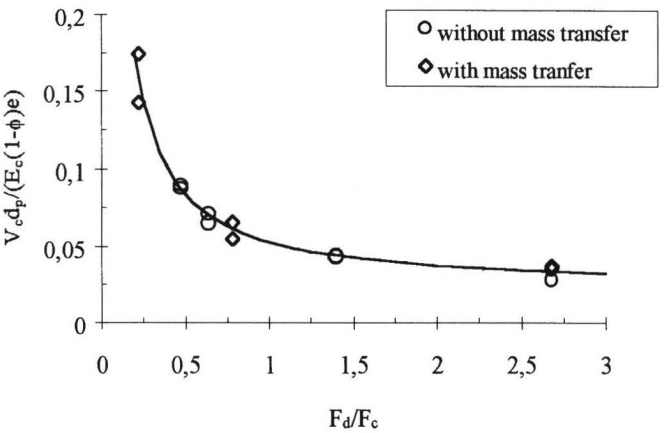

Figure 1. Peclet number for continuous phase *versus* flow ratio. Aqueous phase: $Fe_2(SO_4)_3$ = 0 or 0.134 mol/dm^3, pH=1.60; Organic phase: DEHPA = 20% (v/v), JMT = 10% (v/v), 2-octanol 10% (v/v) in ShellSol T. T = 40°C. Packed column: *L*=5.9 m, diameter=0.08 m; packing – glass Raschig rings, d_p = 0.01 m, e = 0.761.

In this system it was verified that the mass transfer process has no influence on axial mixing. The experimental data were similar to those ones published in literature for packed column.[14] The axial mixing coefficient for dispersed phase was determined assuming a constant value for the Peclet number,[15] namely:

$$\frac{V_d d_p}{E_d \phi} = 0.15$$

Numeric simulation of iron extraction in a packed column

The concentration profiles in packed column were simulated considering that the extraction process was chemical controlled.

The total concentration of free extractant and sulphuric acid along the column height were determined from mass balance considering that extractant consumed / Fe^{3+}extracted is 4 and Fe^{3+}extracted / H^+ released to aqueous phase is 2.[6] Related to the fact that sulphuric acid is not completely dissociated and Fe exists also as sulphate-complexes a set of equations (mass balance and equilibrium) was solved to determine the composition of aqueous solution at Fe^{3+}, H^+ and ionic strength.

The ODE's 1-2 were obtained by the use of the finite differences methodology. The final set of non-linear equations was solved by the aid of the numerical library routine C05PBF from NAG™

In table 1 are presented operating conditions and some parameters used, d_{32} was determined from photographs taken during the experiments.

pH_{exp}	ϕ	d_{32} (cm)	E_c (m^2s^{-1})	E_d (m^2s^{-1})	k^o_F (m/s)	k_R ($kmol^{-1}m^4s^{-1}$)
1.04	0.198	0.295				
1.24	0.204	0.315	6.88×10^{-4}	13.5×10^{-4}	1.65×10^{-5}	8.60×10^{-7}
1.60	0.200	0.315				

Table 1 Parameters used in the simulation of iron extraction in the packed column.

In figure 2 are presented the simulated concentration profiles (lines) which are compared with experimental data (marks). It was noticed that the extraction of iron is enhanced by the increase in pH and the model used predicts an extraction slightly more efficient than the real one. This could be related to the fact of the model used was very sensitive to interfacial area and consequently to drop diameter. The values of d_{32} used are determined on the top of the column that are considerably lower than the correspond values on the bottom of the column (0.46 - 0.49 cm). However when drop analysis was taken 1.5 m from packing support d_{32} it is already equal to the top value.

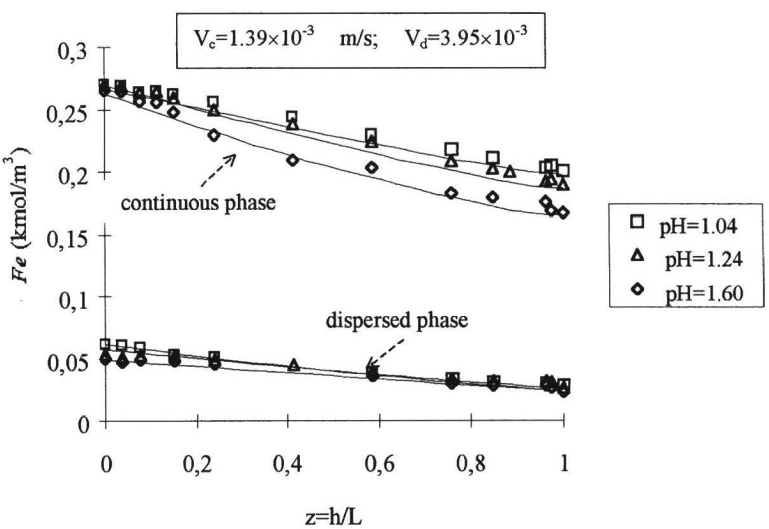

Figure 2. Simulated and experimental concentration profiles in a packed column. Aqueous phase: $Fe_2(SO_4)_3$ = 0.134 mol/dm^3 , pH = 1.0-1.6; Organic phase: DEHPA = 20%, JMT = 10%, 2-octanol 10% in ShellSol T. T = 40°C. Packed column: L = 5.9 m, diameter = 0.08 m; packing d_p = 1 cm, e = 0.761.

NOTATION

a	specific interfacial area (m^{-1})	h	height (m)
c	concentration (kmol m^{-3})	k^o	thermodynamic kinetic constant (m s^{-1})
d_{32}	Sauter mean diameter	k	kinetic constant or mass transfer coefficient (m s^{-1})
d_p	packing size (m)	L	column height (m)
E	axial mixing coefficient (m^2/s)	N	reaction rate, (kmol m^{-2} s^{-1})
e	voidage or free area	V	superficial phase velocity (m s^{-1})
F	flowrate (volumetric)		

z	fraction length
ϕ	hold-up of dispersed phase
γ_i	activity coefficient of species i

subscript

c	continuous phase
B	free extractant
d	dispersed phase
F	forward reaction
R	reverse reaction

REFERENCES

1. Lo TC, Baird MHI and Hanson C (eds), *'Handbook of Solvent Extraction'*, John Wiley & Sons, (1983)
2. Bart H-J and Marr R, *Proc. 2nd. Int. Conf. Sep. Sci. Technol.*, **1**, 274, (1989)
3. Bart H-J and Marr, R., *Chem. Eng. Sci.*, **10**, 291, (1987)
4. Pratt HRC and Stevens GW, *Ind. Eng. Chem. Res.*, **30**, 733, (1991)
5. Ismael MRC, Parreira E, Sequeira AC and Carvalho JMR *Proc. CHEMPOR'98*, **1**,167, (1998)
6. Ismael MRC, *PhD Thesis*, I.S.T. – Technical Univ. of Lisbon Portugal (in press).
7. Lee CK and Tavlarides LL, *Polyhedron*, **4 (1)**, 47, (1985).
8. Clegg SL, Rard JA and Pitzer KS, *J. Chem. Soc. Faraday Trans.*, **90(13)**, 1875, (1994).
9. Zemaitis Jr. JF, Clark DM, Rafal M and Scrivner NC, Ed. *'Handbook of Aqueous Electrolyte Thermodynamics'*, Design Institute for Physical Property Data, N.Y., (1986)
10. Dry MJ and Bryson AW, *Hydrometallurgy*, **21**, 59, (1988).
11. Kreft A and Zuber A, *Chem Eng. Sci*, **33,** 1471. (1978).
12. Rolia E and Dutrizac JE, *Can. Metall. Quart*, **23**, 159, (1984).
13. Pratt HRC and Anderson WJ, *CIM Special*, **21**, 242, (1977).
14. Godfrey JC and Slater MJ, *'Liquid-Liquid Extraction Equipment'*, John Wiley & Sons, (1975).
15. Komasawa I and Ingham J, *Chem. Eng. Sci.*, **33**, 341, (1978).

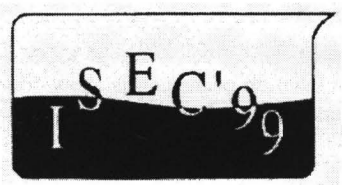

A MASS TRANSFER MODEL FOR THE EXTRACTION OF Te(IV) IN THE PRESENCE OF Se(IV) USING TRI-*n*-BUTYLPHOSPHATE AS EXTRACTANT

M Bandyopadhyay, S Datta and SK Sanyal
Chemical Engineering Department, Jadavpur University, Calcutta 700 032, India

ABSTRACT
Selenium (IV) and Tellurium (IV), two important elements which have many applications in electronic and metal alloy industries, are at present separated from anode slimes (the major source of the two elements), by a pyrometallurgical process which results in low recovery of the elements. The mechanism of Te(IV) separation form Se(IV) in hydrochloric acid media by solvent extraction with tri-n-butylphosphate in dearomatized kerosene was investigated earlier.[3] Mass transfer of Te(IV) from the acid to TBP phase was also studied[1,2] in a modified Lewis cell. The acid concentration in the aqueous phase was maintained at 4.5 mol/dm^3 . At this concentration Te(IV) transfer was appreciable.[3] Based on the results a mass transfer model was developed.[2] In the present paper simultaneous extraction of Te(IV) and Se(IV) was studied in a Lewis cell.[2] Acid concentration was maintained at 6mol/dm^3 so that Se(IV) transfer was significant along with Te(IV). The present model was developed based on the results of the previous model for individual transfer.[2] The model indicates reaction front position and extent of extraction for both Te(IV) and Se(IV) under different experimental conditions. The effect of Reynolds number and extractant concentration on the extent of extraction was also studied both experimentally and theoretically. It was significant that Se(IV) and Te(IV) were extracted in a competitive manner, Te(IV) extraction rate was much higher than Se(IV). A comparative study was made for individual and competitive transfer of Te(IV) and Se(IV) with respect to reaction front movement.

Keywords: mass transfer, modelling, selenium(IV), tellurium(IV), TBP, Lewis cell

INTRODUCTION

Mass transfer of Te(IV) between an aqueous and an organic phase was studied earlier[1,2] in a modified Lewis cell. The organic phase was composed of tri-n-butylphosphate in kerosene. The transfer rate of Te(IV) from aqueous to the organic phase was very fast particularly from 4.5 mol/dm^3 HCl solution. The rate of extraction was found to be dependent upon stirring speed up to 100 min^{-1}; on increasing stirrer speed both kinetics and diffusion can be considered instantaneous. Generally Se(IV) is separated from Te(IV) by using TBP as the extractant at 4.5 mol/dm^3 HCl concentration. This concentration of acid is very much selective for Te(IV) while Se(IV) extraction is found to be negligible due to the low solubility of the extracted compound and slow rate of extraction. At higher acid concentration, Se(IV) extraction increases and at 6 mol/dm^3 or higher acid concentration the extraction becomes simultaneous. Theoretical interpretations of the experimental data at 4.5 M acid concentration was developed earlier.[2]

In the present paper simultaneous extraction of Te(IV) and Se(IV) at 6 mol/dm^3 acid concentration was studied in detail. The present model was developed based on the results of the previous model for individual transfer.[2] The model indicates reaction front position and extent of extraction for both Te(IV) and Se(IV) at 6 mol/dm^3 acid concentration under different experimental conditions.

EXPERIMENTAL

Material

The chemicals used in the experiment were of AR grade. The concentrations of Te(IV) and Se(IV) taken for the experiment were very low, 0.836 mM and 0.0436 mM respectively, so that this does not affect the physical properties of the aqueous and the organic phases. Analytical methods adopted were same as described.[3]

© 2000 Society of Chemical Industry

Procedure

The extraction runs were carried in a batch, stirred, jacketed, Lewis cell made of glass. The detailed description of the cell and procedure are described[1] and an diagram of the cell is shown below where a = variable speed motor, b = stirrer, c = feed point, h = thermowell, e = baffle, f = sample point, g = jacket outlet and d = jacket inlet.

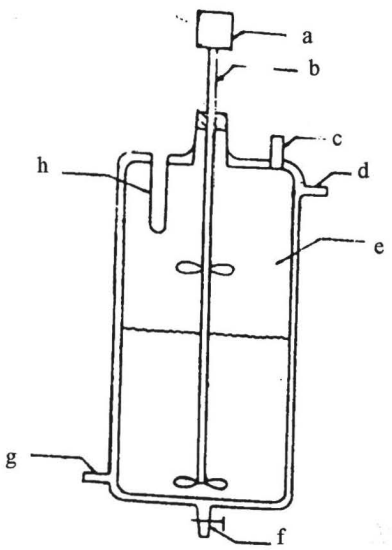

The Model

Experimental studies of the simultaneous extraction of Se(IV) and Te(IV) by TBP, at moderate speed and at HCl concentrations of 6 mol/dm^3 and above was performed earlier.[3] No change in stoichiometry was noticed for Te(IV) at the higher acid concentrations. However for Se(IV) the stoichiometry was totally different.[3]

$$SeO^{2+} + 2H^{+} + 4Cl^{-} + 2TBP = (H_2SeOCl_4).(TBP)_2 \quad (1)$$

For Te(IV) the stoichiometry was as follows:

$$Te^{4+} + 4\,Cl^{-} + 3TBP = (TeCl_4).(TBP)_3 \quad (2)$$

Other conditions remaining the same, the reaction zone thickness would change for the simultaneous extraction of Se(IV) and Te(IV) in the TBP phase. The flux equation of Se(IV) can be expressed by the following expression as the main bulk of both the phases are uniformly stirred:

$$J_{se} = -D_{se}\, a\, d[Se]/dx = -k_L a\,([Se] - [Se]_i) \quad (3)$$

A material balance over the reaction front for Se(IV) and Te(IV) yields the thickness of the reaction layer:

$$2\, d\,(4\pi R^2 L_{RF}\,[TBP]\,)/dt = -D_{se}\, a\, d[Se]/dx \quad (4)$$

For the Te(IV) as the stoichiometry is same, the material balance equation is also the same for a 4.5 mol/dm^3 acid concentration.[2]

$$3\, d(4\,\pi R^2 L_{RF}\,[\,TBP]\,)/dt = D_{Te}\, a\, d[Te]/dx \quad (5)$$

$$J_{Te} = k_L a\,(\,[\,Te] - m1[\,Te]_i\,) \quad (6)$$

$$J_{se} = -k_L a ([Se] - m2 [Se]_i) \quad (7)$$

The rate of change of reaction front for simultaneous transfer of Se(IV) and Te(IV) gives:

$$dL_{RF}/dt = - (J_{Te} + J_{se}) / (5 \times 4 \pi R^2 [TBP]) \quad (8)$$

The individual phase mass transfer co-efficient in the aqueous phase can be evaluated by the following expression :

$$J = k_L a \Delta C = -(v1/a) dc/dt \quad (9)$$

From equations 6, 7 and 9:

$$v1 \, d[Te]/dt = J_{Te} = a [Te] / [1/k_{L1} + m1 (L - L_{RF})/D_{Te}] \quad (10)$$
$$v1 \, d[Se]/dt = J_{Se} = a [Se] / [1/k_{L2} + m2 (L - L_{RF})/D_{Se}] \quad (11)$$

Introducing the dimensionless groups and following variables, three different differential equations are formed.

$h1 = [Te] / [Te]^0$ $\quad$ $h2 = [Se] / [Se]^0$

$E1 = v/3v . [Te]^0 /[TBP]$ $\quad$ $E2 = v/2v . [Se]^0 / [TBP]$

$D = D_{Se} / D_{Te}$ $\quad$ $v/3v$ $\quad$ $AL = v$

$Bi1 = k_{L1} L m1 / D_{Te}$ $\quad$ $Bi2 = k_{L2} L m2 / D_{Se}$

$\beta = L_{RF} / L$ $\quad$ $\tau = DT/L^2$

We get,

$$dh1/d\tau_{Te} = - h1 \, n \, Bi1 /(m1[1+ Bi1 (1-\beta)]) \quad (12)$$
$$dh2/d\tau_{Se} = - h2 \, n \, Bi2 \, D/(m2[1+ Bi2 (1-\beta)]) \quad (13)$$
$$d\beta/d\tau_c = - E1 \, h1 \, Bi1 \, n/ m1 [1 + Bi1 (1-\beta)] - E2 \, h2 \, Bi2 \, n \, D/m2 [1+ Bi2 (1-\beta)] \quad (14)$$

RESULTS AND DISCUSSIONS

It was assumed that the distribution co-efficient at the interface was the same as for the bulk concentrations. The distribution co-efficient was calculated from the equilibrium values of aqueous and organic phase metal concentrations. The Wilke-Chang correlation was used to calculate the diffusion co-efficient. Aqueous phase mass transfer co-efficient was calculated from equations 5 and 6 assuming the overall mass transfer coefficients is effectively the aqueous phase mass transfer coefficient provided both the metals are strongly extracted at 6 mol/dm^3 acid concentration. Detailed calculation of k_L was given earlier.[1]

To use the model, the equations were numerically solved using the fourth order Runge-Kutta method. Experimental and theoretical results were compared using an adjustable parameter, the distribution co-efficient for different TBP concentrations. This experimental and theoretical results are shown in figures 1- 5 for simultaneous extraction of Se(IV) and Te(IV) at 6 mol/dm^3 acid concentration.

From the above figures it was observed that Te(IV) extraction rate is much higher than that of Se(IV) extraction even at 6 mol/dm^3 acid concentration. For the smaller value of t, say 100 x 10^{-5}, the depletion of TBP is mainly due to Te(IV) extraction. From the tables 1 - 4 it is seen that the reaction front increases as the TBP concentration decreases. This is due to the availability of TBP at the interface at higher concentration. Comparison of reaction front movement for single metal transfer, i.e. Te(IV),[2] with the simultaneous extraction of Se(IV) and Te(IV) further indicates that the reaction front movement for the initial period is almost same, i.e., Se(IV) extraction is negligible during this period. But for a larger value of t, the change in reaction front position is much rapid for simultaneous extraction. For increasing consumption of TBP the resistance to diffusion increases because the solutes will now have to move a greater distance to reach the reaction front. Se(IV) has to move a greater distance to reach the reaction front because of the presence of Te(IV).

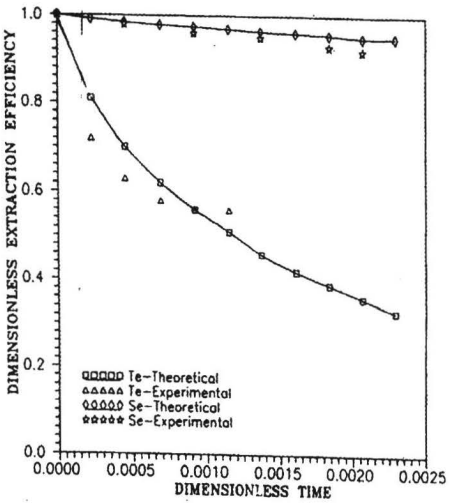

Figure 1. Extraction rate of Se(IV) and Te(IV) from 6 mol/dm acid solution by 1 vol% TBP

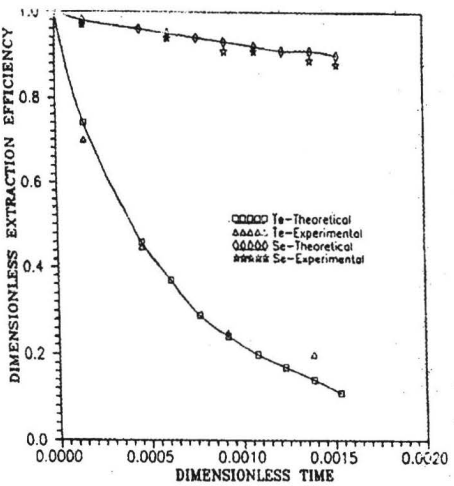

Figure 2. Extraction rate of Se(IV) and Te(IV) from 6 mol/dm^3 acid solution by 3 vol% TBP

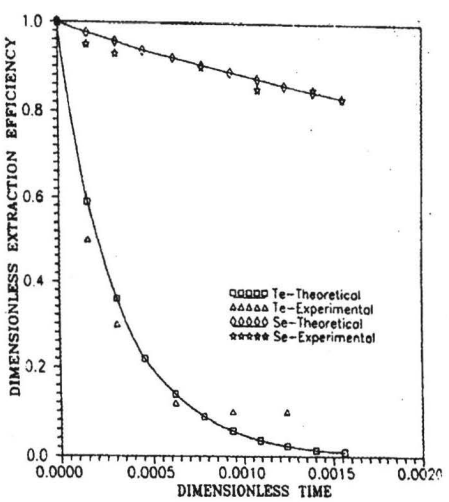

Figure 3. Extraction rate of Se(IV) and Te(IV) from 6 mol/dm^3 acid solution by 10 vol% TBP

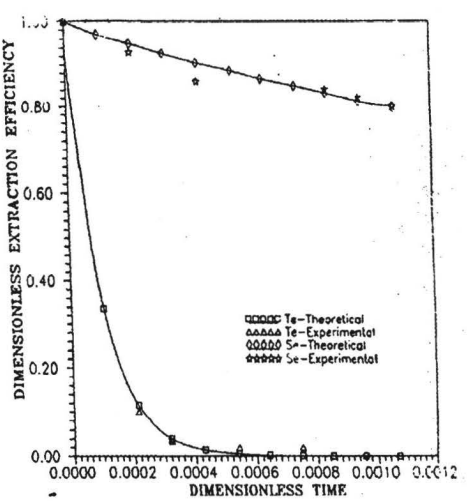

Figure 4. Extraction rate of Se(IV) and Te(IV) from 6 mol/dm^3 acid solution by 30 vol% TBP

Figures 1 and 2 predict higher value of distribution coefficients for Te(IV). This deviation may be due to unavailability of TBP at 1 or 3 vol % TBP since TBP extracts simultaneously, Te, Se, acid and water. Therefore, a crowding effect may occur and it reduces the extraction efficiency. The deviation between the experimental and theoretical results reduces with the increase in TBP concentration.

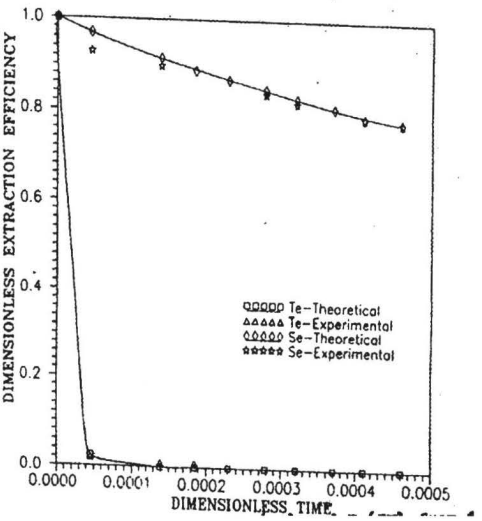

Figure 5. Extraction rate of Se(IV) and Te(IV) from 6mol/dm^3 acid solution by 100 vol% TBP

From the figures it is observed that a large deviation occurs in the experimental and theoretical data for Se extraction at the initial period. The reaction between Te and TBP is favoured compared to Se with TBP even at 6 mol/dm^3 acid concentration. It is presumed that initially the reaction front movement is solely due to reaction between Te and TBP. But in the model, it is assumed that the reaction front moves due to the combined effect of Te and Se starting from the initial stage of extraction. Therefore, the movement of reaction front is faster during the initial period as is evident from the theoretical prediction and the deviation is high for Se at the initial stage.

Dimensionless time $D_{Te}T/L^2$	L_{RF}/L
0.00000	1.0000
0.00023	0.9991
0.00092	0.9979
0.00184	0.9970
0.00229	0.9968

Table 1 Change in reaction front position at 1 vol % TBP for simultaneous extraction of Se and Te at 80 rpm stirrer speed

Dimensionless time $D_{Te}T/L^2$	L_{RF}/L
0.00000	1.0000
0.00031	0.9993
0.00062	0.9989
0.00092	0.9987
0.00123	0.9985
0.00138	0.9985

Table 2 Change in reaction front position at 3 vol % TBP

Dimensionless time $D_{Te}T/L^2$	L_{RF}/L
0.00000	1.00000
0.00016	0.99979
0.00047	0.99958
0.00094	0.99946
0.00104	0.99942

Table 3 Change in reaction front position at 10 vol % TBP.

Dimensionless time $D_{Te}T/L^2$	L_{RF}/L
0.00000	1.00000
0.00005	0.99993
0.00014	0.99988
0.00032	0.99982
0.00042	0.99980

Table 4 Change in reaction front position at 100 vol % TBP

NOMENCLATURE

a	interfacial area
D_{metal}	molecular diffusivity
J	metal flux
k_L	aqueous side mass transfer co-efficient
L	height of the organic liquid phase
L_{RF}	height of the unreacted organic liquid phase
m	distribution co-efficient , [metal]/[metal]
V	volume of organic phase

REFERENCES

1 Bandyopadhyay M, Datta S and Sanya, SK. *Hydrometallurgy*, **42**, 115-123, (1996).
2 Bandyopadhyay M, Datta S and Sanyal SK. *Hydrometallurgy*, **43**, 175-185, (1996).
3 Chowdhury MR and Sanyal SK. *Hydrometallurgy*, **32**, 189-200, (1993).

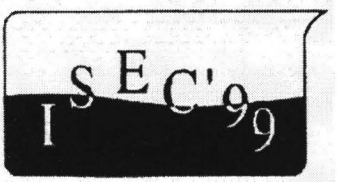

EXTRACTION CHROMATOGRAPHY: EQUILIBRIA AND KINETICS

Alex Schöneberger[1], Hans-Jörg Bart[1], Anshu Nanoti[2] and Andreas Wildberger[1]

[1]Lehrstuhl Thermische Verfahrenstechnik, Universität Kaiserslautern, Germany

[2]Indian Institute of Petroleum, Dehradun, India

ABSTRACT

The separation of zinc from aqueous solutions using solvent-impregnated-polymers (SIR) was examined. Porous resins e.g. Amberlite (XAD 4; XAD 16) and a functionalized inorganic polymer (Deloxan APII) were used as supports and contained di-(2-ethylhexyl)phosphoric acid (D2EHPA) as ion exchanger. The equilibrium distribution of zinc was measured and the mass transfer kinetics have been examined in a stirred cell. Mass transfer kinetics can be increased dramatically when using Deloxan APII instead of the Amberlite supports, due to the different internal pore structures. The transfer of anions with the functionalized Deloxan APII, is also discussed.

Keywords: impregnated polymer, extraction chromatography, aminopoly-siloxane, reactive sorption, extraction kinetics, zinc, D2EHPA, XAD 4, XAD 16

INTRODUCTION

SIR's combine the techniques of adsorption with reactive extraction. In this method liquid ion-exchangers, known for their reactive extraction, are first adsorbed by macroporous polymers to create a SIR. The solute then reacts with the liquid ion-exchanger on the resin. The method combines the advantages of a sorption process, the preferable application in the ppm scale, with that of the reactive extraction with the great variety of available liquid ion-exchangers. One problem of the method is, that kinetics may be slow, depending on the polymers and pore sized used.[3] Investigations with di-(2-ethylhexyl)phosphoric acid immobilised on silica show, that the mass transfer kinetics can be increased dramatically by variation of the support.[4] In this paper equilibria and mass transfer are measured and discussed using different organic porous polymers (Amberlites) and an inorganic material with a hydrophobic and functionalized surface (Deloxan APII). Di-(2-ethylhexyl)phosphoric acid is used for the separation of zinc from aqueous solution. The effects of co-extraction of anions by means of the amino-functions on Deloxan APII are also considered briefly.

EXPERIMENTAL

Materials used

The di-(2-ethylhexyl)phosphoric acid cation exchanger (AH) was used from BAYER (Baysolvex) with the following assay: AH 97.3%, monoacid 0.5%; impurities 2.2%. Hexane (Merck, 96%) used for impregnation was distilled to remove impurities. All the other reagents are standard chemicals of analytical grade and are used without any further purification: [zinc chloride (FLUKA, puriss. p.a.), hydrochloric acid, 1 mol/dm^3, (Fixanal, Riedel de Haen)]. The polymers were washed with distilled water and acetone A.R. and than dried. The physico-chemical properties are summarised in the Table 1. Some experiments were carried out by protonating the functionalized groups of Deloxan APII. Protonation was carried out by mixing 2 mol/dm^3 HCl, followed by water washing (100 bed volumes) to simulate a sorption cycle with acid regeneration.

An impregnation method reported by Traving et al.[5] was used. The AH-loading on the polymer was determined by weight balance as well as by CHN-analysis. The loadings were found to be comparable with both methods. Equilibria and kinetic experiments were carried out at 25°C in a mechanical shaker and in a stirred vessel, respectively. pH was measured using a WTW pH-Ion-Meter (pMX 2000), zinc was analysed by atomic absorption spectrophotometer (HITACHI Z 8100) and the chloride concentration was determined by silver nitrate titration with a METTLER-titrator.

© 2000 Society of Chemical Industry

Carrier material	XAD 4	XAD 16	Deloxan AP II
Manufacturer	Rohm & Haas	Rohm & Haas	DEGUSSA
Surface area	760 m^2/g	860 m^2/g	600 m^2/g
Bead size	0,3 - 1,2 mm	0,3 - 1,2 mm	0,2 - 0,5 mm
Average pore diameter	5,5 - 8 nm	20 - 25 nm	30 nm
Material	styrene/divinylbenzene copolymer	Divinylbenzene polymer	aminopolysiloxane

Table 1 Properties of the polymers

RESULTS AND DISCUSSION

Equilibria

The result of the equilibrium experiments with different initial pH-values is shown in figure 1. Like in solvent extraction, the following mass balance must hold:

$$Zn^{2+} + 2b\ \overline{AH} \leftrightarrow \overline{ZnA_2(AH)_{2\cdot b-2}} + n\ H^+ \qquad (1)$$

The mass balance in its logarithmic form reads as:

$$\log D = n\ pH + (\log K_1 + b\ [AH]) \qquad (2)$$

where D is the distribution coefficient and K_1 the equilibrium constant of equation 1. Slope analysis of both systems (Deloxan APII amd Amberlite) of the zinc extraction reveals 'n' to equal 2, the slope 'b' for the Amberlites is 3, which is in accordance with extraction literature.[6] The distribution coefficients with Deloxane used are higher (figure2) compared to the Amberlite (XAD 4, XAD 16). This indicates the effect of the support on the zinc separation, since obviously the polysiloxan support with even the smallest inner surface has promoted the activity of AH and thus the extraction equilibria. This change in activity causes even a deviation from the slope 'b' with Deloxan (b = 3.7).

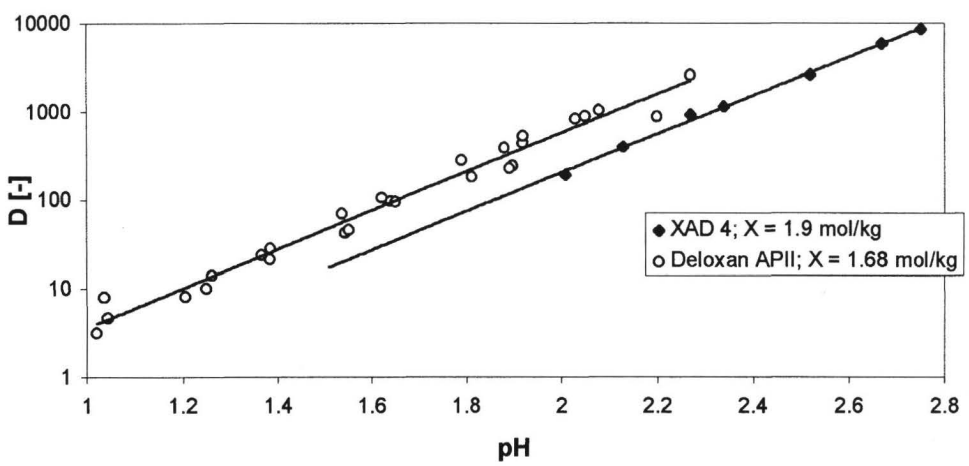

Figure 1. Distribution coefficient v/s pH with different supports

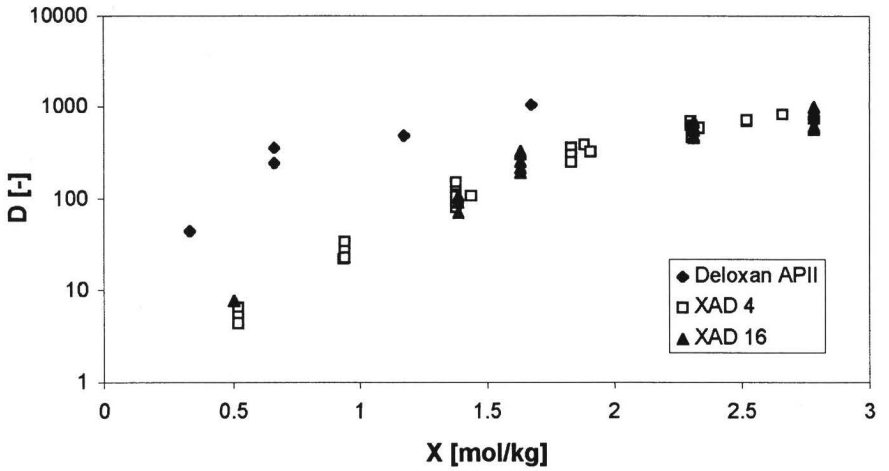

Figure 2. Distribution coefficient v/s AH-loading with different supports

Deloxan with its aminopolysiloxan structure enables also anion extraction according equation 3:

$$HCl + \overline{R_3N} \Leftrightarrow \overline{R_3NHCl} \tag{3}$$

with the equilibrium constant :

$$K_2 = \frac{c_{\overline{R3NHCl}}}{c_{HCl} \cdot c_{\overline{R3N}}} \tag{4}$$

and the mass balance:

$$c_{\overline{R3N}} = c_{\overline{R3N,0}} - c_{\overline{R3NHCl}} \tag{5}$$

Further experiments were carried out with various chloride concentrations to quantify the chloride sorption on protonated as well as on unprotonated Deloxan APII. The results are compared in figure 3 and can be described by the following equation, calculated from equations 4 and 5:

$$C_{Cl,s} = \frac{K_2 \cdot c_{HCl,a} \cdot c_{\overline{R3N,0}}}{1 + K_2 \cdot c_{HCl}} \tag{6}$$

The equilibrium constant K_2 for both curves is 60 dm^3/mol. The concentration of amine-groups $c_{R3N,0}$ that are able to react with chloride is 2.4 mol/kg at the unprotonated Deloxan APII (see upper line in figure 3) which is comparable to the results of the CHN-analyses (2.3 mol/kg nitrogen in the Deloxan APII). The analysis of the protonated Deloxan (bottom line in figure 3) indicates that 1.2 mol/kg amine-groups are available for anion exchange, which is independent of the AH-loading of the polymer.

Kinetics

Experiments were carried out with various loadings of D2EHPA on the polymer XAD 4 (figure 4), which can be interpreted in the following way. In the first step small pores are first filled with the ion exchanger during impregnation. Than the bigger pores are loaded with D2EHPA.[7] This is confirmed by the experiments shown in figure 4, because the equilibrium is reached earlier, if the loading of D2EHPA is high. In the larger pores the diffusion is fast and the zinc complexes can easily be formed. Because at small loadings only tiny pores are filled with the ion exchanger, the mass transfer is decelerated from the start. In comparison Deloxan APII shows a quite different behaviour

(figure 5) since equilibrium was reached within 4 minutes while XAD 4 needs hours under similar conditions. The increasing rate can be explained with the pore structure of the polymer. The pore size is larger and the pore size distribution is narrow in Deloxan APII, so the zinc complexes can easily be formed. This is also confirmed by the works of Tavlarides et al.,[4] who used a macro-porous silica as carrier material instead of Amberlite thus increasing the rate of mass transfer dramatically.

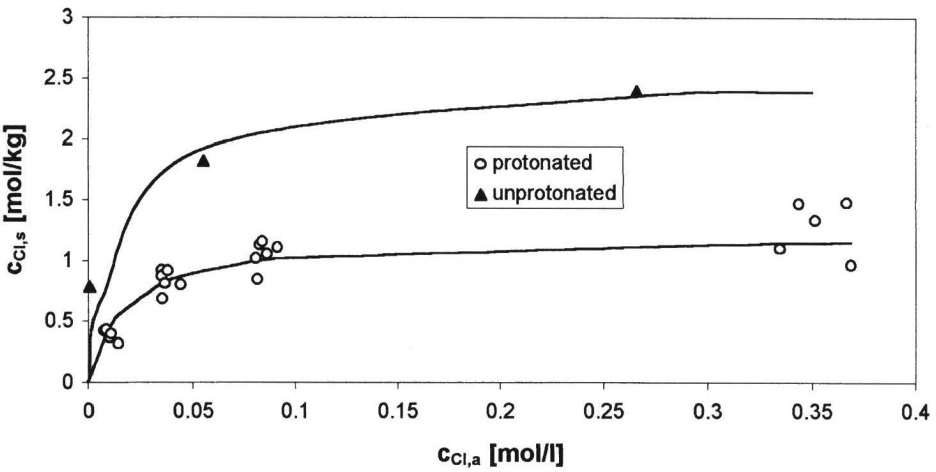

Figure 3. Chloride sorption on Deloxan APII various AH-loadings (0 - 1.67 mol/kg)

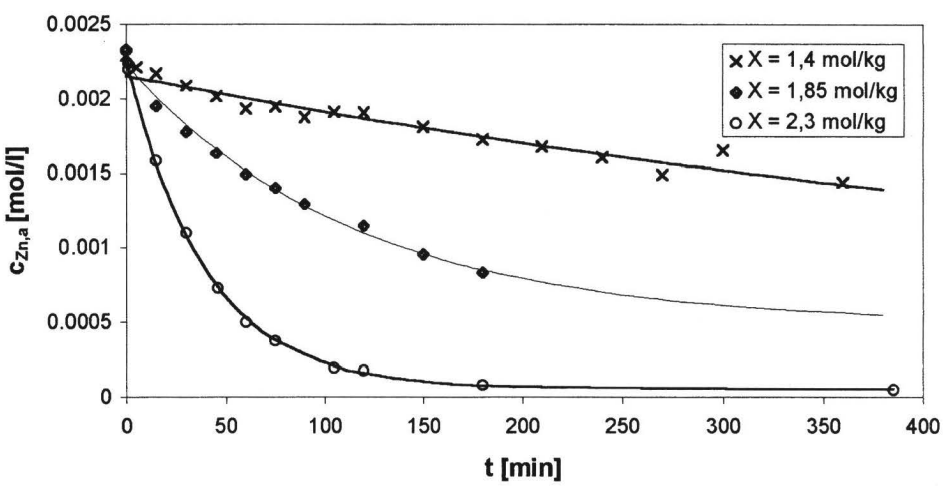

Figure 4. Experiments with various loadings of AH (2.3; 1.85; 1.39 mol/kg) on XAD 4 initial zinc concentration = 2.29 mmol; initial pH-value = 3.5;

The functionalized structure of the Deloxan APII leads to a sorption of chloride, in form of HCl, parallel to the zinc sorption. So experiments with various loadings of AH on the Deloxan APII (figure 6) show that the sorption of chloride at a lower AH-amount is more significant. This may even lead to an increase in pH-value (upper line in figure 6) and a neutralisation of the aqueous solution, according to equation 4. This has a positive effect on the very pH sensitive zinc sorption.

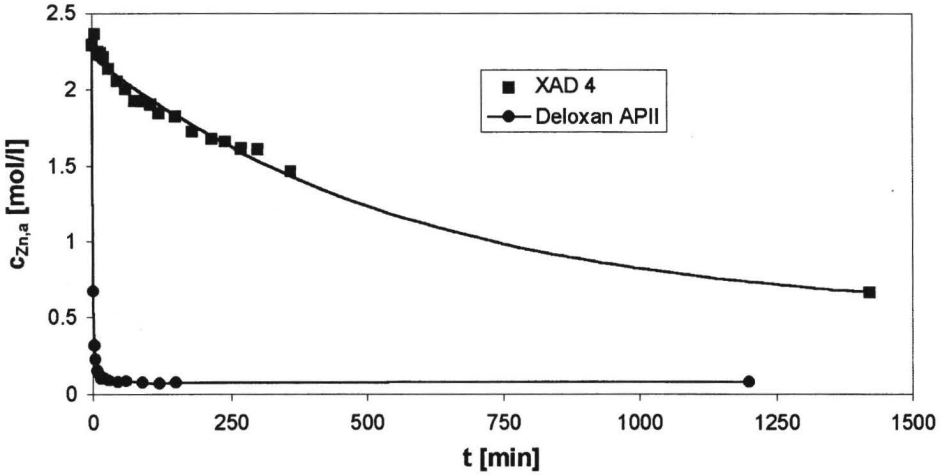

Figure 5. Comparison of XAD 4 and Deloxan APII with equal loading of AH = 1.39 mol/kg initial zinc concentration = 2.29 mmol/l; initial pH-value = 3.5.

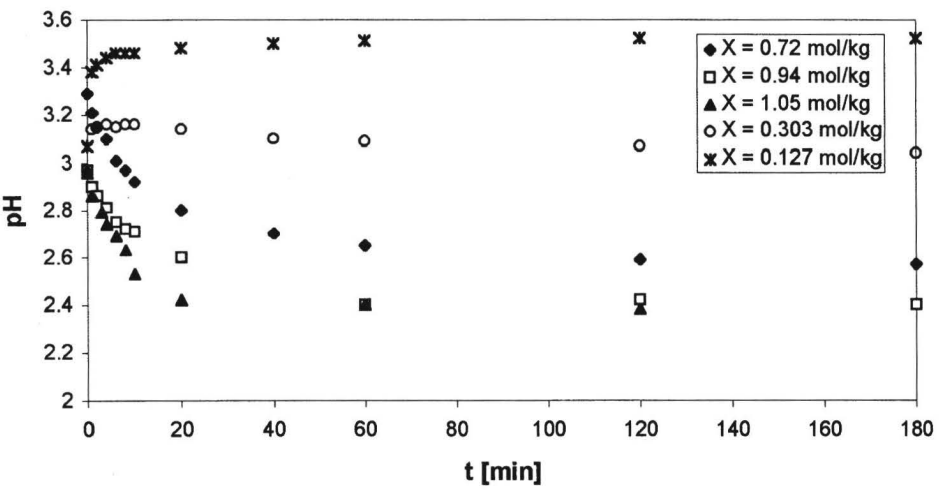

Figure 6. pH v/s time initial zinc concentration = 2.29 mmol/l; initial pH-value = 3

CONCLUSIONS

A problem with Solvent-Impregnated-Polymers is that the mass transfer may be slow, so the technique cannot be used in industrial scale, due to large residence times needed. An alternative carrier is e.g. Deloxan APII (DEGUSSA, Hanau, Germany) with additional functional groups which shows excellent mass transfer characteristics. Another feature is that the amine groups on the polymer react with anions at the same time depending on the regeneration technique. This effect can be turned on and off. The anion reaction mechanism is independent of the D2EHPA-loading and the cationic zinc sorption. It may lead to a neutralisation of the aqueous solution, which has a positive effect to the pH sensitive zinc sorption, giving a further optimisation potential of the overall process.

ACKNOWLEDGEMENT

We express our thanks to "DEUTSCHE BUNDESSTIFTUNG UMWELT, 49007 Osnabrück, Germany" (grant no.: 6000/317), "DEUTSCH FORSCHUNGS-GEMEINSCHAFT, 53170 Bonn, Germany" (grant: DFG-INSA) for supporting this project and "DEGUSSA, Hanau, Germany" for the donation of Deloxan APII.

REFERENCES

1 Juang R-S and Su J-Y, *Ind. Eng. Chem. Res.*, **31**, 2774, (1992)
2 Cortina JL, Miralles N, Aguilar M and Sastre AM, *Solvent Extract. Ion Exch.*, **12(2)**, 371, (1994)
3 Schöneberger A and Bart H-J, *CHISA Prag'98* (1998)
4 Tavlarides LL and Nandkumar VD, *Ind. Eng. Chem. Res.* **36**, 399, (1997)
5 Traving M and Bart H-J, *Proc. ISEC'99*, Barcelona (1999)
6 Sainz-Diaz CI, Klocker H, Marr R and Bart H-J, *Hydrometall.*, **42**, 1, (1995)
7 Jerabek K, Hanková L, Strikovsky AG and Warshawsky A, *React. Func. Polymers*, **28**, 201, (1996)

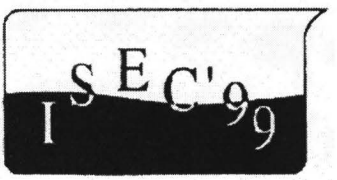

COMPUTER SIMULATION OF INTERFACIAL BEHAVIOUR OF N-8-QUINOLYLSULFONAMIDE FOR THE EXTRACTION KINETICS OF COPPER

F Nakashio, A Sakoguchi, E Zushi, R Ueoka and K Yoshizuka[1]
Department of Applied Chemistry, Kumamoto Institute of Technology, Ikeda 4-22-1, Kumamoto 860-0082, Japan
[1]Department of Applied Chemistry, Saga University, Honjyo 1, Saga 840-8502, Japan

ABSTRACT
Both the semi-empirical molecular orbital method and molecular dynamics at the water-toluene interface are employed in order to elucidate quantitatively the mechanism of formation of Cu(II), Zn(II) and Co(II) complexes with N-8-quinolylsulfonamides (CnphSAQ) at the liquid-liquid interface. The computer simulation reproduced that the experimentally observed extraction rate is affected by the adsorption of CnphSAQ and metal complex at the interface. A quantitative structure property relationship (QSPR) was obtained between the strain energy to the complex formation and extraction equilibrium constant.

Keywords: extraction kinetics, interfacial behaviour, computer simulation, N-8-quinolylsulfonamide, semi-empirical molecular orbital method, molecular dynamics simulation, copper, zinc, cobalt

INTRODUCTION

The common extractants used for metal extraction in hydrometallurgical processes are generally amphiphile, having both the hydrophobic long alkyl chain to reduce the solubility loss into water and hydrophilic coordinating group to metal. Due to this property, the extractant exhibits interfacial activity and is adsorbed at the oil-water interface.
Recently, the computer simulation is one of the important tools in chemistry.[2] In a few published reports, the liquid-liquid interfacial behaviours in the solvent extraction were studied.[4,6,10]

In a previous paper,[11] the effect of hydrophobicity of extractant on extraction kinetics of copper with four kinds of N-8-quinolylsulfonamide (CnphSAQ) of different alkyl-chain length was elucidated using a hollow fiber extractor. It was also reported that the extraction rate is controlled by the interfacial reaction in the range of low pH and by diffusion of the extractant or copper in the range of high pH, and that the effect of hydrophobicity of the extractants on the interfacial reaction is more remarkable as compared with those on diffusion.

In this paper, the computer simulation of the structures of CnphSAQs having different alkyl chains in each solvent (water and toluene) was carried out with the PM3 type of semi-empirical molecular orbital method, and also the molecular dynamics simulation of adsorption behavior of the extractants and metal complexes at the toluene-water interface was carried out. The effect of hydrophobicity of the extractants on the interfacial reaction will be discussed on the basis of the computer simulation.

EXPERIMENTAL

Semi-empirical molecular orbital (MO) calculation

The structural formula of N-8-quinolylsulfonamide (CnphSAQ) is shown in Figure 1. The optimized geometries of CnphSAQ were obtained by the semi-empirical molecular orbital method (PM3) [8] with MOPAC93 [9]. The optimized geometries of CnphSAQ in toluene calculated by the Conductor-like screening model (COSMO) [5] method implemented into MOPAC93 were almost consistent with those in water. The initial geometries of metal complexes were constructed from the optimized geometries of CnphSAQ in toluene.

© 2000 Society of Chemical Industry

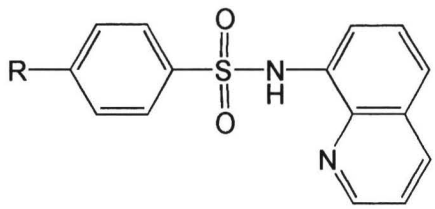

$R=C_nH_{2n+1}$

Figure 1. Structural formula of N-8-quinolylsulfonamide (CnphSAQ).

Molecular dynamics (MD) simulation

The molecular dynamics simulations were performed with the molecular modeling program (HyperChem) and the MM+ force field developed principally for organic molecules as a extension of MM2.[1] The liquid-liquid boundary cell (3 x 3 x 6 nm^3) was prepared by two adjoining rectangular boxes of pure water (892 molecules) and toluene (157 molecules). In these boxes, the experimental densities of water and toluene were reproduced, respectively. The liquid-liquid cell was optimized under NVT ensemble for 1000 ps. After setting CnphSAQ or metal complex at the interface of the cell, the MD simulation were run under NVT ensemble for 100 ps.

Quantitative structure property relationship (QSPR) [3]

The extraction of metal (M^{2+}) with CnphSAQ (HR) are expressed by:

$$M(H_2O)_6^{2+} + 2HR \rightleftarrows MR_2 + 2H_3O^+ + 4H_2O \quad (1)$$

The strain energy contribution to the complex (MR_2) formation is given by:

$$\Delta U_M = (U_{MR2} + 2U_{H3O+} + 4U_{H2O}) - (U_{M(H2O)6\,2+} + 2U_{HR}) \quad (2)$$

where Ui (i = MR2, H+, M2+ and HR) are the strain energies of component i. The relationship of free energy (ΔG_M) for the complex formation and extraction constant ($K_{ex,M}$) is expressed as follows.

$$\Delta G_M = - RT \ln K_{ex,M} \quad (3)$$

From Eqs.(2) and (3), the following equation is obtained :

$$\Delta U_M - \Delta U_{Co} = \alpha \ln (K_{ex,M} / K_{ex,\,Co}) \quad (4)$$

where $\Delta U_M - \Delta U_{Co}$ is the relative strain energy with respect to that of Co(II) compounds. α is the apparent QSPR constant.

RESULTS and DISCUSSION

Optimized geometries of CnphSAQ and metal complexes

The structures of CnphSAQ from quinoline ring to benzene ring were almost the same in spite of alkyl chain length.[7] Longer alkyl chain is attached to CnphSAQ, more bent and coiled alkyl chain is observed.

The Cu-CnphSAQ complexes (1:1 stoichiometries) had almost the same structures corresponding to CnphSAQ. Figure 2 shows that the optimized geometries Cu-C_{12}phSAQ complexes (1:1 stoichiometries) and C_{12}phSAQ. The structures of 1:2 complexes shown in Figure 3, especially from quinoline ring to benzene ring, were different from those of CnphSAQ and 1:1 complexes. Furthermore, the hydrophobic groups of Cu-C_{12}phSAQ (1:2) complex were located on the one side of quinoline ring and Cu-C_{18}phSAQ (1:2) complex was covered with the hydrophobic groups, as shown in Figure 3.

MD simulation of the adsorption of CnphSAQ and metal complexes at the liquid-liquid interface

In our previous work,[7] it was found that the sulfonamidequinoline (SAQ) group of CnphSAQ was adsorbed in a parallel with the interface and that the alkyl chain was elongated in the bulk toluene phase.

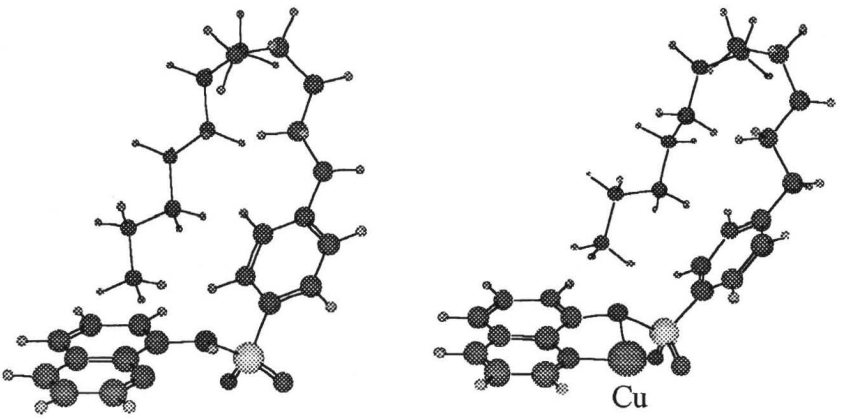

C_{12}phSAQ Cu:C_{12}phSAQ (1:1)

Figure 2. Optimized geometries of C12phSAQ and Cu-C12phSAQ complex (1:1) in vacuo calculated by the semi-empirical molecular orbital method.

The interfacial area occupied by a molecule of CnphSAQ obtained by the measurement of interfacial equilibrium is almost equal to the projected area of SAQ group.[12] Figure 4 shows that the SAQ group of metal complexes (1:1 stoichiometries) was adsorbed perpendicular to the interface. It is suggested that the conformation of the alkyl chain affects the interfacial behaviour, especially the metal complex formation at the interface.

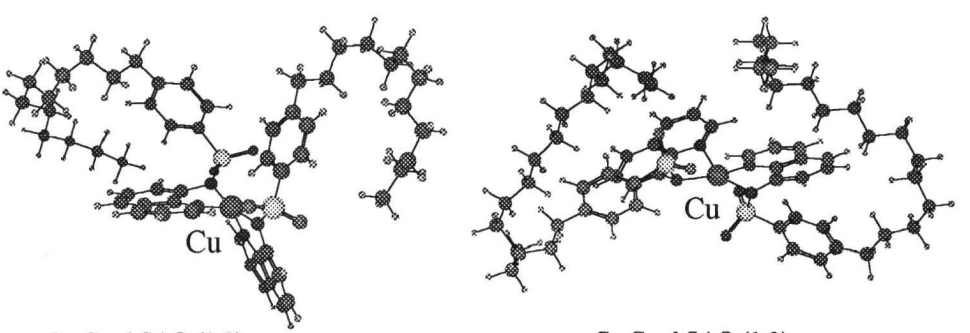

Cu:C_{12}phSAQ (1:2) Cu:C_{18}phSAQ (1:2)

Figure 3. Optimized geometries of Cu-CnphSAQ complex (1:2) in vacuo calculated by the semi-empirical molecular orbital method.

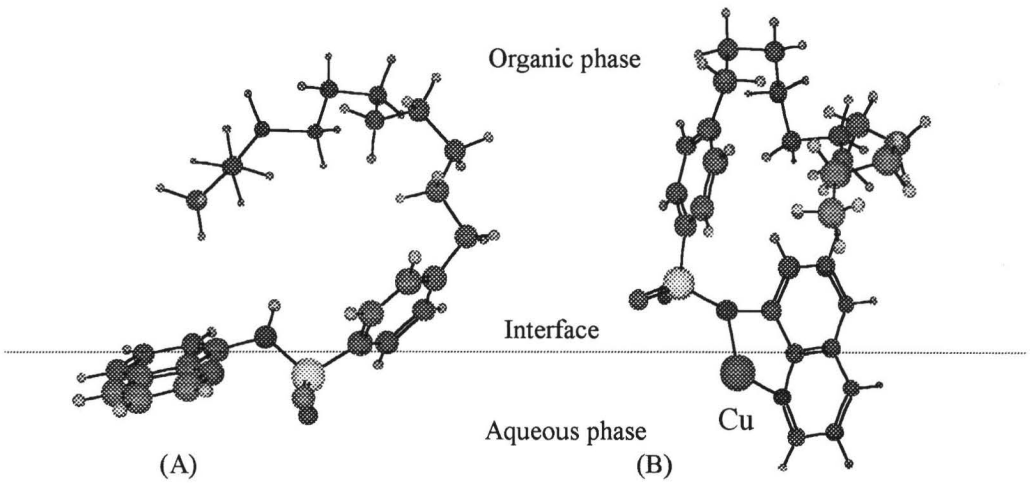

Figure 4. MD simulation of (A) C_{12}phSAQ and (B) Cu-C_{12}phSAQ (1:1) complex at the water-toluene interface.

QSPR of extractability trends of Cu(II), Zn(II) and Co(II) with CnphSAQ

A plot of (ΔU_M - ΔU_{Co}) vs ln ($K_{ex,M}$ / $K_{ex,Co}$) revealed a good linear relationship, as shown in Figure 5. It is suggested that the neglected terms are constant or linearly dependent on the strain energy for compounds in this study.

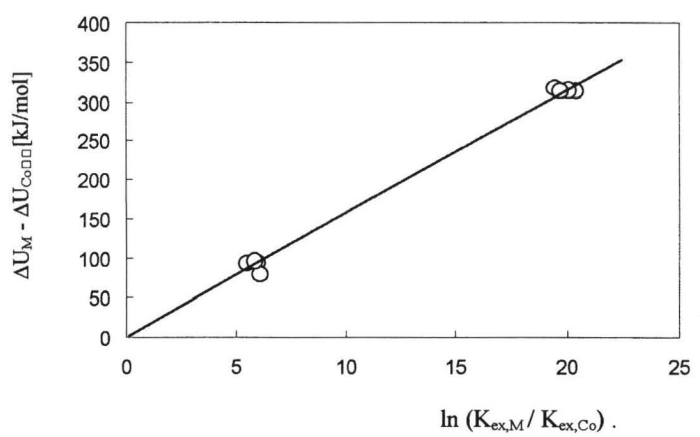

Figure 5. QSPR between (ΔU_M - ΔU_{Co}) and ln ($K_{ex,M}$ / $K_{ex,Co}$)

CONCLUSION

The computer simulation reproduced the mechanism of complex formation at the liquid-liquid interface and the effect of a hydrophobic alkyl chain on the experimentally observed extraction rate. A

quantitative structure property relationship (QSPR) was obtained on the correlation of the calculated strain energy difference for complex formation and the relative extractability.

NOMENCLATURE

ΔG	free energy difference in complex formation	[kJ·mol^{-1}]
K_{ex}	extraction equilibrium constant	[-]
R	gas constant	[kJ·mol^{-1}·K^{-1}]
T	temperature	[K]
U_j	strain energy of species j	[kJ·mol^{-1}]
ΔU_M	strain energy difference in complex formation	[kJ·mol^{-1}]
α	apparent QSPR constant	[-]

REFERENCES

1. Allinge NL, *J. Am. Chem. Soc.*, **99**, 8127, (1987).
2. Clark T, '*Guidebook of Computational Chemistry*', Wiley-Interscience, New York, USA (1988).
3. Comba P, Gloe K, Inoue K, Krüger T, Stephan H and Yoshizuka K, *Inorg. Chem.*, **37**, 3310, (1998).
4. Guilbaud P and Wipff G, *New J. Chem.*, **20**, 631, (1996).
5. Klamt A and Schuurmann G, *J. Chem. Soc. Perkins Trans. 2* , 799 (1993).
6. Lauerbach M, Engler E, Muzet N, Troxler L and Wipff G, *J. Phys. Chem. B*, **102**, 245, (1998).
7. Sakoguchi A, Zushi E, Ueoka R, Nakashio F and Yoshizuka K, *Kagaku Kogaku Ronbunshu*, to be submitted.
8. Stewart JJP, *J. Comput. Chem.*, **10**(2), 221, (1989).
9. Stewart JJP, *'MOPAC93, a molecular orbital package'*, JCPE P081, Stewart Computational Chemistry, Colorado Springs, USA (1993).
10. Watarai H, Gotoh M and Gotoh N, *Bull Chem. Soc. Jpn.*, **70**, 957, (1997).
11. Yoshizuka K, Kondo K and Nakashio F, *J. Chem. Eng. Japan*, **19**, 396, (1986a).
12. Yoshizuka K, Kondo K and Nakashio F, *J. Chem. Eng. Japan.*, **19**, 258, (1986b)

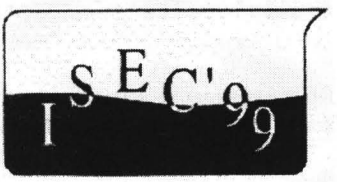

THE *LAP*-MODEL – A NEW APPROACH FOR MODELING KINETICS OF REACTIVE EXTRACTION

M Roos and H-J Bart
Lehrstuhl Thermische Verfahrenstechnik, Universität Kaiserslautern, Germany

ABSTRACT
A new model for extraction kinetics involving interfacial reactions has been developed using a Limited number of Adsorption Places (LAP) in the interfacial area for the formulation of reaction kinetics. This model allows the calculatation of the kinetic constants of each reaction step and makes them transferable to other systems. An extension to multi-component simultaneous transfer reactions has been included.

Keywords: reactive extraction, reaction kinetics, interfacial adsorption, simultaneous mass transfer

INTRODUCTION

In the last decades, a lot of reaction mechanisms for extraction of ions have been developed assuming two or more consecutive reaction steps including two or more species being adsorbed in the liquid interfacial area.[1,2] Transforming all the equations, one expression for the transfer rate can be developed containing several parameters. These can be determined by regression from experimental results. But with none of these models has it been possible to calculate the concentrations of the intermediate (adsorbed) products, since it is impossible to separate all the included kinetic parameters.

The aim of this study was to describe the extraction rates up to equilibrium and to evaluate all included reaction constants. These ought to be transferable to comparable systems. The new model should also be extendable to simultaneous transfer reactions.

In this work, the new LAP-model is introduced for the extraction of organic and inorganic acids with tri-n-octylamine. Additionally it is also applicable for other reactive extraction systems with strongly interfacial active ion exchangers.

THEORETICAL BACKGROUND

It has been known for a long time that it is possible to extract organic and inorganic acids with long chain ternary amines. The reaction site of this extraction is in the interfacial area because of the surface activity of the liquid ion exchangers. For the extraction of hydrochloric acid (HCl) with tri-n-octylamine (TOA) the following reaction steps have been considered by Danesi et al.[3]:

R1: $$TOA_{ad} + H^+ \underset{k_{-1}}{\overset{k_1}{\Leftrightarrow}} TOAH^+_{ad}$$

R2: $$TOAH^+_{ad} + Cl^- \underset{k_{-2}}{\overset{k_2}{\Leftrightarrow}} TOAHCl_{ad}$$

R3: $$TOAHCl_{ad} + \overline{TOA} \underset{k_{-3}}{\overset{k_3}{\Leftrightarrow}} \overline{TOAHCl} + TOA_{ad}$$

Typically the second step is assumed to be fast ($K_{eq2} = k_2 / k_{-2}$).This leads to the total reaction rate R:

$$R = \frac{k_1 \cdot \left(\left[\overline{TOA}\right] \cdot [H^+] \cdot [Cl^-] - \frac{1}{K_{ex}} [TOAHCl] \right)}{\left[\overline{TOA}\right] \cdot [Cl^-] + \frac{k_{-1}}{k_3 \cdot K_{eq2}}} [TOA_{ad}] \qquad (1)$$

Now, the two parameters C_1 and C_2 can be estimated to describe the measurements.

© 2000 Society of Chemical Industry

$$C_1 = k_1 \cdot [TOA_{ad}] \qquad C_2 = \frac{k_{-1}}{k_3 \cdot K_{eq2}}$$

Sometimes it can be seen, that the amount of adsorbed TOA has been calculated according to the Langmuir-equation (two parameters). Then, it is possible to describe the kinetic data with four parameters. Both methods assume that the amount of adsorbed TOA is either constant or only depending on the concentrations of TOA in the organic phase.

The problem with this formulation of the extraction kinetics is, that the reaction kinetic constants of each single step cannot be evaluated. Without them, it is impossible to transfer the parameters (for example of the protonation, which should be independent from the anion) from one acid to another. In particular it is not clear how large the concentrations of the two other adsorbed species are and if they are in a proper order of magnitude.

EXPERIMENTAL

Chemicals and Analytical Procedures.

Hydrochloric acid (FIXANAL, Riedel de Haen), acetic acid (ROTIPURAN, >99.7 %) and sodium acetate (Riedel de Haen, >99 %) are used to prepare the acid solutions of various concentrations. Tri-n-octylamine (TOA, >95 % Henkel) is diluted by toluene (Riedel de Haen, > 99.7 %). All chemicals except TOA (once washed with aqueous NaOH solution) are used as received.

The aqueous and the organic samples were weighed with a Sartorius R300S (0.1 mg) and analyzed for total acid concentration using an autotitrator (Mettler DL25) with NaOH (FIXANAL, Riedel de Haen, different concentrations). For lower hydrochloric acid concentrations, the electrical conductivity was recorded (WTW LF 2000/C).

Mass transfer

For kinetic investigations in this work a vibration cell (V = 323 cm^3, A = 44.1cm^2, f = 50Hz) proposed by Hancil was used. The description can be found elsewhere.[4] For all the results presented , kinetic limitation during mass transfer was achieved.

Interfacial tension

The samples were equilibrated for at least 24 hours and then separated in a centrifuge. Afterwards the interfacial tension was measured in a droplet volume tensiometer (TVT1, LAUDA).

DEVELOPMENT OF THE LAP MODEL

For the development of the LAP-model the previously mentioned three-step reaction mechanism for the extraction of hydrochloric acid is used. Additionally, one important assumption is made:

> ***The number of adsorption places in the interfacial area is limited, but interfacial activity of the species is strong enough to keep all places occupied.***

This means, that the sum of the concentrations of the adsorbed species is equal to the maximum concentration MAX:

$$[TOA_{ad}] + m \cdot [TOAH^+_{ad}] + n \cdot [TOAHCl_{ad}] = MAX \qquad (2)$$

A second assumption is that every adsorbed molecule needs the same surface area (so that m = n = 1). Here, this seems to be reasonable because the size of each species is dominated by the TOA. If more detailed information are available, this could also be rejected.

Substituting the second and the third term of equation (2) by the corresponding rate term, the concentration of adsorbed TOA can be calculated:

$$[TOA_{ad}] = \frac{MAX + R\cdot\left(\frac{1}{k_{-1}} - \frac{1}{k_3\cdot[\overline{TOA}]}\right)}{1+\frac{k_1}{k_{-1}}\cdot[H^+]+\frac{k_{-3}}{k_3}\cdot\frac{[\overline{TOAHCl}]}{[\overline{TOA}]}} \qquad (3)$$

This can be inserted into eq. (1) and solved explicitly in R:

$$R = \left([\overline{TOA}]\cdot[H^+]\cdot[Cl^-] - \frac{1}{K_{ex}}[\overline{TOAHCl}]\right)\cdot\frac{MAX}{denom} \qquad (4a)$$

with

$$denom = \frac{1}{k_1}\cdot[\overline{TOA}]\cdot[Cl^-]+\frac{k_{-1}}{K_{eq2}\cdot k_1\cdot k_3}+\frac{1}{K_{eq2}\cdot k_3}\cdot[H^+]\ldots$$
$$\ldots+\frac{1}{k_3}\cdot[H^+]\cdot[Cl^-]+\frac{k_{-3}}{k_3\cdot k_1}\cdot[\overline{TOAHCl}]\cdot[Cl^-]+\frac{1}{K_{ex}\cdot k_{-1}}[\overline{TOAHCl}] \qquad (4b)$$

The obtained equation contains the kinetic parameters k_1, k_{-1}, K_{eq2} and k_3 (k_{-3} can then be calculated from K_{ex}) and the maximum number of adsorbtion places MAX.

RESULTS AND DISCUSSION

To reduce the number of parameters, the maximum number of adsorption places MAX was estimated by measurements of the interfacial tension of TOA/toluene/water (see figure 1). They show a linear decrease in interfacial tension for increasing TOA concentrations. From the Gibbs equation:

$$\Gamma = -\frac{1}{\Re\cdot T}\cdot\frac{\partial\sigma}{\partial\left(\ln[\overline{TOA}]\right)} \qquad (5)$$

it can be seen, that the interface is saturated and MAX = 1.24 mmol/m².

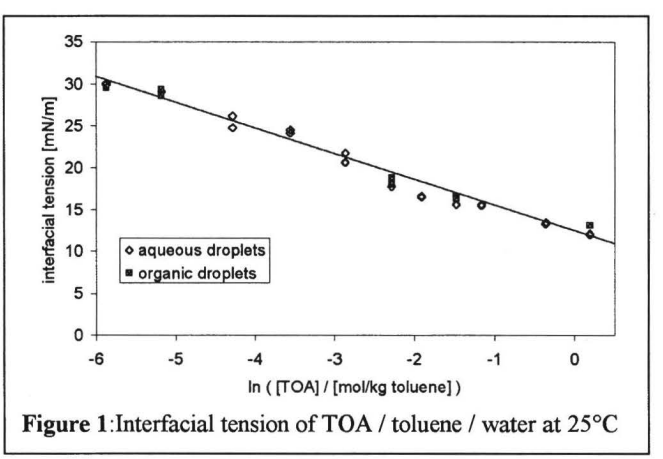

Figure 1:Interfacial tension of TOA / toluene / water at 25°C

With this, good agreement between measurement and calculations are possible for each investigated acid. However, the kinetics of the protonation, which is included for every acid, depends on the kind of anion and for acetic acid on the amount of added sodium acetate, which shifts the pH and the anion concentration.

To avoid this inconsistency, the model was modifed as follow: The protonation is fast and both other reaction steps are slow. This leads to:

$$R = \frac{\left([\overline{TOA}] \cdot [H^+] \cdot [Cl^-] - \frac{1}{K_{ex}} [\overline{TOAHCl}] \right)}{\frac{1}{K_{eq1} \cdot k_2} \cdot [\overline{TOA}] + \frac{k_{-2}}{K_{eq1} \cdot k_2 \cdot k_3}} [TOA_{ad}] \qquad (6)$$

Then, equation 3 can be inserted and solved explicitly in R. This leads to an equation which is similar to equation 4 a+b. Only the denominator changes to:

$$\text{denom} = \frac{1}{k_2} \cdot [\overline{TOA}] \cdot [H^+] + \frac{k_{-2}}{K_{eq1} \cdot k_2 \cdot k_3} + \frac{k_{-2}}{k_2 \cdot k_3} \cdot [H^+] \ldots$$
$$\ldots + \frac{1}{k_3} \cdot [H^+] \cdot [Cl^-] + \frac{1}{K_{eq1} \cdot k_2} \cdot [\overline{TOA}] + \frac{1}{K_{ex} \cdot k_{-2}} [\overline{TOAHCl}] \qquad (7)$$

The equation obtained contains the kinetic parameters K_{eq1}, k_2, k_{-2} and k_3 (k_{-3} from K_{ex}) and the maximum number of adsorption places MAX, which is given above. In figure 2 a comparison between measurements and the LAP-model (equation 7) for hydrochloric acid extraction is given for two mass transfer experiments. The model is able to describe the experiments in a pH-range from 0.5 to 3.

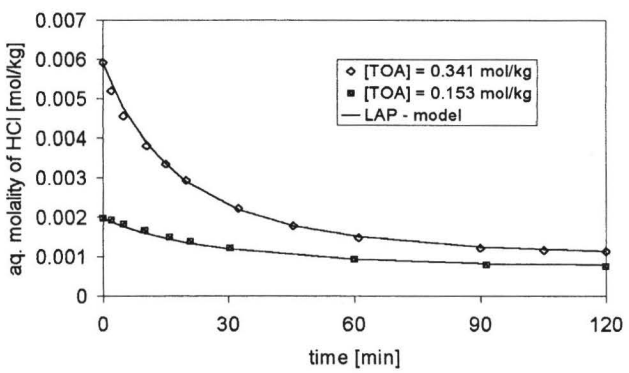

Figure 2: Extraction kinetics of hydrochloric acid at 25°C

The obtained equilibrium constant K_{eq1} for the protonation can be used for the acetic acid extraction. Only three parameters (k_2, k_{-2} and k_3) have to be estimated. For acetic acid, phase equilibria are a little more complicated.[5] In the aqueous phase, most of the acid is undissociated but only the dissociated acid influences the extraction rate. With the addition of sodium acetate, pH and acetate concentration can be varied. At higher acetic acid concentrations in the organic phase, higher complexes (e.g. three HAc for every TOA molecule) have to been taken into account. For these concentrations, no kinetic limitation could be found so this effect has not been included in the model.

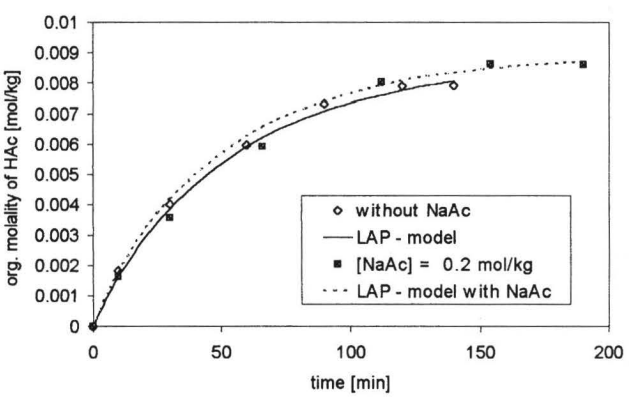

Figure 3: Extraction kinetics of acetic acid at 25°C

Extension to simultaneous mass transfer

For the case that protons and two different anions are present in the aqueous phase (for example simultaneous extraction of two acids or extraction of an organic acid in the presence of a salt) the model can be extended. Then, it is necessary to include two more reactions (e.g. for acetate):

R4: $$TOAH^+_{ad} + Ac^- \underset{k_{-4}}{\overset{k_4}{\Leftrightarrow}} TOAHAc_{ad}$$

R5: $$TOAHAc_{ad} + \overline{TOA} \underset{k_{-5}}{\overset{k_5}{\Leftrightarrow}} \overline{TOAHAc} + TOA_{ad}$$

Now, there are four adsorbed species at the interface:

$$[TOA_{ad}] + [TOAH^+_{ad}] + [TOAHCl_{ad}] + [TOAHAc_{ad}] = MAX \tag{8}$$

The rate equations (one for each transferred acid) can be developed in a similar way. Again the protonation is assumed to be fast. For hydrochloric acid this leads to an equation like equation 7 again, only the denominator has to be extended:

$$denom_{\text{with acetate}} = denom_{\text{without acetate}} \cdots$$

$$\cdots + \frac{\frac{1}{k_2}\cdot[\overline{TOA}] + \frac{k_{-2}}{k_2 \cdot k_3}}{\frac{1}{k_4}\cdot[\overline{TOA}] + \frac{k_{-4}}{k_4 \cdot k_5}} \cdot \left\{ \frac{1}{k_5}\cdot[H^+]\cdot[Ac^-] + \frac{1}{K_{ex,aceticacid}\cdot k_{-4}}[\overline{TOAHAc}] \right\} \tag{9}$$

Without acetate present in the system (neither in the aqueous nor in the organic phase), this extention reduces to zero. The rate equation for the simultaneous acetic acid extraction looks quite similar.

CONCLUSIONS

The LAP-model assumes a limited number of adsorption places to be available at the liquid interface. For the extraction of organic and inorganic acids with tri-n-octylamine (TOA) diluted in toluene, the LAP-model has been applied to a three-step reaction mechanism. The number of adsorption places has been estimated by measurement of the interfacial tension. With the LAP-model, it is possible to evaluate all parameters of the single reaction steps. Especially, the obtained parameters are consistent because the protonation is assumed to be fast with the identical equilibrium constant for all experiments. To describ the simultaneous reaction of two acids, the LAP-model has been extended. In the appendix, some ideas to reduce the number of necessary kinetic parameters are given.

APPENDIX

At equilibrium (no mass transfer, R = 0), the LAP-model delivers also the composition of the adsorbent. From eq. (3), the concentration of adsorbed TOA can be calculated to

$$[TOA_{ad}] = \frac{MAX}{1 + \frac{k_1}{k_{-1}}\cdot[H^+] + \frac{k_{-3}}{k_3}\cdot\frac{[\overline{TOAHCl}]}{[\overline{TOA}]}} \tag{A1}$$

From further measurements of the interfacial tension, it should be possible to gain equilibrium parameters for the single reaction steps and hence to reduce the necessary number of parameters to describe the mass transfer experiments again.

Another point is, with the LAP-model also the concentration of protonated TOA

$$[TOAH^+_{ad}] = \frac{MAX \cdot K_{eq1}\cdot[H^+]}{1 + K_{eq1}\cdot[H^+] + K_{eq1}\cdot K_{eq2}\cdot[H^+]\cdot[Cl^-]} \tag{A2}$$

can be computed. This implies a positive electrical loading to be located at the interface. In Figure A1, the concentration of protonated TOA for hydrochloric and for acetic acid, calculated with the LAP-model, is shown. Between a pH-value of 2 and 3, a maximum in the concentration of protonated TOA, slightly depending on the kind of acid, is predicted. First results show the same tendency, a positive

electrical loading has been measured for acetic acid by Czapla and Bart[6] using a light scattering technique to study the electrophoretic mobility of oil in water emulsions.

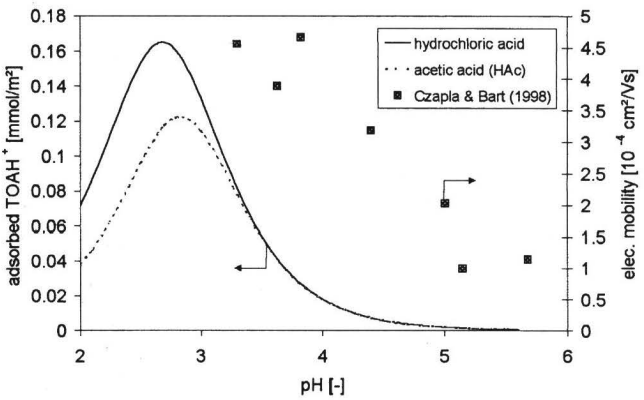

Figure A1: Electrical loading of the liquid interface

REFERENCES

1 Danesi PR in *"Principles and Practices of Solvent Extraction"*, ed. J. Rydberg et al., Marcel Dekker, New York, Chapter 5, (1992)
2 Klocker H, *Dissertation*, Techn. Universität Graz, (1996).
3 Danesi PR, Chiarizia R and Muhammed M., *J. inorg. nucl. Chem.*, **40**, 1581, (1978).
4 Hancil V, Rod V and Rehakova M, *Chem. Eng. J.* **16**, 51, (1978).
5 Roos M, Szitkai Z and Bart H-J, *paper at CHISA '98*, (1998).
6 Czapla C and Bart H-J, *paper at CHISA '98*, (1998).



Liquid Membranes

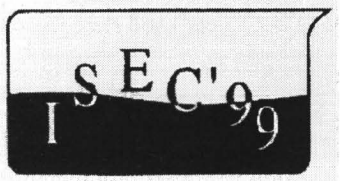

COMPARING CYANEX 301 WITH D2EHPA FOR THE EXTRACTION OF NICKEL THROUGH EMULSION LIQUID MEMBRANES

A Hoffmann, M Verhaege and RF De Ketelaere
Chemical and Biochemical Research Centre CBOK, Dept. KIHO, Gebroeders Desmetstraat 1, B-9000 Gent, Belgium

ABSTRACT
A comparison concerning the transport of nickel from an aqueous phase related to emulsion stability for Cyanex 301 and D2EHPA containing Emulsion Liquid Membrane (ELM) systems has been made. The results of the extractants at two different concentrations (3%, 20%) combined with two surfactants (Span 80 and Parabar 9551) at two concentrations (3%, 20 %) and for different strip acidities (1 mol/dm^3, 3 mol/dm^3 H_2SO_4) have been directly compared to each other. It was found that Cyanex 301 is a better extractant for nickel than D2EHPA. Due to the better stripping kinetics a 3% Cyanex 301 containing membrane is better than 20 %. Furthermore it was found that Cyanex 301 forms very stable with only moderately swelling of emulsions in combination with Parabar 9551. Cyanex 301 in combination with Span 80 shows better extraction results but leads to a higher emulsion swelling. Extraction with D2EHPA is only satisfactory for 20% concentrations in the membrane phase and leads to strip phase leakages in combination with Parabar 9551. Satisfactory nickel extraction with D2EHPA could only be obtained with 3 % Span 80 concentration in the membrane phase

Keywords: emulsion liquid membrane, nickel, Cyanex 301, D2EHPA

INTRODUCTION

European electroplating industries are more and more forced by the European authorities (PARCOM) to increase their efforts for waste water management due to the lowering of the concentration levels for heavy metal ions output in process water. Emulsion Liquid Membranes (ELM) have the ability to work in this concentration range and have been widely investigated for the removal of metal ions from waste waters and separation of organic acids.[1]

For the recovery of nickel from aqueous solutions several investigations have been made. The extractants tested with liquid membranes for nickel extraction are di-(2-ethylhexyl)phosphoric acid (D2EHPA),[1,2,3] di-(2-ethylhexyl)dithiophosphoric acid (DTPA)[1] and LIX 65N.[1,2] Recently investigated extractants are LIX 84 and LIX 860.[1] Among these D2EHPA is seen as the most suitable one for nickel.[2,3]

Bis-(2,4,4-trimethylpentyl)dithiphosphinic acid with the commercial name Cyanex 301 belongs to the dialkyldithiophosphinic acids and was originally developed to recover zinc from effluent streams of viscose rayon plants.[1] It shows also very strong extraction for nickel ions but due to its extremely slow stripping kinetics[1] it is nearly unknown for liquid membranes and di-(2-ethylhexyl)dithiophosphoric acid (DTPA) is recommended for ELM[1] although its chemical stability is a point of discussion.[1]

The purpose of this research was to compare the two extractants Cyanex 301 and D2EHPA in combination with the ELM technique. Matters of interest were the actual feed and strip concentrations and the emulsion stability depending on the choice of surfactants. One being the well documented Sorbitan Monooleate (Span 80) and a polyamine (Parabar 9551).[11,13,14]

EXPERIMENTAL

The experiments were carried out in laboratory scale equipment. The feed phase was a model solution containing 550 ppm Ni^{2+} prepared with $NiSO_4 \cdot 6H_2O$ salt and mQ water. As stripping agent a 95-97 % H_2SO_4 solution was used and diluted with mQ water.

The organic membranes were prepared with Shellsol D100 (Shell) as the solvent, Cyanex 301 (Cytec) and D2EHPA (Merck) were used as extractants and Span 80 (Sigma) or Parabar 9551 (EXXON Chemical) as surfactants.

All chemicals were used as delivered.

© 2000 Society of Chemical Industry

The volume ratio of the feed phase to the emulsion was 5 / 1 (375 / 75 cm^3) and strip phase to organic membrane phase 1 / 2 (25 / 50 cm^3), see also table 1:

Feed	Ni^{2+}; 550 ppm, Starting pH 5.3
Strip	H_2SO_4 1 and 3 mol/dm^3
Volume Proportions:	
Feed/Emulsion:	5/1 (375 cm^3/75 cm^3)
Organic/Strip:	2/1 (50 cm^3/25cm^3)
Organic Membrane:	
Extractant:	3 and 20%
Surfactant:	Parabar 9551, Span 80, 1 and 3%
Solvent:	Shellsol D100
Duration of experiment	60 minutes
Mixer Speed	300 rpm
Emulsion supply	4.5 cm^3/min

Table 1 Experimental conditions

At first the surfactant and the extractant were dissolved in the organic solvent. Then the aqueous strip phase and the organic membrane phase were emulsified with an Heidolph Diax 900 at 24 000 rpm for 1 minute.

The feed solution was placed in an unbaffled separatory funnel (95 mm Ø) containing a pH electrode and a Pt 1000 for temperature measurement. The contents of the separatory funnel were stirred with an Eurostar digital drive from IKA at 300 rpm and an off-centred PP propeller with two pitched plates (15 x 15 x 8 mm, W x H x Ø).

The emulsion was then pumped into the feed phase at a flow rate of 4,5 cm^3/min. The start of the experiment was when the first emulsion droplet fell into the feed phase. Samples of approximately 2 cm^3 aqueous feed were taken out of the solution with a 5 cm^3 pipette at 0, 3, 5, 10, 15, 20, 30, 45, 60 minutes and additionally the temperature and pH values were noted.

After 60 minutes the stirrer was stopped and the emulsion was allowed to separate from the aqueous feed phase. Subsequently the volumes of the feed phase and the emulsion were measured with a 100 cm^3 measuring cylinder.

The emulsions were split in an alternating current electrical field at 50 Mhz and 3000 V in a glass tube with an inner diameter of 13 mm using concentrical electrodes.

The nickel concentration was determined by atomic absorption spectrometry.

RESULTS

The goal for these experiments was to compare directly the results between the two extractants under different conditions as extractant concentrations, different surfactants and acidity of the strip phase. Therefore the carriers were combined at two concentrations (3%, 20 %) with two surfactants (Parabar 9551, Span 80) at two concentrations (1%, 3%) and all these combinations have been tested with two different H_2SO_4 strip solutions (1 mol/dm^3, 3 mol/dm^3).

The poor stripping characteristics of Cyanex 301 at 20% could be confirmed and are not shown. Extraction results with 3% D2EHPA are also not shown due to its extremely low performance. Thus 16 experiments will be explained in detail. They are divided into extraction, stripping and emulsion stability.

Extraction

An example for the different extraction characteristics between Cyanex 301 and D2EHPA is shown in figure 1. Assuming the decrease of the concentration can be expressed as a second order equation (see figure 1) this membrane composition extracts about twice as fast nickel with 3% Cyanex 301 than with 20% D2EHPA.

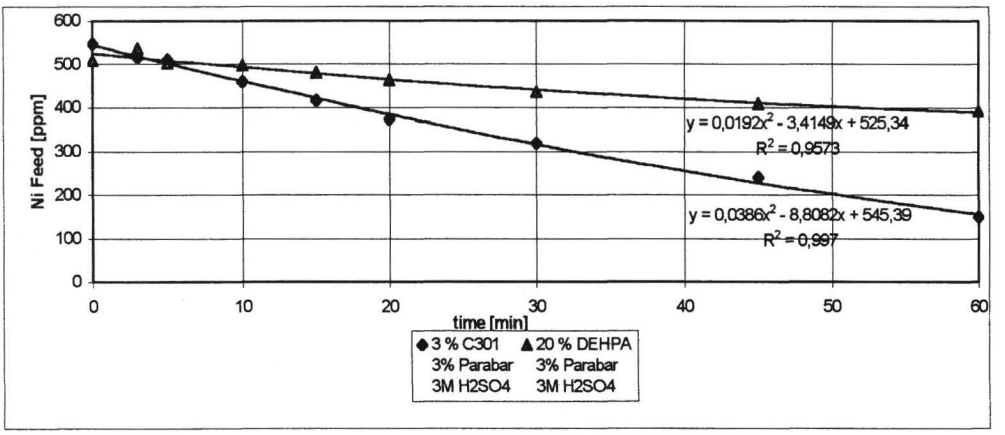

Figure 1. Example for different extraction kinetics for Cyanex 301 and D2EHPA

The concentrations after 60 minutes of extraction time for the chosen experiments are shown in figure 2. Except for one membrane composition the nickel concentrations with 3% Cyanex 301 are always lower than with 20% D2EHPA. Parabar 9551 shows a higher nickel mass transfer resistance than Span 80, which is typical for polyamines.[1]

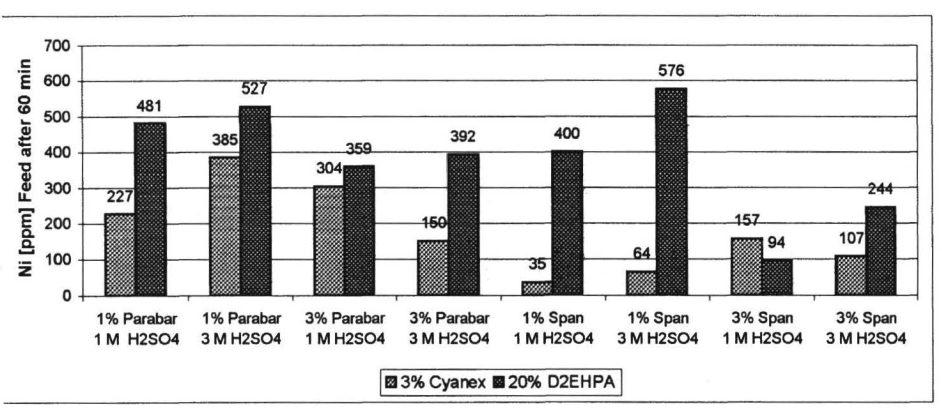

Figure 2. Nickel feed concentrations after 60 minutes extraction

Stripping

Cyanex 301 shows the best stripping characteristics with a 3 mol/dm^3 H_2SO_4 strip solution and 3% Parabar 9551 concentration, as shown in figure 3. Generally 3% Parabar 9551 concentrations and 3 mol/dm^3 H_2SO_4 perform better. At lower surfactant concentrations and 1 mol/dm^3 H_2SO_4 Cyanex 301 strips better with Span 80. The maximum of 1888 ppm nickel in the strip can be reached with 3% Cyanex 301 3% Parabar 9551 and 3 mol/dm^3 H_2SO_4.

D2EHPA shows inhomogeneous results. It strips better at 1% surfactant concentrations and generally better with 1 mol/dm^3 H_2SO_4 but for a 3% Span 80 containing membrane the nickel concentration in the strip phase is higher with a 3 mol/dm^3 H_2SO_4 strip solution.

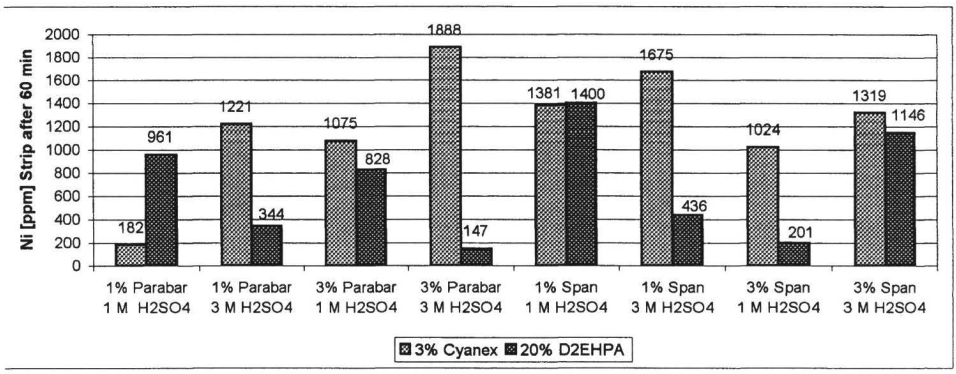

Figure 3. Nickel strip concentration after 60 minutes extraction

Emulsion Stability

Another property of ELMs is the emulsion swelling which is introduced as:

$$S = \frac{V_{E,60} - V_{E,0}}{V_{E,0}},$$

where $V_{E,0}$ is the starting volume of the emulsion end $V_{E,60}$ the emulsion volume after 60 minutes of extraction. This volume change is only due to water permeation across the membrane because the organic membrane phase volume was observed to remain constant.

Cyanex 301 in combination with Parabar 9551 shows less swelling than D2EHPA which even leads to strip phase losses, as shown in figure 4. D2EHPA shows less water permeation for 1% Span 80 and 1 mol/dm^3 H_2SO_4 but the strip phase is also leaking for a 3 mol/dm^3 H_2SO_4 strip solution. Cyanex 301 membranes swell for 1% Span 80 concentration more than D2EHPA and swelling is practically identical for both extractants with 3 % Span 80 concentrations.

CONCLUSIONS

Bis-(2,4,4-trimethylpentyl)dithiophosphinic acid (Cyanex 301) is a very good nickel extractant and due to its low stripping efficiency it is preferably used in concentration of 3% rather than 20%. In combination with the surfactant Parabar 9551 Cyanex 301 shows only moderate swelling. Cyanex 301 has also good extracting and stripping properties in combination with Span 80, however is the emulsion swelling up to 100 %. With none of the surfactants a leakage of the strip phase could be observed.

Compared to Cyanex 301 only one membrane composition with D2EHPA shows lower nickel concentration in the feed and only one shows significantly higher nickel concentrations in the strip. In combination with Parabar 9551 however no stable emulsion can be formed.

Hence Cyanex 301 is a better extractant for nickel extraction than D2EHPA. The surfactant selection depends on the disadvantage that can be accepted. After 60 minutes low nickel concentrations in the feed solution down to 64 ppm and strip concentrations of 1675 ppm can be reached with 3% Cyanex 301, 1% Span 80 and 3 mol/dm^3 H_2SO_4, if an emulsion swelling of 80% can be accepted. If only a moderate swelling can be accepted then Parabar 9551 should be chosen as surfactant.

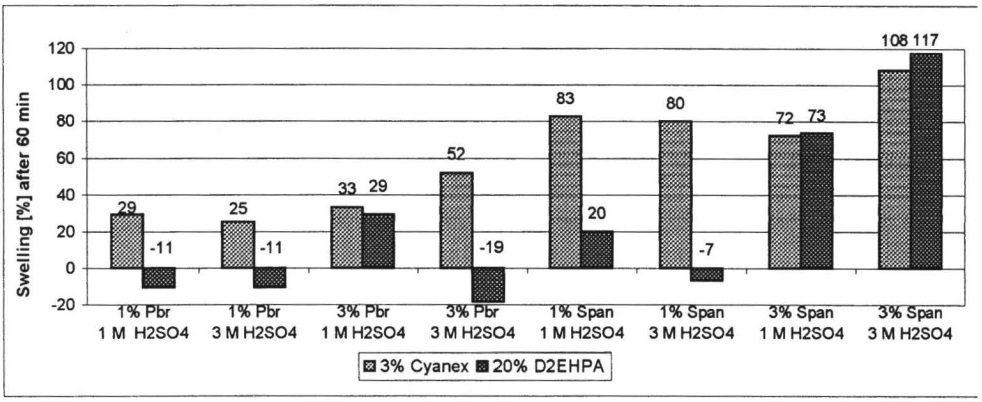

Figure 4. Emulsion swelling after 60 minutes extraction

ACKNOWLEDGEMENTS

The author wishes to thank the European Union for the Marie-Curie research grant [BRMA-CT95-5028]. Furthermore wishes the author to thank Cytec for the samples of Cyanex 301 and Exxon Chemical for the samples of Parabar 9551.

REFERENCES

1 Ho WSW and Li NN. in Ho WSW and Sirkar KK. (Eds.), *Membrane Handbook*, Chapman & Hall, New York, London, 597, (1992).
2 Verhaege M, Wettnick E, Van Robaeys D and Lareyns F. in Davies GA. (Ed.), *Separation Processes in Hydrometallurgy*, Ellis Horwood Ltd. Chichester England, 331, (1987).
3 Juang R-S and Jiang J-D. J. *Memb. Sci.* **100**, 163, (1995).
4 Smit JJ and Koekemoer LR. *Water SA*, **22**, 249, (1996).
5 Marr R, Lackner H and Bart H-J, *European Patent 89112656.7*, (1989)
6 Cussler EL and Evans DF. *J. Membr. Sci.* **6**, 113, (1980).
7 Marr RJ and Kropp A. *Int. Chem. Eng.* **22**, 44, (1982).
8 Kakoi T, Ura T, Kasaini H, Goto M and Nakashio F. *Sep. Sci. Technol.* **33**, 1163, (1998).
9 American Cynamid Corp. (Cytec), Product Information SPT-039, 1989, Wayne N.J., USA
10 Gibson RW and Rice NM in: *Proc.Nickel-Cobalt 97 Int.Symp.* Cooper WC, Michaylov I Eds., Can.Inst.Min.Metal.Petr. **I**, 247, (1997)
11 Gu Z, Ho WSW and Li NN. in Ho WSW, Sirkar KK. (Eds), *Membrane Handbook*, Chapman & Hall, New York, London, 656, (1992).
12 Marr RJ and Draxler J. in Ho WSW and Sirkar KK. (Eds), *Membrane Handbook*, Chapman & Hall, New York, London, 701, (1992)
13 Nakashio F, Goto M, Matsumoto M, Irie J and Kondo K. *J. Membr, Sci.* **38**, 249, (1988).
14 Abouh-Nehmeh I and van Peterghem AP. *Chem.-Ing.-Tech.* **62**, 420, (1990).
15 Draxler J and Marr R. *Chem. Eng. Process.* **20**, 319, (1986).

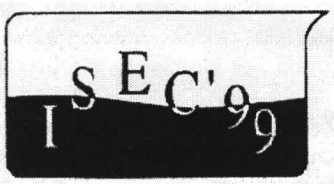

EFFECTS OF SOME PARAMETERS ON COBALT/ NICKEL SEPARATION AND ON COBALT PERMEATION BY A LIQUID SURFACTANT MEMBRANE PROCESS

A Salum[1], GL da Silva[2], MB Mansur[1], TLS Miranda[1] and VST Ciminelli[3]

[1]Dept of Chemical Engineering, Universidade Federal de Minas Gerais, Belo Horizonte, M.G., Brazil

[2] GLS Consultores Associados S.A., M.G., Brazil

[3] Dept of Mining and Material, Universidade Federal de Minas Gerais, Belo Horizonte, M.G., Brazil

ABSTRACT

The cobalt/nickel separation in a sulphate medium containing 1.5g/L of cobalt and 95.0g/L of nickel by the liquid surfactant membrane (LSM) technique was investigated. Permeation experiments were performed using bis-(2,4,4-trimethylpentyl)phosphinic acid (Cyanex 272) as a carrier, the surfactant ECA 4360 and Escaid 110 as a diluent. As internal phase, a solution of sulphuric acid containing Li^+ as a tracer was employed. A buffer solution formed by citric acid and its salts was used in the external phase. The influence of external phase pH, carrier concentration and temperature on the cobalt/nickel separation, as well as on the cobalt permeation, was evaluated, demonstrating the potential of the LSM technique for this application.

Keywords: cobalt, nickel, surfactant liquid membranes, Cyanex 272, surfactant ECA 4360

INTRODUCTION

A membrane can be defined, in a simple manner, as an interphase that separates two phases and limits the transport of different chemical species in a specific way.[1] Thus, a liquid can act as a semipermeable stable barrier, a membrane, between two other liquid phases, if it is immiscible in both of them. Due to its selective permeability, a liquid membrane system can be considered a separation process.[2,3]

Liquid surfactant membranes (LSMs) are based on the multiple emulsion principle. A primary emulsion is mechanically dispersed in a continuous liquid phase. For metal separation, this primary emulsion is a water-in-oil one. The dispersed aqueous phase is called internal phase and the continuous organic one is the membrane phase. The latter contains a surfactant, which is responsible for the emulsion stability, and a solvent, which is formed by a diluent and an extractant. This emulsion is then dispersed in another aqueous phase (the external phase), which contains the solute(s) to be transported, forming a multiple emulsion.

The LSM process consists of four steps: emulsification, permeation, sedimentation and de-emulsification. In the first step the stable emulsions are obtained. During permeation, the transport of the solute(s) from the external to the membrane phase, and from this to the internal phase occurs. In the sedimentation stage, the emulsion enriched in the solute is separated from the external phase. Finally, in de-emulsification, the emulsion is broken up and the aqueous phase rich in the solute is recovered.

The occurrence of cobalt in nature is almost a third of that of nickel. Cobalt occurs always in low- grade ores and associated with other metals, especially nickel. Generally, it is obtained as a by-product of the processing of copper, nickel and silver ores. Thus, for cobalt separation, it is necessary to use an efficient separation technique. Nickel and cobalt are chemically very similar. As they are both found in low-grade ores and have to be obtained as pure as possible for their applications, a lot of studies have been carried out on cobalt and nickel extraction, separation and concentration.

On the industrial scale, nickel and cobalt are extracted from ores by leaching with ammonia, hydrochloric acid, nitric acid, sulphuric acid (most usual) or a mixture of nitric and sulphuric acids.

© 2000 Society of Chemical Industry

For the recovery of these metals, the most common methods are precipitation and liquid-liquid extraction, the use of the latter technique has been increasing because of the development of more selective extractants for nickel/cobalt separation. After this operation, an electrowinning or other solution treatment is normally used to recover the metals.

As the LSMs can commonly use the same extractants as the liquid-liquid extraction process, they can be a possible alternative for the extraction and separation of metals, presenting some advantages in comparison to the solvent extraction.[4] The following acidic extractants have been widely studied for the cobalt/nickel separation in sulphate medium: di-(2-ethylhexyl)phosphoric acid (D2EHPA), 2-ethylhexyl-2-ethylhexylphosphonic acid (PC-88A or Ionquest 801) and bis-(2,4,4-trimethylpentyl)phosphinic acid (Cyanex 272).[5-9] Companhia Níquel-Tocantins, the unique company which products electrolytic cobalt and nickel in Brazil, uses Cyanex 272 in its plant for the extraction of cobalt from sulphuric acid liquors. This reagent has the advantage of not extracting calcium, which would lead to solvent losses in sulphate medium.

Few studies have been performed on cobalt/nickel separation using LSM.[10-12] Danesi *et al.*[13] studied this separation using supported liquid membranes with Cyanex 272 as a carrier. In the current study, the potential of the LSM technique for the cobalt/nickel separation is demonstrated. The optimum temperature, external phase pH, extractant concentration and time for the separation of cobalt in a sulphuric acid liquor containing 1.5g/L of cobalt and 95.0g/L of nickel were obtained. The influence of these parameters on cobalt extraction and on cobalt/nickel separation were also studied.

EXPERIMENTAL

The reagents used to prepare the membrane phase were: the extractant Cyanex 272 (Cyanamid Co.), 85% purity, as a carrier; the polyamine ECA 4360 as a surfactant and the diluent Escaid 110 (Exxon Chemicals Ltd.). The internal phase was prepared using sulphuric acid 97% w/w (Vetec), distilled water and lithium sulphate monohydrate p.a. (Vetec), as a tracer. The external phase was prepared using (Vetec): cobalt (II) sulphate heptahydrate p.a., nickel (II) sulphate hexahydrate p.a. and citric acid p.a./sodium hydroxide p.a., to prepare the buffer solution. All reagents were used as received.

The appropriate amounts of the cobalt and nickel salts were dissolved in distilled water, at 40-50°C, under mechanical agitation, to obtain a synthetic liquor containing 1.5 g/L of cobalt and 95.0 g/L of nickel, which corresponds to the concentrations of these metals in some Brazilian liquors from sulphuric acid leaching. Citric acid (0.50 M) was added to the solution and the pH was adjusted to the desired value by using a saturated sodium hydroxide solution. Then, the external phase prepared was filtered and 200 mL of the solution were heated to the temperature of the experiment. In an emulsification vessel, the internal phase containing lithium (0.10 M) in sulphuric acid (0.50 M) was dispersed, with an agitation speed of 13,000 rpm, for 5 minutes, in the membrane phase previously prepared. The presence of lithium in the external phase, after the permeation experiment, is an indication of membrane break-up. For each experiment, 40 mL of the emulsion were poured into a double wall reactor containing 200 mL of the preheated solution with the cobalt and nickel salts (external phase), linked to a thermostatic bath, to control the temperature of the tests. The position of the impeller was adjusted experimentally to obtain homogeneous and efficient agitation. The agitation speed was 200-210 rpm. When the permeation experiment was concluded, the mixture was transferred to a separation funnel. The external phase volume was measured and a sample was taken for analysis of cobalt, nickel and lithium. The emulsion enriched in cobalt was sent to the de-emulsification step. After the break-up, the emulsion was poured into a separation funnel and a sample of the internal phase was taken for analysis of cobalt, nickel and lithium. An absorption atomic spectrophotometer CG AA 7000 SBC was used for the analysis of cobalt, nickel and lithium. Table I summarizes the operation conditions investigated. The parameters chosen for the evaluation of this study were: the percentage of cobalt extracted from the external phase, the cobalt/nickel

concentrations ratio in the internal phase at the end of the permeation experiment, the percentage of the membrane break-up, defined as shown by the following equations:

$$\%\ (Co)_{EP} = 100\ [(C_{Co}\ .V)_{fin.} - (C_{Co}\ .V)_{in.}]_{EP} / [(C_{Co}\ .V)_{in.}]_{EP} \quad (1)$$

$$(Co/Ni)_{IP} = [(C_{Co})_{IP}/(C_{Ni})_{IP}]_{fin.} \quad (2)$$

$$\%\ \text{membrane break up} = 100[(M_{tr.})_{fin}]_{EP} / [(M_{tr.})_{in}]_{IP} \quad (3)$$

where C = concentration (g/L), M = mass (g) and V = volume (L) and subscripts Co = cobalt; Ni = nickel, tr = tracer; IP = internal phase; EP = external phase; in = initial and fin = final conditions.

RESULTS AND DISCUSSION

Figure 1 shows the influence of the Cyanex 272 concentration on cobalt extraction from the external phase. The experiments were performed at a temperature of 50 °C, with an internal phase containing 0.10M Li^+ in 0.50M H_2SO_4. Each test lasted for 21 minutes. At low concentrations of the carrier, cobalt extraction was not significant because there was not enough reagent to extract the metal. Cobalt extraction increased with the concentration of Cyanex 272 until a limit, about 9.5 g/L of carrier, after which the extraction stabilized. This limit is probably due to the saturation of the surface of the emulsion globules by the extractant, together with a low cobalt concentration in the external phase. An increase in Cyanex 272 concentration improves the reaction kinetics, but further addition does not increase cobalt extraction because, at this level, the cobalt concentration in the external phase is so low that it can be the limiting factor for the extraction. Besides, a high Cyanex 272 concentration can favour the extraction reaction at the external interphase and then the stripping reaction at the internal interphase. As a result, the H^+ ions transport from the internal to external phase increases, diminishing the driving force of the process. As depicted in Figure 2, both cobalt and nickel concentrations in the internal phase increase with Cyanex 272 concentration and, with high concentrations of the carrier, $[Ni]_{FI}$ increases more than $[Co]_{FI}$. The preferential nickel extraction can also explain the stabilization of cobalt extraction shown in Figure 1. Membrane break-up was also evaluated and this increases with the Cyanex 272 concentration.

Operation Variables Studied	Levels
1. External phase pH	3; 4; 5; 6
2. Permeation time (minutes)	From 1 to 60
3. Temperature (°C)	22; 32; 50; 60
4. Extractant (carrier) concentration (g/L)	From 3.8 to 27.0
Fixed Variables	**Levels**
1. Surfactant concentration (% v/v)	3.0
2. Cobalt initial concentration in the external phase (g/L)	1.5
3. Volumes ratio membrane phase/internal phase (MP/IP)	1.0
4. Volumes ratio external phase/emulsion	5:1
5. Buffer solution used	Citric acid and its salts
6. Agitation speed in the permeation step (rpm)	200-210
7. H^+ ions concentration in the internal phase (M)	0.75 and 1.00
8. Initial Ni/Co concentrations ratio in the external phase	63.3:1

Table I - Variables investigated in permeation experiments and their levels.[14]

Further studies in a narrow range of Cyanex 272 concentration (from 8.5 - 11.5 g/L) were performed and confirmed the results presented in Figures 1 and 2. It was observed that the percentage cobalt extraction and cobalt concentration in the internal phase are constant in this range, but nickel

concentration in the internal phase increases. Thus, the appropriate Cyanex 272 concentration for Co/Ni separation is about 9.5 g/L.

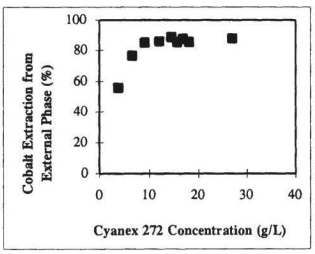

Figure 1 - Influence of Cyanex 272 concentration on Co extraction from the external phase.

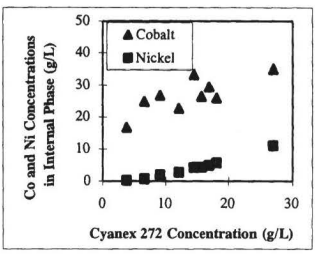

Figure 2 - Influence of Cyanex 272 concentration on Co and Ni concentrations in the internal phase.

The influence of external phase pH with permeation time on cobalt extraction was also studied. It was found that the extraction increases in the following sequence: pH 3 < pH 4 < pH 6 < pH 5. The maximum extraction was attained after about 30 minutes. As shown in Figure 3, the selectivity also depends on the external phase pH and it is higher at pH 5. Nickel extraction has a great increase at pH 6 and $[Ni]_{FI}$ becomes higher than $[Co]_{IP}$. The selectivity decreases with permeation time. Low membrane break- up was observed at the lowest pH values, probably due to the predominance of the non-ionic over the ionic form, which stabilises the membrane in a bigger extension.[15]

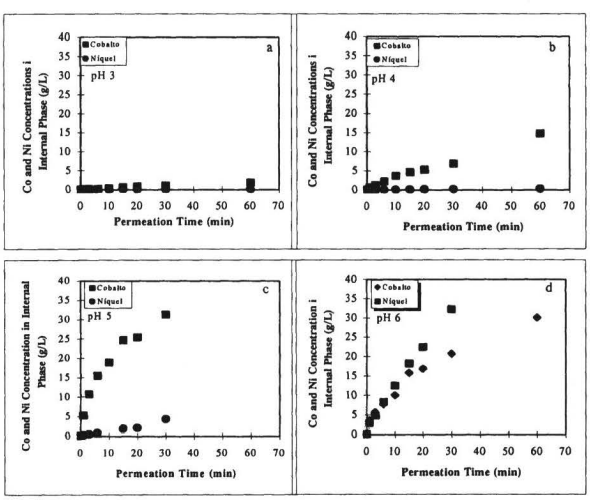

Figure 3 - Variation of cobalt and nickel concentrations in the internal phase with time permeation for different external phase pH values.
(a) pH_{in} = 3,0; (b) pH_{in} = 4,1; (c) pH_{in}= 5,0; (d) pH_{in} = 6,1
Extractant conc. = 12,1 g/L; $(C_{H2SO4})_{FI}$ = 0,50 M; $(C_{Li})_{FI}$ = 0,10 M; T = 41°C.

The influence of temperature on cobalt extraction, as well as on the membrane stability with time, is shown, in figures 5 and 6 respectively. As temperature and permeation time increase, cobalt extraction and membrane break-up also increase. At higher temperatures, membrane viscosity decreases and the internal phase is lost in the nodal region.[15] Analysis of cobalt and nickel in the internal phases showed that the temperature affected nickel extraction, which was not observed in

liquid-liquid extraction studies. The best temperature and permeation time were, respectively, 50°C and 20-30 minutes.

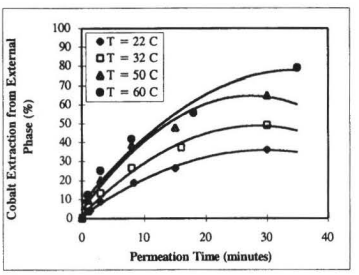

Figure 5 - Influence of temperature on Co extraction from external phase with time $(C_{H2SO4})_{FI}$ = 0,375M; $(C_{Li})_{FI}$ = 0,10M; pH_{ini} = 5,0

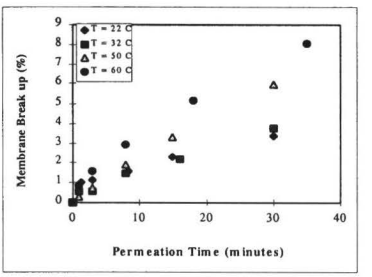

Figure 6 - Influence of temperature on membrane break up with permeation time $(C_{H2SO4})_{FI}$ = 0,375M; $(C_{Li})_{FI}$ = 0,10M, pH_{ini} = 5,0)

Normally, in order to separate cobalt and nickel from liquors containing 1.5 g/L of Co and 95.0 g/l of Ni with Cyanex 272 is necessary to use about 100 g/L of this extractant in a liquid-liquid extraction operation. So, the results presented showed the potential of the liquid surfactant membrane technique for this application in that it is possible to separate cobalt and nickel using only approximately a tenth of the Cyanex 272 concentration in solvent extraction process.

ACKNOWLEDGEMENT

The author would like to thank CAPES (Brazil) for financial support to attend ISEC'99

REFERENCES

1 Strathmann H. *J.Membrane Sci*, **9**, 121, (1981)
2 Halwachs W and Schügerl K. *Int. Chem.Eng.*1, **20**(4), 519, (1980)
3 Noble RD, Way JD and Bunge AL. *'Liquid Membranes'*. Boulder: National Bureau of Standards, Internal Report, (1989)
4 Marr R, Bart H-J and Draxler J. *Sep. Sci. and Technol.* **2**, 403, (1989)
5 Tait BK. *Hydrometallurgy*, **32**, 365, (1993)
6 Dreisinger DB and Cooper WC. *Hydrometallurgy*, **12**, 1, (1984)
7 Ritcey GM, Ashbrook AW and Lucas BH, *CIM Bulletin*, **68**, 111, (1975)
8 Xun F and Golding JA. *Solv. Ext. and Ion Exch.* **5**(2), 205, (1987)
9 Xun F and Golding JA. Proc. 2nd *Int. Conf. on Sep. Sci. and Tech.* Soc. *for Chem. Eng.*, **1**(2), 205, (1989)
10 Strzelbicki J and Charewicz W. *Hydrometallurgy*, **5**, 243, (1980)
11 Duarte AS, Duarte JN, Castro RMZ and Reis RLR, In: *Encontro do Hemisfério Sul sobre Tecnologia Mineral*, **3**, São Lourenço, Minas Gerais, 1992. Anais. Belo Horizonte, MG, ABTM, **2**, 283, (1992)
12 Kakoi T, Goto M, Sugimoto K, Ohto K and Nakashio F. Sep. Sci. and Technol., **30**(4), 637, (1995)
13 Danesi PR, Reicheley-Yinger L, Mason G, Kaplan L, Horwitz EP and Diamond H. Solv. Ext. and Ion Exch. **3**, 435, (1985)
14 Salum A, *Estudo da Parmecao de Cobalto e da Separacoa Cobalto/Niquel em Meio Sulfurico, com Cyanex 272, pela Tecnica de Membranas Liquidas Surfactantes* PhD Thesis, Universidade Federal de Minas Gerais, (1998)
15 Rosen MJ, *Surfactants and Interfacial Phenomena*. John Wiley & Sons, Inc., USA., (1978)
16 Mikucki BA, *Metal Extraction with Liquid Surfactant Membranes: the Role of Emulsifying Agent*. MSc (Metallurgy) Thesis, Pennsylvania State University, 315, (1984)

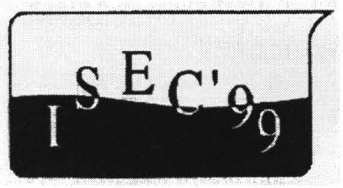

LIQUID MEMBRANE PERMEATION OF ZINC IN A CONTINUOUS COUNTERCURRENT COLUMN

MTA Reis[1], H-J Bart[2] and JMR Carvalho[1]

[1]Dep. Eng. Química, Instituto Superior Técnico, 1096 Lisboa Codex, Portugal

[2]Thermische Verfahrenstechnik, Univ. Kaiserslautern, D-67653 Kaiserslautern, Germany

ABSTRACT

Zinc permeation with emulsion liquid membranes was carried out in a stirred countercurrent column. The carrier used in the membrane phase was bis(2-ethylhexyl)monothiophosphoric acid. The composition of the aqueous feed was zinc sulphate (4.59×10^{-3} kmol m^{-3}) and sulphuric acid. The influence of the stirring speed on zinc extraction was tested in the range of 200-320 rpm. The experimental concentration profiles of the external aqueous phase were compared with the ones predicted by numerical simulation. The mathematical model used takes into account the diffusion and reaction of solutes within the membrane and connects the hydrodynamics with mass transfer.

Keywords: emulsion liquid membranes, zinc, stirred column, numerical simulation, bis-(2-ethylhexyl)monothiophosphoric acid, surfactant ECA 11522

INTRODUCTION

The emulsion liquid membrane (ELM) technique has been noticed as an attractive method for purifying polluted wastewater. In the industrial application of this technology, a continuous operation using a column or a mixer-settler is required. Column operation is desirable by known reasons unless the kinetics of mass transfer has prohibitive values. The studies, which have been done on the ELM permeation process with columns, are not very extensive.[1-6]

In the present paper a set of ELM experiments was carried out in a continuous countercurrent column with mechanical agitation. The extraction of interest was the zinc ion from sulphuric solutions by using MTPA (bis(2-ethylhexyl)monothiophosphoric acid) as carrier. The purpose of this work is to demonstrate that the results obtained can be predicted by numerical simulation.

THEORY

Owing to the complexity of carrier-facilitated transport processes the mass transfer models are usually tedious and involve a lot of parameters. Lorbach *et al.*[7] developed a mass transfer model for the permeation of Cu^{2+} ions with a few parameters. This model accounts for the transient nature of diffusion and reaction of the solutes within the membrane phase and was chosen in the present work to describe the mass transfer. The extractant MTPA was found to be a dimeric form, $(HR)_2$, in non-polar solvents[8] and zinc is extracted according to the following reaction:[9]

$$Zn^{2+} + 1.5\,\overline{(RH)_2} \leftrightarrow \overline{ZnR_2(RH)} + 2H^+ \qquad (\mathrm{Zn} + 1.5\,\mathrm{B} \leftrightarrow \mathrm{C} + 2\mathrm{H})$$

The kinetics of the extraction rate was tested in a modified Lewis cell with vibrational mixing. The forward and reverse reaction rates, n_F and n_R, are expressed as follows:[9]

$$n_F = k_F \frac{c_{Zn}\, c_B}{c_H} - k_R \frac{c_C\, c_H}{c_B^{0.5}} \qquad n_R = k_R \frac{c_C\, c_H}{c_B^{0.5}} - k_F \frac{c_{Zn}\, c_B}{c_H} \qquad (2\text{-}3)$$

The performance of a column is influenced adversely by hydrodynamic features such as axial mixing in both phases. These deviations from the ideal plug flow were introduced by the use of the dispersion model. The connection between mass transfer and hydrodynamics leads to the following equations (considering one class of drops):

© 2000 Society of Chemical Industry

$$E_c \frac{d^2 c_{Zn(III)}}{dh^2} + \frac{V_c}{1-\phi} \frac{dc_{Zn(III)}}{dh} - k_c \frac{6\phi}{d_{32}(1-\phi)} \left(c_{Zn(III)} - c_{Zn(III,i)}\right) = 0 \quad (4)$$

$$E_d \frac{\partial^2 c_B}{\partial h^2} - \frac{V_d}{\phi} \frac{\partial c_B}{\partial h} \frac{D_{B,ef}}{(1-\phi')} \frac{1}{r^2} \frac{\partial}{\partial r} \left(r^2 \frac{\partial c_B}{\partial r}\right) + 1.5 \frac{6\phi'}{d_\mu (1-\phi')} n_R = 0 \quad (5)$$

$$E_d \frac{\partial^2 c_C}{\partial h^2} - \frac{V_d}{\phi} \frac{\partial c_C}{\partial h} \frac{D_{C,ef}}{(1-\phi')} \frac{1}{r^2} \frac{\partial}{\partial r} \left(r^2 \frac{\partial c_C}{\partial r}\right) - \frac{6\phi'}{d_\mu (1-\phi')} n_R = 0 \quad (6)$$

$$E_d \frac{d^2 c_{Zn(I)}}{dh^2} - \frac{V_d}{\phi'} \frac{dc_{Zn(I)}}{dh} + \frac{6}{d_\mu} n_R = 0 \quad (7)$$

The set of equations 2-7 with the adequate boundary conditions[7,10,11] results in a non-linear partial differential equation system in axial and radial directions. After using special discretization techniques a large equation system is obtained which is solved by the block Gauss-Seidel iteration method.[10,11] Due to the incomplete dissociation of sulphuric acid the concentration of H^+ must be calculated by formulating the equilibrium relationships and mass balance components. For instances the presence of the species Zn^{2+}, H^+, SO_4^{2-}, HSO_4^- and $ZnSO_4$ is considered. The dissociation of bisulphate and the formation of zinc sulphate ion-pair are assumed to be instantaneous reactions. The stoichiometry of equation 1 leads to the calculation of total sulphuric acid at each point of the column. The equilibrium constants are written in terms of activities and the activity coefficients are evaluated by Pitzer's equations.[12] The activity coefficients are a function of the ionic strength, concentrations and Pitzer's parameters.[12-14] The set of equations is solved by a simple iteration procedure. The concentrations of the species are calculated by a numerical routine (CO5PBF) written by NAG®, which was introduced in the algorithm of Ortner *et. al.*[11]

Estimation of parameters

The axial mixing coefficients of continuous and dispersed phases, E_c and E_d, can be measured via residence time distribution by using tracer techniques. In literature there are several empirical correlations available which are suitable for agitated columns.[15-17] However the column used is not an equipment standard and analogy must be done. In the present work the coefficient E_c was determined by means of a step-input perturbation into the continuous phase and E_d was obtained from data published by Komasawa *et al.*[16] assuming that the stirred column is similar to the Mixco column.
The mass transfer coefficient for zinc in the continuous phase, k_c, was estimated by the correlation of Bibaud *et al*[15] which is valid for rigid spheres in a Mixco column.

Effective diffusivity, $D_{C,ef}$, can be derived from mass transfer models which take into account facilitated diffusion in the emulsion phase.[18] In this work $D_{C,ef}$ was derived to modify "T-model" in a way similar to that developed for phenol permeation.[19] $D_{C,ef}$ depends on the extraction rate at the interfaces and is also a function of diffusivity of zinc in the internal phase, $D_{Zn(I)}$, diffusivity of zinc complex, D_C, in the membrane phase and volume fraction of phases. The diffusivity $D_{Zn(I)}$ was calculated by the Nernst equation and then corrected for the water viscosity.[20] The Wilke-Chang relationship[20] was used to estimate the diffusion coefficients D_C and D_B. The molar volume of the solute was evaluated by the method of Le Bas.[20] The ratio $D_{C,ef}/D_{B,ef}$ was assumed to be equal to the molecular diffusivity ratio D_C/D_B.

EXPERIMENTAL

Reagents

The external aqueous solution (continuous phase) was prepared with $ZnSO_4$ (4.59×10^{-3} kmol m^{-3} = 300 mg Zn dm^{-3}) and H_2SO_4 (1.98×10^{-4} kmol m^{-3}, pH=3.50). The membrane phase consisted of 5% (=0.1 kmol m^{-3}) MTPA (di(*2*-ethylhexyl)monothiophosphoric acid, Höchst), 2 % ECA 11522 (nonionic polyamine, Exxon) as surfactant in an aliphatic diluent (ShellsolT, Shell). The internal aqueous phase was a solution with H_2SO_4 (2.2 kmol m^{-3}) and LiCl p.a. (0.3 kmol m^{-3}) as a tracer for emulsion break-up. A NaCl p.a. aqueous solution was used to measure the axial mixing in the continuous phase.

Equipment and procedure

The experiments were performed in a continuous countercurrent column at room temperature (291-293 K). The active height was 3.7 m and the internal diameter was 0.05 m. The column was agitated by several turbines (diameter-0.025 m, distance between turbines-0.075 m). The emulsion was prepared by a static low-pressure disperser (ATOMIX-SNDisperser) and splitted in a coaxial electrocoalescer (2 kV AC-10 kHz).

The axial mixing experiments were conducted without the presence of the dispersed phase. The tracer was injected at the middle of the column and the measurements effected at 1.38 m of distance. The samples were analysed by conductimetry.

In the start of the experiments the throughputs were checked (phases III, II and I: 1.39×10^{-5}, 1.39×10^{-6} and 1.39×10^{-7} m^3 s^{-1}, respectively) and the level of agitation fixed. After 3 hours of operation samples of the aqueous continuous phase were collected with the aid of taps distributed along the column. Photographs of the emulsion globules were done during the experiment. Average hold-up of the emulsion phase was measured by a shutdown method.

The measurement of drop size was performed with an image analyser (QuantimedQ520, Cambridge Instruments). In the case of internal droplets the measures were made with the aid of a microscope. The analyses of zinc (and lithium) were effected with an atomic absorption spectrophotometer (AAS IL video 2000).

RESULTS AND DISCUSSION

Axial mixing experiments

The equation of response for a step (cumulative residence-time distribution) depends on the location of the perturbation and measurements. In this work the test section investigated is open with respect to diffusion at both ends and the apparatus may be considered to be of infinite length. The analytical solution of the dispersion model respecting to initial and boundary conditions adequate is published elsewhere.[21] The stirring speed did not affect the Peclet number in the range studied and the value of E_c may be considered constant and approximately equal to 3.0×10^{-4} m^2s^{-1}. This result is in agreement with the one predicted by the correlation of Bibaud *at al.*[15] for single phase ($2.9\text{-}3.0\times10^{-4}$ m^2s^{-1}). The presence of dispersed phase influences the results but due to uncertainly of estimation ($1\text{-}10\times10^{-4}$ m^2s^{-1} [15,17]) the experimental value for single phase was used.

ELM experiments

The influence of stirring speed on Sauter mean diameter of globules and hold-up of the dispersed phase is observed in Figures 1-2.

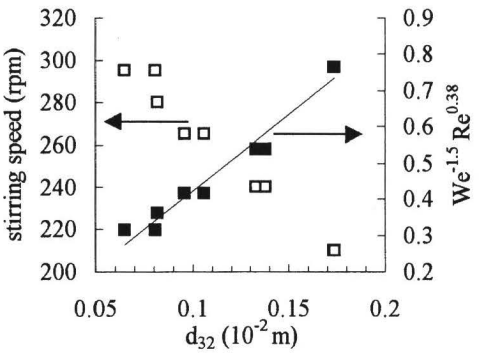

Figure 1. Influence of agitation on d_{32}.

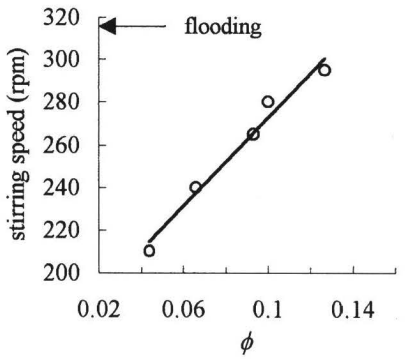

Figure 2. Influence of agitation on hold-up.

The stirring speed influences significantly the size of emulsion globules ($d_{32} \propto N^{-2.6}$). The dependence on Weber and turbine Reynolds numbers is not quite different from the one found by Rautenbach *et al.* ($d_{32} \propto We^{-1.2}Re^{0.6}$) for a stirred column.[17] The actual discrepancies may be due to the swelling and break-up of emulsion effects, which were not taken into account. Analysis of lithium in external and internal phases indicate that break-up is less than 5% but osmosis is more pronounced.

The average hold-up of the dispersed phase is nearly proportional to stirring speed in the range studied as is expected for this type of equipment.[22] In this case the analogy with Mixco column fails when the corresponding correlations for hold-up and characteristic velocity are used ($\phi \propto N^{4.2}$).[15] Due to the lacking of hydrodynamic data to establish a reliable correlation for hold-up the experimental values were employed in the present simulation of zinc permeation.

The list of parameters used for numerical computation is shown in Table 1. The comparison between the measured concentration profiles and the simulated results is shown in Figure 3.

ϕ - (0.044-0.127), ϕ' - 0.091	[-]	k_c - $(3.8\text{-}4.2)\times10^{-5}$	[m s^{-1}]
d_{32} - $(0.65\text{-}1.73)\times10^{-3}$	[m]	$k_F^0(293\ K)$ - 3.2×10^{-5}	[m s^{-1}]
d_μ - $(1.13\text{-}1.45)\times10^{-6}$	[m]	$k_R^0(293\ K)$ - 1.0×10^{-6}	[$kmol^{-0.5}$ $m^{2.5}$ s^{-1}]
V_c - 7.07×10^{-3}, V_d - 7.78×10^{-4}	[m s^{-1}]	$k_F = k_F^0 \frac{\gamma_{Zn^{2+}}}{\gamma_{H^+}} \frac{c_{Zn^{2+}}}{c_{Zn^{total}}}$, $k_R = k_R^0 \gamma_{H^+}$	
E_c - 3.0×10^{-4}, E_d – $(2.7\text{-}9.7)\times10^{-4}$	[m^2 s^{-1}]		

Table 1 List of the parameters employed for simulation.

The extraction of zinc is enhanced by the increase in the stirring due to the increase in mass transfer area. The model is obviously very sensitive to hold-up and globules size. The resistance in mass transfer through the aqueous film decreases about 10% when the stirring speed vary from 210 to 295 rpm and also contributes to a higher extraction. Due to the pH value of external phase the kinetic resistance is relatively less important than the resistance of mass transfer of zinc ions to the interface. The estimation of the effective diffusivity by the "T-model" is reasonable since the simulated results are in agreement with experimental data. In spite of ignoring the effect of surfactant on reaction rate and neglecting the swelling phenomena the zinc profile along the stirred column is satisfactory simulated by the present model.

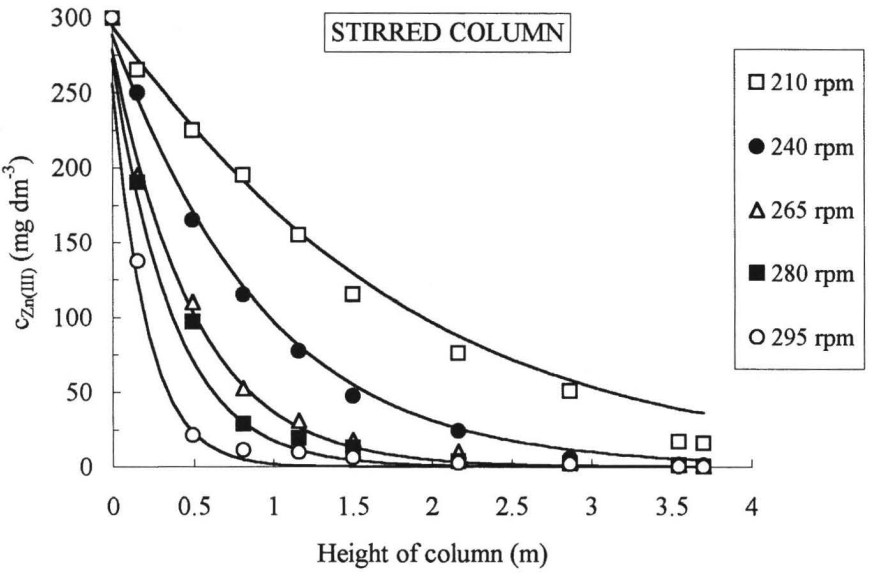

Figure 3. Concentration zinc profile in external aqueous phase at several stirring speeds. Initial pH=3.50 (calculated by Pitzer's method-3.53). Solid lines: numerical simulation; marks: experimental values; see the list of parameters in Table 1.

ADDITIONAL NOTATION

D_{ef}	effective diffusivity, $m^2\ s^{-1}$
d_{32}	Sauter mean diameter of the emulsion globules, m
d_μ	Sauter mean diameter of the internal droplets, m
n	reaction rate, kmol $m^{-2}\ s^{-1}$
k^0	thermodynamic (in terms of aqueous phase) kinetic constant, $m^2\ s^{-1}$or $kmol^{-0.5}m^{2.5}s^{-1}$
ϕ'	volume fraction of the emulsion with internal phase
γ_i	activity coefficient of the specie i

subscripts

B, C	free carrier and zinc complex in the membrane phase, respectively
H	hydrogen ion in the aqueous phase (III or I)
F, R	forward and reverse reaction, respectively
I, II, III	internal, membrane and external phase, respectively

AKNOWLEDGEMENT

Support by EC-COMETT programme and CD-Labor (TU-Graz, Austria) is gratefully acknowledged. The authors wish also to thank Inst. Thermische Verfachrenstechnik und Umwelttechnik (TU-Graz, Austria) where the experiments were carried out.

REFERENCES

1. Xiujuan Z, Jianghong L and Tiansi L, *Water Treatment*, **2**, 127, (1987).
2. Marr RJ and Draxler J, *Membrane Handbook*, Ed. Ho, W.S.W., Sirkar, K.K., (1992).
3. Matsumoto M, Ema K, Kondo K and Nakashio F, *J. Chem. Eng. Jpn.*, **23**, 402, (1990).
4. Kinugasa T, Watanabe K, Utunomiya T and Takeuchi H, *J. Memb. Sci.*, **102**, 177, (1995)
5. Uezu K, Irie S, Yoshimura O, Goto M and Nakashio F, *Trans IChemE*, **75**, 513, (1997).
6. Lee SC, Lee KH, Hyun GH and Lee W K, *J. Memb. Sci.*, **124**, 43, (1997).
7. Lorbach D, Bart H-J and Marr R, *Ger. Chem. Eng.*, **9**, 321, (1986).
8. Hirai T, Hashimoto T, Tsuboi I, Hino A and Komasawa I, *J. Chem. Eng. Jpn.* **28**, 85, (1995)
9. Reis MTA, *Ph.D. Thesis*, IST, Technical University of Lisbon, Portugal (in press).
10. Ortner A, *Diplomarbeit*, Fakultät der Joannes Kepler Universität, Linz, Austria, 1989.
11. Ortner A, Auzinger D, Wacker HJ and Bart H-J, *Computed-Oriented Proc. Eng.*, **1991**, 399.
12. Zemaitis Jr. JF, Clark DM, Rafal M and Scrivner NC, *Handbook of Aqueous Electrolyte Thermodynamics*, Ed. Design Institute for Physical Property Data, N.Y.,(1986).
13. Hovey JK, Pitzer KS and Rard JA, *J. Chem. Thermodynamics*, **25**, 173 (1993).
14. Klocker H, Sainz-Dias CI, Wachter B, Bart H-J and Marr R, *Proc. ISEC'96*, 617, (1996).
15. Bibaud R and Treybal RE, *AIChE J.*, **12**, 472 (1996).
16. Komasawa I and Ingham J, *Chem. Eng. Sci.*, **33**, 479, (1978).
17. Rautenbach R and Machhammer O, *J. Memb. Sci.*, **36**, 425, (1988).
18. Teramoto M, Matsuyama H and Izumo Y, *J. Memb. Sci.*, **68**, 169, (1992).
19. Teramoto M and Matsuyama, *J. Chem. Eng. Jpn.*, **19**, 469, (1986).
20. Perry R and Chilton CH, *Chem. Eng. Handbook*, McGraw-Hill, N.Y., 5th ed., (1973).
21. Sawinsky J, Hunek J and Podmaniczky L, *Int. Chem. Eng.*, **20**, 681, (1980).
22. Kataoka T, Nishiki T, Yamauchi M and Zhong Y, *J. Chem. Eng. Jpn.*, **20**, 410, (1987).

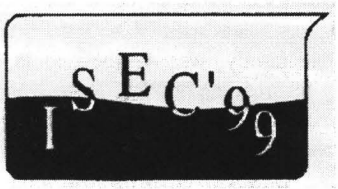

PURIFICATION OF A RADIOACTIVE LIQUID EFFLUENT: ELIMINATION OF CAESIUM BY LIQUID SURFACTANT MEMBRANE EXTRACTION

D Pareau, P Kaplan, M Stambouli and G Durand
Laboratoire de Chimie et Génie des Procédés, Ecole Centrale
Paris 92295 Châtenay-Malabry, France

ABSTRACT
An ELM extraction process scheme is developed for the elimination of caesium from an effluent containing traces of Cs along with high concentrations of sodium and hydroxide. Caesium is selectively extracted and concentrated. Emulsion liquid membrane (ELM) extraction is chosen because of its main advantages: possibility of treating very diluted solutions and possibility of concentration. The desired selectivity is obtained using a new extractant, synthesised in our laboratory: a calixarene formed by the acid-catalyzed condensation of resorcinol and octanal, named resorcarene (PR8). This extractant is first tested in solvent extraction to verify its properties: extraction ability, selectivity and to find a suitable stripping solution. A molar nitric acid is convenient for this last purpose. PARABAR 9220 is used as surfactant. The inner phase of the emulsion is HNO_3 (1 mol/dm^3) and the organic phase contains PR8, PARABAR 9220 and dodecane. Surprisingly, by employing commonly used volume ratios of the emulsion (around 1), it is not possible to extract caesium. Emulsions containing a very low volume of internal phase (10% or less) are nevertheless very efficient. This is a very surprising and original behaviour. The batch extraction studies show an extraction yield of 95% for caesium and less than 1% of sodium is co-extracted. The concentration factor of caesium is then 20. Continuous extraction studies in mixer-settlers and a pulsed column are performed to test the validity of the continuous process. The results in mixer-settlers are deceiving because of high emulsion breakage, due to strong shear stresses in the mixer chamber. A pulsed column is then preferred leading to satisfactory results (> 90% Cs extracted, Cs concentration factor 20 and 1,2% sodium co-extracted). These results could then be improved by optimising chemical and operating conditions.

Keywords: caesium, emulsion liquid membrane, calixarene, resorcarene

INTRODUCTION

Nuclear fuel reprocessing operations generate different types of effluents. Chemical segregation of most or all the radioactive components from the inactive bulk constituents of the waste can reduce the volume of waste requiring vitrification and subsequent burial in a deep geologic repository. Because of their diversity and complexity, highly selective separation processes are required and some new improved schemes have been recently developed for specific types of effluents.[1,2]

This work is focused on a liquid effluent containing high concentrations of sodium hydroxide along with minor amounts of high-level radiation elements such as caesium (^{137}Cs) and strontium (^{90}Sr) which represent more than 99% of the remaining radioactivity after ten years decay. Moreover, because of the potential dispersion of the very soluble ^{137}Cs in the environment during its burial in deep repository, selective extraction of caesium is required. An emulsion liquid membrane extraction process (ELM) seems to be more appropriate for such dilute solutions.[3-5]

The basic requirements that have to be achieved are:[5] high decontamination and concentration factors (DF > 10^3 and CF > 10), low sodium co-extraction ([Na^+] < 0.1 mol/dm^3) and specific atomic composition of the organic solvent, including C, H, O and N atoms only (the so-called «CHON's rule»).

EXPERIMENTAL

Synthesis of a new selective extractant

With respect to the CHON's rule, which prohibits the use of mineral exchangers, the main organic extractants known to form strong compounds with alkali and alkaline earth elements are the

© 2000 Society of Chemical Industry

cyclic compounds crown ethers[6] and calixarenes.[7] Being not very lipophilic, the relatively water soluble crown ethers require the addition of polar diluents which are quite inconvenient with ELM extraction. A new macrocyclic compound extractant, belonging to the calixarene family, was synthesised in our laboratory according to Högberg method.[8] This calixarene, namely resorcarene or PR8, is the reaction product of the acid-catalysed condensation of resorcinol with octanal. The formula of the resorcarene PR8 is deduced according to both spectroscopic (IR & UV) and chromatographic (GPC) analysis of the purified product (figure 1).

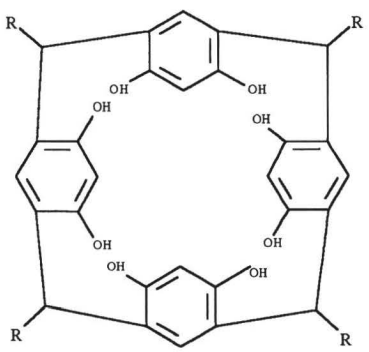

Figure 1: Resorcarene (PR8) developed formula (R : $-C_7H_{15}$)

A review of the extracting behaviour of some similar calixarenes is reported.[9] Heavy alkali element extraction (Na, K, Rb and Cs) is strongly pH-dependent with an optimum between 9 and 12 and a significantly better selectivity for Cs. The decrease of alkali extraction for pH values higher than 12 is related to the increase of the solubility of calixarene in water.

Batch solvent extraction

Preliminary experiments

Alkali concentrations are determined by Flame Emission Spectroscopy. Batch solvent extraction experiments are conducted with the following phases:

- Organic phase: Resorcarene (PR8) mixed with a commonly used diluent, dodecane, and octanol is then added to increase the polarity of the organic phase and prevent third phase formation.
- Aqueous phase: $[Na^+] = [OH^-] + [NO_3^-] = 3$ mol/dm^3; $[Cs^+] = 7{,}52\ 10^{-5}$ mol/dm^3; pH =11,5
- Stripping: nitric acid solution (3 mol/dm^3)

Extraction equilibrium is reached in less than one minute. As expected, the calixarene displays very good selectivity and extraction efficiency (> 90%).

Effect of the surfactant

The effect of the addition of a surfactant, needed for ELM experiments, has been investigated. Three surfactants, kindly supplied by EXXON, have been studied, the most commonly used SPAN 80 (sorbitan monooleate) and ECA 4360 (succinic derived polyamine), and a new one PARABAR 9220 (polyolefin alkyl anhydride), not commonly used for ELM extraction.

With both SPAN 80 and ECA 4360, extraction was surprisingly inhibited. In addition, resorcarene PR8 is no more water-soluble over pH 12, suggesting the formation of a calixarene-surfactant molecular association species. Thus, the two common surfactants may be rejected.

Only a slight calixarene-surfactant interaction was observed with PARABAR 9220, (PARA). Moreover, the stabilisation of the organic phase occurs for hydroxide concentrations as high as 2 mol/dm^3. Interfacial precipitation of resorcarene is only observed for weight ratio of PARA/PR8 lower than 1.

These experimental facts suggest the formation of an organic mixed alkali molecular complex including the extractant, the surfactant and potentially water molecules.

Batch ELM extraction

Extraction efficiency

Surprisingly, extraction was inefficient for the commonly used equi-volume emulsion, i.e., internal phase/emulsion volume ratio around 50%. Emulsions with different reduced volume ratios were formed by a controlled electrocoalescence of an initial equi-volume emulsion. The extraction efficiency was investigated with the following operating conditions:

External aqueous phase (Ext)	Membrane (M)	Internal aqueous phase (Int)
V_{Ext} = 20 cm^3	V_M = 18 cm^3	V_{int} = 2 cm^3
$[Na^+]$ = 3 mol/dm^3	[PR8] = 5.63 10^{-3} mol/dm^3	(emulsion ratio = 10%)
$[OH^-]$ = 2 mol/dm^3	[PARA] = 7.34 10^{-3} mol/dm^3	$[HNO_3]$ = 1mol/dm^3
$[Cs^+]$ = 7.52 10^{-5} mol/dm^3	Diluent :dodecane-octanol 95-5% (volume/volume)	

The experimental results on the kinetics of Cs transfer are shown in table 1. Mass balance was checked with an excellent accuracy and an excellent extraction yield was achieved (>90%). Cs transfer was very fast and the extraction kinetics rate were similar to those for solvent extraction. Thus, no additional interfacial transfer resistance, due to the presence of the surfactant, is observed. The nitric acidic internal phase does not affect the emulsion stability.

Time (minutes)	$[Cs^+]_{ext}$ (mg /dm^3)	Extraction Yield (%)
0	10	0
1	0,69	93
3	0,86	91
5	0,87	91
10	0,89	91

Table 1: Kinetics of ELM extraction of Cs

Effect of membrane/internal phase volume ratio

ELM batch experiments were conducted in a magnetically stirred cell with equal volumes (V_{Ext} = V_{em} = 100 cm^3) of the following phases:

Aqueous phases (internal and external): the same than (3.1)

Membrane composition:

[PR8] = 2.63 10^{-3} mol/dm^3; [PARA] = 1.42 10^{-3} mol/dm^3

Diluent: dodecane 95% + octanol 5% (v/v)

Different emulsion ratios were considered (V_{Int} / V_{em} = 1; 10 and 20 %). As expected, the extraction efficiency was better than 90% with the emulsion ratio having practically no effect on the extraction yield. In addition, the emulsion exhibited an excellent stability with no membrane breakage observed after 1 hour. Nevertheless, this favourable result had to be validated for continuous experiments.

Continuous ELM extraction

Preliminary continuous experiments were conducted in a mixer-settler battery. However, extraction efficiency was surprisingly low and strong shear stresses in the mixer chamber induced the inclusion of some external aqueous phase into the organic emulsion. Moreover, a high emulsion

breakage was observed (80 to 90%) prohibiting the use of this extraction technology.

Therefore because of its low residence times and shear stresses, a pulsed column was chosen to validate the ELM extraction performances. The laboratory scale pulsed column (height: 1m; internal diameter: 2.5 cm) has been described in previous studies.[3,4] The packing consisted of 40 stainless plates (20 disks + 20 doughnuts), regularly spaced (distance 2.4 cm). The column was equipped with a cylindrical upper settler allowing the separation of the phases for spectroscopic alkali analysis. The liquid hold-up is about 475 cm^3 and the transparency is equal to 25%.

A preliminary hydrodynamic study was undertaken to determine the appropriate operating conditions for a countercurrent flow:

Pulsation parameters: 2.5 cm amplitude and 119 min^{-1} frequency, corresponding to a pulsation energy of 179 $cm \cdot min^{-1}$.

Aqueous and emulsion flowrates respectively 1.09 and 1.13 dm^3h^{-1}, corresponding to a total specific flowrate of 0.45 dm^3cm^{-2}

Composition of the phases:

External aqueous phase: as above except $[Cs^+] = 7.02\ 10^{-5}$ mol/dm^3

Internal aqueous phase: as above with a volume ratio equal to 10%

Emulsion:[PR8]=1.67 10^{-3} mol/dm^3 and [PARA] = 1.14 10^{-3} mol/dm^3 in the same dodecane-octanol mixture

The evolution of the concentration of Cs in the final effluent with time is shown in figure 2.

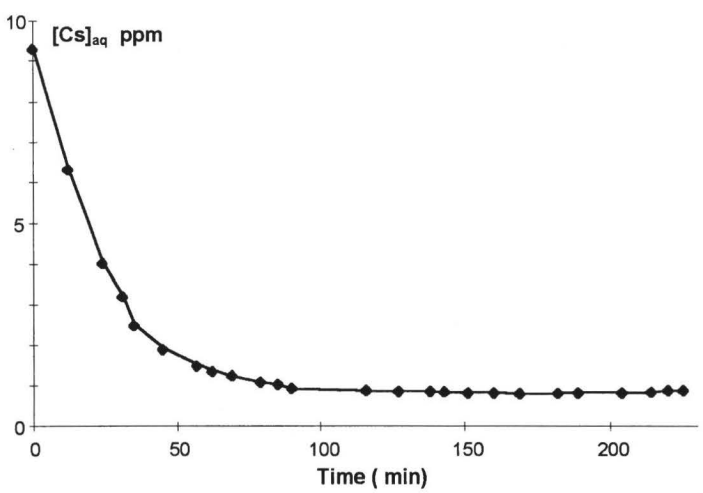

Figure 2: Final Caesium concentration versus time

Cs extraction efficiency is excellent (91%) with the stationary state being reached in less than 2 hours. Following stripping the loaded emulsion, the alkali concentrations in the internal phase were: $[Cs^+]_{int} = 2.07\ 10^{-3}$ mol/dm^3 and $[Na^+]_{int} = 1.9$ mol/dm^3

Thus, concentration and decontamination factors, with respect to Cs, are respectively 27 and 11. In addition, Karl-Fischer determination of water concentration in the organic phase proves that about 50% of water was transferred from the emulsion to the external phase due to both emulsion breakage and osmotic contraction. Even if sodium co-extraction is quite low (1.2%), the surprisingly high sodium concentration in the internal phase is most probably due to imperfect phase disengagement in the upper settler.

Measured retention rate is equal to 17% and mean residence time for the dispersed phase is

about 2.33 minutes.

CONCLUSION

A new ELM extraction process has been developed for the purification of Cs from a concentrated sodium and hydroxide matrix. Continuous extraction was validated on a laboratory scale pulsed column. Excellent extraction performances were achieved (>90%). The process scheme is based on an original association between resorcarene, a new calixarene extractant synthesised in our laboratory, and a surfactant (PARABAR 9220) newly introduced to ELM processes.

The appropriate nature and composition of the emulsion allowed the achievement of excellent extraction performances: efficiency, selectivity and decontamination.

An unfavourable result concerning the surprisingly high sodium concentration in the internal aqueous phase has been observed in relation with the imperfect phase disengagement in the settle, although, emulsion coalescence and settling may be optimised. Significant improvements may result from an exhaustive study of the effect of hydrodynamic parameters and the choice of an appropriate settler. Validation with the industrial effluent may complete the present study.

REFERENCES

1 Bell JT and Bell JH, *Chemical Pre-treatment of Nuclear Waste for Disposal,* Schultz WW and Horwitz EP, Eds. Plenum Publishing Corp., New York, (1994)

2 Horwitz E P, Dietz M L and Jensen MP, *Proc.ISEC'96*, Melbourne, (1996)

3 Hartmann D, Pareau D, Chesne A and Durand G, *Solvent Extraction 1990*, *Proc.ISEC'90,* Ed. Sekine T., Elsevier, 1567, (1994)

4 Samar M, Pareau D, Durand G and Chesne A. *Hydrometallurgy'94*, Chapman & Hall, (1994)

5 Kaplan P, *Thèse de Doctorat de l'Ecole Centrale Paris*, Paris, (1997)

6 Gokel JW, *Crown Ethers and Cryptands*», Ed. Stoddart JF, (1991)

7 Vicens J and Bohmer V, *Calixarenes : A versatile class of macrocyclic compounds*, Ed. Kluver, (1991)

8 Hogberg S, *J. Am. Chem. Soc.*, **102**, 6046, (1980)

9 Koide Y and Oka T, *Bull. Chem. Soc. Jap.*, **66**, 2137, (1993)

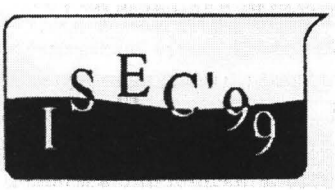

MECHANISM OF TRANSMEMBRANE WATER TRANSFER AND EMULSION SWELLING

MYu Koroleva, NV Bakastova and EV Yurtov
Mendeleev University of Chemical Technology, Moscow, Russia

ABSTRACT
Liquid membrane extraction in multiple emulsion is often accompanied by transmembrane water transfer, which leads to the swelling of extracting emulsions. Mechanism of water transport was studied in experiments with rhodamine C. This substance can penetrate through the liquid membrane only in solubilized form. D2EHPA, oleic acid, sodium oleate, trioctylamine, dioctylamine, and Tween 80 were added to the organic phase. Our results showed that the main form of water transport is one by means of nanodispersion droplets.

Keywords: liquid membrane, emulsion swelling, water diffusion, dioctylamine, tri-*n*-octylamine, oleic acid, sodium oleate, D2EHPA, Tween 80

INTRODUCTION

Transmembrane water transfer leading to emulsion swelling is a negative phenomenon, which takes place during the liquid membrane extraction when internal and external water phases have different substance concentrations. As known, such process takes place in a great extent in emulsion systems with Span 80. Several articles have been published in this field, and the related points of view can be divided into two groups: water can be transported by either microemulsion or nanodispersion[1,2] and water can be transported by single surfactant and carrier molecules.[3,4]

The formation of either microemulsion or nanodispersed droplets is promoted by the presence of a co-surfactant along with the surfactant in the system and by the dis-equilibrium between the phases of the extracting emulsion, i.e. by the mass transfer of the components and the solvents through the interface. Diffusion coefficients of microemulsion are much lower than those of the monomeric individual surfactant molecules.[5]

Data concerning the size distribution of drops in the emulsion before and after the membrane extraction of cholesterol have been presented.[2,6]

States of the Surfactant in the Extracting Emulsions

As published[7], the raising of the surfactant concentration increases the emulsion stability against coalescence. When the surfactant is present in an amount sufficient for the stabilization of all internal phase droplets formed as a result of the dispersing, the maximum stability of the emulsion is reached. With a greater concentration of the surfactant, the excess of the latter can dissolve in liquid membrane with the formation of different types of micelle structures.

The surfactant condition in extracting emulsions was examined with low sorbitanmonooleate concentration. During emulsion phase separation the oil phase was taken away and analysed by optical methods and dye solubilization techniques. Figure 1 illustrates sorbitanmonooleate concentration in the oil phase of the extracting emulsion versus the dependence of the total surfactant concentration. The sharp bend of the Span 80 concentration in the liquid membrane at 0.125 mol/dm^3 sorbitanmonooleate in the emulsion corresponds to the complete adsorption of the surfactant on the interface of all droplets formed as a result of the dispersing. At the higher concentration of the surfactant its amount in oil phase dramatically increases.

The dotted line on the figure 1 corresponds to critical concentration of sorbitanmonooleate micelle formation in the mineral oil. So at the low surfactant concentration in the extracting emulsion (concentrations less than necessary for the complete adsorption) some of the sorbitanmonooleate is present in the liquid membrane in the form of micelles. As our investigations showed, in many cases

© 2000 Society of Chemical Industry

there are solubilized micelles in the oil phase of emulsion, that is micelles with a small amount of water phase in the inner core.

Mechanism of Water Transfer in the Liquid Membrane

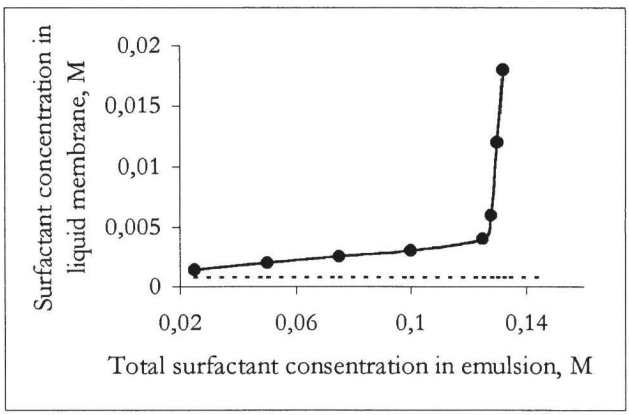

Figure 1. Sorbitanmonooleate concentration in the liquid membrane versus the total surfactant concentration in the extracting emulsion. Dotted line -CCM of sorbitan monooleate in the mineral oil

To clear up the mechanism of this phenomenon transmembrane transfer of different substances in a multiple emulsion was investigated .

Rhodamine C is a substance, which dissolves well in water, does not dissolve in the mineral oil in the liquid membrane, does not interact with single surfactant molecules, but can be solubilized in micelles and water droplets of a nanodispersion. So the dye can be transported through the liquid membrane only by surfactant micelles or nanodispersion, or as a result of coalescence of internal phase droplets leading to water phase separation.

An emulsion W/O was prepared from either 3.5 mol/dm^3 NaCl solution or distilled water, mineral oil, and surfactant - sorbitanmonooleate. This emulsion was placed on a flat surface with an area of 6.5 x 10^{-3} m^2, and contacted with one of the above mentioned water solutions. Rhodamine C was added in the internal or in the external water phase and different variants of rhodamine C transport from the internal water phase to the external one and in the opposite direction were carried out:

- without water transport;
- with water transport in the same direction;
- with water transport in the opposite direction.

Concentration of rhodamine C in the external water phase was determined by optical methods. The extracting emulsion stability against coalescence, that is water phase separation, was controlled by measurements of salt concentration in the external water phase.

Diffusion coefficients of rhodamine C were calculated using the data of the kinetic curves of rhodamine C concentration in the external water phase by means of the equation of non-stationary diffusion (table 1).

The kinetics of ethanol diffusion in the multiple emulsion was also investigated . This substance is highly soluble in water phase, with a very low solubility in mineral oil. Consequently, ethanol can be transported only to a slight extent from the internal water phase to the external one in the molecular form.

The emulsion with containing 2.0 mol/dm^3 ethanol and 3.5 mol/dm^3 NaCl in the internal water phase was contacted with a NaCl solution with the same concentration. During these experiments internal water phase concentration slightly decreased due to the alcohol flux from the emulsion. Ethanol concentration in the external water phase was determined by refractometry and gas-chromatographic methods. Diffusion coefficient was equal to 1.8 x 10^{-14} m^2/s.

Water transmembrane transfer leads to the swelling of the extracting emulsion and the transfer of water takes place during the liquid membrane extraction when the internal and external water phases have different solute concentrations.

In these experiments, the internal water phase of emulsion was a NaCl solution whose concentration varied between the experiments. The organic phase was mineral oil without carrier. External water phase consisted of distilled water.

Internal water phase (in emulsion)	Direction of substance transfer	External water phase (out of emulsion)	$D * 10^{14}$ m^2/s
3.5 mol/dm^3 NaCl	← Rhodamine C	3.5 mol/dm^3 NaCl & $2.4x10^{-5}$ mol/dm^3 Rhodamine C	1.7
3.5 mol/dm^{3}NaCl & $7.2x10^{-5}$ mol/dm^3 Rhodamine C	Rhodamine C →	3.5 mol/dm^{3}NaCl	4.2
H_2O	H_2O → ← Rhodamine C	3.5 mol/dm^3 NaCl & $2.4x10^{-5}$ mol/dm^3 Rhodamine C	1.7
H_2O & $7.2x10^{-5}$ mol/dm^3 Rhodamine C	H_2O → Rhodamine C →	3.5 mol/dm^3 NaCl	4.2
3.5 mol/dm^3 NaCl	← H_2O ← Rhodamine C	H_2O & $2.4x10^{-5}$ mol/dm^3 Rhodamine C	1.5
3.5 mol/dm^3 NaCl & $7.2*10^{-5}$ mol/dm^3 Rhodamine C	← H_2O Rhodamine C →	H_2O	5.6
H_2O	← Rhodamine C	H_2O & 2.410^{-5} mol/dm^3 Rhodamine C	1.4
H_2O & $7.2x10^{-5}$ mol/dm^{3}Rhodamine C	Rhodamine C →	H_2O	5.6

Initial internal water phase concentration in emulsion - 0.65.

Table 1 Diffusion Coefficients of Rhodamine C in Multiple Emulsion

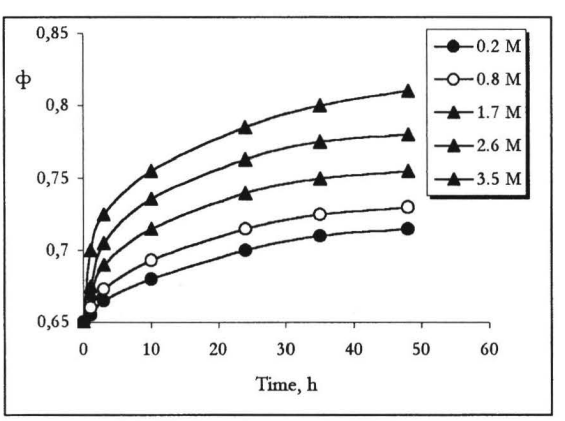

Figure 2. Kinetic curves for water transfer at the different initial NaCl concentrations in the internal phase of the emulsions

Figure 2 shows the kinetic curves of the alteration of ϕ , the internal water phase concentration (or ratio of phases), in emulsions with different initial NaCl concentration. Only starting intervals of kinetic curves are shown on this figure. Water transfer continued approximately 20-25 days, and the internal water phase concentration reached ~ 0.92 in the emulsion of initial NaCl concentration 3.5 mol/dm^3.

Diffusion coefficients of water were calculated on the base of these kinetic curves by means of equation of non-stationary diffusion and were equal ~ 0.30 x 10^{-14} m^2/s.

Investigations were also conducted of the diffusion characteristics in the extracting emulsions with carrier or polar organic substances. Emulsion with 3.5 mol/dm^3 NaCl in the internal water phase and 3 mas.% additives to the mineral oil was contacted with distilled water.

For the comparison of experimental diffusion coefficients of water, Rhodamine C, and ethanol, molecular diffusion coefficients were calculated of by Wilke-Chang equation and the results are in table 2.

Substances diffused	Additives	*D* experimental, m^2/s	*D* calculated, m^2/s
Water	——	0.3×10^{-14}	5.4×10^{-11}
	DEHPA	6.2×10^{-14}	
	Oleic acid	5.8×10^{-14}	
	Natrium oleate	3.6×10^{-14}	
	Trioctylamine	4.4×10^{-14}	
	Dioctylamine	5.6×10^{-14}	
	Tween 80	2.5×10^{-14}	
Rhodamine C	——	$(1.4\text{-}5.6)\times10^{-14}$	0.7×10^{-11}
Ethanol	——	1.8×10^{-14}	3.0×10^{-11}

Table 2 Molecular and Experimental Diffusion Coefficients

So calculated diffusion coefficients are approximately 1000 times higher than the experimental ones. The presence of carriers in the organic phase of the extracting emulsion does not lead to a significant increase of the diffusion coefficients. The value of the diffusion coefficient of water in the system without carrier is approximately 10 times smaller than those in systems with carriers. But these values do not exceed the diffusion coefficient of Rhodamine C, the substance, which can be transported through the liquid membrane only in solubilized form. This fact points out that all these substances, including water, are transported in the form of a nanodispersion.



Figure 3. Photomicrographs Pt/C replicas of emulsion after ethanol transport (magnitude - $1.5*10^5$).

To confirm the formation of nanodispersion droplets during transmembrane transfer of substances photomicrographs of emulsions were obtained before and after extraction. Photomicrographs of Pt/C replicas of emulsion after ethanol transport were prepared by the freezing-cleavage method (figure 3). Internal water phase drops in

emulsion were covered by small droplets of nanodispersion (d = 17 - 25 nm). Initial emulsion before ethanol transport contained smooth water drops without nanodispersion.

So it can concluded that the main form of water transmembrane transfer is by nanodispersion droplets or solubilized micelles. Water, like the other substances investigated, can be transported by surfactant or carrier in molecular form, but the first way prevails.

Extracting Emulsion Swelling and its Stability

Emulsion swelling is a negative phenomenon, which takes place at the liquid membrane extraction. It leads to the dilution of substances in the internal phase of the emulsion, and consequently to a decrease of extraction efficiency.

At the same time emulsion swelling affects extracting emulsion stability. The criterion of the stability against coalescence is the half-separation period of the water phase. The influence of the emulsion swelling ϕ/ϕ_0, (the ratio of the internal phase concentration at time t to that at t=0) on the half-separation period of water phase is shown in figure 4. Extracting emulsion stability against coalescence sharply diminishes at the emulsion swelling, and at $\phi/\phi_0 = 1.4$, i.e. at the swelling emulsion with initial $\phi_0 = 0.65$ to $\phi = 0.90$, decreases to approximately ~ 10 h at 85 °C, and this emulsion can not be used for the extraction. Thus, extracting emulsion swelling is a complicated process connected with the transport of water. The main form of water transport is one by means of nanodispersion droplets or solubilized micelles.

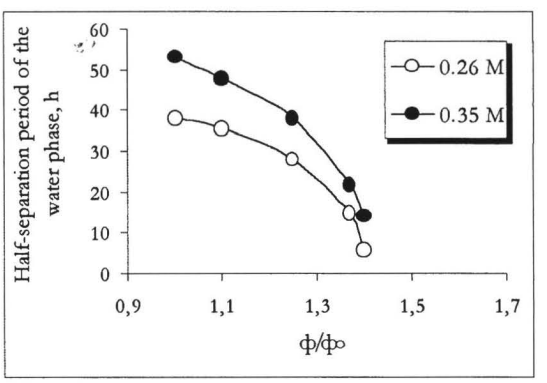

Figure 4. Extracting emulsion stability to coalescence at 85°C versus emulsion swelling at the different initial concentrations of NaCl in the internal phase

ACKNOWLEDGMENTS

Various aspects of the research presented in this paper were supported by Russian Foundation of Fundamental Researches - Grant N° 98-03-32564 and the Ministry of Education of the Russian Federation - the Grant "Fundamental Natural History".

REFERENCES

1. Plucinski P, *J. Membran. Sci.*, **21** (1), 105, (1985).
2. Yurtov EV and Koroleva MYu, *Russian Chemical Reviews*, **60** (11), 1255, (1991).
3. Tsuboi K, Akita S, Takahashi T and Takeuchi H, *Kagaku Kogaku Ronbunshu*, **13** (1), 110, (1987).
4. Colinart P, Delepine S, Trouve G and Renon H, *J. Membran. Sci.*, **20** (2), 167, (1984).
5. Eike HF, *Interfacial Phenomena in Apolar Media*, Marcel Dekker, Inc., New York, 41, (1987).

6. Yurtov EV, Koroleva MYu, Golubkov AS, et al., *Dokl. Akad. Nauk SSSR*, **302** (5), 1164, (1988).
7. Yurtov EV and Koroleva MYu, *ACS Symposium Series, 642*, Washington, DC, 89, (1996).

RECOVERY OF 4-HYDROXYBENZOIC ACID FROM AQUEOUS SOLUTIONS BY EMULSION LIQUID MEMBRANES

Paulo FMM Correia and Jorge MR Carvalho
Instituto Superior Técnico, DEQ - Department of Chemical Engineering, Av. Rovisco Pais 1096 Lisboa Codex Portugal

ABSTRACT
Emulsion liquid membranes were applied to the recovery of 4-hydroxybenzoic acid (a compound present in olive mill wastewater) from aqueous solutions. Models considering solute diffusion through the emulsion as the rate determining step (typically used to describe phenol transport) fail to describe this compound's behaviour. A model considering stripping kinetics effect gave better results.

Keywords: emulsion liquid membranes, olive mill waste-water, hydroxybenzoic acid, Hostarex A327, surfactant ECA 4360

INTRODUCTION

From the processing of products of vegetable nature large environmental impact waste-waters with phenolic compounds result. An example of this is the olive mill waste-water problem that occurs mainly in Mediterranean countries. Olive average world production is 7900 thousand tons per year. About 90% of this production is used in olive oil production. The environmental danger of this activity is that only 20% of the olive mass gives olive oil. The remaining 80% give rise to effluents either solid waste - the husks - (30%) or olive mill waste-water (50%).[1] To give an idea of this huge pollution problem, it is proved that processing 1 ton. of olives generates oxygen demand pollution equivalent to the one produced by 800 people. 4-Hydroxybenzoic acid is a typical phenolic compound present in this kind of wastewater. Recovery of this compound from aqueous solutions by emulsion liquid membranes was tried out.

Emulsion (or surfactant) liquid membranes (ELM) were invented by Li in 1968.[2] From that time on this technology has demonstrated a considerable potential as a technique for separating and concentrating organics, inorganics and metal ions from dilute streams.[3] A schematic diagram of ELM technology is presented in Figure 1. The effluent to be treated is contacted with emulsion globules (with diameters in the mm range). Each globule consists of droplets of an aqueous internal receiving phase (with diameters in the μm range) encapsulated in an organic membrane phase containing a surfactant. This emulsion was previously prepared by stirring at high mixing rates (emulsification). During the contact between wastewater and emulsion (permeation), transport of the products to be recovered occurs through the membrane and into the receiving phase, where they are concentrated. After subsequent separation by gravity of the effluent from the emulsion (settling), splitting of the emulsion (or demulsification) is carried out usually by applying an high voltage electrical field, in order to separate the phases which compose the emulsion - the internal aqueous phase and the organic membrane phase. The stripped membrane phase can be reused and the receiving phase - enriched in recovered solute - can be recycled or recovered for solute. According to its composition, the effluent may be submitted to additional treatment processes or simply discharged.

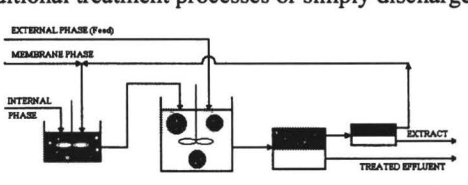

Figure 1. Schematic diagram of ELM process.

© 2000 Society of Chemical Industry

Several studies have been reported and reviewed[4] concerning the application of the emulsion liquid membranes technology to the removal of phenols from aqueous solutions. However studies have been confined to the removal of phenol, nitrophenols, chlorophenols and cresols. The mechanism for the emulsion liquid membranes in this case is usually type I (without the use of a carrier in the membrane phase). Several models have been developed to describe this case. The most successful ones were the advancing front model and the reversible reaction model.

Advancing front model was proposed by Ho et al.[5], as an extension of Marr & Kopp[6] model to spherical co-ordinates. It assumes the emulsion globule as homogeneous and that there is an hypothetical interface - the reaction front - that separates the region where the internal stripping phase is exhausted from the unreacted core. This model assumes that the stripping reaction is instantaneous and irreversible. Their equations can be solved approximately by the perturbation method, giving zero order analytical solutions, which are accurate enough to describe batch permeation results. This model was refined by Fales & Stroeve[7], who introduced an extra external phase mass transfer resistance.

Reversible reaction model was firstly proposed by Teramoto and co-workers[8] and by Bunge et al.[9]. This model does not use the reaction front concept and allows the stripping reaction to be reversible. It gave similar results to advancing front model ones when applied to solutions containing only one phenolic compound, but in opposition to the advancing front model it could describe the behaviour of mixtures of phenols and organic acids (competition effects, etc.)[10]. The obtained equations set has to be solved numerically.

Yan and co-workers[11] have proposed recently a model that takes into account not only the diffusion through the emulsion globule, but also the possible rate determining effect of stripping kinetics. An approximate zero order solution by perturbation method was also obtained. This model was tested for this case and results were compared to the other ones.

Due to lack of space, interested readers are advised to find further information about these models (mathematics, formalism, etc.) in the cited papers.

EXPERIMENTAL

Emulsions were prepared by emulsifying NaOH (MERCK) aqueous solutions (internal phase) in an organic membrane phase composed by a paraffinic solvent (ShellSol T, Shell Chemicals Ltd.) and a non-ionic surfactant (polyamine ECA4360J, Essochem Europe Inc.). In most studies a modifier typically used in liquid-liquid extraction (Isodecanol, Riedel de Haën) was also used. A tertiary amine extractant - Hostarex A327 (Höechst) - composed by 50% tri-n-octylamine and 50% tri-n-decylamine was tested too. This extractant was selected from a set of separation funnel tests with several primary, secondary and tertiary amines, published elsewhere.[12] A rotor-stator type high speed rotative disperser (IKA Ultra Turrax T50 with an IKA G45ff ultrafine turbine) was used at 7000 rpm with a residence time of 15 min. Permeation was made by dispersing this emulsion in the external aqueous phase containing 4-hydroxybenzoic acid (Fluka) in a 1 l cylindrical glass reactor (85 mm internal diameter, round bottom) immersed in a water bath, in order to keep the permeation temperature constant. A set of two stainless steel baffles (with 205 mm × 7 mm × 0.55 mm each) was attached to this reactor. It allowed a gap of 5 mm between each baffle and the reactor wall, in order in order to prevent emulsion accumulation near reactor wall. Agitation was performed through a stainless steel paddle (with 45 mm × 45 mm × 1 mm) centred at 12 mm from reactor top and provided by an Heidolph RZR1 driver. During permeation photographs were taken near the reactor wall. Afterwards an extra sample of the reactor external phase content was obtained and emulsion was poured and broken in a cylindrical double wall coaxial electrocoalescer. The annular space was filled with an electrolyte. Demulsification was performed by applying a 4 kV and 2.7 kHz electric field through an high voltage unit prototype.

Internal and external phase sample analysis was made in a double beam ultra-violet/visible spectrophotometer Hitachi U2000. pH measurement was accomplished by a Metrohm 632 pH Meter

with a combined Metrohm electrode. Emulsion globules Sauter mean diameter was obtained through the use of KS100 image analysis software (Kontron Elektronik GmbH). 4-Hydroxybenzoic acid distribution ratios between external and membrane phase were obtained by agitating the external and membrane (without surfactant) for 24 h. Densities and viscosities were obtained through glass pyknometers and Ubbelohde glass capillary viscometers (Schott). Interfacial tension between external and membrane (without surfactant) phases was obtained through modified drop size method[13].

Implementation of the models was done by the use of MATLAB software. In the case of reversible reaction a Crank and Nicolson version using Thomas algorithm[14] was used.

RESULTS AND DISCUSSION

Based in successful tests with phenol (published elsewhere[12]), the recovery of 4-hydroxybenzoic acid from synthetic aqueous solutions was tested by emulsion liquid membranes. Results are shown in Table 1. Permeation kinetics is very low, suggesting that the behaviour of this compound is somewhat different of that of phenolic compounds that have been studied so far. The introduction of an amine extractant or a modifier typically used in liquid-liquid extraction in the membrane phase enables the increase of the permeation kinetics and an effective removal of 4-hydroxybenzoic acid from an aqueous solution as shown. However care must be taken with external phase pH, because sulphuric acid co-transport may occur and internal phase may be neutralised, aborting the process. This deleterious pH effect can be overcome by the use of a membrane phase with the modifier only. This was the composition used for the rest of the studies.

Internal phase	NaOH 0.2 mol dm^{-3}				
Membrane Phase:					
ShellSol T	98% (p/p)		94% (p/p)		96% (p/p)
Isodecanol	-		2% (p/p)		2% (p/p)
Hostarex A327	-		2% (p/p)		-
ECA4360J	2% (p/p)		2% (p/p)		2 % (p/p)
External phase					
$[C_7H_6O_3]_{III,0}$ (pH)	200 mg/L (pH=3.7)	200 mg/L (pH=2.3*)	200 mg/L (pH=3.7)	200 mg/L (pH=2.3*)	200 mg/L (pH=2.3*)
$[C_7H_6O_3]_{III,after\ permeat.}$ (*E*)	180 mg/l (*E*=0.10)	90 mg/l (*E*=0.55)	7 mg/l (*E*=0.965)	150 mg/l (*E*=0.25)	1.4 mg/l (*E*=0.993)
$[C_7H_6O_3]_{I,after\ demulsif.}$	182 mg/l	825 mg/l	1500 mg/l	626 mg/l	1200 mg/l

*External phase acidification was done by H_2SO_4 addition.

Table 1 Results of preliminary studies to choose membrane phase composition (Operating conditions: $V_{II}/V_I = 1$; emulsification stirring rate: 7000 rpm; emulsification time: 15 min; $V_{III}/V_I = 10$; permeation temperature: 298 K; permeation time: 20 min; permeation stirring rate: 300 rpm)

For modelling permeation results both advancing front[5,7] and reversible reaction[9] models were tried out, but both failed to describe experimental data as shown in Figure 2. On the other hand, Yan et al. model[11] proved to describe quite well the experimental data with the proper choice of this model's adjustable parameter - the Damköhler number (*Da*). Good fitting has been found with *Da*=30 at external phase pH=2.3. As referred by Yan et al.[11], this value of *Da* means that permeation process is controlled by diffusion and reaction jointly. If external phase pH changes to 3.7 best fitting occurs at *Da*=60 (Figure 3). One could argue about *Da* real physical meaning in this case, but one interesting

thing is that the value of *Da*=60 chosen has shown to describe (despite the presence of some non-idealities) permeation stirring rate effect (shown in Figure 4).

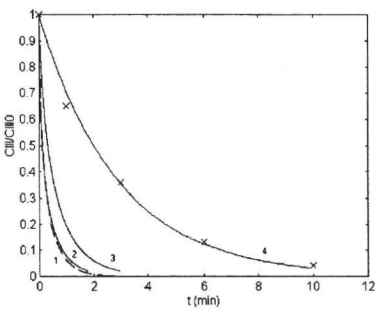

Figure 2. Application of several models to batch permeation data: 1. Bunge et al. model[9]; 2. Advancing front model[5]; 3. Fales and Stroeve model[7]; 4. Yan et al. model[11]; × - Experimental data. (Operating conditions: V_{II}/V_I = 1; emulsification stirring rate: 7000 rpm; emulsification time: 15 min; V_{III}/V_I = 20; permeation temperature: 298 K; permeation time: 10 min; phases composition: the same listed in last column of Table 1).

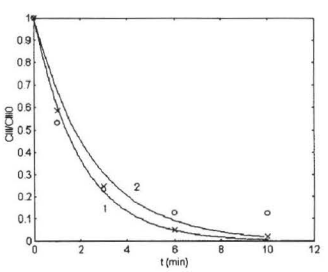

Figure 3. External phase pH effect: pH=2 (line 1- Yan et al. model[11]; × - experimental data) and pH=3.7 (line 2 - Yan et al. model[11]; o - experimental data) (Operating conditions: the same of Figure 2, except external phase pH variations; permeation stirring rate: 400 rpm).

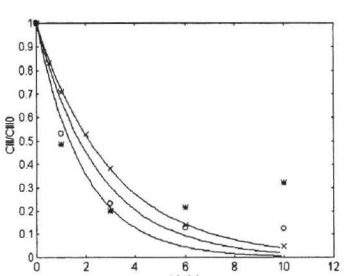

Figure 4. Permeation stirring rate effect: × - 300 rpm; o - 400 rpm; * - 500 rpm; Solid lines - Yan et al. model[11] (Operating conditions: the same of Figure 2, except external phase was not acidified

Permeation temperature effect was also studied and is shown in Figure 5. Yan et al.[11] model description of permeation experimental data was also possible with good fitting using *Da* values shown in Table 2. From these values stripping rate constants assuming pseudo-first order kinetics were obtained. From an Arrhenius regression (with a correlation coefficient of 0.98) the expression $ln\ k_1 = (13\pm2) - (4.3\times10^3\pm6\times10^2)/T$, a value of (36±5) kJ/mol was obtained for the activation energy. Further studies are needed however in order to check either physical meaning of this kinetic treatment (through kinetic studies in a stirred cell) or the possible role of isodecanol as a carrier (as in metals permeation), which has been neglected so far.

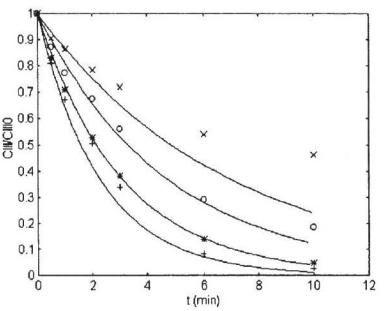

Figure 5. Batch permeation temperature effect: × 278K; o 285K; * 298K; + - 308 K; Solid lines - Yan et al. model[11]. (Operating conditions: $V_{II}/V_I = 1$; emulsification stirring rate: 7000 rpm; emulsification time: 15 min; $V_{III}/V_I = 20$; permeation time: 10 min; permeation stirring rate: 300 rpm; phases composition: the same listed in last column of Table 1, except external phase was not acidified (pH=3.7)).

(Relevant operating parameter: $\phi_1 = 0.5$ ($V_{II}/V_I = 1$))

T (K)	α	D_{eff} (m^2/s)	R (m)	$Da = \phi_1 k_1 R^2 / (\alpha D_{eff})$	k_1 (s^{-1})
	0.524	1.87×10^{-10}	1.96×10^{-4}	20	0.102
	0.519	1.96×10^{-10}	2.03×10^{-4}	40	0.197
	0.516	2.43×10^{-10}	2.07×10^{-4}	60	0.350
	0.514	2.88×10^{-10}	2.00×10^{-4}	65	0.482

Table 2 Results of permeation temperature effect analysis by Yan et al.[11] model

As a final conclusion of these preliminary studies, one should be cautious considering phenolic effluents treatment, because, as proved, there are some phenolic compounds with different behaviour from the most common ones and treatment conditions extrapolation without considering the effluent composition could be a huge risk.

ADDITIONAL NOTATION

Da	Damköhler number (-)	ϕ_1	$[= V_{I0} / (V_{I0} + V_{II0})]$ (-)
D_{eff}	Effective diffusivity in emulsion globules (m^2/s)		
R	Radius of emulsion globule (m)		*Subscripts:*
V	Volume (m^3)	0	Initial
C	4-Hydroxybenzoic acid concentration (mol/m^3)	1	Pseudo-first order
α	Distribution coefficient for the solute between external phase and emulsion at equilibrium $[= (V_{I0} + D\ V_{II0}) / (V_{I0} + V_{II0})]$ (-)	I	Internal phase
		II	Membrane phase
		III	External phase

ACKNOWLEDGEMENTS:

The authors would like to thank Shell Chemicals, Ltd., Höechst AG and Essochem Europe Inc. by the reagent samples offered to this work. The financial support of FCT through PRAXIS XXI Programme is also acknowledged.

REFERENCES

1. Vives-Rego J, Sala C and Díaz O, *Diário de Mallorca*, June 1995.
2. Li NN, *U.S. Pat. 3,410,794*, (1968).
3. Kitagawa T, Nishikawa Y, Frankenfeld JW and Li NN, *Environ. Sci. Technol.*, **11(6),** 602, (1977).
4. Correia PFMM and Carvalho JMR, *V Conf. Nac. Qual. Amb., Aveiro*, 1827, (1966).
5. Ho WS, Hatton TA, Lightfoot EN and Li NN, *AIChE J.*, **28**, 662, (1982).
6. Marr R and Kopp A, *Int. Chem. Eng.*, **22**, 55, (1982).
7. Fales JL and Stroeve P, *J. Memb. Sci.*, **21**, 35, (1984).
8. Teramoto M, Takihana H, Shibutani M, Yuasa T and Hara N, *Sep. Sci. Technol.*, **18(5),** 397, (1983).
9. Bunge AL and Noble RD, *J. Memb. Sci.*, **21**, 55, (1984).
10. Wang CC and Bunge AL, *J. Memb. Sci.*, **53**, 71, (1990).
11. Yan N., Shi Y and Fu YF, *Chem. Eng. Sci.*, **47**, 4365, (1992).
12. Correia PFMM and Carvalho JMR, *CHEMPOR'98*, Lisbon, 1073, (1998).
13. Carvalho JMR, *PhD Thesis*, University of Bradford, 1982.
14. Rice RG and Do DD, *'Applied Mathematics and Modeling for Chemical Engineers'*, John Wiley & Sons, New York, (1995).

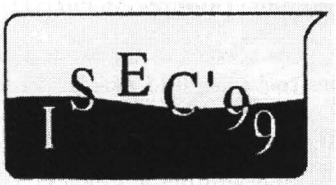

PURIFICATION AND CONCENTRATION OF LACTIC ACID BY EMULSION LIQUID MEMBRANE EXTRACTION

T Berrama, D Pareau, M Stambouli and G Durand
Laboratoire de Chimie et Génie des Procédés, Ecole Centrale Paris, Grande Voie des Vignes, 92295 Chatenay-Malabry Cedex France

ABSTRACT
Lactic acid extraction by emulsion liquid membranes (ELM) was studied and optimal conditions were found in batch experiments by studying the influence of different parameters: concentrations of extractant, surfactant, contact time, etc. These conditions were then adapted to the actual effluent and tested in continuous experiments with one and two stages of mixer- settler; the feasibility of the process was then demonstrated.

Keywords: lactic acid, emulsion liquid membrane, tri-dodecylamine, surfactant ECA 4360, Span 80

INTRODUCTION

The milk industry leads to the formation of a by-product, lactoserum. Many works are performed in Europe to valorise this effluent by producing lactic acid by fermentation; this lactic acid must however be purified before being recycled. The most expensive step of the process is this purification; several techniques are competing in terms of efficiency and cost. Membrane techniques have been evaluated since the 1980's: systems combining immobilization of growing cells and electrodialysis have proven their efficacy.[1] More recently, the continuous isolation of lactic acid by facilitated membrane extraction has been studied.[2] Adsorption on polyvinylpyridine and activated carbon[3] and ion exchange, cation exchange for production and purification of lactic acid[4] and anion exchange for lactate recovery[5] have been successfully investigated. Solvent extraction was the most studied technique using mainly tertiary amines.[6-8] The main result of these works is the feasibility of lactic acid extraction at an intermediate pH between the optimum extraction pH about 3 and the optimum fermentation pH of 5-6. In membrane based solvent extraction using a tertiary amine,[9] the three liquid phases (aqueous feed, organic carrier and stripping phase) are separated by membranes and its feasibility has been demonstrated.

A few studies have been devoted to emulsion liquid membrane extraction (ELM) of lactic acid, the extractant being mainly a secondary amine.[10,11] The feasibility of the process was demonstrated also with a tertiary amine.[12,13] A mathematical model was proposed for lactic acid permeation in such systems. It seemed interesting to follow up such a study with a continuous process proposal and its bench scale test.

EXPERIMENTAL

Synthetic aqueous solutions were prepared by dissolving lactic acid Merck (90%) in water. The extractant is a tertiary amine: tri-dodecylamine (Merck). The other compounds are: sodium hydroxide (Merck), SPAN 80 (Fluka), ECA 4360 (EXXON), dodecane (Prolabo), octanol-1 (Prolabo) and 2- ethylhexane-1,3-diol (Merck).

Lactic acid and lactate concentrations were measured in aqueous solution by acid-base titration (Methrom Herisau E 536 Dosimat 655). Sodium concentrations were measured by atomic absorption spectroscopy (VARIAN A 300).

An agitated vessel of 200 cm^3capacity was used to contact aqueous solutions of lactic acid with the emulsion. Stirring was performed by a turbine impeller. Emulsification was performed using an Ultraturrax emulsifier (Janke & Kunkel IKA).

© 2000 Society of Chemical Industry

Solvent extraction preliminary experiments

A tertiary amine, trilaurylamine or tri-dodecylamine (TLA) was selected as the extractant. A solution of lactic acid was contacted with different organic solutions containing 0.15 mol/dm^3 TLA in various diluents (dodecane, dodecane/octanol, ethylhexanediol (EHD)/octanol). In the case of dodecane, extraction of lactic acid leads to third phase formation; extraction efficiency was good in the presence of octanol and/or EHD, leading to the quantitative formation of ammonium lactate. The extraction is favoured in acidic media where HLa is preponderant. Quantitative stripping was achieved by contacting the loaded organic phase with sodium hydroxide, leading to sodium lactate recovery.

The extraction mechanism is the following:

$$HLa + \overline{R_3N} \leftrightarrow \overline{R_3NH^+La^-}$$

where HLa and La$^-$ are lactic acid and lactate, and R_3N is TLA.

These extraction systems were then tested in ELM.

ELM Experiments

Experiments with SPAN 80

The experimental conditions are shown in table 1:

	Extraction phase (1)	Organic phase (2)	Stripping phase (3)
Composition	lactic acid 0.56 mol/dm^3	TLA 5% (w/w) EHD SPAN 80 Dodecane	NaOH 3.7 mol/dm^3
Volume cm^3	100	10	10

Table 1: Experimental conditions

EHD was varied between 0 and 5% (w/w) and SPAN between 1 and 5 % (w/w). In all cases emulsion breaking was important and always > 50%. As a consequence the extraction yield is reduced to < 5%. Several operating parameters were tested: emulsification time, rotating speed of the emulsifier, volume ratios, contacting time, etc, without any improvement of emulsion stability. This surfactant was consequently not retained.

Experiments with ECA 4360

Preliminary experiments with ECA 4360 showed that emulsion breaking is more limited in this case being < 10%. Under the same conditions as above with EHD 1% and ECA 5% (w/w), extraction yield is still relatively low, about 20% in 10 minutes contact time. In addition a considerable swelling of the emulsion was observed, about 100% in the same time, due to the ionic strength difference between both the aqueous phases. The first concern was then to find optimal conditions to extract lactic acid and reduce swelling.

To obtain quantitative extraction, it is necessary to introduce an excess of sodium hydroxide in the stripping phase. But it is not possible to increase NaOH concentration because of swelling, so it is necessary to increase the relative volume of the emulsion phase. The volume ratios were then altered to: $V_1/V_2/V_3 = 4/1/1$. Several parameters were studied: ECA, EHD and TLA concentrations

ECA concentration

The extraction kinetics of lactic acid were studied for EHD 1%, TLA 5% (w/w) and different concentrations of ECA. Extraction and swelling ratios are represented in figures 1 and 2. ECA has little influence on swelling which is still considerable. On the other hand the extraction yield decreases with increasing ECA concentration. So 2% ECA was the chosen concentration.

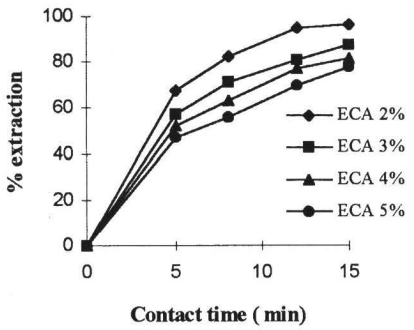

Figure 1: Extraction kinetics of lactic acid

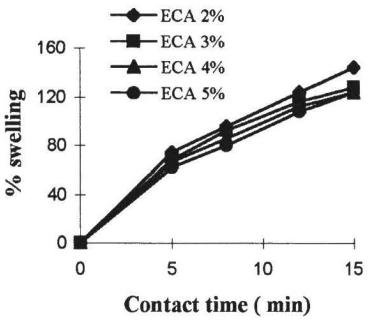

Figure 2: Swelling kinetics

In all cases emulsion breaking is limited to < 3%. ECA concentration has the same influence on both extraction and swelling. Due to the increasing membrane viscosity with increasing ECA concentration, lactic acid is extracted more slowly.

EHD concentration

Experiments with 1% and 0% EHD were compared with ECA 2%; extraction is better in the presence of EHD with 95% extraction against 80% without EHD after 12 minutes contact time. Swelling is more important too in the presence of EHD, showing that water can be transported by it. 1% EHD was the selected concentration because of the better lactic acid transfer.

TLA concentration

TLA was varied from 2 to 5%, all other parameters being constant. The results are reported in figure 3. As expected the extraction yield increases with increasing TLA concentration. 5% TLA was then adopted.

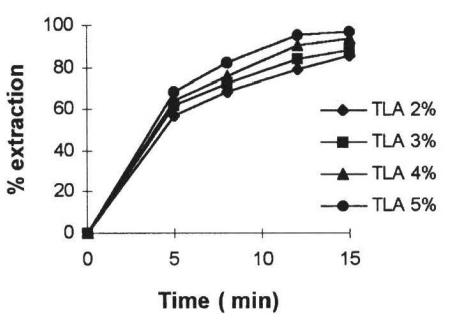

Figure 3: Influence of TLA concentration on lactic acid extraction

Conclusion

Under the following conditions: TLA 5%, ECA 2%, EHD 1%, $V_1/V_2/V_3$ = 4/1/1, the extraction (> 90%) is satisfactory after 10 minutes contact time, but swelling is important due to osmosis. The concentration factor is reduced to about 2 and a solution of about 1 mol/dm^3 lactic acid can be obtained. The initial aqueous solution had a pH lower than lactic acid pK_A (3.9), so the extraction was favoured. This is not the case for the actual effluent.

Extraction in the actual effluent conditions

The actual effluent has a pH of 4.5 so the major species is the lactate ion so the extraction is

then reduced with an extraction yield of 17% and the final pH 5.5.

Sulphuric acid was added to the extraction phase to maintain the pH around 4.5 which then favours lactic acid extraction. The extraction kinetics are limited due to the low HLa concentration compared to lactate ion (figure 4). It was confirmed that sulphuric acid was not co-extracted at this pH as no sulphate was found in the internal phase. By lowering the pH, lactic acid extraction is favoured but then sulphuric acid begins to be co-extracted, competing with lactic acid extraction and stripping. So the limiting pH value of 4.5 was adopted.

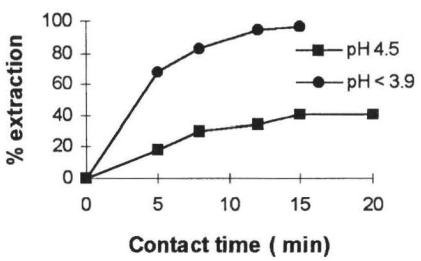

Figure 4: pH influence on lactic acid extraction

The extraction is however possible and this process was then tested in continuous experiments as can be seen below.

It should be noticed that under these pH conditions, a quaternary ammonium salt like Aliquat 336 could have be advantageously chosen; it is however then necessary to consider the stripping step which cannot performed by any mineral anions without polluting the recovered product. The only possible stripping solution is an hydroxide solution whose concentration might need to be very high, because of the exchange difficulties between lactate and hydroxide ions.

Continuous experiments

These were performed in one or two stages of mixer- settlers in the following conditions:

- organic phase: 5% TLA, 2% ECA, 1% EHD, dodecane
- stripping phase: NaOH 2 mol/dm^3
- extraction phase: lactic acid 0.3 mol/dm^3 pH 4.5
- emulsion volume ratio: 1/1
- contact time in each mixer: 10.4 min

The results are shown in figures 5 and 6.

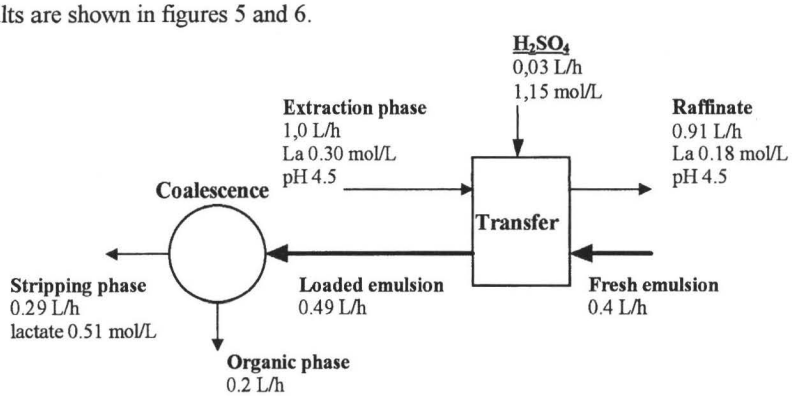

Figure 5: Continuous experiment with one stage of mixer- settler

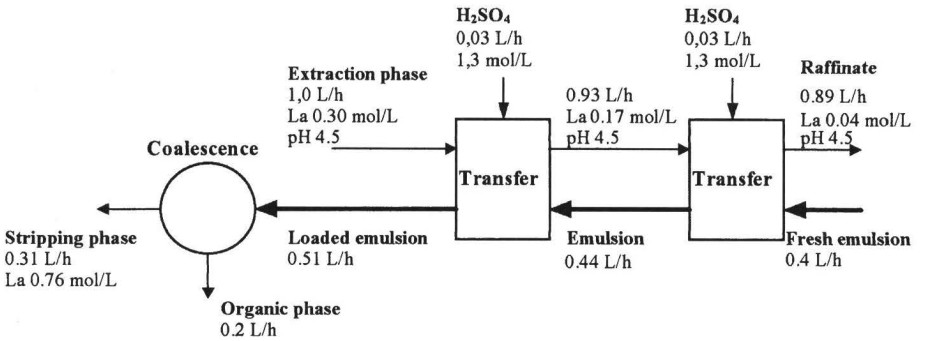

Figure 6: Countercurrent continuous experiments with two stages

The results are compared in table 2:

	% extraction	% swelling	%emulsion breaking	Concentration factor	SO_4 in stripping phase (mol/dm^3)
One stage	45.4	45	7	1.7	~ 2 x 10^{-3}
Two stages	88.1	55	10	2.5	~ 3 x 10^{-3}

Table 2: Comparison of continuous experiments

The extraction yield is directly related to contact time; but swelling is much more reduced with two stages, than with one with 20 minutes of contact in which swelling would be around 80%. The emulsion breaking is quite satisfactory, it was performed by electrocoalescence by the addition of a continuous field of 3.2 kV and an alternative of 0.5 kV (2 kHz). With a residence time of 4 minutes, the coalescence efficiency is greater than 90%.

CONCLUSION

The feasibility of this process has been demonstrated. Further optimisation could be performed on operating parameters to increase the extraction yield. Moreover experiments must be done on actual effluents to investigate possible interferences of lactoserum compounds, especially other organic acids like citric and pyruvic acids. Further work is then necessary before validating this process for lactoserum treatment.

REFERENCES

1. Vonktaveesuk P, Tonokowa M and Ishizaki A, *J. Ferment. Bioeng.*, **77**, 508, (1994)
2. Narebska A and Staniszewski M, *Sep. Sci. Technol.*, **33** (10), 1455, (1998)
3. Chen C and Ju LK, *Sep. Sci. Technol.*, **33** (10), 1423, (1998)
4. Rincon J, Fuertes J, Rodriguez JF, Rodriguez L and Monteagudo JM, *Solv.Extr. Ion Exch.*, **15**(2), 329, (1997)
5. Dave SM, Patil SS and Suresh AK, *Sep. Sci. Technol.*, **32**(7), 1273, (1997)
6. Han H and Hong WH, *Sep. Sci. Technol.*, **31**(8), 1123, (1996)
7. Han H, and Hong WH, *Sep. Sci. Technol.*, **33**(2), 271, (1998)
8. Tong Y, Hirata M, Takanashi H, Hano T, Matsumoto M and Miura S, *Sep. Sci. Technol.*, **33**(10), 1439, (1998)
9. Giorno L, Spicka P and Drioli E, *Sep. Sci. Technol.*, **31** (16), 2159, (1996)
10. Reisinger H and Marr R, *Chem Eng. Technol.*, **15**, 363, (1992)
11. Mok YS and Lee WK, *Sep. Sci. Technol.*, **29** (6), 743, (1994)
12. Chauduri JB and Pyle DL, *Chem. Eng. Sci.*, **47**(1), 41, (1992)
13. Chauduri JB and Pyle DL, *Chem. Eng. Sci.* , **47**(1), 49, (1992)

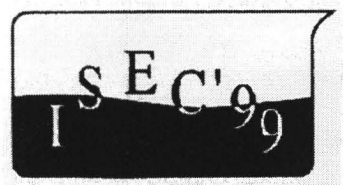

PREPARATION OF METAL–SILICATE MICROBALLOONS WITH LIQUID SURFACTANT MEMBRANE

T Hano[1], M Hirata[1], H Takanashi[1] and Y Nakahara[2]
[1]Department of Applied Chemistry, Oita University, Oita 870-1192, Japan
[2]Research Institute of Innovative Technology for the Earth, Kyoto 619-02, Japan

ABSTRACT
An interfacial reaction method, which is close to liquid surfactant membrane technology, was applied to prepare inorganic microballoons made of a variety of metal silicates. The extent of spherical balloon formation and the smoothness of the surface were controlled by the emulsifying conditions, especially by the concentrations of surfactant in oil phase and inorganic metal salts in both internal and external aqueous phases. The rate of balloon formation was accelerated by adding a metal cation carrier in oil phase. Microballoons made of multiple metal silicates were prepared by changing the metal species in external aqueous phase during the secondary emulsification.

*Keywords:*silicate microballoons, surfactant liquid membrane, silicates, calcium, D2EHPA, Span 80,

INTRODUCTION

Microballoons made of hard inorganic shell have become of interest as a new material due to their attractive properties such as strong resistance against high temperature and organic solvents. These characteristics are not expected with conventional organic microballoons made of organic high polymers. Several methods have been proposed so far to prepare inorganic microballoons, but the interfacial reaction method developed by Nakahara[1,4] is considered to be most favourable in that a wide variety of inorganic precipitation reactions can be applied to form insoluble shell. In this method, ion exchange occurs through an oil membrane between internal and external aqueous phases of (W/O)/W emulsion and the insoluble shell is formed inside the internal aqueous phase. Therefore, the reaction mechanism is quite similar to the transportation process in a liquid surfactant membrane. In the past study, the acceleration of balloons formation by applying the carrier-mediated penetration of ions has been reported, where two kinds of ion-carrier, cation and anion exchangers, were evaluated for their effects on ion exchange rates.[2,3] Together with the increase of formation rate, it is important to prepare the spherical balloons with as smooth a surface as possible. The extent of spherical balloons formation is influenced substantially with preparing conditions of W/O and (W/O)/W emulsions.

The present study focused on the effects of the conditions of emulsion preparation on the surface state of inorganic microballoons made of various metal silicates to clarify the reaction mechanism of shell formation. The technique to prepare the microballoons made of multiple metal silicates shell was developed.

EXPERIMENTAL

Figure 1 shows the experimental procedure to prepare calcium silicate microballoons as an example. An internal aqueous solution, prepared by dissolving sodium silicate ($Na_2O.nSiO_2$) in deionised water, and an organic solution, prepared by dissolving Span 80 as a surfactant and D2EHPA (di-2-ethylhexylphosphoric acid) as a cation carrier in kerosene, were mixed in a homogenizer at 2500 to 5000 rpm. The W/O emulsion thus prepared was then added to an external aqueous solution containing $CaCl_2$ and stirred gently at 200 to 300 rpm in a tank. The salt concentrations in both aqueous solutions were made equal to prevent the swelling of emulsion. Microballoons formed were washed with methanol and dried for scanning electron microscopy observations. A wide variety of metal chlorides or nitrates were used to prepare the metal silicate microballoons.

© 2000 Society of Chemical Industry

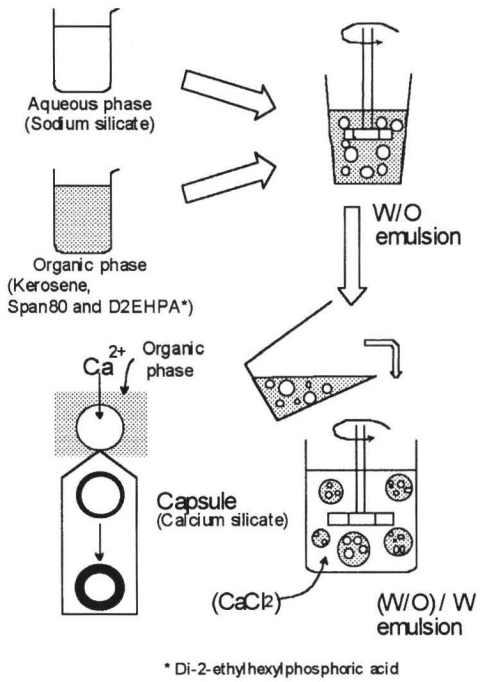

Figure 1 Preparation procedure of calcium silicate microballoons

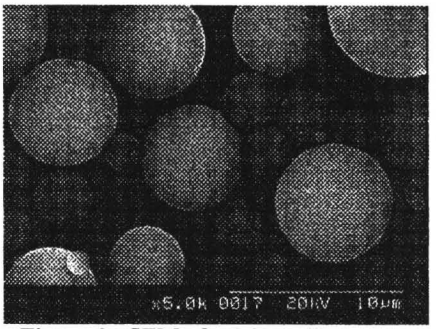

Figure 2 SEM of calcium silicate microballoons

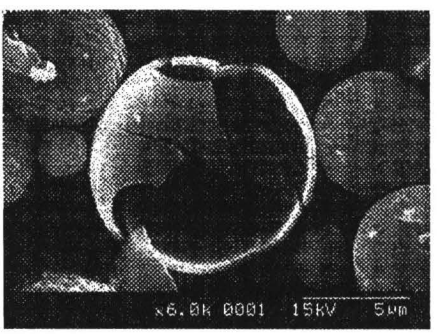

Figure 3 SEM of broken microballoons

RESULTS AND DISCUSSION

Effects of Operating Conditions on the Formation of Spherical Microballoons

The SEM picture of calcium silicate microballoons is shown in figure 2 where almost completely spherical balloons with smooth surface were prepared at high yield. It was also observed that several microballoons were broken as shown in figure 3, which clearly demonstrates the formation of hollow spheres with thin shell. The size of microballoons was dependent on the agitation speed of a homogenizer, oil phase viscosity and surfactant concentration. Figure 4 shows the relationship between the size of sodium silicate microballoons and the drop diameter of internal aqueous solution in the initial W/O emulsion. The size of microballoons increased linearly with drop size of internal aqueous solution with the shrinkage ratio of 75%. The shell thickness of capsules increased with the increase in the initial salt concentration. The effects of operating conditions on the extent of spherical balloon formation were examined based on the SEM observations as follows,

+++ (Almost all balloons are spherical.),
++ (The fraction of spherical balloons is high.),
+ (The fraction of spherical balloons is low.),
– (Spherical balloons are scarce.).

Homogenizer speed

As stated above, the size of balloons is well correlated with that of inner water drops which is principally determined by homogenizer speed, but the extent of spherical balloons formation was not influenced so much.

Sodium silicate concentration in inner aqueous solution

Table 1 predicts the effects of sodium silicate concentration as Na_2O. The increase in Na_2O concentration contributed to raising the fraction of spherical balloons probably due to the increase of shell thickness.

Carrier concentration

Table 2 predicts the effects of concentration of a cation carrier, D2EHPA, added to increase the penetration rate of metal cation through oil membrane. With the increase in D2EHPA concentration, the fraction of spherical balloons also increased although the W/O emulsion became very unstable beyond 0.5 wt% concentration. The effects on the size of balloons were not observed clearly.

Na_2O [M]	Span80 [wt%]	D2EHPA [wt%]	Homogenizer [rpm]	D_W [μm]	D_{MB} [μm]	D_{MB}/D_W [–]	Evaluation
0.38	1.0	0.1	5,000	2.65	1.73	0.65	–
0.75	1.0	0.1	5,000	2.23	1.92	0.86	–
1.12	1.0	0.1	5,000	3.01	2.41	0.80	+
1.43	1.0	0.1	5,000	5.46	3.91	0.72	++
2.24	1.0	0.1	5,000	22.7	3.74	0.17	+

D_W : Diameter of water drop in W/O emulsion. D_{MB}: Diameter of microballoons.

Table 1 Effects of sodium silicate concentration on the state of microballoon

Na_2O [M]	Span80 [wt%]	D2EHPA [wt%]	Homogenizer [rpm]	D_W [μm]	D_{MB} [μm]	D_{MB}/D_W [–]	Evaluation
1.45	1.0	0.1	4,000	6.60	4.46	0.64	++
1.43	1.0	0.1	5,000	5.46	3.91	0.72	++
1.56	1.0	0.1	6,000	4.82	3.22	0.67	+
1.45	1.0	0.2	4,000	5.13	5.49	1.07	++
1.44	1.0	0.2	5,000	4.99	4.45	0.89	++
1.42	1.0	0.2	6,000	3.48	2.89	0.83	+++
1.44	1.0	0.3	5,000	4.32	2.76	0.64	+++
1.42	1.0	0.3	6,000	2.69	3.00	1.12	+++
1.45	1.0	0.4	5,000	4.66	3.66	0.79	+++

Table 2 Effects of cation carrier concentration on the state of microballoon

Na_2O [M]	Span80 [wt%]	D2EHPA [wt%]	Homogenizer [rpm]	D_W [μm]	D_{MB} [μm]	D_{MB}/D_W [–]	Evaluation
1.44	1.0	0.3	5,000	4.32	2.76	0.64	+++
1.56	2.0	0.3	5,000	3.79	3.64	0.96	++
1.56	3.0	0.3	5,000	4.16	3.49	0.84	+++
1.52	4.0	0.3	5,000	3.75	2.90	0.77	+++

Table 3 Effects of surfactant concentration on the state of microballoon

Surfactant concentration

Table 3 predicts the effects of Span 80 concentration. The increase of surfactant concentration was most effective in raising the formation of spherical microballoons, especially when it was difficult

to get beautiful balloons under usual conditions. This was true for transition-metal silicate microballoons. The smooth and clear surface was obtained by increasing a surfactant concentration, but the rate of balloon formation was retarded due to the increase of oil-phase viscosity.

Viscosity of internal aqueous phase

The effects of aqueous phases viscosity were examined by adding glycerol to internal aqueous solution, but a clear effect of viscosity increase was not observed. When the concentration of sodium silicate was as low as 0.34 mol/dm^3, the formation of spherical microballoons was made possible by increasing the viscosity.

Viscosity of oil phase

Since the diffusion-controlled penetration of a metal cation through oil phase may affect the formation of inorganic shell, the effect of oil phase viscosity was examined by adding liquid paraffin to kerosene. However, the drastic change of spherical balloon formation was not observed under the present conditions.

Effects of Operating Conditions on the Formation Rate of Microballoons

The formation of inorganic microballoons proceeds by the ion exchange between internal and external aqueous solutions through oil membrane. Therefore, the formation rate of microballoons may be controlled by the operating factors that influence the rate of ion penetration. In this study, the rate of ion exchange was regarded as the formation rate of microballoons, and the effects of operating conditions were examined for calcium silicate microballoons.

Figure 5 shows the change of calcium ion concentration after pouring the W/O emulsion into aqueous calcium chloride solution. With the increase in stirring speed, the formation rate of microballoons also increased, probably due to the decrease in the size of dispersed W/O emulsion drops and the resultant increase in the specific surface area. In the separate runs, the increase of oil-phase viscosity clearly retarded the balloon formation because of low penetration rates. Figure 6 shows the change of average balloons size during the ion exchange. The increase in salt concentration clearly caused the increase in balloon size. As clearly shown, the formation of microballoons proceeded just after putting the emulsion into external aqueous solution and it took fairly long time to reach the steady state when the salt concentration was low. These findings demonstrate that the transfer of ions controls the overall process.

Preparation of Microballoons Composed of Multiple Metal Silicates

Microballoons made of various metal silicates other than Ca were prepared with the same procedure described in figure 1. The metals tested were Mg, Al, Cu, Mn, Co, Ni, Pb, Zn, Fe(II), Fe(III) and Ba. Although some metals could not give beautiful microballoons under usual preparing conditions, it was improved by increasing the surfactant and inorganic salt concentrations. The microballoons made of multiple metal silicates were prepared as follows. The W/O emulsion was mixed with the aqueous solution of the first metal salt for a while, then it was separated from aqueous solution quickly. Next, the recovered W/O emulsion was poured into the aqueous solution of the second metal salt and stirred to complete the ion-exchange reaction. Figure 7 shows the SEM observations of broken microballoons that were prepared by reacting with Mn^{2+} at first followed with Ca^{2+}. We can ascertain that the double layer of metal silicates was formed by this method. The surface of such a multiple metal-silicates microballoons was analyzed by EDX. Only the metal element used at the second-stage exchange was observed at the surface, which means the complete coverage of the external shell composed of the first metal silicate with the second metal silicate.

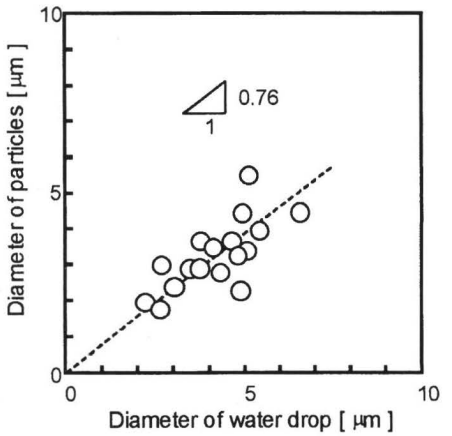

Figure 4 Relation between balloon size and diameter of internal aqueous drop

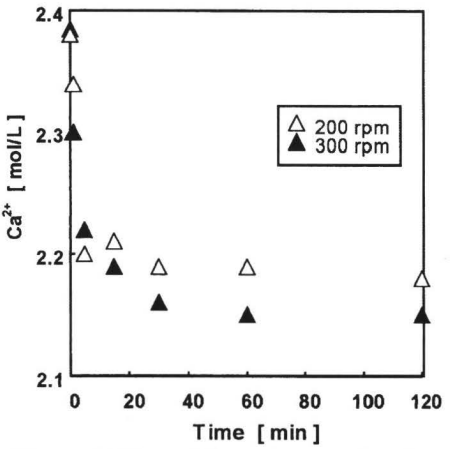

Figure 5 Effect of dispersion speed on the formation rate of microballoons

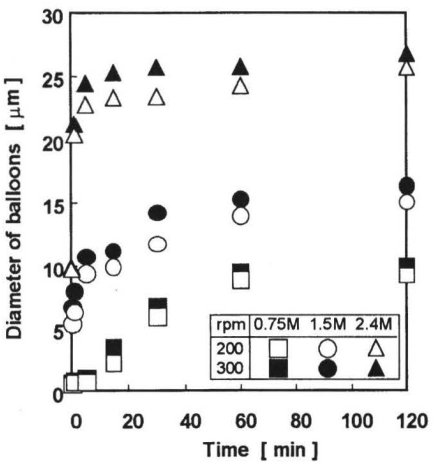

Figure 6 Change of balloon size - Effect of salt concentration and dispersion speed -

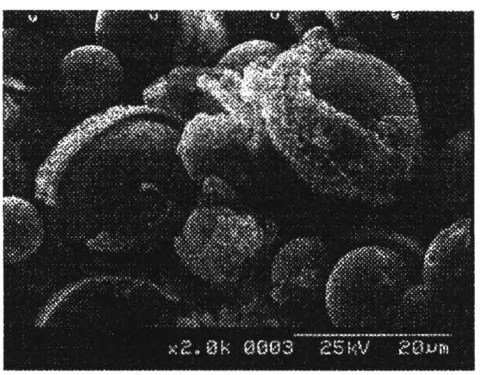

Figure 7 Broken surface of multiple metal silicates microballoons

CONCLUSION

In the preparation of inorganic microballoons based on the interfacial reaction method proposed by Nakahara, the extent of spherical balloon formation was substantially affected by the emulsion-preparing conditions, especially the concentration of surfactant and inorganic salts. The microballoons made of a wide variety of metal silicates could be prepared satisfactorily by increasing the concentration of surfactants. The microballoons made of multiple metal silicates were obtained by changing the inorganic salt solutions during the operation.

REFERENCES

1. Nakahara Y and Miyata K, *Reports of Govern. Ind. Res. Inst., Osaka*, **357**, 59 (1980)
2. Hano T, Hirata M, Takanashi H, Matsumoto M, Ohtake T and Nakahara Y; *Proc. ICOM*, S 8-1-6 (1996)
3. Hano T, Matsumoto M and Ohtake T; *Chemical Engineering (Japan)*, **36**, 873 (1991)
4. Nakahara Y, *Shikizai*, **59**, 543(1986)

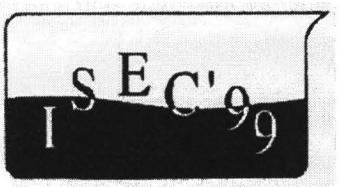

SELECTIVE RECUPERATION OF COPPER BY SUPPORTED LIQUID MEMBRANE (SLM) EXTRACTION

RF De Ketelaere and J Vander Linden
Chemical and Biochemical Research Centre CBOK, Dept. KIHO, KaHo Sint-Lieven, Gebroeders Desmetstraat,1 - 9000 Gent
Belgium

ABSTRACT
Initially a comparison of described and commercialised copper extractants and diluents was made by means of conventional extractions. The investigated criteria were: the distribution ratio, the kinetics and the selectivity of copper extraction and stripping. A salicylaldoxime dissolved in kerosene, LIX 860, gave the best distribution ratio, with a fast extraction and very fast and complete stripping with 300 g/L sulphuric acid. Below pH 2,5, the selectivity for copper is high (only Fe^{3+} was partially co-extracted). However Acorga M 5640 provided the highest selectivity. In the second stage, experimental studies on the lifetime of several supporting membranes as well as on the stability of the supported liquid membrane showed that Celgard© X10-240 has the smallest pore size and provide the highest stability. Finally, the working parameters, investigated in a pilot scale continuous SLM extraction, showed a permeability coefficient, varying between 1 and 7.10^{-2} $m.h^{-1}$. It is not influenced by the flow velocity and is dependent, not only on LIX-860 concentration and pH, but also on the copper feed concentration. Moreover, these three parameters are interacting.

Keywords: copper; LIX 860; Acorga M5640; supported liquid membrane

INTRODUCTION

In metal recovery, extraction by liquid ion exchangers is of growing concern.[1] The use of supported liquid membrane (SLM) can improve this technique and extend its application field to the recovery of metal ions from waste water.[2] Therefore the mass transfer for the SLM extraction of copper ions was studied.[3]

Moreover, much research has been done in the field of preparation of selective metal extractants and in the development of membranes with well controlled pore diameters.[4,5] However, between a principle and an operating process, a large gap has to be filled up with concrete and specialised know-how. Trying to contribute to this goal, this paper presents a comparison of copper extractants and diluents useful in SLM and the selection of supporting membranes and defines the working parameters of an SLM pilot plant.

EXPERIMENTAL

Selection of the extractant and the diluent

To perform an uphill extraction of copper, the extractant has to be a acidic (HL) giving the reaction:

$$Cu_a^{2+} + 2HL_o \longleftrightarrow CuL_{2o} + 2H_a^{+}.$$

In this case, the pH difference between feed and stripping liquid can be the driving force for the extraction. Most of the copper extractants are 8-hydroxyquinoline derivatives (Figure 1.A) or salicylaldo- or keto-oximes (Figure 1.B).[6,7] Five different commercial copper extractants were selected, available in the form of concentrated kerosene solutions .

© 2000 Society of Chemical Industry



(A) (B)

Figure 1 : Copper extractants : (A) 8-hydroxyquinoline derivative, (B) salicylaldo- or keto-oximes

Distribution ratio as a function of time

A total of 35 extraction experiments were carried out with samples of the aqueous phase taken after a shaking time of respectively 30, 120, 300, 600, 1800 seconds for each of the 5 selected extractants in kerosene and for Kelex 100 and Acorga M 5640 in 1-decanol. The results are shown in Figure 2.

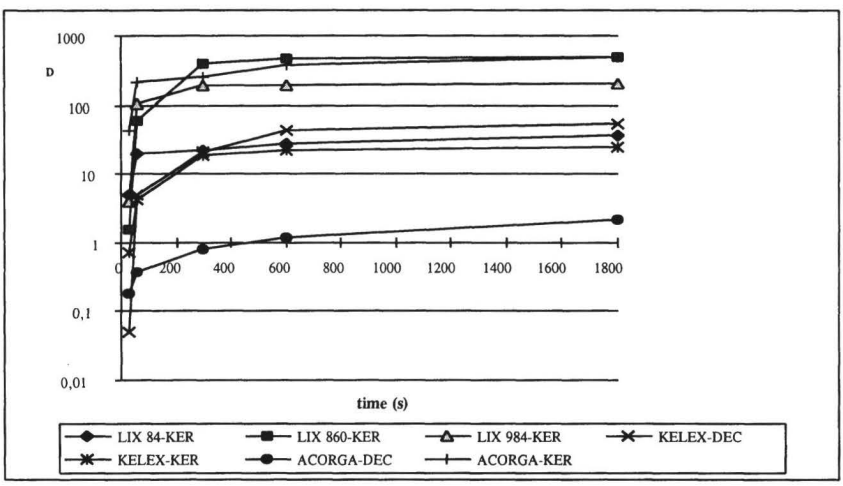

Figure 2: Distribution ratio as a function of time

Selectivity against other metal ions and influence of brighteners and wetting agents

The metals studied were: Fe^{2+}, Fe^{3+}, Cr^{3+}, Zn^{2+}, Pb^{2+}, Ca^{2+} and Ni^{2+} and the galvanic commercial brighteners GM and the wetting agents WA and polyethyleneglycol.

The distribution ratios of copper were never affected. Settling was slower under the influence of wetting agents. Co-extraction of other metals increased with higher pH but below pH 3, only Fe^{3+}, co-extraction was measurable. Thus at pH 2, this was 42% for LIX860, 39% for LIX984, 26% for Kelex 100 and 12% for ACORGA M5640. However, stripping of Fe^{3+} was negligible. This could explain that in continuous SLM, selectivity, even against iron, was already observed.[7]

Distribution ratio as function of time and concentration of sulphuric acid and copper in the stripping phase

With 200g/L sulphuric acid, the stripping reaction was very fast and after a stripping time of 30 seconds the final equilibrium rates were reached for all extractants. This is in contradiction with earlier assertions.[8] Above $C(H_2SO_4)$ = 200 g/L, D was zero for all extractants, except for LIX 860, where D = 0 was only reached above 300 g/L. This was hardly affected by an increasing copper

concentration in the stripping phase and below 5 g/L of copper in the stripping phase, no measurable change in the distribution rate was observed.

Measurement of SLM stability [4]

An organic (apolar) phase filling the pores of a hydrophobic membrane cannot be displaced by water due to the surface tension of water against the membrane material and against the organic phase. It prevents the surface deformation of the water caused by penetration into the pores. This can be quantified by P_C.

P_C was measured directly by applying an increasing pressure on a water circuit closed with a test membrane. This was soaked in a transparent glass containing the organic phase. The pressure producing the first appearance of turbidity near the membrane, due to water droplets in the organic phase, was noted by visual observation.

The critical displacement pressure was calculated from the pore size given by the membrane supplier.

	Experimental		Theoretical	
membrane type	measured pressure (kPa)	calculated pores (x 10^{-6} m)	mentioned pores (x 10^{-6} m)	calculated pressure (kPa)
1E-PP	320,0	0,45	0,29	498,6
TF 450	140,0	1,03	0,45	321,3
HVHP	140,0	1,03	0,45	321,3
Celgard 2500	560,0	0,26	0,075	1928,0
Celgard 2400	> 600,0	< 0,24	0,05	2892,0
TF 200	330,0	0,44	0,2	723,0
Zefluor 1	150,0	0,96	1	144,6
Zefluor 2	40,0	3,61	2	723,0
Verasapor 3000	20,0	7,32	3	48,20
TE 36	220,0	0,66	0,45	321,3
Durapore 0,22	190,0	0,76	0,22	657,2
Fluoropore 0,2	280,0	0,52	0,22	657,3
SciMAT	400,0	0,36	0,17	850,6

Table 1: Comparison table between the experimental pore size and the given mean size of membranes

Table 1 shows that Celgard© X10-240 has the smallest pore size and the highest critical displacement pressure.

Used membranes with a decreased displacement pressure [9,10] can be regenerated to their initial value after purification with hexane.

This is an indication that the most common factor of ageing is not the altering of the membrane surface, but the increasing polarity of the organic phase, by extraction of polar organic compounds, which act as tensides from the feeding water.

Permeation measurements on SLM

After measurement of ageing and selectivity on a lab scale, a pilot plant was started up. Previously, once-through flow experiments were studied. Thereafter, in an experimental design the effects of four parameters were tested: the feed copper concentration, the pH, the flow velocity and the LIX 860 concentration.

Ageing

A two litre feed solution (500 ppm Cu) was circulated at a flow rate of 12 $L.h^{-1}$ (corresponding to a flow velocity of 136 $m.h^{-1}$), through the "Celgard© X-10" polypropylene hollow fibers of a "Liqui-cel" Membrane Contactor SPCM -106 from Hoechst Celanese Co.

The feed concentration was measured twice daily, allowing a speed correction for the copper addition, and allowing calculation of the flux. So the flux was measured in a continuous run of over 500 hours. The flux dropped to half its start value after 250 hours and decreased slowly to 40 % after 500 hours.

Once-through flow experiments

Instead of circulating the feed solution over the membrane module, a feed tank of 200 litre was emptied at various flow rates over a "Liqui-cel" Pilot Membrane Contactor 5PCM-105. It provided an effective surface area of 3.7 m^2 of "Celgard© X-10" polypropylene hollow fiber, which was impregnated with 25 vol % LIX 860. The copper concentration was controlled at its outlet.

Starting with a feed concentration of 47.6 ppm Cu at pH 4.4, the outlet concentration could be held below 0.5 ppm Cu at pH 3 with a flow rate of 12 $L.h^{-1}$ corresponding to a velocity of 31.8 $m.h^{-1}$ over the membranes. The results are important as they show the possibilities of an SLM operation in a once-through flow.

A same flow rate could be obtained with two classic mixer-settler pilot units QVF DN 80 from Corning, showing the following advantages of SLM:

a reduction of installation volume and costs;
a much simpler working control;
a more than 30-fold reduction of the extractant volume;
a much lower risk for emulsifying and foam formation.

Investigation of the working parameters

Proceeding

The feed solution was circulated from a 30 litre tank through the hollow fibers of the pilot membrane contactor. A flow meter was incorporated in the feed circuit.

The stripping solution, containing 200 $g.L^{-1}$ sulphuric acid, in a tank of 60 litre was allowed to circulate around the fibers. A copper ion sensitive electrode was dipped in the feed tank and, to maintain a constant copper concentration, a concentrated copper sulphate solution, containing 6,4 $g.L^{-1}$ Cu, was added with a controlled peristaltic pump. The pH of the feed was continuously measured by a combined glass electrode and a constant pH was achieved by controlled addition of a 0,5 $mole.L^{-1}$ sodium hydroxide solution.

The level settings of both controllers were checked twice daily with AAS for copper and with pH 4 and 7 buffers.

The apparatus was started at the level settings of the starting experiment for two hours to reach a steady state. Then the volume of added copper was measured hourly, over 5 hours, and gave five times the copper flux (expressed in mole/ h).

Checking the four parameters at three levels gives a total number of $3^4 = 81$ experiments.
This was reduced to a third = 27, which corresponds with an experimental design of 3 parameters at 3 levels.

As the preliminary experiments, on a 0,230 m^2 laboratory module, proved that the flow velocity does not influence the permeability, this parameter was left out but reintroduced by confounding its 3 levels with the 3 blocs of combinations from which interactions ^{11} would be calculated.
So the loss of information was minimal as the linear and quadratic influence of each parameter was saved and only information about interactions could be lost if a statistically significant influence of the confounded fourth parameter would appear.
The actual values for each of the 4 parameters are given in Table 2:

Factor	Levels	0	1	2
A	LIX concentration	20 Vol %	25 Vol%	30 Vol %
B	pH	2,0	3,0	4,0
C	Cu concentration	10 ppm	100 ppm	500 ppm
D	Flow rate	40 L/h	110 L/h	180 L/h
	Corresponding Velocity	106 m/h	292 m/h	477 m/h

Table 2: Setted values for three levels of the four investigated parameters

DISCUSSION OF RESULTS

It is demonstrated with a greater than 99% confidence that all parameters except flow velocity have a linear influence on the permeability. As the influence of the flow velocity does not exceed the spreading of measurements, it cannot be seen as significant within the installed levels.

This is in perfect agreement with the findings of Ching-Yeh Shiau and Pai-Zon Chen.[6] This proves that the rate determining step is situated in the organic phase and although the opposite is mostly claimed, the need of a high flow velocity to avoid concentration polarisation or to reduce the stationary layer, is out of question.

This is very important because flow velocity is the main cause of bleeding of the supported liquid, by successive small and local displacements due to local pressure differences caused by turbulence and wall unevenness.[8]

Since in the case of no main effect, the opportunity of interaction with other parameters is very low, it can be accepted that the earlier mentioned confounding is not cause of information loss of the other parameters. Concerning the square influences, they are unremarkable for all parameters except for concentration that shows an influence but with a low confidence of about 80%.

The most important conclusion, on the other hand, is the fact that a linear interaction of the three parameters is demonstrated with a confidence above 99%. This is shown in figure 3, a 3-D graph giving the permeability results for each combination of the three parameter levels: LIX concentration, pH and Cu concentration.

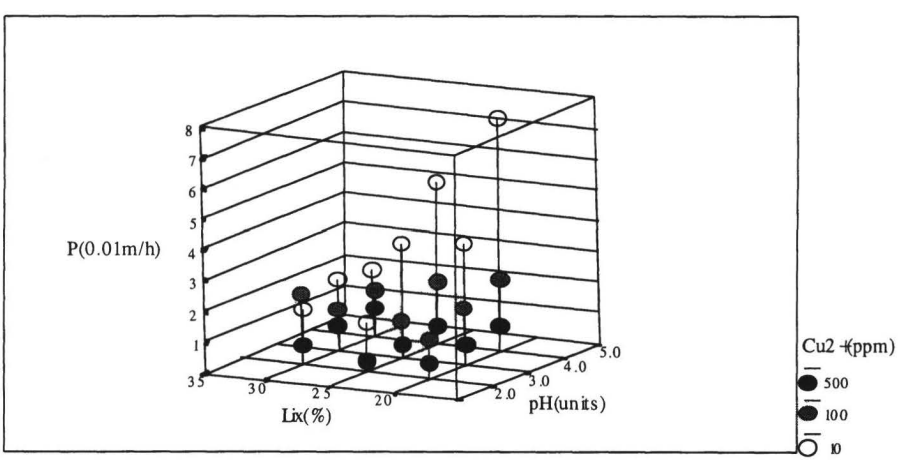

Figure 3: Permeation as a function of [LIX], pH and [Cu] in the feed solution

Figure 3 shows that in general the permeability increases with lower copper concentrations and with higher pH. But the best LIX concentration depends on the other parameters: at pH 2 the permeability increases with higher LIX concentrations even over 30 vol %.
However, at higher pH values, the highest LIX concentration gives only the best permeability for copper concentrations above 500 ppm; for lower copper concentrations the best LIX concentration seems to be far below the lowest measured level of 20 vol %. This explains the contradictions found in earlier publications.

ACKNOWLEDGEMENTS

The financial support of the project by the European Commission, DG XII in the BRITE-EURAM II frame (BE 5436) and the financial support by the Flemish Government, VLIM (0 / 9111) are gratefully acknowledged.

REFERENCES

1 Townsend B and Severs KS, Mining Mag., Jan.1990.
2 de Haan AB, Bartels PV and DeGraauw J, *J. Membrane Sci.*, **45** ,281, (1995).
3 Szpakowska M and Nagy OB, *Bull. Soc. Chim. Belg.*, **99,** 4, (1990).
4 Takeuchi H, Takahashi K and Goto W, *J. Membrane. Sci.*, **34** ,19, (1987).
5 Hiratani K, Hirose T, Fujiwara K and Saito K, *Chem. Letters*, 1921, (1990).
6 Shiau Ching-Yeh and Chen Pai-Zon, *Sep. Sci. and Technol.*, **28** ,2149, (1993).
7 Baker RW, Tuttle ME, D.J. and Lonsdale HK, *J. Membrane Sci.*, **2,** 213, (1977).
8 Neplenbroek AM, Bargemanand D, Smolders CA, *Desalination*, **79**, 303, (1990).
9 Dozol JF, Casas J and Sastre A, *J. Membrane Sci.*, **82 ,** 237, (1993).
10 Takeuchi H. and Nakano M, *J. Membrane. Sci.*, **42**, 183, (1989).
11 Owen L.Davies, for ICI by Oliver and Boyd Edinburgh:Tweeddale Court, 2nd.edit. (1971).

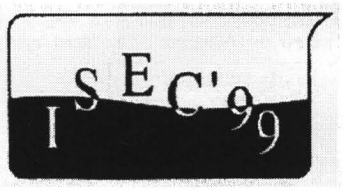

UPHILL TRANSPORT OF SILVER(I) FROM NITRIC ACID MEDIA USING BINARY EXTRACTANTS AS POTENTIAL LIQUID MEMBRANE CARRIERS

Anil Kumar[1*], PK Gautam[2], JP Shukla[3], RK Singh[2] and AM Sastre[1]

[1]Universitat Politècnica de Catalunya, Department of Chemical Engineering, E.T.S.E.I.B., Diagonal 647, E 8028 Barcelona, Spain (* on leave from BARC, Tarapur)

[2]PREFRE Plant, Bhabha Atomic Research Centre, Tarapur 401502, India

[3]Radiochemistry Division, Bhabha Atomic Research Centre, Trombay, Mumbai 400085, India

ABSTRACT

In the present paper, some important aspects of binary extractants as carriers in liquid membrane pertraction of metal ions have been outlined. As a case study, uphill transport of Ag(I) from nitric acid solutions across supported liquid membrane by Cyanex 301 in Solvesso-100 and its binary mixtures with Aliquat 336 has been investigated as a function of chemical parameters. The permeability of Ag(I) with pure Cyanex 301 was very high but stripping from membrane to receiving phase was very poor owing to a highly stable silver complex at the membrane interface. The stripping of Ag(I) with pure Cyanex 301 was never exceeded 10%, in contrast with the binary carrier Cyanex 301 + Aliquat 336, stripping ranged between 95-98%. The highest concentration factor around 88 was obtained with a binary carrier concentration 0.25 M Cyanex 301 + Aliquat 336 and source and receiving phases consisting of 1 M HNO_3 and 1M thiourea + 0.1M HNO_3 respectively.

Keywords: silver(I), Cyanex 301, Aliquat-336, supported liquid membranes, binary extractants

INTRODUCTION

Silver being the precious metal, gains paramount importance in view of its recovery from diverse matrices. The solvent extraction of silver by various thiosubstituted organo-phosphorous reagents has been previously investigated, with particular regard to potential analytical applications.[1,2] Recently, two sulfur-containing organophosphorous extractants have been introduced by American Cyanamid Co.[3] A recent study by Sole *et al.* investigated the extraction of silver(I) from nitric acid media. The stability of the Ag-Cyanex 301 complex was reported to be so great that quantitative extraction occurs even with concentrated nitric acid. Hence, non-destructive stripping of used extractant was observed to be extremely difficult.[4] Therefore, this extractant needs modification to be suitable for solvent extraction applications. To improve the performance of extractants especially stripping behaviour, some attempts have been made to evaluate metal extraction by binary extractants for metal extraction.[5-8] The objectives of testing the usefulness of binary extractants are: i) they are less sensitive to acidity in the aqueous phase than cation exchangers, ii) they have relatively high efficiency in extraction, iii) provide easy regeneration of stripped extractants, and iv) fast separation of metal ion across supported liquid membranes (SLM). Liquid membrane (LM) studies of Ag(I) using other carriers such as Cyanex 471X, Cyanex 302, di-(2-ethylhexyl)-dithiophosphoric acid and crown ethers were reported but stripping results were not promising specially with carriers such as Cyanex 471X and Cyanex 302.[9-12]

Cyanex 301 is an organic acid, (bis(2,4,4-trimethylpentyl)dithio-phosphinic acid), and consequently will react with an organic base, such as Aliquat 336, to form an organic salt, a so called binary extractant. In our previous studies, the concept of binary extractant was adopted for Ag(I) extraction and showed promising results with Cyanex 301+Aliquat336.[13] In view of the several advantages of liquid membranes described elsewhere,[14] binary extractants were tested as liquid membrane carriers across supported liquid membranes. Surprisingly, no study has been carried out to evaluate the effectiveness of binary extractants as liquid membrane carrier for metal separation across a supported liquid membrane.

© 2000 Society of Chemical Industry

This paper deals with the liquid membrane permeation of Ag(I) with Cyanex 301 and its binary salts with trialkylmethyl ammonium chloride, commercially marketed as Aliquat 336, from nitric acid solutions.

EXPERIMENTAL

Cyanex 301 (75-80% pure) was kindly supplied by American Cyanamid (now Cytec Industries, Inc.) and Aliquat 336 were obtained from Henkel Corpn. USA. The extractants were used without further purification. Reagent grade diluent Solvesso-100 (Shell Co., Australia) was used as received. The binary extractants were prepared according to the method described elsewhere.[13] Consequently, all solutions with a low acid concentration were made up in 1.0 M sodium nitrate to provide a constant ionic medium and nitrate ions to promote extraction by mass action.

Silver-110m tracer, obtained in the Ag(I) state from the Isotope Division, Bhabha Atomic Research Centre, India, was used throughout the present study. Its radiochemical purity was ascertained by gamma ray spectrometry. Ag-110 was assayed by a well-type NaI(Tl) scintillation detector coupled to a single channel analyser. Solvent extraction studies of Ag(I) with Cyanex 301 and its binary mixture are presented elsewhere.[13] Details of SLM cells and permeation measurements are also published elsewhere.[15] The permeation coefficient (P) was computed by the following equation:

$$\ln(C/C_0) = - (A/V)P \times t \qquad (1)$$

where V is the volume of the source phase solution (cm^3), A the effective membrane area (cm^2) , C_0 and C concentrations of metal ion in source phase at time zero and at a given time, t, respectively (mol cm^{-3}), and t the elapsed time (s).

Membrane Support

Enka Accurel PP thin flat-sheet type hydrophobic microporous polymeric membranes, coded as 2E HF-PP used were about 130-180 μm thick, and had a nominal porosity of about 70% with an average pore diameter of the order of 0.2 μm. Filling the pores of these dry supports with the carrier was accomplished by immersing the membrane in the organic phase for at least 6-7 hours before use for the sake of uniformity.

RESULTS AND DISCUSSION

Cyanex 301 and its binary mixtures form 1:1 silver extractant complexes.[13]

$$Ag^+ + HA \;==\; AgA + H^+ \qquad \text{(Cyanex 301)}$$
$$R_4NA + Ag^+ + NO_3^- == AgA + R_4NNO_3 \qquad \text{(Cyanex 301+Ali-336)}$$

where HA is the extractant representing Cyanex 301 and R_4NA the Aliquat-336 salt of Cyanex 301. Results on the extraction of Ag(I) from pure Cyanex 301 and Cyanex 301 + Ali-336 and stripping behaviour of Ag(I) from loaded extractant phase are given in Table 1. This indicates that the performance of Cyanex 301 + Ali-336 was superior to that of pure Cyanex 301. In addition, stripping of Ag(I) with various complexing agents gave poor recovery around <15% with pure Cyanex 301 while the binary extractants afforded >95% silver recovery proving better control over back extraction. Based on the liquid-liquid extraction results, the binary extractant was employed as the carrier. To maintain stability of Cyanex 301 and its binary extractants, the concentration of nitric acid used was not greater than 3M as Sole *et al.*, observed decomposition of Cyanex 301 at higher concentrations of nitric acid.[16] Table 2 presents average permeation coefficients as a function of nitric acid concentration. Results indicate that P values increased up to 1M HNO_3 and further decreased with increase in HNO_3 concentration in the source phase. On the other hand, the recovery of silver in the receiving phase was <8% even though its permeation across the membrane phase was quantitative with a measured average permeation coefficient

18.2 10^{-3} m/s with pure Cyanex 301.

Aqueous Phase HNO_3 Conc. (M)	Log D		Stripping of Ag(I) (%)		
	I	II	Strippant[a]	I	II
0.01	2.2	3.0	HNO_3 (8)	4.0	10.3
0.1	2.3	3.2	HCl (8)	6.0	8.5
0.5	2.3	3.1	Oxalic acid (0.5)	6.0	8.2
1.0	2.4	3.0	EDTA (0.5)	4.0	5.7
1.5	2.5	2.8	Thiourea (0.05)[b]	13.2	95.3
2.0	2.2	2.6	Thiourea (0.5)[b]	15.2	98.3
3.0	2.2	2.5	Thiourea (1.0)[b]	13.2	95.3

a, values shown in brackets indicate strippant concentration (mol/L)
b, thiourea in 0.1 M HNO_3

Table 1 Extraction of Ag(I) into Solvesso-100 by pure Cyanex 301 and its binary Cyanex 301 + Ali-336 and stripping behaviour of Ag(I) from loaded organic phase
Extractant : 0.25 M Cyanex 301/Solvesso 100 (I)
Binary extractant : 0.25 M Cyanex 301 + Ali-336 in Solvesso-100 (II)
Volume ratio, org/aq : 1

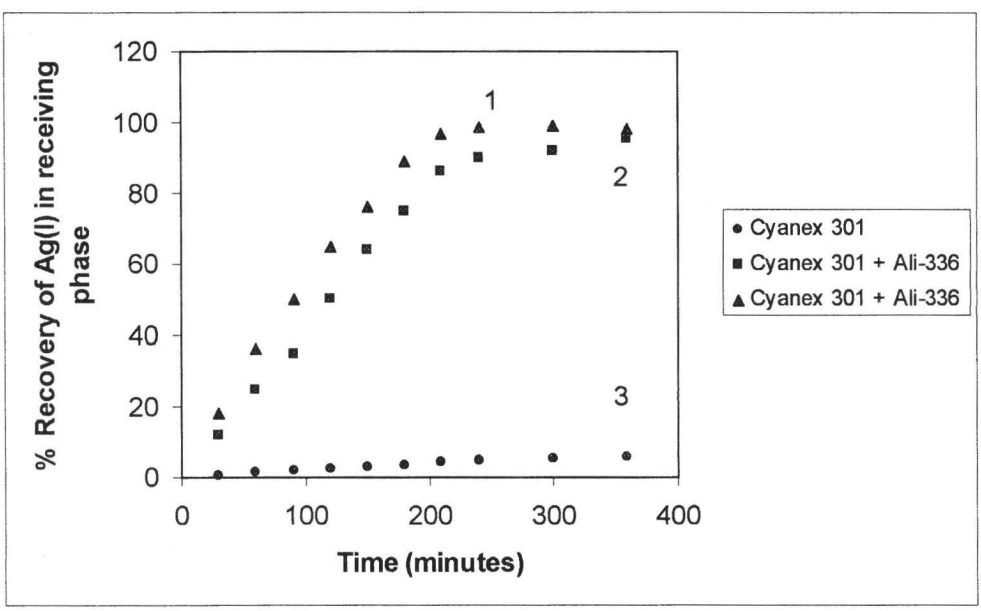

Figure 1. Recovery of Ag(I) with pure and binary liquid membrane carrier into receiving phase. 1) 1.0 M thiourea +0.1M HNO_3; 2) 0.5 M thiourea +0.1M HNO_3; 3) 1.0 M thiourea +0.1M HNO_3

On the other hand, silver (I) permeation was 99.8% with a measured average permeation coefficient 12.2 ± 0.21 m/s with the binary carrier (Cyanex 301 + Ali-336) with 1M HNO_3. As shown in Figure 1, more than 60% of silver permeated within the initial two hours using the binary carrier. On the other hand, recovery of silver was less than 6% when Cyanex 301 was used alone as the liquid membrane carrier. This is probably due to the stability of the metal complex with the binary extractant differs from that with pure Cyanex 301 (less stable complex) which attributes to the greater stripping of Ag(I) in

similar experimental conditions. Permeation coefficients of Ag(I) as a function of binary carrier concentration are presented in Table 3. The P values were observed to increase with binary extractant concentration. The recovery of Ag(I) was more than 95% at extractant concentration 0.15M and furthermore remained in same range with increase in binary extractant concentration. The highest concentration factor of 88 was obtained using 0.25M Cyanex 301 + 0.25M Ali-336 maintaining the source phase acidity at 1 M HNO_3. When experiments were conducted in presence of actinides such as Am(III) and Pu(IV), promising results were obtained indicating more than 97% recovery of Ag(I) from electrolytic waste across the SLM using 0.25M Cyanex 301 + 0.25M Ali-336 maintaining the source phase acidity at 1 M HNO_3 (Table 3).

Source Phase HNO_3 Conc. (M)	Average permeation coefficient (P) 10^{-3} m/s		Recovery in receiving phase after 6h (%)		Concentration factor after 6h	
	I	II	I	II	I	II
0.01	21.5 ± 0.01	3.7 ± 0.31	7.5	82.5	3.1	7.0
0.1	----	6.4± 0.31	---	99.6	---	16.5
0.5	----	7.4± 0.70	---	98.5	---	28.2
1.0	18.2±0.08	12.2± 0.20	5.7	99.8	2.3	87.6
2.0	----	7.7± 0.40	----	94.7	----	19.6
3.0	13.2± 0.06	4.9± 0.31	5.2	74.1	1.8	7.7

Table 2 Permeation Coefficient of Ag(I) using pure Cyanex 301 and Binary Extractants as carriers across SLM

Carrier concentration : 0.25 M Cyanex 301/Solvesso 100 (I)
Binary extractant : 0.25 M Cyanex 301 + Ali-336 in Solvesso-100 (II)
Receiving phase : 1 M thiourea + 0.1M HNO_3

Binary carrier conc. (M)	Permeation Coefficient after 1h, (P) 10^{-3} m/s	Concentration factor after 6h	Permeation after 6h (%)
0.01	4.0 ± 0.31	0.1	9.1
0.05	11.6 ± 0.28	2.3	55.2
0.10	14.1 ± 0.35	9.1	76.0
0.15	15.7 ± 0.58	26.6	96.8
0.20	16.4 ± 0.71	29.6	98.3
0.25	12.2 ± 0.20	87.6	99.8
0.20[a]	15.6± 0.43	84.6	97.4

a, Experiments were conducted in presence of Am(III) and Pu(IV) from waste (see text)

Table 3 Permeation Coefficient of Ag(I) as a function of binary carrier concentration across SLM

Source phase acidity : 1 M HNO_3
Binary extractant : Cyanex 301 + Ali-336 in Solvesso-100
Receiving phase : 1 M thiourea + 0.1M HNO_3

ACKNOWLEDGEMENTS

The authors wish to thank Shri. K. Balu, Director, Fuel Reprocessing and Waste Management, Shri. D.D. Bajpai, Head PREFRE, BARC, India and Dr. S.B. Manoher, Head, Radiochemistry Division, BARC for their keen interest in this work. Dr. Anil Kumar gratefully acknowledges the support of the Spanish Ministry of Education and Culture (CICYT), for awarding the Visiting Scientist fellowship.

REFERENCES

1. Handley TH, *Anal. Chem.*, **35**, 991, (1963).
2. Sevic S, *Proc. Int. Solvent Extr. Conf. ISEC 74*, Society of Chemical Industry, London, **3**, 2733, (1974).
3. American Cyanamid Co., Cyanex 272, Cyanex 302, Cyanex 301, Technical Brochures, Wayne, NJ.
4. Sole KC, Hiskey JB and Furgusan TL, *Solv. Extr. Ion Exch.*, **12**, 1033, (1994).
5. Kholkin AI, Pashkov GL et al., *Hydrometallurgy,* **36**, 109 (1994).
6. Belova BB and Kholkin AI, *Solv. Extr. Ion Exch.*, **16**, 1233, (1998).
7. Eyal AM, Eyal Bressler, Bloch R and Hazan B, *Ind. Eng. Chem. Res.*, **33**, 1067, (1994).
8. Eyal AM, Kogan L and Eyal Bressler, *Ind. Eng. Chem. Res.*, **33**, 1076, (1994).
9. Bromberg L, Isaak Levin, Warshawsky A, *J. Membr. Sci.*, **70,** 31, (1992).
10. Singh RK, Venugopalan AK, Anil Kumar, Gautam PK, Bajpai DD, Shukla JP, XIV National Symposium on Membranes in Chemical and Biochemical Industries, Indian Institute of Technology, New Delhi, India. Feb. 16, (1996)
11. Izatt RM, Clark GA and Christensen JJ, *J. Membr. Sci.*, **24**, 1, (1985).
12. Munoz M, Palet C and Valiente M, *Anal. Lett.*, **23**, 1591, (1990).
13. Anil Kumar, Gautam PK, Shukla JP, Singh RK and Sastre AM, *Proc ISEC'99,* Barcelona, Spain, (1999).
14. Sastre AM, Anil Kumar, Shukla JP, Singh RK, *Sep. Purif. Meth.*, **27**(2), (1998).
15. Shukla JP, Anil Kumar and Singh RK, *Radiochimica Acta*, **57**, 185, (1992).
16. Sole KC, Hiskey JB and Furgusan TL, *Solv. Extr. Ion Exch.*, **11**, 783, (1993)

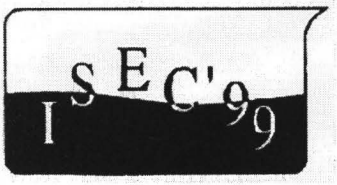

CHROMIUM(VI) AND CHROMIUM(III) SEPARATION BY SUPPORTED LIQUID MEMBRANES AND POLYMERIC INCLUSION MEMBRANES

Jerzy Gega[1], Cezary Kozlowski[1] and Wladyslaw Walkowiak[2]
[1]Technical University of Czestochowa, Department of General Chemistry, Al. Armii Krajowej 19, 42-200 Czestochowa, Poland,
[2]Technical University of Wroclaw, Institute of Inorganic Chemistry and Metallurgy of Rare Elements, Wyb. Wyspianskiego 27, 50-370 Wroclaw, Poland

ABSTRACT
Two types of liquid membranes for separation of Cr(VI) and Cr(III) ions, i.e. supported liquid membranes (SLM), and polymeric inclusion membranes (PIM) are utilized. PIMs were composed of polymeric support (cellulose triacetate), membrane plasticiser (o-nitrophenyl pentyl ether), and metal ions carrier. Both SLM and PIM consist of the same types of carrier: i.e. tri-n-octylamine or tri-n-octylphosphine oxide. Source phase was equimolar mixture of Cr(III) and Cr(VI) ions in sulfuric acid solutions. The influence of several factors on chromium transport selectivity and effectiveness has been explored. These factors included the effect of acidity and concentration of metal ions in the source solution, and concentration of ion carrier and plasticiser (PIM) in membrane material. The comparison of metal ion transport across SLM and PIM has been carried out. The selectivity of competitive transport was higher in the case of PIM. The kinetic studies of SLM and PIM processes are also presented.

Keywords: supported liquid membranes, polymeric inclusion membranes, Cr(VI), Cr(III), tri-*n*-octylamine, Cyanex 921

INTRODUCTION

To obtain metals in hydrometallurgical processing frequently requires the separation of metal ions from technological or waste aqueous solutions. Application of liquid membranes is an alternative method of separation to liquid-liquid extraction process. The liquid membrane process involves the selective transport of the ionic species from a source phase across the liquid membrane (bulk, emulsion or supported) into a receiving phase. The membrane contains an ionic carrier such as an organophosphorus compound or amine.[1,2] Instability of the emulsion and supported liquid membranes is the main problem in application of these methods in industrial practice.

In the last few years the attempts have been made to increase the stability of the liquid membranes through inclusion of the ionic carriers inside the structure of the polymer transparent membrane. Sugiura and coworkers[3-6] reported the use of the plasticised cellulose triacetate (CTA) membranes for the transport of zinc(II) and lanthanide ions. By applying as plasticisers o-nitrophenyl octyl ether and ethyl benzoate they obtained tough, transparent membranes with good metal ion transport ability. More recently, Lamb et al.[7] studied the transport of alkali metal cations across CTA membranes by a crown ether carrier, dicyclohexano-18-crown-6. In another paper, Lamb with co-authors[8] studied the silver(I) ion-selective transport across the polymer inclusion membranes containing new pyridino- and bipyridino-podands. Bartsch with co-authors[9] reported the alkali metal cations selective transport across polymer inclusion membranes using as the ionic carrier proton-ionisable lariat ethers, i.e. sym-(decyl)dibenzo-16-crown-5-oxyacetic acid.

In this study the application of supported liquid membranes for separation of chromium (VI) and chromium (III) ions from acidic sulfate aqueous solutions is shown. As the ionic carrier organophosphorus compound, i.e. Cyanex 921 and tertiary amine, i.e. tri-n-octylamine were applied. Comparison of the transport kinetics of Cr(VI) and Cr(III) ions from equimolar aqueous solutions is presented.

© 2000 Society of Chemical Industry

EXPERIMENTAL

Chemicals

The aqueous solutions (source and receiving phases) were prepared using deionised water. The source phase an equimolar mixture of chromium (VI) and chromium (III) ions was used, which was obtianed by dissolving appropriate amounts of potassium dichromate, chromium (III) sulphate and sulphuric acid. The receiving phase was an 0.01 mol/dm^3 aqueous solution of potassium hydroxide. All inorganic chemicals were reagent grade and were obtained from POCh (Gliwice, Poland).

Two types of the ionic carriers were used:

- Cyanex 921, which contain 93 w.% of tri-n-octylphosphine oxide (TOPO), manufactured by Cyanamid Co.,
- tri-n-octylamine (TOA), manufactured by Serva.

Supported Liquid Membranes (SLM)

The competitive transport of equimolar mixture of Cr(VI) and Cr(III) ions through the supported liquid membranes from sulfuric acid aqueous solutions was studied applying two-compartment cells with a flat-sheet membrane with an effective area of 3.14 cm^2. Microporous polypropylene membrane Celgard® 2500 (Hoechst Celanese Co.) was used as the solid support. The membrane has a porosity of 0.45, a thickness of 0.025 mm, and 0.04 μm effective pore size. The membrane was soaked for 12 hours in 0.0058 to 0.10 mol/dm^3 organic solution of Cyanex 921 or TOA in kerosene. The volumes of both aqueous phases were 50 cm^3. Both aqueous phases were pumped using peristaltic pumps at such flow rate to allow for exchange of whole volume of aqueous phases within 10 minutes.

0.10 cm^3 samples of aqueous phases were periodically removed for determination of chromium (VI) and chromium (III) concentrations. The total chromium concentration was measured by atomic absorption spectroscopy (SOLAAR 939, ATI Unicam, G.B.), and the chromium (III) concentration was determined spectrophotometrically (UV-VIS SOLAAR UV2 spectrometer, ATI Unicam, G.B.).

Polymeric Inclusion Membranes (PIM)

The transport across PIM was performed using the same two compartment cells as for the SLM process To make the transparent polymer film the following organic solutions were prepared:

- a solution of 1 g cellulose triacetate (CTA) from Aldrich in 100 cm^3 dichloro-methane (POCh, Gliwice, Poland),
- a solution of 10 g plasticiser, o-nitrophenyl octyl ether (NPPE) (Aldrich) in 100 cm^3 of dichloromethane,
- a solution of ionic carrier, 0.001 mol/dm^3 of Cyanex 921 or TOA in dichloro-methane.

Aliquots of the solutions: CTA (5 cm^3), NPPE (2 cm^3) and an ionic carrier (0.5 – 8.6 cm^3) were poured into a membrane mold comprised of 9-cm glass ring attached to a glass plate with CTA-dichloromethane glues. The solvent (dichloromethane) was allowed to evaporate for 24 hours and the resulting membrane was separated from the glass plate by immersion in cold water. The membrane was soaked overnight in water. The resulting membrane was transparent and tough and its thickness was from 30 to 40 μm.

To compare both liquid membranes, i.e. SLM and PIM, it was necessary to introduce similar amounts of ionic carrier into membranes. For this reason, the amount of a carrier introduced into the Celgard® 2500 membrane, was determined by weighing the membrane before and after soaking in kerosene solution of ionic carrier, i.e. Cyanex 921 or TOA. It was found that depending on the carrier concentration in kerosene solution, i.e. from 0.058 to 0.1 mol/dm^3, the amount of the carrier introduced into Celgard® 2500 membrane was equal to from 7.5×10^{-9} to 1.3×10^{-7} moles/cm^2 of the

membrane surface. To achieve of similar amount of the carrier introduced into the PIM membranes the volumes of 0.001 mol/dm^3 solution of carrier in dichloromethane required used to prepare membranes ranged from 0.5 to 8.6 cm^3.

RESULTS AND DISCUSSION

Changes of chromium (VI) and chromium (III) concentrations in the source phase as a function of time for both processes, i.e. SLM and PIM, show the transport process may be described as a first-order reaction in metal concentration:[1]

$$\ln \frac{c}{c_i} = -kt \qquad (1)$$

where: c - chromium (VI) or chromium (III) concentration in the source phase, mol/dm^3
c_i - initial Cr(VI) and Cr(III) concentration in the source phase, mol/dm^3
t - process time, s
k - rate constant, s^{-1}

An example of such plot is shown in figure 1.

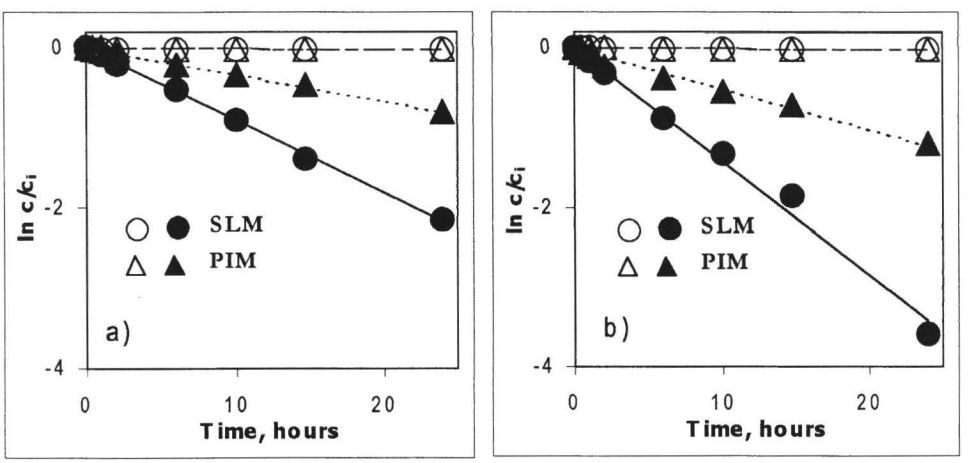

Figure 1 Transport kinetics of Cr(VI) (solid symbols) and Cr(III) (open symbols) through SLM and PIM. The used carriers: a) Cyanex 921, b) TOA. Source phase 0.01 mol/dm^3 Cr(VI) and 0.01 mol/dm^3 Cr(III) in 0.5 mol/dm^3 H_2SO_4. PIM: the amounts of CTA and NPPE – see Experimental, the volume of carrier solution was equal to 8.6 cm^3.

The relationship of ln c/c_i versus transport time is linear, which results from the high values of determination coefficients, i.e. from 0.9522 to 0.9985. The initial flux, i.e. flux at t = 0 can be calculated knowing the values of the rate constant:

$$J_i = \frac{V}{A} k c_i \qquad (2)$$

where: J_i - initial flux, moles m^{-2} s^{-1}
V - volume of source phase, m^3
A - interfacial area, m^2.

Determined values of initial fluxes are shown in Figs. 2 – 4.

From figure 1 it can be seen that the transport rate for both ionic carriers, i.e. for Cyanex 921 and TOA, is much faster for chromium (VI) when compared with chromium (III). Practically no transport occurs in case of chromium (III) ions. Comparing initial fluxes of chromium (VI) it can be noticed that TOA, (fig. 1b) as an ionic carrier allows for faster transport in comparison with Cyanex

921 (fig. 1a). For both ionic carriers initial fluxes of chromium (VI) are higher for the SLM process in comparison with the PIM process.

An important factor influencing the transport of chromium (III) and chromium (VI) ions is acidity of source phase (figure 2). Increasing sulphuric acid concentration in the source phase the transport rate of chromium (VI) increases very strongly for both ionic carriers and in both liquid membrane processes. Also here are observed lower initial fluxes for PIM's process in comparison with SLM's. Since increase of the initial fluxes for chromium (III) is much smaller, the separation ratio for both PIM's and SLM's increases as a function of the source phase pH.

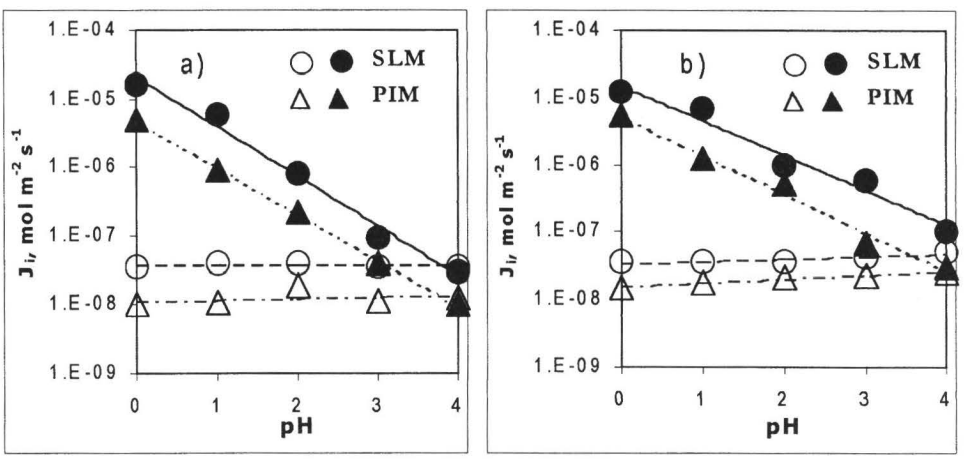

Figure 2 Initial fluxes of chromium (VI) (solid symbols) and chromium (III) (open symbols) ions vs. hydrogen ion concentration in source phase by SLM and PIM: a) Cyanex 921, and b) TOA. Other conditions see figure 1.

Also the concentration of chromium (VI) and chromium (III) in the source phase influences strongly the initial fluxes of both forms of chromium transported across PIM and SLM membranes (figure 3).

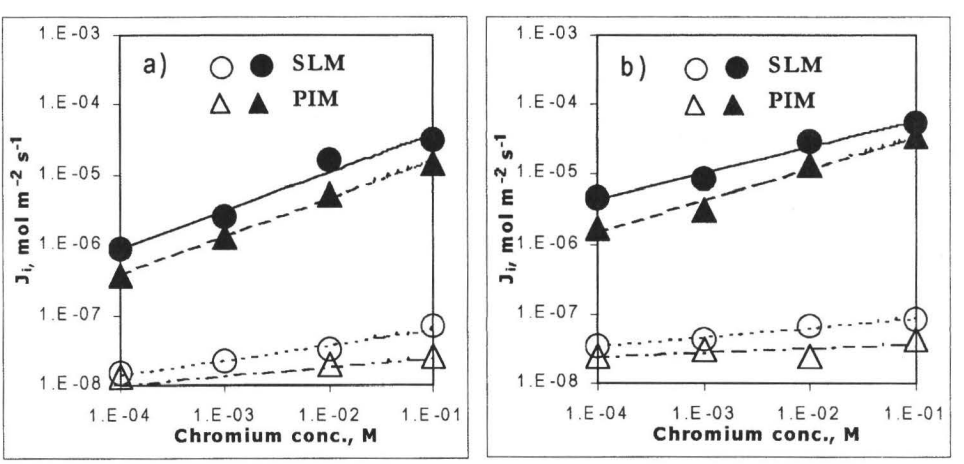

Figure 3 Initial fluxes of chromium (VI) (solid symbols) and chromium (III) (open symbols) ions vs. initial concentration of chromium in source phase by SLM and PIM: a) Cyanex 921, and b) TOA. Concentration of H_2SO_4 in source phase: 0.5 mol/dm^3. Other conditions see figure 1.

But this increase is much slower in comparison with pH increase in the source phase. For 1000-fold increase of chromium concentration the initial fluxes of Cr (VI) with Cyanex 921 as ionic carrier in SLM process increases only 20 times. For TOA as ionic carrier this increase is even lower. Since Cr(III) initial flux is also increasing with increase of metal concentration the separation of Cr(VI) and Cr(III) decreases as a function of chromium concentration in the source phase.

The last studied factor, which influences on the transport rate of chromium, was the amount of the ionic carrier in membrane (figure 4). The amount of the ionic carrier only significantly influences the transport rate of chromium (VI) and for this reason in figure 4 only shows the influence on chromium (VI).

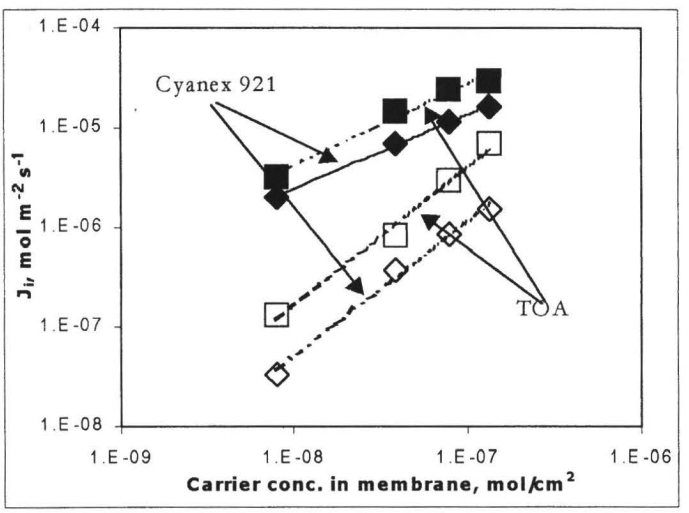

Figure 4 The influence of the amount of the carriers ($n_{carrier}$) in membrane on transport rate of Cr (VI) ions through SLM (solid symbols), and PIM (open symbols). Other conditions of the experiments see figure 1.

When the amount of the carrier increases the initial flux also increases but for TOA these fluxes are higher in comparison with Cyanex 921. This occurs for both liquid membranes but for the SLM process the initial fluxes are higher in comparison with the PIM process.

CONCLUSIONS

The studies presented show the possibility of effective separation of chromium (VI) from chromium (III) ions from aqueous sulphuric acid solutions using as the ionic carriers Cyanex 921 and tri-n-octylamine in both liquid membrane processes i.e. supported liquid membrane and polymeric inclusion membranes. In all experiments chromium (VI) was transported much more effectively in comparison with chromium (III). The initial fluxes of Cr(VI) ranged from 3×10^{-8} to 9×10^{-5} moles m^{-2} s^{-1} and were more than 800-times higher in comparison with Cr(III) fluxes. The highest fluxes for Cr(VI) were obtained for an SLM with TOA as an ionic carrier. The fluxes of chromium (VI) are higher in the supported liquid membrane process, which can be explained by higher mobility of ionic carriers in this type of liquid membranes.

Studying such parameters as acidity and concentration of chromium ions in the source phase as well as the amount of the ionic carrier per unit of interfacial area it was found that with increase of these parameters values of the Cr(VI) fluxes also increase. The highest values of Cr(VI)/Cr(III) separation ratio (which is a fraction of the initial fluxes of Cr(VI) and Cr(III)) were about 815 and were obtained for a polymeric inclusion membrane with TOA as the ionic carrier at the concentration

of chromium (VI) and chromium (III) in the source phase equal to 0.1 mol/dm^3 and at the concentration of sulphuric acid in the same phase equal to 1.0 mol/dm^3.

Polymeric inclusion membranes appear to be more stable and give higher selectivity for chromium (VI) over chromium (III) than supported liquid membranes. On the other hand, the transport of chromium ions across SLM was faster than transport through PIM.

ACKNOWLEDGMENTS

This work was supported by State Committee for Scientific Research in Poland under project 3 T09B 027 12.
The authors thank Cyanamid Co., Canada for free samples of Cyanex 921.

REFERENCES

1. Danesi PR, *Sep. Sci. Technol.*, **19,** 857, (1984-85).
2. Chiarizia R, *J. Membr. Sci.*, **55,** 39, (1991).
3. Sugiura M, Kikawa M and Urita S, *Sep. Sci. Technol.*, **22** , 2263, (1987).
4. Sugiura M, Kikawa M and Urita S, *J. Membr. Sci.*, **42**, 47, (1989).
5. Sugiura M, *Sep. Sci. Technol.*, **25**, 1189, (1990).
6. Sugiura M, *Sep. Sci. Technol.*, **27**, 269, (1992).
7. Schow AJ, Peterson RT and Lamb JD, *J. Membr. Sci.*, **111**, 291, (1996).
8. Lamb JD, Nazarenko AY, Uenishi J and Tsukube H, *Anal. Chem. Acta*, **373**,167, (1998).
9. Bartsch RA, Charewicz WA, Lu J, Walkowiak W and Amiri-Elaisi B, *Proc. of Int.Solv. ExtrConf ISEC'88* Moscow (Russia), 205, (1998).

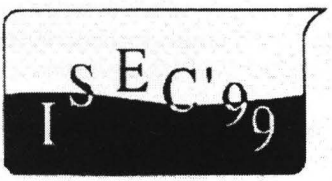

DISPERSION-FREE MEMBRANE BASED EXTRACTION AND STRIPPING OF Pb(II) AND Cd(II) WITH KELEX 100 AS CARRIER

J de Gyves, JC Aguilar and E Rodríguez de San Miguel
Dpto. Química Analítica. D.E.Pg. Facultad de Química. UNAM. Ciudad Universitaria. 04510 México, D.F. México

ABSTRACT
Pb(II) and Cd(II) are recovered from aqueous media using laminar supported liquid membranes (LSLM) and a two module hollow fiber supported liquid membrane (HFSLM) with Kelex 100 dissolved in heptane as carrier. Experimental parameters such as aqueous phase composition, flow rates of feed and strip solutions, extractant concentration, contact area, geometry and pressure differences (HFSLM) are evaluated.

Keyword: supported liquid membrane, cadmium, lead, Kelex 100

INTRODUCTION

Lead and cadmium have many uses in industrial and consumer products such as batteries, metal coatings and plastics. Both metals are recognized as toxic elements and can be found in at least 388 of the 1,300 National Priorities List sites identified by the Environmental Protection Agency (EPA). EPA allows only 0.01 ppm of cadmium and 0.05 ppm of lead in drinking water. These levels are under review and are expected to be further reduced. The EPA also limits how much of these metals can be put into lakes, river dumps and arable land, and does not allow cadmium in pesticides. Some of the methods suggested to reduce discharges of cadmium and lead from industrial sources are: a) recycling of metal-containing wastewater, or otherwise limitation of the use of water in processes where they are handled, b) strict separation of cadmium and lead-containing wastewater from all other effluents, and c) effective treatment of wastewater containing lead and cadmium by the use of common (i.e. precipitation, ion exchange) or other advanced technologies (membrane separations) so that the concentrations and quantities of lead and cadmium in effluents from various industrial sources are reduced to the allowed limits.

Separation techniques based on supported liquid membranes (SLM) allow simultaneous extraction and back-extraction operations with several advantages, i.e. high selectivities, high fluxes, high feed/strip ratios, ease of operation, and low capital and operating costs. In contrast, degradation of the membranes is identified as the main disadvantage. Common configurations available commercially include flat-sheets (FS) and hollow fibres (HF). Extraction of cadmium from chloride and nitrate media with SLM's using amines[1-3] and organophosphorus[4] extractant reagents and of lead with amines[3] has been reported. Recently, Ashrafizadeh et al.[5] studied the permeation of Cd (II) and Pb (II) as impurities in the permeation of Ir (IV) with Kelex 100 in concentrated chloride solutions.

In this work Pb (II) and Cd (II) are separated from aqueous chloride and nitrate media using a laminar supported liquid (LSLM) and a two module hollow fibre supported liquid membrane (HFSLM) with Kelex 100 dissolved in n-heptane as carrier. Experimental parameters such as aqueous phase composition, extractant concentration, flow rates of feed and strip solutions, contact area, geometry and pressure differences (HFSLM) are evaluated. Performance of both configurations under optimal conditions are compared and analysed with proposed theoretical models.

EXPERIMENTAL

Reagents and equipment

$Cd(NO_3)_2$, $CdCl_2$, $Pb(NO_3)_2$ and $PbCl_2$ A.R. (Merck) were used to prepare 0.01mM feed solutions of the metal ions. Ionic strength was fixed at 0.01 with $NaNO_3$ and NaCl respectively. MES

© 2000 Society of Chemical Industry

and TRIS A.R. (Aldrich) buffers were used, adjusting the appropriate pH working values with HNO_3 or NaOH. The commercially available extractant Kelex 100 (Sherex) was kindly supplied by the producers. As organic solvent n-heptane (Baker) was chosen because of the good affinity between the polymeric support and this diluent.

In the LSLM experiments Millipore GVHP04700 flat-sheet membranes (polyvinilydene difluoride) of 125μm thickness, 75% porosity and effective pore size of 0.22μm were used as hydrophobic supports to immobilize the organic phase within the pores. A two-compartment cell was used where the feed and the strip solutions were contained and stirred with mechanical motors located in the top of each compartment. The stirring rate was controlled with the use of an optical tachometer.

For the HFSLM experiments hollow fibre cartridges XAMPLER UFP-5-E3A and UFP-10-E3A (polysulfone, 5000 and 10000 NMWC, respectively, 1mm I.D.) from A/G Technology Corporation served as supports to perform the dispersion free solvent extraction experiments. Masterflex 7520-10 pumps with Viton tubes (1/4" I.D., 5/16" E.D. Cole Palmer) conducted the solutions through the system. Air pressure was supplied with a diaphragm type Gast pump.

The metal concentrations in the feed and strip solutions were measured using flame AAS with a Perkin Elmer 3100 spectrometer. The pH of aqueous phases was controlled with the use of a Metrohm 620 pH meter and a combined glass electrode Cole Palmer 62014.

Procedure

Preliminary solvent extraction experiments were performed in a conventional way to establish appropriate conditions for the dispersion-free experiments and characterize the extraction reactions. Once these conditions were selected, metal extraction was performed in the LSLM.

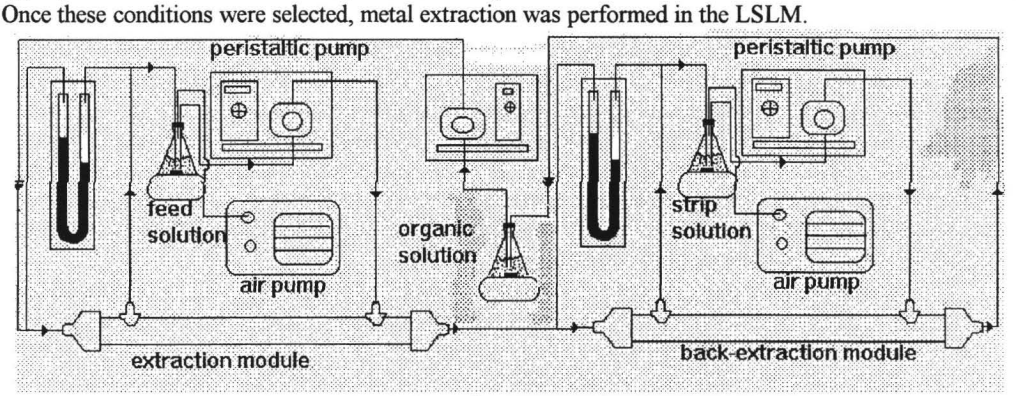

Figure 1. Experimental two-module hollow fibre setup for the dispersion-free solvent extraction experiments.

For the experiments, equal volumes of 200 cm^3 of the feed and strip solutions were used. Subsequently, the extraction system was tested in the HFSLM module, using the setup shown in figure 1. In this case, 200 cm^3 of the aqueous phases and 100 cm^3 of the organic phase were used. Experiments were carried out in each module in a continuous recirculating mode for both phases in counter-current operation.

RESULTS AND DISCUSSION

Liquid-Liquid Extraction

The solvent extraction of 0.01mM of Pb(II) and 0.01 mM Cd(II) from chloride and nitrate media at constant ionic strength of 0.01 using NaCl and $NaNO_3$, respectively, with Kelex100 dissolved in n-heptane was studied over the pH range of 5-9. The results obtained are shown in figure 2. Preliminary experiments showed that Pb(II) and Cd(II) are extracted quantitatively in less than 5

minutes. Plots of log D (distribution constant) as a function of pH and of the total extractant concentration indicated that the extracted species for Pb(II) is PbL in both media; however, for Cd(II) the extraction is explained by the formation of $CdHL_2X$ (where $X = Cl^-$, NO_3^-) and CdL_2.

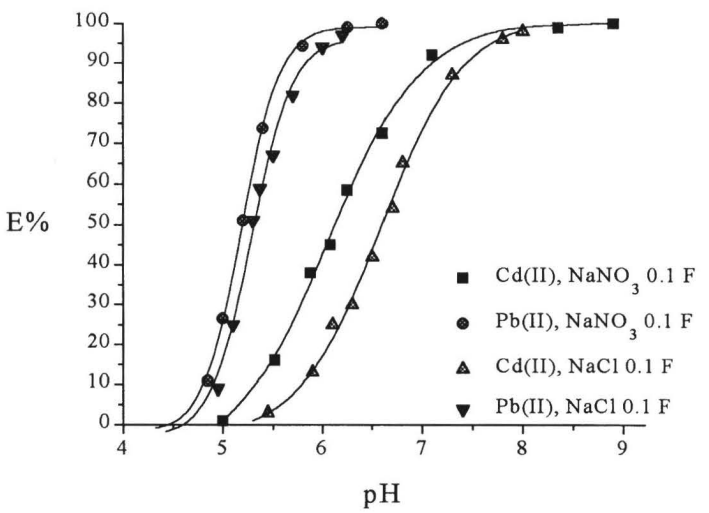

Figure 2 Percentage extraction of Cd(II) and Pb(II) with 5% v/v KELEX 100 as a function of pH in two different ionic media.

LSLM

Carrier concentration

The effects of the carrier concentration were studied using an aqueous solution containing 0.01mM $Cd(NO_3)_2$ + 0.01M TRIS + 0.01 M $NaNO_3$, pH = 8.0 .

Constant permeability coefficients of 0.13 cm min^{-1} and 0.09 cm min^{-1} in the feed solution (P_f) and strip solutions (P_s), respectively, were measured in the 1-5% v/v range of Kelex 100. P_f was evaluated from the slope of the log $[M]_f$ / $[M]_{o,f}$ vs time plot, while P_s from the log $\{[M]_{o,f}$ - $[M]_f\}$ / $[M]_{0,f}$ vs time plot.

The different values obtained for P_f and P_s indicate the presence of some accumulation of the metal ion within the membrane phase. The same permeability coefficients were measured using unpurified Kelex 100 (5%).

Influence of pH

As observe in figure 3, P_f values increase with the increase in pH according to the value of the distribution coefficients in liquid-liquid extraction experiments. In comparison, the P_s values reach a maximum at pH = 8.0. This behaviour seems to indicate that a polarization phenomenon is taking place, possibly because the increasing amount of Cd(II) extracted in the feed phase as the pH increases is not properly (quantitatively) back-extracted in the strip phase, due to the constant rate at which the back-extraction is occurring. In this form, the concentration gradient within the membrane should be decreasing as the pH increases, suggesting that the diffusion of the metal complex in the aqueous phase plays a major role in the permeation rate.

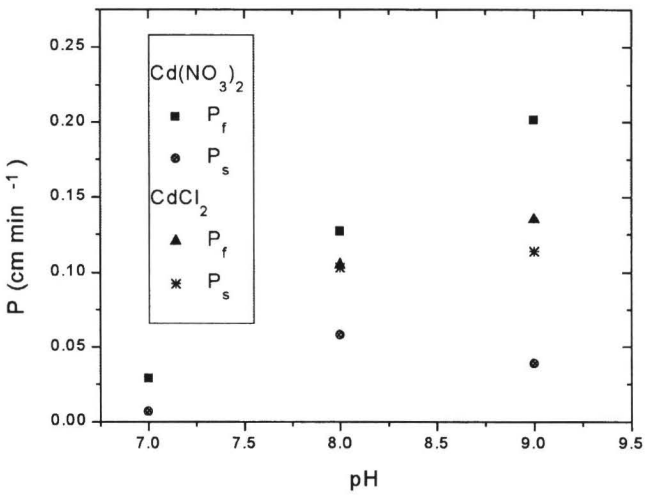

Figure 3. Permeability values of Cd(II) in the feed and strip solutions as a function of pH for two different ionic media.

Influence of Cd(II) total concentration

The dependence of the permeability with respect to Cd(II) concentration in the feed and strip solutions at fixed pH value of 8 and in nitrate aqueous media is shown in figure 4. The results obtained indicate that as the initial total metal ion concentration decreases the permeability in the feed aqueous phase increases, however it decreases in the strip solution. Apparently, as the initial concentration of Cd(II) decreases a strong retention of the metal within the membrane occurs making more difficult its release to the strip solution. This behaviour has also been observed by Hayashita,[3] who suggested that the retention of cadmium is a function of the cadmium concentration in the membrane phase.

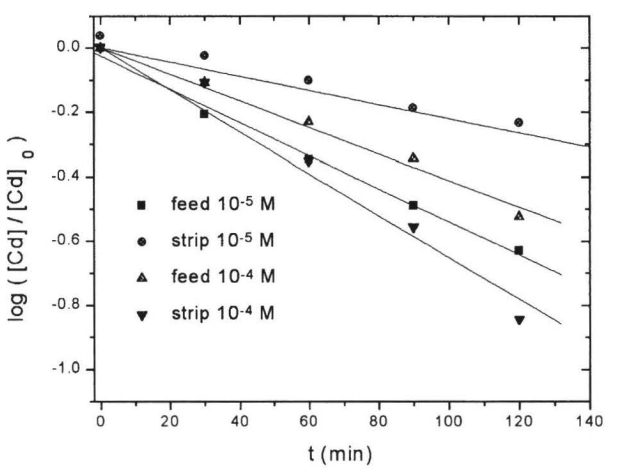

Figure 4. Influence of Cd(II) concentration on the permeabilities measured in the feed and strip solutions.

Membrane selectivity

The permeabilities of Cd(II) and Pb(II) in a solution containing 0.01mM of each metal ion in an aqueous chloride solution (I=0.01) and using 1%v/v of Kelex 100 were determined at pH values of 6.0, 7.0 and 8.0. Separation factors calculated as:

$$S_{Pb}^{Cd} = \frac{[Cd]_s[Pb]_{0,f}}{[Cd]_{0,f}[Pb]_s}$$

were 0, 0.47 and 3.14, respectively, after 160 minutes. Consequently, a good separation between Cd(II) and Pb(II) is obtained at pH 6.0.

HFSLM

According to the results obtained in the LSLM experiments two different total concentrations of Cd(II) were tested in the two-module HFSLM setup described above. The phases were circulated at 20 cm^3min^{-1}, ΔP in the extraction module was 0.3 psi , ΔP in the back-extraction module was 3 psi , and 1% v/v of Kelex 100. At pH = 8.0 in a chloride aqueous media, 0.01mM Cd(II) was quantitatively extracted but not back-extracted. However, when 1 mM Cd(II) was introduced in an aqueous nitrate feed solution (I = 0.01) at pH = 6.8, 50% of Cd(II) was extracted from the feed solution and 24% was back-extracted in the strip solution in 80 min.

Using the double-film model a good description of the performance of the system is possible.

REFERENCES

1. Danesi PR and Reicher-Yinger L, *J. Membr. Sci.*, **27**, 339, (1986).
2. Molinari R Drioli E and Pantano G, *Sep. Sci. Technol.*, **24**, 1015, (1986).
3. Hayashita T, in *Chemical Separations with Liquid Membranes* Eds. Bartsch RA and Way JD, ACS Symposium Series 642: Washington, (1996).
4. Alonso AI, Urtiaga AM, Zamacona S and Ortiz II, *J. Membrane Sci.* **130**, 193, (1997).
5. Ashrafizadeh SN, Demopoulos GF, Rovira M and Sastre AM, *Sep.Sci.Technol.*, **33**, 1145, (1998).

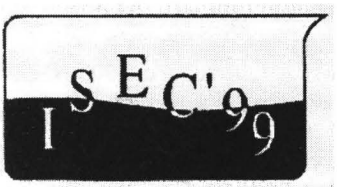

MEMBRANE-BASED SOLVENT EXTRACTION FOR INDIUM(III)–IRON(III) SEPARATION USING A HOLLOW FIBRE CONTACTOR

E Rodríguez de San Miguel and J de Gyves
Dpto. Química Analítica. D.E.Pg. Facultad de Química. UNAM. Ciudad Universitaria. 04510 México, D.F. México.

ABSTRACT
Indium (III) is kinetically separated from iron (III) from nitrate media by a non-dispersive solvent extraction technique using a hollow fibre contactor with Cyanex 272 dissolved in n-heptane as extractant reagent. The influence of several variables such as pressure difference, flow rates of the aqueous and organic phases, extractant concentration and pH are evaluated.

Keywords. supported liquid membrane; hollow fibre contactor; indium; iron; Cyanex 272

INTRODUCTION

Separation techniques based on membranes have received considerable attention in the past 30 years. From a practical point of view, the two most commonly employed types are emulsion and supported liquid membranes. The latter are available in two main configurations: flat-sheets (FS) and hollow fibres (HF). The non-dispersive extraction techniques solve many of the problems traditionally encountered with liquid-liquid extraction, such as: emulsion formation, density differences between phases and swelling limitations. Furthermore, non-dispersive contactors present other advantages: a) no mechanical mobile parts are present in the extractor, b) significant interfacial area without mixing the phases, c) great versatility since they can be connected in series or in parallel and the number, length and diameter of the fibres can be modified in order to provide the required interfacial area , d) the flow rates can be varied in a wide range without flooding or loading as long as the correct relative phase pressure conditions are maintained, e) lower solvent loss, f) the HF extractor can have a very high membrane surface area per unit equipment volume leading to very high extraction rates/volume and g) scaling-up is easier.[1,3,5]

The dispersion-free solvent extraction technique has been widely used for the extraction of pharmaceuticals, organic reagents, proteins and metal ions for many years.[1-4] Some organophosphorus compounds (Cyanex 272, HEHEHP, PC88A and D2EHPA) have been employed in HF modules for the extraction of Mo(VI), Cu(II), Zn(II), Cd(II), and Ni(II).[6-12] Due to the low extraction kinetics of iron, the kinetic separations of U(VI) from Fe(III),[13] and Y(III) from Fe(III)[14] with this type of compound have been reported using flat sheet SLM's. However, concerning the separation In(III)/Fe(III) special types of contactor have been used for this purpose[15,16] but no information on with the use of HF in this separation is available.

In this work In(III) is kinetically separated from Fe(III) in aqueous nitrate media using a HF contactor with Cyanex 272 dissolved in n-heptane as extractant reagent. The influence of variables such as pressure difference, flow rate of the aqueous and organic phases, extractant concentration and iron concentration are evaluated. Optimal conditions for the In(III)/Fe(III) separation are given and discussed.

EXPERIMENTAL

Reagents and Equipment

$Fe(NO_3)_3.9H_2O$ A.R. (Merck) and 1010 ppm atomic absorption solution of In(III) (Aldrich) were used to prepare the feed solutions. As the organic diluent n-heptane (Mallinckrodt) was chosen

© 2000 Society of Chemical Industry

because of the good affinity with the polymeric support. The commercial available extractant Cyanex 272 was kindly supplied by CYTEC. Nitric acid was A.R. grade.

An ultrafiltration hollow fibre cartridge XAMPLER UFP-5-E3A (polysulfone, 5000 NMWC, 1mm I.D. (d), 33.7 cm length (l)) from A/G Technology Corporation served as support to perform the dispersion free solvent extraction experiments. MASTERFLEX 7520-10 pumps with VITON tubes (1/4" I.D., 5/16" E.D. Cole Palmer) fed the solutions through the system. Air pressure was supplied with a diaphragm type GAST pump.

Metal content in the aqueous phases was determined by F-AAS (Perkin Elmer 3100 Spectrophotometer); pH was controlled with the use of a Metrohm 620 pHmeter and a combined glass electrode Cole Palmer 62014.

Procedure

Preliminary solvent extraction experiments were performed in a conventional way to establish appropriate conditions for the dispersion free experiments and characterise the extraction reactions. Once these conditions were selected metal extraction was performed using the membrane module. The volumes of the phases (V_{org} ,V_{ac}) were 200 cm^3 and the total membrane area of the module was 70 cm^2. Experiments were carried out in a continuous recirculating mode for both phases in counter-current operation. The influence of the variables: pressure difference (Δp = 0-3 psi), total extractant concentration (C_{tot} = 0.1, 0.2, 0.4 mol/dm^3), flow rate of the aqueous phase (Q_{ac} = 20-80 cm^3min^{-1}), flow rate of the organic phase (Q_{org} = 4-50 cm^3min^{-1}), in the indium and iron extractions were studied at pH 1.8 to find conditions for selective separation. A 1 to 100 fold excess of Fe(III) respect to In(III) was present in the aqueous solution. The uncertainty in the percent of extraction values reported is ± 2%.

RESULTS AND DISCUSSION

Pressure Influence

The effect of pressure differences between phases was studied at constant flow rates (Q_{org} = 4 and Q_{ac} = 60 cm^3min^{-1}) and total extractant concentration (C_{CYANEX} = 0.2 mol/dm^3). Since the membrane used is hydrophobic in nature, it will be preferentially wetted by the organic solution. Consequently, in the absence of pressure a turbidity is observed in the aqueous phase. As the pressure of the aqueous phase increases (Δp >15 psi) this turbidity disappears indicating the immobilisation of the interface between the pores of the membrane. Further experiments were performed using Δp = 2 psi.

Extractant Concentration

Once the appropriate pressure value for the immobilisation of the interface was established, the influence of the extractant concentration was studied under constant flow rate conditions. From figure 1 it is possible to observe that percent of extraction (E%) of In(III) increases as the extractant concentration increases.

Aqueous Volumetric Flux Rate

Figure 2 shows the variation on E% of 0.1 mM In(III) and 0.1 mM Fe(III), respectively, as a function of time and the aqueous flow rate at constant pressure, total extractant concentration and organic flow rate. For In(III), it is observed that an increase of the flow rate above 20 cm^3min^{-1} favours the extraction until a maximum value is obtained at approximately 60 cm^3min^{-1}; above this value the residence time in the interface of the metal ion is insufficient for a complete reaction with the extractant and the E% of metal extracted into the organic phase decreases. In the case of Fe(III), the kinetics of extraction is much slower. Consequently it is possible to predict a kinetic separation of these two metals. In fact, for a flow rate of 60 cm^3 min^{-1} and a period of time of 30 min, 80% of In(III) and 5% of Fe(III) are extracted, making this separation feasible.

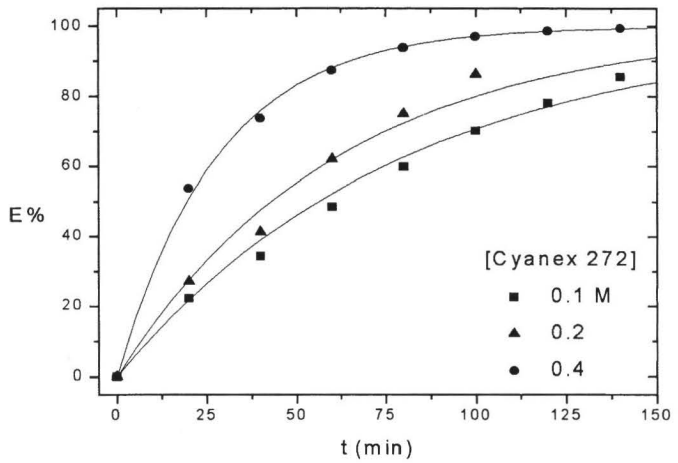

Figure 1. Variation of the percent of extraction of 0.1 mM In(III) as a function of time and total extractant concentration. Q_{org} = 4 cm^3min^{-1}, Q_{ac} = 20 cm^3min^{-1}, Δp = 2 psi.

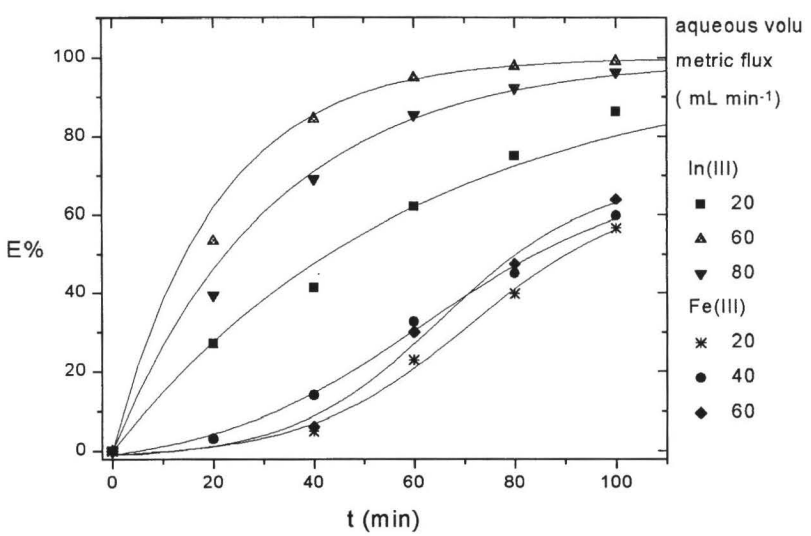

Figure 2. Influence of the aqueous flow rate in In(III) and Fe(III) extractions. C_{CYANEX} = 0.2 mol/dm^3, Q_{org} = 4 cm^3min^{-1}, Δp = 2 psi.

Organic Volumetric Flow Rate

The variation of this parameter gives rise to similar conclusions as above: a maximum in E% vs. time plot is obtained. Indium extraction is more sensitive to the variation in the flow rate than iron extraction. For 0.01mol/dm^3 Fe(III), 20% of In (III) and 3% of Fe(III) are extracted in 15 minutes in aqueous/organic flow rate ratio of 3.

Iron Concentration

The content of Fe(III) after acid leaching of zinc-based minerals is 10-100 times greater than that of indium. The study of the influence of the concentration of this element in the separation is very

important due to the fact that it has been observed that as the Fe(III) concentration increases Y(III)[14] and In(III)[17] transport diminish when using FS-SLM. Figure 3 shows the separation factor defined by:

$$F_{Fe}^{In} = \frac{[In(III)][Fe(III)]_0}{[In(III)]_0[Fe(III)]}$$

as a function of time and three different aqueous/organic flow rate ratios. The separation is accomplished better for small contact-times and it depends on the ratio of the phase flow rates. Moreover, this optimal ratio depends on the iron concentration. For an aqueous/organic flow rate ratio of 15, F_{Fe}^{In} = 52 when the iron and indium concentrations are 0.1mM, and F_{Fe}^{In}=4.2 when a 100-fold excess of iron exists in the aqueous phase, both factors taken for a 20 minute contact-time.

To enhance the In/Fe separation it is suggested that the operation of the system is explored in the once-through mode with a greater membrane area with small contact-times.

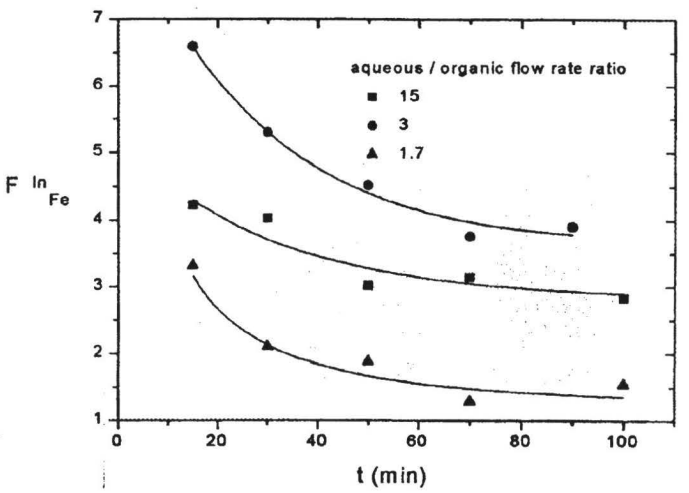

Figure 3. Separation factor as a function of time and three different aqueous/organic flow rate ratios in the presence of a 100-fold excess of Fe(III) respect to In(III).

REFERENCES

1 Prasad R and Sirkar KK. In: *Membrane Handbook*, Sirkar KK and Ho W.S. (Editors). Van Nostrand Reinhold. New York, (1992) and references therein.
2 Prasad R, and Sirkar KK. *J. Membrane. Sci.*, **50**, 153, (1990).
3 Alonso AI and Pantelides CC. *J. Membrane. Sci.*, **110**, 151, (1996).
4 Dahuron L and Cussler EL. *AIChE Journal*, **34**, 130, (1988).
5 Ortiz Y, Galán B and Irabien A. *Ind. Eng. Chem. Res.*, **35**, 1369, (1996).
6 Yinming C and Fumiyuki N. *Huaxue Fanying Gongcheng Yu Gongyi*, **6**, 67, (1990).
7 Sato Y, Kondo K and Fumiyuki N. *J. Chem. Eng. Jpn.*, **23**, 23, (1990).
8 Sato Y, Kondo K and Fumiyuki N. *J. Chem. Eng. Jpn.*, **22**, 686, (1989).
9 Sato Y, Kondo K and Fumiyuki N. *J. Chem. Eng. Jpn.*, **22**, 200, (1989).
10 Sato Y, Akiyoshi Y, Kondo K and Fumiyuki N. *J. Chem. Eng. Jpn.*, **22**, 182, (1989).
11 Shiau C-Y and Chen P-Z. *Sep. Sci. Tech.*, **28**, 2149, (1993).
12 Daiminger UA, Geist AG, Nitsch W and Plucinski PK. *Ind. Eng. Chem. Res.*, **35**, 184, (1996).
13 Chiarizia R and Horwitz EP. *Solvent Extr. Ion Exch.*, **8**, 65, (1990).
14 Akiba K, Ito M and Nakamura S. *J. Membrane. Sci.*, **129**, 9, (1997).
15 Zhou X, Zhou J, Zhang Ch and Yu W. *Sep. Sci. Technol.* **32**, 2705, (1997).
16 Zhang Ch, Zhou J, Zhou X, Yu W and Li F. *Youse Jinshu*, **47**, 78, (1995).

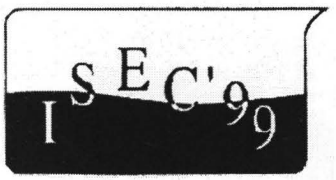

PERTRACTION OF NEODYMIUM AND HOLMIUM IN A HOLLOW FIBRE CONTACTOR

Gabriel Cara[1], Štefan Schlosser[2], Maria Muñoz[1] and Manuel Valiente[1]

[1]Unitat Química Analítica, Autonomous University of Barcelona, E- 08193 Bellaterra, Spain

[2]Dep. Chem. Biochem. Eng., Slovak University of Technology, SK-81237 Bratislava, Slovakia

ABSTRACT

Pertraction of Nd and Ho through liquid membranes (LM) with DEHPA as a carrier has been studied. Reaction kinetics of the metal/carrier complex decomposition influences greatly Nd and Ho transport through layered LM while this influence is relatively small in the transport through LM in a hollow fibre (HF) contactor. HF contactors can be effectively used for the recovery of Nd and Ho from diluted solutions. The overall mass-transfer coefficients and flux densities have been estimated for these systems.

Keywords: pertraction, liquid membranes, hollow fibre contactor, lanthanides, neodymium, holmium, D2EHPA

INTRODUCTION

Pertraction of metals through liquid membranes could be an alternative way of their recovery or removal from different solutions. Hollow fibre (HF) contactors for contacting three phases in pertraction, as discussed,[1,2] could be used effectively. New types of HF pertractors have been presented.[3-5] The pertraction of Nd through supported liquid membranes (LM) has been studied,[6] the transport of neodymium through a well-mixed bulk liquid membranes has been presented by Cara et al.[7] and the solvent extraction of holmium in a HF contactor (two phase) has been studied by Yoshizuka et al.[8,9]

The aim of this work was the experimental study and mass-transfer characteristics of a HF pertractor with two bundles of hydrophobic microporous HF in pertraction of neodymium and holmium with di-(2-ethylhexyl)phosphoric acid (DEHPA) as a carrier.

THEORETICAL

The overall stoichiometry of the extraction equilibrium of neodymium with DEHPA can be written as:[8-10]

$$Nd^{3+} + 3\,\overline{(AH)_2} \rightleftarrows \overline{NdA_3 \cdot 3AH} + 3H^+ \qquad (1)$$

where bars denote species dissolved in the membrane (solvent) phase and the same reaction can be proposed for holmium.

The flux density of Nd in pertraction in a HF contactor for an effective interfacial area ($A_F\varepsilon$) can be defined by equation 2:

$$J = \frac{K_p A_F \varepsilon}{M}\left(c_{F.} - c_{FRm}\right)_{ls} \qquad (2)$$

where c_{FRm} is the concentration of metal in the feed at the surface of the fibre corresponding to its concentration in the stripping solution $c_{FRm} = c_{Rm}\, D_{rR}/D_{rF}$, where D_r is the distribution coefficient on the strip and the extraction interfaces, R and F, respectively. When using a stoichiometric excess of a strong acid in the stripping solution, the metal complex on the strip interface is effectively destroyed and the value of $D_{rR} = c_{MR}/c_{RM}$ is very low, and accordingly the value of c_{FRm} is practically zero especially when the value of the distribution coefficient on the feed interface is high. From equation 2 it follows that:

© 2000 Society of Chemical Industry

$$J = \frac{K_p A_F \varepsilon}{M} c_{Fls} \tag{3}$$

From the overall material balance of the feed and stripping solution streams in the steady-state conditions follows:

$$J = \frac{\dot{V}_F}{M}\left(c_{Fo} - c_F\right) = \frac{\dot{V}_R}{M}\left(c_R - c_{Ro}\right) \tag{4}$$

Combining equations 3 and 4 and assuming a fresh stripping solution, when $c_{Ro} = 0$, the overall mass-transfer coefficient in the pertractor can be calculated as:

$$K_p = \frac{\dot{V}_R c_R}{A_F \varepsilon c_{Fls}} \tag{5}$$

where the logarithmic mean concentration of phenol in the feed stream is

$$c_{Fls} = \frac{c_{Fo} - c_F}{\ln \frac{c_{Fo}}{c_F}} \tag{6}$$

EXPERIMENTAL

Materials

The feed solution consisted of an aqueous solution of $Nd(NO_3)_3$ or $Ho(NO_3)_3$ in 0.1 mol/dm^3 $(Na,H)NO_3$ at a $pH_{Fo} = 2.1$ unless otherwise stated.

The membrane phase was a 0.2 mol/dm^3 solution of di-(2-ethylhexyl)phosphoric acid (DEHPA) in the dodecane fraction of n-alkanes.

1 mol/dm^3 HNO_3 was used as the strip phase unless otherwise stated.

HF contactor

A new pertractor PV-10 with two distributed bundles of hollow fibres (HF), one for the feed and the second one for the stripping solution, has been built, figure 1.[4,5] These two U-shaped bundles with 20 HF each, whose fibres were mixed, were inserted through the bottom ends of two vertical glass tubes. The same microporous polypropylene hollow-fibres Celgard X-10 (Hoechst-Celanese, USA) were used in both bundles. Porosity of the fibre walls was 30%. The inner and outer diameters of HF were 0.20 and 0.264 mm respectively. The basic parameters of the pertractor PV10 are: effective length of fibres 491.5 mm, inner geometrical surface area of one bundle about 61.76 cm^2. The membrane phase was pulsed by a moving piston, with adjustable amplitude, h, and frequency of stroke, ω_M, which was connected to the pertractor. The pulsation velocity was set in the presented experiments to $\omega_M.h$ = 6.6 mm.s^{-1}, a value found to be an optimum in previous works.[3,4] Pertraction of Nd and Ho was studied at 25°C. A steady-state was achieved after about 7 hours of operation.

Two compartment contactor

This has been described in papers,[11,12] with a layered liquid membrane and was used for more detailed study of transport of rare earth through the liquid membrane.

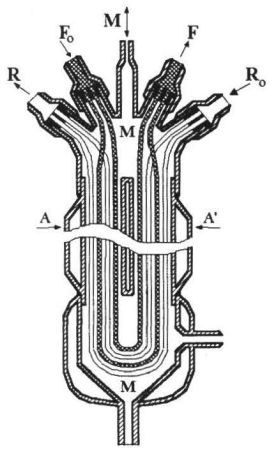

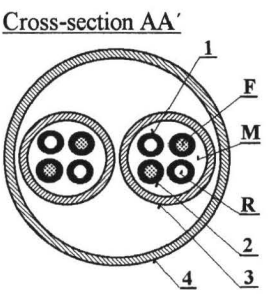

Figure 1. Diagram of the hollow-fibre pertractor PV-10 with two distributed bundles of hollow fibers (HF).[4,5]
F - feed, M - liquid membrane phase, R - stripping solution,
1 - microporous HF for strip, 2 - microporous HF for feed, 3 - glass tube, 4 - glass thermostat jacket.

Analytical method

The concentration of Nd and Ho in the aqueous phases was determined using a FIA spectrophotometric method. A multichannel peristaltic pump equipped with Tygon tubing was used to arrange the flow of the buffer, reagent and sample solution. The set-up consisted of a six-port sample injection valve 5041 (Rheodyne, USA) with 30 µl sample loop. Absorbance was measured at 660 nm by a Unicam 8625 spectrophotometer in a 80 µl flow-cell with 10 mm path length. pH was measured with the Ion Analyser model 3040 (Jenway, UK). For the determination of the concentration of metal, a buffer consisting of 0.2 mol/dm^3 formic acid/sodium formate solution at pH = 3.15 and a solution of reagent with 8.10^{-5} mol/dm^3 Arsenazo III (Fluka Chemie AG, Switzerland) in the mentioned buffer solution were used

RESULTS AND DISCUSSION

Results of transport experiments through layered LM in two compartment contactor are presented in paper.[7] From these results follows that with increasing nitric acid concentration the maximum flux through LM, J_{Rmax}, increases and approaches a steady value at acid concentration of about 1 mol/dm^3, as shown in figure 2a. In the pH interval from 1.3 - 3.5 fluxes through extraction and stripping interfaces are practically constant, as seen in figure 2b.

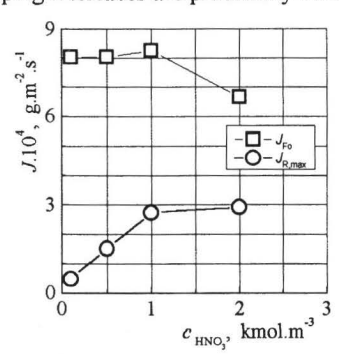

a) pH_{Fo}= 3.5

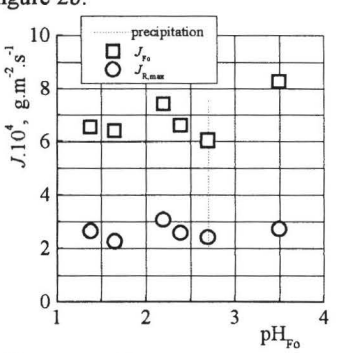

b) c_{HNO3}= 1 M

Figure 2 Influence of the stripping acid concentration (a) and initial pH of the feed (b) on the initial flux density through the extraction interface, J_{Fo}, and on the maximum flux density into stripping solution, J_{Rmax} in pertraction of Nd through the layered LM in a two compartment contactor. c_{Fo} was around 115 g.m^{-3}.

This is different from results in paper[6] and should be examined. In this work a membrane phase is used with more than ten times lower carrier concentration. At pH around 2.7, precipitation at the feed interface was observed, as it was reported earlier.[6] As shown in figure 2, the flux density through the extraction interface is substantially higher than through the stripping interface. This could be interpreted by slower kinetics of the complex decomposition on the stripping interface which influences the overall flux through the membrane.

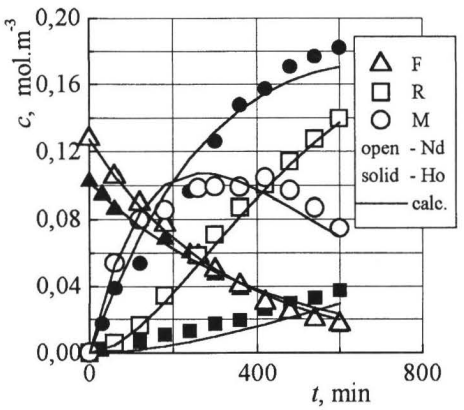

Figure 3 Time dependence of metal concentrations in the three phases of the two chamber contactor in pertraction of neodymium and holmium.

The flux of holmium through LM is much lower, less than one third, comparing with neodymium, figure 3. A much higher build up of Ho in the membrane phase is a consequence of slower decomposition of the Ho/DEHPA complex than decomposition of the Nd/DEHPA complex.

Neodymium is effectively recovered in the HF pertractor PV10 with high yield (99 to 82 %) even in short fibres of the contactor or for a short residence time used, figure 4. With increasing velocity of the feed in the fibre lumen, u_F, the yield of Nd decreases due to the lower residence time (figure 4a), but the overall mass transfer coefficient and flux density increase, figure 5. This suggests that the resistance in the feed phase plays some role. It can be assumed that the value of the overall mass-transfer coefficient, as well as flux, will approach a steady value at the linear velocity of the feed of about 6 $cm.s^{-1}$, figure 5, as it was observed in other systems such as Zn, phenol and butyric acid pertraction.[4,12,13] With increasing feed concentration the value of the overall mass-transfer coefficient decreases while the flux into the stripping solution increases, figure 6. As presented by Cara et al.,[7] the extraction rate constant of Nd through the well mixed layered bulk liquid membrane is practically independent of feed concentration. This indicates that the mass-transfer resistance in a HF bundle is probably responsible for the decrease of K_p. Experimental values of the steady state mean concentration of Nd in the membrane phase are much lower than the equilibrium concentration when considering distribution coefficient of around 100 for actual experimental conditions. Yield of Nd in the stripping solution only slightly decreases with the feed concentration in the concentration interval studied, figure 4b.

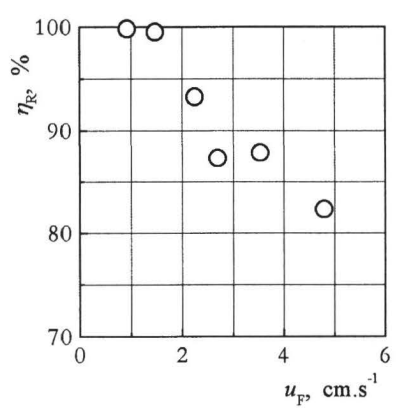

a)

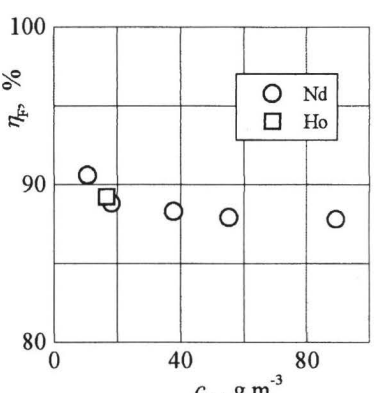

b)

Figure 4. Yield of Nd, Ho in the stripping solution vs. linear velocity of the feed in the fiber lumen of PV10 (a) and initial concentration of Nd in the feed (b).
a) $c_{Fo} = 89.3\ g.m^{-3}$, b) $u_F = 3.5\ cm.s^{-1}$

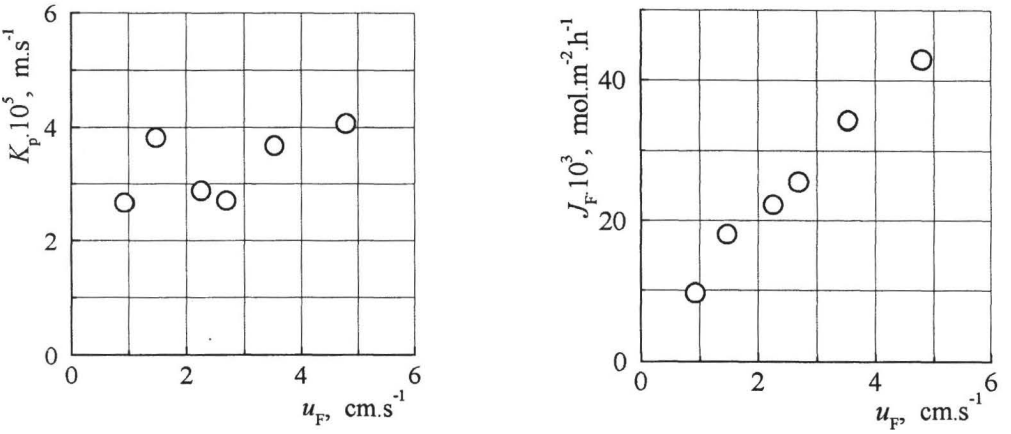

Figure 5. Overall mass-transfer coefficient and flux density of Nd into the stripping solution in pertraction in PV10, vs. linear velocity of the feed in the fiber lumen (c_{FO} = 89.3 g.m^{-3}, u_R = 0.66 cm.s^{-1})

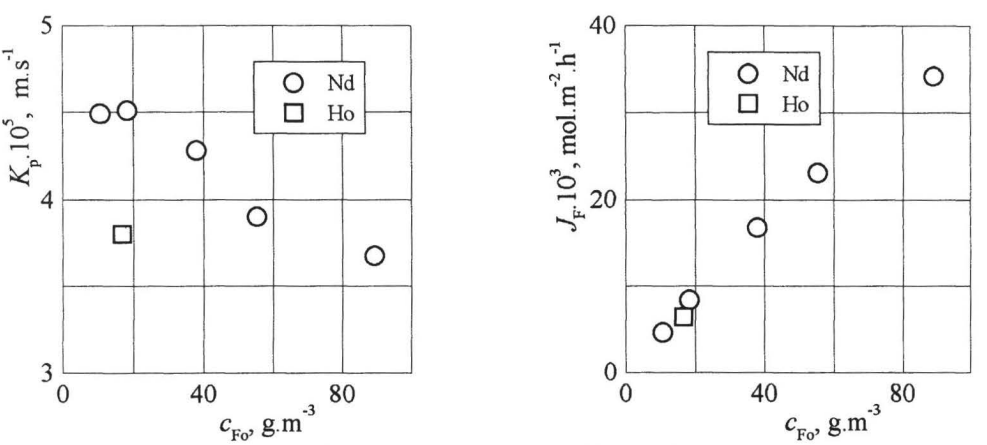

Figure 6. Overall mass-transfer coefficient and flux density of Nd into the stripping solution in pertraction in PV10, vs. initial concentration of Nd in the feed.
u_F = 3.5 cm.s^{-1} , u_R = 0.66 cm.s^{-1}

The overall mass-transfer coefficient and flux of holmium are a little lower than for neodymium, as shown in figure 6, but their differences are much lower than in the pertraction through layered LM, figure 3. This can be explained by a relatively great influence of the rate of complex decomposition on the transfer rate through the layered LM. In the bulk LM in a HF contactor is the main mass-transfer resistance membrane phase in the wall pores and the relative contribution of resistance due to the reaction kinetics is small.

ACKNOWLEDGEMENTS

Support from the EU grant CIPA CT 92-4015 and national grant VEGA No.4215/97 is gratefully acknowledged. The experiments were performed at SUT Bratislava during the study stay of G.C.

NOTATION

A surface area, m^2
c mass concentration, $g.m^{-3}$
D_r distribution coefficient, -
h amplitude of the membrane phase pulsation, m
J flux density, $g.m^{-2}.s^{-1}$
K_p overall mass-transfer coefficient in HF pertractor, $m.s^{-1}$
M molar weight, $g.mol^{-1}$
$\dot{V}$ volumetric flowrate, $m^3.s^{-1}$
u linear velocity in the fiber lumen, $m.s^{-1}$
t time, s
ε tortuosity of pores, -
η yield of metal, %
ω_M frequency of pulsation of the membrane phase, s^{-1}

Indices

F feed phase, interface on the feed side F/M
M membrane phase
o initial value
R stripping solution, interface on the strip side M/R
* equilibrium value

REFERENCES

1 Majumdar S and Sirkar KK. In: Ho WSW and Sirkar KK. (Ed.), *Membrane Handbook*, Van Nostrand Reinhold, 764, (1992).
2 Guha AK, Yun CH, Basu R and Sirkar KK. *AICHE J.*, **40**, 1223, (1994).
3 Schlosser S, Rothova I and Frianova H. *J. Membrane Sci.*, **80**, 99, (1993).
4 Forgová E and Schlosser Š. In: *The First Europen Congress on Chemical Engineering*, Florencia, 1321, (1997).
5 Schlosser Š and Sabolová E. *J. Membrane Sci.* submitted for publication, (1999)
6 Moreno C, Hrdlicka A and Valiente M. *J. Membrane Sci.* **81**, 121, (1993).
7 Cara G, Schlosser Š, Munoz M and Valiente M. In: *Chisa 96, paper No. 1524* Praha, Czech Republic, , 6, (1996).
8 Yoshizuka K, Sakamoto Y, Baba Y et al. In: *Proc. ISEC 90*, p. 805, (1990).
9 Yoshizuka K, Sakamoto Y, Baba Y et al. *Ind. Eng. Chem. Res.* **31**, 1372, (1992).
10 Preston JS and du Preez AC. *Solvent Extr. Ion Exchange*, **9**, 237, (1991).
11 Marták J, Schlosser Š and Stopka J. In: *Proc. 7th Int. Sym. on Synthetic Membranes in Science and Industry*, Tubingen, 293, (1994).
12 Cichy W, Schlosser Š and Szymanowski J. these proceedings.
13 Sabolová E and Schlosser Š. In: *Proc. of the 13th Int. Congress CHISA 98*, Praha, 12, (1998).

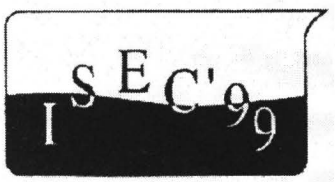

CHARACTERISATION OF THE STABILITY AND EFFICIENCY OF A HOLLOW FIBRE SUPPORTED LIQUID MEMBRANE CONTAINING ALIQUAT 336 AS CARRIER FOR RHODIUM(III) TRANSPORT

Clàudia Fontàs, Cristina Palet, Victòria Salvadó and Manuela Hidalgo

Dept. de Química, Universitat de Girona, 17071 Girona, Spain

ABSTRACT

A hollow fibre supported liquid membrane system (HFSLM) for the transport of rhodium (III) from aqueous feed chloride solutions containing SCN^- has been developed and characterised by using Aliquat 336 as carrier. Under these chemical conditions different experiments have been run to obtain practical information concerning the lifetime of both the supported liquid membrane and the polypropylene hollow fibre. Results demonstrated the feasibility of the SLM system during 6 non-stop days' operation, and also the resistance of the fibres used, which provided the same rate of rhodium (III) transport after 15 washes of the fibre with ethanol. The influence of the hydrodynamic conditions, as well as the configuration of the HFSLM system, have also been studied.

Keywords: rhodium(III), supported liquid membrane, hollow fibre module, Aliquat 336

INTRODUCTION

Supported liquid membranes (SLM) have been widely studied for the separation and concentration of a variety of compounds.[1,2] One of the major problems concerning SLM, especially with laminar SLM, is their low stability due to the easy loss of the liquid membrane from the support.[3,4] In this sense, the configuration of SLM by using tubular hollow fibres (HFSLM) has been found to improve lifetime of the liquid membrane system, due to the hydrodynamic characteristics.[5]

The extraction of rhodium (III) is a very difficult task because of the extremely inert character of its complexes. It is well known that Rh(III) in chloride media forms a large number of aquachloro complexes of the type $RhCl_{6-n}(H_2O)^{(3-n)-}$ (where $0<n<6$) which are highly hydrophilic.[6] To minimise this hydrophilicity, thiocyanate (SCN^-) had been used as a complexing reagent to form the extractable anion complex $Rh(SCN)_6^{3-}$.[7] Taking advantage of this, in previous work the transport of rhodium (III) through a flat SLM containing Aliquat 336 as a carrier was achieved.[8]

To improve the lifetime of this laminar liquid membrane system, a new design of a hollow fibre supported liquid membrane module is proposed, and the lifetime, stability and efficiency of the liquid membrane system are characterised. The influence of operating conditions, such as hydrodynamics and the configuration of the HFSLM system have also been evaluated.

EXPERIMENTAL

Reagents and solutions

The organic phase was prepared by dissolving tricaprylylmethylammonium chloride (Aliquat 336; Fluka Chemie), in dodecane (analytical reagent grade, Merck) modified with 1-dodecanol. A stock solution (500 mg dm^{-3}) of Rh(III) pH = 1 was prepared from $RhCl_3$ (Johnson Matthey) dissolved in concentrated HCl. The feed solution containing 10 mg dm^{-3} of Rh(III) and 10^{-3} mol dm^{-3} thiocyanate was prepared as described previously.[8] The stripping solution consisted of a 0.8 mol dm^{-3} NaSCN solution with $NaHSO_3/Na_2SO_3$ to achieve pH = 5 and 1.0 mol dm^{-3} ionic strength.[9]

Hydrophobic polypropylene hollow fibres from AZKO (Enka E.G., Germany), 75% porosity with o.d. 1.0 mm and i.d. 0.6 mm were used as solid tubular support for the liquid membrane. The effective pore size was 0.2 μm.

© 2000 Society of Chemical Industry

Apparatus and Procedure

The hollow fibre supported liquid membrane module proposed is shown in Figure 1. As seen, the module contains one spiral hollow fibre 57 cm long. The impregnation of the fibre was performed as described elsewhere.[5] In most experiments, the initial feed solution flowed through the hollow fibre (lumen) while the shell-side contained the final receiving solution (stripping solution). Both aqueous phases were continuously recirculated at a flow-rate of 0.35 cm^3 min^{-1} by means of a Gilson peristaltic pump. The pH measurements were carried out by using a pH-meter mode micro pH 2000, Crison Instruments S.A. (Spain).

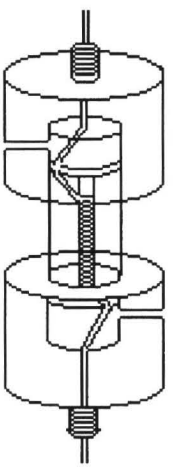

Figure 1: The hollow fibre supported liquid membrane module

A Varian SpectrAA-300 atomic absorption spectrometer (Varian Australia, Mulgrave, Victoria, Australia) was used to determine rhodium (III) concentrations in both aqueous solutions, at λ=343.5 nm.

RESULTS AND DISCUSSION

The permeability data for hollow fibre SLM module operating in a recycling mode were expressed in terms of Rh(III) coefficient permeability, P*, defined by Danesi as:[10]

$$\text{Ln}\,(C/C_0) = -\frac{A}{V} P^* \left[\frac{(\Phi+1)}{\Phi}\right] t$$

where A is the total effective area of the hollow fibre module, V is the total volume of the feed solution and C_0 is the concentration of the metal species in the feed solution at time zero. The parameter Φ, for a membrane containing N fibres, is $\Phi = Q_T / \text{PLNR}\Pi$, being Q_T the total flow rate of the feed solution, P* is the modified permeability coefficient, L the length of the fibre, N the number of the fibres and R its internal radius.

Reproducibility of the HFSLM rhodium (III) transport system was checked in different experiments under the same chemical and hydrodynamic conditions, using a new fibre in each experiment. Figure 2 shows the results of four consecutive experiments. As observed, a good reproducibility is obtained.

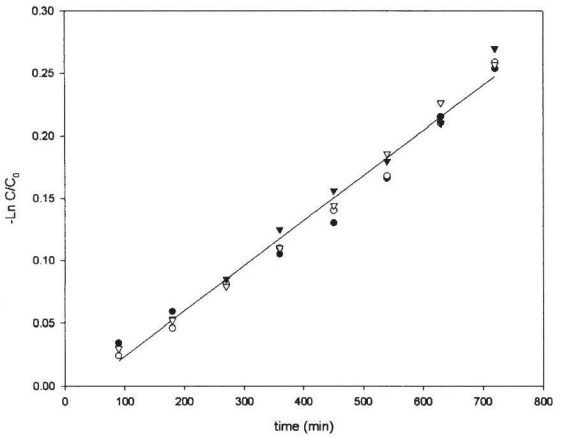

Figure 2: Reproducibility of the HFSLM system for Rh(III) transport

The stability of the liquid membrane system for long-term operation was verified by using a hollow fibre support (Figure 1) impregnated with the liquid membrane at the beginning of the experiment during subsequent cycles of 24 hours. At the end of each cycle feed and stripping solutions were substituted by fresh ones. As can be seen in Figure 3, the HFSLM does not show any appreciable decline in P during a period of 6 days of continuous operation. When a decrease of the efficiency was observed, the fibre was washed and reimpregnated with a fresh liquid membrane solution. After that, the membrane permeability coefficient was restored to its initial value. It is believed that the failure of the HFLMS is due to a loss of organic liquid membrane solution from the support pores, as found previously with laminar supports.[5]

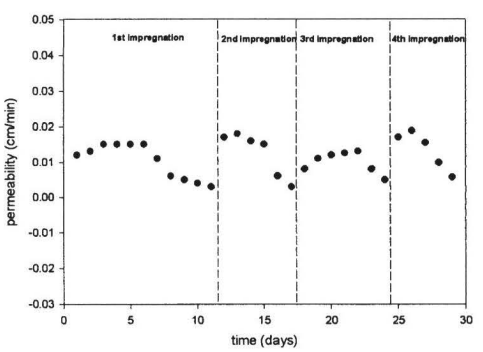

Figure 3: Stability of the liquid membrane system for consecutive impregnations applied to Rh(III) transport

The lifetime of the hydrophobic polypropylene hollow fibre was studied by using a HFSLM module in 24 hour cycles. In this case, at the end of each cycle the fibre was washed with ethanol, dried and reimpregnated with a fresh liquid membrane solution for reuse. The corresponding permeability results (Figure 4) demonstrated that it is possible to use the same fibre under these conditions for 15 cycles. After this period, the permeability of the metal through the membrane slightly decrease probably

due to the damage of the pores of the support, that leads to an increase of pore size which also implies the loss of the LM solution.

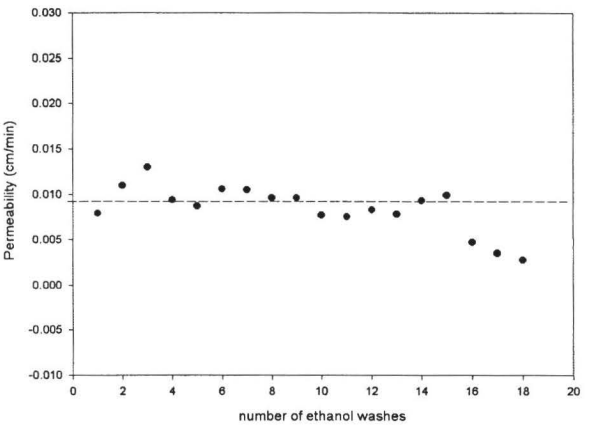

Figure 4: Lifetime of the hydrophobic polypropylene hollow fibre support

Some experiments were carried out with a different configuration of the system, i.e., operating with the feed solution on the shell-side and the stripping through the lumen, both also continuously recirculated. Under these conditions, a 10% decrease in the metal extraction from the feed solution was observed, and, therefore, the permeability value for Rh(III) transport also decreased. This result revealed the extraction as the slowest step of the system. Hence, to favour it, recirculation of the feed though the lumen of the HF where allows a better contact of the solution with the LM due to the hydrodynamic conditions in the spiral fibre.

Another possibility to operate with the described HFSLM module could be as a column system. In this way, corresponding experiments were carried out by recirculating the feed solution through the lumen of the fibre for 24 hours, while the shell-side contained a solution of 1.0 mol dm^{-3} NaCl to keep the ionic strength balanced. After this period of time, the feed solution was replaced by the stripping solution, which was also recirculated for 24 hours. The comparison between results obtained working with the HFSLM module as a column system and in the continuous mode is presented in Figure 5. It can be seen that when the HFSLM module works as a column system it is not possible to recover all the metal extracted, and therefore the efficiency of the system decreased.

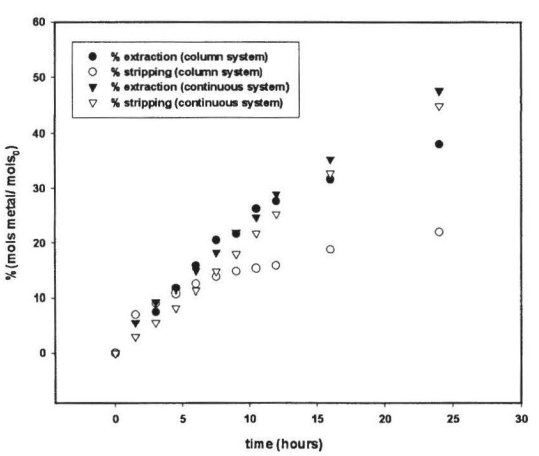

Figure 5: Comparison of two operation configurations of the HFSLM module

Taking into account these results, the flow rate of the aqueous solutions was varied to determine its influence on the rhodium transport and preconcentration. The results obtained are plotted in Figure 6 as P vs. flow rate ($cm^3\ min^{-1}$). The permeability increases with the flow rate, eventually reaching a plateau at over 0.8 $cm^3\ min^{-1}$. The initial increase in transport rate may be attributed to a corresponding decrease in the diffusion layer thickness at the membrane/source solution interface,[11] which reaches a constant minimum value at higher flow rates.

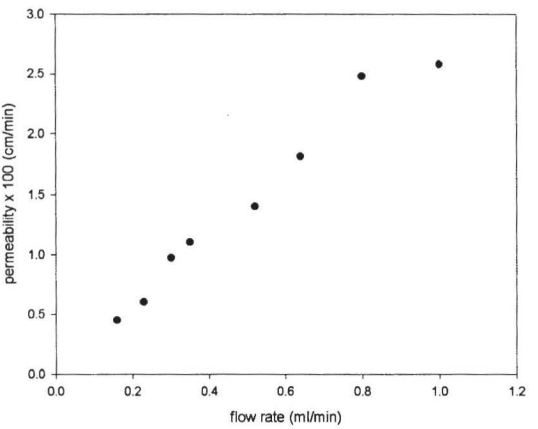

Figure 6: Influence of the flow rate of both aqueous solutions on the Rh(III) transport

ACKNOWLEDGEMENTS

The present work has been carried out under CYCIT (Spanish Commission for Research and Development) financial support, project nº QUI 96-1025-C03-03.

REFERENCES

1. Danesi PR, *Sep. Sci. and Technol.* **19**(11&12), 857, (1984-85).
2. Qi Yand Cabral JMS, *J. Chem. Tech. Biotechnol.* **65,** 137, (1996).
3. Kemperman AJB *et al. Sep. Sci. and Technol.* **31**(20), 2733, (1996).
4. Takenchi H *et al. J. Membr. Sci.* **34**, 19, (1987).
5. Danesi PR and PG Rickert PG, *Solv. Extr. Ion Exch.* **4**(1), 149, (1986).
6. Berengel E *et al. Hydrometallurgy* **40**, 135, (1996).
7. Al-Bazi SJ and Chow A, *Anal. Chem.* **53**, 1073, (1981).
8. Fontàs C *et al.*, *Anal. Chim. Acta* **346**, 199, (1997).
9. Fontàs C *et al.*, submitted to *J. of Membr. Sci.*
10. Danesi PR, *Solv. Extr. Ion Exch.* **2**(1), 115, (1984).
11. Parhasarathy N *et al. Anal. Chim. Acta* **350**,183, (1997).

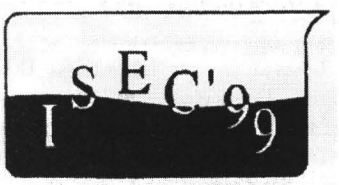

SEPARATION OF AMINE AND AMINO ACID ENANTIOMERS USING SUPPORTED LIQUID MEMBRANES WITH CHIRAL PHOSPHORIC AND PHOSPHONIC ACID ESTERS

P Wieczorek, P Dzygiel and P Kafarski
University of Opole, Institute of Chemistry, Oleska 48,
45-052 Opole, Poland

ABSTRACT
The results of the application of phosphoric and phosphonic acids esters with chiral alcohols namely nopol and menthol as carriers in supported liquid membrane (SLM) system for enantioselective transport of β-phenylethylamine (PEA) and tryptophan (Trp) enantiomers are presented. The dependence of the acceptor phase pH and the carrier concentration on the β-phenylethylamine enantiomers transport is shown. Moreover, the influence of the carrier structure on the chiral discrimination of the PEA and Trp enantiomers has been investigated.

Keywords: supported liquid membrane, amino acids, amines, β–phenylethylamine, chiral separation, phosphoric acid esters, phosphonic acids esters

INTRODUCTION

Chirality of biomolecules plays a very important role in the great number of biochemical processes, where specific and selective interactions take place. Thus, obtaining and identification of the enantiopure compounds is a very important and often difficult requirement to accomplish. To achieve this aim a group of methods known as chiral separations have been widely applied. One of those methods by which chiral separation can be performed is supported liquid membrane (SLM) technology. SLM offers some advantages[1] as a separation method but the most important feature, from chiral separation point of view, is that only minute amounts of the expensive chiral carriers is needed.

Supported liquid membranes have been used for the enantiomeric separation of amines and amino acids. For this reason such carriers as chiral crown ethers,[2-7] chiral complexes of transition metals,[8,9] carriers based on the structure of the sapphyrin ring[10] or macrocyclic peptides[11] have been used. However although these carriers turned out more or less effective chiral selectors, their further application seems to be limited due to their moderate solubility in organic solvents. This disadvantage enables their use in higher concentrations, where it might give the possibility of the simultaneous enrichment of compounds of interest.

From the other side, SLMs have been successfully applied as a sample pre-concentration technique for biomedical and environmental analysis.[1] In this case the most important effect is to obtain as high as possible enrichment of the sample. Various types of the biologically active compounds including amines and amino acids have been prepared in this way followed by analysis.[12-14] One of the possibilities for amino acids pre-treatment is using di-(2-ethylhexyl)phosphoric acid (DEHPA) as a carrier in SLM.[12] In this case the enrichment is achieved by simple adjustment of the pH of the donor and acceptor phases.[14] If the transport and chiral separation of the amine enantiomers is required simultaneously, a chiral environment must be created.

Taking into account these considerations, the possibility of the amine and amino acid enantiomers separation by employing carriers developed from phosphorus acid derivatives has been studied. The carriers were synthesised in our laboratory and applied in an SLM system for transport of β-phenylethylamine (PEA) and tryptophan (Trp) enantiomers as model compounds. In case of Trp, only the influence of the carrier structure on its enantiomers transport has been investigated as the conditions for amino acid transport through SLM with anionic carriers have been presented elsewhere.[12] For PEA the influence of acceptor phase pH and carrier concentration have been additionally examined to find the optimal condition for its transport.

© 2000 Society of Chemical Industry

EXPERIMENTAL

The carriers used for PEA and Trp transport were synthesised in our laboratory. D,L-tryptophan, (R)- and (S)-β-phenylethylamine were obtained from Sigma. Dihexylether (DHE) used as a liquid membrane phase was obtained from Aldrich. Structures of the organophosphorus esters are shown in figure 1. All water used was purified with Millipore Q system. The membrane unit used for separation experiments has been described.[12,15]

The solution of D,L-Trp hydrochloride was prepared by dissolving equimolar quantities of amino acid enantiomers mixture and HCl, yielding a total 1 mM concentration. The solutions of (R)- and (S)-β-phenylethylamine were prepared by dissolving the appropriate amount of R or S enantiomer in water yielding the required concentrations. After that the solutions were adjusted to pH = 7 and were pumped through the donor phase channel with flow rate 0.1 cm^3/min. After which, the acceptor phase (0.1 mol/dm^3 HCl) containing the amino acids was transferred with a pump into a 2cm^3 flask.

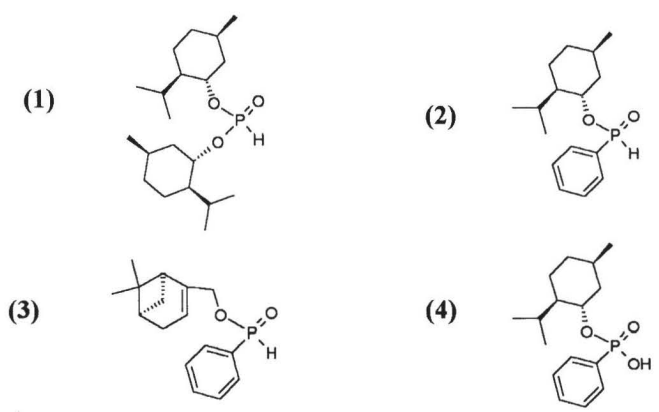

Figure 1. Carrier structures

The collected sample was analysed by capillary electrophoresis (CE) using a Beckman 2100 system with α-cyclodextrin as a chiral selector according to the procedure described elsewhere.[16] In case of the amine, analysis was performed by CE in a 0.1mol/dm^3 phosphate buffer, pH = 7 as a background buffer with application of 12.5 kV voltage and UV detection at 214 nm. The donor and acceptor channels were washed with 20 cm^3 of water before the membrane unit was used for the next experiment. The flux was calculated from the equation $J = dc/dt \times V/A$ where A is an effective membrane area and V is a volume of the collected sample. The chiral discrimination factor, α was calculated as a ratio of fluxes J_D/J_L for Trp and or J_S/J_R for PEA. Each experiment was repeated 2 - 3 times.

RESULTS AND DISCUSSION

A mechanism for the amino acid transport with a phosphoric acid diester has been described by Wieczorek at al.[12] Thus here it is only important to mention that this transport is proton-driven and the H^+ gradient is built over the membrane from acceptor (pH = 1) to donor phase (pH = 3.3). It was assumed that the amine transport mechanism is akin to that for the amino acid, if the similar conditions were applied. In figure 2 the dependence of the pH of acceptor phase on the transport of β-phenylethylamine enantiomers is presented. The pH of the acceptor phase is lowered the transport of amine increases. This confirms that the transport mechanism is the same and that the low pH in the

acceptor is required to achieve effective PEA transport. When there is no driving force present in the SLM system (high acceptor pH) transport is insignificant.

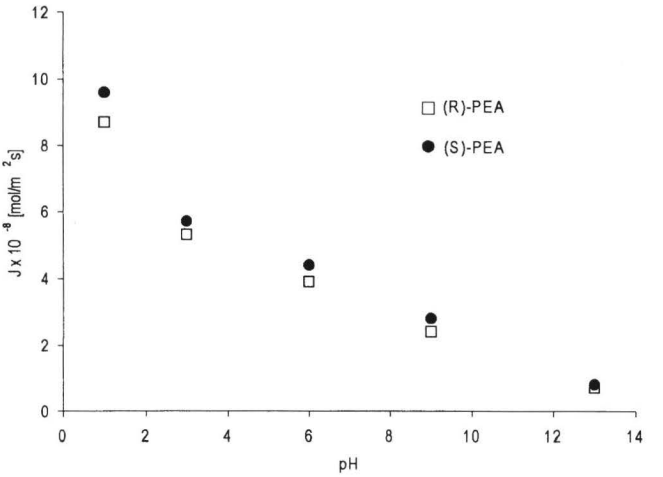

Figure 2. The influence of the acceptor phase pH on the (R)- and (S)-PEA flux J × 10^{-8} [mol/m^{2}s] and discrimination factor, α. Conditions: donor phase: 1 mM (R)- and (S)-PEA, pH = 7, flow rate = 0.1 cm^3/min; membrane phase: 150 mM carrier 2 in DHE, acceptor 0.1 mol/dm^3 HCl;

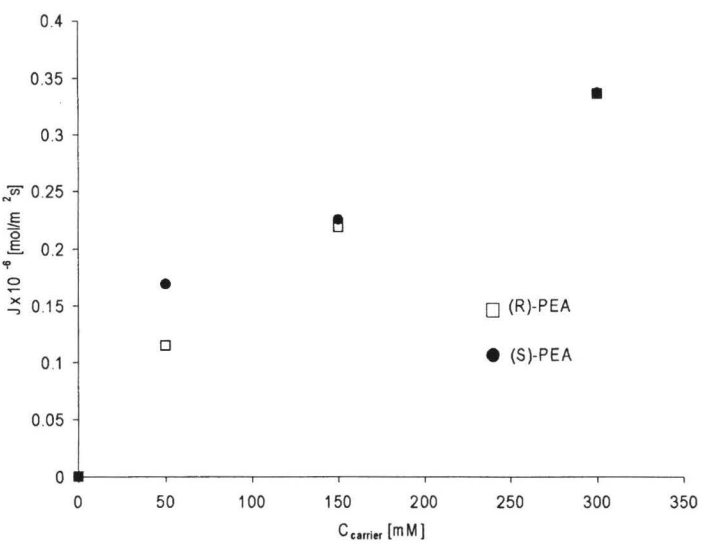

Figure 3. The influence of the carrier concentration on the (R)- and (S)-PEA flux J × 10^{-6} [mol/m^{2}s] and discrimination factor, α. Conditions: donor phase: 10 mM (R)- and (S)-PEA, pH = 7, flow rate = 0.1 cm^3/min; membrane phase: carrier 2 solutions in DHE, acceptor: 0.1 mol/dm^3 HCl;

In figure 3 the influence of the carrier concentration on the PEA enantiomers transport and discrimination factor is shown. With an increase of the carrier concentration, the possibility of the creating amine-carrier complex arises. Thus, more amine molecules can be transported, which results in an increase of the mass transfer over the liquid membrane. In turn, the PEA enantiomers fluxes

grow. It can be also seen at the figure 3 that at given conditions, the discrimination factor diminishes with the increase of carrier concentration. It might suggested that the source of enantioselctivity has a thermodynamic origin (the two diasteroisomeric complexes have different formation constants).[8]

Carrier	R-PEA	S-PEA	α
1*	0.42	0.49	1.16
2	0.36	0.37	1.01
3	0.16	0.20	1.25
4	0.16	0.19	1.19

Table 1. The influence of the type of carrier on the (R)- and (S)-PEA flux J × 10^{-6} [mol/m^{2}s] and discrimination factor, α. Conditions: donor phase: 10 mM (R)- and (S)-PEA, pH = 7, flow rate = 0.1 cm^3/min; membrane phase: 300 mM of carrier in DHE, acceptor: 0.1 mol/dm^3 HCl; (*) saturated solution

Carrier	L-Trp	D-Trp	α
1*	8.20	8.00	1.04
2	0.86	1.11	1.30
3	0.16	0.17	1.06
4	0.31	0.35	1.13

Table 2. The influence of type of carrier on the D- and L-Trp flux J × 10^{-10} [mol/m^{2}s] and discrimination factor: α. Conditions: donor phase: 1 mM D,L-TrpHCl, pH = 3.3, flow rate – 0.1 cm^3/min; membrane phase: 50 mM of carrier DHE; acceptor phase: 0.1 mol/dm^3 HCl; (*) saturated solution

In tables 1 and 2 the effect of the changes in the carrier structure on the transport of PEA and Trp enantiomers and α value is shown. Generally, it can be seen that β-phenylethylamine is transported better through the SLM due to the hydrophobic character of PEA and shows a higher affinity to organic phase. The effect of the carrier structure on the PEA and Trp enantiomers separation is insignificant. In those cases the complexes are created by ion-pair interactions between protonated amino group of PEA or Trp and negatively charged phosphate stabilised by hydrogen bonds. Thus, it might be assumed that the alcohol moieties of the diester are responsible for chiral discrimination. As can be seen from tables 1 and 2 there is little contribution of the ester part of carrier molecule to the enantiomer differentiation. It could be related to weak steric (repulsive) interactions of those substitutents with amine or amino acid molecules caused by too long a distance between them. However, the introduction of a phenyl moiety to the carrier molecule instead of one alcohol group generally increases the α value with simultaneous decrease in the magnitude of the flux. This could be attributed to the changes in the geometry of the complex . These alterations produce a decrease of the complex stability, and in turn smaller fluxes. From the other side, the interactions between the ester moiety of the carrier and PEA or Trp molecule are stronger and thus, the discrimination of enantiomers is more significant.

These preliminary studies have shown that chiral phosphate and phosphonate esters may be considered as a promising group of new carriers for chiral liquid membrane separation.

REFERENCES

1. Jönsson JÅ and Mathiasson L, *Trends Anal. Chem.*, **11,** 106, (1992).
2. Bryjak M, Wieczorek P, Kafarski P and Lejczak B, *J. Membr. Sci.*, **57**, 287, (1998).
3. Yamaguchi T, Nishimura K, Shinibo T and Sugiura M, *Bioelectrochem. and Bioenergetic*, **20**, 109, (1988).
4. Shinibo T, Yamaguchi T, Yangishita H, Sakaki K, Kitamoto D and Sugiura M, *J.Membr.Sci.*, **84**, 241, (1993).
5. Pietraszkiewicz M, Ko□bia□ M and Pietraszkiewicz O, *J. Membr. Sci.*, **138**, 109, (1998).

6. Newcomb M, Toner J, Helgenson R and Cram D, *J. Am. Chem. Soc.*, **101**, 4941, (1979).
7. Martinez-Diaz VM, de Mendoza J and Torres T, *Tetrahedron Lett.*, **35**, 7669, (1994).
8. Scrimin P, Tecilla P and Tonellato U, *Tetrahedron*, **51**, 217, (1995).
9. Tsukube H, Shinoida S, Uenishi J, Kanatami T, Itoh H, Shiode M, Iwachido T and Yonemitsu O, *Inorg. Chem.*, **37**, 1585, (1998).
10. Sessler J and Andrievsky A, *Chem. Eur. J.*, **4**, 159, (1998).
11. Miyake H, Yamashita T, Kojima Y and Tskube H, *Tetrahedron Lett.*, **42**, 7669, (1995).
12. Wieczorek P, Jönsson JÅ and Mathiasson L, *Anal. Chim. Acta*, **346**, 191, (1997).
13. Dzygiel P, Wieczorek P, Jönsson JÅ and Mathiasson L, *Anal. Lett.*, **31**, 1261, (1998).
14. Audunsson G, *Anal. Chem.*, **60**, 1340, (1988).
15. Wieczorek P, Jönsson JÅ and Mathiasson L, *Anal. Chim. Acta*, **337**, 183, (1997).
16. Dzygiel P, Wieczorek P and Jönsson JÅ, *J. Chrom. A*, **793**, 414, (1998).

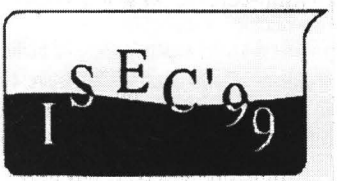

PERTRACTION AND MEMBRANE BASED EXTRACTION OF CARBOXYLIC ACIDS IN HOLLOW FIBRE CONTACTORS

Štefan Schlosser, Erika Sabolová and Ján Marták
Slovak University of Technology, Department of Chemical and Biochemical Engineering, SK-812 37 Bratislava, Slovakia

ABSTRACT
Pertraction of butyric acid (BA) and dimethyl(cyclopropane)carboxylic acid (DMCCA) through bulk liquid membranes in the hollow fibre (HF) contactors with flowing head has been studied. In both systems tertiary amines were used as carriers. The mode of operation of the HF contactors as a result of hydrodynamic conditions (membrane pulsation, feed velocity), formulation of the membrane (distribution coefficient, diffusivity), and feed composition (pH, concentration) can substantially influence performance of the contactors. The main resistance for transport of BA in HF pertractors is in the stagnant layers of the liquid membrane in the wall pores. Preliminary analysis shows that kinetics of the complex decomposition play a role in the overall resistance. The overall mass-transfer coefficient in the pertractor was about 24% higher than in the two-phase HF contactor in membrane based solvent extraction of DMCCA.

Keywords: bulk liquid membranes, hollow fibre contactors, carboxylic acids, trioctylamine

INTRODUCTION

Pertraction through liquid membranes (LM) or membrane-based solvent extraction (MBSE) of organic acids could be an alternative way of their recovery from fermentation broth or from waste solutions.[1-3] Integration of pertraction or MBSE with fermentation can enhance the fermenter performance by decreasing product inhibition.

The aim of the presented work was to study the pertraction of butyric acid (BA) and dimethyl(cyclopropane)carboxylic acid (DMCCA) through bulk liquid membranes and to compare mass-transfer characteristics of HF contactors for the pertraction and MBSE of DMCCA.

EXPERIMENTAL

Components of the membrane phase

Trioctylamine (TOA, Fluka) or Hostarex A327 (trialkylamine with C_8 and C_{10} alkyl groups, Hoechst) were used as carriers alone or with the addition of iso-decanol or iso-tridecanol (Unipar) as modifiers, in n-alkanes (dodecane fraction, Slovnaft) as diluent. Composition of the membrane phases and their characteristics are listed in table 1.

The feed solution consisted of an aqueous solution of BA with c_{F0} = 0.45 kmol.m^{-3} and pH_{F0} = 2.6 or an aqueous solution of DMCCA with c_{F0} = 0.12 kmol.m^{-3} and pH_{F0} = 2.1 if not otherwise stated. The pH of the solutions was in some measurements adjusted by the addition of NH_4OH or H_2SO_4 solutions.

An aqueous solution of NaOH with a concentration of 1.5 kmol.m^{-3} was used for stripping. The experiments were conducted at temperatures of 30°C and 25°C for experiments with BA and DMCCA, respectively.

Analytical Procedure

The concentrations of BA and DMCCA in the aqueous phases were determined with the isotachophoretic analyser EA 100 (Villa, SK). The concentration of acids in the solvent phase was determined after stripping acids with aqueous solution of NaOH.

© 2000 Society of Chemical Industry

Contactors

Two types of three-phase HF contactors of own construction, with distributed bundles of hollow fibres and a flowing head, were used for the pertraction.[4] Both pertractors PV10 and PV20 have two bundles of hollow fibres, one for the feed and the second one for the stripping solution, with the bulk liquid membrane between them (outside the fibres) and the liquid membrane in their pores. Microporous polypropylene hollow fibres were used in both bundles. Basic characteristics of the pertractors and fibres are presented in table 2 and the diagram of the contactor PV20 is shown in figure 1. More details are presented elsewhere.[4-6] The membrane was pulsed by a piston pulsator with an adjustable frequency and amplitude.

The flowsheet of the two-phase HF contactors used in MBSE experiments is shown in figure 2 and described elsewhere in more detail.[7] LiquiCel Extra Flow 2.5 x 8″ contactors (Celgard, USA) with 10000 fibres 15 cm in length and cross flow of phases were used. The feed in MBSE and the solvent in stripping flowed in the fibre lumen.

Kinetics of transport through well mixed layered liquid membranes have been studied in a double Lewis cell described in papers.[7,8]

Membrane phase or solvent	D_r		$\mu^{25}.10^3$	$\mu^{30}.10^3$	$D.10^{10}$, $m^2.s^{-1}$ for $(HA)_2$ or $(HA)_2P$	
	BA^+	$DMCCA^b$	Pa.s	Pa.s	BA	DMCCA
M1: n-alkanes	0.56	8[c]	1.285	1.183	10.23[a]	8.58[b]
M2: 0.4 M TOA in n-alkanes	3.40	26.72	1.665	1.523	3.81[a]	3.30[b]
M3: 0.4 M Hostarex A327 and 1.2 M isotridecanol in n-alkanes	3.26			3.125	1.88[a]	
M4: 0.4 M Hostarex A327 and 1.5M (30 wt.%) isodecanol in n-alkanes		31.92	3.411			1.72[b]

[a] 30°C [b] 25°C [c] at $c_F = 0.08$ kmol.m^{-3} [+] at 30°C and $c_F = 0.5$ kmol.m^{-3}

Table 1 Dynamic viscosity of the membrane phases, distribution coefficient of acids (D_r) and diffusion coefficient (D) of acid dimers $(HA)_2$ and their complexes with carrier P in the membrane phases or solvents

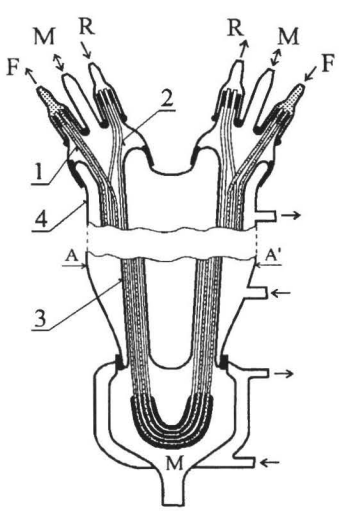

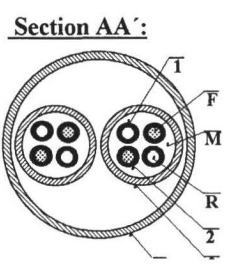

Fig.1. Scheme of the hollow fibre pertractor PV20 with two mixed bundles of fibres with flowing bottom head [4].
F - feed, M - bulk liquid membrane, R - stripping solution,
1 - microporous HF for the feed, 2 - HF for the stripping solution, 3 - glass tube, 4 - glass tempering jacket.

	PV10	PV20
Number of HF in the feed bundle	20	22
Number of HF in the stripping solution bundle	20	22
Effective length of fibres (wetted with M), cm	49.2	51.2
Effective pore size of the fibre wall (data of supplier), μm	0.03	
Porosity of the fibre wall[+], %	30	
Inner and outer diameter of HF, mm	0.20, and 0.264	

Table 2 Basic parameters of the contactors PV10 and PV20 with hollow fibres Celgard X-10 (Celgard, USA)

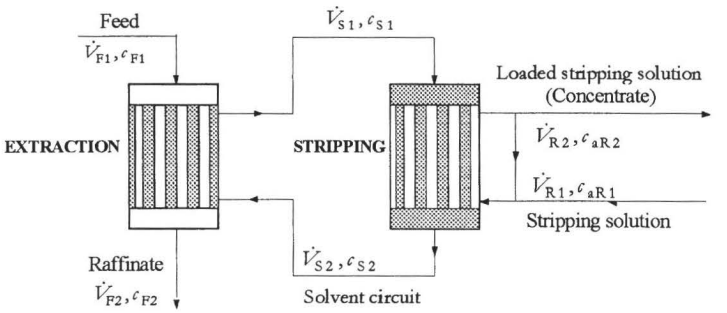

Figure 2. Flowsheet of the MBSE combined with regeneration of the solvent by stripping, both in HF contactor.

RESULTS AND DISCUSSION

Axial pulsation of the membrane phase in hollow fibre pertractor increases the transport rate by 60 to 22% and approaches a plateau value at the pulsation velocity (product of the pulsation frequency and amplitude) of about 6 mm.s^{-1}. [6,8] With increasing axial velocity of the feed in the fibre lumen the mass-transfer coefficient increases and approaches a steady value at a relatively low velocity of about 5 cm.s^{-1}, as can be seen in figure 3.

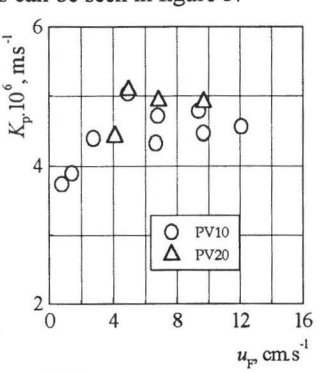

a) BA

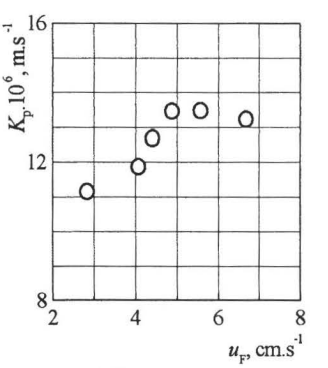

b) DMCCA

Figure 3. Influence of the linear velocity of the feed in the fibre lumen on the overall mass-transfer coefficient in pertraction of BA and DMCCA in the contactor PV10 or PV20. u_R = 1.04 cm.s^{-1}, Membrane: M2

The introduction of carrier and modifier into the membrane increases the distribution coefficient for acids as shown in table 1 and figure 5. This is not accordingly reflected in a proportionally higher mass-transfer coefficient, as is evident from figure 4. In the first approximation, the permeability of the bulk liquid membrane is a product of the distribution coefficient and the diffusivity of the acid dimer or of the acid complex. For membranes with a carrier the mass-transfer coefficient at medium concentrations is more or less independent of concentration. For pure n-alkanes the K_p concentration is dependent reflecting the dependence of D_r on concentration, as follows from comparison of figure 4 and 5. In formulation of the membrane phase for biotechnological applications also toxicity of the solvent for biomass has to be considered.[9]

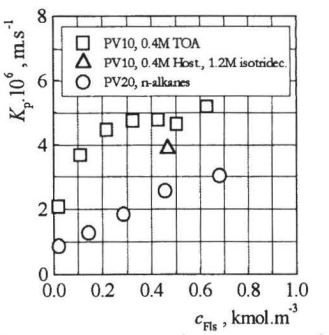

a) BA, u_F=4.8 cm.s^{-1}, u_R =1 cm.s^{-1}

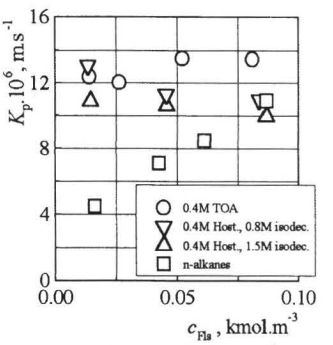

b) DMCCA, PV20, u_F=5.6 cm.s^{-1}, u_R =0.8 cm.s^{-1}

Figure 4. The overall mass-transfer coefficient in pertraction of BA and DMCCA in the HF contactors, vs. mean concentration of acid in the feed.

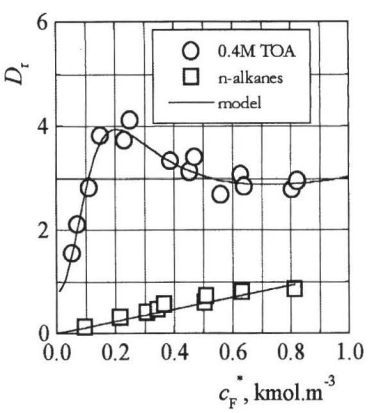

a) BA at 30°C

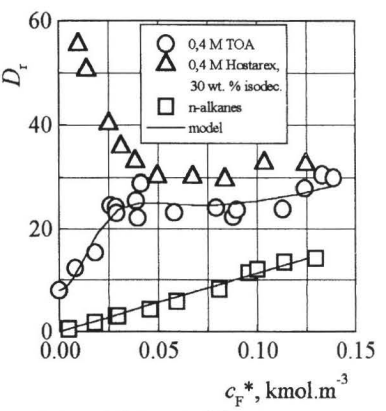

b) DMCCA at 25°C

Figure 5. Extraction equilibria for acids. Lines are calculated according to the model.

The analysis of individual resistances in pertraction, based on the diffusional model and presented in papers,[5,6,10] suggests that the main resistance for transport of BA is in the stagnant layers of the liquid membrane in the wall pores, figure 6. The resistances of LM in the wall and in the bulk liquid membrane outside the pores in pertraction of DMCCA are comparable.[8] The overall resistance of the membrane for DMCCA is much lower than for BA because of higher distribution coefficient of the C_6 acid, as shown in figure 6.

Increasing the pH of the feed with BA decreases the value of the mass-transfer coefficient and above pH 4 this decrease is sharp.[5,6] Acidification of the feed with mineral acids below pH = 2.6 decreases the BA flux due to their competitive transport. Sulphuric and hydrochloric acids decrease the

BA flux by 8 and 36 %, respectively.[11] The values of the mass-transfer coefficient in pertraction of BA and DMCCA in the contactor PV20 using membrane phase M2 are about $4.5.10^{-6}$ m.s^{-1} and $13.5.10^{-6}$ m.s^{-1}, respectively, which are promising values.

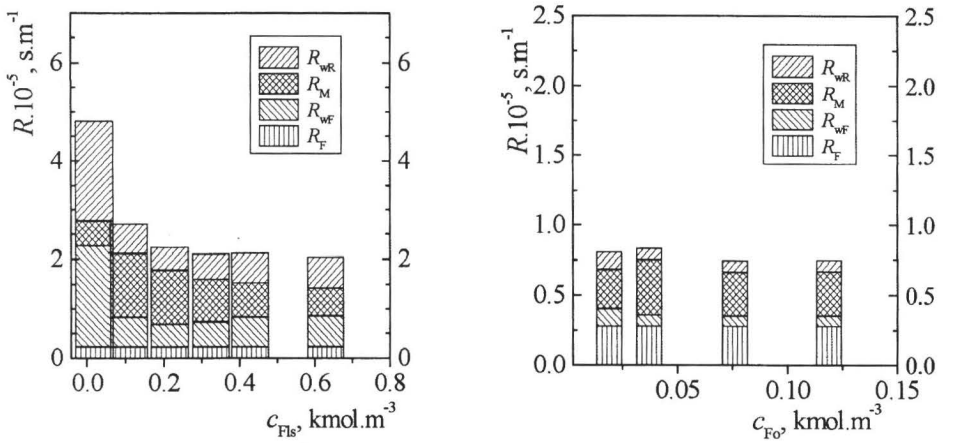

a) BA, PV10,; u_F=6.8 cm.s^{-1} b) DMCCA PV20, u_F=5.6 cm.s^{-1}

Figure 6. Analysis of the mass-transfer resistances in individual layers of the HF contactors in pertraction of acids for different initial concentrations of acid in the feed. Membrane: M2

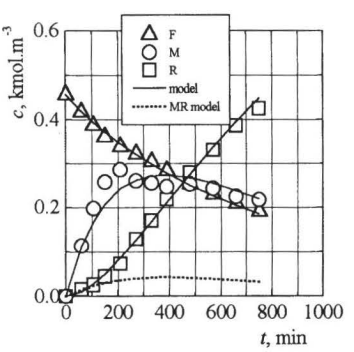

Figure 7. Time dependency of concentrations in three phases of a two-compartment cell in pertraction of BA through the layered liquid membrane.

Full lines are calculated according to the model taking into account the stripping reaction kinetics.

Dotted line - concentration of BA in the membrane at stripping interface, c_{MR}, calculated from the model.

Membrane: M2

The proposed diffusional mass-transfer model of pertraction through the well mixed LM in a two cell contactor describes experimental data well.[11,12] Preliminary analysis of the transport data for BA with this model extended by the equation for reaction kinetics and distribution coefficient variation suggests that diffusional resistances are dominant but also slower kinetics of complex decomposition on the strip interface play a role, figure 7. This is manifested by a non-zero value of acid concentration in the membrane at the stripping interface. The resistance connected with slower kinetics of the stripping reaction contributes about 40% to the overall resistance. In this case it is proved that a new analysis of resistances in the HF contactors is required, but no great changes are assumed because the diffusional resistance of the LM in the wall (not present in the layered LM) is mostly dominant.

The value of the overall mass-transfer coefficient in MBSE of DMCCA with the solvent M4 is about $8.5.10^{-6}$ m.s^{-1} which is one order of magnitude greater than in the membrane based stripping from the loaded solvent into an alkaline solution in the same contactor where the value $0.8.10^{-6}$ m.s^{-1} was found, figure 8.

The mass-transfer rate in pertraction of DMCCA in the HF contactor PV20 with the membrane M4, integrating extraction and stripping in one equipment, was found to be 24% higher than in MBSE (not optimised conditions) in the HF contactor with cross flow of phases.

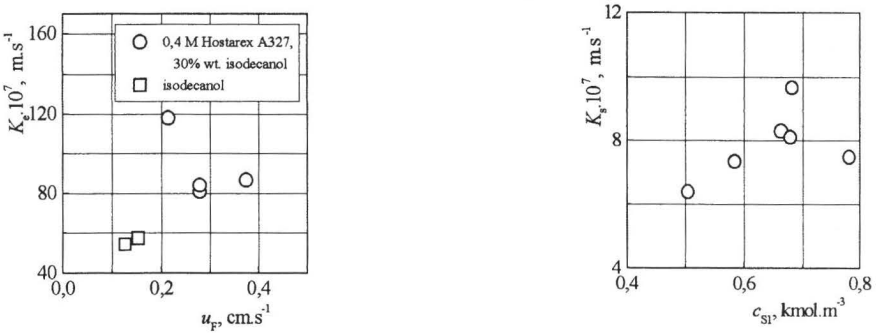

Figure 8. Overall mass-transfer coefficient in extraction and stripping of DMCCA in the HF contactors Extra Flow 2.5 x 8'' vs. linear velocity of the feed in the fibre lumen and vs. concentration of DMCCA in the loaded solvent entering the stripper. Solvent: M4.

ACKNOWLEDGEMENT

Support of the Slovak grant agency VEGA for grants No.4215/97 and No.1/6154/99 is acknowledged.

REFERENCES

1 Majumdar S and Sirkar KK. In: Ho WSW and Sirkar KK. (Ed.), *Membrane Handbook*, Van Nostrand Reinhold, 764, (1992).
2 Prasad R and Sirkar KK. In: Ho WSW and Sirkar KK. (Ed.), *Membrane Handbook*, Van Nostrand Reinhold, 727, (1992).
3 Schlosser S., In: *Proc. 13th Int. Congress CHISA 98*, Praha, 9 (Aug. 1998).
4 Schlosser S and Sabolová E. *J. Membrane Sci.*, submitted for publication (1998) .
5 Sabolová E and Schlosser S. In: as ref [3], p 12.
6 Sabolová E and Schlosser S. *J. Membrane Sci.*, submitted for publication (1998) .
7 Schlosser S and Marták J. In: *Proc. 24th Conf. SSCHI, Castá - Papiernicka (SK),* 447, (1997) (in Slovak).
8 Schlosser S, Sabolová E and Marták J. In: *Proc. 25th Conf. SSCHI*, Jasná, 9, (May. 1998) (in Slovak).
9 Marták J, Sabolová E, Schlosser S et al. *Biotechnol. Techn.*, **11**, 71, (1997).
10 Schlosser S, Rothova I and Frianova H. *J. Membrane Sci.*, **80**, 99, (1993).
11 Sabolová E, Schlosser S and Stopka J. In: *Proc. 24th Conf. SSCHI,* Castá - Papiernièka, p. 147, (June, 1997) (in Slovak).
12 Cichy W, Schlosser S and Szymanowski J. this proceedings.

NOTATION

c molar concentration , kmol.m^{-3}
D diffusion coefficient, m^2·s^{-1}
D_r distribution coefficient, -
K overall mass-transfer coefficient, m.s^{-1}
R mass-transfer resistance, s.m^{-1}
u linear velocity, m.s^{-1}
μ dynamic viscosity, m^2·s^{-1}

Indices: F feed phase
M membrane phase
e extraction
o initial value
p pertraction
s stripping
R stripping solution
* equilibrium value

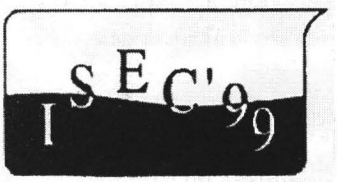

TRANSPORT PROPERTIES OF ACTIVATED COMPOSITE MEMBRANES CONTAINING DI-(2-ETHYLHEXYL)DITHIOPHOSPHORIC ACID AS A CARRIER TOWARDS POLYVALENT METAL IONS

Maria Oleinikova, Jordi Macanas, Maria Muñoz and Manuel Valiente

Unidad de Química Analítica, Universidad Autonoma de Barcelona, E-08193 Bellaterra Barcelona, Spain

ABSTRACT

The paper reports the results on the further development of activated composite membranes (ACM) containing di-(2-ethylhexyl)dithiophosphoric acid (DTPA) as a carrier. The ACM membranes prepared by means of interfacial polymerisation technique demonstrate sufficiently stable transport properties within several weeks of their use, while the corresponding supported liquid membrane (SLM) show no metal ions transport under identical conditions after one day working experiment. The selectivity of DTPA based ACM towards different metal ions is presented and discussed. Such selectivity is based on the dominating role of both equilibrium (complex stability) and non-equilibrium (stripping kinetics) factors.

Keywords: activated composite membranes, di(2-ethylhexyl)dithiophosphoric acid, aluminium, calcium, copper, indium, magnesium, manganese, tin, zinc

INTRODUCTION

Application of extraction techniques for removal and recovery of heavy metals is of immensely growing importance from the viewpoint of environmental protection problems.[1] Supported liquid membranes (SLM) have attracted much interest for separation and concentration of toxic and/or valuable solutes due to the possibility to combine the extraction and stripping processes in one step and because of their high interfacial area.[2] The SLM's have important advantages such as a high selectivity and diffusion rate as compared with solid membranes. At the same time, their main drawback is the lack of stability, which is caused by different factors including the leakage of the organic extractant from the pores of support, the formation of emulsions in these pores, and the loss of the organic solvent.[3-5]

Different approaches have been suggested to stabilize SLM's such as, for example, gel formation in pores of the support.[6] Thus, Neplenbroek et al.[7] reported the use of SLM systems consisting of a poly(vinyl chloride) gelled membrane containing quaternary ammonium salts as carriers for removal of nitrate ions from water. Recently, Kemperman et al.[8] investigated and optimized the application of a thin polyamide layer covering the impregnated support, which partially avoided the loss of the carrier reagent from the membrane phase. In the previous communication of this series we have shown and characterized a set of new Activated Composite Membrane (ACM) suggested as an alternative to Supported Liquid Membrane (SLM).[9]

To extract polyvalent metals from hydrometallurgical effluents, an extractant should posses an extremely high selectivity for the formation of complexes with these metals. For this purpose a number of dialkyldithiophosphoric acids were tested[10] including di-(2-ethylhexyl)dithiophosphoric acid (DTPA), which demonstrates high chemical stability and in the majority of instances does not form any stable emulsion.[11,12] It has been shown that DTPA is a highly selective extractant for a number of metals.[10] Nevertheless, the information about the use of DTPA as a carrier in SLM or ACM is still very limited.

In the present study several ACM systems containing DTPA and their transport properties towards polyvalent metal ions are described. The mechanisms of: 1) interaction of DTPA with different metal ions, and 2) interference of different metal ions in the course of their transport through the membrane phase are proposed and discussed.

© 2000 Society of Chemical Industry

EXPERIMENTAL

Materials and membranes

Di-(2-ethylhexyl)dithiophosphoric acid (DTPA) was synthesized and purified by following the procedures described elsewhere.[13] Solutions of DTPA in hexane (95%, Aldrich, Germany) with concentration from 0.2 to 1.0 mol/dm^3 were used to prepare ACM samples with different carrier content. The other chemicals were all of analytical reagent grade and were used as received. Doubly distilled water was used for preparation of metal containing feed and HCl stripping solutions.

The preparation of ACM containing DTPA as a carrier was carried out by using the procedure recently published elsewhere.[9] Porous thin polysulfone film (PS) (Udel P-3500, Union Carbide) obtained by the phase inversion technique on the surface of a non-woven fabric (3329 Holytex, France) was used as a solid support for ACM. Thin top layers of polyamide containing DTPA of different concentrations (from 200 to 1000 mM) were prepared by interfacial polymerization, thus, an aqueous amine solution (1,3-phenylenediamine 99%) (Merck, Germany) was mixed with water immiscible organic solution (hexane solutions of DTPA). The excess of solution was carefully washed off the surface of the membrane. Finally, the membranes, thus prepared were dried in an oven at 60°C for 10 minutes.

Procedure

The measurements of ion transport were carried out at 20°C ± 0.2 in an air-conditioned room using a two compartments membrane cell of 200 cm^3 each (V_c),[14] the ACM was placed on the circular window separating the two compartments. The membrane working area, S_m, was 12 cm^2. The feed and stripping solutions were placed in each compartment of the cell and vigorously agitated by mechanical stirrers. The pH values in the feed solution were monitored by using a Crison pH meter 507 (Barcelona, Spain) supplied with a combined glass electrode. The stripping phase consisted of 2.2 mol/dm^3 HCl in all experiments carried out. NaCl solution was added to the stock (feed) solution of a mixture of metal ions to equilibrate the ionic strength with that of stripping solution. The concentration of metal ions in both feed and stripping solutions was determined periodically on samples withdrawn from the cell by atomic emission spectrometry (ICP-AES technique) using an ARL Model 3410 spectrometer (Fisons, Beverly, MA) provided with Minitorch. An average uncertainty of metal ions determination was in all cases < 1.5%. The results of the analysis were used for plotting the extraction- and re-extraction-time histories (for the feed and stripping phases, respectively). The stability of ACM was evaluated by carrying out several sequential metal ion transport cycles with the same membrane sample. The efficiency of ion transfer through the membrane was evaluated by determining the permeability values from the slope of respective metal concentration in stripping solution versus time curve. The rate of ion transfer through the membrane (J, mol/cm^2·sec) was evaluated from the initial slope of the concentration vs time plot. The rate can be calculated by using a linear regression technique:

$$J = (V_c / S_m) dc/dt \qquad (1)$$

RESULTS AND DISCUSSION

The experimental data on metal transport were expressed in terms of the degrees their extraction and stripping (%) versus contact time in order to follow up the shape of the metal permeation curves under different experimental conditions.

Monocomponent systems

The typical extraction-re-extraction-time histories obtained in experiments with different metal ions are shown in figures 1, 2 and 3. The concentration of metal ions in the feed solution (Zn^{2+}, $Cu^{2+}$and Cd^{2+}) was constant and equalled 0.75 mM. The results presented in figures 1-3 were obtained by using ACM samples prepared with 500 mM DTPA casting solutions. As seen in figure 1, the

maximum rate of metal transport is observed for zinc, which concentration in the stripping solution increases up to 30 % of the initial concentration in the feed phase after 2 hours. The transfer rates for $Cu^{2+}$and Cd^{2+} measured under the same conditions appeared to be far lower (figures 2 and 3, respectively). The results presented in figures 1, 2 and 3 can be interpreted in terms of the selectivity parameters of DTPA towards metal ions under consideration. The extraction sequence of DTPA for polyvalent metal ions[11, 15] can be written as follows:

$$Ag > Cu > In > Pb > Fe(III) > Cd > Sn > Ni \cong Zn >> Ca \qquad (2)$$

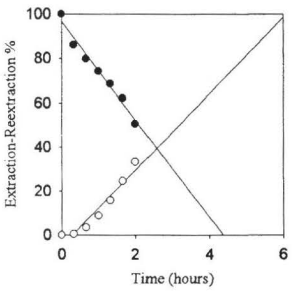

Figure 1. Extraction-reextraction time histories for Zn^{2+} obtained ACM containing 0.5 M DTPA

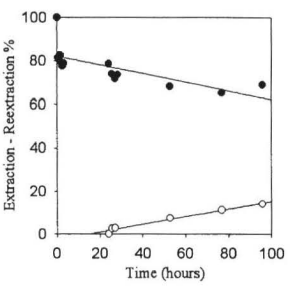

Figure 2. Extraction-reextraction time histories for Cu^{2+}obtained using ACM containing 0.5 M DTPA

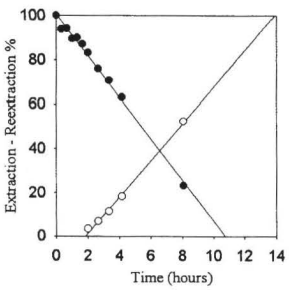

Figure 3. Extraction reextraction time histories for Cd^{2+} obtained using using ACM containing 0.5 M DTPA

The extraction constants, K_{ex}, of DTPA for Cu^{2+}, Cd^{2+} and Zn^{2+} reported by Levin et. al.[11] were determined by using following equation:

$$M^{n+}_{aq} + n(HR)_{org} = (MR_n)_{org} + nH^{+}_{aq} \qquad (3)$$

and equal log K_{ex} = 12.3, 7.01 and 2.25, respectively. As follows from the qualitative comparison of extraction constant values with the results shown in figures 1-3, the lower the K_{ex} value the higher is the rate of metal transfer through the ACM. To quantify this conclusion, the Cu^{2+}, Cd^{2+} and Zn^{2+} ion fluxes through ACM (calculated by using equation 1) are collected in table 1 along with respective extraction constant values. As seen in table 1, a direct proportionality between respective K_{ex} values and metal fluxes is observed for all metal ions studied in the first series of experiments.

Metal ion	Log K_{ex}	J, mol/cm^2·s
Zn^{2+}	2.25	5.12 e-10
Sn^{2+}	5.45	3.55 e-10
Cd^{2+}	7.01	2.07 e-10
In^{3+}	10.22	6.74 e-11
Cu^{2+}	12.31	1.53 e-11

Table 1. Extraction constants and metal ion fluxes through ACM

This result indicates that under given experimental conditions the formation of DTPA complex in the ACM phase can be suggested as the rate-determining step of the metal transfer process. To confirm this hypothesis it was decided to evaluate the rate of transfer of other metal ions through ACM containing DTPA. The second series of experiments was carried out with In^{3+} and Sn^{2+}, whose extraction constants with DTPA have been reported to equal logK_{ex} = 10.22 and 5.45, respectively.[11] The flux values calculated for In^{3+} and Sn^{2+} from the respective experimental data on transport of these metal ions through the ACM are also given in table 1. As seen, the direct proportionality between flux

and extraction constant values is observed for metal ions studied in the second series of experiments. This testifies to the validity of the above hypothesis.

Selective transport of Zn^{2+} versus Al^{3+}, Ca^{2+}, Mg^{2+} and Mn^{2+}.

The experiments on separation of Zn^{2+} from non-extractable by DTPA[10, 12] metal ions like Al^{3+}, Ca^{2+}, Mg^{2+} and Mn^{2+} using DTPA-ACM were carried out on membrane sample prepared with 500 mM DTPA casting solution. The concentration of each metal ion in the mixture in the feed was 1 mM (in presence of 2.2 mol/dm^3 NaCl at pH = 2.0). One of the typical extraction-re-extraction-time histories obtained in this series of experiments is shown in figure 4. As seen, highly selective transport of Zn^{2+} is observed within the whole experiment (3 hours) that allows for recovering high purity (~100%) zinc from the stripping solution. The efficiency of separation process can be easily improved by using more effective membrane unit, such as, for example, hollow fibre modulus.

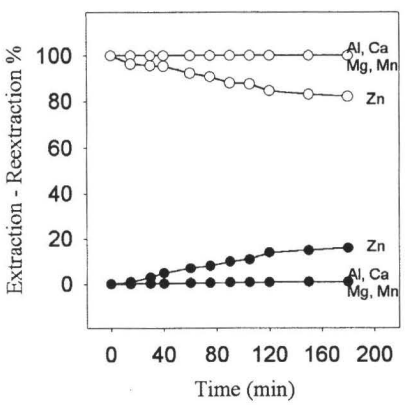

Figure 4. Extraction-reextraction time histories for Zn^{2+}, Al^{3+}, Ca^{2+}, Mg^{2+}, Mn^{2+} mixture obtained

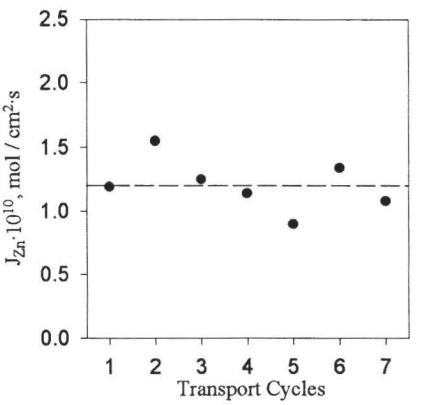

Figure 5. Zinc flux as a function of cycle number for ACM containing 0.5 M DTPA

Membrane stability

Finally, figure 5 shows the results on the experimental evaluation of the stability of ACM sample used in this study. The results shown here were obtained with 7 sequential experiments on Zn^+ transport from feed solution containing 1 mM of Zn^{2+} through the ACM sample prepared with 500 mM DTPA casting solution. As seen, the flux through the ACM under study remains practically constant within all transport cycles carried out that testifies to the high stability of DTPA-ACM and indicates their applicability in the long-term separation experiments.

ACNOWLEDGEMENT

This work was supported by the Spanish Commission for Science and Technology (CICYT), project number: MAT97-0970-C03). MO is a recipient of a fellowship from the Catalan Commission for Research and Technology (CIRIT).

REFERENCES

1. Ferguson JE, *The Heavy Elements. Chemistry, Environmental Impact and Health Effects*. Pergamon, New York (1990).
2. Danesi PR, *Sep. Sci. Technol.*, **19**, 857, (1984/1985).
3. Danesi PR, Reichley-Yinger L and Rickert PG, *J. Membrane Sci.*, **31**, 117, (1987).

4. Neplenbroek AM, Bargeman D and Smolders CA, *J. Membrane Sci.*, **67**, 121, (1992).
5. Neplenbroek AM, Bargeman D and Smolders CA, *J. Membrane Sci.*, **67**, 133, (1992).
6. Bromberg L, Levin G, Libman J and Shanzer A, *J. Membrane Sci.*, **69**, 143, (1992).
7. Neplenbroek AM, Bargeman D and Smolders CA, *J. Membrane Sci.*, **67**, 149, (1992).
8. Kemperman AJB, Rolevink HHM, Bargeman D, Van den Boomgaard T and Strathmann H, *J. Membrane Sci.*, **138**, 43, (1998).
9. Benavente J, Oleinikova M, Muñoz M and Valiente M, *J. Electroanal. Chem.*, **451**, 173, (1998).
10. Alimarin IP, Rodionova TV and Ivanov VM, *Russ. Chem. Rev.*, **58**, 863, (1989).
11. Levin IS et al., in: *Proc. Int. Sol Ext Conf., ISEC'74,* Jeffrens GV (Ed.), SCI London, **3**, 2137, (1974)
12. Levin IS, Sergeeva VV, Tarasova VA, Varentsova VN, Rodina TF, Vorsina IA, Kozlova NE and Kogan BI, *Zh. Neorg. Khim.*, **18**, 1643, (1973).
13. Bromberg L, Lewin I, Gottlieb H and Warshawsky A, *Inorg. Chim. Acta,* **197**, 95, (1992).
14. Palet C, Muñoz M, Daunert S, Bachas L and Valiente M, *Anal. Chem.*, **65**, 1533, (1993).
15. Levin IS and Sergeeva VV, *Izv. Sib. Otd. Acad. Nauk SSSR, Ser. Khim. Nauk*, **3**, 53, (1974).

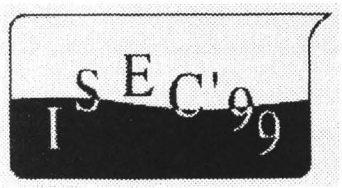

THE USE OF A PVC-BASED ALIQUAT 336 MEMBRANE TO EXTRACT Cd(II) AND Cu(II) FROM CHLORIDE SOLUTIONS

Lijuan Wang[1], Rohani Paimin[1], Robert W Cattrall[2] and Spas D Kolev[2]

[1]Chemical Sciences, School of Life Sciences and Technology, Victoria University of Technology, P.O. Box 14428, MCMC, Melbourne, 8001, Australia

[2]Centre for Scientific Instrumentation, La Trobe University, Bundoora, Melbourne, 3083, Australia

ABSTRACT

Aliquat336 ($R_3CH_3N^+Cl^-$) extracting agent has been used to prepare PVC-based Polymer Membranes (PLMs). These membranes were used in the extraction of Cd(II) and Cu(II) from hydrochloric acid solutions. The membrane showed a higher extraction capacity for Cd(II) than for Cu(II). The extraction of Cd(II) was found to be greater for thicker membranes and for membranes of higher Aliquat336 content. The diffusion coefficients, D_B, for the Cd(II) complex ($R_3CH_3N^+CdCl_3^-$) for 30%, 40% and 50% (m/m) Aliquat336/PVC compositions, were 0.8×10^{-13}, 4.0×10^{-13}, and 8.0×10^{-13} m^2s^{-1} respectively. Due to the extremely small extraction of Cu(II), the diffusion coefficient of the corresponding complex could not be reliably calculated.

Keywords: Aliquat 336, polymer inclusion membrane, copper, cadmium

INTRODUCTION

Liquid membrane separation techniques have become increasingly important in the separation of metals. Liquid membrane systems consist of a liquid barrier between a feed and a strip phase. The main types of liquid membrane systems are; bulk liquid membranes (BLM), emulsion liquid membranes (ELM), supported liquid membranes (SLM), gelled supported liquid membranes (GSLM), and polymer liquid membranes (PLM).

The work reported here made use of the PLM. These membranes are self-supporting membranes containing a commercial extractant, Aliquat 336, immobilised in a polymer matrix, poly(vinyl chloride) (PVC). This type of membrane has been used successfully in the extraction of gold (III) from hydrochloric acid solutions in the presence of a 500-fold higher concentration of copper (II).[1] It has also been shown previously that the rate of loss of the liquid membrane phase components from the PLM was minimal and the membrane exhibited sufficient mechanical strength to enable it to be self-supporting.[1] A PLM extraction system is a 'solvent-less' extraction system, thus giving it an added advantage as disposal of any solvent is eliminated. The membranes also require a small amount of the extractant or reagent, thus, are economically sound.

In this work PVC/Aliquat336 membranes were used to extract Cd(II) and Cu(II) from hydrochloric acid solutions. The extraction capacity of the membrane towards these metals was studied. The effects of extractant compositions in the membrane and membrane thickness were also investigated.

EXPERIMENTAL

Reagents

Aliquat 336 (Fluka), $R_3MeN^+Cl^-$, was obtained as a mixture of quaternary ammonium chlorides and was used as received. High molecular weight poly(vinyl chloride) (Fluka, Selectophore) was used for membrane preparation. Tetrahydrofuran (THF), HPLC grade from BDH, was further purified by passing through an activated alumina column to remove stabilisers and peroxides before use. Hydrochloric acid (HCl), cadmium chloride ($CdCl_2.H_2O$) and cupric chloride ($CuCl_2.2H_2O$) were analytical reagents from BDH. Cd(II) solutions of various concentrations were prepared in 2.0 mol/dm^3

© 2000 Society of Chemical Industry

HCl and Cu(II) solutions of various concentrations were prepared in 3.0 mol/dm^3 HCl. Cd(II) and Cu(II) standard solutions for atomic absorption spectrometry measurements were prepared from 1000 mg/dm^3 spectroscopic standards (BDH Spectrosol).

Membrane Preparation

The membranes used in this study were prepared by dissolving a mixture of known amounts of Aliquat 336 and PVC in 5 - 10 cm^3 of THF. The homogeneous solution obtained was then poured into a glass ring on a flat glass plate. The THF was allowed to evaporate slowly over 12 hours to yield a colourless, flexible, transparent and mechanically strong membrane. The composition of the membrane was expressed in mass percentage of Aliquat 336 in the membrane (%m/m). The membrane was then removed from the glass plate and used for the membrane extraction study. Membranes containing 30%, 40% and 50% Aliquat 336/PVC (m/m) were prepared. Membranes of Aliquat 336 content higher than 50% were soft and sticky and mechanically too weak to be used for the extraction experiments.[1]

Measurement of Membrane Thickness

The measurement of the membrane thickness was carried out using a microscope (ISSCO SZM-4). The membrane was cut as a square piece (54 mm^2) and then vertically mounted on a glass slide for the microscope measurement.

Membrane Extraction Procedure

Membrane extraction studies were carried out in a two-compartment[1] cell that was thermostatted at 25^{0}C in a water bath. Each compartment had a volume capacity of 60 cm^3. The membrane was sandwiched between the two compartments. The stirring rate of each compartment was kept constant throughout the experiment. An aqueous solution of the same composition was placed in each compartment for the Cd(II) and Cu(II) extraction studies. The extraction of the metal was monitored by taking 1 cm^3 aliquots from each compartment at regular time intervals and the metal concentration was analysed by AAS using a GBC Model 902 spectrometer. The solution removed was replaced with an equal volume of fresh metal solution.

RESULTS AND DISCUSSION

The Effect of Membrane Compositions on the Extraction of Cd(II) and Cu(II)

The results for the extraction of Cd(II) and Cu(II) using membranes of various compositions are shown in figures 1 and 2 respectively. The extraction of the metals was followed by monitoring the decrease of the averaged metal concentration in both compartments of the cell.

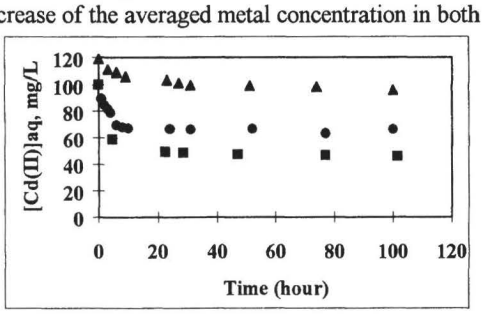

Figure 1. Aqueous Cd(II) concentration vs. extraction time for various membrane compositions ((▲) 30, (●) 40, (■) 50% Aliquat 336/PVCmembranes).

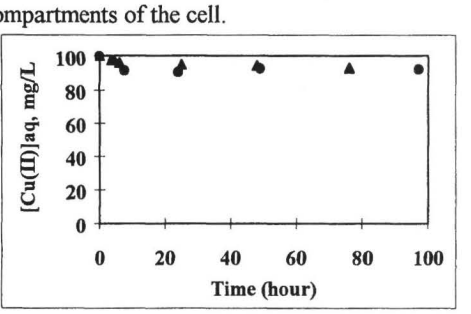

Figure 2. Aqueous Cu(II) concentration vs. extraction time for various membrane compositions ((▲) 30, (●) 40% Aliquat 336/PVC membranes).

In the extraction of Cd(II) (figure 1), for all the membranes used, it was found that the higher the concentration of Aliquat 336 in the membrane, the better was the extraction. In the case of the 50% Aliquat 336/PVC membrane, more than 50% of the metal was extracted by the membrane after 20 hours of contact.

A decrease in the concentration of Cu(II) with time was also observed for the Cu(II) extraction system, although the decrease was extremely small. Figure 2 shows that only about 10% of Cu(II) was extracted into the membrane after 20 hours of contact time. It was also found that the extraction capacity of the membrane for the Cu(II) metal was independent of the Aliquat 336/PVC composition. This is shown by a similar extent of extraction for both 30% and 40% Aliquat 336/PVC membranes (figure 2).

The effect of membrane thickness

Membranes of the same chemical composition but different in the thickness were studied for the extraction of Cd(II) system. Figure 3 shows the greater decrease of the Cd(II) concentration for the thicker membrane (279μm) which is indicative of a better extraction of the metal by this membrane than by the thinner membrane (82μm). Similar results were also observed for the extraction of Au(III) from chloride solutions using various Aliquat 336/PVC compositions.[1]

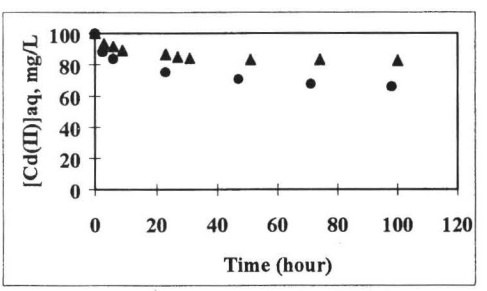

Figure 3. The effect of membrane thickness on the extraction of Cd(II). (30%(m/m) Aliquat 336/PVC membrane, initial Cd(II) concentration was 100 mg/L, membrane thickness: (▲) 82μm and (●) 279μm).

Permeation of Cd(II) and Cu(II) Through the PLMs

The ability of the Aliquat336/PVC membranes to transport Cd(II) and Cu(II) was measured by conducting experiments in which the feed solutions contained the metal of interest and the strip phase contained a low concentration of HCl solution. For the Cd(II) system, the feed solution contained 114 mg/dm^3 of Cd(II) in 2.0mol/dm^3 HCl and the strip phase contained 0.05 mol/dm^3 HCl. Figures 4 and 5 show the permeation results for the Cd(II) and Cu(II) systems, respectively.

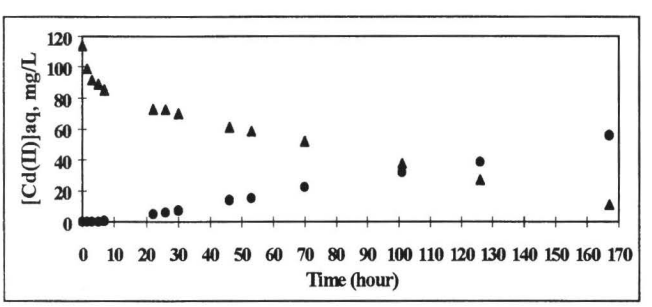

Figure4 Permeation experiment result for the Cd(II) system. (membrane composition: 40% (m/m) Aliquat 336/PVC; Initial Cd(II) concentration was 114 mg/dm^3 in 2.0mol/dm^3 HCl in the feed phase; 0.05mol/dm^3 HCl in the strip phase; (▲) Cd(II) concentration in the feed phase, (●) Cd(II) concentration in the strip phase.

The effectiveness of the transport of Cd(II) through the membrane was characterised by the flux (J_{Cd}, equation 1)

$$J_{Cd} = (V_{strp}/S)(\Delta C_{Cd}/\Delta t) \qquad (1)$$

where V_{strp} is the volume of the strip solution, S is the membrane surface and ΔC_{Cd} is the concentration difference for the time interval Δt.
The J_{Cd} was calculated as 5.77×10^{-4} g.cm^{-2}.s^{-1} at time of 20 hours.

The Cu(II) permeation results are presented in figure 5. The J_{Cu} at 20 hours was calculated by equation 1 as 2.93×10^{-4} g.cm^{-2}.s^{-1} which is similar in value to J_{Cd}. This result shows that the factor responsible for the much lower extraction of Cu(II) into Aliquat336/PVC membranes compared to Cd(II) is the small extraction constant rather than a slow diffusion of the corresponding Cu(II)-Aliquat336 complex.

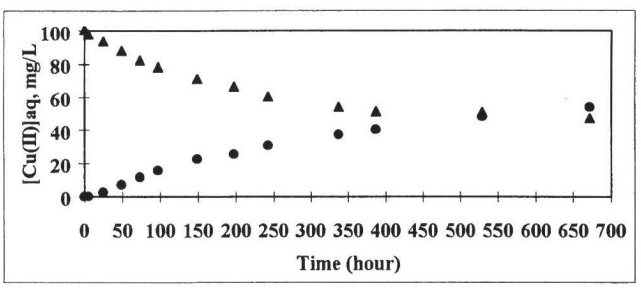

Figure 5 Permeation experiment result for the Cu(II) system. (membrane composition: 40% (m/m) Aliquat 336/PVC; Initial Cu(II) concentration was 100 mg/dm^3 in 3.0mol/dm^3 HCl in the feed solution; 0.10 mol/dm^3 HCl in the strip solution; (▲) Cu(II) concentration in the feed solution, (●) Cu(II) concentration in the strip solution.

Mechanism for the Extraction of Cd(II) Using Aliquat 336/PVC Membrane.

In a previous study of the solvent extraction of Cd(II) and Cu(II) from hydrochloric acid solutions using Aliquat336 in Shellsol AB,[2] it was proposed that the extraction involved an interfacial mechanism. It consists of a fast ion-exchange reaction between the Aliquat336 at the aqueous/organic interface and the anionic chloro species, $CdCl_3^-$ or $CuCl_3^-$, to form extractable ion-pairs which then diffused into the bulk organic phase and were replaced at the interface by fresh Aliquat336. A similar mechanism was also proposed for the solvent extraction of Cd(II) and Cu(II) using Aliquat336 dissolved in chloroform.[3] By analogy, the same mechanism has been assumed for the Aliquat336/PVC membrane extraction system. In this case, both the chemical kinetics and diffusion processes were taken into account.

Mathematical model for the extraction of gold (III) into Aliquat336/PVC membranes based on the mechanism mentioned above was developed previously and experimentally verified.[1] The same model was used in this study. Figure 6 shows the best fit between the experimental data and the model.

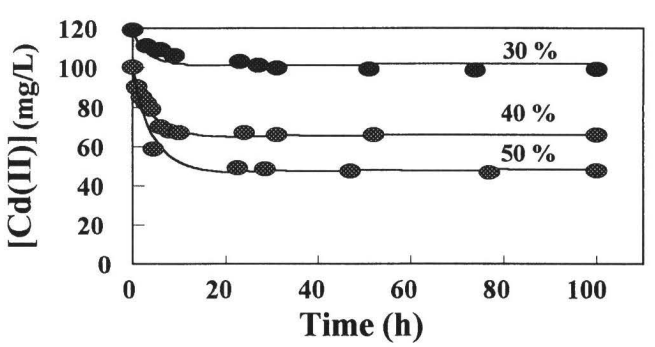

Figure 6. Experimental (•) and theoretically calculated(–) aqueous Cd(II) concentration vs. extraction time for various membrane compositions (Initial aqueous Cd(II) concentration was 120 mg/dm^3 for 30%(m/m) Aliquat 336/PVC and 100 mg/dm^3 for 40% and 50% (m/m).

The values of the model parameters (D: the diffusion coefficient, k_f : the forward kinetic rate constant, k_b: the backward kinetic rate constant and K_{ex}: the extraction equilibrium constant) which

correspond to the best fit (figure 6) are presented in table 1. These values show that the extraction mechanism was governed by both the chemical kinetics and the diffusion within the membrane.

Membrane composition in % Aliquat336/PVC (m/m)	$D_B \times 10^{13}$ (m^2s^{-1})	$k_f \times 10^9$ ($m^4mol^{-1}s^{-1}$)	$k'_b \times 10^9$ ($m\ s^{-1}$)	K_{ex} ($m^3\ mol^{-1}$)
30	0.8	1.5	3.7	0.41
40	4.0	1.5	3.3	0.45
50	8.0	1.7	1.7	1.00

Table 1. Values of D, k_f, k_b and K_{ex} obtained by fitting the model to the experimental Cd(II) data shown in figure 6

The result shows that D_B increases with increasing Aliquat 336 concentration as a result of decreasing membrane viscosity.[4] The values of K_{ex} obtained for membranes containing less than 50% Aliquat 336 were close to each other, but the value for the highest Aliquat 336 concentration (50%) was almost double. This indicates that the properties of the membrane alter considerably at Aliquat336 concentrations higher than 40%.[4]

CONCLUSION

From this study, the Aliquat 336/PVC membrane showed a higher extraction capacity to Cd(II) compare to Cu(II). The extraction capacity of the membrane for Cd(II) was found to be dependent upon the thickness and the Aliquat 336 content of the membrane. The extraction equilibrium constant values were similar for membranes containing Aliquat 336 less than 50% but almost double for the membrane of 50%.

REFERENCES

1. Argiropoulos G, Cattrall RW, Hamilton IC, Kolev SD and Paimin R, *J. Membr Sci* **138**, 279, (1998).
2. Wang L, *Master Thesis,* Victoria University of Technology, Australia, (1999).
3. Daud H and Cattrall RW, *J. Inorg. Nucl. Chem.*, **43**, 779, (1981).
4. Kolev SD, Argiropoulos G, Cattrall RW, Hamilton IC and Paimin R, J. Membr Sci, **137**, 261, (1998).

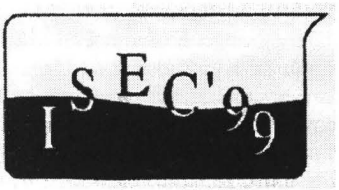

SEPARATION OF ESTERS OF POLYUNSATURATED FATTY ACIDS BY BULK LIQUID MEMBRANE WITH A POROUS PARTITION

Susumu Nii, Ri-e Yokosawa and Katsuroku Takahashi
Department of Chemical Engineering,
Nagoya University, Chikusa-ku, Nagoya, 464-8603, Japan

ABSTRACT
The 'bulk liquid membrane with porous partition (BLM)' was applied to the separation of esters of such polyunsaturated fatty acids (PUFA) as eicosapentanoic acid (EPA) and docosahexanoic acid (DHA) from a mixture of esters of fatty acids. By using 2 mol/dm^3 $AgNO_3$ aqueous solution as a membrane liquid, dodecane as a diluent and *m*-xylene as a recovery solution, esters of PUFA's were successfully separated from the mixture. The transfer experiments of ethyl ester of DHA were performed under various operating conditions. In comparison with the ordinary supported liquid membrane, the BLM has realized a stable operation, a high recovery ratio and a high throughput. The comparison of the recovery fractions for the porous and the nonporous partitions demonstrated the enhancement effect of 'bulk motion' of the membrane liquid on the solute transfer. The effect was quantitatively evaluated from the membrane transfer coefficient.

Keywords: polyunsaturated fatty acid, bulk liquid membrane, silver nitrate

INTRODUCTION

Use of the supported liquid membrane (SLM) suffers from the membrane instability and the low transfer rate. The authors have developed a novel operation mode of liquid membrane, which enables them a fast and very stable operation.[1] That is the 'bulk liquid membrane with porous partition (BLM)'. On both sides of the porous partition membrane, two-phase mixtures, consisting of a large amount of membrane liquid and the feed or the recovery solution, were placed. The partition avoids mixing of the feed and the recovery solution, while the membrane liquid moves across the partition. Such a 'bulk motion' of membrane liquid passing through the pore of the partition was promoted by the flow of a large amount of membrane liquid. The bulk motion of the membrane liquid enhances the solute transfer from the feed side to the recovery side. Another advantage of BLM is simplicity in scale-up because the operation is performed with a module. As shown in the previous study,[2] the BLM is effective for the separation of unstable solutes of large molecular weight such as Penicillin G. A high recovery fraction for Penicillin G was attained in a short residence time.

After the report that esters of polyunsaturated fatty acids (PUFA) were extracted with a silver nitrate solution by Yazawa and Kageyama,[3] separation of esters of PUFA from a fish oil has been attempted by many workers. Teramoto *et al.*[4] have shown the extraction equilibria for various solution systems and found that silver nitrate acts as a carrier for the uphill transport of ethyl ester of EPA in liquid membranes.[5,6] The emulsion liquid membrane was applied for the separation of esters of PUFAs by Nakano *et al.*[7] and they pointed out the low stability of the membrane. Similarly to Penicillin G, PUFA's have large molecular weights and need a rapid separation. Thus the application of BLM is possibly advantageous for effective separation for PUFA's. In the present study, the BLM was used for the separation of esters of PUFA's and transfer characteristics of esters of PUFA in BLM were investigated. The enhancement effect of the bulk motion of the membrane liquid on the solute transfer was also discussed.

EXPERIMENTAL

Esters of unsaturated fatty acids used in the present study are ethyl esters of docosahexysanoic acid (DHA-Et), eicosapentanoic acid (EPA-Et), a palmitic acid and oleic acid. DHA-Et and EPA-Et are kindly supplied from Harima Chemicals, Inc. and Q.P. Corporation, respectively. The feed solution was prepared by dissolving the ethyl esters in dodecane. The membrane liquid was 2 mol/dm^3 $AgNO_3$ aqueous solution. The recovery solution was *m*-xylene. The hydrophilic porous partition is a cellulose acetate membrane whose pore size is 3μm, the porosity being 0.78. On both

© 2000 Society of Chemical Industry

sides of the partition, spacer plates having a flow channel pattern shown in (figure 1) were mounted. Within the channel, a mesh coated with PTFE was set to enhance the mixing. Experimental setup is shown in (figure 2). The organic feed solution was pumped from a reservoir and mixed with the membrane liquid just before the inlet of the module, then the two-phase mixture was sent to the channel on the feed side. Another two-phase mixture of the recovery solution with the membrane liquid was fed to the channel on the recovery side and flowed in parallel with the feed side flow. The solute extracted to the membrane liquid in the feed side channel is transferred from the feed to the recovery solution across the porous partition, then was stripped into the recovery solution.

After leaving the module, the two-phase mixture was separated to aqueous and organic

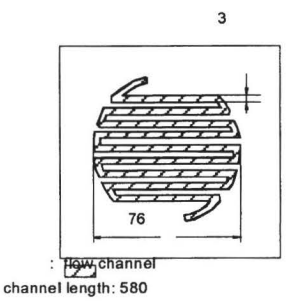

Fig. 1 Detail of flow channel

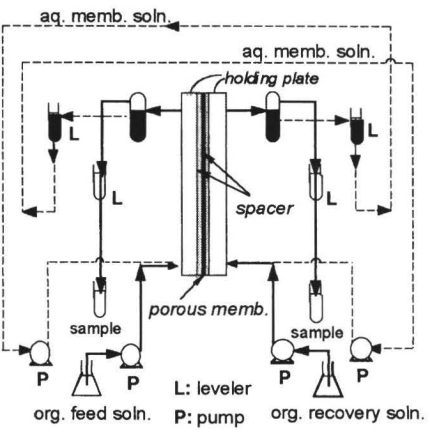

Fig.2 Schematic diagram of experimental apparatus

phases. Then the membrane liquid separated at each side was sent to the opposite side. A small amount of feed and recovery solutions was sampled and the concentration of esters was measured. When the supply of membrane liquid is stopped, the membrane liquid in both side channels flows out with a feed or recovery solution, while in the pore the partition, the membrane liquid stays quiescently. Thus the module works as a SLM contactor. The concentration of esters of fatty acids was determined by a gas chromatograph with a FID detector.

RESULTS AND DISCUSSION

To examine whether the aqueous solution of $AgNO_3$ acts as a liquid membrane and the porous partition inhibits the mixing of the feed and the recovery organic solutions, the experiment was carried out for the separation of PUFA-esters from the mixture of fatty acid esters. Table 1 shows the concentration of fatty acid esters at the feed inlet and that at the recovery outlet. The feed solution was prepared as a model fish oil. Esters of oleic and palmitic acids were not observed at the recovery outlet, which demonstrated that $AgNO_3$ solution works as a selective membrane separation system for PUFA-esters. The analysis of feed or recovery outlet solutions demonstrated that either dodecane or *m*-xylene was not observed in the opposite side, which indicates that no leak of the organic solutions across the partition occurs.

	$C_{F,in}$ [kmol/m^3]	$C_{R,out}$ [kmol/m^3]
DHA-Et	0.032	0.019
EPA-Et	0.017	0.004
Oleic acid-Et	0.02	undetected
Parmitic acid-Et	0.02	undetected

Table 1 Composition of fatty acid esters in feed and recovery solutions for separation of PUFA-Et in BLM

The transfer characteristics of PUFA-esters in BLM were studied for one component system. The dodecane solution of DHA-Et was used as the feed. The recovery fraction of the solute, which is given by the equation, was measured under various operating conditions.

$$R = (C_{F,in} - C_{F,out})/C_{F,in} \quad (1)$$

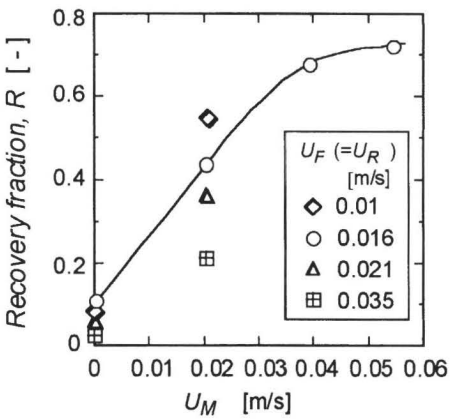

Fig.3 Effect of U_M on recovery fraction

Figure 3 shows an effect of the velocity of the liquid membrane, U_M, on the recovery fraction. When the membrane liquid is not pumped, the apparatus works as a SLM contactor. The fraction significantly increases with increasing U_M, as a result of the increase of the transfer coefficient of the membrane liquid, which will be discussed later, and the increase of overall capacity coefficients on both sides. High recovery fraction of 0.7 is achieved at U_M=0.045m/s which is about three times larger than the organic phase velocity (U_F=U_R=0.016m/s), wherein the residence time of the organic feed solution is only 36 seconds. As was shown in R for U_F=U_R=0.01m/s, more effective separation is possible by changing the ratio of velocity of the aqueous and organic phases. No emulsification or degradation of the membrane liquid was observed during the operation.

Figure 4 shows the effect of organic phases velocity on the recovery fraction for BLM and SLM. The recovery fraction for BLM decreased with the organic phase velocity owing to a decrease of the residence time for the extraction in the feed side. Significant difference was observed between the SLM and the BLM. In the SLM, where U_M=0, the solute transfer rate is controlled by the rate of molecular diffusion driven by the concentration difference between the both sides. In the BLM, three modes contribute to the solute transfer from the feed to the recovery side. One is the transfer by the bulk motion of the membrane liquid. The second is a molecular diffusion in the membrane liquid. The third is the circulation of the membrane liquid containing the solute from the feed side to the recovery side. In this way, for the solute of large molecular weight, the transfer rate is significantly enhanced in the BLM.

Replacement of the porous membrane by a non-porous film limits the solute transfer to the circulation of the membrane liquid. In the figure, the closed key shows the recovery fraction for the nonporous partition. The values are smaller than the BLM operation with a porous partition, which clearly shows the effect of the bulk motion of the membrane liquid on the solute transfer.

The effect of the bulk motion of the membrane solution on the solute transfer is evaluated from the membrane transfer coefficient, k_B. When a mass balance for the solute transfer from the feed to the recovery side is written in the differential section of the module,[1] we have:

$$-h\, d(U_{aqF}C_{aqF}) / dl = k_B (C_{aqF} - C_{aqR}) + v\, C_{aqF} \quad (2)$$

where h is a channel depth and v the apparent velocity of the membrane liquid across the pore of the partition. Since dU_F is equal to $-v\, dl/h$, equation 2 reduced to:

$$- h\, U_{aqF} dC_{aqF} / dl = k_B (C_{aqF} - C_{aqR}) \tag{3}$$

By solving the equation, k_B is obtained as follows.

$$kB = v \frac{ln\left[UaqRin\, UaqFin / \left\{\left(UaqFin + UaqRin\right)CaqFout - UaqFin\, CaqFin\right\}\right]}{ln\left\{UaqRout\, UaqFin / \left(UaqFout\, UaqRin\right)\right\}} \tag{4}$$

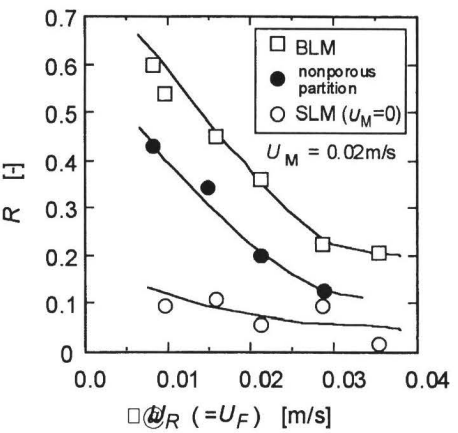

Fig.4 Effect of U_R (= U_F) on R

The contribution of the bulk motion of the membrane liquid on the solute transfer rate depends on the pore properties of the partition such as porosity and the pore structure. The partition having larger pore size and porosity, and also lower tortousity should be effective to enhance the bulk motion of the membrane liquid. The strength of the bulk motion can be evaluated with the value of k_B. For the partition used in the present study, the value of k_B was measured by the apparatus shown in (figure 5) in which the same module was used but the membrane liquid flows in a one path. To examine the transfer of solute in the membrane liquid from the feed to the recovery side, the copper ion was used as a solute in place of the complex of PUFA-Et. Two-phase mixture of an aqueous solution of copper chloride and dodecane flows in the feed side. While in the recovery side, a mixture of deionised water and *m*-xylene was supplied. The outlet concentration of copper ion in the aqueous phase was analyzed by atomic absorption spectroscopy, and the amount of solute transferred by a bulk motion of a membrane liquid and a molecular diffusion was given. The value of k_B was derived from Equation (4). From the plot of k_B vs. U_{Mav} shown in (figure 6), the following correlation for k_B was obtained.

$$k_B = 0.006 U_{Mav}^{1.19} \tag{5}$$

where U_{Mav} is average velocity of the membrane liquid comes out from feed and recovery side. The dashed line shows a correlation obtained in the previous study for the hydrophobic porous polypropylene, whose porosity is 0.45 and 0.4x0.04μm being pore size. From the SEM observation, the pore structure is quite different between the present partition and the previous one. It seems the pore of the present partition is straighter than that of the previous partition. The value of k_B for the present partition is higher than that for the previous one. Furthermore the dependence of $U_{M,av}$ on k_B for the present partition is stronger than that for the previous one. The fact clearly shows that the pore properties have a significant effect on the membrane transfer coefficient which indicates the strength of the bulk motion of membrane liquid.

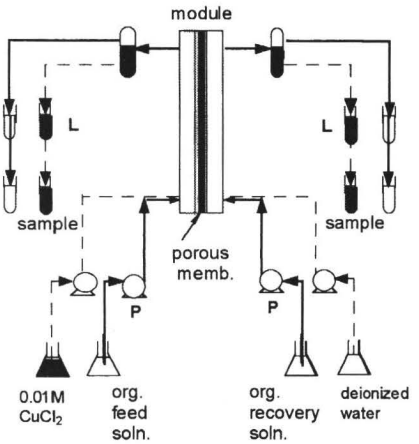

Fig.5 Apparatus for mesurement of k_B

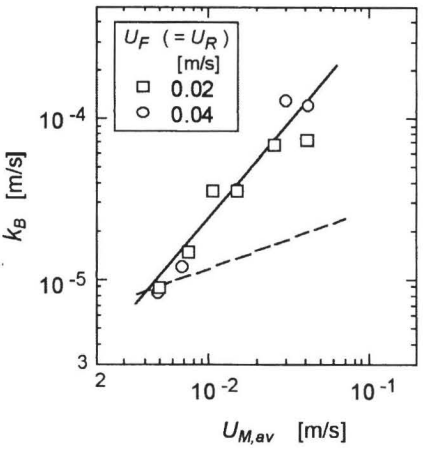

Fig.6 Effect of $U_{M,av}$ on k_B

NOMENCLATURE

C	concentration	[kmol/m^3]
h	channel depth	[m]
k_B	membrane transfer coefficient defined by Equation(4)	[m/s]
l	channel length	[m]
R	recovery fraction defined by Equation(1)	[-]
U	liquid velocity	[m/s]
U_{Mav}	average velocity of membrane liquids comes out from feed and recovery side	[m/s]
v	apparent velocity of membrane liquid across partition	[m/s]

Subscripts

aq	aqueous phase
in	inlet
org	organic phase
out	outlet
F	feed side
M	membrane liquid
R	recovery side

ACKNOWLEDGEMENT

We wish to thank Harima Chemicals Inc. and Q.P. Corporation for supplying samples of ethyl ester of docosahexysanoic acid and eicosapentanoic acid.

REFERENCES

1. Nii S, Haryo I, Takahashi K and Takeuchi H, *J. Chem. Eng. Japan*, **27**, 369, (1994)
2. Nii S and Takahashi K, *'Values Adding through Solvent Extraction' Proc. ISEC'96*, Univ. Melbourne, 839, (1996)
3. Yazawa K and Kageyama K, *Yukagaku*, **40**, 974, (1991)
4. Teramoto M, Matsuyama H, Ohnishi N, Uwagawa S and Nakai K, *Ind. Eng. Chem. Res.*, **33**, 341, (1994)

5. Teramoto M, Matsuyama H, Nakai K, Uesaka T and Ohnishi N, *J. Memb. Sci.*, **91**, 209, (1994)
6. Teramoto M, Matsuyama H and Nakai K, *Sep. Sci. and Technol.*, **31**, 1953, (1996)
7. Nakano K, Kato S, Noritomi H and Nagahama K, *J. Memb. Sci.*, **110**, 219, (1996)

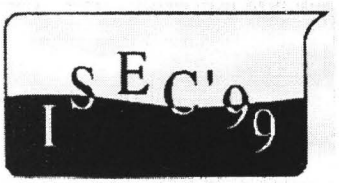

TRANSPORT OF PHENOL THROUGH BULK LIQUID MEMBRANES

Wojciech Cichy[2], Štefan Schlosser[1] and Jan Szymanowski[2]

[1]Dep. Chem. Biochem. Eng., Slovak University of Technology, SK-81237 Bratislava, Slovakia

[2]Inst. Chem. Technol. Eng., Poznañ University of Technology, Poznañ, Poland

ABSTRACT

Pertraction of phenol through a layered bulk liquid membrane (BLM) and through BLM in a hollow fibre (HF) contactor has been studied. Three liquid membranes with dialkylamine, trioctylamine and trialkylphosphine oxide (Cyanex 923) carriers and pure n-alkanes have been tested. The membrane with Cyanex 923 was found to give the highest fluxes in phenol pertraction through the layered BLM. The proposed model of pertraction through layered BLM describes experimental data well and permits a better understanding of the behaviour of the systems studied. Kinetics of the stripping reaction have to be studied closer. The overall mass-transfer coefficient in the HF contactor with trioctylamine carrier is independent of the feed concentration and increases with increasing pulsation velocity of the membrane and the feed velocity in the fibre lumen approaching a steady value at 7.5 $mm.s^{-1}$ and 6 $cm.s^{-1}$, respectively.

Keywords: bulk liquid membranes, pertraction, hollow fibre contactor, phenol, trioctylamine, Amberlite LA-2, Cyanex 923

INTRODUCTION

Phenol is a toxic compound present in waste-waters and process solutions formed in various industries, e.g. processing of coal tar, manufacture of phenol and its processing to resins. Solvent extraction with various solvating and basic reagents is usually considered as a suitable method of phenol recovery.[1,2]

Membrane processes can be now considered as an alternative route of phenol recovery or removal, especially from dilute solutions, both by pertraction through liquid membranes[3-6] and membrane based solvent extraction.[7-10] These methods are also suitable to recover other organic pollutants and various biochemicals.[3,8,9]

The aim of this work was to evaluate carriers for pertraction of phenol and the study of mass transfer of phenol through layered bulk liquid membrane and BLM in a hollow fibre contactor. The former can be considered as the first step before more comprehensive studies in the hollow fibre modules.

THEORETICAL

The following assumptions were taken into account in the development of a mass-transfer model in the two compartment cell with a layered bulk liquid membrane:[11]

(i) fast chemical reactions of formation and decomposition of the complex phenol-carrier on interfaces, which means that the diffusional mass-transfer in boundary layers is decisive;
(ii) all three phases are well mixed and hydrodynamic conditions at both interfaces in the membrane are identical so $k_{MF} = k_{MR} = k_M$;
(iii) equilibrium at both interfaces;
(iv) constant volume of the feed, membrane and the stripping phases;
(v) concentration of undissociated phenol in the stripping solution at the interface R/M is practically zero, what means that the concentration of the complex in the membrane at the strip interface is close to zero, as well.

The resulting model equations are as follows:

$$\frac{dc_F}{dt} = -\frac{k_F k_M A_F (D_{rF} c_F - c_M)}{V_F (k_F + k_M D_{rF})} \qquad (1)$$

© 2000 Society of Chemical Industry

$$\frac{dc_M}{dt} = \frac{k_M A_R}{V_M}\left[\frac{k_F A_F (D_{rF} c_F - c_M)}{A_R (k_F + k_M D_{rF})} - c_M\right] \quad (2)$$

$$\frac{dc_R}{dt} = \frac{k_M A_R}{V_R} c_M \quad (3)$$

$$c_M = \frac{V_F (c_{Fo} - c_F) - V_R c_R}{V_M} \quad (4)$$

Mass-transfer in the HF module is discussed in papers[4,12] and in this proceedings.[6]

EXPERIMENTAL

Components of the membrane phases

Trioctylamine (TOA, Fluka), dialkylamines (Amberlite LA-2, with C_{12} and C_{13} alkyl groups, Fluka) and trialkylphosphine oxides (Cyanex 923, with C_6 and C_8 alkyl groups, Cytec) were used as carriers in n-alkanes (dodecane fraction C_{10}- C_{13}, Slovnaft, SK) as a diluent. Composition of the membranes and their characteristics are shown in table 1.

Membrane phase	D_r	$\nu_M.10^6$ $m^2 \cdot s^{-1}$	$D.10^{10}$ $m^2 \cdot s^{-1}$	$D_r.D.10^{10}$ $m^2 \cdot s^{-1}$
M1 - 0.4 M TOA	1.2	2.03	3.8	4.56
M3 - 0.4 M Cyanex 923	42	2.30	4.7	197.4
M4 - 0.4 M LA-2	2.2	2.22		
M5 - n-alkanes	0.12	1.60	14.2	1.7

Table 1 Distribution coefficient of phenol, D_r, (at c_F= 0,8 g/dm^3 and pH_F = 4), kinematic viscosity and diffusion coefficient of the carrier-phenol complex (1:1) or phenol (in n-alkanes), D, for the membrane phases at 25°C. Diluent used was an n-dodecane fraction of n-alkanes

The feed was an aqueous solution with 1 g/dm^3 of phenol, if not otherwise stated, and 0.1 mol/dm^3 Na_2SO_4 with pH = 1.2 to 6.0 adjusted with the addition of H_2SO_4 or NaOH. A solution of 0.05-2 mol/dm^3 NaOH in water was used for stripping.

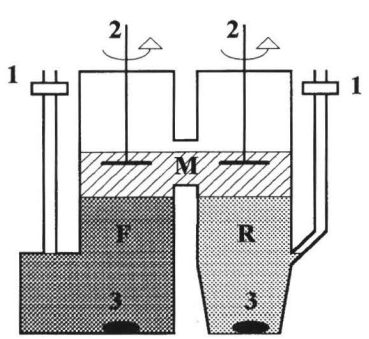

Figure 1. Scheme of a two-compartment pertraction cell.
F - feed, M - membrane phase, R - stripping solution,
1 - sampling ports, 2 - disc mixers,
3 - magnetic Teflon rod mixers.

A two-cell contactor with a well mixed layered BLM (double Lewis cell) was used to study the transport through liquid membranes, as designed earlier,[13] figure 1. The membrane phase was mixed with Teflon disc mixers (29 mm in diameter, distance between the centre of disc and the interface was 12 mm, frequency of mixers around 120 min^{-1}). The aqueous feed and stripping phases were mixed by

magnetic stirrers with a frequency of 95 min^{-1}. The measurements were carried out at a temperature of 25°C. Volumes of phases: feed V_F = 310 cm^3, membrane V_M = 90 cm^3, stripping solution V_R = 130 cm^3. Interfacial areas: A_F = 21.53 cm^2, A_R = 20.19 cm^2.

A hollow fibre contactor of own construction PV20 for pertraction has been used.[12] A more detailed description of this contactor is given elsewhere.[6]

RESULTS AND DISCUSSION

The distribution of phenol between the membrane and aqueous phase depends on the extractant, the acidity of the aqueous phase and the phenol concentration in the feed. For n-alkanes (M5), and solvents M1 or M4 the distribution coefficient does not depend on the concentration of phenol in the aqueous phase, as shown in paper[14] for the concentration interval from about 0.15 to 0.9 g/dm^3. A strong effect of concentration was observed for Cyanex 923 (M3), figure 2b. The distribution coefficient does not depend on pH for Cyanex 923, (figure 2b), and for Amberlite LA-2 at pH<8, which is well below the value of pK_a for phenol i.e. about 10. The effect of pH is observed for a solvent containing TOA (M1) when the distribution coefficient sharply increases with decreasing pH values below 4 following the addition of H_2SO_4, figure 2a, probably as a result of formation of a mixed complex TOA with H_2SO_4, as previously observed.[15] For all solvents tested, the value of the distribution coefficient decreases sharply at pH > 9 because of the dissociation of phenol, when the phenolate anions do not form complexes with extractants and the phenolate anion is not soluble in pure n-alkanes.

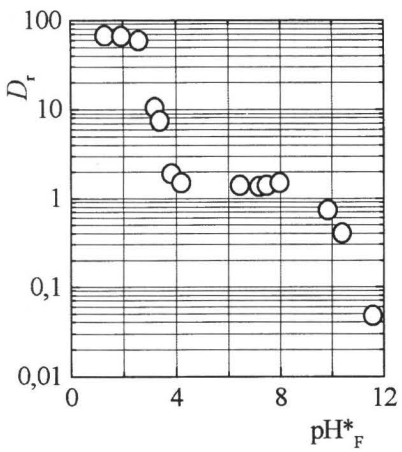

a)

a) 0.4 mol.dm^{-3} TOA (M1),

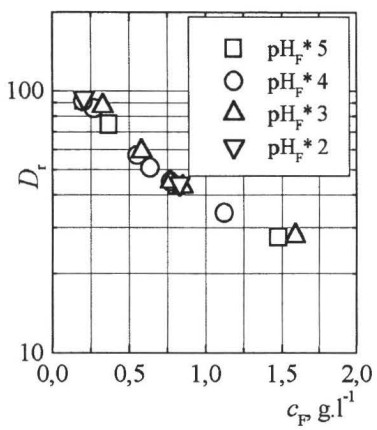

b)

b) 0.4 mol.dm^{-3} Cyanex 923 (M3).

Figure 2. Distribution coefficient of phenol for solvents:

Typical time dependences of phenol concentrations in three phases during pertraction of phenol in a two-cell contactor are presented in figure 3. As can be seen from this figure the suggested model describes experimental data well. In the case of a solvent with Cyanex 923 an empirical equation for the concentration dependence of D_r is included in the model. Model parameters, k_F and k_M, for different membranes are shown in figure 4a.

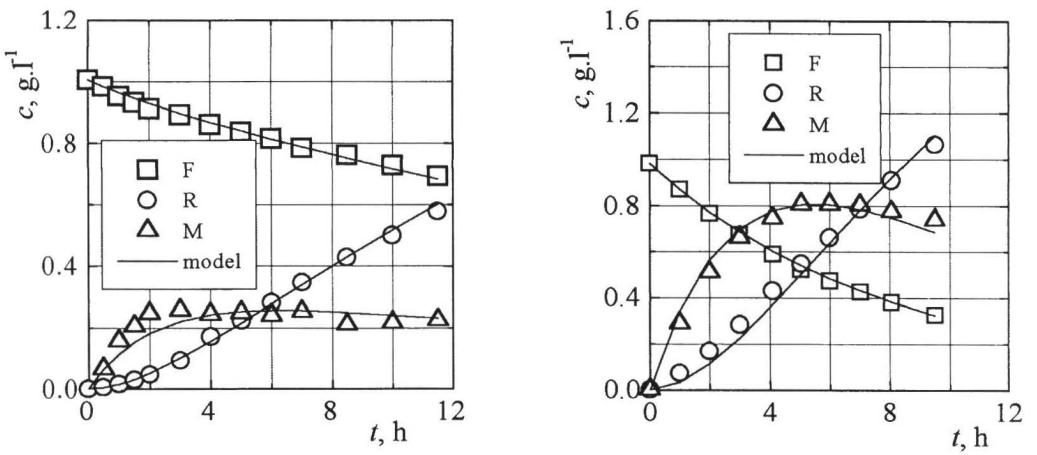

a) Membrane: M1, R: 0.05 mol.dm^{-3} NaOH b) Membrane: M3, R: 2 mol.dm^{-3} NaOH

Figure 3. Pertraction of phenol through layered BLM in a two-cell contactor. pH_{Fo}= 4.0

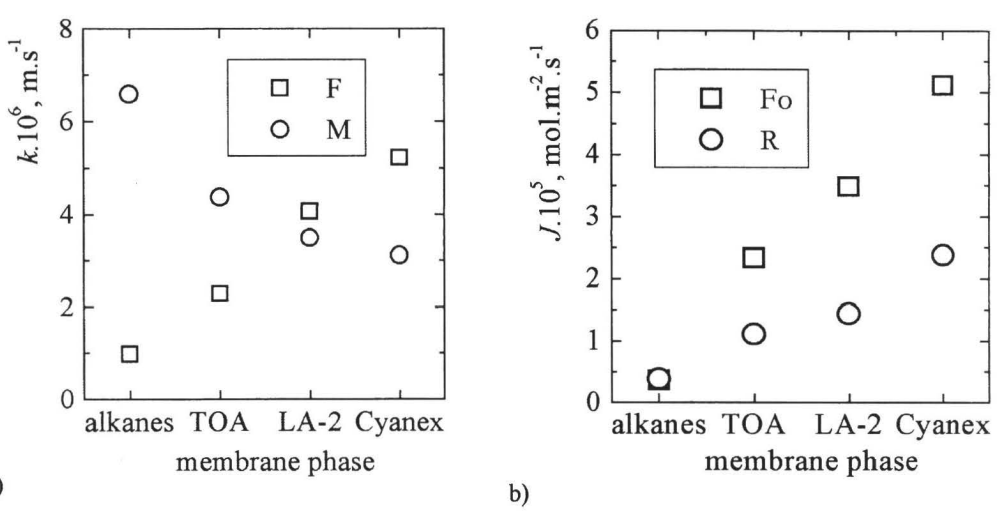

a) b)

Figure 4. Influence of composition of the membrane phases on individual mass transfer coefficients in the feed and membrane phases and on the flux density of phenol in pertraction in a two compartment contactor. pH_{Fo}= 4.0, R: 0.05 mol/dm^3 NaOH

The initial flux through the feed interface, J_{Fo} , and the maximum flux through the stripping interface (at time corresponding to a maximum on the c_M dependence), J_R , has been estimated from the slopes of c_F and c_R dependences and are presented in figure 4b. The highest overall flux through the liquid membrane, represented by J_R in figure 4b, was achieved with the carrier Cyanex 923 (membrane M3) which exhibits also the highest distribution coefficient, as shown in table 1. The permeability of the liquid membrane could be in the first approximation represented by the product of distribution and diffusion coefficients, $D_r.D$, included in table 1.

The value of this product for the membrane M3 is one and two orders of magnitude higher compared with the membranes M1 and M5, respectively. But this is not completely reflected in

differences between flux of the phenol for the membrane M3, which is only 3 and 6 times higher, compared with fluxes for membranes M1 and M5, respectively. Moreover the difference between J_R and J_{Fo} increases with increasing value of J_R, as can be seen in figure 4b. The mass-transfer coefficient in the membrane phase, k_M, decreases with increasing flux through the membrane, as shown in figure 4a. These facts may suggest the explanation that kinetics of the stripping reaction are responsible for these differences, which should be further evaluated. Spontaneous emulsification on the stripping side of the membrane with Cyanex 923 has to be considered in the evaluation of this membrane.

The flux density of phenol through BLM in the HF contactor PV20 proportionally increases with the concentration of phenol in the feed. The value of the overall mass-transfer coefficient is independent of the concentration in the feed, figure 5.

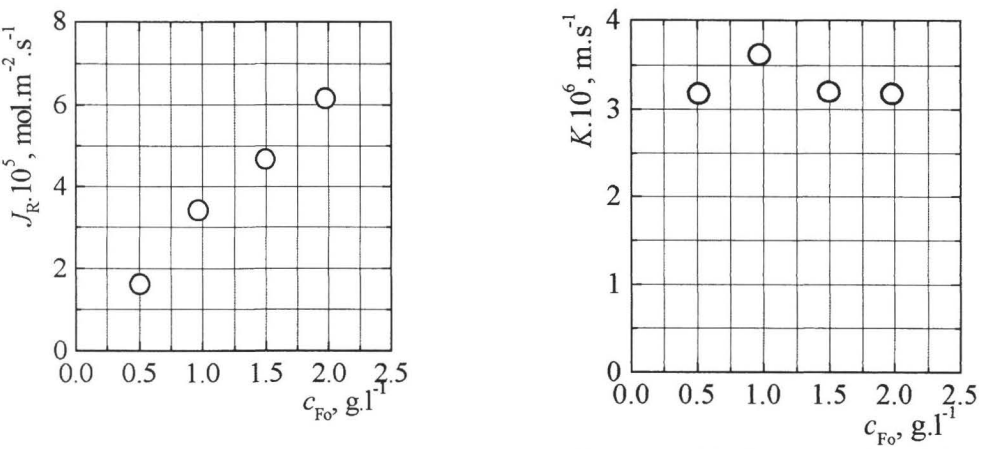

Figure 5. Flux of phenol and overall mass transfer coefficient vs. initial concentration of phenol in pertraction in HF contactor with TOA in membrane phase (M1).

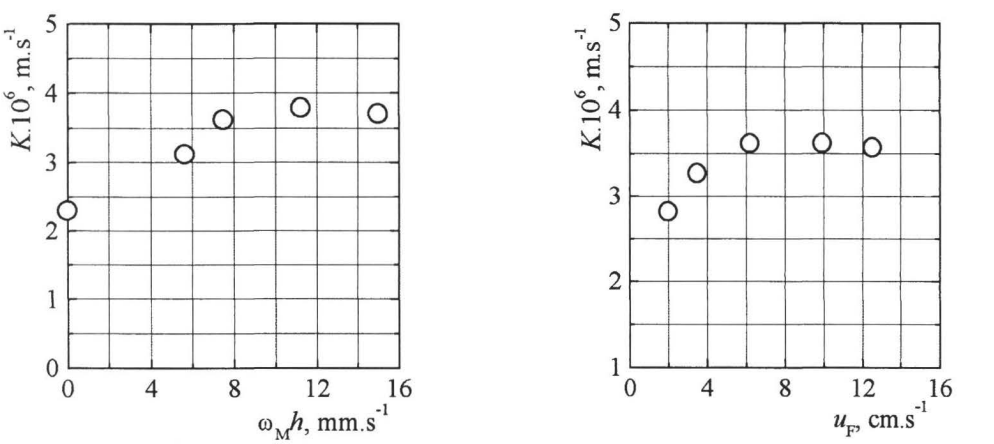

Figure 6. Influence of the velocity of membrane pulsation and of the feed linear velocity in the fibre lumen on the overall mass transfer coefficient of phenol in pertraction in a HF contactor with TOA as carrier (M1). a) $u_F = 6.2$ cm.s^{-1} b) $\omega_M h = 7.5$ mm.s^{-1}

Pulsation of the membrane phase increases the transport rate which approaches a plateau value at the pulsation velocity (product of pulsation frequency and amplitude, $\omega_M h$) of about 7.5 mm.s^{-1}, as shown in figure 6a, with a value of the overall mass-transfer coefficient of about $3.7.10^{-6}$ m.s^{-1}. With

increasing linear velocity of the feed in the fibre lumen the overall mass-transfer coefficient increases and at about a relatively low velocity of 6 cm s^{-1} a steady value is approached, (figure 6b).

NOTATION

A interfacial area, m^2
c mass concentration, $kg.m^{-3}$
D diffusion coefficient, $m^2 \cdot s^{-1}$
D_r distribution coefficient, -
J flux density, $mol.m^{-2}.s^{-1}$
k individual mass-transfer coefficient, $m.s^{-1}$
K overall mass-transfer coefficient, $m.s^{-1}$
V volume, m^3
u linear velocity in fibre lumen, $m.s^{-1}$
t time, h
ν kinematic viscosity, $m^2 \cdot s^{-1}$

Indices

F feed phase, interface on the feed side F/M
M membrane phase
o initial value
R stripping solution, interface on the strip side M/R
* equilibrium value

ACKNOWLEDGEMENTS

Support of the Slovak grant agency VEGA for grants No.4215/97 and No.1/6154/99 are acknowledged. Help of E. Sabolová at experiments is highly appreciated. Experiments performed at SUT Bratislava during the study stay of W. C.

REFERENCES

1 Lo TC, Baird MHI and Hanson C (eds). *Handbook of Solvent Extraction,* J. Wiley, (1983).
2 King CJ and Senetar, in: Marinsky JA and Marcus Y. (Ed.), *Ion Exchange and Solvent Extraction*, M. Dekker. **10**, 35,
3 Majumdar S and Sirkar KK. in: Ho WSW and Sirkar KK. (Ed.), *Membrane Handbook*, Van Nostrand Reinhold, 764, (1992).
4 Schlosser S, Rothova I and Frianova H. *J. Membrane Sci.*, **80**, 99, (1993).
5 Garea A, Urtiaga AM, Ortiz MI et al. *Chem. Eng. Commun.*, **120**, 85, (1993).
6 Schlosser S, Sabolová E and Marták J. In: this proceedings.
7 Basu R, Prasad R and Sirkar KK. *AICHE J.*, **36**, 450, (1990).
8 Prasad R and Sirkar KK. as ref [3], p. 727.
9 C. H. Yun, R. Prasad and K. K. Sirkar, *Ind. Eng. Chem. Res.*, **31**, 1709, (1992).
10 Urtiaga AM, Alonso AI,. Galan B, Irabien JA and Ortiz MI. In: *Proc.Extraction 94*, Edinburgh, 1, (October 1994).
11 Sabolová E, Schlosser S and Stopka J. In: *Proc. of the 24th Conf. SSCHI*, Castá - Papiernièka 147, (June 1997).
12 Schlosser S and Sabolová E. *J. Membrane Sci.*, submitted for publication (1998).
13 Marták J, Schlosser S and Stopka J. In: *Proc. of the 7th Int. Symp. on Synthetic Membranes in Science and Industry*, Tubingen, 293, (1994) .
14 Cichy W, Schlosser S and Szymanowski J. In: *Proc. of the 25th Conf. SSCHI*, Jasná, 9, (May 1998).
15 Wang ML and Hu KH. *Ind. Eng. Chem. Res.*, **33**, 914, (1994).

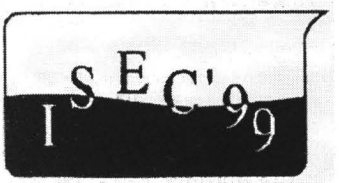

RECOVERY OF SILVER TRACES FROM ELECTRONIC WASTES

G Durand, D Pareau and K Ennassef [1]
Laboratoire de Chimie et Génie des Procédés, Ecole Centrale Paris, 92295 Châtenay-Malabry Cedex, France
[1]Present address: Faculté des Sciences, Université Moulay Ismail, Meknès, Maroc

ABSTRACT
A process for recovering silver from wastes of silvered copper wires has been studied. The difficulty is to separate minor amounts of silver (1%) from large amounts of copper (99%). Selective extraction of silver by Cyanex 471X has been studied. A continuous process has been devised to separate silver (stripping solution) from copper (raffinate) using a surfactant liquid membranes to produce a highly concentrated solution of silver.

Keywords : surfactant liquid membrane, silver, copper, Cyanex 471X, surfactant ECA 4360, Span 80, silvered copper wires

INTRODUCTION

The aeronautic industry uses silvered copper wires. These copper conductors are silvered for two purposes: first to protect wires from corrosion, secondly for conduction of high frequency currents. Wastes generated during coated-wire preparation and wastes from end of life materials may be collected to recover silver which is the most valuable product. The difficulty is that the silver concentration is about 1% (w/w) of the copper; so recovery of silver needs a very selective process to produce a concentrated solution for electrochemical recovery.

EXPERIMENTAL

Reagents:

Cyanex 471X (TIBPS > 95 %) from Cyanamid and D2EHPA (from Sigma) were used as extractants. Span 80 (2% m/m) from Fluka or ECA 4360 (4% w/w) from Exxon were used as surfactants. Technical grade dodecane mixed with small amounts (5% v/v) is used as diluent for solvent extraction, and without octanol for surfactant liquid membrane extraction. All other chemicals are of analytical grade.

Procedure and apparatus:

Experiments were performed at 25°C. Cyanex 471X was purified according to Rikelton and al.[1] Emulsification was carried out by an Ultraturrax T25 (13500 r/min, 5 min). The electrocoalescer was supplied by Micronics System and the corresponding cell was built in the laboratory. A laboratory pulse column (h = 1m, d_V = 2.5 cm, 40 plates, disks and crowns, 25% free area) was used for SLM extraction. Determination of silver and copper were carried out with an atomic absorption spectrometer (Varian SpectrAA 300P).

RESULTS AND DISCUSSION

Solvent Extraction

Selective silver extraction

Solid silvered wires are leached by concentrated nitric acid so that silver and copper are oxidized to their cations Cu^{2+} and Ag^{+}. This solution is then diluted to a HNO_3 concentration of 0.5 mol/dm^3. The amount of wire leached is calculated so that copper and silver concentrations in diluted

© 2000 Society of Chemical Industry

solution were respectively 5g/dm^3 and 50 mg/dm^3. As the extraction is performed in acidic media Cyanex 471X (triisobutylphosphine sulfide, TIBPS) was selected because of its strong affinity for silver. Indeed, preliminary experiments showed that Cyanex 471X extracts silver from a Cu 5g/dm^3 and Ag 50mg/dm^3 solution with a separation ratio [Ag]/[Cu]≥49.5. The distribution isotherm $[\overline{Ag}]$ vs [Ag] shows that the organic phase is saturated at a [Ag]/[TIBPS] ratio around 0.5. So $AgNO_3$ is extracted as $\overline{AgNO_3(TIBPS)_2}$ similarly to AgCl from chloride media as shown by Abe and al.[2] So the extraction reaction is :

$$AgNO_3 + 2\overline{TIBPS} \Leftrightarrow \overline{AgNO_3(TIBPS)_2}$$

with

$$Ag^+ + NO_3^- \Leftrightarrow AgNO_3 \qquad K_1 = 0.63 \text{ (dm}^3\text{/mol) (according to Kotrly and al}^3\text{)}$$

$$K_E = \frac{\left[\overline{AgNO_3(TIBPS)_2}\right]}{\left[AgNO_3\right]\left[\overline{TIBPS}\right]^2} \qquad \text{and } D_{Ag} = \frac{\left[\overline{AgNO_3(TIBPS)_2}\right]}{\left[Ag^+\right]+\left[AgNO_3\right]}$$

Plot of logD vs $\log\left[\overline{TIBPS}\right]$ confirms the stoichiometry of extracted species and gives the value of extraction constant, $K_E = (5.4 \pm 0.4) \times 10^7$ (mol/dm^3)$^{-2}$.

Whatever the concentration between 50mg/dm^3 and 10 g/dm^3, copper is not extracted by $\left[\overline{TIBPS}\right]$ 5.10^{-3} mol/dm^3. Copper concentration in the organic phase < 0.1 mg/dm^3. ($D_{Cu} \approx 8.10^{-5}$).

Silver stripping

The stripping of silver from the organic phase was examined with different reagents (NH_3, HNO_3, $P_2O_7^{4-}$, $S_2O_3^{2-}$ and $SC(NH_2)_2$). The most efficient reagent is thiosulfate, but in acidic media it is not stable and leads to a precipitate. So we have chosen thiourea (Tu) 0.01 mol/dm^3 in HNO_3 0.1 mol/dm^3. Gaspar and al[4] have already demonstrated the ability of thiourea to strip silver in acidic media. A systematic study of silver stripping with acidified thiourea (Tu) led to the determination of AgTu complex stoichiometry (1:1 in the aqueous stripping phase) and to the estimation of the formation constant $K_{AgTu^+} = (6.4 \pm 0.8) \times 10^6$ (mol/dm^3)$^{-1}$.

So the stripping reaction is :

$$\overline{AgNO_3(TIBPS)_2} + Tu \Leftrightarrow AgTu^+ + NO_3^- + 2\overline{TIBPS}$$

Plot of $\log D'_{Ag} + 2\log\left[\overline{TIBPS}\right]$ vs log[Tu], where $D'_{Ag} = \frac{[Ag]}{[\overline{Ag}]}$ is the stripping coefficient confims the stoichiometry 1:1 of silver-thiourea complex and allows the determination of stripping constant $K_S = (0.19 \pm 0.02)$ (mol/dm^3)^2

Small concentrations of copper extracted with silver are also entirely stripped by thiourea.

Flow-sheet for silver-copper separation

Because of the very good separation of silver from copper, a flow-sheet comprising only two steps, extraction and stripping, without scrubbing, has been calculated (figure 1)

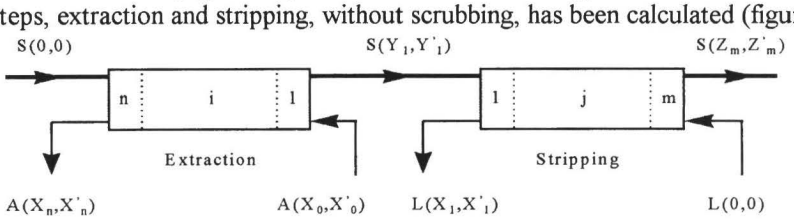

Figure 1. Flow-sheet for silver-copper separation

The parameters are :

S : organic phase flow (dm^3/h)
A : feed aqueous phase flow (dm^3/h)
L : stripping aqueous phase flow (dm^3/h)
X_0, X'_0 : silver and copper concentrations in the feed solution
X_n, X'_n : silver and copper concentrations in the outflow of extraction
Y_1, Y'_1 : silver and copper concentrations in the outflow of the extraction organic phase
Z_m, Z'_m : silver and copper concentrations in the outflow of the stripping organic phase
X_1, X'_1 : silver and copper concentrations in the outflow of the stripping aqueous phase

The initial conditions are :

feed solution :
$X_0 = 50$ mg/dm^3 (4.63×10^{-4} mol/dm^3)
$X'_0 = 5$ g/dm^3 (7.87×10^{-2} mol/dm^3)

organic phase :
[TIBPS] = 5×10^{-3} mol/dm^3
dodecane-octanol (95:5)

stripping solution :
[HNO_3] = 0.1 mol/dm^3
[Tu] = 10^{-2} mol/dm^3

For silver concentrations we impose that X_n and $Z_m < 0.1$ mg/dm^3.

Extraction step

Considering the global silver balance [$Y_1 = A/S(X_0 - X_n)$] and the operating balance for stage i [$Y_{i+1} = Y_1 + A/S(X_i - X_0)$], the equilibria equation is $X_i = \dfrac{\alpha Y_i}{K_E([S]_0 - 2Y_i)^2}$

with $\alpha = 1 + \dfrac{1}{K_1[NO_3^-]} = 5.233$

To determine the minimum flow of solvent, the maximum A/S ratio is calculated according to the previous equations. This lead to $A/S \leq 4.68$.

For copper, owing to the fact that its distribution coefficient varies from one stage to another, we must calculate Y'_i stage by stage.

The results obtained are collected in Table 1

A/S	X_1 X'_1	Y_1 Y'_1	X_2 X'_2	Y_2 Y'_2	X_3 X'_3	Y_3 Y'_3	X_4 X'_4	Y_4 Y'_4	stage required
1	0.294 5.000	49.99 0.398	0.0011 5.000	0.293 0.598					2
2	0.985 5.000	99.98 0.237	0.0077 5.000	1.954 0.589					2
3	2.958 5.000	149.89 0.118	0.0365 5.000	8.764 0.562					2
4	11.61 5.000	199.98 0.040	0.2645 5.000	46.436 0.411	0.0041 5.000	1.041 0.595			3
4.68	40.88 5.000	229.98 0.0137	7.976 5.000	188.07 0.0549	0.192 5.000	36.67 0.521	0.0034 5.000	0.866 0.596	4

Table 1 Profile of extraction concentrations (mg/dm^3)

It appears that a small number of stages is sufficient, even for A/S = 4.68, which allows a highly concentrated silver solution.

Stripping step

Considering the global silver balance [$X_1 = S/L(Y_1 - Z_m)$] and the operating balance for stage j [$Y_{j+1} = S/L(Z_j - Z_m)$], the equilibria equation is :

$$K_D = \frac{X_j\left[NO_3^-\right]([S]_0 - 2Z_j)^2}{Z_j([Tu]_0 - X_j)}.$$

Supposing that $[S]_0 - 2Z_j \approx [S]_0$ (credible for L/S>0.25), we have :

$$Z_j = \beta\frac{X_j}{[Tu]_0 - X_j} \qquad \text{with} \qquad \beta = \frac{[S]_0^2\left[NO_3^-\right]_0}{K_D} = 2.63 \text{mol/L}$$

Values of parameters and number of stages have been calculated in order that silver concentration in the organic phase flowing out of the stripping step be < 0.1 mg/dm^3.

Copper concentration is very low in the extraction outflow (≤ 0.596 mg/dm^3 i.e. 5.52x10^{-6} mol/dm^3). So the whole copper is stripped at the first stage and the organic phase outflow does not contain copper. Results are collected in Table 2

(A/S,S/L)	(1,3)	(2,3)	(3,3)	(4,3)	(4.7,3)	(1,4)	(2,4)	(3,4)	(4,4)	(4.7,4)
X_1	151.5	302.9	454.2	605.9	696.9	199.98	399.9	59905	799.8	919.7
X'_1	1.194	0.819	0.354	0.12	0.04	1.59	1.092	0.472	0.16	0.052
X_2	0.700	1.67	3.003	5.483	7.802	1.285	3.325	7.055	16.14	32.45
Z_1	0.232	0.554	1.031	1.817	2.585	0.323	0.836	1.77	4.06	8.156
Z_2	0.0009	0.002	0.0004	0.007	0.01	0.0017	0.004	0.009	0.02	0.044
n_1	2	2	2	3	4	2	2	2	3	4
n_2	2	2	2	2	2	2	2	2	2	2

where n_1, n_2,number of respectively extraction and stripping stages.

Table 2 Profile of stripping concentrations (mg/dm^3)

From table 2 it can be seen that silver may be concentrated from 5 mg/dm^3 to about 0.5-1 g/dm^3. The efficiency of separation may be expressed by the global separation factor (SF) :

$SF = \frac{([Ag]/[Cu])_{outlet}}{([Ag]/[Cu])_{inlet}}$ and by the purity percentage of each metal (silver in the outlet of stripping aqueous phase, copper in the raffinate of extraction). Results are collected in Table 3.

(A/S,S/L)	(1,3)	(2,3)	(3,3)	(4,3)	(4.7,3)	(1,4)	(2,4)	(3,4)	(4,4)	(4.7,4)
SF (x10^{-4})	1.3	3.7	13.1	51.1	171	1.3	3.7	1.3	50	181
% Ag	99.22	99.73	99.92	99.99	99.99	99.21	99.73	99.92	99.98	99.98
% Cu	99.99	99.99	99.99	99.99	99.99	99.99	99.99	99.99	99.99	99.99
$[Ag]_{stripping}$ (mg/dm^3)	151	303	454	606	697	200	400	600	800	920

Table 3 Performance of mixer-settler separation

It can be observed that silver and copper are efficiently separated and that according to the experimental conditions (flow ratio A/O at extraction and O/A at stripping), it is possible to recover silver in the strip solution between 150 and 920 mg/dm^3. These concentrations are slightly too small for an efficient electrodeposition of metal with plane cathodes. So we have studied the selective extraction of silver by surfactant liquid membranes.

Surfactant Liquid Membrane Extraction

As it is planned to recover silver metal by electrowinning, silver/copper separation by surfactant liquid membrane has been studied. It is expected to achieve a higher concentration factor than in solvent extraction. Many works have been published about liquid membrane extraction of cations. [5-8]

The physicochemical results of liquid-liquid distribution have been used to determine the composition of liquid membrane. So the organic phase was a solution of Cyanex 471X in dodecane and thiourea was the ligand used for stripping. Span 80 or ECA 4360 were used as surfactant. Several values of the volumetric ratios $A = V_{org}/V_{aq}$ and $B = V_{ext}/V_{emul}$, of the three phases have been studied.

Silver extraction

The experimental conditions chosen were first : external phase : Ag^+ 50 mg/dm^3 + HNO_3 0.25 mol/dm^3, membrane: TIBPS 1.5×10^{-3} mol/dm^3 + Span 80, 2% (in weight) + dodecane; inner aqueous phase: thiourea 0.5 mol/dm^3 + HNO_3 0.5 mol/dm^3. Kinetics of extraction shows that after 5 min the equilibria is obtained, but the extraction is not complete (90%). An increase of TIBPS concentration increases the amount of extracted silver. With [TIBPS] $\geq$ 10 [Ag], the remaining silver in the raffinate is negligible.

Copper/silver extraction

Selective extraction of silver from a mixture Cu 5 g/dm^3 + Ag 50 mg/dm^3 has been studied under the following conditions : TIBPS 5×10^{-3} mol/dm^3, inner phase HNO_3 0.25 mol/dm^3 + thiourea concentration varying from 0 to 1 mol/dm^3. The balance of soluble silver is not 100%, because it appears that $AgNO_3$(TIBPS) is not very soluble in dodecane. So a part of silver is precipitated on the wall of reactor. To avoid this precipitation octanol has been added to dodecane (0-4%). But addition of octanol diminishes the emulsion stability. So the extraction of silver is not so good. For this reason di-(2-ethylhexyl)phosphoric acid (D2EHPA) was added to replace octanol. In acidic media D2EHPA is not an extractant, but only a solvating species (hydrogen bonding) which increases the solubility of $AgNO_3$(TIBPS). The effect of D2EHPA was studied in the range of concentration 0-10%. Span 80 causes large emulsion swelling and a bad decantation. To avoid these phenomena ECA 4360 (4%) was used instead of Span 80. Finally we operated under the following conditions:

outer phase: Ag^+ 50 mg/dm^3; Cu^{2+} 5 g/dm^3 in HNO_3 0.25 mol/dm^3
membrane: TIBPS 2.5 10^{-2} mol/dm^3; D2EHPA 10%; ECA 4%; dodecane
inner phase: Thiourea 0.75 mol/dm^3 in H_2SO_4 0.5 mol/dm^3 + $LiNO_3$ 0.1 mol/dm^3
A = 2; B = 11.25. Time transfer: 5 min. Stirring: 300 r/min.

With these conditions 95% of silver is extracted from the external phase, and 94% is stripped. Silver in internal phase is highly concentrated (985 mg/dm^3) with only traces of copper (70 mg/dm^3)

CONCLUSION

This work shows that traces of silver (1%) may be separated from copper (99%) either by liquid-liquid extraction or by surfactant liquid membrane. Very efficient separation of silver (99.98%) from copper (99.99%) may be achieved by solvent extraction (separation factor $\approx$ 180). Silver is recovered at high concentration (concentration factor 18.4), allowing a direct electrowinning step. In order to increase concentration of silver recovered, surfactant liquid membrane extraction was tested.

Its performances are similar to those of solvent extraction, but the process is simpler, then cheaper, because only one contactor is necessary to separate traces of silver from copper.

ACKNOWLEDGEMENTS

The authors wish to thank Cytec Co. which kindly provided the extractant Cyanex 471X.

REFERENCES

1. Rickelton WA and Robertson AJ, SME-AIME Fall meeting, Denver, Colorado USA. Preprint N° 84-357
2. Abe Y and Flett DS, *"Solvent Extraction 1990" Proc. ISEC'90* ed Sekine T Elsevier 1127, (1992).
3. Kotrly S and Sucha L, *Handbook of Chemical Equilibria in Analytical Chemistry*, Ellis Horwood, Chichester (1985)
4. Gaspar V, Mejerovich AS, Meretukov MA and Schmiedl J, *Hydrometallurgy* **34**, 369, (1994).
5. Bromberg L, Lewin I, Warshawsky A, *Hydrometallurgy* **33**, 59, (1992)
6. Nishiki T and Bautista RG, *AIChE J.* **31**, 2093, (1985)
7. Imato T, Ogawa H, Morooka S and Kato Y, *J. Chem. Eng. Jpn* **14**, 289, (1981)
8. Samar M, Pareau D, Chesné A and Durand G, *Bull. Soc. Chim. Fr.* **129**, 259, (1992)



Metal and Non-metal Extraction

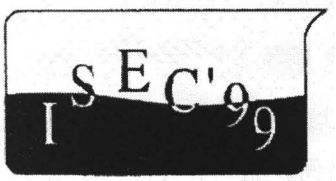

RARE EARTHS SEPARATION STUDY

Deqian Li
Laboratory of Rare Earth Chemistry and Physics, Changchun Institute of Applied Chemistry, Chinese Academy of Sciences, Changchun 130022, China

ABSTRACT
A review on some new extraction systems of rare earth separation in the Laboratory of Rare Earth Chemistry and Physics, Changchun Institute of Applied Chemistry, Chinese Academy of Sciences, is given with 17 references. The systems considered are: (I) new extraction systems for RE separation: Cyanex 272 and Cyanex 302; (II) new extraction systems for Sc separation: (1) Cyanex 272 (HBTMPP), (2) Cyanex 302 and Cyanex 301, (3) Stripping of Sc, (4) Role of the different components of Cyanex 302 in Sc extraction and (5) Cyanex 923.

Keywords: rare earths, Cyanex 301, Cyanex 302, Cyanex 923, Cyanex 272

INTRODUCTION

At present the rare earth separation process demonstrated by our laboratory using HEH/EHP (marketed as P507 in China) and naphthenic acid (denote as HA) solvent extraction combined with P507 extraction resin and ion exchange chromatography, etc. has been applied widely in China. This process provides industrial production of all the individual RE (except Pm) up to 4N or even greater purity.[1-6] However, the industrial practice indicates that the shortcoming of P507 extraction process is the high acidities required to strip heavy RE, especially Sc, small separation factors (1.4 - 1.8) for some RE pairs such as Pr-Nd, Eu-Gd, Y-Er, Yb-Lu, slower extraction rates for heavy RE in HCl system, etc. Consequently, to explore some new extractants that possess extracting, stripping, separation selectivity and mass transfer properties superior to P507 has been an interesting subject for many researchers.[7]

This paper introduces briefly what we have been studying on some new extraction systems of RE separation in recent years.

NEW EXTRACTION SYSTEMS FOR RARE EARTH SEPARATION

Cyanex 272 system[8,9]

Bis(2,4,4-trimethylpentyl)phosphinic acid (HBTMPP), the active component of commercial extractant Cyanex 272, has a similar structure to di(2-ethylhexyl)phosphinic acid (H[DEHP]). With two alkyl groups attached to the phosphorus atom, the pK_a of extractants increase in the order HDEHP < HEH/EHP < HBTMPP or H[DEHP], which is consistent with the decreasing order of extraction and stripping acidity HDEHP > HEH/EHP > HBTMPP or H[DEHP]. Extractants with more highly branched alkyl chains attached to the P atom than those of H[DEHP], HBTMPP will probably show higher selectivity for separating RE including Sc.

Figure 1 shows that the extractability for RE with HBTMPP increases with the increase in atomic number, and the slopes of the log D plot against pH for all RE are about 3, which indicates 3 moles of hydrogen ions are released as one mole of RE(III) is extracted at lower aqueous acidity. The separation factors of adjacent RE(III) are given in Table 1, and the average separation factors (β_Z^{Z+1}) is 3.24, which is superior to P507 extraction system. The average separation factors of extracting mixed RE with Cyanex 272-Kerosene from HCl or HNO_3 solutions are consistent with those in Table 1. The stripping properties of Cyanex 272 loaded mixed heavy RE are shown in Figure 2, and the stripping curves mean that there are two extraction mechanisms of RE(III). The stripping coefficients of RE(III) in a single stage are about 87% and 92% by 1.5 mol/dm^3 HCl or HNO_3 solutions respectively, it indicates that the stripping efficiency of Cyanex272 is considerably superior to P507 system.

© 2000 Society of Chemical Industry

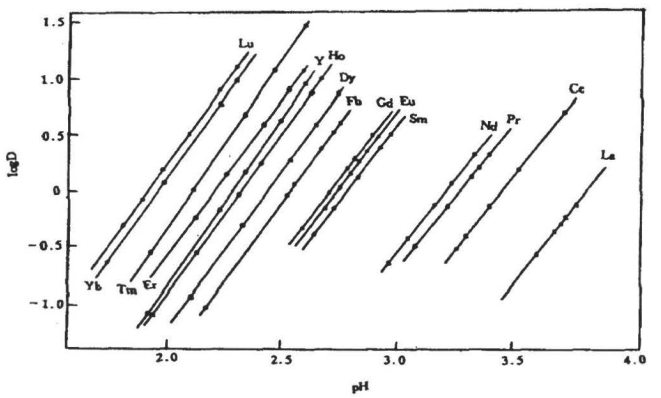

Figure 1 Effect of equilibrium pH in aqueous phase on the extraction of RE(III) with HBTMPP RE(III) = 4.0 x 10^{-4} mol/dm^3; $[HL]_{(o)}$ =2.0 x 10^{-2} mol/dm^3, t= 25°C

	Ce	Pr	Nd	Sm	Eu	Gd	Tb	Dy	Ho	Y	Er	Tm	Yb	Lu
La	11.7	39.7	51.4	679	910	1052	3389	6515	14525	23388	28056	74655	179077	236073
Ce		3.39	4.39	58.0	77.8	89.9	290	557	1241	1998	2397	6379	15301	20171
Pr			1.30	17.1	23.0	26.5	85.4	164	366	590	707	1882	4515	5952
Nd				13.2	17.7	20.5	66.0	127	283	455	546	1453	3486	4596
Sm					1.34	1.55	4.99	9.59	21.4	34.4	41.3	110	264	347
Eu						1.16	3.72	7.16	16.0	25.7	30.8	82.0	197	259
Gd							3.22	6.19	13.8	22.2	26.7	71.0	170	224
Tb								1.92	4.29	6.9	8.28	22.0	52.8	69.7
Dy									2.23	3.59	4.31	11.4	27.5	36.2
Ho										1.61	1.93	5.14	12.3	16.2
Y											1.20	3.19	7.66	10.1
Er												2.66	6.38	8.41
Tm													2.40	3.16
Yb														1.32
Lu														

Table 1. Separation factors of RE(III) in the system of HBTMPP-HCl

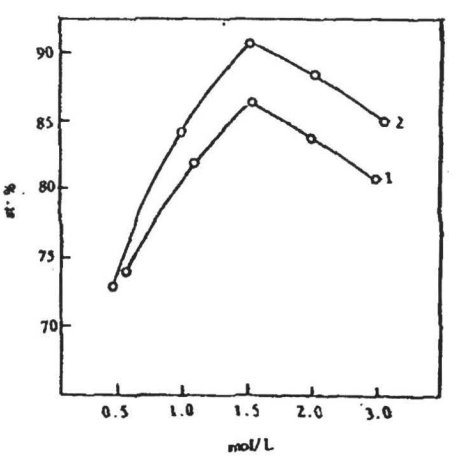

Figure 2 Stripping curves for heavy rare earths (III): 1. HCl; 2. HNO_3

Cyanex 302 system[10-12]

Thiosubstituted organophosphorus compounds have been studied widely for analytical applications and hydrometallurgical processes. According to Pearson's Hard-Soft Acid-Base (HSAB) principle, sulfur substitution of organophosphorus reagents is generally considered to have high efficiency on the extraction of most soft and borderline metals such as Pd(II), Pt(II), Cd(II), Ag(I), Co(II), Ni(II), Cu(II), Zn(II), etc. However, less work has been conducted on the extraction of "hard acid" metals such as lanthanides, Sc(III), Zr(IV), Th(IV), etc. More recently, the extractants Cyanex 302 and Cyanex 301, which are the respective the monothio- and dithio- analogues of Cyanex 272, have been commercially available from Cyanamid (CYTEC) Canada Co. A series of papers concerning the extraction of Zn(II), Co(II), Ni(II), Cu(II),Fe(III), etc. with these reagents have been published. Here the RE extraction with raw and purified Cyanex 302 (denote HBTMPTP, HL) from mineral acid solutions is discussed systematically.

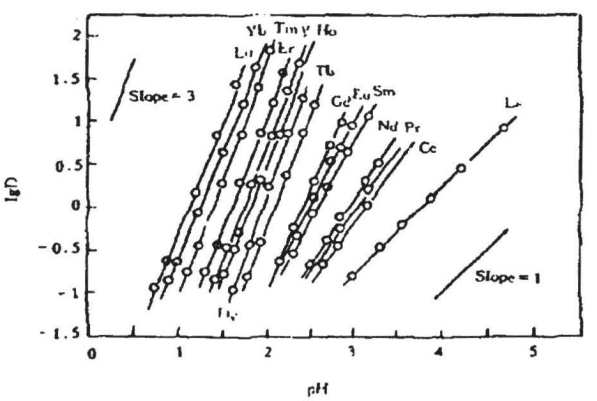

Figure 3 Effect of pH values on the extraction of RE(III) from nitrate solutions with Cyanex 302 at 25°C

	Ce	Pr	Nd	Sm	Eu	Gd	Tb	Dy	Ho	Y	Er	Tm	Yb	Lu
La	7..32	10.5	14.8	71.0	115	201	1382	3635	8822	13325	30966	1227032	319404	65636
Ce		1.44	2.02	9.70	15.7	27.4	189	496	1205	1820	4229	16757	43621	89636
Pr			1.40	6.74	10.9	19.5	131	345	837	1265	2939	11646	30314	62293
Nd				4.80	7.79	13.6	93.4	246	596	901	2094	8296	21594	44373
Sm					1.62	2.82	19.5	51.2	124	188	436	1727	4496	9239
Eu						1.74	12.0	31.6	76.6	116	269	1065	2773	5697
Gd							6.89	18.1	44.0	66.4	154	611	1592	3271
Tb								2.63	6.38	9.64	22.4	88.8	231	475
Dy									2.43	3.67	8.52	33.8	87.9	181
Ho										1.51	3.51	13.9	36.2	74.4
Y											2.32	9.21	24.0	49.3
Er												3.96	10.3	21.2
Tm													2.60	5.35
Yb														2.05
Lu														

Table 2. Separation factors of RE(III) from HNO_3 medium with Cyanex 302 at 25°C

Figure 3 shows that the extraction efficiency for RE(III) with HBTMPTP from HNO_3 solutions is in the order of $La^{3+} < Ce^{3+} < Pr^{3+} < Nd^{3+} < Sm^{3+} < Eu^{3+} < Gd^{3+} < Tb^{3+} < Dy^{3+} < Ho^{3+} < Y^{3+} < Er^{3+} < Tm^{3+} < Yb^{3+} < Lu^{3+}$, which rises with the increase of atomic number or the decrease of atomic

radius. The slopes of log D vs pH from Lu^{3+} to Tb^{3+} are almost 3 whereas the slopes from Gd^{3+} to La^{3+} decrease from 3 to 1 gradually. This means that the extractions of these metal ions proceed by other reaction stoichiometries, which may attribute to the presence of intermediate water-soluble complexes at the higher aqueous pH values. The extraction mechanisms of RE(III) in the H_2SO_4 system are more complex. The average separation factors of Gd-Lu are 4.2 (H_2SO_4), >3.4 (HCl or HNO_3), which is superior to HEH/EHP extraction system. Table 2 shows that the separation factors of RE(III) in the HBTMPTP-HNO_3 system. The average separation factor (β_Z^{Z+1}) is 3.26, which is smaller than that of HBTMPP-octane-chloride system (β_Z^{Z+1}=3.69), but the average separation factor of adjacent heavy RE(III)(Gd-Lu) is 3.44, which is greater than that of HBTMPP (β_Z^{Z+1}=2.24). In contrast, it seems that HBTMPTP is more useful for the separation of heavy RE(III).

NEW EXTRACTION SYSTEMS OF Sc(III) SEPARATION

Cyanex 272 (HBTMPP) system[13,14]

The log D plots against log [H_2SO_4] for Sc(III), Zr(IV), Ti(IV), Th(IV), Fe(III) and Lu(III) are shown in Figure 4 and the results indicate that in ranges 0.1- 0.5 mol/dm^3 H_2SO_4, significant extraction of Sc(III) is possible with little or no extraction of Th(IV), Fe(III), and Lu(III) with HBTMPP by controlling the aqueous sulphuric acid concentration. The separation of Sc(III) from Ti(IV) can be achieved using selective stripping, but it is difficult to separate Zr(IV) from Sc(III). However, HBTMPP is superior to HDEHP or HEH/EHP for separation of Sc(III) from Th(IV), RE(III), Fe(III), etc.

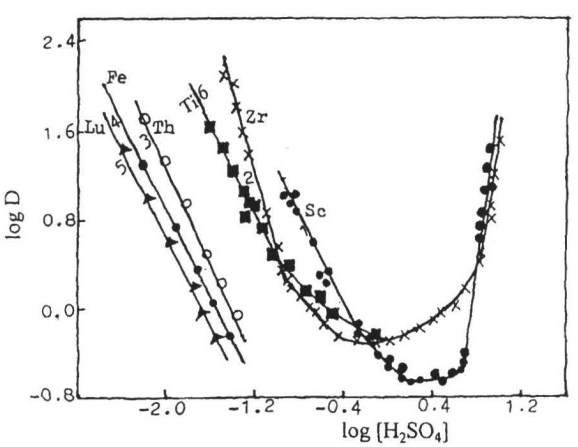

Figure 4 The extraction of metal ions from sulphuric acid solutions with HBTMPP

Cyanex 302 systems[15]

The effect of equilibrium aqueous acidity on the extraction of Sc(III), Zr(IV), Th(IV), Fe(III) and Lu(III) with Cyanex 302 from sulphuric acid solutions in Figure 5. It was found that the extractabilities of the metals decrease in the order: Zr(IV) > Sc(III) > Th(IV) > Fe(III) >Lu(III) and Ti(IV). The results indicate that it is possible to separate Th(IV), Fe(III) and Lu(III) from Sc(III) with Cyanex 302 by controlling the aqueous acidity. For instance, in the 0.4 mol/dm^3 H_2SO_4 solution, the extraction percentage of Sc(III) is close to 96%, while those of Th(IV), Fe(III) and Lu(III) are 40% 15% and 50%, respectively. It is difficult to separate Zr(IV) from Sc(III) due to the stronger affinity of the extractant toward Zr(IV), which will be more readily extracted into the organic phase than Sc(III).

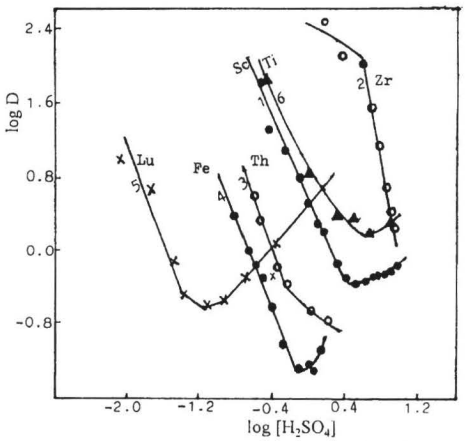

Figure 5 The extraction of metal ions from sulphuric acid solutions with Cyanex 302

Stripping of Sc(III) from Cyanex 272, Cyanex 302 and Cyanex 301[15]

To investigate the stripping of Sc(III) from Cyanex 272, Cyanex 302 and Cyanex 301, the loaded organic phases were stripped by sulphuric acid solutions of different concentrations. From the experimental results it has been demonstrated that Cyanex 272, Cyanex 302 and Cyanex 301 become stronger extractants for Sc(III) in the order shown. Consequently, it might be expected that stripping Sc(III) would become progressively more difficult in the same order. This is in fact the case as shown by the stripping percentage for Cyanex 272, Cyanex 302 and Cyanex 301 plotted in Figure 6.

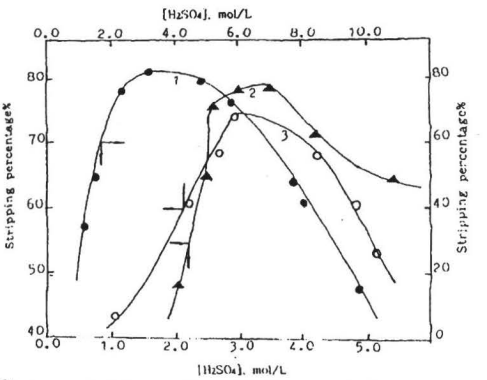

Figure 6 Stripping of Sc^{3+} from H_2SO_4 media with Cyanex 272, Cyanex 302 and Cyanex 301
1. [Cyanex 272]=4.81 x 10^{-2} mol/dm^3, [Sc(III)]=5.46 x 10^{-4} mol/dm^3
2. [Cyanex 302]=4.83 x 10^{-2} mol/dm^3, [Sc(III)]=5.12 x 10^{-4} mol/dm^3
3. [Cyanex 301]=4.82 x 10^{-2} mol/dm^3, [Sc(III)]=5.10 x 10^{-4} mol/dm^3

The results indicate that Sc(III)can be stripped readily by sulphuric acid solutions of certain concentrations even though the stripping acidity increases gradually according to the order shown. In fact, the stripping percentages of Sc(III) in a single stage for Cyanex 272, Cyanex 302 and Cyanex 301 are near 82%, 78% and 75% by 1.5 mol/dm^3, 3.5 mol/dm^3 and 5.8 mol/dm^3 H_2SO_4 solution, respectively. In contrast with the Cyanex extractants, the stripping percentages of Sc(III) for HDEHP and HEH/EHP are only 5% and 20% by 5 mol/dm^3 H_2SO_4 solution, respectively. Therefore, Cyanex 272 and Cyanex 302 show a better stripping performance with respect to Sc(III) than HDEHP and HEH/EHP.

Role of the different components of Cyanex 302 in the Sc(III) extraction[15,16]

It has been found that the extraction ability of the purified Cyanex 302 (HBTMPTP) is significantly lower than that of the as-received Cyanex 302. According to the composition of Cyanex302, n-hexane solutions of tri-n-octylphosphine oxide (TOPO), HBTMPTP and HBTMPP, or mixed solutions of TOPO with either HBTMPTP or HBTMPP, were prepared. The extractability of Sc(III) increases when TOPO is added to either of the HBTMPTP or HBTMPP solutions, especially at the lower aqueous acidity, but is still considerably lower than that by the raw Cyanex 302. This result indicates that there may be a synergistic effect in the extraction when TOPO is present together with HBTMPTP or HBTMPP, particularly at the lower aqueous acidity. The reason why the raw Cyanex 302 can extract Sc(III) more efficiently than the purified Cyanex 302 is still not clear, but at least is not attributed to the presence of HBTMPP. It is interesting to study the roles of the branched trialkylphosphine oxide and pure dialkyldithiophosphinic acid in the Sc(III) extraction. Recently, it has been found that the extractability of Sc(III) increases considerably when the branched trialkylphosphine oxide (Cyanex 925, B) is added to HBTMPTP solution, and this result indicates that there is a significant synergistic effect in the HBTMPTP-Cyanex 925-Sc(III) system. From results of IR, NMR and FAB-MS spectra for Sc(III) extracted complex, it can be suggested that the stoichiometry of Sc(III) extracted complex is $Sc(SO_4)_{0.5}(HL_2)_2 \bullet 3B$.

Cyanex 923 system[17]

The extraction equilibria of Sc(III), Zr(IV), Ti(IV), Th(IV), Fe(III) and Lu(III) from sulphuric or hydrochloric acid media by Cyanex 923 (mixture of straight chain alkylated phosphine oxides) were studied at various aqueous acidities. The results obtained are shown in Figures 7 and 8 respectively. The metals are extracted as a function of aqueous acidity in the order: Zr(IV) > Sc(III) > Ti(IV) ~ Lu(III) > Fe(III) (H_2SO_4 medium) or Sc(III) > Th(IV) > Lu(III) (HCl medium). The separation of Sc(III) from Ti(IV), Fe(III) and Lu(III) can possibly be achieved by controlling the aqueous acidity. For example, the extraction percentage of Sc(III) is 96% at an acidity of 2.0 mol/dm^3 H_2SO_4, while those of Ti(IV), Lu(III) and Fe(III) are 48%, 50% and 10% respectively.

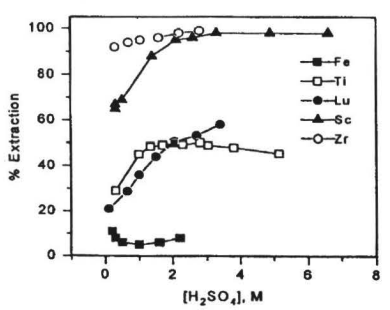

Figure 7. The extraction of metal ions by Cyanex 923 from H_2SO_4 medium
Organic phase: 5% v/v Cyanex 923
Aqueous phase: [Sc^{3+}]=5.49E-4 mol/dm^3, [Zr^{4+}]=3.07E-4 mol/dm^3, [Ti^{4+}]=4.89E-4 mol/dm^3, [Fe^{3+}]=6.00E-4 mol/dm^3, [Lu^{3+}]=2.66E-4 mol/dm^3

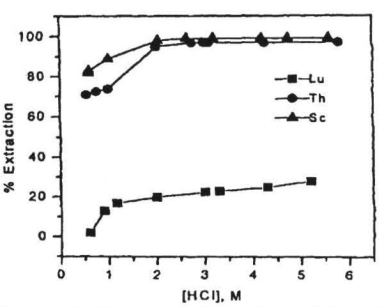

Figure 8. The extraction of metal ions by Cyanex 923 from HCl medium
Organic phase: 5% v/v Cyanex 923
Aqueous phase: [Sc^{3+}]=6.34E-4 mol/dm^3, [Th^{4+}]=1.85E-4 mol/dm^3, [Lu^{3+}]=2.38E-4 mol/dm^3

Thus the separation factors(β) of Sc(III) toward Ti(IV), Lu(III) and Fe(III) are 26, 24 and 218 respectively. A new technology, which is superior to those using TBP or HDEHP, was developed with the advantage of a high Sc(III) yield and a good selectivity for impurity metal ions. The purity of the final scandium product is above 95% with a yield > 94%.

CONCLUSION

Superior extraction behavior of rare earths separation with some new excellent extractants including extracting, stripping, separation selectivity were discussed in the paper. It is apparent that for trivalent

rare earths separation, especially for heavy RE(III) separation Cyanex 272 and Cyanex 302 are two potential extractants which could be applied in industrial processes with high average separation factors and high stripping efficiency. For the same reason Cyanex 272, Cyanex 302 and Cyanex 923 may be used to separate Sc(III) from RE(III) instead of HEH/EHP and HDEHP in the future.

ACKNOWLEDGEMENT

This work was supported by the National Natural Science Foundation of China

REFERENCES

1. Li DQ, Wan X, Lin DZ et al., *Proc ISEC'80*, Liege, Belgium, 80, (1980).
2. Li DQ, Xu W, Wang ZH et al., *CN pat., No.85102244.8*, (1985).
3. Dai ZR, Wang CX and Wang ZR, *CN pat., No. 85102220.0*, (1985).
4. Peng CL, Niu W, Cao WG et al., *CN pat., No.85101874.0*, (1985).
5. Lin SX and Yuan P, *CN pat., No.85101611.0*, (1985).
6. Li DQ, Wang ZH, Song WZ et al., *Hydrometallurgy'94*, Chapman & Hall, London. 627, (1994).
7. Li DQ, *Progress in Chemistry* (in Chinese), **7**(3), 209, (1995).
8. Zhang XF and Li DQ, *Chinese Journal of Applied. Chemistry*, **10**(4), 72, (1993).
9. Wang ZH, Meng SL, Li DQ et al., *Chinese Journal Analytical Chemistry*, **23**(4), 391, (1995).
10. Xue LZ, Li DQ, Luo AQ et al., *Journal Rare Earths* (Special issue), **2**, 657, (1995).
11. Li DQ, Luo AQ, Yuan M et al., *Value adding through Solvent Extraction*, Edited by Shallcross DC, Melbourne University, **1**, 165, (1996).
12. Yuan M, Luo AQ and Li DQ, *Acta Metallurgica Sinica*, **8**(1), 10, (1995).
13. Wang C and Li DQ, *Solv. Extr.Ion Exch.*, **12**(3), 615, (1994).
14. Ma GX and Li DQ, *Chinese Journal of Analytical Chemistry*, **20**(10), 1113, (1992).
15. Wang C and Li DQ, *Solv. Extr.Ion Exch.*, **13**(3), 503, (1995).
16. Wei ZG, Li DQ, Wang C et al., *Chemical Journal of Chinese University*, **18**(8), 1281, (1997).
17. Li DQ and Wang C, *Hydrometallurgy*, **48**, 301, (1998).

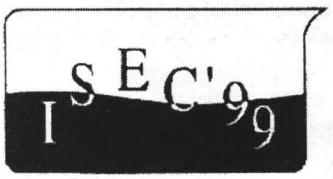

SOLVENT EXTRACTION SEPARATIONS OF TRIVALENT LANTHANIDE AND ACTINIDE IONS USING AN AQUEOUS AMINOMETHANE-DIPHOSPHONIC ACID

Mark P Jensen and Kenneth L Nash
Chemistry Division Argonne National Laboratory Argonne, Illinois 60439-4831, USA

ABSTRACT
The possibility of separating the trivalent lanthanides, represented by Eu^{3+}, and actinides, represented by Cf^{3+}, using bis-(2-ethylhexyl)phosphoric acid (HDEHP) in toluene and an aqueous phase containing N-piperidinomethane-1,1-diphosphonic acid (PMDPA), has been investigated. This modified aqueous phase offers potential advantages over the diethylenetriaminepentaacetic acid based TALSPEAK process because of the improved complexation properties of PMDPA in acidic solutions, and the ability to decompose PMDPA before disposal. Extraction experiments were conducted at 25°C in 2 M $NaClO_4$ between -log $[H^+]$ 1 and 2. The studies enabled us to derive the aqueous phase speciation, the stability constants of the aqueous complexes, and the Cf/Eu separation factors. Despite the presence of an amino group in PMDPA that should favor the retention of the actinides in the aqueous phase, the Cf/Eu separation factors are near unity under the conditions studied.

Keywords: lanthanide, actinide, bis-(2-ethylhexyl)phosphoric acid, N-piperidinomethane-1,1-diphosphonic acid, TALSPEAK

INTRODUCTION

Given the similar ionic radii of the trivalent lanthanide (Ln^{3+}) and actinide (An^{3+}) cations, practical intergroup separation of these elements remains a challenge for separation science. One key to achieving this separation is to exploit the small differences in the chemical hardness of the two groups. Experimentally the An^{3+} cations appear to be slightly softer Lewis acids, interacting more strongly with softer donors than the Ln^{3+} cations. Recently, the objective of incorporating nitrogen and sulfur donors into extractant molecules has made progress toward useful extractants capable of effecting this separation.[1,2] Historically, however, most Ln/An group separation schemes have incorporated modified aqueous phases.[3] The most thoroughly studied of these schemes, the TALSPEAK process, involves the preferential extraction of Ln^{3+} cations by bis-(2-ethylhexyl)phosphoric acid (HDEHP) from pH 2-3 aqueous phases containing 1 M lactic acid and 0.05 M diethylenetriaminepentaacetic acid (DTPA).[4] The separation is based on the extraction of the 1:1 metal:lactate complexes and the stronger interaction of the An^{3+} with the nitrogen donors of DTPA.

While the TALSPEAK process has been shown effective for separating Ln^{3+} from An^{3+}, the concentrations of lactic acid and the moderate pH require substantial adjustment to the nitric acid feed solutions usually encountered in nuclear processing. An alternative to the original TALSPEAK aqueous phase that could function in more acidic solutions, such as 1 M HNO_3, would be desirable. Methanediphosphonic acid ligands are powerful Ln/An complexants, even in 1 M acid,[5-8] that have been studied as stripping agents for the TRUEX process.[9] They are members of a class of ligands known as thermally unstable complexants or TUC's, so called because they can be degraded by gentle heating in the presence of mild oxidizing agents. A ligand that combines the powerful complexing properties of the methanediphosphonate group with the softer nitrogen donor might favor An^{3+} complexation in the aqueous phase and allow selective extraction of Ln^{3+} ions. N-piperidinomethane-1,1-diphosphonic acid (PMDPA), Figure 1, is one such ligand whose Eu^{3+} extraction has been studied previously.[8] To explore the possibility of a PMDPA based Ln/An separation, we have studied the HDEHP/toluene extraction of an An^{3+} cation, Cf^{3+}, from aqueous solutions of 2 M H/$NaClO_4$ between -log $[H^+]$ 1 and 2. This actinide was chosen because it has a

© 2000 Society of Chemical Industry

similar crystal radius to Eu^{3+} (109 pm vs. 108.7 pm CN=6).[10] An observation of stronger Cf^{3+} complexation by PMDPA could thus be attributed to a greater covalent character in the Cf-ligand bonds since the electrostatic component of M-L bonding for Eu^{3+} and Cf^{3+} are the same.

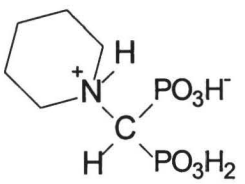

$pKa_5 = 11.5$
$pKa_4 = 7.76$
$pKa_3 = 4.62$
$pKa_2 = 2.02$
$pKa_1 = 0.3$

Figure 1. N-piperidinomethane-1,1-diphosphonic acid, H_4(PMDPA)

EXPERIMENTAL

The ^{249}Cf tracer ($t_{1/2}$ = 351 yr.) was obtained as the daughter of ^{249}Bk supplied by Oak Ridge National Laboratory. A 0.13 M HNO_3 solution of ^{249}Cf was evaporated to dryness and taken up in 0.01 M HNO_3. A high resolution γ-ray spectrum showed only ^{249}Cf emissions. The initial aqueous phase concentration of ^{249}Cf was ca. 3 x 10^{-8} M (3 x 10^4 cpm).

Other reagents, procedures, equipment, and data analysis have been previously described,[8] except that the distribution ratio of Cf^{3+}, *D*, was determined radiometrically by γ-counting between 300 and 450 keV with a NaI detector. Each combination of aqueous and organic phase was run in duplicate. All uncertainties are expressed at the ±2σ level.

RESULTS AND DISCUSSION

Characterization of Cf^{3+} extraction by HDEHP/toluene in the absence of PMDPA was the first step. Slope analysis of the extractant and acid dependencies gave 2.98 ± 0.05 and 3.16 ± 0.08 respectively, confirming the expected extraction equilibrium,

$$Cf^{3+}_{aq} + 3\,(HDEHP)_{2,\,org} \Leftrightarrow Cf(DEHP)_3(HDEHP)_{3,org} + 3\,H^+_{aq} \qquad (1)$$

in agreement with the Eu^{3+} results. The extraction constant for Cf^{3+}, K_{ex}, was determined to be 0.493 ± 0.048.

$-\log [H^+]_{aq}$	$[(HDEHP)_2]_{org}$, M	$[PMDPA]_{aq}$, M	Number of Concentrations
0.981	0.0250 - 0.250	0	8
0.981 - 1.998	0.0250	0	8
0.981	0.250	0 - 0.020	10
1.266	0.125	0 - 0.016	10
1.656	0.050	0 - 0.012	10
1.998	0.025	0 - 0.008	10

Table 1. Solution Compositions for Extraction Studies

The effect of PMDPA on the Cf^{3+} extraction equilibrium was measured by varying the concentration of PMDPA at four different sets of -log $[H^+]$ and HDEHP concentrations, as summarized in Table 1. The normalized extraction data are shown in Figure 2. Slope analysis of the extraction data indicate that Cf complexes containing 1, 2, and 3 molecules of PMDPA form in the

aqueous phase under these experimental conditions. If we assume that only mononuclear complexes are formed and that Cf-PMDPA complexes are not extracted, the stability constant, β_n^*, of the hypothetical equilibrium,

$$Cf^{3+} + n\ PMDPA^{4-} = Cf(PMDPA)_n^{3-4n} \quad (2)$$

can be calculated at each -log [H^+] for n = 1, 2, and 3 according to the standard solvent extraction equation

$$\frac{D_o}{D} = 1 + \sum_{n=1}^{3} \beta_n^* [PMDPA^{4-}]^n \quad (3)$$

where D_o is the distribution coefficient of Cf^{3+} in the absence of PMDPA. D_o is calculated from K_{ex}, [(HEDHP)$_2$], [H^+], and the slopes of the extractant and acid dependencies. Slope analysis of the dependence of log β_1^*, log β_2^*, and log β_3^* on log [H^+] gives three lines representing the average H^+ stoichiometry of the 1:1, 1:2, and 1:3 Cf:PMDPA complexes respectively.[5] Next, the full set of distribution ratios were systematically fit to the expression

$$\frac{D_o}{D} - 1 = \sum_{n=1}^{3} \sum_{h=0}^{2n} \beta_{hn} [H^+]^h [H_2PMDPA^{2-}]^n \quad (4)$$

by weighted non-linear least squares regression to obtain the stoichiometries and stability constants, β_{hn}, of the $CfH_h(H_2PMDPA)_n^{3+h-2n}$ complexes. The parameters giving the best fit and the uncertainties are summarized in Table 2.

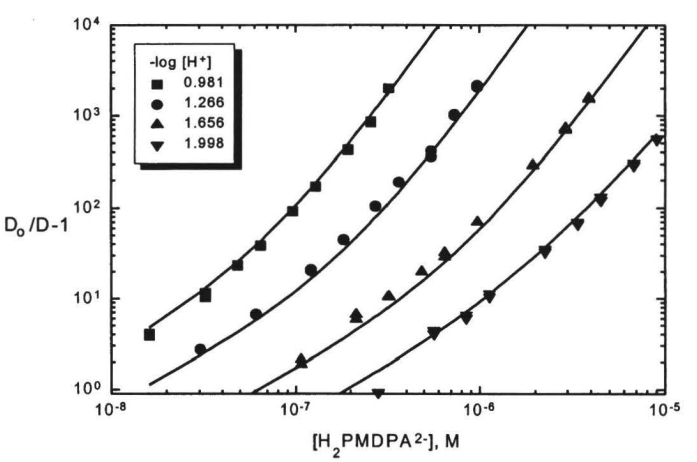

Figure 2. HDEHP/toluene extraction of Cf^{3+} from 2 M H/$NaClO_4$ at 25°C fit to Equation 4. Lines are the fit of the data to the model of Table 2.

The stoichiometries of the Cf-PMDPA complexes derived from the extraction experiments (Table 2) are the same as those previously observed for the Eu-PMDPA complexes in the same range of acidity and ligand concentration. The stability constants of the Cf-PMDPA complexes are comparable to those of Eu^{3+}, and are the same within experimental error for the 11, 21, and 42 complexes. The stability constants are slightly higher for Cf^{3+} in the case of $Cf(H_3PMDPA)_2^+$ and $CfH_2(H_3PMDPA)_3^{2+}$, which may also be written as $Cf(H_3PMDPA)(H_4PMDPA)_2^{2+}$.

Species	Stoichiometry, *h n*	Cf^{3+} Log β_{hn}	Eu^{3+} Log β_{hn}
$Cf(H_3PMDPA)^{2+}$	1 1	8.42 ± 0.16	8.56
$Cf(H_4PMDPA)^{3+}$	2 1	10.22 ± 0.11	9.92
$Cf(H_3PMDPA)_2^{+}$	2 2	16.62 ± 0.06	16.21
$Cf(H_4PMDPA)_2^{3+}$	4 2	19.56 ± 0.12	19.47
$CfH_2(H_3PMDPA)_3^{2+}$	5 3	27.47 ± 0.06	27.13

Table 2. Measured Cf^{3+}-H^{+}-H_2PMDPA^{2-} stability constants compared with Eu^{3+} stability constants[8]

These differences in the stability of the aqueous phase complexes are not sufficient, however, to separate Eu^{3+} from Cf^{3+} by HDEHP extraction. Using the constants measured for Eu^{3+} and Cf^{3+}, the distribution of these metal ions into HDEHP/toluene may be calculated for comparison. Between -log $[H^{+}]$ 0 and 3 and in the presence of 0.01 M PMDPA, the separation factor Eu/Cf = 1.0 ± 0.1 for HDEHP/toluene extraction. This is comparable to the value 0.9 reported by Stary in the absence of PMDPA.[11] There is no significant separation between the trivalent lanthanides and actinides, unlike the original TALSPEAK process, which gives a Eu/Cf separation factor of 16.[4]

The lack of Ln/An separation by PMDPA indicates that the piperidino nitrogen does not bind the metal center under the conditions studied. The affinity of the piperidino nitrogen for H^{+} is substantial, as indicated by pK_a=11.5. However, the basicity of this amino group can be compared to the amino groups of 1,2-dimethylethylenedinitrilotetraacetic acid (pK_a = 11.53, I=0.1 M), nitrilotriacetic acid (pK_a=9.34, I=1.0 M), and iminodiacetic acid (pK_a=9.26, I=1.0 M).[12] In each of these ligand systems the amino nitrogen is coordinated to Ln or An cations in the respective 1:1 complexes. Therefore, the H^{+} affinity of PMDPA's nitrogen probably is not an intrinsic limitation on metal binding and does not account for the absence of an interaction with Eu^{3+} or Cf^{3+}. With this in mind, it is likely that the ligand geometry is responsible for the absence of direct complexation of the metal cations by the PMDPA nitrogen. These results suggest that a ligand incorporating aliphatic amines and phosphonate groups not bound to the same methylene group might be a more promising reagent for Ln/An separations.

CONCLUSIONS

Despite the simplifications in aqueous phase feed adjustment and waste disposal that would be realized if an aminomethanediphosphonic acid could be substituted for lactic acid and DTPA in a TALSPEAK flowsheet, PMDPA shows no significant preference for trivalent actinides over trivalent lanthanides in 2 M H/$NaClO_4$ between -log $[H^{+}]$ 1 and 2. The lack of differentiation between the Eu and Cf cations, implies that the piperidino nitrogen of PMDPA, which would bind Cf^{3+} more strongly, does not bind either metal ion under the conditions studied due to the geometric constraints of the ligand.

ACKNOWLEDGMENTS

The ^{249}Cf tracer was provided by REDC/HFIR at Oak Ridge National Laboratory. This work was performed under the auspices of the US Department of Energy, Office of Basic Energy Science, Division of Chemical Sciences under Contract number W-31-109-ENG-38.

REFERENCES

1. Smith, BF, Jarvinen, GD, Miller, GG, Ryan, RR and Peterson, EJ, *Solv. Extr. Ion Exch.* **5**, 895, (1987).
2. Musikas, C., "Actinide-Lanthanide Group Separation Using Sulfur and Nitrogen Donor Extractants" in *Actinide/Lanthanide Separations* Proceedings of an International Symposium, Honolulu, Hawaii, 16-22 December, 1984. (G. R. Choppin, J. D. Navratil, and W. W. Schulz eds.), World Scientific Publishing, Singapore, p. 19. (1985)
3. Nash, KL, *Solv. Extr. Ion Exch.* **11,** 729, (1993)
4. Weaver, B and Kappelmann, FA, *J. Inorg. Nucl. Chem.*, **30**, 263, (1968).
5. Nash, KL, Horwitz, EP, *Inorg. Chim. Acta*, **169**, 245, (1990).
6. Nash, KL, *Radiochim. Acta*, **54**, 171, (1991).
7. Nash, KL, *Radiochim. Acta*, **61**, 147, (1993).
8. Jensen, MP, Rickert, PG, Schmidt, MA and Nash, KL, *J. Alloys and Compounds*, **249**, 86, (1997).
9. Lumetta, GJ and Swanson, J. L., *Sep. Sci. Tech.*, **28**, 43, (1993).
10. Shannon, RD, *Acta Crystallographica*, **A32,** 751, (1976).
11. Stary, J, *Talanta*, **13**, 421, (1966).
12. Martell, AE, Smith, RM and Motekaitis, RJ, '*Critically Selected Stability Constants of Metal Complexes Database Version 3.0*', Gaithersburg, Maryland, USA, 1997.

EXTRACTION AND SEPARATION OF LANTHANIDES AND ACTINIDES IN AQUEOUS NITRIC ACID BY 'CMPO-LIKE' CALIXARENES

A García-Carrera, H Rouquette, JF Dozol, V Böhmer[1] and AM Sastre[2]

C.E.A./ D.C.C./ D.E.S.D./ S.E.P./ L.P.T.E. Atomique Energy Commissariat, C.E.A. Cadarache, 13108 Saint Paul lez Durance, France

[1] Institut für Organische Chemie, Johanes-Gutenberg-Universität, J.J.BecherWeg 34, SBI, D-5509 Mainz, Germany

[2] Department of Chemical Engineering, E.T.S.E.I.B., Universitat Politècnica de Catalunya, Diagonal 647, E-08028 Barcelona, Spain

ABSTRACT

Calix[4]arenes substituted by acetoamidophosphine oxide groups (CMPO moieties) at their wider (upper) and narrower (lower) rim are exceptionally powerful extractants towards trivalent lanthanides and actinides from aqueous nitric acid media, allowing a separation of actinides from the most of the lanthanides, except the lightest ones. These separative properties determined by solvent extraction measurements are kept when supported liquid membrane (SLM's) transport experiments are performed.

Keywords: Extraction, separation, lanthanide, actinide, calixarene, acetoamidophosphine oxide groups (CMPO)

INTRODUCTION

High and medium level activity liquid wastes are produced during the reprocessing of spent nuclear fuel by the PUREX process, used to recover Plutonium and Uranium. Acid nitric liquid wastes contain important concentrations of transplutonium elements, the most harmful long lived radionuclides, and fission products, like trivalent lanthanides.

Separation of the trivalent actinides (transplutonium elements) from lanthanides is one of the problems in separation science, being a strategy for the clean-up, to enable their destruction by incineration, and reducing the volume of high radioactive liquid wastes from reprocessing of nuclear reactor fuels (PUREX raffinate).

Separation of these elements by solvent extraction has been carried using different extractants, most of them are not efficient in acidic medium. CMPO (octyl(phenyl)-N,N-di-isobutyl-carbamoylmethylphosphine oxide) (figure 1), used in TRUEX process, has been extensively studied for the extraction of lanthanides (Ln) and actinides (An), but displays a low discrimination of An from Ln.[1]

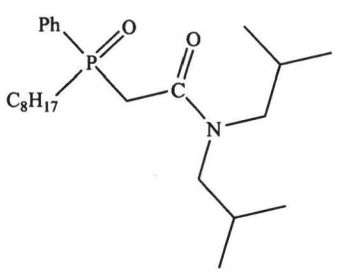

Figure 1. Structure of the CMPO molecule

On the contrary, calix[4]arenes [2] bearing CMPO moieties are stronger extractants than CMPO and they are able to separate light lanthanides from heavy ones and the smallest transplutonium (III)

© 2000 Society of Chemical Industry

elements from lanthanides (III) in aqueous nitric acid media. These liquid-liquid extraction measurements are confirmed by transport experiments through supported liquid membranes (SLM).

EXPERIMENTAL

The calixarenes bearing CMPO moieties, used in this study, were synthesised by Böhmer (University of Mainz). This new class of extractants combines the extracting ability of carbamoylmethylphosphine oxide groups with the preorganization of calixarenes (Figure 2).

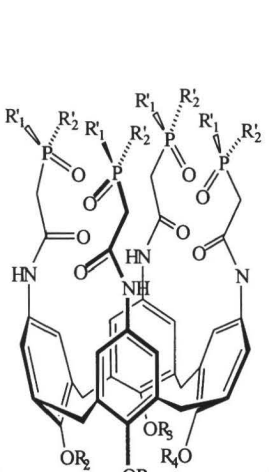

(1)(1')

(1) (R'_1=R'_2=Ph)
MN1:R_1=R_2=R_3=R_4=C_5H_{11}
MN49:R_1=R_2=R_3=R_4=CH_3
MN50:R_1=R_2=R_3=R_4=C_3H_7
MN23:R_1=R_3=C_5H_{11} ; R_2=R_4=CH_3
MN37:R_1=R_2=C_3H_7;R_3=R_4=CH_3
MN51:R_1=R_3=CH_3 ; R_2=R_4=C_3H_7
MN52:R_1= R_2=R_3=CH_3 ; R_4=C_3H_7
MN53:R_1= R_2=R_3=C_3H_7 ; R_4=CH_3
MN36:R_1=R_2=R_3=R_4=C_5H_{11} (linear tetramer)

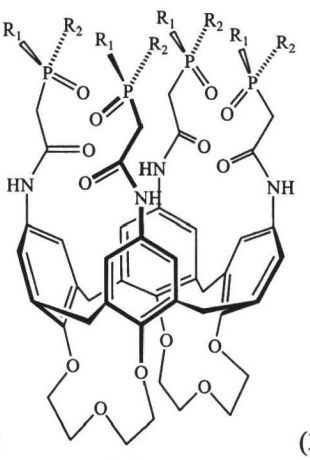

(2)

MN47:R_1=R_2=OC_2H_5
MN48:R_1=Ph; R_2=OC_2H_5

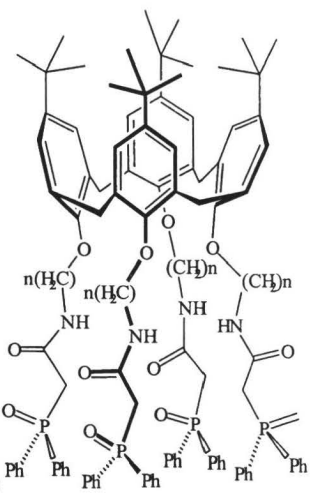

(3)

MN54: n=2
MN45: n=3
MN46: n=4

(1')(R_1=R_2=R_3=R_4=C_5H_{11})
MN38: R'_1=OC_2H_5; R'_2=Ph
MN39: R'_1= R'_2=OC_2H_5

Figure 2. Structure of the CMPO-like calix[4]arenes

Solvent Extraction

An aqueous phase was prepared varying concentrations of nitric acid (0.01 - 4 mol/dm^3). Inactive lanthanides were included at concentrations of 10^{-5} mol/dm^3. Americium, as the radioisotope ^{241}Am, and ^{244}Cm, were used at a concentration of ~10^{-9} mol/dm^3 to give an activity of approximately 1000-1500 kBq/dm^3. An aliquot of aqueous phase was then shaken at room temperature for one hour with an aliquot of the organic phase (C_L= 10^{-3} mol/dm^3 in 1,2-nitrophenylhexyl ether (NPHE)). After centrifugation the concentration of the lanthanides and ^{241}Am was determined by ICP-MSS in the aqueous phase. Alfa activity of Curium-244 was determined by liquid scintillation in the aqueous and organic phase. Distribution Coefficient D was calculated from:

$$D = \frac{[M]_{org}}{[M]_{aq}}$$

Supported liquid membranes

The thin flat sheet supported liquid membrane (SLM) device, described by Stolwijk *et al.*[3], was used. Equal volumes of feed and stripping solutions, varying from 45 to 50 cm^3 were used with membrane areas between 15 to 16 cm^2 (Figure 3). The support used was a Celgard 2500 membrane possessing the following characteristics : thickness: 25 µm, porosity: 45%, average pore diameter: 0.04 µm. The SLM was prepared by soaking the Celgard membrane in the organic phase containing the calixarene ($C_L = 10^{-3}$ mol/dm^3) diluted in NPHE.

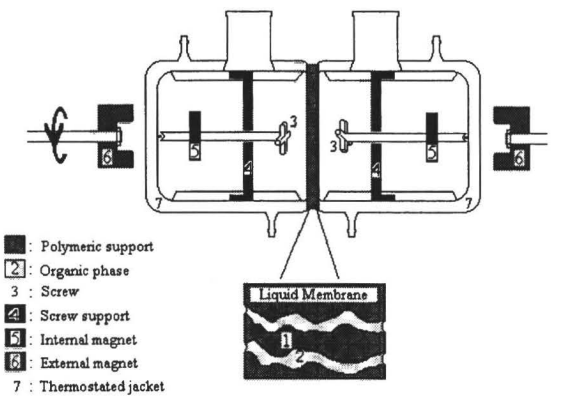

Figure 3 Supported liquid membrane set-up

The transport of the cations from the feed solution, spiked with radionuclides was followed by regular measurement of the decrease of radioactivity in the feed solution or its increase in the stripping solution. This allows graphical determination of the constant permeabilities P_f and P_S (cm h^{-1}) of M, respectively from feed and stripping solutions, by plotting the logarithm of the ratio C/C° (or 1-C'/C°) versus time, as described in the model proposed by Danesi:[4]

$$\mathrm{Ln}\left(\frac{C}{C_0}\right) = -\frac{\varepsilon S}{V} P_f t \qquad \mathrm{Ln}\left(1-\frac{C'}{C_0}\right) = -\frac{\varepsilon S}{V} P_s t$$

where:
C, C' : concentration of the cation respectively in the feed or stripping solution at time *t*.
C : initial concentration of the cation in the feed solution.
ε : volumetric porosity of the S.L.M. (%).
S : membrane surface area (cm^2).
V : volume of feed or stripping solution (cm^3)
t : time (h)

RESULTS AND DISCUSSION

The CMPO molecule and different calix[4]arenes bearing CMPO moieties on the large rim (*upper rim*) and on the narrow rim (*lower rim*) have been studied, extraction measurements of some lanthanides and the two main trivalent transuranium elements present in spent nuclear fuel were carried out.

CMPO, although used at a concentration 250 higher than calixarenes (0.25 mol/dm^3), is less efficient than most of the calix[4]arenes-CMPO,[5,6] moreover like the tetramer it displays a low selectivity towards the lanthanides or the two actinides. These results show the role of the calixarene

platform, as lanthanide distribution coefficients are enhanced and a discrimination of lanthanides, not easily discernible for CMPO and linear tetramer, is important for most of the calixarenes bearing CMPO moieties (Figure 4).

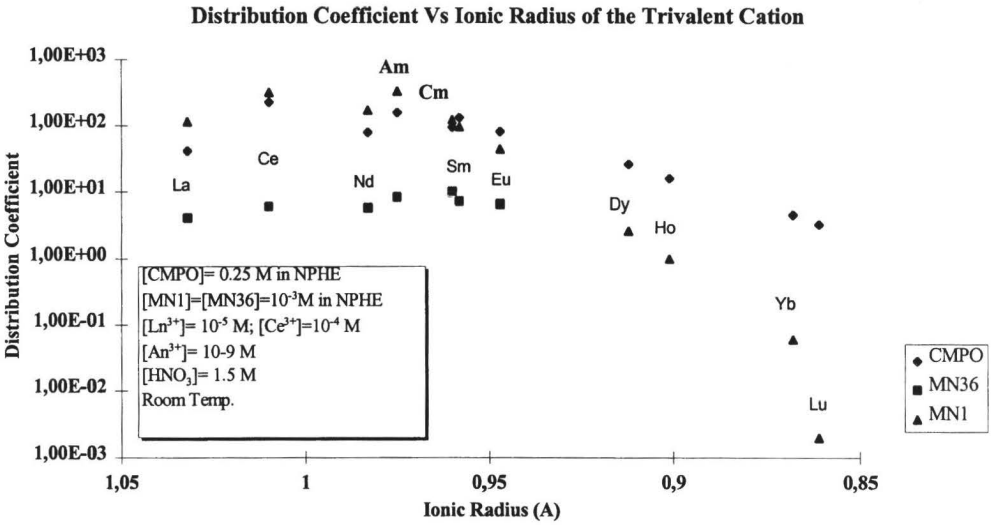

Figure 4. Plots of the distribution coefficients vs. ionic radius of the trivalent cation for CMPO, MN36 (linear tetramer) and MN1.

The conformational mobile wide rim CMPO-calix[4]arenes, which bear shorter alkoxy chains than pentoxy on the lower rim, (MN23, MN37, MN49, MN50, MN51, MN52, MN53) display a similar behaviour to MN1, however americium distribution coefficients are higher and otherwise, the separation factor americium/lanthanides (Figure 5). This fact could be explained since the conformational flexibility of the compounds can favour the interaction of the americium (*softer* cation than trivalent lanthanides) with the π-electron cloud of the arene rings. This effect has been described[7] for the interactions between caesium cation and the calix[4]arenecrowns in 1,3-alternate conformation.

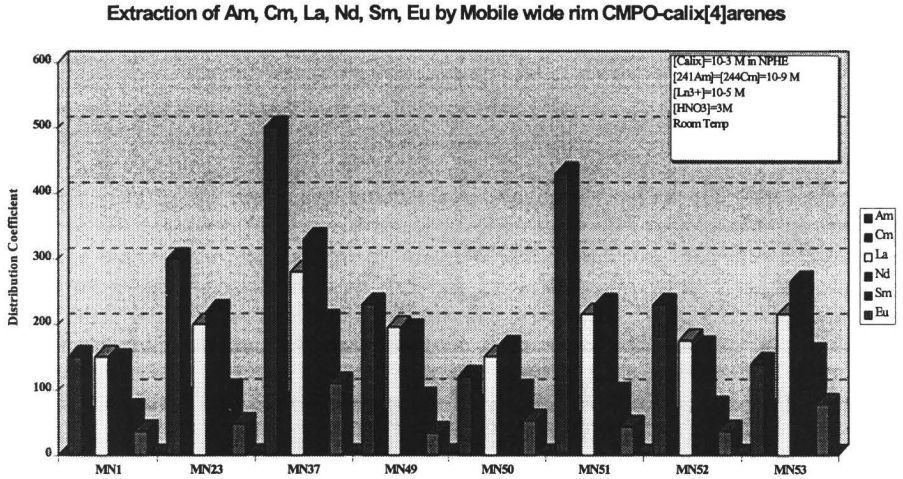

Figure 5. Plots of the distribution coefficients of Am, Cm, La, Nd, Sm and Eu vs. extractant (mobile calix[4]arenes).

Narrow rim CMPO-calixarenes are less efficient extractants for all the cations examined than MN1 although extraction efficiency increases at higher acidities, this can be explained by a cavity too small to accept cations. However MN46 and MN45 have different selectivity profiles to that seen for the upper rim molecules. With upper rim calixarenes the light lanthanides (larger cationic radius) are extracted more efficiently than the heavy lanthanides (smaller cationic radius). In contrast a reverse order is seen for compounds MN45 and MN46, where the lightest lanthanides (La, Nd) are less extracted than heavier ones (Eu). Thus D_{Am}/D_{Eu} for MN46 in 3 mol/dm^3 HNO_3 is 1.3 and for MN1 is 4.9 whereas D_{Am}/D_{La} is 2.0 for MN46 and 1.0 for MN1. It is interesting to observe a maximum extraction for curium from 3 mol/dm^3 HNO_3 concentration, a smaller cation than Am(III), using MN45 as extractant (Figure 6).

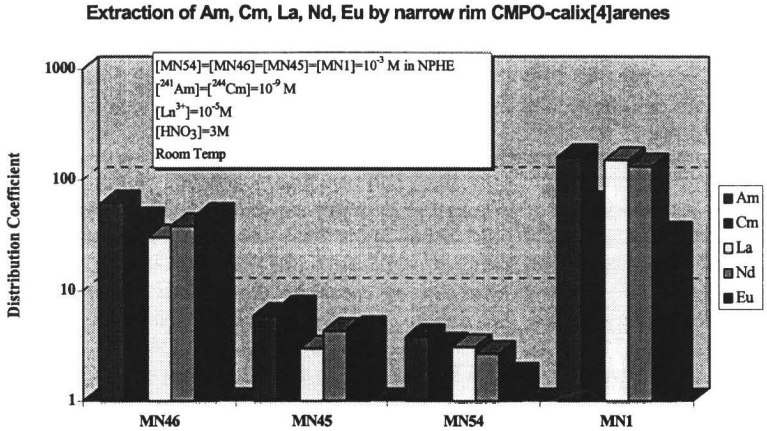

Figure 6. Distribution coefficients of Am, Cm, La, Nd and Eu vs extractant (narrow rim calixarenes).

Horwitz et al.[8] showed that the extraction efficiency was improved when phenyl groups were attached to the phosphoryl group. Replacing the phenyl units attached to phosphoryl group of CMPO

moieties by ethoxy chains (MN38, MN39), caused the actinide/lanthanide extraction to decrease strongly when compared to MN1.

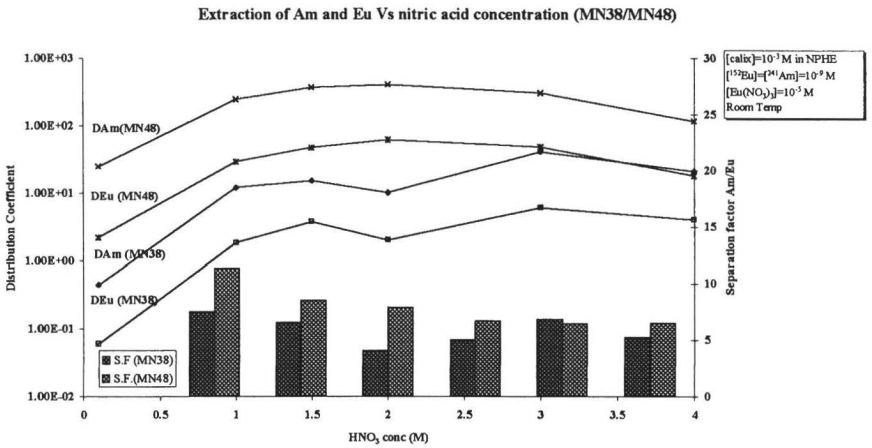

Figure 7. Distribution coefficients and separation factors Am/Eu vs extractant. Influence of the structure rigidity.

In addition, the *rigid* calixarene MN48, presenting the same phosphoryl substituents as those of MN38 but having crown-3 bridges on the lower rim between adjacent phenyl units of the calixarene skeleton, gives a significant improvement in the extraction efficiency in comparison with MN38, but selectivity Am/Eu remains similar (Figure 7).

MN39, bearing two ethoxy chains attached to the phosphoryl groups of the CMPO moieties, shows a different extraction behaviour. The basicity of the phosphoryl group is affected (lower basicity than MN38 or MN1) and consequently selectivity is changed. Extraction of americium decreases and becomes lower than that of the lightest lanthanides (La-Nd).

To assess the actinide/lanthanide ability separation of the extractants, CMPO (0.25 mol/dm^3) and CMPO-like calix[4]arenes, competitive transport experiments have been carried out using aqueous feed solutions containing ^{241}Am and different mixtures of lanthanides in the nitric acid medium which gives the best extraction/separation results (2 mol/dm^3 HNO_3) and narrow rim CMPO-calixarenes. MDP 1mol/dm^3 was used as stripping solution to allow back extraction of the cation from the SLM. Under these conditions, transports follow Danesi's model, allowing the determination of permeability coefficients (Table 1).

	^{152}Eu			^{241}Am			
	P_S (cm/h)	P_F (cm/h)	Tr_{2h} (%)	P_S (cm/h)	P_F (cm/h)	Tr_{2h} (%)	P_SAm/P_SEu
CMPO	8.80	9.49	87	11.06	11.73	81	1.26
MN1	12.22	10.35	90	22.84	18.41	99	1.87
MN23	7.68	8.43	77	19.35	20.10	91	2.52
MN37	16.03	11.20	93	14.36	13.88	93	0.89
MN54	0.21	1.31	3	0.61	5.91	8	2.90
MN45	0.71	1.22	15	1.18	3.52	24	1.66
MN46	1.25	1.18	25	1.63	2.54	33	1.30

Tr_{2h} (%): % transported to the stripping solution after 2 hours

Table 1. Experimental Americium and Europium Permeabilities.
Organic Phase: 10^{-3} mol/dm^3 of extractant- 0.25 mol/dm^3 CMPO- in NPHE.
Aqueous Feed Solution (900 rpm): HNO_3 2 mol/dm^3 + ^{241}Am + ^{152}Eu (10^{-9} mol/dm^3)
Aqueous Stripping Solution (900 rpm): MDP 1mol/dm^3

Table 1. Experimental Americium and Europium Permeabilities.
Organic Phase: 10^{-3} mol/dm^3 of extractant- 0.25 mol/dm^3 CMPO- in NPHE.
Aqueous Feed Solution (900 rpm): HNO_3 2 mol/dm^3 + ^{241}Am + ^{152}Eu (10^{-9} mol/dm^3)
Aqueous Stripping Solution (900 rpm): MDP 1mol/dm^3

Just like the solvent extraction results for the upper rim calixarenes, MN23 (mobile conformation), provides the best separation factor Am/Eu, but due to the excellent ligand *extraction* and MDP *stripping*, it is so difficult to appreciate the differences of performance of the extractants.

Due to the relative "discrimination" Americium/lanthanides of MDP like stripping reagent, experiments using different concentration (0.5 and 1mol/dm^3) have been made. Results show the influence of MDP on the separation actinide/lanthanide, when MDP 0.5 mol/dm^3 has been used like stripping solution permeability coefficients decrease as compared to MDP 1M, but, on the contrary, ratio $P_S Am/P_S Eu$ increase (Figure 8). This strong difference of permeability when the MDP concentration is divided by a factor 2 seems to indicate that the limiting step in the transfer is the *back-extraction*.

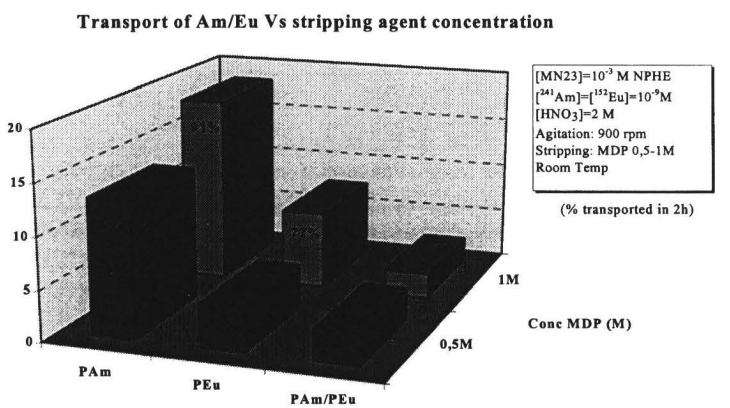

Figure 8. Plots of permeability coefficients of Am/Eu vs stripping agent concentration for the calixarene MN23.

REFERENCES

1. Horwitz EP, Kalina DG, Vandergrift GF and Schulz WW, *Solv. Extr.Ion Exch.*, **3** (1-2), 75, (1985).
2. Böhmer V, *Angew. Chem.*, **107**, 785, (1995).
3. Stolwijk TV, Sudhölter EJR and Reinhoudt DN, *J. Am. Chem, Soc*, **109**, 7042, (1987).
4. Danesi PR, Sep. Sci. and Technol., **19**, (11&12), 857, (1984-85).
5. Delmau L, Simon N, Schwing-Weill MJ, Arnaud-Neu F, Dozol JF, Eymard S, Tournois B, Böhmer V, Grüttner C, Musigmann C and Tunayar A, *Chem Commun.*, 1627, (1998)
6. Arnaud-Neu F, Böhmer V, Dozol JF, Grüttner C, Jakobi RA, Kraft D, Mauprivez O, Rouquette H, Schwing-Weill MJ, Simon N and Vogt W, *J. Chem. Soc. Perkin Trans.*, **2**, 1175, (1996).
7. Ungaro R, Casnati A, Ugozzoli F, Pochini A, Dozol JF, Hill C and Rouquette H, *Angew. Chem*; Int. Ed; Engl., **33** (14), 1506, (1994).
8. Horwitz EP, Martin KA, Diamond H and Kaplan L, *Solv. Extr. Ion Exch.*, **4** (3), 449, (1986).

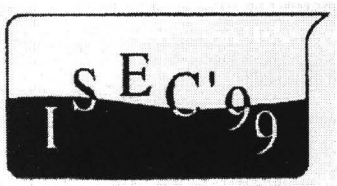

SOLVENT EXTRACTION OF RARE EARTH ELEMENTS(III) WITH A BIFUNCTIONAL PHOSPHINIC ACID

Yoshito Wakui, Toshirou Yokoyama and Kenichi Akiba[1]
Tohoku National Industrial Research Institute, 4-2-1, Nigatake, Miyagino, Sendai 983-8551, Japan
[1]Institute for Advanced Materials Processing, Tohoku University, Katahira 2-1-1, Aoba, Sendai 980-8577, Japan

ABSTRACT
A novel bifunctional compound, 1,3-benzenedimethylbis(phenylphosphinic acid) (m-xylenebis(phenylphosphinic acid); XPPA) was synthesized as a model of a dimer of monofunctional phosphorus extractants. Distribution ratios (D) of rare earth elements(III) were obtained between a chloroform solution of XPPA and an acidic aqueous solution. Extractability of XPPA was very high compared with those of conventional monoacidic extractants. Difference in log D value between La(III) and Lu(III) was about 5. An extracted species was estimated to be $[M(HR)_3(H_2R)_x]$ (x = 1, 2), and then XPPA molecule seems to behave as a bidentate ligand, and to successfully simulate the properties of a dimer of monofunctional extractants.

Keywords: rare earths, bifunctional extractant, 1,3-benzenedimethylbis(phenylphosphinic acid),La, Lu.

INTRODUCTION

Solvent extraction by organophosphorus compounds have been extensively applied for the separation of rare earth (RE) elements, in experimental and industrial solvent extraction.[1,2] Acidic organophosphorus extractants have been commonly employed owing to large separation factors between RE elements(III), in spite of their simple molecular structures. For example, bis(2-ethylhexyl)hydrogen phosphate (D2EHPA), 2-ethylhexylhydrogen 2-ethylhexyl-phosphonate (EHEHPA) and bis(2,4,4-trimethylpentyl)phosphinic acid (DTMPPA) are well known to have high separation efficiencies for a series of RE(III) elements.[3-6] These extractants ordinarily exist as dimers in nonpolar solvents, and the dimer behaves like a chelating ligand having two coordinating groups to a metal ion.[7] However, the information on functions of such a dimeric structure is still insufficient.

In this paper, we aimed at developing an extractant having double acidic organophosphorus groups as a model of the dimer of monofunctional extractants. A novel compound, 1,3-benzenedimethylbis(phenylphosphinic acid) (XPPA), was synthesized. It was expected to have a fairly rigid structure to keep an appropriate distance between two functional groups. The distribution ratio of RE(III) elements was obtained between a chloroform solution of XPPA and an acidic aqueous solution, and extracted species in the organic phase are also estimated.

EXPERIMENTAL

Equipment

The concentrations of metals were measured with a ICP atomic emission spectrophotometer (ICP-AES, SEIKO SPS-1200A). A digital pH meter (TOA AUT-301) was used for the pH measurement. Osmometric concentration of the product in chloroform was determined with a vapor pressure osmometer (UIC Inc. 070B).

© 2000 Society of Chemical Industry

Reagents

The extractant, 1,3-dimethylbenzene-bis(phenylphosphinic acid) (m-xylene-bis(phenylphosphinic acid); XPPA; Fig. 1), was synthesized by the method of Boyd *et al.*[8]

The product was purified by solvent extraction between dichloromethane and water, and by

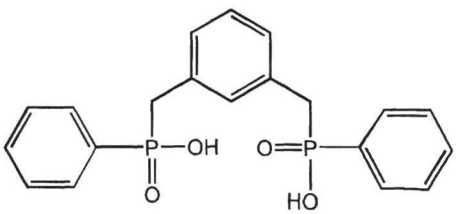

Fig. 1
1,3 - Benzenedimethyl bis(phenylphosphinic acid)
(XPPA)

reprecipitation. A white powder was obtained; yield: 98%; mp 194 - 199°C; calcd. for $C_{20}H_{20}O_4P_2$: C, 62.2; H, 5.2; P, 16.0%; found: C, 60.7; H, 5.1; P, 15.5%; molar absorption coefficient (ε / $dm^3mol^{-1}cm^{-1}$) in chloroform: 1200 at 259 nm, 1600 at 265 nm and 1400 at 272 nm. The compound was identified by ^1H NMR, ^{13}C NMR and infrared spectrometry. Solubility was approximately 2 x 10^{-3} M (M = mol dm^{-3}) in chloroform saturated with water.

RE(III) solutions were prepared by dissolving the corresponding oxides (99.9%) into hydrochloric acid. Chloroform (Dojindo Laboratories) was of analytical grade and was contacted with water prior to use. Benzil (zone refined, Tokyo Kasei Kogyo Co.,Ltd.) was employed as a reference material for calibration of the osmometer. Hydrochloric acid was of analytical grade, and the other chemicals were of guaranteed grade.

Solvent extraction

An aqueous solution containing RE(III) and a chloroform solution containing XPPA were equilibrated by a shaker (Yamato KC-30) for 30 min in a room thermostated at 25°C. After centrifuging, an aliquot of the aqueous phase was taken out for ICP measurement. The distribution ratio (D) was obtained as the ratio of the concentration of metal in the organic phase to that in the aqueous phase.

RESULTS AND DISCUSSION

To elucidate the aggregation phenomenon of the extractant, we measured the osmometric concentration of 1 x 10^{-3} M XPPA in chloroform at 25°C. The observed concentration was found to be about half of that calculated for monomeric molecules, indicating that XPPA exists as a dimer in chloroform.

The effect of metal concentration on the distribution ratio was examined in order to check the possibility whether polynuclear complexes[9] are formed or not with XPPA having two ion exchangeable groups. In a concentration region of La(III) from 2 x 10^{-6} to 3 x 10^{-5} M, the D value with 10^{-3} M $[XPPA]_o$ at pH 1.1 was observed to be almost constant, log D = 0.39 ± 0.12, implying that no polynuclear species were formed in the extraction.

In subsequent experiments, the initial concentration of metal in the aqueous phase was fixed at 10^{-5} M.

The equilibrium for the extraction of RE(III) ions (M^{3+}) with XPPA (H_2R) was assumed to be as follows:

$$M^{3+} + m\,((H_2R)_2)_o \rightleftharpoons (MH_nR_{2m})_o + (4m-n)\,H^+. \qquad (1)$$

Subscript o refers the species in the organic solution. The extraction constant (K_{ex}) and the D value are given by Eqs. (2) and (3), respectively.

$$K_{ex} = \frac{[MH_nR2m]_o[H^+]^{(4m-n)}}{[M^{3+}][(H_2R)_2]_o{}^m} \quad (2)$$

$$D = \frac{[MH_nR2m]_o}{[M^{3+}]} \quad (3)$$

From Eqs. (2) and (3), following relationship is obtained:

$$\log D = \log K_{ex} + m \log [(H_2R)_2]_o + (4m-n)\ pH. \quad (4)$$

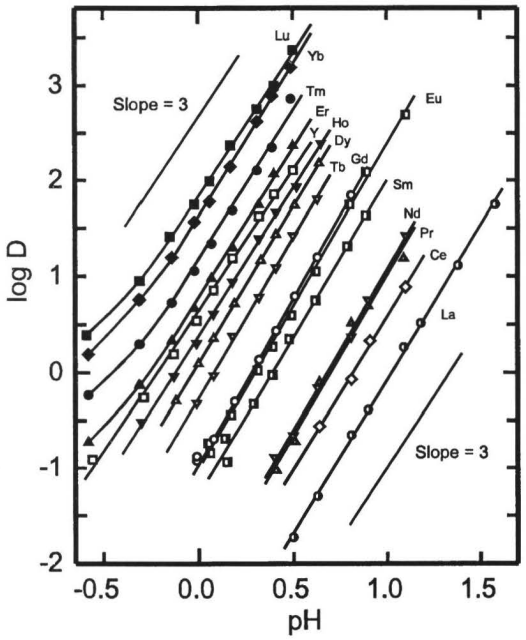

Fig. 2 Distribution ratio of rare earth elements(III) as a function of pH.
1 x 10^{-3} M XPPA in $CHCl_3$; 1 x 10^{-5} M each RE(III); V_a, V_o: 10 cm^3; 30 min; 25 °C; 0.1 M (H, Na)Cl when [HCl] < 0.1 M.

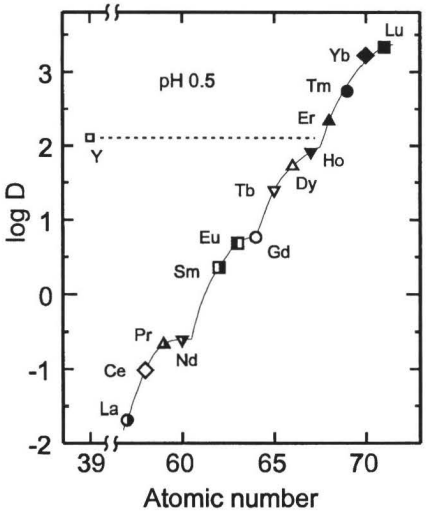

Fig. 3 Relationship between log D value and an atomic number of rare earth elements(III).
1 x 10^{-3} M XPPA in $CHCl_3$; 30 min; 25 °C;
1 x 10^{-5} M each RE(III); V_o, V_a: 10 cm^3.

Figure 2 shows log D *vs.* pH profiles for RE(III). For each element, linear plots have slopes of around 3, which indicate that three protons are released on extracting the metal ion: *i.e.*, 4m - n = 3.

Figure 3 shows relationship between log D at pH 0.5 and atomic number of RE(III). Tetrad effect[10] composed of divided curves is clearly observed on the plot. The difference in distribution ratios between La(III) and Lu(III) was fairly large; *i.e.*, about 5 in log units, which was comparable to those of traditional extractants[3,4] such as D2EHPA. The D value of Y(III) was located between Ho(III) and Er(III) similarly to the cases with D2EHPA *etc.*[3,10] These facts indicate some similarity in the extracted species with XPPA and monofunctional reagents having high separation efficiency.

The extractability of XPPA was found to be very high compared with those of conventional monofunctional extractants.[11] For example, log D of Ce(III) was 0.58 with 10^{-3} M XPPA in $CHCl_3$ at pH 1, while the value was estimated to be -5.4 for diphenylphosphinic acid under comparable conditions. This suggest that XPPA has higher extractability than that of monofunctional ones, which corresponds to the fact that a bidentate ligand forms a more stable complex than monodentate ones in various combinations of metal ions and reagents.[12,13] XPPA seems to have the potentiality as a strong extractant for RE(III) ions in low pH region.

Plots of log D against the concentration of XPPA dimer gave straight lines, as typically shown in Fig. 4. Slopes of the plots for RE(III) examined were illustrated in Fig. 5, in which the slope of nearly 2 was obtained for heavy lanthanides(III) and Y(III) while larger slopes for light lanthanides(III). According to Eq. (4), the extraction proceeds by the reaction in which 2 - 2.5 XPPA dimers participate, that is, about 5 molecules of XPPA monomer with respect to La(III), and 4 molecules with heavy lanthanides(III) and Y(III). Extraction constants (log K_{ex}) were estimated from Eq. (2) as shown in Table 1.

Since three protons are released upon complex formation, the extracted species would consequently contain three anionic extractants and one or two neutral ones: *i.e.*, $M(HR)_3(H_2R)$ or $M(HR)_3(H_2R)_2$.

This difference in composition corresponds to a decrease in a coordination number of lanthanide series, *i.e.*, from 9 or 10 for light lanthanides(III) to 8 for heavy ones.[14,15] XPPA molecules form RE(III) complexes filling the coordination number of the ion, implying that each ligand has two coordination bonds.

The ^{31}P NMR spectrum of Lu(III) complex extracted to an organic phase (Lu(III) : XPPA = 1 : 4) showed 8 peaks which shifted from the original signal of XPPA free acid. This finding suggests that XPPA acts like a chelating ligand.

A XPPA molecule acting as a bidentate

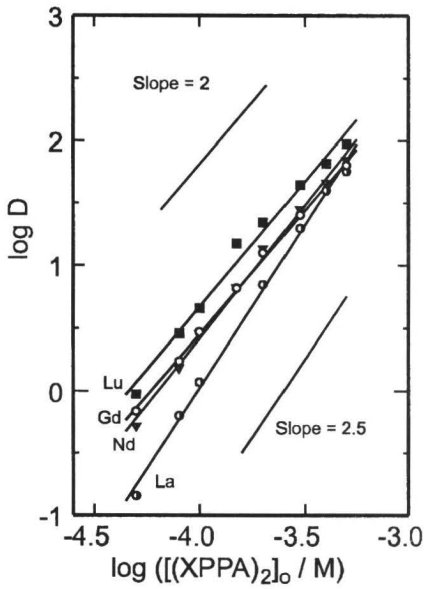

Fig. 4 Distribution ratio of rare earth elements(III) as a function of a concentration of XPPA dimer in chloroform.
pH: 1.6 for La(III), 1.2 for Nd(III), 0.8 for Gd(III), 0.1 for Lu(III); 1 x 10^{-5} M each RE(III); V_a, V_o: 10 cm^3; 30 min; 25°C; 0.1 M (H, Na)Cl when [HCl] < 0.1 M.

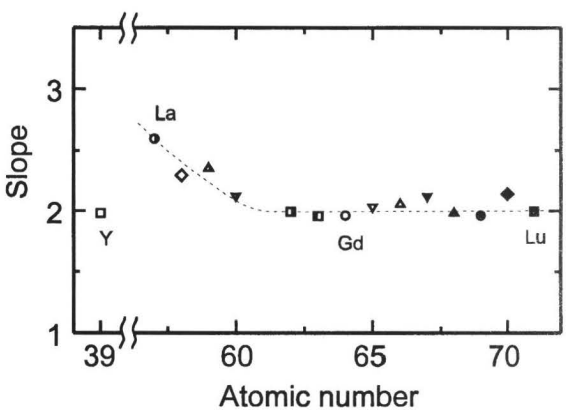

Fig. 5 Variation of slope of log D *vs.* log $((XPPA)_2)_o$ graphs, with atomic number of rare earth elements(III).
1 x 10^{-5} M each RE(III); V_a, V_o: 10 cm^3; 30 min; 25°C; 0.1 M (H, Na)Cl when [HCl] < 0.1 M.

ligand can successfully simulate the separation properties of a dimer of conventional monofunctional extractants. A coordinating structure including neighboring acidic phosphorus groups is essential for the excellent separation efficiency, and that such function can be produced by a bifunctional reagent without using dimers of monofunctional extractant. In addition, very high extractability enables quantitative extraction at low pH region by a diluted extractant. Further development of extractants having an analogous structure will contribute to improve the separation techniques of RE(III) ions both in analytical and industrial fields.

Table 1 Extraction constant of RE(III) with XPPA.

Element	m value* in Eq. (1)	log K_{ex}
Y	2.0	7.3 ± 0.1
La	2.5	5.2 ± 0.1
Ce	2.3	5.5 ± 0.3
Pr	2.3	5.7 ± 0.2
Nd	2.1	5.0 ± 0.1
Sm	2.0	5.5 ± 0.1
Eu	2.0	5.8 ± 0.1
Gd	2.0	5.9 ± 0.1
Tb	2.0	6.5 ± 0.1
Dy	2.0	6.8 ± 0.1
Ho	2.0	7.1 ± 0.1
Er	2.0	7.4 ± 0.1
Tm	2.0	7.8 ± 0.1
Yb	2.0	8.2 ± 0.1
Lu	2.0	8.5 ± 0.1

$CHCl_3$, V_a, V_o: 10 cm^3; 25 °C; 0.1 M (H, Na)Cl when [HCl] < 0.1 M.
*: Estimated value to calculate K_{ex}.

NOMENCLATURE

H_2R: XPPA in the neutral form.
M: trivalent rare earth element.
o: species in organic phase.
XPPA: 1,3-benzenedimethylbis(phenylphosphinic acid); extractant.

REFERENCES

1. Minczewski J, Chwastowska J and Dybczyński R, *"Separation and Preconcentration Methods in Inorganic Trace Analysis"*, Ellis Horwood Limited, Chichester, (1982).
2. Weaver B, *"Ion Exchange and Solvent Extraction"*, ed. J. A. Marinsky and Y. Marcus, **6**, chap. 4, Marcel Dekker, Inc., New York, (1974).
3. Peppard DP, Mason GW, Maier JL and Driscoll WJ, *J. Inorg. Nucl. Chem.*, **4**, 334 (1957).
4. Wakui Y, Matsunaga H and Suzuki TM, *Anal. Sci.*, **4**(3), 325 (1988).
5. Nakamura S, Takeyasu M and Akiba K, *Proc. Symp. Solvent Extr. 1991*, 45 (1991).
6. Komatsu Y, Freiser H, *Anal. Chim. Acta*, **227**(2), 397 (1989).
7. Peppard DF, Mason GW, Driscoll WJ and Sironen RJ, *J. Inorg. Nucl. Chem.*, **7**, 276 (1958).
8. Boyd EA, Regan AC and James K, *Tetrahedron Lett.*, **35**(24), 4223 (1994).
9. Noro J and Sekine T, *Bull. Chem. Soc. Jpn.*, **66**(8), 2242 (1993).
10. Peppard DF, Mason GW and Lewey S, *J. Inorg. Nucl. Chem.*, **31**, 2271 (1960).
11. Motomizu S and Freiser H, *Solv. Extn. Ion Exch.*, **3**(5), 637 (1985).
12. Hancock RD and Marsicano F, *J. Chem. Soc., Dalton Trans*, **1976**(12), 1096.
13. Hancock RD, Jackson G and Evers A, *J. Chem. Soc., Dalton Trans*, **1979**(9), 1384.
14. Bünzli J-C G, Metabanzoulou J-P, Froidevaux P and Jin L, *Inorg. Chem.*, **29**(19), 3875 (1990).
15. Helm L and Merbach AE, *Eur. J. Solid State Inorg. Chem.*, **28**(suppl), 245 (1991).

SOLVENT EXTRACTION OF LANTHANIDES AND YTTRIUM FROM NITRATE SOLUTIONS WITH CYANEX 923

Deqing Chu, Genxiang Ma and Deqian Li
Lab of Rare Earth Chemistry and Physics, Changchun Institute of Applied Chemistry, Chinese Academy of Sciences, Changchun, 130022 China

ABSTRACT
The extraction of lanthanides (La ~ Lu except Pm) and yttrium from nitrate solutions with Cyanex 923 in heptane has been systematically investigated. The extraction equilibrium constants and mechanism have been determined. The separation factors of lanthanides and yttrium from nitrate solutions have been evaluated and it has been found that their separation factors with purified Cyanex 923 are different from those with non-purified Cyanex 923. Also the dependence of temperatures on the extraction of lanthanides and yttrium has been studied with purified and non-purified Cyanex 923 and the thermodynamic parameters such as free energy (ΔG), enthalpy (ΔH) and entropy (ΔS) have been calculated. The results show that temperature significantly affects the separation of lanthanum and yttrium from rare earths. The well-regulated changes of these parameters with increasing atomic number of rare earth elements take place. The results of the separations with Cyanex 923 of lanthanum from light rare earths and yttrium from heavy rare earths have demonstrated their practicality.

Keywords: Cyanex 923, lanthanides, yttrium, mechanism of extraction, thermodynamics

INTRODUCTION

It is well-known that the P=O group of the neutral organophosphorus extractants plays an important role in the process of solvent extraction of metal ions. The extraction ability of metal ions increases with increasing oxygen electronic density in the P=O group, that is, $(RO)_3P=O$ < $(RO)_2RP=O$ < $(RO)R_2P=O$ < $R_3P=O$. Accordingly, extractants such as $(RO)R_2P$, $R_3P=O$ with higher extraction ability have become more and more important in the extraction of metal ions. Cyanex 923 is a mixture of four trialkylphosphine oxides (R_3PO), which has been recently produced by American Cyanamid Company, U.S.A.[1]

This extractant has the advantage of being liquid, completely miscible with all hydrocarbons, low solubility in the water, low extraction acidity and high extraction capacity.[2,3] It has been suggested as a potential extractant for the separation of zirconium and hafnium.[4] In spite of the reported extraction of several lanthanides and yttrium from thiocyanate and nitrate solutions with Cyanex 923,[5,6] the effects of temperature, the use of purified and non-purified extractants, and the effect different proportions of metal ions on the extraction and separation of all lanthanides and yttrium, provide still challenges. In the present study, the extraction of all lanthanides (except Pm) and yttrium from nitrate solutions with Cyanex 923 in heptane has been systematically investigated.

EXPERIMENTAL

Reagents and Solutions

Cyanex 923, supplied by Cyanamid Canada Inc., was used both as received without further purification, and with purification as described.[7] The contents of the extractant are similar to those published.[5] Heptane, analytical reagent quality, was used as a diluent in the present work.

Stock solutions of all lanthanide and yttrium ions were prepared by dissolving their corresponding oxides (>99.9%) with nitric acid. The concentrations of rare earth ions were determined either by EDTA titration or spectrophotometrically using Arsenazo III as an indicator. The initial concentration of Cyanex 923 was determined by the method of acid saturation.[7] The pH values in aqueous phase were measured by a pHS-3 model meter. All other reagents used were of analytical grade.

Distribution ratios were determined by shaking equal volumes of aqueous and organic phases for 30 minutes in a glass stopped vial placed in a thermostat box with help of a mechanical shaker at

© 2000 Society of Chemical Industry

298 ± 1°K except in the experiments with varying temperature. The initial concentration of lanthanides and yttrium was $2.0\sim4.0\times10^{-4}$ mol/dm^3. The concentration of metal ions in equilibrium aqueous phase was determined by spectrophotometer using Arsenazo III as an indicator and the concentration of metal ions in equilibrium organic phase was obtained by difference. These concentration values were used to obtain the distribution ratio, D.

RESULTS AND DISCUSSION

Extraction of lanthanides and yttrium with purified and non-purified Cyanex 923

At constant concentration of sodium nitrate (0.5 mol/dm^3) and Cyanex 923 (0.023 mol/dm^3) and constant pH (2.2), the extraction of lanthanides and yttrium from nitrate solutions with purified and non-purified Cyanex 923 has been studied. The relationship of logarithm of distribution ratio (log D) vs atomic number of lanthanides and yttrium are plotted in Figure 1. It is clearly seen that the D values increase with increasing atomic number of light rare earths with both purified and non-purified Cyanex 923, while D values decrease with increasing atomic number of heavy rare earths with purified Cyanex 923 but still increase with non-purified Cyanex 923. The position of yttrium is between Ce and Pr for non-purified Cyanex 923 but either between Ce and Pr or between Er and Tm for purified Cyanex 923, which demonstrates the significant possibility of complete separation of yttrium from heavy rare earths with non-purified Cyanex 923. It is also apparent that the extractability of rare earths(III) with purified Cyanex 923 was lower than that with non-purified Cyanex 923, this have been calculated under the present conditions, which provides important data for the analysis and selection of separation of rare earths. The results showed the acidic impurity in non-purified Cyanex 923 may increase the extractability. The separation factors of lanthanides and yttrium are given in Tables 1 and 2.

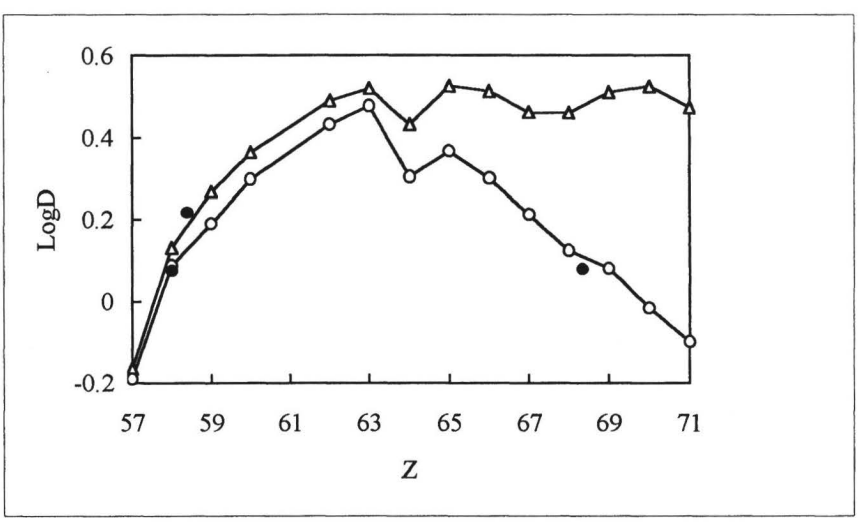

Figure 1. Relationship of Log D vs atomic number of rare earths (Z)
O purified Cyanex 923; Δ non-purified Cyanex 923; •-Yttrium

symb	Ce	Pr	Nd	Sm	Eu	Gd	Tb	Dy	Ho	Er	Tm	Yb	Lu	Y
La	1.98	2.72	3.38	4.52	4.84	3.95	4.91	4.76	4.24	4.22	4.73	4.90	4.36	2.78
Ce		1.37	1.71	2.28	2.44	2.00	2.48	2.40	2.14	2.13	2.39	2.47	2.20	1.40
Pr			1.25	1.66	1.78	1.46	1.81	1.75	1.56	1.55	1.74	1.80	1.60	1.02
Nd				1.34	1.43	1.17	1.45	1.41	1.25	1.25	1.40	1.45	1.29	0.82
Sm					1.07	0.88	1.09	1.05	0.94	0.93	1.05	1.08	0.96	0.62
Eu						0.82	1.01	0.98	0.88	0.87	0.98	1.01	0.90	0.57
Gd							1.24	1.21	1.07	1.07	1.20	1.24	1.10	0.70
Tb								0.97	0.86	0.86	0.96	1.00	0.89	0.57
Dy									0.89	0.89	0.99	1.03	0.91	0.58
Ho										1.04	1.17	1.21	1.08	0.69
Er											1.12	1.16	1.03	0.66
Tm												1.04	0.92	0.59
Yb													0.89	0.57
Lu														0.64

Table 1. Separation factors of rare earths with non-purified Cyanex 923

symb	Ce	Pr	Nd	Sm	Eu	Gd	Tb	Dy	Ho	Er	Tm	Yb	Lu	Y
La	1.89	2.40	3.08	4.19	4.65	3.13	3.61	3.10	2.53	2.00	1.80	1.49	1.23	1.96
Ce		1.27	1.63	2.21	2.46	1.64	1.91	1.64	1.34	1.06	0.95	0.79	0.65	1.04
Pr			1.28	1.75	1.94	1.31	1.50	1.29	1.05	0.83	0.75	0.62	0.51	0.82
Nd				1.36	1.51	1.02	1.17	1.01	0.82	0.65	0.58	0.48	0.40	0.64
Sm					1.11	0.75	0.86	0.74	0.60	0.48	0.43	0.36	0.29	0.47
Eu						0.68	0.78	0.67	0.55	0.43	0.39	0.32	0.27	0.42
Gd							1.15	0.99	0.81	0.64	0.57	0.48	0.39	0.63
Tb								0.86	0.70	0.56	0.50	0.41	0.34	0.55
Dy									0.82	0.65	0.58	0.48	0.40	0.63
Ho										0.79	0.71	0.59	0.49	0.78
Er											0.90	0.75	0.62	0.98
Tm												0.83	0.69	1.09
Yb													0.83	1.32
Lu														1.59

Table 2. Separation factors of rare earths with purified Cyanex 923

Effect of La/Ce ratio in the mixture on the separation of La and Ce

Usually a change of separation factor of adjacent rare earth ions takes place depending on the different concentration ratio of rare earths ions.

For example, as seen from Figure 2, the separation factor of La and Ce is obviously changed with different ratios of La and Ce. It is evident from Figure 2 that the separation factors of rare earth ions slightly decreases with increasing the concentration of Cyanex 923 but increases largely with increasing the ratio of La/Ce. For example, the β values of rare earth ions with the line of symbol 'o' are largest for the ratio of La/Ce=9 and the β values decrease in the order of decreasing ratio of La/Ce. However, the β values with larger concentration of total rare earth ions are smaller than those with lower concentration..

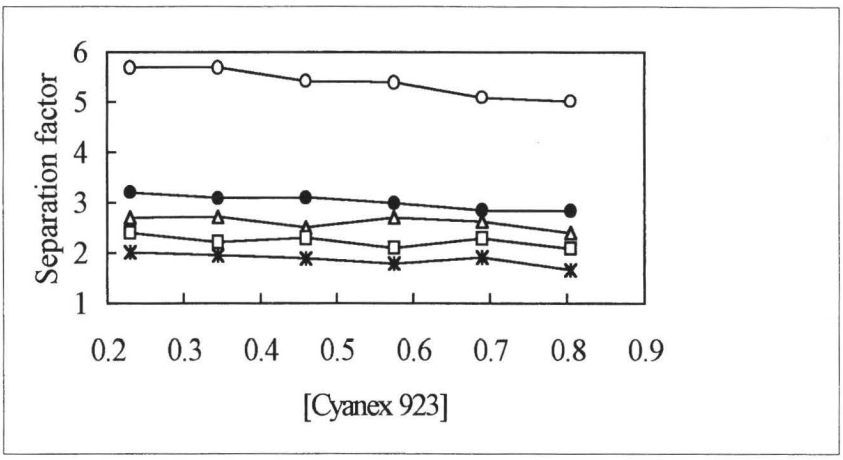

Figure 2. Effect of the concentration of Cyanex 923 and the different ratios of La and Ce on the separation factors of La and Ce
o-$[RE^{3+}]$=0.42 mol/dm^3, Ce/La=1:9; Δ-$[RE^{3+}]$=0.50 mol/dm^3, Ce/La=1:4.6;
□-$[RE^{3+}]$=0.50 mol/dm^3, Ce/La=1:3; •-$[RE^{3+}]$=0.83 mol/dm^3, Ce/La=1:9;
*-$[RE^{3+}]$=0.50 mol/dm^3, Ce/La=1:1

Determination of extraction mechanism

The results of the plots of Log D vs Log [Cyanex 923] and Log D vs Log [$NaNO_3$] show that the extraction reaction of rare earths ions with purified Cyanex 923 is expressed by the following equation:

$$RE^{3+} + 3NO_3^- + 3Cyanex923_{(o)} \Leftrightarrow RE(NO_3)_3 \cdot 3Cyanex923_{(o)}$$

$$K_{ex} = \frac{[RE(NO_3)_3 \cdot 3Cyanex923]_{(o)}}{[RE^{3+}][NO_3^-]^3[Cyanex923]^3_{(o)}} = \frac{D(1+\sum_1^i \beta_i[NO_3^-]^i}{[NO_3^-]^3 \cdot [Cyanex923]^3_{(o)}}$$

Under the present conditions, the species extracted are mainly in the form of $[RE(NO_3)^+_2$ and $RE(NO_3)^{2+}$. The above reaction has been confirmed by IR spectra of the extracted complexes.[6]

Effect of temperature on the extraction of rare earths with Cyanex 923

This was studied by keeping all other parameters constant and only varying temperature. The effect of atomic number of the rare earths on their extraction with both purified and non-purified Cyanex 923 is shown in Figures 3a and 3b. It is very interesting that the D values of rare earths increase obviously with decrease of temperature and the yttrium position shifts gradually with change of temperature. Particularly, the yttrium position can shift outside lanthanides at lower temperatures when using purified Cyanex 923, which might provide a significant method for the separation of yttrium from lanthanides.

According to the Gibbs-Helmhotz's equation, the equation of $\Delta(\log K)/\Delta(1/T) = -\Delta H/2.303R$ can be easily obtained with the help of thermodynamic equations such as $\Delta G° = -RT\ln K$ and $\Delta G° = \Delta H - \Delta S°$, the values of log K (from literature[8]), enthalpy, entropy and free energy with purified Cyanex 923 have been calculated and are given in Table 3.

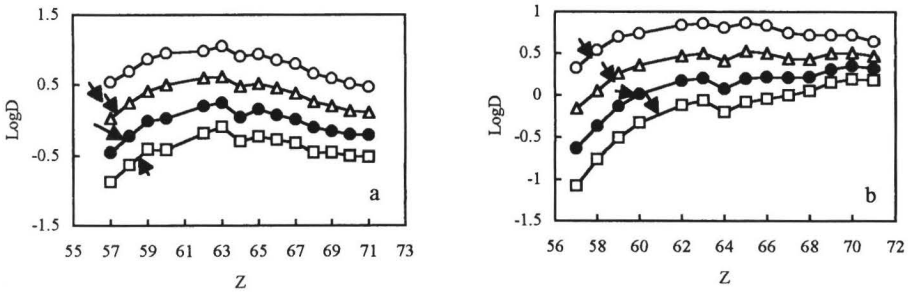

Figure 3. Effect of atomic number of rare earths on the distribution ratio of rare earths at different temperatures with Cyanex 923

o-T=283K; □-T=293K; □-T=303K; □-T=313K; ➔yttrium position
a: purified Cyanex 923; b: non-purified Cyanex 923

Table 3. The values of ΔH, ΔS°, ΔG° and log K with purified Cyanex 923 at 25°C

	La	Ce	Pr	Nd	Sm	Eu	Gd	Tb
Log K	5.98	6.26	6.36	6.47	6.61	6.65	6.48	6.54
-ΔH	83.9	76.1	72.7	76.5	66.8	65.2	69.7	66.4
-ΔG°	34.1	35.7	36.3	36.9	37.7	37.9	37	37.3
ΔS°	-161.9	-131.1	-103.0	-86.2	-61.4	-52.9	-74.6	-62.0
	Dy	Ho	Er	Tm	Yb	Lu	Y	
Log K	6.47	6.39	6.28	6.24	6.15	6.07	6.28	
-ΔH	64.5	64.4	63.4	60.3	58.2	56.5	47.4	
-ΔG°	36.9	36.4	35.9	35.6	35.1	34.7	35.8	
ΔS°	-47.8	-22.7	-11.2	8.4	15.4	23.3	-2.0	

As seen from Table 3, It is evident that the "tetra effect" of thermodynamic functions as function of atomic number of rare earth elements has been observed. The values of ΔH and ΔS° increase with increase of atomic number of rare earths, but those of ΔG° and log K decrease with increase of atomic number of heavy rare earths. Most of the ΔS° values of rare earths are negative, which is mainly due to the decease of molecular number in the extraction reaction. However, those for heavy rare earths such as Tm, Yb and Lu are positive, which might be explained by the fact that many hydrated molecules are released, which result from decrease of atomic radii of rare earths with increase of atomic number of rare earths, which compensate for the decrease of molecular numbers in extraction reaction when the heavy rare earths are extracted into the organic phase.

CONCLUSIONS

The extraction of lanthanides (La ~ Lu except Pm) and yttrium from nitrate solutions has been systematically investigated using both purified and non-purified Cyanex 923 in heptane. The results clearly demonstrate that: 1) the separation factors of rare earths with purified Cyanex 923 are different from those with non-purified Cyanex 923; 2) the separation factors of metal ions are mainly dependent on the ratio of metal ions to be separated in the mixture, that is, the larger the ratio of metal ions, the larger the separation factors of metal ions; 3) the yttrium position can shift at different temperatures,

thus the separation of yttrium from lanthanides with Cyanex 923 can be easily obtained from this temperature effect. The well-regulated changes such as 'tetra effect' of thermodynamic functions (ΔH, $\Delta G°$, $\Delta S°$, and log K) with increasing atomic number of rare earth elements have been observed.

ACKNOWLEDGEMENT

This project was supported by the National Natural Science Foundation of China

REFERENCES

1. Rickelton WA and Boyle RJ, *Sep Sci Technol*, **23**, 1227, (1988).
2. *Cyanex 923, Cyanex 925, Technical Brochures,* West Paterson New Jersey, Cytec Industries Inc..
3. Chun Wang, *Ph. D. Dissertation*, Changchun Institute of Applied Chemistry, Chinese Academy of Sciences, (1996)
4. Ammouri E El and Distin PA, *Solv Extr Ion Exch*, **14**, 871, (1986).
5. Reddy MLP, Luxmi Varma R and Ramamohan TR, *Solv Extr Ion Exch,* **16**(3), 795, (1998).
6. Chu Deqing , Ma Genxiang and Li Deqian, Chin J Analyt Chem, **26**(11), 1346, (1998).
7. Zheng Gui Wei, *Dissertation of Master Degree*,Changchun Institute of Applied Chemistry, Chinese Academy of Sciences, (1997).
8. Peppard DF, Mason GW and Hucher I, J Inorg Nucl Chem, **24**, 881, (1962).

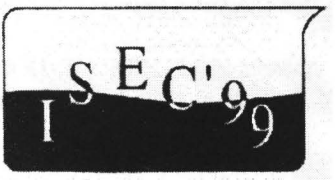

SEPARATION OF YTTRIUM AND NEODYMIUM FROM NITRATE SOLUTIONS BY DI(2-ETHYLHEXYL)-PHOSPHORIC ACID IMPREGNATED ON AMBERLITE XAD-2 RESIN

M Iglesias, E Anticó and V Salvadó
Dept. de Química, Universitat de Girona. Campus de Montilivi, 17071 Girona, Spain.

ABSTRACT
Solvent impregnated resins (SIR) containing di(2-ethylhexyl)phosphoric acid (D2EHPA), were prepared by direct adsorption of the extractant onto Amberlite XAD-2. Extractant adsorption was studied as a function of both the nature of the organic solution and the extractant concentration used. The best conditions for a successful separation of Y(III) and Nd(III) have been evaluated. Previously the distribution equilibrium of yttrium were determined graphically and numerically as a function of both the metal concentration in the aqueous phase and the extractant concentration on the resin phase

Keywords: yttrium(III), di(2-ethylhexyl)phosphoric acid, Amberlite XAD-2, solvent impregnated resin

INTRODUCTION

Solvent extraction of rare earths has been studied extensively as a separation and purification method of these metals. Among the extractants commonly employed di(2-ethylhexyl)phosphoric acid (D2EHPA) has the advantage of its separation efficiency, fast kinetics and low solubility in aqueous solution.

The use of solvent impregnated resins (SIR) in metal extraction, separation and recovery offers many advantages over liquid-liquid extraction.[1] These new materials combine the versatility of extractants reagents used in solvent extraction with the properties of the solid phase. In this sense, the selectivity and kinetics of both techniques are comparable, increasing the efficiency in SIR. On the other hand, the elution process is easier than in the case of chelating resins.

One of the characteristics of SIR, reported by Warshawsky[2] and Muraviev;[3] is the low solubility in water required for both the extractant and the solvent employed in its preparation. Nevertheless, the solvents most usually employed are acetone,[4] ethanol or even mixtures of ethanol and water.[5] The objectives of this work are the comparison of the impregnation process when solutions of D2EHPA are prepared using kerosene or Ethanol:H_2O 2:1 mixtures and the thermodynamic characterisation of the yttrium adsorption by the D2EHPA(kerosene)-XAD-2 system. The results of these studies have been applied to the separation of yttrium and neodymium from aqueous solutions containing different concentrations of these metals.

EXPERIMENTAL

Reagents and solutions

Amberlite XAD-2 (20-60 mesh) was washed several times with different ratios of Dioxane:H_2O, Dioxane:Acetone and Dioxane:Ether. Afterwards, it was purified with a solution of 50% methanol and 4 mol/dm^3 hydrochloric acid overnight.

Di(2-ethylhexyl)phosphoric acid (D2EHPA), 97% Aldrich-Chemie (Germany), was used as received. The purity of the reagent was evaluated by titration against a 0.1 mol/dm^3 NaOH standardised solution.

Aqueous stock solutions of yttrium at H^+ concentration of 0.1 mol/dm^3 and mixtures of yttrium and neodymium were prepared from $Y(NO_3)_3.5H_2O$, 99.9% Aldrich (USA) and $Nd(NO_3)_3$, analytical

© 2000 Society of Chemical Industry

grade Fluka (Switzerland). The H^+ concentration was adjusted using standardised HNO_3 solution. The metal concentration of the stock solution was determined after EDTA titration using Arsenazo III as indicator.[6] Working solutions were prepared by dilution and appropriate volumes of HNO_3 and $NaNO_3$ standardised solution were added to adjust the H^+ concentration and the ionic strength to the desired value.

Kerosene "purum", Fluka (Switzerland), was employed as organic diluent after washing with H_2SO_4, then several times with distilled water and finally dropped through KOH. Other reagents used were Panreac (Spain) of analytical grade.

Apparatus

A Labinco rotary mixer was employed to agitate aqueous solution with the resin. The concentration of the metal in the aqueous solution was determined by measuring the absorbance of their Arsenazo (III) complexes with a Hitachi U-1100 UV-visible spectrophotometer.[7] pH measurements were carried out using a pH-meter model micro pH-2000, Crison Instruments S.A. (Spain) and a Crison Model 50-02 combined electrode. For solutions containing a mixture of metals, the concentration was determined by Inductively Coupled Plasma (ICP) Emission Analysis, ARL model 3410 Minitorch (USA).

Impregnation procedure

The impregnation of XAD-2 beads was carried out by using the "wet method".[2] Appropriated amounts of dry XAD-2 (0.3 g) was placed into organic solutions containing different concentrations of D2EHPA in kerosene (0.06-0.6mg/cm^3) or in ethanol:H_2O 2:1 (0.02-0.1mg/cm^3) for 6 hours until equilibrium was reached. After filtration, the impregnated resin was washed several times with water. The amount of adsorbed D2EHPA was evaluated after quantitative stripping with ethanol, and subsequent titration with standardised NaOH solution 0.1 mol/dm^3.

Yttrium extraction by SIR

An amount of SIR (0.3 g) was contacted with 10 cm^3 of Y(III) solution for 5 hours until equilibrium was reached. After separation of the solid phase, the yttrium remaining in the aqueous solution was analysed. The amount of yttrium adsorbed by the SIR was determined by mass balance. In some experiments, yttrium concentration in the resin phase was determined after elution with 6 mol/dm^3 hydrochloric acid to verify the mass balance.

Yttrium-Neodymium separations.

Yttrium-Neodymium mixtures at two different HNO_3 concentrations, 1.0 and 0.032 mol/dm^3, were kept in contact for 6 hours with 0.3 g of impregnated D2EHPA-XAD-2. After that, the metal adsorbed on the resin phase was stripped with 10 cm^3 of HCl 6 mol/dm^3 over two hours.

All experiments were carried out at a controlled room temperature of 22 ± 2°C and their reproducibility was verified in duplicate.

RESULTS AND DISCUSSION

Evaluation of the impregnation process.

Data on D2EHPA adsorbed in XAD-2 at different extractant concentrations in the impregnation solution using kerosene and Ethanol:H_2O 2:1 are plotted in Figure 1. From this figure it can be observed that the quantity of extractant adsorbed in the polymer increases with the extractant concentration. Moreover, it also shows that the extractant retention in the polymer increases with the hydrophilicity of the organic solvent, this behaviour, which was also observed by Cortina et al.,[5] can be explained by the

formation of a dimer species of D2EHPA in kerosene[8] that restricts the diffusion of the extractant into the polymer matrix.

Yttrium extraction

The kinetic studies of the extraction of Y(III) by D2EHPA impregnated XAD-2 resin in kerosene of ethanol:H_2O 2:1 are summarised in Figure 2. It shows that after 3 hours of contact equilibrium was reached and is no difference between the resin impregnated with kerosene than the one impregnated with ethanol:H_2O 2:1.

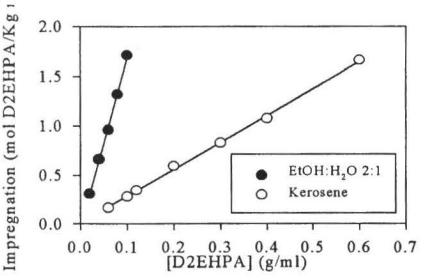

Figure 1. Dependence of the resin loadings on the D2EHPA concentration in the impregnation solution.

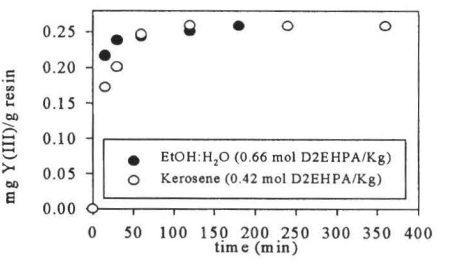

Figure 2. Rate of adsorption of Y(III) by D2EHPA/XAD-2 resins from 1.0 M HNO_3 aqueous solutions.

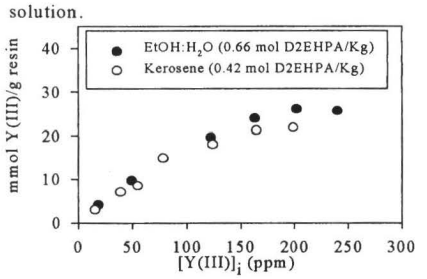

Figure 3. Adsorption of Y(III) from 1.0 M HNO_3 aqueous solutions by D2EHPA/XAD-2 resins.

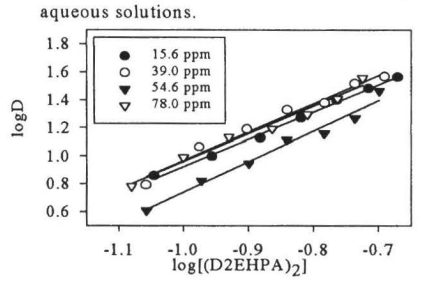

Figure 4. Experimental distribution data at different metal concentration. [HNO_3]=1.0M.

Data on the amount of Y(III) extracted at different aqueous metal concentrations are plotted in Figure 3. It can be seen that, for both kerosene and ethanol:H_2O 2:1 organic solvents, a plateau is reached. The maximum yttrium adsorbed by the resin was 0.025 mol/Kg resin when XAD-2 with 0.66 mol D2EHPA/Kg impregnated in EtOH:H_2O 2:1 is used, and 0.021mol Y(III)/Kg resin when the XAD-2 was impregnated with a kerosene organic solution giving a D2EHPA concentration of 0.422 mol/Kg.

By analogy with liquid-liquid extraction, the distribution coefficient of the metal between the resin and the aqueous phase can be defined as the ratio of the total metal concentration in the resin phase and the total metal concentration in the aqueous phase, corrected by taking into account the volumes of the organic and aqueous phases. The organic phase volume was calculated taking into account the volumetric uptake of Amberlite XAD-2 according to Muraviev for toluene[3] as data for kerosene are not available. Yttrium distribution data were plotted as log D versus log $[(D2EHPA)_2]_{free}$, where $(D2EHPA)_2$ accounts for the dimer of D2EHPA (Figure 4).

The extraction of yttrium with D2EHPA can be described by the following general reaction:

$$Y^{3+} + n\,(HA)_{2,r} \leftrightarrow YA_3.(2n-3)HA_r + 3\,H^+ \qquad K_{ex} \qquad (1)$$

where HA symbolises a D2EHPA molecule and the subscript 'r' refers to the resin phase. Under the experimental conditions, i.e. 1.0 mol/dm^3 HNO_3, the hydrolysis of yttrium can be neglected, but the

formation of metal complexes with nitrate ions must be taken into account.[9] In this way, the equilibrium constant associated to reaction (1) in logarithmic form can be written as:

$$\log D = \log K_{ex} - 3 \log [H^+] - \log\alpha + n \log [(HA)_2] \quad (2)$$

where $\alpha = 1 + \beta_1 [NO_3] + \beta_2 [NO_3]^2 + \beta_3 [NO_3]^3 + \beta_4 [NO_3]^4 + \beta_5 [NO_3]^5 + \beta_6 [NO_3]$.[6]
Thus, a plot of log D vs log $[(HA)_2]$ should give a straight line with an intercept equal to $\log K_{ex} - 3 \log[H^+] - \log\alpha$ and a slope equal to n. From Figure 4 log K_{ex} and n values can be determined. The values obtained are collected in Table 1.

$[Y^{3+}]_{tot}$ (ppm)	slope $\pm$ t .S_{slope}	intercept $\pm$ t . $S_{intercept}$	$\log K_{ex}$
15.6	1.94±0.14	2.87±0.12	2.93
39.0	2.03±0.35	3.00±0.30	3.07
54.6	2.19±0.39	2.93±0.33	2.99
78.0	1.98±0.33	2.94±0.30	3.01

Table 1. Results of the equilibrium study using graphical treatment.

The experimental data were analysed numerically with the program LETAGROP-DISTR,[10] which is based on minimisation of the error-square sum, U:

$$U = \Sigma_N (\log D_{calc} - \log D_{exp})^2 \quad (3)$$

where D_{exp} are the experimental values of the distribution coefficient and D_{calc} the corresponding values from the relevant mass-balance equation for a proposed model. N is the total number of experimental points.

The input of the program includes the data corresponding to the equilibria involved in the system.[9] For these calculations D2EHPA concentration was introduced as a monomer. In table 2, results of some chemical models are presented. The goodness of the fit of any model is evaluated by the values of U and standard deviation defined as $\sigma(\log D) = (U/N\text{-}N_k)^{1/2}$ where N_k is the number of constants to be determined. As seen in Table 2, slight differences are observed between the models III, IV and V. A special computational procedure was applied by allowing the programme to choose statistically from different possible stoichiometries. The calculation rejected all the proposed species considered besides $YA_3.HA$ with a formation constant $\log K_{ex} = 3.35$ which has been corrected taking into account the dimerisation of D2EHPA in the organic solvent.[11] This value is in good agreement with the results obtained in the graphical analysis of the experimental data.

	MODEL	log β	U	σ
I	$YA_3.3HA$	19.749±0.087	0.437	0.127
II	$YA_3.2HA$	16.647±0.062	0.240	0.094
III	$YA_3.HA$	13.553±0.050	0.176	0.081
IV	$YA_3.2HA$	15.629MAX16.632		
	$YA_3.HA$	13.509MAX13.806	0.175	0.082 GK
V	$YA_3.3HA$	18.415MAX19.462		
	$YA_3.HA$	13.531±0.232	0.175	0.082 GK

where β stands for the reaction, $Y^{3+} + 2n\,(HA)_r \leftrightarrow YA_3.(2n\text{-}3)HA_r + 3H^+$

Table 2. Results of the equilibrium study using the LETAGROP-DISTR program.

Yttrium-Neodymium separation

To apply the SIR system to the separation of neodymium and yttrium, solutions with different amounts of both metals have been tested. It is very difficult to choose a ratio of concentrations that could be similar to the relative abundance of these metals in nature due to the great differences between the ratios of light and heavy rare earth metals in the different mineral sources. In Tables 3 and 4 the results of separation of neodymium and yttrium using a D2EHPA /XAD-2 impregnated resin are presented. The impregnation has been carried out in kerosene (table 3) or in EtOH:H_2O 2:1 (table 4).

$[H^+]$=1.0 mol/dm^3					$[H^+]$=0.032 mol/dm^3					
$[Y^{3+}]_i$	$[Nd^{3+}]_i$	% Y_{ext}	%Nd_{ext}	%Y_{elu}	$[Y^{3+}]_i$	$[Nd^{3+}]_i$	% Y_{ext}	%Nd_{ext}	%Y_{elu}	%Nd_{elu}
12.8	13.5	**48.5**	**2.0**	89.5	10.5	10.4	**99.4**	**87.7**	108.3	89.0
12.8	50.9	**50.4**	**2.6**	85.1	11.8	41.8	**99.5**	**81.0**	95.6	83.2
50.3	13.2	**46.2**	**4.8**	86.2	40.9	10.7	**99.8**	**80.0**	101.5	84.5
52.6	51.8	**47.5**	**5.8**	76.8	42.2	40.9	**99.8**	**67.1**	98.0	86.4

Table 3. Separation of Y(III) and Nd(III) with 0.42 mol D2EHPA/Kg impregnated onto XAD-2 polymeric matrix with kerosene.

The experiments have been carried out at different HNO_3 concentration (1.0 and 0.032 mol/dm^3) due to the pH-dependence of the extraction process with D2EHPA. As can be seen in the tables, neodymium extraction increases at pH = 1.5 and the metal uptake for both metals is greater when kerosene is used as solvent in the SIR preparation. This fact can be explained by the loss of the solvent during the rinsing process, when EtOH:H_2O 2:1 is used to impregnate the resin.

$[H^+]$=1.0 mol/dm^3					$[H^+]$=0.032 mol/dm^3					
$[Y^{3+}]_i$	$[Nd^{3+}]_i$	% Y_{ext}	%Nd_{ext}	%Y_{elu}	$[Y^{3+}]_i$	$[Nd^{3+}]_i$	% Y_{ext}	%Nd_{ext}	%Y_{elu}	%Nd_{elu}
11.6	11.6	**30.9**	**2.1**	91.8	10.6	10.4	**98.6**	**65.5**	109.4	110.6
11.7	46.3	**31.1**	**2.1**	87.5	11.8	41.8	**99.0**	**55.0**	92.5	94.6
45.1	11.7	**26.5**	**0.0**	82.7	40.9	10.7	**98.8**	**53.0**	99.7	98.7
44.8	46.4	**26.6**	**2.6**	86.6	42.2	40.9	**96.3**	**34.2**	92.8	83.7

Table 4. Separation of Y(III) and Nd(III) with 0.42 mol D2EHPA/Kg impregnated onto XAD-2 polymeric matrix with EtOH:H_2O 2:1.

To improve the separation of both metals, another experiment with a higher D2EHPA concentration on the SIR has been carried out. The acidity of the aqueous phase was adjusted to 1.0 mol/dm^3 to favour only the yttrium adsorption (Table 5). In these conditions, the separation of yttrium and neodymium is almost achieved and the elution of yttrium using HCl 6 mol/dm^3 is nearly quantitative.

$[Y^{3+}]_i$	$[Nd^{3+}]_i$	% $Y_{extraction}$	% $Nd_{extraction}$	% $Y_{elution}$
11.6	11.6	**79.9**	**0**	86.0
11.7	46.3	**82.7**	**2.3**	90.3
45.1	11.7	**83.9**	**1.0**	86.4
44.8	46.4	**80.8**	**1.1**	89.3

Table 5. Separations of Y(III) and Nd(III) with [D2EHPA] =1.34 mol/Kg impregnated onto XAD-2 polymeric matrix with EtOH:H_2O 2:1. Aqueous phase $[H^+]$=1.0 mol/dm^3.

ACKNOWLEDGEMENTS

This work was carried out under CICYT (Spanish Commission for Research and Development) Project No. QUI96-1025-CO3-03.

REFERENCES

1 Flett DS. *Chemistry and Industry*, 6 August (1977) 641-646.
2 Warshawsky A, *Ion Exchange and Solvent Extraction.* Eds. Marinsky JA and Marcus Y. Marcel-Dekker, New York **8**, 229, (1981).
3 Muraviev D. *Solv Extr Ion Exch,* **16**(1) 381, (1998).
4 Wakui Y, Matsunaga H and Suzuki TM, *Anal. Sci.*, **5**, 189, (1989).
5 Cortina JL, Miralles N and Aguilar M, *Solv Extr. Ion Exch.*, **12**(2), 349, (1994).
6 Fritz JS, Oliver RT and Pietrzyk DJ. *Anal. Chem.*,**30**(6), 111, (1958).
7 Marczenko Z *"Separation and Spectrophotometric Determination of Elements"*. Ellis Horwood Ltd. Chichester, England (1986).
8 Liem DH. *Acta Chem. Scan.*, **26** , 191, (1972).
9 Sillen and Martell. *"Stability constants. Special publication n°7"*. The Chemical Society (1964).
10 Liem DH. *Acta Chem. Scan.*, **25,** 1521, (1971).
11 Liem DH. *Acta Chem. Scan.*, **26**,191, (1972).

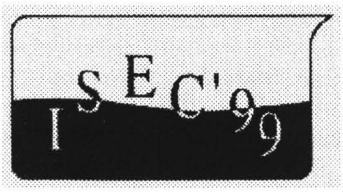

DISTRIBUTION OF NEODYMIUM(III) BETWEEN ACIDIC AQUEOUS NITRATE SOLUTIONS AND ORGANIC SOLUTIONS OF DI-(2-ETHYLHEXYL)-PHOSPHORIC ACID IN KEROSENE AT LOW METAL CONCENTRATION

JM Sánchez[1], M Hidalgo[1], M Valiente[2] and V Salvadó[1]

[1]Dept. Química, Universitat de Girona, Facultat de Ciències, Campus Montilivi s/n, 17071-Girona, Spain

[2]Dept. Química, Universitat Autònoma de Barcelona, Facultat de Ciències Edifici CN, 08193-Bellaterra, Barcelona, Spain

ABSTRACT

The solvent extraction of neodymium (III) from 0.1M nitrate solutions by di-(2-ethylhexyl)phosphoric acid (D2EHPA) in kerosene has been characterized at low metal concentration. The influence of the diluent on the speciation of the system has been studied by graphical and numerical analysis of the metal distribution data and compared to the results obtained in hexane. Nd(III) was extracted by ion-exchange reactions via the species $NdA_3 \cdot 3HA$, $NdA_3 \cdot 2HA$ and NdA_3 in the organic phase, with logarithm of stability constants equal to 15.42, 12.32 and 4.12 respectively.

Keywords: neodymium, D2EHPA, diluent effect

INTRODUCTION

The separation of Rare Earth Elements (REE) by liquid-liquid extraction is one of the most extensively used methods to obtain high purity metals. Among the extractants developed for this purpose, organophosphorous compounds present a high selectivity and extraction efficiency in the separation of these chemically similar elements.[1] The extraction constants with these extractants are high compared to solvating reagents due to the complex formation reaction between the acidic compound and the metal ion. Among the alkylphosphoric acids, di-(2-ethylhexyl)phosphoric acid (D2EHPA) presents the advantages of its chemical stability, good kinetics of extraction, versatility of extraction of various metal ions and commercially available.

The diluent used in the organic phase has a great influence on the extraction process using organophosphorous acidic extractants[2] because the different polymerization of the extractants depends on the diluent. In diluents of low polarity, the formation of dimer species (H_2A_2) with stable eight-member ring has been reported.[1] This cyclic structure is maintained when the complex with the metal ion is formed in presence of an excess of extractant in relation to metal concentration. In this situation, only one hydrogen ion is displaced and the anion HA_2^- acts as a ligand.[3,4] Aliphatic hydrocarbons, such hexane, are the diluents most used in the extraction of REE with D2EHPA, but its high volatility prevents its use in industrial applications. Thus kerosene is a good low cost alternative to hexane.

The aim of this work is to carry out a systematic study on the speciation of the organic phase in the distribution of neodymium (III) between aqueous nitrate media and D2EHPA/kerosene organic solutions.

EXPERIMENTAL

Neodymium nitrate, analytical grade, was purchased from Fluka (Switzerland). A stock solution of 25 mmol dm^{-3} of neodymium in 0.1mol dm^{-3} nitric acid was standardized chelatometrically with EDTA in acetate buffer using Xylenol Orange as indicator.[5] Working solutions, in the range $1 \cdot 10^{-5}$ to $1 \cdot 10^{-4}$ mol dm^{-3}, were prepared by dilution. Appropriate volumes of nitric acid and sodium nitrate standardized solutions were added to adjust the proton concentration and the ionic strength to the desired value. Ionic strength was kept equal to 0.1mol dm^{-3} in all the experiments. Kerosene used as a

© 2000 Society of Chemical Industry

diluent was obtained from Fluka (Switzerland). The composition was 60% of aliphatic hydrocarbons and 40% of aromatic, with a major predominance of the molecules with 11 and 12 carbon atoms (50%)*. It was washed several times with sulfuric acid, potassium hydroxide and water before use. Di-(2-ethylhexyl)phosphoric acid (D2EHPA), 97% purity, was obtained from Aldrich (Germany). Appropriate concentrations of the acidic extractant were prepared by dilution in kerosene. The D2EHPA concentration in the organic solutions ranged from 0.01 to 30 mmol dm^{-3}. All other reagents used were of analytical grade.

The experimental data were obtained by a two phases titration with NaOH using an automatic setup composed of a potentiometric system and a flow injection analysis system, described in a previous work.[6] A thermostated bath was used to keep the temperature at 25 ± 1°C within the extraction cell. The concentration of neodymium in the aqueous phase was measured "in situ" by a Flow Injection Analysis (FIA) system with Arsenazo III as a colorimetric reagent (r.s.d. 1.5%).

To verify the equilibrium of the chemical system and the metal mass balance, some stripping experiments were carried out with HNO_3 solutions. The good agreement between potentiometric curves corresponding to extraction and stripping experiments indicates that both have been accomplished.

All constants related to the equilibrium involved in the system are used for the calculations: formation of neodymium nitrates and hydroxides in aqueous phase,[7] dimerization of D2EHPA in organic phase (K_2), its distribution between phases (K_D) and its acidity in aqueous phase (K_a).[8]

RESULTS AND DISCUSSION

The extraction of neodymium with D2EHPA occurs via an ion exchange mechanism that can be expressed by the following reaction:

$$Nd^{3+}_{(aq)} + 3(HA)_{2(org)} \leftrightarrow NdA_3 \cdot 3HA_{(org)} + 3H^+_{(aq)} \qquad (1)$$

This equation shows the dependence of the extraction system on the pH and D2EHPA concentration in the organic phase. The equilibrium constant, K, associated to the extraction reaction is:

$$K = \frac{[NdA_3 \cdot 3HA]_{org}\,[H^+]^3}{[Nd^{3+}][(HA)_2]^3_{org}} \qquad (2)$$

and in logarithmic form:

$$\log K = \log D + 3\log[H^+] - 3\log[(HA)_2] \qquad (3)$$

where D is the metal distribution coefficient defined by:

$$D = \frac{C_{Nd(III)_{org}}}{C_{Nd(III)_{aq}}} \qquad (4)$$

The experimental data are represented in Fig.1 in terms of the logarithm of D as function of the dimer concentration in the organic phase at different pH values (all these points were obtained with D2EHPA concentrations higher than 10 mmol dm^{-3}). According to equation 3, a linear relationship with slopes equal to 3 is obtained if log D is plotted against either $\log[(HA)_2]$ or pH. The slopes calculated from Figure 1 are all close to 3. This result verifies the assumption made in equation 1 that three molecules of dimer are associated to each metal ion and allows the graphical calculation of the extraction constant from equation 3 ($\log K = 2.71 \pm 0.29$).

* Information supplied by Fluka Chemie AG

In Figure 2, the representation of log D vs pH at different D2EHPA concentrations gives more information about the extraction system. The slopes found when the concentration of D2EHPA is over 10 mmol dm^{-3} are close to 3 according to equation 3; for concentrations lower than 10 mmol dm^{-3}, two slopes of approximately 1.0 and 2.5 were obtained. This fact seems to indicate that other species than $NdA_3 \cdot 3HA$ are present in the organic phase.

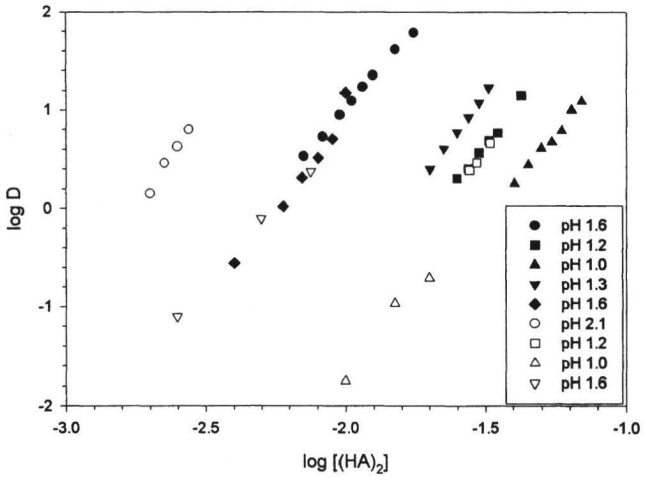

Figure 1. Extraction of Nd at fixed pH values and varying D2EHPA concentrations.

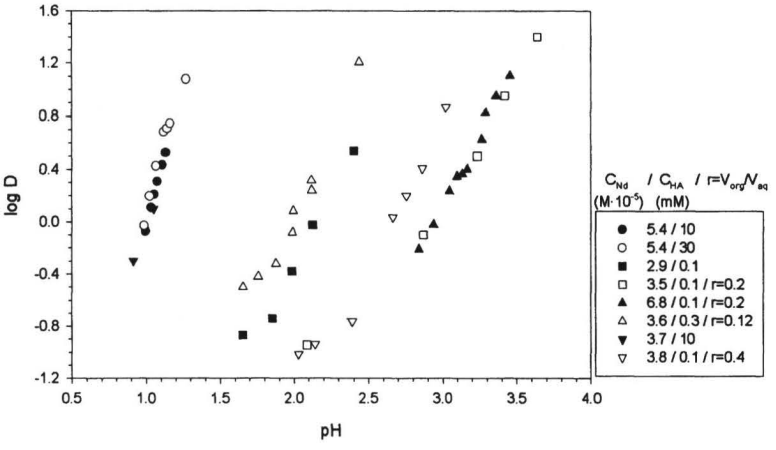

Figure 2 Extraction of Nd at fixed D2EHPA concentration and varying pH values.

To elucidate the stoichiometries of the species formed in the organic phase and the values of their stability constants, a numerical treatment of the data has been carried out using the LETAGROP-DISTR program.[9] The results of the computer analysis are collected in Table 1. As can be seen in this table, when D2EHPA concentrations are higher than 10 mmol dm^{-3}, the model that best fit the experimental data is composed of the species $NdA_3 \cdot 3HA$ and $NdA_3 \cdot 2HA$. At lower concentrations, a new species, NdA_3, is also present in the organic phase.

Based on this model, the distribution diagram of Nd(III) species was calculated in Figure 3. This diagram shows that species NdA_3 is predominant in the interval 0.1 to 20 mmol dm^{-3}, while $NdA_3 \cdot 3HA$ is the main species for total D2EHPA concentrations above 20 mmol dm^{-3}. Besides these, the $NdA_3 \cdot 2HA$ fraction has a maximum value of 30% and is present at D2EHPA concentrations between 1 and 100 mmol dm^{-3}.

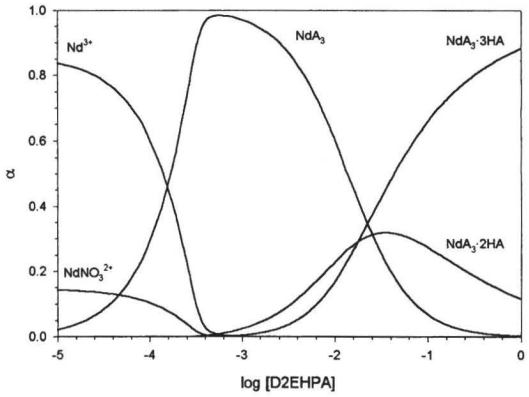

Figure 3. Distribution diagram of Nd(III) species calculated from the constant values in Table 1 (pH = 3 and 0.1 mmol dm^{-3} Nd(III)).

Model	log β	σ	U
[D2EHPA] > 10 mmol dm^{-3}			
NdA_3	5.99±0.25	0.26	5.01
$NdA_3 \cdot 3HA$	15.43±0.17	0.12	1.49
$NdA_3 \cdot 2HA$	12.29±0.12	0.17	2.03
$NdA_3 \cdot 3HA$	15.42±0.18	0.10	1.15
$NdA_3 \cdot 2HA$	12.27±0.13		
NdA_3	MAX 5.09		
[D2EHPA]<10 mmol dm^{-3}			
NdA_3	5.94±0.25	0.28	9.16
$NdA_3 \cdot 3HA$	15.64±0.22	0.23	6.38
$NdA_3 \cdot 2HA$	12.39±0.13	0.15	2.05
$NdA_3 \cdot 3HA$	15.42±0.23	0.19	3.8
NdA_3	4.82 MAX 5.20		
$NdA_3 \cdot 3HA$	16.01 MAX	0.12	2.3
$NdA_3 \cdot 2HA$	16.30		
NdA_3	12.37±0.15		
	4.12±0.14		

* The goodness of the fit of any model is evaluated by the values of U and standard deviation, defined as $U = \Sigma (\log D_{calc.} - \text{Log } D_{exp})^2$ and $\sigma (\log D) = (U/N\text{-}N_k)^{0.5}$, where N is the number of experimental points and N_k is the number of constants to be determined.

Table 1. Results obtained by numerical treatment of the experimental data for the extraction of Nd(III) by D2EHPA in kerosene using LETAGROP-DISTR computer program.

The formation of NdA_3 has been previously reported in hexane with a log β=4.94±0.05, very similar to the calculated value in kerosene (Table 1). At this low concentration, the dimerization of D2EHPA is

not significant and the extractant mainly exists as a monomer. Moreover, the alkylphosphorous acids tend to saturate the interface,[10] and interact with water molecules by hydrogen bonding.[11] In these conditions, the formation of the complex NdA_3 can be written in the form:

$$Nd^{3+}_{(aq)} + 3HA_{(org)} \leftrightarrow NdA_{3(org)} + 3H^{+}_{(aq)} \quad (5)$$

When the concentration of the extractant increases, the formation of the species $NdA_3 \cdot 2HA$ and $NdA_3 \cdot 3HA$ take place in the organic phase. The influence of the diluent on the speciation of neodymium (III)-D2EHPA extraction system became evident from the formation of the species $NdA_3 \cdot 2HA$ when kerosene is used as diluent. This species has not been reported in the case of D2EHPA-hexane solutions. On the other hand, the stability constants of $NdA_3 \cdot 3HA$ and NdA_3 species are slightly different in both diluents.

ACKNOWLEDGEMENTS

This work was carried out under CICYT (Spanish Commission for Research and Development) Project nº QUI96-1025-C03-03.

REFERENCES

1. Kolarik Z and Pankova H, *J. Inorg. Nucl. Chem.*, **28,** 2325, (1966).
2. Sekine T and Hasegawa Y, in *Solvent Extraction Chemistry*, Sekine T and Hasegawa Y Eds., Marcel Dekker, New York, (1977).
3. Baes CF, *J. Inorg. Nucl. Chem.*, **24,** 707, (1962).
4. Peppard DF, Mason GW, Driscoll WJ and Sironen RJ, *J. Inorg. Nucl. Chem.*, **7,** 276, (1958).
5. Kinnunen J and Wennestrand B, *Chemist-Analyst*, **46,** 92, (1957).
6. Sánchez JM, Hidalgo M, Salvadó V and Valiente M, *Solv. Extr. Ion Exch.*, **3** (17), (1999) in press.
7. Högfeldt E, *Stability Constants of Metal Ion-Complexes*, Pergamon Press, Oxford, (1982).
8. Kolarik Z, *Pure & Appl. Chem.*, **54**(12), 2593, (1982).
9. Liem DH, *Acta Chem. Scand.*, **26,** 191, (1972).
10. Vandegrift GF and Horwitz EP, *J. Inorg. Nucl. Chem.*, **42,** 119, (1980).
11. Miyake Y, Matsuyama H, Nishida N, Nakai M, Nagase N and Teramoto M, *Hydrometallurgy*, **23,** 19, (1990).

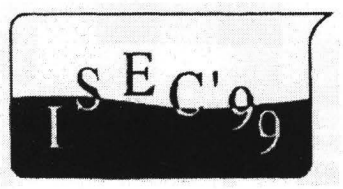

SOLVENT EXTRACTION STUDIES OF ERBIUM(III) BY 2-ETHYLHEXYLPHOSPHONIC ACID MONO-2-ETHYLHEXYL ESTER (IONQUEST 801) FROM HYDROCHLORIC ACID SOLUTIONS

IO Masson[1], PSM Soares[1], M Aguilar[2] and JL Cortina[2]

[1] CETEM, National Council for Cientific and Technological Development, Rio de Janeiro, 21941-590, Brazil.

[2] Chemical Engineering Dep, Universitat Politecnica de Catalunya, Barcelona, Spain.

ABSTRACT

In this work the chemical modelling of Er(III) extraction from HCl solutions reproducing processing conditions at high Er(III) metal contents (g/dm^3) using a phosphonic acid ester (Ionquest 801) dissolved in isoparaffin was carried out. Analysis of the metal distribution showed that Er(III) extraction could be explained assuming the formation of metal complexes such as $ErL_3(HL)_{3,o}$. The extraction constants for different ionic strength are given.

Keywords: erbium, Ionquest 801, modelling.

INTRODUCTION

Rare earth (RE) elements have been used in several applications, mainly in chemical, materials and electronic industries. To achieve high purity compounds (or elements) suitable for these advanced technologies, very complex processes are commonly used.[1] The purification of aqueous solutions containing lanthanides aiming to obtain high purity single elements or groups of elements is most usually performed by solvent extraction (SX). For the last several years, a systematic investigation of the extraction behaviour of selected trivalent lanthanides at equilibrium has been undertaken. These studies have been performed using a variety of chelating agent families. Their purpose was to know how chelating extractants of improved selectivity towards an individual lanthanide could be obtained.[2] The separation of rare earths by SX is usually carried out with acidic alkylphosphorous extractants, phosphoric, phosphonic and phosphinic derivatives.[3-7] Although, the alkylphosphonic acid derivatives are usually less effective regarding extraction of the rare earth cations than the corresponding alkylphosphoric derivatives, they lead to higher separation factors. In addition, alkylphosphonic derivatives are more easily stripped and have good hydrodynamic behaviour.[4-7]

Several studies are described in the literature involving rare earth extraction from hydrochloric acid media using phosphonic acid derivatives such as Ionquest 801 (2-ethylhexylphosphonic acid, mono-2-ethylhexyl ester). Yet different aspects of these systems have been addressed, the studies are usually carried at low rare earth metal concentrations (μg/dm^3 to mg/dm^3).[5-7] Interest in these systems has recently increased mainly because of their close connections to some hydrometallurgical processes. Thus, rare earth chloride hydrometallurgy at high concentrations, seems to demand further investigation concerning the behaviour of individual extraction systems over a relatively wide chloride concentration range. Such investigations require precise determination of the extent of the influence of the different parameters associated with the extraction process, e.g. composition of organic and aqueous phases, stoichiometry of extracted products, mass action law, mass-transfer kinetics, etc.

Therefore the objective of this work is the study of Er(III) SX from solutions reproducing processing conditions at high proton and Er(III) contents (g/dm^3) using a phosphonic acid derivative (Ionquest 801) dissolved in isoparaffin. The distribution coefficient (D) was determined as a function of acidity, Er(III) concentration and ionic strength. The data were analysed graphically and numerically using the program LETAGROP-DISTR.[8]

© 2000 Society of Chemical Industry

EXPERIMENTAL

Reagents and solutions

Ionquest 801, 2-ethylhexylphosphonic acid, mono-2-ethylhexyl ester (HL), kindly supplied by Albright & Wilson, was conditioned before use by treatment with aqueous hydrochloric acid solutions. Stock solutions of Er(III) (1 g/dm^3) were prepared by dissolving the corresponding oxide (Er_2O_3) (Aldrich a.r.) in the stoichiometric amount of HCl (Merck, a.r.), and were standardised by the usual titrations.[9] Isoparaffin, a mixture of hydrocarbons with a distillation range 170-210C was used as received (Unipar Química, Brazil).

Erbium (III) distribution with Ionquest 801-isoparaffin solutions

The extraction of Er(III) was carried out with batch experiments at room temperature (25 ± 1C). Equal volumes of Ionquest 801 diluted in isoparaffin and aqueous solution were mixed mechanically in glass tubes with an aqueous solution (10 cm^3). Six different ionic strength levels were examined: 0.5, 1, 1.5, 2, 2.5 and 3 mol/dm^3 (Er(III), H^+/Cl^-. To standardise the shaking step of the experiment, Er(III) concentration was determined as a function of time. Ten minutes were considered enough to achieve equilibrium. A high-speed centrifuge was used for phase separation and the equilibrium proton concentration was measured by acid-base titration. Er(III) content in both phases was determined by ICP and complexometric titrations[9] at low and high concentrations respectively.

$[Er]_o$	$[H^+]_i$	$[H^+]_e$	I (mol/dm^3)	Log D	$[Er]_o$	$[H^+]_i$	$[H^+]_e$	I (mol/dm^3)	Log D
0.044	0.737	0.841	1.0	0.49	0.252	0.726	0.976	2.2	-0.38
0.043	0.518	0.704	0.8	0.80	0.251	0.516	0.886	2.o	-0.25
0.043	0.306	0.490	0.6	1.18	0.255	0.315	0.641	1.8	-0.16
0.044	0.104	0.358	0.4	1.00	0.249	0.103	0.539	1.6	-0.04
					0.252	0.012	0.407	1.5	-0.01
0.084	0.730	0.999	1.2	0.19	0.337	0.003	1.751	2.0	-0.20
0.084	0.517	0.808	1.0	0.47	0.344	0.739	0.992	2.8	-0.50
0.084	0.312	0.584	0.8	0.75	0.340	0.513	0.774	2.6	-0.40
0.084	0.103	0.451	0.6	1.21	0.341	0.307	0.646	2.4	-0.33
0.085	0.015	0.274	0.5	1.38	0.341	0.100	0.482	2.1	-0.23
0.085	0.002	0.283	0.5	1.52	0.335	0.010	0.411	2.0	-0.23
0.167	0.729	0.952	1.7	-0.14	0.417	0.723	0.983	3.2	-0.60
0.168	0.518	0.752	1.5	0.01	0.417	0.517	0.429	3.0	-0.55
0.168	0.304	0.606	1.3	0.13	0.421	0.314	0.729	2.8	-0.44
0.168	0.100	0.523	1.1	0.31	0.418	0.102	0.473	2.6	-0.40
0.167	0.013	0.380	1.0	0.36	0.418	0.011	0.402	2.5	-0.36
0.169	0.003	1.601	1.0	0.38	0.415	0.003	0.371	2.5	-0.36

Table 1. Log D values as function of the initial molar concentrations of Er^{3+} ($[Er^{3+}]_o$) and hydrogen ion concentration ($[H^+]_i$]) for 1mol/dm^3 [Ionquest] in isoparaffin.

RESULTS AND DISCUSSION

Graphical and computer modelling

The distribution of Er(III) between the organic phase, containing Ionquest 801 (HL), and the aqueous phase can be obtained directly as:

$$D = \frac{[Er(III)]_o}{[Er(III)]} \quad (1)$$

where $[Er(III)]_o$ and [Er(III)] denote the total concentration of Er(III) in the organic and in the aqueous phase respectively.
In general, the extraction behaviour of Er(III) ions with Ionquest 801 could be described by the following general reaction:

$$Er^{3+} + (p+q-t)\,HL_r + t\,X^- \Leftrightarrow MX_t\,L_{3-t}(HL)_{q,r} + (3-t)\,H^+ \quad (2)$$

Determination of stoichiometric coefficients(p,q,t).

Data in Table 1 were classified into six different groups according to their total ionic strengths: 0.5, 1.0, 1.5, 2.0, 2.5 and 3.0 mol/dm^3 for their graphical and numerical treatment. The number of exchanged protons per mole of extracted metal (p) was calculated from the acidity balance:

$$[H^+]_{eq} = [H^+]_i + p[Er]_o$$

p = 3 being the number which better explain the acidity balance and indicating that chloride ions are non-extracted to the organic phase i.e. t = 0.

Finally, and taking into account that all sets of experiments where carried out at 1mol/dm^3 extractant concentration, it was not possible to determine the number of extractant molecules in the extracted complex. A literature survey indicated that in all studies published for Er and other rare earth metals[5-7] a total number of six molecules was selected to explain the extraction results. Thus, equation (2) can be expressed as:

$$Er^{3+} + 6\,HL_o \Leftrightarrow M\,L_3(HL)_{3,r} + 3\,H^+ \quad (3)$$

Following the approach developed[10,11] in the study of metal extraction reactions the corresponding equilibrium constant of the extraction process (K^o) is defined:

$$K^o = \frac{[ErL_3(HL)_3]_o [H^+]^3 \gamma_{ML_3(HL)_{3,o}} \gamma^3_{H^+}}{[Er^{3+}][HL]^6_o \gamma_{M^{3+}} \gamma^6_{HL_r}} \quad (4)$$

where γ_i and $\gamma_{i,o}$ denote the activity coefficients of "i" species in the aqueous and the organic phase, respectively. Rearranging equation (6), the following expression may obtained:

$$K^o = K^*_I \Gamma(I) \quad (5)$$

where K^*_I is the stoichiometric equilibrium constant for the extraction reaction for a given ionic strength (I):

$$K^*_I = \frac{[ErL_3(HL)_3]_o [H^+]^3}{[Er^{3+}][HL]^6_o} \quad (6)$$

and " $\Gamma(I)$" is the term containing all the activity coefficients. As a preliminary hypothesis, the term $\Gamma(I)$ can be expected to remain constant as long as the ionic strength in the aqueous phase is constant and the variations in organic phase concentrations are small.

Taking into account the extraction reaction and the speciation of Er(III) in the aqueous phase[12]:

$$[Er(III)]_o = [ErL_3(HL)_3]_o$$

$$[Er(III)]_a = [Er^{3+}] + [ErCl^{+}] = [Er^{3+}](1 + \beta_{ErCl}[Cl^{-}]) = [Er^{3+}]\alpha \qquad (7)$$

$$\alpha = \beta_{ErCl}[Cl^{-}]$$

where β_{ErCl} is the stability constant for the formation of the $ErCl^{2+}$ in the aqueous phase. At constant ionic strength $[Cl^-]$ is constant and thus α constant.

To obtain the extraction constant for the different ionic strengths the stability constant of the erbium-chloride complex needs to be known at each ionic strength. Using the Bromley equation[13] the formation constants can be related to the values can be related to the determined values[12] at the ionic strength I = 0.1 mol/dm^3 in the in the following way:

$$\log \beta_{ErCl}(I) = \log \beta_{ErCl}(0.1) + \log(\gamma_{Cl}(I)/\gamma_{Cl}(0.1)) + 0.51(3-1)^2[\sqrt{0.1}/(1+1.5\sqrt{0.1}) - \sqrt{I}/(1+1.5\sqrt{I})] \qquad (8)$$

where $\beta_{ErCl}(I)$ stability constant for formation of $ErCl^{2+}$ at ionic strength I. From this equation the stability constants β_{ErCl} and α have been computed at each ionic strength.

Experimental data obtained were evaluated by the computer program LETAGROP-DISTR. In this program, for a given model, the computer searches for the best set of equilibrium constants K^*_I, that would minimise the sum squared error defined by:

$$U = \Sigma(\log D_{exp} - \log D_{calc})^2 \qquad 9$$

where D_{exp} is the distribution ratio of metal (II) determined experimentally and D_{cal} is the value calculated by the program solving the mass balance equations, assuming a particular set of species and constants. Furthermore the equilibrium constants for the extracted complex were also determined for the different ionic strength and are shown in Table 2.

The good agreement obtained between experimental and calculated values give as confidence of the proposed model as can be seen in Figure 1.

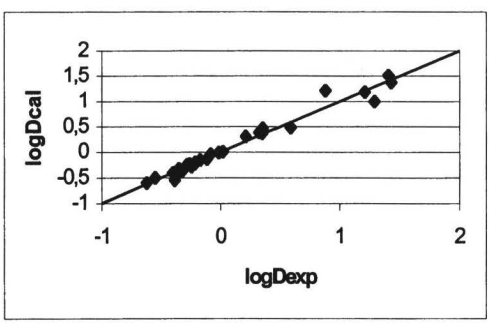

Figure 1. Comparison between logD experimental and logD predicted for Er(III) extraction for the different ionic strength values

I(mol/dm^3)	log K*(I)	I(mol/dm^3)	log K*(I)
0.5	11.63±0.21	2.0	11.85±0.16
1.0	11.73±0.18	2.5	11.95±0.12
1.5	11.78±0.12	3.0	12.07±0.11

Table 2. Values of the extraction constant K*(I) at different ionic strengths. T=298K.

Dependence of the extraction constant K^*_I on the ionic strength (I)

The results at different I values indicate as expected that the composition of the extracted species is independent on the ionic strength whereas the formation constants varies with I. To correlate the values of these constants with the ionic strengths the Guggenheim and Vasilev approach has been used.[14] According to these authors the dependence of the formation constants on **I**, is given by:

$$\log K = \log K^\circ - \frac{\Delta z^2 A\sqrt{I}}{1 + 1.5\sqrt{I}} + \sum b(i,k) I_k \qquad 10$$

with

$$\Delta z^2 = \sum n_j z^2{}_j - \sum r_1 z^2{}_1 \qquad 11$$

where n_j denotes the stoichiometric coefficients of the reacting ionic species of charge z_j (Er^{3+} in equation (2)) and r_1 are the corresponding coefficient for the ionic species formed in reaction (3). K_I and K° represent, formation constants at the ionic strength I and 0 respectively, b is the ionic interaction coefficient of the species i and K, A = 0.511 and I is expressed in $mol.dm^{-3}$.
In our case j represents Er^{3+} and 1 = 0 because the species in the organic phase are associated (non-ionic). Then, $Z^2 = 9$ and equation (10) can be written:

$$\log\beta^*{}_I + - \frac{9A\sqrt{I}}{1 + 1.5\sqrt{I}} = \log\beta^\circ + \sum bI \qquad 12$$

so plotting $\log\beta^*_I + 9A\sqrt{I}/(1+1.5\sqrt{I})$ versus I a straight line is obtained (Figure 2)

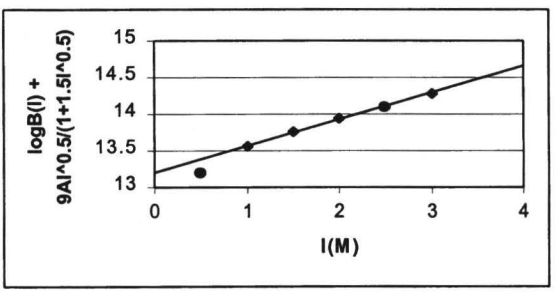

Figure 2. The function $\log\beta^*_I + 9A\sqrt{I}/(1+1.5\sqrt{I})$ (equation 12) plotted for different ionic strengths.

From the intercept and the slope of these lines the formation constant at zero ionic strength and the sum of the specific interaction coefficient, Σb, has been determined. In the present case $\Sigma b = \varepsilon(Er^{3+}, Cl^-)$ Neglecting the first point, the data extrapolated to log K° = 13.20 and the interaction coefficient = $\varepsilon(Er^{3+}, Cl^-)$ was determined as 0.35 estimated from the slope of the straight line in Figure 2. This value seems to be consistent with the present literature.[15,16] For $\varepsilon(Er^{3+}, Cl^-)$ the value is 0.33 and for = $\varepsilon(In^{3+}, Cl^-)$ it is 0.45, which are consistent since the interaction coefficient is expected to increase as the ionic radius rises.

REFERENCES

1 Ritcey GM and Ashbrook AM. *Solvent Extraction in Process Metallurgy*, Elsevier, Toronto, (1984).
2 Freiser H, *Rare Earths Extraction, Preparation and Applications*, The Minerals Metals and Materials Society, (1988).
3 Motomuzi S and Freiser H. *Solv. Extr. & Ion Exch.*, **3**, 637, (1985).
4 Preston JS and du Prez AC. *Solvent Extraction 1990*, Elsevier Science Publishers, B.V., (1992).
5 Han KS, Kim YS and Tozawa T. *Proc. Symp. on Solvent Extraction*, Sendai, Japan, 125, (1986).
6 Han KS, Tozawa T and Kim YS. *Bull. Res. Inst. Min. Dressing and Metall.*, **43**, 184, (1987).

7 Han KS and Tozawa T. *Rare Earths Extraction, Preparation and Applications*, The Minerals Metals and Materials Society, (1988).
8 Liem DH. *Acta Chem. Scand*, **25**, 1521, (1971).
9 Vogel AI. *Textbook of Quantitative Inorganic Analysis*, Longmans, London, (1964).
10 Marcus Y. *Ion Exchange, A series of Advances*. Marcel Dekker, New York, (1966).
11 Aguilar M. *Developments in Solvent Extraction*, Ellis Horword Limited, (1988).
12 Marcus Y. *J. Inorg. Nucl. Chem.*, **28**, 209, (1966).
13 Bromley LA. *A.I.Ch.E, Journal*, **19**, 313, (1973).
14 Vasilev VP. *Russ. J. Inorg. Chem.*, **7**, 924, (1962).
15 Ciavatta L. *Annali di Chimica*, **12**, 550, (1980).
16 Aguilar M, de Pablo J, Valiente M and. Hoegfelt E. *Chemica Scripta*, **26**, 635, (1986).

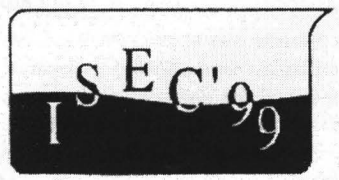

SYNERGISTIC AND ANTAGONISTIC BEHAVIOUR IN THE STRIPPING OF HEAVY RARE EARTH ELEMENTS FROM SOLVENT MIXTURES CONTAINING PHOSPHONIC AND PHOSPHINIC ACIDS AND TRIALKYLPHOSPHINE OXIDES

Donato Nucciarone, Christina D Pagnucco, Boban Jakovljevic and William A Rickelton

Cytec Canada, Inc., Phosphine Technical Centre, P.O. Box 240, Niagara Falls, Ontario L2E 6T4, Canada

ABSTRACT

The stripping behaviour of ytterbium loaded organic solvent mixtures containing the mono-(2-ethylhexyl) ester of 2-ethylhexylphosphonic acid and bis-(2,4,4-trimethylpentyl)phosphinic acid was examined as a function of trialkylphosphine oxide concentration. Depending on the acid used, either a synergetic or antagonistic effect was observed. Stripping with HCl of varying concentrations showed a synergic effect as trialkylphosphine oxide concentration increased, while stripping with HNO_3 showed an antagonistic effect.

Keywords: lanthanide (ytterbium) stripping,, Cyanex 921, 2-ethylhexylphosphonic acid mono-(2-ethylhexyl)ester, bis-(2,4,4-trimethylpentyl)phosphinic acid, Cyanex 272,

INTRODUCTION

The recovery of high purity rare earth elements (REE) by solvent extraction has and continues to be the subject of much study.[1,2,3] Organophosphorus acids have been examined extensively and the mono-2-ethylhexyl ester of ethylhexylphosphonic acid currently appears to be the reagent of choice within the industry. One exception is in the recovery of the heavy rare earths that are very strongly extracted by phosphonic and phosphoric acids and require, for example, 6 mol/dm^3 HCl for stripping. This leads to high neutralisation costs in the recovery of these elements and in contamination of the final product by chlorides.

Phosphinic acids have not been used commercially for REE separation. While, in some cases, they exhibit higher selectivity than their phosphoric and phosphonic acid counterparts, they have, disadvantageously, significantly lower loading capacities and distribution coefficients. However, it has been found that synergetic mixtures of phosphonic and phosphinic acids can be stripped of heavy REE quite readily while, simultaneously, maintaining the selectivity, loading capacity and distribution coefficients associated with phosphonic acid derivatives.[4,5]

However, commercial grade phosphinic acids, particularly CYANEX® 272* extractant, contains significant quantities of a trialkylphosphine oxide impurity. This investigation has determined that this impurity can have a significant effect of the stripping characteristics of the phosphonic/phosphinic acid mixtures.

EXPERIMENTAL

The bulk of the studies were done using Yb^{3+} as representative of the heavy REE. A 0.1mol/dm^3 stock solution was prepared by dissolving solid $YbCl_3 \cdot 6H_2O$ (Alfa-Aesar, 99.9% purity). A stock solution of Lu^{3+} was prepared in a similar manner.

The various solvents were prepared by combining the appropriate amount of phosphinic acid, phosphonic acid and trialkylphosphine oxide then diluting with EXXSOL® D80 (Exxon Corporation).

The Cytec extractant CYANEX® 272 contains bis-(2,4,4-trimethylpentyl)phosphinic acid (BTMPPA) as the principal component at levels of 85-89% by weight. Also present is tri-(2,4,4-trimethylpentyl)phosphine oxide (TTMPPO) at levels of 10-12% and mono-(2,4,4-trimethylpentyl)phosphonic acid at levels of up to 1%. BTMPPA was obtained from CYANEX® 272

* Trademark and Registered Trademark

© 2000 Society of Chemical Industry

by removal of TTMPPO. This was accomplished using a modification of the procedure reported by Fu Xun, et al.[6] A 1 dm^3 volume of 20% by volume CYANEX® 272 in hexane was shaken with a 1 dm^3 solution containing 26 g Na_2SO_4 and 33 g NaOH. The resulting three phases were allowed to separate. The upper phase was enriched with TTMPPO. The lower phase contained the sodium salt of mono-(2,4,4-trimethyl-pentyl)phosphonic acid. The middle phase consisted of a microemulsion enriched in the sodium salt of BTMPPA and residual TTMPPO. The middle phase was separated from the upper and lower phases. This middle phase was then extracted five times with equal volumes of hexane. Each successive wash removed additional TTMPPO. After the final wash the acid form of BTMPPA was obtained by washing with 100 g/dm^3 sulphuric acid. Hexane was removed by distilling under vacuum using a rotary evaporator. The resultant BTMPPA contained <50 mg/dm^3 TTMPPO.

The phosphonic acid, EHEHPA, obtained from Albright & Wilson (IONQUEST® 801), contained 97.4% by weight phosphonic acid and used as received.

The phosphine oxides used were either TTMPPO present naturally in CYANEX® 272 or trioctylphosphine oxide (TOPO) from Cytec as CYANEX® 921, which contained >93% TOPO.

Solvents with the compositions listed in Table 1 were prepared. Each solvent mixture was washed with an equal volume of 100 g/dm^3 HCl, followed by a wash with deionized water. The solvent was then centrifuged (2000 rpm, 30 minutes) to remove any entrained water.

Loading of the solvents was carried out as follows. To a 2 dm^3 baffled flask was added 500 cm^3 of 0.1mol/dm^3 Yb^{3+}. With vigorous stirring an equal volume of solvent was added. Using 100 g/dm^3 NaOH the mixture was adjusted to pH = 3.0. The mixture was allowed to stir for an additional ten minutes then poured into a separatory funnel and the phases separated. For solvents A-D a precipitate was observed settling at the organic/aqueous interface. In all cases the organic phase was centrifuged and the resultant clear organic phase collected.

The following procedure was used to determine solvent loading. A 25 cm^3 aliquot of loaded solvent was shaken with an equal volume of 3 mol/dm^3 HCl on a Burrell wrist action shaker for 25 minutes. The two phases were separated and centrifuged. The aqueous strip liquor was kept for ICP analysis. The stripped organic was mixed with a fresh volume of 3 mol/dm^3 HCl. This stripping process was repeated three times, each time with a fresh aliquot of 3 mol/m^3 HCl. The strip liquors were combined, diluted to volume and Yb concentration determined.

Solvent	BTMPPA (mol/dm^3)	EHEHPA (mol/dm^3)	TTMPPO (mol/dm^3)	TOPO (mol/dm^3)	Yb (mol/dm^3)
A	0.5	0.5	0	0	0.093
B	0.5	0.5	0.07	0	0.090
C	0.5	0.5	0	0.1	0.093
D	0.5	0.5	0	0.2	0.093
E	0.75	0.75	0	0	0.092
F	0.75	0.75	0.1	0	0.100
G	0.75	0.75	0	0.2	0.094

Table 1. Solvent Compositions

The stripping studies were carried out as follows. Stock solutions of HCl and HNO_3 were prepared having the following concentrations: 0.5, 1.0, 1.5, 2.0, 4.0, 6.0 mol/dm^3. For each test 25 cm^3 of acid and 25 cm^3 of loaded organic were combined in an iodine flask. The flasks were shaken for 25 minutes on a Burrell wrist-action shaker at 21°C. The phases were allowed to separate. The aqueous phase was sampled and analysed after dilution.

Rare earth analyses were by ICP spectroscopy using matrix matched standards. Serial dilutions were with 2% HNO_3. The wavelengths used were 369.419 and 339.707 nm for Yb and Lu, respectively.

RESULTS AND DISCUSSION

Loading of the solvents did not reveal any apparent trends as indicated by the results listed in Table 1. Yb concentration in the solvents ranging from 0.09 to 0.10 mol/dm^3 indicated that the loading conditions transferred the bulk of the Yb from the aqueous to the organic phase.

Loading of the solvents A-D resulted in the formation of precipitates. This was not observed for solvents E and F but was seen for solvent G. The precipitates from G however slowly dissolved upon standing for several hours. The formation of these precipitates has also been reported by Hino et. al. and was thought to be rare earth hydroxides being formed during pH adjustment.[7] This occurred only under high loading conditions. They attributed this to steric effects of the bulky terminal substituents on the phosphinic acid alkyl chain. This interfered with the formation of bimetallic species under high loading conditions. Since, in our studies, the loaded solvents A-D had a higher metal/extractant ratio than solvents E-G this behaviour would be expected to be more important for the former solvents.

Presented in Figures 1-4 are the results from the stripping studies. The percent Yb stripped versus acid strength was plotted. Data from the 0.5 mol/dm^3 solutions A-D are represented separately from the 0.75 mol/dm^3 solutions. Data from the Lu studies are presented in Table 2.

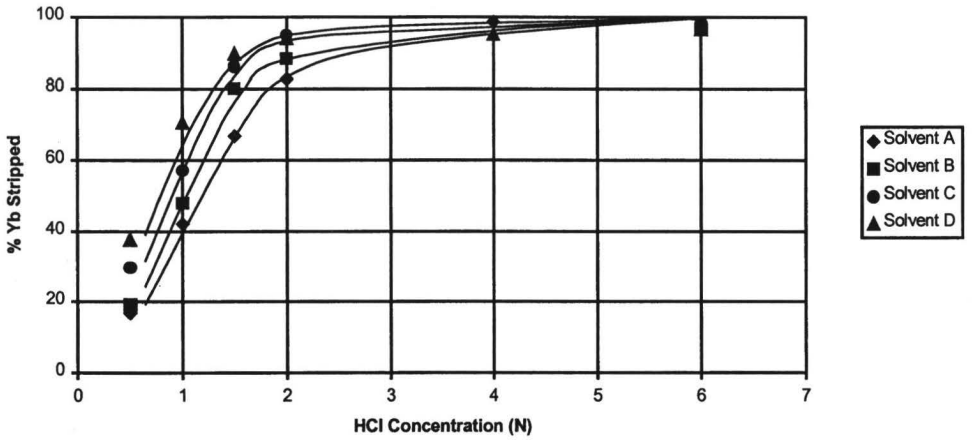

Figure 1. HCl Stripping of Solvents A-D

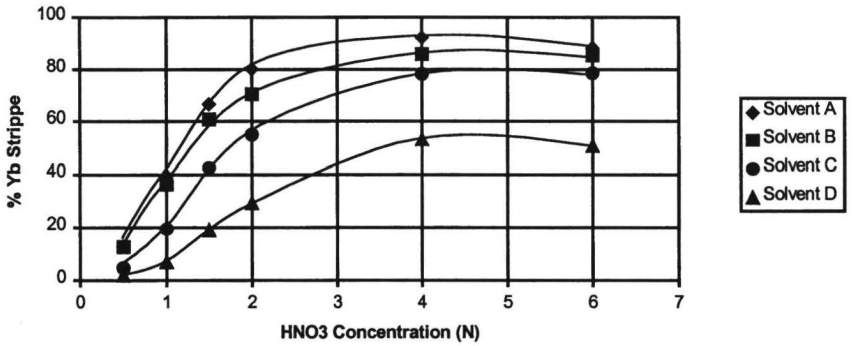

Figure 2. HNO_3 Stripping of Solvents A-D

For the tests using HCl the stripping efficiency improved as the concentration of trialkylphosphine oxide increased. This effect was particularly pronounced at lower acid strengths. For

example, for 1.0 mol/dm^3 HCl in Figure 1, the amount of Yb stripped increased from 42% to 70% upon increasing the TOPO concentration from none to 0.2 mol/dm^3. At higher acid concentrations the effect became insignificant as the amount of Yb stripped approached 100%.

In tests using HNO_3 stripping efficiency decreased as the amount of trialkylphosphine oxide increased. For example, in Figure 2, for 2 mol/dm^3 HNO_3, 80% of the Yb^{3+} was stripped in the absence of any trialkylphosphine oxide (solvent A) compared to 30% stripped in the presence of 0.2 mol/dm^3 TOPO.

Stripping studies for Lu loaded solvents were also conducted, but not as extensively as for Yb. The results, shown in Table 2, indicated similar trends, i.e. the presence of trialkylphosphine oxide improved stripping with HCl but worsened for HNO_3.

Figures 3 and 4 show the results using 0.75 mol/dm^3 concentrations each of phosphonic and phosphinic acids. While the magnitude of the effects was not as large, similar trends were observed.

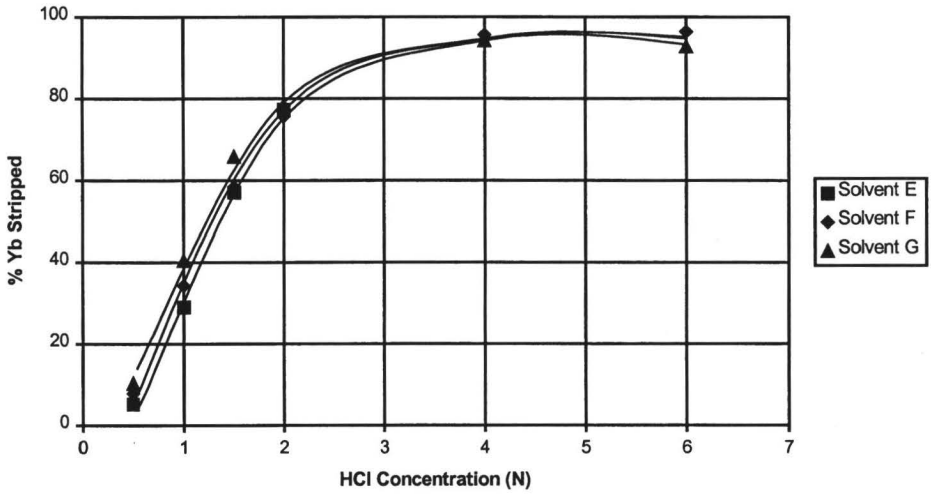

Figure 3 HCl Stripping of Solvents E-G

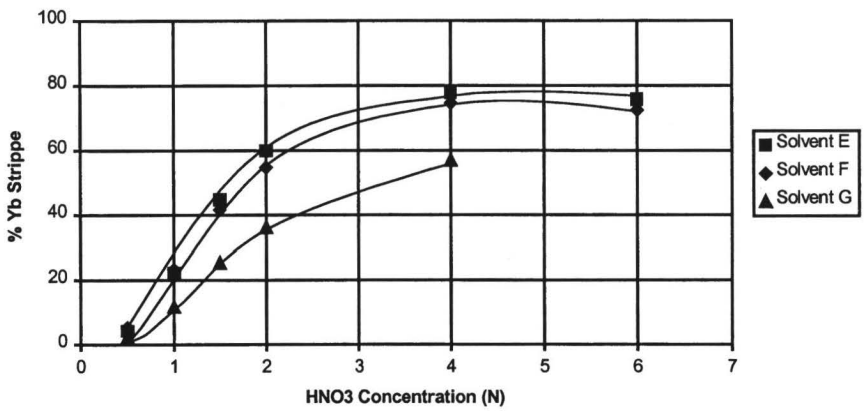

Figure 4 HNO_3 Stripping of Solvents E-G

Strip Acid	Solvent A (% stripped)	Solvent D (% stripped)
HCl (1.0 mol/dm^3)	46	68
HNO_3 (1.5 mol/dm^3)	54	17

Table 2 Lutetium Stripping

The deterioration in stripping performance of HNO_3 with increasing trialkylphosphine oxide concentration may in part be due to the formation of REE nitrate complexes that are re-extracted during the stripping process:

$$\overline{M^{3+} + 3TOPO} + 3NO_3^- = \overline{M(TOPO)_3(NO_3)_3}$$

This suggests that if stripping with HNO_3, an extractant free of trialkylphosphine oxide would be most effective.

The enhanced performance observed in stripping with HCl as trialkylphosphine oxide concentration increased may be due to several factors including the formation of organic REE complexes containing trialkylphosphine oxide as an adduct[8,9,10] or the extraction of HCl into the organic phase by trialkylphosphine oxide.[11]

CONCLUSIONS

An examination of the effect of trialkylphosphine oxide concentration on stripping of heavy REE showed that for solvent systems containing mixtures of EHEHPA and BTMPPA as the trialkylphosphine oxide concentration increased stripping efficiency increased when using HCl as the strip acid and decreased when using HNO_3.

REFERENCES

1. Sherrington L, in *"Handbook of Solvent Extraction"*, Lo TC, Baird MHI, Hanson C edit, Krieger Publishing Co., Malabar, Florida, 717, (1991).
2. Preston JS and Du Preez AC, *"Solvent Extraction 1990, Proceedings of the International Solvent Extraction Conference, Part A"*, Sekine T, editor, Elsevier, Amsterdam, 883, (1992).
3. Cox M in *"Principles and Practices of Solvent Extraction"* RydbergJ, Musikas C and Choppin GR edits., Marcel Dekker Inc., New York, 393, (1992)
4. Yuan C, Ma H, Pan C and Rickelton WA, *"Value Adding Through Solvent Extraction", Proceedings of ISEC'96*, Shallcross DC, Paimin R, Prvcic LM, edits., University of Melbourne Publishing, **1**, 733, (1996).
5. Yuan C and Ma H, *United States Patent 5,622,679*, April 22, 1997.
6. Hu Zhengshui, Pan Ying, Ma Wanwu, Fu Xun, *Solv Extr Ion Exch*, **13** (5), 965, (1995).
7. Hino A, Nishihama S, Hirai T and Komasawa I, *J. Chem. Eng. Japan*, **30**(6), 1040, (1997)
8. Li K and Freiser H, *Solv Extr Ion Exch*, **4**(4), 739, (1986).
9. Komatsu Y and Freiser H, *Anal. Chim. Acta*, **227**, 397, (1989).
10. Reddy MLP, Luxmi Varma R and Ramamohan TR, *Solv Extr Ion Exch*, **16**(3), 795, (1998).
11. Alguacil FJ and Lopez FA, *Hydrometallurgy*, **42**, 245, (1996).

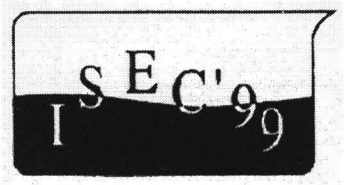

EXTRACTION OF CHLORO COMPLEX ACIDS OF PLATINUM GROUP METALS WITH BINARY EXTRACTANTS

Vera V Belova[1], AI Kholkin[1] and TI Jidkova[2]

[1]N.S. Kurnakov Institute of General and Inorganic Chemistry. Russian Academy of Sciences. 31 Leninskii pr., Moscow, 117907, Russia

[2]Institute of Chemistry and Chemical Technology. Siberian Branch of Russian Academy of Sciences. 42 Marksa, Krasnoyarsk, 660049, Russia

ABSTRACT

The salts of quaternary ammonium bases and strong organic acids were shown to be of most interest for practical purposes. Platinum Group Metals are easily stripped from the organic phase by water, which is practically impossible in the more classical systems involving salts of quaternary ammonium bases with mineral anions.

Keywords: platinum group metals, binary extractants, alkylammonium alkylbenzenesulphonates

INTRODUCTION

Salts of quaternary ammonium bases (QAB) and trialkylammonium possess high extraction efficiency towards Platinum Group Metals.[1-3] Extracted species often have high thermodynamic stability. As a result, such systems suffer from the disadvantage of slow stripping of the platinum metals from the organic phase. The difficulty in stripping has become a problem in the application of these processes. Earlier it was shown[4-6] that salts of organic bases and organic acids (binary extractants) extract mineral acids and metal salts which can then be stripped from the organic phase more easily than for QAB and amine halide extractants. Binary extractants are, therefore, of great interest for studying extraction and stripping of platinum metals.

RESULTS AND DISCUSSION

The extraction processes of chloro complex acids of Platinum Group Metals, H_mMCl_n by binary extractants (R_4NA and R_3NHA respectively, where A^- is anion of an organic acid) can be described in general form as follows:

$$m\,H^+_{(aq)} + MCl_n^{m-}{}_{(aq)} + m\,R_4NA_{(o)} \Leftrightarrow (R_4N)_mMCl_{n(o)} + m\,HA_{(o)} \quad (1)$$

$$m\,H^+_{(aq)} + MCl_n^{m-}{}_{(aq)} + m\,R_3NHA_{(o)} \Leftrightarrow (R_3NH)_mMCl_{n(o)} + m\,HA_{(o)} \quad (2)$$

From equations (1) and (2) it follows that the distribution of complex acids of platinum metals in binary extractant systems depends on the acidity of the aqueous phase, in contrast to anion-exchange extraction. With increasing pH values, the distribution coefficients of metals decrease. Depression of extraction is assumed to result from the formation of a stable binary extractant in the organic phase, which reduces the amount of free extractant available for metal complex formation.

In the systems involving salts of trialkylammonium ions co-ordination mechanism can also take place[7] and as a result slow stripping is observed. Owing to this fact, binary extractants based on QAB are preferable, because ionic associates are only formed in these systems. The systems involving salts of QAB and strong organic acids, for example, alkylbenzenesulphonic acids appear to be the most practical systems, because the stripping processes occur more easily with these reagents.

For example, the extraction of Pt by trialkylbenzylammonium alkylbenzenesulphonate was studied as a function of the concentrations of HCl, the extractant and platinum metal. Table 1 shows that platinum is effectively extracted from 1 mol/dm^3 HCl solution by a 1 mol/dm^3 solution of the binary extractant in toluene and then it is stripped from the organic phase by water in one mixing step. With increasing HCl concentration, the extraction of platinum is enhanced accordingly to regularities

© 2000 Society of Chemical Industry

of binary extraction of mineral acids. The high extent of the extraction and stripping is observed over a wide region of platinum concentration (Table 1).

C_{HCl}, mol/dm^3	C_e, mol/dm^3	$C_{Pt(init.)}$, g/dm^3	Extraction, %	Stripping for 1 Step, by Water, %
0.2	0.10	0.500	52.1	80.6
0.5			67.7	97.9
1.3			89.3	~100
2.3			96.9	~100
3.3			~100	~100
2.0	0.05	0.560	91.8	~100
	0.10		97.9	~100
	0.15		~100	90.6
	0.20		~100	72.8
	0.25		~100	60.4
2.0	0.10	0.197	~100	~100
		0.394	95.4	~100
		0.780	95.3	90.6
		1.18	92.4	72.8
		1.93	88.6	60.4

Table 1 Extraction and Stripping of Pt (IV) from Hydrochloric Solutions, Extractant - Trialkylbenzylammonium Alkylbenzenesulphonate in Toluene

Solvent	C_{HCl}, mol/dm^3	C_e, mol/dm^3	$C_{Ir(init.)}$ 10^3, mol/dm^3	Extraction, %	Stripping for 1 Step by Water, %
Benzene	1.8	0.084	1.03	58.6	~100
	2.3			72.2	97.9
	3.1			83.3	95.8
Toluene	0.8	0.070	1.23	24.9	98.0
	1.4			56.1	~100
	2.0			75.1	97.0
	2.5			78.6	~100
	3.0			85.7	~100

Table 2 Extraction and Stripping of Ir (IV) from Hydrochloric Solutions Extractant - Trialkylbenzylammonium Alkylbenzenesulphonate in Solvents

When the binary extractant system is used, concentrated stripped solutions of platinum in water can be obtained. Thus, using a loaded solution with 1.6 g/dm^3 Pt concentration, after four stripping steps with water (Vo : Va = 1 : 1), a strip solution of platinum with 6.4 g/dm^3 concentration was obtained and platinum stripping was 93-100 % for each step (Extractant concentration was 0.1 mol/dm^3).

Experimental results showed also the improvement of iridium (IV) extraction from chloride solutions by binary extractants with increasing HCl concentration and effective iridium stripping from the organic phase by water (Table 2).

The data for the extraction of palladium from hydrochloric solutions by tetraoctylammonium 4-hexadecyloxybenzenesulphonate in toluene and palladium stripping from the organic phase by water are given in Table 3. The results obtained show the effective extraction of palladium and subsequent stripping with water or diluted solutions of ammonia.

C_{HCl}, mol/dm^3	CH_2SO_4, mol/dm^3	C_e, mol/dm^3	$C_{Pd(init.)} \cdot 10^3$, mol/dm^3	D_{Pd}	Stripping for 1 Step, %	
					by Water	by 1 mol/dm^3 NH_3 soln
0.5	-	0.01	17.8	0.837	61.8	-
2.1				0.968	64.5	
3.0				0.948	61.9	
0.5	-	0.10	10.7	35	30.2	
		0.05		8.9	38.2	
		0.01		0.188	~100	
1.0	-	0.01	6.58	0.600	59.5	87.8
1.0	0.5			0.720	72.7	76.7

Table 3 Extraction and Stripping of Pd (II) from Chloride and Sulphate-chloride Solutions
Extractant - Tetraoctylammonium 4-hexadecyloxybenzenesulphonate in Toluene

In the extraction of chlorocomplexes of Pt(IV), Pd(II), Ir(IV) by 0.1 mol/dm^3 solutions of trialkylbenzylammonium alkylbenzenesulphonate in toluene, the distribution coefficients of metals in the region of 0.5 - 4 mol/dm^3 HCl were in the range 5 - 150, while D_M values for Rh(III), Ru(III) and Ir (III) were less than 0.1 (Figure 1), which creates possibilities for the separation of Platinum Group Metals. The calculated coefficients of the platinum metal separation are $\beta_{Pt/Ir(IV)} \sim 20$; $\beta_{Ir(IV)/Ru(III)} \sim 10$; $\beta_{Ir(IV)/Rh} \sim 50$; $\beta_{Pt/Pd} \sim 12$; $\beta_{Pt\ /Ir(IV)} \sim 20$; $\beta_{Pt/Ru(III)} \sim 2 \cdot 10^2$; $\beta_{Pt/Rh} \sim 1 \cdot 10^3$; $\beta_{Pt/Ir(III)} \sim 2 \cdot 10^3$.

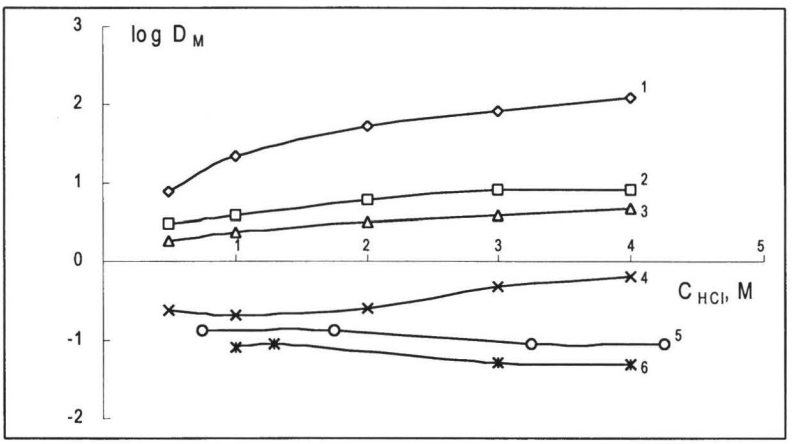

Figure 1. Extraction of Pt(IV) (1), Pd(II) (2), Ir(IV) (3), Ru(III) (4), Ir (III) (5), Rh(III) (6) from chloride solutions by 0.1 mol/dm^{3}solution of trialkylbenzylammonium alkylbenzene-sulphonate in toluene.
$C_{M(init.)}$, g/L: 2.0 (Pt); 0.95 (Pd); 1.9 (Ir); 0.55 (Rh); 0.13 (Ru).

Thus, the results obtained have shown that extracted species resulting from the extraction of platinum metals by binary extractants are labile in these systems and can effectively be stripped in some cases by water. Platinum metals can be separated at both of the extraction and stripping steps.

REFERENCES

1 Maeck WJ, Boman GL, Kussy ME et. al. *Anal. Chem.*, **33**, 1775, (1961).
2 Gindin LM *Extraction Processes and their Application*, Nauka, Moscow, (1984).
3 Markus Y and Kertes AS. *Ion Exchange and Solvent Extraction of Metal Complexes*, Wiley Interscience, New York, (1969).
4 Kholkin AI, Pashkov GL et. al. *Hydrometallurgy*, **36**, 109, (1994).
5 Kholkin AI and Kuzmin VI *Zh. Neorg. khim*, **27**, 2070, (1982).
6 Belova VV and Kholkin AI. *Solv. Extr. Ion Exch.*, **16**, 1233, (1998).
7 Belova VV, Jidkova TI, Vasilevich SA and Kholkin AI. *Solv. Extr. Ion Exch.*, **15**, 1023, (1997).

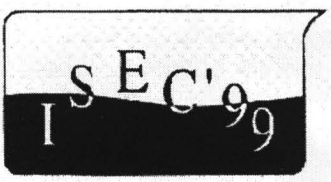

THERMODYNAMIC AND KINETIC STUDIES OF PALLADIUM(II) EXTRACTION BY LIX 63–ALIQUAT 336 MIXTURES

C Foulon, S Pareau, M Stambouli and G Durand
Laboratoire de Chimie et Génie des Procédés, Ecole Centrale Paris, Grande Voie des Vignes, 92295 Châtenay-Malabry Cedex, France

ABSTRACT
The thermodynamic aspects of palladium extraction by LIX 63-Aliquat 336 mixtures from HCl 1 mol/dm^3 were examined showing a synergistic effect, explained by the formation of a mixed complex, in addition to those formed with the individual extractants. The values of the three equilibrium constants were calculated. The kinetics of the system was studied for different conditions and allowed to propose a complete reaction scheme whose limiting step is interfacial. The kinetic enhancement compared to individual LIX 63, is explained by a catalytic effect of Aliquat 336.

Keywords : palladium, LIX63, Aliquat 336, interfacial kinetics, thermodynamics

INTRODUCTION

Since palladium is a precious metal, many investigations of its purification and concentration from HCl media by solvent extraction have been performed. It is however quite difficult to find an extractant that combines a quantitative, selective and quick extraction of Pd(II), with easy stripping. Anionic extractants[1,2] allow high extraction rates, but sometimes lead to a third phase formation, even if a polar solvent is used and stripping is rather difficult. Besides, most of the other extractants exhibit a high degree of extraction, but a low extraction rate, such as solvating extractants[3,4] and chelating extractants.[5,6] Although 5,8-diethyl-7-hydroxy-6-dodecanone oxime (LIX 63), a commercial α-hydroxyoxime, leads to a very slow extraction, it is particularly interesting because it allows a quantitative extraction of Pd(II) and its separation from platinum (IV) in hydrochloric acid solution. The addition of amines or ammonium salts to a chelating or solvating extractants often leads to a catalytic extraction of Pd(II).[7,8,9] This work is therefore devoted to study the extracting properties of LIX 63-Aliquat 336 (quaternary ammonium salt) mixtures.

EXPERIMENTAL

The following reagents were used: palladium (II) chloride (Prolabo, 59% Pd), hydrochloric acid (Prolabo, analytical grade), dodecane (Prolabo, technical grade: 35 % n-dodecane), octanol-1 (Prolabo, purity above 98 %), LIX 63 (Henkel, purity above 70 % (V) (anti + syn isomers)) and Aliquat 336 (Acros). LIX 63 was purified before use according to Tammi[10] and after purification LIX 63 contained 93 % of anti isomer.

Palladium (II) extraction by LIX 63, Aliquat 336 and their mixture was studied in dodecane-octanol 95/5 (V/V). The aqueous phase was prepared by dissolving palladium (II) chloride in 1 mol/dm^3 hydrochloric acid; the resulting palladium concentration was 100 mg/dm^3 (9.4 x 10^{-4} mol/dm^3). The palladium (II) concentration in the aqueous phase was determined after extraction by atomic absorption spectroscopy using a Varian SpectrAA 300/400 atomic absorption spectrometer. The palladium (II) concentration in the organic phase was calculated by mass balance.

RESULTS AND DISCUSSION

Preliminary kinetic study

LIX 63 exhibits a high percentage extraction, but the extraction rate is slow; thus under these conditions, 120 minutes are required to reach equilibrium, as observed by Dhaskali.[11] Aliquat 336

© 2000 Society of Chemical Industry

extracts Pd(II) poorly but rapidly however, in combination with LIX 63, a rapid extraction of Pd(II) ($6 < t_{equilibrium} < 10$ min) is obtained, whereas equilibrium would theoretically be obtained within 1 hour without acceleration. LIX 63-Aliquat 336 is thus a powerful system and has therefore been used for the following studies.

Thermodynamics of Pd(II) extraction by LIX 63-Aliquat 336 mixtures

Distribution curves obtained for Pd(II) extraction by LIX 63, Aliquat 336 and LIX 63-Aliquat 336 mixtures are presented in figure 1, where [Pd(II)] and $\overline{[Pd(II)]}$ denote Pd(II) concentrations in aqueous and organic phases respectively; the points represent the experimental results.

The extracting power of Aliquat 336 is negligible compared to that of LIX 63. Distribution curves relative to LIX 63-Aliquat 336 mixtures indicate that a significant synergism occurs, since: $D_{LIX\ 63\ +\ Aliquat\ 336} > D_{LIX\ 63} + D_{Aliquat\ 336}$, where D is Pd (II) distribution ratio.

The maximum absorption wavelength (395 nm) observed for organic phases containing Pd(II) and LIX 63, is characteristic of a species containing $PdCl_2$ and is consistent with the mechanism proposed by Dhaskali[11] in pure dodecane, i.e:

$$PdCl_4^{2-} + 2\,\overline{H_2Ox} \underset{}{\overset{K_1}{\rightleftharpoons}} \overline{PdCl_2(H_2Ox)_2} + 2\,Cl^-$$

The thermodynamic constant relative to this mechanism has been calculated: $K_1 = (1.5 \pm 0.25)\ x10^6$

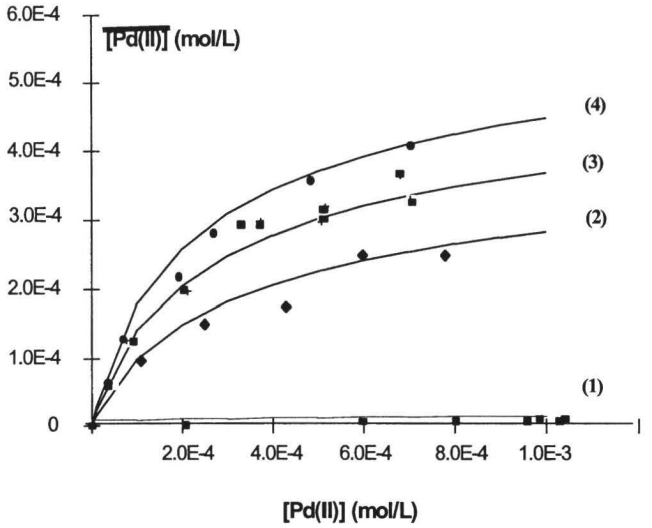

Figure 1:. Distribution isotherms of palladium (II) at 25 ± 1°C.

(1) $\overline{AliCl}]_0 = 5.10^{-4}$ mol/dm^3; (2) $\overline{H_2Ox}]_0 = 10^{-3}$ mol/dm^3
(3) $\overline{AliCl}]_0 = 2.5.10^{-4}$ mol/dm^3 + $\overline{H_2Ox}]_0 = 10^{-3}$ mol/dm^3
(4) $\overline{AliCl}]_0 = 5.10^{-4}$ mol/dm^3 + $\overline{H_2Ox}]_0 = 10^{-3}$ mol/dm^3.

When Pd(II) is extracted by Aliquat 336, the UV-visible spectrum of the organic phase shows a maximum absorption band at 475 nm, which is characteristic of $PdCl_4^{2-}$. This result suggests that the extraction proceeds according to the following mechanism:[2]

$$PdCl_4^{2-} + 2\ \overline{ALICl} \underset{\longleftarrow}{\overset{K_2}{\longrightarrow}} \overline{PdCl_4(ALI)_2} + 2\ Cl^-$$

The thermodynamic constant relative to this mechanism has been calculated: $K_2 = (3.4 \pm 0.5) \times 10^4$

Concerning Pd(II) extraction by LIX 63-Aliquat 336 mixtures, the absorbance band wavelength of organic phase increases with increasing Aliquat 336 concentration. It is comprised of the wavelengths of $PdCl_2$ (λ = 396 nm) and of $PdCl_3^-$ (about 420 nm). These results are explained by the presence of different palladium (II) complexes in the organic phase, containing at least $PdCl_2$ and $PdCl_3^-$. Synergism is explained by the formation of a mixed complex $\overline{PdCl_3(Ali)(H_2Ox)_n}$ which exhibits a higher extractability than the two base complexes ($\overline{PdCl_2(H_2Ox)_2}$ and $\overline{PdCl_4(Ali)_2}$). Taking Pd(II) co-ordination number into account, n may be equal to 1 or 2. The following equilibrium is then involved, simultaneously with both previous equilibria:

$$PdCl_4^{2-} + n\ \overline{H_2Ox} + \overline{ALICl} \leftrightarrow \overline{PdCl_3(ALI)(H_2Ox)_n} + 2\ Cl^- \qquad K_3$$

If n = 2, the calculated K_3 value depends on the experimental conditions: this hypothesis is thus not valid. On the other hand, if n = 1, K_3 is constant whatever the experimental conditions: $K_3 = (3.7 \pm 0.7) \times 10^6$

To validate these mechanisms, the experimental distribution curves have been compared to the theoretical ones (figure 1, where the solid lines are the calculated isotherms). The theoretical curves fit the experimental points. This model is then correct.

Kinetics of Pd(II) extraction by LIX 63-Aliquat 336 mixtures

The experiments were performed in a highly stirred cell at 25°C; the dispersed phase was the aqueous one and the interfacial area was estimated photographically.

Modelling

Consider the three extraction mechanisms; one, i, is limiting:

$$Pd(II) \Leftrightarrow \overline{Pd(II)_i} \qquad i = 1,\ 2 \text{ or } 3$$

$$-V_{aq}\frac{dX}{dt} = k_i\ X - k'_i\ Y_i \qquad X = [Pd(II)] = [PdCl_4^-] \qquad Y_i = \overline{[Pd(II)]_i}$$

The other mechanisms are equilibrated:

$$Y_k = K_k\ X \qquad k = 1,2,3 \qquad k \neq i$$

$$P = \sum_{j=1}^{3} Y_j = Y_i + K\ X$$

where P is the total Pd concentration in organic phase, and K, k_i and k'_i are apparent constants, including chloride and extractant concentrations.

Using mass balance one can obtain the following equation, with X_0, initial aqueous concentration of Pd (II) and X_{eq} its equilibrium aqueous concentration:

$$-V_{aq}\ \frac{dX}{dt} = \left[k_i + k'_i\left(\frac{V_{aq}}{V_{org}} + K\right)\right] X - \frac{k'_i\ V_{aq}\ X_0}{V_{org}} \qquad X_{eq} = \frac{k'_i\ V_{aq}\ X_0}{k_i + k'_i\left(\frac{V_{aq}}{V_{org}} + K\right)}$$

By integration: $\ln\left(\frac{X_0 - X_{eq}}{X - X_{eq}}\right) = \beta\ t \qquad \beta = \frac{k_i}{V_{aq}} + k'_i\left(\frac{1}{V_{org}} + \frac{K}{V_{aq}}\right)$

k_i and k'_i depend on the reaction site.

Limiting reaction site

β depends on both phase volumes. In its previous expression, only k_i and k'_i are depending on reaction site S: $k_i = k\ S$ and $k'_i = k'\ S$, with $S = V_{aq}$, V_{org} or A (interfacial area).

Bulk aqueous phase: the limiting reaction takes place in aqueous phase as for individual LIX 63. Aliquat 336 being insoluble in aqueous phase, this reaction then involves only LIX 63 and might have the same rate than the reaction with individual LIX 63. The extraction by LIX 63- Aliquat 336 mixtures being much quicker, the limiting reaction site is not the aqueous bulk.

Bulk organic phase: In this case the expression for β is the following:

$$\beta = (k + K \quad k') \frac{V_{org}}{V_{aq}} + k'.$$

The variation of β versus V_{org} / V_{aq} has to lie on a straight line. The experimental points being very dispersed, the limiting reaction site might not be the organic bulk.

Interfacial reaction: The expression of β is now:

$$\beta = (k + K \quad k') \frac{A}{V_{aq}} + \frac{k' \quad A}{V_{org}}.$$

The variation of $\beta\ V_{aq} / A$ versus V_{aq} / V_{org} are presented in figure 2. The experimental points roughly lie on a straight line, the limiting reaction is therefore probably interfacial. At least one of the extractants is involved in an interfacial reaction.

Interfacial tension measurements

Interface tension was measured in various cases: individual LIX 63 or Aliquat 336 and their mixtures. LIX interfacial concentration is always negligible; only Aliquat is adsorbed at the interface and its interfacial concentration was calculated. The results of these measurements and calculations are presented in another paper.[12]

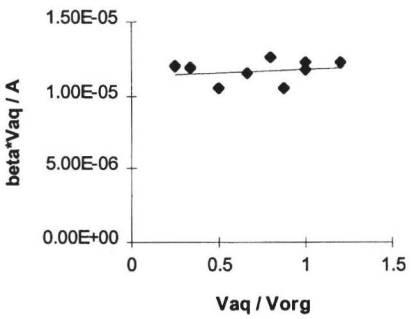

Figure 2: Determination of the limiting reaction site

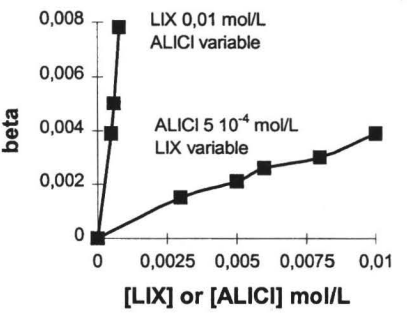

Figure 3: Variations of β with extractant concentration

Proposed Mechanism

As the main result (figure 3), β increases with concentrations of both extractant a mechanism involving one Aliquat adsorbed molecule and one LIX organic molecule is then proposed:

$$PdCl_4^{2-} + ALICl_{ad} \leftrightarrow PdCl_4(ALI)_{ad} + Cl^- \qquad rapid$$

$$PdCl_4(ALI)_{ad} + \overline{H_2Ox} \leftrightarrow PdCl_3(ALI)(H_2Ox)_{ad} + \overline{ALICl} \qquad slow$$

$$PdCl_3(ALI)(H_2Ox)_{ad} \leftrightarrow \overline{PdCl_3(ALI)(H_2Ox)} \qquad rapid$$

$$\overline{PdCl_3(ALI)(H_2Ox)} + \overline{H_2Ox} \leftrightarrow \overline{PdCl_2(H_2Ox)_2} + \overline{ALICl} \qquad rapid$$

The expression for β is the following:

$$\beta = k_0 \ [\overline{H_2Ox}] + \frac{k'_0 \ [\overline{ALICl}]}{[ALICl]_{ad} \ (1 + \frac{K_1}{K_3} \frac{[\overline{H_2Ox}]}{[\overline{ALICl}]})}$$

By plotting $Y = \frac{\overline{\beta}}{[\overline{H_2Ox}]}$ versus $X = \frac{[\overline{ALICl}]}{[ALICl]_{ad} \ [\overline{H_2Ox}] \ (1 + \frac{K_1}{K_3} \frac{[\overline{H_2Ox}]}{[\overline{ALICl}]})}$,

a straight line must be obtained as represented in figure 4. Several other mechanisms were tested without success. The proposed reaction scheme is in good agreement with the experimental results.

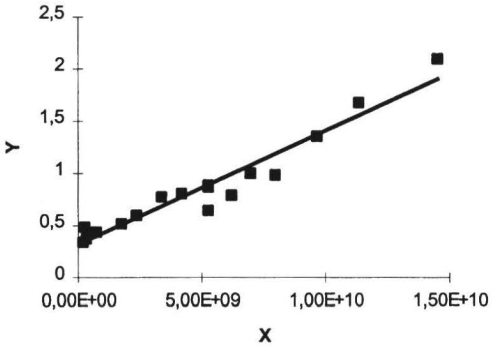

Figure 4: Confirmation of the proposed mechanism

CONCLUSION

This work lead to several significant results: determination of three different mechanisms for Pd (II) extraction by LIX 63-Aliquat 336 mixtures and estimation of their equilibrium constants. In addition the extraction kinetics were studied, showing that the limiting step is an interfacial reaction; a reaction scheme was proposed in good accordance with experimental results.

REFERENCES

1 Mazurova AA and Gindin LM, *Russ. J. Inorg. Chem.*, **10**(2), 263, (1965)
2 Zveguintzoff D, *Thèse de doctorat d'état ès Sciences Physiques*, Université Pierre et Marie Curie, Paris VI, (1981).
3 Inoue K and Baba Y, *Proc. Int. Solvent Ext. Conf. (ISEC'86)*, Munich, **2**, 263, (1986)
4 Baba Y and Shimizu Y, *Proc. Int. Solvent Ext. Conf. (ISEC'93)*, York, **1**, 565, (1993).
5 Inoue K and Maruchi T, *Hydrometallurgy*, **16**, 93, (1986).
6 Ma E and Freiser H, *Solv. Ext. and Ion Exch.*, **1**(3), 485, (1983).

7 Rong Q and Freiser H, *Solv. Extr. Ion Exch.*, **5** (5), 923, (1987).
8 Al-bazi SJ and Freiser H, *Inorg. Chem.*, **28,** 417, (1989).
9 Bauer D and Cote G, *Proc. Int. Solvent Extr. Conf. (ISEC'88)*, Moscow, **2**, 79, (1988).
10 Tammi T, *Hydrometallurgy*, **2**, 371, (1976).
11 Dhaskali G, *Thèse de Doctorat,* l'Université de Paris VI , (1990)
12 Foulon C, *Thèse de Doctorat,* l'Université de Paris VI (1997)

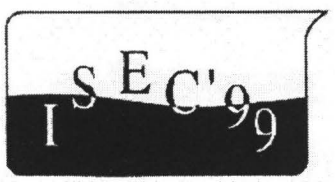

EXTRACTION BEHAVIOUR OF PLATINUM(IV) IN CHLOROFORM WITH A CROWN ETHER FROM ACIDIC MEDIA

Kazi Zakir Hossain and Takaharu Honjo
Department of Chemistry, Faculty of Science Kanazawa University, Kakuma-machi, Kanazawa Ishikawa 920-1192, Japan

ABSTRACT
A new method for the extraction of platinum from hydrochloric acid media has been established based on the formation of ion-pair complex of platinum hexachloro anion with dicyclohexyl-18-crown-6 (DC18C6) oxonium cation in chloroform by means of liquid-liquid extraction and back-extraction combined with inductively coupled plasma atomic emission spectrometry (ICP-AES). The effect of various factors (solvent, crown ether, reagent concentration, acid concentration, shaking time, and foreign ions etc.) on the extraction and back-extraction of platinum has been investigated in detail. The platinum hexachloro anion in 8 mol/L hydrochloric acid forms a stable ion-association complex with protonated DC18C6 (0.05 mol/L DC18C6) as $[H_3O{\cdot}DC18C6^+]_2[PtCl_6^{2-}]$, and can be extracted quantitatively (97%) in chloroform within 5 min. Stripping of the extracted platinum was achieved with 0.1 mol/L hydrochloric acid. No extraction was observed when extracting palladium and rhodium under the same analytical conditions for platinum extraction. The content of platinum in palladium chloride and rhodium chloride of guaranteed reagent grade was determined after its separation by DC18C6 extraction at 8 mol/L hydrochloric acid and it was found to be 16.39 μg/g and 8.94 μg/g, respectively.

Keywords: crown ether, platinum(IV), hydrochloric acid, ICP-AES.

INTRODUCTION

Platinum group metals, such as platinum (IV), palladium (II) and rhodium (III) have been used as catalytic converters in automobiles. Platinum- and gold-based medicines have also been used as anti-cancer and anti-rheumatic drugs[1]. The high values of these metals have prompted investigations of their separation, concentration and purification by solvent extraction techniques. Crown ethers along with thenoyltrifluoroacetone (TTA) have been used as a versatile synergistic extractant for alkali and alkaline earth metals[2] and heavy metals[3]. Anionic palladium complex of 4-(2-pyridyl-azo)-resorcinol (PAR)[4] has been readily extracted in 1,2-dichloroethane as an ion-pair complex with cationic potassium complex of dicyclohexyl-18-crown-6. Palladium complexes of Cl^-, Br^-, I^-, and SCN^- have been extracted in chloroform-acetonitrile (3:1) solution as ion-association products with cationic potassium complex of dibenzo-18-crown-6 (DB18C6) and its derivatives[5]. Complexation[6] of the hydronium ion (H_3O^+) with DC18C6 and its uses[7,8,9,10] as a counter-cation in the ion-association extraction of anionic complexes of various metals, such as $PMo_{12}O_{40}^{3-}$, TaF_6^-, $MoO(SCN)_5^-$, $WO_2(SCN)_3^-$, $WO(SCN)_5^-$, $FeCl_4^-$, $AuCl_4^-$, $GaCl_4^-$, $TlCl_4^-$, $SbCl_4^-$ and $SbCl_6^-$, have been reported.

Platinum mainly exists as anionic hexachloro complex in 8 mol/dm^3 hydrochloric acid. Therefore, protonated crown ethers may have excellent promise to extract the platinum hexachloro anion in a suitable organic solvent. There has been no report on the ion-association extraction of platinum with crown ethers[11]. In preliminary experiments on the extraction of platinum (IV) with DC18C6 in various organic solvents (chloroform, 1-octanol, dichloromethane, o-dichlorobenzene, nitrobenzene, toluene etc.) from 8 mol/dm^3 hydrochloric acid, it has been found that platinum (IV) can be extracted quantitatively and selectively with DC18C6 in chloroform. On the basis of these results, the extraction behaviour of platinum (IV) with 0.05 mol/dm^3 DC18C6 in chloroform at 8 mol/dm^3 hydrochloric acid solution has been investigated in detail, and a new method for the quantitative extraction and separation of platinum from palladium and rhodium has been established by means of extraction and back-extraction combined with inductively coupled plasma atomic emission spectrometry (ICP-AES).

© 2000 Society of Chemical Industry

EXPERIMENTAL

Apparatus

A Shimadzu Sequential Type Plasma Emission Spectrometer, model ICPS-1000 III (Kyoto, Japan); a Taiyo Recipro Shaker, model SR-II; a Tomy Seiko Low Speed Centrifuge, model LC-100 were used.

Reagents

A 1000 $\mu g/cm^3$ of platinum standard stock solution (f = 1.008) in 1 mol/dm^3 hydrochloric acid (Cica-MERCK, Japan) was used after suitable dilution with distilled-deionized water prepared by Nanopure system (Barnstead Ltd., USA). 12-crown-4 (12C4) (TCI Ltd, Japan), 18-crown-6 (18C6) (Katayama, Japan), 15-crown-5 (15C5), dibenzo-18-crown-6 (DB18C6), dicyclohexyl-18-crown-6 (DC18C6) and dibenzo-24-crown-8 (DB24C8) (Merck-Schuchardt, Germany) were used without further purification. All other chemicals were of guaranteed grade and were used without further purification.

Solvent extraction

An aliquot (10 cm^3) of a sample solution containing platinum (50 $\mu g/cm^3$) in 8 mol/dm^3 hydrochloric acid was placed into a 30 cm^3 glass-stoppered centrifuge tube. A 10 cm^3 of chloroform solution containing 0.05 $moldm^3$ DC18C6 was added to the centrifuge tube, and the mixtures were shaken on a shaking machine for 5 min. The two phases were separated by centrifugation at 2000 rpm for 5 min and then taken by pipetting into another tube.

Back-extraction

The organic phase (10 cm^3) containing the extracted platinum was shaken with 10 cm^3 of 0.1 mol/dm^3 hydrochloric acid solution for 5 min. The amount of platinum stripped from the organic phase was determined by ICP-AES at 214.423 nm.

RESULTS AND DISCUSSION

Effect of solvent

The effect of organic solvent on the extractability of platinum with DC18C6 from 8 mol/L hydrochloric acid solution was investigated by various organic solvents such as benzene, toluene, nitrobenzene, *o*-dichlorobenzene, cyclohexane, dichloromethane, 1-octanol and chloroform. The results are summarized in Table 1.

The extractability of platinum as the ion-pair complex with protonated DC18C6 in chloroform, $[H_3O.DC18C6^+]_2[PtCl_6^{2-}]$, gave higher values than that of all other solvents investigated. Taking into account the low solubility of the organic solvent in water and its high extractability for platinum, chloroform was selected as the solvent for subsequent experiments.

Solvent	Solubility in water (W/W%)	%E
Benzene	0.18	0
Toluene	0.05	0
Nitrobenzene	0.21	96
o-Dichlorobenzene	0.01	70
Cyclohexane	0.01	0
Dichloromethane	0.05	95
1-Octanol	0.1	62
Chloroform	0.01	97

Pt: 50 μg/cm^3, DC18C6: 0.05 mol/dm^3, HCl: 8 mol/dm^3, Shaking time: 5 minutes

Table 1 Effect of organic solvent on the extraction of platinum with DC18C6

Effect of hydrochloric acid concentration

The optimum hydrochloric acid concentration for quantitative extraction of platinum was ascertained with DC18C6 in chloroform by carrying out extraction from 1 to 10 mol/dm^3 hydrochloric acid. The phase volume ratio was maintained at 1:1. The results are shown in Fig.1. The quantitative extraction (97%) was achieved in an acid concentration range of 8 to 10 mol/dm^3. From these results; A 8 mol/dm^3 hydrochloric acid was selected as the optimum concentration for quantitative extraction of platinum. An attempt was made to extract palladium and rhodium under the same analytical conditions and, it was found that the %E of both the metals was zero at 8 mol/dm^3 hydrochloric acid region (Fig.1).

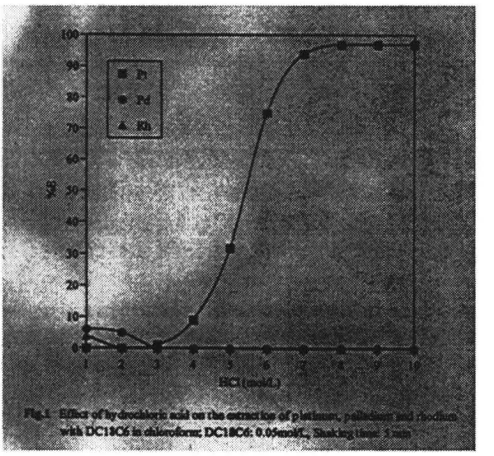

Fig.1 Effect of hydrochloric acid on the extraction of platinum, palladium and rhodium with DC18C6 in chloroform; DC18C6: 0.05mol/L, Shaking time: 5 min

Effect of various crown ethers

Various crown ethers were investigated as extractants for platinum in chloroform at 8 mol/dm^3 hydrochloric acid. The crown ethers used were 12C4, 15C5, 18C6, DB18C6, DC18C6 and DB24C8. The results are summarized in Table 2. It was found that DC18C6 was the best extracting agent for quantitative extraction of platinum.

Crown ether	%E
None	3.0
12C4	3.0
15C5	3.0
18C6	4.0
DB18C6	7.0
DC18C6	97.0
DB24C8	4.0

Pt: 50 μg/cm^3, Crown ether: 0.05 mol/dm^3, HCl: 8 mol/dm^3, Shaking time: 5 minutes

Table 2 Effect of crown ether on the extraction of platinum in chloroform

Effect of DC18C6 concentration

The optimum concentration of DC18C6 for the quantitative extraction of platinum was ascertained by extracting it with the various concentration of the crown ether in the concentration range of $5.0x10^{-4}$ to $1.0x10^{-1}$ mol/dm^3. The extraction was quantitative from $5.0x10^{-2}$ mol/dm^3 of DC18C6. Therefore, $5.0x10^{-2}$ mol/dm^3 of DC18C6 was selected as optimum crown ether concentration for the present method.

Effect of shaking time

The optimum shaking time required to reach the extraction equilibrium was ascertained by measuring the recovery of platinum at various shaking times (0~10 min). It was found that the extraction equilibrium is attained rapidly within 5 min. The stripping of platinum contents from organic phase by 0.1 mol/dm^3 hydrochloric acid solution was fast also, and completed within 2 min. From these data; A 5 min was adopted as optimum shaking time for both extraction and back-extraction procedure to ensure the complete extraction.

Composition of the extracted species

The composition of the extracted species on the extraction of platinum with DC18C6 in chloroform was ascertained by plotting log D vs. log $[DC18C6]_{org}$ at a fixed hydrochloric acid concentration of 6 mol/dm^3 (Fig.2). The plot gives a straight line having a slope of 2. As DC18C6 forms stable oxonium cation in the presence of high acid concentration[6], anionic platinum hexachloro complex may be extracted as an ion-association product of $[H_3O.DC18C6^+]_2[PtCl_6^{2-}]$, the metal to crown ether ratio being 1:2.

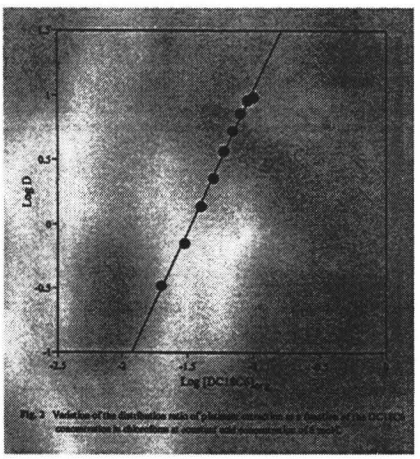

Effect of foreign ions

The effect of foreign ions which may cause interference in the extraction of platinum was studied by using a series of synthetic samples containing platinum (50 μg/cm^3) and various amounts of foreign ions. The recoveries obtained for binary mixtures are summarized in Table 3. It was noted that the procedure is free from the interferences by foreign ions at a concentration of several hundred times that of platinum, except for iron(III) at 10 times. Iron(III), which co-extracted along with platinum can be pre-removed[12] completely by extracting it with 0.05 mol/dm^3 DC18C6 in chloroform at hydrochloric acid range of 3~4 mol/dm^3.

Foreign ion	Concentration (times that of platinum)	Recovery of platinum (%)
Li^+	200	98
Na^+	200	96
K^+	200	95
Rb^+	100	96
Mg^{2+}	200	97
Ca^{2+}	200	96
Fe^{2+}	10	88
NO_3^-	300	98
SO_4^{2-}	300	96

Pt: 50 μg/cm^3, DC18C6: 0.05 mol/dm^3, HCl: 8 mol/dm^3, Solvent: Chloroform, Shaking time: 5 min

Table 3 Effect of foreign ions on the extraction of platinum

Determination of platinum in chemical reagents

The extraction method was applied to the separation and determination of platinum traces in chemical reagents of $PdCl_4$ and $RhCl_3$. A linear calibration curve (r^2=0.9999) of 0~50 μg/cm^3 platinum in 0.1 mol/dm^3 hydrochloric acid was prepared by measuring its intensity with ICP-AES. A weighed amount of reagent sample (21.7 mg) was dissolved in 10 mL of hydrochloric acid (8 mol/dm^3) solution and 1 μg/cm^3 and 5 μg/cm^3 platinum standard was spiked to it. The platinum content was analyzed by the proposed method in Fig.3. In this analysis, the recovery of platinum was 66% for 1 μg/cm^3 platinum and 97% for 5 μg/cm^3 platinum. The content of platinum in palladium chloride and rhodium chloride of guaranteed reagent grade dissolved in 8 mol/dm^3 hydrochloric acid was found to be 16.39 μg/g and 8.94 μg/g, respectively.

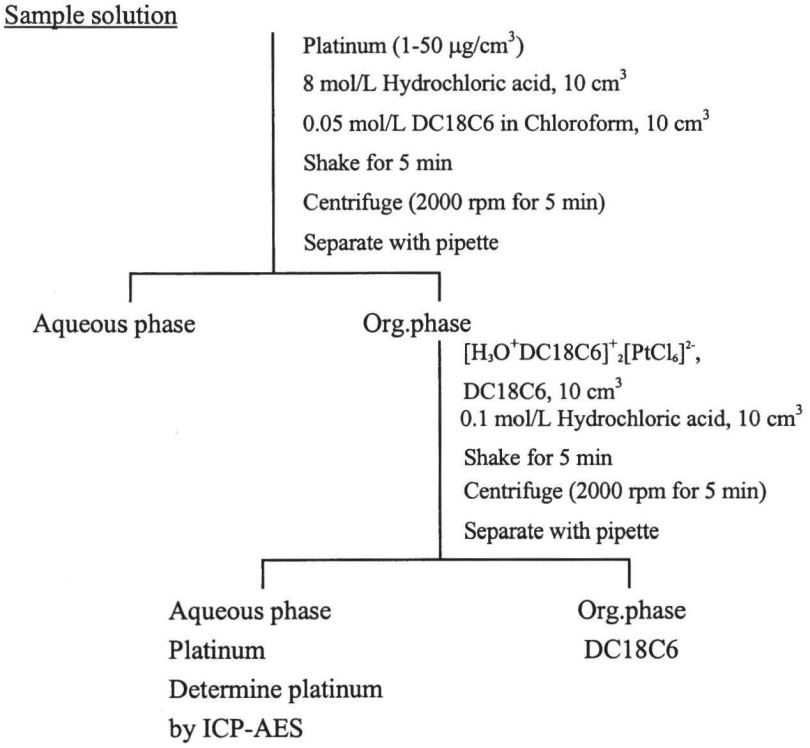

Figure 3 Analytical scheme for the determination of platinum traces in hydrochloric acid media

ACKNOWLEDGEMENTS

This work was supported by grant-in-aid for Scientific Research from the Ministry of Education, Science, Sports and Culture, Japan (No.10640586).

REFERENCES

1. Begerow J, Turfeld M and Dunemann L, *Anal. Chem. Acta.*, **340**, 277, (1997).
2. Itoh T, Billah M, Honjo T and Terada K, *Anal. Sci.*, **7** (supplement), 47, (1991).
3. Hossain KZ and Honjo T, *Fresenius J. Anal. Chem.*, **361**, 451, (1998).
4. Gaikwad AG, Noguchi H and Yoshio M, *Anal. Lett.*, **1991**, 1625.
5. Poladyan VE, Burtnenko LM, Avlasovich LM and Andrianov AM, *Russ J Inorg. Chem.*, **32**, 413, (1987).
6. Izatt RM, Haymore BL and Christensen JJ, *J. Chem. Soc. Chem. Comm.*,**1972**, 1308.
7. Noguchi H, Yoshio M, Nakamura H, and Nagamatsu M, *Chem. Abstr.*, **97**, 192365, (1982).
8. Caletka R, Hausbeck R and Krivan V, *Fresenius J. Anal. Chem.*, **320**, 665, (1985).
9. Caletka R, Hausbeck R and Krivan V, Talanta, **33**, 315, (1986).
10. Koshima H and Onishi H, *Analyst*, **111**, 1261, (1986).
11. Honjo T, *Bunseki*, **1997**, 127.
12. Koshima H and Onishi H, *Anal. Sci.*, **1**, 389, (1985).

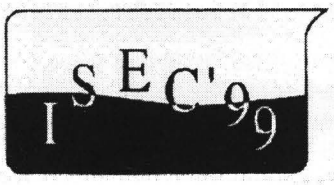

COMPARATIVE STUDIES OF SOLVENT EXTRACTION AND LIQUID MEMBRANE PERMEATION OF GOLD(III) FROM CHLORIDE MEDIA

Réda Haddad[1], Anil Kumar[1], FJ Alguacil[2] and AM Sastre[1]

[1] Department of Chemical Engineering, Universitat Politecnica de Catalunya E.T.S.E.I.B., Diagonal 647, E-8028 Barcelona, Spain

[2] Centro Nacional de Investigaciones Metalurgicas, Avda. Gregorio del Amo 8, Ciudad Universitaria, 28040 Madrid, Spain

ABSTRACT

Selective solvent extraction and liquid membrane permeation of Au(III) from aqueous chloride media into cumene by pure Cyanex 471X, Cyanex 925, Cyanex 301, Cyanex 302 and their binary salts with trioctylmethylammonium chloride (TOMAC) i.e. Cyanex 301+TOMAC , Cyanex 302 + TOMAC has been investigated to compare the performance of these extractants or as liquid membrane carrier under similar experimental conditions. Cyanex 301, Cyanex 302 and their binary extractants with TOMAC afforded very high extraction of Au(III) but stripping of metal from loaded organic phase was found to be extremely difficult. Among all these extractants, Cyanex 925 was found to be the best extractant and liquid membrane carrier with respect to Au(III) recovery and its easy regeneration. Optimum conditions were established for extraction separation of Au(III) with Cyanex 925 in solvent extraction as well as liquid membrane studies. For all the extractants studied, experimental data has been treated graphically and numerically by means of the computer programme LETAGROP-DISTR to calculate K_{ex} values except Cyanex 925 and Cyanex 471X (taken from published literature). The metal species formed with extractants are also proposed. The permeability coefficients of Au(III) were determined with all liquid membrane carriers under the similar experimental conditions to compare their performance.

Keywords: gold(III), supported liquid membrane, Cyanex 301, Cyanex 302, Cyanex 925, binary extractants, trioctylmethylammonium chloride

INTRODUCTION

Gold is one of the most useful and precious noble metals, due to its excellent physcochemical properties. A great interest in the recovery of gold from primary and secondary resources still continues to meet the high metal demand. Mostly, processes dealing with these types of resource use acid leaching for gold recovery. Therefore, studies on recovery of gold from chloride media are of great importance. In previous studies the selective extraction-separation of gold (III) from base metals using thiourea derivatives as extractants have been reported.[1] In the present study, commercially available extractants introduced by Cytec Industries i.e. Cyanex 301 [bis (2,4,4-trimethylpentyl) dithiophosphinic acid], Cyanex 302 ([bis (2,4,4-trimethyl)monohiophosphinic acid],), Cyanex 471X (tri-isobutylphosphine sulphide), Cyanex 925 (2,4,4-trimethylpentyl-n-octyl phosphine oxide) have been chosen.[2] In addition Cyanex 301 and Cyanex 302 were also used in the form of binary extractants with TOMAC (Trioctyl methyl ammonium chloride). This has been done to ease the regeneration of the extractant as proposed by Eyal et al.[3,4] The binary extractants behave like neutral extractants in solvent extraction. Earlier work performed by Kakoi et al[5] and Sole[6] have indicated that stripping of metal was extremely difficult with Cyanex 301 and Cyanex 302. More details of binary extractants and their advantages are published elsewhere.[7] The solvent extraction and liquid membrane studies of gold from chloride media with Cyanex 471X have been reported by Hidalgo et al.[8,9] In previous publications, solvent extraction of Au(III) from chloride media using Cyanex 925 has been reported.[10] This paper presents the comparative studies of liquid-liquid extraction of Au(III) and liquid membrane permeation studies from chloride media using Cyanex 471X, Cyanex 925, Cyanex 301, Cyanex 302 and their binary salts with TOMAC i.e. Cyanex 301 + TOMAC, Cyanex 302 + TOMAC.

© 2000 Society of Chemical Industry

EXPERIMENTAL

All the chemicals used were of A.R or G.R grade unless stated otherwise. Analytical grade diluent namely cumene (A.R.Fluka), was obtained and used as such. Extractants Cyanex 301, Cyanex 302, Cyanex 925 and Cyanex 471X, were kindly supplied by Cyanamid (now Cytec Inc.) and TOMAC was obtained from Merck. The extractants were used without further purification. A stock solution of Au(III) (1g/dm^3) was prepared from 48.92% pure solid $HAuCl_4$, Johnson Mathey, by dilution with HCl.

Distribution Ratio measurements

Equal volumes (10 cm^3) of Au(III) in desired acid molarity and the organic extractant dissolved in an organic diluent, were pipetted into a 20 cm^3 glass stoppered equilibration vial and stirred mechanically for one hour at room temperature (25 ± 1C). Equilibrium was established rapidly, although a contact time of 15 minutes was used in the case of Cyanex 301 and Cyanex 302; and in the case of binary Cyanex 301 + TOMC and Cyanex 302 + TOMAC the contact time was 10 minutes. The binary extractants were prepared by mixing equimolar quantities of Cyanex 301 and Cyanex 302 with TOMAC. The formation of the acid-base couple is an exothermic reaction, and can be expressed as

$$HA_o / H_2A_{2,0} + R_4NCl_0 \Rightarrow R_4NA_o / R_4NHA_{2,o} + HCl_o$$

where HA_0 and H_2A_2 denotes Cyanex 301, Cyanex 302 respectively and R_4NCl denotes TOMAC. Vapour pressure osmometry measurements have shown that Cyanex 302 exist predominantly as dimeric species (H_2A_2), while Cyanex 301 is monomeric.[11] The formation of the binary extractant, R_4NA, results in the generation of hydrochloric acid in the organic phase. This inorganic acid was removed by washing with water. The extractants were dissolved in cumene to the required concentration. After phase separation, the equilibrium pH was measured, and the metal concentration was determined by atomic absorption spectrometry using a 2380 Perkin Elmer Absorption Spectrometer. The gold content of the organic phase was measured after stripping of the metal ion into 0.5 mol/dm^3 NaSCN in 0.5 mol/dm^3 NaCl. All the measurements were performed at least in duplicate and the agreement of the D values obtained was within ± 2% with good material balance (>95%). For studying the back extraction, 10 cm^3 of loaded organic was withdrawn into a equilibration tube and back extracted for about 30 minutes with the same volume of the strippant.

PILM Preparation and Measurements

Single stage PILM measurements were carried out with a simple two compartments permeation cell which consisted of a source phase (generally 180 cm^3) separated from the receiving phase chamber (180 cm^3) by a liquid membrane having an effective membrane area 11.33 cm^2. The source and receiving phases were mechanically stirred at about 1400 rpm at room temperature (25 ± 1C) to avoid concentration polarisation conditions at the membrane interfaces and in the bulk of the solutions. Membrane permeabilities were determined by monitoring Au(III) concentration by atomic absorption spectrometer (2380 Perkin Elmer Absorption Spectrometer) in the source phase as a function of time. The Au(III) concentration in the various phases was found to be reproducible within ±10%. Permeation coefficient (P_{au}) was computed by the following equation :

$$\mathrm{Ln}\left(\frac{[\mathrm{Au(III)}]}{[\mathrm{Au(III)}]_o}\right) = -\frac{A}{V} P\, t$$

where V is the volume of the source phase solution (cm^3), A the effective membrane area (cm^2) , $[Au(III)]_0$ and [Au(III)] are concentrations of metal ion in source phase at time zero and at a given time t, respectively (mol/dm^3), and t the elapsed time (s).

Membrane Support

The organic membrane phase was prepared by dissolving a weighed quantity of extractants in organic diluent to obtain a carrier solution of various concentrations. The polymeric support, Durapore (polyvinylldenedifluoride) used was about 125 μm thick, and had a nominal porosity of about 75% and pore diameter of the order of 0.22 μm and tortuosity 1.67. The polymeric support was impregnated with the carrier solutions containing the extractant in cumene by immersion for 24 hours, then leaving it to drip for a few seconds before being placed in the PILM cell.

RESULTS AND DISCUSSION

The extractability of Au(III) with extractants Cyanex 301, Cyanex 302, Cyanex 301+TOMAC, Cyanex 302+TOMAC, followed the order: Cyanex 301 + TOMAC > Cyanex 302 +TOMAC > Cyanex 301 > Cyanex 471X > Cyanex 302 > Cyanex 925. Figure 1 shows log D values plotted against extractant concentrations. Cyanex 301, Cyanex 302 and their binary salts with TOMAC afforded very high extraction. On the other hand log D values varies 0 to 2.5 for Cyanex 471X and –1 to 0 for Cyanex 925. Table 1 presents log K_{ex} values for the extraction at different HCl concentrations with the model of extracted species. The K_{ex} values for Cyanex 471X and Cyanex 925 were taken from published literature.[8,11]

The complex formation with various extractants from chloride media is given below:

$$AuCl_4^- + HL \Leftrightarrow AuCl_3HL + Cl^- \quad \text{[Cyanex301]}$$

$$AuCl_4^- + HL \Leftrightarrow AuCl_3HL + Cl^- \quad \text{[Cyanex302]}$$

$$H^+ + AuCl_4^- + R_4NA \Leftrightarrow AuCl_4R_3NH^+ + Cl^- \quad \text{[Cyanex301+TOMAC]}$$

$$H^+ + AuCl_4^- + R_4NA \Leftrightarrow AuCl_4R_3NH^+ + Cl^- \quad \text{[Cyanex302+TOMAC]}$$

$$H^+ + AuCl_4^- + 2L \Leftrightarrow HAuCl_4L_2 \quad \text{[Cyanex925]}$$

$$Au^{+3} + 3Cl^- + L \Leftrightarrow AuCl_3L \quad \text{[Cyanex471X]}$$

$$Au^{+3} + 3Cl^- + 2L \Leftrightarrow AuCl_3L_2 \quad \text{[Cyanex471X]}$$

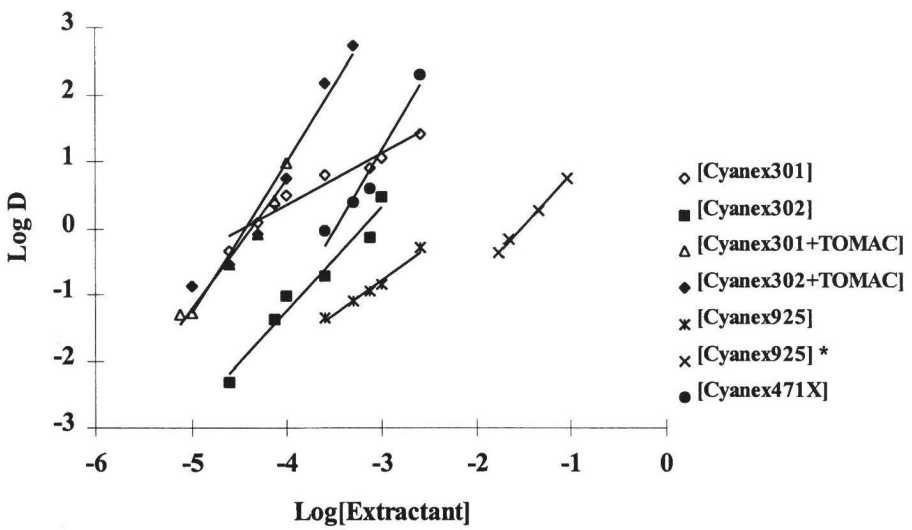

Figure 1 : Variation of Log D as a function of extractants concentrations dissolved in cumene for the extraction of Au(III) from a 1 mol/l HCl medium.
(*) Variation of Log D as a function of Cyanex 925 dissolved in xylene for the extraction of Au(III) from a 5 mol/l HCl medium (10) .

Extractants	[HCl] = 1 mol/dm^3	Model extracted species	Reference
	log K_{ext}		
Cyanex 301	4.169	$AuCl_3HL$	this work
Cyanex 302	3.082	$AuCl_3HL$	this work
Cyanex 301+TOMAC	3.812	$AuCl_4R_3NH^+$	this work
Cyanex 302+TOMAC	2.243	$AuCl_4R_3NH^+$	this work
Cyanex 925	7.870	$HAuCl_4L_2$	(11)
Cyanex 471X	34.840	$AuCl_3L$	(8)
	42.040	$AuCl_3L_2$	(8)

Table 1 Log K_{ex} for the extraction of Au(III) with different extractants .

The stripping behaviour of Au(III) with all the extractants using 0.5 mol/dm^3 NaSCN + 0.5mol/dm^3 NaCl is depicted in Figure 2. Binary extractants afforded gold stripping between 25-30% whereas from pure Cyanex 301 and Cyanex 302 loaded organic phase, stripping was around 26 % for both the extractants. For the other neutral extractants such as Cyanex 471X and Cyanex 925, stripping was almost 30 and 90 % respectively. The findings are contrary to the results of Eyal[3,4] and Tait,[12] with respect to the performance of binary extractant metal stripping from loaded organic phase. The reason for this behaviour may be the strong complexation of Au(III) with TOMAC alone in binary phase which overall affects the metal stripping from loaded organic phase.

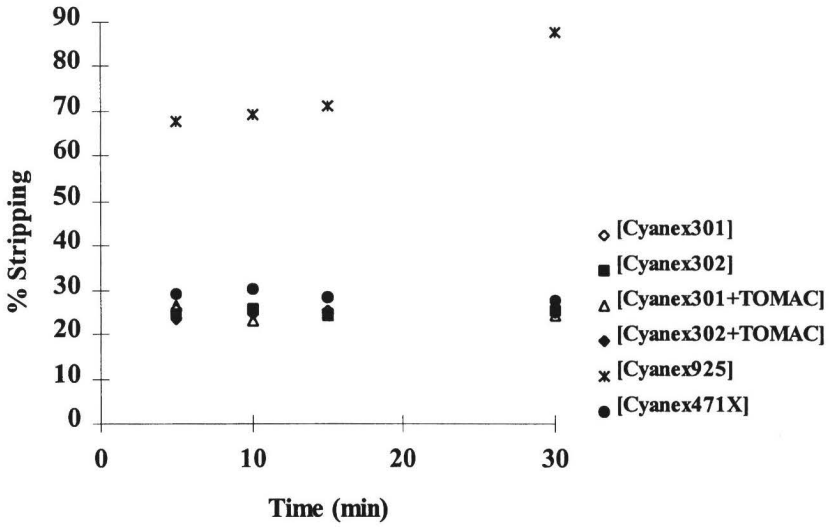

Figure 2 Stripping behaviour of Au(III) from loaded organic phase of different extractants dissolved in cumene

Carriers	P (cm/s) (after 60 minutes)	Au(III) recovery in receiving phase (%)
Cyanex 301	0.012	55
Cyanex 302	0.010	67
Cyanex 301+TOMAC	0.010	47
Cyanex 302+TOMAC	0.013	59
Cyanex 925	0.017	94
Cyanex 471X	0.019	81

Table 2 Values of the permeability coefficient P and percentage of stripping S for different carriers.[Au(III)]=10mg/dm^3 ; [Carrier]=0.1mol/dm^3

Based on the solvent extraction data, all these extractants were tested as liquid membrane carriers to evaluate their performance. Table 2 summarises the values of permeability coefficient (P) with carriers studied and % recovery of Au(III) in receiving phase. As indicated by the results, P values range between $1.0x10^{-2}$ to $1.3x10^{-2}$ cm/s for Cyanex 301, Cyanex 302 and their binary carriers but stripping from membrane in receiving phase was only between 45 to 65%.

[Cyanex925] (mol/dm^3)	0.025	0.05	0.075	0.1	0.2
P (cm/s) (after 60 min)	0.008	0.011	0.015	0.017	0.027

Table 3 Values of the permeability coefficient P at different concentrations of Cyanex 925 in cumene .[Au(III)]=10mg/dm^3; $[HCl]_{feed}$=1mol/dm^3 ; $[NaSCN]_{strip}$=0.5mol/dm^3 ; [NaCl]=0.5mol/dm^3

[HCl] (mol/dm^3)	P (cm/s) (after 60 min)	Au(III) recovery in receiving phase(%)
0.1	0.019	89
1	0.017	94
3	0.012	100
5	0.008	100

Table 4 Values of the permeability coefficient P at different concentrations of HCl. $[Au(III)]_{feed}$ = 10mg/dm^3; [Cyanex 925] = 0.1mol/dm^3 ; $[NaSCN]_{strip}$ = 0.5mol/dm^3 ; [NaCl] = 0.5mol/dm^3

On the other hand, Cyanex 471X and Cyanex 925 respectively could attain around 81 and 94% stripping of Au(III) using 0.5 mol/dm^3 NaSCN + 0.5 mol/dm^3 NaCl. Hence, based on overall performance, Cyanex 925 seems to be the most efficient carrier in LM studies. Tables 3 and 4 present the permeability coefficient values as a function of HCl concentration and extractant concentration (Cyanex 925) respectively. The permeability was found to increase with decrease in HCl concentration. This behaviour was in contrast to solvent extraction.[11] This was probably due to the co-transport of HCl which starts competing with metal ion (10 mg/dm^3) and affects the permeability at higher concentration of HCl. On the other hand P values increased with increase in concentration of liquid membrane carrier i.e. Cyanex 925/cumene. The maximum permeability was found to be $2.7x10^{-2}$ cm/s at 0.2 mol/dm^3 Cyanex 925 maintaining feed acidity at 1mol/dm^3 HCl.

ACKNOWLEDGEMENT

This work was supported by CICYT (QUJ 96-1025).
R Haddad acknowledges the support from AECI for fellowship. Anil Kumar gratefully acknowledge the support of Universitat Politecnica de Catalunya and Generalitat de Catalunya for awarding the fellowship as Visiting Scientist (CIRIT) (SGR 96-101). R Haddad is also thankful to Shri M El Gharbi for his contribution to the experimental work.

REFERENCES

1. El Aamrani FZ, Kumar A, Bayer L, Cortina JL and Sastre AM, *Solv. Extr. Ion Exch.*, **16**, 1389, (1998).
2. American Cyanamid Company, *Cyanex 272, Cyanex 302 and Cyanex301*, Technical Brochures, Wayne, NJ.
3. Eyal AM, Bressler E, Bloch R and Hazan B, *Ind. Eng. Chem. Res.*, **33**, 1067, (1994).
4. Eyal AM, Kogan L and Bressler E, *Ind. Eng. Chem. Res.*, **33**, 1076, (1994).
5. Kakoi T, Goto M and Nakashio F, *Solv. Extr. Ion Exch.*, **12**, 541, (1994).
6. Sole KC, Hiskey JB and Fergusson TL, *Solv. Extr. Ion Exch.*, **12**, 1033, (1994).
7. Kumar A, Gautam PK, Shukla JP, Singh RK and Sastre AM, *ISEC'99*, 11-16 July, Barcelona, Spain.
8. Salvado V, Hidalgo M, Masana A, Munoz A, Valiente M and Muhammed M, *Solv. Extr. Ion Exch.*, **8**, 491, (1990).
9. Salvado V, Hidalgo M, Masana A, Muñoz M, Valiente M and Muhammed M, *Solvent Extraction, 1990 , Proceedings of ISEC 90*, (ed.) T. Sekine, Elsevier, (1992)
10. Barroso MA, Lopez FA, Sastre A and Alguacil FJ, *Hydrometallurgy*, **45**, 199, (1997).
11. Sole KC, Hiskey JB and Fergusson TL, *Solv. Extr. Ion Exch*,**12**, 1033, (1994).
12. Tait BK, *Solv. Extr. Ion Exch.*, **10**, 799, (1992).

EXTRACTION OF PENTACHLOROAQUAOSMATE(IV) ION FROM SULPHURIC ACID SOLUTIONS

AB Maiboroda, ID Troshkina and AM Chekmarev
D.I. Mendeleyev University of Chemical Technology, 9,
Miusskaya Sq., Moscow 125047, Russia

ABSTRACT
The possibility of effective recovery of $[OsCl_5(H_2O)]^-$ ion by means of solvent extraction with aliphatic amines and tri-n-butylphosphate (TBP) has been established. The values of the equilibrium constants of osmium extractions with amines have been measured. The behaviour of osmium in the organic phases is discussed.

Keywords: osmium(IV), amines, di-*n*-octylamine, dodecylamine, tri-*n*-octylamine, tributylphosphate

INTRODUCTION

The pentachloroaquaosmate (IV) ion was obtained in aqueous solution for the first time as a product of the hydrolysis of a hexachloroosmate (IV) ion.[3] The presence of this ion in some sulphuric acid solutions of copper production plants has recently been proved.[4] At the same time, the extraction behaviour of this osmium complex has not been studied up until now. The purpose of the present work was to study extraction of pentachloroaquaosmate (IV) ion with some of common extractants.

EXPERIMENTAL

Pure osmium tetroxide (Merck) has been used as starting material for the synthesis of $[OsCl_5(H_2O)]^-$. Trioctylamine, dioctylamine, dodecylamine and tri-n-butylphosphate of "rein zur Synthese" grade (Merck) were used as extractants. Osmium was determined by a photometric method with thiourea following osmium tetroxide distillation.[1] UV-VIS spectra were recorded on a Perkin Elmer Lambda 40 spectrophotometer, the same device was used for the photometric determination of osmium. The concentration of chloride in solutions was determined according to Volhard's method.[2]

The solutions of tri-n-octylamine (TOA), di-n-octylamine (DOA), and dodecylamine in decane were used for the recovery of $[OsCl_5(H_2O)]^-$ ions from aqueous solutions. The solutions of the extractant contained 2-ethylhexanol (10 % v/v in the case of TOA and 20% in the case of DOA and DA) as modifier, which prevented the formation of a third phase after the conversion of the amine into the salt form. The experiments on extraction were carried out at a temperature 20°C using a contact time of 5 minutes. The concentration of osmium in initial aqueous solutions was in the range of $1 \times 10^{-4} - 2 \times 10^{-4}$ mole/dm^3.

RESULTS AND DISCUSSION

The $[OsCl_5(H_2O)]^-$ ion was synthesised by the reduction of osmium tetroxide with sodium sulphite in a solution of 3 mole/dm^3 H_2SO_4 in the presence of 0.5 mole/dm^3 NaCl. The process was carried out at a temperature of 100°C. Equilibrium was reached under these conditions within 15 minutes. The increase of chloride ion concentration in the solution resulted in an increase in absorption in the wavelength range 345-350 nm. It was proved through electrodialysis, that anionic species of osmium prevail in this solution.

The osmium complex with a maximum absorption at 345 nm was separated from the other products by means of ion-exchange chromatography by using a strong base resin. The ratio Os:Cl in the complex was equal to 1:5, which confirms the assumption of the formation of the $[OsCl_5(H_2O)]^-$ ion in solution. The value of the extinction coefficient $\varepsilon = 7 \times 10^3$ dm^3 mole^{-1}·cm agrees with data presented[3,5] for the extinction coefficient of this complex at λ_{max} =345 nm.

© 2000 Society of Chemical Industry

The OsO_4 reduction in sulphuric acid solutions results in the formation of osmium species with low distribution coefficients in addition to $[OsCl_5(H_2O)]^-$. Therefore, the extraction of $[OsCl_5(H_2O)]^-$ ion occurs in the presence of poorly extractable impurities. The spectrum of the raffinate given in Figure 1 is considerably different from the spectrum of the feed solution. The absorption maximum of the raffinate was observed at λ=375 nm. Comparison of the obtained spectra with the published data[5] confirms the presence of the osmium complex $[Os(H_2O)(OH)Cl_5]^-$ with λ_{max} =376 nm in the raffinate.

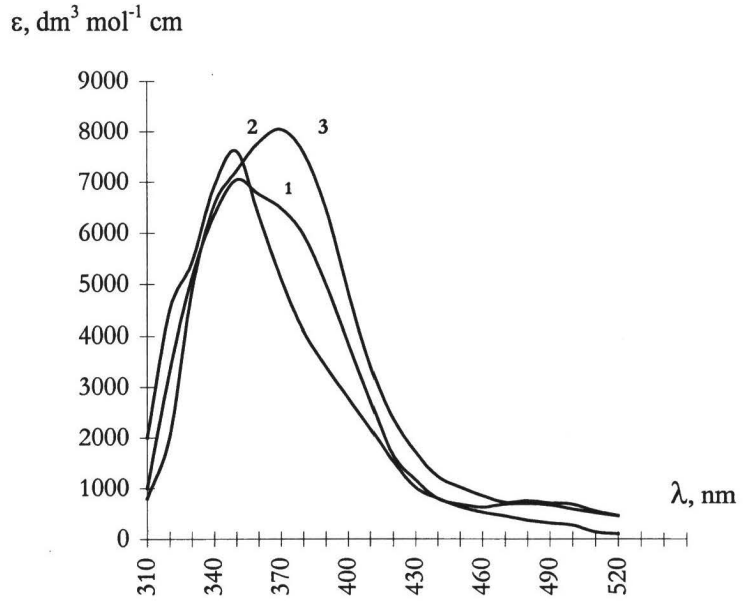

Figure 1. Extraction of $[OsH_2OCl_5]^-$ ion with trioctylamine: UV-VIS spectra of the feed aqueous phase (1), the organic extract (2) and the raffinate (3).

Calculation of the distribution coefficient was carried out by taking into account the presence of poorly extractable impurities in the solution, as described earlier.[6] The osmium solution was contacted sequentially with a few portions of freshly made solvent. The fraction of poorly extractable impurities was determined. Then, the distribution coefficient of extractable species was calculated. The data presented in Table 1 indicates an increase in osmium distribution coefficient with increasing amine basicity.

Amine	Trioctylamine	Dioctylamine	Dodecylamine
D_{Os}	56.6	7.1	5.0

Conditions: aqueous phase: 3 mole/dm³ H_2SO_4, 0.5 mole/dm³ NaCl;
organic phase: 0.1 mole/dm³ extractant in decane

Table 1 Effect of amine nature on distribution coefficient of osmium.

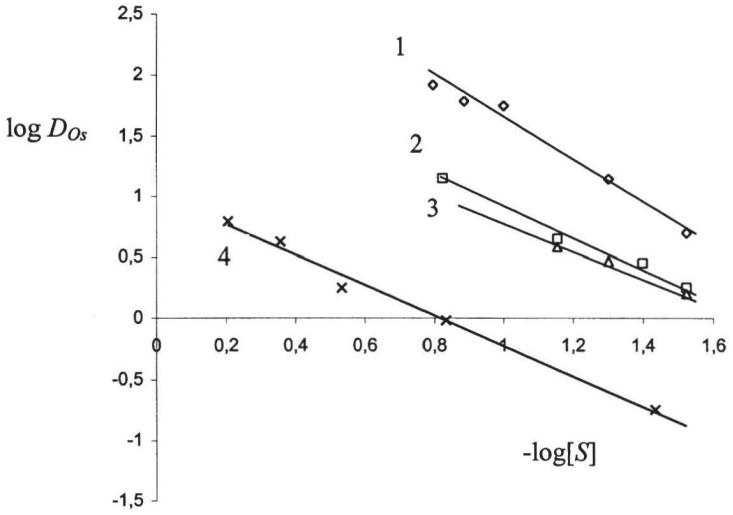

Figure 2. The effect of extractant concentration on distribution coefficient of osmium: 1: trioctylamine, 2: dioctylamine, 3: dodecylamine, 4: tributylphosphate, [*S*] – extractant concentration .

Slope analysis[7] was used to determine the composition of the extracted species. Figure 2 illustrates the effect of amine concentration on the distribution coefficient of osmium. The slope of function logD - f(log[Am]) is equal to 1.30 for TOA, 1.10 for DOA and 0.93 for DA. This data allows the assumption of the formation of compounds containing one amine molecule. Since the amine exists in the organic phase in two forms, as chloride and as bisulphate, the equations of extraction can be written in following form:

$$\overline{H[OsH_2OCl_5]} + \overline{AmHCl} = \overline{AmH[OsH_2OCl_5]} + H^+ + Cl^- \quad (1)$$

$$\overline{H[OsH_2OCl_5]} + \overline{AmH_2SO_4} = \overline{AmH[OsH_2OCl_5]} + H^+ + HSO_4^- \quad (2)$$

Each of the given reactions can be characterised by the concentration equilibrium constants given in equations (3) and (4).

$$K_1 = \frac{\{\overline{AmH[OsH_2OCl_5]}\} \cdot [H^+] \cdot [Cl^-]}{\{\overline{H[OsH_2OCl_5]}\} \cdot [\overline{AmHCl}]} \quad (3)$$

If the distribution coefficient of osmium is equal to:

$$K_2 = \frac{\{\overline{AmH[OsH_2OCl_5]}\} \cdot [H^+] \cdot [HSO_4^-]}{\{\overline{H[OsH_2OCl_5]}\} \cdot [\overline{AmH_2SO_4}]} \quad (4)$$

$$D_{Os} = \frac{\{\overline{AmH[OsH_2OCl_5]}\}}{\{\overline{H[OsH_2OCl_5]}\}} \quad (5)$$

then equations for calculation of the equilibrium constant will be as follows:

$$K_1 = D_{Os} \cdot \frac{[H^+] \cdot [Cl^-]}{[\overline{AmHCl}]} \quad (6)$$

$$K_2 = D_{Os} \cdot \frac{[H^+] \cdot [HSO_4^-]}{[\overline{AmH_2SO_4}]} \qquad (7)$$

Stripping with ammonium hydroxide causes complete deprotonation of the amine. The chloride content in ammoniacal stripping solutions was determined, and the concentration of the chloride form of the amine in organic phase was calculated. The bisulphate amine concentration was found by means of subtraction of the amine chloride salt concentration from the total amine concentration in organic solution. The values of extraction constants for the three amines studied are presented in Table 2.

Amine	Trioctylamine	Dioctylamine	Dodecylamine
[AmHCl], mole/l	0.030	0.029	0.028
$K_1 \cdot 10^{-2}$	27.9	3.66	2.67
$K_2 \cdot 10^{-2}$	71.6	8.95	6.21

Table 2. The concentration equilibrium constants of extraction of $[OsCl_5(H_2O)]^-$ ion with amines

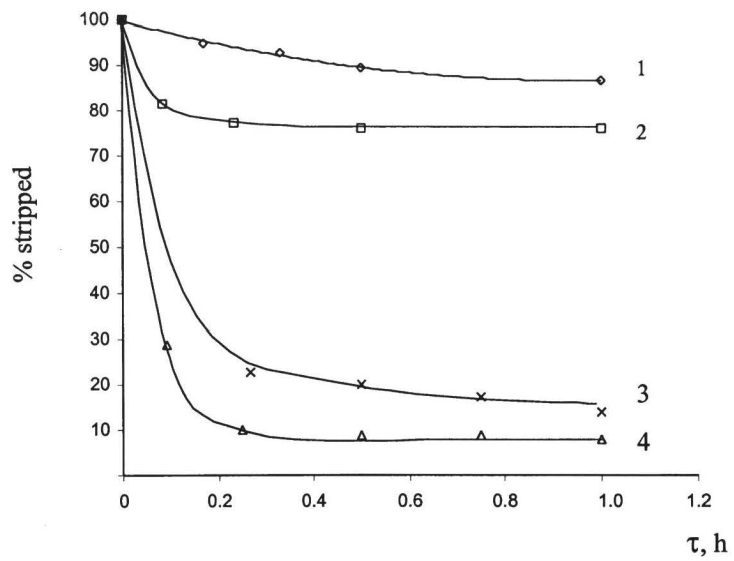

Figure 3. The function of the stripping degree with time of holding of extract at 60°C:
1: trioctylamine (0.1 mole/dm^3), 2: dioctylamine (0.1 mole/dm^3),
3: trialkylamine (10% v/v), 4: dodecylamine (0.05 mole/dm^3).

The commercially pure trialkylamine is widely used in hydrometallurgy in former USSR as an extraction agent. This product contains 70% weight tertiary amines (alkyl radical C_7-C_9), 25 % secondary amines and 5 % primary amines.[8] The analogues of trialkylamine are Adogen 364 and Alamin 336 containing 95-96% weight of tertiary amines.[9] Experiments on the extraction of $[OsCl_5(H_2O)]^-$ ion with trialkylamine showed that the osmium distribution coefficient is close to the value of D_{Os} in extraction with trioctylamine. At the same time, incomplete stripping of osmium by an ammonium hydroxide solution was observed. To explain this phenomenon the assumption was made that part of the osmium remaining in the organic phase is in the form of amino-complexes, which are poorly soluble in water. It is known, that under amine extraction of some platinum group metals, such

as iridium and palladium, the implantation of amine molecule in the interior sphere of the complex can take place.[10] The ability of amines to form complexes with platinum metals decreases in the following order: primary>secondary>tertiary. Heating and exposure to light of extracts promote the process of amino-complex formation.[11]

The behaviour of osmium in trialkylamine organic extractant was studied. The organic phase contained $[OsCl_5(H_2O)]^-$ ion extracted from an aqueous solution. After extraction, the organic solution was washed with water (O/A = 1:1) and thermostated at 60°C. Figure 3 shows that the degree of osmium stripping decreases in the first 15 minutes and after approximately 30 minutes of heating, 80 % osmium turns into unstrippable species.

In order to ascertain a cause for this phenomenon, similar experiments using trioctylamine, dioctylamine and dodecylamine as extractants were carried out. The plot of the percentage stripping against time of holding of extract at 60°C indicates that almost complete stripping occurs in the case of tri- and dioctyl-amine, and that the formation of amino complexes does not take place. In the case of dodecylamine, the stripping decreases during first 5 minutes of heating and then becomes settled at a value of 5-7%.

The UV-VIS spectra of the extracts provide information about the reorganisation of the interior co-ordination sphere of the osmium complex. As the spectra of the TOA and DOA extracts are almost identical to the spectrum of $[OsCl_5(H_2O)]^-$ ion in aqueous solutions, the appearance of new light absorption maximum under λ_{max}=510 nm in the spectrum of extract containing dodecylamine was observed. It should be noted that as a result of stripping from dodecylamine extracts, osmium formed a deep violet precipitate at the phase boundary. Both the organic solvent and the aqueous phase contained only traces of osmium.

Tri-n-butyl phosphate was used as a neutral extraction agent for the recovery of osmium. The quantity of osmium extracted from sulphuric acid solutions increased with an increase of chloride ion concentration up to 0.5 mole/dm^3. Further increase of chloride ion concentration in the aqueous phase had little effect on the quantity of osmium extraction. The organic extracts obtained by osmium extraction with TBP have a similar spectra to that of the aqueous solutions, that contain $[OsCl_5(H_2O)]^-$ ion. It was established by means of a slope analysis, that the solvate formed by osmium extraction with TBP contains one amine molecule. The slope coefficient of the logarithmic distribution curve given in figure 1 is 1.17.

CONCLUSIONS

The study of the extraction of pentachloroaquaosmate (IV) ion with aliphatic amines and tributylphosphate from sulphuric acid solutions has been carried out. It was established that extracted compound contains one molecule of extractant. The increase in amine basicity resulted in increase in osmium extraction. The reason for incomplete stripping of osmium from commercial trialkylamine solutions is the interaction of osmium complex with primary amine impurities.

REFERENCES

1. Beamish FE, *The Analytical Chemistry of Noble Metals*, Pergamon Press New York:, 185, (1966).
2. Gubitz T, Haubold G, and Stoll C, *Analytische Praktikum: Quantitative Analyse*, VCH Weinheim, **Band 2b**, 111, (1989).
3. Miano RR and Gardner CS, *Inorg. Chem.*, **4** (3), 337, (1965).
4. Chekmarev AM, Troshkina ID, and Maiboroda AM, *Inter.Symp. on Rhenium and Rhenium Alloys,* Orlando, Florida, USA, February 10-13, 1997.,109, (1997).
5. Muller H, Scheible H, Martin S, *Z. anorg. allg. Chem.*, **462** , 18, (1980).
6. Fomin VV, *Chemistry of Extractions Processes*, Atomizdat, Moscow, 147, (1962) (in Rus.)
7. Y.A.Zolotov YA, *Solvent Extraction in Inorganic Analysis*, MGU, Moscow , 33, (1988) (in Rus.).
8. *Chemical Encyclopaedic Dictionary* (Moscow: Sovetskaja encyclopedia), 588, (1983) (in Rus.).
9. Lo TC, Baird MHI, and Hanson C eds, *Handbook of Solvent Extraction,* (Malabar: Kreiger Pub Co, 638, (1991).
10. Tougarinoff B at al.in *Advances in Hydrometallurgy*, IMM, London, 741, (1968).
11. Smidt VS, *Extraction with Amines*, Atomizdat, Moscow, 312, (1970), (in Rus.)

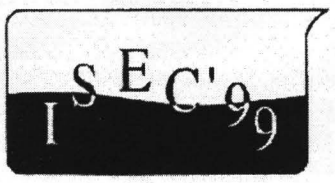

SOLVENT EXTRACTION OF RUTHENIUM(III) AS A THIOCYANATE COMPLEX

B Tamhina, V Vojkovic and N Brajenovic
Laboratory of Analytical Chemistry, Faculty of Science, University of Zagreb, Strossmayerov trg 14, 10000 Zagreb, Croatia

ABSTRACT
The extraction of ruthenium(III) as a thiocyanate complex from hydrochloric acid solution with tetraphenylarsonium (TPA), tetraphenylphosphonium (TPP) and cetylpyridinium (CP) chloride and cetyltrimethylammonium (CTMA) bromide dissolved in chloroform was investigated. The optimum conditions for quantitative extraction (over 99%) by all extractants were determined. The extraction described can be used as a very simple method for ruthenium separation and also for the spectrophotometric determination of ruthenium (III) in the organic phase, which is more sensitive than in the aqueous phase. The extraction behaviour of CTMA and CP was found to be more efficacious than that of TPA and TPP, because lower excess of extractant and less shaking time of the aqueous and organic phases were required. Distribution and spectrophotometric methods showed that the mechanism of extraction was based on the formation of ion-associated compounds between two onium cations and one ruthenium (III) thiocyanate anion bearing two negative charges.

Keywords: ruthenium, thiocyanate, spectrophotometry, tetraphenylarsonium, tetraphenylphosphonium, cetylpyridinium, cetyltrimethylammonium ions

INTRODUCTION

Ruthenium (III) forms a deep-blue complex with thiocyanate which can be used for the spectrophotometric determination of ruthenium in the aqueous phase or in the organic phase after extraction with some organic solvents, or by polyurethane foam.[1-4] The selective separation of ruthenium from other platinum group elements by extraction as thiocyanate complexes has also been described.[3-6]

The present experiments were undertaken to study the extraction of ruthenium (III) as a thiocyanate complex with tetraphenylarsonium (TPA) and tetraphenylphosphonium (TPP) chlorides, which are ion-pair extractants. The presence of surfactants can influence complex formation.[7-9] Therefore, extraction of the ruthenium (III) thiocyanate complex was carried out also with cetyltrimethylammonium (CTMA) bromide and cetylpyridine (CP) chloride as cationic surfactants and as ion-pair extractants.

The results show that CTMA and CP are better extractants for ruthenium (III) thiocyanate than TPA and TPP. A more efficacious extraction behaviour of CTMA and CP in comparison with that of TPA and TPP is discussed. The extraction described can serve as a potential method for ruthenium separation and also for the spectrophotometric determination of ruthenium (III) in the organic phase, a determination that is more sensitive than the one in the aqueous phase.

EXPERIMENTAL

Reagents

Standard ruthenium (III) solution (8×10^{-3} mol/dm^3) was prepared by dissolving $(NH_4)_2RuCl_5X\ H_2O$ (analytical grade, Johnson Matthey) in 1mol/dm^3 HCl. The solution was standardized spectrophotometrically with thiourea[10] and checked with ruthenium atomic absorption standard solution (Johnson Matthey). Solutions of lower concentrations were made by dilution with deionized water. TPA and TPP chloride (analytical grade, Fluka), CTMA bromide (cryst. pure, Serva) and CP chloride-monohydrate (analytical grade, Merck) were dissolved in reagent grade chloroform. All chemicals used were of p.a. purity grade.

© 2000 Society of Chemical Industry

Extraction Procedures

The aqueous phases of a given composition were heated at 85C for 45 min. After cooling to room temperature an aliquot was used for absorbance measurement using a Varian Cary 3 spectrometer. Another aliquot (5 cm^3) was shaken with an equal volume of the organic phase of a given composition in a 50 cm^3 conical flask with a mechanical shaker for 25 minutes (CTMA and CP) or 70 minutes (TPA and TPP). After the phases were separated by gravity for each experimental point, aliquots of the organic and aqueous phases were used for absorbance measurements.

Distribution Ratio

Ruthenium distribution was determined by absorbance measurements in the aqueous phase at 585 nm before and after extraction. Ruthenium concentrations in the organic phase were calculated from the difference in ruthenium concentrations in the aqueous phase before and after extraction. Ruthenium distribution was also determined by absorbance measurements in the organic phase at 575 nm (TPA and TPP) or at 568 nm (CTMA and CP). Ruthenium concentrations in the aqueous phase were calculated from the difference between the maximum and constant absorbance of the organic phase at optimum conditions for extraction and the measured absorbance value of a given composition.

RESULTS AND DISCUSSION

The extraction of ruthenium (III) as a thiocyanate complex from hydrochloric acid solution with TPA, TPP and CP chloride and CTMA bromide dissolved in chloroform was investigated. Ruthenium (III) could be extracted only after the formation of a thiocyanate complex in the aqueous phase. As ruthenium (III) formed a thiocyanate complex quantitatively only by heating, the effect of temperature and the heating time on the formation of the thiocyanate complex in the aqueous phase and on its extraction with all investigated extractants dissolved in chloroform was determined by heating the aqueous phase before extraction. The optimum heating time was 45 minutes at 85C. Without heating complex formation and its extraction were about 50%, independent of the time of standing of the aqueous phase at room temperature before extraction.

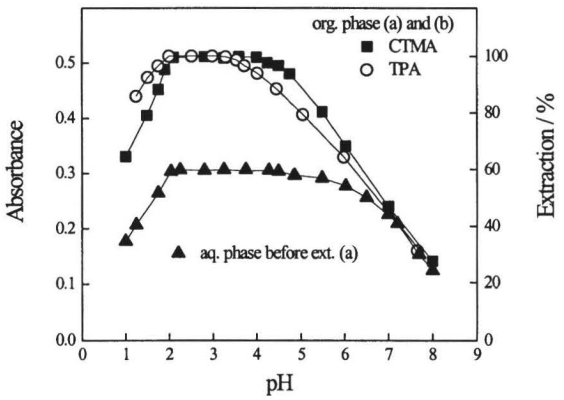

Figure 1 Dependence of absorbance (a) and per cent extraction (b) on initial pH

The absorption spectrum of the ruthenium (III) thiocyanate complex in the aqueous phase showed a maximum absorbance at 585 nm ($\varepsilon = 5.0 \times 10^3$ L mol^{-1} cm^{-1}), in the organic phase extracted with TPA or TPP at 575 nm and with CTMA or CP at 568 nm ($\varepsilon = 8.4 \times 10^3$ L mol^{-1} cm^{-1}). The maximum and constant absorbances of the organic phase were in the same thiocyanate and extractants

concentration range and pH range as for quantitative extraction. This showed that the formation of the extractable ruthenium (III) thiocyanate complex with all investigated extractants could be determined spectrophotometically by measuring the absorbance of the organic phase at 575 nm for TPA or TPP and at 568 nm for CTMA or CP as extractants. The absorbances of the organic phase were stable for at least 5 hours regardless of the extractant used and the determination of ruthenium (III) in the organic phase was more sensitive than in the aqueous phase.

The optimum pH of the aqueous phase before heating was 2.0-4.5. In this pH range the absorbance values of the aqueous phase were constant. From this solution the ruthenium(III) thiocyanate complex was quantitatively extracted (over 99%) in the pH range 2-3 (TPA or TPP) and 2-4 (CTMA or CP). At higher or lower acidity complex formation and its extraction decreased (Fig. 1). At pH < 1 no complex was formed and the absorption spectra of the aqueous and organic phases showed no absorption maximum in the 400-700 nm wavelength range.

The effect of thiocyanate concentration on the formation and extraction of the ruthenium (III) thiocyanate complex was examined by varying the thiocyanate concentration in the aqueous phase. The extraction started from solutions containing an initial ruthenium (III) concentration of 6.1×10^{-5} mol/dm^3 at optimum acidity (pH = 2.5) using an excess of extractants in chloroform (Figure 2). For complete formation of the complex in the aqueous phase and its extraction with all investigated extractants in chloroform a thiocyanate concentration ≥ 0.05 mol/dm^3 was required; the minimum molar ratio of thiocyanate to ruthenium was 800:1. A thiocyanate concentration >0.05 mol/dm^3 produced no influence on the formation of the thiocyanate complex in the aqueous phase and absorbances of the aqueous phase had constant values. All the extractants used extracted the ruthenium (III) thiocyanate complex quantitatively in the thiocyanate concentration range 0.05-0.16 mol/dm^3. At a higher thiocyanate concentration the extraction with TPA and TPP very strongly decreased and at a thiocyanate concentration ≥ 0.3 mol/dm^3 the extraction was about 50%. In contrast, if thiocyanate concentration increased above 0.16 mol/dm^3, the extraction with CTMA and CP very slowly decreased. This may have been due to the excess of thiocyanate which formed with extractants ion-pairs that were also extractable in chloroform[11,12] and therefore coextracted a thiocyanate complex with ruthenium (III) decreasing ruthenium (III) extraction. Thiocyanate ion-pairs with TPA and TPP were probably more extractable in chloroform than with CTMA and CP and consequently strongly decreased ruthenium extraction.

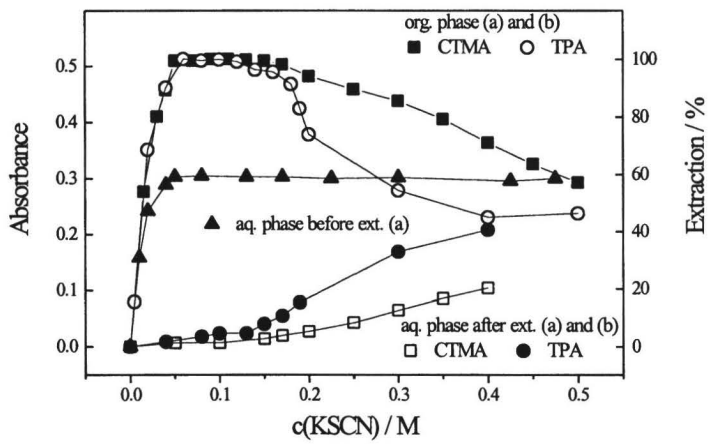

Figure 2. Dependence of absorbance (a) and per cent extraction (b) on initial thiocyanate concentration

The influence of extractant concentration in the organic phase on the extraction of ruthenium (III) from the aqueous phase at optimum acidity (pH = 2.5) and thiocyanate concentration (0.1 mol/dm^3) was also studied (Figure 3). For the quantitative extraction of ruthenium as a thiocyanate complex the molar ratio of TPA or TPP to Ru(III) had to be at least 160:1, of CP to Ru(III) 12:1 and of CTMA to Ru(III) 6:1.

At optimum conditions for extraction the distribution equilibrium was attained after 5 minutes with CTMA or CP but only after 60 minutes with TPA or TPP (Table 1). The shaking time of the aqueous and organic phases sufficient to achieve reproducible results by measuring the absorbances of the organic phase was 15 minutes with CTMA or CP as extractants and 70 minutes with TPA or TPP.

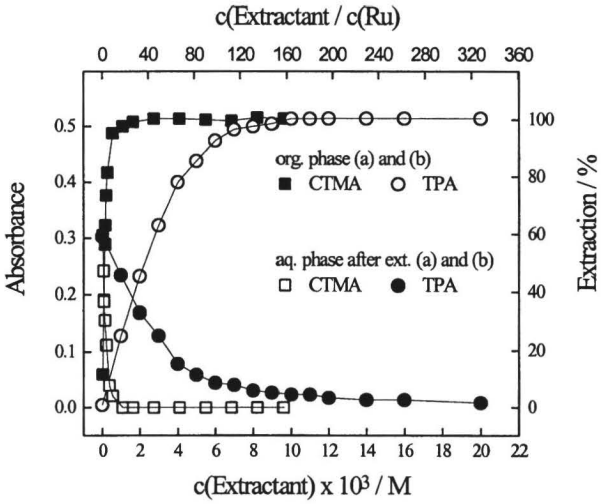

Figure 3. Dependence of absorbance (a) and per cent extraction (b) on initial TPA and CTMA concentrations

Shaking time / min	Extraction / %			
	TPA	TPP	CTMA	CP
2	81.8	79.8	97.9	97.3
4	83.3	80.7	98.2	98.5
5	85.8	81.6	99.9	99.9
15	94.8	91.3	100.0	99.9
50	97.7	97.3	99.9	99.9
60	100.0	99.8	99.9	99.9
70	99.9	99.9	99.9	99.8

Table 1 Effect of shaking time on per cent extraction depending on extractant

All these results showed that for the quantitative extraction of the ruthenium (III) thiocyanate complex with CTMA or CP a lower excess of extractant and less shaking time of the aqueous and organic phases were required than with TPA or TPP. A different, more efficacious extraction behaviour of CTMA and CP in comparison to TPA and TPP was due to the fact that CTMA and CP are not only ion-pair extractants, but also cationic surfactants. It is known that the presence at a surfactant can influence complex formation.[7-9] CTMA and CP as surfactants were more soluble in water than TPA and TPP, and therefore accelerated the formation of the ion-associated compounds

between the onium cation and the ruthenium (III) thiocyanate anion and their transfer into the organic phase.

The composition of the extracted ruthenium (III) complex was determined by distribution (slope analysis) and spectrophotometric, Job's method of continuous variation, methods (Figure 4). The molar ratio of ruthenium(III) to onium ion in the extracted complex with all the extractants investigated was 1:2. This indicates that the mechanism of extraction was based on the formation of ion-associated compounds between two onium cations and one ruthenium (III) thiocyanate anion bearing two negative charges, probably having the formula $[R_4X]_2[RuO(SCN)_3]$ (R_4X^+ = TPA, TPP, CTMA or CP).

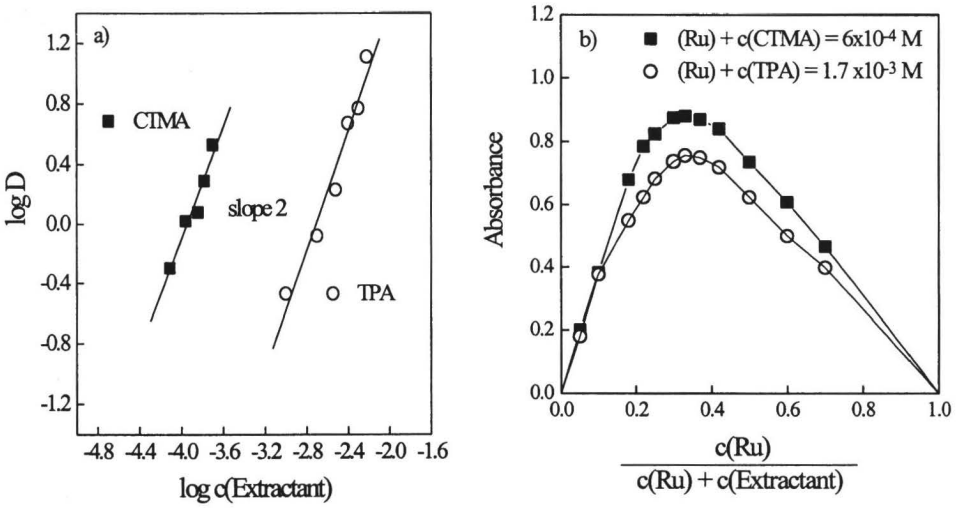

Figure 4. Determination of complex composition by (a) slope analysis, b) Job's method

REFERENCES

1. Belew WL, Wilson GR and Corbin LT, *Anal.Chem.*, **33**, 886, (1961).
2. Tagashira S, Murakami Y, Nishiyama M, Harada N and Sasaki Y, *Bull. Chem. Soc.Jpn,* **69**, 3195, (1996)
3. Marczenko Z and Balcerzak M, *Anal. Chim. Acta*, **109**, 123, (1979).
4. Al-Bazi SJ and Chow A, *Talanta*, **31**, 189, (1984).
5. Jaya S and Ramakrishna TV, *Bull. Chem. Soc. Jpn.*, **57**, 267, (1984).
6. Warshawsky A, *Sep. Purif. Methods*, **12**, 119, (1983); *Chem. Abstr.*, **100**, 89314j, (1984).
7. Cheng KL, Ueno K and Imamura T, *Handbook of Organic Analytical Reagents*, CRC Press, Boca Raton, Fla, (1982)
8. Savvin SB, Chernova RK and Kudryavtseva LM, *Zh. Anal. Khim.*, **34**, 66, (1979).
9. Attwood D and Florence AT, *Surfactant Systems*, Chapman and Hall, London, (1985).
0. Ayres GH and Young F, *Anal. Chem.*, **22**, 1227, (1950).
1. Bock R and Jainz J, *Z. Anal. Chem.*, **198**, 315, (1963).
2. Bock R and Beilstein GM, *Z. Anal. Chem.*, **192**, 44, (1963).

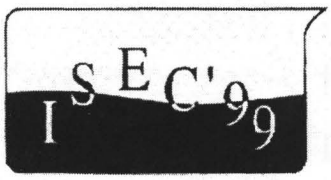

EXTRACTION OF IRON(III) FROM HYDROCHLORIC ACID SOLUTIONS BY AN α-HYDROXYOXIME

Taichi Sato,[1,2] Masahiko Ito[1] and Masuyuki Hotta[1]
[1]Faculty of Engineering, Shizuoka University, Hamamutsu, 432 Japan
[2]Metallurgical Engineering Department,
Queen's University, Kingston, Ontario K7L 3N6, Canada

ABSTRACT
The extraction of iron(III) from hydrochloric acid solutions was investigated using LIX 63 (5,8-diethyl-7-hydroxy-6-dodecanone oxime, H_2Ox) in kerosene under various conditions. The organic extracts were examined by infrared and ultraviolet spectroscopies. In consequence, the following equilibrium equations have been proposed: at $2 > pH > 1$, $Fe(OH)^{2+}(aq) + 2H_2Ox(org)$ $Fe(OH)(HOx)_2(org) + 2H^+(aq)$; at [HCl] = 1-10 mol dm^{-3}, $FeCl_3(aq) + HCl(aq) + H_2Ox(org)$ $HFeCl_4.H_2Ox(org)$.

Keywords: iron(III), LIX 63 (5,8-diethyl-7-hydroxy-6-dodecanone oxime), hydrochloric acid

INTRODUCTION

The extraction of metal ions from aqueous solutions by α-hydroxyoximes, such as 5,8-diethyl-7-hydroxy-6-dodecanone oxime (H_2Ox), the active component of LIX 63) and its equivalent, has been reported previously.[1] The current studies were also conducted on the complexes formed in the extraction of copper from hydrochloric acid solutions by an α-hydroxyoxime, as well as the extraction of divalent cobalt, nickel and copper and trivlent gallium, indium an thallium.[2-4] In this study, the work was extended to include the extraction of iron(III) from hydrochloric acid solutions by α-hydroxyoxime.

EXPERIMENTAL

Reagents

LIX 63 (Henkel Corp.), used as an α-hydroxyoxime, was purified by the method reported in an earlier paper[5] and diluted with purified kerosene. Aqueous solutions of iron were prepared by dissolving ferric chloride ($FeCl_3 \cdot 6H_2O$) in hydrochloric acid of the required concentration. In general, the aqueous metal concentration was 1 g dm^{-3} ferric chloride except for the loading test. Other chemicals were of analytical reagent grade.

Extraction and analytical procedures

Equal volumes (15 cm^3 each) of the aqueous and organic phases were shaken for 20 min in a 50 cm^3 stoppered conical flask at 20°C. Preliminary experiments showed that equilibration was complete in 20 min. The mixture was centrifuged and separated, and then the aliquots of both phases were pipetted out to determine the distribution coefficient (E: the ratio of the equilibrated concentration of metal in the organic phase to that in the aqueous phase). Iron was stripped from the organic phase with 1 mol dm^{-3} hydrochloric acid solution. The concentration of iron in aqueous solution was determined by EDTA titration using xylenol orange (XO) as the indicator. The chloride concentration and the water content of the organic phase were determined by the use of Volhard's method in the presence of nitrobenzene and by Karl Fisher titration, respectively.

© 2000 Society of Chemical Industry

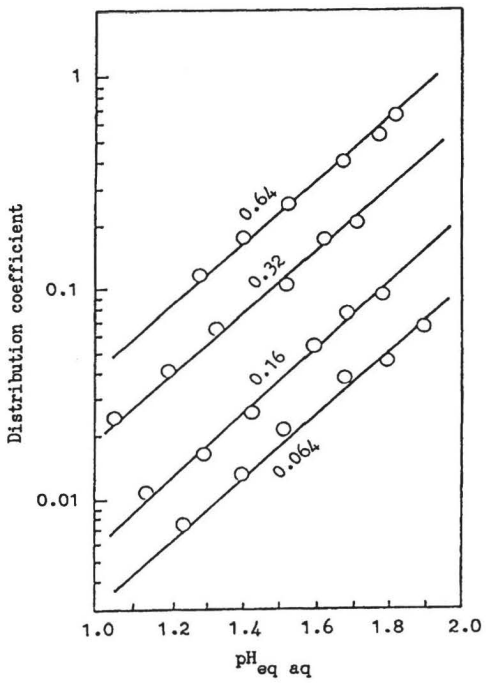

Figure 1. Extraction of iron(III) from aqueous solutions as a function of pH with LIX 63 in kerosene ($pH_{eq\ aq}$ denotes equilibrated aqueous pH; numerals on lines are LIX 63 concs., mol dm^{-3}).

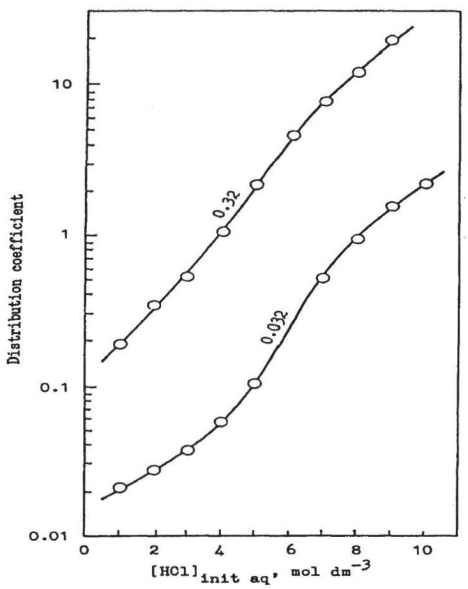

Figure 2. Extraction of iron(III) from hydrochloric acid solutions with LIX 63 in kerosene (numerals on lines are LIX 63 concs., mol dm^{-3}).

IR and UV spectral measurements.

The infrared (IR) spectra of the organic extracts were determined on JASCO models IRA-1 (4000-650 cm^{-1}) and IR-F (700-200 cm^{-1}) using a capillary film between thallium halides or polyethylene films. The ultraviolet (UV) absorption spectra were recorded on a Hitachi model 340 spectrophotometer using 1.0 x 1.0 cm fused silica cells.

RESULTS AND DISCUSSION

Extraction isotherms.

The extraction of iron(III) from aqueous solutions of low acidity at $1 < pH < 2$ showed a gradual decrease in the distribution coefficient when lowering the pH value as indicated in Figure 1. At higher acidities in [HCl} = 1-10 mol dm^{-3}, the distribution coefficient rose with increasing aqueous acidity (Figure 2). From these results it was deduced that there are two different regions in which the extraction occurs through different mechanisms.

In the weak acid region, the variation of the distribution coefficient was attributed to a chelation mechanism similar to the cation-exchange mechanism. It was thus assumed that the extraction of metal from aqueous solutions in the pH region by LIX 63 can be expressed by the equation:

$$M^{m+}(a) + nH_2Ox(o) \longleftrightarrow MH_{2n-m}Ox_n(o) + mH^+(a), \qquad (1)$$

where (a) and (c) denote aqueous and organic phases, respectively, and M represents the metal species. If the extraction of iron (III) follows Equation (1), the distribution coefficients are proportional to $[H^+]^m$. The plots of E vs $pH_{eq\ aq}$ at $[H_2Ox]_{init} = 0.064$ -0.64 mol dm^{-3} showed that the distribution coefficients are proportional to the second-power hydrogen ion concentration in the region of $1 \leq pH \leq 2$, meaning $m = 2$ (Figure 1). Also the plots of log E vs log $[H_2Ox]_{eq}$ revealed straight lines with a slope of ~2. This corresponded to the result obtained for the continuous variation of $[Fe]_{org}$ as a function $[Fe]_{init\ aq}/([Fe]_{init\ aq} + [H_2Ox]_{init})$ at pH 1.6, giving the maximum at 0.33. In addition, as the hydroxo species such as $[Fe(OH)(H_2O)6]^{2+}$ exists in aqueous solutions at the pH region, it was inferred that the extraction of iron(III) from aqueous solutions at $2 \geq pH \geq 1$ by LIX 63 can be expressed by the equilibrium equation:

$$Fe(OH)^{2+}(a) + 2H_2Ox(o) \longleftrightarrow Fe(OH)(HOx)_2(o) + 2H^+(a)(2).$$

In the extraction of iron (III) from aqueous solutions with 0.032 mol dm^{-3} LIX 63, when the concentration of iron in aqueous solutions was increased at the constant pH = 1.6, it was found that the metal-loaded organic phases do not contain either water molecules or chloride ions. This suggested that the species formed in the organic phase has the stoichiometric composition of $Fe(OH)(HOx)_2$.

At hydrochloric acid concentrations above 1 mol dm^{-3}, the distribution behavior was similar to that for the extraction using the neutral organophosphorus compounds such as TBP (tri-n-butyl phosphate) and TOPO (trioctylphosphine oxide). When hydrochloric acid in the aqueous phase was replaced by lithium chloride, the extraction behavior of iron (III) resembled that from hydrochloric acid solutions alone. The plots of log E vs log $[H_2Ox]_{eq}$ gave straight lines with a slope of ~1, showing the first-power dependency on LIX 63 concentration. This was in accordance with the results for the continuous variation method. $[Fe]_{org}$, plotted as a function of mole fraction of $[Fe]_{init\ ac}/([Fe]_{init\ aq} + [H_2Ox]_{init})$ at a fixed concentration of $[Fe]_{init\ aq} + [H_2Ox]_{init} = 0.05$ mol dm^{-3} at 5 mol dm^{-3} HCl, revealed a maximum at 0.5. The loading test of iron in the organic phase indicated the stoichiometry of the extracted species: when increasing the iron concentration in the aqueous

phase at 5 mol dm^{-3} HCl, the molar ratio [Fe]/[Cl]/H_2Ox]/H_2O] in the organic phase approached 1 : 1 : 4 : 2, indicating the composition $HFeCl_4 \cdot H_2Ox.2H_2O$.

Hence it was deduced that the extraction of iron (III) from hydrochloric acid solutions by LIX 63 should be written as:

$$FeCl_3(a) + HCl(a) + H_2Ox(o) \longleftrightarrow HFeCl_4.H_2Ox(o). \qquad (3)$$

IR and UV spectral studies.

Organic extracts with 0.032 mol dm^{-3} LIX 63 in n-hexane, from aqueous solutions containing ferric chloride at 1, 10 and 20 g dm^{-3} at pH 1.6 and with 1, 10 and 100 g dm^{-3} HCl, were examined by IR spectroscopy. These extracts exhibited an OH stretching vibration at 3300 cm^{-1} and an OH bending band at 1640 cm^{-1} for free extractant shifts to higher and lower frequencies, respectively. Simultaneously, the bands due to the N-O stretching vibration at 1270 cm^{-1} and the C=N-O skeletal vibration at 830 cm^{-1} shifted to lower frequencies in the extraction of iron (III) from aqueous solutions in the pH region, while the N-O stretching vibration at 940 cm^{-1} and the C-H-O out-of-plane vibration at 760 cm^{-1} shifted to higher frequencies in the extraction from hydrochloric acid solutions at higher acidities. From these results, it was deduced that the species forming organic phases possess the structure in which the oxime group coordinates to iron through the oxygen and nitrogen atoms.

The absorption spectra of the organic extracts were examined in the extraction with 0.032 mol dm^{-3} LIX 63 in cyclohexane from aqueous solutions containing iron(III) chloride of 1 g dm^{-3} in pH 1.6 and in 3, 5 and 7 mol dm^{-3} HCl. The spectra revealed the absorption at 334 nm due to the species $Fe_2OOH)_2^{4+}$ in the extraction from aqueous solution in the pH region,[6] and absorptions at 316 and 364 nm due to the species $FeCl_4^-$ in the extraction from hydrochloric acid solutions at higher acidities.[7] Therefore, the IR and UV spectral results confirmed the relevance of Equations (2) and (3) for the extraction of iron (III) from hydrochloric acid solutions by LIX 63.

CONCLUSION

The extraction of iron (III) from hydrochloric acid solutions by LIX 63 was examined under various conditions. From the results, it can be seen that the extraction of iron (III) from aqueous solutions in the pH region involved the chelating reaction expressed in Equation (2); and the solvating reactions according to Equation (3) were the result of hydrochloric acid solutions at higher acidities.

REFERENCES

1. Ritcey GM and Ashbrook AW, *Solvent Extraction, Part I*, Elsevier, Amsterdam, 117, (1984).
2. Sato T, Ito M, Sakamoto T and Otsuka R, *Hydrometallurgy*, **18**, 105, (1987).
3. Sato T, Sato K and Ito M, *Value Adding through Solvent Extraction Proc. ISEC'96*, ed. Shallcross, University of Melbourne, **1**, (1996).
4. Sato T, Suzuki K and Sato K, Proc. 2nd Int. Conf. on Separation Science and Technology, Hamilton, Can. Soc. Chem. Eng. Ottawa, **2**, 567, (1989).
5. Al-Diwan TAB, Hughes MA and Whewell RJ, *J. Inorg. Nucl. Chem.*, **39**, 1419, (1977).
6. Knight RJ and Sylva RN, *J. Inorg. Nucl. Chem.*, **37**, 779, (1974).
7. Brady GM, Robin MB and Varmbi J, *Inorg. Chem.*, **3**, 1168, (1964).

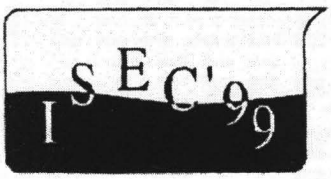

THIRD PHASE APPEARANCE IN COBALT(II) AND NICKEL(II) EXTRACTION WITH MONO-(2-ETHYL-HEXYL)PHOSPHONIC ACID-2-ETHYLHEXYL ESTER (MOOP)

Da Maljkovic, Z Lenhard and Du Maljkovic
Faculty of Metallurgy, University of Zagreb, Aleja narodnih heroja 3, 44000, Sisak, Croatia

ABSTRACT
During investigation of cobalt(II) and nickel(II) extraction with mono-(2-ethylhexyl)phosphonic acid 2-ethylhexyl ester (MOOP) in kerosene a third phase was observed under certain conditions. Systems containing cobalt(II) and nickel(II) or both metals were investigated at different initial pH values and initial phase volume ratios under conditions of the third phase formation. Partial distribution ratios and separation factors were calculated.

Keywords: nickel, cobalt, mono-(2-ethylhexyl)phosphonic acid 2-ethylhexyl ester, (MOOP), third phase

INTRODUCTION

Coexistence of three liquid phases was observed in a number of extraction systems. The third liquid phase appears as a result of splitting of the organic phase into the light and heavy ones. In the case of metal extraction the heavy organic phase, known as the third phase, usually contains a much higher metal concentration than the light organic phase. The approach to the third phase appearance in extraction systems can be twofold. Namely, in systems containing ethers (e.g. diisopropyl ether) the appearance of the third phase should be stimulated, because it can serve to improve separation efficiency due to a very high metal content. In contrast to that, there are numerous extraction systems (such as the ones containing long-chain amines) in which the third phase formation should be avoided because of unfavourable distribution.

When the partial distribution ratio of the heavy organic phase to the light organic phase, D^{h}_{l}, is small, two organic phases can be treated as integral organic phase and can be separated from the extraction system together using an average distribution ratio, D_{av}, to express metal distribution.

To stimulate as well as to prevent the third phase formation, it is necessary to examine the factors influencing the behaviour of systems where, under certain conditions, three liquid phases can be present simultaneously. However, there are large differences in the behaviour of specific extraction systems even when they belong to the same group of systems according to the extraction mechanism, for instance different properties of the third phase which appears during the extraction of iron(III) and gold(III) with di-isopropyl ether or solvents containing di-isopropyl ether.[1,2] This indicates that the phenomenon of the third phase formation is by no means simple and that apparently, it involves simultaneous operation of a number of factors. Hence, there is no general rule for the third phase formation and the literature on the subject is confined to data concerning conditions of its appearance in specific systems.

There are no data in literature related to the third liquid phase appearance in extraction systems containing mono-(2-ethylhexyl) phosphonic acid 2-ethylhexyl ester. However the use of the third phase modifiers can be an indication that the third phase was observed under certain circumstances.[3] During our examination of cobalt(II) and nickel(II) extraction with MOOP the third phase was observed and results concerning that phenomenon are discussed in this paper.

© 2000 Society of Chemical Industry

EXPERIMENTAL

Materials

Mono-octyloctanphosphonate, MOOP, kindly supplied by Bayer AG was used without further purification. The reagent contains 97.5% of pure compound mono-(2-ethylhexyl)phosphonic acid (2-ethylhexyl)ester and has a density (20°C) of 0.950 $g.cm^{-3}$.

Procedure

The experiments were carried out in graduated cuvettes (15 cm^3). Samples prepared by dissolution of metal sulphates in sulphuric acid were adjusted to appropriate pH using a concentrated solution of ammonium hydroxide and mixed in a chosen ratio with a 10% solution of MOOP in kerosene. The initial volume ratios of the aqueous to the organic phase, r^i, were 1 and 2. Systems were thermostatted for 15 minutes at 25 °C and after that vigorously shaken four times for 30 seconds at three-minute intervals. In between shaking the systems were thermostatted.

Methods of Analysis

Determination of equilibrated phase volumes was carried out in graduated cuvettes before sampling with the accuracy of ± 0.05 cm^3. Concentration of cobalt (II) (using nitroso-R salt) and nickel (II) (using dimethylglyoxime and $K_2S_2O_8$) were determined by absorbance measurements.

RESULTS AND DISCUSSION

In the investigation of cobalt (II) and nickel (II) extraction by MOOP in kerosene the presence of the third phase was observed at higher pH values.

The relationship between the initial pH value (pH^I = 8-10) and the number of coexisting liquid phases in systems containing nickel (II) (1.8 x 10^{-1} mol/dm^3), cobalt (II) (1.2 x 10^{-2} mol/dm^3) and a mixture of the two metals (with identical metal content) is shown in Table 1.

r^i	Metals in sample	Number of phases at pH^I					
		8.0	8.5	8.75	9.0	9.5	10.0
1	Co	2	2	2	2	2	3
	Ni	2	2	3	3	3	3
	Co+Ni	2	2	3	3	3	3
2	Co	2	2	2	2	3	3
	Ni	2	3	3	3	3	3
	Co+Ni	2	3	3	3	3	3

Table 1 The number of co-existing liquid phases at different initial pH values, pH^i, and initial volume ratios, r^i, in the extraction of cobalt (II) and nickel (II) by MOOP in kerosene. Initial metal concentrations: c^i_{Co} = 1.2 x 10^{-2} mol/dm^3 and c^i_{Ni} = 1.8 x 10^{-1} mol/dm^3

The system containing cobalt (II) consisted of two phases at pH^i = 6.0 - 9.5 and pH^i = 6.0 - 9.0 for initial phase volume ratios, r^i = 1 and 2 respectively. The systems containing nickel (II) were not prepared in the same pH^i range, because the solution of a given nickel (II) sulphate concentration was unstable at pH values lower than 8.0. In these systems the third phase appeared at a lower initial pH value than in those containing cobalt (II). Its appearance was also noted at a lower initial pH value for a higher initial phase volume ratio (r^i = 2).

So, in the system containing nickel (II) for r^i = 2 the third phase appeared at pH^i = 8.5 but in the system containing cobalt(II) for same r^i, it appeared at pH^i = 9.5. In system containing a mixture of the metals a third phase appears at same initial pH as in system containing the single

nickel (II) species. This leads to the conclusion that nickel contributes to the appearance of the third phase at lower initial pH values in systems containing both metals.

Determination of metal concentration in the co-existing organic phases showed that the heavy organic phase (the third phase) contained a much higher metal concentration than the light one, as in the extraction of cobalt and nickel with Cyanex 272.[4]

For all the systems investigated the partial distribution ratio between organic phases D^{h}_{l} for both metals increased with increase in initial pH values and was mostly higher at $r^{i} = 2$. The highest values were obtained at $pH^{i} = 10.0$ (Table 2).

r^{i}	D^{h}_{l}			
	Co	Co(Co+Ni)	Ni	Ni(Co+Ni)
1	44.2	42.3	51.1	45.0
2	55.9	43.2	54.3	31.4

Table 2 Partial distribution ratio of the heavy organic phase to the light organic phase, D^{h}_{l}, of cobalt (II) and nickel (II) for different initial phase volume ratios, r^{i}, in extraction systems containing single or both metals. Experimental conditions: MOOP (10%) in kerosene, initial pH, pH^{i} =10, initial metal concentrations: $c^{i}_{Co} = 1.2 \times 10^{-2}$ mol/dm^3 and $c^{i}_{Ni} = 1.8 \times 10^{-1}$ mol/dm^3.

Although the values of the partial distribution ratio of the heavy organic phase to the light organic phase, D^{h}_{l}, were higher than those obtained in cobalt (II) and nickel (II) extraction with Cyanex 272,[4] the partial distribution ratio of the heavy organic phase to the aqueous phase, D^{h}_{a}, were much lower. Namely, the high partial distribution ratio between the organic phases is here more the result of a very low metal content in the light organic phase than of the metal content in the heavy organic phase. In other words, it is the result of the low partial distribution ratio of the light organic phase to the aqueous phase (Table 3).

r^{i}	Metals in sample	pH = 9.0		pH = 10.0	
		D^{h}_{a}	D^{l}_{a}	D^{h}_{a}	D^{l}_{a}
1	Ni	1.3	0.04	0.4	0.01
	Co	*	*	1.1	0.03
	Co(Co+Ni)	7.6	0.69	1.2	0.03
	Ni(Co+Ni)	0.8	0.06	0.3	0.01
2	Ni	1.0	0.02	0.4	0.01
	Co	*	*	1.2	0.02
	Co(Co+Ni)	4.7	0.30	1.3	0.03
	Ni(Co+Ni)	0.6	0.03	0.3	0.01

Table 3 Partial distribution ratios of the heavy organic phase to the aqueous phase, D^{h}_{a}, and of the light organic phase to the aqueous phase, D^{l}_{a}, of cobalt(II) and nickel(II) for different initial pH values, pH^{i}, and initial phase volume ratios, r^{i}.
Experimental conditions: MOOP (10%) in kerosene, initial metal concentrations: $c^{i}_{Co} = 1.2 \times 10^{-2}$ mol/dm^3 and $c^{i}_{Ni} = 1.8 \times 10^{-1}$ mol/dm^3.

Two-phase system

Partial distribution ratios D^{h}_{a} and D^{l}_{a} were much higher at lower initial pH. Also, the partial distribution ratio D^{h}_{a} was different in systems containing single metals and a mixture of metals, indicating a mutual influence of metals on their distribution. For cobalt (II), partial distribution ratio D^{h}_{a} in the system containing a single metal was lower than in the system containing a mixture of

metals, contrary to the partial distribution ratio D^h_a for nickel (II) which was higher for systems containing a single metal.
Maximum D value of cobalt (II) was found at $pH^i = 9.0$. It was 86.9 and 31.8 for both initial phase volume ratios, $r^i = 1$ and 2 respectively. However, in the system containing both metals at $pH^i = 9.0$, the third phase appeared and distribution of cobalt (II) was determined by partial distribution ratio $D^h_a = 7.6$ and 4.7 for the initial phase volume ratios, $r^i = 1$ and 2 respectively (Table 3).

The separation factor of cobalt (II) over nickel (II), α^{Co}_{Ni} in extraction with MOOP under conditions of the third phase was calculated from the partial distribution ratio D^h_a. The separation factor of cobalt (II) over nickel (II), α^{Co}_{Ni} obtained at $pH^i = 9.0$ was higher than at $pH^i = 10.0$ (Table 4).

r^i	α^{Co}_{Ni}	
	$pH^i = 9$	$pH^i = 10$
1	9.4	3.7
2	7.6	4.5

Table 4 Separation factor α^{Co}_{Ni} obtained by MOOP in kerosene and calculated from the partial distribution ratio D^h_a of cobalt(II) and nickel(II) at different initial pH, pH^i and initial phase volume ratios, r^i. Initial metal concentrations: $c^i_{Co} = 1.2 \times 10^{-2}$ mol/dm^3 and $c^i_{Ni} = 1.8 \times 10^{-1}$ mol/dm^3.

The distribution and separation of metals with MOOP under conditions of the third phase formation are not as efficient as e.g. in systems containing di-isopropyl ether.[1,2] However, when the choice of initial pH is stipulated by the presence of other metals in solution results of extraction of cobalt (II) and nickel (II) by MOOP in a three-phase system can also be satisfactory.

ACKNOWLEDGEMENT

This work has been supported by the Ministry of Science and Technology of the Republic of Croatia.

NOMENCLATURE

- D^h_l - partial distribution ratio of the heavy organic phase to the light phase
- D^h_a - partial distribution ratio of the heavy organic phase to the aqueous phase
- D^l_a - partial distribution ratio of the light organic phase to the aqueous phase
- D_{av} - average distribution ratio in three phase systems
- r - volume ratios of the aqueous to the organic phase
- α - separation factor

Subscripts and superscripts

- Co - cobalt
- Ni - nickel
- i - initial

REFERENCES

1. Maljkovic Da and Branica M, *Proc Int. Solv Ext Conf (ISEC'77)*, Toronto, CIM, Spec.Vol. **21/I**, 173, (1979)
2. Maljkovic Du, Maljkovic Da and Paulin A, *Solv Extr. Ion Exch.*, **10**, 477 (1992).
3. Devi NB, Nathsarma KC and Chakravortty V, *Hydrometallurgy*, **49**, 47, (1998).
4. Maljkovic Da, Lenhard Z and Balen M, *Proc. First Europ. Metals Conf. (EMC'91): Non-ferrous Metallurgy Present and Future, Brussels, 1991*; Elsevier Appl. Sci., London, 175, (1991).

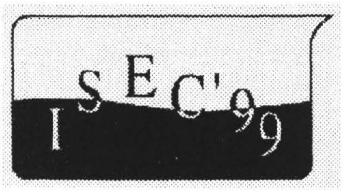

EXTRACTION EQUILIBRIA OF NICKEL WITH LIX860 AND DEHPA

Takashi Sana[2], Koichiro Shiomori[1], Yoshinobu Kawano[1] and Koji Nagayoshi[2]

[1]Dept. Materials Science, Miyazaki Univ., Miyazaki 889-21, Japan

[2]Yoshitama Surface Finishing Co.,Ltd, Nobeoka, Japan

ABSTRACT

The extraction equilibria of nickel in aqueous ammonium sulphate with LIX860 and DEHPA in kerosene were investigated at 303K. For LIX860, the fractional extraction of nickel increased with pH in the aqueous solution and with concentration of the extractant. For DEHPA, the fractional extraction increased to the maximum value at pH = 7, and decreased drastically with increasing pH. The maximum fractional extraction increased with the concentration of the extractant. The extraction reactions for each extractant were established by slope analysis method and their formation constants were estimated as:

$$K=\{[(NiR_2)\cdot[H^+]\}/\{[Ni^{2+}]\cdot[RH]^2\}= 5.2 \times 10^{-4}\ dm^3/mol \text{ for LIX860,}$$

and

$$K=\{[NiR_2RH]\cdot[H^+]\}/\{[Ni^{2+}]\cdot[(RH)_2]^{1.5}\} = 2.3 \times 10^{-3}\ (dm^3/mol)^{0.5} \text{ for DEHPA.}$$

Keywords: nickel, LIX860, DEHPA

INTRODUCTION

Usually, wastewaters involving base metals have been treated by multi-stage precipitation operations. The treatments are effective, because the operations are quite simple and can be widely applied for various metals in the wastewater. The precipitates formed in this method are a mixed solid of various metals and the aggregating agent. Separation and recovery of the metals from this process is difficult. To obtain fundamental information of solvent extraction operations, the separation and recovery of nickel from sulphate solution using solvent extraction with 5-dodecylsalicylaldoxime (LIX860) and di-(2-ethylhexyl)phosphoric acid (DEHPA) as extractants was investigated.

EXPERIMENTAL

LIX860 (65% pure, Henkel Hakusui Co.) and DEHPA (95% pure, Tokyo Chemicals Co.) were used without further purification. Ni_2SO_4, NH_4OH and H_2SO_4 were guaranteed grade regents from Wako Chemicals Co. The organic solutions were prepared by dissolving the extractants in kerosene at the desired concentration. The aqueous solution was prepared by dissolving $NiSO_4$ in 0.50 mol/dm^3 $(NH_4)_2SO_4$ aqueous solution. The pH values of the aqueous solution were adjusted by addition of H_2SO_4 or $(NH_4)OH$. Initial concentration of nickel in the aqueous solution was 230 ppm (4.0×10^{-3} mol/dm^3). Nickel concentrations were measured using atomic absorption spectrophotometer.

Equal volumes of the aqueous and the organic solution were put into a sample vial with stopper. The sample vials were mechanically shaken for 12 hours in a water bath at 303K. After both phases were separated, pH values and the concentrations of nickel in the aqueous solutions were measured. The concentrations of nickel in the organic solution after equilibration were determined from mass-balance for nickel in the aqueous solution.

RESULTS AND DISCUSSION

The extraction of nickel with LIX860

The fractional equilibrium of nickel, E, was plotted against pH in figure 1. The extraction of nickel was affected by the concentration of the extractant and pH with E increasing with pH. The reaction is

© 2000 Society of Chemical Industry

assumed to follow the simple model of chelate extraction.[1,2]

$Ni^{2+} + mRH \Leftrightarrow NiR_m + ZH^+$ (1)

The equilibrium constant, K for eq. (1) is written as follows:

$$K = \frac{[NiR_m]\cdot[H^+]^Z}{[Ni^{2+}]\cdot[RH]^m} \quad (2)$$

Substituting the distribution coefficient, $D(=[Ni]_{org}/[Ni]_{aq})$, into eq.(2) and rearranging gives:

$$D = K[RH]^m / [H^+]^Z \quad (3)$$

Taking logarithms of eq.(3), the following equation is obtained:

$$\log D = m\log[RH] + zpH + \log K \quad (4)$$

Log$D$ is plotted against log[RH] in figure 2. The experimental results are plotted on the straight lines having a slope of 2.0 at each pH. Hence, the value of m were determined as 2.0. Substituting m value into eq.(4) and rearranging gives:

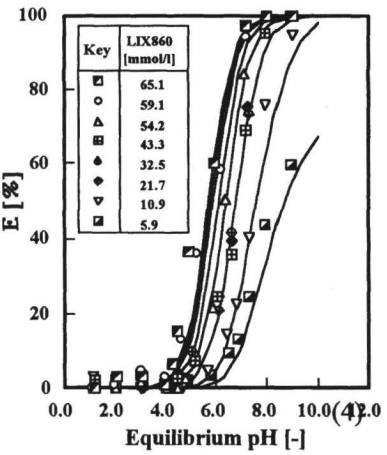

Figure 1 Effect of pH on the extraction of nickel with LIX860

$$\log(D/([RH]^2) = zpH + \log K \quad (5)$$

$\log(D/[RH]^2)$ is plotted against pH in figure 3. All of the experimental values were scattered on a straight line having a slope of 1.0. Therefore the value of z was determined as 1.0.

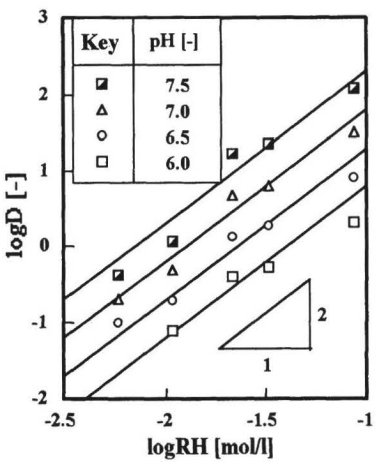

Figure 2 Effect of logRH on the logD at various pH

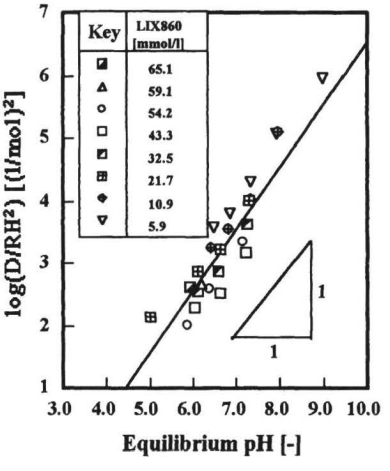

Figure 3 Plot of $\log(D/RH^2)$ against pH at various LIX860 concentrations

Substituting m and z values into eq.(4) and rearranging gives:

$$\log D = \log(RH^2 / H^+) + \log K \quad (6)$$

log$D$ values are plotted against $\log(RH^2 / H^+)$ in figure 4. The experimental points all converge on a straight line having a slope of 1.0. Using the intercept of the line, the apparent equilibrium constant, K is

determined as 5.2×10^{-4} mol/dm^3.
Substituting the values of m and z into eq.(1), the overall reaction is written as follows :

$$Ni^{2+} + 2RH \Leftrightarrow NiR_2 + H^+$$

Disagreement of the charge above the results is due to very high concentration of sulphate and ammonium ion in aqueous solution. The solid line calculated using the value of K, m and z in figure 1 agrees well with the experimental results.

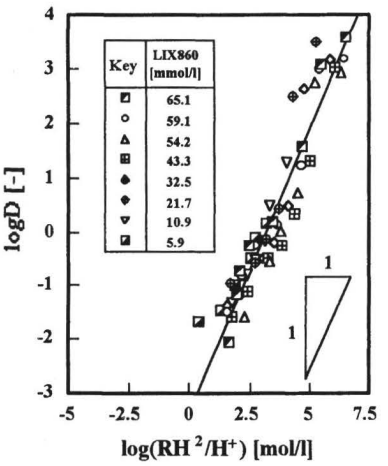

Figure 4 Plot of logD against $\log(RH^2/H^+)$

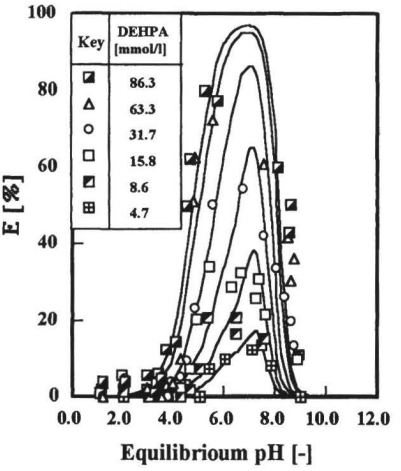

Figure 5 Effect of pH on the extraction of nickel with DEHPA

Extraction of nickel with DEHPA

Values of E are plotted against pH in figure 5. E increases to a maximum value at pH = 7 and then decreases with increasing pH. The Ni^{2+} was assumed to react with dimer of DEHPA as the most simple model.[3,4,5]

$$Ni^{2+} + m(RH)_2 \Leftrightarrow NiR_nlRH + zH^+ \qquad (m = n+l) \tag{7}$$

The equilibrium constant, K for eq.(7) is written as:

$$K = \frac{[NiR_nlRH] \cdot [H^+]^z}{[Ni^{2+}] \cdot [(RH)_2]^m} \tag{8}$$

Substituting $D = ([Ni]_{org}/[Ni^{2+}]_{aq})$into eq.(8) ,

$$D = K[(RH)_2]^m / [H^+]^Z \tag{9}$$

Taking logarithms eq.(9), the following equation is obtained:

$$\log D = m\log[(RH)_2] + zpH + \log K \tag{10}$$

Taking into account the following reactions and mass balance equations.

$$[Ni(NH_3)_{(i-1)}]^{2+} + NH_3 \Leftrightarrow [Ni(NH_3)_i]^{2+} \ (i = 1\text{-}6) \tag{11}$$

$$[Ni]0=[Ni]aq+[Ni]org \tag{12}$$

$$NH_4^+ \Leftrightarrow NH_3+H^+ \tag{13}$$

$$[NH_3]_0 = [NH_4^+] + [NH_3] + \Sigma \{i\cdot[\ [Ni(NH_3)_i]^{2+}]_0\} \tag{14}$$

D is given by:

$$D = \frac{[Ni]_{org}}{[Ni]_{aq}(1 + \sum_{1}^{6} \beta_i (Ka/(Ka + [H^+])^i)} \quad (15)$$

where Ka is acid dissociation constant of ammonium ion, i is the co-ordination number of ammonia to nickel and β_i are overall formation constants of each nickel-ammine complex.
log$D$ are plotted against log[$(RH)_2$] in figure 6.

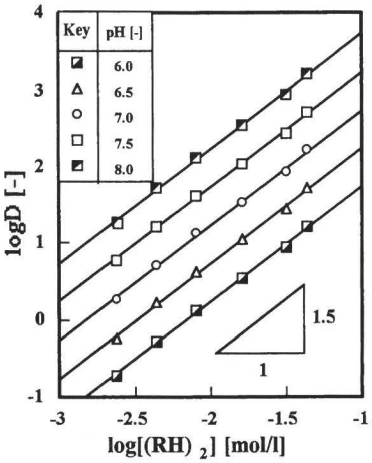

Figure 6 Effect of log[$(RH)_2$] on logD at various pH values

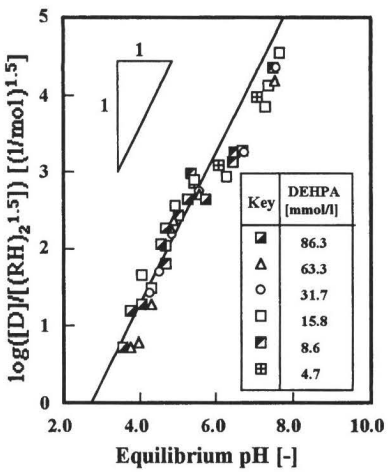

Figure 7 Plot of log[$D/(RH)_2^{1.5}$] against pH

The experimental results are plotted on the straight lines having of a slope of 1.5 at each pH. Hence the value of m is determined as 1.5.
Substituting m value into eq.(10) and rearranging gives:

$$\log(D/([(RH)_2]^{1.5}) = zpH + \log K \quad (16)$$

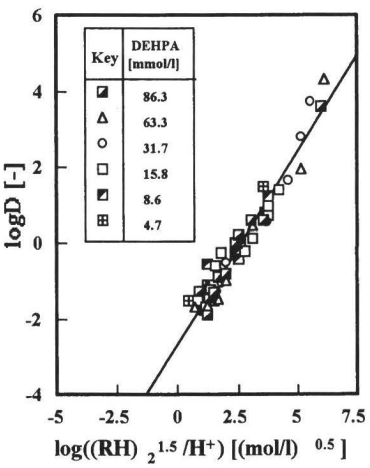

Figure 8 Plot of logD against log[$(RH)_2^{1.5}/H^+$]

log(D/([$(RH)_2$]$^{1.5}$) were plotted against pH in figure 7. All of the experimental values were plotted on a straight line having a slope of 1.0. Thus the value of z was determined as 1.0.
Substituting m and z values into eq.(10) and rearranging gives:

$$\log D = \log((RH)_2^{1.5} / H^+) + \log K$$

log$D$ values are plotted against the log($(RH)_2^{1.5}$ /H^+) in figure 8. The points at all concentrations converge on a straight line having a slope of 1.0. The apparent equilibrium constant, K is determined by the intercept of the line as 2.3 x 10^{-3} $(dm^3/mol)^{0.5}$.
Substituting the values of m and z into eq.(7), the overall reaction is written as follows:

$$Ni^{2+} + 1.5(RH)_2 \Leftrightarrow NiR_2RH + H^+$$

The solid line calculated using the value of K, m and z in figure 5 agrees well with experimental results.
The charges involved in the reaction is not satisfactory. The

reason for this is not clear and will be considered that further analysis in necessary in future work.

CONCLUSION

Extraction equilibria of nickel from aqueous nickel sulphate with LIX860 and DEHPA in kerosene were examined at various pH values in aqueous solution and various concentrations of the extractants in the organic solution. The overall extraction reactions and their constants were estimated as follows;

(1) for LIX860, nickel reacts with LIX860 to form nickel/LIX860 complexes NiR_2 having following equilibrium constant;

$$K=\{[(NiR_2]\cdot[H^+]\}/\{[Ni^{2+}]\cdot[RH]^2\}= 5.2 \times 10^{-4} dm^3/mol$$

(2) for DEHPA, nickel reacts as Ni^{2+} alone with DEHPA to form the nickel/DEHPA complex NiR_2RH having a equilibrium constant;

$$K=\{[NiR_2RH]\cdot[H^+]\}/\{[Ni^{2+}]\cdot[(RH)_2]^{1.5}\} = 2.3\times 10^{-3} (dm^3/mol)^{0.5}$$

REFERENCES

1 K.Srinivasa K et al. *Minerals and Metallurgical Processing*,8, (November 1997)
2 Yamashita K et al *Sep.Sci.and Technol,* **33**, 369, (1998)
3 Komasawa I et al. *J.Chem.Eng. Jpn.*, **16**, 210, (1983)
4 Kim S-G et al. *Hydrometallugy*, **38**, 7, (1995)
5 Park, S-J et al.;*Solv. Extr.*,201, (1992)

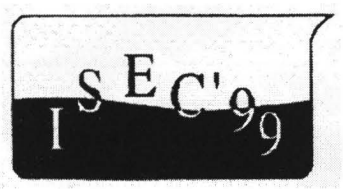

STOICHIOMETRY OF THE EXTRACTION OF NICKEL WITH ORGANOPHOSPHORUS ACIDS

C C Bourget, M Cox and D S Flett
Department of Physical Sciences, University of Hertfordshire, Hatfield, Hertfordshire AL10 9AB, UK

ABSTRACT
A systematic study of nickel extraction has been carried out with a range of commercial organophosphoric, phosphonic and phosphinic acid extractants and the stoichiometry of the extracted nickel species determined graphically (slope analysis) and numerically by using the LETAGROP procedure. The co-extraction of water has also been studied. Consistent results were obtained from both methods leading to the general conclusion that the extracted nickel complexes have the general form $NiR_2(RH)_x(H_2O)_y$ where $x + y = 4$. The amount of water present in the complexes depends on the nature of the extractant and, although there is an equilibrium between several species, in general it is found that $y = 2$ with alkylphosphoric acids, $y = 1$ for phosphonic acids and $y = 0$ for phosphinic acids.

Keywords: nickel, Cyanex 272, PC-88A, Ionquest 801, PIA-8, water content of extracted complexes

INTRODUCTION

In the course of an investigation of the recovery of nickel from leach liquors arising from the Greek laterite ores[1,2] it became apparent that, unlike cobalt, there was lack of agreement in the literature regarding the stoichiometry of the extracted nickel complexes with organophosphorus acids. No resolution of these discrepancies regarding the nickel extracted species has as yet been made and so it was decided to study in more detail the stoichiometry of the nickel complexes with organophosphorus acids by means of graphical (slope analysis) and numerical (LETAGROP) techniques. At the same time the amount of water associated with the extracted nickel species was also determined.

EXPERIMENTAL

The acids used in this study were DEHPA (di-(2-ethylhexyl)phosphoric acid, Albright & Wilson (A&W)), 2-ethylhexylphosphonic acid mono-2-ethylhexyl ester, (PC-88A Daihachi Chemical Industry Co. Ltd (DCI) and (Ionquest 801 A&W)), CYANEX 272 (bis-(2,4,4-trimethylpentyl)phosphinic acid, Cytec Inc.) and PIA-8 (di-(2-ethylhexyl)phosphinic acid, DCI). These were used without further purification. Their purity and pK_a values have been reported earlier.[1] The diluent used in this study was Phillips Orform SX7. All other chemicals were of reagent grade purity.

The equilibrium distribution of nickel with these alkylphosphorus acids was determined as a function of pH and reagent concentration by contacting equal volumes (300 ml) of the aqueous and organic phases by rapid mechanical stirring for 60 minutes at room temperature. Adjustment of the pH was made by additions of H_2SO_4 (3 M) or NH_4OH (6 M) and the pH measured using a combined electrode. The initial aqueous phase contained nickel sulphate (10^{-3} M) and Na_2SO_4 (1 M) to maintain ionic strength. For all experiments the metal contents of both the aqueous and organic (after stripping with H_2SO_4) phases were analysed by ICP. The mass balances for each organic and aqueous phase measurement agreed to within ± 5%.

The water content of the organic phases in the presence and absence of extracted nickel were measured by Karl Fischer analysis using an Aquapal 11-02 Moisture Meter.

RESULTS AND DISCUSSION

At low nickel concentrations it is assumed that the extracted nickel complexes are monomeric. Thus the extraction can be represented by the following equation:

© 2000 Society of Chemical Industry

$$Ni^{2+} + (2+q)/2\ \overline{R_2H_2} = \overline{NiR_2(HR)_q} + 2p\ H^+ \qquad (1)$$

where R_2H_2 is the organophosphorus acid dimer and bars denote organic phase species.
Defining the reaction equilibrium constant, K_{2q} and the nickel distribution coefficient, D_{Ni}, in the usual way, substituting, rearranging and taking logs results in the following equations:

$$\log(D_{Ni}) = \log K_{2q} + (2+q)/2\ \overline{\log(R_2H_2)} + 2p\ H^+ \qquad (2)$$

$$\log(D_{Ni}[H^+]^2) = \log(K_{2q}) + (2+q)/2\ \overline{\log(R_2H_2)} \qquad (3)$$

Thus a plot of $\log(D_{Ni}[H^+]^2)$ against $\log(\overline{R_2H_2})$ at constant pH gives a straight line with an intercept equal to $\log(K_{2q})$ and a slope equal to $(2+q)/2$. These plots are shown in Figure 1. The values of q determined from the slopes are: DEHPA, 2.0; PC-88A, 3.6; Ionquest 801, 3.2; PIA-8, 3.8 and CYANEX 272, 3.2.

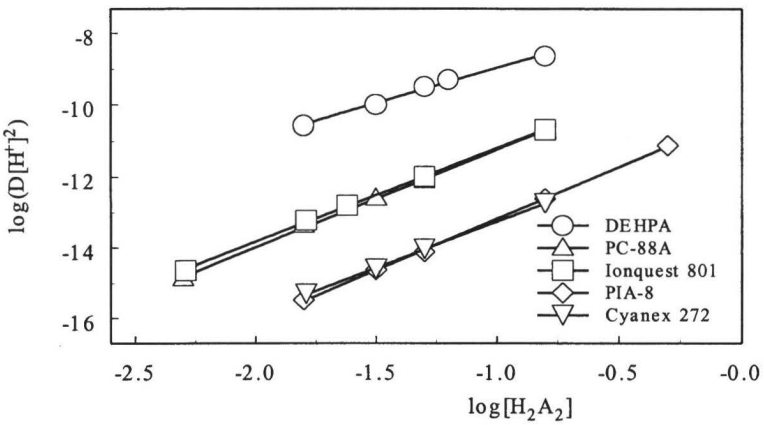

Figure 1 Effect of reagent concentration on extraction of nickel

For DEHPA the extracted species is therefore concluded to be $NiR_2.R_2H_2$. For the other acids the q values are between 3 and 4 indicating the formation of the species $NiR_2(RH)_3$ and $NiR_2(R_2H_2)_2$ respectively. Similar equations to those above can be derived for the formation of these complexes. The appropriate formation constants can be determined from a plot of $D_{Ni}(H^+)_2(R_2H_2)^{-3}$ against $(R_2H_2)^{-0.5}$ which gives a straight line of slope K_{23} and an intercept equal to K_{24}. These data are shown in Table 1.

The extraction stoichiometries and formation constants were reconfirmed by analysis of the experimental equilibrium data by the LETAGROP-DISTR program.[3] For the calculation literature values [4,5,6] were taken for the required dimerisation, distribution and dissociation constants of the acids themselves as well as the complexation constants for the interactions between Ni^{2+} and the sulphate anion. Calculation showed that the best fit was obtained when the species were the same as those inferred from the graphical treatment.

Graphically and numerically determined constants are compared in Table 1 from which it can be seen that the equilibrium constants for nickel using the five organophosphorus acids determined graphically and numerically agree reasonably well (less than one unit difference) considering that the equilibrium constants used from the literature to run LETAGROP differ slightly from the ones which would have matched the conditions of the present work.

Extractant	Graphical			Numerical		
	$\log K_{22}$	$\log K_{23}$	$\log K_{24}$	$\log K_{22}$	$\log K_{23}$	$\log K_{24}$
DEHPA	-7.01	-	-	-6.74	-	-
PC-88A	-	-8.95	-8.73	-	-9.44	-8.03
Ionquest 801	-	-8.78	-8.95	-	-8.64	-8.50
PIA-8	-	-11.41	-10.26	-	-10.56	-10.62
CYANEX 272	-	-10.89	-10.86	-	-10.72	-9.80

Table 1 Comparison of Graphically and Computer Generated Equilibrium Constants

For DEHPA the extracted nickel species found in this study agrees with a number of other workers [7,8,9] from both sulphate and nitrate media. However different stoichiometries are reported by other workers [6,10,11,12] who conclude that three dimer molecules of DEHPA are involved in the complex viz. either $NiR_2.4RH$ or $NiR_2.2(RH)_2$. For the phosphonic and phosphinic acids the present work has shown that both $NiR_2(RH)_3$ and $NiR_2(RH)_4$ complexes are formed in the organic phase. However the formation of a single species, $Ni(R_2H)_2(R_2H_2)$, has been reported [11] for PC-88A from perchlorate solution. Other workers [13,14] have found the same species from nitrate media with PC-88A while Komasawa et al [15] concluded that the extracted species was $NiR_2.2(RH)_2$. For PIA-8, Nagaosa and Binghua,[5] using both graphical and numeric methods, found contradictions between the stoichiometries determined by both methods with slope analysis agreeing with the current work but the best fit from LETAGROP gave $NiR_2(RH)_3$ and $NiR_2(RH)_6$. Danesi et al.[14,16] found their data was best represented by a single species $Ni(R_2H)_2(R_2H_2)$ and found the same species for CYANEX 272 which was later confirmed by Sole and Hiskey [17] and Tait [18] for sulphate media. Different experimental conditions between the current work and that of other workers may explain many of these discrepancies in the stoichiometries of the nickel complexes.

Nickel is known to exist in the organic phase as an octahedral complex. Thus some at least of the reported complexes including the $NiR_2.R_2H_2$ and $NiR_2(RH)_3$ species found in this study are not co-ordinately saturated. It is logical therefore to assume that co-ordination saturation is achieved through addition of water molecules. The uptake of water by the five extractants was therefore determined over a range of nickel contents in the organic phase. The results are shown in Figure 2 which, in agreement with Nakano et al (19), shows that the amount of water associated with the extracted species decreases in the order phosphoric>phosphonic>phosphinic which follows the same order of polarity of the organophosphorus compounds.[11] From the water to metal concentration ratios, Figure 3, it is clear that the number of water molecules associated with the metal-extractant complex is related to the nickel complex concentration in the organic phase as also observed by Nakano et al.[18] However the number of water molecules involved in the nickel-extractant complex is far too high to come only from the co-ordination of water to the nickel. An examination of the water to metal concentration ratio (R) in the organic phase for each nickel-extractant system indicates that the water content for the nickel complex with the phosphoric acid DEHPA ($0<R<40.9$) is about twice as high as for the phosphonic acids PC-88A and Ionquest 801 ($0<R<17.5$) which in turn is about twice as high or more as that for the phosphinic acids, CYANEX 272 and PIA-8 ($0<R<8.0$). This suggests that the number of water molecules present in the nickel complex to be in the ratio of 2:1:0 for the series phosphoric, phosphonic and phosphinic acids.

This is supported by Nakano et al (19) who also found the water content of DEHPA to be twice as high as for PC-88A. Thus the following stoichiometries are proposed for the nickel complexes: DEHPA: $NiR_2(RH)_2(H_2O)_2$; and $NiR_2(RH)_3(H_2O)$ and $NiR_2(RH)_4$ for the other systems. From the suggested variation in the water:nickel ratio of 2:1:0 it may be inferred that the species $NiR_2(RH)_3(H_2O)$ is more predominant for the phosphonic acids and $NiR_2(RH)_4$ for the phosphinic acids. It is therefore believed that the stoichiometry of the nickel complexes with organophosphorus acids can be represented by an equilibrium wherein the molecules of water are progressively replaced by molecules of extractant through the series phosphoric, phosphonic and phosphinic acids as follows:

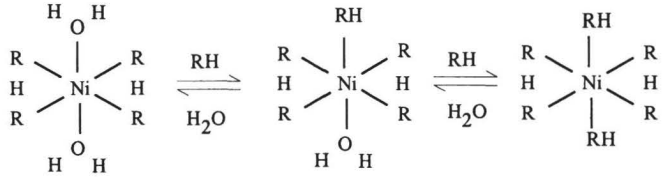

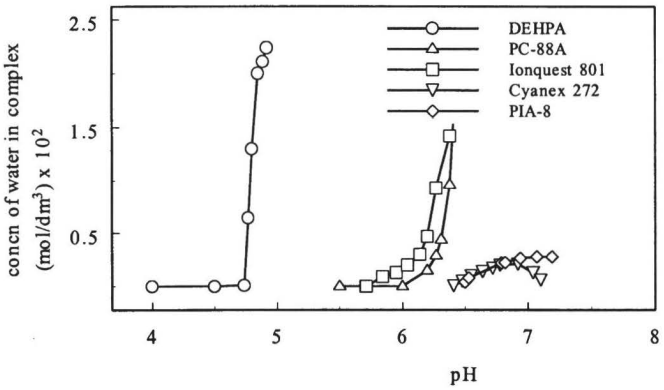

Figure 2 Water content of nickel complexes

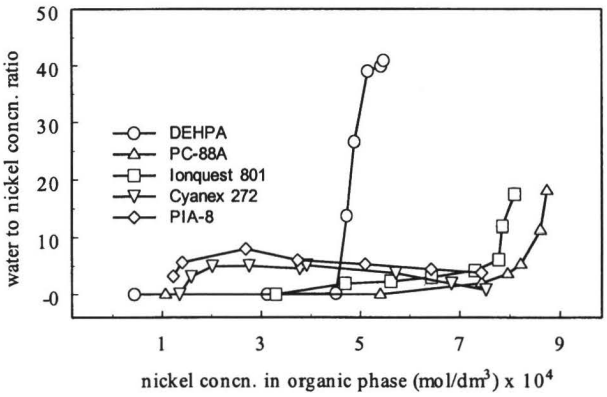

Figure 3 Number of water molecules per nickel ion

In accordance with this work Sato and Nakamura [20] and Nakano et al.[19] found two molecules of water associated with the nickel-DEHPA complex from sulphate and nitrate media respectively. Preston and Du Preez [21,22] and Preston [13] have surveyed the extraction of nickel with many organophosphorus acids and concluded that the nickel complexes were best represented by the general formula $Ni(R_2H)_2(R_2H_2)_x(H_2O)_{2-x}$ where x = 0, 1 or 2 depending on the extractant concentration. At low extractant concentration (0.2 M) the nickel species were found to be $Ni(R_2H)_2(H_2O)_2$ which was later confirmed by Yuan et al.[23] who reported the presence of the same species on extraction from sulphate media.

CONCLUSIONS

In this study both graphical and numerical analyses have given a consistent general stoichiometry of $NiR_2(RH)_x(H_2O)_y$ for the extracted nickel species with organophosphoric, phosphonic and phosphinic acids where $x + y = 4$. The amount of water present in the complexes is shown to depend on the nature of the extractant and, although there is an equilibrium between several species, in general it is found that y = 2 with alkylphosphoric acids, y = 1 for phosphonic acids and y = 0 for phosphinic acids. Different working conditions between the current work and that of other workers may explain the many discrepancies in the stoichiometries of the nickel complexes with organophosphorus acids.

ACKNOWLEDGEMENTS

This work was carried out as part of an EU Brite-Euram project contract number BRE2-CT94-1020. The authors would like to acknowledge gifts of the reagents from the manufacturers and of Orform SX7 from Phillips Petroleum Inc.

REFERENCES

1. Bourget CG, Cox M and Flett DS. *Value Adding Through Solvent Extraction. Proc ISEC'96*, eds D C Shallcross, R Paimin and L M Prvcic, The University of Melbourne, **1**, 505-510, (1996),.
2. Bourget C, Cox M and Flett DS *Nickel/Cobalt'97, Vol 1, Hydrometallurgy and Refining of Nickel and Cobalt,* eds W C Cooper and I Mihaylov, CIM, 305-318, (1997).
3. Liem DH. *Acta Chem. Scand*, **25**, 1521, (1971)
4. Sella C and Bauer D *Solv. Extr. and Ion Exch*, **6**(5), 819, (1988)
5. Nagaosa Y and Binghua Y. *Talanta*, **44**, 327, (1997)
6. Huang TC and Tsai TH. *Ind Eng Chem Res*, **28**, 1557, (1989)
7. Brisk ML and McManamey WJ. *J Appl Chem*, **19**, 103, (1984)
8. Smelov VS and Chubukov VV. *Radiokhimiya*, **15**, 530, (1973)
9. Fernandez LA, Elizalde MP and Castresana JM. *Solv Extr and Ion Exch* , **3**(6), 807, (1985)
10. Grimm R and Kolarik Z. *J inorg nucl Chem*, **36**(1), 189, (1974)
11. Dianyun Q, Longao Z and Rongjun M. *Solv Extr & Ion Exch* , **7**(6), 937. (1989)
12. Komasawa I, Otake T and Higaki I. *J inorg nucl Chem,* **43**(12), 3351, (1981)
13. Preston JS. *Hydrometallurgy*, **9**, 115-133, (1982)
14. Danesi PR, Reichley-Yinger L, Mason G, Kaplan L, Horwitz EP and Diamond D. *Solv Extr & Ion Exch* , **3**, 435, (1985)
15. Komasawa I, Otake T and Hattori I. *J Chem Eng Japan*, **16**(3), 210, (1983)
16. Danesi PR, Reichley-Yinger L, Cianetti C and Rickert PG. *Solv Extr & Ion Exch*, **2**(6), 781, (1984)
17. Sole KC and Hiskey JB. *Hydrometallurgy*, **30**, 345-365, (1992)
18. Tait BK. *Hydrometallurgy*, **32**, 365-372, (1993)
19. Nakano M, Takahashi K and Takeuchi H. *Proc Symp on Solvent Extraction,* Kansai University, Osaka, Japan, **1987**, 81-86.
20. Sato T and Nakamura T. *J inorg nucl Chem*, **34**, 3721, (1972)
21. Preston JS and Du Preez AC. *MINTEK Report*, M378, (1988)
22. Preston JS and Du Preez AC. *Proc ISEC'86, Dechema*, **2**, 83-90, (1986)
23. Yuan CY, Xu Q, Yuan S, Long H, Shen D, Jiang Y, Feng H, Wu F and Chen W.*Solv Extr & Ion Exch*, **6**(3),

393, (1988)

COPPER EXTRACTION FROM AMMONIACAL SOLUTIONS WITH COMMERCIAL CHELATING EXTRACTANTS AND THEIR MIXTURES

George Kyuchoukov[1], Mariusz B Bogacki[2] and Jan Szymanowski[2]

[1] Institute of Chemical Engineering of Bulgarian Academy of Science, Sofia, Bulgaria,

[2] Institute of Chemical Technology and Engineering, Poznan University of Technology, Pl. M. Sklodowskiej – Curie 2, 60-965 Poznan, Poland

ABSTRACT

Extraction of copper from ammoniacal solutions with LIX 84 and LIX 54 used alone and as a mixture was studied and a chemical model was proposed and verified. The equilibrium extraction constant was correlated with the ionic strength. The effect is weak for the strong extractant LIX 84 and its mixture but very strong for the weak extractant LIX 54.

Keywords: copper, ammoniacal solution, LIX 84, LIX 54

INTRODUCTION

LIX 84 and LIX 54 manufactured by HENKEL differ significantly in their extraction ability.[1] LIX 84 is a strong hydroxyoxime extractant and extracts copper from highly acidic sulphuric solutions. LIX 54 is a weak β-diketone extractant[2,3] and is used to recover copper from various ammoniacal solutions. Both reagents are able to associate and co-associate via intermolecular hydrogen bonds forming the 2:1 co-associate (2 molecules of hydroxyoxime and 1 molecule of β-diketone). As a result, LIX 54 can be considered as a modifier of LIX 84.[4-7]

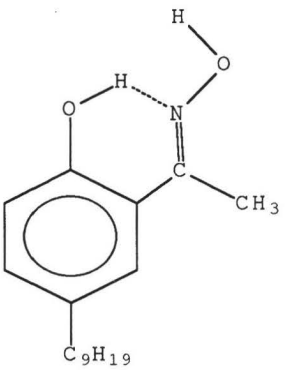

LIX 84

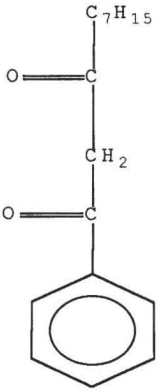

LIX 54

The aim of the work was to model the extraction of copper from ammoniacal chloride solutions with individual LIX 84 and LIX 54 and their mixtures. Such a system is important from a technological point of view. The recovery of copper from ammoniacal solutions obtained from printed circuit board manufacture may be considered as the most important application.[1,8]

EXPERIMENTAL

LIX 84 and LIX 54 were used as kindly delivered by HENKEL. The initial feed used for extraction contained 134 ± 2 g/dm^3 Cu^{2+}, ~ 4.8 mol/dm^3 Cl^- and 8 ± 0.3 mol/dm^3 NH_3. The raffinate

© 2000 Society of Chemical Industry

obtained in the first extraction was used as a feed in the second extraction step. LIX 84, LIX 54 and their 1:1 v/v mixture without any added diluent were used for extraction, which was carried out at room temperature.

RESULTS AND DISCUSSION

Extraction isotherms shown in Figure 1 confirm the different extraction strengths of the reagents. The isotherm obtained for the 1:1 v/v mixture of LIX 54 and LIX 84 lies approximately in the middle of the isotherms determined for the individual extractants. As a result, a synergistic effect is not observed and the concentration of copper in the organic phase can be predicted from the results obtained for the individual extractants (Table 1).

Copper in raffinate,	Copper in extract, g/dm^3	
g/dm^3	Found	Calculated
92.38	43.6	40.33
59.71	34.7	36.19
31.29	26.57	30.42
7.19	19.04	17.33
0.52	7.66	3.00
0.33	0.44	2.28

Table 1. Observed and calculated equilibrium concentrations of copper in the organic phase after extraction with the mixture of extractants (initial concentration in the feed: 4.7 mol/dm^3 Cl^-, 136.15 g/dm^3 Cu^{2+}, 7.81 mol/dm^3 NH_3).

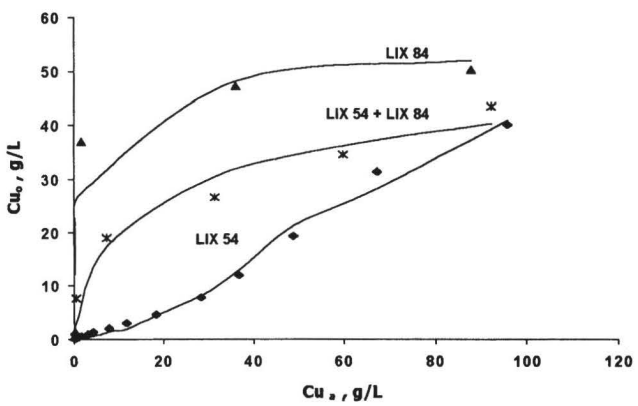

Figure 1. Extraction isotherms for copper extraction with LIX 84 and LIX 54 and their 1:1 v/v mixture.

The extraction from ammoniacal solutions is complex because several different equilibria must be considered. They include:

- extraction of Cu(II)

$$Cu_a^{2+} + 2HL_o = CuL_{2o} + 2H_a^+, \qquad K_1 = \frac{[CuL_2]_o [H^+]_a^2}{[Cu^{2+}]_a [HL]_o^2} \tag{1}$$

- formation of ammonia complexes

$$Cu_a^{2+} + iNH_{3a} = Cu(NH_3)_{i\ a}^{2+}, \qquad \beta_i = \frac{[Cu(NH_3)_i^{2+}]_a}{[Cu_a^{2+}][NH_3]_a^i} \tag{2}$$

- formation of ammonium cation

$$NH_{3a} + H_a^+ = NH_{4\ a}^+, \qquad K_3 = \frac{[NH_4^+]_a}{[NH_3]_a[H^+]_a} \tag{3}$$

The mass balance of copper is as follows:

$$[Cu_t]_a = [Cu^{2+}]_a \cdot \left(1 + \sum_{i=1}^{4} \beta_i \cdot [NH_3]_a^i\right) \tag{4}$$

and the extraction equilibrium constant can be expressed in the following form:

$$K_1 = \frac{1}{K_5^2} \frac{[CuL_2]_o [NH_4^+]_a^2}{[Cu_t]_a [HL]_o^2 [NH_3]_a^2} \cdot \left(1 + \sum_{i=1}^{4} \beta_i \cdot [NH_3]_a^i\right) \tag{5}$$

The equation can be simplified for higher ammonium concentration to equation:

$$K_{ex} = \frac{[CuL_2]_o [NH_4^+]_a^2 [NH_3]_a^2}{[Cu_t]_a [HL]_o^2} \tag{6}$$

where $K_{ex} = K_1 . K_3^2 . \beta_4^{-1}$

The extraction equilibrium depends on the ionic strength I and the equilibrium constant increases as the ionic strength rises. As a result, the additional equation was considered:

$$\ln(K_{ex}) = a + b.I \tag{7}$$

where a and b are the regression coefficients.

Such a model (solid lines in Figure 1) agrees well with the experimental data. The extraction constants given in Table 2 and calculated according to the model indicate that the linear approximation of K_{ex} with I is fully justified.

Extractant	$\ln(K_{ex}) = a + b.I$		$[RH]_T$, mol		MSE
	a	b	exp.	calc.	
LIX 54	-6.088	1.970	0.596	0.854	0.0005
LIX 84	8.159	0.111	0.768	0.862	0.015
LIX 54 + LIX84 1:1 v/v	4.611	0.374	1.372	1.524	0.014

Table 2. Effect of ion strength on the extraction equilibrium constant. ($[RH]_T$ denotes the total molar concentration of extractants calculated from the model (calc.) and estimated from the maximum loading given in Figure 1. (exp.) and MSE stands for model variance).

CONCLUSIONS

Copper extraction from ammoniacal solutions changes in the following order of extractants LIX 84 > LIX 84 + LIX 54 > LIX 54. These differences are important for low copper concentrations in the feed. The extraction can be well described by a chemical model that takes into account the positive effect of the ionic strength. This effect is strong for LIX 54 and small for LIX 84 and LIX 84 + LIX 54 (1:1 v/v) mixture.

ACKNOWLEDGMENT

M. B. Bogacki and J. Szymanowski thank for the grant No. 3T09B05114 from the Polish Research Committee KBN

NOMENCLATURE

K_{ex} extraction equilibrium constant,
K_1 extraction equilibrium constant,
K_3 ammonia complex equilibrium constant,
β_i ammonia complex formation constants,

REFERENCES

1. Szymanowski J, *Hydroxyoximes and Copper Hydrometallurgy*, CRC Press, Boca Raton, FL., (1993).
2. Dziwinski E, Szymanowski J. *Solv. Extr. Ion Exch.*, **14**, 219, (1996).
3. Mickler W, Uhlemann E, Herzschuh R, Wenclawiak B and Plaggenborg L, *Sep. Sci. Technol.*, **27**, 1171, (1992).
4. Majdan M, Sperline RP, Gu W-G, Yu W-H and Freiser H, *Solv. Extr. Ion Exch.*, 7, 987,(1989).
5. Szymanowski J, *Crit. Rev. Anal. Chem.*, **25**, 143, (1995).
6. Szymanowski J, *Solvent Extr. Res. Dev. Jpn*, **1**, 97, (1994).
7. Bogacki MB and Szymanowski J, *Solv. Extr. Res. Dev., Jpn*, **3**, 10, (1996).
8. Transaco MX International AB, *MECER, a Solvent Extraction Process for the Recovery of Ammoniacal Etching Liquors*, Stockholm, Sweden

EXTRACTION OF COPPER FROM CHLORIDE MEDIA WITH NEW ALKYL DERIVATIVES OF PYRIDINE-3,5-DICARBOXAMIDE

Aleksandra Borowiak-Resterna[1], Gerard Cote[2] and Jan Szymanowski[1]

[1]Institute of Chemical Technology and Engineering, Poznan University of Technology, Pl. Skodowskiej-Curie 2, 60-965 Poznan, Poland

[2]Laboratoire d'Electrochimie et de Chimie Analytique, Ecole Nationale Superieure de Chimie de Paris, France

ABSTRACT

Model individual N,N'-dialkyl- and N,N,N',N'-tetraalkylpyridine-3,5-dicarboxamides were used to recover copper(II) from chloride solutions at constant water activity and constant total concentration of dissolved species in aqueous solution. It was found, that N,N'-di(2-ethylhexyl)pyridine-3,5-dicarboxamide is a stronger extractant than N,N,N',N'-tetraalkyldiamides. N,N,N',N'-tetraalkylpyridine-3,5-dicaboxamides, and N,N'-dialkylpyridine-3,5-dicarboxamides with branched chains and their copper complexes are well soluble in hydrocarbon diluents. N,N,N',N'-tetraalkyldiamides form with copper complexes $CuCl_2(Ext)_2$. However, $Cu(NO_3)_2(Ext)_2$ and $CuClNO_3(Ext)_2$ are also formed in significant amounts at low chloride concentration ($\leq$ 0.5 M) and high concentration of nitrate (3.5 - 4 M).

Keywords: copper, pyridine-3,5-dicarboxamides, chloride media.

INTRODUCTION

The success of the hydrometallurgical technique for extraction of copper in the processing of oxide ores and various wastes has induced interest in applying this technology to copper recovery from other raw materials, including sulphidic ores, constituting the principal raw material for copper production.

Esters and amides of pyridinecarboxylic and pyridinedicarboxylic acids have been proposed by ICI (now ZENECA) for copper extraction from concentrated chloride solutions[1] . In the 1980's ICI patented extractant DS5443 (now known as ACORGA CLX-50), which contains a diester of pyridine-3,5-dicarboxylic acid. The extraction-stripping process can be described by the following equation:

$$Cu^{2+}_w + 2\,Cl^-_w + 2\,Ext_o \Leftrightarrow [CuCl_2(Ext)_2]_o \qquad (1)$$

The extraction properties of pyridinecarboxylic and pyridinedicarboxylic acid esters were previously studied[2]. Equilibrium studies of extraction for selected alkyl derivatives of pyridinecarboxamides were also described in our previous work[3,4].

The aim of this work is the synthesis of model N,N'-dialkyl- and N,N,N',N'-tetraalkylpyridine-3,5-dicarboxamides and studies of equilibrium extraction at constant water activity. Such extractants with dialkyl substituents at amide nitrogen should perform a better extraction performance in comparison to amides studied previously.

EXPERIMENTAL

N,N'-di(2-ethylhexyl)pyridine-3,5-dicarboxamide (1), N,N,N',N'-tetrabutyl-pyridine-3,5-dicarboxamide (2) and N,N,N',N'-tetrahexylpyridine-3,5-dicarboxamide (3) were synthesized with yield of 30 % in the following two-stage process:

1) the synthesis of pyridine-3,5-dicarboxyl dichloride from pyridine-3,5-dicarboxylic acid and thionyl chloride in presence of pyridine,
2) the acylation reaction of the appropriate amine by raw pyridine-3,5-dicarboxyl dichloride.

Reaction conditions were the same as in synthesis of N,N-dihexylpyridine-3-carboxamide[3].

© 2000 Society of Chemical Industry

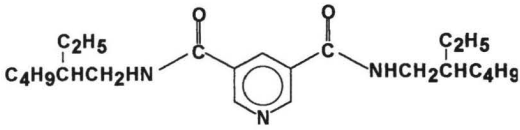

1

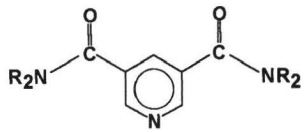

or R = C_4H_9 - 2
R = C_6H_{13} - 3

A purity of 98-99 % was demonstrated by GC/MS for all amides. UV, IR, PMR and MS spectra prove the structure of the obtained compounds.

Extraction was carried out at constant water activity a_w = 0.8352 and constant total concentration of ions and molecules dissolved in aqueous solution σ = 8.0 mol/dm^3. As exposed previously, the fact of keeping constant a_w and σ permits to maintain constant the activity coefficients. $CuCl_2$, $LiNO_3$, $NaNO_3$, and NaCl of analytical grade were used[2].

The chloride concentration was changed from 0.02 to 3.0 mol/dm^3. In all experiments the pH of the aqueous phase was close to 3.5. The studies were carried out at constant copper(II) concentration equal to 0.01 mol/dm^3. The concentration of extractants in the organic phase was changed from 8 x 10^{-2} to 3.5 x 10^{-1} mol/dm^3. Toluene was used as a diluent. The phase volume ratio was 1.

Extraction was carried out in a typical manner at room temperature[3]. Copper(II) was completely stripped from the organic phase after extraction by pure water. Copper concentration was determined by titration with EDTA, in the aqueous feed and raffinate solutions and in the aqueous solution obtained after stripping.

Acid transfer to the organic phase by the extractants was determined in the same way as described previously[4].

RESULTS AND DISCUSSION

N,N,N',N'-tetrabutyl(and tetrahexyl)pyridine-3,5-dicarboxamides (2 and 3) and N,N'-di(2-ethylhexyl)pyridine-3,5-dicarboxamide (1), and their copper complexes are well soluble in hydrocarbon diluents. Analogs of 1 containing normal alkyl groups, e.g. dodecyl group, exhibit low solubilities in hydrocarbon diluents and cannot be used for extraction.

The extraction of copper from aqueous solutions does not depend on the concentration of hydrogen ions above pH 3.

Acid transfer to organic phase by tetraalkylpyridine-3,5-dicarboxamides (2 and 3) is small (Table 1). Proton concentration in toluene solution of these amides (c_{amide} = 0.2 mol/dm^3) increases from (2-8) x 10^{-4} mol/dm^3 at 0.1 mol/dm^3 HCl to 8 x 10^{-3} mol/dm^3 at 4 mol/dm^3 HCl in aqueous solution, which corresponds to (1-4) x 10^{-3} – 4 x 10^{-2} molecules of HCl per 1 molecule of the amide. Acid transfer to the toluene phase by N,N'-dialkylpyridine-3,5-dicarboxamide (1) is higher than by amides 2 and 3 and strongly depends on the concentration of hydrogen ions. The hydrochloric acid concentration in the organic phase increases with an increase of aqueous HCl concentration between 0 and 1 mol/dm^3. Above 1 M HCl, the organic proton concentration is constant and amounts about 2.5 x 10^{-1} mol/dm^3.

This value corresponds to 1.25 molecules of HCl per molecule of amide. As the basicity of pyridine nitrogen is higher than that of amide nitrogen, the preceding results indicates that the pyridine nitrogen is completely protonated ($N_{pyridine}$*HCl). The excess of hydrogen ions extracted may be as a result of partial protonation of amide nitrogen (N_{amide}*HCl) or of the formation of ($N_{pyridine}$*HCl*HCl) species, as in the case of alkyl derivatives of 8-hydroxyquinoline[5,6].

HCl in feed	Organic phase		
	1	2	3
mol/dm^3	mol/dm^3	mol/dm^3	mol/dm^3
0.01	$4.8*10^{-3}$	-	-
0.1	$4.9*10^{-2}$	$1.95*10^{-4}$	$7.95*10^{-4}$
0.2	$8.8*10^{-2}$	-	-
1.0	$2.3*10^{-1}$	$6.8*10^{-4}$	$2.1*10^{-3}$
2.0	-	$1.9*10^{-3}$	$3.9*10^{-3}$
3.0	$2.4*10^{-1}$	-	-
4.0	$2.5*10^{-1}$	$8.0*10^{-3}$	$8.2*10^{-3}$

Table 1 Acid transfer to the organic phase by diamides (c_{amide} = 0.2 mol/dm^3; ionic strength was adjusted in each case to 4 mol/dm^3 with NaCl)

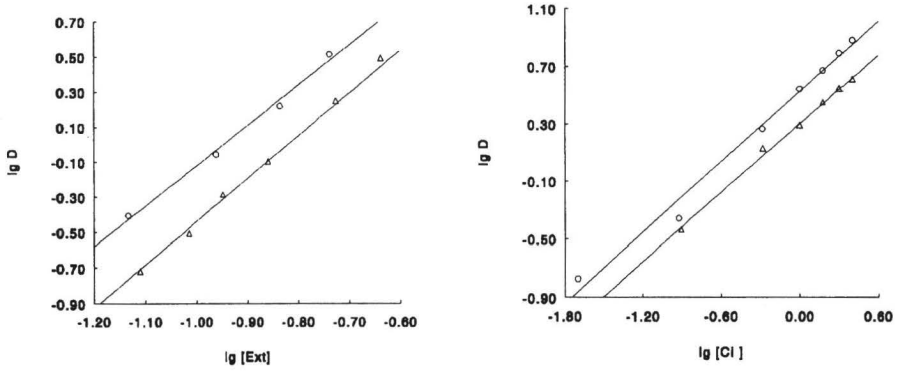

a) **b)**

Figure 1. Influence of reagent concentration (a, extractant-corrected; b, chloride) on copper distribution ratio (O, amide 2; Δ, amide 3; c_{Cu} = 10^{-2} mol/dm^3; a, chloride concentration = 1 mol/dm^3; b, amide concentration = 0.2 mol/dm^3).

Examination of the plots lg D = f(lg[Ext]) (Figure 1a) shows that extraction data obtained with tetraalkyldiamides are rather consistent with Equation (1), i.e. with the formation of extracted species exhibiting a 1 : 2 metal : extractant molar ratio. The slopes of lines are equal to 2.30 (r^2 = 0.992) and 2.44 (r^2 = 0.997) for extractants 2 and 3, respectively. It appears that amide 2 is slightly more efficient than amide 3.

The logarithmic plots of the copper distribution ratio versus chloride concentration at constant extractant concentration are shown in Figure 1b for N,N,N',N'-tetraalkyl-pyridine-3,5-dicarboxamides. These plots can be roughly simulated by straight lines the slopes of which are equal to 0.82 (r^2 = 0.988)

and 0.80 ($r^2 = 0.992$) for extractants 2 and 3, respectively. Thus, the results deviate from the value of 2 expected from Equation (1), but the slopes are similar to those obtained previously for copper extraction with decylpyridinecarboxylates (0.70)[2]. The formation of chlorocomplexes in the aqueous phase according to Equation (2) generates such large deviations[2].

$$Cu^{2+} + i\,Cl^- \Leftrightarrow CuCl_i^{2-i} \qquad \text{with } i = 1 \text{ to } 4 \qquad (2)$$

It is of interest that a weak extraction occurs in the systems which do not contain chloride ions ($[Cl^-] = 0$, copper nitrate was used to prepare the feed), but a high nitrate concentration (i.e., $[NO_3^-] = 4$ mol/dm^3). Indeed, copper forms a very weak $CuNO_3^+$ complex with nitrate ion ($\beta_1 = 0.07 \pm 0.02$ at 25°C in the region of nitrate concentration similar to that considered in the present work)[7] and it is likely that the weak extraction observed at $[Cl^-] = 0$ arises from the competing formation of species such as $Cu(NO_3)_2(Ext)_2$ and/or $CuClNO_3(Ext)_2$. A similar feature was observed by Cote et al.[8] in the system containing perchlorate ions. As a result, the three following additional equilibria were taken into account for further modelling:

$$Cu^{2+}_w + 2\,NO_3^-{}_w + 2\,Ext_o \Leftrightarrow [Cu(NO_3)_2(Ext)_2]_o \qquad (3)$$

$$Cu^{2+}_w + NO_3^-{}_w + Cl^-{}_w + 2\,Ext_o \Leftrightarrow [CuClNO_3(Ext)_2]_o \qquad (4)$$

$$Cu^{2+}_w + NO_3^-{}_w \Leftrightarrow Cu(NO_3)^+{}_w \qquad (5)$$

The TOT program[9] was used for the modelling of extraction equilibrium. In the first step, the formation of $CuCl_2(Ext)_2$ and of the two first copper chlorocomplexes was considered (the formation of upper copper chlorocomplexes can be legitimately neglected at the considered ionic strength and water activity). The formation constants of copper chlorocomplexes estimated in the work of Cote et al.[2] for the same water activity ($a_w = 0.835$) and the same total concentration of ionic species ($\sigma = 8$ mol/dm^3) were used for computing. The following values of the extraction constant were obtained by a trial and error method: $\lg K_{ex} = 2.70$ and 2.40, for 2 and 3, respectively. The agreement of the model represented by Equations (1) and (2) with the experimental data can be considered as satisfactory, except for the low chloride concentrations (i.e., $[Cl^-] < 0.5$ mol/dm^3) (Table 2).

$[Cl^-]$	$[Cu^{2+}]_{org}*10^3$ Experimental	$[Cu^{2+}]_{org}*10^3$ Theoretical from Eq (1) + Eq (2)	$[Cu^{2+}]_{org}*10^3$ Theoretical from Eq (1) + Eq (2) + Eq (3) + Eq (4) + Eq (5)	Molar fraction of $CuCl_2(Ext)_2$ From Eq (1) + Eq (2) + Eq (3) + Eq (4) + Eq (5)
mol/dm^3	mol/dm^3	mol/dm^3	mol/dm^3	
0.0	0.66	0	0.67	0
0.02	1.51	0.07	1.15	0.04
0.12	3.20	1.55	3.14	0.33
0.52	6.82	6.20	6.74	0.74
1.0	8.17	7.94	8.13	0.87
1.5	8.67	8.66	8.75	0.92
2.0	9.05	9.05	9.09	0.95
2.5	9.29	9.28	9.30	0.97

Table 2 Modelling of extraction data for N,N,N',N'-tetrabutyl pyridine-3,5-dicarboxamide ($a_w = 0.835$, $\sigma = 8.0$ mol/dm^3, see experimental) $[Cu^{2+}] = 1.05*10^{-2}$ mol/dm^3, [Ext] = 0.2 mol/dm^3. Modelling conditions: $\lg\beta(CuCl) = 0.60$; $\lg\beta(CuCl_2) = -0.40$; $\lg\beta(CuNO_3) = -1.15$ (see Table 3).

Extraction equation	2	3
Eq. 1	2.70	2.40
Eq. 3	-0.86	-0.70
Eq. 4	1.40	1.35

Table 3 Logarithmic values of selected constants (lg K_{ex})

On the other hand in a second step, Equations (3), (4) and (5) were also taken into account and it was found that the full model represented by Equations (1) to (5) is satisfactory in the whole range of chloride concentration investigated (i.e., from 0 to 2.5 mol/dm^3) (Table 2). The selected constants are given in Table 3. The extraction ability of copper decreases in the following order: $CuCl_2(Ext)_2$ > $CuClNO_3(Ext)_2$ >> $Cu(NO_3)_2(Ext)_2$. Examination of the data given in Table 2 suggests that the formation of $CuClNO_3(Ext)_2$ significantly competes with that of $CuCl_2(Ext)_2$ only up to about 0.5 mol/dm^3 Cl^-.

c_{amide}	$[Cu^{2+}]_{org}*10^3$	D	lg D
M	M	-	-
0.06	10.1	16.4	1.21
0.07	10.1	16.4	1.21
0.08	10.3	28.3	1.45
0.09	10.2	20.4	1.31
0.10	10.3	25.7	1.41
0.11	10.3	24.8	1.39
0.18	10.4	34.7	1.54

Table 4 Extraction data for N,N'-di(2-ethylhexyl)pyridine-3,5-dicarboxamide
(a_w = 0.835, σ = 8 mol/dm^3, $[Cu^{2+}] = 1.07*10^{-2}$ mol/dm^3, $[Cl^-]$ = 1 mol/dm^3)

From all the preceding results it appears that 2 and 3 behave very similarly as far as the extraction of copper from chloride media is concerned. On the opposite, examination of Table 4 shows that N,N'-di(2-ethylhexyl)pyridine-3,5-dicarboxamide extracts copper(II) from chloride media much more efficiently than the two preceding model extractants. As compared to previously studied analogs with the normal alkyl group[3] 1 is well soluble in the organic phase and can be considered as a strong perspective extractant. It is probable that a chelate with copper is formed instead of the considered solvate as in the case of nicotinamidoxime[10].

ACKNOWLEDGEMENT

The work was supported by KBN grant No.3 T09B 051 14.

REFERENCES

1. Dalton RF, Price R, Quan PM and Steward D, *Eur. Patent 57,797*, (1982).
2. Cote G, Jakubiak A, Bauer D, Szymanowski J, Mokili B and Poitrenaud C, *Solv. Extr. Ion Exch.* , **12**, 99 (1994).
3. Borowiak-Resterna A, *Solv. Extr. Ion. Exch.*, **12**, 557, (1994).
4. Borowiak-Resterna, *Solv. Extr. Ion. Exch.* (in press).
5. Kyuchoukov G, Jakubiak A, Szymanowski J and Cote G, *Solv. Extr. Res. Dev., Japan*, **5**, 172, (1998).
6. Cote B and Demopoulos GP, *Solv. Extr. Ion Exch.*, **11**, 349, (1993).
7. Davis AR and C. Chong C, *Inorg. Chem.* , 11, 1891, (1972).

8. Bouvier C, Cote G, Cierpiszewski R and Szymanowski J, *Solv. Extr. Ion Exch.*, submitted
9. Rosset R, Bauer D and Desbarres J, *Chimie Analytique des Solutions et Informatique*, 2nd edition, Masson, Paris, (1991).
10. Tripathi KKand Banerjea D, *Z. Anal. Chem.*, **168**, 407, (1959).



EXTRACTION OF COPPER AND ZINC FROM CHLORIDE SOLUTIONS BY AN HYDROPHOBIC ALKYL DERIVATIVE OF 8-HYDROXYQUINOLINE

G Kyuchoukov[1], A Jakubiak[2] and J Szymanowski[2]
[1]Institute of Chemical Engineering, Bulgarian Academy of Sciences, 1113 Sofia, Acad. Bonchev str. Bl.103, Bulgaria
[2]Poznan University of Technology, Institute of Chemical Technology and Engineering, Pl. Sklodowskiej-Curie 2, 60-965 Poznan, Poland

ABSTRACT
The extraction of copper and zinc with the Kelex 100 was studied in a broad range of acidities and chloride concentrations. Depending on acidity and chloride concentration in the aqueous phase as well as on extractant pre-treatment (conditioning or deprotonation), at pH < 1 copper was extracted simultaneously by cation and anion exchange mechanism whereas zinc was extracted only by the anion exchange mechanism.

Keywords: Kelex 100, copper(II), zinc(II), chloride media

INTRODUCTION

In the last ten years a lot of work has been done to develop processes for copper and zinc extraction from chloride solutions.[1-3] For this approach a new technology for electrowinning from chloride electrolytes and reprocessing of metal granules formed during this operation must be used. To avoid electrowinning from chloride media the extraction with the transfer of extracted metal ions into sulphate solutions was proposed.[4-6]. Mixtures of basic and chelating extractants, e.g. ALAMINE 336 and LIX 54 was used.
The purpose of this work is to study the extraction of copper(II) and zinc(II) with KELEX 100 at broad range of acidity and chloride concentration, up to 8 mol/dm^3 chloride.

EXPERIMENTAL

Aqueous solutions containing $ZnCl_2$ or $CuCl_2$ and adjusted with LiCl and HCl were used. The organic phase contained 65 v/v% kerosene, 15 v/v% decanol and 20 v/v% of KELEX 100®. The experiments were performed at room temperature for 5 minutes. Prior to extraction, the extractant was fixed in the hydrochloride or deprotonated form. Deprotonation was performed by repeated scrubbing with water until the pH of the scrub solution reached about 4.6. To convert the extractant from the hydrosulphate form (obtained during stripping of the metal ions with sulphuric acid), back to the hydrochloride form, conditioning was performed with an aqueous solution of NaCl ([NaCl] > 4.5 mol/dm^3).

The concentration of metal ions, chloride ions and hydrogen cations in the aqueous phase was determined by titration with aqueous solutions of EDTA, $AgNO_3$ and NaOH, respectively.

RESULTS AND DISCUSSION

Under conditions providing protonation of the tertiary nitrogen atom in the quinoline nucleus, the chloride or complex metal chloride anions present in the solution are extracted according to:

$$\overline{HORN} + H^+ + Cl^- \leftrightarrow \overline{HORN * HCl} \quad (1)$$

$$\overline{2HORN} + 2H^+ + MeCl_4^{2-} \leftrightarrow \overline{(HORNH^+)_2 MeCl_4^{2-}} \quad (2)$$

where the bar denotes a species in the organic phase.

© 2000 Society of Chemical Industry

The ratio between reagent-metal complex and free reagent is related to the extraction constants and to the composition of the aqueous phase ($[MeCl_4^{2-}]$, $[Cl^-]$, $[H^+]$).

When an extractant conditioned as the hydrochloride is used and its deprotonation can be neglected the processes taking place can be described by:

$$2\overline{HORN * HCl} + MeCl_4^{2-} \leftrightarrow \overline{\left(HORNH^+\right)_2 MeCl_4^{2-}} + 2Cl^- \tag{3}$$

with extraction constant:

$$K_{MeCl_4^{2-}/Cl^-} = \frac{\left[\overline{\left(HORNH^+\right)_2 MeCl_4^{2-}}\right]\left(1+\sum_{i=1}^{4}\beta_i\left[Cl^-\right]^i\right)}{\left[Me_T\right]\beta_4\left[Cl^-\right]^2\left[\overline{HORN * HCl}\right]^2} \tag{4}$$

where β_i is the overall stability constant of the i-th complex, and Me_T is the total concentration of metal ions.

It follows from eqn (4) that $[Me_T] \approx [M^{2+}]$ for $\Sigma\beta_i[Cl^-]^i << 1$. An increase in the chloride content favours the extraction of metal chloride complex. And vice versa, $[Me_T] \approx [MeCl_4^{2-}]$ for $\Sigma\beta_i[Cl^-]^i = \beta_4[Cl^-]^4 \approx \beta_4[Cl^-]^4$ and the metal extraction falls when the chloride concentration further rises. The effect depend on the value of :

$$\frac{\beta_4[Cl^-]^2}{1+\sum_{i=1}^{4}\beta_i[Cl^-]^i}$$

compared to the other terms in eqn (4) which after taking logarithms becomes:

$$\log\left[\overline{\left(HORNH^+\right)_2 MeCl_4^{2-}}\right] = \log K_{MeCl_4^{2-}/Cl^-} + \log[Me_T] + 2\log\left[\overline{HORN * HCl}\right] + \log\frac{\beta_4[Cl^-]^2}{1+\sum_{i=1}^{4}\beta_i[Cl]^i} \tag{5}$$

Chloride ions have a stronger effect on copper extraction (Fig.1, curve 1), than on zinc extraction (Fig.1, curve 2), since copper forms weaker complexes than zinc.[7] The amount of copper extracted as $(HORNH^+)_2CuCl_4^{2-}$ increases several times over the range examined, whereas the corresponding increase in zinc extraction is about 30%.

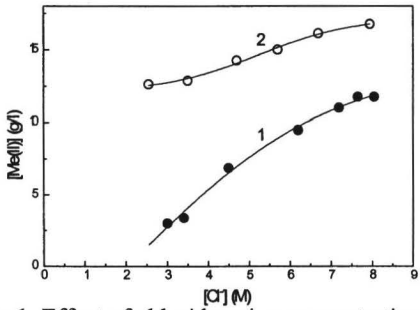

Figure 1. Effect of chloride anion concentration on extraction of copper (curve 1) and zinc (curve 2) for $[H^+]$ = 1.8 ± 0.1 mol/dm^3, $[M^{2+}]$ = 40 ± 2 g/dm^3 and solvent composition: 20 v/v% KELEX 100, 15 v/v% decanol and 65 v/v% kerosene.

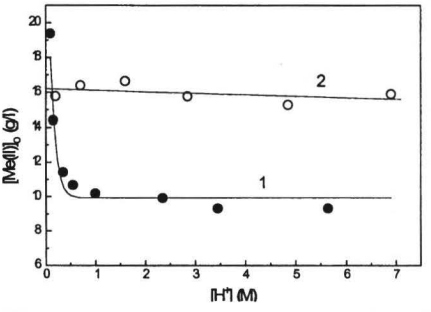

Figure 2. Dependence of the extraction of copper (curve 1) and zinc (curve 2) on the acidity of the aqueous phase for $[Cl^-]$ ~ 7.5 mol/dm^3, $[M^{2+}]$ = 40 ± 2 g/dm^3 and solvent composition as given in Fig. 1.

According to eqn (4) no effect of acidity on the concentration of the extracted metal complex is to be expected for chloride anion concentrations providing complete performance of reactions (1) and (2). This is the case for zinc extraction (Fig. 2, curve 2). The mass balance of extracted and stripped zinc ions points to the compound $(HORNH^+)_2ZnCl_4^{2-}$. A different picture is observed in copper extraction; the concentration of copper in the extractant sharply increases at the low acidities (Fig. 2, curve 1). Since the concentration of chloride anions in the extractant corresponds to the $CuCl_2$ species and there is no acidity change between initial solution and raffinate, a solvation mechanism of copper extraction[8] was previously assumed.

The identification of the extracted zinc species in the present work as $(HORNH^+)_2ZnCl_4^{2-}$ and not as $(HORN)_2ZnCl_2$ prompted the detailed studies on copper and zinc extraction at low acidities of the initial aqueous solution. Parallel experiments were performed with conditioned (HORN*HCl) and deprotonated (HORN) extractant. The concentration of zinc in the initial aqueous solution was $\approx 0.48 \pm 0.01$ mol/dm^3 and that of hydrogen cations 0.15 ± 0.01 mol/dm^3. Theoretically, competition of reactions 1 and 2 could be expected. The shape of the obtained curves (Fig. 3) reveals that KELEX 100 protonation has proceeded mainly by $ZnCl_4^{2-}$ addition according to eqn (2). A noticeable contribution of reaction (1) would yield higher values of curve 2 and lower values of curve 3. The maximum value of extracted zinc corresponds to the equivalent concentration of hydrogen cations present in the initial solution, i.e. to 0.15 mol/dm^3. The overlap between curves 1 and 2 and the higher with a factor 2 values of curve 3 reveal that zinc(II) is extracted with the deprotonated reagent according to eqn (2). The contribution of reaction 1 is negligible. Thus, the tertiary nitrogen atom in the quinoline nucleus has a higher affinity for $ZnCl_4^{2-}$ than for Cl^-. The changes observed in the two-phase system using conditioned extractant HORN*HCl are shown in Fig. 4. Curve 1 corresponds to zinc extraction, curve 2, to the increase in acidity of the aqueous phase and curve 3, to the extraction of chloride anions. The latter is a result of extractant deprotonation caused by the change in the chloride anion content in the raffinate. There is a significant difference between curve 1 in Fig. 3 and curve 1 in Fig. 4.

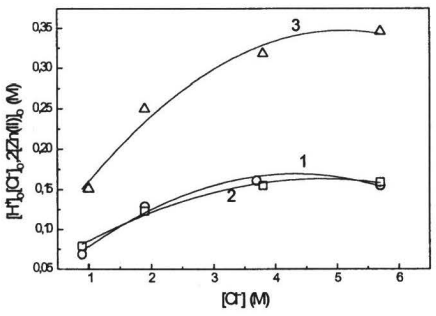

Figure 3. Dependence of $[Zn^{2+}]$ (curve 1), $[H^+]$ (curve 2) and $[Cl^-]$ (curve 3) in the organic phase on the chloride content in the aqueous phase for $[Zn^{2+}] = 0.48 \pm 0.01$ mol/dm^3, $[H^+] = 0.15 \pm 0.01$ mol/dm^3 and solvent composition as given in Fig. 1.

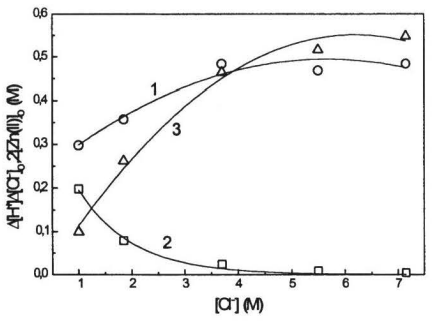

Figure 4. Effect of chloride content in the aqueous phase on the extraction of Zn^{2+} (curve 1), the acidity of the aqueous phase - (curve 2) and $[Cl^-]$ (curve 3) with the conditioned extractant for $[Zn^{2+}] = 0.48 \pm 0.01$ mol/dm^3, $[H^+] = 0.15 \pm 0.01$ mol/dm^3 and solvent composition as given in Fig. 1.

The extraction takes place according to eqn (6). At low acidity of the feed the extraction is not limited by low hydrogen concentration because the hydrogen ion is already present in the extractant molecule. As a result, significantly higher amounts of zinc(II) can be extracted in comparison to the deprotonated reagent. Simultaneously, at the low chloride and hydrogen ion concentrations in the

initial aqueous solution a significant part of the extractant is deprotonated according to eqn (1). As a result, the concentration of HORN*HCl decreases, whereas the concentration of hydrogen cations in the aqueous phase rises (curve 2). Different from Fig. 3, the lower transfer of chloride anions into the organic phase (curve 3) is not equivalent to the extracted zinc chloride complex since during extraction the aqueous phase is also enriched with chloride anions according to eqns (1) and (3). The increase in chloride concentration shifts the equilibrium of eqn (1) to the right and favours the extraction of the zinc chloride complex. As is shown in eqn (5) the complex concentration depends on the equilibrium extraction constant, metal and chloride ions and extractant hydrochloride concentrations. The effect of the changes in the term containing chlorocomplex formation constants is relatively low for zinc extraction and the effect of extractant hydrochloride concentration is then clearly observed.

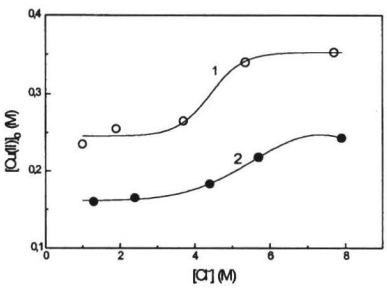

Figure 5. Effect of chloride content in the aqueous phase on the extraction of copper with deprotonated (curve 1) and conditioned (curve 2) extractant for $[Cu^{2+}] = 0.52 \pm 0.02$ mol/dm^3, pH ~ 2.5 and solvent composition as given in Fig. 1

There is no extractant deprotonation ($\Delta[H^+]=0$) at the high chloride content ($[Cl^-]\geq 4$) (curve 2) and the acidity of the raffinate becomes equal to that of the initial solution. At such high chloride concentration zinc is almost totally present as $ZnCl_4^{2-}$ and the effect of chloride concentration on zinc extraction is small. The transfer of chloride ions to the organic phase is approximately equivalent to the zinc(II) extraction, i.e. two Cl^- for one Zn^{2+}.

By taking into account that KELEX 100 extracts copper by the cation exchange mechanism at low acidities[9] (Fig.5):

$$\overline{2NROH} + Cu^{2+} \leftrightarrow \overline{(NRO)_2 Cu} + 2H^+ \qquad (6)$$

The shape of the copper curves is fundamentally different from that of the zinc curves (curve 1 in Figs 3 and 4). The concentration of extracted copper with the deprotonated extractant is limited by the extractant capacity, whereas the concentration of extracted zinc is limited by the equivalent concentration of hydrogen cations present in the two-phase system. The effect of chloride anion concentration is particularly expressed in the range > 4 mol/dm^3. The low concentration of hydrogen cations in the initial solution favours reaction (6) yielding hydrogen cations which increase the acidity of the aqueous solution. The increased acidity, together with the increased chloride anion concentration favours on its turn reactions (1) and (2).

By describing the processes taking place with reactions (1), (2) and (6) it may be assumed that the increase in chloride anion concentration and hence in extracted copper would affect the ratio between copper extracted as a cation (Cu^{2+}) and that extracted as a complex anion ($CuCl_4^{2-}$). This ratio cannot be, however, precisely determined. For the case of deprotonated extractant these reactions may be expressed as:

$$(x+2y+2z)\overline{HORN} + XCl^- + yCuCl_4^{2-} + zCu^{2+} \leftrightarrow x\overline{HORN.HCl} + y\overline{(HORNH^+)_2 MeCl_4^{2-}}$$
$$+ z\overline{(NRO)_2 Cu} + (2z-x-2y)H^+ \qquad (7)$$

The increase in the concentration of chloride anions leads to a decrease in the concentration of the copper chelate. This may be related to the effect of two factors: (i) the shift of the equilibrium of reactions (1) and (2) to the right; and (ii) the decrease in the concentration of copper cations. The latter may be expressed with the following dependence:

$$[Cu^{2+}] = \frac{[Cu_T]}{1 + \sum_{i=1}^{4} \beta_i [Cl^-]^i} \quad (8)$$

At low chloride concentration one may assume that the organic phase contains mainly $(NRO)_2Cu$ with only small amounts of $(HORNH^+)_2CuCl_4^{2-}$. Such statements finds its support in the chloride ion content in the organic phase. The estimation gives the complex ratio $[(NRO)_2Cu]/[(HORNH^+)_2CuCl_4^{2-}]$ about 12. This conclusion is supported by a high concentration of hydrogen ions in the raffinate (0.372 mol/dm^3) and small amounts of copper (0.0035 mol/dm^3) and hydrogen ions (0.042 mol/dm^3) liberated in the scrubbing.

At the high chloride concentration a high extraction of copper is observed. The concentration of hydrogen ions in the raffinate is small (the difference between the raffinate and the feed amounts to 0.006 mol/dm^3) and large amounts of hydrogen ions are liberated in the scrubbing. Simultaneously, copper and chloride ions are scrubbed.

The negligible change in acidity between the feed and the raffinate suggests that the hydrogen ions liberated in eqn (6) are consumed in eqn (2) and the complex ratio $[(NRO)_2Cu]/[(HORNH^+)_2CuCl_4^{2-}]$ is near 1 with the concentrations of each component about 0.18 M. Scrubbing shifts reaction (2) to the left liberating copper(II) (0.115 mol/dm^3), chloride ions (0.635 mol/dm^3) and hydrogen ions (0.407 mol/dm^3). The amounts of liberated copper and chloride ions are lower and higher, respectively, from those estimated as present in $(HORNH^+)_2CuCl_4^{2-}$ because the part of the liberated copper (32.7%) is complexed by the liberated extractant forming the stable chelate.

The processes taking place with the conditioned extractant may be expressed with the overall reaction:

$$(x+2y+2z)\overline{HORN*HCl} + yCuCl_4^{2-} + zCu^{2+} \leftrightarrow y\overline{(HORNH^+)_2CuCl_4^{2-}} + z\overline{(NRO)_2Cu} + \\ + (x+4z)H^+ + (x+2y+2z)Cl^- + x\overline{HORN} \quad (9)$$

The use of the conditioned extractant yields a higher concentration of hydrogen ions in both raffinate and scrubbings since significant deprotonation according to eqn (1) takes place at the lower concentrations of chloride ions. Moreover, extractant deprotonation is a precondition for reaction (6) to take place.

At low chloride concentration large amounts of hydrogen ions are liberated in extraction. Simultaneously, the concentration of chloride ions increases. Both these changes can be explained by a significant extractant deprotonation (eqn (1)) and subsequent chelate formation (eqn (6)). However, some important amounts of ions are liberated in scrubbing which proves the coexistence of two different complexes. The mass balance analysis gives the complex ratio $[(NRO)_2Cu]/[(HORNH^+)_2CuCl_4^{2-}]$ about 2; thus, close to that obtained with the deprotonated extractant at the high chloride content.

At high chloride concentration a raffinate of low acidity is obtained which is an evidence for copper extraction as $(HORNH^+)_2CuCl_4^{2-}$ and for the lack of deprotonation of the extractant. Scrubbing liberates copper ions and extractant molecules according to eqns (2) and (1) with their subsequent chelation (65.7% of liberated copper). As a result, high amounts of hydrogen and chloride ions are observed in the scrubbing solution.

ACKNOWLEDGEMENTS

The financial support of Polish Research Committee (KBN) grant No. 3 T09B 051 14, Poland is gratefully acknowledged.

REFERENCES

1. Dalton RF, Price R, Quan PM and Steward D, *Eur. Pat. Spec, 57797*, 1982.
2. Devonald DP, Nelson AJ, Quan PM and Stewart D, *Eur Pat Spec, 196153*, (1989).
3. Dalton RF, Burgess A and Quan PM, *Hydrometallurgy*, **30**, 385, (1992).
4. Kyuchoukov G and Mihaylov I, *Hydrometallurgy*, **27**, 361, (1991).
5. Kyuchoukov G and Mishonov I, *Solv Extr Ion Exch*, **11**, 555, (1993).
6. Kyuchoukov G, Fletcher AW, Mihaylov I, Elenkov D and Boydziev L, *Bulg Pat, 80754*, (1987).
7. Aguilar A, Valiente M, Massana A, Coello J, Aparicio JL, Fernandez LA and Muhammed M, In: *Proc. ISEC'86*, Munich, **2**, 239, (1986).
8. Kyuchoukov G and Kounev R, *Hydrometallurgy*, **35**, 321, (1994).
9. Sato T, Oishi H and Otsuka R, *Hydrometallurgy*, **18**, 277, (1987).

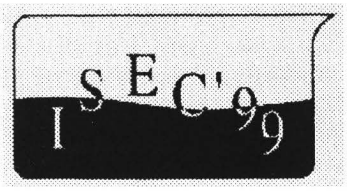

LIQUID–LIQUID EXTRACTION OF ZINC(II) BY SOLVATING EXTRACTANTS FROM HCl/H_2SO_4 MIXED MEDIA

JA Barron Zambrano[1], M Avila-Rodríguez[1], TI Saucedo Medina[1], R Navarro Mendoza[1] and AM Sastre[2]

[1]Instituto de Investigaciones Científicas, Universidad de Guanajuato, L. de Retana No. 5, Guanajuato, Gto., Mexico

[2] Chemical Engineering Department, Universitat Politècnica de Catalunya, ETSEIB, Barcelona, Spain

ABSTRACT

The extraction of Zn(II) by 1-(dodecyloxy)-3-methyl-oxo-Δ^3-phospholene (DMPL) and 1-(2, 6-dimethylhept-4-yloxy)-3 methyl-1-oxo-Δ^3-phospholene (NMPL) from concentrated HCl/ H_2SO_4 mixed media, has been studied and compared to the extraction when the extractant is tri-butyl phosphate (TBP). The extraction of water and mineral acids (HCl and H_2SO_4) by these compounds has also been considered. The results obtained show that the extraction of water and mineral acids plays an important role in the efficiency of extraction of zinc(II) using all these compounds. The evaluated percentage of extraction (E%) of mineral acids and water, is higher in the case of phospholene derivatives than in the case of the TBP. The extraction of Zn(II) by the compounds thus studied, follows the order NMPL > DMPL > TBP. Finally, a thermodynamic model, which considers the nature of the hydrated solvates extracted into the organic phase, is proposed to explain the experimental results.

Keywords: zinc, acid extraction, tri-butylphosphate, 1-(dodecyloxy)-3-methyl-oxo-Δ^3-phospholene, 1-(2,6-dimethyl-hept-4-yloxy)-3-methyl-1-oxo-Δ^3-phospholene

INTRODUCTION

The extraction of metal ions from concentrated media by liquid-liquid extraction is very important in the metallurgical industry. Different kinds of solvating extractants have been used for this purpose, such as tri-n-butylphosphate (TBP),[1-3] tri-n-octylphosphine oxide (TOPO),[4-5] etc. Recently, phospholene derivatives have been used in the recovery of precious metals such as gold (III).[6] However, the influence of the presence of concentrated mineral acids in the efficiency of extraction has not been sufficiently considered. In this paper, the extraction of Zn(II) by 1-(dodecyloxy)-3-methyl-oxo-Δ^3-phospholen (DMPL) and 1-(2, 6-dimethylhept-4-yloxy)-3 methyl-1-oxo-Δ^3-phospholen (NMPL) from HCl/H_2SO_4 concentrated media is studied and compared to the extraction when the extractant is tri-butyl phosphate (TBP), considering the extraction of water and mineral acids (HCl and H_2SO_4) by these compounds. In the first part of this work, the distribution curves of Zn(II) with phospholene derivatives, as a function of HCl concentration in the presence and absence of H_2SO_4 are obtained and the influence of the extraction of acid and water is pointed out. In the second one, a thermodynamic model considering the activities of different species involved in the process of extraction is proposed.

EXPERIMENTAL

All the reagents used were analytical grade. The extractants, 1-(dodecyloxy)-3-methyl-oxo-Δ^3-phospholene (DMPL) and 1-(2,6-dimethylhept-4-yloxy)-3-methyl-1-oxo-Δ^3-phospholene (NMPL) were kindly supplied by Bayer Leverkussen. Tri-n-butyl phosphate (TBP) was kindly donated by the Daihachi Chemical Industry Co, Ltd. The organic phase consisted of concentrated phospholene derivatives or TBP. The aqueous phase consisted of Zn(II) and HCl and H_2SO_4. Given that solvating extractants are capable of extracting water, it is necessary to equilibrate them previously with an aqueous phase, which contains HCl and H_2SO_4 only, for 20 minutes. The phases are separated and the organic phase treated in this way is used to obtain the distribution curves of Zn(II), under the same acidic conditions. The ratio of volumes of the organic phase (V_{org}) and aqueous phase (V_{aq}) was in every

© 2000 Society of Chemical Industry

case equal to one ($V_{aq} = V_{org} = 10$ mL). The solutions (aqueous phase /organic phase) are shaken with a (Cole Palmer 51502) ping-pong shaker at 150 rpm at 25°C for 20 minutes, which is enough time to reach equilibrium. Once equilibrium is attained, the phases are separated and the concentration of Zn(II) in the aqueous phase is determined with a (Perkin-Elmer 3110) atomic absorption spectrometer. The concentrations of Zn(II) in the organic phase are calculated by mass balance. The concentrations of HCl and H_2SO_4 extracted by the TBP were obtained by potentiometric titration of H^+ ions in the organic phase (Titrino 716 Metrohm) with NaOH 0.1 M, and as a function of Cl^- concentration, obtained by the Mohr's method.[7] The water extracted in the organic phase was determined by a Karl-Fisher titration.

RESULTS AND DISCUSSION

Extraction of Zn(II) by TBP, DMPL and NMPL from the HCl/H_2SO_4 mixed media.

The results obtained in the study of the extraction of Zn(II) by the different organophosphorated extractants (TBP, NMPL and DMPL) are shown in figure 1, where the variation of the zinc distribution coefficient ($D_{Zn(II)}$) is presented as a function of HCl concentration at equilibrium, in the absence (figure 1A) and presence (figure 1B) of H_2SO_4 (initial concentration = 1 mol/L).

It can be observed that the distribution curves of Zn(II) show a similar behavior with each one of the studied extractants. That is, the value of the distribution coefficient increases with HCl concentration, reaching a maximum ($D_{Zn(II)} = 25$ for TBP, $D_{Zn(II)} = 80$ for NMPL and $D_{Zn(II)} = 38$ for DMPL) and then decreases. The forms of the distribution curves can be explained if, on one hand, one considers a salting out effect, and on the other hand, the extraction of acid (HCl and H_2SO_4) by the extractants. When the aqueous phase has a high concentration of electrolytes, the water activity decreases and causes a variation in the activity coefficient of the species present in solution. Thus, there is a better association between the ions (anions and cations) to form neutral molecules or ion pairs. The net result is an increase in the extraction yields of zinc.

The decrease in the value of the Zn(II) distribution coefficient at high concentrations of HCl can be explained on one hand, if a strong competition is assumed between the acid and the zinc (II) for the active extractant contained in the organic phase. On the other hand, the zinc extraction mechanism by those specific extractants is through solvation. By this mechanism, Zn(II) is preferably extracted as a neutral complex, $ZnCl_2$. When the chloride ion concentration in the medium is increased, the tendency to form higher complexes $ZnCl_j^{(2-j)}$ increases, which makes the transfer of this metallic ion to the organic phase more difficult.

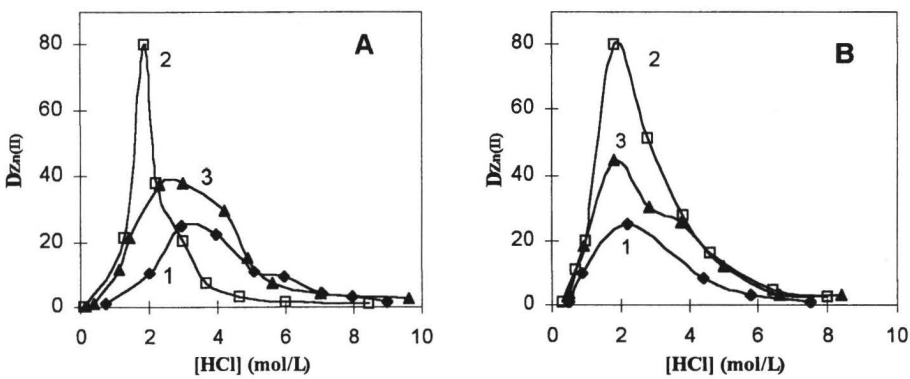

Figure 1. Variation of $D_{Zn(II)}$ as a function of [HCl], in the absence (A) and presence of H_2SO_4 (B) of initial concentration = 1 M. $V_{org}/V_{ac} = 1$.[Zn(II)]in = 1 x 10-3 M. 1) TBP; 2) NMPL ; 3) DMPL .

The presence of H_2SO_4 in the medium provides in general an increase in the extraction of Zn(II) by the extractants studied. This is noted by an increase in the value of $D_{Zn(II)}$ (for DMPL see curves 3A and 3B in figure 1), or else by shifting the distribution curve of Zn(II) towards lower HCl concentration values (for TBP, see curves 1A and 1B, in figure 1), or as in the case of NMPL (curves 2A and 2B in figure 1) where a widening of the zone where it is possible to perform the extraction of Zn(II) is observed.

The increase of the transfer of Zn(II) to the organic phase resulting from the presence of H_2SO_4 in aqueous phase can be explained by taking into account that the dissociation of H_2SO_4 causes a decrease in water activity, favoring the extraction of Zn(II).

The order of affinity for Zn(II) by the three extractants studied (NMPL > DMPL > TBP), can be explained if one considers that the extraction capacity of the organophosphorated compounds increases with the basicity of the donor phosphoryl group, following the order: $(RO)_3PO < (RO)_2RPO < (RO)R_2PO < R_3PO$. On the other hand, the extraction capacity of neutral organophosphorated compounds increases with the branching of the alkyl chain. Such an effect is more pronounced if the branching is close to the alkoxy oxygen. This is related to the basicity of the compound, which increases with chain branching. According to this, one would expect that the extraction of Zn(II) by the extractants studied earlier would follow the order: NMPL > DMPL > TBP, which agrees well with the experimental results obtained in the present work.

Extraction of HCl, H_2SO_4 and H_2O by TBP, DMPL and NMPL from HCl/H_2SO_4 mixed media.

The extraction study of HCl by concentrated TBP, DMPL and NMPL shows that in the three cases the concentration of HCl in the organic phase increases with HCl concentration in the aqueous phase. A higher extraction capacity for HCl was observed in the case of the phospholene derivatives than in the extraction by TBP. When the HCl concentration in the aqueous phase is 6 mol/L the concentration of HCl extracted by TBP is 1.64 mol/L, while in the case of NMPL and DMPL, the HCl concentration in the organic phase is close to 3 mol/L. This behavior is also observed in the presence of H_2SO_4 (initial concentration = 1 mol/L). The increase in HCl concentration in the organic phase can be explained by considering, on one hand, a mass action effect, and on the other, a salting out effect.

In the case of the H_2SO_4 extraction, the phospholene derivatives have a higher affinity for this acid than TBP. The yield of extraction of H_2SO_4 in concentrated TBP is of the order of 11% in HCl solution (7 mol/L), while at the same concentration of HCl in the aqueous phase, NMPL and DMPL are capable of extracting almost 30% of the H_2SO_4.

The water extraction into the organic phase increases with HCl concentration, while the presence of H_2SO_4 results in a decrease in water concentration in the organic phase, compared with the amount extracted in its absence, the magnitude of this effect being different for each extractant. The extraction of water by these extractants follows the order: DMPL > NMPL > TBP. This order is similar to that observed in the extraction of HCl, which indicates that most of the water that is transferred to the organic phase goes through by forming part of the hydration sphere of the H^+ ions.[8]

Thermodynamic considerations.

The general extraction reaction of Zn(II) from an HCl medium can be written as follows:

$$ZnCl_2 + n\,HCl + m\,H_2O + p\,\overline{X} \Leftrightarrow \overline{[ZnCl_2.(HCl)_n.(H_2O)_m.X_p]} \qquad (1)$$

where: X represents the extractant (TBP, NMPL or DMPL), and the barred species are those found in the organic phase.

The thermodynamic reaction constant $K^{\circ}_{ext,i}$ for each of the extracted species is:

$$K^{0}_{ext,i} = \frac{a_{\overline{ZnCl_2.(HCl)_n.(H_2O)_m.X_p}}}{a_{ZnCl_2} a^{n}_{HCl} a^{m}_{H_2O} a^{p}_{\overline{X}}} \qquad (2)$$

Introducing the concentration of Zn(II) and its activity coefficient, both in aqueous phase and in organic phase, equation (2) becomes:

$$K^{0}_{ext,i} = \frac{\gamma_{\overline{ZnCl_2.(HCl)_n.(H_2O)_m.X_p}} * [\overline{ZnCl_2.(HCl)_n.(H_2O)_m.X_p}]}{\gamma_{ZnCl_2} * a^{n}_{HCl} a^{m}_{H_2O} a^{p}_{\overline{X}} * [ZnCl_2]} \qquad (3)$$

It is possible to obtain an apparent extraction $K_{ext,i}$ constant if the variation of the activity coefficients of the metallic species in the organic phase and the aqueous phase is considered as similar. Such a constant can be written as follows:

$$K_{ext,i} = \frac{[\overline{ZnCl_2.(HCl)_n.(H_2O)_m.X_p}]}{a^{n}_{HCl} a^{m}_{H_2O} a^{p}_{\overline{X}} * [ZnCl_2]} \qquad (4)$$

Equation (4) shows an apparent constant $K_{ext,i}$ that depends on the activities of HCl and H_2O in the aqueous phase, and on the activity of the extractant. This permits consideration of the extraction of HCl and H_2O because the activities in both phases are functions of the equilibrium concentration and of the activity coefficient of each of the species. This is important because, as discussed earlier, the Zn(II) distribution curves are strongly influenced by the extraction of acids and water by the three extractants studied. In addition, due to its dependence on the activities, the apparent extraction constant also considers the interactions with the medium resulting from the high electrolyte concentration (salting out effect).

The distribution coefficient is defined as:

$$D_{Zn} = \frac{[\overline{Zn(II)}]}{[Zn(II)]} \qquad (5)$$

where: $[\overline{Zn(II)}]$ and [Zn(II)] represent the concentration of Zn(II) in all its forms in the organic phase and in the aqueous phase, respectively.

In the extraction systems with solvating extractants the metallic ions can be extracted as solvates of different composition.[3] Then, the concentration of Zn(II) in the organic phase can be represented as follows:

$$[\overline{Zn(II)}] = \sum_n \sum_m \sum_p [\overline{ZnCl_2.(HCl)_n.(H_2O)_m.X_p}] = \sum_n \sum_m \sum_p K_{ext,i} [ZnCl_2] * a^{n}_{HCl} a^{m}_{H_2O} a^{p}_{\overline{X}} \qquad (6)$$

In the case of the aqueous phase:

$$[Zn(II)] = [Zn^{2+}] + \sum_j [ZnCl_j^{(2-j)}] + \ldots\ldots \qquad (7)$$

The presence of the different complex species of Zn(II) and Cl^- in the aqueous phase has an effect on the equilibrium of the extraction of the $ZnCl_2$, for which it is necessary to introduce the complexation coefficient defined as follows:

$$\alpha_{ZnCl_2} = \frac{1}{\beta_2 a_{Cl^-}^2} + \frac{\beta_1}{\beta_2 a_{Cl^-}} + 1 + \frac{\beta_3}{\beta_2} a_{Cl^-} + \ldots \qquad (8)$$

where: βj is the overall formation constant of the $ZnCl_j$ complex.

Introducing the complexation coefficient and considering the possible formation of more than one solvate of Zn(II) in the organic phase, the distribution coefficient takes the form:

$$D_{Zn(II)} = \frac{\sum_n \sum_m \sum_p K_{ext,i} a_{HCl}^n a_{H_2O}^m a_{\bar{X}}^p}{\alpha_{ZnCl_2}} \qquad (9)$$

From equation (9), the value of $D_{Zn,calc}$ was calculated for the case of the extraction of Zn(II) by TBP. The activity values of TBP were taken from reference 9. The values of a_{HCl} were obtained from the activities of the ions H^+ and Cl^-, as reported by Sella and Bauer,[10] and the values of a_{H2O} are those reported by Hamer and Wu[11]. The calculation of the latter was done using the values of global formation constants $\log \beta_1 = 0.43$; $\log \beta_2 = 0.61$; $\log \beta_3 = 0.53$; $\log \beta_4 = 0.2$ at zero ionic strength.[12] The solvates $ZnCl_2.(TBP)_2$, $ZnCl_2.(TBP)_3$, $HZnCl_3.(TBP)_2$ and $HZnCl_3.(TBP)_3$ reported by Kolarik,[3] were used as the base for the calculations of $D_{Zn,calc}$. In addition, the water molecules that are part of the complex were considered, as well as the water molecules that are part of the solvation sphere of the H^+ ion. In this way, the solvates have the following form: $ZnCl_2.(H_2O)_2.(TBP)_2$, $ZnCl_2.(H_2O).(TBP)_3$, $ZnCl_2.(HCl).(H_2O)_5.(TBP)_2$ and $ZnCl_2.(HCl).(H_2O)_4.(TBP)_3$. The best set of constants were calculated by minimization of the sum of the error squares (U) defined by:

$$U = \sum (\log D_{exp} - \log D_{calc})^2 \qquad (10)$$

A good correlation (U = 0.3209) between the experimental data and the model developed in the present paper is obtained upon consideration of the formation of the solvate $ZnCl_2(H_2O)_5(TBP)_2$, with an apparent extraction constant value $K_{ext} = 33.8$. Consideration of other solvates in the extraction model does not improve the correlation obtained with the solvate $ZnCl_2(H_2O)_5(TBP)_2$, which indicates that this is the predominant species under the extraction conditions studied. The results obtained are shown in figure 4, where the variation of $\log D_{Zn}$ as a function of HCl concentration is plotted.

The application of the model in the case of Zn(II) extraction by NMPL and DMPL requires knowledge of the activities of these extractants. Such activities are not available in the literature, and thus the application of the model developed here to these extraction systems is not possible at present.

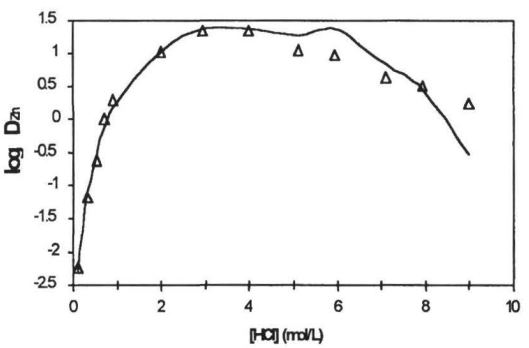

Figure 4 Variation of $\log D_{Zn}$, as a function of [HCl]. The continuous line represents the $\log D_{Zn,calc}$, whereas the symbol Δ represents the experimental values. Solvate: $ZnCl_2(H_2O)_5(TBP)_2$. U = 0.3209, Kext = 33.8.

CONCLUSIONS

The extraction of Zn by the extractants TBP, NMPL and DMPL from concentrated HCl/H_2SO_4 mixed media, has been studied. The results show that the order of affinity of these extractants for Zn(II) is NMPL > DMPL > TBP. The extraction of acid and water plays an important role in the Zn(II) extraction process. This influence is confirmed with the aid of the thermodynamic model developed for the extraction of Zn(II) by TBP from an HCl medium. Such a model is a function of the activities of HCl, H_2O and TBP, and of the complexation coefficient. The results obtained with the model indicate that the solvate $ZnCl_2(H_2O)_5(TBP)_2$ adequately represents the extraction process of Zn(II) by concentrated TBP in HCl medium.

REFERENCES

1. Sato T, *J. Appl. Chem. Biotechnol.*, **22**, 1233, (1972).
2. Mühl P, Gloe K, Fisher C, Ziengelbelg S and Hoffman H, *Hydrometallurgy*, **5**, 161, (1980).
3. Jorger R and Kolarik Z, *Solv. Extr. Ion. Exch.* **11**, 33, (1993).
4. Sato T, Watanabe H and Suzuki H, *Hydrometallurgy*, **23**, 297, (1990).
5. Bunus F and Dumitrescu P, *Hydrometallurgy*, 1986, **16**, 167, (1986).
6. Madi A, Miralles N, Cortina JL, Arnaldos J and Sastre A, in *Proceedings of ISEC'96.* University of Melbourne. Melbourne **1**, 463, (1996)
7. Vogel AI, *Química Analítica Cuantitativa.* Ed. Kapelusz, Argentina, 354, (1960).
8. Osseo-Asare K, *Advances in Colloid and Interface Science*, **37**, 123, (1991).
9. Apelblat A, *J. Chem. Soc. (A)*, **1970**, 1271.
10. Sella C and Bauer D, *Hydrometallurgy*, **23,** 353, (1990).
11. Hamer WJ and Wu CY, *J. Phys. Chem. Ref. Data*, **1**, 1047, (1972).
12. Dean J, *Lange's Handbook of Chemistry*, McGraw Hill, 14th edition, 1992.

SOLVENT EXTRACTION OF DIVALENT ZINC AND CADMIUM FROM HYDROCHLORIC ACID SOLUTIONS BY DIHEXYLSULPHOXIDE

Taichi Sato,[1,2] Izumi Ishikawa[1] and Keiichi Sato[1]

[1] Faculty of Engineering, Shizuoka University, Hamamutsu, 432 Japan

[2]Metallurgical Engineering Department, Queen's University, Kingston, Ontario K7L 3N6, Canada

ABSTRACT

The extraction of divalent zinc and cadmium from aqueous solutions containing hydrochloric acid and/or lithium chloride was carried out using dihexylsulphoxide (DHSO, R_2SO) in benzene. The distribution coefficient increases with increasing chloride concentration of aqueous solutions. The extraction efficiency of DHSO for zinc (II) is higher than that for cadmium (II) at $[HCl)_{init\ aq} \leq 4$ mol dm^{-3}, while the extraction order reverses above this acidity. As a consequence, it was found that the extraction of zinc II) and cadmium (II) from hydrochloric acid solutions can be expressed by the equilibrium equations: $MCl_2(aq) + 2R_2SO(org) = MCl_2 \cdot 2R_2SO(org)$, $MCl^-_3(aq) + H^+(aq) + 3R_2SO(org) = HMCl_3 \cdot 3R_2SO(org)$ and $MCl^{2-}_4(aq) + 2H^+(aq) + 2R_2SO(org) = H_2MCl_4 \cdot 2R_2SO(org)$, where M = Zn or Cd.

Keywords: zinc(II), cadmium(II), dihexylsulphoxide, hydrochloric acid

INTRODUCTION

It is known that the presence of sulphur atom facilitates the combination of ligands with class B metal ions. Accordingly, sulphur-containing compounds such as dihexylsulphide (DHS, R_2S) and dihexylsulphoxide (DHSO, R_2SO) have been studied as solvent extractants for mercury(II).[1-3] However, since DHSO also contains an oxygen atom in addition to a sulphur atom, the extractability of metals by DHSO is generally higher than that by DHS. The present study extended the work to obtain further information on the extraction of divalent zinc and cadmium belonging to the IIB group from hydrochloric acid solutions by DHSO.

EXPERIMENTAL

Reagents

DHSO was synthesized by oxidation of DHS (Daihachi Chem. Ind. Co., Ltd.).[3]as follows: 1) 35 cm^3 each of acetic acid and acetic anhydride and 20 cm^3 of a 30% aqueous solution of hydrogen peroxide were added to 50 cm^3 of DHS dropwise during 2 hr; the mixture was cooled with ice, and then strirred for 3 h at 0°C. 2) After the reaction was confirmed by TLC, DHSO was extracted into chloroform, and the extract then washed first with water followed with 10% sodium carbonate, and finally with water again. 3) The white crystals obtained upon removal of chloroform by evaporation were purified by recrystallization. The DHSO was dissolved in benzene.

Aqueous solutions of zinc and cadmium were prepared by dissolving their chlorides, $ZnCl_2$ and $CdCl_2 \cdot 2.5H_2O$, respectively, in hydrochloric acid of selected concentrations; in general the concentration of the metal salts was 1 g dm^{-3} except for the loading test. All chemicals were of analytical reagent grade.

Extraction and analytical procedures.

Equal volumes (15 cm^3 each) of organic and aqueous phases were placed in 50 cm^3 stoppered conical flasks and shaken for a selected time in a water bath thermostated at 20°C, with the exception of the experiments on the effect of temperature. Preliminary experiments showed that equilibrium was complete in 10 min for both metals. The mixture was readily separated by centrifuge, and then

© 2000 Society of Chemical Industry

both phases were assayed to determine the distribution coefficient (E, the ratio of the equilibrium concentration of metal in the organic phase to that in the aqueous phase). Metals in the organic phases were stripped with 1 mol dm^{-3} hydrochloric acid. The concentration of metal in the aqueous solution was determined by EDTA titration using as indicators, Eriochrome Black T (BT) for cadmium and Xylenol Orange (XO) for zinc. The concentration of chloride and the water content in the organic phase were determined by Volhard's method with nitrobenzene and by Karl Fischer titration, respectively.

Raman and NMR spectral measurements.

The Raman spectra of the organic extracts were measured on a JASCO laser Raman spectrometer model R-300. Nuclear magnetic resonance (NMR) spectra were obtained for the organic extracts dissolved in carbon tetrachloride using a JEOL model JNM-PMX 60SO NMR spectrometer with tetramethylsilane as an internal reference.

RESULTS AND DISCUSSION

Extraction isotherms.

The extraction of zinc (II) from hydrochloric acid solutions by DHSO was carried out in solutions of different aqueous acidity. The distribution coefficient of zinc (II) rose when the initial concentration of hydrochloric acid was increased (Figure 1). When hydrochloric acid in the aqueous phase was replaced by lithium chloride, the extraction behavior of zinc (II) resembled that of hydrochloric acid solutions alone (Figure 1). The log - log plots of E vs $[R_2SO]_{aq} = [R_2SO]_{init} - 2[Zn]_{org}$ at constant hydrochloric acid concentration gave straight lines with slopes of 2.6, 2.5 and 2.6 at 2, 4 and 6 mol dm^{-3} HCl, and, in addition, 2.6 and 2.2 at 0.5 mol dm^{-3} HCl + LiCl (8 and 10 mol dm^{-3}), respectively. These results indicated that the dependencies of the distribution coefficient on the DHSO concentration were of second- and third- and/or second-powers at low ($[HCl]_{init} \leq 2$ mol dm^{-3}) and higher ($[HCl]_{init} \geq 2$ mol dm^{-3}) aqueous acidities, respectively.

In the extraction of zinc (II) from hydrochloric acid solutions by DHSO, continuous variation plots of $[Zn]_{org}$ as a function of the zinc mole fraction $[Zn]_{init\ aq}/([Zn]_{init\ ac} + [R_2SO]_{init})$, at a fixed total concentration of $[Zn]_{init\ aq} + [R_2SO]_{init} = 0.1$ or 0.2 mol dm^{-3}, and at initial aqueous hydrochloric acid concentrations of 2, 4 and 7 mol dm^{-3}, gave maxima at 0.33, 0.25, and 0.25, respectively, indicating that the combination of DHSO with zinc is in the molar ratio of 2 : 1 and 3 : 1, depending on aqueous acidities. However, because the distribution coefficient from acid alone was higher than that from a mixture of hydrochloric acid and lithium chloride, the effect of proton concentration on the distribution coefficient was examined.

When the initial hydrochloric acid concentration was varied at a constant total chloride concentration in the aqueous phase ($[Cl]_{init\ aq} = [HCl]_{init\ aq} + [LiCl]_{init\ aq}$), the distribution coefficient increased linearly when increasing the proton concentration in the aqueous phase. These results lead to the presumption that in analogy with the distribution of aqueous chloro species of zinc (II),[4] the dependencies of the distribution coefficient on the proton concentration in the aqueous phase were of first- and/or second-powers. Accordingly, the stoichiometric species $ZnCl_2 \cdot 2R_2SO$, $ZnCl_2 \cdot HCl \cdot 3R_2SO$ (as $HZnCl \cdot 3R_2SO$) and $ZnCl_2 \cdot 2HCl \cdot 2R_2SO$ (as $H_2ZnCl_2 \cdot 2R_2SO$) are formed gradually when increasing the initial aqueous hydrochloric acid concentration. For these reasons, the following equilibrium equations have been proposed for the extraction of zinc (II) from hydrochloric acid solutions by DHSO, as the aqueous species of zinc (II) depends on the aqueous chloride concentration[4]:

$$ZnCl_2(a) + 2R_2SO(o) \Leftrightarrow ZnCl_2 \cdot 2R_2SO(o) \quad (1)$$

$$ZnCl_3^-(a) + H^+(a) + 3R_3SO(o) \Leftrightarrow HZnCl_3 \cdot 3R_2SO(o) \quad (2)$$

and

$$ZnCl^{2-}_4(a) + 2H^+(a) + 2R_2SO(o) \Leftrightarrow H_2ZnCl_4{\cdot}2R_2SO(o) \quad (3)$$

where (a) and (o) denote aqueous and organic phases, respectively. Based on these equations, it can be seen that the variation of the distribution coefficient with the aqueous acid concentration (Figure 1) corresponds to the distribution of the aqueous zinc chloro species $ZnCl_2$, $ZnCl_3^-$ and $ZnCl_4^{2-}$.

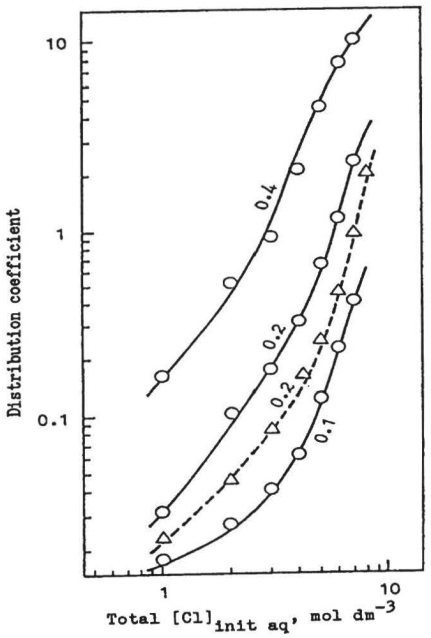

Figure 1. Extraction of zinc (II) from HCl solutions with DHSO in benzene (continuous and broken lines represent the extraction from HCl solutions and mixed 0.5 mol dm^{-3} HCl/LiCl solns., respectively; numerals on curves are DHSO concns., mol dm^{-3}).

Extraction isotherms of cadmium(II).

The extraction of cadmium (II) from hydrochloric acid solutions by DHSO indicated an extraction behavior resembling that of zinc (II). The distribution coefficient rose when increasing the aqueous acidity (Figure 2). The extraction efficiency of DHSO for zinc (II) was higher than that of cadmium (II) at $[HCl]_{init\ aq} \leq 4$ mol dm^{-3}, but this order was reversed above this acidity. Thus, log-log plots of E vs $[R_2SO]_{aq}$, and continuous variation plots of $[Cd]_{aq}$ as a function of mole fraction of $[Cd]_{init\ aq}/([Cd]_{init\ aq} + [R_2SO]_{init})$ at a fixed total concentration of $[Cd]_{init\ ac} + [R_2SO]_{init}$, were carried out. The results allowed the conclusion that the extraction of cadmium (II) from hydrochloric acid solutions by DHSO can be expressed by equilibrium equations similar to Equations. (1) - (3).

Spectral studies.

The Raman spectra of the organic extracts of zinc (II) from aqueous solutions containing 200 g dm^{-3} $ZnCl_2$ in 2, 3, 5 and 7 mol dm^{-3} HCl with 2 mol dm^{-3} DHSO in benzene gave absorption bands at 298, 298 (shoulder) + 283, 280 and 278 + 265 cm^{-1}, assigned to the species $ZnCl_2$, $ZnCl_2$ + $ZnCl_3^-$, $ZnCl_3^-$ and $ZnCl_3^-$ + $ZnCl_4^{2-}$, respectively, corresponding to the equilibrium equations (1) - (3). In similar experiments for the organic extracts of cadmium (II), the Raman spectra exhibited respective absorptions at 262, 262, 262 and 260 cm^{-1}, assigned to the species $CdCl_3^-$.

The organic phases after the extraction of zinc (II) and cadmium (II) from aqueous solutions containing 10 and 50 g dm^{-3} $ZnCl_2$ or $CdCl_2$ in 5 mol dm^{-3} HCl with 0.5 mol dm^{-3} DHSO in carbon tetrachloride were examined by NMR spectroscopy. The NMR spectrum for DHSO revealed a sharp peak at $\tau = 9.14$ in a doublet due to the methyl protons, a multiplet at 8.66, which arises from most of the methylenic protons, and a triplet at 7.52, from the methylenic protons attached to the carbon atoms immediately adjacent to the oxygen atom; in addition, the water proton resonance at 7.81 indicated the formation of the compound $R_2SO.H_2O$[5]. In the extraction from 3 and 5 mol dm^{-3} hydrochloric acid solutions only, the water proton signal shifted to 7.24 and 3.88, respectively, confirming the formation of a hydrogen bond in the compound $HCl{\cdot}R_2SO{\cdot}H_2O$. The spectra of the organic solutions from the extraction of aqueous solutions containing 10 and 50 g dm^{-3} $ZnCl_2$ or $CdCl_2$ showed a water proton resonance at 2.20 and 1.56, respectively, or 2.32 and 1.56, respectively. It was interpreted that the shift of the water proton to a higher field caused by the extraction of zinc (II) or cadmium (II) into the organic phase probably arose from the displacement of the compound $HCl{\cdot}R_2SO{\cdot}H_2O$ by the complexes $HZnCl_3{\cdot}3R_2SO$ and/or $H_2ZnCl_4{\cdot}2R_2SO$ or $HCdCl_3{\cdot}3R_2SO$ and/or $H_2CdCl_4{\cdot}2R_2SO$. Similar phenomena were also observed in other extraction systems involving TBP and TOPO.[6,7]

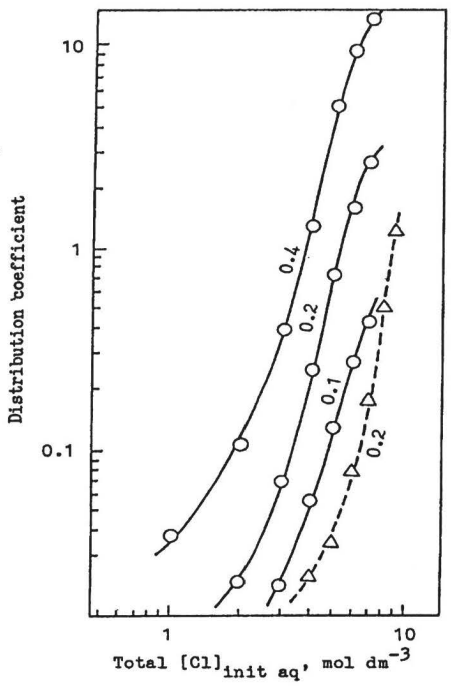

Figure 2. Extraction of cadmium (II) from HCl solutions with DHSO in benzene (continuous and broken lines represent the extraction from HCl solutions and mixed 0.5 mol dm^{-3} HCl/LiCl solns., respectively; numerals on curves are DHSO concns., mol dm^{-3}).

Temperature effect.

The extraction of zinc (II) and cadmium (II) from 6 mol dm^{-3} hydrochloric acid solution with 0.1 mol dm^{-3} DHSO in benzene was carried out at temperatures between 10 and 50°C. The results showed that the distribution coefficients decreased with rising temperature. The values of the heat of reaction (change of enthalpy, $-\Delta H$) for zinc (II) and cadmium (II) were estimated as 36.9 and 38.4 kJ mol^{-1}, respectively, that is, close to those expected for the energy of hydrogen bonds.

CONCLUSION

The extraction of zinc (II) and cadmium (II) from aqueous solutions containing hydrochloric acid and/or lithium chloride was carried out using DHSO in benzene. It was found that the distribution coefficient rose when increasing the chloride concentration of aqueous solutions, and the extraction behavior of zinc (II) was analogous to that of cadmium (II). In consequence, it was determined that the extraction of divalent zinc and cadmium from hydrochloric acid solutions by DHSO can be expressed by the equilibrium equations:

$$MCl_2(a) + 2R_2SO(o) \Leftrightarrow MCl_2 \cdot 2R_2SO(o) \quad (4)$$

$$MCl^-_3(a) + H^+(a) + 3R_2SO(o) \Leftrightarrow HMCl_3 \cdot 3R_2SO(o) \quad (5)$$

and

$$MCl^{2-}_4(a) + 2H^+(a) + 2R_2SO(o) \Leftrightarrow H_2MCl_4 \cdot 2R_2SO(o) \quad (6)$$

where M = Zn or Cd.

When the results obtained in the extraction of zinc (II) and cadmium (II) were compared with those for the extraction of mercury (II)[3], it was seen that the extraction behavior of all these metal species is similar. The extraction efficiency of metals by DHSO was in the order of Hg > Zn > Cd at [HCl] $\leq$ 4 mol dm^{-3} and Hg > Cd > Zn at higher acidities.

REFERENCES

1. Sato T, Ishikawa T and Nakamura T, *Solv. Extr. Ion Exchg.*, **1**, 541, (1983).
2. Sato Y, Ishikawa I and Sato K, *Proc ISEC'86*, **3**, 156, (1986); *Proc ISEC'90*, **Part A**, 913, (1992).
3. Sato T, Ishikawa I and Sato K, *J. Min. Mater. Process. Inst. Jpn.*, **114**, 33, (1998).
4. Sato T and Kato T, *J. Inorg. Nucl. Chem.*, **39**, 1205, (1977).
5. Sato T, *Anal. Chim. Acta*, **52**, 489, (1965).
6. Sato T, Sato K, Noguchi Y and Ishikawa I, *J. Min. Mater. Process. Inst. Jpn.*, **113**, 185, (1997).
7. Sato T, *J. Min. Mater. Process. Inst. Jpn.*, **112**, 123, (1996).

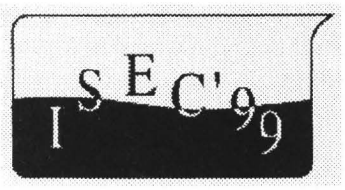

SOLVENT EXTRACTION OF DIVALENT ZINC AND LEAD FROM SODIUM HYDROXIDE SOLUTIONS BY AN ALKYLATED HYDROXYQUINOLINE

Taichi Sato,[1,2] Keiichi Sato[1] and Françoise Tahiani[2]

[1] Faculty of Engineering, Shizuoka University, Hamamatsu, 432 Japan

[2] Alcan International, Kingston Laboratories, P.O. Box 8400, Kingston, Ontario K7L 5L9, Canada

ABSTRACT

The extraction of zinc (II) and lead (II) from sodium hydroxide solutions by Kelex 100 (7-(5,5,7,7-tetramethyl-l-octen-3-yl)-8-hydroxyquinoline) in kerosene has been investigated under different conditions with the addition of alcohol. It was found that when alcohol is added to the organic phase, the extraction of zinc(II) and lead(II) is enhanced with the limited amounts of alcohol added at low alkali concentration, although the extraction efficiency for zinc (II) is higher than that for lead (II). In contrast, the extraction is supressed on addition of alcohol at higher alkali concentrations.

Keywords: zinc (II), lead (II), hydroxide media, Kelex 100, alcohol

INTRODUCTION

Some metals contained in bauxite accompany the aluminate ion in Bayer liquor. Therefore the removal of these metals from alkaline solutions is investigated using solvent extraction.[1] It has been reported that alkylated hydroxyquinolines such as 7-(5,5,7,7-tetramethyl-l-octen-3-yl)-8-hydroxyquinoline (Kelex 100, HQ) has an excellent ability to extract zinc (II) , lead (II) and gallium (III) from concentrated sodium hydroxide solutions.[2-4] In these extraction systems, since the extractant forms an insoluble salt in the organic and aqueous phases in the process of back-extraction with acid, an aliphatic alcohol is often added to exclude the formation of an insoluble salt. Therefore the effect of the addition of alcohol on the extraction of gallium (III) has been examined previously[3]. The present study extends the work to obtain further information for the effect of the presence of alcohol (for 2-ethylhexyl) an the extraction of zinc (II) and lead (II) from alkaline solutions by Kelex 100.

As the extraction of gallium (III) from sodium hydroxide solutions by alkylalkylated hydroxyquinoline is related to the Bayer process, several researchers have investigated its extraction system from both thermodynamic and kinetic points of view.[1,5-7] The extraction rate of gallium (III) from alkaline solutions by Kelex 100 is very slow in comparison with those of zinc (II) and lead (II),[2] and the use of some surfactants has been shown to increase the extraction rate of gallium (III). A mixture of an alcohol and the sodium salt of long chain carboxylic acid was added to the organic phase.[8] It has been reported that the organic phase of such extraction system is a water-in-oil microemulsion,[9] which is an optically transparent and thermodynamically stable water-in-oil (or oil-in-water) dispersion formed by adding a surfactant and alcohol.[10]

In these cases, water-in-oil microemulsions should be described as micro-droplets of water, surrounded by surfactant and alcohol molecules and dispersed in a continuous organic phase. Accordingly the presence of alcohol is regarded as the addition of modifier to the solvent. However, since the results for the effect of the addition of alcohol as a modifier on the extraction efficiency of metal are limited, its effect on the extraction of zinc (II) and lead (II) is surveyed in this paper.

EXPERIMENTAL

Reagents

Kelex 100 (Schering AG) was distilled twice under a reduced pressure of 33.33 Pa at 147-159C to remove 8-hydroxyquinoline. The purified Kelex 100, a pale yellow liquid, was diluted with kerosene or hexane. Aqueous alkaline solutions of zinc (II) and lead (II) were prepared by dissolving

© 2000 Society of Chemical Industry

their oxides in sodium hydroxide solution of selected concentration. In general the aqueous metal concentrations were adjusted to respective 0.01 mol dm^{-3}. 2-Ethylhexyl alcohol was used as an alcohol added to the organic phase. Chemicals were of analytical reagent grade.

Extraction and analytical procedures

Equal volumes (15 cm^3 each) of organic and aqueous phases placed in 50 cm^3 stoppered centrifugal glass tube were shaken for 20 min at 20C except for the examination of the temperature effect. Preliminary experiments showed that equilibration was complete in 20 minutes. The mixture was centrifuged and separated, and then the portions of both phases were removed by pipette to determine the distribution coefficient (E_a^0 the ratio of the equilibrium concentration of metal in the organic phase to that in the aqueous phase). Zinc was stripped from the organic phases with 2 mol dm^{-3} hydrochloric acid with the addition of 2-ethylhexyl alcohol for better phase separation, and lead with 2 mol dm^{-3} nitric acid and 2-ethyl alcohol. The concentration of metal in the aqueous solution was determined by EDTA titration using xylenol orange (XO) as indicator.

RESULTS AND DISCUSSION

Extraction isotherms of zinc (II)

In the extraction of zinc(II) from aqueous sodium hydroxide solutions, the distribution coefficient decreases with increasing concentration of sodium hydroxide below ~4 mol dm^{-3}; above this concentration there is an anomalous change in distribution coefficient which has a maximum at 6 mol dm^{-3} (Figure 1).[2] It has been previously suggested that the extraction of zinc (II) from sodium hydroxide solutions by Kelex 100 is expressed by the equilibrium equations:

$$Zn(OH)_4^{2-}(a) + 2HQ(o) \leftrightarrow ZnQ_2(o) + 2OH^-(a) + 2H_2O(a) \quad (1)$$

where (a) and (o) denote aqueous and organic phases, respectively, and at higher alkali concentrations

$$Zn(OH)_4^{2-}(a) + 2Na^+(a) + 2HQ(o) \leftrightarrow ZnQ_2 \cdot 2NaOH(o) + 2H_2O(a) \quad (2)$$

When alcohol was added to the organic phase, the extraction of zinc (II) was enhanced at low alkali concentration ([NaOH] <2 mol dm^{-3}) and supressed at higher alkali concentrations ([NaOH] >2 mol dm^{-3}) as shown in Figure 1.

The distribution coefficient of zinc (II) followed different behaviour depending on the concentration of the aqueous alkaline solutions. At [NaOH] < 0.4 mol dm^{-3} the distribution coefficient increased and attained almost a constant value with increasing amounts of added alcohol. At [NaOH] = 0.6 - 4 mol dm^{-3} the distribution coefficient also increased with the limited amounts of alcohol added (50, 20 and 10 % (v/v) at [NaOH] = 0. 6 - 2, 3 and 4 mol dm^{-3}, respectively), and decreased beyond these amounts. Finally at [NaOH] > 6 mol dm^{-3} the distribution coefficient decreased on addition of alcohol. Thus the increase in distribution coefficient at higher concentrations of alkaline solutions disappeared in the presence of alcohol.

In a previous paper,[2] it was shown that drastic extraction of sodium occurs at the concentration of aqueous sodium hydroxide above 5 mol dm^{-3} owing to the formation of the species NaQ, and that the increase in the distribution coefficient at concentrations of sodium hydroxide above 4 mol dm^{-3} is due to the up-take of zinc (II) accompanied by sodium ions as represented in Equation (2). However, since the distribution coefficient decreased on addition of alcohol at higher alkaline concentrations, the distribution behaviour of sodium hydroxide to the organic phase was examined under the different amounts of alcohol added for the sodium hydroxide solution at 4 mol dm^{-3} in the absence of metal. As a result, it was observed that the concentration of sodium in the organic phase increases with increasing the amount of alcohol added up to 50 % (v/v) and then attains an almost constant value on addition of above 50 % (v/v) of alcohol. From this it is deduced that the increase in the distribution coefficient of zinc (II) at higher alkaline concentrations may be attributed to the decrease of effective extractant concentration due to the extraction of sodium in the organic phase caused by addition of alcohol.

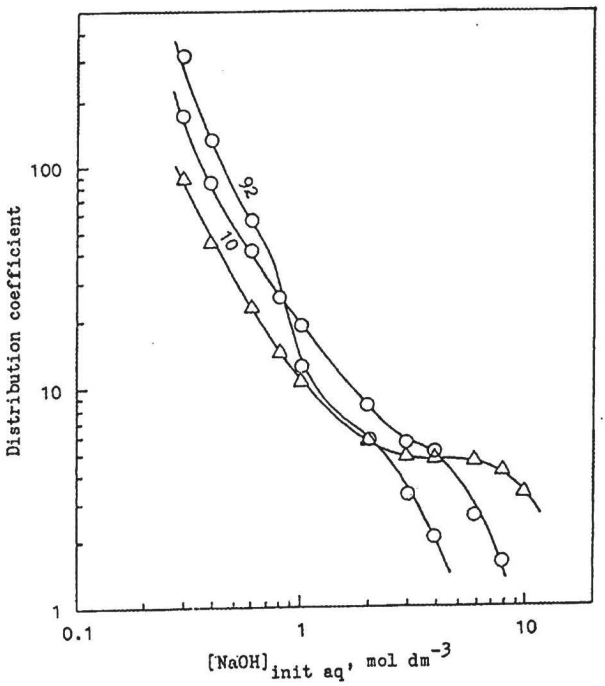

Figure 1. Extraction of zinc (II) from sodium hydroxide solutions with 0.02 mol dm^{-3} Kelex 100 in kerosene in the presence of alcohol (triangles and circles denote the extraction with Kelex 100 in kerosene and kerosene/alcohol, respectively; numerals on curves are the amount of alcohol added, % (v/v)».

Extraction isotherms of lead (II)

The shape of the extraction curve of lead (II) resembles that of zinc (II), although the extraction efficiency of former is lower than the latter.[2] On addition of alcohol to the organic phase, the extraction of lead (II) is enhanced at low alkali concentration ([NaOH] <3 mol dm^{-3}) and supressed at higher alkali concentrations ([NaOH] >3 mol dm^{-3}) as indicated in Figure 2. The distribution coefficient of lead (II) followed a similar effect to that of zinc (II), depending on the concentration of the aqueous sodium hydroxide solutions. At [NaOH] <1 mol dm^{-3} the distribution coefficient was increased and attained almost a constant value with increasing amount of alcohol added. At [NaOH] = 2 - 6 mol dm^{-3} the distribution coefficient increased under the limited amounts of alcohol added (50, 20 and 5 % (v/v) at (NaOH] = 2, 3 - 4 and 6 mol dm^{-3}, respectively), and decreased beyond these amounts. Finally at (NaOH] >8 mol dm^{-3} the distribution coefficient increased on addition of alcohol.

Temperature effect

The extraction of zinc (II) or lead (II) from aqueous solution containing 0.4 or 0.8 mol dm^{-3} sodium hydroxide, respectively, with 0.02 mol dm^{-3} Kelex 100 in kerosene in the presence of 2-ethylhexyl alcohol was carried out at temperatures between 10 and 40C. The results indicated that the distribution coefficients decrease with increasing temperature, and that the values of heat of reactions (change of enthalpy, $-\Delta H$) in Equations (1) and (2) were estimated to be 138, 166, 181 and 205 kJ mol- for zinc (II) and 132, 142, 156 and 158 kJ mol^{-1} for the addition of alcohol at 0, 5, 10 and 20% (v/v), respectively. From these it is inferred that as the values of heat of reactions are not much different on addition of alcohol, the metal extraction mechanism may not be much influenced by the presence of alcohol added as a modifier.

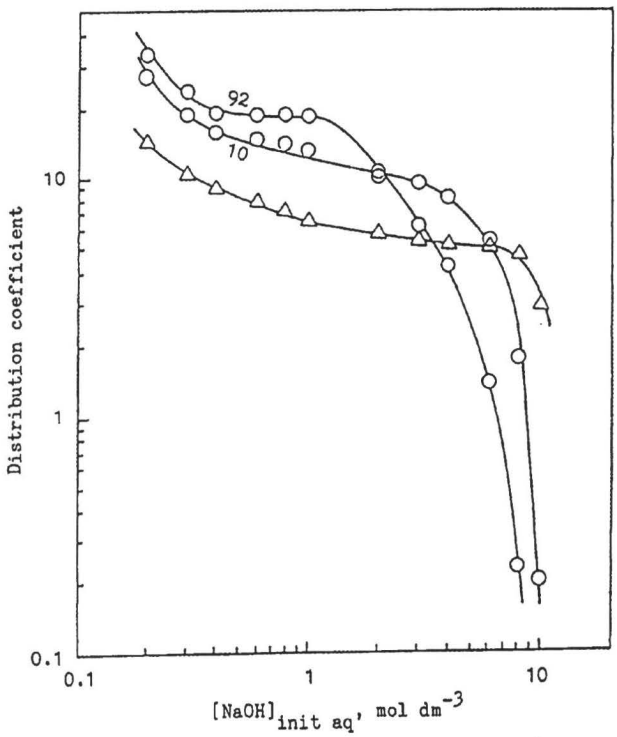

Figure 2. Extraction of lead (II) from sodium hydroxide solutions with 0.02 mol dm^{-3} Kelex 100 in kerosene in the presence of alcohol (triangles and cycles denote the extraction with Kelex 100 in kerosene and kerosene/alcohol, respectively; numerals on curves are the amount of alcohol added, % (v/v)».

CONCLUSIONS

The effect of the presence of alcohol on the extraction of zinc (II) and lead (II) from sodium hydroxide solutions by Kelex 100 in kerosene has been examined under different conditions. It was seen that when alcohol is added to the organic phase, the extraction of zinc (II) and lead (II) is enhanced when limited amounts of alcohol are added at low alkali concentration, although the extraction efficiency for zinc (II) is higher than that for lead (II). But these extraction systems are supressed on the addition of alcohol at higher alkali concentrations. It is therefore seen that the effect of alcohol addition on the extraction of zinc (II) and lead (II) does not depend on the kind of metal.

In addition, as an alcohol alone does not extract the metal, it is expected that the extraction mechanism of zinc (II) and lead (II) by Kelex 100 in the presence of alcohol follows Equations (1) and (2). Accordingly it is presumed that the interactions of the mixed solutions containing extractant and alcohol and/or the extracted metal complexes and such mixed solutions influence the extractability of metal in the present extraction system. Besides, when the relation between the distribution coefficient of zinc (II) or lead (II) and the physical properties of solvent (e.g. solubility parameter, refractive index, specific gravity, viscosity and dielectric constant) were checked by varying the concentration of alcohol added, no special observations were seen except for the refractive index.

ACKNOWLEDGEMENT

The authors wish to thank Mr. Hiroyuki Watanabe for assistance with experimental work.

REFERENCES

1 Leveque A and Helgorsky J. *Proc. ISEC'77*, CIM Special **2**, 439, (1979).
2 Sato T, Nakamura T and Oishi H. *Solv. Extr. Ion Exch.*, **2**, 45, (1984).
3 Sato T. *Chemical Separations*, (King CJ and Navratil JD, eds.), Litarvan Literature, Denver, **1**, 285, (1986).
4 Sato T and Oishi H. *Hydrometallurgy*, **16**, 315, (1986).
5 Bauer D and Pescher-Cluzeau Y. *Hydrometallurgy*, **18**, 293, (1987).
6 Pesic B and Zhou T. *J.Metals*, **40**, 24, (1988); **41**, 42, (1989).
7 Fourre P and Bauer D. *Solv. Extr. Ion Exch.* **1**, 465, (1983).
8 Fourre P and Bauer D. *C.R. Acad. Sc. Paris, II*, **292**, 1077, (1981).
9 Bauer D, Fourre P and Lemerle J. *C.R. Acad. Sc. Paris, II*, **292**, 1019, (1981).
10 Shinoda K and Friberg S. *Adv. Colloid Interface Sci.* **4**, 282, (1975).

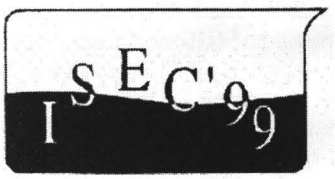

EXTRACTION OF LEAD(II) BY CYANEX 302 AND CYANEX 301 FROM 2.19 MOL/DM^3 PHOSPHORIC ACID MEDIUM

B Menoyo and MP Elizalde
Dpto. Química Analítica, Universidad del País Vasco, Bilbao, Spain

ABSTRACT
The extraction of Pb(II) from 2.19 mol/dm^3 phosphoric acid medium by the commercial extractants Cyanex 302 and Cyanex 301 dissolved in toluene has been studied. Numerical treatment was carried out to establish the extraction stoichiometry as well as the conditional equilibrium constants of the extraction processes, at this phosphoric acid concentration. The effect of aqueous acidity on the extraction of Pb(II) by Cyanex 302 from phosphoric acid solutions has also been investigated.

Keywords: lead, phosphoric acid, Cyanex 302, Cyanex 301

INTRODUCTION

Industrial phosphoric acid, used in the manufacturing of phosphated fertilizers, contains among other impurities, Pb(II), whose recovery from these acidic media can be of interest. Studies have been made on the solvent extraction of lead from chloride solutions[1,2] with the organothiophosphinic acids Cyanex 302 and Cyanex 301, that have proved able to extract Pb(II) at very low pH values. Also Cd(II) extraction from H_3PO_4 acid solutions by Cyanex 302 has been studied,[3] and high metal extraction recoveries reported. So, the new organothiophosphinic acids seem to be promising reagents to remove the impurities present in the industrial formulation.

The present report, deals with the extraction of Pb(II) from 2.19 M H_3PO_4 medium by Cyanex 302 and Cyanex 301, and is a part of a study covering an extensive range of phosphorus acid concentrations where the variation of the ionic strength and its influence on the extraction equilibrium constants is being considered. Since the variation of the phosphoric acid concentration also involves a change in the free hydrogen ion concentration, this magnitude must be estimated so as to calculate the extraction equilibrium constants. In this sense, following the phosphoric acid model proposed by Elmore,[4] data of $[H^+]$ concentration at 2.19 mol/dm^3 H_3PO_4 acid concentration has been taken from Stenström.[5]

EXPERIMENTAL

Reagents and solutions

Samples of Cyanex 302 and Cyanex 301 were kindly supplied by Cytec Canada Inc. and used without further purification. Cyanex 302 and Cyanex 301 were considered to be 85.0% bis(2,4,4-trimethylpentyl)monothiophosphinic acid (HR) and 77.2% bis(2,4,4-trimethylpentyl)dithiophosphinic acid (HL) respectively, according to the purity percentage given in the Cytec brochure. The percentage of (HL) present in Cyanex 302 was determined by GC using an NPD detector and the mean value of 0.47% was taken. The extractants were dissolved in toluene (Riedel and Haën, p.a.). Aqueous solutions were prepared by dissolving $Pb(NO_3)_2$ (Merck, p.a.) in H_3PO_4 (Scharlau, p.a.) acid solutions.

Experimental technique

The extraction experiments were carried out by shaking equal volumes (10 cm^3) of aqueous and organic solutions in special stoppered tubes for 30 minutes. The aqueous lead concentration was 0.5 mmol/dm^3 in all the experiments. Phosphoric acid concentration was 2.19 mol/dm^3, except in the study of the acid dependency where it was varied betwen 0.36 and 5.83 mol/dm^3. The organic phases

© 2000 Society of Chemical Industry

contained either Cyanex 302 in the concentration range from 10.2 to 212.5 mmol/dm^3 (HR) in toluene or Cyanex 301 in a concentration ranging from 0.2 to 1.2 mmol/dm^3 (HL) in toluene. Organic solutions were prepared daily.

The analysis of lead in both phases was carried out by atomic absorption spectroscopy (Perkin-Elmer 560). The lead content of the organic phase was measured by stripping the metal into 5.0 mol/dm^3 nitric acid. All the data which did not fulfill the mass balance for lead within 3% were rejected.

RESULTS AND DISCUSSION

Pb(II) extraction by Cyanex 301

To fully understand the extraction of Pb(II) by Cyanex 302, it is necessary to consider that this reagent has bis(2,4,4-trimethylpentyl)dithiophosphinic acid (HL) as a minor component that is able to extract Pb(II) very efficiently at very low pH values as reported in a previous paper.[2] For this reason, the extraction of Pb(II) by Cyanex 301 was studied in the range of concentration between 0.2 and 1.2 mmol/dm^3 HL, which would approximately correspond to the amounts present in Cyanex 302 in the range of concentrations used in the present work.

The results obtained on the extraction of Pb(II) by Cyanex 301 are shown in Figure 1 where it can be appreciated that small amounts of Cyanex 301 can extract Pb(II) very efficiently under these experimental conditions. So, it is probable that its active component plays an important role on the extraction of Pb(II) by Cyanex 302.

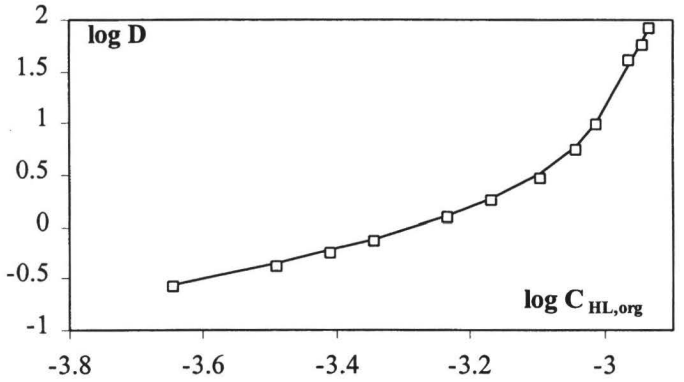

Figure 1. Variation of the distribution coefficient as a function of total HL concentration for the extraction of Pb(II) by Cyanex 301. The continuous line represents the theoretical curve calculated with the proposed model.

Data on Pb(II) extraction by Cyanex 301 were treated using the computer program LETAGROP-DISTR.[6] In this program the function to be minimized is the error square sum (U). For each combination of species the program calculates both U_{min} and the mean standard deviation, (log D). The best fit to the data corresponded to either the formation of the species Pb_2L_4 or PbL_2 as shown in Table 1(a). The formation of polynuclear metallic species, such as Pb_2L_4 in the organic phase is favoured when the metal concentration is high compared with the ligand concentration, as in this study. However, this species cannot be proposed as responsible for the extraction process, due to the lack of additional experiments varying the metal concentration to confirm the extraction of this polynuclear species. Thus, the species PbL_2 can be proposed as responsible for the extraction of Pb(II) by Cyanex 301 under the experimental conditions of this study, the conditional extraction

constant being log k'_{ex} =8.69 ± 0.064. The good fit to the data obtained with this species is illustrated in Figure 1 where the experimental behaviour is compared with the theoretical one obtained with the proposed model (continuous line).

Pb(II) extraction by Cyanex 302

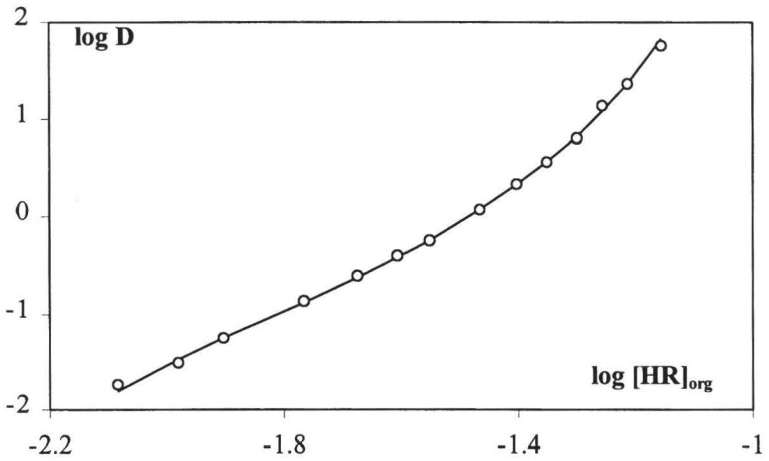

Figure 2. Variation of the distribution coefficient as a function of the free HR concentration for the extraction of Pb(II) by Cyanex 302. The continuous line represents the theoretical curve calculated with the proposed model.

Figure 2 shows the variation of log D as a function of the free HR concentration (log $[HR]_{org}$). The free HR concentration has been calculated taking into account the mass balance equation for the extractant and considering its dimerization constant in toluene.[7]
The extraction of Pb(II) by Cyanex 302, by analogy with the extraction from KCl media, can be expressed by the general equation:

$$Pb^{2+} + (2+m)\, HR_{org} + n\, HL_{org} \Leftrightarrow [PbR_2(HR)_m(HL)_n]_{org} + 2\, H^+ \qquad (1)$$

In the above equation, the formation of general mixed species has been considered, although these species could be formulated in a different way, L being directly bound to the metal ion and HR solvating the complex.
The distribution coefficient can be expressed as:

$$D = \sum_{2mn} k'_{ex} \left[H^+\right]^{-2} \left[HR\right]_{org}^{(2+m)} \left[HL\right]_{org}^{n} \qquad (2)$$

k'_{ex} being the conditional extraction constant which takes into account the effect of the ionic strength as well as the formation of Pb(II) complexes with phosphoric acid. According to equation (2) the variation of the distribution coefficient with the free HR concentration should give a straight line if only R containing species were extracted. However, examination of Figure 2 shows clearly that the plot has more the shape of a curve rather than straight lines. So, it is again clear that the contribution of HL to the extraction process has to be considered. However, as it can not be assumed the constancy of the free HL concentration, no graphical treatment considering the participation of this minor component can be applied.

Data on Pb(II) extraction by Cyanex 302 were treated using the computer program LETAGROP-DISTR.[6] It was considered, as a first step, that HR, the major component of Cyanex

302 was the only responsible for the extraction process. As it can be seen from Table 1(b), high values of both (log D) and U_{min} were obtained.

Model of species	U_{min}	(log D) 10^2
a) PbL_2	0.010	3.01 (+)
$PbL_2(HL)$	6.436	76.19
PbL_2, $PbL_2(HL)$*	0.010	3.01
Pb_2L_4	0.008	2.66
b) PbR_2*, $PbR_2(HR)$	0.828	25.24
PbR_2, $PbR_2(HR)_2$	0.225	13.68
$PbR_2(HR)$, $PbR_2(HR)_2$	0.309	16.06
$PbR_2(HR)$, $PbR_2(HR)_3$	0.160	11.56
$PbR_2(HR)$, PbL_2	0.655	23.37
$PbR_2(HR)_2$, PbL_2	0.184	12.37
$PbR_2(HR)$, $PbL_2(HR)$	0.392	18.08
$PbR_2(HR)$, $PbR_2(HL)$	0.754	25.06
$PbR_2(HR)$, $PbR_2(HR)_2$	0.126	10.27
$PbR_2(HR)$, $PbR_2(HR)_3$	0.305	15.94
$PbR_2(HR)_2$, $PbL_2(HR)$	0.058	6.94
$PbR_2(HR)_2$, $PbR_2(HR)$	0.175	12.08
$PbR_2(HR)_2$, $PbR_2(HL)_2$	0.017	3.73 (+)
$PbR_2(HR)_2$, $PbR_2(HR)_3$	0.020	4.08
$PbR_2(HR)_2$, $PbR_2(HL)_2$, PbR_2	0.012	3.27
$PbR_2(HR)_2$, $PbR_2(HL)_2$, $PbR_2(HR)$	0.014	3.56

(+) proposed model
(*) rejected species

Table 1 Results of the numerical calculations in the system (a) Pb(II)-2.19 mol/dm^3 H_3PO_4/Cyanex 301-toluene and (b) Pb(II)-2.19 mol/dm^3 H_3PO_4/Cyanex 302-toluene

The presence of HL in Cyanex 302 was considered by introducing in the input its concentration according to the percentage value of 0.47%. Firstly, the possibility of the formation of one species with HR together with either a PbL_2 species or a mixed species was checked. An essential improvement of the fit was obtained when a mixed species of stoichiometry $PbR_2(HL)_2$ was supposed to be formed together with the species $PbR_2(HR)_2$. A slightly better improvement of the fit was achieved when a third species was included in this model. The little importance of this third species is corroborated by the fact that variation of its composition caused minimal changes of both (log D) and U_{min}. So, to confirm the formation of this third species, more experimental data at different phosphoric acid concentrations would be necessary. On the other hand, the set of species $PbR_2(HR)_2$ and $PbR_2(HL)_2$ seems to explain by itself the experimental data obtained at 2.19 mol/dm^3 H_3PO_4 concentration, as can be seen from Figure 2, where the experimental behaviour is compared with the theoretical obtained with the proposed model (continuous line). The values of the conditional equilibrium constants obtained by this treatment, are $\log k'_{ex}(PbR_2(HR)_2) = 4.79 \pm 0.07$ and $\log k'_{ex}(PbR_2(HL)_2) = 10.27 \pm 0.14$.

The contribution of the different extracted species as a function of the reagent concentration is illustrated in Figure 3, where it can be seen that the mixed species $PbR_2(HL)_2$ is the most important extracted species whereas the importance of $PbR_2(HR)_2$ decreases with increasing extractant concentration.

Phosphoric Acid Dependency

Finally, additional experiments at different H_3PO_4 acid concentrations were carried out and are presented in Figure 4. As can be seen from this figure, the distribution coefficient depend on the

initial concentration of phosphoric acid in the aqueous phase. Thus, the extraction curves show that the extraction of Pb(II) decreases with increasing phosphoric acid concentration. However, even at the more acidic conditions, an extraction efficiency around 40% can be achieved by increasing the extractant concentration to approximately 125 mmol/dm^3 HR. An accurate treatment of this series of data would need more experimental points since the variation of H_3PO_4 concentration involves variation of the ionic strength and data at each phosphoric acid concentration have to be treated separately.

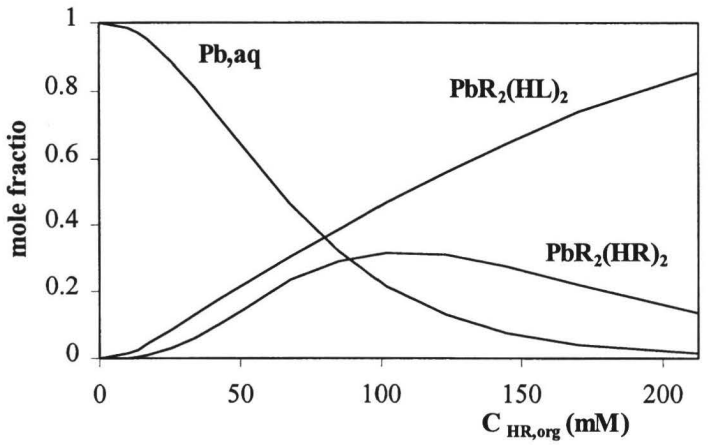

Figure 3. Pb(II) distribution diagram as a function of total HR concentration.

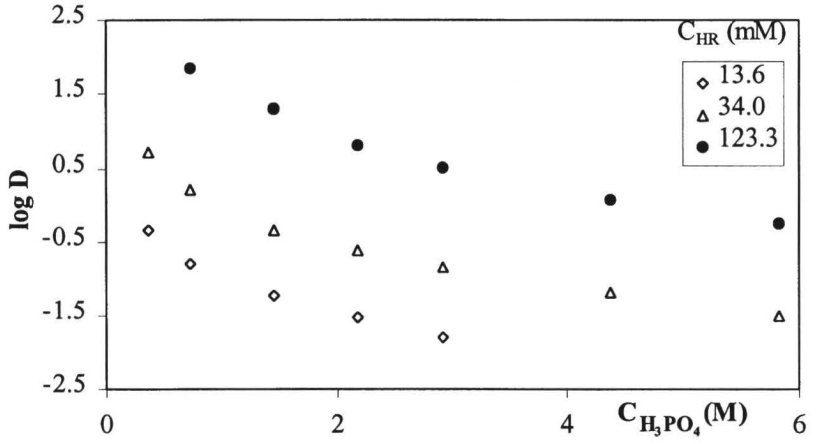

Figure 4. Variation of the distribution coefficient as a function of aqueous phase phosphoric acid concentration at different HR concentrations.

CONCLUSIONS

The results obtained on the extraction of Pb(II) from 2.19 mol/dm^3 phosphoric acid by Cyanex 302 and Cyanex 301 confirm the superior behaviour of Cyanex 301 towards the extraction of this metal ion. Concerning the extraction stoichiometry, Cyanex 301 was found to extract the metal ion as PbL_2 while in the case of the extraction by Cyanex 302 the fact that HL, present at small amounts in

this extractant, is able to extract Pb(II) very efficiently has to be taken into consideration. This is confirmed by the numerical treatment where the formation of species having only HR as participant in the extraction process cannot explain the experimental data. Thus the species $PbR_2(HR)_2$ and $PbR_2(HL)_2$, which could also be formulated as $PbL_2(HR)_2$, can be proposed as the main extracted species by Cyanex 302.

Finally, it should be pointed out that in order to confirm the proposed extraction model further experiments covering a wide range of H_3PO_4 acid concentrations are needed. Such investigations are in progress, which also consider the thermodynamics of the variation of the stoichiometric extraction constants with the phosphoric acid concentration.

REFERENCES

1 Facon S, Cote G and Bauer D. *Solvent Extr. Ion Exch.*, **9(5)**, 717, (1991).
2 Menoyo B, Benito R and Elizalde MP. *Solvent Extr. Ion Exch.*, **14(1)**, 69, (1996).
3 Almela A, Elizalde MP and Gómez JM. *Fluid Phase Equilibria*, **145**, 301, (1998).
4 Elmore KL, Hatfield JD, Dunn RL and Jones AD. *J. Phys. Chem.*, **69**, 3520, (1965).
5 Stenström S, Wingefors S and Aly G. *Solvent Extr. Ion Exch.*, **4(5)**, 883, (1986).
6 Liem DH. *Acta Chem. Scand.*, **25**, 1521, (1971).
7 Almela A, Elizalde MP and Menoyo B. *J. Solution Chem.*, **23**, 685, (1994).

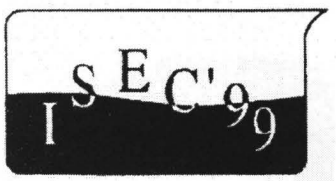

SOLVENT EXTRACTION OF SCANDIUM(III) WITH CYANEX 302 AND H[BTMPTP]

Deqian Li [1], Chun Wang [2] and Zhengui Wei [1]

[1]Laboratory of Rare Earth Chemistry & Physics, Changchun Institute of Applied Chemistry, Chinese Academy of Sciences, Changchun 130022, China

[2] Department of Metallurgy, Beijing General Research Institute of Mining & Metallurgy, Beijing 100044, China

ABSTRACT

The solvent extraction of Sc(III) from acidic sulphate media with as-received Cyanex 302 and purified Cyanex 302 (hereafter abbreviated as H[BTMPTP], HA) was studied. H[BTMPTP] has a weaker extracting ability for Sc(III) than the as-received Cyanex 302. The results of FAB-MS spectra of the extractants indicate that the content of R_3PO decreases sharply and those of $R_2PS(OH)$ and $R_2PO(OH)$ increase significantly in H[BTMPTP] (where R represents 2,4,4-trimethylpentyl). According to the composition of Cyanex 302, the extraction of Sc(III) with H[BTMPTP], purified Cyanex 272 (H[BTMPP]), Cyanex 925 (branched chain alkylated phosphine oxide mixture), and their mixed solutions were carried out. It was found that there was a synergistic effect in the extraction when Cyanex 925 was present together with H[BTMPTP] at the lower aqueous acidities, and the extraction ability is relatively close to that of the as-received Cyanex 302. This means that the stronger extraction ability of Cyanex 302 may be primarily ascribed to the synergistic extraction effect of its components $R_2PS(OH)$, R_3PO and $R_2PO(OH)$. The results of FAB-MS spectra of Sc(III) complexes with Cyanex 302 and H[BTMPTP] confirmed the conjecture proposed. A synergistic effect was observed between H[BTMPTP] and Cyanex 925 on the Sc(III) extraction at the lower aqueous acidity less than 0.25 M H_2SO_4. The stoichiometry of the synergistic extraction reaction was postulated based on slope analysis. The composition of the extracted complex was determined to be $Sc(HA_2)_2C_3(SO_4^{2-})_{1/2}$.

Keywords: scandium, sulphate, Cyanex 302, bis(2,4,4-trimethylpentyl)mono-thiophosphinic acid, FAB-MS spectra

INTRODUCTION

Thiosubstituted organophosphorus compounds have been widely studied for the extraction of most soft and borderline metals such as Pd(II), Pt(II), Ag(I), Cd(II) and Zn(II), etc.[1,2] More recently, the extractant Cyanex 302 (bis(2,4,4-trimethylpentyl)-mono-thiophosphinic acid), which is the monothio analogue of Cyanex 272, has been introduced by Cytec Industries Inc.[3] It has been reported that this reagent is significantly more resistant toward decomposition by hydrolysis than its phosphoro analogues.[4] Many papers have been published concerning the general characteristics and extraction performance of first transition metals such as Zn(II), Co(II), and Cu(II) etc. with this reagent.[5,6,7] However, less work has been conducted on the extraction of rare earths with Cyanex 302.

The extraction distribution of lanthanides and scandium by as-received Cyanex 302 and purified Cyanex 302 (H[BTMPTP]) was studied in earlier works.[8,9] It was found that Cyanex 302 has a higher affinity toward these metals than H[BTMPTP]. This is believed to be ascribed to the presence of impurity components such as organophosphine oxide in Cyanex 302.

In this paper, FAB-MS spectra of Cyanex 302, H[BTMPTP] and their scandium complexes were measured to study the role of the different components in Cyanex 302. Cyanex 925 (a branched chain alkylated phosphine oxide mixture), commercially available solvating reagent from Cytec Industries Inc., was added to H[BTMPTP] solution as an alkylphosphine oxide to simulate the extraction ability difference. The synergistic extraction of Sc(III) with H[BTMPTP] and Cyanex 925 was also studied.

EXPERIMENTAL

Reagents

The extractants Cyanex 302 and Cyanex 925 was kindly supplied by Cytec Canada Inc. Cyanex 302 was used as received or purified by precipitation of the cobalt salt. Cyanex 925 was used without further purification. The diluent was n-hexane of analytical grade.

© 2000 Society of Chemical Industry

The stock solution of scandium was prepared by dissolved its oxide into the sulphuric acid solution of appropriate concentration. All other reagents were analytical grade.

Extraction and Analytical Procedures

Equal volumes of aqueous and organic phases were placed into equilibrium tubes and shaken for 30 min at room temperature (25±1°C). After equilibration both phases were separated by centrifuging. Metal contents of the aqueous phases were determined by spectrophotometry using a Shimadzu model UV-365 instrument. Metal contents of the organic phases were determined by difference. The aqueous acidity was determined by titration with standard sodium hydroxide solution using phenolphthalein as indicator. The concentrations of Cyanex 302 and H[BTMPTP] were determined by titration with standard NaOH solution in ethanol-water mixture.

Mass spectra of the extractants and scandium complexes were determined using a fast-atom (caesium) bombardment excitation source (FAB-MS) on a VG Quattro instrument. The samples were dissolved in nitrobenzylalcohol. Fragments having a mass-to-charge ratio from 100 to 2000 were detected.

RESULTS AND DISCUSSION

Extraction Equilibria of Sc(III) with Cyanex 302 and H[BTMPTP]

The extraction equilibrium data of Sc(III) with as-received Cyanex 302 and purified Cyanex 302 (H[BTMPTP) from sulphuric acid solutions were obtained. The result is shown in Figure 1. The distribution ratio (D) of Sc(III) decreases with increasing aqueous acidity, up to 3.0 mol/dm^3 H_2SO_4, and increases with increasing aqueous acidity at higher acidity than 3.5 mol/dm^3 H_2SO_4. This means that the extraction of Sc(III) proceeds by a cation exchange reaction in the range of lower aqueous acidity and a solvation reaction in the range of higher aqueous acidity. It was found that the extraction ability of H[BTMPTP] is significantly lower than that of the as-received Cyanex 302.

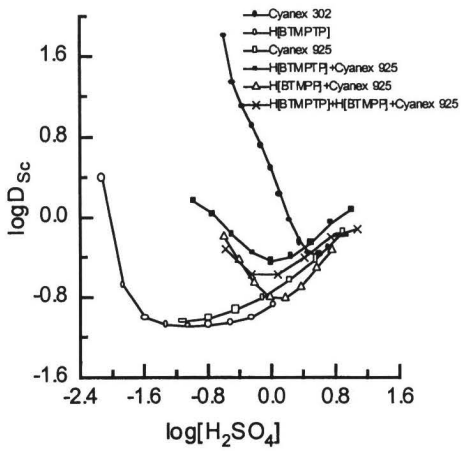

Figure 1. Extraction of Sc(III) with Cyanex 302, H[BTMPTP], Cyanex 925, H[BTMPP] and their mixture solutions. (●) 4.83×10^{-2} mol/dm^3 Cyanex 302; (○) 4.83×10^{-2} mol/dm^3 H[BTMPTP]; (□) 4.83×10^{-3} mol/dm^3 Cyanex 925; (■) 4.83×10^{-2} mol/dm^3 H[BTMPTP]+1.20×10^{-2} mol/dm^3 Cyanex 925; (Δ) 4.83×10^{-2} mol/dm^3 H[BTMPP] + 4.83×10^{-3} mol/dm^3 Cyanex 925; (×) 4.83×10^{-2} mol/dm^3 H[BTMPTP] + 1.50×10^{-3} mol/dm^3 H[BTMPP] + 4.83×10^{-3} mol/dm^3 Cyanex 925.

According to the composition of Cyanex 302 reported by Sole et al.,[5] Cyanex 302 consists of 78-80% bis(2,4,4-trimethylpentyl)monothiophosphinic acid ($R_2PS(OH)$), 10-12% tris(2,4,4-trimethylpentyl)phosphine oxide (R_3PO), 2-3% bis(2,4,4-trimethylpentyl)-phosphinic acid ($R_2PO(OH)$),

2% bis(2,4,4-trimethylpentyl)dithiophosphinic acid ($R_2PS(SH)$), and 8% unknown components. Based on this analysis, n-hexane solutions of H[BTMPTP], Cyanex 925, H[BTMPP] (denoting the purified Cyanex 272) and their binary or ternary mixture were used to simulate the difference in extractability of Sc(III) by Cyanex 302 and H[BTMPTP]. The result is also shown in Figure 1.

The results show that the extraction of Sc(III) with Cyanex 925 proceeds by a solvation reaction, the distribution ratio of Sc(III) increases with increasing aqueous acidity, especially at the higher aqueous acidity. The extractability of Sc(III) increases when Cyanex 925 is added to either of H[BTMPTP] or H[BTMPP] solutions, especially at the lower aqueous acidity. The extractability by binary mixture of H[BTMPTP] and Cyanex 925 is relatively close to that of the as-received Cyanex 302. Although the ternary mixture of H[BTMPTP], H[BTMPP] and Cyanex 925 cannot extract Sc(III) as well as the as-received Cyanex 302, it can be inferred that there may be a synergistic effect in the extraction of Sc(III) with H[BTMPTP], H[BTMPP] and the trialkylphosphine oxide components in Cyanex 302.

FAB-MS Spectra of Cyanex 302 and H[BTMPTP]

The FAB mass spectra of Cyanex 302 and H[BTMPTP] are shown in Figure 2 (where A = R_2PSO^-, L = R_2POO^-, B = R_3PO). In the mass spectrum of Cyanex 302, HA (+ H^+: M/e = 307), $(HA)_2$ (+ H^+: M/e = 613), HL (+ H^+: M/e = 291), $(HL)_2$ (+ H^+: M/e = 581), and B (+ H^+: M/e = 387) were observed.

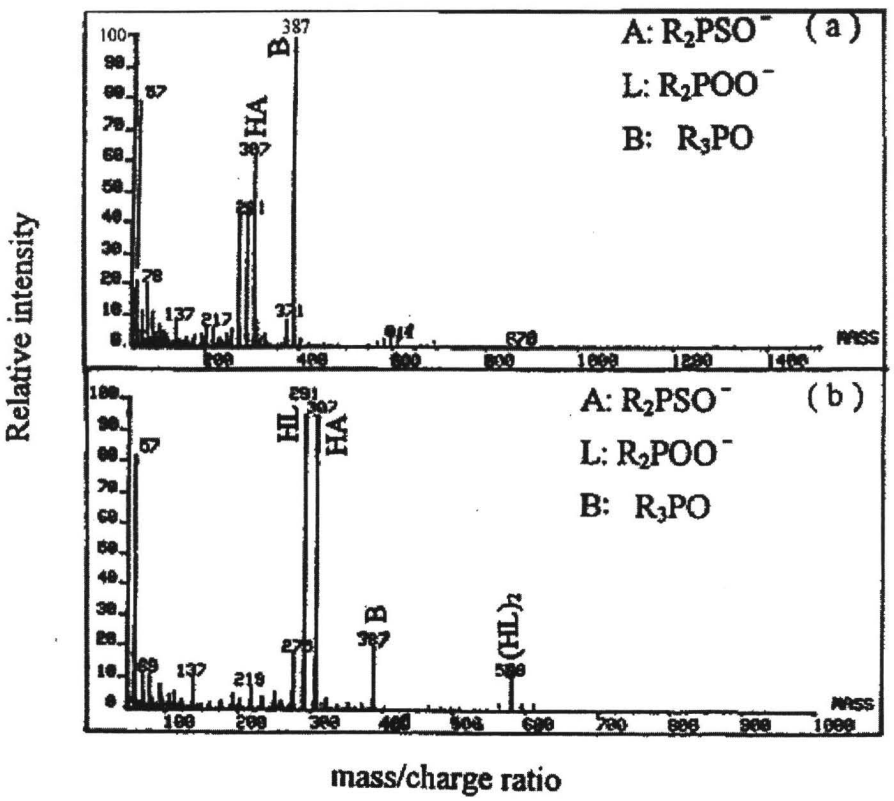

Figure 2. FAB-MS Spectra of Cyanex 302 and H[BTMPTP]. (a) Cyanex 302; (b) H[BTMPTP]

The spectrum illustrates the presence of monomer and dimer of bis-(2,4,4-trimethylpentyl)monothiophosphinic acid, monomer and dimer of bis-(2,4,4-trimethylpentyl)phosphinic acid, and trialkylphosphine oxide (R_3PO) in Cyanex 302. In the mass

spectrum of H[BTMPTP], the relative intensities of species HA, HL and $(HL)_2$ increase, while that of species B decreases. The comparison of these mass spectra indicates that the content of dialkylmonothiophosphinic acid and dialkylphosphinic acid increases, while that of trialkylphosphine oxide impurity decreases significantly in H[BTMPTP].

FAB-MS Spectra of Sc(III) Complexes with Cyanex 302 and H[BTMPTP]

The FAB mass spectra of the Sc(III) complexes with Cyanex 302 and H[BTMPTP] are shown in Figure 3.

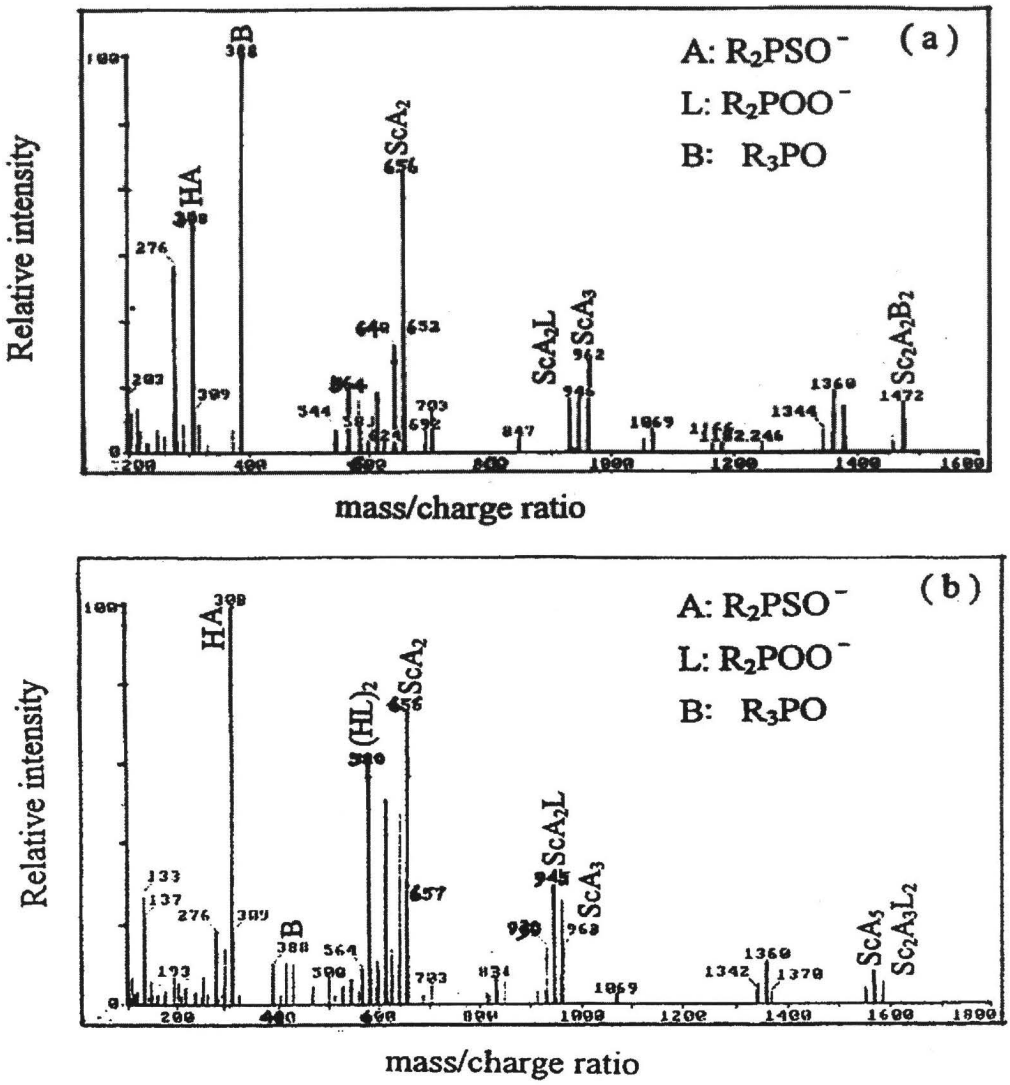

Figure 3. FAB-MS Spectra of Sc(III) complexes with Cyanex 302 (a) and H[BTMPTP] (b).

This fragmentation pattern illustrates the formation of multinuclear species and association of complexes. In the mass spectrum of Sc(III) complex with Cyanex 302 (Figure 3(a)), the species ScA_2, ScA_3, Sc_2A_2L, and $Sc_2A_2B_2$ were detected (charges on fragments not shown). The observation of species of Sc_2A_2L, and $Sc_2A_2B_2$ provides further evidence that Sc(III) is co-ordinated to both the R_3PO, R_2POO^- impurities and R_2PSO^- in Cyanex 302. Therefore, these impurity components in Cyanex 302 contribute to the extraction of Sc(III). In the mass spectrum of Sc(III) complex with H[BTMPTP] (Figure 3(b)), the species ScA_2, ScA_3, ScA_2L, ScA_5, and $Sc_2A_3L_2$ were detected. It is interesting to notice that there is no species, which consists of A and B, appears in the spectrum. The comparison of these spectra indicates that the lower extractability of Sc(III) with H[BTMPTP] can be ascribed primarily to the removal of the trialkylphosphine oxide impurity from Cyanex 302.

To study the synergistic effect of $R_2PS(OH)$ and R_3PO in Cyanex 302, H[BTMPTP] and Cyanex 925 were adopted as the dialkylmonothiophosphinic acid and trialkylphosphine oxide, respectively. A synergistic effect was observed on the Sc(III) extraction with H[BTMPTP] and Cyanex 925 at the aqueous acidity less than 0.25 mol/dm^3 H_2SO_4. The synergistic extraction reaction has been studied systematically in a previous paper.[10] The stoichiometry, based on slope analysis, was postulated as the following equation: [10]

$$Sc^{3+} + 2(HA)_{2(o)} + 3C_{(o)} + 1/2\ SO_4^{2-} \rightleftharpoons Sc(HA_2)_2C_3(SO_4^{2-})_{1/2\,(o)} + 2H^+ \qquad (1)$$

Where HA and C denote H[BTMPTP] and Cyanex 923, respectively. The composition of the extracted complex was determined to be $Sc(HA_2)_2C_3(SO_4^{2-})_{1/2}$.

CONCLUSIONS

Cyanex 302 can extract more Sc(III) than H[BTMPTP]. The comparison of the results of FAB-MS spectra indicates that the stronger extraction ability of Cyanex 302 is primarily attributed to the synergistic extraction effect of its components $R_2PS(OH)$, R_3PO and $R_2PO(OH)$, especially that of $R_2PS(OH)$ and R_3PO. The study on the synergistic extraction of Sc(III) with H[BTMPTP] and Cyanex 925 provides further evidence on explanation of the extraction ability difference between Cyanex 302 and H[BTMPTP].

ACKNOWLEDGEMENTS

The authors wish to thank Dr. W. A. Rickelton of Cytec Canada, Inc., for the samples of Cyanex 272, Cyanex 302 and Cyanex 925. Dr. Yiming Se is acknowledged for experimental assistance and helpful discussions about FAB-MS spectra of this work.
This work was supported by the National Program "The Basic Research of Rare Earths" of China.

REFERENCES

1. Handley TH. *Talanta*, **12**, 893, (1965).
2. Cote G and Bauer D, *Rev. Inorg. Chem.* **10**, 121, (1989).
3. Rickelton WA and Boyle RJ, *Sep. Sci. Technol.*, **23**, 1227, (1988).
4. Rickelton WA and Boyle RJ, *Solv Extr. Ion Exch.*, **8**, 783, (1990).
5. Sole KC and Hiskey JB, *Hydrometallurgy*, **30**, 345, (1992).
6. Alguacil FJ, Cobo A and Caravaca, *Hydrometallurgy*, **31**, 174, (1992).
7. Tait BK, *Hydrometallurgy*, **32**, 365, (1993).
8. Yuan M, Wang C and Li D, *Acta Metallurgica Sinica* (English Letters), **8**, 10, (1995).
9. Wang C and Li D, *Solv Extr. Ion Exch.*, **13**, 503, (1995).
10. Wei Z, Li D, Wang C and Jiang Z, *Chemical J. Chinese Universities*, **18**, 1281, (1997).

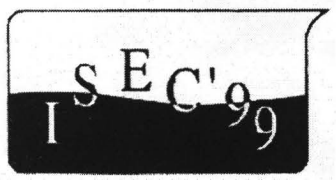

SOLVENT EXTRACTION OF SCANDIUM(III) BY CYANEX 272 AND H[BTMPP]

Chun Wang[1] and Deqian Li[2]

[1] Department of Metallurgy, Beijing General Research Institute of Mining & Metallurgy,
Beijing 100044, China

[2] Laboratory of Rare Earth Chemistry & Physics, Changchun Institute of Applied Chemistry, Chinese Academy of Sciences, Changchun 130022, China

ABSTRACT

The extraction equilibrium data of scandium from sulphuric acid media by as-received Cyanex 272 (bis(2,4,4-trimethylpentyl) phosphinic acid) and purified Cyanex 272 (hereafter abbreviated as H[BTMPP]) were obtained. It was found that the extraction ability of Cyanex 272 toward scandium is slightly greater than that of H[BTMPP]. The stoichiometry of extraction reaction and the geometry of the extracted complexes are postulated. Cyanex 272 behaves as a bidentate ligand and combines in a 1:3 stoichiometric ratio with scandium. The FAB-MS spectra of Cyanex 272 and H[BTMPP] indicate that the content of R_3PO in H[BTMPP] decreases and the content of R_2POOH increases in contrast with those in Cyanex 272 (where R represents 2,4,4-trimethylpentyl). In the FAB-MS fragmentation spectrum of scandium complex with Cyanex 272, the fragments ScL_2, ScL_3, Sc_2L_2B, ScL_4, Sc_2L_3B and Sc_2L_5 ($L=R_2POO^-$, $B=R_3PO$) are observed. These results provide the evidence that scandium is coordinated to the R_3PO species in Cyanex 272. The greater Sc(III) extraction ability of Cyanex 272 can be attributed to the presence of R_3PO in Cyanex 272.

Keywords: scandium(III), sulphate, Cyanex 272, bis(2,4,4-trimethylpentyl)phosphinic acid, FAB-MS Spectra

INTRODUCTION

The organophosphorus extractant Cyanex 272, which was originally developed for the separation of cobalt and nickel from weakly acidic sulfuric media, has been commercially available from American Cyanamid Company (now Cytec Industries Inc.) for about a decade.[1,2] To date, a number of fundamental studies of cobalt and nickel extraction by Cyanex 272 has been published.[3,4] Recently, the solvent extraction of trivalent lanthanides and scandium by Cyanex 272 from various acidic media has been investigated.[5,6,7] The potential application of Cyanex 272 in the separation of rare earths, especially the heavy rare earths, was evaluated.[6]

Cyanex 272 contains bis(2,4,4-trimethylpentyl)phosphinic acid (H[BTMPP]) as the main component and tri(2,4,4-trimethylpentyl)phosphine oxide as an impurity. The amount of alkylphosphine oxides in the Cyanex 272 was analyzed to be about 10%.[8]

Although solvent extraction of first-row transition metals and rare earths by Cyanex 272 have been widely studied, less work has been conducted on the role of the components of Cyanex 272 in the extraction.[9,10] E. Paatero et al. studied the extraction of copper by as-received Cyanex 272 and purified Cyanex 272 (H[BTMPP]) from perchloride acid media, and observed that the as-received Cyanex 272 could extracts more copper than H[BTMPP]. The difference was ascribed to the presence of alkylphosphine oxide in Cyanex 272. [10]

The extraction of scandium by H[BTMPP] from acidic sulfate or chloride media has been previously reported.[6,7] In this work the extraction of scandium by Cyanex 272 and H[BTMPP] from sulphuric acid media are compared to study the role the alkylphosphine oxide in Cyanex 272. The stoichiometry of extraction reaction and the geometry of the extracted complexes are postulated.

© 2000 Society of Chemical Industry

EXPERIMENTAL

Reagents

Cyanex 272 was kindly supplied by Cytec Canada Inc. The extractant was used as received or purified by precipitation of the copper salt. The mono acid contents of Cyanex 272 and H[BTMPP] were 87% and 98%, respectively. The diluent was n-hexane of analytical grade.
The stock solution of scandium was prepared by dissolved its oxide into the sulphuric acid solution of appropriate concentration. All other reagents were analytical grade.

Extraction and Analytical Procedures

Equal volumes of aqueous and organic phases were placed into equilibrium tubes and shaken for 30 min at room temperature (25±1°C). Both phases were separated by centrifuging after equilibrium was reached. Metal contents of the aqueous phases were determined by spectrophotometry using a Shimadzu model UV-365 instrument. Metal contents of the organic phases were determined by difference. The aqueous acidity was determined by titration with standard sodium hydroxide solution using phenolphthalein as indicator. The concentrations of Cyanex 272 and H[BTMPP] were determined by titration with standard NaOH solution in ethanol-water mixture.

Mass spectra of the extractant and scandium complex were determined using a fast-atom (cesium) bombardment excitation source (FAB-MS) on a VG Quattro instrument. The samples were dissolved in nitrobenzylalcohol. Fragments having a mass-to-charge ratio from 100 to 2000 were detected. Infrared spectroscopy (IR) spectra of extractant and scandium complex were measured across the wavenumber range 4000-500 cm^{-1}, using a Brucker model IFS-113V instrument.

RESULTS AND DISCUSSION

Extraction of Scandium by Cyanex 272 and H[BTMPP]

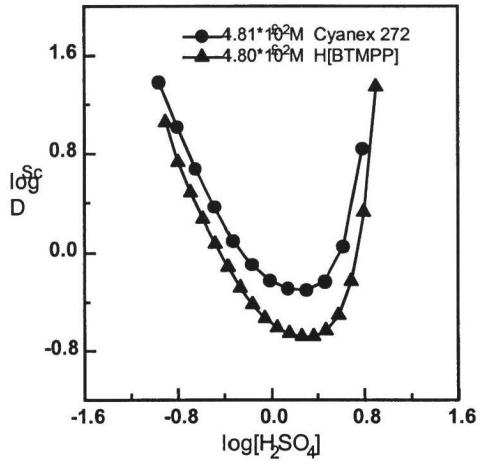

Figure 1. Extraction of Scandium by Cyanex 272 and H[BTMPP]. Aqueous phase: 5.04×10^{-4} M Sc as sulfate. Organic phase: (●) 4.81×10^{-2} M Cyanex 272; (▲) 4.80×10^{-2} M H[BTMPP].

The extraction equilibria of scandium by as-received Cyanex 272 and purified Cyanex 272 (H[BTMPP]) from sulfuric acid media were studied under different aqueous acidities. Cyanex 272 was used at an equivalent H[BTMPP] concentration for comparison. The results are shown in Figure 1.

The distribution ratio of scandium by either Cyanex 272 or H[BTMPP] decreases with increasing aqueous acidity, up to 1.5 M H_2SO_4, and increases with increasing acidity at higher acidity than 2.0 M H_2SO_4. This means that solvent extraction of scandium by Cyanex 272 and H[BTMPP] occurs via a cation exchange reaction in the range of lower aqueous acidity and a solvation reaction in the range of higher aqueous acidity. It is interesting to notice that Cyanex 272 extracts more scandium than H[BTMPP] under the aqueous acidities studied. This difference in extractability of scandium may be attributed to the presence of the trialkylphosphine oxide in Cyanex 272.

Stoichiometry of the Extracted Scandium Complex

Equal volumes of organic phase (0.06 M Cyanex 272 in hexane) and aqueous phase (0.045 M $Sc_2(SO_4)_3$) were contacted at aqueous acidity of 0.05 M H_2SO_4 in an separatory funnel. After equilibrium, the raffinate was measured to determine scandium concentration and the loaded organic phase was re-contacted with fresh aqueous phase until the scandium concentration in the raffinate was the same as the initial concentration. The scandium concentration in the saturated loaded organic phase was determined by mass balance. The result is shown in Table 1, where subscript (o) represents organic phase, and HL, Cyanex 272. The ratio of scandium to Cyanex 272 in the organic phase is 1:2.92, closes to 1:3. The concentration of sulfate ion in the organic phase could be neglected in comparison with that of scandium. The saturated scandium complex formed with Cyanex 272, thus, is postulated to be ScL_3. The scandium extraction by Cyanex 272 can be expressed as follow: [11]

$$Sc^{3+} + \longrightarrow 1.5(HL)_{2(o)} \qquad ScL_{3(o)} + 3H^{+} \qquad (1)$$

$[Sc(III)]_{(o)}$ (M)	$[SO_4^{2-}]_{(o)}$ (M)	$[HL]_{(o)}$ (M)	[Sc(III)]/[HL]	$[SO_4^{2-}]$/[Sc(III)]
0.027	6.77×10^{-5}	0.062	1:2.92	3.25×10^{-3}

Table 1 Composition of the Saturated Scandium Complex with Cyanex 272

IR Spectra of Cyanex 272 and Scandium Complex with Cyanex 272

The extracted scandium complex was examined by IR spectrophotometry. IR spectrum of Cyanex 272 shows P-O-H stretching and bending bands at 2500-1700 cm^{-1}, P=O stretching band at 1172 cm^{-1}, P-O-H stretching band at 960 cm^{-1}. In the spectrum of scandium complex, the intensities of P-O-H stretching and bending bands at 2500-1700 cm^{-1} decrease significantly, P=O absorption band at 1172 cm^{-1} shifts to lower frequency 1142 cm^{-1}, symmetrical and asymmetrical stretching bands of POO^- appear at 1144-1061 cm^{-1}. P-OH stretching band at 960 cm^{-1} becomes weaker remarkably. The IR result provides evidence that the hydroxy proton of P-OH is substituted by scandium in the extracted complex and confirms that the extraction proceeds by a cation exchange reaction.

FAB-MS Spectra of Cyanex 272 and H[BTMPP]

The FAB mass spectra of Cyanex 272 and H[BTMPP] are shown in Figure 2 (where L=R_2POO^-, B=R_3PO). In the mass spectrum of Cyanex 272, HL (+ H^+: M/e=291), $(HL)_2$ (+ H^+: M/e=581) and B (+ H^+: M/e=387) were observed. The spectrum illustrates the presence of monomer and dimer of bis(2,4,4-trimethylpentyl)phosphinic acid, and trialkylphosphine oxide (R_3PO) in Cyanex 272. In the mass spectrum of H[BTMPP], the relative intensity of species $(HL)_2$ increases, while that of species B decreases. The comparison of these mass spectra indicates that the content dialkylphosphinic acid increases and trialkylphosphine oxide impurity decreases significantly in H[BTMPP].

FAB-MS Spectrum of Scandium Complex with Cyanex 272

The FAB mass spectrum of the scandium complex with Cyanex 272 is shown in Figure 3. This fragmentation pattern illustrates the formation of multinuclear species. The species ScL_2, ScL_3, Sc_2L_2B,

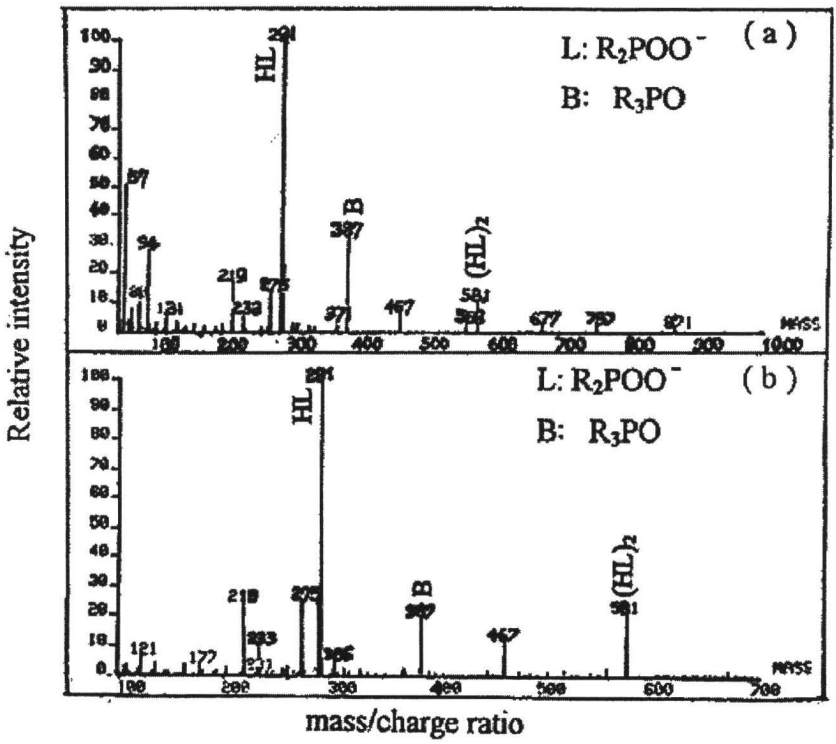

Figure 3. FAB-MS Spectrum of Scandium Complex with Cyanex 272

ScL_4, Sc_2L_3B and Sc_2L_5 were detected in the mass spectrum (charges on fragments not shown). The observation of species of ScL_3 provides further evidence that Cyanex 272 combines in a 1:3 stoichiometric ratio with scandium. The species Sc_2L_2B and Sc_2L_3B occur in the mass spectrum indicate that scandium coordinates with the R_3PO component of Cyanex 272. This result confirms that the greater extractability of scandium by Cyanex 272 can be ascribed to solvation of the trialkylphosphine oxide impurity. The proposed oligomeric structure of species Sc_2L_3B is shown in Figure 4.

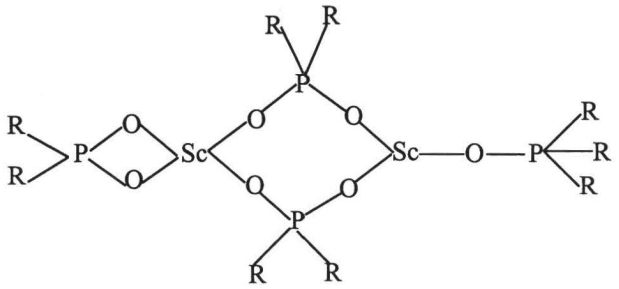

Figure 4. Postulated Oligomeric Structure of Species Sc_2L_3B

CONCLUSIONS

Comparison of the solvent extraction of scandium by as-received Cyanex 272 and purified Cyanex 272 (H[BTMPP]) shows that Cyanex 272 extracts more scandium than H[BTMPP]. The FAB-MS spectra of Cyanex 272, H[BTMPP] and scandium complex with Cyanex 272 demonstrate that oligomeric multinuclear scandium complex is formed. Scandium is coordinated primarily to the R_2POO^- species and also to R_3PO impurity in Cyanex 272. Therefore, the greater extractability of scandium by Cyanex 272 can be ascribed to the solvation of the trialkylphosphine oxide impurity.

ACKNOWLEDGEMENTS

The authors wish to thank Dr. W. A. Rickelton of Cytec Canada, Inc. for the sample of Cyanex 272. Dr. Yiming Se is acknowledged for experimental assistance and helpful discussions about FAB-MS fragment spectra of this work.
This work was supported by the National Program "The Basic Research of Rare Earths" of China.

REFERENCES

1. Rickelton WA, Flett DS and West DW, *Solv. Extr. Ion Exch.*, **2**, 815, (1984).
2. Rickelton WA and Boyle RJ, *Sep. Sci. Technol.*, **23**, 1227, (1988).
3. Danesi PR, Reichley-Yinger L, Mason G, Kaplan L, Horwitz EP and Diamond H, *Solv Extr. Ion Exch.*, **3**, 435, (1985).
4. Yuan CY, Xu Q, Yuan S, Long H, Shen D, Jiang Y, Feng H, Wu F and Chen W, *Solv Extr. Ion Exch.*, **6**, 393, (1988).
5. Li K and Freiser H. *Solv. Extr. Ion Exch.*, **4**, 739, (1986).
6. Li D, Ma G and Zhang X, *Proc. Int Solv Extr Conf (ISEC'93)*, SCI/Elsevier Science Pub, **1**, 384, (1993).
7. Wang C and Li D, *Solv Extr. Ion Exch.*, **12**, 615, (1994).
8. Sole KC and Hiskey JB, *Hydrometallurgy*, **30**, 345, (1992).
9. Danesi PR, Reichley-Yinger L, Cianetti C and Rickert PG, *Solv Extr. Ion Exch.*, **2**, 781, (1984).
10. Paatero E, Lantto T and Ernola P, *Solv Extr. Ion Exch.*, **8**, 371, (1990).
11. Wang C, *Ph D Thesis*, Changchun Institute of Applied Chemistry, (1996).

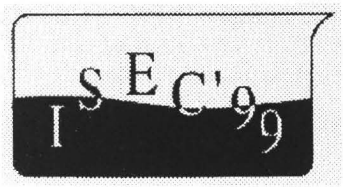

SOLVENT EXTRACTION OF TIN(IV) FROM HYDROCHLORIC ACID SOLUTIONS BY HIGH MOLECULAR WEIGHT AMINES

Taichi Sato,[1,2] Keiichi Sato[1] and Yoshitomo Noguchi[1]

[1]Faculty of Engineering, Shizuoka University, Hamamutsu, 432 Japan

[2]Metallurgical Engineering Department, Queen's University, Kingston, Ontario K7L 3N6, Canada

ABSTRACT

The extraction of tin(IV) from hydrochloric acid solutions by trioctylamine (TOA) and trioctylmethylammonium chloride (TOMAC) in benzene was investigated under various conditions. The organic extracts were also examined by infrared and nuclear magnetic resonance spectroscopies. On the basis of the results obtained, the equilibrium expressions for the extraction by TOA and TOMAC are proposed as follows: for TOA, $SnCl_4(aq) + 2R_3NHCl(org)$ ...$(R_3NH)_2SnCl_6(org)$; for TOMAC, $SnCl^{2-}(aq) + 2R_3R'NCl(org)$...$(R_3R'\text{-}N)_2SnCl_6(org) + 2Cl^-(aq)$, in which the extraction efficiency for $tin(IV)^3$ is in the order TOMAC > TOA.

Keywords: tin(IV), chloride, trioctylamine, trioctylmethylammonium chloride

INTRODUCTION

In a previous study,[1] the extraction of tin(IV) from hydrochloric acid solutions was investigated using di-(2-ethylhexyl)phosphoric acid (DEHPA). In addition, studies have been made of the extraction of some metals from aqueous solutions by trioctylamine (TOA) or trioctylmethylammonium chloride (TOMAC). The present paper extends this work to include the extraction of tin(IV) from hydrochloric acid solutions by TOA and TOMAC.

EXPERIMENTAL

Reagents.

TOA and TOMAC (Koei Chem. Co., Ltd.) of high purity were used without further purification and diluted with benzene. Aqueous solutions containing tin were prepared by dissolving stannic chloride ($SnCl_4.xH_2O$) in hydrochloric acid of the required concentration. In general, the aqueous metal concentration was 1g dm^{-3} stannic chloride except for the loading test. Other chemicals were of analytical reagent grade.

Extraction and analytical procedures.

Equal volumes (15 cm^3 each) of organic and aqueous phases placed in 50 cm^3 stoppered conical flasks were shaken for 10 minutes in a thermostatic water bath at 20°C except for the examination of temperature effect. Preliminary experiments showed that equilibration was complete in 10 minutes. The mixture was centrifuged and separated, and then both phases were assayed to determine the distribution coefficient (E, the ratio of the equilibrium concentration of tin in the organic phase to that in the aqueous phase). Tin was stripped from the organic phase with 0.1 mol dm^{-3} hydrochloric acid solution. The tin concentration in the aqueous solution was determined by titration with EDTA using xylenol orange (XO) as the indicator. The concentration of chloride and the water content in the organic phase were examined by Volhard's method with nitrobenzene and by Karl Fisher titration, respectively.

IR and NMR spectroscopies.

Infrared (IR) spectra of the samples prepared by evaporation of the organic diluent were measured on JASCO models IRA-1 (4000-650 cm^{-1}) and IR-F (700-200 cm^{-1}) using capillary film

© 2000 Society of Chemical Industry

between thallium halide plates or polyethylene films. Nuclear magnetic resonance (NMR) spectra of the organic solutions from the extraction with carbon tetrachloride as diluent were obtained on a JEOL model JNM-PMX60SI NMR spectrometer by using tetramethylsilane as an internal reference.

RESULTS AND DISCUSSION

Extraction isotherms.

The extraction of tin(IV) from hydrochloric acid solutions by TOA gave the results shown in Figure 1. This indicated that the distribution coefficient rose with increasing aqueous acidity to the maximum, which occurred at initial hydrochloric acid concentration of 7 mol dm^{-3}, and then fell. When hydrochloric acid in the aqueous phase was partly replaced by lithium chloride, it was observed that the distribution coefficient from the mixed aqueous phase, 0.2 mol dm^{-3} hydrochloric acid-lithium chloride solutions, by TOA increased continuously with chloride ion concentration. In the extraction of tin(IV) by TOMAC, as indicated in Figure 2, the shape of the extraction curve was similar to that by TOA, although the extraction efficiency for tin(IV) was in the order TOMAC>TOA: the distribution coefficient from hydrochloric acid solutions passed through the maximum at 5 - 7 mol dm^{-3} hydrochloric acid concentration; while the distribution coefficient from aqueous mixed solutions of 1 mol dm^{-3} hydrochloric acid and lithium chloride increased gradually with aqueous chloride concentration.

The log-log plots of E vs. [TOA] or [TOMAC] $-n[Sn]_{org}$, where n is the solvation number, at constant hydrochloric acid concentration gave straight lines with slopes of ~2 for TOA and ~2 for TOMAC in the cases of n = 2 and 2, respectively; 2.0, 2.0, 2.4, 2.4 and 2.1 for TOA and 1.8, 1.9, 1.9, 2.0 and 2.0 for TOMAC at 1, 3, 5, 7 and 10 mol dm^{-3} hydrochloric acid, respectively. These results revealed the second- and second-power dependencies on TOA and TOMAC concentrations, respectively. In addition, the stoichiometry of the extracted species was examined by a loading test of tin to the organic phase: with increasing tin concentration in the aqueous phase, the molar ratios [Sn]/[Cl]/[TOA]/[H_2O] and [Sn]/[Cl]/[TOMAC]/[H_2O] approached 1 : 6 : 2 : 9, in the extraction of tin(IV) from 7 mol dm^{-3} hydrochloric acid solution with 0.02 mol dm^{-3} TOA and TOMAC in benzene. Hence, it was considered that the extraction of tin(IV) from hydrochloric acid solutions by TOA and TOMAC can be expressed by the following equilibrium equations:

for the extraction by TOA

$$SnCl_4(a) + 2R_3NHCl(o) \leftrightarrow (R_3NH)_2SnCl_6(o), \quad (1)$$

and for the extraction by TOMAC

$$SnCl^{2-}_6(a) + 2R_3R'NCl(o) \leftrightarrow (R_3R'N)_2SnCl_6(o) + 2Cl^-(a) \quad (2)$$

in which (a) and (o) denote aqueous and organic phases, respectively.

IR and NMR spectra.

The organic extracts of tin(IV) from hydrochloric acid solutions by TOA and TOMAC in benzene were examined by IR spectrophotometry. With increasing the tin concentration in the organic phase, the OH stretching band at 3400 cm^{-1} and the OH bending band at 1640 cm^{-1} decreased in intensity, and the bands almost disappeared completely in the metal-saturated organic extracts. These results suggested that the extracted species have no water molecules, corresponding to the results for the measurement of water content in the organic phase. Further, the organic extracts exhibited the following absorptions in addition to the absorption bands of alkyl groups due to TOA and TOMAC:[2,3] for the extracts by TOA, the NH^+ stretching band which appeared at 2430 cm^{-1} for the TOA HCl salt shifted to 3060 cm^{-1} and the Sn-Cl stretching vibration appeared as the band centred at 300 cm^{-1}; for the extracts by TOMAC, the absorption around 29 cm^{-1} was the result of the Sn-Cl stretching frequency. Accordingly, the IR spectra indicated the formation of a species which co-ordinates the chloride ion to tin; this was supported by the results obtained in the organic phase.

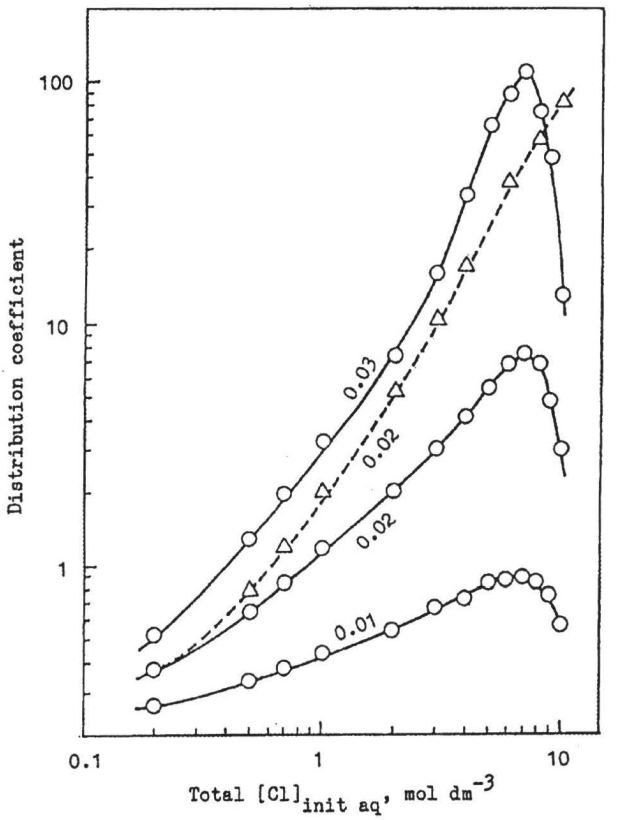

Figure 1. Extraction of tin(IV) from HCl solutions with TOA in benzene (continuous and broken lines represent the extraction from HCl solutions and mixed 0.2 mol dm_3 HCl/LiCl solutions, respectively; numerals on curves are TOA concentrations, mol dm^{-3}).

Further, the organic phases from the extraction of aqueous solutions containing stannic chloride in hydrochloric acid by TOA and TOMAC in carbon tetrachloride were examined by NMR spectroscopy. The organic extracts showed shifts of the methylene protons (and/or methyl proton for TOMAC), attached immediately adjacent to the nitrogen, to a lower field and the disappearance of the water proton signal in addition to the peaks due to the methyl and methylene protons of TOA and TOMAC, while increasing the concentration of tin in the organic phase.[4] These results correspond to those obtained by IR spectra.

It was thus inferred that the extracted species of tin(IV) according to Equations 1 and 2 consist of the complexes $(R_3NHCl)_2SnCl_6$ and $(R_3R'N)_2SnCl_6$, respectively, displaying a co-ordination number of six.

Temperature effect.

The extraction of tin(IV) from aqueous solutions containing 1 g dm^{-3} stannic chloride in 1 and 5 mol dm^{-3} hydrochloric acid with 0.01 mol dm^{-3} TOA and TOMAC in benzene was carried out at temperatures between 10 and 50°C. The results indicated that the distribution coefficients decreased when temperatures increased, and the values of heat of reaction (change of enthalpy, $-\Delta H$) in Equations 1 and 2 were estimated to be 22.4 and 23.6 kJ mol^{-1} for TOA and 79.1 and 87.5 kJ mol^{-1} for TOMAC, respectively.

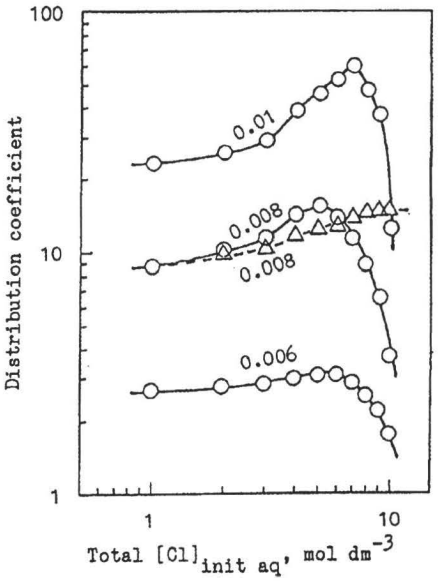

Figure 2. Extraction of tin(IV) from HCl solutions with TOMAC in benzene (continuous and broken lines represent the extraction from HCl solutions and mixed 1 mol dm^{-3} HCl/LiCl solutions, respectively; numerals on curves are TOMAC concentrations, mol dm^{-3}).

CONCLUSION

The extraction of tin(IV) from hydrochloric acid solutions containing stannic chloride was examined under various conditions. In consequence, it was seen that although the extraction efficiency for tin(IV) is in the order TOMAC > TOA, the shape of the extraction curve is similar in both extraction systems. Further, it was determined that these extractions can be expressed by the equilibrium equations:

$$SnCl_4(a) + 2R_3NHCl(o) \leftrightarrow (R_3NH)_2SnCl_6(o)$$

and

$$SnCl^{2-}{}_6(a) + 2R_3R'NCl(o) \leftrightarrow (R_3R'N)_2SnCl_6(o) + 2Cl^-(a).$$

ACKNOWLEDGEMENT

The authors wish to thank Messrs. K. Suga and S. Morita for their assistance with the experimental work.

REFERENCES

1 Sato T and Kikuchi S. *Hydrometallurgy*, **20**, 97, (1988).
2 Sato T *J. Appl. Chem.*, **15**, 10, (1965).
3 Sato T, Watanabe H and Kikuchi S. *J. Appl. Chem. Biotechnol.*, **25**, 63, (1975).
4 Sato T and Watanabe H. *Anal. Chim. Acta*, **49**, 463, (1970); **54**, 439, (1971).

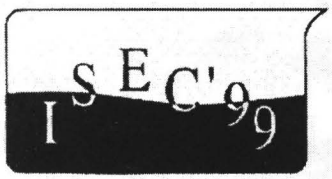

SEPARATION OF CESIUM AND STRONTIUM FROM S-BLOCK METAL IONS BY DOUBLE AND TRIPLE PHASE SYSTEMS

Yu Komatsu[1], Shigeo Umetani[2] and Shigekazu Tsurubou[3]

[1]National Institute for Research in Inorganic Materials, 1-1 Namiki, Tsukuba, Ibaraki 305-0044, Japan

[2]Institute for Chemical Research, Kyoto University, Uji, Kyoto 611-0011, Japan

[3]Department of Chemistry, Asahi University, Hozumi-cho, Gifu 501-0296, Japan

ABSTRACT

Both Sr^{2+} and Cs^{+} have been recognised as toxic components of high level radioactive wastes. To separate Sr^{2+} and Cs^{+} from other s-block metal ions, all metal ions were separated into two groups, namely alkali metal and alkaline earth metal groups by solvent extraction using thenoyltrifluoroacetone (TTA) as the chelating ligand and trioctylphosphine oxide (TOPO) as the auxiliary ligand. The large ion exchangeability of Cs^{+} over other alkali metal ions was used to separate it by ion-exchange using dihydrogen tetratitanate hydrate fibers (DTHF) which has the selectivity $Cs^{+} > Rb^{+} > K^{+} > Na^{+} > Li^{+}$. The separation of Sr^{2+} from other alkaline earth metal ions by solvent-extraction and ion-exchange is not simple as Sr^{2+} lies in the middle of the order of selectivity, namely $Mg^{2+} > Ca^{2+} > Sr^{2+} > Ba^{2+}$ in the former using TTA and TOPO and $Ba^{2+} > Sr^{2+} > Ca^{2+} > Mg^{2+}$ in the latter using DTHF. The complete separation of Sr^{2+} and Ca^{2+} has been achieved by a combination (IX-SX) of ion-exchange with DTHF and solvent extraction with TTA and TOPO by adding the organic phase containing TTA and TOPO to the DTHF ion-exchange system.

Keywords: alkali metals, alkaline earth metals, thenoyltrifluoroacetone, double and triple phase separation (IX-SX), dihydrogen tetratitanate hydrate

INTRODUCTION

The separation of alkali and alkaline earth metal ions has been investigated by solvent-extraction and ion exchange methods. The ligands such as thenoyltrifluoroacetone (TTA),[1,2] tributyl phosphate (TBP)[3] and isopropyl tropolone (IPT),[4] have been used to extract alkaline earth metal ions by solvent extraction. Inorganic ion-exchange materials such as antimonate,[5] zirconium phosphate,[6] and dihydrogen tetratitanate hydrate fibres (DTHF)[7,8] have also been used to separate these metal ions. The complete separation of Sr^{2+} from other alkaline earth metal ions is extremely difficult to accomplish by solvent extraction or ion exchange. This is mainly due to the fact that Sr^{2+} lies in the middle of the order of selectivity for the alkaline earth metals by either solvent extraction or ion exchange. In the present study, the complete separation of Sr^{2+} from Mg^{2+}, Ca^{2+}, and Ba^{2+} has been investigated by employing a triple phase approach which combines solvent extraction with ion exchange methods. This new approach is called IX-SX whereby an organic solvent containing a suitable ligand is added to an aqueous phase - ion-exchange phase pair to obtain the triple phase separation system. The feasibility of IX-SX for difficult separations has been demonstrated by employing it for the separation of Sr^{2+} and Ca^{2+} from a mixture of alkaline earth metal ions. This approach resulted in the separation of Ca^{2+} and Sr^{2+} by the former being extracted into the organic phase and the latter being retained on the ion exchange material. These studies are described.

EXPERIMENTAL

Chemicals

TTA and TOPO were obtained from Dojindo Laboratories. Titanium dioxide used was 99.9% pure. All the other reagents were of analytical grade. Distilled and deionized water was used throughout the experiments. The aqueous standard solutions of alkali metal ions (Cs^{+}, Rb^{+}, K^{+}, Na^{+} and Li^{+}) and alkaline earth metal ions (Ba^{2+}, Sr^{2+}, Ca^{2+} and Mg^{2+}) were prepared by dissolving corresponding chloride salts in water. Layered potassium tetratitanate fibres, $K_2Ti_4O_9$ were first

© 2000 Society of Chemical Industry

synthesized[9] by slow cooling of a K_2MoO_4 flux melt containing K_2CO_3 and TiO_2 (1:3 molar ratio). The $K_2Ti_4O_9$ was converted into an H form according to the following reaction.

$$K_2Ti_4O_9 + nH_2O = H_2Ti_4O_9 \cdot nH_2O + 2K^+ \quad (1)$$

The fibres were washed with water at a rate of 1 dm^3/day until the pH of the effluent was > 5.5 after the potassium ion concentration in the effluent became less than 1 x 10^{-5} mol dm^{-3} as determined by atomic absorption spectrophotometry. The solid product was kept in a constant humidity box controlled by a saturated NaCl solution (relative humidity 70%) to keep the original amount of the interlayer water in the fibres. The fibres on the average were 1 mm in length and 0.01 mm in diameter.

Solvent extraction separation of metal ions

Stoppered glass tubes of 23 cm^3 were used to contact 10 cm^3 of an aqueous solution and 10 cm^3 of benzene containing TTA and TOPO. The aqueous solution contained the alkaline earth metal ion in the form of chloride with the concentration of $1x10^{-4}$ mol dm^{-3} and acetate buffer of $5x10^{-3}$ mol dm^{-3}. The pH of the aqueous solution was adjusted with perchloric acid or sodium hydroxide solution. The tubes were shaken by a mechanical shaker that was placed in the thermostated room at 298 K. The ionic strength of the aqueous solution was controlled at 0.1 mol dm^{-3} with sodium perchlorate. The time required to attain extraction equilibrium for the alkaline earth metal ions was determined by agitating for various times. The pH of the aqueous solution was measured after equilibration by a pH meter (TOA model, HM 60s). The metal content in the aqueous solution was determined by an atomic absorption spectrophotometer (Hitachi Zeeman Spectrophotometer, model 180-80) or an inductively coupled plasma spectrophotometer (Seiko Denshi, model SPS 1100). From the analytical data, the distribution equilibria of the alkaline earth metal ions were determined at 298 K.

Ion exchange separation of metal ions

The solid (0.1 g of DTHF) and the aqueous solution (10 cm^3) were used to equilibrate the ion exchange reaction of alkali and alkaline earth metal ions. The initial metal chloride concentration in the aqueous solution was 1 x 10^{-3} mol dm^{-3} for alkali metal ions and 1 x 10^{-4} mol dm^{-3} for alkaline earth metal ions and the pH was adjusted with HCl solution. The content of the tubes was agitated 100 times a day by hand for 3 days for alkali metal ions and 15 days for alkaline earth metal ions. The ion exchange equilibrium for alkaline earth metal ions was attained within this period. The materials were separated by centrifugation for 20 minutes at 4000 rpm after standing the tubes for one day. The metal content in the supernatant liquor and its pH were measured by the same methods as the solvent extraction experiment. The metal content in the solid phase was calculated from the initial and equilibrium concentration in the aqueous solution.

Triple phase separation of metal ions

As the ion exchange reaction takes long time to reach equilibrium, the aqueous solution containing alkaline earth metal ions was first contacted with dihydrogen tetratitanate hydrate fibres. The organic solution containing TTA and TOPO was added to the solid-liquid system after 10 days. The triple phase mixture, organic-aqueous-solid was slowly agitated for 5 days to achieve the equilibrium. Other experimental procedures were the same as those described above.

RESULTS

DTHF was used to separate alkali metal ions by ion exchange method. The X-ray diffraction pattern of potassium tetratitanate fibres is shown in Figure 1. The (200) peak of ca.10 denotes the layered structure of the potassium tetratitanate fibres. After potassium ion in the layer of the fibres was replaced with hydrogen ion, the potassium tetratitanate was converted to DTHF. The hydrogen ion in the layer is exchangeable with metal ions.

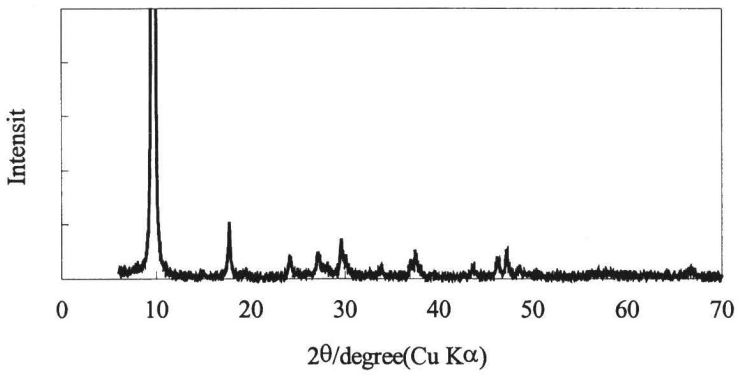

Figure 1. X-ray diffraction pattern of the potassium tetratitanate

The solvent extraction of alkaline earth metal ions is expressed in terms of the distribution ratio, D:

$$D = C_{M(o)} / C_M \quad (2)$$

where C represents the total concentration and the subscript "o" denotes the organic solution.

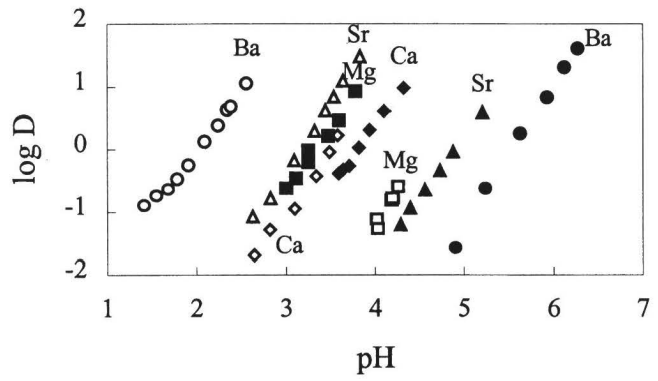

Figure 2. Solvent extraction of alkaline earth metal ions into benzene with TTA (0.1 mol dm^{-3}) and TOPO (0.1 mol dm^{-3}) (closed symbols). Ion exchange of alkaline earth metal ions in the aqueous solution (10 cm^3) onto dihydrogen tetratitanate hydrate fibres (0.1 g) (open symbols).

Figure 2 gives the log D values as a function of pH in the aqueous phase. The log D is proportional to the pH of the aqueous solution since the organic phase contains a large excess of the ligand compared to the concentration of metal ions in the aqueous phase. The slopes of the plots in Figure 2 are +2 and previous studies have shown that two TOPO molecules are complexed with a metal ion. This indicates that the solvent extraction reaction of alkaline earth metal ions can be written as follows.

$$M^{2+} + 2HA_{(o)} + 2TOPO_{(o)} = MA_2(TOPO)_{2(o)} + 2H^+ \quad (3)$$

where HA denotes TTA and the subscript "o" represents the chemical species in the organic phase.

The ion exchange of alkaline earth metal ions is expressed in terms of the distribution ratio, D, similar to equation 2.

$$D = C_{M(s)} / C_M \quad (4)$$

where C represents the total concentration and the subscript "s" denotes the solid phase. Figure 2 also shows the log D values as a function of pH in the aqueous solution for ion exchange with DTHF. The slope +2 indicates that the ion exchange of alkaline earth metal ions can be represented by equation 5.

$$M^{2+} + H_2Ti_4O_9 \cdot nH_2O_{(s)} = MTi_4O_9 \cdot nH_2O_{(s)} + 2H^+ \quad (5)$$

where the subscript "s" represents the chemical species in the solid phase.

To separate Ca^{2+} and Sr^{2+}, the triple phase separation system was used to partition Ca^{2+} into the organic phase and Sr^{2+} onto the ion exchange material. Figure 3 gives the ratio of extracted Ca^{2+} and Sr^{2+} by triple phase separation and solvent extraction system.

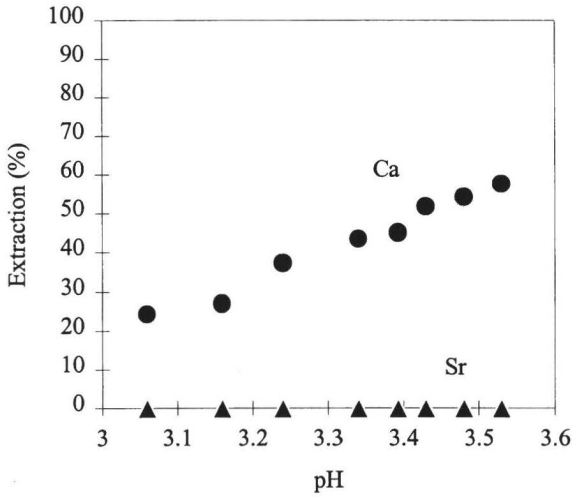

Figure 3. The triple phase separation of Ca^{2+} (circles)and Sr^{2+}(triangles). Organic phase: 10 cm^3 of benzene containing 0.2 mol dm^{-3} TTA and 0.2 mol dm^{-3} OPO. Solid phase: 0.1 g of DTHF. Aqueous solution: 10cm^3 containing 10^{-4} mol dm^{-3} Ca^{2+} and Sr^{2+}.

DISCUSSION

As is shown in Figure 2, the order of extraction in the solvent extraction system is $Mg^{2+} > Ca^{2+} > Sr^{2+} > Ba^{2+}$ which can be rationalised by solvation, charge density, and steric effect in forming the chelate ring. The order for ion exchange reaction $Ba^{2+} > Sr^{2+} > Ca^{2+} > Mg^{2+}$ as seen from Figure 2 is the opposite of that observed by solvent extraction. This order of selectivity can be rationalised by the hydration energy of the alkaline earth metal ions in the aqueous solution. The $pH_{1/2}$ values defined as pH at 50% solvent extraction or ion exchange of alkaline earth metal ions and the separation factors Sf defined in equation 6 are listed in Table 1.

$$\log Sf = pH_{1/2\,(M1)} - pH_{1/2\,(M2)} \quad (6)$$

It is evident from Table 1 that the separation factors of Ba - Sr and Ca - Mg are also large enough for separation by ion exchange. However, the separation factors for Ca and Sr by solvent extraction and ion exchange are not large enough for complete separation.

From the data in Figure 3, Ca^{2+} can extract even in the condition including DTHF, while Sr^{2+} does not extract in the presence of DTHF. The separation between Ca^{2+} and Sr^{2+} is large enough to separate each other by this triple phase separation method.

$pH_{1/2}$ values

	Solvent extraction	Ion exchange
Ba	5.50	2.02
Sr	4.80	3.14
Ca	3.80	3.50
Mg	3.35	4.62

Separation factors of alkali and alkaline earth metal ions

	Solvent extraction	Ion exchange
Ba -Sr	25.1	174
Sr-Ca	100	5.25
Ca -Mg	795	913

Table 1 $pH_{1/2}$ values and the calculated separation factors for alkaline earth metal ions

REFERENCES

1. Hasegawa Y, Kawashima H and Sekine T, *Bull. Chem. Soc. Jpn.*,**43**, 1718, (1970).
2. Komatsu Y, Fujiki Y and Sasaki T, *Solv. Extr. Ion Exch.*,**9**(3), 471, (1991).
3. Poluekotov NS and Beltyukova SV, *Zh. Anal. Khim.*,**25**, 2106, (1970).
4. Lapitskaya EV and Gorbenko FB, *Radiokhimiya*, **10**, 90, (1967).
5. Abe M, Chitrakar R, Tsuji M and Fujimoto K, *Solv. Extr. Ion Exch.*,**3**(1), 149, (1985)
6. Sekino H and Tomita I, *Bull. Chem. Soc. Jpn.*, **46**,1005, (1973).
7. Komatsu Y, Fujiki Y and Sasaki T, *Bunseki Kagaku* **32**, E33, (1983).
8. Komatsu Y, Fujiki Y and Sasaki T, *Bunseki Kagaku* **31**, E225, (1982).
9. Fujiki Y and Ohta N, *Yogyo-Kyokai-Shi*, **88**,111, (1980).

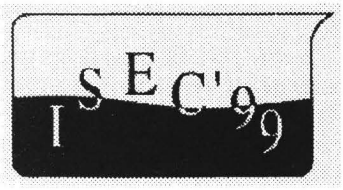

THE STOICHIOMETRIC MODELLING OF THE EXCHANGE EXTRACTION OF Mg, Ca AND Na WITH POTASSIUM DI-2-ETHYLHEXYLPHOSPHATE FROM CONCENTRATED BRINES

NM Rice and MA Tomlinson[1]
Department of Mining and Mineral Engineering, University of Leeds, Leeds LS2 9JT, West Yorkshire, U.K.
[1]Present address: Fluor Daniel Wright, Vancouver, BC, Canada

ABSTRACT
An organic phase comprising potassium di-2-ethylhexylphosphate (KD) with some free acid (HD) in xylene diluent was used to extract calcium, magnesium and sodium from chloride brine containing each of the elements. The stoichiometry of two possible extraction reactions was studied by testing the agreement between the experimental data and the respective equilibrium models. For calcium and magnesium the reactions tested were:

$$M^{2+}_a + 2KD_{org} \leftrightarrow MD_{2\,org} + 2K^+_a$$

and

$$M^{2+}_a + KD_{org} + HD_{org} \leftrightarrow MD_{2\,org} + K^+_a + H^+_a$$

Whilst the former reaction gave good agreement only at higher concentrations of potassium, the latter equation involving the free acid, gave an excellent fit. The equilibrium constant was $K_{ex} = 1.82 \times 10^{-3}$. Extraction of sodium from a synthetic brine containing 0.1 mol/dm^3 NaCl in 2.0 mol/dm^3 KCl provided evidence that the extracted complex is polymerised to a variable extent and contains excess extractant of formula, Na_mD_{m+1} with m = 4 to 12 including one extra HD or KD unit.

Keywords: Exchange extraction, magnesium, calcium, sodium, potassium, di-2-ethylhexylphosphate salts, chloride, brine.

INTRODUCTION

"Potash", the potassium content of potassium chloride, is of great importance as a raw material in the fertiliser and pharmaceutical industries. In Britain potash is recovered at Boulby mine, County Cleveland, by Cleveland Potash Ltd (CPL) as sylvite (KCl) from a Triassic evaporate ore, using flotation from a brine saturated with respect to KCl and NaCl of approximate composition, 4.1 mol/dm^3 NaCl, 1.7 mol/dm^3 KCl, 0.06 mol/dm^3 $MgCl_2$ and 0.05 mol/dm^3 $CaCl_2$, whose exact concentration depends on ore feed composition and ambient process temperature. The production of brine enriched in KCl or a pure saturated KCl brine would be useful for upgrading the coarse flotation concentrate by leaching. The replacement of fractional crystallisation for recovering pure high grade KCl from the fine concentrate might also permit an overall reduction in energy consumption and process costs. Solvent extraction is potentially useful for both these applications and also in the processing of ores containing carnallite ($KCl.MgCl_2.6H_2O$). Previous publications have described possible solvents and process routes using a mixed solvent system,[1, 2] and the potassium salt (KD) of di-2-ethylhexylphosphoric acid (HD).[3,4] The present work is concerned with the stoichiometry of the extraction reactions in the latter system. Although much has been published on the extraction of alkaline earth metals[4,5] very little of this work refers to extraction from concentrated brine media.

THEORY

The direct use of `slope analysis' to determine the stoichiometry is difficult to apply in the present system owing to its complexity. The system includes two extractants, KD and HD, as well as three metallic species, Ca, Mg and Na. Whilst it would be easy to isolate the individual metals, the possibility exists that their mutual presence could influence the stoichiometry. Furthermore, the method of preparing the organic phase precluded the separate study of the individual extractant species. In addition the transfer of water from this organic phase[4] must be taken into account. Therefore the approach adopted was to derive an equilibrium model based upon an assumed stoichiometry for the extraction reaction and then to observe the agreement between the slope of an experimental data plot for the variation of log D with some function of the extractant concentration and the behaviour predicted by the model for that particular stoichiometry.

© 2000 Society of Chemical Industry

Calcium and Magnesium

Since the object of the extraction process was the removal of the metals from the brine rather than their mutual separation and also to simplify the model, the two alkaline earth metals were treated as a single entity. This was also the approach used previously to the plot McCabe-Thiele diagrams.[3] The experimental test-work reported below did include analysis for both metals individually and although Ca is extracted slightly more strongly than Mg,[4] their overall extraction behaviour is very similar. Ritcey and Ashbrook[6] have indicated, at high metal loading the extracted species for divalent metals with HD is MD_2 so that each will consume the same amount of extractant in molar terms.

The initial assumption was made that because of its superior extraction power[4] only KD was active as the extractant, i.e. the extraction equilibrium may be written as:

$$M^{2+}_a + 2KD_{org} \leftrightarrow MD_{2\,org} + 2K^+_a \qquad (1)$$

where M represents Ca and Mg. The extraction equilibrium constant is given by:

$$K_{ex} = \frac{[MD_2]_{org}[K^+]_a^2}{[M^{2+}]_a[KD]_{org}^2} \qquad (2)$$

and the distribution ratio of metal M, (Ca + Mg), $D_M = [M]_{org}/[M]_a$, whence for a concentrated brine of constant potassium ion activity:

$$\log D_M = 2 \log [KD] + \log C \qquad (3)$$

where C is a constant including K_{ex} as well as the potassium concentration of the brine and any activity coefficients which were assumed to remain unchanged as other conditions vary due to the high ionic strength of the brine. Hence a plot of log D_M v log [KD] should have a constant slope = 2 if equation 1 is a correct representation of the extraction equilibrium.

Alternatively if the acid component of the solvent takes part in the extraction as well the potassium salt, the extraction reaction may be written as:

$$M^{2+}_a + KD_{org} + HD_{org} \leftrightarrow KD_{2\,org} + K^+_a + H^+_a \qquad (4)$$

with equilibrium constant:

$$K_{ex} = \frac{[MD_2]_{org}[K^+]_a[H^+]_a}{[M^{2+}]_a[KD]_{org}[HD]_{org}} \qquad (5)$$

An organic phase containing 1 mol/dm^3 D2EHPA in xylene was pre-equilibrated with 1.33 mol/dm^3 K_2CO_3 to give a solvent containing 66.25% KD : 33.25% HD with a water content of 20% by weight of which 90% was found to transfer back to the aqueous phase on contact with the brine.[4] The extractant concentration was varied by dilution of this solvent with xylene. From this information the 'initial' concentrations of KD and HD (allowing for the transfer of water) were calculated prior to transfer of the Ca and Mg as $[KD]_{iw}$ and $[HD]_{iw}$ respectively.[4] The equilibrium concentrations of KD and HD, $[KD]_e$ and $[HD]_e$, could then be calculated from the equilibrium aqueous total metal (Ca+Mg) concentration, $[M]_e$, and the hydrogen ion concentration, $[H^+]$ respectively where the $[H^+]$ value was estimated from the measured pH corrected for the varying chloride concentration using the relationship:[4]

$$-\log [H^+] = pH + p, \qquad \text{where } p = 0.214\,[Cl^-] - 0.085 \qquad (6)$$

Substitution of these values into equation 5 gives:

$$K_{ex} = \frac{D_M[K^+]_e[H^+]_e}{([KD]_{iw} - 2[M]_{org} + 2R_e[H^+]_e)([HD]_{iw} - R_e[H^+]_e)} \qquad (7)$$

Where R_e is the equilibrium aqueous:organic phase ratio, and, as $[H^+]_e$ is small in comparison with $[KD]_{iw}$ and $[HD]_{iw}$, equation 7 may be approximated to:

$$K_{ex} = \frac{D_M[K^+]_e[H^+]_e}{([KD]_{iw} - 2[M]_{org})[HD]_{iw}} \quad (8)$$

so that,

$$\log D_M = \log (([KD]_{iw} - 2[M]_{org})[HD]_{iw}/[H^+]_e) + \log (K_{ex}/[K^+]) \quad (9)$$

which may be validated by plotting log D_M versus the log variable on the RHS of equation 9 to give a slope of 1 or by testing the constancy of K_{ex}.

Sodium

Initial loading tests indicated that sodium was loaded with a slight excess of extractant[4] so that the extraction equilibrium for sodium in the absence of alkaline earth metals, which are preferentially extracted, may be written as:

$$Na^+_a + nKD_{org} \leftrightarrow NaD_{n\,org} + nK^+_a \quad (10)$$

for which:

$$K_{ex} = \frac{[NaD_n][K^+]^n_a}{[KD]^n_{org}[Na^+]_a} \text{ so that } K_{ex} = D_{Na}/D_K^n$$

and the model equation may be written as:

$$\log D_{Na} = n \log D_K + \log K_{ex} \quad (11)$$

which should give a linear plot of slope = n. However equation 10 is unbalanced with respect to charge so that clearly some other species is involved in the reaction and the above theory can only be regarded as a first approximation.

EXPERIMENTAL

The initial organic phase consisted of a 1.00 mol/dm^3 solution of di-2-ethylhexylphosphoric acid (BDH), used as received, in xylene diluent. This was pre-equilibrated to form the potassium salt[2, 4] by contacting it with 1.33 mol/dm^3 K_2CO_3 solution at a phase ratio (A/O) of 4 to give a solvent phase containing 20% H_2O (Karl Fischer) and KD and HD concentrations of 0.534 and 0.266 mol/dm^3 respectively (KD:HD = 66.75 %: 33.25 %) as measured by potentiometric titration. This was further diluted with xylene as required. The aqueous phase for calcium and magnesium extraction was a slightly diluted plant brine from CPL of approximate original composition (in mol/dm^3): NaCl 4.10, KCl 1.70, $MgCl_2$ 0.06, $CaCl_2$, 0.05. The actual concentrations of K and total alkaline earths were 1.530 and 0.1046 mol/dm^3 respectively. For sodium extraction synthetic brines containing either 1.996 mol/dm^3 NaCl with zero KCl or 0.087 mol/dm^3 NaCl with 1.869 mol/dm^3 KCl were used. Neither of these contained any alkaline earth metals as the latter were preferentially extracted.

Phases were contacted at ambient temperature (20 ± 3)°C either manually or in a stirred vessel at a phase ratio of either unity or 2:1 (A/O) usually for at least 5 minutes, which in most cases was sufficient to establish equilibrium. Organic phases were filtered through phase separation paper prior to stripping and analysis of the strip solutions.

Analysis of Ca and Mg was performed by EDTA titration using standard methods and indicators.[7,8,9,10] Ca was titrated using 0.004 mol/dm^3 EDTA and calcein indicator after pH adjustment and buffering with triethanolamine. Very low concentrations were determined by Atomic Absorption (AA)[11] using an N_2O/acetylene flame at 422.7 nm on a Varian AA-10 spectrophotometer calibrated with matrix matched standards. Mg was calculated by difference after titration of the total Ca + Mg content with 0.004 mol/dm^3 EDTA using a buffered solution and methylthymol blue indicator.[10] Low concentrations of Mg were measured by AA using an air/acetylene flame at 202.6 nm and matrix matched standards for calibration. Na was measured by AA with an air/ acetylene flame at 330.3 nm (0 - 400 ppm) with the addition of a suitable amount of K and also CsCl as an ionisation depressant.[11] K was determined by AA at 404.4 nm (0 - 800 ppm) using ionisation suppressants and matrix matching. Chloride in the brine was determined by the Volhard

back titration method[7] with $AgNO_3$ and KSCN using Fe(III) indicator but omitting nitrobenzene for safety reasons. Measurements of organic phase chloride concentration were not reliable owing to the low levels present.

RESULTS AND DISCUSSION

Calcium and Magnesium

Figures 1 and 2 show plots of log D_M, for Ca + Mg, against the log of the equilibrium concentration of KD (in mmol/dm^3) according to equation 3, where D_M is the total distribution ratio for Ca and Mg. In figure 1 the slope of the regression line through 8 data points with r = 0.965, is 1.34 ± 0.15 (the ± figure represents 1 standard deviation). However, if the two lowest concentrations are omitted as in figure 2 the linearity improves (r = 0.993) and the slope is 1.91 ± 0.013. This indicates that at the highest extractant tenor the extraction mechanism might be as in equation 1 implying that the extracted species are CaD_2 and MgD_2.

Figure 1: Variation of log D for Ca + Mg with equilibrium extractant concentration

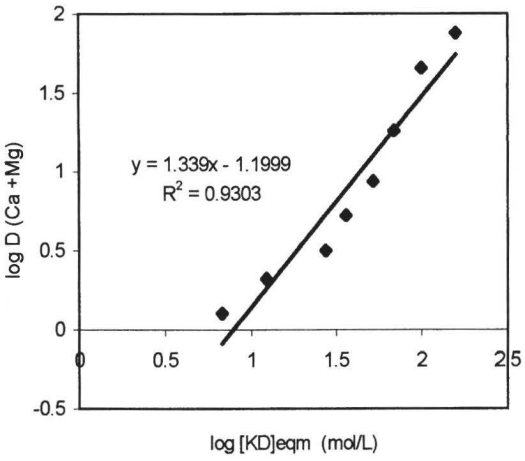

Figure 2: Variation of lof D for Ca + Mg with equilibrium extractant concentration at high metal loading

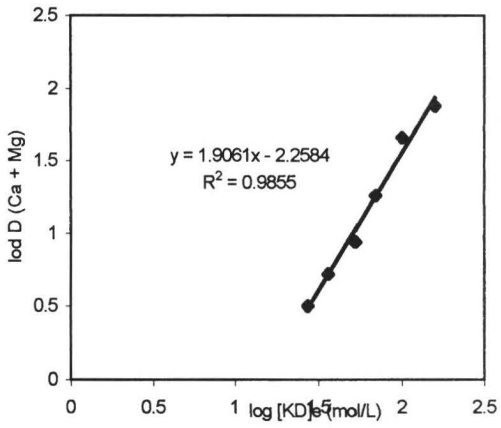

Figure 3 shows a plot of log D_M, for Ca + Mg, against the model parameter $(([KD]_{iw} - 2[M]_{org})[HD]_{iw}/[H^+]_e)$ according to equation 9 taking into account both the presence of free acid, HD, in the organic phase and the back extraction of water. For all 8 data points the plot is linear (r = 0.986) with a slope of 0.930 ± 0.065. Thus the slope is equal to 1 within experimental error as predicted by equation 9. Furthermore the value of K_{ex}, calculated using equation 8, was (1.82 ± 0.50) x10^{-3} (to one standard deviation) which is effectively constant to within the overall error considering the assumptions made in deriving the model. From figure 3 the intercept in equation 9, log $(K_{ex}/[K^+])$ = -5.455 ± 0.200 giving a value of K_{ex} = (5.37 ± 3.14)x10^{-3}, which is of the same order of magnitude. The statistical agreement between the respective models and the experimental data does not lead to a very clear choice between reactions 1 and 4 but as equation 4 fits the experimental conditions better and leads to slightly better agreement it is the preferred model for the extraction of Ca and Mg.

Figure 3: Variation of log D for Ca + Mg with the model parameter log X, where X = ([KD]iw - 2[M]e) [HD]iw/ [H+]e

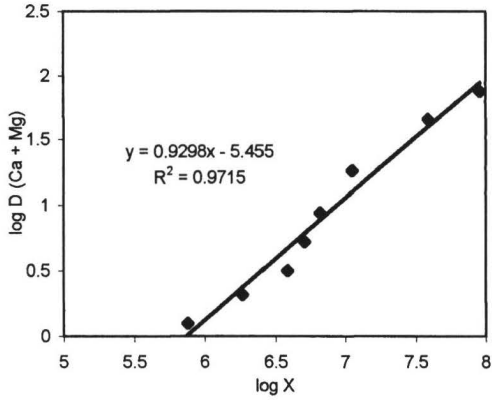

Sodium

Figure 4 shows the variation of log D_{Na} with log D_K following equation 11 after extraction from a brine containing 1.996 mol/dm^3 NaCl initially and no potassium using a pre-equilibrated organic phase diluted with xylene to give various extractant concentrations. The regression line has a slope of 0.45 ± 0.028 with r = 0.988 indicating that the extracted species is Na_2D. This is difficult to explain but if only the highest concentrations are considered the slope is 1.08 ± 0.065 with r = 0.991. Furthermore, the ratio of initial D2EHPA present to the Na stripped from the respective organic phases for each data point averaged 1.09 ± 0.03 indicating that n was probably > 1. Application of activity coefficients to the data did not improve the agreement and it was suspected that because of the high sodium tenor in the brine equilibrium had not been properly established at the lower extractant concentrations.

Figure 4: Extraction of sodium from a brine at initial concentration of 1.996 mol/L NaCl and zero KCl

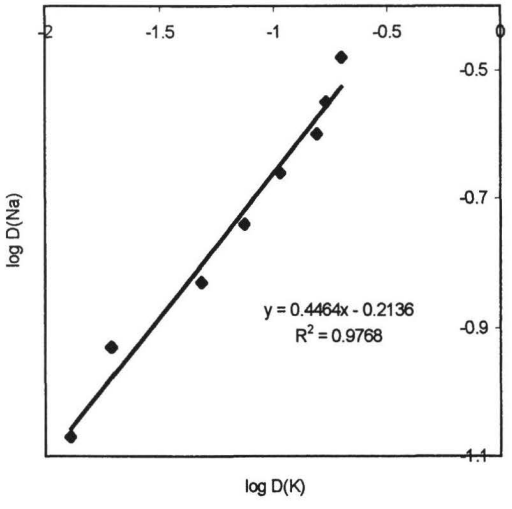

Figure 5: Extraction of sodium from a dilute brine containing initial concentrations of 0.087 mol/L NaCl and 1.869 mol/L KCl

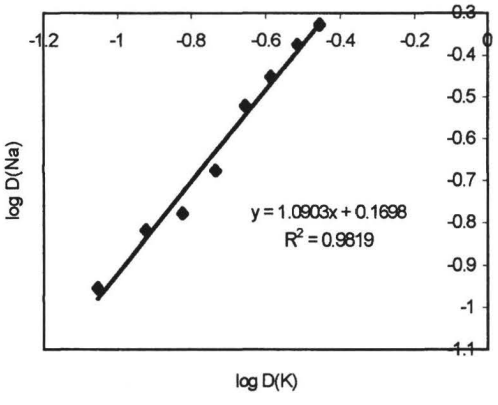

A further series of tests using a synthetic brine of lower sodium concentration (NaCl 0.087 mol/dm^3, KCl 1.869 mol/dm^3) in which the aqueous KCl concentration would be virtually constant was studied. The results are shown in figure 5 where a linear plot (r = 0.991) with a slope = 1.09 ± 0.061 was obtained in good agreement with the previous results. The figure of 1.09 appears consistently indicating either polymerisation and/or solvation of the extracted sodium complex, i.e. a polymer of formula Na_mD_{m+1} containing also either HD or KD. Using this formula, all values of n between 1.07 and 1.12 can be reconciled with a polymer with n between 9 and 12. Other data for the counter-current extraction and stripping of sodium[4] gave a value of n = 1.25 corresponding to m = 4 so it appears that, depending on conditions such as the concentration of the various components, the chain length of the polymer can vary. Further study is necessary to fully characterise this behaviour in detail, however it may be concluded that equilibrium 10 with n = about 1.1 gives a fair representation of the exchange extraction of Na^+ with KD. From figure 5 the intercept of the line is 0.1698 ± 0.0449, which from equation 11 corresponds to log K_{ex} so that K_{ex} = 1.48 ± 0.16 for the sodium/potassium exchange reaction.

CONCLUSIONS

Calcium and magnesium are extracted from concentrated brines by the potassium salt of di-2-ethylhexyl phosphoric acid (KD) and the free acid (HD) according to the equilibrium:

$$M^{2+}_a + KD_{org} + HD_{org} \leftrightarrow MD_{2\,org} + K^+_a + H^+_a$$

with equilibrium constant $K_{ex} = (1.82 \pm 0.50) \times 10^{-3}$

Sodium is extracted as a polymeric species, Na_mD_{m+1} with m =9-12 according to the reaction:

$$Na^+_a + nKD_{org} \leftrightharpoons NaD_{n\,org} + nK^+_a$$

with equilibrium constant K_{ex} = 1.48 ± 0.16.

ACKNOWLEDGEMENTS

The authors wish to thank the SERC (now EPSRC) for the provision of a studentship for M.A.Tomlinson. They also wish to thank the management of Cleveland Potash Ltd for additional financial support and the provision of facilities and samples. Particular thanks are due to Mr G.Holyfield and also to Mr M.Greenhalgh (formerly of CPL). Thanks are also due to Mr S.Lloyd for technical assistance with analytical equipment and to Dr N.Taylor (formerly of the Department of Chemistry, University of Leeds) for advice and the provision of laboratory space.

REFERENCES

1. Rice NM and Chapman RJ *Trans.Inst.Mining.Metall. (Section C.)*, **99**(3), C125, (1990).
2. Chapman RJ *PhD Thesis*, University of Leeds.UK (1989).
3. Rice NM and Tomlinson MA *Proc. ISEC'93*, Ed. Logsdail DH and Slater MJ, London, Elsevier/ SCI, 753, (1993).
4. Tomlinson MA *PhD Thesis*, University of Leeds, UK, (1991).
5. Komatsu Y *Proc. ISEC'93*, Ed. Logsdail DH and Slater MJ, London, Elsevier/ SCI, 775, (1993).
6. Ritcey GM and Ashbrook AW *Solvent Extraction Principles and Applications to Process Metallurgy, Part 1*, Elsevier, Amsterdam, (1984).
7. Vogel AI *Textbook of Quantitative Analysis, (3rd Edition)*, Longmans, London (1961).
8. Schwarzenbach G *Complexometric Titrations*, Methuen, London, (1957).
9. Gibson FH and Ode WH *U.S. Bureau of Mines RI 6036*, (1962).
10. West TS *Complexometry, (3rd Edition)*, BDH Chemicals Poole Dorset UK, (1969)
11. Slavin W *Atomic Absorption Spectroscopy*, Interscience, New York, (1968).

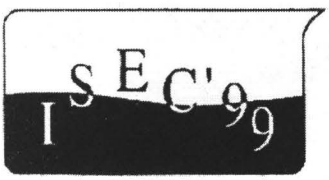

EXTRACTION OF ARSENIC(III) AND ARSENIC(V) FROM SULPHURIC ACID SOLUTIONS WITH TRIALKYLPHOSPHINE OXIDES AND HYDROXAMIC ACIDS

M Wisniewski, L Iberhan and J Szymanowski
Institute of Chemical Technology and Engineering, Poznan University of Technology, Poznan, Poland

ABSTRACT
The extraction of As(III) and As(V) from sulphuric acid solutions of various concentrations (50-200 g/dm^3) with Cyanex 923, Cyanex 925 and neo-decanohydroxamic acids, was studied. These extractants were dissolved in toluene, and in Exxsol D 220/230. Cyanex 923, Cyanex 925 and neo-decanohydroxamic acids can be considered as effective arsenic extractants. Sulphuric acid is co-extracted into the organic phase. Extraction of both As(III) and As(V) occurs rapidly and the equilibrium is obtained after 5-15 minutes. The isotherms of As(III) and As(V) extraction at various sulphuric acid concentrations were determined. The diluent affects significantly the extraction of As(III) with Cyanex 923 and Cyanex 925. Toluene is a better diluent than Exxsol D 220/230. In the case of neo-decanohydroxamic acids the effect of diluent on extraction efficiency is very small. Arsenic (V) is always extracted better with the reagents diluted with toluene. Arsenic can be stripped with water.

Keywords: arsenic(III), arsenic(V), Cyanex 923, Cyanex 925, neo-decanohydroxamic acid

INTRODUCTION

In the electrorefining of copper to produce cathodes of high purity from impure anode copper, certain impurity elements such as nickel, arsenic, antimony and bismuth dissolve in the copper bearing acidic electrolyte solution. If crude ores rich in these elements are smelted and processed in the subsequent refining procedures such contaminating elements are rapidly accumulated, particularly in strongly acidic sulphuric acid solutions. Arsenic, however, is the major impurity in such solutions, and must be removed. Many methods were described to separate arsenic from copper electrolyte bleeds. Solvent extraction is one of the methods developed and used in few installations including Hoboken Refinery in Belgium and Copper Refineries in Townsville, Australia. Tributylphosphate (TBP) is used as an arsenic extractant.[1] Various extractants are proposed for the extraction of arsenic. They can be used alone or together with various modifiers. They include alcohols and polyglycols, hydrophobic polyphenols, hydroxamic acids, trialkylphosphine oxides and full esters of phosphoric and phosphinic acids.[2-5]

EXPERIMENTAL

Cyanex 923 and Cyanex 925 were used as delivered by Cyanamid Canada Inc. without purification. Cyanex 923 contains four trialkylphosphine oxides:

$(R_2)R'P=O$	$(R'_2)RP=O$	$R'_3P=O$	$R_3P=O$
31%	42%	14%	8%

where: $R=C_6H_{13}$ $R'=C_8H_{17}$ and 5% water.

Cyanex 925 contains bis(2,4,4-trimethylpenthyl)octylphosphine oxide, the structure of which is shown below. The composition of the sample used in this work was presented recently by Dziwi | ski et al.[6]

Neo-decanohydroxamic acids were synthesised from Versatic acid 9-10 where: $R_1+R_2+R_3=8$. The composition of the Versatic acids was not studied. However, their full conversion to hydroxamic acids was proven.

© 2000 Society of Chemical Industry

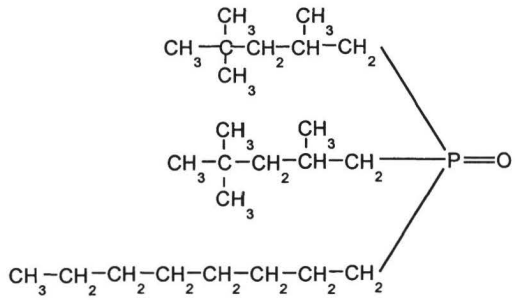

Structure of bis(2,4,4-trimethylpenthyl)octylphosphine oxide

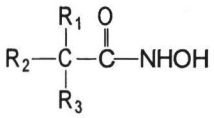

Structure of neo-decanohydroxamic acids

Cyanex 923 and Cyanex 925 were diluted with Exxsol D 220/230 (kerosene without aromatics, Exxon Co., USA) or with toluene, and used as 50% v/v solutions. Neo-decanohydroxamic acids were diluted with Exxsol D 220/230 or with toluene, and 0.1 mol/dm^3 solutions were used.

Synthetic arsenic solutions in sulphuric acid were used.

Extraction of As(III) and As(V) was carried out using equal volumes of both phases (20 cm^3 each) at 50^{0}C under vigorous mixing (1000 min^{-1}) for 5 minutes (Cyanex 923 and Cyanex 925) and 15 minutes (neo-decanohydroxamic acids). The equilibrium of extraction was achieved in each case. The content of arsenic in the sulphuric acid solutions was determined spectrophotometrically by arsenomolybdate extraction.

Arsenic was stripped from the organic phase by mixing with the same volume of distilled water at 50^{0}C under effective mixing (1000 min^{-1}) for 5 minutes for loaded Cyanex 923 and Cyanex 925 and 15 minutes for loaded neo-decanohydroxamic acids. The content of arsenic in the aqueous phase was determined using the same method and conditions as in the extraction studies.

Sulphuric acid co-extracted with arsenic was determined in the aqueous phase after its extraction into the organic phase, by direct titration with NaOH in the presence of methyl orange.

RESULTS AND DISCUSSION

The extraction of arsenic was studied under different concentrations of sulphuric acid. Figures 1 and 2 show the effect of sulphuric acid concentration on arsenic extraction. Sulphuric acid affects the extraction both of As(III) and As(V), which significantly increases when the sulphuric acid concentration increases from 50 to 200 g/dm^3.

Figure 3 shows the extraction of As(III) and As(V) with the studied extractants dissolved in toluene versus the initial concentration of sulphuric acid. Cyanex 925 and neo-decanohydroxamic acids extract As(III) and As(V) with similar efficiency. A significant difference in extraction ability for Cyanex 923 towards arsenic is, however, observed. Arsenic (V) is transferred in higher quantity into the organic phase.

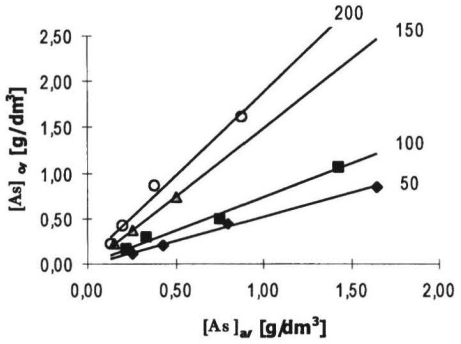

Figure 1. Isotherms for As(V) extraction with Cyanex 923 (50% v/v) in toluene from sulphuric acid solutions of various concentrations (from 50 to 200 g/dm^3).

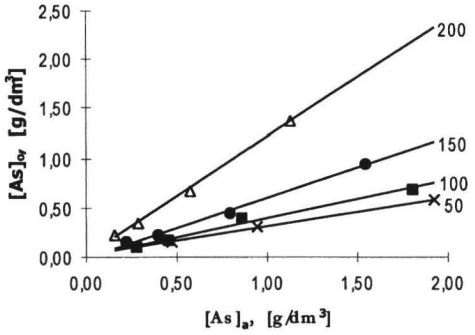

Figure 2. Isotherms for As(V) extraction with neo-decanohydroxamic acids (0.1 M) in toluene from sulphuric acid solutions of various concentrations (from 50 to 200 g/dm^3).

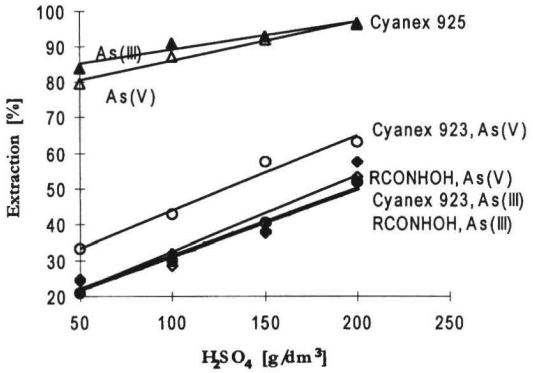

Figure 3. Extraction of As(III) and As(V) with Cyanex 923 (50% v/v) in toluene, Cyanex 925 (50% v/v) in toluene and with neo-decanohydroxamic acids (0.1 M) in toluene, (1.25 g/dm^3 arsenic in the feed).

The influence of diluent and oxidation state of arsenic on the extraction is shown in Table 1. Trialkylphosphine oxides diluted with Exxsol D 220/230 extract As(V) better than As(III). The diluent affects significantly As(III) extraction with Cyanex 923 and Cyanex 925. Toluene is a better diluent than Exxsol D 220/230. In the case of neo-decanohydroxamic acids the differences are very small. As(V) is always better extracted with reagents diluted with toluene.

Extractant	Diluent	Extracted Arsenic [%]	
		As(III)	As(V)
Cyanex 923	Exxsol D 220/230	35.9	47.9
Cyanex 923	Toluene	43.0	59.5
Cyanex 925	Exxsol D 220/230	44.8	62.2
Cyanex 925	Toluene	95.0	91.0
Neo-decanohydroxamic acids	Exxsol D 220/230	38.8	22.0
Neo-decanohydroxamic acids	Toluene	39.0	36.0

Table 1. The extraction of arsenic (1.25 g/dm^3 As(III) and As(V)) from 150 g/dm^3 H_2SO_4 solutions with Cyanex 923 (50% v/v), Cyanex 925 (50% v/v) and with neo-decanohydroxamic acids (0.1 mol/dm^3).

As(III) and As(V) can be stripped with water from the loaded organic phase. The isotherms for As(III) stripping are given in Figure 4. Stripping increases when the concentration of the sulphuric acid increases in the feed used for extraction. The stripping of As(III) and As(V) with water is better from the loaded Cyanex 923 dissolved in Exxsol D 220/230. No difference was observed between the stripping of As(III) and As(V) with water. The stripping of As(III) and As(V) with water from the loaded Cyanex 925 dissolved in toluene is very low; however 70% of arsenic can be easily stripped from the loaded Cyanex 925 in Exxsol D 220/230. As(III) as well as As(V) can be removed from the loaded neo-decanohydroxamic acids dissolved in toluene. As(V) is removed better from the loaded neo-decanohydroxamic acids dissolved in Exxsol D 220/230. Among all the studied reagents dissolved in toluene, the most efficient As(V) stripping is obtained from the loaded Cyanex 923. If the reagents are dissolved in Exxsol D 220/230, the most efficient strip is observed when the loaded Cyanex 925 is used.

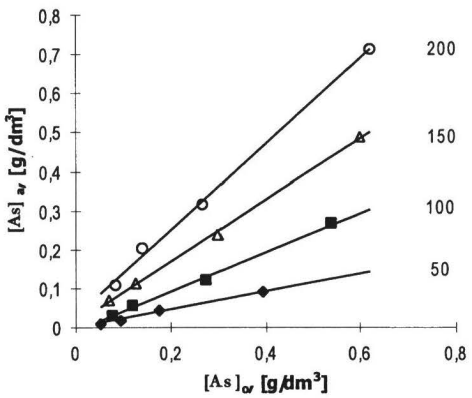

Figure 4. Isotherms for As(III) stripping with water (loaded Cyanex 923 (50% v/v) in toluene was obtained by As(III) extraction from sulphuric acid solutions of various concentrations from 50 to 200 g/dm^3).

These observations cannot be explained only by differences in structures (straight and branched chain) of the alkyl substituents in Cyanex 923 and Cyanex 925. Thus, they indirectly support our analytical data in which we report the complex composition of the sample of Cyanex 925 used by us in which the presence of sulphur analogues was found.[6]

Sulphuric acid is also co-extracted and its content in the organic phase increases with increasing initial concentration in the feed. Figure 5 shows that the presence of arsenic species decreases slightly the extraction of sulphuric acid by Cyanex 925. A stronger effect is observed in the presence of As(III).

The studies can be summarised as follows. The extraction of both As(III) and As(V) takes place rapidly with Cyanex 923 and Cyanex 925, and the equilibrium is established after 5 minutes of phase mixing, and in the case of neo-decanohydroxamic acids after 15 minutes of phase contact. The extraction of arsenic increases from feeds containing higher concentrations of sulphuric acid. Simultaneously, increased co-extraction of sulphuric acid is observed. Cyanex 923 dissolved in toluene extracts better As(V) than As(III). Other extractants transfer similar quantities of As(III) and As(V) to the organic phase. Toluene is a better diluent for Cyanex 923 and Cyanex 925 than Exxsol D 220/230, for the extraction of arsenic. In the case of neo-decanohydroxamic acids the type of diluent has no significant effect on extraction of arsenic. Stripping of arsenic with water increases when the initial sulphuric acid concentration increases. The highest re-extraction of arsenic with water is obtained for the loaded extractants dissolved in Exxsol D 220/230. As(V) is more easily stripped with water than As(III). More sulphuric acid is transferred to the organic phase in the case of As(V) extraction with Cyanex 925. Cyanex 923, Cyanex 925 and neo-decanohydroxamic acids seem to be promising reagents for arsenic recovery from various sulphuric acid solutions, including those obtained from copper refining.

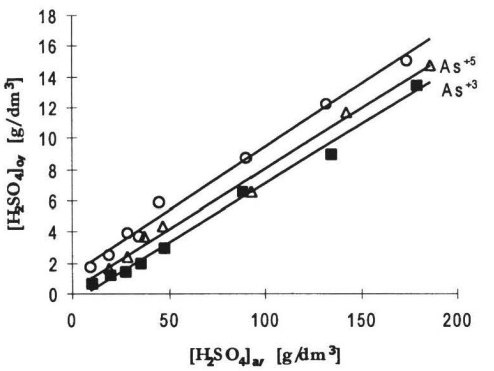

Figure 5. Extraction of sulphuric acid with Cyanex 925 (50% v/v) in toluene from sulphuric acid solutions of various concentration (10-200 g/dm^3 H_2SO_4).

ACKNOWLEDGEMENTS

The work was supported by KBN donation for Institute activity DS PP No. 32/221/98.

REFERENCES

1. Hall PG, Armstrong RW and Middlin B, *114th TMS AIME Annual Meeting*, Townsville, Australia. 6, (1985).
2. Bogacki MB, Wisniewski M and Szymanowski J, *J. Radioanal. Nucl. Chem.* **228**, 57, (1998).
3. Wisniewski M, *Hydrometallurgy,* **46**, 235, (1997).
4. Wisniewski M, *J. Radioanal. Nucl. Chem*, **228**, 105, (1998).
5. Szymanowski J and Wisniewski M, *Polish J. Appl. Chem.*, **40**, 3, (1996).
6. Dziwi | ski E and Szymanowski J, *Solv Extr. Ion Exch.*, **16**, 1515, (1998).

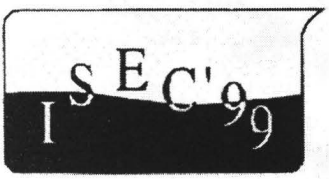

NEW DEVELOPMENTS IN SOLVENT IMPREGNATED RESINS. AN OVERVIEW

A Warshawsky,[1] JL Cortina[2], M Aguilar[2] and K Jerabek[3]

[1]Department of Organic Chemistry, Weizmann Institute of Science, Rehovot, Israel.

[2]Department of Chemical Engineering, Universitat Politecnica de Catalunya, Barcelona, Spain.

[3]Department of Chemical Engineering Czech Academie of Science, Prague, Czech Republic

ABSTRACT

This paper discusses the trends in the design and development of highly selective and efficient Solvent Impregnated Resins (SIR) combining the physico-chemical data of the materials (equilibrium, kinetic and morphological data) with the mass transport parameters. The use of both spectroscopic and surface analysis techniques provides complementary information on the influence of the solid phase structure and ligand activity on the extraction process.

Keywords: impregnated resins, extraction chromatography, new supports

INTRODUCTION

The concept of Solvent-Impregnated-Resins (SIR) was introduced in the seventies[1] as a way of solving one of the major drawbacks of solvent extraction such as organic solvent losses, by substitution of the "Solvent" with a "Solid phase". Taking into account the limitations in the preparation of chelating and ion exchange resins, due to the complexity and time-consuming procedures needed for covalently linking the functional group to the backbone of the resin added to their high cost. All this together with the recent advances in the synthesis of new organic reagents for solvent extraction- the development of impregnated resins as a link between solvent extraction processes and ion exchange processes was established as an important and developing field in separation science. Macroporous polymeric supports with a number of the desired properties (high surface area, high porosity, high chemical and mechanical resistance) where selected as the ligand-containing solid phase and since that time the research and applications of Solvent Impregnated Resins (SIR) grew steadily as reflected in the large number of scientific contributions during the last three decades. Basically, the impetus has been directed to the development of new metal separation processes, particularly for liquid wastes and effluents[1,2]

This paper will deal with the most recent investigations and developments in the preparation, characterisation and application of impregnated resins in extraction, separation and recovery of metals. The introduction of reactive polymeric macroporous supports is shown, to be as one of the most promising new developments. Recent results on the application of these new type of materials in metal extraction, separation and recovery of metal ions in hydrometallurgical, environmental and in analytical applications for the separation and/or preconcentration of metal ions will be presented.

INTRODUCTION OF NEW POLYMERIC SUPPORTS AND IMPREGNATION PROCEDURES

Improvements in SIR preparation were primarily aimed to solve the major problems to the implementation of SIR columns which is the leakage of the Ligand into the aqueous phase. This leakage can be multiplied by use of the SIR column in several extraction-elution cycles. The problem remained how to ensure the highest possible efficiency for removing low levels of metal ions and to increase the kinetics of the extraction process by improving the hydrophilic nature of the polymer matrix. To solve these problems different approaches were evaluated:

© 2000 Society of Chemical Industry

New polymeric supports.

Typical non-reactive macroporous polymeric supports based on polystyrene-divinylbenzene were substituted by reactive polymeric supports including polyvinylpiride (PVP) weak or strong ion-exchange resins[3-8]. All these new types of polymeric supports for SIR are characterised by the presence of either acid or base groups. The selection of a suitable reactive polymeric support should be controlled by the following rules:

a) when impregnating an acidic ligand (HL) (organophosphoric (DEHPA)[8] and organothiophosphoric (DEHPTA)[4-7]) and neutral (TBP, TOPO)[8] derivatives a polymeric support containing a basic functionality should be selected (e.g. PVP or weak base ion exchange resins). The acid-base interaction could be described as:

$$PS\text{-}R_2N + (RO)_2P(O)\text{-}OH \Leftrightarrow PS\text{-}R_2N\cdots\cdots OH\ P(O)(RO)_2 \text{ (hydrogen bond)}$$

e.g. for a tertiary anion-exchange resin and organophosphoric derivative (DEHPA):
Where PS indicated the polymeric support network

b) when impregnating a basic extractant (B), amine type extractants as (Alamine 336)[9] and LIX79[10] a polymer containing an acidic functionality is to be selected (e.g. strong and weak acid ion exchange resins). The acid-base interaction could be described as:

$$PS\text{-}XOOH + B \Leftrightarrow (PSXOOH.....B)$$

e.g. for a sulphonic cation-exchange resin and a tertiary amine derivative (Alamine 336):

$$PS\text{-}S(O)OH + R_3N \Leftrightarrow PS\text{-}S(O)OH\cdots\cdots NR_3 \text{ (hydrogen bond)}$$

The interactions described in the equations above may be detected by FTIR measurements and in general, interactions are much stronger than the physical adsorption of the extractant on non-functional (inert) polymeric supports.

Modifying impregnation procedures.

Improvements in the kinetic properties of the materials were achieved by modification of the impregnation procedures in several different ways. When using the direct adsorption of the extractant onto the polymeric a mixture of a solution of the reagent in an aqueous miscible organic solvent is imbibed in the polymer. In this case, using a good solvent for the polymer, that means a solvent with a high solubility in the polymer phase, it may be possible to increase the distribution of the extractant in the polymer phase. Combined with the use of a water containing solvents SIR materials with better wetting properties can be reached. Mixtures of methanol, acetone, ethanol with water allowed to prepare SIR containing both acidic and basic extractants which show mass transfer data similar to those shown typically by hydrophilic ion exchange resins.[2,10-11]

Increasing Extractant Loading

For making SIR competitive as metal removal materials, there is a need to increase the extractant loadings. Two different options were evaluated: 1) the use of high surface polymeric materials such as gel type polymers and a new type of macroreticular polymeric supports Macronet (Purolite) and, 2) the use of reactive supports (ion exchange resins)[3-7]. The use of gel type and Macroreticular polymeric supports with high surface areas (around 1000 m^2/g) did not produce substantial increase in extractant loading or in subsequent metal loadings[10]. But the use of ion exchange materials as supports for SIR allowed reaching extractant loadings close to 0.8-1.0 mol/Kg with metal ion exchange or extraction capacities very similar to capacities of ion exchange resins (between 2-5 mol/Kg). However, while these values of capacity are achievable, the activity of the reagent adsorbed on the SIR need to be carefully studied considering the fact that the increase of the extractant loading is very likely to affect some other important properties of the SIR when applied on

a technological scale. Firstly, the increase of loading implies an increase in the extractant losses, in some cases when loadings are very high the appearance of third phases was observed. Secondly the increase in the loadings also causes increase in the hydrophobic nature of the SIR resin. Hence it is very important to define in what is the range of optimum loadings and how they compromise with a different number of objectives which need to be accomplished: a) maximum capacity; b) low hydrophobic nature (affecting kinetics); c) low extraction losses

MODELLING METAL EXTRACTION PROCESSES

When comparing SIR to conventional ion exchange resins the SIR's provide increased selectivity for a metal without reduction in the kinetics and capacity shown by chelating ion exchange resins. On the other hand comparing SIR's with liquid-liquid extraction systems the SIR systems show a more efficient extractant use with minimal use of organic solvents (in the SIR preparation step, but no organic solvent is used in the metal extraction step). The early papers did not discern any differences in the behaviour of these SIR's[1]. However, recently it has been shown in a number of cases that the polymer matrix influences not only the extraction kinetics, but also the formation of metal complexes in the organic phase and then the extraction reactions. Description of the metal extraction reactions and the influence of the solid carrier have been studied[4-6]. Knowledge and understanding of the metal extraction processes was a useful tool for designing new separation and preconcentration schemes based on SIR[2]. Then, extensive efforts to develop a unified approach to describe the metal extraction and separation properties of solid supported ligands and compare their behaviour with those found when these supported ligands are used in liquid-liquid extraction. We have made during the last years, a concerted effort to describe simultaneously the chemical and physical processes involved in the preparation and application of SIR in metal extraction coupled with definition of their surface and morphological properties. This was brought about by the combination of the expertise vested in the three groups writing this paper: the Solvent Extraction Chemistry expertise of the group in Barcelona, the SIR and polymer chemistry expertise of the group in Rehovot and the Surface studies expertise of the group in Prague. At the starting point the thermodynamic approaches developed to describe liquid-liquid and solid ion exchange extraction systems were used as models. The thermodynamic evaluation was accomplished by:

a) description of the support-extractant system, in order to determine the extractant distribution between the aqueous and the polymer phases, as well as the aggregation state of the extractant in the polymer phase.

b) description of the extractant-metal reactions, in order to identify exactly the metal extraction species responsible for the metal extraction process.

Typically, different families of acidic organophosphorous extractants (DEHPA[2], Cyanex 272[2,11], DEHPTA[3-7]) and basic ligands (Alamine 336 and LIX79)[11-14] in the removal of heavy and precious metals have been thermodynamically characterised. As a general trend, behaviour of these extractants retained on the solid matrix and the extracted metal-ligand species follow similar trends to those found when dissolved in organic solvents. However, in specific cases some changes in the pH dependence order were found. This provides great confidence in the use of liquid-liquid distribution data as the initial step required in the design of new SIR's and those economise in the characterisation of the metal extraction properties of any new SIR's.

MORPHOLOGICAL CHARACTERISATION

The differences observed in metal removal by liquid extractant and by SIR's obtained by the immobilisation of the same extractant unto a porous polymeric carrier are the result of the influence inserted by the polymeric carrier matrix on the state of the extractant. We have only recently observed and reported such interactions[3-7]. The affirmation of this influence is of great significance, and the

elucidation of the mechanism by which the supporting matrix influences metal complex formation may enable new and more efficient methods of metal separation and recovery to be devised.

Determination of the morphology of the original polymers and the SIR's obtained from them by impregnation is very helpful in elucidation of the adsorption mechanism of the extractant. The results of specific surface area determinations and mercury intrusion porosimetry were used to determine the different mechanism involved in extractant retention in the polymer phase as a function of the polymer structure and the type of mechanism involved on the retention: a) physical adsorption or b) chemical interaction. For comparison, the results of specific surface area measurements on the starting reactive macroporous polymeric supports (e.g. PVP, ion exchange resins) and after the impregnation with a dithiophosphoric derivative (DEHPTA) only small changes of the specific surface area and total Hg intrusion volume of the resin samples with the supported extractant were found. However, there is evidently a very great decrease in the surface area when using non-reactive macroporous supports (Amberlite XAD2, XAD4) with increase of the ligand loading. These observations are consistent with the existence of two different mechanisms of DEHTPA sorption on reactive supports as (Reillex™ and ion weak base ion exchange resins as MP62, MP64 (Bayer AG) and Amberlite XAD supports. On reactive resins the impregnation proceeds via a chemical interaction of DEHTPA with the pyridine groups of the functional polymeric support. The predominant part of the extractant is adsorbed into the polymer phase where it is held by chemical rather then by physical interaction, however, a small amount of the extractant, physically adsorbed in the pores may be present too. The presence of DEHTPA-Pyridine complexes in the DEHTPA-Reillex™ SIR's was further proven by FTIR analysis. In the case of Amberlite XAD based SIR's absorption proceeds via creation of a separate extractant phase filling the pore volume. A pioneering Study of the extractant state and activity in the porous carriers by means of IR and 31P, 1H NMR spectroscopic methods supports this conclusion[4-7].

This novel phenomenon may be of general importance. First, if it is needed to find out if the migration equilibrium constants are related to some molecular factors, e.g. molecular weight, hydrophobic constant, molecular volume. If differences are found, this could be the basis for a new separation technique. Second, it was found[9] that the metal, DEHDTPA, complex is a hydrophobic entity, which can be readily removed from the non-complexed DEHDTPA by extraction with toluene. Hence, here is a basis for a new type of process using SIRs. The first step involves removal of a toxic metal from an aqueous stream using a solid [(SIR)]. The second step is regeneration of the metal complex using an organic solvent.

DEVELOPMENT OF SIR FOR HYDROMETALLURGICAL APPLICATIONS

Dilute solution of gold cyanide and other metal cyanide complexes (Ag, Fe, Cu, Ni, Co) are currently purified and concentrated by activated carbon. However in the last years the following innovations were attempted: substitution of activated carbon by ion-exchange systems and implantation of processes combining leaching and adsorption steps. The main objective for the implantation of IX was solving existing problems associated with activated carbon for example the need to improve the selective recovery of gold cyanide; the need to prepare ion exchange materials with high loadings and stripping efficiencies; and developing integrated process of leaching and extraction as Resin in Leach and Resin in Pulp processes. In this last case, the ion exchange material to be used should fit the experimental conditions of the system, and being able to extract gold from the leaching solutions containing $Au(CN)_2^-$ at about pH 10. The objective might be accomplished if it is possible to develop a polymeric support with a functional group (R), which would operate on the hydrogen ion cycle shown in the following reaction:

$$PS\text{--}Rres + H^+ \Leftrightarrow P\text{--}RH^+res$$

Where the equilibrium lies far to the right at pH < 10 and far to the left a pH>12.5. The functional

group in the protonated form, (RH+), at pH<10 would be an active anion extractant, the functional group in the neutral form R at pH>12.5, would not be an anion extractant. Then, gold cyanide extraction will be accomplished by the following reaction:

$$PS\text{--}RH^{+}res + Au(CN)^{2-} \Leftrightarrow PS\text{--}RH^{+}\ Au(CN)^{2-}\ res$$

Available single extractants tested do not meet the above objectives on pH cycle with the exception for recently developed family of reagents from Henkel Co containing a guanidine functionality with pKa values around 12, or greater, depending on the R groups attached to the various nitrogen atoms. This is the case of N,N'-bis(2-ethylhexyl)guanidine which is being nowadays commercialised under the name of LIX79. The pH extraction behaviour of LIX79 has been studied in cumene and impregnated onto Amberlite XAD2 shown a typical S function shape with a quantitative extraction in the range 9-10 and shifting the pH to values of 12 the back reaction proceeds allowing the elution of the goldcyanide complex. This guanidine functionality appears to fit the chemistry of gold cyanide leaching solution quite nicely, extracting gold well at pH<10.5. Such system will fit the process operation when applying in Resin in Pulp and Resin in Leach, in terms of the extraction and stripping steps[12].

SIR AS EXTRACTION CHROMATOGRAPHIC MATERIALS IN ANALYTICAL APPLICATIONS

Solvent Impregnated Resins could be used as stationary phases with high efficiency for Extraction Chromatographic schemes as an excellent alternative to ion exchange resins. Thus, the use of impregnated resins for preconcentration and clean-up in metal ions analysis in complex matrices offers the following benefits: a) the active part of the resin (complexing group), can be selected depending on the nature of the metal ion, the sample matrix and the analytical procedure which is going to be applied; b) the impregnation procedures of the complexing molecules are very simple and c) their structure and composition can be designed to be compatible with integrated detection systems, when used in solid phase spectroscopic measurements. In the determination of trace metals in surface waters by means of fully automated analytical methodologies based on UV-VIS spectrophotometry, separation is an important issue. Some non toxic metal ions, such as Fe(III) and Zn(II), can be in surface waters at relatively high concentration levels, which may become a serious interference problem when the aim of the analysis is the determination of toxic metal ions (e.g. Cu(II), Cd(II), Pb(II), Ni(II)) . Under this situation the best approach to solve this problem is a separation process based on the use of SIR. Literature search on liquid-liquid extraction systems allowing the separation factors needed indicated that the use of a phosphinic derivative Cyanex 272 containing di(2,4,4-tri-methylpentyl) phosphinic acid was the right solution to solve this problem. Evaluation of Cyanex 272 impregnated resins in on-line analytical schemes for the separation of Zn and Ni from the target toxic metal group (Cu, Cd and Pb), as a pre-treatment step before the spectrophotometric analysis of these metal ions was suitable to fit the separation patterns required[12-14].

ACKNOWLEDGEMENTS

We wish to acknowledge to Purolite, Bayer AG, Reilly Chemicals and Rohm & Haas Hispania for resin supply and to Henkel and Cyanamid Co for extractants supply. Finally, this work was supported by CICYT Project QUI96-1025-C03-02 (MEC, Spain). The support of the AID-CDR grant C13-085 (A. Warshawsky, K. Jerabek 1993-7) is gratefully acknowledged. A.Warshwasky is the holder of the Rebbeca and Israel Sieff professorial chair in organic chemistry.

REFERENCES

1. Warshawsky A, *Ion Exchange and Solvent Extraction*, J.A. Marinsky and Y. Marcus, Eds., Marcel Dekker, New York, **8,** 229, (1981).
2. Cortina JL and Warshawsky A, *Ion Exchange and Solvent Extraction*, J.A. Marinsky and Y. Marcus, Eds., Marcel Dekker, New York, **13**, 209, (1996).
3. Warshawsky A, Strikosky AG, Jerabek J and Cortina JL, *Solv. Extr. & Ion Exch.*, **15**(2), 259-283, (1997).
4. Jerabek J, Hankova L, Strikosky AG and Warshawsky A, *React. Polym.*, **28**, 149, (1996).
5. Strikovsky A, Jerabek K, Cortina JL, Sastre AM and Warshawsky A, *React. Funct. Polym.*, **28**, 149-158 (1996).
6. Strikovsky AG, Warshawsky A, Hankova L and Jerabek K, *Acta Polymerica* in press.
7. Cortina JL and Warshawsky A, unpublished data.
8. Jerabek J, unpublished data.
9. Warshawsky A and Jerabek K, Israel Patent pending.
10. Meinhardt E, Kautzmann RM, Ruiz N, Sastre AM, Sampaio CH and Cortina JL, in *Ion Exchange 98, Proceedings*, in press (1998).
11. Rovira M, Cortina JL, Arnaldos J and Sastre AM, *Solv. Extr. & Ion Exch.*, **16**(5), 1279, (1998).
12. Castillo E, Granados M, Prat MD and Cortina JL, *Solv. Extr. & Ion Exch.*, (submitted).
13. Roijals O, Martí V, Meinhardt E and Cortina JL, *React.& Functional Polym*, in press.
14. Castillo E, Granados M, Prat MD and Cortina JL, *Analytica Chimica Acta* (submitted).

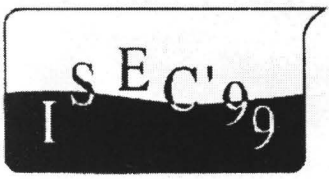

INFLUENCE OF POLYMERIC SUPPORT ON SELECTIVITY OF EXTRACTANT IN SOLVENT IMPREGNATED RESINS

Anna Gonzalo, Dmitri Muraviev and Manuel Valiente
Unitat de Química Anlítica, Universitat Autònoma de Barcelona, E-08193 Bellaterra, Barcelona, Spain.

ABSTRACT
The paper reports the results obtained by studying the influence of temperature on selectivity of Solvent Impregnated Resins (SIR) prepared by immobilisation of DEHPA in granulated macroporous polymeric matrices of different types. SIR represents a convenient model system to study the temperature dependencies of extractant selectivity by using a column mode of operation. The same technique can also be applied to evaluate the influence of the polymeric support on the properties of immobilised extractant. Capacity and stability of prepared SIR have been determined by sequential conversion of the resins to the proton and sodium form. Different SIR samples have been characterised in terms of their capacity and selectivity at different temperatures towards Cu^{2+} and Zn^{2+}. The comparison of temperature dependencies of SIR selectivity with that of DEHPA in different liquid-liquid extraction systems is carried out and discussed.

Keywords: zinc, copper, di-2-ethylhexylphosphoric acid, impregnated resins, XAD-2, XAD-4, XAD-7

INTRODUCTION

The Solvent Impregnated Resin (SIR) concept is known as one of the routes of conversion of a liquid-liquid extraction system into a solid-liquid one[1-12] Immobilization (impregnation) of the organic phase (extractant) of a bi-phase liquid-liquid system on (or in) an appropriate granulated solid, mainly polymeric support offers the following advantages in comparison with conventional extraction systems: 1) ease of phase separation due to elimination of problems concerned with the formation of stable emulsions; 2) the use of a dynamic mode of operation in columns; 3) the ease of designing a continuous separation process by using counter-current columns, and some others. In addition SIR represent a convenient model system to evaluate a possible influence of the polymeric support on the extractant properties, such as temperature dependence of its selectivity. This information is not available in the literature although it is of particular importance for both practical applications and theoretical interpretation of SIR based separation processes. Another field, where this information can be of great practical importance, is the design and tailored synthesis of ion-exchange resins with temperature-responsive selectivity [13,14] which are not commercially available. Their development must dramatically stimulate the development of ecologically-clean ion-exchange separation methods. The properties of extractant in a liquid-liquid extraction system ("free" extractant) can differ dramatically from those of the same extractant when introduced into a polymeric matrix ("semi-free" extractant).[13] Nevertheless, most of publications dedicated to SIR use an approach, which suggests, a priori, identical properties of both "free" and "semi-free" extractant.[4-6]

EXPERIMENTAL

All chemicals (of p.a. grade) were purchased from Panreac (Barcelona, Spain). Di-2-ethylhexylphosphate (DEHPA) of r.p.e grade was from Carlo Erba (Milano, Italy). Amberlite XAD-2 and XAD-4 macroporous polymeric supports (both of polysterene-divinylbenzene type, PS-DVB) were from Aldrich (Germany), and Amberlite XAD-7 polymer (polyacrylic ester, PAE) from Fluka (Germany). The main characteristics of these supports are shown in Table 1.

Stabilization of resins and determination of their capacity were carried out in 1 cm i.d., 20 cm long glass-columns from BioRad (USA). Before impregnation XAD-2, XAD-4 and XAD-7 non-ionic supports were treated with HCl 2 mol/dm^3 to eliminate possible inorganic impurities, followed by rinsing with water and ethanol. Finally all resins were dried at 60C. Overnight impregnation of 2 grams of each dry polymer with 25 cm^3 of a solution of 20% (v/v) DEHPA in DMF was carried out in

© 2000 Society of Chemical Industry

a vortex mixer (Fisher, USA). SIR samples were filtered and rinsed with a few cubic centimeters of ethanol/water (80/20) mixture to remove excess of impregnating solution and then placed in water.

Resin	Matrix	Porosity volume, %	Surface area, m^2/g	Pore diameter, Å
XAD-2	PS-DVB	42	330	90
XAD-4	PS-DVB	51	750	50
XAD-7	PAE	55	450	80

Table 1 Characteristics of polymeric supports

Determination of SIR capacities and their stabilization was carried out by sequential conversion of SIR samples to Na- and H-form as described elsewhere.[10,12,13] The Cu^{2+}- Zn^{2+} exchange equilibrium at different temperatures was studied using SIR samples with stable capacity as described elsewhere.[14] The capacity values of SIR samples were found to be 0.125 (XAD-2), 0.46 (XAD-4) and 0.087 mmol/g (XAD-7). The concentration of metal ions was determined by the ICP technique using ARL Model 3410 spectrometer (USA) provided with Minitorch. The effect of temperature on extraction of copper and zinc in the liquid-liquid (L-L) systems using equal volumes ($V_{Org}/V_{Aq} = 1$) of 0.1 mol/dm^3 DEHPA in cumene (isopropylbenzene) and 0.0075 mol/dm^3 solution of copper or zinc sulphate at pH = 2.4 was studied using a magnetically agitated thermostated cell provided with a refrigerator. The results obtained in both series of experiments were expressed in terms of temperature dependencies of metal distribution coefficients, D_M, which were calculated as follows:

$$D_M = \frac{[M]_0 - [M]_f}{[M]_f} (L-L \text{ systems}); \; D_M = \frac{[M]_R}{[M]_0} (\text{SIR systems}) \qquad (1)$$

where $[M]_0$ and $[M]_f$ are the initial and the final metal concentration in the aqueous phase, and $[M]_R$ is the equilibrium concentration of metal ion in the resin (SIR) phase (mols of metal/gram of resin). $[M]_R$ was determined by the analysis of the stripping solution collected from the outlet of the column. For SIR system, D_M does not depend on the ratio between amount of resin and volume of aqueous phase since the metal solution was passed through the resin until the equilibrium was achieved.

RESULTS AND DISCUSSION

The typical D_M versus temperature dependencies for Cu^{2+} and Zn^{2+} ions determined in SIR and L-L systems are shown in Figures 1a and 1b, respectively. As seen, the absolute values of both D_{Cu} and D_{Zn}, when determined in SIR and L-L systems, differ dramatically from each other. At the same time, the general trend of temperature dependencies of D_M remains essentially unchanged. Indeed, D_{Zn} values determined in all systems under study increase (see Figure 1b) while those of D_{Cu} do not essentially change with temperature. The only exception is the D_{Cu} vs t dependence determined in the Cu-DEHPA in kerosene system, where unlike other Cu-DEHPA systems studied a slight increase of D_{Cu} values with temperature is observed.[15] The higher D_M values obtained in SIR systems, in comparison with corresponding L-L ones, can be attributed by both higher concentration of extractant in the polymer and the influence of the polymeric environment on its properties[13]. Indeed, the order of both D_{Cu} and D_{Zn} values for different SIR samples follow the increase of their specific capacities. Higher D_M values are obtained for the SIR samples with hydrophobic PS-DVB matrix, XAD-2 and XAD-4, in particular. The different influence of the polymeric support on the properties of DEHPA when incorporated in the polymer can be attributed to different polarity and hydrophilicity, as the result, of the PS-DVB (XAD-2 and XAD-4) and PAE matrices. The different nature of the polymeric support strongly influences the interaction of the extractant molecules with fragments of the polymeric skeleton of the polymer. Thus, in XAD-4 and XAD-2 matrices only hydrophobic interactions between

extractant and polymer can occur while in XAD-7 both hydrophobic and hydrophyllic interactions can be expected to occur.

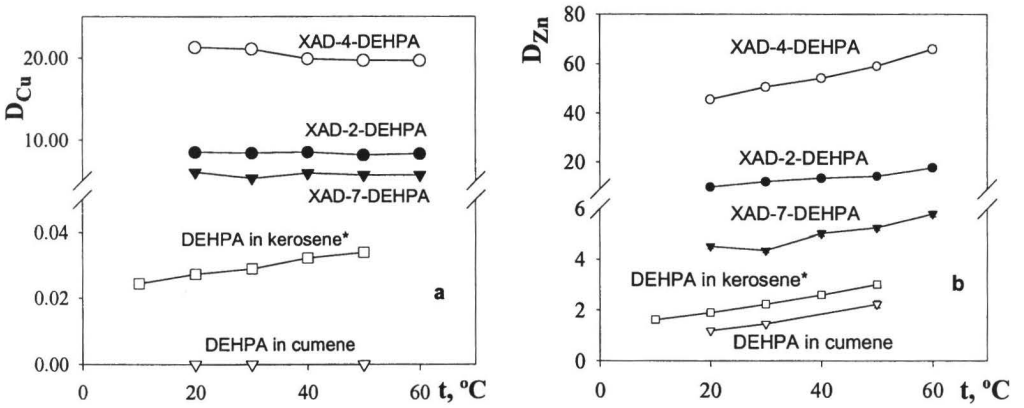

Figure 1. Temperature dependencies D_{Cu} (a) and D_{Zn} (b) for different DEHPA-SIR samples and DEHPA liquid-liquid systems (see text). *Data adapted from Ref. 15

Figure 2 shows normalised D_M vs t dependencies presented in Figure 1. Normalisation was carried out by dividing all $D_M(t_i)$ values with respective $D_M(20^o)$ determined in each system. As seen in Figure 1a, the normalised D_{Cu} vs t dependencies obtained in different SIR systems satisfactorily coincide with each other and also with that obtained in the DEHPA-cumene L-L system. For normalised D_{Zn} vs t dependencies shown in Figure 2b a better correlation between the results obtained in SIR and L-L systems is observed for the XAD-2 SIR samples. It is interesting to note that unlike the absolute D_M vs t dependencies (see Figure 1), after normalisation these dependencies for all SIR samples become very similar (cf., for example respective data for XAD-4-DEHPA and XAD-7-DEHPA systems). The results, shown in Figs. 1a and 1b, can also be interpreted in terms of metal ion sorbabilities.

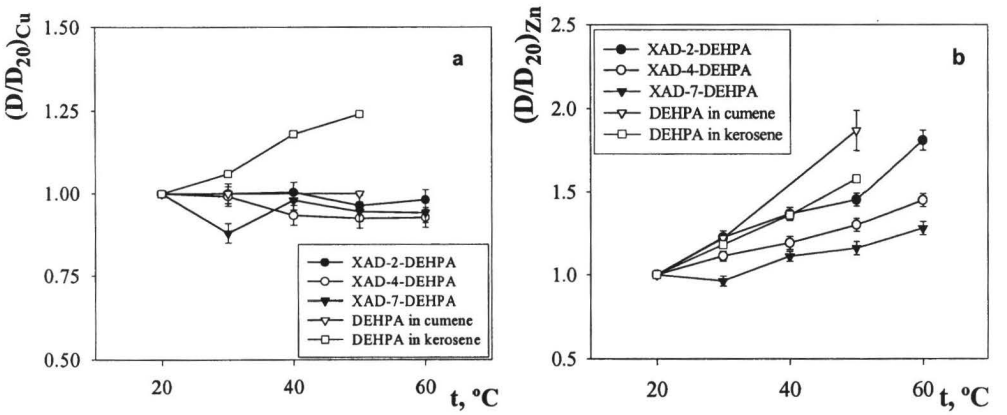

Figure 2. Temperature dependencies of normalised distribution coefficients of Cu^{2+} (a) and Zn^{2+} (b) for different DEHPA-SIR samples and DEHPA liquid-liquid systems (see text).

As follows from equation (1), the increase of D_{Zn} with temperature in the SIR systems under study (see Fig. 1b) reflects, in fact, the variation of zinc content in the resin phase as the composition of solution phase is identical in all cases. In other words, the variation of the partial capacity of the resin towards Zn^{2+} appears to be the parameter, which is responsible for the dependence of D_{Zn} on

temperature. At the same time, the relative constancy of D_{Cu} at different temperatures for all SIR samples studied (see Fig. 1a) indicates that the sorbability of this ionic species does not depend on temperature. Hence, the characterisation of the variation of SIR sample selectivities with temperature can be adequately carried out in terms of the resin capacities towards zinc. To simplify the comparison of different SIR samples and to allow comparison of the temperature dependence of DEHPA-SIR selectivities with that of the polymeric phosphoric resin KF-7, it seems convenient to express the partial capacities of all resins under comparison towards Zn^{2+} in terms of equivalent fractions of this ionic species in the resin phase, Y_{Zn}. Note that KF-7 resin can be considered as a polymeric analogue of DEHPA-SIR due to the identity of its polymeric matrix to that of SIR (also of PS-DVB type), and the similarity of the functional group of this resin to that of the extractant (DEHPA) incorporated in SIR. The properties of KF-7 resin are described elsewhere.[16] The normalised equivalent fractions of Zn^{2+} in the resin phase ($Y_{n,Zn} = Y_{Zn}(T_i)/Y_{Zn}(20^{\circ}C)$, see above) at different temperatures for DEHPA-SIR samples and KF-7 resin are shown in Figure 3.

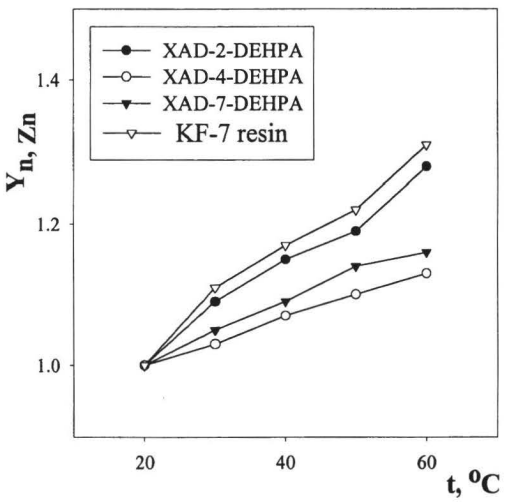

Figure 3. Normalised Y_{Zn} values versus temperature for different DEHPA-SIR samples and phosphoric resin KF-7 (see text).

As seen, both SIR and KF-7 resin demonstrate quite similar trends in changing $Y_{n,Zn}$ values with temperature, i.e. all $Y_{n,Zn}$ values increase when the temperature rises. At the same time, it is interesting to emphasise that, unlike XAD-4 and XAD-7 based SIR, the XAD-2-SIR sample demonstrates behaviour, which is far closer to that of phosphoric resin. This testifies to a far better suitability of this particular polymeric support for the preparation of DEHPA-SIR to model the properties of analogous ion-exchange resins. Two important conclusions follow from the results presented in Figure 3: 1) SIR systems can be successfully applied to model the properties of polymeric ion-exchange resins with similar functionality, and 2) this modelling allows for selection of both the extractant and the polymeric matrix for the tailored synthesis of ion-exchange resins with temperature responsive selectivity (see Introduction).

ACKNOWLEDGEMENTS

This work was supported by the Research Grant No. EV5V-CT94-556 from the Commission of the European Communities, Programme Environment 1990-1994. Bayer Hispania Industrial, S.A., is gratefully acknowledged for kindly supplying samples of Lewatit resin. A.G. is a recipient of a fellowship from CIRIT (Commission for Science and Technology of Catalunya), which is also acknowledged with thanks. Thanks are also due for the financial support to Dmitri Muraviev during his Visiting Professorship at Universitat Autonoma de Barcelona.

REFERENCES

1. Warshawsky A, *Talanta*, **21**, 624, 962, (1974).
2. Parrish JR, *Anal. Chem.*, **49**, 1188, (1977).

3. Vernon F, *Hydrometallurgy*, **3**, 65, (1978).
4. Cortina JL, Mirales N, Sastre AM, Aguilar M, Profumo A and Pesavento M, *React. Polym.*, **21**, 103, (1993).
5. Cortina JL, Mirales N, Sastre AM and Aguilar M, *Solv. Extr. Ion Exch.*, **12**, 371, (1994).
6. Strikovsky AG, Jerábek K, Cortina JL, Sastre AM and Warshawsky A, *React. Funct. Polym.*, **28**, 201, (1996).
7. Warshawsky A, Strikovsky AG, Jerábek D and Cortina JL, *Solv. Extr. Ion Exch.*, **15**, 259, (1997).
8. Warshawsky A, in Marinsky JA and Marcus Y (Editors), *Ion Exchange and Solvent Extraction*, Marcel Dekker, New York, **8**, Chap.3, (1981).
9. Cortina JL and Warshawsky A, in Marinsky JA and Marcus Y (Editors), *Ion Exchange and Solvent Extraction*, Marcel Dekker, New York, **13**, Chap.5, (1997).
10. Muraviev D, *Solv. Extr. Ion Exch.*, **16**, 381, (1998).
11. Muraviev D and Högfeldt E, *React. Polym.*, **8**, 97, (1988).
12. Muraviev D, *Chemica Scripta*, **29**, 9, (1989).
13. Muraviev D, Noguerol J and Valiente M, *Solv. Extr. Ion Exch.*, in press (1999).
14. Muraviev D, Gonzalo A and Valiente M, *Anal. Chem.*, **67**, 3028, (1995).
15. Sato T, Kawamura M, Nakamura T and Ueda M, *J. Appl. Chem. Biotechnol.*, **28**, 85, (1978).
16. Muraviev D, Torrado A and Valiente M, this issue.

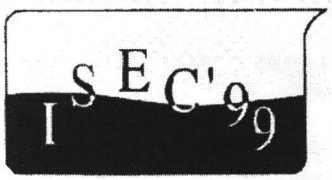

EXTRACTION OF HEAVY METAL IONS USING ENCAPSULATED EXTRACTANT-IMPREGNATED RESIN

Susumu Nii, Masataka Masutani and Hiroshi Takeuchi
Department of Chemical Engineering, Nagoya University, Chikusa-ku, Nagoya 464-8603, Japan

ABSTRACT
The pores of the polymeric microporous resin were filled with an organic solution of tri-*n*-octylamine (TOA) and LIX84I, and the surface of the resin was covered with Nylon 6-10 film formed by interfacial polymerisation of sebacoyl chloride and hexamethylenediamine. The extractant-impregnated resin is successfully encapsulated with a polymer membrane. The extraction of Zn^{2+} or Cu^{2+} from an aqueous phase was carried out with a stirred vessel using the capsule containing both extractants. The capsule is so stable that the extraction capacity remained constant after five operation cycles of forward and back extraction. The extraction equilibrium for both types of capsules suggested that extraction mechanisms are the same as in liquid-liquid extraction. For the capsule containing TOA, the increase of sebacoyl chloride concentration leads to a decrease in Zn^{2+} transfer rate, which suggests that the rate-controlling step is diffusion in the membrane. For the capsule containing LIX84I, the initial extraction rate was given by the expression $1.2 \times 10^{-8}[Cu^{2+}]^{0.5}[RH][H^+]^{0.5}$. Using a packed bed of the capsule containing LIX84I, A stable column operation was carried out.

Keywords: zinc, copper, tri-*n*-octylamine, LIX84I, extractant-impregnated resin

INTRODUCTION

The recovery of valuable or toxic metal ions from aqueous solutions is important for recycling of resources or wastewater treatment. For this purpose, ion exchange and chelating resins have been applied. Although handling and scale-up for these systems, is quite easy, these resins have the disadvantages that only the functional groups of the surface are effective and the extraction rate is not high enough. By applying solvent extraction, the rate and the capacity can be improved. However, the dissolution of extractants or solvents in the aqueous phase is a problem when treating a large amount of aqueous solution. For the purpose of developing a novel separation material of easy handling, some attempts have been made to encapsulate the extractant[1] or to use extractant-impregnated resins.[2,3,4] Although the encapsulation of the extractant successfully prevented the dissolution of extractant in aqueous phase, the mechanical strength of the capsules is not enough for a packed bed operation. On the other hand, extractant-impregnated resins are enough strong for the packed bed operation, but they also have a serious disadvantage concerning their rapid degradation due to the dissolution of extractant in the aqueous phase.

The present study is aimed to develop a highly stable microsphere containing an extractant by encapsulating a microporous resin that is impregnated with an extractant solution. The dissolution of the extractant is prevented by encapsulation, and the microporous resin likely keeps the mechanical strength. When the extractant was encapsulated and fixed in a solid support, the handling is quite improved, and the process of phase separation is not required. A column operation was also carried out for testing feasibility of continuous operation.

EXPERIMENTAL

Capsule preparation.

Extractants used were tri-*n*-octylamine (TOA) and LIX84I for zinc and copper extraction, respectively. They were diluted with dodecane or Shellsol. For the later step of polymerisation, sebacoyl chloride was added to the solution. A polymeric microporous resin, Amberlite XAD-II was soaked in the solution. The porosity of the resin is 0.42, the average pore diameter being 9nm, and the average particle diameter 560μm. After removing the remaining solution by filtration, the resin impregnated with the corresponding extractant was obtained.

© 2000 Society of Chemical Industry

An amount of the resin was poured into 100cm^3 of water containing gum Arabic at 2 wt%. The mixture was stirred at 12.5 s^{-1} in a vessel for one hour. A given amount of hexamethylenediamine was dissolved into the 0.1mol/dm^3 NaOH to prepare the solution of 0.45 mol/dm^3 . The interfacial polymerisation of sebacoyl chloride and hexamethylenediamine was started by adding 10 cm^3 of the aqueous solution of hexamethylenediamine to the mixture of the resin and water. The surface of the resin was coated with the membrane of Nylon 6-10, and the encapsulated resin was prepared. For stabilising the membrane, the mixing was continued more than thirty minutes. The mixture of the capsule and the aqueous solution was then filtered. The capsule was washed with the detergent several times and rinsed with deionized water.

Batch operation.

The separation of Zn and Cu from a dilute aqueous solution was performed in a vessel using capsules containing TOA and LIX84I, respectively. The zinc solution was prepared by dissolving $ZnCl_2$ into a solution of 1 mol/dm^3 HCl. To prepare the copper solution, known amounts of $CuCl_2 \cdot 2H_2O$ were mixed with a buffer solution of acetic acid and sodium acetate. 100 cm^3 of the metal ion solution were poured into the vessel and stirred at a constant speed. The extraction was started by adding a given amount of the capsule into the solution, and the aqueous solution was sampled at fixed time intervals. The concentration of the metal ion in the aqueous solution was analysed with atomic absorption spectroscopy (AAS). After the extraction, the capsule was regenerated and used repeatedly. For regenerating the capsules used for zinc extraction, they were washed with 1mol/dm^{3}HCl and the zinc was stripped with deionized water. Capsules used for copper extraction were regenerated with 1mol/dm^3 HCl.

Continuous operation.

For a continuous column operation of copper recovery from aqueous solution, a packed bed of the capsule containing LIX84I was used with a diameter of 9.6 mm and a height of 65 mm. The feed solution consisted in an aqueous solution of copper chloride buffered with an acetic acid/sodium acetate solution. The feed was supplied to the top of the bed and the flow direction was downward. Fractions of the effluent were collected at different time intervals and their copper concentration was analysed with AAS.

RESULTS AND DISCUSSION

Separation of zinc ion from its dilute solutions was carried out in a batch mode by using a capsule containing TOA. Figure 1 shows the typical zinc concentration histories obtained. The initial flux was obtained from the initial slope $-dC/dt$. After the operation for 120 minutes, the concentration changed only slightly, which means that about 180 minutes was enough to reach the equilibrium under the experimental conditions. The extraction capacity of the capsule was determined from the operation for longer than 180 minutes. The curve does not change with the number of operation cycles, which implies that there is no 'wash out' of the extractant and demonstrates the high stability of the capsule. Figure 2 shows the extraction capacity of the capsule containing TOA. The capacity is proportional to the TOA concentration. It was reported that zinc and TOA form a 1:2 complex in the liquid-liquid extraction[5]. By assuming that the extraction mechanism in the capsule is the same as for the liquid-liquid extraction system, the amount of TOA used for extraction corresponds to about 80% of the moles of TOA involved. Such a reasonable agreement suggests that the extraction ability of the extractant is maintained after encapsulation and that no significant change in extraction mechanism is observed. The initial zinc extraction rates were examined under various conditions, wherein the interfacial area was taken as the total outer surface area of the capsule calculated on the basis of its average diameter of 570μm. There were no significant effects of stirring speed, the amount of capsule and the initial zinc concentration on the transfer rate, which suggests that mass transfer resistance in the aqueous boundary film is negligibly small.

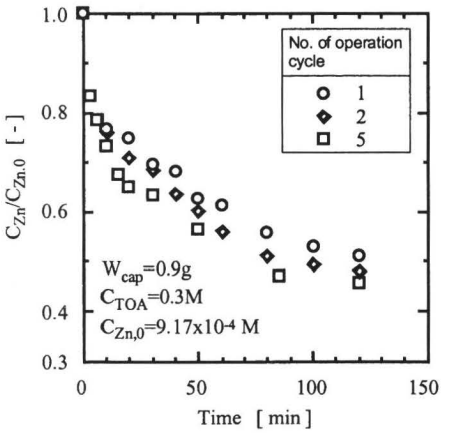

Fig. 1 Zinc concentration histories

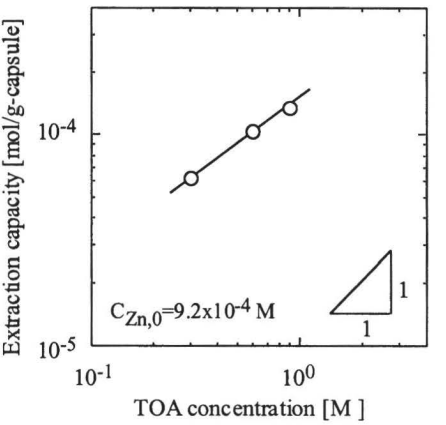

Fig. 2 Effect of TOA concentration on extraction capacity for zinc

Further experiments were carried out with various concentrations of TOA. The rate was constant for the concentration range from 0.3*M* to 0.9*M*, which indicates that the mass transfer is not controlled by the diffusion within the pore of the resin. Figure 3 shows the effect of sebacoyl chloride concentration on the extraction rate. Since the concentration of sebacoyl chloride was smaller than that of hexamethylenediamine, the concentration of sebacoyl chloride controls the degree of polymerisation, which possibly changes the thickness of the membrane. By assuming the membrane thickness is proportional to the concentration of sebacoyl chloride, the transfer rate is reduced when thickness of the membrane increases. These results suggest that the rate-controlling step for zinc extraction is the diffusion in the coating membrane.

After the extraction experiments, stripping was performed by mixing the capsule with deionized water. Almost all the zinc was removed from the capsule and the rate of back extraction was larger than that of the forward extraction.

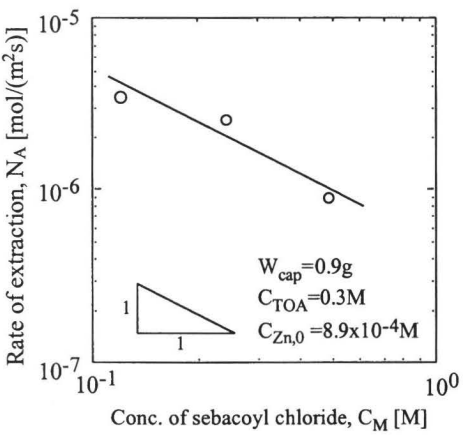

Fig.3 Effect of monomer concentration on extraction rate for capsule involving TOA

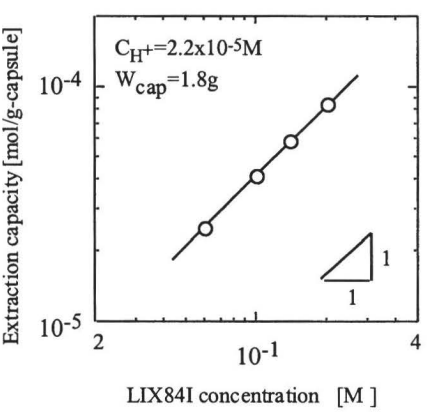

Fig.4 Effect of LIX84I concentration on extraction capacity for copper.

The extraction of copper from a dilute solution was carried out with the capsule containing LIX84I. The extraction capacity was examined five times, and the capacity remained constant, which demonstrates the mechanical stability of the capsule and the reversibility of the extraction reaction. Since the LIX84I was used without purification, its effective concentration was determined from the maximum loading of copper. Figure 4 shows the effect of LIX84I concentration on the extraction capacity.

The capacity linearly increased with the increase of extractant concentration. The extraction mechanism is discussed in terms of the distribution ratio of copper, which is determined by the equation.

$$D=(C_0/C_{eq}-1)(V_{aq}/V_{org}) \quad (1)$$

where, C_0 is the initial concentration, C_{eq} the copper concentration at equilibrium, V_{aq} the volume of aqueous phase, and V_{org} the volume of organic phase involved in the porous resin. Figure 5 shows the dependence of pH on the distribution ratio. In the lower pH region, the slope of the curve approaches -2, which suggests that two hydrogen ions are released by the extraction of a copper ion. In the higher pH region, the distribution ratio approaches a constant value due to the saturation of the extractant.

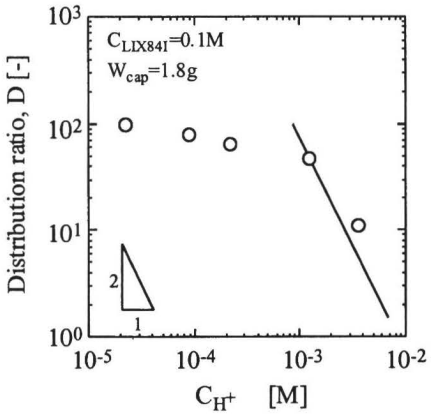

Fig.5 Effect of pH on distribution ratio

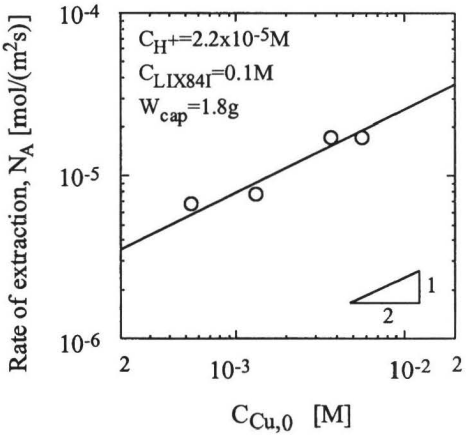

Fig. 6 Effect of initial concentration of copper on extraction rate

The initial extraction rate was observed under various conditions. The change in stirring speed did not affect the extraction rate in the range from 2.8 s^{-1} to 15 s^{-1}, which suggests that the mass transfer rate is not controlled by the diffusion in the aqueous boundary film. Figure 6 shows the effect of initial concentration of copper on the extraction rate. The rate increases with increasing copper concentration with a slope 0.5. The effect of LIX84I concentration on the extraction rate is shown in Fig. 7. The rate increases with increasing LIX84I concentration with a slope of 1, which indicates that the extraction rate is affected by the rate of reaction and/or the diffusion within the capsule. The effect of pH on the extraction rate was also examined. The result showed the rate varies with $[H^+]^{-0.5}$. Therefore, the initial extraction rate was expressed by $k\,[Cu_0^{2+}]^{0.5}[RH]/[H^+]^{0.5}$. The rate coefficient was determined from the plot of $N_A[H^+]^{0.5}/[RH]$ versus $[Cu_0^{2+}]$, and the following equation was obtained.

$$N_A = 1.2\text{x}10^{-8}\,[Cu_0^{2+}]^{0.5}[RH]/[H^+]^{0.5} \quad (2)$$

The predicted values of initial extraction rate were calculated and are plotted as a solid curve in Figs. 5 and 6. A reasonable agreement is observed between the observed and predicted values.

After the extraction experiments, the capsule was regenerated by contact with 1mol/dm^3 HCl. After about 10 minutes operation, almost all the copper was removed from the capsule and the rate of back extraction was larger than that for the forward extraction rate.

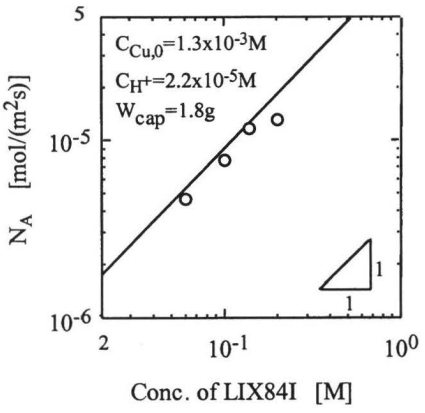

Fig.7 Effect of LIX84I concentration on extraction rate

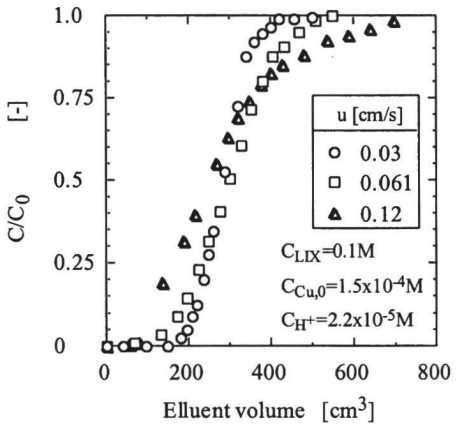

Fig.8 Breakthrough curve for copper extraction using packed bed of capsule involving LIX84I

The mechanical strength of the encapsulated resin is enough for a packed bed operation. The continuous stable operation was possible and the bed could be regenerated with 1mol/dm^3 HCl. Figure 8 shows the breakthrough curve for the packed bed of the capsule containing LIX84I. With increasing liquid velocity, the absorption band expands, what suggests an effect of diffusional mass transfer in the boundary film in the aqueous phase.

REFERENCES

1 Yoshizawa H, Uemura Y, Kawano Y and Hatate Y. *J. Chem. Eng. Japan*, **26**, 198, (1993).
2 Tavlarides LL, Baw JH and Lee CK. *Sep. Sci and Technol.*, **22**, 581, (1987).
3 Inoue K, Baba Y and Sakamoto Y. *Sep. Sci and Technol.*, **22**, 1349, (1987).
4 Akita S and Takeuchi H. *J. Chem. Eng. Japan*, **23**, 439, (1990).
5 Sato T, Adachi K, Kato T and Nakamura T. *Sep. Sci and Technol.*, **17**, 1565, (1982).

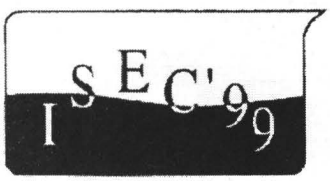

DESIGN OF A TRULY CONTINUOUS FLUIDIZED BED SYSTEM FOR METAL RECOVERY USING IMPREGNATED RESINS

M Rovira, J Herranz, JL Cortina, N Miralles, J Arnaldos and AM Sastre
Department of Chemical Engineering, ETSEIB, Universitat Politècnica de Catalunya, Diagonal 647, E-08028, Barcelona, Spain

ABSTRACT
A continuous fluidized bed system for metal recovery using impregnated resins with high wide versatility has been designed. The plant consists of two columns, one for extraction and another for stripping, both of a single stage. The circulation system and transport of resin is based on the use of peristaltic pumps. The capacity of treatment of the plant can be enlarged by connecting more than a column in series to achieve the required degree of extraction. Also, the hydraulic capacity of the plant can be increased putting more than one column in parallel.

Keywords: copper, LIX84, impregnated resins, XAD-2, continuous fluidized bed design

INTRODUCTION

Over the past years the development of impregnated resins as a link between solvent extraction and ion-exchange has been an important field of development in separation science.[1,2] Although the good performance exhibited by impregnated resins for the recovery of different metals, their application in industrial processes and commercial scale can present some difficulties such as handling solids in terms of continuous operation, process control, number of required units, etc. Therefore a suitable combination of impregnated resins and an appropriate technology for their optimum use is required. Our research group has been working on the development of impregnated resins for recovery and separation of metal ions from dilute solutions and their technological implementation by means of fluidized bed technology.[2-5]

Model systems to evaluate this concept of metal extraction schemes based on pH dependent extraction and stripping steps have been selected. Impregnated resins have been prepared by selecting highly selective metal extraction reagents with suitable acidic and basic properties which have been thoroughly characterized and studied in impregnated resins. These types of materials work with extraction-stripping steps following a pH cycle dependency as follows:

a) for acidic extractants (HL) (e.g. organophosphorous extractants):

extraction step: $M^{n+} + (n+q)HL_{res} \Leftrightarrow ML_n(HL)_{q,\,res} + nH^+$

stripping step: $ML_n(HL)_{q,\,res} + nH^+ \Leftrightarrow M^{n+} + (n+q)HL_{res}$

b) for basic extractants (B) (e.g. primary, secondary and tertiary alkylamine extractants):

extraction step: $MX_n^- + (BH^+Y^-)_{res} \Leftrightarrow (BH^+\,MX_n^-)_{res} + Y^-$

stripping step: $(BH^+\,MX_n^-)_{res} + OH^- \Leftrightarrow B_{res} + MX_n^- + H_2O$

Both systems present suitable properties for application in a continuous fluidized bed system because the stripping step using strong acid or base conditioning of resin between runs is easily achieved for further use by the addition or strong acid or bases (depending on the type (a,b)).

Some of the engineering design difficulties of continuous systems may be overcome by using fluidized beds of resins. In this work, the design of a truly continuous fluidized bed column device for the use of impregnated resins is reported. The system consists of two columns: an absorption or extraction column, where impregnated resin is fluidized by the upward flow of liquor from which ions are to be removed and an elution column, where the regeneration of the resin takes place. Extraction and elution columns operate simultaneously and during operation the resin moves through both columns by means of peristaltic pumps. A scheme of the system is shown in Figure 1.

© 2000 Society of Chemical Industry

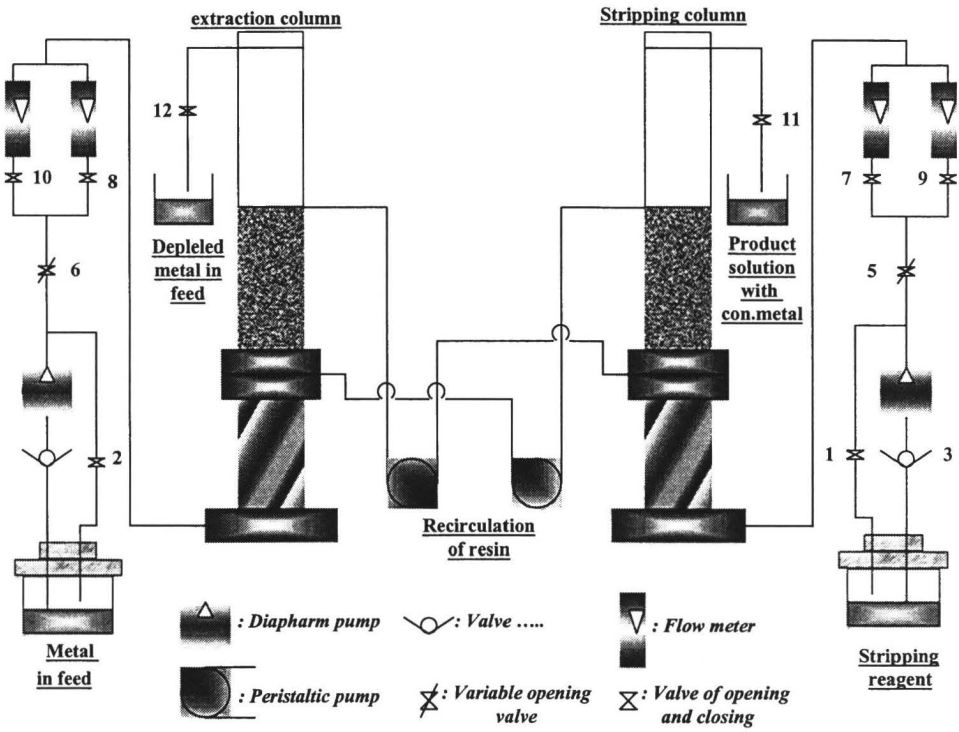

Figure 1. Simplified scheme of the pilot plant.

PILOT PLANT DESIGN

As a starting point, plant design and dimensioning has to operate with the parameters of the basic solid-liquid system. The chosen system was water-Amberlite XAD2 recognising that metal solutions to be processed are aqueous solutions at ambient temperature. The chosen resin support Amberlite XAD-2 is a high surface macroporous polymeric resin widely used when preparing impregnated resins,[1,2] although other resin adsorbents could be used with the designed pilot plant. Table 1 shows the characteristics of the chosen solid-liquid system.

	ρ (kg/m^3)	μ (Pa·s)	ρ_w (kg/m^3)	ρ_p (kg/m^3)	d_p (mm)	ϕ	ε_i
Water	998	$1 \cdot 10^{-3}$	-	-	-	-	-
XAD-2	-	-	1020	750	0.32-0.8	0.7	0.4

Table 1. Characteristics of the solid-liquid system.

The dimensions of the fluidization columns, both for extraction and stripping, was fixed according to previous studies described in the literature.[7-10] The different fluidized plant designs described used column diameters between 51 and 600 and in the present design, 150 mm has been chosen as column diameters to allow later extrapolation of the results. Then taking into account the solid-liquid properties and the column diameters fluidization parameters of both columns have been calculated by using the appropriate equations.[11] The calming section has the same diameter that the column. Fluidization parameters and design parameters are shown in Tables 2 and 3.

u_{mf} (mm/s)	u_t (mm/s)	$u_{t,min}$ (mm/s)	ε_{mf}	ε_{max}	ΔP (Pa)	ΔP_d (Pa)
0.23	9.8	2	0.4	0.7	78	10

Table 2. Fluidization parameters.

Diameter of the columns	150 mm
Thickness of the column walls	3 mm
Height of the columns	1 m
Maximum operation velocity	10 u_{mf}
Height of the calming section	0.3 m
Distributor free area	2.3%

Table 3. Design values of the fluidization columns.

Polymethylmethacrylate (PMM) was selected as the material for both columns due to both its resistance to the operation conditions (ambient temperature and pressure < 0.2 bar rel.) and, being transparent it allows the observation of any incident during column installation. The liquid distributor is a perforated plate built in PMM with 1 mm diameter holes in a centered hexagonal disposition with a 6 mm separation between them.

The recirculation of the resin between the columns is carried out by a peristaltic pump and it will be shown later this transport of resin does not generate fines and the resin capacity was constant over a number of runs. The characteristics of the peristaltic pumps (Masterflex model 7553-75, with bolster Quick Load) used are: 5.5 mm i.d. tubes, with 3 cylinders in the drive bolster, variable rotation speed between 6 and 600 rpm, and a range of flow-rates between 10 and 1000 cm^3/min

The resin feed in the two columns is made inside the bed just above the distributor. Generally, this type of feeding demands the injection of an auxiliary fluid, however in the different tests carried out this was found not to be necessary. Discharge is carried out by means of overflows located in the walls of the columns, with heights between 5 cm and 60 cm from the distributor. This ensures a wide versatility of the pilot plant. The resin feed and discharge are located on opposed sides of the columns, assuring the resin has the maximum time inside the bed.

Liquid circulation is carried out by means of centrifugal pumps to ensure a constant flow without pulsation that could affect the good operation of the installation. The chosen pumps (HEIDOLPH, model KrP 800) had a flow-rate of 2.8 dm^3/min and a pressure of 0.14 bar rel. The parts of the pump in contact with the solution were made of polypropylene.

Auxiliary equipment consisted of three reservoirs of 50 dm^3 capacity to feed each of the centrifugal pumps. This arrangement allowed one reservoir working, another in reserve and another to prepare the solution that feeds the columns. Reservoirs for the reception of the solutions that leave the columns were also provided. The connecting pipes of the installation were PVC with a nominal diameter of 25 mm and 1.5 mm thick. Different types of valves were used for the control of the circulation of liquid and solid. Thus valves with variable opening of the seat were placed in the installation to regulate the flow-rate of liquid that the columns receive, as well as ball valves to cut off the flow of liquid in a pipe when it is necessary. Also, a check valve was installed so that when the centrifugal pump was stopped, the column of liquid above the pump is retained and does not flow back through the pump allowing the liquid to return to the feed reservoir and mix with this solution. Two rotameters with Teflon floats with ranges from 2 to 20 dm^3/h and of 15 to 150 dm^3/h, respectively were installed to measuring the flow-rates of the liquids. The plant has a by-pass line so that the spare flow returns to the feeding reservoir. For the control of the circulation of the resin clip valves were used (flexible tubes). The flow of the resin was controlled by the rotational speed of the peristaltic pumps.

Finally, operation of the installation was studied for different types of impregnated resins and ion exchange resins, and it was found that the pilot plant worked in a satisfactory way hydrodynamically up to the most unfavorable case (i.e. a resin with ρ_p = 1280 kg/m^3, d_p = 0.8 mm and u_{max}/u_{mf} = 1.5),

Feasibility of impregnated resin transfer between the columns through a peristaltic pump

The feasibility of resin movement between the columns by means of a peristaltic pump is considered in this separate section since this is one of the key points of the plant design. Impregnated resins are based on the idea of adsorbing an organic solvent extraction reagent onto a polymeric support. Therefore, when impregnated resins are transported using a peristaltic pump, special attention must be taken to prevent damage of the solid due to the strong mechanic action of the pump cylinders. If damage of the resins occurs, loss of metal extraction ability and generation of fine particles could be expected.

A simple experiment was performed to ensure the feasibility of resin transfer, as proposed in the plant design section. A certain amount of impregnated resin, particle size 0.5-0.9 mm, was contacted with water in a vessel and agitated with a magnetic stirrer to simulate a fluidized bed. The same solid was transported several times to another vessel by means of the peristaltic pump described in the previous section. After each transport the metal extraction capacity was tested. As can be seen in figure 2, the impregnated resin extraction capacity was not affected. Moreover, at the end of the experience the resin was sieved, and the amount of fines produced was negligible.

Therefore, these experimental results demonstrate that the peristaltic pump may transport the resin efficiently between the columns.

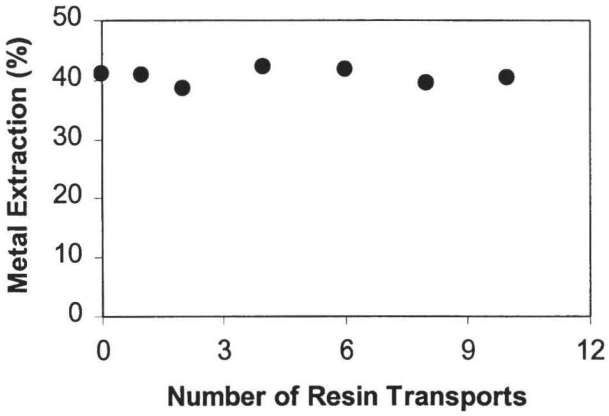

Figure 2. The influence of the number of impregnated resin transfers through a peristaltic pump on metal extraction.
Experimental conditions: 20 cm^3 of solution containing 500 mg/dm^3 Cu^{+2} in 0.1 mol/dm^3 Na_2SO_4/H_2SO_4 at pH = 4 were contacted with 0.2g of impregnated resins [LIX84(Henkel)/XAD2].

CONCLUSIONS

A continuous fluidized bed system with wide versatility, to process the extraction of heavy and precious metals with impregnated resins has been designed and evaluated. The plant consists of two columns, one for extraction and another for stripping, both of a single stage. The circulation system and transport of resin is made by peristaltic pumps that it has been shown do not cause attrition of the solid resin and thus loss of extraction capacity. The capacity of treatment of the plant can be enlarged by connecting more than one column in series to make the required degree of extraction. Also, the hydraulic capacity of the plant can be increased putting more than one column in parallel.

NOMENCLATURE

d_p particle diameter.
ΔP pressure drop in the bed.
ΔP_d pressure drop in the distributor.
u_{mf} minimum fluidization velocity.
u_t terminal velocity.
ε_i internal porosity of the particle.
ε_{mf} bed voidage at incipient fluidization.
ε_{max} maximum bed voidage.
ρ liquid density.
ρ_p apparent density of the particle.
ρ_w density of the wet particle.
μ liquid viscosity.
ϕ shape factor.

ACKNOWLEDGMENTS

This work was supported by CICYT Project QUI 96-1025-CO3 (Ministry of Science and Culture of Spain) and 96SGR 00101 (Autonomous Government of Catalonia).

REFERENCES

1. Warshawsky A, in *Ion Exchange and Solvent Extraction* ed Marinsky J and Marcus Y, Marcel Dekker, **8**, 229, (1991).
2. Cortina JL and Warshawsky A, in *Ion Exchange and Solvent Extraction,* ed Marinsky J and Marcus Y, Marcel Dekker, **12,** 199, (1996).
3. Cortina JL, Miralles N, Sastre A, Aguilar M, Profumo A and Pesavento M, *Reactive Polymers,* (a) **23**, 81, (1993) and (b) **23**, 103, (1993).
4. Meinhardt E, Kautzmann RM, Ruiz N, Sastre AM, Sampaio CH and Cortina JL, in *"Proceedings of the Ion Exchange '98 Conference*", in press (1998).
5. Rovira M, Hurtado L, Cortina JL, Arnaldos J and Sastre AM, *React and Funct Polym.*, in press, 1998.
6. Cortina JL, Meinhardt E, Roijals O and Martí V, *React. and Funct. Polym.*, **36**, 149, (1998).
7. Anderson NJ, Dixon DR and Swinton, E.A.. *J. Chem. Tech. Biotech.*, **29**, 332, (1979).
8. Cosmen P, Ruiz ML and Gasós P, *Ingeniería Química*, **7**, 177, (1991).
9. Himsley A, *Annual Meeting International Water Conference 41st*, 236. Pittsburgh. October 20-22 (1980).
10. Slater MJ, *Can J. Chem. Eng.* **52**, 43, (1974).
11. M. Rovira M, L. Hurtado L, J. L. Cortina JL, J. Arnaldos J and A. M. Sastre AM in *"Second European Meeting on Chemical Industry and Environment"*. Eds. Piccinini N and Delorenzo R, Politecnico di Torino, **2**, 469, (1996).

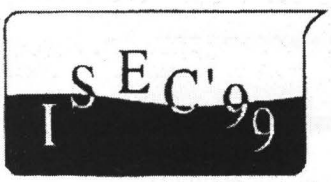

EXTRACTION OF NON-EXTRACTABLE IONIC SPECIES IN AQUA IMPREGNATED RESIN SYSTEMS

Dmitri Muraviev, Anna Torrado and Manuel Valiente
Departament de Química, Unitad de Química Analítica, Universitat Autònoma de Barcelona, E-08193 Bellaterra, Barcelona, Spain

ABSTRACT
The paper reports the results on the further development of the Aqua Impregnate Resin (AIR) concept. The AIR concept represents one of two possible routes to convert liquid-liquid (aqueous-organic, Aq-Org) extraction system to a solid-liquid one through the immobilisation of the aqueous phase in a polymeric matrix. It has been shown that metal ions, which are not extracted in conventional Aq-Org systems (non-extractable ionic species) can be extracted in a corresponding AIR system. The results obtained by studying Aq-Org and AIR systems including di-2-ethylhexylphosphoric and di-2-ethyhexyldithiophosphoric acids, carboxylic, iminodiacetic and phosphoric resins and aqueous solution of Cu^{2+} and Zn^{2+} mixtures of different compositions are reported and discussed.

Keywords: zinc, copper, di-2-ethylhexylphosphoric acid, di-2-ethyhexyldithiophosphoric acid, aqua impregnated resins, carboxylic acid, iminodiacetic acid, phosphoric acid resins

INTRODUCTION

Triphase solid-liquid-liquid (S-L-L) systems including a solid resin and two immiscible liquid phases (aqueous and organic) are known in the literature mainly as triphase catalytic systems.[1,2] Phase-transfer catalysis with ion-exchange resins[3,4] and reactive extraction with ion-exchange membranes[5,6] are comparable mass-transfer process taking place in S-L-L systems. Two versions of S-L-L systems including either ion-exchange membranes[6] or granulated ion-exchange resins,[7-9] simultaneously contacting both organic and aqueous phases, have been applied to the effective hydrogen-deuterium, H-D, exchange on (trimethylamino)borane dissolved in water-immiscible solvents. The H-D exchange reaction has been demonstrated to occur at the interface between the water swollen (aqua-impregnated) ion-exchange material and the organic phase. In this case the aqueous phase (D_2O) can be withdrawn from S-L-L systems in such a way that it is substituted by the D_2O taken up in the swollen polymer.[8,9] Thus, the triphase S-L-L system is transformed into the corresponding biphase one where the aqua-impregnated resins (AIR) phase is in contact with the organic solution of the substrate.[9] Recently it has been demonstrated that AIR systems can be effectively applied to the separation of metal ions.[10]

EXPERIMENTAL

All chemicals (of p.a. quality) were purchased from Panreac P.A. (Barcelona, Spain). Iminodiacetic ion exchanger, Lewatit TP-207, and carboxylic resin, Lewatit S 8528, were kindly supplied by Bayer Hispania Industrial, S.A. A phosphoric resin, KF-7, was from IREA (Moscow, Russia). All resins were of the polystyrene-divinylbenzene (PS-DVB) type. Di-(2-ethylhexyl-phosphoric acid (DEHPA), 99%, was purchased from Carlo Erba R.S. (Italy). Di-(2-ethylhexyl)-dithiophosphoric acid (DEHDTPA) was synthesized as described elsewhere.[11] The purity of the final product appeared to be ~85 %. Doubly distilled water was used in all experiments. The pH of metal ion solutions was controlled by using a Crison pH meter 507 (Barcelona, Spain), supplied with a combined glass electrode. The concentration of metal ions was determined by the ICP technique using an ARL Model 3410 spectrometer provided with Minitorch. The relative uncertainty of metal ion determination was <1.5 %. All experiments were accomplished at 22 ± 0.5C. Experiments on extractive stripping of Cu^{2+} and Zn^{2+} from KF-7 resin in AIR systems were carried out under dynamic conditions in columns packed with 0.3 g of the resin pre-equilibrated with a stock solution of 0.02 mol/dm^3 (Cu,Zn)SO_4 of 1:4 Cu:Zn molar ratio at pH = 3.8. After equilibration, the resin was rinsed with water followed by a consecutive rinsing with ethanol (from water) and heptane (from ethanol).

© 2000 Society of Chemical Industry

The stripping solutions (0.2 mol/dm^3 DEHPA or DEHDTPA solutions in heptane) were passed at a constant flow rate (~0.2 cm^3/min) and collected in portions in pre-weighted vials. The eluate sample volumes were determined by dividing the weight of eluate samples by the density of the respective stripping solution. The accuracy of volume determination was ± 0.005cm^3. The concentration of metal ions was determined in all samples. Samples of DEHPA and DEHDTPA eluate were first treated with 5 cm^3 of 0.2 mol/dm^3 NaEDTA to strip metal ions from the organic phase. The stripping was carried out under vigorous agitation for 15 minutes. Experiments studying the extraction and ion-exchange equilibrium in the triphase systems involving solid resin (R), organic solution of extractant (Org) and aqueous solution of metal ions (Aq) were carried out in batch mode by following the procedure described elsewhere.[10] The volumes of Aq (0.06 mol/dm^3 (Cu,Zn)SO_4 with Cu:Zn ratio of 2.5:1 in acetate buffer at pH = 3.8 ± 0.05) and Org (0.2 mol/dm^3 DEHPA or DEHDTPA solution in heptane) were in all cases 10 and 3 cm^3, respectively. The amount of R varied from 0.025 to 0.100 g.

RESULTS AND DISCUSSION

Typical concentration-volume histories obtained by extractive stripping of Cu^{2+} and Zn^{2+} from KF-7 resin using either DEHPA or DEHDTPA solutions in heptane are shown in Figure 1. As seen in Figure 1a, the treatment of the resin with DEHPA, known to be highly selective towards zinc over copper[12] leads to the preferential extraction of Zn^{2+} from the resin phase so that the eluate, except first three portions, contains essentially pure zinc. At the same time, some Cu^{2+} is also co-extracted in the first eluate portions. Note, that practically no extraction of Cu^{2+} is observed in conventional Aq-Org system of similar composition.[10,12] A far more substantial extraction of "non-extractable" ionic species is observed in the KF-7-DEHDTPA AIR system. Indeed, as seen in Figure 1b, elution of metal ions from the resin with DEHDTPA, which is highly selective towards copper over zinc in conventional Aq-Org extraction systems,[11] results in the preferential stripping of zinc from the resin phase. The results presented in Figure 1, which are in good agreement with the previously reported data,[10] can be interpreted in terms of the following parameters: 1) selectivity of the Org; 2) selectivity of the R; 3) hydration of metal ions, and 4) pH in the resin phase. The selectivity of the resin and extractant towards the ion couple under study can be characterised by the selectivity factor, α, which is defined as follows:

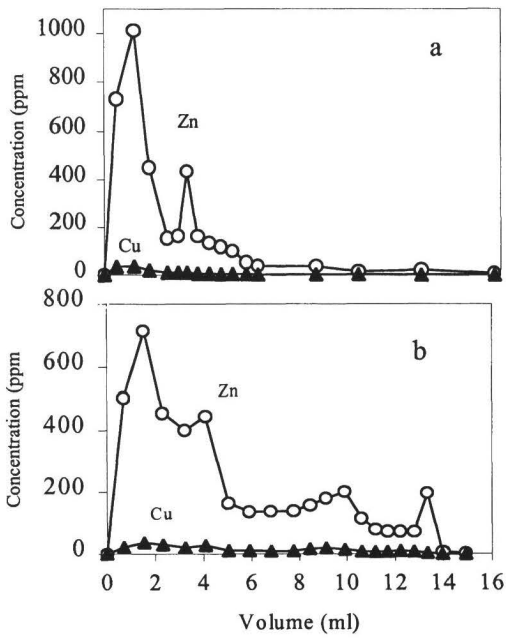

Figure 1. Concentration-volume histories obtained in KF-7-DEHPA (a) and KF-7-DEHDTPA (b) AIR systems (see text).

$$\alpha_{Zn}^{Cu} = \frac{Y_{Cu}\, X_{Zn}}{Y_{Zn}\, X_{Cu}} \qquad (1)$$

where Y and X are the equivalent fractions of metal ions in the resin or extractant and aqueous solution phases, respectively. The α_{Zn}^{Cu} values determined in biphase R (KF-7)-Aq and Org

(DEHPA)-Aq biphase systems appeared to equal 1.78 and 0.0072 (α_{Cu}^{Zn} = 139.3), respectively, that indicates a higher selectivity of the resin towards Cu^{2+} and a higher selectivity of the extractant for Zn^{2+}. The determination of α_{Zn}^{Cu} value in the Org (DEHDTPA)-Aq system was not possible due to the extremely high selectivity of this extractant towards Cu^{2+}.

A comparison between the extractants and the resin selectivities reveals that extraction of Cu^{2+} in KF-7-DEHPA system (see Figure 1a) proceeds "against" the selectivity of both the resin and the extractant. In other words, this ionic species is extracted *from copper-selective resin with a copper-non-selective extractant*. This effect can be explained by alteration of both Cu^{2+} hydration and pH in the resin phase. Indeed, immobilisation of the Aq in the R, or impregnation of the R with the Aq, leads to the remarkable changes in the chemistry of the metal ions when sorbed by the KF-7 resin. Firstly, both Zn^{2+} and Cu^{2+} appear to be less hydrated in the R than in the respective Aq since water molecules can only occupy the co-ordination vacancies of metal ions that are not saturated with the functional (ligand) groups of the ion exchanger. Secondly, as a rule, the pH in the R is higher than in the Aq at equilibrium.[13] Hence, lower hydration and higher pH enhance the extraction of Cu^{2+} from the R. Similar reasonings can be used to explain extraction of Zn^{2+} in the KF-7-DEHDTPA system. The low extraction of Cu^{2+} in this system can be attributed, in turn, by the strong binding of this ion by the functional groups of the R.

The results obtained by studying the distribution equilibrium in the triphase Aq-R-Org systems are shown in Figures 2, 3 and 4.

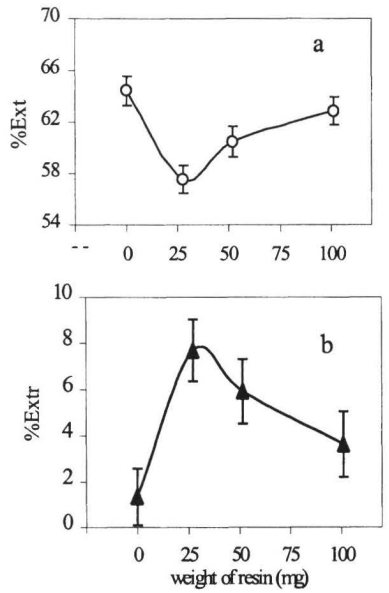

Figure 2. Extraction degrees of Zn^{2+} (a) and Cu^{2+} (b) in triphase R-Org-Aq system including KF-7 resin and DEHPA.

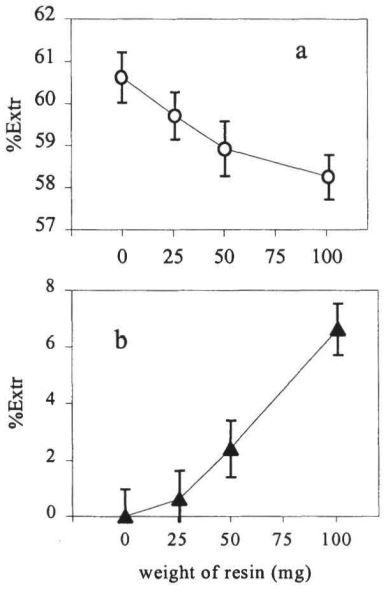

Figure 3. Extraction degrees of Zn^{2+} (a) and Cu^{2+} (b) in triphase R-Org-Aq system including Lewatit S 8528 resin and DEHPA.

The variable parameters in these series of experiments were the type and amount of the R introduced in the biphase Aq-Org system after equilibration. The KF-7 resin was pre-equilibrated with the initial stock solution of Cu^{2+} and Zn^{2+} mixture. In other cases the R was pre-equilibrated with solution of metal ions, whose composition corresponded to that of the Aq in the Aq-Org system at equilibrium. After achieving the equilibrium in the triphase system, the Aq phase was analysed to calculate the extraction degrees of metal ions, E, in presence of the R.

As seen in Figures 2 and 3, introduction of the resin phase in the Org-Aq system results to the remarkable redistribution of metal ions between the R and the Org, despite both of these phases having

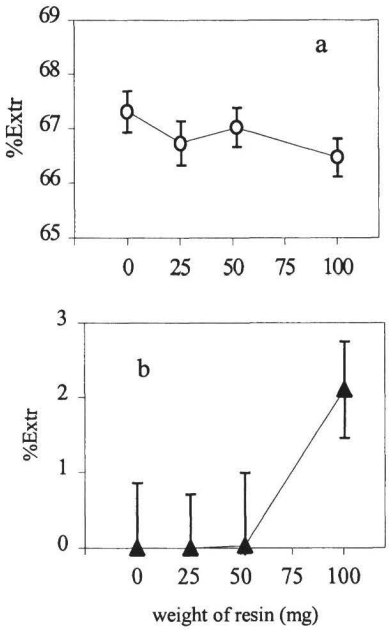

Figure 4. Extraction degrees of Zn^{2+} (a) and Cu^{2+} (b) in triphase R-Org-Aq system including Lewatit TP-207 resin and DEHPA.

been equilibrated with the Aq of the same composition. Indeed, introduction of small amount of the phosphoric resin (KF-7) in the Org-Aq system (see Figure 2) leads to a substantial increase of Cu^{2+} extraction accompanied by the decrease of Zn^{2+} concentration in the Org phase. The further increase of R content in this system results to the decrease of copper extraction while that of zinc increases. As seen in Figure 3, the influence of carboxylic resin (Lewatit S 8528) on the extraction behaviour of Cu^{2+} differs from that of KF-7 resin. The increase of the amount of resin introduced in the R-Org-Aq system leads to a nearly linear rise of Cu^{2+} extraction and to a simultaneous drop of Zn^{2+} content in the Org. A far weaker effect of the R on the extraction of both Cu^{2+} and Zn^{2+} is observed in the R-Org-Aq system involving the iminodiacetic resin (Lewatit TP-207) as is clearly seen in Figure 4. Introduction of small amounts (25 or 50 mg) of the R in the Org-Aq does not essentially affect the distribution equilibrium of metal ions. The increase of the amount of R to 100 mg results in a slight decrease of Zn^{2+} extraction and also slightly increases extraction of Cu^{2+}.

The results presented in Figures 2, 3 and 4 can be interpreted by viewing all distribution equilibria in the R-Org-Aq systems under study. The triphase systems of this type are characterised by three interfaces: Org-Aq, R-Org and R-Aq. Each interface represents a possible pathway for the transfer of metal ions and therefore can be associated with the respective ion-exchange (or extraction) reaction as follows:

R-Aq interface:

$$R\text{-}Zn + Cu^{2+} \leftrightarrow R\text{-}Cu + Zn^{2+} \qquad (2)$$

Org-Aq interface:

$$Org\text{-}Zn + Cu^{2+} \leftrightarrow Org\text{-}Cu + Zn^{2+} \qquad (3)$$

R-Org interface:

$$R\text{-}Cu + Org\text{-}Zn \leftrightarrow R\text{-}Zn + Org\text{-}Cu \qquad (4)$$

Reactions (2) and (3) are at equilibrium as both the R and the Org phases have been pre-equilibrated with the Aq of the same composition. Therefore, no mass transfer can be expected to proceed through the R-Aq and Org-Aq interfaces. At the same time, the R and the Org phases are not at equilibrium. Hence, the R-Org interface appears to be responsible for the redistribution of metal ions in the triphase systems considered under reaction (4). In other words, this particular interface is responsible for the extraction of "non-extractable" ionic species. The equilibrium in reaction (4) can be described by the ratio of separation factors characterising the selectivity of the Org (α_{Org}) and the R (α_R) (see equation 1) in respective Org-Aq and R-Aq systems.[10] The α_{Org} values are nearly identical in all triphase systems under study. Therefore, the difference in distribution of metal ions in the R-Org-Aq systems (see Figures 2, 3 and 4) can be evidently attributed to the different selectivity of the resins under study towards Cu^{2+} and Zn^{2+} ions.[14,15] The mechanism of mass transfer in the R-Org-Aq systems, through the R-Org interface, can be considered to be similar to that in the phase-transfer catalytic systems involving ion-exchange resins.[1-4] The transfer of ions in this case proceeds through the following steps: 1) sorption of ions by the R from the Aq accompanied by their partial dehydration, and 2) extraction of metal ions from the R by Org. The last process appears to be enhanced in comparison with respective Aq-Org extraction due to the alteration of both ion hydration and the pH in the R phase.[10]

ACKNOWLEDGEMENTS

This work was supported by Research Grant No. QUI-96-1025-C03-01 from CICYT (the Spanish Commision for Research and Development). Bayer Hispania Industrial, S.A. is gratefully acknowledged for kindly supplying samples of Lewatit resins. A.T. is the recipient of a fellowship from CIRIT (Commission for Science and Technology of Catalonia). The Catalan Research Council (CIRIT) of the Catalonian Government is acknowledged with thanks for the financial support to Dmitri Muraviev during his Visiting Professorship at Universitat Autonoma de Barcelona.

REFERENCES

1. Regen SL, *J. Am. Chem. Soc.*, **97**, 5956, (1975).
2. Regen SL, *J. Am. Chem. Soc.*, **98**, 6370, (1976).
3. Starks CM and Liotta C, *Phase Transfer Catalysis,* Academic Press, New York (1978).
4. Sherington DC, in: *Polymer-Supported Reactions in Organic Synthesis*, P Hodge and DC Sherington, Eds., John Wiley & Sons, New York, p.157, (1980).
5. Kedem O and Bromberg L, *J. Membr. Sci.*, **78**, 225, (1993).
6. Bromberg L, Muraviev D and Warshawsky A, *J. Phys. Chem.*, **97**, 967, (1993).
7. Bromberg L, Muraviev D and Warshawsky A, *J. Phys. Chem.*, **97**, 13927, (1993).
8. Muraviev D, Rogachev I, Bromberg L and Warshawsky A, *J. Phys. Chem.*, **98**, 718, (1994).
9. Muraviev D and Warshawsky A, *React. Polym.*, **22**, 55, (1994).
10. Muraviev D, Oleinikova M and Valiente M, *Langmuir*, **13**, 4915, (1997).
11. Levin IS, Sergeeva VV, Tarasova VA, Varentsova VI, Rodina TF, Vorsina IA, Kozlova NE and Kogan BI, *Zh. Neorg. Khim.*, **18**, 1643, (1973).
12. Preston JS and du Preez AC, *MINTEK Report No M 378*, the Council of Mineral Technology, ISBN 086999851X (1988).
13. Szabadka O, *Talanta*, **29**, 183, (1982).
14. Muraviev D, Gonzalo A and Valiente M, *Anal. Chem.*, **67**, 3028, (1995).
15. Muraviev D, Noguerol J and Valiente M, *Anal. Chem.*, **69**, 4234, (1997).

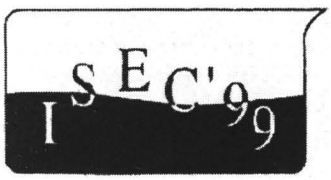

EXTRACTION OF RARE EARTH METALS WITH PC-88A BY A HOLLOW FIBRE MEMBRANE SYSTEM

F Kubota[1], M Goto[1], S Furusaki[1], K Yoshizuka[2], F Nakashio[3] and T Hano[4]

[1] Department of Chemical Systems and Engineering, Graduate School of Engineering, Kyushu University, Fukuoka 812-8581, Japan

[2] Department of Applied Chemistry, Saga University, Saga 840-8502, Japan

[3] Department of Applied Chemistry, Kumamoto Institute of Technology, Kumamoto 860-0082, Japan

[4] Department of Applied Chemistry, Oita University, Oita 870-1192, Japan

ABSTRACT

The extraction and stripping of rare earth metals, Sm and Gd, with PC-88A as an extractant were performed simultaneously by a novel extractor composed of a membrane module utilizing microporous hydrophobic hollow fibre. It was found that the permeation of metals from the aqueous feed solution to the stripping solution was achieved through an organic solution containing the extractant. The experimental results were simulated by a diffusion model combined with chemical reaction at the aqueous-organic interface at both extraction and stripping sides. The model well explained the permeation behaviour of rare earth metals in a hollow-fibre membrane extractor.

Keywords: gadolinium, samarium, supported liquid membrane, hollow fibre membrane extractor, PC-88A

INTRODUCTION

Conventional solvent extraction has been used for the separation and concentration of rare earth metals on an industrial scale. However, for preparation of high-purity products, it requires a large number of stages, because the separation factors among adjacent elements are very small.[1] Thus, the development of more efficient separation techniques is desired.

A membrane-based solvent extraction method has been recently developed as an efficient technology for the separation of various metals and organic compounds.[2-7] In this novel system, phase separation stages are unnecessary because the aqueous and organic solutions come into contact through a membrane. Several disadvantages such as loading, flooding and emulsification caused by phase dispersion in solvent extraction method can be eliminated. Furthermore, the module of hollow fibre type provides a very large interfacial area necessary to promote the extraction with a compact device.

The purpose of this study is to apply this novel membrane extraction system to the separation and purification of rare earth metals. The extraction equilibrium of rare earth metals[8] and their permeation mechanisms through a single hollow-fibre membrane independently for extraction and back-extraction have been elucidated.[9] In the present work, the extraction and stripping of the middle rare earth metals, samarium (Sm) and gadolinium (Gd), with 2-ethylhexylphosphonic acid mono-2-ethylhexyl ester (commercial name PC-88A, abbreviated as HR) as an extractant was carried out by a membrane extractor consisting of a module of microporous hydrophobic hollow fibre. The experimental results were simulated to clarify the permeation mechanism necessary for the optimization and scale-up of the metal recovery system.

EXPERIMENTAL

Reagents

PC-88A, from Daihachi Chemical Industry Co. Ltd. (Lot No. N10102) was used without further purification. The organic solution was prepared by dissolving PC-88A in n-heptane of analytical grade. The aqueous feed solution containing Sm and Gd was prepared by dissolving the hexahydrate of each metal chloride in a nitric acid solution. The pH of the aqueous solution was adjusted in

© 2000 Society of Chemical Industry

sequence with 100 mol/m^3 nitric acid and 100 mol/m^3 sodium acetate solutions. Aqueous nitric acid solution was used as the strip solution. All the other inorganic and organic reagents used were of analytical grade.

Procedure

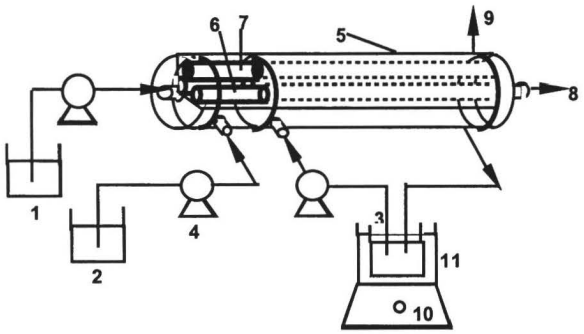

1 Aqueous feed solution
2 Stripping solution
3 Organic solution
4 Glass tube
5 Hollow fiber module
6 Hollow fiber for extraction
7 Hollow fiber for stripping
8 Raffinate
9 Recovery solution
10 Magnetic stirrer
11 Water bath

Figure 1 Schematic diagram of a membrane extractor

Figure 1 shows schematically a membrane extractor composed of two sets of microporous hydrophobic hollow fibres, made of polytetrafluoroethylene (Japan Gore-Tex Inc.). The numbers of fibres used for extraction and stripping are n and n′, respectively. The specification of the extractor is listed in Table 1. Aqueous feed and stripping solutions were fed separately and cocurrently into the inner sides of each set of hollow fibres. An organic solution containing the extractant PC-88A was also fed cocurrently into the outer side of hollow fibres and was recirculated as shown in Figure 1. At the steady state, the concentration of rare earth metals in the effluent solutions was measured by an ICP-atomic emission spectrometer (SHIMADZU ICP-5000). In this study, the total number of hollow fibres (n + n′) was four.

Inner diameter of extractor	4.9×10^{-3} m
Inner diameter of hollow fibre (d_I)	1.02×10^{-3} m
Outer diameter of hollow fibre (d_o)	1.86×10^{-3} m
Length of hollow fibre	0.25 m
Porosity (ε)	0.43
Tortuosity (τ)	1.14

Table 1 Specification of the membrane extractor

RESULTS AND DISCUSSION

Extraction and stripping behavior of rare earth metals

Figure 2 shows the schematic illustration for modeling of rare earth metal permeation in a hollow-fibre module, where subscripts 1, 2 and 3 represent extraction, organic and stripping sides, respectively. Subscript Mi, Ci and B indicate metal species, metal complex (i = Sm and Gd) and dimer species of extractant. J and J′ are the fluxes (mol/(m^2•s) for extraction and stripping sides, respectively, and v is the volumetric flow rate (m^3/s). Figure 3 shows the typical time-course of rare earth metal concentrations in the outlet solutions of the extraction and stripping sides expressed by the dimensionless terms defined as follows:

$$X_{Mi}=C_{Mi,1,e}/C_{Mi,1,0},\ Y_{Mi}=C_{Mi,3,e}/C_{Mi,1,0} \quad (2)$$

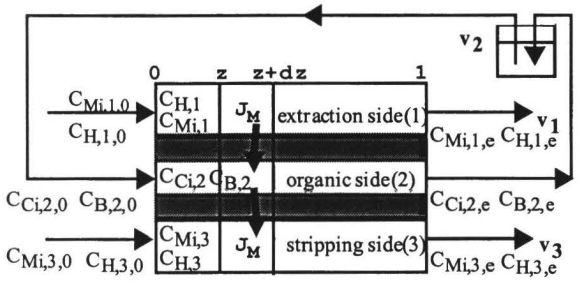

Fig.2(a) Schematic diagram of a membrane extractor

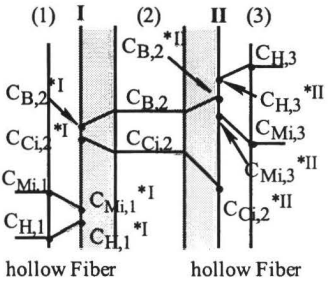

Fig.2 (b) Concentration profiles of chemical species

Under the present experimental conditions, the extent of metal remaining in the feed solution, X_{Mi}, reached a steady value within 20-35 hours and the extent of metal enrichment in the stripping solution, Y_{Mi}, within 40-50 hours. Furthermore, these times were influenced neither by the ratio of n to n′ nor by that of v_1 to v_3. The membrane was confirmed to be stable for more than 80 hours of use because the flux was maintained constant after the mass transfer reached the steady state, as shown in Figure 3.

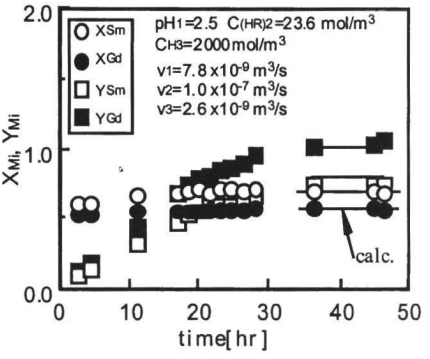

Figure 3 Time course of rare earth metal

The number of fibres, that is, the contact area provided by membranes extremely affected the efficiency of metal recovery. When the membrane extractor of n = 3 and n' = 1 was used to obtain a higher extent of extraction, for example, the concentration of metals in the stripping solution was very low and the resultant accumulation of metals occurred in the membrane phase due to the deficiency of the contact area for stripping. Then, a subsequent experiment was carried out with the membrane extractor of n = 2 and n' = 2. Figure 4 shows the effect of pH in the feed solution on X_{Mi} and Y_{Mi} when the hydrogen ion concentration of the stripping solution, C_{H0}, was held constant at 2000 mol/m^3 in all runs. It was found that both rare earth metals in the feed solution were extracted well by increasing pH and the concentrations of metals in the stripping solution increased concomitantly. Figure 5 shows the effect of the inlet concentration of the dimeric extractant in the organic feed solution, $C_{(HR)20}$, on X_{Mi} and Y_{Mi}. Extraction and stripping of rare earth metals were promoted by increasing $C_{(HR)20}$. It was found in the separate runs that excessively high concentration of acid such as 4000 mol/m^3 in the stripping solution reduced the degree of metal recovery. The extraction and enrichment of metal are expected to improve by increasing the number of hollow fibres for extraction and stripping steps in the extractor of same size.

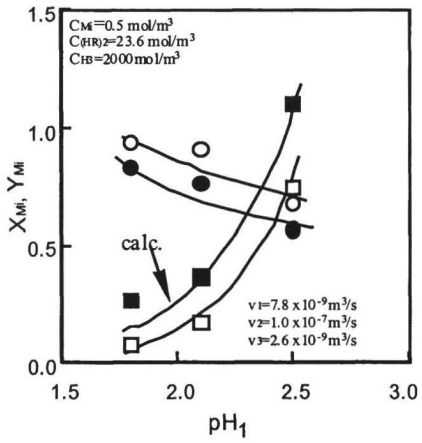

Figure 4. The effect of pH_1 on X_{Mi} and Y_{Mi}

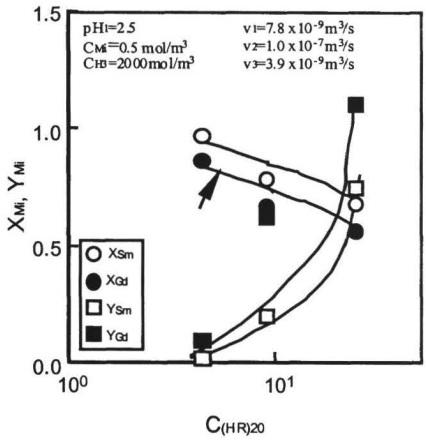

Figure 5. The effect of $C_{(HR)20}$ on X_{Mi} and Y_{Mi}

Analysis of permeation rate

Rare earth metal is known to be extracted with the dimer of PC-88A, $(HR)_2$, as follows[8]:

$$M^{3+}_{aq} + 3(HR)_{20,org} = MR_3 \bullet 3HR_{org} + 3H^{+}_{aq} \qquad : K_{ex} \tag{3}$$

where K_{ex} denotes the extraction equilibrium constant.

In the present hollow-fibre membrane system, aqueous-organic interfaces are formed at the inner surface of hollow fibres for extraction (interface I) and for stripping (interface II), respectively, as shown in Figure 2, because the fibres used are hydrophobic. Rare earth metals are extracted at the interface I by the forward reaction of Equation (3) and the complex, $MR_3 \bullet 3HR$, is stripped at the interface II to the strip side through the backward reaction. In the previous paper,[9] the permeation rates of rare earth metals through a single hollow-fibre membrane with PC-88A were examined independently for extraction and stripping . Consequently, the interfacial reaction rate for extraction, $R(I)_i^{*I}$ (mol/(m^2•s)), was derived as follows:

$$R(I)_i^{*I} = k_{fi} \frac{\{C_{Mi,1}^{*I} \cdot (C_{B,2}^{*I})^3 / (C_{H,1}^{*I})^3 - C_{Ci,2}^{*I} / K_{exi}}{1 + (1 + K_a / C_{H,1}^{*I}) \cdot K_{HR} K_D^{-1/2} (C_{B,2}^{*I})^{1/2} + K_{(HR)2} C_{B,2}^{*I}} \tag{4}$$

where, K_a, K_D, K_{HR} and $K_{(HR)2}$ are the acid dissociation constant, the dimerization constant, the interfacial adsorption equilibrium constant of monomer and that of dimer species of PC-88A, respectively. The values of the interfacial reaction rate constants, k_{fi}, are listed in Table 2 together with K_{exi}. For stripping, however, the interfacial reaction rate was assumed to be very fast, that is, the stripping reaction was considered to be at equilibrium.

Considering the segment of length dz in the membrane extractor, where z is the dimensionless axial distance(l/L), as shown in Figure 2(a), the governing equations for mass transfer at the steady state in each region are expressed as follows:

For extraction side:

$$-v_1(dC_{Mi,1}/dz) = k_{M,1} \bullet a_I (C_{Mi,1} - C_{Mi,1}^{*I}) \tag{5}$$

For organic side:

$$v_2(dC_{B,2}/dz) = k_B \bullet a_{II} (C_{B,2}^{*II} - C_{B,2}) - k_B \bullet a_I (C_{B,2} - C_{B,2}^{*I}) \tag{6}$$

$$v_2(dC_{Ci,2}/dz) = k_{Ci} \bullet a_I (C_{Ci,2}^{*I} - C_{Ci,2}) - k_C \bullet a_{II} (C_{Ci,2} - C_{Ci,2}^{*II}) \tag{7}$$

For strip side:

$$v_3(dC_{Mi,3}/dz) = k_{M.3} \bullet a_{II} (C_{Mi,3}^{*II} - C_{Mi,3}) \tag{8}$$

Here, the buffer was used as the feed solution and the hydrogen ion concentration of stripping solution was very high, so the hydrogen ion concentration in each aqueous solution was considered to be constant through the membrane extractor. k_M, k_C and k_B are the mass transfer coefficients (m/s) of metal in the aqueous solution, complex and extractant in the organic solution, respectively, where the same values of k_M and k_C were used for Sm and Gd. a_I ($=n\pi Ld_i$) and a_{II} ($=n'\pi Ld_i$) are the interfacial area (m^2) of interfaces I and II. C^{*I} and C^{*II} indicate the concentration of chemical species at the interfaces I and II, respectively, which are derived from the mass balance equations of chemical species at each interface.

At interface **I** :

$$J_{Mi} = k_{M,1}(C_{Mi,1} - C_{Mi,1}^{*I}) = k_C(C_{Ci,2}^{*I} - C_{Ci,2}) = R(I)_i^{*I} \quad (9)$$

$$k_B (C_{B,2} - C_{B,2}^{*I}) = 3\Sigma R(I)_i^{*I} \quad (10)$$

where, Equation (4) is employed for the extraction rate at the interface I, $R(I)_i^{*I}$.

At interface II :

$$J_{Mi}' = k_{M.3}(C_{Mi,3}^{*II} - C_{Mi,3}) = k_C(C_{Ci,2} - C_{Ci,2}^{*II}) \quad (11)$$

where the concentrations of chemical species satisfy Equation (12) in the equilibrium state according to Equation (3).

$$K_{exi} = C_{Ci,2}^{*II} \cdot (C_{H,3}^{*II})^3 / C_{Mi,3}^{*II} \cdot (C_{B,2}^{*II})^3 \quad (12)$$

$$C_{B,2}^{*II} - C_{B,2} = 3 \quad (C_{Mi,3}^{*II} - C_{Mi,3}) \quad (13)$$

Under the present experimental conditions, the concentrations of chemical species at $l = 0$ ($z = 0$) are written as follows:

$$C_{Mi,1} = C_{Mi,1,0}, \quad C_{Mi,3} = C_{Mi,3,0} \quad (14)$$

$$C_{H,1} = C_{H,1,0}, \quad C_{H,3} = C_{H,3,0} \quad (15)$$

$$C_{B,2} = C_{B,2,0} = C_{B,2(z=1)} \quad C_{Ci,2} = C_{Ci,2,0} = C_{Ci,2(z=1)} \quad (16)$$

The basic equations, Equations (5)-(8), can be solved by the Runge-Kutta-Gill method by using Equations (9)-(16), according to the procedure described in the previous paper.[5] The values of $k_{M,1}$ and $k_{M,3}$ were estimated from the values of diffusivity of metals, D_M, by taking account of the laminar flow.[10] The values of k_j (j = B and Ci) were evaluated with the following equation by using the values of D_j estimated in the previous paper[9] (Table 2) and the thickness of a hollow fibre, δ ($=d_o/2-d_i/2$), ε and τ (Table 1):

$$k_j = D_j \times (\varepsilon/\delta\tau)$$

The exit (l = L) concentrations of chemical species are estimated by numerical calculations. X_{Mi} and Y_{Mi} obtained are drawn by the solid lines in Figures 4 and 5. The experimental results are entirely agreed with those calculated, suggesting that the interfacial chemical reaction played a predominant roll in the permeation of rare earth metals in the membrane module.

	Sm	Gd
K_{ex} (-)	1.0	3.6
k_f (m/s)	1.6×10^{-5}	5.7×10^{-5}
D_M (m^2/s)	7.2×10^{-10}	
D_B (m^2/s)	1.1×10^{-9}	
D_C (m^2/s)	4.5×10^{-10}	

Table 2 Constants used for analysis[9]

CONCLUSION

The permeation behaviour of rare earth metals from an aqueous feed solution to the recovery solution through an organic liquid membrane containing an extractant was investigated by using a novel membrane extractor consisted of microporous hydrophobic hollow fibres. The membrane phase,

which was flowing continuously during the operation, was ascertained to be stable even for long term use. The permeation behavior of rare earth metals through the module could be explained well by the permeation mechanism proposed for each step of the extraction and stripping through a single membrane. It was suggested that the extraction and enrichment of metals is promoted by the increase in the number of fibres for extraction and stripping.

ACKNOWLEDGEMENT

We are grateful to Mr. Horiuchi of Kyushu University for his technical assistance in construction of the membrane extractor. The authors are also grateful to Daihachi Chemical Industry Co.,Ltd., and Japan Gore-Tex Inc. for the supply of extractant PC-88A and hollow fibre membranes, respectively.

REFERENCES

1. Koch DFA, *Materials Australasia*, 12, May, 1987.
2. Kim BM, *J. Membr.Sci.*, **21**, 5, (1984).
3. Sengupta A, Basu R and Sirkar KK, *AIChE J.*, **34**, 1698, (1988).
4. Teramoto M, Tohno N, Ohnishi N and Matsuyama H, *Sep.Sci.Technol.*, **24**, 981,(1989).
5. Sato Y, Kondo K and Nakashio F, *J.Chem.Eng.Japan*, **23**, 23, (1990).
6. Kubota F, Goto M, Nakashio F and Hano T, *Sep.Sci.Technol.*, **32**, 1529, (1997).
7. Tong Y, Hirata M, Takanashi H, Hano T, et al., *J.Membrane Sci.*, **43**, 81, (1998).
8. Kubota F, Goto M and Nakashio F, *Solv. Extr. Ion Exch.*,**11**, 437, (1993).
9. Kubota F, Goto M, Nakashio F and Hano T, *Sep.Sci.Technol.*,**30**, 777, (1995).
10. Hausen H, *Verfarenstecnick Beih.Z.Ver.deut.Ing.*, **4**, 91, (1943).

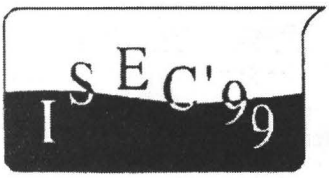

HOLLOW FIBRE NON-DISPERSIVE SOLVENT EXTRACTION: A PROMISING APPROACH TO ENVIRONMENTAL AND HYDROMETALLURGICAL APPLICATIONS

Anil Kumar[1] and AM Sastre

Department d'Enginyeria Quimica, ETSEIB, Universitat Politecnica de Catalunya, Av. Diagonal 647, E 8028 Barcelona, Spain

[1]On leave from PREFRE, Bhabha Atomic Research Centre, Tarapur, India

ABSTRACT

A feasibility study of a non-dispersive hollow fibre solvent extraction (HFNDSX) system for the environmental and hydrometallurgical applications has been considered. For environmental purposes, non-dispersive solvent extraction studies were conducted for the removal of toxic heavy metals such as Cu(II), Cd(II) and Zn(II) from aqueous waste streams using a hydrophobic hollow fibre module (MHF). The organic extractant used for this purpose was 0.1 mol/dm^3 Cyanex 272 [bis (2,4,4-trimethylpentyl)phosphinic acid] in n-heptane. Cd (II) and Cu(II) were extracted together between pH 3.8 - 4.0 and Zn(II) in the pH range of 2.0 - 2.5 from aqueous nitrate solutions. It was possible to achieve extraction of metals in the range of 80-90%. For, hydrometallurgical applications, extraction of gold (I) from alkaline cyanide media is considered. A recently developed new solvent extraction reagent, LIX79 (Henkel Corporation) has been employed as extractant. It was possible to extract Au(I) in presence of other metal cyanide salts such as Fe(II), Cu(II), Ni(II), Ag(I) and Zn(II) (NaCN = 500 ppm) by employing this technique.

Keywords: copper, cadmium, gold, zinc, Cyanex 272, LIX79, non-dispersive solvent extraction

INTRODUCTION

Research and developments in membrane separation technologies are rapidly expanding all over the world and new membrane separation technologies are overcoming the barrier to commercialisation.[1] Among developing techniques, hollow fibre non-dispersive membrane extraction has been extensively deployed in the field of environmental and hydrometallurgy for example, metal recovery from leaching and waste waters, winning of precious and strategic metals from neutral waters, treatment of large volumes of effluents including toxic and hazardous wastes generated by industries.[1-6] Thus the promising idea is to use non-dispersive hollow fibre solvent extraction (HFNDSX) which affords high mass transfer rates of solutes, especially high selectivities by the use of extractants. The basic principle of non-dispersive extraction is the immobilisation of the interface in the pores of hydrophobic membranes, by impregnation of lumen of the fibre and appropriate applied pressure.

The technique also overcomes other shortcomings of conventional liquid extraction such as flooding limitations from independent variation of phase flow rates, requirement of density difference, and the inability to handle particulates. This paper presents a feasibility study of a HFNDSX process for removal of heavy metals (environmental) from an aqueous stream and recovery of gold (I) from alkaline cyanide media in presence of base metals for hydrometallurgical application.

EXPERIMENTAL

A stock solution of Au(I) (5 g/dm^3) was prepared from pure solid $KAu(CN)_2$, and $KAg(CN)_2$, $Zn(CN)_2$, $KNi(CN)_4$, and CuCN (Johnson Mathey Chemicals, Karlsruhe, Germany), $K_4Fe(CN)_6.3H_2O$, NaCN (Merck, Darmstadt, Germany). Metal cyanide salts were dissoved in NaCN ($KNi(CN)_4$, and CuCN salts in excess of NaCN) in deionized water. The commercially available organic solvent *n*-heptane was used as diluent for both the extractants. All chemicals were used as received. LIX 79 (N,N'-bis(2-ethylhexyl)guanidine) was kindly donated by Henkel Corp. and Cyanex 272 was supplied by Cytec Inc.

© 2000 Society of Chemical Industry

The HFM is manufactured by Hoechst Celanese, Charlotte, NC (Liqui-Cel, 8x28 cm 5PCG-259 contactor and 5 PCS-1002 Liqui-cel laboratory LLE) and specified as below:

Type of module	Number of fibres	Module diameter (cm)	Module length(cm)	Active interfacial area (m^2)
5PCG-259 (contactor)	10,000	8	28	1.4

Hollow fibre Membrane details:

Fibre i.d. (cm) 24.0×10^{-3},	Fibre o.d. (cm) 30.0×10^{-3}
Fibre wall thickness (cm) 3.0×10^{-3}	Fibre length (cm) 15
Porosity (%) 30%	Pore size(μm) 0.03
Area per unit volume 29.3 (cm^2/cm^3)	Polymeric Material Polypropylene

Partition coefficients

Partition coefficients (H) of Au(I) from alkaline cyanide media with LIX 79 [7] and of heavy metals such as copper, cadmium and zinc with Cyanex 272 [8] were previously determined and described elsewhere.

Non-dispersive membrane extraction set-up

A Schematic view of the membrane based extraction process of Au(I) from Cyanide media or heavy metals from nitrate solutions using hollow fibre contactor is shown in Fig. 1.

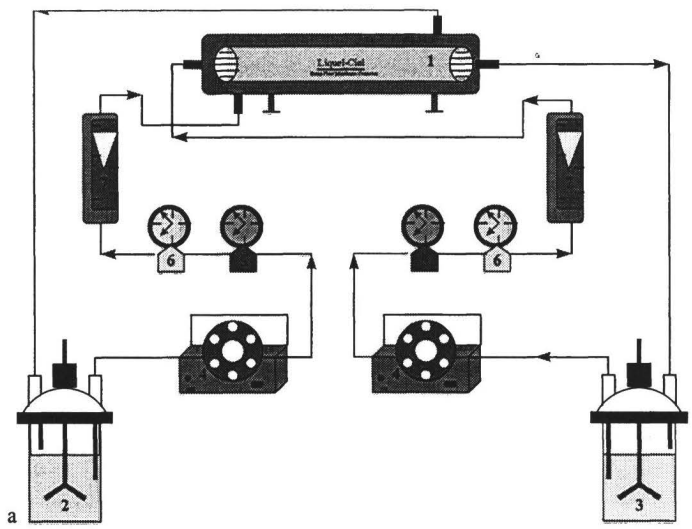

Figure 1. A Schematic view of the membrane based extraction process of Au(I) from cyanide media and heavy metals from nitrate solutions using hollow fibre contactor (1) hollow fibre contactor (2,3) feed and organic extractant (4) feed and organic pump (5,6) Inlet and outlet pressure gauge respectively for organic and feed (7) Flow meters for feed and organic.

Hydrometallurgical Application.

Both the aqueous phase, Au(I) in alkaline cyanide media at pH 10.3, and organic phase, 8 -12% LIX79/n-heptane, were contacted in the hollow fibre module in co-current and recirculating mode. In the extraction module, the organic phase flows through the lumen of the fibres, wetting the wall of the hydrophobic fibres while the aqueous phase circulates through the shell side. The pressure of the aqueous phase was held 0.4 bar higher than the pressure in the organic phase ensuring that no displacement of the organic phase from the pores of the hollow fibre occurred. The Au(I) concentration in the feed varied between 10-200 mg/dm^3.

Environmental Application.

The organic phase, Cyanex 272 in n-heptane (0.05 to 0.2 mol/dm^3) flowed through lumens (20-25 dm^3/h) and the aqueous feed of Cd(II), Cu(II) at pH 4 and Zn(II) at pH 2.5 flowed through the shell side (18-23 dm^3/h) in co-current mode in the hollow fibre module. The pressure of the aqueous phase was held 0.4 - 0.6 bar higher than the pressure in the organic phase. The initial concentration of metal ion was 100 mg/dm^3.

The organic phase was a 1000 cm^3 solution of 8 and 12% LIX 79 or Cyanex 272 in n-heptane (0.05 - 0.2 mol/dm^3). 1.0 litre of aqueous feed solution of desired concentration of Au(I) or heavy metals was prepared by taking suitable aliquots from the stock solution. Further the desired feed pH was adjusted by adding 1mol/dm^3 NaOH or HCl solution.

Extraction Equilibrium

The mechanism of gold extraction with LIX79 is by ion pair formation[9,10]. The Au(I) ions in alkaline cyanide media (present as $Au(CN)_2^-$) form a complex with the extractant LIX 79 (N,N'-bis(2-ethylhexyl)guanidine, RH), expressed as:

$$R_{org} + H^+_{aq} + Au(CN)_2^-{}_{aq} \Leftrightarrow [HAu(CN)_2R]_o \qquad K_{ex} \qquad (1)$$

The extraction equilibrium can be described by the following reactions and extraction constants:

$$K_{ex} = \frac{[HAu(CN)_2R]_{org}}{[Au(CN)_2^-][H^+][R]_{org}} \qquad (2)$$

where L is the organic extractant. The values of log K_{ex} for Au(I) with LIX 79 were found to be 11.34 ±0.15.[7] Similarly, extraction of cadmium, copper and zinc from nitrate solutions with Cyanex 272 (HA) can be described by the following reaction:[8]

$$M^{2+} + (p+2)\,HA_{org} \Leftrightarrow MA_2(HA)_{p,org} + 2\,H^+ \qquad (3)$$

The extraction equilibrium can be described by the following reactions and extraction constants:

$$K_{ex} = \frac{[MA_2(HA)_p][H^+]^2}{[M^{2+}][HA]^{p+2}} \qquad (4)$$

The log K_{ex} (stoichiometric equilibrium coefficient) value for copper ($CuA_2(HA)_2$) was 1.51 ± 0.09. For cadmium, K_{ex} values were 0.5 ± 0.1 ($CdA_2(HA)_2$) and 2.07 ± 0.1 ($CdA_2(HA)_3$) and for zinc values were 1.96 ± 0.1 ($ZnA_2(HA)$) and 4.48 ± 0.09 ($ZnA_2(HA)_2$) respectively.

Non-dispersive membrane extraction

The results of metal concentration measurements allowed the calculation of the overall mass transfer coefficient, K_A,[11] defined by:

$$J_M = K_A(C_A - C_{e/R}/H) \qquad (5)$$

$$\left[\frac{\frac{1}{Q_A}+\frac{1}{Q_{e/R}H}}{\frac{1}{V_A}+\frac{1}{V_{e/R}H}}\right]\ln\left[\frac{C^0_{e/R}/H-C^0_A)}{(C^0_{e/R}-C^0_A)+(V_A/HV_{e/R})(C^0_A-C_A)}\right]= \tag{6}$$

$$=t\left[1-\exp(-4K_A V_M/d\{1/Q_{e/R}H\})\right]$$

where J is the solute flux, C_f is the concentration in the feed solution, $C_{e/s}$ is the concentration in the extract or strip solution, and H is partition coefficient of metal with organic extractant. Thus, K_A is based on a feed driving force. For co-current flow, the key equation for the calculation of K_A is where Q_A and $Q_{e/R}$ are the feed and extract/strip flows; V_A and $V_{e/R}$ are the feed and extract/strip volumes; C_A^0 and $C^0_{e/R}$ are the concentrations of the solute in the feed and in the extract/strip solutions at time zero; C_A is the concentration of the solute in the feed at time t; V_m is the volume of all the hollow fibres; and d the diameter of one fibre.

RESULTS AND DISCUSSION

Environmental

The liquid-liquid extraction studies of Cd(II), Cu(II) and Zn(II) were performed earlier with Cyanex 272 and described elsewhere.[8] The extraction of copper and zinc using MHF ranged between 90 - 95% in 4-5 hours while Zn(II) was in the range of 85 - 90%. The extractant concentration has a influence on exit concentration of metal ion and 0.1mol/dm^3 was found to be suitable for the removal of these metal ions. The effect of organic flow rate in the tube side indicated that flow rate greater than 25 dm^3/h will affect the contact time between aqueous and organic phase resulting in poor extraction of metal ions. The mass transfer coefficients were calculated from equation 6 and are presented in Table 1.

Cyanex 272 Concentration, (mol/dm^3)	% removal			Mass tranfer coeff., K_A (10^{-7} cm/s)		
	Cu(II)	Cd(II)	Zn(II)	Cu(II)	Cd(II)	Zn(II)
0.05	65	55	65	0.7	0.5	0.7
0.10	90	85	90	7.2	6.5	7.0
0.15	95	90	92	8.2	7.9	8.0
0.20	95	91	95	8.3	8.0	8.5

Table 1 Removal of Cu(II), Cd(II) and Zn(II) using non-dispersive extraction technique as a function of extractant concentration

Feed : Cu(II), Cd(II) and Zn(II) =100 ppm in 0.1mol/dm^3 NO_3^- media, pH 3.8-4.0
Cu(II), Cd(II)] for Zn(II) 2.0-2.5;
Extractant : Cyanex 272 in in n-heptane
Flow rate (organic) : 23 dm^3/h ; Flow rate (aqueous) : 18 dm^3/h

Hydrometallurgical Application

Liquid-liquid extraction studies of Au(I) with LIX79 were performed earlier and described elsewhere.[7] A plot of concentration differences versus time as predicted by equation 6 for extraction and stripping of Au(I) into LIX79 were plotted to determine mass transfer coefficients. The results of these calculations are given in Table 2. Mass transfer coefficients (K_A) for the extraction and stripping process are 0.4 x 10^{-6} cm/s and 0.1 x 10^{-6} cm/s respectively. The extraction of Au(I) using MHF was

ranging between 90 - 95% in 4-5 hours. Therefore, 12% (v/v) LIX 79 was found to be suitable for the efficient removal of Au(I) from alkaline cyanide media. The Au(I) could be separated efficiently from other base metals except zinc from alkaline cyanide media using 12% LIX79 at pH 10.3 - 10.5 as shown in Figure 2 which indicates the potential of this technique to recover gold from hydrometallurgical alkaline cyanide leach solutions. Research work is in progress to improve the selectivity of gold against zinc and silver by using mixtures of LIX79 with organophosphorous extractants such as TOPO and TBP. Several changes in HFNDSX set-up are being carried out in addition to checking various chemical parameters to obtain better mass transfer coefficients.

Run	Aqueous Flow rate (cm^3/s)	LIX79 flow Rate (cm^3/s)	K_f ($\times 10^{-6}$ cm/s)
Extraction			
1[a]	5.55	6.94	0.4
2[b]	5.55	6.94	1.0
Stripping		6.94	
4*	5.55	6.94	0.1
5*	7.75	6.94	0.1

a, 8% (v/v) LIX79 in *n*-heptane b, 12% (v/v) LIX79 in *n*-heptane

Table 2. Mass transfer coefficients for extraction and stripping of Au(I) from aqueous alkaline cyanide media (pH=10.3) using LIX 79 in n-heptane using HFNDSX technique

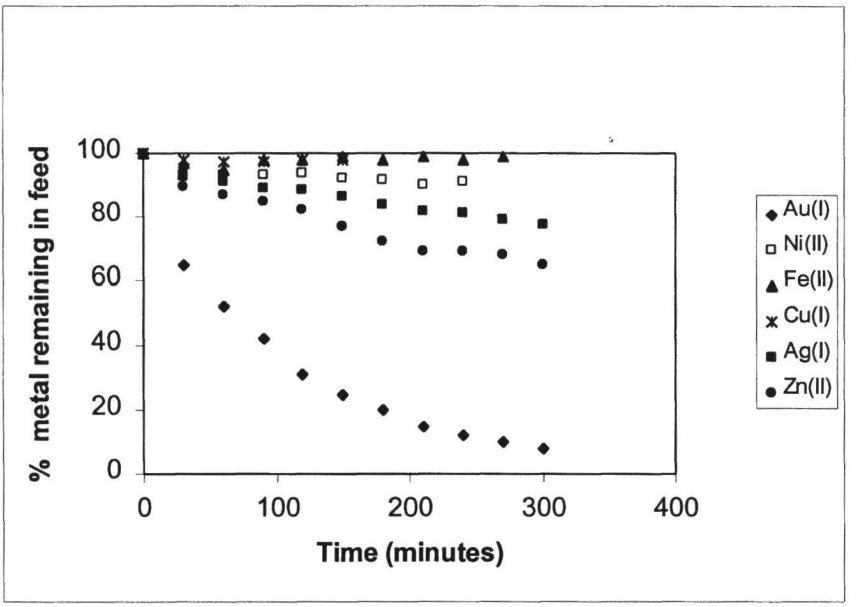

Figure 2 Separation of Au(I) from Fe(II), Cu(II), Ag(I), Ni(II) and Zn(II) with 12 % (v/v) LIX79 using HFNDSX technique, Au(I): 10.0 mg/dm^3, Fe(II): 30 mg/dm^3, Cu(II): 30 mg/dm^3, Ni(II): 10 mg/dm^3, Ag(I): 3 mg/dm^3 and Zn(II): 5 mg/dm^3 at pH 10.35, NaCN = 500 ppm

ACKNOWLEDGEMENTS

This work was supported by the CICYT (QUI 96-1025). Anil Kumar acknowledges the financial support from Comisión Interministerial de Ciencia y Tecnología, Spain for awarding Visiting Scientist fellowship. Authors gratefully acknowledge Henkel Corporation, U.S.A. for supplying LIX79, Cytec Inc. for supplying Cyanex 272 and Hoechst AG for the discount on the hollow fibre modules.

REFERENCES

1. Sirkar KK, *Chem. Eng. Comm*, **157**, 145, (1997).
2. Noble RD, Way JD and Bunge AL, Ion Exch. and Solv. Extr.,**10**, 63, (1988).
3. Winston Ho WS and Sirkar KK, *Membrane Handbook*, Van Nostrand Reinhold, New York, (1992).
4. Alonso AI, Urtiaga AM, Zamacona S, Irabien A and Ortiz I, *J. Membr. Sci.***130**, 193, (1997).
5. Sastre AM, Kumar A, Shukla JP and Singh RK, *Sep. Purif. Meth.*, **27**, 215, (1998).
6. Kumar A and Sastre AM, *Spanish Patent, No. 98 01736*, August, 1998.
7. Madi A, *Ph.D Thesis*, Universitàt Pòletecnica de Cataluyña, Barcelona, Spain, (1998).
8. Sastre AM, Mirrales N and Fuguerola E, *Solv. Extr. Ion Exch.*,**8**, 597, (1990).
9. Kordosky GA, Sierakoski JM, Virning MJ and Mattison PL, *Hydrometallurgy*, **30**, 291, (1992).
10. Virnig MJ and Wolfe GA, *Value Adding through Solvent Extraction, Proc. ISEC'96*, ed. D C Shallcross et al, University of Melbourne, **1**, 311, (1996)
11. D'ellia NA, Dahuron L and Cussler EL, *J.Membr. Sci*, **29**, 309, (1986).

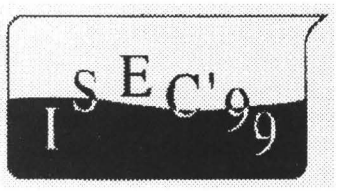

HYDRATION OF METAL PERCHLORATES EXTRACTED WITH TRIOCTYLPHOSPHINE OXIDE IN HEXANE

S Kusakabe
Department of Chemistry, Science University of Tokyo
Kagurazaka, Shinjuku, Tokyo 162-8601 Japan

ABSTRACT
A series of metal perchlorates were extracted with trioctylphosphine oxide (TOPO) in hexane and the hydration number of the extracted species as well as the solvation number of TOPO (n) were determined. From a comparison of these numbers with the coordination number of each metal ion, TOPO seems to coordinate in the inner-sphere (n </= 4), in the outer-sphere (n >/= 6), and in both spheres. TOPO is a stronger ligand than water. However, the bulkiness of TOPO molecule allows up to only four molecules to coordinate directly to the metal ion and the remaining coordination sites are available for water of hydration. In some cases the species that retain hydration water show good extraction.

Keywords: metal perchlorates, alkali metals, alkaline earth metals, lanthanides, transition metals, trioctylphosphine oxide, ion hydration, ion solvation

INTRODUCTION

In solvent extraction systems the organic phase is saturated with water and the extracted species often carry hydration water into the organic phase. Since the perchlorate ion coordinates poorly to metal ions, a metal ion should have the highest hydration number when it is extracted as the perchlorate. Metal perchlorates can be extracted with solvating extractants such as trioctylphosphine oxide (TOPO) into a non-polar solvent. The solvation number of TOPO can be calculated from the dependence of the distribution ratio of the metal ion on the TOPO concentration. The hydration number of the extracted species can be estimated from the amount of water taken into the organic phase. In the present study, results for several trivalent metal ions are added to the previous ones[1-4] on the extraction equilibria of a series of metal perchlorates with TOPO in hexane. The relationship between the solvation and hydration in this extraction system is discussed.

EXPERIMENTAL

The ionic strength of aqueous media was adjusted to unity except for the sodium salt solution (4 mol dm^{-3}). The initial concentrations of lithium perchlorate was 1 mol dm^{-3} and the divalent metal ions was 0.33 mol dm^{-3}. The initial concentrations of tri-valent metal perchlorates were 0.1mol dm^{-3} in 0.4 mol dm^{-3} sodium perchlorate containing an amount of perchloric acid to prevent the hydrolysis of the metal ion. Aliquots of the metal salt solutions and hexane solutions containing various amount of TOPO were placed in stoppered glass tubes. They were agitated for one or half an hour by a mechanical shaker in a room at 25°C. The distribution ratio of the metal ion was measured by atomic absorption spectroscopy or colorimetry. The concentration of water in the equilibrated organic phase was measured with a Hiranuma AQ-6 type Aquacounter by a coulometric Karl Fischer titration.

The extraction equilibrium of m-charged metal ion is expressed as:

$$D = [M^{m+}]_{org,total}/[M^{m+}] = [M(ClO_4)_m(TOPO)_n]_{org}/[M^{m+}] = SK_{ex,n}*[ClO_4^-]^m x^n \quad (1)$$

where n is the solvation number with TOPO on the extracted metal ion, and x represents the equilibrated concentration of unbonded TOPO after the co-extraction of water was taken into account.[2] The extraction constant is defined as: $K_{ex,n}* = [M(ClO_4)_m(TOPO)_n]_{org}/ [M^{m+}][ClO_4^-]^m x^n$. The asterisk indicates that the constant is obtained by using the free TOPO concentration excluding the TOPO associated with water. The latter quantity was calculated by a successive approximation from the TOPO mass balance:

© 2000 Society of Chemical Industry

$$[TOPO]_{org,total} = [TOPO]_{org} + [TOPO \cdot H_2O]_{org} + 2[(TOPO)_2(H_2O)_3]_{org} + Sn[M(ClO_4)_m(TOPO)_n]_{org}$$
$$= x + K_{11}c_w x + 2K_{23}c_w^3 x^2 + SnK_{ex,n}*[M^{m+}][ClO_4^-]^m x^n \quad (2)$$

The association constants of TOPO with water are $K_{11}c_w=[TOPO\cdot H_2O]_{org} / [TOPO]_{org} = 0.8$ and $K_{23}c_w^3 = [(TOPO)_2(H_2O)_3]_{org}/[TOPO]_{org}^2 = 10$, respectively. The c_w is concentration of water dissolved in pure hexane, $3x10^{-3}$ mol dm^{-3}. The measured concentration of water is given by Eq. 3:

$$[H_2O]_{org,total} = [H_2O]_{org} + [TOPO \cdot H_2O]_{org} + 3[(TOPO)_2(H_2O)_3]_{org} + Sh[M(ClO_4)_m(TOPO)_n\cdot(H_2O)_h]_{org}$$
$$= c_w + K_{11}c_w x + 3K_{23}c_w^3 x^2 + h_n K_{ex,n}*[M^{m+}][ClO_4^-]^m x^n \quad (3)$$

The average hydration number of the extracted metal salt is calculated by Eq. 4:

$$h_{av} = ([H_2O]_{org,total} - c_w - K_{11}c_w x - 3K_{23}c_w^3 x^2)/[M^{m+}]_{org,total} \quad (4)$$

The value of x, which was obtained in the process of calculation of extraction constants, is used here. When a single metal species is extracted, the hydration number is equal to h_{av}. When, however, two species are extracted together, for example n = 4 and 6, the hydration number of each can be estimated by curve fitting to the plot of h_{av} against x. The h_ns are related to h_{av} in this case as shown in Eq. 5 and a pair of suitable value of h_4 and h_6 should give a fit to the curve.

$$h_{av} = (h_4[M(ClO_4)_m(TOPO)_4(H_2O)_{h4}]_{org} + h_6[M(ClO_4)_m(TOPO)_6(H_2O)_{h6}]_{org}/[M^{m+}]_{org,total}$$
$$= (h_4 K_{ex,4}*x^4 + h_6 K_{ex,6}*x^6)/(K_{ex,4}*x^4 + K_{ex,6}*x^6) \quad (5)$$

RESULTS AND DISCUSSION

The results of the present study are shown in Table 1 together with those reported previously:

M^{m+}	h_{aq} [a)]	CN [b)]	n [c)]	$h_{3\text{-}4}$	$h_{6\text{-}8}$	$\text{Log}K_{ex,3\text{-}4}$*	$\text{Log}K_{ex,6\text{-}8}$*
Li^+	5.2	4	3	1-2		3.34	
Na^+	3.5	6	3	1-2		2.73	
Mg^{2+}	100	6	4, 7	5-6	10-13	5.70	11.76
Ca^{2+}	7.2	6	4, 6	2	3	7.09	11.41
Mn^{2+}	8.7	6	4, 6	5	5	6.79	11.6
Co^{2+}	9.6	4-6	4, 7	1	10-11	5.47	12.0
Ni^{2+}	10.4	4	4, 7	0	13	4.81	10.3
Cu^{2+}	9.9	5	4, 7	1.5	5, 10	6.34	12.4
Zn^{2+}	9.6	6	4, 6	3	3	6.53	12.0
Sc^{3+}	14.4	7	4, 6	2.0	4.2	11.56	17.92
Y^{3+}	12.0	8	4, 6	3.2	4.7	8.88	14.24
La^{3+}	10.3	9	4, 8	3.9	5.1	9.00	20.05
Eu^{3+}	11.4	8-9	4, 6	1.9	4.6	8.83	14.28
Nd^{3+} [d)]	11.0	9	4, 6	2.1	4.6	8.78	14.19
Sm^{3+} [d)]	11.3	8-9	4, 6	1.7	4.7	8.87	14.26
Dy^{3+} [d)]	11.9	8	4, 6	3.3	4.7	8.91	14.26
Ga^{3+} [d)]	17.4	6	4, 8	4.9	8<	7.30	17.08
In^{3+} [d)]	13.7	6	4, 6	3.9	4.7	9.41	15.39
Cr^{3+} [e)]	17.4	6	6		18.0		10.13

a) Hydration number in aqueous solution (ref.5). b) Coordination number in aqueous solution (ref.6). c) Solvation number with TOPO in extracted species. d) Present work. e) To be submitted.

Table 1 Hydration numbers and solvation numbers of metal ions and extraction constants of metal perchlorates with TOPO in hexane

In the table the results are compared with the hydration number (h_{aq})[5] and coordination number(CN)[6] of a metal ion in aqueous solution. Most of the metal ions are extracted as two species: one is smaller and the other is larger in solvation and hydration numbers. Some of the metal ions are extracted with very large hydration number, for example, Ni^{2+}, Mg^{2+}, and Cr^{3+}. As discussed previously, metal ions transfer form an aqueous solution into nitrobenzene holding almost the whole hydration sphere around them.[2,7] These three metal ions seem to behave in a similar way. Contrary to the extraction into nitrobenzene in which the salts are completely dissociated, metal ions should be extracted as ion-pairs into hexane. Since the paired anion is located in the outer-sphere, it disturbs the outer-sphere hydration layer. Although this effect will reduce the hydration number, the hydration molecules at the most outside position are still interacting with bulk water molecules in the aqueous solution. In the organic phase, however this interaction should be less than in the aqueous phase, which will result in an increase of the hydration number in the organic phase.

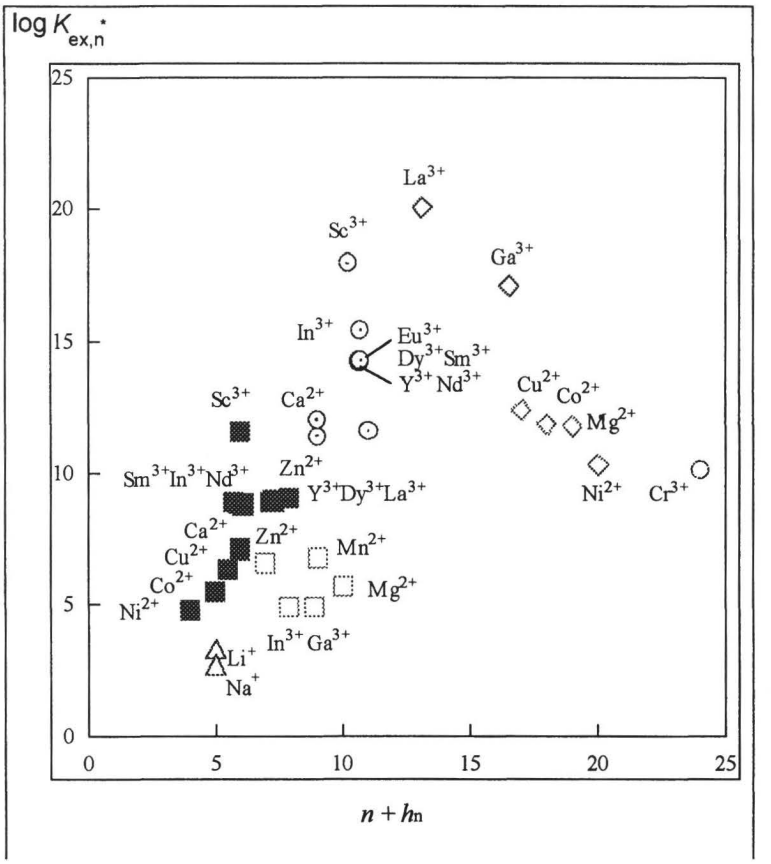

Figure 1 Extraction constants of metal perchlorates with TOPO in hexane vs sum of solvation number (n) and hydration number of the extracted species. Symbols are n=3(Δ), 4(′,≤), 6(□,□), 7 or 8(″,↓). Filled squares indicate when all the TOPO molecules are solvated in the inner-sphere.Open symbols for n=6, 7, and 8 indicate when all of the TOPO molecules lie in the outer-sphere.

As shown in Table 1, hydration tendencies of metal ions are not simple to rationalise. This

may be because the TOPO and water molecules compete with each other for the coordination sites of a metal ion with. In order to understand the solvation-hydration relationship, the number of hydration and solvation were summed and plotted vs the logarithm of the extraction constants are in Fig. 1: TOPO molecules can combine with the metal ion and hydrating water. Water molecules can combine with the metal ion and hydration water but not with the solvated TOPO molecule. Consequently, the hydration water should preferentially enter into the coordination sites of the metal ion. Strictly speaking, a water molecule can bridge over two TOPO molecules, as is proposed in the 2:3 hydrate of TOPO. When the hydration number of an extracted metal ion (h_n) is less than its coordination number, namely $h_n < CN$, the metal ion should have un-hydrated site(s) which TOPO molecules can occupy in the inner coordination sphere. When h_n is larger than CN, all the inner coordination sites are already filled with water molecules and TOPO should remain in the outer-coordination sphere.

The uni-charged metal ions are extracted with either three (Li^+, Na^+, K^+, and Tl^+) or four (Rb^+, Cs^+, and Ag^+)[1] TOPO molecules. Although only two metal ions were examined, both Li^+ and Na^+ have one hydration water molecule. Thus, the coordination number four may be common among these uni-charged ions.

Solvation with four TOPO molecules is common for the di- and tri-valent metal ions except Cr^{3+}. Some of them show better extraction when the hydration number is larger (closed circles in Fig. 1). Even when more than four coordination sites are available for TOPO, no more than four TOPO molecules enter into the inner-sphere probably because of the bulkiness of this ligand. The remaining coordination sites if any occupied with water, which saves the dehydration energy on the transfer from water to the organic phase.

A solvation number of TOPO larger than six is found when the metal ions are fully hydrated (open symbols in Fig. 1) or when some of the TOPO molecules enter both into the inner and outer coordination sphere (semi-closed symbols in Fig. 1). In the latter case, assuming that all the hydration water is regarded as inner-sphere hydration water and that the coordination number of these metal ions is as usual (see Table 1), the number of remaining coordination site are mostly three ($CN - h_n$ = 3). The reason for this behavior is not clear.

Concluding, the results of competition of water and TOPO molecules around the coordination sites of a metal ion are very complicated. However, complete dehydration is not always necessary for the extraction of metal ion. In some cases hydration in the extracted species may improve its extractability because it can save the dehydration energy on transfer from water to the organic phase.

REFERENCES

1. Kusakabe S, *"Value Adding Through Solvent Extraction", Proc ISEC'96,* Ed.D C Shallcross, R Paimin, and L M Prvcic, University of Melbourne, **1**, 189, (1996).
2. Kusakabe S, *Solv.Extr.Ion Exch.*, **15**, 219 (1997).
3. Kusakabe S, *Solv.Extr.Res.Develop.Japan*, **4**, 147 (1997).
4. Kusakabe S, *J.Radioanal.Nucl.Chem.*, **228**, 27 (1998).
5. Marcus Y, *"Ion Properties"*,Chapter 12, Marcel Dekker, New York (1997).
6. Richens D T, *"The Chemistry of Aqua Ions"*, John Wiley & Sons, Chichester (1997).
7. Osakai T, Ogata A and Ebine K, *J.Phys.Chem.B*, **101**, 8341, (1997).

SOLVENT AND SOLID EXTRACTION OF METAL IONS WITH 4-*n*-DODECYL-6-(2-THIAZOLYLAZO)-RESORCINOL

Hideyuki Matsunaga
Tohoku National Industrial Research Institute, 4-2-1 Nigatake, Miyagino-ku, Sendai 983-8551 Japan

ABSTRACT
The solvent extraction characteristics of several transition metal ions with 4-n-dodecyl-6-(2-thiazolylazo)resorcinol (DTAR) in 4-methyl-2-pentanone (MIBK) have been investigated. Copper (II) has been well extracted with DTAR and MIBK. An acid-base equilibrium of DTAR has been also checked in the solvent extraction system with MIBK. The second acid dissociation constant of DTAR has been measured to be $10^{-9.97}$. The extraction constant of DTAR has been simultaneously obtained to be $10^{5.3}$, which is a large value compared with other extraction reagents. Solid extraction of the same metal ions with DTAR-impregnated polymer beads (DTAR-XAD-7) and DTAR-embedded Langmuir-Blodgett membrane coated on a quartz plate (DTAR-LB) has been also studied. It was found that copper (II) can be also successfully extracted with DTAR-LB as well as DTAR-XAD-7. The change in adsorption spectra of the plate to that of Cu(II)-complex from that of the reagent itself was observed upon immersing it in a Cu(II) solution. The extraction characteristics of several heavy metal ions with DTAR-XAD-7 have been compared with those of DTAR in MIBK. The order of the extractability with DTAR-XAD-7 is Cu(II) > Co(II) > Ni(II), which is similar to that with DTAR in MIBK. It was concluded that DTAR could be widely used as an extractant in a solid extraction system as well as in an ordinary solvent extraction.

Keywords: copper, cobalt, nickel, 4-n-dodecyl-6-(2-thiazolylazo)resorcinol, XAD-7, Langmuir-Blodgett membrane

INTRODUCTION

Long alkyl or alkenyl derivatives of common extracting agents are known as excellent extractants with specific performances. A derivative of 8-quinolinol or Kelex 100 is one of the most famous reagents having a structure which provides a good extractant for gallium from alkaline media.[1] The author has proposed other example of these types of extractants with some interesting characteristics in solvent extraction.[2] Some of the extraction characteristics of 4-dodecyl-6-(2-thiazolylazo)resorcinol (DTAR, **I**) toward several heavy metal ions were previously reported briefly.[2] Strong hydrophobicity of DTAR was also observed in the previous study on the solvent extraction with 4-methyl-2-pentanone (MIBK). It was also suggested that DTAR may be used as a reagent for a reagent-impregnated polymer material (RIPOM) as a solid extractant for metal ions.[3]

In this paper, solvent and solid extraction of several metal ions with DTAR is reported in more detail. A quartz plate coated with a Langmuir-Blodgett (LB) membrane has been investigated as a solid material as well as an ordinary RIPOM system using Amberlite XAD-7. A typical structure of the LB film is a self-assembly of a kind of surfactant. Thus, it is expected that the LB films should have a hydrophobic phase inside against a contacting water phase. The extraction characteristics of several heavy metal ions with DTAR-embedded LB film (DTAR-LB) and DTAR-impregnated polymer beads (DTAR-XAD-7) has been studied as compared with solvent extraction using the same reagent.

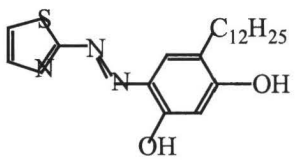

1

EXPERIMENTAL

Reagents and Apparatus

The extractant, DTAR, was prepared as reported by Matsunaga.[2] This long alkyl derivative is as stable as the original TAR in the redox system. It can be stored at room temperature and in air. Amberlite XAD-7 beads (20-60 mesh) were washed with a sodium hydroxide solution, nitric acid followed by acetone and water. Poly-n-dodecylacrylamide (PDDA, Mn = 6200) was synthesised and

© 2000 Society of Chemical Industry

kindly donated by Dr. Sen[4] and used for the base LB film. All other chemicals used were of analytical grade. DTAR was impregnated in XAD-7 as described in the previous paper.[5] DTAR was embedded into a LB film using a Kyowa Kaimen Kagaku HBM-AP automatic Langmuir trough.

The concentration of metal ion was determined with a SEIKO SP-1200 ICP Atomic Emission Spectrometer. The UV-VIS spectra were measured with a HITACHI U3410 UV-VIS spectrophotometer. A TOA HM-50V pH-meter with a glass electrode was used for the measurement of pH.

Extraction Procedure with MIBK

An aliquot of the stock solution of the metal ion was placed in a 50 cm^3 glass bottle. The acidity of the solution was adjusted with hydrochloric acid or a suitable buffer solution and diluted to the desired volume with distilled water. Into the solution was added the same volume of MIBK containing an appropriate amount of DTAR. Then, the mixture was shaken until equilibrium was attained. The distribution ratios for solvent extraction (D_L) were calculated from the concentrations of the metal ion in the solution before and after shaking, based on the following equation:

$$D_L = \frac{\text{The amount of the metal ion extracted into MIBK (mol } cm^{-3})}{\text{The amount of the metal ion left in the solution (mol } cm^{-3})}$$

Extraction Procedure with RIPOM

The fundamental procedure is the almost same as that in the solvent extraction. An aliquot of the stock solution of the metal ion was placed in a 50 cm^3 glass bottle. The acidity of the solution was adjusted with a hydrochloric acid or a suitable buffer solution and diluted to the desired volume with distilled water. Into the solution was added a certain amount of RIPOM. The mixture was shaken until equilibrium was attained. The distribution ratios (D_S, cm^3/g) for solid extraction were calculated also from the concentrations of the metal ion in the solution before and after shaking, based on the following equation:

$$D_S = \frac{\text{The amount of the metal ion in the RIPOM (mol } g^{-1})}{\text{The amount of the metal ion left in the solution (mol } cm^{-3})}$$

Extraction Procedure with LB film

A quartz plate (10 mm x 50 mm x 1mm) coated with DTAR embedded PDDA film was immersed into a metal ion solution in different pH conditions and left it until equilibrium was attained. After drying the plate in the air for a while, a change in UV-VIS spectra after a contact with the metal solution was checked to confirm the formation of metal complexes of DTAR. The concentration of metal ions in the aqueous phase was also measured to calculate the amount of the metal ions taken up.

RESULTS AND DISCUSSION

Extraction with MIBK

Distribution ratio of DTAR as a function of pH in water-MIBK system is shown in Figure 1. The value of log D_L is relatively small at pH 13, whereas it increases with further increase in pH. It is suggested that the mono-anionic species HR^- should be extracted into MIBK as a sodium salt. This is supported by the fact that some of the sodium ions were extracted together with DTAR in these conditions. The data can be analysed based on the following equilibrium, assuming that the other species are not participating in the equilibrium under these conditions.

$$R^{2-} \underset{H^+}{\overset{Ka2}{\rightleftharpoons}} HR^- \underset{Na^+}{\overset{Kex1}{\rightleftharpoons}} NaHR$$

where Ka2 and Kex1 represent the second acid dissociation constant and the extraction constant for mono-anionic species, respectively.

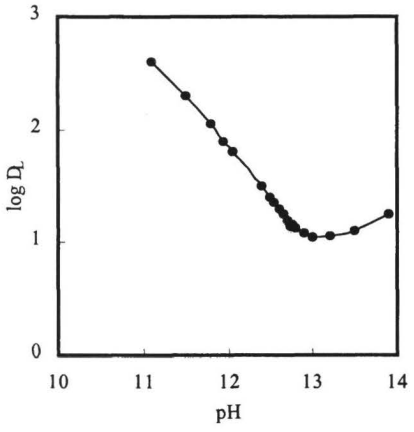

Figure 1 Effect of pH on the extraction of DTAR

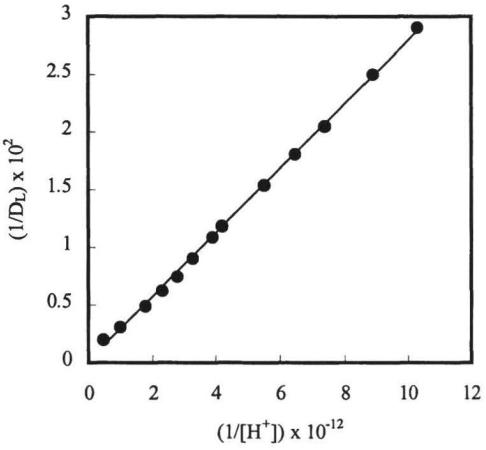

Figure 2 Plots of $1/D_L$ against $1/[H^+]$

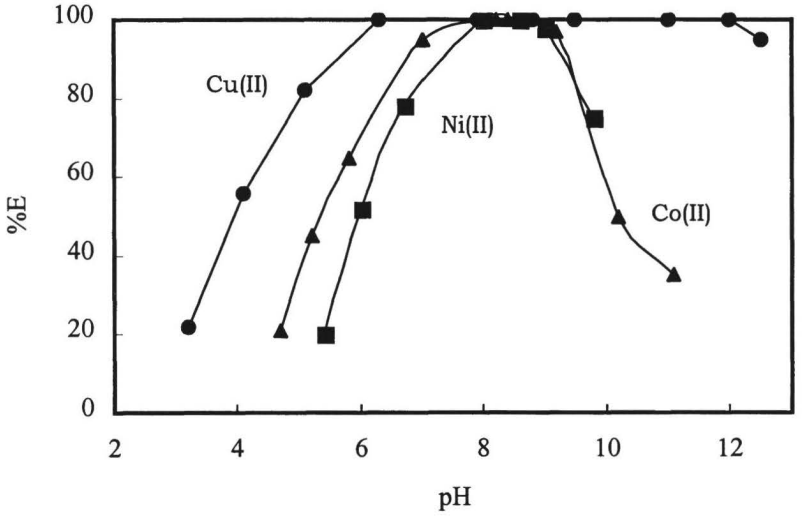

Figure 3 Effect of pH on the extraction of metal ions with DTAR
[metal] = 2 x 10^{-5} mol dm^{-3}, [DTAR] = 2 x 10^{-4} mol dm^{-3}.

Taking mass balance of the above equilibria using two constants, the following equation is obtained with regard to the distribution ratio of the reagent and the concentrations of each species.

$$D_L = [NaHR]/([HR^-] + [R^{2-}]) = Kex1[Na^+][HR^-]/[HR^-](1 + Ka2/[H^+]) \quad (1)$$

Taking reciprocal of D_L gives the next equation.

$$1/D_L = 1/Kex1[Na^+] + Ka2/Kex1[Na^+][H^+] \quad (2)$$

According to the equation (2), if $[Na^+]$ is constant, plots of $1/D_L$ against $1/[H^+]$ should give a straight line with $1/Kex1[Na^+]$ as the interception and $Ka2/Kex1[Na^+]$ as the slope. Figure 2 shows the linear relationship between $1/D_L$ and $1/[H^+]$. Thus, the second acid dissociation constant of DTAR has been calculated to be $10^{-9.97}$. The extraction constant of DTAR has been simultaneously obtained to be $10^{5.3}$, which is a considerably larger value compared with those of other extracting reagents

Figure 3 shows the effect of pH on the extraction of several metal ions with DTAR into MIBK. Copper (II) was found to be strongly extracted and the order of the extractability was Cu(II) > Co(II) > Ni(II). The composition of the Cu(II)-DTAR complex is 1:1 (Metal : Reagent) according to the results on both the molar ratio and the continuous variation method, in contrast to the Ni and Co complexes which are both 1:2.

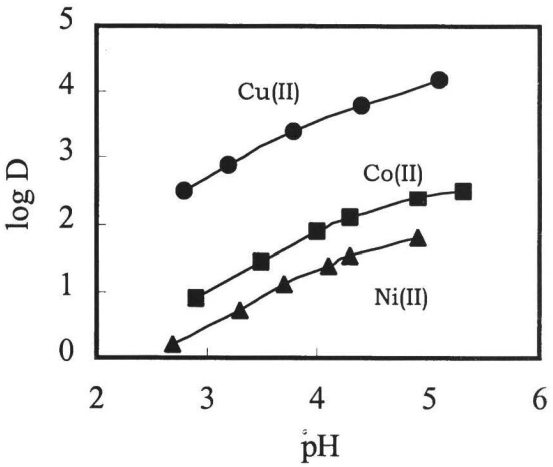

Figure 4 Effect of pH on the extraction of metal ions with DTAR-XAD-7.
DTAR-XAD-7; 100mg, $[M]=10^{-4}$ mol dm^{-3}

Extraction with DTAR-XAD-7

Figure 4 shows the effect of pH on the distribution ratio of several heavy metal ions with DTAR-XAD7. It was found that copper (II) was strongly extracted as is in the solvent extraction into MIBK. Comparing the formation constants[6,7] of TAR complexes with the distribution ratios of the metal ions on DTAR-XAD7, the order of the formation constants of 1:2 TAR complexes, Ni(II) > Co(II) > Cu(II), does not agree with that of distribution ratios in the RIPOM system with DTAR. It matches to that of solvent extraction with MIBK. Hence, if the effect of alkyl group on the complex formation is small, the difference in these orders could be attributed to the difference in the structures of the complexes in MIBK and on XAD-7, where 1:1 copper (II) complex is the predominant species under the experimental conditions.

Measurement of time dependency of the extraction with DTAR-XAD-7 showed that copper (II) was extracted within 30 minutes. As was expected, it took a longer time to extract the metal ions with RIPOM than into MIBK. The rate of extraction, however, is large enough to

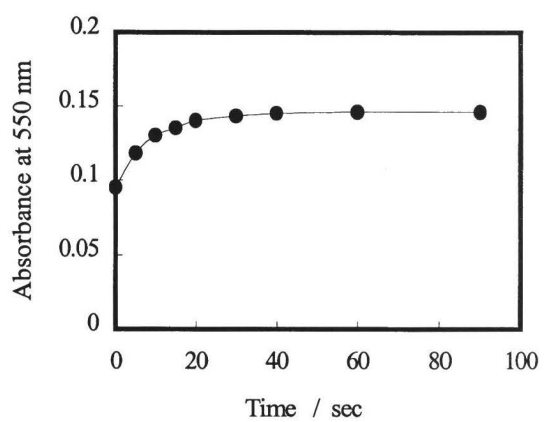

Figure 5 Time-course of the change in colour of DTAR-LB in the presence of C(II) ion.
$[Cu] = 1 \times 10^{-4}$ mol dm^{-3}, pH = 9.3

concentrate the metal ions with the flow system using the column packed with DTAR-XAD-7.

Extraction with DTAR-LB

The adsorption spectra of DTAR-LB film phase on a quartz plate along with the plate after Cu(II) was measured. The plate turned from orange to purple when it was immersed into a Cu(II) solution. The wavelength of maximum adsorption of the DTAR plate was 472 nm and changed to 550 nm after immersion, which are similar to that of DTAR and of Cu(II) complex in the MIBK phase, respectively. It means that DTAR-LB extracts Cu(II) to make a Cu(II) complex on the film. Detailed studies indicate that DTAR is a co-component in the LB film with PDDA. Thus, the position of species extracted should be also in the same position as that of the monomer unit of PDDA in the LB membrane. In contrast, dithizone (DZ) and 8-quinolinol (OX) do not make a LB film themselves. It was found, however, that DZ is present also in the membrane phase, while OX is not in it. It is suggested that DZ should be dissolved in a hydrophobic part of the film which is formed with dodecyl groups of PDDA.

The rate of uptake of metal ions with DTAR-LB was also checked by monitoring the colour change of the plate upon immersing it into a Cu(II) solution at pH 9.2. The result is shown in Figure 5. It was found that copper (II) was extracted into the LB film phase within a few minutes. It was confirmed that almost all the DTAR in the film can easily reacts with Cu(II) in the aqueous phase with which it is in contact. The DTAR-LB film turns yellow again after contacting with a 1 mol dm^{-3} HCl solution. This change in colour was reproducible during at least five cycles of extraction – stripping.

CONCLUSION

Solvent and solid extraction of several transition metal ions with three extraction systems using DTAR have been studied to explore the application of extracting reagents having long alkyl chains. In the ordinary solvent extraction, copper, cobalt and nickel have been well extracted with DTAR into MIBK under neutral pH conditions. Solid extraction of the same metal ions with DTAR-impregnated polymer beads (DTAR-XAD-7) and DTAR-embedded Langmuir-Blodgett membrane coated on a quartz plate (DTAR-LB) has been also studied. It was found that copper can be also successfully extracted with DTAR-LB as well as DTAR-XAD-7. The change in adsorption spectra of the plate to that of Cu(II)-complex from that of the reagent itself was observed upon dipping it into a Cu(II) solution. The extraction characteristics of several heavy metal ions with DTAR-XAD-7 have been compared with those of DTAR in MIBK. The order of the extractability with DTAR-XAD-7 is Cu(II) > Co(II) > Ni(II), which is similar to that with DTAR in MIBK.

It was concluded that DTAR could be widely used as an extractant in solid extraction system. Extracting reagents having long alkyl chains must have a wide potential in the application including sensing systems for ultra trace amount of metal ions.

REFERENCES

1. Helgorsky J and Leveque A, *French Patent, 2 307 047* (1976); *Chemical Abstract*, **87**, 42333, (1977).
2. Matsunaga H and Suzuki TM, *Chem Letters*, 225, (1986).
3. Matsunaga H, Wakui Y and Suzuki TM, *Proc ISEC'93*, York, 615, (1993).
4. Miyashita T, Sakai J, Mizuta Y, Matsuda M, *Thin Solid Films*, **244**, 718, (1994).
5. Wakui Y, Matsunaga H and Suzuki TM, *Analyt Sci*, **4**, 325, (1998).
6. Stanley RW and Cheney GE, *Talanta*, **13**, 1619, (1966).
7. Nickles G, Polland FH and Samuelson TJ, *Anal Chim. Acta*, **39**, 37, (1967).

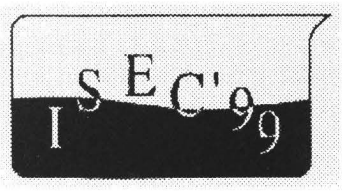

THE SEPARATION OF PHENOL FROM NEUTRAL OILS BY LIQUID–LIQUID EXTRACTION

Denise L Venter and Izak Nieuwoudt
Department of Chemical Engineering, University of Stellenbosch, Banhoekweg, 7600 Stellenbosch, South Africa

ABSTRACT
In this study, the separation of phenol from neutral oils by means of liquid-liquid extraction is investigated. Liquid-liquid equilibria for the systems phenol + aniline + benzonitrile + 5-ethyl-2-methylpyridine + mesitylene + hexane + water + triethylene glycol have been determined at 313.15 K to evaluate the suitability of triethylene glycol as a high-boiling solvent for the separation of phenol from neutral oils. The effect of parameters such as solvent ratios on the desired separation is illustrated on the basis of phenol-benzonitrile separation factors and percentage recoveries of phenol. From the experimental results it was concluded that triethylene glycol is suitable for the proposed separation.

Keywords: phenols, glycols, nitriles, nitrogen bases, aromatics, neutral oils

INTRODUCTION

The recovery of valuable phenolic compounds from coal pyrolysis liquors has long been of interest. The separation of the phenolic compounds from the neutral oils, also present in the pyrolysis liquors, is difficult due to low relative volatilities, the formation of azeotropes and eutectics.[1] The separation of phenol from benzonitrile and aniline is especially difficult.

Separation of phenolic compounds from neutral oils by solvent extraction with solvents such as: aqueous acetamide,[2] sodium xylenesulphonate, isobutyl acetate and aqueous methanol solutions[3] and sodium phenolate[4] have been investigated. Disadvantages of these processes include the high solvent ratios required and complex post-purification of the phenolic product.

A high-boiling solvent, triethylene glycol, was chosen for the separation of phenol from neutral oils with the assistance of a computer aided molecular design program. In addition to triethylene glycol, a co-solvent, water, and an anti-solvent, hexane, were used in an extraction system with a feed stream consisting of a mixture of phenol, benzonitrile, aniline, 5-ethyl-2-methylpyridine and mesitylene. The composition of the feed stream was based on the analysis of a typical industrial coal pyrolysis liquor fraction.

SOLVENT SELECTION

Benzonitrile was identified as the neutral oil potentially most difficult to separate from phenol. A computer aided molecular design program based on a genetic algorithm, using the modified Unifac method, was therefore used to predict a solvent suitable for the separation of phenol from benzonitrile. Favourable phenol-benzonitrile separation factors were predicted for ethylene glycol as well as for molecules containing ether, carbonyl and unsaturated hydroxyl functional groups. Triethylene glycol was consequently identified as a likely solvent for the proposed separation. Batch extractions with triethylene glycol, water, hexane and a feed stream consisting of phenol, aniline, benzonitrile, 5-ethyl-2-methylpyridine and mesitylene were simulated with PROII®. The results obtained were highly satisfactory.

EXPERIMENTAL

Batch extraction tests were executed to determine the effect of solvent ratios on the separation of phenol from neutral oils. Ratios of high-boiling solvent to feed water to high-boiling solvent and anti-solvent to feed were varied from 0.5 to 3.0, 0.0 to 0.7 and 0.5 to 5.0 respectively. The concentrations of

© 2000 Society of Chemical Industry

the components in each resulting liquid phase, with the exception of water, were determined by capillary gas chromatography with a FID detector. The water concentrations were determined by Karl-Fischer titrations. In all extractions the feed stream was defined as a mixture of phenol + benzonitrile + aniline + 5-ethyl-2-methylpyridine + mesitylene in the ratio 10.65: 1 : 1 : 1 : 1.35.

RESULTS AND DISCUSSION

The post-purification removal of benzonitrile from the phenolic product is extremely difficult. The efficiency of triethylene glycol for the separation of phenol from neutral oils was therefore evaluated according to the degree of separation achieved between phenol and benzonitrile and the recovery of phenol.

The phenol-benzonitrile separation factor β_{12} is defined as follows:

$$\beta_{12} = (p_1^{I} / p_1^{II}) / (p_2^{I} / p_2^{II}) \quad (1)$$

where p_1^{I} and p_1^{II} are the mass percentages of phenol, and p_2^{I} and p_2^{II} are the mass percentages of benzonitrile in the extract and raffinate phases respectively.

The compositions of the batch extraction phases, as well as the phenol-benzonitrile separation factors and phenol recoveries are shown in Table 1.

The effect of the water to high-boiling solvent ratio on the phenol-benzonitrile separation factors (β_{12}) and phenol recoveries are shown in Figures 1 and 2 respectively.

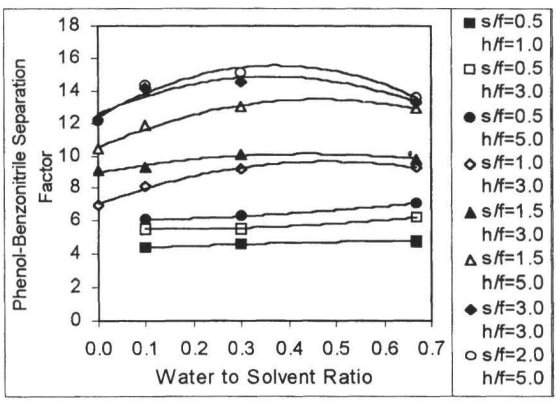

Figure 1. Effect of Water to Solvent Ratio on Phenol-Benzonitrile Separation Factors at Constant Solvent to Feed and Hexane to Feed Ratios.

As can be seen from Table 1, the β_{12} values and phenol recoveries achieved are very good. With the exception of extractions where a low solvent to feed ratio (0.5) is combined with a high hexane to feed ratio (5.0), phenol recoveries in excess of 90% are achieved for a single extraction.

It can be seen from Figure 1 that an increase in the water to solvent ratio from 0.0 to 0.3 leads to a rise in β_{12} for all solvent to feed and hexane to feed ratios. A further increase in the water to solvent ratio leads to a decrease in β_{12} where the solvent to feed ratios are greater than 1.5 and the hexane to feed ratios greater than 3.0. At lower solvent to feed and hexane to feed ratios an increase in the water to solvent ratio leads to an increase in β_{12}.

S/f	h/f	w/s	p_1^I	p_2^I	p_3^I	p_4^I	p_5^I	p_6^I	p_7^{II}	p_1^{II}	p_2^{II}	p_3^{II}	p_4^{II}	p_5^{II}	p_6^{II}	p_7^{II}	β_{12}	E_1 [%]
Phenol (1)+Benzonitrile (2)+Aniline (3)+Mesitylene (4)+5-Ethyl-2-methylpyridine (5)+ Water (6)+Hexane (7)+Triethylene Glycol (8)																		
1.0	3.0	0.3	30.64	2.05	2.67	0.18	1.50	15.27	1.11	1.44	0.88	0.33	2.87	1.23	0.04	92.89	9.2	93.9
1.0	1.0	0.3	31.16	2.57	2.85	0.53	2.15	14.84	1.48	2.02	1.18	0.40	7.24	1.80	0.05	87.17	7.1	96.9
1.0	0.5	0.3	30.28	2.70	2.77	0.88	2.29	14.57	1.51	2.65	1.45	0.48	11.56	2.38	0.04	81.35	6.1	98.0
1.5	4.9	0.7	19.40	0.93	1.72	0.04	0.58	31.96	0.47	1.25	0.77	0.32	1.65	0.95	0.02	94.91	12.9	90.6
1.0	4.9	0.3	30.45	1.72	2.56	0.12	1.07	15.71	1.23	1.05	0.60	0.26	1.74	0.86	0.03	95.46	10.1	92.4
1.0	1.0	0.7	26.72	2.09	2.41	0.29	1.64	27.34	0.73	2.64	1.49	0.45	7.68	2.16	0.04	85.53	7.2	95.9
1.0	3.0	0.7	26.60	1.57	2.24	0.12	1.08	27.07	0.66	1.73	0.95	0.36	2.91	1.32	0.06	92.49	9.3	92.3
0.5	3.0	0.7	39.38	2.49	3.42	0.22	1.65	20.93	1.06	2.42	0.95	0.39	2.79	1.37	0.05	91.97	6.2	89.8
1.5	3.0	0.7	19.68	1.23	1.69	0.06	0.75	31.02	0.32	1.51	0.93	0.31	2.73	1.38	0.03	93.08	9.8	93.0
3.0	3.0	0.7	11.68	0.76	1.06	0.04	0.43	35.02	0.33	1.15	1.00	0.27	3.04	1.39	0.03	93.09	13.3	95.3
1.5	3.0	0.1	26.60	1.88	2.28	0.28	1.45	6.72	1.11	1.04	0.68	0.23	2.60	1.02	0.03	94.32	9.3	95.4
1.0	5.0	0.1	34.47	2.05	2.84	0.19	1.37	5.80	2.00	1.17	0.60	0.28	1.67	0.77	0.02	95.42	8.7	91.5
0.5	3.1	0.1	47.06	3.05	3.74	0.44	2.34	4.12	3.92	2.16	0.77	0.35	2.50	0.98	0.02	93.13	5.5	90.4
1.0	3.0	0.1	34.22	2.40	3.04	0.36	1.86	5.72	2.00	1.22	0.70	0.28	2.61	0.97	0.02	94.15	8.2	94.6
2.0	3.0	0.1	22.95	1.50	1.98	0.28	1.23	7.12	1.07	0.98	0.70	0.26	2.62	1.02	0.01	94.34	10.9	95.9
3.0	3.0	0.1	16.61	1.18	1.49	0.25	1.02	7.90	0.97	0.52	0.52	0.15	2.61	0.84	0.02	95.35	14.2	97.8
0.5	4.9	0.7	38.36	2.15	3.08	0.15	1.35	21.65	2.15	1.87	0.75	0.38	1.72	0.89	0.02	94.32	7.1	86.1
2.0	5.0	0.7	15.75	0.74	1.32	0.03	0.46	32.62	0.65	1.15	0.73	0.29	1.73	0.93	0.02	95.13	13.6	91.6
0.5	1.0	0.7	38.94	3.03	3.53	0.68	2.66	20.01	1.96	3.39	1.26	0.50	6.95	1.86	0.07	85.94	4.8	94.5
1.5	1.0	0.7	20.56	1.54	1.98	0.19	1.23	29.53	0.58	2.48	1.42	0.45	7.06	2.39	0.04	86.11	7.7	95.9
2.0	1.1	0.7	15.73	1.17	1.44	0.11	0.89	34.51	0.47	2.22	1.45	0.39	6.99	2.32	0.03	86.55	8.8	96.3
3.0	0.8	0.7	11.79	0.96	1.15	0.11	0.80	34.34	0.54	1.96	1.53	0.34	9.28	2.56	0.03	84.25	9.6	97.5
3.0	1.0	0.7	11.46	0.91	1.11	0.08	0.73	34.84	0.27	1.69	1.37	0.31	7.48	2.33	0.03	86.12	10.1	97.3
0.5	3.0	0.3	43.16	2.98	4.01	0.34	2.23	11.38	3.13	2.11	0.82	0.37	2.74	1.05	0.03	92.82	5.6	90.5
1.5	3.0	0.3	23.24	1.57	2.19	0.15	1.16	18.50	0.95	1.18	0.80	0.29	2.87	1.11	0.02	93.70	10.1	94.6
3.0	3.0	0.3	14.10	1.00	1.31	0.09	0.76	20.62	0.84	0.66	0.68	0.19	2.86	1.05	0.01	94.25	14.5	97.1
1.5	1.0	0.3	23.61	2.04	2.23	0.37	1.65	17.92	0.98	1.72	1.18	0.36	7.27	1.82	0.03	87.53	7.9	97.4
0.5	1.0	0.3	42.15	3.70	4.12	1.03	3.40	11.28	2.10	2.93	1.17	0.53	6.91	1.79	0.04	86.50	4.6	95.5
2.0	1.0	0.3	18.86	1.57	1.73	0.27	1.42	18.92	0.93	1.33	1.00	0.27	7.45	1.78	0.02	88.06	9.1	97.9
2.9	1.0	0.3	14.45	1.17	1.36	0.23	1.08	20.26	0.44	1.06	0.95	0.22	8.26	1.70	0.02	87.72	11.1	98.5
1.5	0.5	0.3	23.79	2.16	2.31	0.68	1.98	17.71	1.15	2.02	1.32	0.38	13.49	2.20	0.03	80.52	7.3	98.5
0.5	0.5	0.3	42.53	3.95	4.10	1.72	3.52	10.69	1.56	3.36	1.24	0.53	11.05	1.78	0.05	81.96	4.0	97.4
2.0	0.5	0.3	19.22	1.72	1.89	0.48	1.52	18.81	1.07	1.71	1.28	0.33	12.88	2.07	0.03	81.70	8.3	98.6
3.0	0.5	0.3	14.39	1.26	1.37	0.37	1.16	20.84	0.81	1.39	1.11	0.26	15.48	1.96	0.02	79.71	9.1	99.1
0.5	1.0	0.1	44.56	3.87	4.16	1.25	3.50	4.15	4.75	2.80	1.08	0.49	6.79	1.42	0.03	87.33	4.4	95.8
0.5	5.2	0.3	40.44	2.59	3.67	0.18	1.62	12.44	2.18	1.71	0.70	0.30	1.58	0.76	0.01	94.88	6.3	86.3
1.5	5.0	0.3	23.57	1.33	2.05	0.07	0.92	18.05	1.06	0.87	0.64	0.25	1.69	0.81	0.01	95.36	13.0	93.5
2.0	4.9	0.3	19.23	1.06	1.70	0.07	0.76	19.22	0.81	0.69	0.58	0.21	1.72	0.76	0.01	95.51	15.2	94.8
3.0	5.0	0.3	13.79	0.85	1.24	0.05	0.62	20.61	0.59	0.51	0.54	0.17	1.69	0.76	0.01	96.21	17.1	96.1
0.5	5.0	0.1	45.12	2.66	3.68	0.25	1.97	4.82	4.10	1.76	0.64	0.34	1.68	0.78	0.02	94.68	6.1	86.8
1.5	4.9	0.1	26.59	1.72	2.22	0.17	1.22	6.63	1.96	0.74	0.57	0.20	1.65	0.76	0.01	95.97	11.8	94.5
2.0	5.0	0.1	22.33	1.42	1.94	0.21	1.04	7.12	1.16	0.58	0.53	0.17	1.67	0.70	0.01	96.24	14.4	95.8
3.0	5.0	0.1	16.35	1.10	1.49	0.20	0.83	7.73	1.05	0.39	0.44	0.13	1.55	0.60	0.01	96.79	17.0	97.2
1.5	5.0	0.0	28.11	1.90	2.46	0.49	1.49	0.00	2.63	0.71	0.50	0.17	1.53	0.69	0.00	96.29	10.4	94.8
2.0	5.0	0.0	23.92	1.61	2.13	0.47	1.31	0.00	2.25	0.57	0.46	0.15	1.49	0.62	0.00	96.64	12.1	96.0
1.5	3.0	0.0	27.83	2.07	2.54	0.50	1.80	0.00	3.45	0.87	0.59	0.18	2.54	0.94	0.00	94.78	9.0	96.1
3.0	3.0	0.0	17.60	1.50	1.68	0.48	1.17	0.00	1.93	0.44	0.46	0.12	2.36	0.76	0.00	95.73	12.3	98.1
1.0	3.0	0.0	35.08	2.33	2.99	0.50	2.06	0.00	4.60	1.44	0.67	0.28	2.60	0.87	0.00	94.04	7.0	93.9

Table 1. Isothermal Liquid-liquid Equilibrium Data, Solvent Phase Mass Percentages p_i^I, Antisolvent Phase Mass Percentages p_i^{II}, Separation Factors β_{12}, and Recoveries E_1, for Phenol (1) + Benzonitrile (2) + Aniline (3) + Mesitylene (4) + 5-Ethyl-2-methyl-Pyridine (5) Water (6) + Hexane (7) + Triethylene Glycol (8) at 313.15 K and 101.3 kPa.

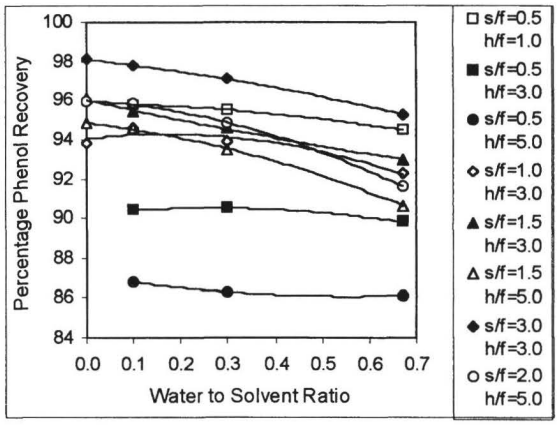

Figure 2. Effect of Water to Solvent Ratio on Percentage Phenol Recovery at Constant Solvent to Feed and Hexane to Feed Ratios.

From Figure 2 it is clear that the phenol recoveries without exception decrease with an increase in the water to solvent ratio.

From Figures 1 and 2 it can also be seen that an increase in the hexane to feed ratio at constant water to solvent and solvent to feed ratios leads to significant increases in β_{12} and decreases in the phenol recoveries. Thus for a solvent to feed ratio of 0.5, and a water to solvent of 0.7, β_{12} increases from 4.8 to 6.8 and the phenol recovery decreases from 94.5% to 86.1% as the hexane to feed ratio increase from 1.0 to 5.0.

The effect of the solvent to feed ratio on β_{12} and the phenol recoveries are shown in Figures 3 and 4 respectively and show respectively that both β_{12} and the phenol recoveries increase with an increase in the solvent to feed ratio.

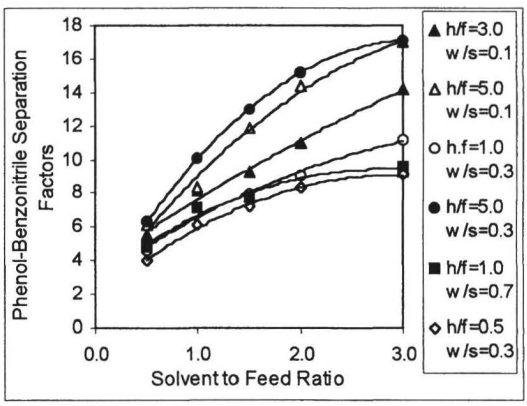

Figure 3. Effect of Solvent to Feed Ratio on Phenol-Benzonitrile Separation Factors at Constant Water to Solvent and Hexane to Feed Ratios.

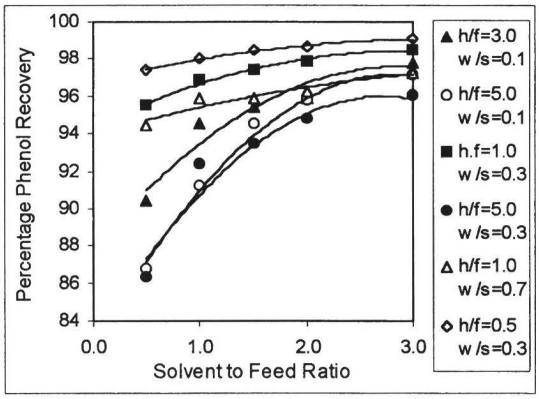

Figure 4. Effect of Solvent to Feed Ratio on Percentage Phenol Recovery at Constant Water to Solvent and Hexane to Feed Ratios.

Phenol-analine (β_{13}), phenol-mesitylene (β_{14}) and phenol-5-ethyl-2-methylpyridine (β_{15}) separation factors can be calculated from Table 1, in an analogous manner to the phenol-benzonitrile separation factor. The values obtained are 1.6-3.7, 81.4-842.6 and 6.4-33.1 for β_{13}, β_{14} and β_{15} respectively.

CONCLUSIONS

Triethylene glycol is an effective solvent for the separation of phenol from neutral oils. Average values obtained for phenol-benzonitrile (β_{12}), phenol-analine (β_{13}), phenol-mesitylene (β_{14}) and phenol-5-ethyl-2-methylpyridine (β_{15}) separation factors are 9.5, 2.5, 340 and 18.3 respectively. Phenol recoveries in excess of 90 % can be achieved in a single batch extraction. An increase in the solvent to feed ratio leads to a significant increase in both the phenol-benzonitrile separation factors (β_{12}) and the phenol recoveries. An increase in the hexane to feed ratio leads to an increase in β_{12} and a decrease in phenol recovery. An increase in the water to solvent ratio leads to a decrease in phenol recovery. Water to solvent ratios should thus not exceed 0.3. Hexane to feed ratios greater than 3.0 should not be used in combination with solvent to feed ratios smaller than 1.0.

NOMENCLATURE

p	equilibrium mass percentage
E	mass percentage recovery in extract (solvent = triethylene glycol) phase
w/s	Water to solvent (triethylene glycol) mass ratio
s/f	Solvent (triethylene glycol) to feed mass ratio
h/f	Hexane to feed mass ratio
β	Separation Factor (defined in equation 1)

Superscripts

I	extract (solvent = triethylene glycol) phase
II	raffinate (anti-solvent = hexane) phase

ACKNOWLEDGEMENTS

The authors would like to thank Braam van Dyk for assistance in the selection of a solvent by means of computer aided molecular design.

REFERENCES

1. Fiege H and Bayer AG , *Ullman's. Encyc. Ind. Chem.* **A8**, 25, (1987).
2. Nair C S B , Sen D K and Basu A N , *J. Appl. Chem.* **17**(4), 113, (1967).
3. Kodera Y, Ukegawa K and Nakayama T , *Pre-prints Div. Petr. Chem. ACS.* **35**(4), 827, (1990).
4. Bizek V, Horacek J, Kousova M, Komers R, Prochazka J and Heyberger A, *Can. J. Chem. Eng.* **71**(2), 256, (1993).

EXTRACTION OF ACETIC AND PROPIONIC ACIDS FROM AQUEOUS NaCl SOLUTIONS BY TRIOCTYLPHOSPHINE OXIDE

HF Al-Mudhaf, AI Abu-Shady, SA Amer and MF Hegazi
College of Technological Studies, Shuwaikh, Kuwait
P. O. Box 43886 Hawalli, 32053 Kuwait, State of Kuwait.

ABSTRACT
Partition data for transfer of acetic and propionic acids from aqueous (NaCl) solutions to cyclohexane in the absence and in the presence of tri-n-octylphosphine oxide (TOPO) were determined at 30°C. The monomer partition constants, the dimerization constants, and the association constant for TOPO-acid complexes have been evaluated. Salting out parameters were found to increase with increasing (TOPO) level in the organic phase as a result of stabilization of acid by complexing with (TOPO).

Keywords: acetic acid, propionic acid, tri-n-octylphosphine oxide, salting out, association constant.

INTRODUCTION

The use of tri-n-octylphosphine oxide (TOPO) as an extractant for removal of fatty acids from aqueous solutions is now well documented.[1-3] Because of its high hydrogen bonding acceptor basisity,[3-6] TOPO forms a stable hydrogen bonded complex with an organic acid, thereby enhancing the transfer of an organic acid to the extract phase. In addition TOPO is characterized by its excellent stability, high boiling point, and low solubility in water. However, due to the increased cost of TOPO, a search for procedures leading to better extraction results with a minimum used quantities of TOPO is highly desirable. Among the procedures to achieve this goal are lowering of temperature, changing the diluent, and salting out processes.

The intent of the present paper is to study the transfer of acetic and propionic acids from aqueous (NaCl) solutions to TOPO dissolved in cyclohexane as a diluent. The data obtained from this work are crucial in evaluating these systems in various contactors.

EXPERIMENTAL

Acetic acid, propionic acid, and sodium chloride (Analytical Univar Reagent), cyclohexane (Merk), and tri-n-octylphosphine oxide (Fluka) were used without further purification. Double distilled water was used throughout the work.

Experimental Procedure.

All aqueous acetic and propionic acids solutions containing various concentrations of NaCl as well as TOPO-cyclohexane solutions were prepared by weight and the concentration of the acid in these solutions was checked by titration. Appropriate amounts of concentated HCl were added to all the aqueous solutions so that the final HCl concentration was always 0.01 M. Partition experiments were made by shaking equal volumes of aqueous and organic phases (20.0 cm^3 each) in a stoppered conical flask in a flask shaker (200 rpm) for two hours. The contents were transferred into a glass-stoppered test tube and incubated in a thermostated water bath at 30°C ± 0.1, for 30 min. A test tube was removed from the water bath for few seconds during which it is shaked vigorously on a Vortex test tube shaker to reequilibrate at the desired temperature. This was followed by incubation in the water bath overnight for complete phase separation. The acid concentration in the organic layer was determined by titrating an aliquot with standardized NaOH using phenolphthalein as an indicator. Duplicate determinations were made for each organic layer and the organic acid concentration in the aqueous phase was determined by difference from initial acetic acid concentration in the aqueous phase. A blank partition experiment, in the absence of organic acid was carried out similarly for each NaCl concentration used and the volumes of NaOH required in the main partition experiment were corrected accordingly. Partition experiments involving TOPO were carried out in a similar way.

© 2000 Society of Chemical Industry

RESULTS AND DISCUSSION

The system under study involves the extraction of acetic and propionic acids from aqueous solutions of NaCl by cyclohexane containing TOPO. The use of NaCl in the aqueous phase generates two effects; the first results from the salting out of the acid from aqueous phase and the second arises from complexation of acid with TOPO in the organic phase. In order to resolve these effects, it is necessary to study the partition of these acids between aqueous solutions containing NaCl and cyclohexane in the absence and in the presence of TOPO. Data of transfer of acetic acid from aqueous NaCl solution to cyclohexane in the absence of TOPO have previously been reported at 30°C.[7]

The partition coefficient (D), defined as the ratio of total acid concentration in the organic and the aqueous phases, is related to the partition constant of monomer (K_d) and the dimerization constant (K_{dim}) by equation (1):[8]

$$D = (K_d + 2K_d^2 K_{dim} c_a) / (1 + K_a / [H^+]) \qquad (1)$$

where c_a is the concentration of undissociated acid in the aqueous phase.

The partition data in this study were made under conditions where the pH of the aqueous phase is well below the pK_a values of the acid studied. The partition coefficients, at 30°C for propionic acid between aqueous phases containing various concentrations of sodium chloride and cyclohexane as a function of concentration of undissociated acid are listed in Table 1.

NaCl] mole dm^{-3}	10^2 D ([propionic acid]$_a$, mole dm^{-3})
0.0	1.29 (0.050); 1.99 (0.098); 2.61 (0.147); 3.62 (0.219); 4.78 (0.289); 5.72 (0.358); 6.32 (0.403); 7.22 (0.470).
1.0	3.19 (0.097); 5.53 (0.191); 7.69 (0.280); 9.75 (0.366); 11.6 (0.450).
2.0	4.98 (0.096); 9.08 (0.185); 12.6 (0.268); 16.3 (0.347); 19.4 (0.422).
3.0	1.16 (0.093); 14.7 (0.175); 20.9 (0.250); 25.9 (0.320); 30.8 (0.385).
4.0	23.4 (0.163); 31.9 (0.229); 40.2(0.287); 46.8 (0.343).

Table 1 Partition Coefficients of Propionic Acid between Cyclohexane and Aqueous Solutions Containing Various NaCl Concentrations at 30°C.

The values of (K_d) and (K_{dim}) in the absence of salt were deduced from the intercept and slope of the linear least square (D – C_{aq}) plot of the corresponding data. The values for log K_d and log K_{dim} were found to be –2.25 and 3.35, respectively in a close agreement with those reported by Sekine *et al.*[1] The (K_d) values at various NaCl concentrations were deduced from solving equation (2)

$$2K_{dim} [HA]_o^2 + [HA]_o = c_o \qquad (2)$$

where $[HA]_o$ and(c_o) are the concentration of acid monomer and the total acid concentration in the organic phase, respectively. The K_d values for acetic and propionic acids are included in Table 2.

Acid	[NaCl] mole dm^{-3}	$10^3 K_d^*$	K_{ex}	Log K
Acetic Acid	0.0	0.70 ± 0.09	7.24 ± 0.11	4.01
	1.0	0.84 ± 0.11	11.6 ± 0.7	4.14
	2.0	1.05 ± 0.29	16.5 ± 1.3	4.19
	3.0	1.31 ±0.10	19.2 ± 1.2	4.12
Propionic Acid	0.0	5.6 ± 0.6	54.6 ± 2.9	4.07
	1.0	7.4 ± 0.7	74.4 ± 6.7	4.00
	2.0	9.8 ± 1.1	108.2 ± 4.2	4.04
	3.0	13.0 ± 3.0	151.0 ± 9.0	4.06

* K_d values for acetic acid were taken from reference 5.

Table 2 Summary of Equilibrium Constants at 30°C.

Extraction of carboxylic acids by TOPO dissolved in an organic diluent involves the formation of a carboxylic acid – TOPO complex, (HAE), with an association constant, K:

$$K = [HAE]_o / [HA]_o [E]_o \quad (3)$$

where $[E]_o$ is the concentration of free TOPO in the organic phase which equals $[E]_{total, o} - [HAE]_o$. The partition coefficient (D) can be expressed as a function of free (TOPO) concentration by the equation;[7]

$$D = D' + K_{ex} [E]_o \quad (4)$$

Where (D') represents the partition coefficient in the absence of extractant at the specified salt concentration used. In our study its magnitude is insignificant compared to the observed partition coefficient for all experiments involving TOPO. The extraction constant K_{ex}, defined by equation (5):

$$K_{ex} = [HAE]_o / (c_a) [E]_o \quad (5)$$

is related to the association constant K by the equation:

$$K_{ex} = K_d K \quad (6)$$

The dependence of partition coefficients of acetic and propionic acids as a function of both TOPO concentration in the organic phase and salt concentration in the aqueous phase at 30°C are displayed in Table 3. The concentrations of acetic and propionic acids were kept constant for these partition experiments at 0.206 and 0.101 mole dm^{-3}, respectively. The values of K_{ex} and K for both acids at various NaCl concentrations are listed in Table 2.

[NaCl] mole dm^{-3}	10 D ($[Acid]_a$, mole dm^{-3})				
$[TOPO]_{total}$ ⇒ mole dm^{-3}	0.02	0.04	0.06	0.08	0.10
	Acetic Acid				
0.0	0.645 (0.198)	1.31 (0.186)	1.96 (0.176)	2.69 (0.166)	3.46 (0.157)
1.0	0.789 (0.191)	1.66 (0.177)	2.57 (0.164)	3.51 (0.152)	4.45 (0.142)
2.0	0.836 (0.190)	1.75 (0.176)	2.67 (0.163)	3.73 (0.151)	5.20 (0.136)
3.0	0.878 (0.189)	1.88 (0.174)	2.95 (0.159)	4.02 (0.147)	5.53 (0.133)
	Propionic Acid				
0.0	2.34 (0.082)	5.11 (0.067)	9.19 (0.053)	14.0 (0.042)	19.4 (0.034)
1.0	2.62 (0.080)	5.79 (0.064)	10.20 (0.050)	17.3 (0.037)	23.6 (0.030)
2.0	3.04 (0.077)	6.54 (0.061)	11.90 (0.046)	19.1 (0.035)	30.6 (0.025)
3.0	3.56 (0.074)	7.46 (0.058)	14.00 (0.042)	22.9 (0.031)	38.5 (0.021)

Table 3 Partition Coefficients for Acetic and Propionic Acids as a Function of Total Concentration of (TOPO) in Cyclohexane and the Concentration of (NaCl) in Aqueous Phase at 30°C.

It can be seen that the change of K_{ex} with salt concentration is larger for propionic acid compared with acetic acid. This result substantiates the earlier finding that the hydrophobicity of the acid controls not only the magnitude of K_{ex} but also the sensitivity of the acid towards salting out.[3,10,11] In addition, the values of K are nearly the same for both acids and also independent on the concentration of salt in the aqueous phase, as excepted. The association constant reported here is very close to that found by Sekine *et al*[1] in hexane at 25°C using 1 mole dm^{-3} hydrochloric acid in aqueous solution.

The partition coefficient data obtained in the present work using various levels of TOPO in cyclohexane at various NaCl concentrations in the aqueous phase have permitted the evaluation of salting out parameter (k_s) associated with each TOPO level using the well known Sechenov equation:[9]

$$\text{Log}(D / D_o) = k_s [\text{salt}] \qquad (8)$$

where D and D_o denote the partition coefficients in the presence and in the absence of NaCl in an aqueous phase, respectively. It is known that k_s is a measure of sensitivity of a solute to be salted in (salted out) by changing the salt concentration in an aqueous phase. Since in the present study only one salt and one solute, either acetic or propionic acid, is being used and the concentration of TOPO in cyclohexane is variable. It is not unreasonable, therefore to consider k_s as a measure of sensitivity of the solvent with a certain TOPO level towards salting out of a given carboxylic acid from an aqueous phase. The variation of k_s as a function of TOPO concentrations are listed in Table 4.

The magnitude of k_s values is, in general, small and their standard errors may lead to overlapping of some of determined values. Nevertheless, there is a gradual increase, although not uniform, as TOPO level increases. In view of hydrophobicity of both acids, it is not unexpected to see that the values obtained for propionic acid are higher than the corresponding values for acetic acid at the same TOPO level. The increase in k_s with TOPO concentration may reflect the ability of TOPO to complex with the extra acid molecules transferred as a result of salting out process.

$[TOPO]_{T,o}$ mole dm^{-3}	Acetic Acid	Propionic Acid
0.02	0.024 ± 0.001	0.067 ± 0.001
0.04	0.027 ± 0.002	0.105 ± 0.030
0.06	0.029 ± 0.008	0.069 ± 0.001
0.08	0.030 ± 0.002	0.062 ± 0.011
0.10	0.048 ± 0.011	0.107 ± 0.004

Table 4 Values of the salting out parameter (k_s) for Acetic and Propionic Acids at Various TOPO Levels.

The magnitude of k_s values is, in general, small and their standard errors may lead to overlapping of some of determined values. Nevertheless, there is a gradual increase, although not uniform, as TOPO level increases. In view of hydrophobicity of both acids, it is not unexpected to see that the values obtained for propionic acid are higher than the corresponding values for acetic acid at the same TOPO level. The increase in k_s with TOPO concentration may reflect the ability of TOPO to complex with the extra acid molecules transferred as a result of salting out process.

In summary, the present data provide a quantitative evaluation of the effect of addition of NaCl to the aqueous solution on the extraction of acetic and propionic acids by TOPO dissolved in cyclohexane. The high partition coefficients obtained in this work may be attributed to two effects which reinforce each other (i) the stabilization of the carboxylic acid in the organic phase through complexing with TOPO, and (ii) the salting out of the acid as a result of addition of NaCl to the aqueous phase. Work is being conducted in our laboratory in order to find out the possibility of "overloading" of TOPO with two or more molecules of acid particularly at higher concentration levels of both salt and acid.

REFERENCES

1. Niitsu M and Sekine T, *Bull. Chem. Soc. Jpn.*, **51**, 705, (1978).
2. Ricker NL, Michaels JN and King CJ, *J. Separ. Proc. Technol.*, **1**, 36, (1979).
3. Hano T, Matsumoto M, Ohtake T, Sasaki K, Hori F and Kawano Y, *J. Chem. Eng. Japan,* **23**, 734.G, (1990)
4. Malmary M, Faizal J, Albet J and Molinier J. *Chem. Eng. Data*, **42**, 982 (1997).
5. Hegazi MF, *J. Chem. Tech. Biotechnol.*, **34A**, 251, (1984).
6. Kamlet MJ, Abboud J-L M, Abraham MH and Taft RW, *J. Org. Chem.*, **48**, 2877, (1983).
7. Abu-Shady A-S I, Amer SA and Hegazi MF, *J. Chem. Tech. Biotechnol.*, **52**, 177.I, (1991).
8. Kojima, Yoshida M and Tanaka M, *J. Inorg. Nucl. Chem.*, **32**, 987, (1970).
9. Hegazi MF, *Bull. Chem. Soc. Jpn.*, **59**, 3945, (1986).
10. Jenckes WP, *Catalysis in Chemistry and Enzymology*, McGraw-Hill, New York, (1969).
11. Long FA and McDevit WF, *Chem. Rev.*, **51**, 119, (1952).



Nuclear Applications

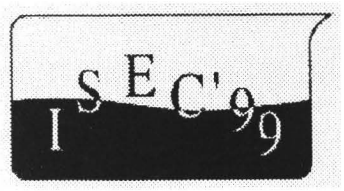

EXTRACTION OF LANTHANIDES(III) AND ACTINIDES(III) BY N,N'-SUBSTITUTED MALONAMIDES: THERMODYNAMIC AND KINETIC DATA

MC Charbonnel[1], M Daldon[1], C Berthon[1], MT Presson[1], C Madic[1] and C Moulin[2]

[1]Commissariat à l'Énergie Atomique, CEN Valrho, Marcoule, BP 171, 30207 Bagnols-sur-Cèze Cedex, France

[2]Commissariat à l'Énergie Atomique, CEN Saclay, 91191 Gif-Sur-Yvette Cedex, France

ABSTRACT

Fundamental studies related to the thermodynamics and kinetics of extraction were carried out as part of the development of the DIAMEX process. The work presented here focused on extraction of trivalent actinides and lanthanides using the extractant DMDBTDMA (N,N'-dimethyl-N,N'-dibutyltetradecylmalonic diamide). The influence of nitric acid and diamide concentrations on extraction of lanthanide(III) nitrates was considered for alkyl and aryl diluents. Spectroscopic investigations (uv/visible, Time-Resolved Laser-Induced Fluorescence (TRLIF), Nuclear Magnetic Resonance spectroscopy) were performed with toluene solutions to study the occurrence of $M(III)/NO_3^-$ ion-pair mechanisms in high acidic conditions but no influence of acidity on the organic metal environment was found. A comprehensive study of the extraction kinetics of lanthanide (III), Am(III) and Cm(III) nitrates was performed using an optimised Lewis cell. The lighter lanthanides exhibit higher extraction rates than the others. This behaviour differs from that observed for M(III) nitrates distribution ratios, which exhibit a tetrad effect.

Keywords: lanthanides, actinides, malonamides, extraction kinetics, mechanism of extraction, Lewis cell, time resolved laser induced fluorescence, NMR, uv-visible spectroscopy

INTRODUCTION

This study was carried out under the CEA programme for the separation and transmutation of long-lived radionuclides, particularly the minor actinides contained in high-level radioactive liquid waste produced by reprocessing nuclear fuel. The first step in the separation strategy is the DIAMEX process, designed to co-extract trivalent actinides and lanthanides using a diamide extractant. Preliminary counter-current hot tests confirmed the feasibility of the concept.[1,2] The malonamide DMDBTDMA (N,N'-dimethyl-N,N'-dibutyltetradecylmalonic diamide) is the first reference extractant; extensive data were therefore compiled to understand its extraction mechanism(s) and to define a computer model of the DIAMEX process. Although some data have been published related to the extraction of trivalent lanthanide nitrates (Nd, Eu, Ce) and of some actinide (III) nitrates (Am and Cm),[2,3] these results needed to be substantiated by a more comprehensive study, the results of which are briefly presented here.

EXPERIMENTAL

Materials

DMDBTDMA was provided by Panchim, Lisses, 91, France. The purity as determined by mass spectrometry was better than 99%. The diamide was then purified on a silica column to avoid the presence of surface-active compounds.[2] Lanthanide (III) n-hydrate nitrates or oxides, lithium nitrate and toluene were reagent grade with better than 99% purity.

Procedure and apparatus

Organic phases were systematically pre-equilibrated with suitable nitric acid solutions a few hours before the tests. The nitric acid distribution was determined by potentiometric titration of aliquots of each phase using a Metrohm 670 potentiometer. The water content of the organic phase was

© 2000 Society of Chemical Industry

determined using a Karl Fisher Metrohm KF737 coulometer. The rare earth concentration in each phase was determined by Arsenazo III visible spectrometric analysis. UV-visible spectra were recorded on a Cary 2315 spectrometer and NMR spectra on a Varian VXR 300 MHz spectrometer. A triple Nd-YAG laser (Continuum) operating at 355 nm was used as the excitation source of a Time-Resolved-Induced-Laser-Fluorescence Spectrometer (TRLIFS). The laser beam was focused into the cell of a "FLUO 2001" (Dilor)[4] spectrofluorometer.

To study An(III) and Ln(III) extraction kinetics, a new constant interface-area stirred cell based on the Armollex-Lewis concept was first built. The main characteristics of our Lewis cells were their modular design (3-piece cell with Teflon seals), their small volume (less than 35 cm^3 for each phase for the smaller cell used) and combined magnetic-mechanical stirring (Figure 1).

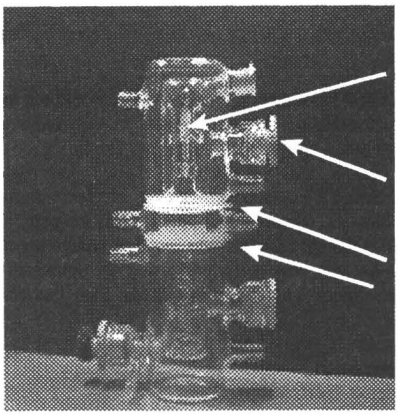

Figure 1. Modified Lewis cell used for kinetic study

RESULTS AND DISCUSSION

Mechanism of lanthanide(III) extraction at thermodynamic equilibrium

The main goal of the studies presented here was to determine whether or not two mechanisms exist, depending on the nitric acid concentration of the aqueous phase. Previous publications indicated the formation of a solvate under neutral conditions, $Nd(NO_3)_3L_x$ where L is the diamide extractant, and an ion-pair complex, L_xH^+ $Nd(NO_3)_4^-$, during Ln(III) extraction under acidic conditions.[3,5] This was based essentially on the analysis of the slopes of the $D_{Nd} = f([HNO_3])$ curves and on the knowledge of nitric acid extraction, which led to the presence of protonated diamide at high acidities.[2,3]

New studies were carried out in an attempt to identify this Ln(III) ion-pair complex. The first issue was the selection of a suitable diluent. We first checked that diamide extraction of nitric acid, water and Ln(III) nitrates proceeds by the same global mechanisms for aromatic or aliphatic diluents. The extraction of nitric acid and Nd(III) nitrate was investigated for TPH and toluene (Figures 2, 3, 4).

The apparent HNO_3 extraction constants K_{21}, K_{11}, K_{12} and K_{13} relative to the formation of the respective complexes $2L{\cdot}HNO_3$, $L{\cdot}HNO_3$, $L{\cdot}2HNO_3$ and $L{\cdot}3HNO_3$ were determined (Table I). The close values of each pair of constants suggest identical mechanisms for HNO_3 and H_2O extraction in these two diluents.

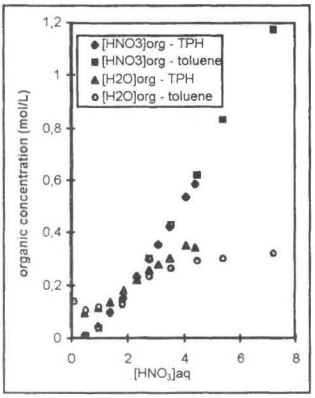

Figure 2. Extraction of HNO_3 and H_2O by DMDBTDMA 0,50+/-0,02 mol/dm^3 in TPH and toluene (Temperature 25C)

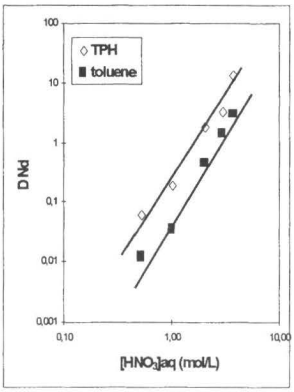

Figure 3. Extraction of Nd(III) by DMDBTDMA 0,64+/-0,01 mol/dm^3 versus aqueous nitric acidity (Temperature 25C)

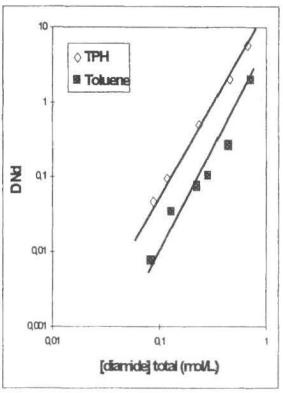

Figure 4. Extraction of Nd(III) by DMDBTDMA versus total extractant concentration (Temp. 25C [NO_3]=3 mol/dm^3; [H^+] = 1 mol/dm^3 and [Li^+] = 2 mol/dm^3)

For neodymium(III) extraction, the $D_{Nd} = f([H^+])$ and $D_{Nd} = f([\text{diamide}])$ curves were compared for both diluents. The calculated slopes were similar (2.7 in TPH and 2.9 in toluene for the variation with aqueous acidity, and 2.36 for both [diamide] curves). These results indicate also a comparable global mechanism for Nd(III) extraction in both diluents and are consistent with a 2/1 ligand/Nd(III) stoichiometry even in toluene.

Table I
Extraction constants for species $2L{\cdot}HNO_3$, $L{\cdot}HNO_3$, $L{\cdot}2HNO_3$ and $L{\cdot}3HNO_3$ ([diamide]=0,5 mol/dm^3 - 25°C)

	TPH	Toluene
K_{21} ($mol^{-2}{\cdot}L^2$)	0.3133	0.4130
K_{11} ($mol^{-1}{\cdot}L$)	0.1632	0.1693
K_{12} ($mol^{-2}{\cdot}L^2$)	0.00210	0.00282
K_{13} ($mol^{-3}{\cdot}L^3$)	1.0×10^{-7}	1.0×10^{-5}

Studies aiming to identify the existence of an ion-pair mechanism were based on three different experimental techniques: UV-visible absorption, TRLIF and ^1H and ^{13}C NMR spectrometries. The following conditions were explored:

- neutral conditions to obtain the Ln(NO3)3Ln solvate complex in the organic phase (high LiNO3 concentration and absence of H^+ in aqueous phase),
- high acidic conditions (in aqueous and organic phases) to obtain the largest possible amount of the assumed $LH^+,M(NO_3)_4^-$ ion-pair complex.

The neodymium(III) environment in these organic phases was investigated by visible absorption spectroscopy (hypersensitive transition at 582 nm: Figure 5) and that of europium (III) by TRLIF. Figure 6 presents the Eu(III) fluorescence spectra in the presence of DMDBTDMA with different acidic conditions. Several comments can be made. The fluorescence spectra were equivalent regardless of the chemical conditions, and the inversion of peak intensities was observed at the hypersensitive transition. The (618 nm / 593 nm) ratio that reflects complexation was equal to 5 and can be compared with the values for Eu(III) aqua ion (0.25) and the europium aqua tricarbonato complex (6).[6] The lifetimes of Eu(III) exited states in 'neutral' and 'acidic' conditions were also very similar (700 ± 80 μs), indicating that there is no more than one water molecule remaining in the Eu(III) inner sphere of co-ordination. *These data indicate a similar coordination polyhedron for lanthanide (III) ion in both cases, neutral and acidic conditions.*

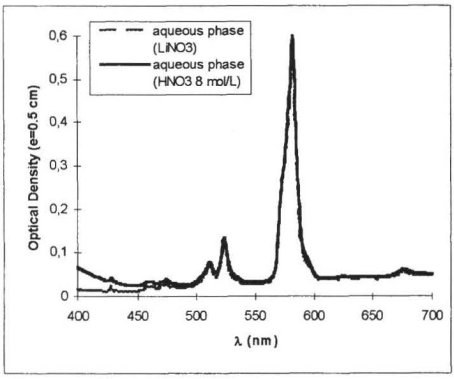

Figure 5. UV-visible spectra of two Nd(III) solutions in DMDBTDMA 0.5 mol/dm^3 in toluene (① $[LiNO_3]_{aq} = 5$ mol/dm^3 and $[Nd]_{org} = 0.048$ mol/dm^3 and ② $[HNO_3]_{aq} = 8$ mol/dm^3 and $[Nd]_{org} = 0.051$ mol/dm^3)

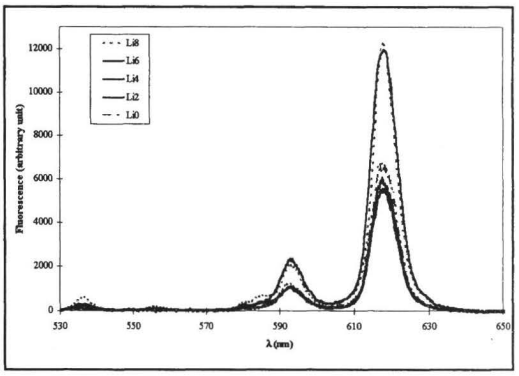

Figure 6. Fluorescence spectra of Eu(III) in DMDBTDMA 0.51 ± 0.01 mol/dm^3 in toluene (initial $[Eu]_{aq} = 2.00 \pm 0.02 \times 10^{-2}$ mol/dm^3 and $[LiNO_3]$ in aqueous phase in equilibrium = 8.0, 6.0, 4.0, 2.0 and 0 when [H+] = 0, 2.0, 4.0, 6.0 and 8.0 mol/dm^3, respectively)

An additional study was carried out using NMR spectroscopy, based on the paramagnetic properties of Nd(III). The presence of Nd(III) induces chemical shifts and increasing relaxation time on each nucleus of an extractant molecule bound or close to the metal ion. The basic assumption was that in the assumed L_xH^+, $Nd(NO_3)_4^-$ ion-pair complex the distance r between metal centre and the extractant carbon atoms should be greater than in the case of the $Nd(NO_3)_3L_x$ solvate complex. We focused on relaxation times T_1 of ^{13}C nuclei 2, 3, 6, 7 and 4 (Figure 7) for solutions described in Table II, because T_1 decreases very rapidly when r increases[7]: $(1/T_1) \square (1/r^6)$. Surprisingly, the results in Table II were consistent with a distance r longer in the case of "neutral" conditions (solution C) than for "acidic" ones.

TABLE II

Samples analysed by NMR and measured relaxation time T_1 for ^{13}C nuclei ([DMDBTDMA] = 0.5 mol /dm^3 in toluene) in absence or presence of Nd(III)

Nature of solutions	A	B	C	D
$[LiNO_3]_{aq}$ (mol.L^{-1})	8	0	8	0
$[HNO_3]_{aq}$ (mol.L^{-1})	0	8	0	8
$[Nd^{3+}]_{aq}$ (mol.L^{-1})	0	0	0.05	0.05
Carbon numbering	Measured T_1 (s)			
4	0.77*	0.26*	0.28	0.19*
3 and 6 (trans)	0.48	0.29	0.29	0.20
3 and 6 (cis)	0.5	0.32	0.30*	0.20
2 and 7 (trans)	2.6	1.25	1.14	0.76
2 and 7 (cis)	2.9	1.5	1.36	0.75

* average value relative to the different observed signals.

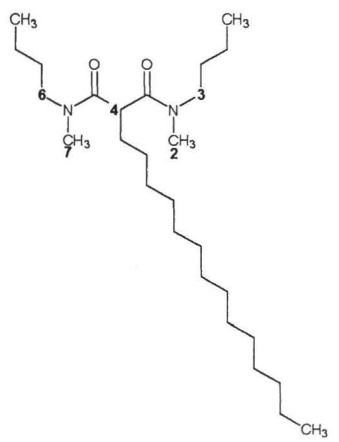

Figure 7. Selected numbering of carbons in DMDBTDMA

These data concerning either the metal or ligand environment suggest that, if a dual extraction mechanism does exist, the second mechanism does not seem to be an ion-pair mechanism. We therefore propose the following overall extraction equilibrium for Nd(III) extraction by DMDBTDMA in TPH and toluene:

$$Nd^{3+} + 3\ NO_3^- + 2\ DMDBTDMA \rightleftarrows Nd(NO_3)_3(DMDBTDMA)_2$$

Variation in the lanthanides series (distribution ratios and kinetics extraction rates)

A systematic investigation of extraction was conducted on a number of lanthanides (La, Ce, Pr, Nd, Sm, Eu, Gd, Dy and Lu). Distribution ratios were found to decrease with increasing Ln(III) Z, but the variation was not monotonic for the first lanthanides (Figure 8). This tendency has already been observed for other ligands[8] and has been described as tetrad effect.[9]

Until now kinetics of rare earths and actinides extraction with malonamides has not been described in the literature, except for some preliminary studies.[10] The importance of such a study was justified by the possible use of centrifugal extractors with short residence time for both phases.

After a qualification step of our new Lewis cell (where the influence of different hydrodynamic parameters was tested), the conditions under which the transfer rate of metallic nitrate kinetics was chemically controlled were determined (i.e. diffusional limitations on kinetics could be considered negligible). This was achieved through a study of the kinetic rate constant as a function of the Reynolds number of the Lewis cell impeller.

The form of the Ln(III) extraction rate law was established: $k\ [Nd(III)][L][NO_3^-]^3$. The curve of kinetic rate constant k versus Ln atomic number (Figure 9) was different from that observed for Ln(III) distribution ratios. Two sets of values were observed: one close to 20×10^{-7} m/s for the first rare earths (La, Pr, Ce) of the series, and a second close to $3 - 7 \times 10^{-7}$ m/s for the other lanthanides. The extraction kinetic rate constants appeared to depend on the size (and hence the co-ordination number) of the lanthanides.

The kinetic extraction rates were also measured for Am(III) and Cm(III) and found to be close to the value for Eu(III), as previously observed by Toulemonde.[10]

We can now propose and discuss an extraction mechanism based on malonamide DMDBTDMA molecules adsorbed at the solvent/aqueous interface.

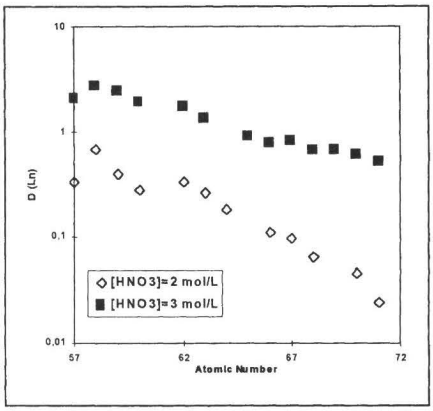

Figure 8. Ln(III) distribution ratios by DMDBTDMA 0.51 mol/dm^3 in TPH ($[Ln]_{init}$ = 0.03 mol/dm^3; Temperature = 25C)

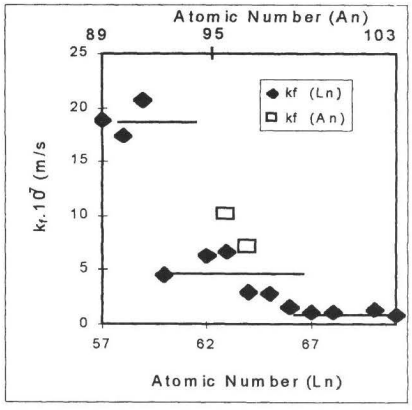

Figure 9. Kinetic rate constant for Ln(III) and An(III) extraction by DMDBTDMA 0.5 mol/dm^3 in TPH($[Ln]_{init}$ = 0.06 mol/dm^3; HNO_3 = 2 mol/dm^3; Temperature = 25C)

CONCLUSION

The studies presented here focused on trivalent lanthanide extraction by the malonamide DMDBTDMA. The mechanisms of HNO_3 and $Nd(NO_3)_3$ extraction are similar in both alkyl and aryl diluents. Three different methods were used in an unsuccessful attempt to identify the occurrence of an ion-pair mechanism for high acidity conditions. The Ln(III) environment appears to be the same as after Ln(III) extraction from neutral conditions. An exhaustive study of extraction and kinetics was performed on most of the elements of the Ln(III)series. While a tetrad effect was observed for the extraction of Ln(III) nitrates (D_{Ln} vs. Z_{Ln}), two sets of extraction rate constants were observed within Ln(III) series: 20×10^{-7} m/s for La, Ce, Pr and $3 - 7 \times 10^{-7}$ m/s for the remaining lanthanides. The Am(III) and Cm(III) extraction rate constants were found to be near those of the heavy lanthanides.

ACKNOWLEDGEMENTS

The authors are grateful for the financial support from the COGEMA and from the Commission of the European Communities (Contract NEWPART - FI41-CT-96-0010).

REFERENCES

1 Madic C *et al. RECOD '94*, 24-28 April, London UK (1994).
2 Madic C and Hudson MJ. *Report EUR 18038* (1998).
3 Nigond-Berthon L. *CEA R-5610,* (1992).
4 Moulin C, Decambox P and Mauchien P. *J. Radio. Nucl. Sci.*, **226**, 135, (1997).
5 Chan GYS *et al. J. Chem. Soc., Dalton Trans.*, 649-660, (1997).
6 Moulin C, Larpent C and Gazeau D. *Anal. Chim. Acta*, **49**, 378, (1999).
7 Bloembergen N and Morgan LO. *J. Chem. Phys.*, **34**, 842, (1961).
8 Nakamura T and Miyake C. *Solv. Extr. Ion Exch.*, **13**, 252, (1995).
9 Mioduski T and Sierirski S. *J. Inorg. Nucl. Chem.* **37**, 1647, (1975).
10 Toulemonde V, *CEA R-5746,* (1997).

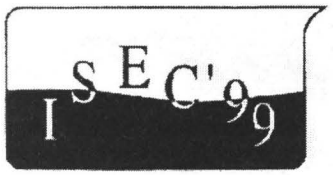

THE SOLVENT EXTRACTION BEHAVIOUR OF TETRAVALENT ACTINIDES IN THE PRESENCE OF SIMPLE HYDROXAMIC ACIDS

RJ Taylor[1], I May[1] and NJ Hill[2]

[1]Research and Technology, BNFL Sellafield, Seascale, Cumbria, CA20 1PG, UK

[2]Research and Technology, BNFL Risley, WA3 6AS, UK

ABSTRACT

Advanced Purex processes based on single cycle flowsheets are currently under development at BNFL. Flowsheet design requires the accumulation of fundamental solvent extraction data. To support the development of complexant based flowsheets distribution data for tetravalent actinides in the presence of simple hydroxamic acid complexants have been obtained and are reported.

Keywords: tetravalent actinides, hydroxamic acids, Purex process

INTRODUCTION

Nuclear fuel reprocessing involves the purification of reusable uranium and plutonium products from irradiated fuel. Reprocessed U and Pu can then be recycled as UO_2 and mixed oxide fuels for further electricity generation. BNFL currently operates two commercial reprocessing plants for the reprocessing of Magnox and oxide fuels.[1] Both these reprocessing plants are based on the Purex process, which involves the solvent extraction of U and Pu from aqueous nitric acid in to tri-n-butylphosphate diluted in odourless kerosene (TBP/OK). U and Pu can also be separated from each other by control of the Pu oxidation state.

BNFL is currently engaged in research and development programmes to both enhance operations of current plants[2] and to develop Advanced Purex processes.[3] Previous papers have described the development of single cycle flowsheets using centrifugal contactors and enhanced control of Np.[3,4] In particular, the development of complexant based flowsheets to separate tetravalent actinides (Np(IV), Pu(IV)) from hexavalent actinides (U(VI)) using hydroxamic acid complexants (XHA) has been a major feature of the *Advanced Purex* project.[5,6] Both acetohydroxamic acid (AHA) and formohydroxamic acid (FHA) readily complex An(IV) in nitric acid rendering the metal ions largely inextractable into TBP/OK.

A companion paper[7] reports the results of a counter-current trial of a Np Rejection flowsheet and the computer simulation of this trial. This paper discusses the accumulation and manipulation of fundamental solvent extraction data that supports counter-current trials and flowsheet modelling.

EXPERIMENTAL

Experimental methods have been described in detail elsewhere.[5,6,8] Briefly, simple batch distribution experiments were used to measure distribution coefficients. Np stock solutions were obtained by the dissolution of NpO_2 in HNO_3 and then the chemical manipulation of Np oxidation state. A pre-existing Pu(IV) stock solution was used and simply diluted to the required concentration. U(IV) stock solutions were purified by the solvent extraction of any U(VI) present and stabilised by hydrazine. FHA, AHA and uranyl nitrate hexahydrate were obtained from Tokris Cookson, Aldrich and Fluka chemical companies respectively. Np and U oxidation states were monitored by uv/vis/nir spectrophotometry. Pu was not monitored spectroscopically during the distribution experiments but Pu(IV) in HNO_3, at the acidities used, is adequately stable unlike U(IV) and Np(IV). Np

© 2000 Society of Chemical Industry

concentration was determined by low energy photon spectroscopy; U by x-ray fluorescence; Pu was analysed radiometrically and acidity by acid-base titration.

RESULTS AND DISCUSSION

Neptunium (IV)

Distribution experiments were undertaken to determine $D_{Np(IV)}$ as a function of [XHA] and [HNO_3]. Initially, in order to validate the experimental methods and to provide distribution data for the mathematical algorithm (particularly at low acidities) the extraction of Np(IV) in the absence of hydroxamic acids was studied.[8]

The results are illustrated in Figure 1. Briefly, the data can be split in to four regions: (1) Above 1 mol/dm^3 HNO_3 good agreement with the literature data was found. (2) Between 0.4-1 mol/dm^3 HNO_3 the distribution data has been reliably extended to show that the trend above 1 mol/dm^3 HNO_3 is continued in this region. (3) Below 0.4 mol/dm^3 HNO_3 the data becomes very scattered due to the difficulties in obtaining Np(IV) distribution data at low acidity (due to hydrolysis, oxidation to Np(V) and solvent phase analyses at low [Np]). However, our data in this region appears to reach a plateau rather than a maximum and so higher Np(IV) distribution coefficients than expected are predicted. This behaviour can be more easily explained in terms of the Np(IV)-nitrate species formed.

In the presence of hydrophilic hydroxamic acids, increased [XHA] and decreased [HNO_3] cause $D_{Np(IV)}$ to decrease to very low levels, characteristic of inextractable species.[5,6] Since the development of the Np Rejection flowsheet has been a priority,[3] a substantial body of distribution data has been accumulated. This body of data can be mathematically manipulated to (a) evaluate the reliability of the data (b) provide information on the effects of complexation on solvent extraction and (c) produce the mathematical algorithm that describes the solvent extraction behaviour of Np(IV) in HNO_3/TBP systems in the presence of hydroxamic acids.

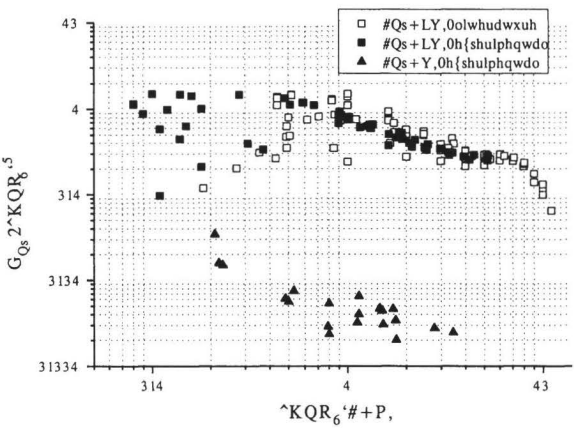

Figure 1. Trends in Np distribution coefficients in nitric acid

When hydroxamic acid is present, the solvent extraction of Np(IV) is modified and, assuming that no complexed Np is extracted, a relationship between the ratio of distribution coefficients in nitric acid only ($D_{Np(IV)}$) and in the presence of XHA ($D_{Np(IV)\text{-}XHA}$) and the concentrations of HNO_3 and XHA is observed. Figure 2 illustrates this relationship for both FHA and AHA, and Figure 3 shows a clearer correlation is obtained when solely FHA at 22C and in 29.24% TBP/OK is plotted.

(Note that U(VI) is not present in these data and, therefore, the only metal ion present in trace quantities is Np(IV)). The linearity of this graph and the good correlation of the data are evidence of this mathematical correlation and the self-consistency of the data-set. The data becomes increasingly scattered at low acidity and this is due to the difficulties in obtaining accurate distribution data in this region (discussed above). The uncertainty in the Np(IV)-XHA algorithm at low acidity was emphasized during a flowsheet trial of the Np Rejection flowsheet[7] and this is clearly an area which requires further work.

Further mathematical manipulation of the distribution data leads to the definition of the extraction algorithm which is a combination of an empirical fitting of the data and functions of all the relevant process variables (e.g. $[H^+]$, $[NO_3^-]$, [XHA], temp, $[U(VI)]$, $[TBP]_{free}$ etc.). This algorithm is then used in process modelling.[7]

Although it has already been reported that FHA and AHA can selectively strip Np(IV) from 30% TBP/OK in the presence of U(VI),[5] further distribution data in the presence of U(VI) were needed to allow the mathematical description of Np(IV) in the presence of hydroxamic acids to be extended to include the effect of [U(VI)].

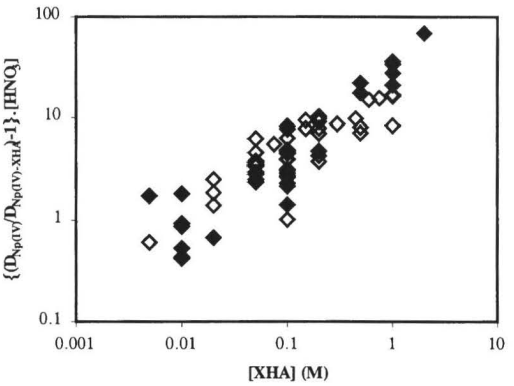

Figure 2. The complexation of Np(IV) by FHA (closed symbols) and AHA (open symbols) in HNO_3 and the effect on extraction in to ~30% TBP/OK. Correlation of data.

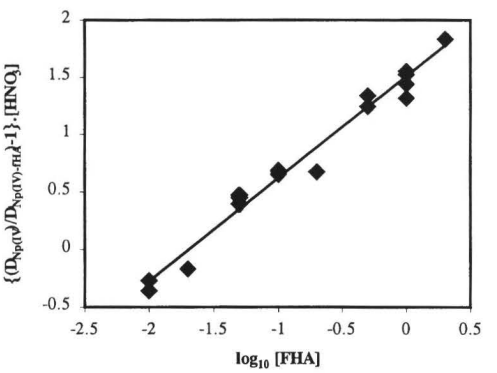

Figure 3. The complexation of Np(IV) by FHA in HNO_3 and the effect on extraction in to 30% TBP/OK

Several key trends were clearly visible in the U(VI) loaded distribution data:

- As expected, even in the absence of AHA or FHA, U(VI) inhibits Np(IV) extraction into 30% TBP/OK [e.g. in 0.68 mol/dm^3 HNO_3: $[U(VI)_{total}] = 0$; $D_{Np(IV)} = 0.50$ cf. $[U(VI)_{total}] = 59.8 g/dm^3$; $D_{Np(IV)} = 0.21$].
- The addition of AHA/FHA leads to increased stripping of Np(IV) leaving the extractability of U(VI) unaffected.
- Increasing the U(VI) loading and decreasing $[HNO_3]$, increased Np(IV) stripping in the presence and absence of FHA and AHA.
- There appears to be a limiting point where lowering the acidity, increasing the ligand concentration or the U(VI) loading does not lead to a decrease in $D_{Np(IV)}$ ($D_{Np(IV)} \sim 0.01$). A likely explanation was that low quantities of aqueous entrainment led to the carry over of Np(IV) in to the solvent phase in these simple distribution experiments. However, flowsheet trials[7] have suggested that the mathematical correlation over predicts Np rejection in the presence of uranyl nitrate and that modifications are needed. Further work is ongoing to clarify this issue.

Uranium (IV) and Plutonium (IV)

The variation of $D_{U(IV)}$ with hydroxamic acid (XHA) concentration is illustrated in Figure 4. Both FHA and AHA stripped U(IV) in to HNO_3 from 30% TBP/OK, with increased stripping at higher ligand and lower HNO_3 concentrations.

UV/vis spectra of the post-equilibrium phases showed that measurable quantities of U(VI) were present in the organic phase. As the organic phase spectra were recorded almost immediately after phase contact, it must be assumed that some U(IV)ÛU(VI) oxidation had occurred during the 10 minute mixing time. By comparing the distribution coefficients obtained in the absence of FHA and AHA with known literature values, it was observed that the experimental values are significantly higher. This discrepancy was almost certainly due to the presence of U(VI), which is more extractable into 30% TBP/OK than U(IV). As the FHA or AHA concentration was raised, more U(IV) was held back in the aqueous phase and thus there was less U(IV) present in the organic phase and less oxidation occurred. Therefore, as the ligand concentration was raised the distribution value more readily represented solely U(IV) behaviour. Further experiments at lower contact times with accurate spectroscopic measurement of U(IV) and U(VI) are planned to reduce the effects of U(VI) on the measured distribution coefficient.

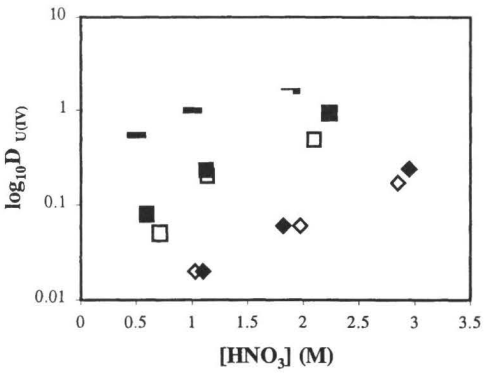

Figure 4. U(IV) distribution data in the presence of FHA and AHA ([XHA]=0 (0); 0.1 (¦); 1.0 (?) mol/dm^3 respectively; FHA = closed and AHA = open symbols)

The variation of $D_{Pu(IV)}$ with $[HNO_3]$ is illustrated graphically in Figure 5. The observed trends with both $[HNO_3]$ and [ligand] again follow the expected patterns, i.e. increased [XHA], [U(VI)] and decreased $[HNO_3]$ decrease $D_{Pu(IV)}$.

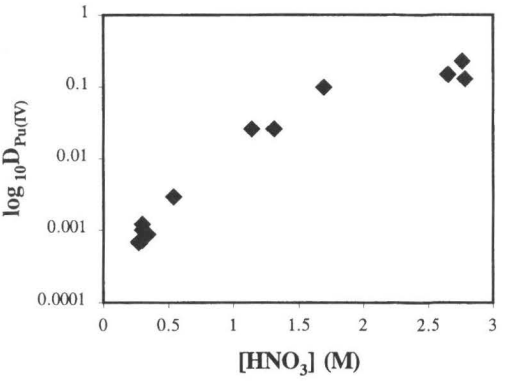

Figure 5. Variation of $D_{Pu(IV)}$ with equilibrium aqueous acidity ([XHA]=0.5 mol/dm^3)

CONCLUSIONS

Simple hydroxamic acids are good complexants for tetravalent actinides, particularly Np(IV) and Pu(IV), in nitric acid solution. Experimental distribution data have been obtained showing how hydroxamic acids inhibit the extraction of tetravalent actinides in to 30% TBP/OK and these distribution data have been used to construct extraction algorithms suitable for use in process modelling.

Modelling of a recent counter-current trial[7] has shown that further work is needed to improve the accuracy of the mathematical algorithm at low acidity in the presence of high [U(VI)] and [NO_3^-] and to determine the rate of mass transfer of Np(IV) in the presence of hydrophilic hydroxamic acids. Furthermore, structural studies of An(IV)-XHA complexes in solution are needed to understand how the hydroxamic acid complexes and retards extraction. It is hoped that these structural studies will complement inferences made from the solvent extraction data.

REFERENCES

1. Wilson PD (ed.), *'The Nuclear Fuel Cycle'*, Oxford Science Publications, Oxford, (1996).
2. Riley A et al., *Proc. RECOD '98*, (1998).
3. Taylor RJ et al., *Proc. RECOD '98*, (1998).
4. Taylor RJ et al., *Nuclear Energy*, **36**, 39, (1997).
5. Taylor RJ et al.,*J. Alloys & Compounds*, **271**, 534, (1998).
6. May I et al., *J. Alloys & Compounds*, **271**, 650, (1998).
7. Wallwork AL et al., *Proc. ISEC'99*, (1999).
8. May I et al., *Radiochim. Acta*, accepted for publication.

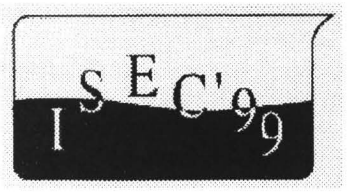

DEVELOPMENT OF A UNIVERSAL COBALT DICARBOLLIDE SOLVENT FOR THE REMOVAL OF ACTINIDES, CESIUM AND STRONTIUM FROM ACIDIC WASTES

TA Todd, KN Brewer, JD Law, RS Herbst and DJ Wood
Lockheed Martin Idaho Technologies Co., Idaho Falls, Idaho, USA
VN Romanovskiy, V Esimantovskiy, IV Smirnov, VA Babain and B Zaitsev
VG Khlopin Radium Institute, St. Petersburg, Russia

ABSTRACT
The cobalt dicarbollide solvent extraction process, originally developed in the mid-1970's by Czechoslovakian researchers, and later developed and implemented in Russia, has been demonstrated to be effective at removing cesium from acidic solutions. Strontium removal can also be achieved by the addition of polyethylene glycol to the solvent. A collaborative development programme has been ongoing for the past five years between the Idaho National Engineering and Environmental Laboratory (INEEL) and the VG Khlopin Radium Institute (KRI) in St. Petersburg, Russia. Initial efforts centered on development of a non-aromatic diluent which was successfully tested in batch contact and countercurrent demonstrations at the INEEL. A universal solvent has been developed, based on the cobalt dicarbollide process, to facilitate removal of actinides, cesium and strontium in a single process. The solvent contains chlorinated cobalt dicarbollide, polyethylene glycol and an organophosphate complexing agent in a non-aromatic diluent. This solvent was tested at the INEEL in a shielded hot cell facility, in a series of batch contacts with actual radioactive waste. Decontamination factors of 98% for Cs, 99.8% for Sr and >99.99% for actinides were achieved in four successive batch contacts with actual tank waste. Testing of the universal extraction process in centrifugal contactor pilot plants using simulated and actual waste has been completed. Results indicate the process is viable and can achieve very high levels of decontamination of acidic radioactive liquid wastes.

Keywords: cesium, strontium, actinides, cobalt dicarbollide, centrifugal contactor

INTRODUCTION

The cobalt dicarbollide solvent extraction process, originally developed in the mid-1970's by Czechoslovakian researchers,[1,2] and later developed and implemented in Russia[3,4] has been demonstrated to be effective at removing cesium from acidic solutions. Strontium removal can also be achieved by the addition of polyethylene glycol to the solvent. A collaborative development programme has been ongoing for the past five years between the Idaho National Engineering and Environmental Laboratory and the VG Khlopin Radium Institute in St. Petersburg, Russia. The focus of this programme has been the development and demonstration of the cobalt dicarbollide process on simulated and actual INEEL acidic waste streams.[5,6]

Recently, a tertiary solvent containing chlorinated cobalt dicarbollide, polyethylene glycol and diphenylcarbamoylmethylphosphine oxide (dϕ-CMPO) was developed for the simultaneous removal of cesium, strontium, actinides and rare earth elements from acidic wastes.[7,8]. The removal of these radionuclides from the waste in a single unit operation offers significant potential capital and operating cost savings.

Testing and demonstration of the universal extraction process (UEP) has been completed on batch contact studies using simulated and actual tank waste as well as four counter-current pilot plant tests in centrifugal contactors; two with simulated waste at the INEEL, one with simulated waste at KRI, and one with actual waste at the INEEL.

EXPERIMENTAL

Two experimental cross-current flowsheets were used in batch contact tests with actual waste using the universal solvent. One test utilized a diluent that was less dense than the aqueous phase. The

© 2000 Society of Chemical Industry

light solvent flowsheet consisted of four extraction contacts to determine decontamination factors for the radionuclides. Solvent from the first contact was further tested after another contact with fresh waste to load the solvent more completely with the extractable species. Two sequential strip contacts were performed to remove Cs, Sr and other extracted metals (primarily Zr) that could form precipitates in the second strip solution. The second strip solution was intended to remove the remaining radionuclides from the solvent.

The second test utilized a diluent that was more dense than the aqueous phase and was designed simply to elucidate potential decontamination factors. The heavy solvent flowsheet contained four sequential batch contacts with fresh solvent being used in each contact. Both experiments were conducted in a hot cell at the Remote Analytical Laboratory (RAL) at the INEEL.

A counter-current test of the universal extraction process was performed at the VG Khlopin Radium Institute (Gatchina), with simulated INEEL tank waste spiked with actual concentrations of radionuclides. The test was performed in two extraction cascades of 12 stage centrifugal contactors (type MZE 12-30). The centrifugal contactors are configured in a circle, with one electric motor drive for all 12 stages, via a gear mechanism. The radionuclides were extracted from the sodium-bearing waste simulant in stages 1-8. The solvent was then washed in stage 9 and the rare earths, Sr, and actinides were stripped in stages 10-14. Cesium was stripped in stages 15-20, and the solvent was washed in stages 21-24. The solvent used for the test was comprised of chlorinated cobalt dicarbollide, polyethylene glycol and df-CMPO in metanitrobenzotrifluoride.

Flowsheet testing was performed at the INEEL using 3.3-cm diameter centrifugal contactors procured from the Research and Development Institute of Construction Technology (NIKIMT) in Moscow, Russia. The 3.3-cm Centrifugal Contactor Pilot Plant consist of 26 stages of 3.3-cm diameter centrifugal contactors, feed and receiving vessels, feed pumps, and an air purge system for the feed and product vessels

Tank waste simulant was prepared to emulate the average composition of the waste currently stored in the INEEL tank farm. The components used as surrogates for the fission products (stable Cs and Sr) and actinides (Eu) were added to the simulant at higher concentrations than found in the actual wastes to facilitate detection limits for analytical chemistry.

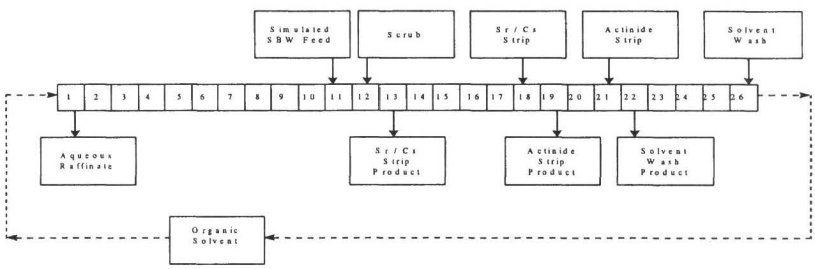

Figure 1. Universal extraction process flowsheet

Two tests were performed with the flowsheet, as shown in Figure 1, consisting of eleven stages of extraction at an organic to aqueous phase ratio (O/A) of 1.4, one stage of scrub (O/A = 5.0), six stages of Cs/Sr strip (O/A = 2.0), three stages of actinide strip (O/A = 5.0), and five stages of solvent wash (O/A = 1.3). The second flowsheet test included addition of citric acid to the aqueous feed, the scrub stream, the Cs/Sr strip solution, and the increase of the Cs/Sr strip flowrate. The flowsheet modifications were necessary in order to reduce the quantity of Zr extracted by the solvent

and to prevent the formation of a precipitate in the Cs/Sr strip section.

The countercurrent flowsheet test performed at the INEEL in a shielded hot cell with actual radioactive tank waste was performed in a pilot plant utilizing 24-stages of 2-cm centrifugal contactors designed and built by Argonne National Laboratory. The flowsheet tested was similar to previous tests, but had minor adjustments. The flowsheet consisted of eight stages of extraction (O/A = 2.0), two stages of scrub (O/A=10), six stages of Cs/Sr strip (O/A = 2.3), three stages of actinide strip (O/A=4.1), and five stages of solvent wash (O/A = 2.2). The composition of the actual radioactive waste used for this test is shown in Table 1. Compositions of simulants used in earlier testing were similar to that shown in Table 1.

Component	Units	Concentration
H^+	mol/dm^3	1.7
Al	mol/dm^3	0.55
B	mol/dm^3	0.02
Ca	mol/dm^3	0.03
Cd	mol/dm^3	0.001
Fe	mol/dm^3	0.05
Hg	mol/dm^3	0.004
K	mol/dm^3	0.08
Na	mol/dm^3	0.74
NO_3	mol/dm^3	5.1
Pb	mol/dm^3	0.001
Zr	mol/dm^3	4.2E-04
gross a	Bq/dm^3	2.15E+07
^{137}Cs	Bq/dm^3	6.78E+09
^{90}Sr	Bq/dm^3	6.62E+09

Table 1. INEEL tank waste composition

RESULTS AND DISCUSSION

KRI Flowsheet Test

The universal solvent tested at KRI (Gatchina) using simulated INEEL tank waste with actual concentrations of radionuclides was completed with no observation of flooding, third phase formation or precipitation. The removal efficiencies obtained for the radionuclides were all >99.8% except for Am, which was 99.2%.

The organic solvent was recycled for about 3 cycles total, with no apparent decrease in extraction efficiency over the duration of the test.

INEEL Batch Contact Tests

Four sequential contacts between actual tank waste and fresh solvent aliquots were performed. Cesium distribution coefficients ranged from 1.4 to 2.1, resulting in a decontamination factor of 89 (98.9% Cs removed).

Extraction coefficients greater than 2 were typically observed for ^{90}Sr. A strontium decontamination factor of 600 (99.8% Sr removed) was achieved in 4 contacts with the universal solvent.

All of the actinides showed very large extraction distribution coefficients. Gross-a and actinide decontamination factors ranged between 9,400 and 160,000. These results are in excess of the necessary decontamination factors required to produce a non-TRU waste.

INEEL Flowsheet Tests

Three counter-current flowsheet tests were performed at the INEEL, two with simulated waste and one with actual highly radioactive tank waste. In the first counter-current flowsheet test using simulated waste, flooding was observed in the aqueous solution exiting the Cs strip section. Inspection of the Cs strip stages after completion of the test revealed large quantities of rust colored precipitate in each of the stages. X-ray diffraction analysis of the precipitate indicate it was an insoluble zirconium complex formed when the extracted Zr entered the strip section. Complexing the Zr to prevent its extraction is expected to prevent the formation of this precipitate.

The extraction section of the flowsheet operated without problems and removal efficiencies for the radionuclides were determined. The removal efficiencies obtained for Cs, Sr, and Eu (Am surrogate) were 99.7%, >99.98%, and >99.92%, respectively.

The flowsheet utilized for the first test was modified by the addition of citric acid to the waste feed and scrub solutions to prevent the extraction, and subsequent precipitation of Zr. A second flowsheet test was then performed without flooding or precipitate formation in the contactors; however, some precipitate formation was observed in the solvent feed vessel and tubes leading to the contactors. This precipitate formed at the bottom of the feed vessel and was pumped through the feed lines to the contactors. The quantity of precipitate in the feed container was significant enough to cause some plugging in the feed line which was alleviated by pumping out of the top of the solvent feed container. Samples of the precipitate were not obtained, or subsequently analyzed, therefore the composition of the precipitate cannot be known with certainty. It is suspected that the precipitate was the CMPO component of the solvent. The solvent used in the second flowsheet test was the same solvent used in the first flowsheet test, but had undergone extensive solvent washing procedures between tests. These washing procedures likely altered the composition of the solvent, resulting in lower solubility of the CMPO, or the precipitate formed in the first flowsheet test could have also changed the composition of the solvent. Removal efficiencies of 99.7%, 99.97% and 4.3% for Cs, Sr and Eu, respectively, were obtained. It is important to note that both INEEL flowsheets using simulated wastes, were performed with a "light" solvent that provided a much lower CMPO solubility. This was a likely cause of the problems encountered in the second flowsheet test.

	Flowsheet Test #1	Flowsheet Test #2	Flowsheet Test #3
Type of Waste	Simulated Waste	Simulated Waste	Actual Radioactive Waste
Volume of Waste Processed	2.4 dm^3	2.5 dm^3	1.7 dm^3
Waste Cs Conc.	126 mg/dm^3	127 mg/dm^3	6.78E+06 Bq/cm^3
Raffinate Cs Conc.	0.321 mg/dm^3	0.50 mg/dm^3	2.76E+03 Bq/cm^3
Cs Removal Efficiency	99.7%	99.7%	99.95%
Cs Decon. Factor	393	254	2,457
Waste Sr Conc.	104.5 mg/dm^3	96.8 mg/dm^3	6.62E+06 Bq/cm^3
Raffinate Sr Conc.	<0.01 mg/dm^3	0.021 mg/dm^3	800 Bq/cm^3
Sr Removal Efficiency	>99.98%	99.97%	99.985%
Sr Decon. Factor	>10,450	4,610	8,275
Waste Alpha Conc.	81.7 mg/dm^3 (Eu)	74.3 mg/dm^3 (Eu)	2.15E+04 Bq/cm^3
Raffinate Alpha Conc.	<0.05 mg/dm^3 (Eu)	61.4 mg/dm^3 (Eu)	821 Bq/cm^3
Alpha Removal Efficiency	>99.92% (Eu)	4.3% (Eu)	95.2%
Alpha Decon. Factor	>1,630 (Eu)	1.2 (Eu)	26

Table 2. Summary of results from the three flowsheet tests performed

Results from the two flowsheet tests with simulated were used to develop a flowsheet for demonstration of the universal extraction process with actual tank waste. The flowsheet test using actual tank waste and a heavy solvent was successfully demonstrated within a shielded hot cell facility. No precipitates or flooding problems were observed during the test. Removal efficiencies of 99.95%, 99.985%, and 95.2% were obtained for ^{137}Cs, ^{90}Sr, and total alpha activity, respectively. The alpha removal efficiency was slightly lower than expected due to loading of the CMPO in the solvent with extracted metals such as Fe and Mo.

Results of the three flowsheet tests are summarized in Table 2. Removal efficiencies, decontamination factors, initial and final waste activities or concentrations, and volumes of waste solution processed are presented for each test. Cs and Sr results are consistent for each of the flowsheet tests. Alpha removal efficiencies were considerably lower in the second and third flowsheet tests. With the second flowsheet test, the CMPO in the universal solvent precipitated resulting in a poor removal efficiency for the actinides. In the third flowsheet test, using actual waste, the extraction of metals loaded the CMPO in the solvent, reducing the removal efficiency of the actinides.

CONCLUSIONS

The universal extraction process, based on cobalt dicarbollide and non-hazardous diluents has been successfully demonstrated in centrifugal contactors. The UEP is a viable technology for the separation of cesium, strontium and actinides from acidic waste streams.

ACKNOWLEDGMENT

This work was supported by the Office of Science and Technology (Efficient Separations and Processing Programme), United States Department of Energy, and the DOE/MINATOM Joint Coordinating Committee for Environmental Restoration and Waste Management.

REFERENCES

1. Rais J, Selucky P and Kyrs M, *J. Inorg. Nucl. Chem.*, **38**, 1376, (1976).
2. Rais J, Sebestova E, Selucky P and Kyrs M, *J. Inorg. Nucl. Chem.*, **38**, 1742, (1976).
3. Galkin B, Esimantovskiy V, Lazarev L, Lyubtsev R, Romanovskiy V, Shishkin D, Kadlekova L, Kyrs M, Rais J and Selucky P, *Proc. Inter. Solv. Extr. Conf.e (ISEC 88),* Moscow, USSR, (1988).
4. Esimantovskiy V, Galkin B, Lazarev L, Lyubtsev R, Romanovskiy V, Shishkin D and Dzekun E, *Proc. Waste Management 92*, Tucson, Arizona, (1992).
5. Todd T, Brewer K, Herbst R, Tranter T, Romanovskiy V, Lazarev L, Zaitsev B, Esimantovskiy V and Smirnov I, *Proc. Inter.l Solv. Extr. Conf. (ISEC 96),* Melbourne, Australia, (1996).
6. Law JD, Herbst RS, Todd TA, Brewer KN, Romanovskiy VN, Esimantovskiy VM, Smirnov IV, Babain VA and Zaitsev BN: *Flowsheet Testing of the Cobalt Dicarbollide Solvent Extraction Process for the Partitioning of ^{137}Cs and ^{90}Sr from Actual ICPP Sodium-Bearing Waste Using Centrifugal Contactors in a Shielded Cell Facility, INEL-96/0192,* Lockheed Martin Idaho Technologies Co. (1996).
7. Todd TA, Brewer KN, Law JD, Wood DJ, Herbst RS, Romanovskiy VN, Esimantovskiy VM, Smirnov IV and Babain VA, *Proc. 13th Radiochemical Conference,* Marianske Lazne, Czech Rep., (1998).
8. Todd T, Brewer K, Law J, Herbst R, Romanovskiy V, Esimantovskiy V, Smirnov I, Babain V and Zaitsev B, *Proc, SPECTRUM 98,* Denver, Colorado, USA, (1998).

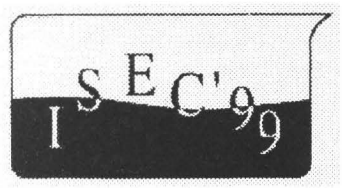

EXTRACTION OF TETRAVALENT URANIUM FROM PHOSPHATE MEDIUM BY HDEHP AND OPAP

JA Daoud, MM Zeid and HF Aly
Hot Laboratories Centre, Atomic Energy Authority, Cairo 13759, Egypt

ABSTRACT
The extraction of U(IV) from phosphoric acid by di-(2-ethylhexyl)phosphoric acid (HDEHP) or octylphenyl acid phosphate (OPAP) in kerosene was carried out under equilibrium conditions. The effect of anions and cations found in the commercial wet-process phosphoric acid on the extraction process of uranium by either extractants was investigated. Experimental results indicated that HDEHP is of higher capacity and gives higher distribution of uranium in the presence of interfering ions. The effect of the different ion concentrations on the extraction process was separately investigated. Stripping of U(VI) from loaded organic solutions by high concentration phosphoric acid, sulphuric acid, oxalic acid and sodium carbonate were tested. The number of stages required for the extraction and stripping of uranium for wet-process phosphoric acid was evaluated.

Keywords: uranium(IV), di-(2-ethylhexyl)phosphoric acid, octylphenyl acid phosphate, phosphoric acid

INTRODUCTION

Wet-process phosphoric acid contains traces of uranium as U(IV) or U(VI) or their mixture together with other metals. Recovery techniques of uranium from phosphoric acid depends mainly on its oxidation state and studies on selective extractants and assessment of conditions for its maximum recovery is therefore an important research area. Hexavalent uranium is commonly extracted from phosphoric acid by a synergistic mixer of HDEHP and trioctylphosphine oxide (TOPO)[1,2] or di-butylbutylphosphonate (DBBP) in kerosene.[3] The mixed extraction of U(VI) from phosphate medium by HDEHP and tri-isodecylamine (Alamine 310), tributylphosphate (TBP), tri-n-phenylsulphoxide (DPSO) and their mixtures in benzene are also reported.[4] Octylphenyl acid phosphate (OPAP) is the most versatile extractant commonly used for the extraction of tetravalent uranium from phosphate medium.[5,6] Tsai and Shuang[7] used OPAP in kerosene for the extraction of U(IV) from wet-process phosphoric acid and used concentrated phosphoric acid as stripping solution. Arnold et al[5] investigated the effect of the different components found in phosphoric acid and reported that uranium extraction decreased with increase in the concentration of ferric ions, hydrofluoric acid or total phosphate and sulphate concentration.

In a previous publication,[8] studies on the extraction of tetravalent uranium from phosphate medium by OPAP or HDEHP in kerosene indicated that HDEHP could be preferred as extractant under certain experimental conditions. Detailed studies of the extraction of U(IV) by HDEHP from phosphoric acid have also shown that the increase in the extractant and Fe(III) concentration enhances the extraction process.[9] In this work these studies are extended to explore the effect of the different cations and anions which are present in industrial phosphoric acid on the extraction of U(IV) by OPAP or HDEHP-kerosene solutions. The results are compared and discussed to select the suitable extractant and assess the conditions for the maximum recovery of uranium from wet-process phosphoric acid.

EXPERIMENTAL

Chemicals and reagents:

Di-(2-ethylhexyl)phosphoric acid (HDEHP) was a product of Union Carbide Corporation ,USA. Octylphenyl acid phosphate was supplied by Mobil Chemical Company and used without purification. Kerosene was obtained from Misr Petrol Ltd., Egypt. Uranyl nitrate and copper (II) chloride were AR products of Fluka-Garantie Ltd., Switzerland. Phosphoric acid, sulphuric acid (source of SO_4^{2-}), and Arzenazo III were supplied from Merck, Germany. Iron(II) sulphate (used for the reduction of U(VI) solution), and iron metal (source of iron (III)) were obtained from Aldrich

© 2000 Society of Chemical Industry

Chemical Co. Ltd., Germany . Aluminium metal, the source of Al(III), was supplied from Veb-Berlin Ltd., Germany. Hydrofluoric acid, the source of F^-, was a product of Reachim Ltd., USSR. Zinc chloride and cadmium chloride were obtained from S.D.Fine Chem. Ltd., India.

Determination of Uranium:

The concentration of uranium in the aqueous phosphoric acid solution was determined spectrophotometrically using a Shimadzu UV-Visible recording spectrophotometer type UV-160A. Arzenazo III was used as colorimetric reagent with 665nm chosen for the detection of tetravalent uranium.

Procedures:

Tetravalent uranium was prepared by adding appropriate amount of iron (II) sulphate to uranyl nitrate in 5 mol/dm^3 phosphoric acid solution.

In the extraction experiments, the concentrations of HDEHP, H_3PO_4, and U(IV) were fixed at 2.5 x 10^{-2} mol/dm^3, 5 mol/dm^3, and 100 ppm, respectively, unless otherwise stated.

The equilibrium for the extraction of uranium was reached after 5 minutes of vigorous shaking in a thermostatted shaker at room temperature. After phase separation, the concentration of uranium in the aqueous phase was determined spectrophotometrically as described. In the stripping experiments, the aqueous and organic phases were equilibrated for 15 minutes, and the uranium concentration was determined colorimetrically in the organic phase.

The simulated solution used in this work was formed by adding some of the anions and cations which are present in the industrial acid to a 5 mol/dm^3 phosphoric acid solution containing 100 ppm uranium as given in Table1.

Component	Concentration, mol/dm^3	Component	Concentration , mol/dm^3
Fe(III)	0 .102	Cd(II)	9.63 x 10^{-5}
Al(III)	6.767 x 10^{-3}	Cu(II)	2.6 x 10^{-4}
Mg(II)	0.178	SO_4^{--}	0.594
Zn(II)	2.79 x 10^{-3}	F^-	0.525

Table 1 Composition of simulated 5 mol/dm^3 phosphoric acid containing 100 ppm uranium.

RESULTS AND DISCUSSION

The effect of HDEHP or OPAP concentration on the extraction of tetravalent uranium was studied by shaking equal volumes of kerosene solution containing the extractant with 5mol/dm^3 aqueous phosphoric solution containing 100 ppm of U(IV). The results obtained indicate that the percentage extraction of U(IV) increases by increasing HDEHP concentration in the range 3.2 x 10^{-2} g/dm^3 to 160 g/dm^3 and reaches a maximum extraction of 94%, Figure 1. Increase in OPAP concentration decreased its solubility in kerosene and a maximum extraction percent of 88% was reached at 10g/dm^3 OPAP solution, Figure1.

The loading capacity of HDEHP was determined by contacting 5 cm^3 of 0.2 mol/dm^3 HDEHP-kerosene solution with fresh volumes of aqueous phase containing 100 ppm U(IV) in 5 mol/dm^3 H_3PO_4 with the organic: aqueous phase ratio is 1:1. The results represented in Figure 2 indicate that a maximum loading of 15.708 g/dm^3 (6.6 x 10^{-2} mol/dm^3) is reached after 8 extraction stages. In a similar experiment carried out with 10g/dm^3 OPAP solution the maximum loading, after 7 stages, was 0.674 g/dm^3 (2.83 x 10^{-3} mol/dm^3), Figure 2.

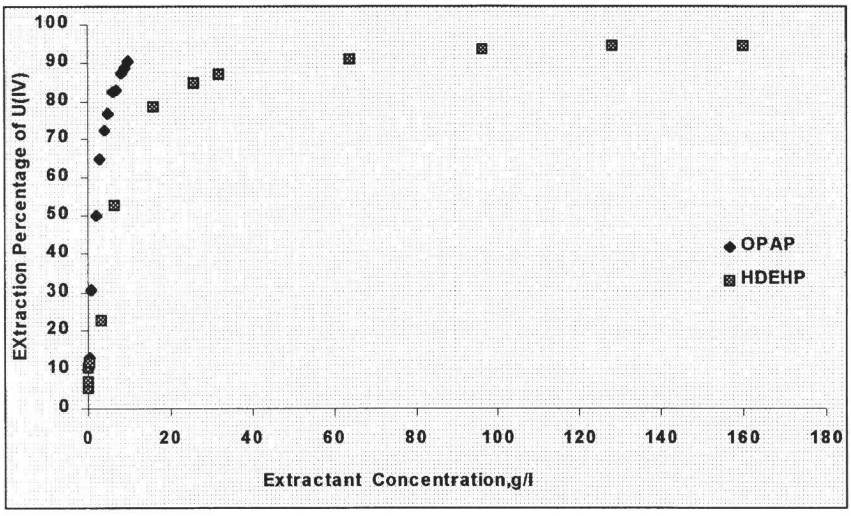

Fig.(1) Effect of Extractant Concentration on the Extraction of U(IV) from Phosphoric Acid Medium

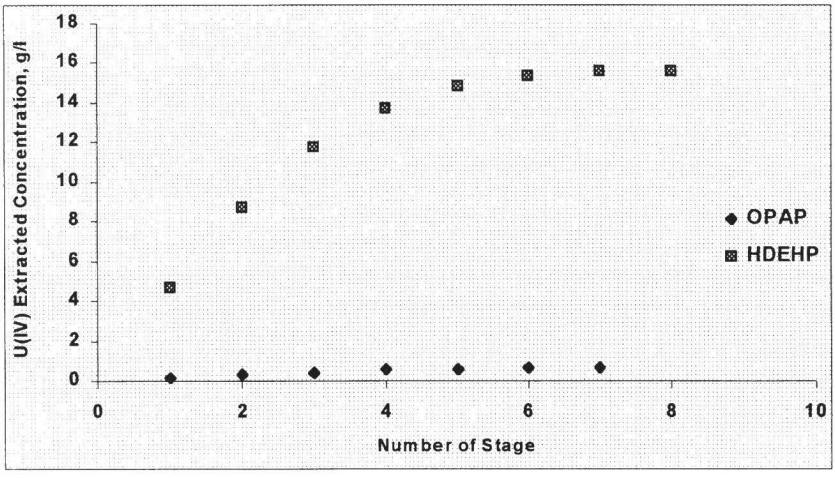

Fig.(2) Loading Capacity of Extractant in Kerosene in the extraction of U(IV) from phosphoric acid

The loading capacity of the investigated extractants was also tested by contacting 0.2 mol/dm^3 (160g/dm^3) HDEHP or 10g/dm^3 OPAP kerosene solutions with aqueous phosphoric acid solutions containing 100 ppm U(IV) at different organic:aqueous phase ratios of 1:1, 1:2, 1:3, 1:4, 1:5 and vice versa. The results represented in Figure 3 indicate that maximum loading of 94% and 92% were reached at phase ratio of about 1:1 for HDEHP and OPAP systems, respectively.

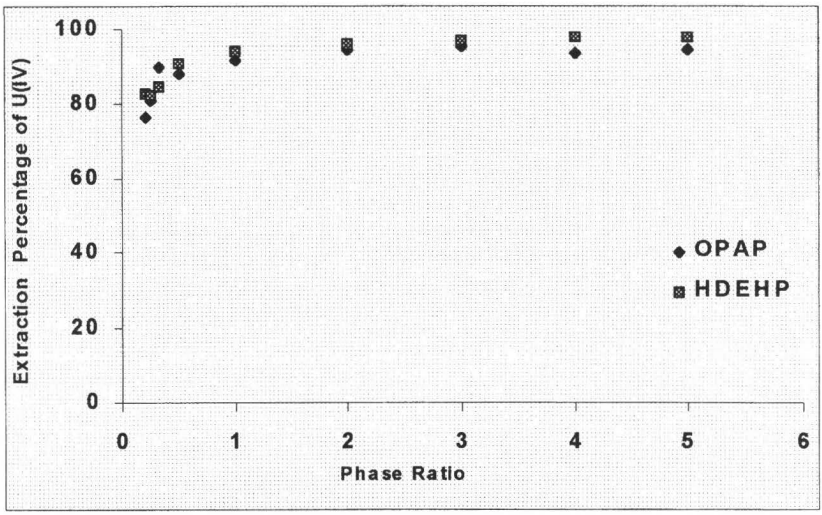

Fig.(3) Effect of Phase Ratio on the Extraction of U(IV) from Phosphoric Acid Medium .

The equilibrium data at organic:aqueous ratio of 1:1 were used to calculate the number of theoretical stages using McCabe-Thiele diagram. It is found that the number of theoretical stages is four while that experimentally obtained was three. Therefore, the efficiency of the process is 0.75.

The extraction of 100 ppm U(IV) from a simulated phosphoric acid solution containing Fe (III) , Al^{3+}, Cd^{2+} ,Cu^{2+}, Zn^{2+}, Mg^{2+}, as well as SO_4^{2-} and F^- ions by HDEHP and OPAP -solutions was then carried out. Increase in HDEHP concentration from 2.5 x 10^{-2} mol/dm^3 to 0.2 mol/dm^3 increased the extraction percent of U(IV) from 85.9% to 87.5% while the increase in OPAP concentration from 5 – 10 g/dm^3 has almost no effect on the extraction percent (~ 85%).

The above results indicated that the extraction of U(IV) from simulated phosphoric acid solution by HDEHP is slightly higher than OPAP solution. Similar behaviour was previously reported by Yun et al.[10] The higher loading capacity of HDEHP (Figures 2, 3) together with the low solubility of OPAP favours the use of HDEHP for the extraction of U(IV) from wet-process phosphoric acid.

Further studies on the extraction of U(IV) were therefore carried out on the HDEHP- kerosene system. The individual effect of the different ions on the extraction of U(IV) in 5 mol/dm^3 H_3PO_4 by 2.5 x 10^{-2} mol/dm^3 HDEHP was carried out at organic:aqueous ratio of 1:1. The increase in the concentration of Fe^{3+}, in the range 3.13 x 10^{-2} mol/dm^3 to 0.25 mol/dm^3, and Al^{3+}, range 1.96 x 10^{-2} mol/dm^3 to 0.196 mol/dm^3, decreased the percentage extraction of U(IV) while a smaller decrease was obtained with increase in Mg^{2+}, from 2.48 x 10^{-2} mol/dm^3 to 0.198 mol/dm^3, Cd^{2+}, from 2.18 x 10^{-5} mol/dm^3 to 1.74 x 10^{-4} mol/dm^3, Cu^{2+}, from 7.43 x 10^{-5} mol/dm^3 to 3.71 x 10^{-4} mol/dm^3 and Zn^{2+} 7.34 x 10^{-4} mol/dm^3 to 3.67 x 10^{-3} mol/dm^3. On the other hand, the extraction of U(IV) increased with increase in SO_4^{2-} from 0.188 to 1.504 mol/dm^3 and F^- ions from 0.113 to 0.9 mol/dm^3, Figures 4a and 4b.

The back extraction of U(IV) from loaded HDEHP-kerosene solution was tested by using different molarities of phosphoric (4 – 12 mol/dm^3), sulphuric (6 – 12 mol/dm^3) and oxalic (5 x 10^{-2} mol/dm^3 to 0.3 mol/dm^3) acids as well as sodium carbonate solution (0.2 – 1 mol/dm^3). The results obtained indicate that among the above reagents, only phosphoric acid could be used for stripping. Increase in phosphoric acid concentration from 4 to 12 mol/dm^3 increased the stripping percentage to 71.4%.

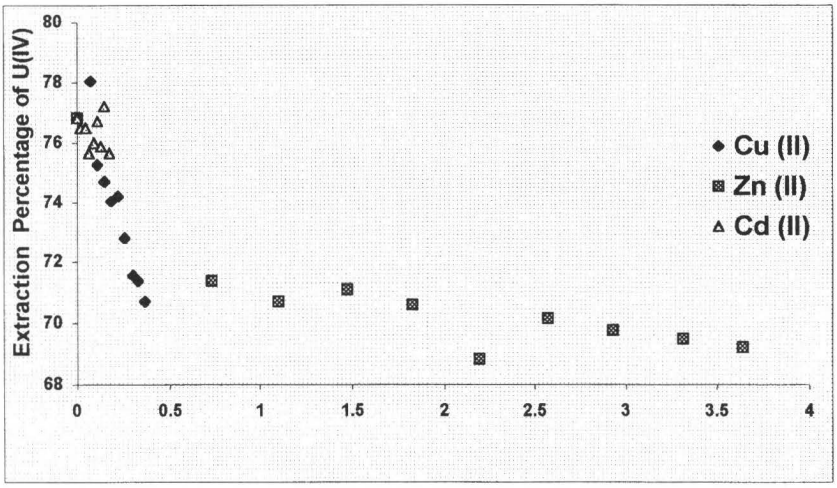

Fig.(4a) Effect of Ions Concentration on the Extraction of U(IV) from Phosphoric Acid Medium

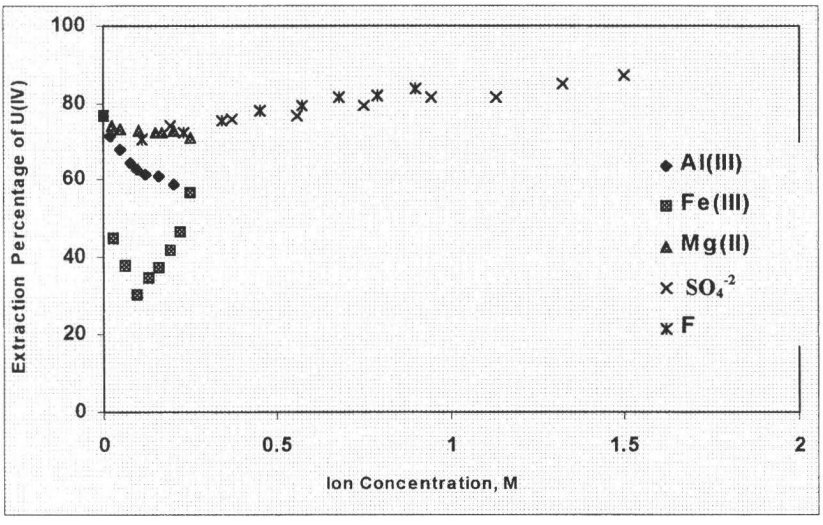

Fig.(4b) Effect of Ions Concentration on the Extraction of U(IV) from Phosphoric Acid Medium .

ACKNOWLEDGMENT

The authors would like to thank Dr Amal I Ali for her valuable help in the experimental work. The collaboration of Mr Ismail M Ahmed is also appreciated.

REFERENCES

1. Albright and Wilson Americas, *DEHPA Bulletin No 5xB1* (1992).
2. Hurst FJ, *Nuclear Fuel Cycle Information Workshop Conference*, Oak Ridge, TN (USA), (1983).
3. Chen HS, Tsai HJ, Tsai YM, Lee TW and Ting G, *Int. Conf. Sep. Sci. Technol.*, New York (USA), 15-17 April (1986).
4. Chen Yude, Fan Shimey, Fu Lei and Li Xintai, *J.Radioanal.Nucl.Chem., Articles*, **131**, 121 (1989).
5. Arnold WD, McKamey DR and Baes CF. *ORNL-TM-7182* (1980).
6. Hurst FJ, *Advisory Group Meeting on the Recovery of Uranium from Phosphoric Acid*, Vienna (Austria) (1987)
7. Tsai MS and Shuang YD, *Mining Engineering* Littleton, Colorado, USA, Aug. (1983).
8. Daoud JA, Zeid MM and Aly HF, *Third Arab Conference on the Peaceful Uses of Atomic Energy*, Damascus (Syria) (1996)
9. Daoud JA, Zeid MM and Aly HF, *Solv.Extr. Ion Exch.*, **15**, 203, (1997).
10. Yun CK, Cho SK, Kwon YS, Lee JK and Seo JH, *AIChE-Symposium-Series* **78**, 76, (1982).

SYNERGISTIC EXTRACTION OF U(VI) AND Th(IV) FROM NITRIC ACID WITH HBMPPT AND TOPO IN TOLUENE

Shao-ning Yu, Li Ma
Naval Medical Research Institute, Shanghai 200433, China
Bo-rong Bao
Institute of Nuclear Research, Shanghai 201800, China

ABSTRACT
The synergistic extraction of U(VI) and Th(IV) from nitric acid solution by HBMPPT(4-benzoyl-2,4-dihydro-5-methyl-2-phenyl-3H-pyrazol-3-thione) and tri-n-octylphosphine oxide (TOPO) in toluene was studied. The extraction ability of HBMPPT was not so high as that of its parent (HBMPP), but when a little TOPO was added in, the ability to extract U(VI) and Th(IV) was greatly improved. The stoichiometry of the synergistic extracted complexes may be presented as $UO_2NO_3 \cdot HBMPPT \cdot TOPO$ and $UO_2(HBMPPT)_2 \cdot TOPO$ for U(VI), and $Th(NO_3)_3 \cdot HBMPPT \cdot TOPO$ and $Th(NO_3)_2(HBMPPT)_2 \cdot TOPO$ for Th(IV) respectively.

Keywords: uranium, thorium, 2-phenyl-3H-pyrazol-3-thione, tri-*n*-phosphine oxide, synergistic extraction

INTRODUCTION

The extraction of An(III) and Ln(III) from aqueous solution with HBMPPT and TOPO has been studied by some authors.[1-5] Under certain conditions, the synergistic effect between HBMPPT and TOPO is able to make An(III) and Ln(III) reach a high separation coefficient. We here report the synergistic extraction of U(VI) and Th(IV) in nitric acid media with HBMPPT and TOPO in toluene.

EXPERIMENTAL

Reagents

HBMPPT was synthesized from HBMPP(4-benzoyl-2,4-dihydro-5-methyl-2-phenyl-3H-pyrazol-3-one) using a procedure similar to that of Jarvinen.[3] TOPO was provided by Fudan University. Uranyl nitric solution and thorium nitric solution were obtained by dissolving $UO_2(NO_3)_2 \cdot 6H_2O$ and $Th(NO_3)_4 \cdot 6H_2O$ (AR grade) in nitric acid solution to the desired pH, and adjusting the ionic strength (0.1) with 0.1 mol/dm^3 NH_4NO_3. Toluene and other reagents were all of AR grade. All aqueous solutions, which contained 0.1 mol/dm^3 NH_4NO_3 were made with distilled water. The pH of the aqueous solutions was adjusted with 0.1 mol/dm^3 NaOH. The aqueous solutions were pre-equilibrated with toluene. The organic phases were toluene solutions of HBMPPT and synergist TOPO dissolved in it.

Distribution Determination

The extraction procedures were as follows: 5 cm^3 of the aqueous phase containing a certain amount of U(VI) or Th(IV) and HNO_3 was shaken for 15 minutes with 2 cm^3 of the organic phase containing a given concentration of HBMPPT and TOPO. The diluent was toluene. Sample of aqueous phase was analyzed immediately after the phase separation by the Arsenazo(III) spectro-photometric method, and the concentration of U(VI) or Th(IV) in organic phase was obtained by calculating $[M]_{a,o}$-$[M]_{a,e}$ where $[M]_{a,o}$ is the concentration of U(VI) or Th(IV) at the beginning, and $[M]_{a,e}$ is concentration of U(VI) or Th(IV) after equilibrium. The distribution ratio was calculated.[6-7] The pH of aqueous was measured after equilibrium. The experimental temperature was controlled at 25 ± 2C.

RESULTS AND DISCUSSION

Synergistic extraction of U(VI) and Th(IV) with HBMPPT and TOPO

The relationship of $\log D_U$ - pH and $\log D_{Th}$ - pH are shown in Tables 1 and 2. The

© 2000 Society of Chemical Industry

distribution ratio of U(VI) and Th(IV) increases with the increase of pH.

pH	0.83	1.00	1.16	1.22	1.30	1.39
D_U	11.22	13.80	22.39	25.12	28.18	34.67

*$[HBMPPT]_{(O)}$ = 0.10mol/dm^3, $[TOPO]_{(O)}$ = 0.005mol/dm^3, $[UO_2^{2+}]_{(a)}$ = 5.48 x 10^{-4}mol/dm^3, $[NH_4NO_3]_{(a)}$ = 0.1mol/dm^3, 25C.

Table 1, the relationship of D_U-pH

pH	2.26	2.42	2.46	2.51	2.56	2.59
D_{Th}	2.04	2.82	3.47	4.47	6.31	7.08

*$[HBMPPT]_{(O)}$= 0.10mol/dm^3, $[TOPO]_{(O)}$ = 0.01mol/dm^3, $[Th^{4+}]_{(a)}$ = 5.68 x 10^{-4}mol/dm^3, $[NH_4NO_3]_{(a)}$ = 0.1mol/dm^3, 25C.

Table 2, the relationship of D_{Th} - pH

The relationship of logD -$log[TOPO]_{(O)}$ is shown in Figure 1. LogD - $log[TOPO]_{(O)}$ is linear with the slope of 1.0 and 0.9 for U(VI) and Th(IV) respectively. It indicates that when HBMPPT exists, the extracted complex has just one TOPO.

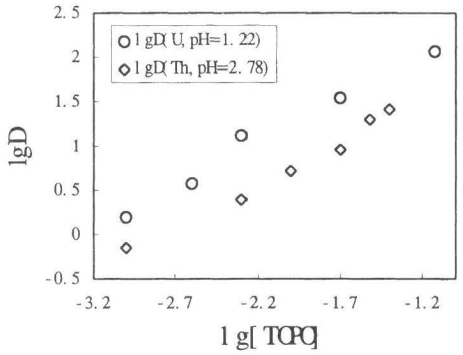

($[UO_2^{2+}]_{(a)}$=5.48x10^{-4}mol/dm^3, $[Th^{4+}]_{(a)}$ =5.685x10^{-4} mol/dm^3, $[HBMPPT]_{(O)}$ = 0.10 mol/dm^3, $[NH_4NO_3]$ = 0.1mol/dm^3, 25C).

Figure 1 Plots of D_U and D_{Th} versus $log[TOPO]_{(O)}$

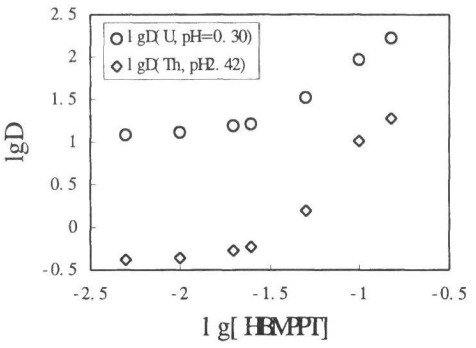

($[UO_2^{2+}]_{(a)}$=5.48x10^{-4}mol/dm^3/$[TOPO]_{(O)}$=0.005mol/dm^3;
$[Th^{4+}]_{(a)}$=5.68x10^{-4}mol/dm^3/$[TOPO]_{(O)}$=0.01mol/dm^3; $[NH_4NO_3]_{(a)}$ = 0.1 mol/dm^3, 25C)

Figure 2 Plots of $logD_U$ and $logD_{Th}$ as a function of $[HBMPPT]_{(a)}$

The relationship of $\log D_U$ - $\log[HBMPPT]_{(O)}$ and that of $\log D_{Th}$ - $\log[HBMPPT]_{(O)}$ are linear with the slope of 1.52 and 1.63 ($[HBMPPT]_{(O)}$ = 0.05 - 0.2 mol/dm^3) respectively (shown in Figure 2). From the log-log plots the extracted complexes should have the following stiochiometries: UO_2NO_3.HBMPPT·TOPO and $UO_2(HBMPPT)_2$·TOPO for U(VI), and $Th(NO_3)_3$·HBMPPT·TOPO and $Th(NO_3)_2(HBMPPT)_2$·TOPO for Th(IV) respectively ($[HBMPPT]_{(O)}$ = 0.05 - 0.2 mol/dm^3).

Separation of U(VI), Th(IV) and Eu(III)

The distribution ratio of U(VI), Th(IV) and Eu(III) under some conditions are shown in Table 3. The comparison between Figure 1 and Figure 2 shows that a small amount of TOPO greatly increases the ability of HBMPPT to extract U(VI) and Th(IV). At the same HNO_3 concentration, the extraction of U(VI) and Th(IV) with TOPO can be neglected.

The extraction with HBMPPT alone basically cannot separate U(VI) and Th(IV), but to add a little TOPO can make its separation coefficient ($b_{U/Th}$) reaches 324 (pH=1.3). The system can also easily separate U(VI) from Eu(III).

Extraction conditions	D_U (pH)	D_{Th} (pH)	D_{Eu} (pH)	$b_{U/Th}$ (pH)	$b_{U/Eu}$ (pH)
0.10 mol/dm^3 BMPPT	0.94 (3.0)	0.67 (3.0)	<0.05 (3.5)	1.4 (3.0)	> 10 (3.0)
0.10 mol/dm^3 HBMPPT+ 0.01mol/dm^3 TOPO	38.9(1.3)	0.12 (1.3)	0.07 (3.5)	324 (1.3)	>556 (1.3)

$[UO_2^{2+}]_{(a)}$=5.48x10^{-4}mol/dm^3, $[Th^{4+}]_{(a)}$=5.68x10^{-4}mol/dm^3, $[NH_4NO_3]_{(a)}$=0.1mol/dm^3, 25C

Table 3, Separation coefficient for U(VI), Th(IV), and Eu(III)

CONCLUSIONS

In this study, we have studied the synergistic effect of U(VI) and Th(IV) with HBMPPT and TOPO for the first time. The extraction ability of HBMPPT is not high, but when a small amount of TOPO is added to the HBMPPT solution, the extraction increases rapidly. According to the experimental results, the synergistic extracted complexes may be represented as UO_2NO_3·HBMPPT·TOPO and $UO_2(HBMPPT)_2$·TOPO for U(VI), and $Th(NO_3)_3$·HBMPPT·TOPO and $Th(NO_3)_2(HBMPPT)_2$·TOPO for Th(IV) respectively. The separation coefficient of U(VI) and Th(IV)($b_{U/Th}$) is 324 (pH=1.3). The extraction system can also easily separate U(VI) from Eu(III).

REFERENCES

1. Smith BF, Jarvinen GD, Miller GG, et al., *Solv. Extr. Ion Exch.*, **5**(5), 895, (1987).
2. Ensor DD, Jarvinen GD and, Smith BF, *Solv. Extr. Ion Exch.*, **6**(3), 439, (1988).
3. Smith BF, Jarvinen GD, Jones MM, et al., *Solv. Extr. Ion Exch.*, **7**(5), 749, (1989).
4. Hannink NJ, Hoffman DC and Smith BF, *Solv. Extr. Ion Exch.*, **10**(3), 431, (1992).
5. Jarvinen GD, Smith BF and Ritchey JM, *Inorg. Chim. Acta*, **129,** 139, (1987).
6. Heng-Li Ma, *Atomic Energy Science and Technology* (in Chinese), **6,** 748, (1964).
7. Jin-Hua Wang, Zu-Ming Zhou and De-Min Xu. *J. Nucl. Radiochem.* (in Chinese), **14**(4),226, (1992).
8. Yude Cheng, Wengji Wang, Zhilin Wang et al., *Nuclear Fuel Chemistry*. Nuclear Energy Publication Co.(in Chinese), 210, (1985).

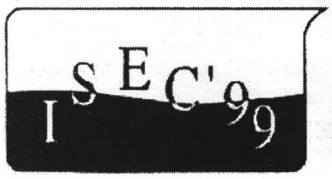

STUDY OF THE SOLVENT EXTRACTION OF U(VI) AND Th(IV) FROM NITRIC ACID WITH HBMPPT

Shao-ning Yu, Teng-jia Wang
Naval Medical Research Institute, Shanghai 200433, China
Bo-rong Bao
Institute of Nuclear Research, Shanghai 201800, China

ABSTRACT
The extraction agent HBMPPT(4-benzoyl-2,4-dihydro-5-methyl-2-phenyl-3H-pyrazol-3-thione) was synthesized from HBMPP with a melting point of 106-108C and elemental analysis in agreement with the theoretical values. The solvent extraction of UO_2^{2+} and Th^{4+} from nitric acid solution by HBMPPT in benzene has been studied. The extraction ability of HBMPPT is not as high as that of its parent (HBMPP). The UO_2^{2+} and Th^{4+} distribution ratios (D_U and D_{Th}) increase with increasing pH of the aqueous phase, and $pH_{0.5}$ was 3.0 and 3.2 for UO_2^{2+} and Th^{4+} respectively. When the pH increases, the distribution ratio of UO_2^{2+}(or Th^{4+}) increases linearly with the slope being 1.56 and 1.59 respectively. When the concentration of HBMPPT increases, the distribution ratio of UO_2^{2+}(or Th^{4+}) increases rapidly. Log D_U vs log[HBMPPT] is linear with a slope of 1.43; logD_{Th} vs log[HBMPPT] is linear with a slope of 1.42. The extraction mechanism is by cation ion exchange.

Keywords: uranium, thorium, 4-benzoyl-2,4-dihydro-5-methyl-2-phenyl-3H-pyrazol-3-thione

INTRODUCTION

To some extent, HBMPPT is a very useful extraction agent for separation of An(III) and Ln(III).[1-5] The extraction mechanism of UO_2^{2+} and Th^{4+} from aqueous solution with HBMPPT has not been studied ever, so we here report the extraction behavior of UO_2^{2+} and Th^{4+} in nitric acid media with HBMPPT in benzene.

EXPERIMENTAL

Synthesis of HBMPPT

HBMPPT was synthesized from BMPP (4-benzoyl-2,4-dihydro-5-methyl-2-phenyl-3H-pyrazol-3-one). 25 g BMPP and 25 cm^3 $POCl_3$ were refluxed for 4 hours at 125C, and then 100 cm^3 H_2O was added. The organic phase was extracted by 100 cm^3 dichloromethane followed by removal of the solvent by vacuum distillation. The product (Cl-BMPP) was re-crystallized from 30 cm^3 ether and 30 cm^3 light petroleum solution with the yield about 75%, and m.p. 79-81C. HBMPPT was synthesized with a procedure similar to that of Jarvinen[5] by refluxing (6 hours) 30 g Cl-BMPP with 38 g $NaSH.H_2O$ (4 equivalents) in ethanol (350 cm^3). The nitrogen-purged reaction mixture was cooled and allowed to settle. The product was isolated by transferring the supernatant liquid under reduced pressure through a teflon tube and subsequently, vacuum reduction of the solvent volume. H_2O (400 cm^3) was added and the solution (pH >11) was extracted with chloroform (60 cm^3) to remove neutral materials. The aqueous layer was made acidic (pH 5-6) with 120 cm^3 of 3 mol/dm^3 HCl, and extracted 3 times with chloroform (50 cm^3 each). The organic fractions were combined, washed with 120 cm^3 water, and dried over anhydrous Na_2SO_4. The solvent was subsequently removed under vacuum and the solid residue dissolved in 60 cm^3 hot ethanol and re-crystallized to yield 27 g of orange crystals, m.p. 106-108C.

Distribution Ratio Determination

The extraction procedure was as follows: 2 cm^3 of the aqueous phase which contained a certain amount of UO_2^{2+} or Th^{4+} and HNO_3 was shaken for 15 minutes with 5 cm^3 of the

© 2000 Society of Chemical Industry

organic phase containing a given concentration of HBMPPT, which had been pre-equilibrated with a suitable nitric acid solution. The diluent was benzene. The concentration of UO_2^{2+} or Th^{4+} in aqueous phase was analyzed immediately by the Arsenazo-III spectrophotometric method [6-7] after the phase separation, and the distribution ratio was calculated. Lower concentrations of UO_2^{2+} or Th^{4+} in aqueous phase, and lower phase ratio(V_o:V_a=1:5), were chosen to reduce the change of pH in aqueous phase. The pH of aqueous solution was measured after equilibrium.

RESULTS AND DISCUSSION

Appraisal of HBMPPT

The result of elemental analysis is as follows: C, 67.51%, H, 4.35%, N, 9.16%, S, 11.97%, which agrees with the theoretical values: C, 69.15%, H, 4.76%, N, 9.52%, S, 10.90%. The mass spectra shows the molecular weight of HBMPPT is 295 (theory 295), and the strong fragment mass of 105 show that the sulfur is not on the -benzoyl group (the mass weight is 105). The IR(KBr) is similar to that given by Jarvinen.[5]

Effect of diluent on distribution ratio of UO_2^{2++}

The HBMPPT is insoluble in diluents such as light petroleum, kerosene, cyclohexane etc., and is slightly soluble in ether and ethyl acetate, but it is easily dissolved in toluene, benzene, dichloromethane, chloroform, etc.. There is little difference in distribution ratio of UO_2^{2+} in benzene, toluene, dichloromethane and chloroform. The distribution ratio of U(VI) in some diluents at 25C, with $[UO_2^{2+}]$ = 2.10 x 10^{-4} mol/dm^3, [HBMPPT] = 0.10 mol/dm^3, pH = 3.4, $[NH_4NO_3]$ = 0.1 mol/dm^3: toluene 2.85; benzene 2.86; dichloromethane 2.75; chloroform 2.85 In ether solution, the HBMPPT can extract UO_2^{2+} in quantity under the conditions above.

Effect of temperature on the distribution ratio

The effect of temperature on the distribution ratio of UO_2^{2+} is shown in table 1. The results show that temperature has little effect on the distribution ratio of $UO_2^{2+}$and Th^{4+}.

T (C)	15	20	25	30	35	40
D_U	1.50	1.48	1.49	1.47	1.42	1.37
D_{Th}	1.31	1.28	1.33	1.29	1.32	1.22

($[UO_2^{2+}]$ = 2.10 x 10^{-4} mol/dm^3; $[Th^{4+}]$ = 5.68 x 10^{-4} mol/dm^3; pH = 3.40 (for U); pH = 3.1 (for Th); [HBMPPT] = 0.10 mol/dm^3; $[NH_4NO_3]$ = 0.1 mol/dm^3)

Table 1, The effect of temperature on the distribution ratio of UO_2^{2+} and Th^{4+}

Effect of concentration of UO_2^{2+} on the distribution ratio

The effect of concentration of UO_2^{2+} on the distribution ratio of UO_2^{2+} is shown in table 2. The distribution ratio (D) of UO_2^{2+} decreases with the increase of concentration of UO_2^{2+}. It probably results from the increase of pH in aqueous after the ion exchange reaction.

$[UO_2^{2+}]$ (7.5 x 10^{-4} mol/dm^3)	2.74	5.48	8.22	10.96	13.7
D_U	6.23	6.15	5.43	4.85	4.65

(t = 25C; pH = 3.11; [HBMPPT]=0.10 mol/dm^3; $[NH_4NO_3]$ = 0.1mol/dm^3)

Table 2, The effect of UO_2^{2+} concentration on the distribution ratio

Effect of acidity of aqueous phase on the distribution ratio

The effect of pH on the distribution ratio of UO_2^{2+} and $Th^{4+}$is shown in figure 1. The logarithm of distribution ratio of U(VI)(or Th^{4+}) and pH have a linear relationship. The slope of log D(U) vs pH is 1.56, and the slope of log D(Th) vs pH is 1.59.

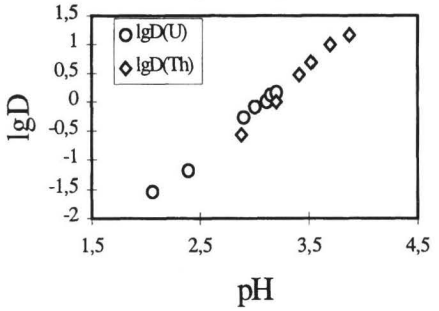

Figure 1 Plots of distribution ratio of UO_2^{2+} and Th^{4+} versus pH.
(t = 25C; $[UO_2^{2+}]$ = 2.10 x 10^{-4} mol/dm^3; $[Th^{4+}]$ = 5.68 x 10^{-4} mol/dm^3; [HBMPPT] = 0.10 mol/dm^3; $[NH_4NO_3]$ = 0.1mol/dm^3.)

Effect of [HBMPPT] on the distribution ratio

The effect of [HBMPPT] on the distribution ratio (D) of UO_2^{2+} and $Th^{4+}$is shown in figure 2. The equilibrium pH was measured, and all the values of log D have been rectified with the relationship shown in figure 1. The logarithm of distribution ratio of UO_2^{2+}(or Th^{4+}) and log [HBMPPT] are in linear relationship. The slope of log D(U) vs log [HBMPPT] is 1.43, and the slope of log D(Th) vs log [HBMPPT] is 1.42.

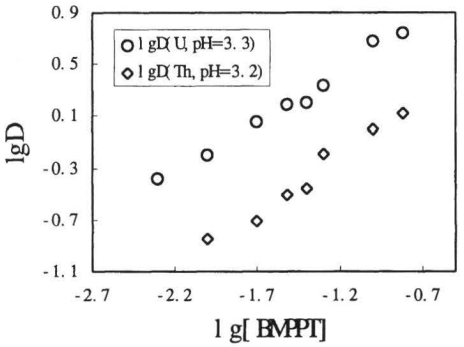

Figure 2 Plots of distribution ratio of UO_2^{2+} and Th^{4+} versus [HBMPPT] in benzene.
(t = 25C; $[UO_2^{2+}]$ = 2.10 x 10^{-4}mol/dm^3; $[Th^{4+}]$ = 5.68 x 10^{-4} mol/dm^3; pH = 3.2 for UO_2^{2+}, pH = 2.8 for Th^{4+}; $[NH_4NO_3]$ = 0.1mol/dm^3.)

From this extraction rule, the extraction reaction between HBMPPT and UO_2^{2+} (or Th^{4+}) is a cation ion exchange reaction, the slopes of log D vs pH and log D vs log [HBMPPT] are not whole numbers, the extraction reaction can be described as follows:

$$HA === A^- + H^+$$
$$UO_2^{2+} + 2A^- === UO_2A_2$$
$$UO_2^{2+} + NO_3^- + A^- === UO_2NO_3A$$

CONCLUSION

The synthetic product is HBMPP and the extraction ability of HBMPPT is not as high as that of its parent (BMPP). The extraction reaction with uranium or thorium is a cation ion exchange. The relation of logD vs pH is linear with slopes of 1.56 and 1.59 for UO_2^{2+} and Th^{4+} respectively and logD vs log[HBMPPT] is also linear with slopes of 1.43 and 1.42 for UO_2^{2+} and Th^{4+} respectively.

REFERENCES

1 Smith BF, Jarvinen GD, Miller GG, et al *Solv. Extr. Ion Exch.* **5**(5), 895, (1987).
2 Ensor DD, Jarvinen GD, Smith BF. *Solv. Extr. Ion Exch.* **6**(3), 439, (1988).
3 Smith BF, Jarvinen GD, Jones MM, et al. *Solv. Extr. Ion Exch.* **7**(5), 749, (1989).
4 Hannink NJ, Hoffman DC and Smith BF. *Solv. Extr. Ion Exch.* **10**(3), 431, (1992).
5 Jarvinen GD, Smith BF and Ritchey JM *Inorg. Chim. Acta.* **129**,139, (1987).
6 Heng-Li Ma, *Atomic Energy Science and Technology*(in Chinese), **6**, 748, (1964).
7 Jin-Hua Wang, Zu-Ming Zhou and De-Min Xu. *J. Nuclear and Radiochemistry* (in Chinese). **14**(4), 226, (1992).

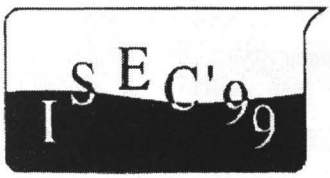

SOLVENT EXTRACTION OF Tc AND Cs FROM ALKALINE NITRATE WASTES

Bruce A Moyer,[1] Peter V Bonnesen,[1] Lætitia H Delmau,[1] Tamara J Haverlock,[1] Richard A Sachleben[1], Ralph A Leonard,[2] Cliff Conner[2] and Gregg J Lumetta[3]

[1]Chemical and Analytical Sciences Division, Oak Ridge National Laboratory, P. O. Box 2008, Bldg. 4500S, MS-6119, Oak Ridge, Tennessee 37831-6119

[2]Argonne National Laboratory, 9700 South Cass Avenue, Building 205, Argonne, IL 60439-4837

[3]Pacific Northwest National Laboratory, P.O. Box 999, Richland, WA 99352

ABSTRACT

This paper summarises progress at three collaborating U.S. national laboratories on the extraction of the fission products ^{99}Tc and ^{137}Cs from alkaline high-level wastes (HLW). Efficient, economical processes for Tc and Cs extraction, SRTALK and alkaline-side CSEX respectively, have been developed, and testing has progressed through batch tests on actual wastes and continuous countercurrent centrifugal-contactor tests on simulants.

Keywords: caesium, technetium, crown ether, calixarene, alkaline high level nuclear waste, centrifugal contactor

INTRODUCTION

The need has arisen at several U.S. Department of Energy sites for separating the key fission products ^{99}Tc, ^{90}Sr, and ^{137}Cs from alkaline defence wastes.[1] At the Hanford site, wastes stored in underground tanks will be retrieved and subjected to separations mainly aimed at concentrating actinides, Tc, Sr, and Cs in a high-activity fraction that will be vitrified and stored in a geologic repository.[1b] Similar goals are being pursued at the Savannah River Site for the removal of actinides, Sr, and Cs.[1c] Aqueous wastes that must be treated include tank supernatant liquids, dissolved salt cake, and sludge-wash solutions.

Significant progress has been made toward solvent-extraction methodology for removal of ^{137}Cs, ^{90}Sr, and ^{99}Tc either individually or simultaneously from nitrate wastes. In particular, crown-type extractants,[2-5] including the novel class of calix[4]arene mono- and bis-crown compounds,[4,5] make possible new technologies featuring high selectivity, good stability, and compatibility with process conditions. These technologies offer the major advantage of stripping with water or dilute acid, in principle yielding a stream concentrated in the target fission products but containing little else. This translates to potentially large cost savings by reducing the need for further downstream processing and reducing the volume of the final HLW form. Efforts have focused largely on the acid side, but recent results[3,4e,5] have extended applicability to alkaline-side separations as well, obviating the need for re-acidification. Indeed, processes have been optimised so that little or no adjustment of the wastes (which tend to lie in the range 5-8 mol/dm^3 Na) is required at all.[3,5]

For appropriately sized neutral crown extractants in low-polarity media, the extraction behaviour may often be rationalised in terms of simple 1:1 metal:ligand complexes:[6a]

$$M^{q+}(aq) + qX^-(aq) + L(org) \rightleftharpoons MLX_q(org) \qquad (1)$$

where M^{q+} is a metal ion of charge q = +1 or +2, X^- is the co-anion, and L is the extractant. Abundant anions in the wastes include nitrate, nitrite, hydroxide, chloride, aluminate, and carbonate, where the most easily transferred to the solvent phase is nitrate.[6b] Owing to the high nitrate concentration in the waste, the equilibrium in Equation 1 is driven to the right. On stripping with water or dilute salt or acid solutions, Equation 1 is driven to the left, decomposing the complexes and releasing the metal ions and co-anions.

Although technetium in its common pertechnetate form TcO_4^- does not complex directly with crown ethers, pertechnetate extraction may be facilitated by crown ethers as the co-anion X^- for M^+ =

© 2000 Society of Chemical Industry

Na^+ and K^+ in Equation 1. In this case, it is the high concentration of sodium and potassium in the waste that drives Equation 1 to the right. Since pertechnetate is at trace levels (of the magnitude 10^{-4} mol/dm^3 on average) in the waste, selectivity over the highly abundant anions, especially nitrate, becomes a critical extraction property. Depending on the solvent environment, pertechnetate anion may be more than a thousand-fold more extractable than the smaller nitrate anion in ion-pair extraction processes.[6] The origin of selectivity in the ion-pair extraction for pertechnetate in Equation 1 in fact arises effectively from the same solvation principles governing anion exchange.[6] Whereas quaternary ammonium extractants and resins are difficult to strip, however, the cationic crown ether complex is readily decomposed on contact with water. It is this easy regenerability that represents the major advantage of crown ethers vs. anion exchange in pertechnetate removal from waste.

RESULTS AND DISCUSSION

SRTALK Process for Tc Extraction.

The crown ether (Figure 1) used in the SRTALK process affords a good balance of properties, but a modifier is additionally required for adequate extraction and stripping when the diluent is an aliphatic hydrocarbon.[3] Using a solvent consisting of 0.04 mol/dm^{3}DtBuCH18C6 in 1:1 v:v TBP:Isopar®M,

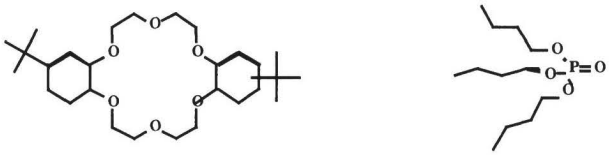

DtBuCH18C6
Di-(t-butylcyclohexano)-18-crown-6
(Mixture of isomers)

TBP
Tributyl phosphate

Figure 1. Crown ether and modifier used in SRTALK process

Tc distribution ratios of 9.3 on extraction of actual Hanford Double-Shell Slurry Feed (DSSF) and 0.3 on stripping with distilled water were obtained in batch tests. These results were similar to those of pertechnetate extraction and stripping in tests with waste simulants.

As shown in Figure 2, a 12-stage SRTALK flowsheet has been developed using a solvent consisting of 0.04 mol/dm^3 DtBuCH18C6 (CE_Sr in Figure 2) and 1.8 mol/dm^3 TBP in Isopar® L (1:1 v:v TBP:Isopar® L).[3c] The flowsheet was designed for a test of SRTALK on a simplified Hanford DSSF simulant using 2-cm centrifugal contactors. The scrub section employed 0.5 mol/dm^3 NaOH to reduce the sodium and potassium nitrate loading of the solvent and to improve the performance of the stripping with 0.01 mol/dm^3 HNO_3. The SRTALK centrifugal-contactor test performed as designed, demonstrating the clean separation of Tc from the bulk waste constituents, especially sodium. While Tc was concentrated by a factor of 9.9 with a DF of 10.7, the sodium concentration was reduced by a factor of 5800 to 0.0010 mol/dm^3 in the strip solution. Potassium and aluminium were rejected to an even greater degree. Assuming that the entire Hanford tank inventory could be treated with comparable performance by the SRTALK process, the additional amount of sodium that would have to be vitrified would be only 1400 kg. Based upon the test results, a plant-scale process utilising 24 stages of 30 cm contactors would treat waste at 100 dm^3/min and require a solvent inventory of approximately 3000 dm^3, costing $1.7M at retail price. Thus, the high efficiency of centrifugal contactors allows the expensive crown ether to be used at acceptable cost.

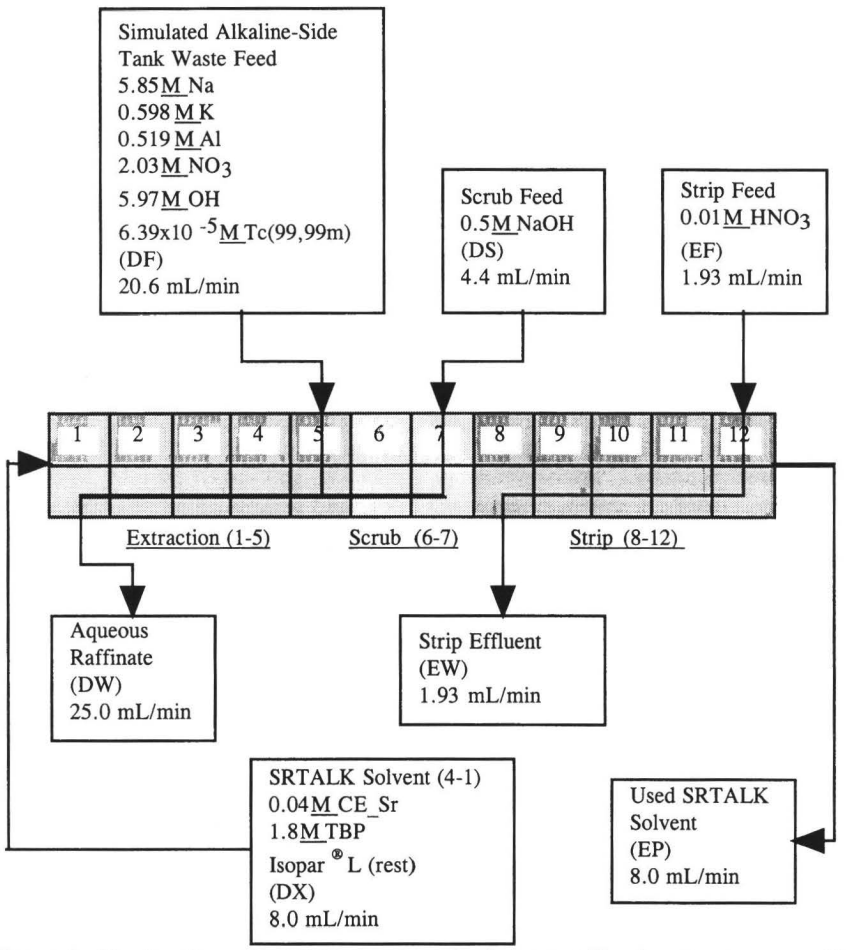

Figure 2. Twelve-Stage SRTALK flowsheet for 2-cm centrifugal contactor test at ANL.

Alkaline-Side CSEX Process for Cs.

The recent advent[4] of calix[4]arene-crown-6 compounds having Cs/Na selectivities exceeding 10^4 constitutes a breakthrough in the search for Cs-selective extractants. Attributed to significant pi-interactions of the aromatic rings with the guest Cs^+ cation,[4d] this unprecedented selectivity makes it practical to employ a crown compound in a solvent-extraction process for Cs removal from alkaline nitrate wastes.[5] A calix[4]arene bis-crown-6 compound with enhanced solubility is shown in Figure 3. It may be seen that either of two identical cavities, each formed by facing aromatic rings and the crown ether, may host the Cs^+ cation.

Analogous to SRTALK, use of BoBCalixC6 in an aliphatic diluent requires the addition of a polar modifier, both to increase solubility and to raise the Cs distribution ratios (D_{Cs}) on extraction to a useful range at affordable concentrations (<0.02 mol/dm^3) of the expensive calixarene. In tests of various modifiers in Isopar® L, lipophilic alcohols proved to be particularly effective, whereas non hydrogen-bond donating compounds such as TBP were weak, as expected if anion solvation by the modifier is important.[6] Experiments on alcohols having the economical alkylphenoxy group showed that phase disengagement and D_{Cs} depend markedly on the modifier structure. Of the modifiers synthesised and evaluated thus far, the modifier "Cs-3" (Figure 3) afforded the best overall combination of desirable attributes. These attributes include a strong synergistic effect with the calixarene, excellent phase disengagement, and negligible distribution to the aqueous phase. This

modifier has also been the most carefully studied in process flowsheet development experiments. During these experiments, Cs-3 modifier exhibited good chemical stability when continuously contacted with an alkaline waste simulant for one month at 25 °C, but at 53 °C more than half of the modifier decomposes.[5b] A new modifier has since been prepared that appears to be stable to alkaline solutions at elevated temperatures.

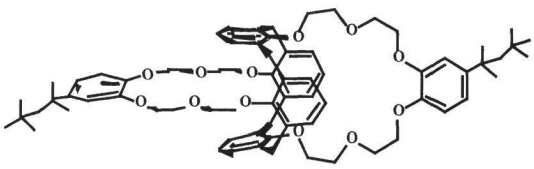

BoBCalixC6
Calix[4]arene-bis(*t*-octylbenzo-crown-6)

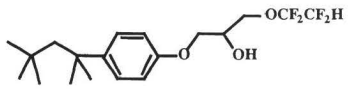

Cs-3
1-(1,1,2,2-tetrafluoroethoxy),
-3-[4-(*t*-octyl)phenoxy]-2-propanol

Figure 3. Extractant and modifier recently employed in the alkaline-side CSEX process.

As shown by the batch results in Table 1, Cs was extracted from two Hanford supernatant tank wastes and stripped with 10 mmol/dm^3 nitric acid. The DSSF waste represents a severe case, since extraction of K^+ ion (at ca. 1 mol/dm^3 in the waste) competes significantly with Cs^+ ion extraction.[5a] By comparison, excellent extraction was obtained from the CC waste, which contains low levels of K^+ ion but a high concentration of organic complexants.

Tank	D_{Cs} Extract #1	D_{Cs} Extract #2	Total % Extracted	D_{Cs} Strip #1	D_{Cs} Strip #2	Total % Stripped
DSSF blend[b]	1.8	2.0	89%	0.7	0.3	90%
CC waste[c]	18	20	99.7%	0.8	0.6	85%

[a] Two extractions each with fresh solvent (0.02 mol/dm^3 BoBCalixC6 + 0.25 mol/dm^3 Cs-3 in Isopar® L) followed by two strips each with fresh 10 mmol/dm^3 HNO_3; 5-min contacts at O:A = 1:1 by vortexing.
[b] Blend of supernatant liquids from three tanks: 70% AW-101 (DSSF), 20% AP-106, and 10% AP-102.
[c] Undiluted complexant concentrate from tank SY-101.

Table 1 Caesium extraction and stripping from Hanford tank waste by ORNL extractant.[a]

Excellent results were achieved in more extensive process development toward adapting alkaline-side CSEX to the HLW at the Savannah River Site (SRS).[5b] In this waste, the competing K^+ concentration is only 0.02 mol/dm^3, making low calixarene concentrations effective. It was found that good overall performance could be obtained with a solvent containing 0.01 mol/dm^3 BoBCalixC6, 0.2 mol/dm^3 Cs-3, and 1 x 10^{-4} mol/dm^3 trioctylamine (TOA) in Isopar® L (Table 2). Two scrub stages employing 0.05 mol/dm^3 HNO_3 sufficed to remove practically all other salts from the solvent to near analytical detection limits. Stripping may be effected by dilute HNO_3 at 0.005 mol/dm^3 or lower. Having negligible effect on extraction, the TOA promotes stripping to low organic-phase Cs concentrations and to counteract potential deleterious effects of lipophilic anion impurities that may accumulate in the solvent. The fact that even low concentrations (e.g., 5 x 10^{-5} mol/dm^3) of lipophilic anions, such as the common surfactant dodecylsulphonate present in many detergents, interfere with effective stripping may be a general vulnerability of crown compounds as applied to waste treatment. Fortunately, the use of TOA corrects this problem. The TOA may be omitted if a stripping solution containing 5 X 10^{-4} mol/dm^3 HNO_3 and 1 x 10^{-4} mol/dm^3 $CsNO_3$ is employed, but we encountered somewhat weaker stripping and difficulties with anionic impurities.[5b]

Extract #1	Extract #2	Scrub #1	Scrub #2	Strip #1	Strip #2	Strip #3
10.4	8.8	0.58	0.64	0.092	0.057	0.043

[a] Two extractions at O:A = 0.5 each with fresh simulant; two scrubs at O:A = 5 each with fresh 0.01 mol/dm^3 HNO_3; and three strips at O:A = 3 with fresh 0.002mol/dm^3 HNO_3. Phases were contacted for 5 minutes at 25 °C by vortexing.

Key simulant constituents: 7.1 X 10^{-4} mol/dm^3 Cs^+, 7 mol/dm^3 Na^+, 0.02 mol/dm^3 K^+, 0.4 mol/dm^3 Al(III), 0.015 mol/dm^3 Cr(VI), 1.9 mol/dm^3 free OH^-, 2.7 mol/dm^3 NO_3^-, 1 mol/dm^3 NO_2^-, 0.2 mol/dm^3 CO_3^{2-}, 0.22 mol/dm^3 SO_4^{2-}, 0.1 mol/dm^3 Cl^-, and 0.05 mol/dm^3 F^-.

Table 2 Caesium distribution ratios in batch tests using SRS waste simulant.[a]

ACKNOWLEDGEMENTS

This research was sponsored by the Efficient Separations and Processing Crosscutting Program, USDOE Office of Environmental Management, under contract number 1) DE-AC05-96OR22464 with Oak Ridge National Laboratory (ORNL), managed by Lockheed Martin Energy Research Corp.; 2) W-31-109-Eng-38 with Argonne National Laboratory, and 3) DE-AC06-76RLO1830 with Pacific Northwest National Laboratory operated by Batelle Memorial Institute. LHD thanks the ORNL Postdoctoral Research Associates Programme administered by ORNL and the Oak Ridge Institute for Science and Education.

REFERENCES

1 (a) Stewart TL, Frey JA, Geiser DW and Manke KL. in *Science and Technology for Disposal of Radioactive Tank Wastes*, Schulz WW and Lombardo NJ. Eds., Plenum, New York, 3-13, (1998).
(b) Bunker B, Virden J, Kuhn B and Quinn R. in *Encyclopedia of Energy Technology and the Environment,* Wiley, 2023-2032, (1995).
(c) Hobbs DT and Walker DD. in *Chemical Pretreatment of Nuclear Waste for Disposal*, Schulz WW and Horwitz EP. Eds., Plenum, New York, 17-24, (1995).

2 (a) Horwitz EP, Dietz ML and Fisher DE. *Solv. Extr. Ion Exch.*, **9**, 1, (1991).
(b) Dietz ML, Horwitz EP and Rogers RD. *Solv. Extr. Ion Exch.*, **13**, 1, (1995).
(c) Dietz ML, Horwitz EP, Jensen MP, Rhoads S, Bartsch RA, Palka A, Krzykawski J and Nam J. *Solv. Extr. Ion Exch.*, **14**, 357, (1996).

3 (a) Bonnesen PV, Moyer BA, Presley DJ, Armstrong VS, Haverlock TJ, Counce RM and Sachleben RA. *Alkaline-Side Extraction of Technetium from Tank Waste Using Crown Ethers and Other Extractants,* Report ORNL/TM-13241, Oak Ridge National Laboratory, (1996).
(b) Moyer BA, Sachleben RA and Bonnesen PV. *U.S. Patent 5,443,731*, (1995).
(c) Leonard RA, Conner C, Liberatore MW, Bonnesen PV, Moyer BA, Presley DJ and Lumetta GJ. *Sep. Sci. Technol.* In Press.

4. (a) Dozol JF, Asfari Z, Hill C and Vicens J, E. *Patent 9214245*, (1992).
(b) Dozol JF, Rouquette H, Ungaro R and Casnati A, E. *Patent 9304566*, (1993).
(c) Hill C, *Ph.D. Thesis*, Universite Louis Pasteur de Strasbourg, (1994).
(d) Hill C, Dozol J-F, Lamare V, Rouquette H, Tournois B, Vicens J, Asfari Z, Ungaro R and Casnati A, *J. Incl. Phenom.*, **19**, 399, (1994).
(e) Dozol J-F, Simon N, Lamare V, Rouquette H, Eymard S, Tournois B, De Marc D and Macias RM. *Sep. Sci. Technol.*, In Press.

5 (a) Haverlock TJ, Bonnesen PV, Sachleben RA and Moyer BA, *Radiochim. Acta.* **76**, 103, (1997).
(b) Bonnesen PV, Delmau LH, Haverlock TJ and Moyer BA, *Alkaline-Side Extraction of Caesium from Savannah River Tank Waste Using a Calixarene-Crown Ether Extractant,* Report ORNL/TM-13704, Oak Ridge National Laboratory, (1998).

6 (a) Moyer BA. in *Molecular Recognition: Receptors for Cationic Guests*, Gokel GW, Ed., Vol. 1, Comprehensive Supramolecular Chemistry, JL Atwood, JED Davies, DD MacNicol, F Vögtle, and J-M Lehn, Eds., Pergamon, Oxford, 1996; Chap. 10.
(b) Moyer BA and Bonnesen PV. in *The Supramolecular Chemistry of Anions,* Bianchi A, Bowman-James K and Garcia-Espana E. Eds., VCH, Chap. 1, (1997).

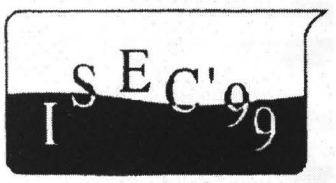

EXTRACTION OF STRONTIUM AND CESIUM USING A SYNERGISTIC SOLVENT MIXTURE

TA Todd and DJ Wood
Lockheed Martin Idaho Technologies Co., Idaho Falls, Idaho, USA
MA Afonin
St. Petersburg Institute of Technology, St. Petersburg, Russia
VV Romanovski
Glenn T Seaborg Institute for Transactinium Science at Lawrence Livermore National Laboratory, Livermore, California, USA

ABSTRACT
A new solvent mixture, based on combining chlorinated cobalt dicarbollide and a macrocyclic polyether extractant, has been shown to extract both cesium and strontium. When the two extractants are combined in a single solvent, the distribution coefficient for cesium is primarily a function of the concentration of the cobalt dicarbollide extractant, as expected. A significant increase, up to five orders of magnitude, in the strontium distribution coefficient is realized in the presence of both extractants, over the distribution coefficient that is measured for the macrocyclic polyether alone. This synergistic effect allows for lower concentrations of extractant to be used, making the process more economical. Batch extraction contacts were performed to determine equilibrium distribution coefficients over a range of solvent compositions and acid concentrations. The extraction of cesium, strontium, europium, americium and sodium was studied and the results are presented.

Keywords: americium, cesium, europium, sodium, strontium, synergistic extraction, cobalt dicarbollide, crown ether

INTRODUCTION

The cobalt dicarbollide extractant (CoDiC), originally developed in Czechoslovakia and later developed and implemented in Russia, has been demonstrated to be an effective extractant for the removal of cesium from acidic radioactive wastes.[1] The Mayak Production Association, Ozersk, Russia processed more than 320 m^3 of highly radioactive waste in 1996, recovering a total of 7.1 MCi of cesium and strontium. The concentrated cesium and strontium rich-stream was prepared for subsequent vitrification. Strontium extraction was realized by the addition of polyethylene glycol (PEG) to the solvent.

A recent collaborative effort between the Idaho National Engineering and Environmental Laboratory (INEEL), Idaho Falls, USA and the VG Khlopin Radium Institute, St. Petersburg, Russia, has successfully demonstrated the extraction and recovery of cesium and strontium from actual acidic radioactive wastes using chlorinated CoDiC/PEG in a non-nitroaromatic solvent.[2,3] Actinide and rare earth elements are not appreciably extracted by the CoDiC/PEG solvent. Separation of other radionuclides, including technetium, actinides and rare earth elements, from INEEL radioactive wastes is also of interest. Therefore, the investigation of synergistic effects for the extraction on strontium, actinides and rare earth elements from solvents containing cobalt dicarbollide and potentially synergistic secondary extractants was initiated.

Macrocyclic polyethers, commonly known as crown ethers, are widely known to selectively extract alkaline and alkaline earth elements. The extraction of strontium from solvents containing 18-crown-6 molecules has received significant attention over the past 10 years.[4,5] Initial studies of the extraction of Am, Cm, Eu and Ce (III) from nitrate media by mixtures of chlorinated CoDiC and unsubstituted 18-crown-6 were performed at the Pacific Northwest Laboratory (PNL).[6]

This study involved the fundamental investigation of the extraction of cesium, sodium, strontium, europium and americium from nitric acid solutions using a mixture of chlorinated CoDiC and the polyether extractants 18-crown-6 and di-(tert-butylcyclohexano)-18-crown-6 (DtBuCH18C6).

© 2000 Society of Chemical Industry

EXPERIMENTAL

Preparation of the solvent included dissolution of the cesium salt of chlorinated cobalt dicarbollide in nitrobenzene (0.34 g/cm^3), followed by 10 successive contacts with equal volumes of fresh 8 mol/dm^3 HNO_3, then five successive contacts with deionized water at a volume ratio of 1:5 (O/A). Contacts were performed by vortex mixing for 5 minutes followed by centrifugation at 3000-4000 rpm. Cobalt dicarbollide concentration in the stock solvent was determined by X-ray Fluorescence Analysis (XRF). Solvent compositions for subsequent experiments were made by diluting the stock solution with nitrobenzene and/or addition of crown ether.

Batch extraction contacts were conducted by vortex mixing equal volumes of solvent and nitric acid solutions containing trace concentrations of ^{241}Am, ^{137}Cs, ^{90}Sr, ^{22}Na and ^{152,154}Eu. Mixing times in initial contacts varied from 1 minute up to 6 minutes to determine the kinetics of extraction. After establishing that the extraction kinetics were rapid, all subsequent contacts were performed for 3 minutes. Nitric acid concentrations in the aqueous solutions were varied between 0.3 - 0.7 mol/dm^3, while solvent compositions ranged from 0 - 0.25 mol/dm^3 in CoDiC and 0 - 0.12 mol/dm^3 in 18-crown-6. The aqueous phase was simultaneously spiked with all radionuclides mentioned above (approximately 1000 - 2000 Bq/cm^3 for each radionuclide) prior to contacting the organic phase. The phases were separated by centrifugation and analytical measurements of both aqueous and organic phases were performed directly by gamma spectroscopy.

RESULTS AND DISCUSSION

Results of batch distribution contacts for cesium, strontium, europium and americium in 0.5 mol/dm^3 HNO_3 are summarized graphically in Figures 1 and 2.

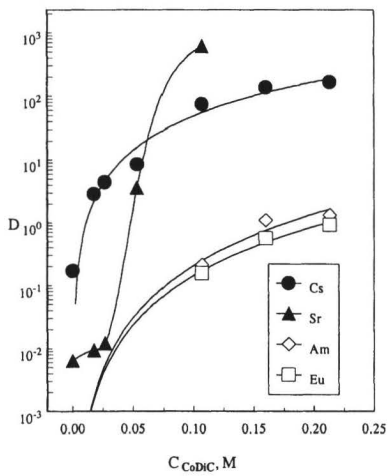

Figure 1. Extraction of Cs, Sr and trivalent Am and Eu tracers by CoDiC/18-crown-6 mixtures in nitrobenzene from 0.5 mol/dm^3 HNO_3, $C_{18\text{-crown-6}}$ = 0.0533 mol/dm^3.

Cesium distribution coefficients in the presence of 0.053 mol/dm^3 18-crown-6 ranged from 0.2 with no CoDiC present in the solvent to 164 with 0.213 mol/dm^3 CoDiC in the solvent for 0.5 mol/dm^3 HNO_3 solutions. The cesium distribution coefficient was also determined for solvent compositions containing 0.16 mol/dm^3 CoDiC with and without 0.053 mol/dm^3 18-crown-6. The distribution coefficients were nearly identical (134 - 135) for both solvent compositions. When the CoDiC concentration was held constant at 0.16 mol/dm^3 and the 18-crown-6 composition was varied from 0 -

0.12 mol/dm^3, the distribution coefficient decreased to a minimum at 0.08 mol/dm^3 18-crown-6, then increased four-fold at 0.12 mol/dm^3 18-crown-6. Distribution coefficients in this test ranged from 58 - 259, which is nearly quantitative extraction of cesium for all solvent compositions tested. In general, the extraction of cesium is occurring predominately by the cobalt dicarbollide extractant, which is expected.

Strontium is only slightly extracted by cobalt dicarbollide in 0.5 mol/dm^3 HNO_3 as demonstrated by a distribution coefficient of 0.59 using 0.16 mol/dm^3 CoDiC. The strontium distribution increases to over 700 when 0.019 mol/dm^3 18-crown-6 is added to the solvent. Addition of larger concentrations of 18-crown-6 to the solvent result in quantitative extraction of strontium. Strontium distribution coefficients in the presence of 0.053 mol/dm^3 18-crown-6 ranged from 0.007 with no CoDiC present in the solvent to 613 with 0.107 mol/dm^3 CoDiC in the solvent for 0.5 mol/dm^3 HNO_3 solutions. There was very little change in the strontium distribution coefficient until CoDiC concentration in the solvent exceeded 0.027 mol/dm^3, resulting in a substantial increase of nearly 5 orders of magnitude at a CoDiC concentration of 0.107 mol/dm^3. The sudden and rapid increase in strontium distribution coefficients as a function of CoDiC concentration was not expected and appears to be the result of a synergistic effect from the presence of both extractants.

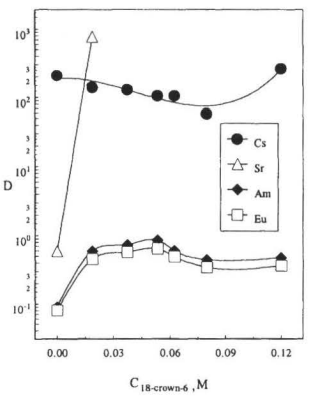

Figure 2. Extraction of Cs, Sr and trivalent Am and Eu tracers by CoDiC/18-crown-6 mixtures in nitrobenzene from 0.5 mol/dm^3HNO_3, C_{CoDiC} = 0.16 mol/dm^3.

Europium and americium distribution coefficients were determined for the same conditions as described above. Distribution coefficients for 0.16 mol/dm^3 CoDiC without 18-crown-6, ranged from 0.08 - 0.1, while the distribution coefficients for 0.0533 mol/dm^3 18-crown-6 without CoDiC were near zero (no detectable Eu or Am in the organic phase after contact). These results indicate that Eu and Am are not appreciably extracted from either extractant. When small concentrations of 18-crown-6 (0.019 to 0.12 mol/dm^3) are added to solvent containing 0.16 mol/dm^3 CoDiC, distributions ranged from 0.34 - 0.64. Likewise, when CoDiC (0.018 - 0.213 mol/dm^3) was added to solvent containing 0.0533 mol/dm^3 18-crown-6, distributions increased to as much as unity (at 0.213 mol/dm^3 CoDiC).

Similar results were obtained at 0.3 and 0.7 mol/dm^3 HNO_3 feed concentrations. Each of the radionuclides exhibits similar behavior in various nitric acid concentrations.

CONCLUSIONS

The extraction of cesium and sodium from a solvent containing cobalt dicarbollide and 18-crown-6 derivatives appears to be primarily a function of cobalt dicarbollide concentration. Strontium, europium and americium all extract at higher levels in the solvent containing both extractants. The

levels of extraction appear to be significantly higher than the expected additive effects of individual extractants, suggesting that synergistic effects are present.

ACKNOWLEDGMENT

This work was supported by funding provided by Lockheed Martin Idaho Technologies Company and NATO grant DISRM CRG 941020.

NOMENCLATURE

Bq	Becquerel
Ci	Curie
O/A	Organic/aqueous phase ratio

REFERENCES

1. Esimantovskiy V, Galkin B, Lazarev L, Lyubtsev R, Romanovskiy V, Shishkin D, and Dzekun E, *Proc. Waste Management 92*, Tucson, Arizona, (1992).
2. Todd T, Brewer K, Herbst R, Tranter T, Romanovskiy V, Lazarev L, Zaitsev B, Esimantovskiy V and Smirnov I, *Proc. Inter. Solv. Extr. Conf. (ISEC 96)*, Melbourne, Australia, (1996).
3. Law JD, Herbst RS, Todd TA, Brewer KN, Romanovskiy VN, Esimantovskiy VM, Smirnov IV, Babain VA, Zaitsev BN: *INEL-96/0192*, Lockheed Martin Idaho Technologies Co., (1996).
4. Horwitz EP, et al., *Solvent Extraction and Ion Exchange,* **8**(4&5), 557, (1990).
5. Wood DJ, Law JD, and Todd TA, *Science and Technology for Disposal of Radioactive Tank Waste*, WW Schulz and NJ Lombardo editors, Plenum Publishing Co., NY, ISBN:0-306-45904-3, pp. 255, (1998).
6. Romanovski VV, Proyaev VV and Wester DW, *Proc. International Topical Meeting on Nuclear and Hazardous Waste Management (Spectrum'94)*, Atlanta, GA, American Nuclear Society, La Grange Park, IL, **2**, 1550, (1994).

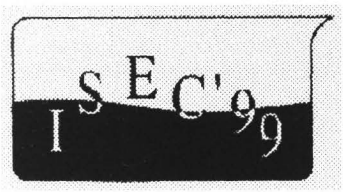

USE OF BINARY EXTRACTANTS FOR RECOVERY OF SILVER(I) FROM WASTE: A NOVEL CONCEPT IN SOLVENT EXTRACTION

Anil Kumar[2], PK Gautam[2], JP Shukla[3], RK Singh[2] and AM Sastre[1]

[1]Universitat Politècnica de Catalunya, Department of Chemical Engineering ETSEIB, Diagonal 647, E 08028 Barcelona, Spain

[2]PREFRE Plant, Bhabha Atomic Research Centre, Tarapur 401502, India

[3]Radiochemistry Division, Bhabha Atomic Research Centre, Trombay, Mumbai 400085, India

ABSTRACT

The solvent extraction of silver(I) from nitric acid solutions by bis(2,4,4-trimethylpentyl)dithiophosphinic acid (Cyanex 301), and bis(2,4,4-trimethylpentyl)monothiophosphinic acid, (Cyanex 302) in Solvesso-100 and their binary mixtures with Aliquat-336 was investigated. The stripping behaviour of silver complexes with Cyanex 301, Cyanex 302 and with binary extractants were carried out in detail and it was found that Cyanex-301 + Aliquat-336 (I) and Cyanex-302 + Aliquat-336 (II) provide better control over stripping and easy regeneration of the extractant than pure Cyanex 301 and Cyanex 302 individually. Among the aqueous reagents tested, thiourea + 0.1mol/dm^3 HNO_3 and ammonium thiocyanate + 0.1mol/dm^3 HNO_3 proved to be efficient stripping reagents for silver. Application of the developed method was extended for the recovery of silver from electrolytic wastes.

Keywords: silver(I), Cyanex 301, Cyanex 302, Aliquat 336, binary extractants, electronic waste

INTRODUCTION

In solvent extraction, the choice of a suitable extractant for metal selectivity is a key problem, therefore many investigations are carried out to develop new extractants. Recently, two sulphur containing organophosphorus extractants have been introduced by American Cynamid.[1-3] Cyanex 301 and Cyanex 302 are organic acids and consequently will react with an organic base, such as Aliquat-336, to form an organic salt, a so-called binary extractant. Binary extractants operate at lower pH values than cation-exchangers and at higher temperatures and concentrations than oxygenated reagents. Consequently, less time is required to reach equilibrium than with for example hydroximes, and relatively few counter-current stages are required. A few attempts have been made to evaluate metal extraction by binary extractants by Eyal and co-workers.[4,5] Binary extractants have been proposed for use in many diverse processes, such as the recovery of copper from leaching solutions and eluates,[6] and the recovery of zinc from electrowinning waste streams.[7] The extraction of salts of copper, cobalt, nickel and lanthanides by binary extractants is the basis of several patents.[8,9] This study compares the extraction behaviour of Ag(I) with Cyanex 301 and Cyanex 302 and their binary mixtures with Aliquat 336 from nitric acid solutions. The parameters studied include: nitric acid concentration in aqueous phase, loading capacity, type of metal organic species with pure and binary extractants and nature and type of strippant for back extraction of Ag(I) from the loaded organic phases.

EXPERIMENTAL

Cyanex 301 (75-80% pure) and Cyanex 302 (84% pure) were kindly supplied by American Cyanamid (now Cytec Industries, Inc.) and Aliquat 336 (Ali-336) were obtained from General Mills Inc, USA. Reagent grade diluent Solvesso-100 (Shell Co., Australia) was used as received. The binary extractants were prepared by mixing equimolar quantities of Cyanex 301 and Cyanex 302 with Aliquat-336. The formation of the base couple is an exothermic reaction, and can be expressed as:

$$R_4NCl_o + HA_o/H_2A_{2o} \;===\; R_4NA_o/\,R4NHA_{2}0 + HCl_o$$

© 2000 Society of Chemical Industry

where R_4NCl denotes Aliquat-336 and HA and H_2A_2 denotes Cyanex 301 and Cyanex 302 respectively. The formation of the binary extractant, R_4NA, results in the generation of hydrochloric acid in the organic phase. The inorganic acid was removed by washing with water. Silver-110m tracer, obtained in the Ag(I) state from the Isotope Division, Bhabha Atomic Research Centre, India, was used throughout the present study. Its radiochemical purity was ascertained by gamma ray spectrometry. Pu-239, U-233, Ru-106 and Cs-137 were used to study the extraction characteristics of the respective metal cations as these nuclides are the main component of electrolytic waste generated during solid PuO_2 dissolution catalysed by Ag^{2+} reactive species.[12] All the isotopes were radiochemically pure. Uranium and plutonium were assayed by alpha scintillation counting. Ag-110 and Cs-137 were assayed by a well type NaI(Tl) scintillation detector coupled to a single channel analyser. Ru-106 was assayed by beta scintillation counting.

Synthetic Electrolytic Waste

Simulated electrolytic waste containing silver, spiked with plutonium (1 mg dm^{-3}) and Am(III) (0.052 mg dm^{-3}) and various fission products of the following composition: Ru-106: 57.2 μc dm^{-3}, Cs-137: 2513.2 μc dm^{-3}, Ce-144: 46.4 μc dm^{-3} was employed for extraction studies. Electrolytic waste was spiked with Ag-110m to evaluate the estimation of silver by gamma spectrometry. Plutonium and americium were assayed by alpha spectrometry. High purity germanium detector coupled to 4K PC linked multichannel analyser was used for the estimation of fission product nuclides such as Cs-137, Ce-144 and Ru-106.
Distribution ratio (D) measurements were carried out as described in earlier publication.[10]

RESULTS AND DISCUSSION

The extraction of Ag(I) is quantitative from nitric acid solutions from pure Cyanex 301 and Cyanex 302, Cyanex 301 + Ali-336 (I) and Cyanex 302 + Ali-336 (II). The extraction kinetics were better for binary mixtures than for pure extractants. Thus, it appears that combining an acid extractant such as Cyanex 301 or Cyanex 302 with an organic base such as Aliquat-336 results in the enhancement of the extraction of Ag(I). This has practical applications in reducing the number of extraction stages during metal recovery by solvent extraction. In addition, binary extractants afford greater control over the back extraction. This is ascribed to the stability of the binary extractants which must dissociate to effect extraction. Sole et al. reported the decomposition of the Cyanex 301 and Cyanex 302 in acidic nitrate media.[11] In addition, it has recently been shown that Cyanex 301 is unstable in the presence of high nitric acid concentrations, resulting in oxidation of the extractant. So, HNO_3 concentration did not exceed 4 mol/dm^3, throughout the study.

To assess the dependence of the extraction capacity on the aqueous phase acidity, the extractability of silver from 4 mol/dm^3 HNO_3 down to solutions in the pH range (ca. 0.01 mol/dm^3) into Solvesso 100 by Cyanex 301, Cyanex 302, Cyanex 301 + Ali-336 (I) and Cyanex 302 + Ali-336 (II) from unbuffered aqueous solutions was systematically studied. The data presented in Figure 1 indicate little acid dependence except for Cyanex 302. On the other hand, binary salts of Cyanex 301 and Cyanex 302 did not show any HNO_3 effect in the 2-4 mol/dm^3 acid range. The performance of Cyanex 301 + Ali-336 was superior to that of Cyanex 301 alone. The extraction of Ag(I) by Cyanex 301, Cyanex 302, Cyanex 301 + Ali-336 and Cyanex 302 + Ali-336 with varying extractant concentration is presented in Figure 2. The log D values were found to increase with the extractant concentration. In addition, the binary salt of Cyanex 301 resulted in higher log D values than the pure reagent.

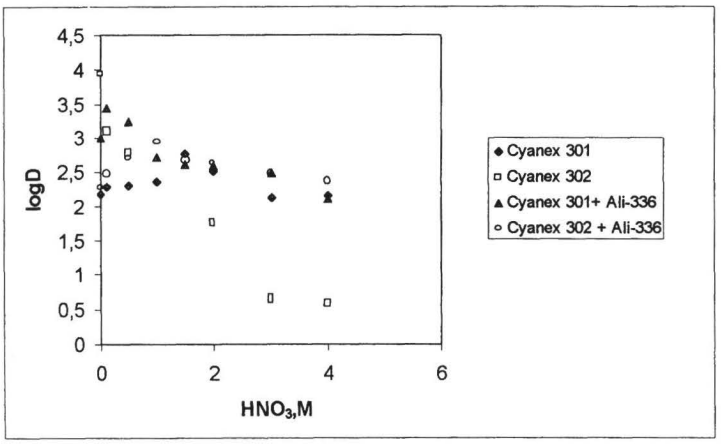

Figure 1 Extraction of Ag(I) with pure Cyanex 301, Cyanex 302 and their binary extractants as a function of nitric acid concentration, Extractant concentration (each): 0.25 mol/dm^3

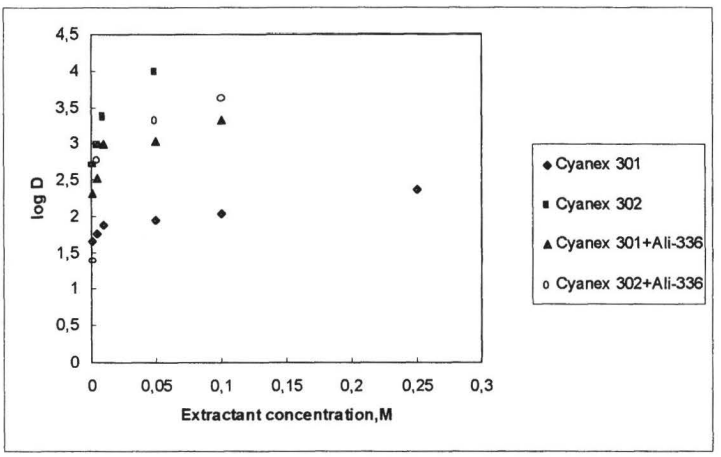

Figure 2 Extraction of Ag(I) with pure Cyanex 301, Cyanex 302 and their binary extractants from nitric acid as a function of extractant concentration, HNO_3 =1mol/dm^3

Silver can be quantitatively extracted, if the extractant is contained in the system at more than the theoretical equivalent amount. Therefore, the extracted species of silver cannot be determined by slope analysis. So the measurement of the silver-loading capacity is tested. Figure 3 shows the relationship between the ratio of the initial concentration of extractant to the concentration of silver extracted, $C_{HA}/C_{Ag,org}$, and the initial concentration of silver in aqueous solutions. From these results, it is found that Cyanex 301, Cyanex 302 and their binary mixtures formed 1:1 silver-extractant complexes.

$$Ag^+ + H_2A_2 \;==\; Ag(HA_2) + H^+ \qquad \text{(Cyanex 302)}$$

$$Ag^+ + HA \;==\; AgA + H^+ \qquad \text{(Cyanex 301)}$$

$$R_4NA + Ag^+ + NO_3^- == AgA + R_4NNO_3 \qquad \text{(Cyanex 301+Ali-336)}$$

$$R4NHA_2 + Ag^+ + NO_3^- == AgHA_2 + R_4NNO_3 \qquad \text{(Cyanex 302+Ali-336)}$$

where HA or H_2A_2 is the extractant. These results were confirmed by other experiments in which the extractant concentration was changed.

Quite high values of D were obtained from low to high concentrations of nitric acid and so stripping became almost impractical with nitric acid solutions alone. Complexing agents like EDTA (0.2 - 0.5 mol/dm^3) or sodium carbonate (0.5 mol/dm^3) fail to recover Ag from the loaded organic phases of Cyanex 301, Cyanex 302 and their binary extractants. Stripping behaviour of silver extracted by the binary extractant indicated quantitative recovery from Cyanex-301 + Ali-336 using 0.1 mol/dm^3 HNO_3 + thiourea or 0.1 mol/dm^3 HNO_3 + NH_4SCN. Stripping of silver extracted by Cyanex 301 seems to be extremely difficult. Stripping from loaded phases of Cyanex 302 and Cyanex 302 + Ali-336 also showed quantitative recovery but fewer contacts in case of latter of the latter stripping reagent were required. This suggests a reduced number of stages in the stripping cycle. Binary mixtures showed improved behaviour proving better control over back extraction than pure Cyanex 301 and Cyanex 302.

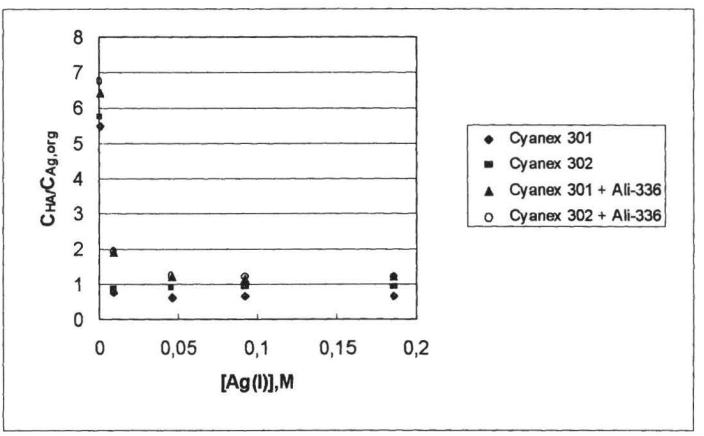

Figure 3 Silver(I)-loading capacity of the extractants,
Extractant concentration (each): 0.005 mol/dm^3, HNO_3 = 1 mol/dm^3

Silver Recovery From Electrolytic Waste Solution

The extractability of Ag(I) from an electrolytic waste solution generated during recovery of plutonium from solid waste[12] by employing a silver catalysed electrooxidative process was explored. Silver recovery into Solvesso 100 solutions of binary mixtures of Cyanex 301, Cyanex 302 and Ali-336 was examined from electrolytic waste. From the data summarized in Table 1, it is quite clear that problematic actinides like Pu(IV), Am(III) and fission product contaminants were poorly extracted (<5%). More than 90% of Ag(I) could be recovered in single contact (O/A = 1) from 1 mol/dm^3 (HNO_3) aqueous medium into Solvesso-100 by Cyanex 301 + Ali-336. Finally, Ag could be readily back extracted almost completely (> 98%) from the loaded Cyanex 301 + Ali-336 with an aqueous 1 mol/dm^3 thiourea + 0.1 mol/dm^3 HNO_3 or 1mol/dm^3 NH_4SCN + 0.1mol/dm^3 HNO_3 solution. It is thus proved that Ag (I) could be efficiently and reversibly extracted from electrolytic waste solutions.

Fission product	F.P.activity[a] in the feed ($\mu ci\ dm^{-3}$)	F.P. activity in the organic phase ($\mu ci\ dm^{-3}$)	Recovery (%) Cyanex 301 + Ali-336
Ru-106	57.2	3.4	5.0
Cs-137	2513.2	125.1	4.0
Sb-125	23.3	1.0	4.0
Ce-144	46.4	1.2	2.2
Ag-110m	1.0[b]	0.9[b]	92.6
Ag(inactive)	5.0[c]	4.9[c]	98.0
Pu(IV)	5.0[b]	0.2[b]	3.0
Am (III)	5.2×10^{-2}[b]	1.0×10^{-3}[b]	1.5

a, Activity of fission products was estimated by multichannel analyser using a High Purity Germanium detector (HPGe).
b, Values are expressed in mg/dm^3
c, Values are expressed in g/dm^3

Feed : Electrolytic Waste in 1.0 $mol/dm^3 HNO_3$; Extractant concentration: 0.25 mol/dm^3
Strippant: 1.0 mol/dm^3 Thiourea in 0.1 mol/dm^3 HNO_3

Table 1 Recovery of Silver from Acidic Electrolytic Waste Generated during Recovery of Plutonium by Silver Catalysed Electroxidative Process

ACKNOWLEDGEMENTS

The authors wish to thank Shri.K.Balu, Director, Fuel Reprocessing and Waste Management, Shri.D.D.Bajpai, Head PREFRE, BARC, India and Dr.S.B.Manoher, Head, Radiochemistry Division, BARC for their keen interest in this work. Dr. Anil Kumar gratefully acknowledges the financial support from Comisión Interministerial de Ciencia y Tecnología, Spain for awarding a Visiting Scientist fellowship during his leave from PREFRE, Bhabha Atomic Research Centre, Tarapur, India.

REFERENCES

1. American Cyanamid Co., Cyanex 272, Cyanex 302 and Cyanex 301, Technical Brochures, Wayne, NJ.
2. Rickelton WA and Boyle RJ, *Sep. Sci. Technol.*, **23**, 1227, (1988).
3. Eyal AM, Bressler E, Bloch R and Hazan B, *Ind. Eng. Chem. Res.*, **33**, 1067, (1994).
4. Eyal AM, Kogan L and Bressler E, *Ind. Eng. Chem. Res.*, **33**, 1076, (1994).
5. Kholkin AI, Sergeev VV, Pashkov GL, Savkina LY, Kalish NK and Kopanev AM, *Soviet Journal of Non-Ferrous Metals*, **28**, 18.
6. Eyal AM, Baniel AM, Hajdu K and Mizrahi J, *Solv. Extr.Ion Exch.*, **8**, 209, (1990).
7. Nishimura S and Watanabe M, *Japanese Patent, 51/151280*, (1976).
8. Minagawa Y and Yazima F, *Japanese Patent, 54/9200*, (1979).
9. Shukla JP, Singh RK and Kumar A, *Radiochim. Acta*, **54**, 73, (1991).
10. Sole KC, Hiskey JB and Fergusson TL, *Solv. Extr. Ion Exch.*, **11**, 783, (1993).
11. Singh RK, Bajpai DD, Venugopalan AK, Gurba PB and Singh RR, *Electrochemical Process for the Recovery of Plutonium from Laboratory Solid Waste, BARC Report*, 1994/I/008.

NEW REDUCING AGENTS FOR NEPTUNIUM(VI) AND PLUTONIUM(IV)

RJ Taylor[1], I May[1], IS Denniss[1], VS Koltunov[2], SM Baranov[2], VI Marchenko[2], EA Mezhov[2], VG Pastuschak[2], GI Zhuravleva[2] and OA Savilova[2]

[1]Research and Technology, BNFL Sellafield, Seascale, Cumbria, CA20 1PG, UK

[2]VNIINM, PO Box 369, Moscow, 123060, Russia

ABSTRACT

The management of neptunium and plutonium within a single cycle flowsheet is a key component of BNFL's *Advanced Purex Project*. One option under development is the routing of Np with the Pu product in the U/Pu split. Salt-free reducing agents capable of achieving this include hydroxylamine and organic derivatives of hydroxylamine and also oximes. A new reductant, ethyl(hydroxy)ethyl hydroxylamine, has been shown to very rapidly reduce both Np(VI) and Pu(IV) which makes it particularly suitable for use in centrifugal contactors which have very short residence times.

Keywords: neptunium, plutonium, hydroxylamine derivatives, reducing agents, extraction kinetics, Purex process, centrifugal contactor

INTRODUCTION

Commercial nuclear fuel reprocessing separates the actinide elements, uranium and plutonium, from irradiated nuclear fuel so that they can be recycled as either uranium dioxide or mixed oxide fuels for further electricity generation. Commercial reprocessing plants use the well established Purex process which separates U and Pu from fission product wastes by solvent extraction from nitric acid into diluted tri-n-butylphosphate.[1,2]

BNFL is currently engaged in research programmes to both enhance current reprocessing operations[3] and to develop Advanced Purex processes.[4] The development of a single cycle flowsheet and the improved control of Np within the single cycle have been identified as important objectives of this '*Advanced Purex*' project.[4,5] One option for the routing of Np in a single cycle flowsheet is with the Pu product (Figure 1).

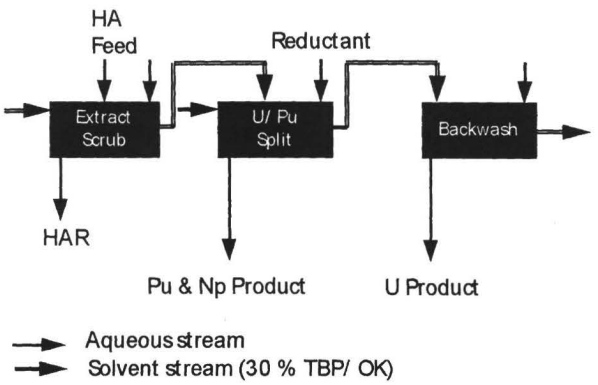

Figure 1. A single cycle flowsheet in which Np is routed with the Pu product

In order to achieve this, Np(VI) must be reduced to inextractable Np(V) without further reduction to Np(IV) and Pu(IV) must be reduced to Pu(III).[5] Rapid kinetics are needed if the

© 2000 Society of Chemical Industry

reductant is to be compatible with centrifugal contactors, which are being developed for these Advanced Purex processes,[4] since they have very low residence times.

Hydroxylamine derivatives are known to reduce both Np(VI) and Pu(IV)[6] and this paper reports kinetic studies of a new co-reductant: ethyl(hydroxy)ethyl hydroxylamine (EHEH; $HOC_2H_4(C_2H_5)NOH$).

EXPERIMENTAL METHODS

The experimental methods used in these studies have been described in detail in previous publications.[7-9] Briefly, a Np(VI) stock solution (17 g/dm^3 in $HClO_4$; >98.5 % Np(VI)) was prepared by the dissolution of NpO_2 followed by ion exchange, acidification, evaporation and dilution. Pu(IV) was purified by solvent extraction and stripping, acidification and the addition of H_2O_2 to stabilise Pu as Pu(IV). The stock solution was ~32 g/dm^3 and 98.5 % Pu(IV). The reduction of Np(VI) and Pu(IV) ions was then followed in the standard manner by spectrophotometry using the Np(V) absorption band at 980 nm and the Pu(IV) or Pu(III) peaks at 477 nm or 602 nm.

RESULTS AND DISCUSSION

Reduction of Np(VI) ions

The stoichiometric coefficients of the Np(VI)+EHEH reaction were determined by mixing the reagent solutions at different mole ratios with a deficiency of reductant. When the reaction was finished completely, the concentration of Np(V) was determined spectrophotometrically. The results in a 0.1 mol/dm^3 $HClO_4$ solution at 25C are given below:

$[Np(VI)]_0/[EHEH]_0$	6	9	12	16	20	25
$[Np(V)]_f/[EHEH]_0$	3.5	4.9	4.9	4.6	4.6	3.1

These results indicate that ca. 4 moles of Np(VI) are consumed per 1 mole of the oxidized reductant. Equation (1) corresponds to this stoichiometric coefficient ratio, although confirmation of this equation by the identification of the reaction products is needed.

$$4NpO_2^{2+} + HOC_2H_4(C_2H_5)NHOH^+ + 3H_2O = 4NpO_2^+ + 2C_2H_5OH + HNO_3 + 5H^+ \quad (1)$$

An example of the results of the kinetics experiments is shown in Figure 2 and from the kinetic results the rate equation (2) was derived. The mean value of the reaction order relative to H^+-ions is approximately equal to -0.8 and this is explained by a mechanism involving two parallel reactions.

$$-\frac{d[Np(VI)]}{dt} = k\frac{[Np(VI)][HOC_2H_4(C_2H_5)NHOH^+]}{[H^+]^{0.8}} \quad (2)$$

The mean value of the general rate constant is $k = 334 \pm 12$ $l^{0.2}mol^{-0.2}min^{-1}$ at 25.6C. There was no effect of ionic strength observed in this reaction. The temperature dependence of the reaction rate was investigated in a 1 mol/dm^3 HNO_3 solution and this led to the calculation of the activation energy, $E = 42.3 \pm 2.7$ kJmol^{-1}, as well as the enthalpy $\Delta H^* = 39.8 \pm 2.7$ kJmol^{-1}, the free energy $\Delta G^* = 68.8 \pm 0.1$ kJmol^{-1} and the activation entropy $\Delta S^* = -97 \pm 9$ Jmol^{-1}K^{-1}.

Reduction of Pu(IV) ions

The reaction stoichiometry was investigated in the same manner as for Np(VI) above. In 0.3 mol/dm^3 $HClO_4$ solution at room temperature this gave:

$[Pu(IV)]_0/[HOC_2H_4(C_2H_5)NHOH^+]_0$	8	8	8	12	12
$[Pu(III)]_f/[HOC_2H_4(C_2H_5)NHOH^+]_0$	6.1	5.6	6.3	5.7	5.6

The stoichiometric coefficient ratio of 6:1 corresponds to the following equation, although again confirmation by the identification of the reaction products is needed.

$$6Pu^{4+} + HOC_2H_4(C_2H_5)NHOH^+ + 3H_2O = 6Pu^{3+} + C_2H_5OH + CH_3CHO + HNO_3 + 7H^+$$

(3)

An example of the results of the kinetics experiments is given in Figure 3. It was found that the reduction of Pu(IV) was second order with respect to Pu(IV) ions and ~1.4 order with respect to EHEH. At constant ionic strength, the kinetic equation was found to be described by equation (4) where $k = 12350 \pm 410\ s^{-1}$ at 11.0C.

$$-\frac{d[Pu(IV)]}{dt} = k\frac{[Pu(IV)]^2[HOC_2H_4(C_2H_5)NHOH^+]^{1.4}}{[H^+]^{2.4}}$$

(4)

When the ionic strength of the solution is varied (Table 1) the rate equation is described by (5) where $k_1 = 58700 \pm 10300\ mol^{1.3}l^{-1.3}s^{-1}$ at 11°C.

$$-\frac{d[Pu(IV)]}{dt} = k_1\frac{[Pu(IV)]^2[HOC_2H_4(C_2H_5)NHOH^+]^{1.4}}{[HNO_3]^{3.7}}$$

(5)

The temperature dependence of the reaction was studied at $[H^+] = 2.3\ mol/dm^3$ and $[EHEH] = 2\times10^{-2}\ mol/dm^3$. This led to $E = 127.2 \pm 8.4\ kJmol^{-1}$ which is close to the activation energy of the Pu(IV) - N,N-diethylhydroxylamine reaction.[10] It can be concluded that the reduction of Pu(IV) by EHEH compared to diethylhydroxylamine is accelerated by introducing the OH-group and this is a consequence of the increased activation entropy, ΔS^*, whilst the activation enthalpy, ΔH^*, remains fairly constant. This conclusion is illustrated by the data of Table 2.

$[HNO_3]\ (mol/dm^3)$	$k''\ (lmol^{-1}s^{-1})$	$k_1'\ (l^{2.4}mol^{-2.4}s^{-1})$	$k_1\ (mol^{1.3}l^{-1.3}s^{-1})^a$
1.06	244	42690	52940
1.52	78.0	13650	64260
2.20	20.0	3500	64750
2.91	5.8	1015	52830
		Mean	*58700 ±10300*

Table 1. The effect of variable $[HNO_3]$ on the rate constants k'' and k_1' (T = 11.0C; [EHEH] = 0.025 mol/dm^3). Note that: $k_1 = k''[HNO_3]^{3.7}/[HOC_2H_4(C_2H_5)NHOH^+]^{1.4}$.

Oxidant	Reductant	ΔG^* $(kJmol^{-1})$	ΔH^* $(kJmol^{-1})$	ΔS^* $(Jmol^{-1}K^{-1})$
Pu(IV)	diethyl hydroxylamine[10]	55.9	110.5	+54
Pu(IV)	EHEH	44.0	124.7	+270

Table 2. Pu(IV) thermodynamic activation parameters with diethyl derivatives of hydroxylamine (T = 25C)

Figure 2. The reduction of Np(VI) by EHEH (T=25.6C;[EHEH]=0.001mol/dm^3;[HNO_3]=0.3 (♦); 0.50 (■); 0.83 (▲); 1.22 (X) and 2.00 (□) mol/dm^3)

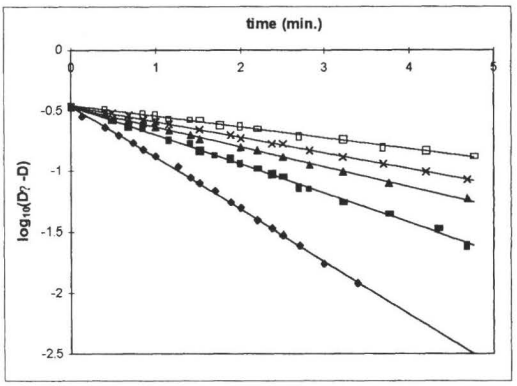

Figure 3. The reduction of Pu(IV) by EHEH (T=11C; [H^+]=2.3mol/dm^3; μ=3; [EHEH]=0.02 (♦); 0.04 (■); 0.08 (▲) mol/dm^3).

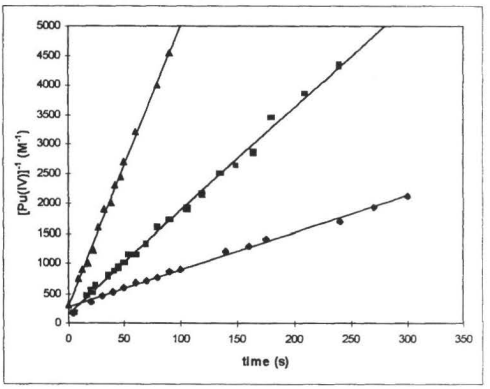

Comparison of various organic reducing agents

Many other organic reducing agents have been reported in the literature.[6,11] Table 3 compares the times taken for 99% of Np(VI) and Pu(IV) ions to be reduced by a selection of organic reductants at two different temperatures. It can be seen that under the quoted conditions, EHEH reduces Np(VI) within similar time-scales to the other reductants but it is a more rapid reductant for Pu(IV) than all these alternatives. This enhanced efficiency for Pu(IV) reduction is due to the introduction of the OH group into the di-substituted hydroxylamine (this is also observed for substituted hydrazines[12]).

It should, however, be noted that, by careful control and optimisation of process conditions, partitioning flowsheets using slower reductants can be operated. For instance, hydroxylamine has been used to successfully separate U and Pu in a centrifugal contactor trial. The Pu decontamination factors (DF_{Pu}) obtained were equal to 1200 and 1000.[13]

Further investigation of a new class of organic reducing agents, oximes, has shown that acetaldoxime in particular is also an effective reductant for Np(VI) and Pu(IV)[14] (see data in Table 3).

Reductant	20C		35C	
	Np(VI)	Pu(IV)	Np(VI)	Pu(IV)
$HOC_2H_4N_2H_3$	0.27	160	0.09	18
$C_6H_5N_2H_3$	0.008	0.8	0.0016	-
NH_2OH	0.28	10500	0.055	240
CH_3NHOH	1.00	3.4	0.29	2.0
$(CH_3)_2NOH$	0.29	0.8	0.087	0.2
$(C_2H_5)_2NOH$	2.43	0.2	0.63	0.02
$(C_4H_9)_2NOH$	4.22	0.5	1.20	0.12
$HOC_2H_4(C_2H_5)NOH$	0.45	0.064	0.20	0.005
$CH_3CH{=}NOH$	0.30	23	0.085	3.1
$C_3H_7CH{=}NOH$	0.32	240	0.081	12

Table 3. A comparison of the time needed for the reaction to reach 99% completion for various organic reducing agents ([HNO_3] = 1.0 M; [Reductant] = 0.1 M)

CONCLUSION

The routing of Np with the Pu product in Advanced Purex processes is one option for Np control in alternative single cycle flowsheets.[5] The kinetics of Np(VI) and Pu(IV) reduction reactions by the novel reagent EHEH have been investigated and these indicate that EHEH is a very rapid reductant for these ions. EHEH may, therefore, be suitable as a new co-reductant for Np and Pu in an Advanced Purex process although much further work is necessary.

REFERENCES

1. Wilson PD (ed.), *'The Nuclear Fuel Cycle'*, Oxford Science Publications, Oxford, (1996).
2. Baron P et al., *Proc. GLOBAL '93*, American Nuclear Society Inc., Illinois (1993).
3. Riley A et al., *Proc. RECOD '98*, (1998).
4. Taylor RJ et al., *Proc. RECOD '98*, (1998).
5. Taylor RJ et al., Nucl. Ener., **36**, 39, (1997).
6. Koltunov VS and Baranov SM, *Proc. GLOBAL '95*, Versailles, (1995).
7. Koltunov VS et al., *Radiochim. Acta*, **76**, 45, (1997).
8. Koltunov VS et al., *Radiochim. Acta*, **76**, 71, (1997).
9. Taylor RJ et al., *Radiochim. Acta*, forthcoming.
10. Koltunov VS et al., *Radiokhimiya*, **19**, 611, (1977).
11. Uchiyama g et al., *Nucl. Tech.*, **102**, 341, (1993).
12. Koltunov VS and Baranov SM, *Inorg. Chim. Acta*, **140**, 31, (1987).
13. Denniss IS et al., in: 'Solvent Extraction in the Process Industries', Proc ISEC'93, Elsevier, London (1993).
14. Koltunov VS and Taylor RJ, Unpublished data.

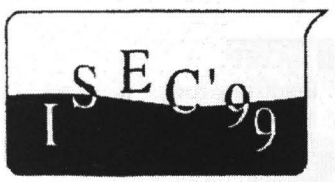

THERMODYNAMICS OF EXTRACTION BEHAVIOR OF Eu(III) AND Tm(III) BY THENOYL-TRIFLUOROACETONE AND CROWN ETHERS IN ORGANIC SOLVENTS FROM NITRATE MEDIUM

FA Shehata, N El-Hefny and HF Aly
Hot Laboratories Centre, Atomic Energy Authority, Cairo 13759, Egypt

ABSTRACT
The behaviour of lanthanide elements, Eu(III) and Tm(III), in synergistic extraction has been investigated in detail by HTTA and/or 18C6 or 15C5 in different organic diluents from nitrate medium. The effect of diluents on the extraction was investigated and the distribution of TTA and crown ethers between different diluents and 0.2 mol/dm^3 $NaNO_3$ solution has been determined at five different temperatures (5 - 45°C). The thermodynamic parameters for the extraction of both Eu(III) and Tm(III) were evaluated and discussed.

Keywords: lanthanides, Eu, Tm, nitrate medium, diluents, thenoyltrifluoroacetone, crown ethers

INTRODUCTION

The effect of solvents on the relative extraction efficiencies of the lanthanides has been observed by Masake and Hideyuki[1] and Tang and Wai[2] in crown ether systems. Krejzler and Fidelis[3] studied the effect of temperature on the selectivity of the extraction of all lanthanides with dibutylphosphoric acid from thiocyanate solution in the temperature range of 15 – 20°C. The influence of temperature on the separation factors was discussed and compared with that obtained during extraction from nitric acid solutions. The results were discussed in the light of the double-double effect within the whole lanthanide series and the investigated temperature range.The extraction of Eu(III) by dinonylnaphthalene sulfonic acid (HDNNS) in benzene from nitrate and perchlorate solutions has been investigated at different temperatures.[4] Stoichiometric formulae were derived as $Eu[(NO_3H_{n-1})(DNNS)_n]_2$ and $Eu(H_{n-1})(DNNS)_n]_3$ for nitrate and perchlorate medium, respectively (n being 1, 2 or 3). The extraction behavior of HTTA and its mixture with the crown ethers 15C5 or 18C6 in benzene towards Eu(III) and Gd(III) from nitrate medium were shown to be different from perchlorate medium[5] and the extracted species were $M(NO_3)(TTA)_2HTTA$ and $M(NO_3)(TTA)_2.CE$ for the chelates and the adducts respectively. The thermodynamic data show that the positive ΔH for all species indicates the endothermic character for both chelates and adducts. Results obtained by Rais et al[6] showed that the extraction of Eu(III) by chlorinated cobalt dicarbollide (CCD) was dramatically enhanced by changing a diluent from non-polar to polar solvents. Majdan and Kolorik[7] studied the synergistic action of TBP (B) in the extraction of La^{3+}, Pr^{3+}, Nd^{3+}, Sm^{3+}, Eu^{3+}, Gd^{3+}, Dy^{3+}, Er^{3+}, and Y^{3+} with trioctylmethylammonium nitrate (A) and found the synergistic effect is diluent dependent. The composition of synergistic complexes formed are $Ln(NO_3)_4\ A^+.2B$; $Ln(NO_3)_4\ A^+.3B^-$ and $Ln(NO_3)_5.2A_2^+.B^{2-}$.

The present work is directed to study the effect of temperature on the extraction behavior of both Eu and Tm ions from nitrate medium by HTTA alone and mixed with 15C5 or 18C6 in nine different diluents. The thermodynamic parameters associated with the extractions are calculated from the constants of the respective reactions.

EXPERIMENTAL

Reagents

The main extractant and the synergistic ligand used are 2-thenoyltrifluoroacetone, HTTA, and 15-crown-5 (15C5) or 18-crown-6 (18C6) respectively. HTTA was supplied by Fluka and the crown ethers used were supplied by Sigma Chemicals. All the other chemicals used were of analytical reagent (AR) and used directly as received.

© 2000 Society of Chemical Industry

The organic diluents used nitrobenzene (B), o-dichlorobenzene (C), chlorobenzene (D), chloroform (E), trichloroethylene (F), toluene (G), benzene (H), carbon tetrachloride (I) and cyclohexane (J) were of analytical purity grade and used without further purification.
The radioactive $^{152+154}$Eu and ^{170}Tm tracers were obtained by irradiating their oxides in 2MW-RR-1 reactor at Inshas, and used in concentration less than 10^{-5} mol/dm^3.

Procedures

In all experiments the aqueous phases used were 0.001mol/dm^3 acetate buffer solutions containing 0.2 mol/dm^3 $NaNO_3$ to fix the ionic strength. The pH was set at 3.5 Ý0.01. The organic phases contained the extractants of known molar composition diluted with different solvents used.

The extraction procedures were carried out as previously described.[5]

RESULTS AND DISCUSSION

Previous work[8] showed a very large change in the equilibrium behaviour in the extraction of Eu(III) and Tm(III) by HTTA and its mixture with crown ethers 15C5 or 18C6, in nine different diluents from nitrate medium at 25 Ý1°C.

The composition of the extracted species were proposed on the basis of the slope analysis method. It was concluded that the stoichiometry of the complexes extracted in nitrobenzene, o-dichlorobenzene, chlorobenzene and chloroform were $M(TTA)_3$ for the chelates and $M(TTA)_3$.CE for the adducts (CE ¤18C6 or 15C5) for both Eu and Tm. When using benzene, toluene, trichloroethylene, carbon tetrachloride and cyclohexane as diluents the extracted species for both Eu and Tm chelates were $M(NO_3)(TTA)_2HTTA$ and $M(NO_3)(TTA)_2$.CE adduct.

Effect of temperature on the extraction

The extraction of Eu(III) and Tm(III) by HTTA alone and in a mixture with 15C5 or 18C6 in nine different diluents was investigated using aqueous nitrate medium with constant 0.2 mol/dm^3 $NaNO_3$ and pH = 3.5 at 5, 15, 35 and 45°C.
The extraction constant values K_{ex} of the extracted species were evaluated in each diluent at the respective temperatures for both Eu(III) and Tm(III) according to the following equations.
In case of using nitrobenzene, o-dichlorobenzene, chlorobenzene and chloroform, the extraction can be represented by the following equilibrium:

$$M^{3+} + \overline{3HTTA} \rightleftharpoons \overline{M(TTA)_3} + 3H^+ \qquad (1)$$

and the K_{ex} for chelates equals:

$$K_{ex} = D\,[H^+]^3 \,/\, \overline{[HTTA]}^3 \qquad M \qquad (2)$$

For adducts, the extraction can be represented by the following equilibrium:

$$M^{3+} + \overline{3HTTA} + \overline{CE} \rightleftharpoons \overline{M(TTA)_3 .CE} + 3H^+ \qquad (3)$$

and the K_{ex} equals:

$$K_{ex} = D\,[H^+]^3 \,/\, \overline{[HTTA]}^3\,\overline{[CE]} \qquad M^{-1} \qquad (4)$$

In case of using benzene, toluene, trichloroethylene, carbon tetrachloride and cyclohexane the extraction equilibrium can be represented by:

$$M^{3+} + NO_3^- + \overline{3HTTA} \rightleftharpoons \overline{M(NO_3)\,(TTA)_2\,HTTA} + 2H^+ \qquad (5)$$

and the K_{ex} for chelates equals:

$$K_{ex} = D\,[H^+]^2 \;/\; \overline{[HTTA]^3}\,[NO_3^-] \qquad M^{-2} \qquad (6)$$

and for adducts, the extraction equilibrium can be represented by:

$$M^{3+} + NO_3^- + 2\overline{HTTA} + \overline{CE} \rightleftharpoons \overline{M(NO_3)\,(TTA)_2\,.CE} + 2H^+ \qquad (7)$$

With the K_{ex} given by:

$$K_{ex} = D\,[H^+]^2 \;/\; \overline{[HTTA]^2}\,\overline{[CE]}\,[NO_3^-] \qquad M^{-2} \qquad (8)$$

Contribution of the acetate anions with the complex formation was considered and the distribution ratio values were corrected according to reference (9). It was found that the effect of the acetate anions is very small and not exceeds 2% of the experimental data, therefore the contribution of the acetate anions was neglected.

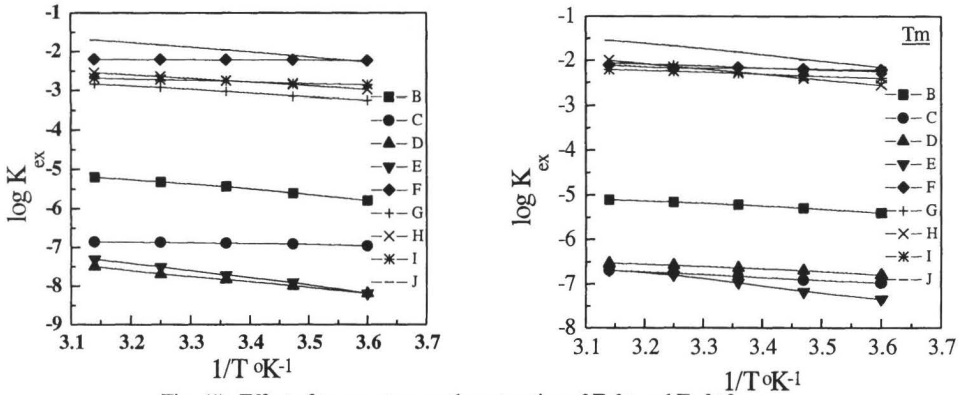

Fig. (1): Effect of temperature on the extraction of Eu^{3+} and Tm^{3+} from 0.2M $NaNO_3$ at pH=3.5 by 0.04M HTTA in different diluents.

The thermodynamics of distribution of Eu and Tm are given by equations:

$$DG^\circ = -RT \ln K_{ex} \qquad (9)$$

$$\ln K_{ex} = -DH\,\hat{E}\,RT + D\,S\,\hat{E}\,R \qquad (10)$$

where DG°, DH°, and DS° are the partial free energy change, enthalpy and entropy change respectively, R and T are the universal gas constant (8.314 J $mole^{-1}$ k^{-1}) and absolute temperature (K). K_{ex} is the extraction constant of the chelate or the adduct species. By applying equation (10) to the data for the extraction constants obtained over a temperature range of 5 - 45°C, DH° and DS° are calculated from the slope and the intercept of the plot of $\log K_{ex}$ against 1/T, respectively.

Figures (1-3) show the Van't Hoff plots obtained for all data with good linearity between log K_{ex} - 1/T. The extraction constants increase with increasing the temperature for all the diluents studied. The results obtained and calculated are summarized in Table (1).

From these thermodynamic data, the following can be elucidated:

A. the positive DH° values obtained for the chelate and adduct formation indicate the endothermic character of the complex formation process;
B. the positive enthalpy values (DH°) obtained for all the extraction systems studied are expected as a main result of the deprotonation of the chelate extractants used;

C. the negative entropy values (DS^{o}) obtained can be explained in terms of the complexation of the extracted Eu(III) and Tm(III) and formation of bonds contributing ordering in the extracted species with negative entropy contribution;

D. the positive DS^{o} obtained for some diluents indicates a net increase in the randomness of the system. This can be related to the dehydration of the extracted Eu(III) and Tm(III) with the release of water with subsequent increase in the randomness of the systems.

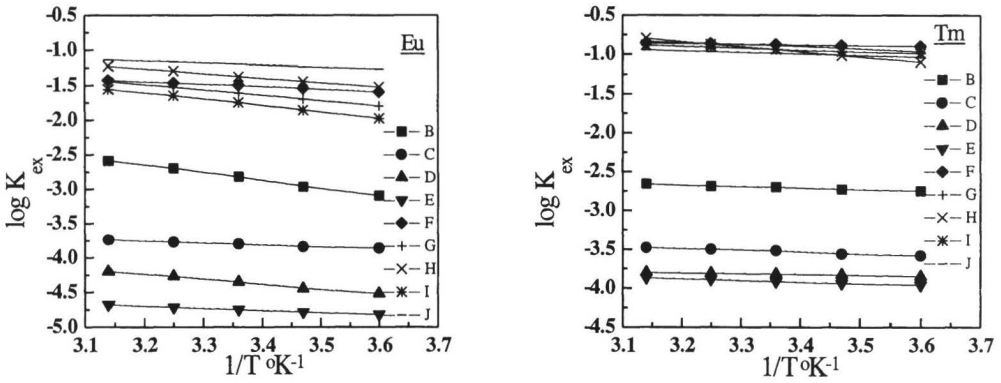

Fig. (2): Effect of temperature on the extraction of Eu^{3+} and Tm^{3+} from 0.2M $NaNO_3$ at pH = 3.5 by 0.05M(HTTA+15C5) in different diluents.

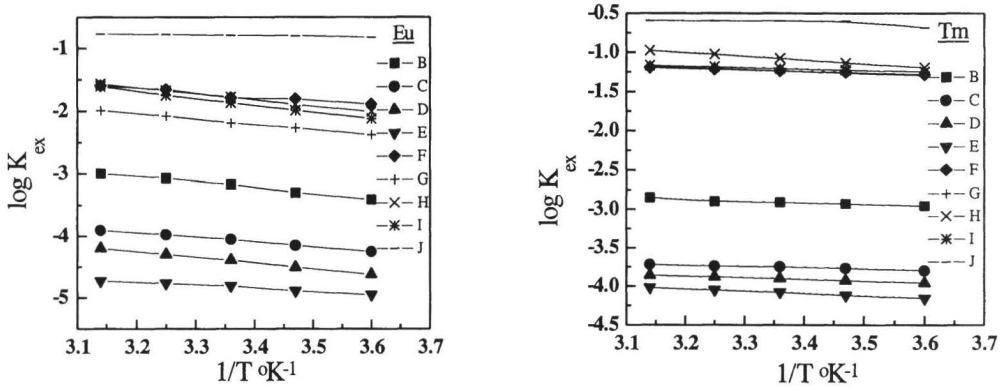

Fig. (3): Effect of temperature on the extraction of Eu^{3+} and Tm^{3+} from 0.2 $NaNO_3$ at pH =3.5 by 0.05M(HTTA+18C6) in different diluents.

B = nitrobenzene, C = o-dichlorobenzene, D = chlorobenzene, E = chloroform , F = trichloroethylene, G = toluene, H = benzene, I = carbon tetrachloride and J = cyclohexane.

$\Delta G^{o}, \Delta H^{o}$ and ΔS^{o} values of the synergistic species with the formation constants, b_{ex}, represented by:

$$b_{ex} = K_{ex \text{ for the adducts}} / K_{ex \text{ for the chelates}}$$

were calculated by subtracting the values obtained with the chelate species from those obtained for the adduct species. The constants obtained are given in Table 2. It is clear that, the negative DH^{o} values obtained for the synergistic reaction with all the diluents indicate an exothermic reactions for the formation of these complexes (with deviation for Eu-TTA-CE- o-dichlorobenzene

and benzene). The positive ΔS^{o} values indicate an increase in the randomness of the system caused by the dehydration of the metal ion and restructuring of the secondary hydration sphere.
On the other hand, it was found that, ΔG^{o} values show two trends. The first values of ΔG^{o} obtained using diluents, nitrobenzene, o-dichlorobenzene, chlorobenzene and chloroform, which are less than -11.4 KJ mol^{-1} ranged between -19.87 to -12.95 for all the systems studied. The second trend obtained when using trichloroethylene, toluene, benzene, carbon tetrachloride and cyclohexane, the values of ΔG^{o} are greater than -11,4 KJ mol^{-1} (ranged between -8.03 to -2.82). These results are related to the change in the hydration sphere of the species formed. Fig.(4) represents the relation of the formation constants, $logb_{ex}$, with the change in free energy (ΔG^{o}) . A linear relation was obtained with both Eu and Tm and all the diluents used.

Diluents	DG^{o} $KJ.mol^{-1}$	DH^{o} $KJ.mol^{-1}$	DS^{o} $J.K^{-1}\ mol^{-1}$	DG^{o} $KJ.mol^{-1}$	DH^{o} $KJ.mol^{-1}$	DS^{o} $J.K^{-1}\ mol^{-1}$
		Eu-TTA			Tm-TTA	
Nitrobenzene	31.05	24.91	-20.04	29.75	11.98	-59.97
o-dichlorobenzene	39.32	4.07	-118.4	28.96	11.92	-90.8
Chlorobenzene	44.67	28.21	-55.28	37.9	11.12	-89.9
Chloroform	44.01	37.88	-20.91	39.84	28.55	-37.99
Trichloroethylene	12.64	1.52	-37.36	12.34	4.7	-25.58
Toluene	17.27	17.45	0.50	12.28	8.21	-13.61
Benzene	15.66	17.97	7.64	12.9	23.17	34.37
Carbontetrachloride	15.77	7.38	-28.3	13.09	8.06	-16.91
Cyclohexane	11.17	23.86	42.45	10.25	25.38	50.3
		Eu-TTA-15C5			Tm-TTA-15C5	
Nitrobenzene	16.06	21.66	18.55	15.42	3.69	-39.4
o-dichlorobenzene	21.67	5.19	-55.34	20.11	4.36	-52.88
Chlorobenzene	24.83	13.75	-37.18	21.8	2.02	-66.36
Chloroform	27.1	5.87	-71.25	22.35	3.85	-62.02
Trichloroethylene	8.61	7.06	-5.15	5.02	1.68	-11.2
Toluene	9.24	14.62	18.19	5.09	5.23	0.4
Benzene	7.91	12.59	15.95	5.36	12.43	23.65
Carbontetrachloride	9.95	17.64	25.66	5.36	4.36	-3.35
Cyclohexane	6.85	5.54	-4.42	5.66	3.7	-6.53
		Eu-TTA-18C6			Tm-TTA-18C6	
Nitrobenzene	18.1	17.64	-1.72	16.6	4.19	-41.61
o-dichlorobenzene	23.11	14.29	-29.81	21.39	3.2	-61.14
Chlorobenzene	25.09	17.63	-25.01	22.25	4.21	-60.64
Chloroform	27.45	9.42	-60.79	23.28	5.88	-58.44
Trichloroethylene	9.82	12.26	7.98	7.05	3.7	-11.32
Toluene	12.52	16.28	13.0	7.05	4.7	-7.97
Benzene	10.09	18.46	27.86	6.17	9.24	10.28
Carbontetrachloride	10.76	21.14	-35.35	6.89	3.36	-11.87
Cyclohexane	4.52	2.02	-8.35	3.41	0.51	-9.75

Table 1: Thermodynamic values for the extraction constants of Eu(III)and Tm(III) extracted by HTTA or HTTA-CE in different diluent from nitrate medium of m =0.2 mol/dm^{3} .

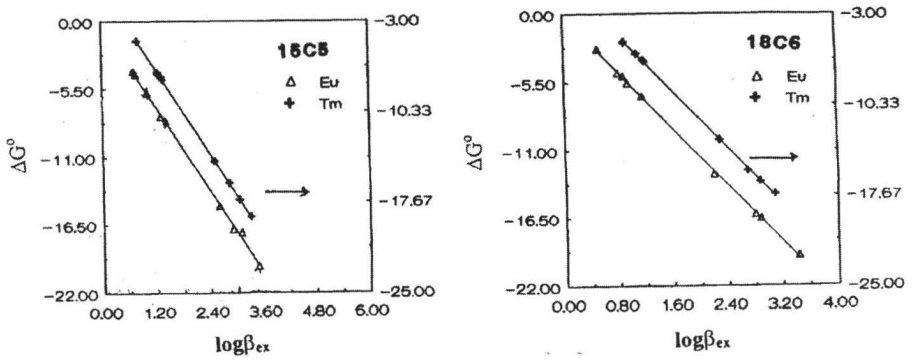

Fig.(4):Variation of ΔG° with $\log\beta_{ex}$ for Eu(III) and Tm(III) species in different diluents.

diluents	$\log b_{ex}$	ΔG° KJ.mol^{-1}	ΔH° KJ.mol^{-1}	ΔS° J.K^{-1} mol^{-1}	$\log b_{ex}$	ΔG° KJ. mol^{-1}	ΔH° KJ.mol^{-1}	ΔS° J.K^{-1} mol^{-1}
		Eu-TTA-15C5				Tm-TTA-15C5		
nitrobenzene	2.6	-14.99	-3.11	39.9	2.5	-14.33	-8.25	20.4
o-dichlorobenzene	3.09	-17.15	1.23	63.4	3.31	-18.86	-7.84	37.0
chlorobenzene	3.48	-19.87	-14.1	19.4	2.82	-16.1	-9.16	23.3
chloroform	2.9	-16.92	-32.3	-51.6	3.05	-17.48	-24.9	-24.9
trichloroethylene	0.7	-4.03	-5.7	32.7	1.27	-7.32	-3.14	14.0
toluene	1.4	-8.03	-2.9	4.4	1.25	-7.19	-3.13	13.6
benzene	1.3	-7.75	-5.4	-3.4	1.33	-7.54	-10.9	-11.3
carbontetrachloride	1.01	-5.82	10.2	53.7	1.36	-7.73	-3.85	13.0
cyclohexane	0.76	-4.32	-18.5	-47.4	0.8	-4.58	-21.7	-57.5
	$\log b_{ex}$	Eu-TTA-18C6			$\log b_{ex}$	Tm-TTA-18C6		
nitrobenzene	2.2	-12.95	-7.11	19.6	2.29	-13.15	-7.9	17.6
o-dichlorobenzene	2.8	-16.21	10.4	89.4	3.09	-17.57	-8.96	28.9
chlorobenzene	3.43	-19.58	-10.6	30.3	2.7	-15.65	-7.03	28.9
chloroform	2.88	-16.56	-28.7	-40.8	2.88	-16.55	-22.83	-21.1
trichloroethylene	0.5	-2.82	10.9	28.9	0.9	-5.29	-1.2	13.7
toluene	0.8	-4.76	-1.4	11.4	0.9	-5.23	-3.64	5.3
benzene	0.95	-5.57	0.58	20.6	1.18	-6.73	-13.75	-23.6
carbontetrachloride	0.88	-5.01	13.5	62.2	1.08	-6.2	-4.87	4.5
cyclohexane	1.1	-6.65	-22.2	-52.1	1.2	-6.83	-24.88	-60.6

Table 2 Thermodynamic values for the formation constants of Eu(III) and Tm(III) extracted by HTTA or HTTA-CE in different diluents from nitrate medium of m =0.2 mol/dm^3

REFERENCES

1. Masake Y and Hideyuki N, *Anal. Lett.*, **15**, 1197 (1982).
2. Tang J and Wai CM, *Anal. Chem.* **58**, 3235 (986).
3. Krejzler J and Fidelis IK, *J. Radioanal. Nucl. Chem.*, **85**(1), 57, (1984).
4. Ramadan A, Khalifa SM, Mahmoud M and Souka N, *J. Radioanal. Nucl. Chem.*, **176**(8), 457, (1993).
5. Shehata FA, El-Dessouky SI and Khalifa SM, *J. Radioanal. Nucl. Chem.*, **196**, 369, (1995).
6. Rais J, Tachimori S, Selucky P and Kadlecova L, *Sep. Sci. Tech.*, **29**(2), 261, (1994).

7. Majdan M and Kolarik Z *Solv. Extr. Ion Exch.*, **11**(2), 331 (1993).
8. Shehata FA, El-Hefny N and Aly HF Si*xth Conference of Nuclear Sciences and Applications*, Cairo, 15-20 March (1996).
9. Shehata FA, Khalifa SM and Aly HF, *J. Radioanal. Nucl. Chem.*, **159**(2), 353, (1992).



Petroleum Applications

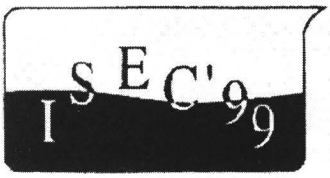

A DEEP DESULFURIZATION PROCESS FOR LIGHT OIL BY PHOTOCHEMICAL REACTION IN AN ORGANIC TWO-PHASE LIQUID–LIQUID EXTRACTION SYSTEM

Yasuhiro Shiraishi,[1] Takayuki Hirai[1] and Isao Komasawa[1,2]

[1]Department of Chemical Science and Engineering, Graduate School of Engineering Science, Osaka University, Toyonaka, Osaka 560-8531, Japan

[2]Research Center for Photoenergetics of Organic Materials, Osaka University, Toyonaka, Osaka 560-8531, Japan

ABSTRACT

A novel deep desulfurization process for light oil, based on uv-irradiation and organic two-phase liquid-liquid extraction, has been investigated. The light oil and acetonitrile are contacted and photoirradiated using a high pressure mercury lamp. The sulfur-containing compounds in light oil, distributed into the acetonitrile phase due to their large polarities, are photooxidized to form highly polarized compounds, which do not distribute into the non-polar light oil phase. Thus in this way, successive removal of sulfur containing compounds from light oil to acetonitrile is carried out under moderate conditions; the sulfur content being reduced from 0.2 to less than 0.05 wt%, meeting with the new regulation in Japan. The overall desulfurization process, involving the separation of the co-extracted aromatics from the acetonitrile, was developed.

Keywords: extraction, photochemical reaction, desulfurization, light oil, dibenzothiophene (DBT), ultraviolet irradiation

INTRODUCTION

Air pollution, caused by diesel exhaust gas, is one of the most serious problems in the world, and much attention has been focused on the deep desulfurization of light oil.[1] A novel desulfurization process for dibenzothiophenes (DBTs) and several sulfur-containing compounds, contained in light oils, by photochemical reaction and liquid-liquid extraction using organic/water two-phase system, has been proposed in previous papers.[2,3] These compounds, when dissolved in tetradecane, were found to be photo-decomposed by the use of a high-pressure mercury lamp and were removed into the water phase. However, the removal of DBT's from light oils was depressed markedly by the presence of naphthalene, because of the triplet energy transfer from the photo-excited DBT to the ground state of naphthalene. The desulfurization was improved by the addition of H_2O_2 alone into the water phase,[4,5] or by the addition of both a triplet photo-sensitizer and H_2O_2 in light oil/water two-phases.[6] In these studies, the basic idea for desulfurization was that of the photo-decomposition of sulfur-containing compounds in the light oil phase, followed by the transfer of the resulting compounds into the aqueous phase. Thus, deactivation of the photo-excited DBTs by naphthalene appeared to be inevitable.

Here a different extraction and photo-reaction system is employed. The basic idea is to transfer the sulfur-containing compounds to another phase, and then to photo-oxidize and decompose them there.[7] Polar solvents, immiscible with the feed oil phase,[8] can be employed as the extraction phase to form an organic two-phase extraction system.

EXPERIMENTAL

The commercial light oil, meeting with the former regulation in Japan (sulfur content: 0.2 wt%) was mixed vigorously using a magnetic stirrer with polar solvent solution in the volume ratio from 50 cm^3/350 cm^3 to 200 cm^3/200 cm^3 with total solution volume of 400 cm3. The solutions were photo-irradiated by the immersion of a high-pressure mercury lamp (300 W, Eikohsha Co., Ltd., Osaka), combined with air bubbling (500 cm^3/min) at atmospheric pressure. The DBT/solvent solution was also employed for photo-reaction studies. The temperature of the solutions was about 323 K during photo-irradiation.

© 2000 Society of Chemical Industry

RESULTS AND DISCUSSION

Liquid-liquid extraction of sulfur-containing compounds.

The extractability of the sulfur-containing compounds and aromatic hydrocarbons from light oil, was studied by contacting the light oil with several polar solvents at room temperature. Table 1 shows a comparison of the sulfur and aromatics content of the feed and treated light oil. In these experiments, acetonitrile is shown to be the most effective solvent for the extraction of the sulfur-containing compounds. The acetonitrile has a lower boiling point and a higher dielectric constant than other solvents, and thus allows the effective extraction of sulfur-containing compounds, which has a relatively large polarity, even at room temperature.

		Before contact	After contact with		
			DMSO	Sulfolane	Acetonitrile
Saturated hydrocarbon	(vol%)	76.2	78.7	79.6	82.0
One-ring aromatics	(vol%)	19.5	18.2	17.7	15.5
Two-ring aromatics	(vol%)	4.3	3.1	2.7	2.5
Total sulfur content	(wt%)	0.1896	0.1644	0.1511	0.1322

Table 1 Aromatic and sulfur content of light oil before and after contact with polar solvents. The volume ratio of light oil/solvents = 1/3

Photoreaction of DBT in polar solvents.

Figure 1 shows the variation with time of the concentration of DBT during photo-irradiation, when dissolved in various solvents. In acetonitrile, DBT was effectively photo-decomposed. This is because the peroxidic intermediates[9] formed by the photo-excitation of DBT are stabilized in the aprotic solvents. Therefore, acetonitrile is regarded to be the most suitable solvent for the photo-reaction of DBT. In acetonitrile, although the decomposition rate for DBT is slightly decreased by the presence of naphthalene, DBT was nevertheless still photo-decomposed satisfactorily. Substituted DBT's, such as 4-methyl-DBT and 4,6-dimethyl-DBT, which are the most difficult components to be desulfurized in the hydrodesulfurization (HDS) process,[1] were effectively photo-decomposed by UV-irradiation. The order of photo-reactivity was: DBT < 4-methyl-DBT < 4,6-dimethyl-DBT, and this tendency was different from the case of HDS.[1] Thus, the present photo-processes are suitable for the deep desulfurization of these compounds.

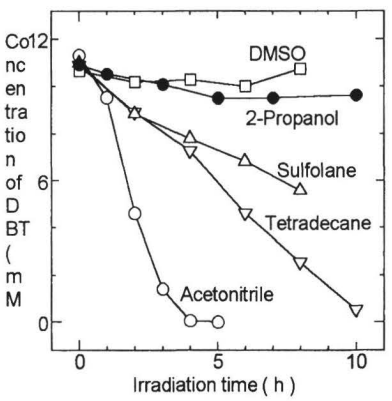

Figure 1. Variation with time of the concentration of DBT dissolved in various solvents, during photo-irradiation

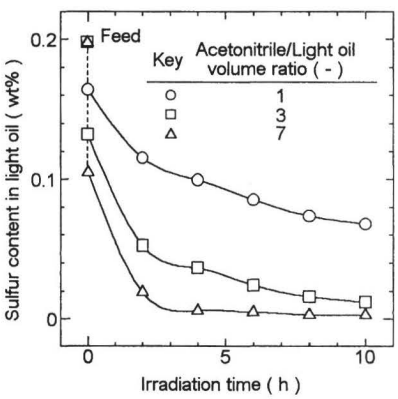

Figure 2. Variation with time of the sulfur content in light oil at various acetonitrile/light oil volume ratio

DBTs were photo-oxygenated and photo-decomposed to form corresponding sulfoxide, sulfone and acidic components, such as sulfonic and carboxylic acid, conjugated with aromatic nuclei.[10] Therefore, DBT is converted to compounds which exist only in the acetonitrile phase. By employing electron-transfer type photo-sensitizers, DBT's were easily photo-oxygenated by the irradiation of visible wavelength radiation ($\lambda > 400$ nm),[11] thus allowing the development of energy-saving desulfurization process.

Desulfurization of light oil using an organic two-phase liquid-liquid extraction system.

Liquid-liquid extraction using an organic two-phase system, combined with the photo-reaction was employed. Figure 2 shows the variations in the sulfur content of light oil with respect to irradiation time, as a function of the oil/solvent volume ratio. The data at an irradiation time of zero are those obtained simply by mixing the two phases, and show the distribution equilibria for the sulfur contents in the organic two-phase system. In combination with photo-irradiation, the desulfurization yield is shown to be much enhanced. At the higher acetonitrile/light oil phase with a volume ratio of 7, 2 hours irradiation decreased the sulfur content to 0.02 wt%, and 10 hours irradiation decreased it to less than 0.005 wt%, which is the value presently strictly legislated in Sweden. The relatively long reaction time required in these studies may be expected to be considerably reduced for industrial use with the development of a photo-reactor of an appropriate advanced design.

The values for the sulfur distribution ratio, D_s, defined as the ratio of the total sulfur content in the acetonitrile and in light oil, are shown in Figure 3. Although the values of D_s for the feed are hardly changed by the volume ratio without photo-irradiation, the ratio increased with increasing volume ratio, when irradiation was applied. At a volume ratio of 7, the values of D_s are increased 11-fold when compared to no photo-irradiation. This indicates that the photo-reaction of DBT's in acetonitrile proceeds more effectively with increasing the volume ratio of acetonitrile. This may probably be the result of a decrease in the photo-scattering and light exclusion by the light oil phase, since the photo-reaction proceeds in acetonitrile phase.

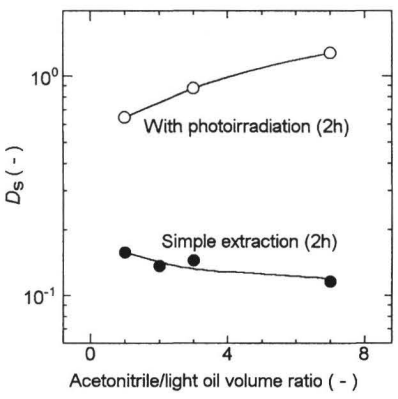

Figure 3. Effect of the photo-irradiation on the sulfur distribution ratio, Ds

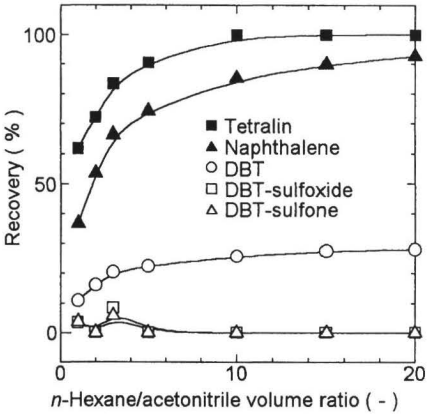

Figure 4. Extractability of aromatic hydrocarbons and photo-oxygenated compounds of DBT from acetonitrile

Recovery of aromatics from acetonitrile and effect of addition of water.

Aromatic hydrocarbons are distributed between the two phases together with the sulfur-containing compounds, as shown in Table 1. To recover them from the acetonitrile, a liquid-liquid extraction procedure was employed, using n-hexane as stripping solvent. Figure 4 shows the extractability of these compounds as a function of the n-hexane/acetonitrile volume ratio. At volume ratios of up to 10, sulfur-free aromatic recoveries of over 85% were obtained for naphthalene and

100% for tetralin. DBT also tends to be extracted, however, it is possible to suppress the transfer to the paraffinic phase by further irradiative conversion to highly polarized components, such as sulfoxide and sulfone.

When contacted, a quantity of acetonitrile is actually distributed into the light oil. Some water is usually added to the polar solvents such as DMSO, sulfolane and tetraethylene glycol to improve the selectivity in the separation and purification of the aromatics.[8] Thus, the effect of the addition of water on the desulfurization was then investigated. The results were shown in Figure 5. Dissolution of the acetonitrile into the light oil was suppressed by the addition of water, especially 10-20 vol%. At this water content region, the desulfurization of light oil by photo-irradiation found to be reasonably feasible.

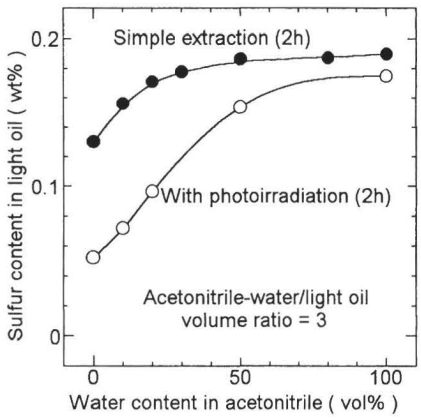

Figure 5. Effect of the water content on the desulfurization of light oil in the case with and without photoirradiation

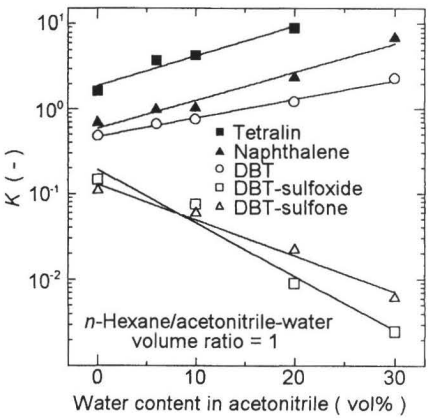

Figure 6. Effect of the water content in acetonitrile on the distribution coefficient, *K*, of each compound

Figure 6 shows the effect of the water content on the distribution coefficient, *K*, defined as the ratio of the concentration of the aromatic hydrocarbons and DBT derivatives in n-hexane to those in the acetonitrile-water mixture. With increasing water content, the values of *K* for the aromatic hydrocarbons are increased, because of the increase in the polarity of the acetonitrile phase. Thus, the addition of water positively affects the separation of aromatic components from the desulfurized sulfur compounds, without decreasing the desulfurization yields. On distilling the resulting mixed solvent following re-extraction, an azeotropic mixture (86% acetonitrile and 14% water, 76) containing no sulfur compounds was obtained, thus the pure azeotropic mixture can be reused as the extraction solvent.

Organization of the process.

A basic flow scheme of the overall process is given in Figure 7. Feed light oil and azeotropic mixture are introduced to the photo-reactor (1). Then, the acetonitrile phase is introduced into the aromatics extractor (2). The aromatic compounds are extracted by a light paraffinic solvent such as n-hexane, leaving the photo-decomposed sulfur-containing compounds. The n-hexane phase was mixed with desulfurized light oil (3) and recovered by light distillation, and therefore, all the sulfur-free aromatics from the feed are mixed with the raffinate light oil phase. The water is used to wash the raffinate for recovery of dissolved acetonitrile (4), and the water phase is then mixed with the remaining acetonitrile phase, which contains sulfur-containing compounds. A pure azeotropic mixture is recovered by the distillation (5), and the pure water was recovered by the sequential distillation (6), leaving the photo-decomposed sulfur-containing compounds at the bottom. The water can be recovered and reused for the washing of raffinate. In this overall process, therefore, the extraction phase (acetonitrile-water azeotropic mixture), aromatic recovery solvent (n-paraffin), and

water can be recirculated.

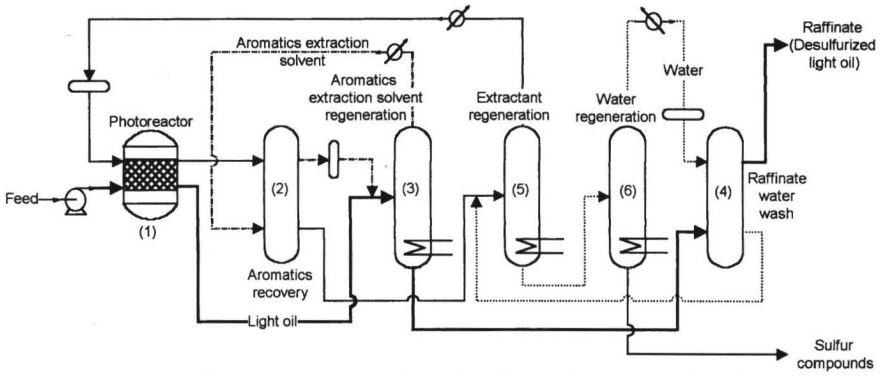

Figure 7. Flow scheme of the deep desulfurization process for light oil

CONCLUSION

A novel deep desulfurization process for light oil by photochemical reaction in an organic two-phase liquid-liquid extraction has been investigated, with the following results.

1) The photo-conversion of DBT's was found to proceed effectively in acetonitrile. The products were highly polarized and are therefore not distributed into the light oil phase.
2) The deep desulfurization of light oil was achieved, by employing the present combination process. The sulfur contents for light oil was reduced to less than 0.005 wt % and thus meeting the new regulation being applied in the near future.
3) The co-extracted sulfur-free aromatics were easily recovered by extraction from the acetonitrile phase using light paraffinic hydrocarbons, leaving the photo-products of DBT in the acetonitrile. This separation was performed with greater ease by the addition of 10 - 20 % water into the acetonitrile. The overall flow scheme of desulfurization process for light oil was proposed, in which all the solvents and water can be recirculated.

REFERENCES

1. Kabe T, Ishihara A and Tajima H, *Ind. Eng. Chem. Res.*, **31**, 1577, (1992).
2. Hirai T, Ogawa K and Komasawa I, *Ind. Eng. Chem. Res.*, **35**, 586, (1996).
3. Hirai T, Shiraishi Y and Komasawa I, *J. Chem. Eng. Jpn.*, **30**, 171, (1997).
4. Hirai T, Shiraishi Y, Ogawa K and Komasawa I, *Ind. Eng. Chem. Res.*, **36**, 530, (1997).
5. Shiraishi Y, Hirai T and Komasawa I, *J. Chem. Eng. Jpn.*, **32**, 158, (1999).
6. Shiraishi Y, Hara H, Hirai T and Komasawa I, *Ind. Eng. Chem. Res.*, **38**, in press, (1999).
7. Shiraishi Y, Hirai T and Komasawa I, *Ind. Eng. Chem. Res.*, **37**, 203, (1998).
8. Lo TC, Baird MHI and Hanson C, *'Handbook of Solvent Extraction'*, John Wiley & Sons, New York, (1983).
9. Sheu C, Foote CS and Gu CL, *J. Am. Chem. Soc.*, **114**, 3015, (1992).
10. Shiraishi Y, Hirai T and Komasawa I, *Ind. Eng. Chem. Res.* (submitted)
11. Shiraishi Y, Taki Y, Hirai T and Komasawa I, *Chem. Comm.*, 2601, (1998).

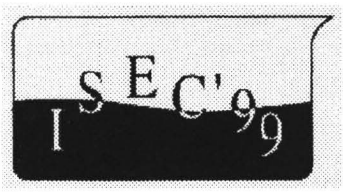

HYDROGEN SULFIDE REMOVAL FROM HYDROCARBONS C_3-C_4

Stratula Costica,[1] Florin Oprea[1] and Florin Enachescu[2]
[1]Universitatea "PETROL-GAZE" Ploiesti, Romania
[2]S.C. ARPECHIM S.A. Pitesti, Romania

ABSTRACT
The subject of the present work is the study of some theoretical and practical aspects concerning H_2S removal from liquid fraction of C_3-C_4. To obtain experimental data concerning H_2S extraction from a C_6 fraction at 20°C, a large number of experiments were made using a column with fine dispersion. Based on the experimental data, the extent of extraction was calculated as function of NaOH solution concentration and of the height of NaOH solution layer as well. Using these experimental data, a new industrial system for H_2S and mercaptans removal was designed. Such a system was successfully applied in two refineries, leading to a reduction of the annual NaOH consumption with more than 50%.

Keywords: Hydrogen sulphide removal, C_3-C_4 fraction, spray column, sodium hydroxide

INTRODUCTION

The liquid fraction of C_3-C_4 hydrocarbons resulted from the catalytic cracking gases by absorption-desorption-distillation is mainly contaminated with hydrogen sulfide (H_2S), mercaptans (RSH) and also carbonyl sulfide. The concentrations of these compounds in the C_3-C_4 fraction is variable, depending on the sulfur content of the processed oil and on the parameters of the stripping column. If the oil is more sulfurous, the sulfur compounds content of the fraction is higher. Also, if the temperature in the bottom of the stripping column is higher, the H_2S content is lower, but the recovery of propylene is lower too. Therefore, the parameters of the stripping column have to be chosen in order to obtain the highest propylene recovery, simultaneous with the highest removal of H_2S.

Even in case of optimizing the stripping column, the liquid fraction of C_3-C_4 hydrocarbons still contains H_2S in the limits 300 - 1800 ppm weight and mercaptan sulfur in the limits 100 - 1100 ppm weight.

When the H_2S content in C_3-C_4 liquid fraction is high, there are three steps of removal for the sulfur compounds in the industrial flow sheets. (Figure 1)

1. The H_2S removal step with aqueous solution of ethanolamine (EA) in regenerative system. This step is used when the initial content of sulfur is high (1000 - 1800 ppm) for the reduction of the sodium hydroxide (NaOH) consumption in the second step. This step can be missing when the initial content of sulfur is low.
2. The H_2S removal step using extraction with aqueous solution of NAOH 10°Bé, a pre-wash step, having the role to protect the concentration of the NAOH solution in the third step (mercaptan sulfur removal).
3. The mercaptan sulfur removal by extraction with aqueous solution of NAOH 20°Bé followed by solution regeneration according to MEROX process.[1,2,3,4]

Some theoretical and practical aspects concerning the second step are presented below.

The study of the H_2S removal from C_3-C_4 liquid fraction by extraction with NaOH solution started from the fact that, in some industrial installations, the pre-wash step (the second step) used a single bubbling vessel provided at the bottom with a distribution system of the C_3-C_4 fraction through NaOH solution. Our analysis of such a bubbling vessel showed that the H_2S could be removed only in a small proportion, the most important part of H_2S was removed in the third step, with unfavourable consequences concerning the concentration of the NaOH solution in this step, the RSH removal and the operation costs.

© 2000 Society of Chemical Industry

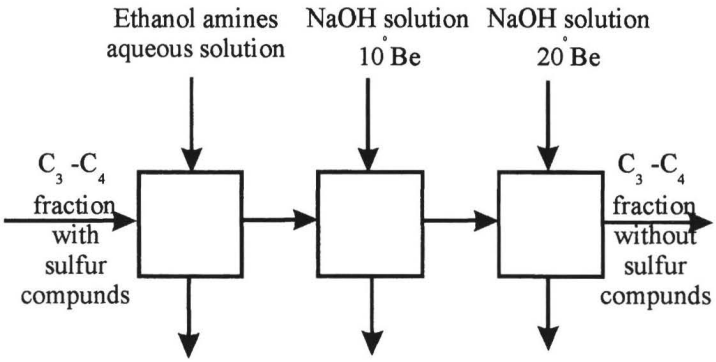

Figure 1. The three steps for sulfur compounds removal from the liquid fraction of C_3-C_4 hydrocarbons

It can be assumed that using one single bubbling vessel for H_2S removal is based on the fact that reaction (1) between NaOH and H_2S is a fast non-reversible reaction and a simple contact is sufficient to entirely remove the H_2S:

$$2NaOH + H_2S \rightarrow Na_2S + 2H_2O \qquad (1)$$

In fact, in the liquid-liquid extraction with chemical reaction, similar to absorption with chemical reaction, the literature[5,6,7] shows that mass transfer based on an extremely quick chemical reaction is not controlled by the reaction speed, but by the coefficient of the physical mass transfer. Thus the overall resistance at mass transfer is controlled by the diffusion through liquid phases and not by the reaction rate. Therefore, to entirely remove the H_2S from the C_3-C_4 liquid fraction, the vessel must be replaced with an extraction column equipped with more contacting trays as in the case of the systems with extraction without chemical reaction or with reversible chemical reaction. Similarly, for removal of H_2S and CO_2 from pyrolysis gas using extraction in NaOH solution, there are two absorption steps with 15 - 20 practical trays each. This number of trays was highlighted by Picciotti.[8]

EXPERIMENTS ON HYDROGEN SULFIDE REMOVAL

Most literature data describe only the H_2S removal from gaseous hydrocarbons by absorption in NaOH solution. The experimental part of the present work proposes to study H_2S removal from liquid hydrocarbons with the same NaOH solution. It uses an extraction column having at the bottom a simple porous plate for distribution of the liquid phase (hydrocarbons) through the stationary phase of NaOH solution. The scheme of the experimental set with the involved streams is presented in the figure 2. This study tried to determine the influence of two parameters versus the extraction degree of H_2S, namely:

- the concentration of NaOH solution;
- the height of the liquid layer.

NaOH solutions were used with the following concentrations: 0.5% weight, 1.0% weight, 3.0% weight, 5.0% weight, 7.0% weight, 10.0% weight. The height of the liquid layer in the column was 0.45 m, 0.90 m, 1.35 m (figure 2).

The experiment consisted of the following: the extraction column was filled with NaOH solution to a certain level. The hydrocarbons liquid fraction (hexane fraction) was saturated with a maximum 110 - 120 ppm weight H_2S to avoid H_2S losses by evaporation during the experiment and was fed by a pump. The distribution system at the bottom of the column produces a fine dispersion with drop size 0.2 - 0.6 mm diameter. Only 200 cm^3 hexane fraction was used each time to avoid

significant decrease in the concentration of the NaOH solution. The concentration of H_2S in the hexane fraction, before and after the column, was analyzed using UOP method.[9]

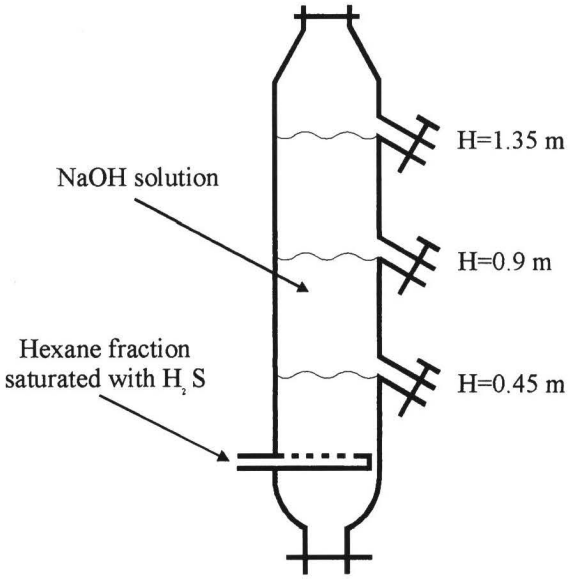

Figure 2. Experimental installation

50 experimental determinations were made and, based on the results, the extent of extraction was calculated using the following formula:

$$\varphi_e = \frac{Y_i - Y_e}{Y_i} \cdot 100 \qquad (2)$$

The calculated data are graphically represented in figures 3 and 4.

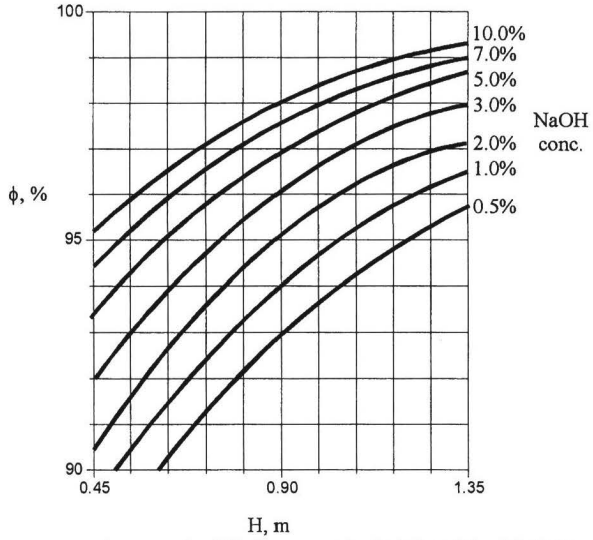

Figure 3. The extent of removal of H_2S versus the height of the NaOH solution layer for different NaOH concentrations

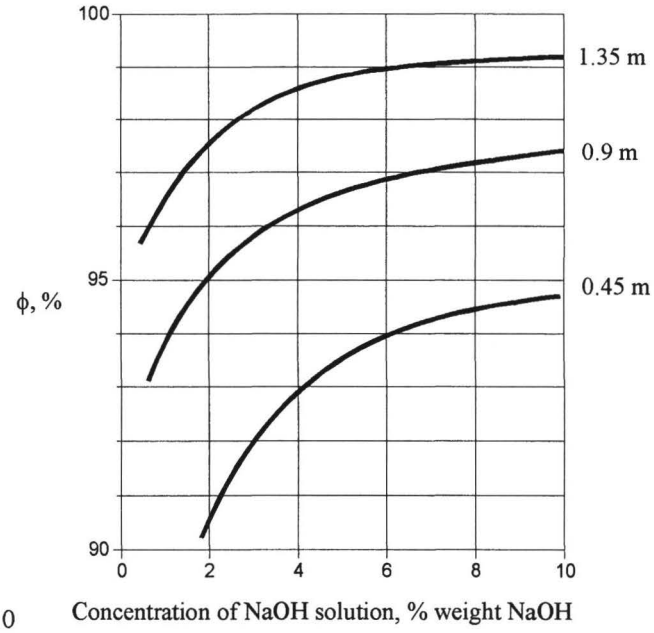

Figure 4. The extent of removal of H_2S versus the concentration of NaOH solution for different heights of NaOH solution layer

DISCUSSION

The analysis of these figures lead to the following conclusions:

1. The H_2S extraction degree is a function both of the NaOH solution concentration and of the height of the solution layer.
2. The extent of H_2S extraction increases with the increase of the NaOH solution concentration, but this increase diminishes in the range of concentration higher than 7% weight NaOH. As result, for pre-washing of C_3-C_4 liquid fraction it is not recommended to use NaOH solutions with more than 7% weight concentration.
3. The H_2S removal is important even at low concentration of NaOH solution (0.5 - 1% weight) leading to a H_2S extraction degree of by 80 - 95%, but only in conditions of a good contacting between the disperse liquid phase and the stationary solution i.e a fine dispersion and enough height of the solution layer.
4. The extent of extraction increases rapidly with the increase of the height of the solution level up to 0.9m, after that, the increase becomes much slower. The explanation is that at the beginning, the mass transfer, which takes place at the exterior surface of the drop, is rapid. After that, the mass transfer decreases because it is limited by the speed of the physical mass transfer, which takes place between the interior of the drop and the exterior surface, and then in the entire solution. Therefore, to be sure, a second dispersion system of the hexane fraction was introduced after the liquid level of 0.45m; this will lead to an increase of the H_2S extraction up to the level of 0.9m, comparative with the case without supplementary dispersion for the same 0.9m height. To highlight this, the experiment was simulated on the same column by taking the fraction after 0.45 m and reintroducing it again at the bottom of the column. Thus the hexane fraction was taken after 0.9m, but with two distribution systems. In this experiment the H_2S concentration decreased from

118 ppm to 8 ppm, comparated with the system with one dispersion that decreased only to 16 ppm for the same height (0.9 m). The extraction degrees are:

for the system with one dispersion:

$$\varphi_e = \frac{118-16}{118} \cdot 100 = 86\%;$$

for the system with two dispersions:

$$\varphi_e = \frac{118-8}{118} \cdot 100 = 93\%;$$

The conclusion is clear, using a single extraction vessel with a single dispersion system at the bottom does not represent an efficient technical solution for high H_2S removal. The industrial dispersion systems do not generate fine particles like those in the laboratory column. Therefore, to obtain high H_2S removal from the C_3-C_4 liquid fraction the use of an extraction column with more distribution systems (sieve trays) is recommended, even if the reaction between NaOH and H_2S is irreversible and proceeds rapidly. Also, the experimental data show that, by using an extraction column with more sieve trays, high removal of H_2S can be achieved even at a low concentration of NaOH solution (0.5 - 1%). Therefore it is recommended to use two distinctive extraction steps: the stage with low concentration of NaOH must be the first contact with C_3-C_4 liquid fraction and the stage with high concentration (fresh solution) must be the final concentration stage. In this way, the NaOH solution can be used until completely exhausted and the NaOH consumption will be reduced by more than 50%. Also, the exhausted solutions, which represent an ecological problem, are reduced in the same proportion. Such a system was applied with success in two refineries.

NOMENCLATURE:

Y_i - H_2S input concentration, ppm weight;

Y_e - H_2S output concentration, ppm weight;

φ_e - extraction degree, %.

REFERENCES

1. Brown KM, Verachtert T, Assolin F and Salazar JR, *"Applications and Developments in the UOP MEROX Process", UOP Technology Conference*, March 1978.
2. Holbrook LD, Arena BJ, Verachtert T and Bricker JO, *"MEROX Processes for Caustic Minimization and Management"*, UOP, Des Plaines, Illinois, Revision 1, July, 1994.
3. Salaper JR, *"UOP MEROX Process", Handbook of Petroleum Refining Processes,* McGraw Hill Book Comp., (1986).
4. Stachle BE, *"MEROX Twenty-five Years of Change. Technical for a Changing Industry", UOP Technology Conference,* September 1985.
5. Van Krevelen DW, and Hoftyzer PJ, *Chem. Eng. Progr.*, **44**, 7, 529, (1948) and *Chem. Eng. Sci.*, **2**, 145, (1953).
6. Van Krevelen DW, *Chem. Eng. Techn.*, **30**, 9, 556, (1958).
7. Nonhebel G, *Gas Purification Processes for Air Pollution Control,* Newnes-Bulter-Warths, London (1972).
8. Picciotti M, *Hydroc. Proc.*, **4**, 89, (1978).
9. UOP method 3131/1967.



Pharmaceutical Applications

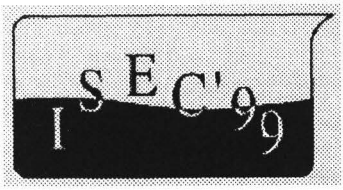

EXTRACTION OF CITRIC ACID IN HOLLOW FIBRE MODULES

Ireneusz Miesiac, Piotr Kirschling and Jan Szymanowski
Poznan University of Technology, Institute of Chemical Technology and Engineering, Poznan, Poland

ABSTRACT
Extraction of citric acid was investigated in the batch extraction-stripping system containing two Liqui-Cel 2.5x 8" modules from Hoechst Celanese. Kerosene containing 6 - 14% trioctylamine or sec-tridecylamine as carrier and 5 - 15% of iso-tridecanol as a modifier was used as the organic phase. The feed phase consisted of 3% citric acid solution and the strip phase was 0.1 - 0.5 mol/dm^3 sodium hydroxide. Both the aqueous phases were circulated in the tube-side of hollow fibre contactors, whereas the organic phase was circulated in the shell-side. The distribution coefficients of citric acid in the extraction system varied from 0.4 to 7.5 and increased considerably with the carrier concentration.
The citric acid flux from the feed to the strip phase was strongly affected by the carrier concentration in the organic phase and the NaOH concentration in the strip phase. It attained a maximal value of about 17 mM/m^{2}h when the carrier concentration was above 10%, regardless of the kind of carrier, and for NaOH concentration at least 0.25 mol/dm^3. The flux was practically independent on the flow rate of the organic phase in the range of 20 - 120cm^3/min and on the flow rate of both aqueous phases of 0.2 - 0.8 dm^3/min.

Keywords: citric acid, hollow fibre, extraction, amine

INTRODUCTION

Among the fruit acids used in the beverage and food industry citric acid holds a cardinal place; it also finds application in the pharmaceutical and in the chemical industry generally. More than 90% of citric acid is produced by fermentation of sugar containing raw materials. The process occurs in the large volume fermentation tanks for 6 - 10 days and gives a final product at a concentration of 15 - 20%. Conventionally, the fermentation broth is first filtered, then the citric acid is precipitated as the calcium salt by adding lime and then liberated as a fairly pure compound by adding sulphuric acid. It is further purified by ion exchange and decolourised by active carbon. The final product is obtained after evaporation and crystallisation as a monohydrate.[1]

The repeated precipitation, filtration, and disposal of unusable calcium sulphate are the main drawbacks of the conventional process. An alternative route, liquid extraction using reversible chemical complexation, could lead to continuous recovery of citric acid and to eliminate the batch process. The recovery rate should correspond to fermentation productivity, which is 0.8 -1 kg/m^{3}h (4.2 - 5.2 mM/dm^3 h).[1]

In several works the use of amines and amides as complexing agents has been described.[2,3] For the extraction of citric acid, the use of tertiary alkylamines is preferred and the extraction constants for different diluents reported.[4] Also various diluents have been proposed using different temperatures for extraction and stripping.[5,6] To overcome the problems of emulsion formation during the extraction process, especially from natural fermentation broths, novel membrane techniques were introduced to separate both the contacting phases. In the so-called supported liquid membrane a carrier solution in an organic solvent is placed in a microporous support that separates both feed and strip aqueous phases. Nevertheless, such a membrane is not enough stable for a lengthy use due to its partial solubility in water, osmotic flow of water and progressive wetting of the support pores.[7] For this reason, nowadays the most commonly investigated membrane system for extraction processes consists of two hollow fibre modules, where the circulating membrane phase facilitates the transport of extracted species from the feed phase to the strip. An important advantage of such a system is the enormous specific area of phase contact in the range of 3000 m^2/m^3. The obtained fluxes of citric acid vary from 8.2 to 109 mM/m^{2}h, depending on the experimental conditions.[3]

© 2000 Society of Chemical Industry

EXPERIMENTAL

Reagents and Apparatus

The experimental system consisted of two hollow fibre Liqui-Cel 2.5 x 8" contactors (Hoechst Celanese) with crossflow configuration. A double Masterflex peristaltic pump was used to circulate both the aqueous phases inside the fibres. The circulation flow rate was in the range of 200 - 800 cm^3/min., and the total volume of each phase, including the associated piping, was 420 cm^3. The membrane phase was circulating through both the contactors on their shell sides at the flow rate of 20 - 120 cm^3/min by using a membrane pump (Prominent Gamma/4W 0408 PP, Germany). The total volume of circulating membrane phase was also 420 cm^3.

The distribution coefficients were measured for given membrane phase and 3% citric acid aqueous solution in volume ratio of 1:1, after shake time of 30 min.

The membrane phase consisted of: kerosene (Exsol D 200/240, Esso); Amberlite LA 2, (N-lauryl-trialkylmethylamine, M = 351-393, (Serva), TOA (trioctylamine), (Serva), HOE F 2562 (di-tridecylamine), (Hoechst) were used as carriers at concentrations of 6 - 14%; with modifiers: iso-tridecanol, (Hüls) and n-decanol, (Serva) at 10% concentration.

The feed phase consisted of citric acid, reagent grade monohydrate (98%, Fluka), as a 3% solution (156 mM) in distilled water, while the stripping phase was an alkaline solution of 0.05 - 0.5 mol/dm^3 NaOH.

Analytical methods used to determine the extent of extraction: potentiometric titration of aqueous phases using 0.1 mol/dm^3 NaOH or HCl and measurement of refraction coefficients of both aqueous phases using a Jamin interferometer (Zeiss Jena)

RESULTS AND DISCUSSION

Transport of citric acid, one of the most hydrophilic compounds, through an organic membrane phase requires an appropriate hydrophilicity of the membrane. On the other hand, many of suitable organic solvents are not neutral enough in relation to live fermentation media and act as a poison.[8] For this reason, the solvent of choice in biotechnological systems is kerosene, free of aromatics, accompanied with appropriate carriers and modifiers to improve its hydrophilicity.

Carrier Type	Carrier conc. %	Modifier conc. %	Distribution coeff
HOE F2562	6	10	0.87
HOE F2562	10	10	2.46
HOE F2562	14	10	7.47
HOE F2562	6	5	0.88
HOE F2562	6	15	0.96
TOA	6	10	0.37
TOA	6	10 (decanol)	0.39
LA 2	6	10	0.37

Table 1 Distribution coefficients of citric acid between kerosene (with carrier and modifier) and 3 % aqueous solution (20C)

Three different alkyl amines were used as carriers, because of their complexing ability as liquid anion exchangers. Surprisingly, the distribution coefficients of citric acid (Table 1) in the system containing TOA, the most basic from the carriers investigated, were the lowest and did not exceed 1. Higher values of the distribution coefficient were obtained for a secondary tridecylamine (HOE F 2562) and they increased strongly to about 7.5 with increasing carrier concentration in the organic phase in

the range of 6 to 14%. The effect of modifier concentration and its alkyl chain length was weak and could be neglected.

A typical change of citric acid concentration in the feed and strip phase during the extraction process is shown in Figure 1. From the linear slope of the strip phase concentrations, the overall fluxes of citric acid were calculated. Such values were in an agreement with those obtained from pH change in the strip (Figure 2). The inflection point at pH ca. 5 corresponds to disodium citrate, which means the neutralisation of 0.25 mol/dm^3 NaOH by 0.125 mol/dm^3 citric acid after a given time, e.g. 110 minutes. Then the flux calculated was equal to about 20 mM/m^{2}h. The value obtained from corresponding slope of strip concentration was equal to 16.9 mM/m^{2}h.

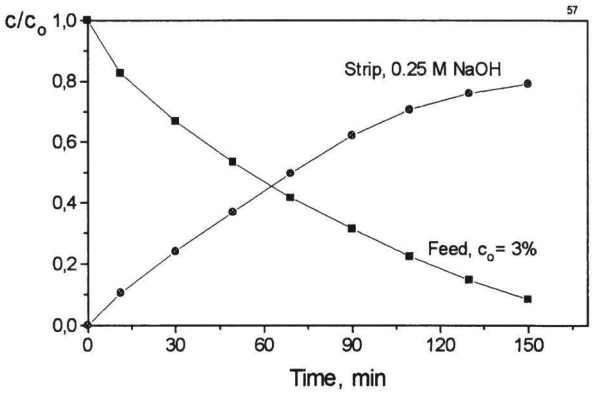

Figure 1. Citric acid concentration in the feed and strip phase for the typical extraction process in the hollow fibre system (carrier HOE F 2562, 14%).

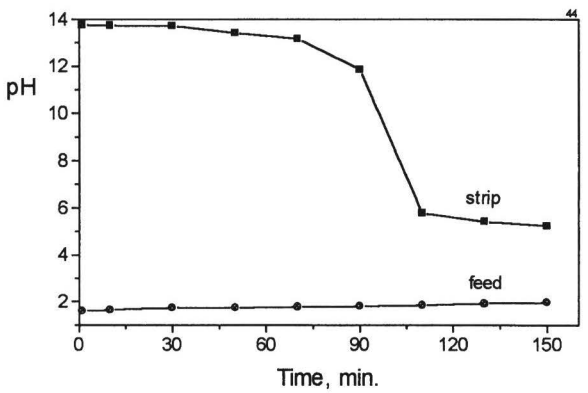

Figure 2. Change of pH in the feed and strip phase during the extraction of citric acid (carrier HOE F 2562, 10%; initial citric acid concentration, 3%; initial NaOH concentration in the strip phase, 0.25 M).

The flux increases linearly when the carrier concentration rises until ca. 10% and then maintains its maximal value of about 17 mM/m^{2}h (Figure 3). The effect of the carrier employed can be neglected. It means that at the concentration of alkylamines above 10% in the membrane phase, the system becomes hydrophilic enough to transport the citric acid efficiently, regardless of the nature of amines

used. The formation of a specific microemulsion system containing the hydrated amine-citric acid complex and amine in the aprotic form as a co-surfactant cannot be excluded.

According to the anion exchange mechanism, alkalinity of the stripping solution is necessary to make the extraction process reversible and to regenerate the used carrier molecules. A similar effect can be also obtained by increasing temperature on the stripping side.[6] At normal temperature in the absence of NaOH no stripping is observed. The flux of citric acid increases sharply until the concentration of NaOH equals 0.1 mol/dm^3, then it becomes constant over 0.25 mol/dm^3 NaOH (Figure 4). It means that the stripping stage behaves as an interfacial chemical reaction with the equilibrium depending on the NaOH concentration and such a reaction or wetting process at the interface can limit the whole process kinetics being more important than the diffusion resistance in the membrane pores.

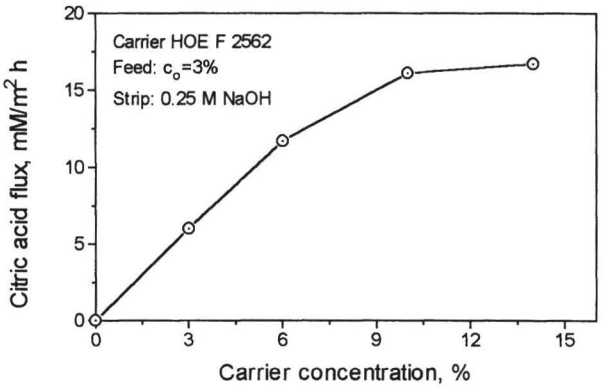

Figure 3. Effect of carrier concentration (HOE F 2562) in the membrane phase on the flux of citric acid.

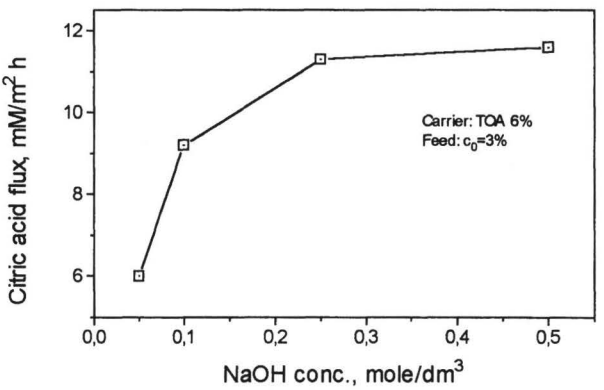

Figure 4. Effect of NaOH concentration in the strip phase on the flux of citric acid (TOA, 6% as carrier).

The observed flux of citric acid slightly increases with an increasing flow rate in the range of 20 -120 cm^3/min (Figure 5). With further increase of membrane phase flow rate up to 10 dm^3/min one may expect considerably greater mass transfer efficiency due to cross flow mechanism.[9]

On the contrary the flow rate of both aqueous phases in the range of 0.2 - 0.8 dm^3/min did not significantly influence the citric acid flux. This supports the assumption that the chemical reaction at the interface water-organic phase is the limiting step for the whole extraction process.

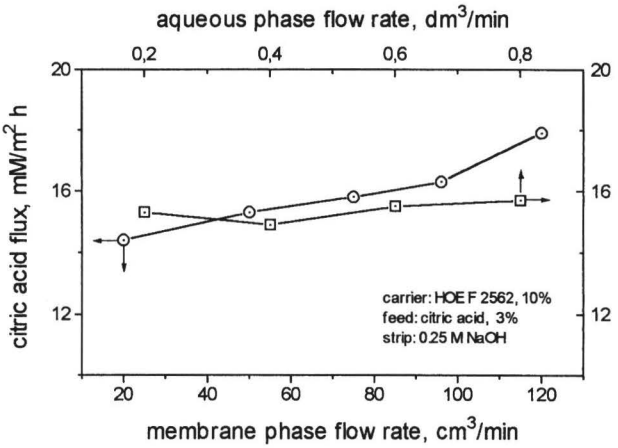

Figure 5 Effect of flow rates of the membrane phase and both the aqueous phases on citric acid flux

ACKNOWLEDGEMENT

The work was supported by the University grant BW 32/285/98.

REFERENCES

1. Messing W and Schmitz R, *Chemie Exper.Didakt.*, **2,** 309, (1976).
2. Baniel AM, Blumberg R and Hajdu K, *US Pat. 4 275 234* (1981).
3. Basu R and Sirkar KK, *AIChE Journal*, **37**, 383, (1991).
4. Bizek V, Horacek J and Kousova M, *Chem. Eng. Sci.*, **48,** 1447, (1993).
5. Wennersten R, *Proc. ISEC 1980*, **2**, 63-67, (1980).
6. Rockman JT, Kehat E and Lavie R, *Proc. ISEC 1996*, 857, (1996).
7. Danesi PR, Reichley-Yinger L and Rickert PR, *J. Membrane Sci*, **31**, 117, (1987)
8. Reschke IM and Schügerl K, *Chem.Biochem. Eng.J.*, **28**, B1-B4, (1984).
9. Cussler EL, *NATO Advanced Study, Inst. Membr. Proc. in Separation and Purification, Curia, Portugal*, (1993).

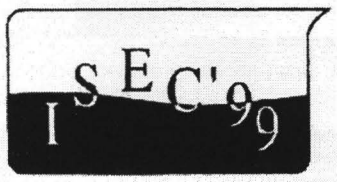

SOLVENT EXTRACTION OF PHTHALIC ACID WITH BASIC EXTRACTANTS, AND THE STRUCTURE OF THE COMPLEXES FORMED

Subhas Rambocus, Neil Kelly and Bryan G Reuben
Division of Chemical Engineering, South Bank University, London SE1 0AA, UK
Alex Drake
Department of Pharmacy, King's College, Manresa Road, London SW3 6LX, UK

ABSTRACT
The extraction of phthalic acid from aqueous solution into dichloromethane containing a range of extractants was studied. At low pH, the basic extractants differed little in extraction capability but came in the order: tetraoctylammonium chloride > Aliquat 336 > Alamine 336 = Alamine 304-1 > tetrabutylphosphonium chloride > tetrabutylammonium chloride. All the basic extractants were much more effective than the solvating extractant, trioctylphosphine oxide. The extraction level rose with rising pH, peaked at about pH 4, and then decreased. Distribution coefficients and free energies of ion exchange were calculated. Measurement of extraction at various pH values indicated that the singly charged hydrogen phthalate ion was the main species extracted, and a model was developed to predict the variation of extraction with pH. Nonetheless, a small amount of phase transfer at high and low pH's indicated extraction of doubly charged phthalate ions and of neutral phthalic acid. The structures of the complexes were investigated by a range of spectroscopic techniques notably FTIR and NMR (^{13}C and ^{1}H) at pH values 1.0, 4.2 and 8.0 corresponding to neutral, singly and doubly charged phthalate ions. Co-extraction of water was also measured by Karl Fischer titrations. Phthalate:extractant 1:1 complexes were formed in the neutral and singly charged regions, and 1:2 complexes in the doubly charged region. On the other hand, UV and FTIR monitoring of the complex of solid phthalic acid with Aliquat 336/dichloromethane in the absence of water indicated a 1:2 acid:quaternary ammonium complex at pH 1.0, showing that when phthalic acid is extracted from aqueous solutions, water is ultimately involved in the complex formed.

Keywords: phthalic acid, quaternary ammonium salts, tertiary amines, hydrogen phthalate ions, basic extractants.

INTRODUCTION

We have reported previously on factors governing the selectivity of liquid-liquid ion exchange of anions[1] and the theory underlying such extractions.[2] We have also described the extraction of amino acids with cationic extractants,[3,4] the point being that that amino acids can exist as cations, anions or zwitterions. The singly charged cations are easily extracted with dinonylnaphthalenesulphonic acid, and there is some evidence that doubly charged ions of amino acids containing two amino groups are extracted by two molecules of extractant.

The work reported here describes the extraction of phthalic acid (a dicarboxylic acid; pK_1 = 2.95 and pK_2 = 5.41) with anionic extractants. We shall report elsewhere on the extraction of a wider range of dibasic acids.[5] King *et al* have published a series of papers on extraction of carboxylic acids with tertiary amines and quaternary ammonium salts,[6,7] although they admitted that the stoichiometry of the complexes that they deduced required further independent evidence, perhaps from spectroscopy to confirm their structures.

THEORY

Initial inspection of results indicated that overwhelmingly the dominant process is extraction of the single charged hydrogen phthalate ion. It is thus possible to write a simple mechanism, made up of the dissociation of the acid in the aqueous phase:

$$H_2A \xleftrightarrow{K_1} HA^- + H^+ \xleftrightarrow{K_2} A^= + 2H^+ \qquad (1)$$

© 2000 Society of Chemical Industry

where K_1 and K_2 are the first and second acid dissociation constants, followed by an extraction stage, equilibrium constant D:

$$HA^-_a + QCl_{org} \xleftrightarrow{D} QHA^-_{org} + Cl^-_a \qquad (2)$$

where QCl_{org} is the extractant. If the volumes of aqueous and organic layers are equal, the initial concentrations of acid and extractant are a and b, and the hydrogen ion concentration is H, then the fractional extraction E is the solution to the quadratic equation:[5]

$$(aH + K_2a - DHa + aH^2/K_1)E^2 + DH(a + b)E - DHb = 0 \qquad (3)$$

Because the ionic strengths of the solutions remain constant, the activity coefficients cancel out, to a first and even a second approximation. The positive sign on the square root term in the solution to the quadratic equation is appropriate.

EXPERIMENTAL

Henkel kindly donated the extractants Aliquat 336 (tri-*n*-C_8/C_{10}-alkylmethylammonium chloride; Aliq 336), Alamine 336 (tri-*n*-C_8/C_{10}-alkylamine; Ala 336), and Alamine 304-1 (trilaurylamine; Ala 304-1). Phthalic acid, tetrabutylammonium chloride (TBACl), tetraoctylammonium bromide (TOABr), tetrabutylphosphonium chloride (TBPCl) and trioctylphosphine oxide (TOPO) were obtained from Aldrich, and dichloromethane from BDH. The Alamine 304-1 and TOABr were converted to the chloride salt before use. Otherwise the materials were used as received.

Aqueous phthalic acid concentrations were measured by UV-spectrometry with a Perkin-Elmer lambda 2 UV/VIS version 3.4 or by ion chromatography. Other spectra were run on a Brucker AMX-400 NMR spectrometer and a Perkin Elmer 1605 FTIR spectrometer. Chloride concentrations were measured with a Dionex 4000*i* ion chromatograph fitted with an OmniPak PAX-100 column. Extraction of water into organic phases was measured with a conventional Karl Fischer apparatus.

In a typical extraction, 10 cm^3 of 50 mM phthalic acid was shaken vigorously for about 10 minutes with an equal volume of 100 mM extractant in dichloromethane (chosen partly because CD_2Cl_2 was suitable as an NMR solvent). The phases were allowed to settle and, if necessary, centrifuged. All experiments were performed at room temperature.

RESULTS

Variation of extraction with pH

Figure 1 shows the extraction of 50 mM phthalic acid by 100 mM solutions of four of the extractants. Data for the others were similar but crowded the diagram. The percentage of acid extracted rose with rising pH, went through a maximum at about pH 4 and then decreased with further increase in pH.

The basic extractants in order of effectiveness about pH 4 were: tetraoctylammonium chloride (TOACl) > Aliq 336 > Ala 336 = Ala 304-1 > TBPCl > TBACl. The extraction efficiencies were broadly similar to the proportion of singly charged ions in the phthalic acid at the different pH values, and this was evidently the species most easily extracted. The basic extractants were all more effective than the solvating extractant, TOPO, whose extraction curve did not go through a peak and which followed broadly the concentration of undissociated phthalic acid molecules in the system.

The results were modeled in terms of equation (3), the parameters K_2 and D being optimized by the non-linear regression programme Microsoft Excel "Solver". As most of the extractions approached 100%, and the experimental measurement was of phthalic acid remaining in aqueous solution, the sum of the squared percentage errors in $(1-E)$ compared with the theoretical model was minimized. The K_2 values were included in the optimization on the advice of M.M. Anwar, who pointed out the susceptibility of dissociation constants, especially second dissociation constants, to apparently trivial

factors such as dissolved carbon dioxide.[8] The regression lines, shown in Figure 1, are an excellent fit. The optimized values of D and K_2 and the derived free energies of phase transfer for the hydrogen phthalate ion are given in Table 1. The TOPO figures and theoretical line refer to the undissociated phthalic acid molecule.

	TOPO	TBPCl	TOACl	TBACl	Ala 304-1	Ala 336	Aliq 336
$K_2 \times 10^{-5}$		28.9	45.8	3.54	10.5	6.46	6.46
D	1.86	357	2186	87.2	697	657	1205
ΔG_t° kJ/mol	-1.53	-14.6	-19.1	-11.1	-16.2	-16.1	-17.6

Table 1 K_2, D and ΔG_t° for the extraction of phthalic acid with basic extractants

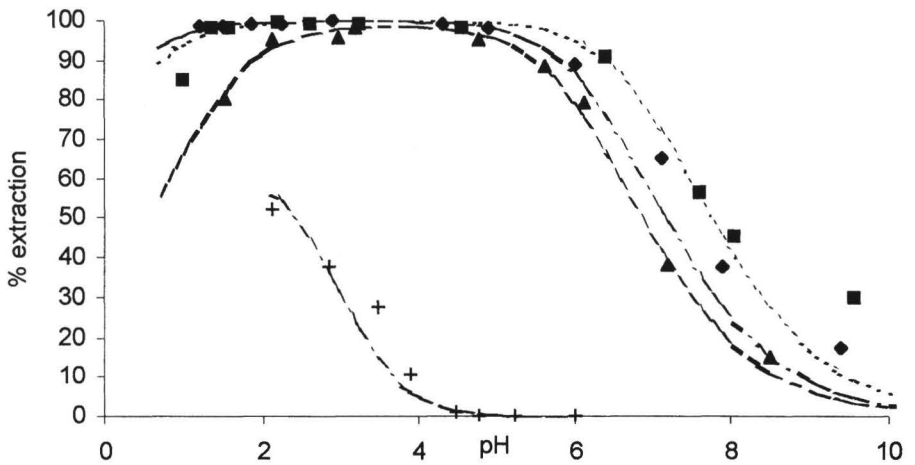

Figure 1. Extraction of 50 mM phthalic acid by 100 mM basic extractants in CH_2Cl_2
◆ TOACl ■ Aliq 336 ▲ TBACl + TOPO

Apart from TOPO, the free energies cluster between −14.6 and −19.1 kJ/mol. The two numerically lowest figures (for TBACl and TBPCl) reflect their lower lipophilicity and higher water solubility. The highest figure reflects that TOACl is the most lipophilic of all the extractants. Evidently the large quaternary ammonium and alkylammonium cations do not bind in a particularly structure-specific way to chloride and hydrogen phthalate ions. This is not a trivial conclusion. One might have expected a tertiary ammonium ion, where one side is open and allows access to small ions, to behave differently from a spherically symmetrical ion.

Spectroscopic studies

In spite of the quality of the fit, experiments at high and low pH with large excess of extractant indicated that phthalic acid was being extracted at pH values where it would be expected to exist as either undissociated molecules or doubly charged cations. The extracts with Aliquat 336 at different pHs were examined by ^{15}N, ^{13}C and ^{1}H NMR. The ^{15}N spectra showed only one nitrogen peak between 38.62 and 38.74 ppm and not the hoped-for bonding to an anion. This may have been due to the low abundance and poor receptivity of ^{15}N. The ^{13}C chemical shifts of the Aliquat 336-phthalic acid complex at pH 1, 4.2 and 8 are shown in Table 2. The peaks due to N-CH_3, N-CH_2, and terminal CH_3 did not alter and have not been listed. A shift of 0.5 ppm is significant in ^{13}C NMR. $C_{aromatic}$, C-$H_{aromatic}$

and C=O all experienced shifts too large to be pH induced and must be due to complexation at pH 8. The fact that only two signals are observed for C-$H_{aromatic}$ indicates that the complex is symmetrical and supports the hypothesis of a 2:1 complex.

In the ^1H spectra, the C-$H_{aromatic}$ peaks appeared at 7.50 and 8.09 ppm at pH 1; 7.487 and 8.307 at pH 4.2; and 7.28 and 7.80 at pH 8. A shift of 0.2 ppm is significant. At pH 8, the peak of C-$H_{aromatic}$ closer to the carboxyl group has shifted by 0.5 ppm upfield. Like the ^{13}C spectrum, this shift supports the formation of a 1:2 acid: ammonium ion complex. It is probably a straightforward ion pair with an ammonium group pairing with each carboxyl.

Peaks	pH 1.0	pH 4.2	pH 8
C=O	170.45	170.51	173.5
$C_{aromatic}$	135.02	135.73	138.66
C-$H_{aromatic}$	131.26 & 132.17	131.18 & 133.72	128.67 & 129.92

Table 2 ^{13}C NMR chemical shifts (ppm) for phthalic acid (50 mM) extracted with Aliquat 336 in CD_2Cl_2

The spectrum at pH 1 also indicates a symmetrical complex. In the unpaired phthalic acid molecule, it is likely that weak hydrogen bonding occurs between the C=O group of one carboxyl and the C-OH of the other. In the ion-paired complex, one can either envisage the quaternary ion interacting with this system, or with the hydrogen bond breaking and the quaternary ion interacting simultaneously with the negative charge of the two carboxyls.

The identity of the 1:1 complex at pH 4.2 is less clear. Experiments with monomethyl phthalate show that Aliquat 336 binds strongly to its singly charged ion, so that in this case the quaternary ion probably pairs with the singly charged COO^-, but only two signals are observed in the ^{13}C spectrum. Perhaps the hydrogen atoms in the meta positions are too distant to be affected.

We hope to elucidate these problems by a comparison with spectra obtained from extraction of sulphobenzoic acid.

The FTIR spectra of phthalic acid extracted from aqueous solutions indicated marked uptake of water especially at pH 1, and this might have been involved in the ion pairing. Experiments were therefore conducted with solid phthalic acid "dissolved" in Aliquat 336/dichloromethane. Attempts to mimic higher pHs by uses of mono- and dipotassium phthalates failed because they were not appreciably soluble.

Solid phthalic acid was treated with Aliquat 336/dichloromethane, in quantities that would have given acid:extractant molar ratios of between 1:0.5 to 1:12, and the extracts analyzed. FTIR and UV spectra both showed a linear rise of C=O peak height with Aliquat 336 concentration up to a molar ratio of 1:2, which then leveled off. This was taken as evidence of a 1:2 complex.

^1H NMR spectra of the phthalic acid extracted from aqueous solution and from solid were not identical. The C-$H_{aromatic}$ peaks from the solid extract appeared at 7.50 and 7.81 ppm instead of 7.50 and 8.09. Thus the peak due to the ortho C-H has changed its charge environment, presumably because of some interaction with water that reduces the charge intensity around the undissociated carboxyl groups.

In spite of careful drying of the reagents, a small water peak at ~3300 cm^{-1} was visible in the FTIR spectrum of Aliquat 336 and this was partly suppressed when the phthalic acid was added. This indicates strong bonding between phthalic acid and water.

Solutions of Aliquat 336 were shaken with water and with phthalic acid solutions, and the water in the organic layers measured. Graphs of water extracted against Aliquat concentrations were linear and had slopes of 1.59 in the presence of phthalic acid and 1.79 in its absence. Further experiments with Aliquat 336 bromide and Aliquat 336 iodide indicated that the chloride (i.e. Aliquat 336 itself) took up two molecules of water per molecule Aliquat. The bromide took up 0.9 and the iodide 0.4. The

implication of the chloride/bromide/iodide results is that the co-extracted water is associated with the extractant anion

Other experiments

The above hypotheses were tested further by measurement of the variation of percentage extraction with excess extractant at pH 1, 4.2 and 8, and by measurement of the concentrations of chloride ions in the aqueous layer after extraction, also at various pH values. The results will be reported elsewhere.[5]

CONCLUSIONS

Phthalic acid can be extracted from solution by basic extractants in dichloromethane. The hydrogen phthalate ion is most easily extracted, with free energies of ion exchange varying between –14.6 and –19.1 kJ/mol. The less lipophilic quaternaries TBACl and TBPCl had the lowest (i.e. least negative) values, while the most lipophilic – TOACl – had the highest.

The hydrogen phthalate ion is extracted as a complex with one molecule of extractant, as is the uncharged phthalic acid molecule. The doubly charged phthalate ion is extracted as a complex with two molecules of extractant. Single, uncharged molecules are also extracted by TOPO. The free energies of ion exchange of these last three processes are far lower (i.e. less negative) than those of the hydrogen phthalate extraction. The identities of the complexes were confirmed by spectroscopic methods.

Solid phthalic acid was found to form a complex with Aliquat 336 in dichloromethane with a 2:1 extractant:phthalic acid ratio. Water appears to play an important role, which was not fully elucidated.

Tamada and King[6] claimed that dicarboxylic acids that form intramolecular hydrogen bonds cannot form complexes with more than one amine per acid but they did not study phthalic acid. Phthalic acid is only weakly hydrogen bonded and only forms weak complexes. Nonetheless, we suggest that Tamada and King's conclusion does not apply to such a lipophilic acid.

ACKNOWLEDGEMENTS

We thank Dr M.M. Anwar, Prof. L. Dunne and Mrs J. Hawkes for advice and assistance, together with the Brucker AMX 400 University of London Intercollegiate Research Service for NMR at King's College.

REFERENCES

1. Reuben BG, Ibrahim N, McGillivary A and Dunne L, *Separations for Biotechnology* 3, ed. D.L. Pyle SCI/RSC, London 221, (1994).
2. Lukhezo M, Dunne LJ, Reuben BG and Verrall MS, *Chemical Physics*, **220**, 53, (1997).
3. Lukhezo M, Kelly NA, Reuben BG, Dunne LJ and Verrall MS, *Proc. ISEC '96*, , eds Shallcross DC, Paimin R and Prvcic LM, University of Melbourne, **1**, 87, (1996).
4. Kelly NA, Lukhezo M, Reuben BG, Dunne LJ and Verrall MS, *J. Chem. Technol. Biotechnol*, **72**, 347, (1998).
5. Rambocus S, Kelly N, Dunne L and Reuben BG in preparation.
6. Tamada JA and King CJ, *Ind. Eng. Chem. Res*, **29**, 1319-26; ibid, 1327-32, ibid 1333-38. (1990).
7. Tung LA and King CJ, *Ind. Eng. Chem. Res.*, **33**, 3217-24, (1994); ibid, 3224-29; Reisenberg and King CJ, ibid, **34**, 845-52, (1995).
8. Anwar MM., Private communication.

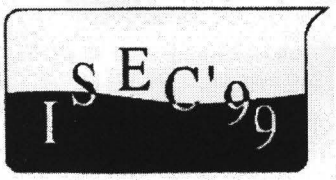

SPECIFIC INHIBITORY EFFECTS OF HYBRID MEMBRANES ON THE GROWTH OF TUMORS *IN VITRO* AND *IN VIVO*

Ryuichi Ueoka, Yoko Matsumoto, Toshihiro Kato, Akihiro Kanno, Makoto Tsuchiya, Kenji Tsuzaki and Yukito Murakami

Graduate Course of Applied Chemistry, Kumamoto Institute of Technology, Kumamoto 860-0082, Japan

ABSTRACT

We have recently produced new type hybrid membranes (liposomes) composed of vesicular and micellar molecules. The physical properties of these liposomes can be controlled by changing the composition of hybrid membranes. In this study, the high inhibitory effect of the hybrid membranes composed of 90 mol% dimyristoyl-phosphatidylcholine (DMPC) and 10 mol% polyoxyethylene-10-dodecyl ether ($C_{12}(EO)_{10}$) on the growth of leukemia cells (HL-60) was obtained. The induction of apoptosis with the hybrid membranes was found in HL-60 cells using flow cytometer and DNA agalose gel electrophoresis. The uniform and stable structure of hybrid membranes was revealed on the basis of dynamic light scattering measurements. Furthermore, the significantly prolonged survival was obtained in mice inoculated melanoma cells after the administration of hybrid membranes.

Keywords: liposome, antitumor effect, apoptosis, leukemia, melanoma

INTRODUCTION

Liquid membranes have recently attracted attention in connection with reducing the toxicity of anti-tumour drugs.[1] We have prepared specific hybrid membranes composed of vesicular and micellar molecules and their physical properties, such as size, membrane fluidity, phase transition temperature, and hydrophobicity can be controlled by changing the composition of hybrid membranes.[2] In the course of this study, remarkably high inhibitory effects of hybrid membranes without drugs on lymphoma growth *in vitro* have been obtained.[3~6] Furthermore, it was found that the hybrid membranes including anti-tumour drugs have a highly inhibitory effect on the growth of glioma *in vitro* and *in vivo*.[7] No toxicity of the hybrid membranes was observed in normal rats *in vivo* without any side effects.[8]

In this study, we report on the specific inhibitory effects of hybrid membranes on the growth of tumors *in vitro* and *in vivo*.

EXPERIMENTAL

Materials

Commercially available phosphatidylcholine (DMPC, DPPC) and micellar surfactants ($C_{12}(EO)_n$, n = 4, 8, 10, 12, 23) were used without purification.

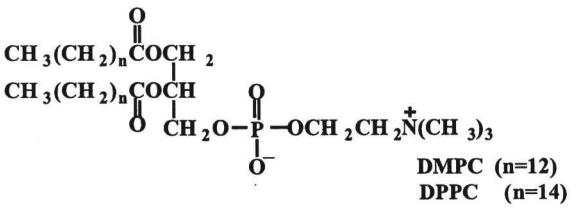

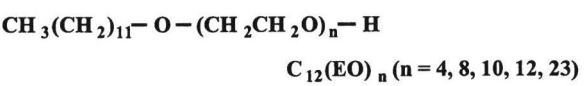

© 2000 Society of Chemical Industry

Preparation of Hybrid Membranes

The hybrid membranes were prepared by dissolving both phospholipids and $C_{12}(EO)_n$ in phosphate-buffered saline with sonication (BRANSONIC Model B2210 apparatus, 90 W) at 45C for 5 minutes.

Cell Culture

The cells were cultured for 4 days in a 5% CO_2 incubator at 37C after adding the hybrid membranes. The inhibitory effects of hybrid membranes on the growth of tumour cells were evaluated by $100(N_a-N_p)/N_a$, where N_a and N_p denote the live cell numbers in the absence and presence of the hybrid membranes, respectively.

Flow Cytometry

The DNA content was determined in a flow cytometer (Epics XL system II, Coulter) with the propidium iodide staining method.

Dynamic Light Scattering

The dynamic light scattering measurements were performed with a Brookhaven BI-90 particle sizer as described previously.[2] The hydrodynamic diameter (d_{hy}) was evaluated by equation (1)

$$d_{hy}=kT/3\pi\eta D \qquad (1)$$

where k is Boltzmann's constant, T is the absolute temperature, η is the solvent viscosity and D is the diffusion coefficient.

Animal Test

Female C57BL/6 mice 5-week-old were purchased from the Charles River Japan Inc. Animals were randomly grouped on the basis of the body weight on the day of tumour cells inoculation using the stratified randomization method. B-16 Melanoma cells (5×10^5 cells) were intraperitonealy inoculated. Hybrid liposomes were intraperitonealy administered to mice. The median life span was calculated according to equation (2).

Median Life Span (%) = (Mean survival days of treated group)/(Mean survival days of control group) (2)

RESULTS AND DISCUSSION

Specific Inhibitry Effects of Hybrid Membranes on the Growth of Leukemia cells *in vitro*

The inhibitory effect of hybrid membranes composed of dimyristoylphosphatidylcholine (DMPC) and polyoxyethylenedodecyl ether ($C_{12}(EO)_n$: n = 4, 8, 10, 12, 23) on the growth of human promyelocytic leukemia (HL-60) cells *in vitro* were examined .

The results are summarized in Table 1 and the noteworthy aspects are as follows :

a. The inhibitory effects of the hybrid membranes composed of DMPC and $C_{12}(EO)_n$ are moderately enhanced as compared with those of the membranes of DMPC.

b The inhibitory effects of DMPC/ $C_{12}(EO)_8$ and DMPC/ $C_{12}(EO)_{23}$ hybrid membranes were fairly enhanced.

c Almost completely inhibitory effects were attained by employing the hybrid membranes of DMPC/ $C_{12}(EO)_{10}$ and DMPC/ $C_{12}(EO)_{12}$.

It is deduced that the hydrophilic-hydrophobic balance in polyoxyethylenealkyl ethers is important for the enhancement of the inhibitory effect on the growth of tumor cells. Relative DNA contents in HL-60 cells treated with the hybrid membranes composed of DMPC/10 mol% $C_{12}(EO)_{10}$ are shown in Figure 1. The DNA of HL-60 cells was found to be almost completely fragmented after the addition of hybrid membranes. On the basis of DNA agarose gel electrophoresis, it was also found that exposure of HL-60 cells to hybrid membranes caused the DNA fragmentation characteristic of apoptosis (data not shown). These results suggest that the DMPC/ $C_{12}(EO)_{10}$ hybrid membranes

can induce the apoptosis of HL-60 cells.

Sample	Inhibitory effect (%)
DMPC	25
DMPC/10 mol% $C_{12}(EO)_4$	64 (0)
DMPC/10 mol% $C_{12}(EO)_8$	89 (77)
DMPC/10 mol% $C_{12}(EO)_{10}$	96 (83)
DMPC/10 mol% $C_{12}(EO)_{12}$	99 (75)
DMPC/10 mol% $C_{12}(EO)_{23}$	79 (3)

DMPC = 7.5×10^{-5} mol/dm^3; $C_{12}(EO)_n = 8.3 \times 10^{-6}$ mol/dm^3
Initial cell number = 1.0×10^4 cells/cm^3
Values in parentheses are $C_{12}(EO)_n$ micelles ($C_{12}(EO)_n = 8.3 \times 10^{-6}$ mol/dm^3)
Inhibitory effects have maximum error of $\pm$ 6%

Table 1 Inhibitory Effects of Hybrid Membranes Composed of 90 mol% DMPC and 10 mol% $C_{12}(EO)_n$ on the Growth of HL-60 Cells

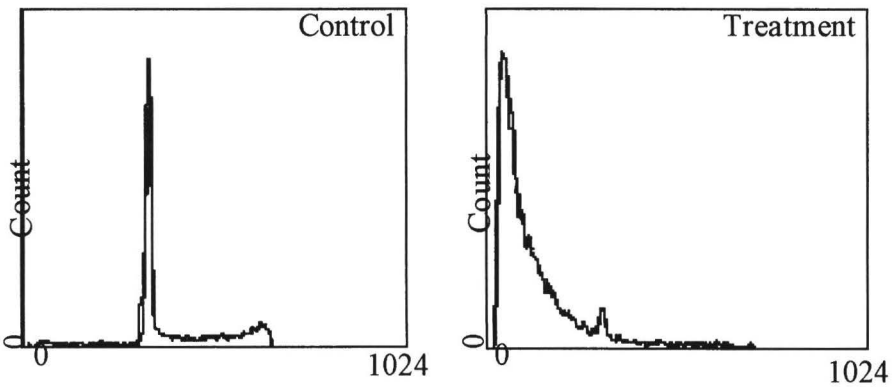

Figure 1. Rerative DNA contents for HL-60 cells treated with the hybrid membranes composed of 90mol% DMPC and 10mol% $C_{12}(EO)_{10}$

Therapeutic Effects of hybrid membranes in mice model of carcinoma *in vivo*

The inhibitory effects of the hybrid membranes composed of phosphatidylcholine (DMPC, DPPC) and $C_{12}(EO)_n$ (n=10, 23) on the growth of melanoma cells *in vitro* and *in vivo* were examined.

The 50% inhibitory concentration of the hybrid membranes composed of DMPC and $C_{12}(EO)_n$ (0.045mM) was one-twelfth of that (0.55mM) of DMPC membranes. A clear solution of the hybrid membranes having a hydrodynamic diameter of 80 nm with a single and narrow distribution could be kept over 30 days, as shown in Figure 2. These results suggest that these hybrid membranes might be suitable for clinical chemotherapy. Screening for therapeutic effects is generally carried out in mice or rats belonging tumour cells. In the primary screening, tumour cells are intraperitonealy inoculated into animals, and the test agents are intraperitonealy administered. So, the effects of hybrid membranes on intraperitonealy inoculated melanoma cells were examined using mice model of carcinoma. The results are summarized in Table 2 and Figure 3. It is attractive that the markedly prolonged survival of mice was obtained for the treatment with DMPC/ 10mol% $C_{12}(EO)_{10}$ and DMPC/ 10mol% $C_{12}(EO)_{23}$ hybrid membranes. On the other hand, DPPC/ 10mol% $C_{12}(EO)_{23}$ hybrid membranes had no life prolonging effects. It is presumed that the fusion between hybrid membranes

and the tumor cells membranes may not proceed in vivo in the case of DPPC, since the temperature of phase transition of DPPC (40C) is higher than the body temperature of mice.

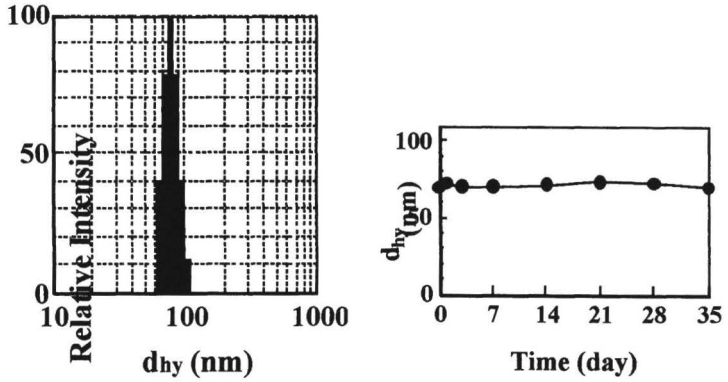

Figure 2. Distribution (A) and time course (B) of size (d_{hy}) for hybrid membranes composed of 90mol% DMPC and 10mol% $C_{12}(EO)_{10}$

Table 2. Median Life Span of Mice Treated with Hybrid Liposomes Composed of 90mol%Lipid and 10mol%$C_{12}(EO)_n$ after the Inoculation of B16-Melanoma Cells

Sample	Dose (mg / kg)	Median survival (days) (Median life span)	
		Experiment 1	Experiment 2
Control	–	14.8± 1.3	14.7± 1.9
DMPC/10mol%$C_{12}(EO)_{10}$	680	23.5± 4.8 (162%)	24.0± 5.3 (166%)
DMPC/10mol%$C_{12}(EO)_{23}$	680	25.2± 2.6 (170%)	24.7± 5.1 (168%)
DPPC/10mol%$C_{12}(EO)_{23}$	734	16.3± 2.4 (110%)	16.5± 1.9 (112%)

Values represent mean± S.D. of 6 mice.

[DMPC]=[DPPC]=5.0* 10^{-2}M, $[C_{12}(EO)_{10}]=[C_{12}(EO)_{23}]=5.6*\ 10^{-3}$M

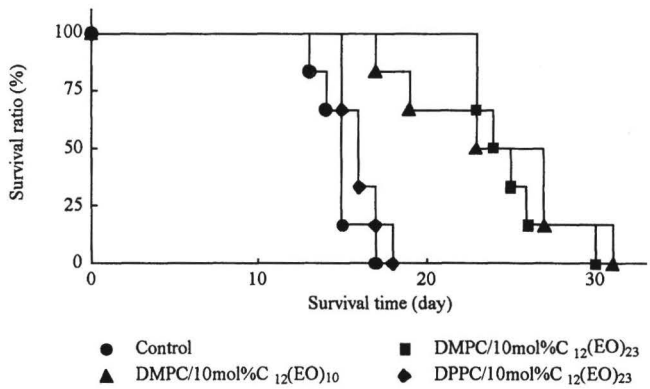

Figure 3. Survival curves of mice treated with hybrid membranes composed of 90mol% phospholipid and 10mol% $C_{12}(EO)_n$ (n=10,23).

CONCLUSION

A summary of noteworthy aspects of this study is as follows: (a) The hybrid membranes (90 mol% DMPC /10mol% $C_{12}(EO)_{10}$) have a highly inhibitory effect on the growth of leukemia cells (HL-60). (b) The induction of apoptosis with the hybrid membranes was found in HL-60 cells using flow cytometer and DNA agalose gel electrophoresis. (c) The uniform and stable structure of hybrid membranes was revealed on the basis of dynamic light scattering measurements. (d) The significantly prolonged survival was obtained in mice inoculated melanoma cells after the administration of hybrid membranes (90 mol% DMPC /10mol% $C_{12}(EO)_{10}$ and 90 mol% DMPC /10mol% $C_{12}(EO)_{23}$).

ACKNOWLEDGMENT

This work was supported in part by a Grant-in-Aid for Science Research from the Ministry of Education, Science, and Culture of Japan (No.10145255, 10680811) and the Science Research Promotion Fund from the Japan Private School Promotion Foundation.

REFERENCES

1. Lasic DD *et al.*, "*Liposomes : from Physics to Application*", Elsevier, Netherlands, 261 (1993).
2. Ueoka R, Matsumoto Y, Moss RA, Swarup S, Sugii A, Harada K, Kikuchi J and Murakami Y, *J. Am. Chem. Soc.*, **110**, 1588 (1988).
3. Ueoka R, Matsumoto Y, Oyama H, Takekuma H and Iio M, *Chem. Pham. Bull.*, **36**, 4640 (1988).
4. Matsumoto Y, Yamada E, Hirano J, Oshige M, Iio M, Iwahara M and Ueoka R, *Biol. Pham. Bull.*, **16**, 213 (1993).
5. Matsumoto Y, Imamura C, Ito T, Taniguchi C and Ueoka R, *Biol. Pham. Bull.*, **18**, 1456, (1995).
6. Imamura C, Kemura Y, Matsumoto Y and Ueoka R, *Biol. Pham. Bull.*, **20**, 1119, (1997).
7. Kitamura I, Kochi M, Matsumoto Y, Ueoka R, Kuratsu J and Ushio Y, *Cancer Res.*,**56**, 3986 (1996).
8. Imamura C, Kanno A, Mitsuoka C, Kitajima S, Inoue H, Iwahara M, Matsumoto Y and Ueoka R, *Yakugaku Zasshi*, **116**, 992 (1996).



Plant Experience

THE THERMAL OXIDE REPROCESSING PLANT AT SELLAFIELD: FOUR YEARS OF ACTIVE OPERATION OF THE SOLVENT EXTRACTION PLANT

C Phillips
British Nuclear Fuels Plc, Thorp Group, Sellafield, Cumbria, CA20 1PG, UK

ABSTRACT
The Thermal Oxide Reprocessing Plant (Thorp) at British Nuclear Fuels' Sellafield site is designed to treat irradiated fuel from UK Advanced Gas-Cooled Reactors and European and Japanese Light Water Reactors. It started operating in March 1984 with the shearing and dissolution of irradiated fuel in the Head End Plant, and in January 1995 the Chemical Separation Plant commenced processing this dissolved fuel. By late 1998 over 1700te of irradiated fuel had been reprocessed in Thorp. The performance of the Thorp Chemical Separation Plant Purex process has been excellent. Decontamination of the uranium and plutonium products from fission products, and uranium-plutonium separation have in general been better than flowsheet requirements. The solvent extraction equipment has operated stably under the automatic controls developed during the R&D programme. Losses of uranium and plutonium to waste streams have been in line with, or better than, expectation.

Keywords: irradiated fuel, Purex, Thorp, uranium-plutonium separation, technetium

INTRODUCTION

The Thermal Oxide Reprocessing Plant (Thorp) at the Sellafield, UK site of British Nuclear Fuels Plc reprocesses irradiated oxide nuclear fuel from British, Japanese and European Light Water and Gas Cooled Reactors. In the Head End Plant irradiated fuel is received, stored under water, sheared into 50mm lengths, dissolved in nitric acid and residual solids removed by centrifuge (Figure1).

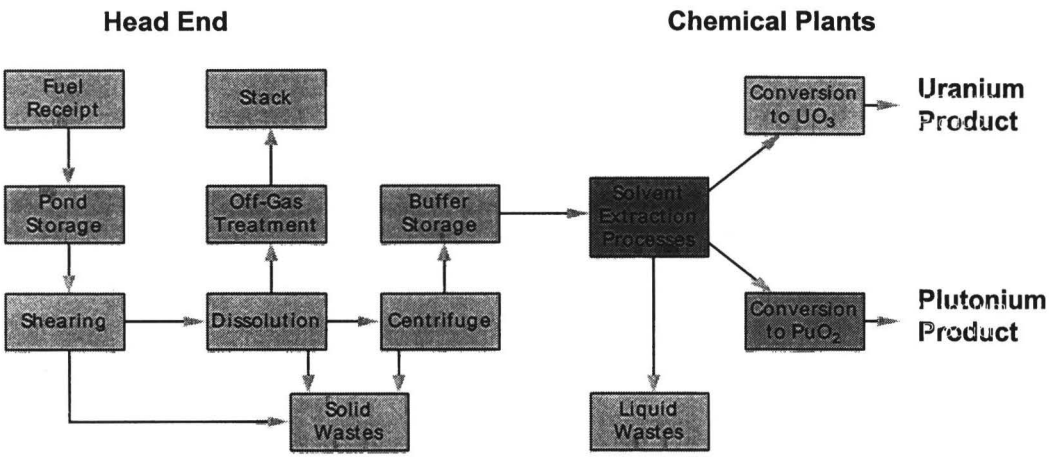

Figure 1. Thorp Unit Processes

In the Chemical Plant the Purex solvent extraction process with tri-n-butylphosphate in kerosene as solvent is used in a three-cycle process to separate uranium, plutonium and fission products. There are further facilities for the conversion of plutonium nitrate to plutonium dioxide by oxalate precipitation and uranyl nitrate to uranium trioxide by thermal denitration. These products are then suitable for recycle into fresh reactor fuel.

© 2000 Society of Chemical Industry

The Head End processes generate mainly solid wastes and these are encapsulated in cement for long term storage. The Chemical Plants generate High Level and Intermediate Level liquid wastes which are vitrified, and a small amount of Low Level liquid waste which is floc-treated to remove residual activity before discharge to sea. The floc so formed is encapsulated in cement. The Head End and Chemical Plants are integrated, with all process stages and services in one building.

During the first 10 years of operation of Thorp there is a committed throughput of 7,000 tonnes based on irradiations up to 40 GW days per tonne and out-of-reactor cooling time of 5 years. Subsequently, the reprocessing of more highly irradiated fuels is planned. A full account of the development, design and construction of Thorp is given elsewhere.[1, 2, 3]

Construction of Thorp was completed to programme and budget in 1992, and commissioning with water, acid and uranium was finished during 1994. Irradiated fuel was introduced into the Head End in early 1994 and into the Chemical Plants a year later. By late 1998, Thorp had processed a total of over 1733t of UK Advanced Gas-Cooled (AGR) fuel, Boiling Water Reactor (BWR) fuel and Pressurised Water Reactor (PWR) fuel from UK, European and Japanese customers.

CHEMICAL PLANT DESIGN PRINCIPLES

Five principles underpinned the design of Chemical Plants and the Purex solvent extraction processes:

a) In order to minimise the amount of activity discharged in liquid wastes, the chemical reagents fed to the process to adjust valency states are "salt-free" so that they do not restrict the ability to concentrate and encapsulate waste streams.
b) It was required to minimise the extent, size and complexity of the process equipment in contact with radioactive material, so as to minimise operator radiation dose, reduce capital and operating costs, and reduce the number of waste streams. This was achieved by using an "early-split" flowsheet with U-Pu separation in the first solvent extraction cycle. Careful flowsheet design, development and proving also allowed single cycles only to be used for the subsequent uranium and plutonium purification stages. In particular the chemistry of neptunium was paid close attention[4] so as to direct it into the appropriate waste streams. This allowed a three-cycle flowsheet to be used rather than the previous typical five-cycle one, thus reducing at source the number of waste streams produced.
c) Pulsed, perforated plate columns are used as the solvent extraction contactors in the Highly Active (HA) and Plutonium Purification (PP) cycles to allow critically safe operation with the higher plutonium concentrations of oxide fuel. Their relatively short aqueous-solvent contact time also minimises solvent degradation from the increased amounts of fission products in oxide fuel.
d) All equipment in contact with radioactive material is designed for minimum or no maintenance throughout the life of the plant. In the highly active parts of the Chemical Plant, no moving mechanical parts are used, and fluidic and compressed air devices are employed for liquid pumping and instrumentation
e) Thorp is built on an existing nuclear site which contains a uranium metal fuel reprocessing plant, and its associated upstream and downstream plants. A major design target for Thorp was that it should contribute no more than 10% of the activity discharge limit for liquid wastes from the site as a whole.

Development Work

The realisation of these design principles necessitated a comprehensive research and development programme that was carried out during the period from the late 1970's to the late 1980's. A large number of pilot plants were designed, built and operated during this period, ranging from full size inactive replicas of major sections of Thorp, through intermediate scale plutonium-containing pilot plants operated in glove boxes, to small scale fully active replicas of most of Thorp using actual irradiated fuel.[1, 3] To underpin this pilot plant work and the extensive safety assessments that were

required for Thorp, a range of fundamental studies was also done of the process chemistry and mechanical engineering of the Thorp processes.

CHEMICAL PLANT FLOWSHEET

The three-cycle Purex flowsheet is shown in Figure 2. The HA and HS pulsed columns in the HA cycle primary separation section extract the uranium and plutonium from the nitric acid solution of the fuel into the 30% TBP in kerosene solvent, leaving almost all the fission products in the acid aqueous phase, which flows to the Vitrification Plant. The uranium and plutonium are then separated in the 1BX and 1BS pulsed columns and 1BXX mixer-settler by chemically reducing the plutonium using salt-free uranium IV produced on site from uranium VI. The presence of significant technetium, which is completely extracted in HA/HS, adversely affects the chemistry of plutonium reduction. Extensive development work[5, 6] allowed this problem to be overcome by careful control of residence times, temperatures and the dispersed phase hold-up in the 1BX and 1BS pulsed columns.

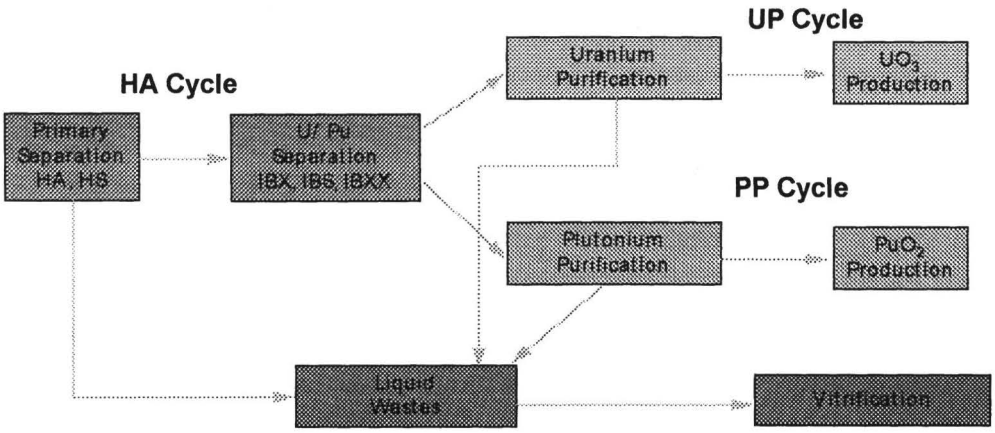

Figure 2. Thorp Chemical Plant Flowsheet

The plutonium stream passes to the single plutonium purification (PP) cycle where pulsed columns and 30% TBP/kerosene are again used to purify the plutonium product from the principal contaminant technetium and residual uranium, ruthenium, caesium and cerium. The single uranium purification (UP) cycle uses 20% TBP/kerosene and mixer-settlers to remove neptunium, plutonium, ruthenium, caesium and cerium from the uranium product. Careful valency conditioning of the neptunium and plutonium prior to solvent extraction, and the use of hydroxylamine nitrate reductant, achieves high simultaneous neptunium and plutonium decontamination in a single solvent extraction cycle.[4] Single Intermediate Level waste streams are produced by the UP and PP cycles, and because they are salt free, these streams can be routed to vitrification along with the High Level waste.

PERFORMANCE OF THE SOLVENT EXTRACTION PROCESSES

Irradiated Fuels Processed

A comparison of the irradiated fuels reprocessed in Thorp up to late 1998 with the design reference fuel is given in Table 1.

It can be seen that, with the exception of ruthenium-106, caesium-134 and cerium-144, fuel characteristic of the design reference has been reprocessed. The exceptions arise because, thus far, the higher burn-up fuel processed has been the longer cooled, allowing these relatively short half-life species to decay significantly.

	Design Reference	Fuel Processed
Irradiation GWD/t	40	10 to 39
Cooling Time Years	5	5 to 19
Plutonium Content %	100	28 to 96
Neptunium 237 Content %	100	23 to 95
Technetium 99 Content %	100	23 to 85
Ruthenium 106 Content %	100	1 to 17
Caesium 134 Content %	100	1 to 22
Caesium 137 Content %	100	19 to 98
Cerium 144 Content %	100	1 to 14

Table 1. Comparison of Fuel Processed with Design Reference

Chemical Plant Separation Efficiency

The performance of the Chemical Plant was studied by looking at fission product separation efficiency, uranium and plutonium product qualities, losses of uranium and plutonium to waste streams and uranium-plutonium separation efficiency. Table 2 illustrates typical fission product decontamination factors (DF's) across the HA and HS pulsed columns for technetium, ruthenium, caesium and cerium, compared with the THORP reference flowsheet.

Fission Product	Ref Flowsheet DF (HA & HS)	Observed DF (HA & HS)
Technetium 99	1.0	1.0 to 1.3
Ruthenium 106	1.0 e 3	1.2 e 3 to 7.0 e 3
Caesium 134+137	4.5 e 3	6.9 e 4 to 1.9 e 5
Cerium 144	3.3 e 3	1.1 e 4 to 1.7 e 5

Where $DF = \frac{\textit{Amount of FP in Feed per g of Uranium}}{\textit{Amount of FP in Product per g Uranium}}$

Table 2. Comparison of Observed Fission Product DF's with Flowsheet (HA&HS)

Tables 3 and 4 show the overall DF's for fission products, neptunium, uranium and plutonium through to the uranium and plutonium products. These tables demonstrate the excellent performance of the solvent extraction plant. Fission product decontamination factors (DF's) in the HA cycle have been consistently better than the flowsheet expectation. Across the whole plant to the UO_3 and PuO_2 products the achieved DF's for fission products and other radioactive contaminants have also been higher than design expectation, resulting in products well within International Specifications and thus fully suitable for recycle into new reactor fuel.

Contaminant	Ref Flowsheet DF	Observed DF to UO_3 Product
Technetium 99	4.0 e 3	8.17 e 3 to 1.16 e 4
Ruthenium 106	8.7 e 5	4.32 e 6 to 1.33 e 7
Caesium 134+137	6.5 e 8	5.66 e 9 to 1.38 e 10
Cerium 144	3.3 e 7	9.36 e 5 to 4.96 e 6
Neptunium 237	1.5 e 4	3.31 e 4 to 6.76 e 4
Plutonium	5.0 e 6	8.60 e 6 to 2.03 e 7

Where $DF = \frac{\textit{Amount of Contaminant in Feed per g of Uranium}}{\textit{Amount of Contaminant in Product per g Uranium}}$

Table 3. Comparison of Observed Contaminant DF's with Flowsheet (Whole Plant to UO_3 Product)

Contaminant	Ref Flowsheet DF	Observed Average DF to Plutonium Nitrate Product	Observed DF to PuO_2 Product
All fission products	2.8 e 8	-	3.37 e 8 to 7.06 e 8
Technetium 99	1.0 e 2	1.00 e 2	-
Ruthenium 106	3.2 e 5	1.04 e 6	-
Caesium 134+137	5.0 e 6	1.31 e 8	-
Cerium 144	3.7 e 6	2.10 e 7	-
Neptunium 237	4.5 e 1	6.60 e 1	-
Uranium (to nitrate)	4.2 e 3	4.62 e 4	-
Uranium (to PuO_2)	2.1 e 5	-	5.80 e 6 to 5.55 e 8

Where $DF = \frac{\text{Amount of Contaminant in Feed per g of Plutonium}}{\text{Amount of Contaminant in Product per g of Plutonium}}$

Table 4. Comparison of Observed Contaminant DF's with Flowsheet (Whole Plant to Plutonium Nitrate and PuO_2 Products)

It will be noted that the cerium-144 DF to the UO_3 product is apparently lower than design expectation. However, the cerium content in the fuel feed to the plant has, up to present, been much lower than the reference flowsheet, leading to analytical limit-of-detection restrictions for the low levels that are therefore present in the uranyl nitrate product. That this is an analytical artefact is supported by the overall gamma activity of the UO_3 product, which at 35Bq/gU is well within the ASTM International Specification value of 524 Bq/gU.

The overall neptunium DF for the UO_3 product is seen to be higher than the already large flowsheet expectation. This shows the effectiveness of the specially developed flowsheet[4] for the simultaneous removal of neptunium and plutonium in the UP Cycle.

Uranium and plutonium losses to waste streams from the Chemical Plant are very low, amounting to no more than 0.013% and 0.049% of the feed amounts respectively.

Uranium - Plutonium Separation Performance

Table 5 shows the typical uranium-plutonium separation performance of the 1B (1BX, 1BXX, 1BS) system compared with reference flowsheet expectations. It can be seen that removal of plutonium from the uranium stream has been an order of magnitude higher than the design requirement and flowsheet expectation. The fuel processed so far has contained up to 85% of the flowsheeted amount of technetium and, with no technetium removal in the HA/HS system, the stability and reductive capacity of the 1B system has thus been fully tested and found to be satisfactory.

	Ref Flowsheet DF	Observed DF
Removal of Pu from U product*	3.3 e 3	1.4 e 4 to 6.5 e 4
Removal of U from Pu product#	2.1 e 3	4.5 e 3 to 8.4 e 4

$*DF = \frac{\text{Amount of Pu in feed per g of U}}{\text{Amount of Pu in U product per g of U}}$ $\quad\quad$ $\#DF = \frac{\text{Amount of U in feed per g of Pu}}{\text{Amount of U in Pu product per g of Pu}}$

Table 5. Comparison of Observed U-Pu Separation Performance with Flowsheet

This demonstrates the benefits of the extensive process chemistry and process equipment pilot plant development work that was carried out on the 1B system.[5, 6] This work was done when initial fully active pilot plant trials showed that there would be no technetium DF across the HA/HS system when zirconium was also present in the feed, and that technetium destabilised the chemical reduction of

plutonium.[7] As a result of this work the 1BX column is operated solvent continuous so as to limit the residence time for the technetium reactions in the aqueous phase. This then requires high pulse energies to be applied so as to maintain satisfactory dispersed phase hold-ups. The 1BS column temperature is also reduced to 20C, to reduce the technetium reactions further. The very satisfactory operation of the Thorp 1B system shows the value of this work and vindicates the decision not to modify the plant design to insert a technetium removal step prior to the 1B system.

The removal of uranium from the plutonium stream has also exceeded original expectations. This excellent performance of the 1BS uranium re-extraction pulsed column is achieved despite the presence of the less extractable UIV, and the lower operating temperature in the column. Further uranium removal occurs across the oxalate precipitation production process for plutonium dioxide, resulting in the very high uranium DF's shown in Table 4.

CONCLUSIONS

The design, construction and commissioning of THORP has been the most challenging single project ever undertaken by BNFL. The plant was commissioned and set to work without significant difficulty and has quickly ramped up to expected throughputs. This has been in large part due to extensive development work and close liaison between developers, designers and the commissioning teams during design, construction and commissioning. The plant uses well established reprocessing technology in an innovative way so as to minimise the number of processing steps needed to meet product quality specifications, and minimise the number of waste streams produced. Product qualities are excellent and allow ready recycle into fresh reactor fuel, preserving separative work and allowing considerably more energy to be extracted from the original fuel. Thorp has thus met or exceeded its design intentions, has operated safely and efficiently, and is an advantageous and environmentally responsible method of treating spent irradiated fuel from the world's nuclear reactors.

REFERENCES

1. Phillips C *Atom,* (394), 13, (1989)
2. Harrop G and Phillips C, *Spectrum,* Boise, USA, (1992)
3. Phillips C *Trans I Chem E* **71(A),** 132, (1993)
4. Dennis IS and Phillips C, *Proc ISEC'90,* Elsevier, 549, (1992)
5. Phillips C *Proc WM99,* Tucson, USA, 1041, (1992)
6. Phillips C *Int Symp on Reprocessing and Waste Management,* Amer. I. Chem E, Pittsburg USA (1991)
7. Garraway J, *I Chem E Symp. Series* **No 88,** 47, (1984)

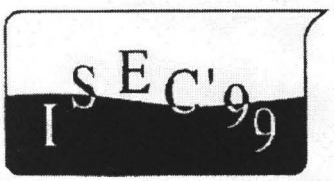

MINI-PLANT TRIALS ON THE RECOVERY OF NICKEL BY SOLVENT EXTRACTION

VM Nagel, BM Davies and PM Cole
Mintek, Randburg, South Africa

ABSTRACT
Several extraction systems for nickel have been evaluated in mini-plant trials to compare their efficiencies and relative selectivity for nickel over other elements under continuous counter-current conditions. The aqueous feed solution was a sulphate liquor derived from the biologically assisted leaching of low-grade sulphide ore, and contained ~9 g/dm^3 nickel, 0.5 g/dm^3 calcium, 0.2 g/dm^3 cobalt, 1.6 g/dm^3 magnesium, and 0.5 g/dm^3 manganese. The extractants tested were Versatic acid, Versatic acid in a synergistic mixture with 4-nonylpyridine, and di(2-ethylhexyl)phosphoric acid in synergistic combination with isodecyl 4-pyridine carboxylate. An aliphatic hydrocarbon diluent was employed.

Keywords: nickel, calcium, Versatic acid, D2EPHA, synergism, alkylpyridine, alkylpyridine carboxylic ester.

INTRODUCTION

Biologically assisted processes are currently being developed for the extraction of nickel from low-grade sulphide ores.[1] Extractants need to be selective for nickel over other impurities present in the leach solutions.[2] This is particularly true with regards to calcium, as the solubility of this sulphate limits the upgrading ratio to a value below that which produces gypsum-saturated strip liquor.

Previous testwork at Mintek investigated the influence of a nitrogen-donor synergist in mixtures with either di(2-ethylhexyl)phosphoric acid (D2EPHA) or a carboxylic acid (Versatic acid) on the separation achievable between nickel and calcium.[2,3] This work identified appropriate mixtures for further continuous counter-current testwork.

Mini-plant trials were conducted using these extractant systems, together with Versatic acid on its own, using a typical bio-leach solution. The extraction efficiencies for nickel and relative selectivity for nickel over other metals were tested under continuous counter-current conditions. Stripping efficiencies, pH of operation, and consumption of NaOH as a neutralising agent were also monitored. The results obtained from the mini-plant runs are discussed in this paper.

PROCESS DESCRIPTON

Mixtures of pyridine derivatives (L) and acid extractants (HA) extract nickel[4] according to Reaction 1

$$Ni^{2+}_{(Aq)} + 2\,HA_{(Org)} + n\,L_{(Org)} \Leftrightarrow NiA_2L_{n(Org)} + 2\,H^+_{(Aq)} \qquad (1)$$

Because protons are released during extraction, the reaction is pH dependent. The appropriate pH was maintained by the addition of base to the mixers in the extraction stages. In the mini-plant trials, NaOH was used. Industrial practice is to pre-load the organic phase with sodium or ammonium ions in a separate stage, before extraction of the metal, to prevent excessive dilution of the aqueous phase. This practice is not favoured for the Versatic systems because of the high aqueous solubility of the sodium Versatic salt.

Nickel is stripped from the loaded organic phase by contacting it counter-currently with aqueous solution containing sulphuric acid, to effect the reverse of Reaction 1. By employing nickel-containing anolyte from nickel electrowinning as the aqueous strip liquor, the net consumption of acid is minimised.

© 2000 Society of Chemical Industry

EXPERIMENTAL

Aqueous solutions

The aqueous feed solution was a leach liquor derived from a biologically assisted process, which had been treated for the removal of iron. The composition is given in Table 1. The strip liquor was a synthetic solution made up from chemically pure grade nickel sulphate, and contained 50 g/dm^3 H_2SO_4, 65 g/dm^3 nickel, 0.1 g/dm^3 magnesium and traces of other metal impurities.

Element	Concentration (g/dm^3)	Element	Concentration (g/dm^3)
Ni	9.0	Fe	< 0.002
Co	0.175	Zn	0.001
Cu	0.062	Ca	0.480
Mn	0.475	Mg	1.6

Table 1. Composition of the aqueous feed solution.

Organic reagents

The various components of the organic phase systems tested are listed in Table 2. Isodecanol (Henkel) was used as a phase modifier where appropriate, and C_{12}-C_{13} *n*-paraffin (SasolChem) was used as the diluent in all cases.

Reagent	Supplier
D_2EHPA	Bayer
Versatic acid	Shell SA
4-nonylpyridine *(SYN1)*	Aldrich
Isodecyl 4-pyridine carboxylate *(SYN2)**	Mintek

* Prepared as described in Reference 3.

Table 2. Organic reagents.

Laboratory batch procedures

The operating pH values for each extractant, pH_{90} (defined as the pH at which 90% of the nickel present in the feed solution was extracted), were determined by plotting the fractional extraction as a function of pH at an organic-to-aqueous phase ratio (O:A) of 3. The number of extraction stages required for continuous counter-current operation was determined from extraction equilibrium isotherms generated at appropriate pH_{90} values at different O:A ratios. Stripping equilibrium isotherms were generated in a similar manner, but without pH control.

The batch tests were carried out by contacting the two phases in the appropriate O:A ratio using magnetic stirring. Where applicable, pH was controlled by the drop-wise addition of 100 g/dm^3 NaOH solution.

Aqueous- and organic-phase samples were taken for the analysis of the elements of interest. The organic-phase samples were stripped with 100 g/dm^3 H_2SO_4 and the acid solutions analysed, together with the aqueous samples, by inductively coupled plasma emission spectroscopy.

The relative phase-separation characteristics of the various extractant systems were tested by contacting equal volumes of the aqueous and organic phases in a beaker and noting the time required for separation.

Continuous counter-current trials

The mini-plant comprised a series of conventional box-type mixer-settler units, each with a 100 cm^3 mixer and 400 cm^3 settler (settling area of 110 cm^2), constructed of clear PVC. Electrically driven pump-mix impellers accomplished mixing and inter-stage transfer of the

aqueous and organic phases. Watson Marlow peristaltic pumps were used to pump the solutions to the plant.

The pH in the mixers of the extraction stages was controlled by the addition of an 80 to 100 g/dm^3 NaOH solution. A loaded organic reservoir was used to minimise carry-over of the aqueous phase with the loaded organic phase to the stripping circuit.

The general layout for a plant with three extraction and two stripping stages is shown in Figure 1. Aqueous and organic samples were taken at regular intervals from each stage. The samples were analysed in the same manner as for the laboratory batch procedures.

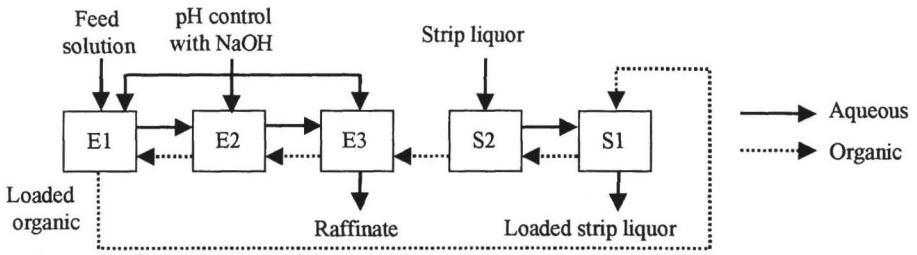

Figure 1. General layout of the continuous counter-current mini-plant.

RESULTS

Laboratory batch experiments

The different extractant systems tested are shown in Table 3. From plots of pH versus fractional extraction, and the extraction and stripping equilibrium isotherms, the operating conditions and plant layout for each extractant system were determined as shown in Table 4.

System	Composition
1	0.5 mol/dm^3 versatic acid
2	0.25 mol/dm^3 versatic acid, 0.25 mol/dm^3 SYN1, 10 volume % isodecanol
3	0.25 mol/dm^3 D2EHPA, 0.25 mol/dm^3 SYN2

Table 3. Composition of extractant systems tested in mini-plant trials.

The criteria applied to the McCabe-Thiele constructions were a nickel raffinate concentration below 0.1 g/dm^3, approximately 80 percent utilisation of the capacity on the organic phase, and a stage efficiency of 90 percent.

System	No. of extraction Stages	No. of stripping Stages	Operating pH (pH_{90})	Extraction O:A	Stripping O:A
1	4	2*	6.5	2	3.3
2	4	2	5.5	2.5	8.6
3	3**	2	3	3	9.2

* McCabe-Thiele construction predicted 1 stage required.

** McCabe-Thiele constructions predicted 2 stages required.

Table 4. Plant layout and operating conditions for the different extractant systems.

Figure 2 shows the nickel/calcium separations achievable with systems 1 and 2. It can clearly be seen that system 2 exhibits better separation of nickel from calcium compared with system 1. The

extraction isotherms for systems 1 and 2 are shown in Figures 3 (a) and (b), respectively. System 1 has better nickel extraction properties than system 2.

It is interesting to note that the loading on the organic phase achieved with system 2 was similar to system 1, even with the reduced Versatic acid concentration.

All systems except for system 2 (without the addition of isodecanol) exhibited acceptable phase-separation characteristics. With the addition of 10 vol. % isodecanol, the time required for complete phase separation of system 2 was comparable to those of the other systems.

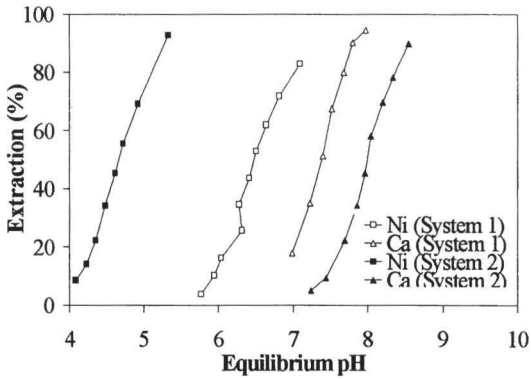

Figure 2. pH *vs.* extraction for system 1 and 2 (0.5 mol/dm^3 of each constituent - system 2)[4].

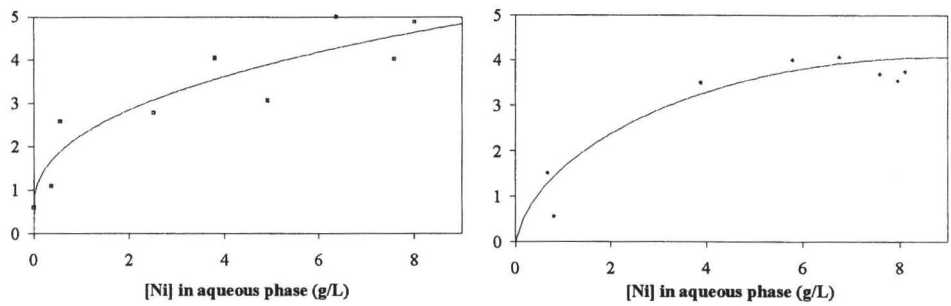

(a) (b)

Figure 3. Equilibrium extraction isotherms (a) system 1 and (b) system 2 using feed solution. ([Ni] in organic phase (g/L) versus [Ni] in aqueous phase (g/L))

Mini-plant trials

For systems 1 and 2 (see Table 5), an additional extraction stage would have reduced the nickel concentration of the raffinate significantly, and raffinate concentrations of less than 0.1 g/dm^3 should be readily attainable with a slight increase in the operating pH of the extraction section. For circuits in which it is desirable to co-extract a large portion of the cobalt along with the nickel, systems 1 and 2 could be employed, operated at higher pH values. Both systems would be successful, but system 1 would co-extract more calcium and other impurities than system 2. This could be overcome by scrubbing the loaded organic phase of system 1 with loaded strip liquor. System 2 should co-extract significantly less calcium and other impurities, and the addition of scrubbing stages may not be required.

The excessive NaOH consumption experienced with system 2 was thought to be caused by the protonation of the synergist component. This will be investigated further. The soluble Versatic salt lost to the aqueous phase for system 1 can be recovered into the plant organic phase by contacting the raffinate with the stripped organic phase at pH 3 in one stage. For system 3, the quantity of nickel extracted was higher than for systems 1 and 2 but so was the co-extraction of impurities. This system would not be used in practice.

Parameter	System 1	System 2	System 3
Raffinate [Ni] (mg/dm^3)	250	600	100
pH profile (E1 – last stage)	6.3 – 6.8	5.8 – 6.0	3
Extraction efficiency (%): Co	78	40	> 80
Cu	100	100	100
Mn	50	< 20	> 90
Ca	1	Negligible	> 80
Mg	4	Negligible	< 20
NaOH consumption (g NaOH/g Ni extracted)	1.5	1.9	2
Ni stripping efficiency (%)	> 98	> 95	> 80
Versatic acid lost (g/dm^3 aqueous phase)	1.4	Negligible	NA
Residence time in extraction mixers (min)	3	5	3

Table 5. Summary of results obtained from mini-plant trials.

CONCLUSIONS

Under the conditions employed, systems 1 and 2 were identified as likely extractant systems for the selective extraction of nickel and cobalt from bioleach liquors. System 3 exhibited unfavourable selectivity characteristics and excessive NaOH consumption.

The high operating pH value required for acceptable cobalt recovery, and the possible high co-extraction of calcium for system 1, can be overcome by an increase in the extractant concentration and the introduction of scrubbing stages.

Further testwork is required on system 2 to quantify the high NaOH consumption and long-term stability of 4-nonylpyridine. The relationship between operating pH and nickel, cobalt and calcium extractions will be interesting, as this system has the potential to eliminate the need for scrubbing stages for any co-extracted calcium and impurities.

ACKNOWLEDGEMENTS

The paper is published by permission of Billiton SA (Ltd) and Mintek.

REFERENCES

1. Miller DM, Dew DW, Norton AE, Cole PM and Benetis G. *Nickel-Cobalt' 97 International Symposium,* Sudbury, Canada, August 17-20, (1997).
2. Preston JS and du Preez AC. *J. Chem. Tech. Biotechnol.*, **61**, 159, (1994)..
3. Preston JS and du Preez AC. *Solv. Extr. Ion Exch.*, **13**, 465, (1995).
4. Preston JS and du Preez AC. Mintek internal communication (1996).

PILOT-PLANT EVALUATION OF MANGANESE REMOVAL AND COBALT PURIFICATION BY SOLVENT EXTRACTION

Angus Feather, Kathryn C Sole and David B Dreisinger[1]
Mintek, Randburg, South Africa
[1]The University of British Columbia, Vancouver, Canada

ABSTRACT
A process flowsheet for the recovery of copper and cobalt from the Kakanda tailings in the Democratic Republic of Congo has been developed. Pilot-scale evaluations of the two solvent-extraction systems for processing a bleed stream from the copper-recovery circuit are discussed. The bulk of the manganese is removed from the copper raffinate bleed with minimal (less than 0.5%) cobalt loss by extraction with di(2-ethylhexyl)phosphoric acid. The cobalt is then upgraded and separated from magnesium by extraction with Cyanex 272. Cobalt recovery in excess of 99% is achieved, and a concentrated cobalt electrolyte suitable for the electrowinning of high-purity cathode is produced.

Keywords: manganese, cobalt, Cyanex 272, D2EHPA, pilot-plant, Kakanda tailings

INTRODUCTION

The electrowinning (EW) of cobalt requires a manganese concentration of at least 2 g/dm^3 in the electrolyte to minimise the oxidation of Co(II) to Co(III) at the anode. Excessive manganese levels can, however, be problematical as unstable Mn(III) formed at the anode disproportionates to Mn(II) and Mn(IV), the latter precipitates as manganese dioxide sludge which needs to be removed from the cell. The removal of manganese from cobalt-containing solutions is usually accomplished by sulphide precipitation.[1] Alternatively, the removal of the bulk of any manganese in solution by a solvent-extraction (SX) route may offer benefits in terms of both cost and ease of operation.

Magnesium concentrations of greater than 10 g/dm^3 in a cobalt electrolyte adversely affect current efficiency and may cause pitting of the cathode. Phosphinic acid extractants can successfully be used to separate cobalt from high concentrations of magnesium.

Manganese removal and the subsequent purification of a cobalt-bearing acidic sulphate liquor by solvent extraction has been evaluated in a continuous operation during an integrated pilot-plant campaign carried out to assess the technical feasibility of a proposed process to recover copper and cobalt from the Kakanda tailings dump material in the Democratic Republic of Congo.

PROCESS DESCRIPTION

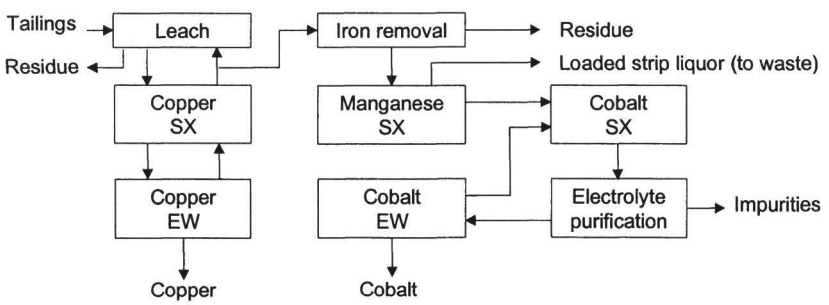

Figure 1. Proposed flowsheet for the recovery of copper and cobalt cathode from Kakanda tailings dump material.

© 2000 Society of Chemical Industry

The flowsheet proposed for the treatment of the Kakanda tailings is shown in Figure 1. Copper is recovered in a conventional leach-SX-EW circuit. Cobalt is then recovered from a bleed from the raffinate of the copper SX circuit. After treatment for iron removal, this stream contains approximately 1.3 g/dm^3 Mn, 3 g/dm^3 Co, and 12 g/dm^3 Mg. The bulk of the manganese is removed by solvent extraction with di(2-ethylhexyl)phosphoric acid (D2EPHA). Cobalt is then upgraded and separated from magnesium by extraction with Cyanex 272. The cobalt-rich loaded strip liquor is purified by ion exchange (IX), and the cobalt recovered as high-purity metal cathode. Process details and results of the integrated pilot campaign are published elsewhere.[2]

PILOT-PLANT EQUIPMENT AND PROCEDURES

Conventional mixer-settler units, each with a mixer volume of 500 cm^3 and settling area of 256 cm^2, were operated in a countercurrent configuration. Solutions were pumped into the plant using peristaltic pumps. As necessary, stages were operated with an internal recycle to maintain aqueous phase continuity in the mixers. The pH was adjusted as required by PID-controlled addition of dilute NaOH into the mixers. To simulate full-scale operational conditions, the extraction stages of the manganese circuit were maintained at 40C by circulating hot water through stainless-steel heat exchangers in the settlers. The initial start-up conditions were selected based on results of laboratory-scale testwork combined with flowsheet simulation modelling using Aspen software.

Each SX circuit was operated continuously for a total running time of 450 h, and treated 1.6 m^3 of the copper SX raffinate bleed solution. All aqueous and organic streams were sampled once per 8-hour shift, and analysed by inductively coupled plasma emission spectroscopy.

D2EHPA was supplied by Albright & Wilson, USA, and Cyanex 272 by Cytec, Canada. Both circuits used C_{12}-C_{13} *n*-paraffin (SasolChem, South Africa) as the aliphatic hydrocarbon diluent.

MANGANESE SOLVENT EXTRACTION

The composition of the feed solution to the manganese circuit is given in Table 1. Mass-balance modelling indicated that 75% of the contained manganese would have to be removed to minimise detrimental effects in the cobalt EW operation. The circuit configuration is shown in Figure 2.

Element	Concentration (g/dm^3)	Element	Concentration (g/dm^3)
Mn	1.25	Zn	0.05
Co	3.2	Ca	0.6
Fe	0.003	Al	0.02
Cu	0.1	Mg	12.0
Ni	0.02	pH	3.8

Table 1. Typical composition of copper SX raffinate bleed stream after iron removal.

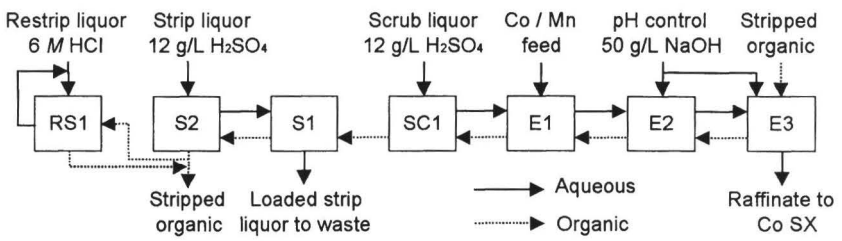

Figure 2. Manganese SX circuit.

Extraction

Typical extraction efficiencies of the various elements in the feed solution are compared in Table 2. Conditions were optimised by maintaining the pH of the extraction circuit between 2.2 and 2.3, and using an advance volume phase ratio (O:A) of unity. Manganese extraction could be increased to better than 90% by increasing the phase ratio to 1.5, however cobalt losses exceeded 1% under these conditions. Copper and magnesium extraction also increased at higher phase ratios.

Element	Extraction (%)	Organic loading (g/dm^3)	Element	Extraction (%)	Organic loading (g/dm^3)
Mn	77.0	1.0	Zn	> 99.9	0.06
Co	< 0.5	0.04	Ca	98.0	0.6
Fe	> 99.9	0.1	Al	89.4	0.04
Cu	21.2	0.03	Mg	3.1	0.45

Table 2. Extraction efficiencies of major elements in the manganese SX circuit.

Scrubbing

Co-extracted cobalt was scrubbed from the loaded organic phase with 12 g/dm^3 H_2SO_4. The scrubbing efficiency was optimised at approximately 80% using an O:A of 8 to 12, and controlling the pH at 2.2. Inclusion of the single scrubbing stage reduced the overall cobalt loss from about 1.8% to less than 0.5%. In most instances, the cobalt concentration on the scrubbed organic phase was below the analytical detection limit.

Some magnesium and copper were also scrubbed. Maximum rejection of both of these elements is desirable as this reduces the difficulty of downstream purification of the cobalt electrolyte.

Stripping

Because of site-specific constraints, dilute sulphuric acid was chosen as the stripping agent. It was therefore not possible to concentrate the impurities because of the calcium sulphate solubility limit. With the exceptions of iron and aluminium, all the elements in the scrubbed organic phase were efficiently stripped in two stages using 12 g/dm^3 H_2SO_4.

Iron (III) is extracted by D2EHPA, but is not stripped by sulphuric acid, and the organic-phase build-up eventually becomes detrimental to manganese extraction. A bleed stream of the stripped organic phase was treated with 6 mol/dm^3 HCl in a single restrip stage. The ferric ion build-up was limited to approximately 0.1 g/dm^3 by bleeding a volume of 30% of the stripped organic phase.

A typical organic-phase profile across the entire manganese SX circuit is shown in Figure 3.

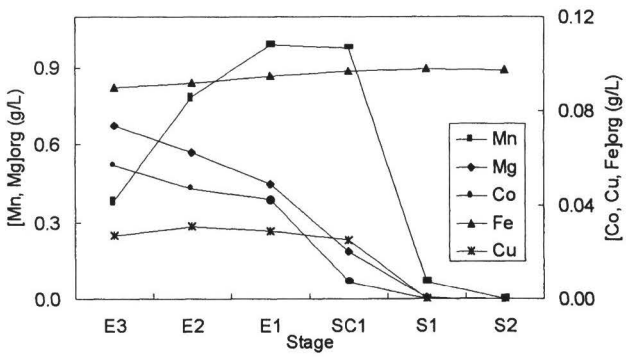

Figure 3. Organic-phase profile across the manganese SX circuit.

COBALT SOLVENT EXTRACTION

Cyanex 272 is commonly employed to separate cobalt and nickel.[3] In this application it was used for the more difficult separation of cobalt from magnesium. The operating philosophy was to load the organic phase as fully as possible with cobalt, thereby 'squeezing off' most of the co-extracted magnesium, and minimising the magnesium scrubbing requirements.

Raffinate from the manganese circuit was passed through a column of coal-based activated carbon to remove any dissolved D2EHPA. The pH was then raised from 2.3 to 6.0 using NaOH. A typical composition of the feed to the cobalt SX circuit is shown in Table 3. Some degree of dilution of the feed solution relative to Table 1 is evident. This results from the addition of NaOH to the manganese SX circuit in the various pH-control operations, as well as dilution from the scrub liquor. The optimised configuration of the cobalt SX circuit is shown in Figure 4.

Element	Concentration (g/dm^3)	Element	Concentration (g/dm^3)
Mn	0.30	Ni	0.02
Co	2.9	Zn	< 0.001
Fe	< 0.001	Ca	0.01
Cu	0.06	Mg	10.1

Table 3. Composition of the feed to the cobalt SX circuit.

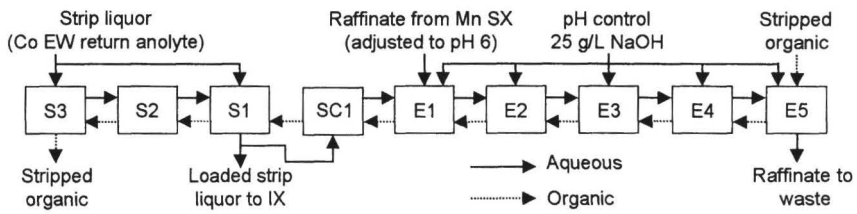

Figure 4. Cobalt SX circuit.

Extraction

The extraction efficiencies of the various elements are shown in Table 4. The use of five extraction stages limited the overall transfer of magnesium to the EW circuit, and the cobalt concentration of the raffinate was maintained at less than 0.005 g/dm^3. The pH across the extraction bank was optimally controlled between 5.6 and 5.9. Lower pH values lead to deterioration in cobalt extraction efficiency, while maintaining a higher pH increased the co-extraction of magnesium, calcium, and nickel.

Element	Extraction (%)	Organic loading (g/dm^3)	Element	Extraction (%)	Organic loading (g/dm^3)
Mn	> 99.9	0.22	Zn	> 99.9	< 0.001
Co	> 99.9	3.6	Ni	4.8	< 0.001
Fe	> 99.9	0.013	Ca	< 0.5	< 0.001
Cu	> 99.9	0.07	Mg	3.6	1.2

Table 4. Extraction efficiencies of major elements in the cobalt SX circuit.

Scrubbing

Co-extracted magnesium was scrubbed with a portion of the loaded strip liquor at an O:A of approximately 30. A single-stage scrubbing efficiency of up to 70% was achieved by maintaining the pH of

the scrub at 4.5. This allowed only 3 to 4% of the magnesium through to the EW circuit. For higher magnesium rejection, an extra scrubbing stage would be required.

Stripping

All elements in the loaded organic phase were quantitatively stripped with return anolyte from the cobalt EW circuit (Table 5). The pH of the loaded strip liquor was maintained at 2.5 to ensure that manganese (as well as minor amounts of copper and zinc) were adequately stripped. At this pH, iron is not efficiently removed from Cyanex 272, and gradually accumulates in the stripping section. Provision for an organic bleed stream for iron removal should be considered in the full-scale plant design. The loaded strip liquor was treated by ion exchange for the removal of trace amounts of copper and zinc, prior to cobalt recovery by electrowinning.

Element	Strip liquor (g/dm^3)	Loaded strip liquor (g/dm^3)	Stripping efficiency (%)
Mn	21.1	22.3	~100
Co	49.5	56.0	99.8
Fe	< 0.001	< 0.001	0.0
Cu	< 0.001	0.07	~100
Zn	0.001	0.004	~100
Mg	6.1	6.8	~100

Table 5. Characteristics of the cobalt SX stripping circuit.

A typical organic-phase profile over the cobalt SX circuit is shown in Figure 5.

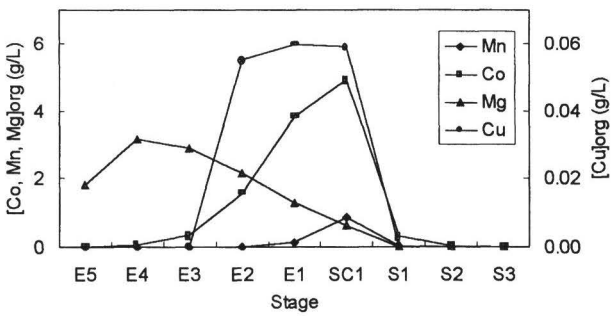

Figure 5. Organic-phase profile across the cobalt SX circuit.

CONCLUSIONS

Technical viabilities of the proposed SX processes for manganese removal and cobalt purification from a copper-circuit bleed stream have been successfully demonstrated in an integrated pilot-plant campaign that treated 1.6 m^3 of feed solution.

At steady state, the manganese SX circuit achieved a manganese removal efficiency of 75 to 80%, with cobalt losses of below 0.5% in the loaded strip liquor that is sent to waste. The Co:Mn ratio was upgraded from 2.5 in the feed liquor to 9.6 in the raffinate stream. Manganese removal efficiency could be increased to about 90%, but at the cost of a 1% cobalt loss.

The optimised cobalt SX circuit achieved cobalt extraction and stripping efficiencies of better than 99.9%, with cobalt losses to the raffinate limited to below 0.005 g/dm^3. Overall magnesium rejection of 94 to 97% was attained. A loaded strip liquor suitable for cobalt electrowinning was produced.

ACKNOWLEDGEMENTS

This paper is published by permission of Mintek. Initial development of the manganese SX system was carried out by John Preston. The Aspen process simulation was modelled by Mike Dry. Cytec and Albright & Wilson are thanked for providing the extractants used in this work. Successful completion of the pilot-plant campaigns would not have been possible without the significant contributions of staff of the Hydrometallurgy and Analytical Science Divisions at Mintek.

REFERENCES

1. Hayward N *et al.*, *ALTA 1997 Nickel/Cobalt Pressure Leaching and Hydr-metallurgy Forum*, ALTA Metallurgical Services, Melbourne, Australia, (1997).
2. Dry MJ *et al.*, *ALTA 1998 Nickel/Cobalt Pressure Leaching and Hydrometallurgy Forum*, ALTA Metallurgical Services, Melbourne, Australia, (1998).
3. Rickelton WA, Flett DS and West DW, *Solv. Extr. Ion Exch.*, **2** (6) 815-838, (1984).

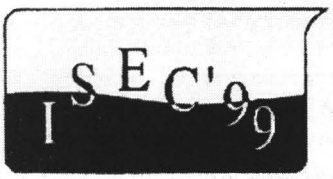

UPDATED AVAILABLE SOLVENT EXTRACTION TECHNOLOGIES

G Díaz, D Martín, C Frías and O Pérez
Técnicas Reunidas,S.A. R&D Division, C/ Sierra Nevada, 16, 28830 San Fernando de Henares, Madrid, Spain

ABSTRACT
This paper deals with a brief description of the industrial application of some updated solvent extraction technologies developed by Técnicas Reunidas S.A. during last few years. Basic process description, suitable raw materials, main products and overall process performance are compiled for five solvent extraction processes. Four of them have been developed either to industrial or demonstration plant level, in which core technology has reached industrial size at least for crucial main components. The fifth is actually in development at laboratory and pilot plant level. A single application of each process is also included. General specification of the industrial facility, year of construction and start up date, productions, main events if any, present status and future trends are briefly described. Industrial applications are mentioned and illustrated with schemes and photographs. Specifically the five processes are: Modified ZINCEX Process, ZINCLOR Process, Copper Metal Extraction Process (CUPREX), MERCUREX Process and Acid Recovery by Solvent Extraction Process (ARSEP). Their fields of application, respectively, are: zinc recovery from secondary materials; zinc recovery from concentrates and ores with no iron residue production; copper recovery from concentrates by chloride hydrometallurgy; mercury removal from brines and aqueous effluents; and acid removal from electrolyte bleeds, diluted acids and spent pickling liquors. The main conclusion of the authors is that the solvent extraction technological package of Técnicas Reunidas S.A. offers a great potential of applications, which could be industrially implemented in specific base metals recovery and removal field. The technological background is also suitable for easy application for the solution of other non-ferrous metal problems with considerable advantages and cost plus time savings.

Keywords: ZINCEX, ZINCLOR, CUPREX, MERCUREX and ARSEP processes

INTRODUCTION

Técnicas Reunidas Research & Development Division has developed an important number of industrial processes which use solvent extraction as a way to produce a pure solution (industrial production) or a cleaned effluent (environmental treatment) from ores, concentrates, secondary materials and bleeds.

Modified ZINCEX Process, ZINCLOR Process, Copper Metal Extraction Process (CUPREX), MERCUREX Process and Acid Recovery by Solvent Extraction Process (ARSEP) are some of the main process developed by TR with demonstrated industrial application.

Modified ZINCEX Process (MZP)

The process treats flue dust from smelting furnaces, ashes from hot dip galvanising baths, Waelz oxide, electric arc furnace dust (EAFD), carbonate and silicate concentrates and ores, etc.

As shown in the simplified process scheme (figure 1) there are three main stages: leaching, solvent extraction and electrowinning. Leaching yield varies from 80 to 99% according to the material treated. The purity of the zinc produced can be up to 99.99% (SHG). Lead, copper and cadmium metals are by-products if they are present in the feed material. In this way, a clean effluent is produced.

The methodology that use the solvent extraction section of the process is the following:

- Extraction: The zinc is extracted by the unloaded organic phase (D2EHPA) from the aqueous phase in a countercurrent system of three stages.
- Washing: Acid aqueous phase is contacted with the loaded organic solution to remove aqueous entrainment and co-extracted impurities and to obtain an ultra pure organic phase.
- Stripping: The zinc content in the organic phase is stripped by an aqueous phase with a high acid concentration. The unloaded organic phase is recycled and the aqueous phase is a high purity zinc solution that can be used to obtain SHG zinc plates by electrowinning.

© 2000 Society of Chemical Industry

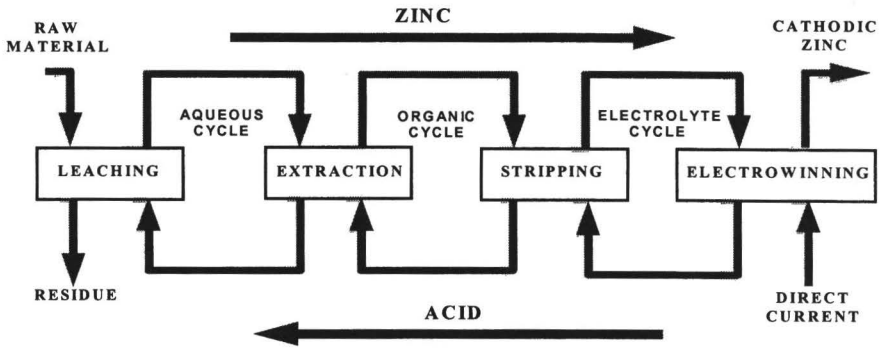

Figure 1 Conceptual Process Flowsheet

This process and the former version ZINCEX has been successfully operated in several plants, such as Metalquímica (Spain) and QUIMIGAL (Portugal) with a capacity of 8000 and 11500 t/y of zinc respectively. Further, a spent battery recycling plant is operating in Cataluña (Spain) with MZP as main section to recover the zinc content in the batteries. Furthermore, an important number of Pilot Plants have been operated in the TR's Research & Development Centre in Madrid (Spain).

Recently two Pilot Plants for new projects called SKORPION and SANYATI for Reunion Mining Company have been finished:

- Skorpion Process is an industrial plant of 150000 t/y of zinc which produce a SHG zinc plates from a silicate ore from a deposit located in Namibia, while
- Sanyati Process is an industrial plant of 5000 t/y of zinc to treat the bleed of an existing copper plant in Zimbabwe.

ZINCLOR Process

This process allows the recovery of zinc from commercial concentrates or zinc ores. The process starts (figure 2) with ferric chloride leaching followed by solvent extraction and electrowinning by the METCLOR cell developed by TR. The ZINCLOR electrowinning cell has been developed and operated at commercial scale. Very pure metal (SHG) is obtained along with chlorine that is recycled and used to re-oxidize the leaching agent. The overall zinc recovery is about 98%.

A simplification of this process without leaching or cementation the PICKLEX Process, has been successfully confirmed for the recovery of zinc from spent pickling acid solutions from galvanising industries. Overall zinc recovery is greater than 97%. Electrowinning products allow the production a very high zinc metal quality and spent pickling acid regeneration and recycling.

The methodology used to operate the solvent extraction section is as follows:

- Extraction: The aqueous feed is contacted counter-currently with an organic solution consisting of a $ZnCl_2$ selective extractant, such as di-pentylpentyl-phosphonate (DPPP), diluted in kerosene, or ACORGA ZNX-50. $ZnCl_2$ is transferred from the aqueous feed to the organic solvent, resulting in a $ZnCl_2$ loaded organic extract and in an aqueous raffinate which is recycled to the leaching operation.

- Washing: An aqueous phase solution is contacted with the loaded organic solution to remove aqueous entrainment and co-extracted impurities and to obtain an ultra pure organic phase.
- Stripping: The organic extract is sent to the stripping section where it is contacted in several countercurrent stages with hot water or spent electrolyte. $ZnCl_2$ is fully stripped from the organic solvent resulting in a barren organic and in an extraordinarily pure aqueous extract with a relatively high $ZnCl_2$ concentration because of the high selectivity of the extractant for zinc. This solution can be fed to the electrowinning cell to produce zinc plates SHG, while the unloaded organic is recycled to the extraction stages to extract $ZnCl_2$ again.

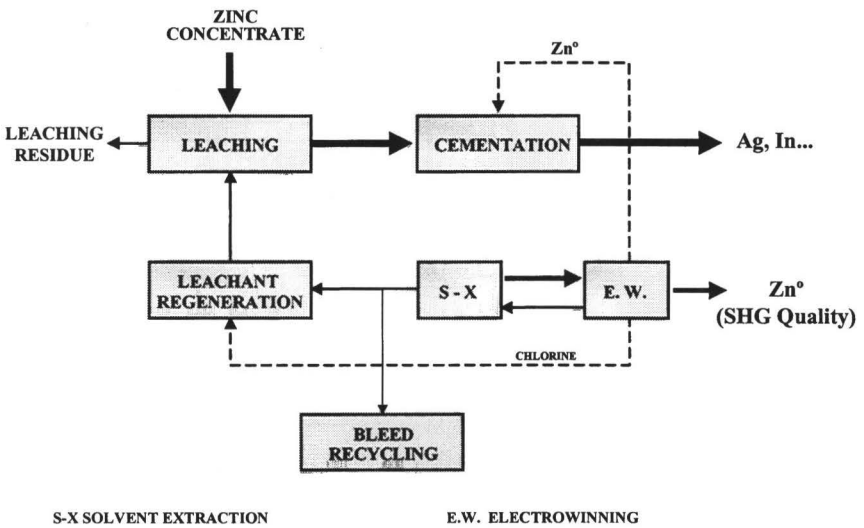

Figure 2 The ZINCLOR Process

This process has been developed at Pilot Plant level in the TR's Research & Development Centre in Madrid (Spain) with excellent results.

CUPREX Process

The CUPREX Process allows the recovery of copper from commercial concentrates. The process (figure 3) starts with ferric chloride leaching followed by solvent extraction and electrowinning in the METCLOR cell developed by TR. Grade 1 copper metal (99,99%) is electrowon along with chlorine which is recycled and used to re-oxidize the leaching agent. The leaching residue contains elemental sulphur produced in the reaction together with any gold fed with the concentrate. The process recovers the main chemicals used and any bleed stream is processed to discharge clean effluents. Overall, the copper recovery is above 98%.

The methodology used by the solvent extraction stage is as follows:

- Extraction: A clarified pregnant liquor containing cupric chloride and ferrous chloride and minor impurities (mainly Zn, Pb and Ag) and 5.5 to 6 mol/dm^3 chloride ion is contacted at ambient temperature with a kerosene solution of ACORGA CLX50, and the copper is transferred selectively to the organic phase.

- Scrubbing: There are three stages where the aqueous entrainment and last traces of co-extracted impurities are removed from the organic phase with an acid aqueous phase to obtain a clean organic phase.
- Stripping: The scrubbed organic solution is stripped with water or spent catholyte at 65°C to produce an aqueous solution containing above 100 g/dm^3 Cu which is sent to the electrolysis section as catholyte to produce a copper metal of grade 1.

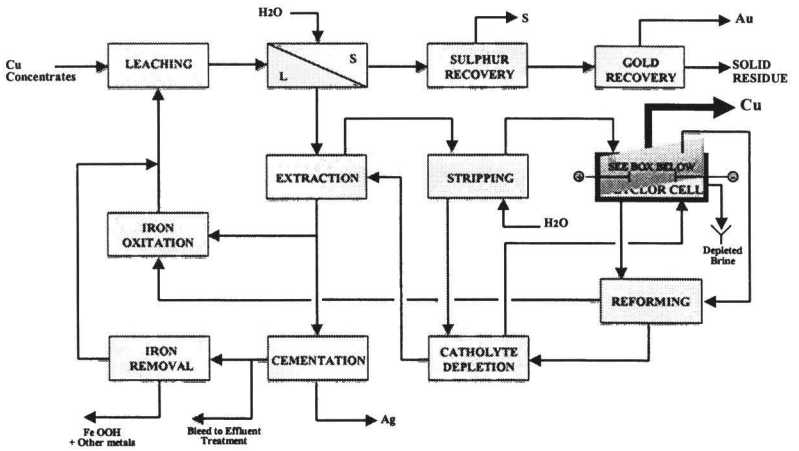

Figure 3 The CUPREX Metal Extraction Process

This process has been developed in a demonstration pilot plant of 300 Kg/d in the TR Research & Development Centre in Madrid (Spain) with excellent results.

MERCUREX Process

The MERCUREX Process may treat any waste-water whose mercury concentration is below 60 ppm. Waste-waters whose mercury content is higher than this must be diluted before treatment.

The final process effluent has a mercury concentration below 10 ppb and over 99.9% of the mercury may be recovered. The mercury is in the form of free mercury chloride which could be re-introduced in the salt circuit before electrolysis..

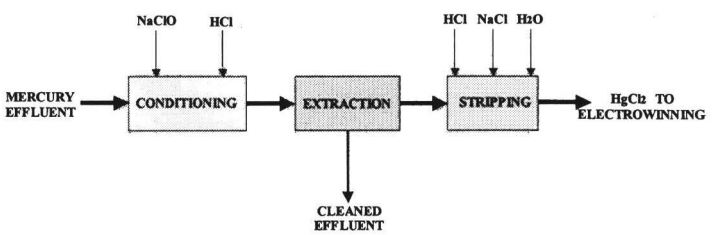

Figure 4 The MERCUREX Process

The MERCUREX Process (figure 4) operates by selective liquid-liquid extraction, employing a highly selective reagent, which is specially modified to accentuate the physical chemical properties and distribution coefficients.

The methodology used in the solvent extraction stage is as follows:

- Extraction: Before extraction, the waste-water is modified and the mercury is oxidised to a cationic state with hypochlorite solution. After complete oxidation, the mercury cation is extracted by an organic phase that contains the extractant. The final concentration of mercury existing in the residual water depends on the conditions of design, operation and initial concentration. This final concentration may be adjusted to any specifications down to 2 ppb.
- Stripping: The mercury in the organic phase is stripped by an acidified brine stream. Once the stripping is completed, this brine, which contains about 1000 ppm of mercury is recycled. The operation is completely automatic.

TR have built three industrial plants with a capacity of 2 m^3/h for Energia e Industrias Aragonesas (EIASA) in Spain. These plants treat a bleed from a sodium-chloride brine feeding chlor-alkali electrowinning cells. The mercury content in the bleed is 20 ppm and MERCUREX Process reduces this value down to 10 ppb.

Acid Recovery by Solvent Extraction Process (ARSEP)

Técnicas Reunidas is developing a series of new processes able to extract free and complex acids from different effluents (figure 5).

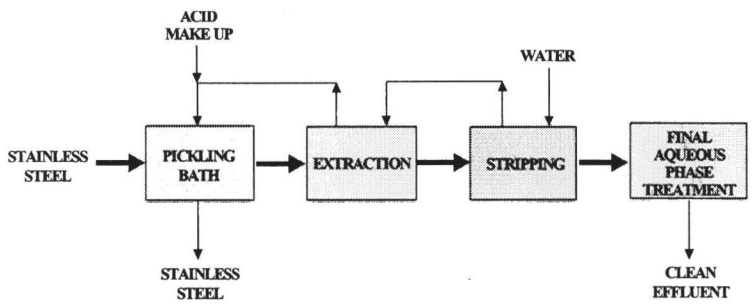

Figure 5 Acid Recovery by Solvent Extraction Process (ARSEP)

Typical recoverable acids are: H_2SO_4, HNO_3 and HCl from electroplating, stainless steel pickling, diluted acids from sulphuric acid plants, etc.

At the moment, the methodology of the solvent extraction section is rather well defined and it is recommended that tests are performed with real solutions for every particular application. The description of the process is as follows:

- Extraction: An effluent with different compositions of free and/or complexed acids is contacted with an organophosphine oxide extractant (CYANEX 923) at 25°C. This temperature should be adjusted to suit each case. The result is extraction of 98% of the total acid content in the aqueous feed.
- Stripping: The acid of the organic phase is stripped by a water stream at 50-70°C. The resulting aqueous extract solution has an acid concentration which depends on the particular process conditions.

TR is presently working on a BRITE-EURAM project devoted to acid recovery from stainless steel pickling baths. A pilot plant will be likely operated within 1999 for continuous testing of this process.

REFERENCES

1. ZINCEX Process:
   Díaz G and Martín D. *Resources, Conservation and Recycling* **10**, 43, (1994).
   Díaz G, Martín D and Lombera C. Paper presented at: *2nd International Conference on the Recycling of Metals*, Amsterdam, Netherlands, October 1994; *5th European Electric Steel Congress*, Paris, France, June 1995.
   Díaz G, Martín D and Lombera C. *J. Metals*. **47**(10), 22, (1995).
2. ZINCLOR Process:
   Parkinson G. *Chem. Eng*. **99**(6), 37, (1992).
   Alvarez JL, Cazorla A, Menéndez M and Parrilla F. *Congreso Mundial de Minería*, Madrid, Spain, 851, (1992).
   Díaz G, Frías C, Parrilla F and Regife JM. *World Zinc'93 Conference*, Hobart (Tasmania), Australia, 341, (1993).
3. CUPREX Process:
   McLean DC, *AIME Annual Meeting*, Dallas, Texas, February 14-18, 1992.
   Peters E, *Chloride Metallurgy*, Benelux Metallurgie, Brussels, 1, (1997).
   Dalton RF et al. *Separation Processes in Hydrometallurgy*, ed Davies GA, Ellis Horwood, London
4. MERCUREX Process:
   Nogueira E and Hermana E. *Innovación Tecnológica* **25**, 2, (1978).
   Nogueira E, Redondo A, Baile M and Regife J. *Patente española nº 447417*.
5. Acid Recovery by Solvent Extraction Process:
   Frías C and Pérez O. *Rev.Metal., 8º Congreso Nacional de Ciencia y Tecnología Metalurgicas*, Madrid, 34, (1998).

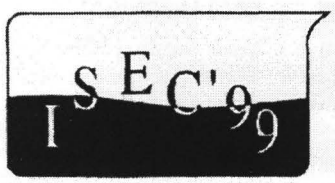

COMPARISON OF THE PERFORMANCE OF FULL SCALE PULSED COLUMNS VS MIXER–SETTLERS FOR URANIUM SOLVENT EXTRACTION

RL Movsowitz, R Kleinberger, EM Buchalier, B Grinbaum and S Hall[1]
Bateman Projects Limited, P.O. Box 15, Yokneam, Israel
[1]Western Mining Corporation (WMC), Australia

ABSTRACT
A rare opportunity to compare the performance of pulsed columns vs. mixer settlers in an industrial site, for a long period, occurred in the Uranium Solvent Extraction Plant of WMC at Olympic Dam, South Australia. The plant was operated for years with two trains of 2 mixer-settler batteries for the extraction of the uranium. When the company decided to increase the yield of the plant, the existing two trains of mixer-settlers for U-extraction were put in series, giving one 4-stage battery. In parallel, two Bateman Pulsed Columns, of the disc-and-doughnut type, were installed, to compare the performance of both types of equipment over an extended period. The parallel operation started two years ago. The intermediate results show, that the performance of the columns is excellent: the extraction yield is similar to the 4 mixer-settlers - about 98%, the entrainment of solvent is lower, there are less mechanical failures, less problems with crud, smaller solvent losses and the operation is simpler. The results convinced WMC to install 10 similar columns for the expansion of their plant. This paper includes quantitative comparison of both types of equipment, including data generated.

Keywords: mixer-settlers, pulsed columns, uranium extraction

INTRODUCTION

WMC's Olympic Dam Operation consists of copper and uranium production plants. Separation and purification of both metals involves SX. Historically both SX processes were carried out in mixer settlers. Part of WMC's 3rd stage expansion program was to improve uranium extraction by installing additional equipment. In 1995 WMC requested Bateman to test the possibility of replacing the mixer-settlers with Pulsed Columns for this purpose. The main emphasis of the tests was therefore uranium extraction, which is the topic of this paper.

The Bateman Pulsed Column is air pulsed with disc and doughnut internals. Earlier versions of this type of pulsed column were used for uranium extraction in the 1970's.

The Process for Extraction of Uranium

The solvent extraction processing at Olympic Dam starts with the extraction of copper from the pregnant leach liquor. The copper raffinate is then fed to the uranium circuit to extract the uranium. The extractant used in ODO Uranium SX circuit is Alamine 336, a tertiary amine, in Shellsol as diluent and decanol as modifier.

Extraction occurs according to the reactions:

$$2R_3N + H_2SO_4 \rightarrow (R_3NH^+)_2SO_4 \quad (1)$$

$$2\left(R_3NH^+\right)_2SO_4^{2-} + UO_2(SO_4)_3^{4-} \rightarrow \left(R_3NH^+\right)_4 UO_2(SO_4)_3^{4-} + 2SO_4^{2-} \quad (2)$$

Standard Operating Conditions.

250-500 ppm U_3O_8 in copper raffinate and 500 ppm U_3O_8 in the barren solvent. The concentration of Alamine 336 in the solvent is 4.0%. This concentration allows the theoretical loading of up to 5,000 ppm U_3O_8 in the solvent.

Phase Ratio:

The desired phase ratio is derived from the concentration of the uranium in the feed on one hand, and the maximum possible loading of the solvent on the other. The design ratio for the plant is 1:7.

© 2000 Society of Chemical Industry

Dispersion Type:

The process should be run with W:O (water in oil) dispersion because the dispersion of O:W causes heavy emulsions in the mixer-settlers. This means that the *major phase* (i.e. the one which is present in excess) is dispersed. In pulsed columns, it is sometimes possible to disperse the *major phase* and keep the *minor* one as continuous (unlike mixer-settlers, where the minor phase must be dispersed, which often leads to internal recycles). This is also the case in the extraction of uranium.

Number of theoretical Stages:

Computer simulation, based on plant data, confirmed that three theoretical stages are sufficient to achieve over 99% yield at standard operating conditions. Similar values were reported by Ritcey.[2] The flow sheet for Uranium extraction using one train of pulse columns and one of mixer-settlers is presented in Figure 1.

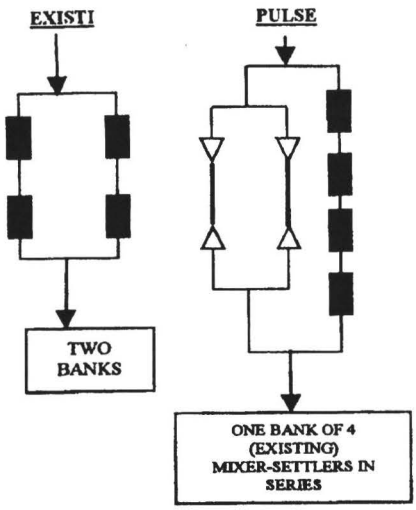

Figure 1. Flow sheet options and effect on recovery

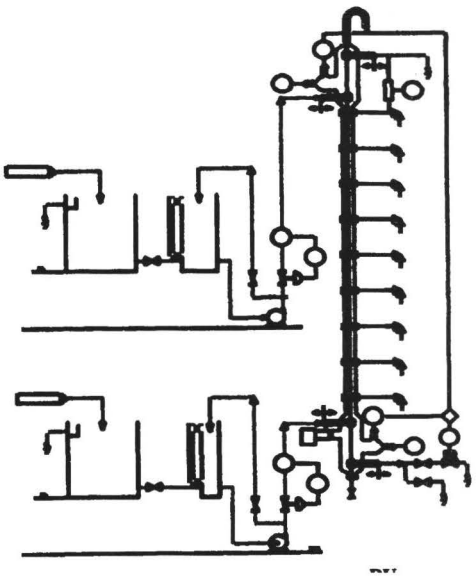

Figure 2

EXPERIMENTAL

Pilot Plant for Verification of the Process

In the first stage, a pilot plant, for verification of the process, was installed. The Pilot Pulsed Column used in the experiments was built from four one-meter glass segments and two glass decanters, as shown in Figure 2. The aqueous and solvent streams were fed to their respective header tanks. Using magnetic drive Richter pumps, the two liquids were pumped to their respective inlets to the column. The flow rates were controlled manually using two rotameters. The column was pulsed using a Bran+Lubbe mechanical pulsator, with variable stroke (0 - 30 mm) and variable frequency (16 - 144 spm).

The experiments were carried out by running copper raffinate against barren solvent, both taken from the plant. The dispersion was always W:O.

After reaching a steady state and verifying that the column was stable, samples of the inlets and the outlets were taken and analysed for concentration of U_3O_8. The results were compared with the routine analysis of the plant. The pilot plant was considered hydrodynamically unstable if one of the following occurred:

Flooding, i. e. plug of aqueous phase blocking the column.

Accumulation of the aqueous phase in the upper settler, with correct solvent level in the lower settler.
Phase inversion.

The parameters that were varied were flow rates and pulsation intensity, to obtain the flooding curve. The flooding curve indicates the hydrodynamic operating limits of the column which are required for scale-up. The experiments were carried out at phase ratio O:W = 1:5-6, according to the phase ratio in the plant.

Full Scale Columns vs. Mixer Settlers

The data were collected from the plant sheets on a daily basis and are presented in Table 3 and Figure 3.

RESULTS

I. Pilot Plant vs. Mixer Settlers

The results of the pilot plant vs. the plant experiments are summarised in Table 1

Test No	Phase Ratio	Pulse (cm/s)	Flux $m^3/m^2/h$	U_3O_8 Feed	U_3O_8 Plant	Raffinate Pilot	Raffinate Plant	Efficiency % Pilot	Efficiency % Diff.
UEX- 1	6.8	2.4	44	400	60	37	85	91	6
UEX- 2	5.7	2.4	30	400	60	32	85	92	7
UEX- 3	5.8	2.4	37	400	60	54	85	87	2
UEX- 4	5.6	2.4	45	400	60	49	85	88	3
UEX- 5	5.6	2.4	48	400	60	14	85	96	11
UEX- 6	5.2	2.4	49	304	28	10	91	97	6
UEX- 7	5.2	2.4	49	304	28	2	91	99	8
UEX- 8	5.2	2.4	49	304	28	7	91	98	7
UEX- 9	4.9	2.4	52	304	28	8	91	97	6
UEX-10	4.5	4	50	333	20	22	94	93	- 1
UEX-12	4.4	4.8	39	333	20	15	94	96	2
UEX-13	4.3	4.8	45	333	20	14	94	96	2
UEX-14	4.6	4.8	47	333	20	2	94	99	5
UEX-15	5.6	2.4	50	386	22	34	94	88	- 6
UEX-24	5.6	2.4	49	264	75	28	72	89	17
UEX-25	5.6	2.4	49	264	75	13	72	94	22
UEX-26	5.2	2.4	49	256	75	1	72	100	28
UEX-31	5	2.4	57	430	20	10	95	98	3

Table 1 U_3O_8 Extraction Efficiency (Plant vs. Pilot)

Entrainment.

The W:O entrainment at the top of the column was below 0.1% in all experiments. The O:W entrainment in the Pilot Plant it was 50-70 ppm while in the Production Plant it was above 220 ppm.

Visual Observations

In addition to the numerical values, the following visual observations were made:

1. Real flooding, i.e. plug of water in the column, was observed only in a blank experiment which was carried out without any pulsation. The flooding which occurred was usually expansion of the aqueous phase over the upper settler or high entrainment of aqueous phase in the top settler.
2. In the region of the aqueous feed entrance, phase inversion often occurred, i.e. the solvent was the dispersed phase. This was probably due to poor design of the feeder. Yet *this dispersion caused no problems*, unlike the situation in the mixer-settlers, where such an inversion is quite harmful. After

less than 0.5 meter, the dispersion re-inverted, reverted to the desired W:O dispersion, which in the given system seems to be more stable.

3. When the feed of the aqueous phase to the column was stopped for 5 minutes, the aqueous phase drained completely. Yet, when the aqueous feed was restarted, the column returned to hydrodynamic steady state in 3 minutes.
4. When the feed of the solvent was stopped for 15 minutes, it had no influence on the hydrodynamic behaviour of the column.
5. The column was operated twice with a problematic high silica feed. In the first run, the column behaved visually normally, without any extraordinary interface phenomena, and with high yield (89-100%), while the yield of the plant was only 72%, i.e. 17 - 28% lower. During this run the entire column section was required for mass transfer (UEX-24, UEX-25). In the second run, the feed was worse. The column operated well all day, and the only problem was difficulty in phase separation in the lower settler. Decreasing the flux by 10% solved the problem. The mixer-settler plant was unable to cope with the high silica levels, with phase inversion occurring almost every hour.
6. During all the experiments no precipitation of solids, neither in the column nor on the walls of settlers was observed. After two months of continuous operation, no problems of crud accumulation were observed.

II. Full Scale Columns vs. Mixer-Settlers

1. Maximum Flux and Turn down Ratio of the Columns

One column was tested at aqueous flow rates in the range 200 to 240 m^3/h and organic flow rates in the range 30 to 38 m^3/h. Simultaneously, the second column was tested at aqueous and organic flows of 100 and 30 to 35 m^3/h respectively. The air pressure was varied between 0 and 20 kpa, Once an operating condition had been selected, the column was allowed to stabilise for four hours before the first set of samples were taken.

At one point during the testwork both air blowers were stopped, and the columns were operated without pulsation for 4 hours.

The column operated for more than 24 hours at aqueous/organic flow rates of 220/31 m^3/h without any hydrodynamic problems and with full saturation of the solvent. The measured hold-up during this period was of the order of 20 to 30"/o aqueous.

At an aqueous flow of 240 m^3/h and an organic flow of 35 m^3/h, the column operation was stable for the first 8 hours, after about 8.5 hours the hold-up in the entire column increased and the column became unstable. Unstable in this sense means that the hold-up rises sharply and within a few minutes the interface rises or falls very quickly.

The columns can operate stably at a tumdown of 100 m^3/h aqueous at constant solvent flow.

The yield of both columns was equal, during the entire experiment, including the period of operation without pulsation, to the yield in the mixer-settler plant.

2. Comparison of Extraction Efficiency

	Mixer-Settlers	Pulse Columns
Settler/Column area (m^2)	30	4.9
Max. aqueous flow rate (m^3/h)	425	220
Normal Aqueous flow rate (m^3/h)	210 – 240	140 – 160 (limited by solvent rates)
Solvent flow rate (m^3/h)	41 – 44	30 – 34
Extraction efficiency (%)	98	98
U concn. in loaded solvent (ppm)	2800 – 3100	2700 - 2900
Downtime due to SX problems	None	None
Organic entrainment in raffinate (ppm)	140	<100

Table 2 Summary of U_3O_8 Extraction Efficiency (Mixer-Settlers vs. Columns)

Table 2 is based on the daily reports of the SX plant. The values given are the arithmetic averages for both the columns and the mixer-settlers.

Table 3 and Figure 3 show the comparison of the pulse columns and mixer-settlers over a 3-week period.

			Column 57			Column 58			Mixer-settlers		
Date	Copper raffinate	Barren solvent	Copper raffinate	Barren solvent	Uranium raffinate	Copper raffinate	Barren solvent	Uranium raffinate	Copper raffinate	Barren solvent	Uranium raffinate
	U ppm	U ppm	m3/h	m3/h	m3/h	m3/h	m3/h	U ppm	m3/h	m3/h	U ppm
21/11	319	65	140	17	8	140	17	9	230	36	2
22/11	346	87	140	22	5	140	22	5	230	42	4
23/11	416	74	140	22	7	140	22	9	230	44	10
24/11	349	91	140	223	5	140	23	5	230	50	0
25/11	423	99	140	27	7	140	27	12	230	47	0
26/11	610	213	140	25	7	140	25	14	230	45	92
27/11	689	123	140	27	9	140	27	13	230	48	271
28/11	664	128	140	27	19	140	27	21	225	48	252
29/11	539	164	140	26	49	140	26	50	210	39	226
30/11	534	82	140	27	11	140	27	11	230	48	161
1/12	515	93	150	25	6	150	25	7	230	46	29
2/12	697	97	140	27	21	140	27	26	230	48	202
3/12	603	101	140	25	15	140	25	27	230	45	197
4/12	463	121	140	22	10	140	22	15	230	40	162
5/12	472	112	140	22	9	140	22	8	240	40	30
6/12	453	99	140	22	6	140	22	9	240	45	12
7/12	417	74	140	22	7	140	22	11	240	45	7
8/12	419	82	140	27	8	140	27	10	240	46	3
9/12	440	21	140	23	5	140	23	8	240	42	2
10/12	431	56	140	22	7	140	22	9	240	42	3

Table 3 U_3O_8 Extraction Efficiency (Mixer-Settlers vs. Columns)

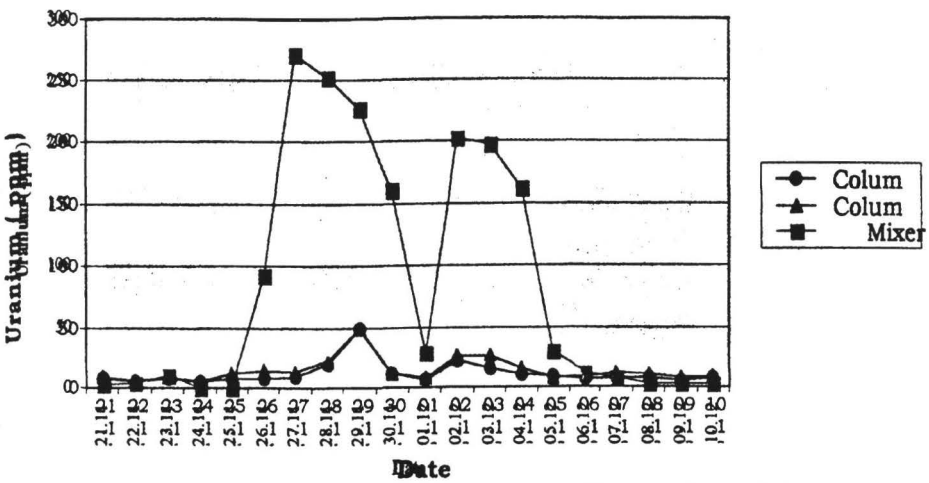

Figure 3. Comparison of Uranium Concentration in the Raffinate of Pulse Columns and Mixer-Settlers

3.General Observations

The observations were made by WMC staff in the plant during 1997-8.

a. High Silica Feed

Silica problems are rare, but there is still a potential to have silica excursions. Last time a high silica feed occurred when both the columns and the mixer-settlers were in the circuit, the columns were not affected, and emulsion was isolated to the mixer settlers. The columns enabled the continuation of solvent circulation through the mixer settlers. Without the columns, the aqueous and

solvent flows would have to be stopped through the mixer settlers, and left until the emulsion had completely settled, which could take several hours, with the potential for cleaning the settlers out before being able to restart. The columns did display an emulsion at the interface, however the units remained on line with the only impact observed being slightly higher aqueous and organic entrainment. The columns on line allowed relatively clean solvent to continue to be circulated, allowing the emulsion in the mixer settler extraction train to be broken down much quicker.

b. Crud Formation and Shutdown for Cleaning

Solids, which are present in the feed, cause crud formation. In mixer-settlers the crud accumulates, and causes a periodical shutdown for cleaning. Cleaning of four settlers can take up to 60 hours, resulting in the loss of significant amounts of solvent which is entrained in the crud (70% of the crud weight is solvent). During the two years of operation, the pulsed columns have not been shutdown for cleaning.

c. Step change in uranium feed

A 50% increase in uranium feed concentration had a significant deleterious effect on the mixer-settler performance whereas the column performance dropped only slightly. The columns returned to their original performance the same day whereas the mixer-settlers took 2 days to return. This demonstrates that the tolerance of the columns to surges and their quick response.

ANALYSIS OF RESULTS AND CONCLUSIONS

The parallel operation of industrial pulsed columns vs. mixer-settlers, for the extraction of uranium from ODO's copper raffinate, started two years ago. The results show, that the performance of the columns is the operation is simpler. The columns are less sensitive to fluctuations in feed composition than the mixer- settlers and show a much faster response

The column can be run in the desired W:O dispersion with phase ratio of 7:1 without any solvent recycle. The dispersion is stable and disturbances in the flow of one of the phases are not expected to cause phase inversion. The entrainment of solvent in the raffinate was much smaller, between 30 - 50%, in the columns relatively to the mixer-settlers.

Flow rates

The industrial columns are able to operate in the entire operating range (100 - 220 m^3/h aqueous and 30 - 35 m^3/h organic) for at least a few hours without pulsation while maintaining hydrodynamic stability and nominal recovery.

The average flux is about 50 $m^3/m^2/hr$, compared to 4 $m^3/m^2/hr$ in the plant. This means that the desired area of the column is 10 times smaller than that of the settler.

The maximum flux in the columns is 55 $m^3/m^2/hr$. On the other hand, fluxes as low as 22 $m^3/m^2/hr$ in the column enabled stable and efficient operation.

Mass transfer

The mass transfer was rapid and not affected by the flow rates. In most cases the column had higher yield than a two stage mixer-settler battery and similar to the 4 stage battery in the plant. The columns succeeded in operating with high silica feed without any special problems, and no solids deposition occurred, while the mixer-settlers had to be shutdown for periodical cleaning.

The results convinced WMC to install 10 similar columns for the expansion of their plant.

REFERENCES

1 *Technical Description of Olympic Dam Operations*, ODO Internal. Publication.

2 Ritcey GM and Ashbrook AW. *Solvent Extraction Principles and Applications to Process Metallurgy*, Elsevier, **II**, 452, (1984).



Process Development

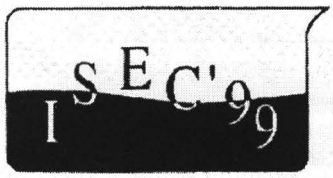

THE DEVELOPMENT OF CHEMICAL FLOWSHEETS FOR AN ADVANCED PUREX PROCESS

AL Wallwork, P Bothwell, JE Birkett, IS Denniss, RJ Taylor and I May
Research and Technology, BNFL, Sellafield, Seascale, Cumbria, CA20 1PG, UK

ABSTRACT
BNFL is developing an *Advanced Purex* reprocessing plant that will reduce costs and have less environmental impact than current plants. This paper describes the design and operation of a miniature alpha active counter-current test rig and includes the results of a typical trial; a Neptunium Rejection flowsheet using the hydrophilic complexing agent acetohydroxamic acid.

Keywords: Purex, Neptunium Rejection, flowsheet trial, acetohydroxamic acid, centrifugal contactors

INTRODUCTION

Nuclear fuel is reprocessed by solvent extraction using tri-butylphosphate dissolved in odourless kerosene (TBP/OK) to recover uranium and plutonium for reuse (the PUREX process). BNFL operates two reprocessing plants at Sellafield to reprocess Magnox (uranium metal) and oxide fuels respectively. These plants both use multiple solvent extraction cycles to separate U and Pu from fission products and then from each other and neptunium[1].

BNFL is now carrying out research and development programmes to enhance the performance of current plants[2] and to develop Advanced Purex processes using single solvent extraction cycles[3]. The latter project is an integrated programme including the investigation of fundamental chemistry, modelling and simulation work and counter-current experimental trials to minimise the amount of development work needed. The development of flowsheets using hydroxamic acid complexants to separate tetravalent actinides such as Np(IV) from hexavalent actinides such as U(VI) is an important part of the programme[4,5]. A companion paper reports the results of typical solvent extraction studies of hydroxamic acid complexants[6]. This paper presents the results of a counter-current trial of a Neptunium Rejection flowsheet using acetohydroxamic acid.

EXPERIMENTAL

All work was carried out at ambient temperature and constant rotor speed in identical centrifugal contactors with 1 cm diameter rotors. Mass transfer was studied in a single stage annular centrifugal contactor operated in a fume hood. Counter-current runs were carried out in a glove box using up to 36 centrifugal contactor stages engineered in banks of 4 which can be connected in a variety of ways to suit the flowsheet under test. Feeds are provided from peristaltic or syringe pumps and the product streams from contactors pass into flow through spectrophotometric cells connected by fibre optic cables to a UV/vis/NIR spectrometer. Samples are taken from the end streams during operation at steady state and then the feeds and rotors are turned off simultaneously and profile samples are removed from each stage. A small number of 'interstage' samples can be taken during the run to compare with the results of profile samples taken after the run.

In this work the counter-current rig was first operated with a uranium-only feed to test the stability of the feed pumps and to generate samples to demonstrate the limit of detection for Np. A feed containing U and Np, conditioned as Np(IV) with an excess of ferrous sulphamate, was then used to carry out the flowsheet test. The extract/scrub and Np backwash contactors were operated simultaneously as shown in Figure 1 and the U loaded solvent was backwashed later. Feed compositions are listed in Table 1.

© 2000 Society of Chemical Industry

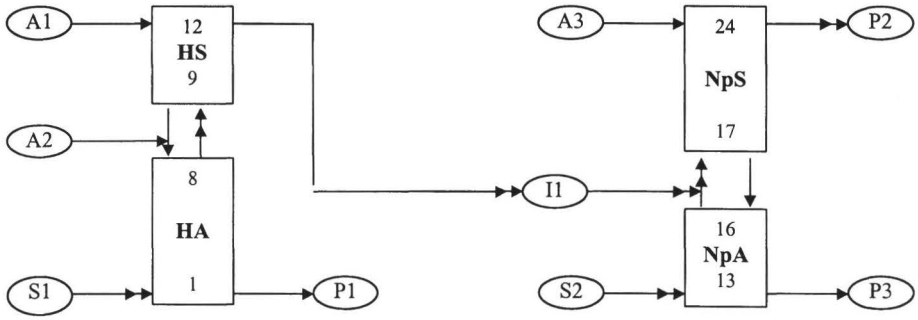

Figure 1 Neptunium Rejection flowsheet

A1	A2	A3	S1	S2	P1	P2	P3
HNO_3	HNO_3	HNO_3	TBP/OK	TBP/OK	HNO_3	TBP/OK	HNO_3
N_2H_4	U(VI)	N_2H_4				U(VI)	Np (99.63% I1)
	Np(IV)	AHA				Np (0.37% I1)	
	N_2H_4						

Table 1. Feed and product concentrations in the Neptunium Rejection flowsheet

Mass transfer trials were carried out in a single stage contactor using solvent preloaded with Np(IV) and aqueous phase containing acid only or acid plus hydroxamic acid to measure the rate of backwashing of Np.

The models were developed using SpeedUp from AspenTech UK Ltd and can be run in either steady state or dynamic mode. Model development has been described in detail elsewhere[7]. The most important features of the model for this assessment included contactor data, distribution algorithms for nitric acid, U(VI) and Np(VI,V,IV), mass transfer kinetics, reaction kinetics and entrainment. Initial simulations used the rate of mass transfer that had been measured for the extraction of U for all transferring metals.

RESULTS AND DISCUSSION

The proposed full single cycle flowsheet comprises U, Np, Pu co-extraction and scrubbing, Tc Rejection, U/Pu partition, Np Rejection and finally U backwash[3]. However, in this trial, U and Np were initially co-extracted using flowsheet conditions designed to replicate the expected composition of the solvent product from the U/Pu split in the single cycle flowsheet (i.e. a conventional HA/HS and Tc Rejection stages were not included). This stream was then fed to the Np Rejection contactor (NpA/S). The trial was primarily designed to test the NpA/S flowsheet and so attention was concentrated on this contactor. Therefore, a limited preliminary mass transfer trial was carried out to measure the rate of backwashing of Np in the presence and absence of hydroxamic acid. The results indicated that mass transfer of Np into acid was slower than for U but that AHA increased the rate of transfer of Np.

Product compositions are shown in Table 1. Good mass balances for nitric acid, U, Np and Fe were calculated from the analytical results so this trial provided an excellent opportunity to validate BNFL computational process models. The analytical results obtained for the profile samples were assessed separately and are discussed below.

Dynamic simulations were carried out before the trial using the estimated volume of each contactor stage to calculate the time required to attain steady state and hence the length of run required. This result was verified by a comparison of the calculated time to remove U from the system when the U feed was turned off, with the U concentration measured by on-line UV spectrophotometry (stream P2). The results are shown in Fig. 2 which demonstrates good agreement between the experimental and simulated U concentrations and so gives confidence in the dynamic responses predicted by the model.

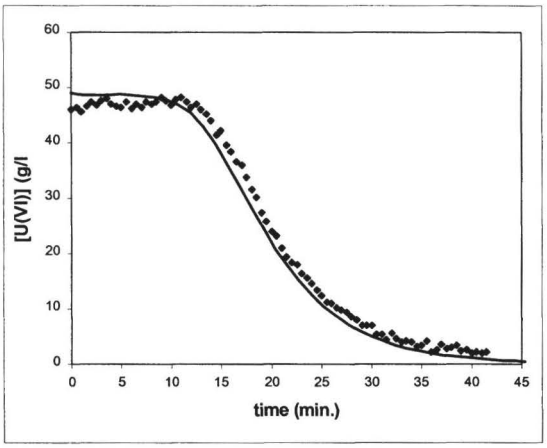

Figure 2. The effect of stopping the U(VI) loaded feed flow on [U(VI)]. Comparison of [U(VI)] in P2 measured by UV/vis spectrometry (♦) with the dynamic simulation (—).

The performance of each contactor was assessed by a comparison of the analysed and predicted profiles. In this flowsheet trial, Np(IV) is extracted in the "HA" contactor and so the concentration in the aqueous phase decreases as it passes from stages 8 to 1. This is demonstrated in Figure 3 where it can be seen that the experimental profile is significantly worse than the initial simulation. This prediction assumed that the rate of Np(IV) mass transfer equalled that measured for U. The solvent extraction behaviour of Np(IV) has been extensively studied[8] and it is well understood at acidities above 1M HNO_3[9]. Therefore, the Np(IV) distribution algorithm at the acidity of the "HA" contactor (1.5M) is considered reliable, so the effect of the rate of Np(IV) mass transfer was investigated. In preliminary single stage experiments, Np(IV) had been found to backwash more slowly than U(VI) and consequently reducing its rate of extraction in the model by a similar factor improved the fit between measured and predicted profiles markedly (Figure 3). This, however, must be confirmed by measuring the mass transfer rate for the extraction of Np.

Np was backwashed in NpS and so the concentration in the solvent and aqueous phases reduced from stages 17-24. This is shown in Figure 4 which again demonstrates that the experimental profile was not as good as the initial simulation. (Note that good agreement between the interstage and profile samples was obtained). In this case, the preliminary mass transfer experiments had shown that AHA increased the rate of backwashing of Np but had not demonstrated the exact dependence on [AHA]. However, it is likely that a change in the mass transfer rate was not the sole cause of the discrepancy between the experimental and predicted profiles. The NpS contactor operated at low

acidity and high [U] in the presence of AHA and it is in this region that Np(IV) extraction is less well characterised due to difficulties inherent in obtaining experimental distribution data[6,9]. A careful re-examination of the Np(IV)-AHA distribution algorithm indicated that it was probably underestimating the effect of [U] and [nitrate] under these conditions. The algorithm was adjusted for these effects and this led to improved agreement between the model and the measured profiles (Figure 4). Further work is in progress to confirm the distribution algorithm for Np(IV) under relevant conditions and to investigate the rate of mass transfer of Np(IV) in more detail.

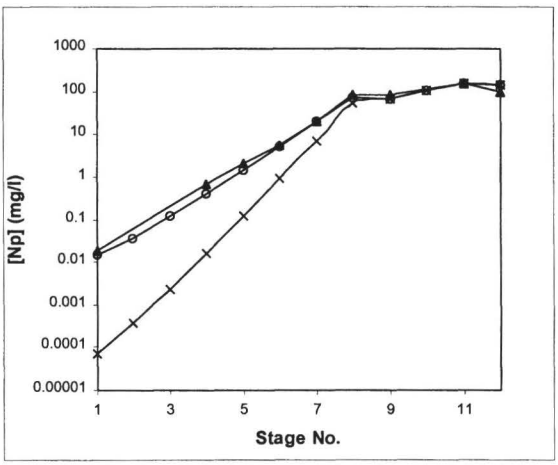

Figure 3. [Np] aqueous profile in the HA/HS cascade (▲ = observed profile; × = initial simulation with mass transfer rate equal to U(VI); ❍ = simulation with Np(IV) mass transfer rate reduced to 0.15 l/h).

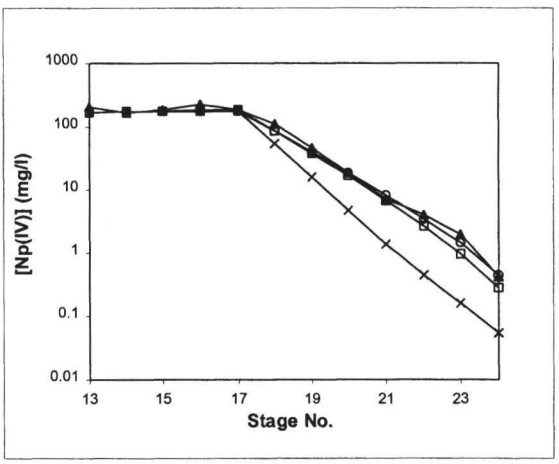

Figure 4. [Np] aqueous profile in the Np Rejection cascade (▲ = observed profile; ×= initial simulation ❍ = simulation with Np(IV) mass transfer rate reduced to 0.56 l/h;□= simulation with new Np(IV) algorithm)

The observed Np decontamination factor (NpDF) to the NpS organic product (P2) was at least 270 thereby demonstrating the separation of Np(IV) from a U(VI) loaded organic stream. The actual NpDF may have been greater than that observed because the Np concentration in P2 was at the analytical limits of detection. This was the first counter-current trial of the Neptunium Rejection flowsheet at Sellafield and it has demonstrated the importance of two effects that had not been identified previously. Further modelling has shown that the flowsheet can be modified to improve NpDF but that the design of the flowsheet will depend crucially on the distribution algorithm for Np(IV) in the presence of U and hydroxamic acid and its rate of mass transfer.

Accordingly, the Np profiles of this trial demonstrate the value of experimental data from miniature contactor rigs because errors in computational process models have been readily identified. Moreover, additional experimental work can be commissioned that is most relevant to developing these models further.

CONCLUSIONS

BNFL has powerful simulation tools with which to investigate flowsheet designs. An important part of modelling development is validation and data reconciliation so that the models can be used with increased confidence. This validation process has included the commissioning of an alpha active miniature counter-current centrifugal contactor rig at Sellafield.

The Np Rejection trial undertaken at Sellafield successfully demonstrated the technically difficult separation of Np(IV) from a U(VI) loaded organic stream using acetohydroxamic acid. Computational process models successfully reproduced the results of the trial and further development work has been identified.

ACKNOWLEDGEMENTS

The authors would like to thank Sellafield Analytical Services for their assistance.

REFERENCES

1. Wilson PD (ed.), '*The Nuclear Fuel Cycle*', Oxford Science Publications, Oxford, (1996).
2. Riley A, Donaldson N and Parkes P, *Proc. RECOD '98*, (1998).
3. Taylor RJ, May I, Denniss IS, Wallwork AL, Hunt G, Hutchison S, Richards V and Hill NJ, *Proc. RECOD '98*, (1998).
4. Taylor RJ, May I, Wallwork AL, Denniss IS, Hill NJ, Galkin B Ya, Zilberman B Ya and Fedorov Yu S, *J. Alloys & Compounds*, **271**, 534 (1998).
5. May I, Taylor RJ, Denniss IS, Brown G, Wallwork AL, Hill NJ, Rawson JM and Less R, *J. Alloys & Compounds*, **275**, 769, (1998).
6. Taylor RJ, May I and Hill NJ, *Proc. ISEC '99*, (1999).
7. Wallwork AL, Denniss IS, Taylor RJ, Bothwell P, Birkett JE and Baker S, *Nucl. Ener.*, forthcoming.
8. Kolarik Z and Dressler P, Unpublished report, KfK 4667, (1990).
9. May I, Taylor RJ, Brown G and Hill NJ, *Radiochim. Acta*, forthcoming.

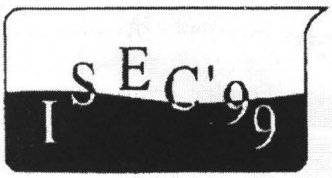

DISTRIBUTION BEHAVIOUR OF URANIUM, PLUTONIUM, NEPTUNIUM AND TECHNETIUM IN AN ADVANCED PUREX PROCESS (PARC PROCESS)

G Uchiyama, T Kihara, H Mineo, T Asakura, S Hotoku, M Watanabe, K Kamei, Y Nakano, S Kimura, M Goto and S Fujine

Process Engineering Laboratory, Japan Atomic Energy Research Institute, Tokai-mura, Naka-gun, Ibaraki-ken, Japan, 319-1195

ABSTRACT

An advanced PUREX process, PARC process (Partitioning Conundrum key process), has been developed which can reduce the radioactive waste volume containing TRU elements and the environmental hazard risk due to long-lived. In the separation of neptunium and technetium from plutonium and uranium solutions before the U/Pu partitioning step in the PARC process, the selective reduction of Np(VI) to Np(V) by normal-butyraldehyde and the high acid scrubbing of technetium are considered.The distribution behaviour of neptunium and technetium in both the PARC process and a current PUREX process as a reference were studied in chemical flow sheet experiments using spent fuel of 8,000 MWD/tU in an α-γ cell in NUCEF. The experimental data show that n-butyraldehyde was an effective reductant of Np(VI) in the presence of uranium and plutonium and that the high acid scrubbing was effective for Tc separation.

Keywords: nuclear reprocessing, neptunium, technetium, butyraldehyde, PUREX.

INTRODUCTION

An advanced PUREX process, PARC process (Partitioning Conundrum key process), has been developed which can reduce the radioactive waste volume containing TRU elements (Np, Pu, Am and Cm) and the environmental hazard risk due to long-lived nuclides such as ^{99}Tc, ^{14}C and ^{129}I.[1,2,3] In the separation of neptunium and technetium from plutonium and uranium solutions before the U/Pu partitioning step in the PARC process, the selective reduction of Np(VI) to Np(V) by normal-butyraldehyde and the high acid scrubbing of technetium are considered.[4]

The distribution behaviour of neptunium and technetium in both the PARC process and a current PUREX process as a reference were studied in chemical flow sheet experiments using miniature mixer-settlers in an α-γ cell in NUCEF. The extraction behaviour of uranium, plutonium and other tracers (zirconium, ruthenium, cesium and iodine) in the experiments were measured. This paper describes the major experimental results on the chemical flowsheet study

CURRENT PUREX PROCESS FLOW SHEET EXPRIMENT

EXPERIMENTAL

Five mixer-settlers (MX-1A, MX-1B, MX-2, MX-3 and MX-4) were used to measure the extraction behaviour of uranium, plutonium, neptunium, technetium and tracers (zirconium, ruthenium, cesium and iodine) in the solvent extraction steps. In the current PUREX process, the flow-sheet consists of six steps: co-decontamination, Tc scrubbing, U recovery, U/Pu partitioning, U stripping and solvent-washing steps as shown in Fig. 1. The volumes of the mixer and the settler sections of MX-1A, MX-1B and MX-2 having 20 stages were 6 cm^3 and 17 cm^3, respectively. The volumes of the mixer and the settler sections of MX-3 with 20 stages were 15 cm^3 and 88 cm^3, respectively. The volumes of the mixer and the settler sections of MX-4 with 6 stages were 15 cm^3 and 33 cm^3, respectively.

Purchased reagents such as n-butyraldehyde, TBP and n-dodecane were used without any special pretreatment. The dissolver solution of spent fuel of 8,000 MWD/tU as a feed contained 257 g/dm^3 uranium, 900 mg/dm^3 plutonium, 15 mg/dm^3 neptunium and 54 mg/dm^3 technetium, 263

© 2000 Society of Chemical Industry

mg/dm^3 zirconium, 118 mg/dm^3 ruthenium, 149 mg/dm^3 cesium and 3.1 mol/dm^3 nitric acid. The valence states of plutonium and neptunium in the feed solution were mainly Pu(VI) and Np(VI), respectively from spectrophotometric analysis. The concentration of nitrous acid in the feed solution was less than 8×10^{-5} mol/dm^3. Tracers of ^{239}Np, ^{95m}Tc, ^{95}Zr, ^{103}Ru and ^{131}I were added into the feed solution after diluted with nitric acid solution.

Uranium and nitric acid were analyzed by alkalimetric titration. N-butyraldehyde was analyzed by liquid chromatography. Alpha-ray and gamma-ray spectrometers were used to analyze the concentrations of plutonium and the tracer elements and a spectrophotometer was used to analyze the valency state of the elements in nitric acid solutions. Nitrous acid and hydrazine were spectrophotometrically analyzed by using chromogenic reagents. Di-n-butylphosphoric acid (HDBP) and hydrogen azides were analyzed by ion chromatography.

RESULTS AND DISCUSSION

The uranium, plutonium, neptunium and technetium fractions distributed to the products and raffinates are shown in Figure 1. In the co-decontamination step (MX-1A), more than 99.9 % of both the total uranium and the total plutonium, about 50 % of the total neptunium and 99 % of the total technetium fed to the co-decontamination step were extracted by the TBP solvent. The distribution fraction of neptunium to the raffinate was larger than those of commercial plants.[5, 6] The distribution fraction of technetium to the raffinate was almost the same as those of commercial plants.[5, 6] The uranium concentration in the organic stream from the co- decontamination step was 118 g/dm^3. This implies TBP was saturated by uranium in the solvent. It is considered that the highly saturated TBP caused the distribution fractions of technetium and neptunium.

In the Tc separation step (MX-1B), the concentrations of uranium, plutonium and neptunium are almost constant in both the organic and the aqueous phases. As for technetium, 90 % that flowed to the Tc separation step was back-extracted from the solvent stream and flowed to the Tc product. It is considered that the mixed complexes of $UO_2(NO_3)(TcO_4)\cdot2TBP$, $Pu(NO_3)_3(TcO_4)\cdot2TBP$ or $Zr(NO_3)_3(TcO_4)\cdot2TBP$ in the organic phase were decomposed to $UO_2(NO_3)_2\cdot2TBP$, $Pu(NO_3)_4\cdot2TBP$ or $Zr(NO_3)_4\cdot2TBP$ in high nitric acid in the Tc separation step.[7]

In the U/Pu partitioning step (MX-2), the uranium concentration in the organic phase was almost constant. The uranium that flowed to the step was not back-extracted from the solvent stream and flowed to the U stripping step. As for Pu, the concentration in both the organic and the aqueous phases decreased with approximately the same gradient as in the U/Pu partitioning step.

The concentrations of neptunium and technetium in both the organic and the aqueous phases decreased with approximately the same gradient as in the U/Pu partitioning step. About 50 % of the neptunium and technetium that flowed to the step (MX-2) was back-extracted from the solvent stream loaded with uranium and flowed as Pu product.

The concentration of hydrogen azide in organic phase was less than 10^{-3} mol/dm^3. The nitrous acid concentrations in both the organic and aqueous phases were less than 10^{-5} mol/dm^3 in both the U/Pu partitioning and U recovery steps. The concentration of HDBP in the U stripped solvent was 4.6 mg/dm^3.

In the solvent washing step (MX-4), alpha, beta and ^{95}Zr activities and HDBP concentration in the uranium stripped solvent decreased from 1,17o to 51.9, from 25 to 0.33, from 3,675 Bq/cm^3 to 16.8 Bq/cm^3 and from 230 mg/dm^3 to 10 mg/dm^3, respectively.

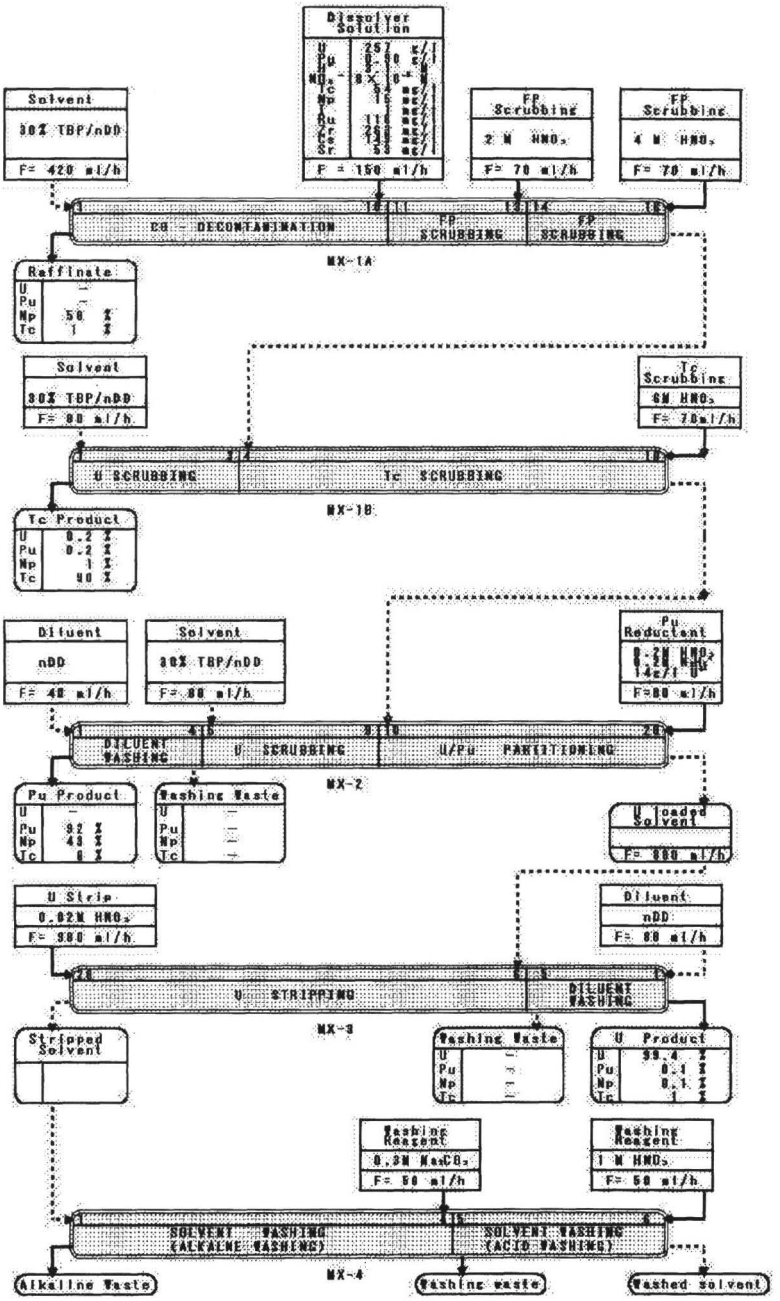

Fig.1 Distributions of U, Pu, Np and Tc in solutions in current PUREX process.

PARC PROCESS FLOW SHEET EXPERIMENT

EXPERIMENTAL

In the PARC process, the flow sheet consists of five steps: co-decontamination, Np separation, Tc separation, U recovery and U/Pu partitioning steps as shown in Figure 2. Normal-butyraldehyde used as a Np(VI) reductant was fed at stage 1 of the MX-1B. The scrubbing solutions for neptunium and technetium fed at stage 10 and 20, respectively were 3 mol/dm^3 and 6 mol/dm^3 nitric acid, respectively.

RESULTS AND DISCUSSION

The uranium, plutonium, neptunium and technetium fractions distributed to the products and raffinates are shown in Figure 2.

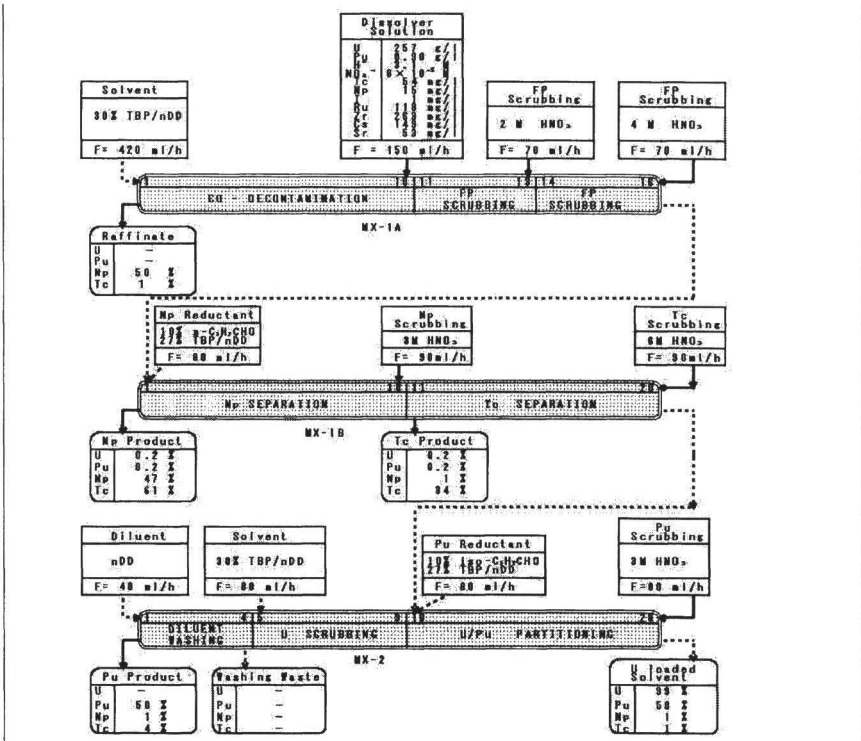

Fig. 2 Distributions of U, Pu, Np and Tc in solutions in PARC process.

In the Np separation step (MX-1B), the concentrations of U and Pu were almost constant in both the organic and the aqueous phases in the Np and the Tc separation steps. As for Np and Tc, concentrations in both the organic and the aqueous phases decreased with approximately the same gradient as in both the Np and the Tc separation steps. About 95 % of the Np that flowed to the Np separation step was back-extracted from the solvent stream loaded with uranium and plutonium and flowed to the Np product. This implies that Np(VI) was reduced to Np(V) by n-butyraldehyde.

As for technetium, about 60 % of the technetium that flowed to the Np separation step was back-extracted from the solvent stream and flowed to the Np product. In a kinetic study, it was found that the reduction rate of Tc(VII) by n-butyraldehyde was very small in 3 mol/dm^3 nitric acid solution.[8] The decrease of U and Pu concentrations in the aqueous and organic solutions by addition of organic solvent

with n-butyraldehyde affected the Tc back-extraction in the Np separation step (MX-1B). The rest of the technetium was back-extracted with 6 mol/dm^3 nitric acid in the Tc separation step.

In the U/Pu partitioning step (MX-2), the uranium concentration in the organic phase was almost constant. The uranium that flowed to the step was not back-extracted from the solvent stream and flowed to the U stripping step. As for plutonium, the concentration in both the organic and the aqueous phases decreased with approximately the same gradient as in the U/Pu partitioning step. About 50 % of the Pu that flowed to the U/Pu partitioning step was back-extracted from the solvent stream and flowed to the Pu product. The separation efficiency was very small, compared with those of previous works[9),10)]. It is considered that the short residence time of the Pu reductant in the U/Pu partitioning step is responsible for the results. The absorption spectrum of the Pu product solution showed that the Pu in the product solution was trivalent. Thus Pu(IV) was reduced to Pu(III) by iso-butyraldehyde.

As for neptunium and technetium, the concentrations in both the organic and the aqueous phases decreased with approximately the same gradient as in the U/Pu partitioning step. About 50 % of the neptunium and technetium that flowed to the step (MX-2) were back-extracted from the solvent stream loaded with uranium and flowed as Pu product.

The nitrous acid concentrations in both the organic and aqueous phases were less than 8×10^{-5} mol/dm^3 in both the U/Pu partitioning and U recovery steps. This indicates that Pu(III) was not re-oxidized by nitrous acid in the step without hydrazine as a decomposing reagent of nitrous acid.

CONCLUSIONS

The PARC process has been developed in which salt-free techniques using organic compounds are considered. The distribution behaviors of neptunium and technetium in both PARC process and current PUREX process as a reference were studied in chemical flow sheet experiments using spent fuel of 8,000 MWD/tU in an α-γ cell in NUCEF.

It was found that n-butyraldehyde was a selective reductant of neptunium(VI) in the presence of uranium, plutonium and technetium. It was confirmed that high acid scrubbing was effective for technetium separation.

REFERENCES

1. Maeda M, Fujine S, Uchiyama G, Kihara T, Sakurai T and Tsujino T, *Proc. GLOBAL 1995*, Versailles, France, 556, (1195).
2. Fujine S, Uchiyama G, Kihara T, Asakura T, Maeda M and Sakurai T, *Proc. 10th Pacific Basin Nuclear Conference*, **1**, 125, (1996).
3. Fujine S, Uchiyama G, Kihara T, Asakura T and Sakurai T, *Progress in Nuclear Energy*, **32**, 357, (1998).
4. Uchiyama G, Asakura H, Watanabe M, Fujine S and Maeda M, *Proc. ISEC'96*, 1291 (1996).
5. Viala M, Salvatores M, Mounney H, *Proc. 4th Information Exchange Meeting on Partitioning-Transmutation*, OECD/NEA, 60, (1996).
6. Phillips C, *Proc. ISEC'96*, 783, (1996).
7. Kanellakopules B and Koning CP, *Radiochimica Acta*, **33**, 169, (1983).
8. Asakura T, Uchiyama G, Fujine S and Maeda M, *Extraction '94*, 25, (1994).
9. Uchiyama G, Asakura H, Hotoku S and Fujine S, *Proc. RECOD'98*, (1998).
10. Uchiyama G, Asakura H, Hotoku S and Fujine S, *Solv. Extr. Ion Exch.*, 1191, (1998).

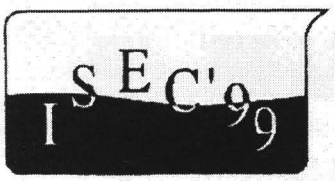

DEVELOPMENT OF FISSION PRODUCT (ARTIFICIAL) PALLADIUM LIQUID–LIQUID EXTRACTIVE RECOVERY AND REFINING OPERATIONS

Ed V Renard[1], VG Torgov[2], VV Tatarchuk[2], TM Korda[2] and IA Druzhinina[2]

[1]VNIINM, 123060, Moscow, Russia,

[2]IChI SB RAS, pr. Lavrentjeva, 3, 630090, Novosibirsk, Russia

ABSTRACT

A multi-stage process has been developed and experimentally tested to recover and further purify (up to 10^7-10^8) fission product palladium from PUREX-process modelling nitrate solutions through two extraction cycles by petroleum sulphides in an aromatic diluent.

Keywords: fission products, palladium, PUREX-process, organic sulphides

INTRODUCTION

Spent nuclear fuel is essentially an alternative to mineral contributors of natural platinoids and is expected to be a major source of Pd, Ru and Rh in the century to come.[1,2] Besides, 'radwaste' vitrification and ecological considerations about their disposal, necessitate the recovery of platinoids mentioned from high-level PUREX nitrate solutions. No commercial fission platinoids recovery procedure is available although efforts are in progress to implement their co-separation by means of reduction of denitrated radwaste raffinates by sugars, assay melting or chemical and electrochemical extraction into organic diluents and salt melts.[1-3]

Comparative analysis of a variety of extractants shows the benefits of using organic sulphides for nitrate solutions involving those from a lead collector dissolution.[3-5] This correlates well with published data [6,7] demonstrating a high Pd selectivity by dialkylsulphides and sulphur - containing concentrates (diesel fuel - gasoline, petroleum sulfides, etc). The feasibility of the desired separation factors (10^3) for Pd from attendant Ag, Rh, Ru radionuclides (this factor is much higher than that for natural Pd purification) using reagent-grade di-n-hexyl sulphide (DHS) or diesel fuel (DF) was not treated previously.[3,4] At present, industrial demand for Pd exceeds the total for other platinoids and is increasing progressively.[8]

This report deals with the Pd separation process involving two extraction cycles: the first one concerns the Pd separation from basic fission radionuclides directly from high-level nitrate solutions followed by its concentration; the second cycle is used as a supplement to separate Pd from noble metal (Ag, Rh, Ru) radionuclides by extraction from hydrochloride solutions. Both cycles use petroleum sulfide (PS) as an extractant; chemical and electrochemical treatment of ammoniacal re-extract, with a subsequent conversion to hydrochloric medium enables two cycles to be combined.

EXPERIMENTAL

Extractants and diluents.

Reagent grade DHS and di-n-octylsulfide (DOS), "summer" diesel fuel (0.15% sulphide sulphur) treated as Arseenkov,[3] and petroleum sulphides (a mixture of mono- and di-thiocyclanes, 10% sulfide sulfur, boiling point 234-360C) extracted from petroleum by 86% H_2SO_4 were used as extractants. Aromatic hydrocarbons (triethylbenzene, TEB), paraffinic hydrocarbons (printing ink thinners, PIT, with <0,2% of aromatic compounds), isostructural isomer mixtures of hydrogenated pentapropylenes (HPP) and paraffin-aromatic mixtures (containing 15-17% of aromatic compounds) served as diluents. The diluent flash point varies from 76C (TEB) to 130C (PIT).

© 2000 Society of Chemical Industry

Noble metals nitrates.

The palladium feed was made by dissolving 99.9% Pd in strong HNO_3 by long refluxing followed by dilution to desired metal and acid concentrations. Silver nitrate was also recrystallised from strong HNO_3. Nitrosoruthenium nitrate solutions were prepared by dissolving a $Na_2[Ru(NO_2)_4OH]$ sample in 8 mol/dm^3 HNO_3 solution by boiling for 1h, evaporating the solution to crystallisation and dissolving in 3 mol/dm^3 HNO_3. RhI_3 was first dissolved in boiling HNO_3-H_2O_2 mixture, evaporated until the iodine was totally removed, and then dissolved in 3mol/dm^3 HNO_3 to get a rhodium solution. The solution was nitrated by a 100-fold excess of sodium nitrite for 3 hours. Prior to extraction, nitrate solutions of single metals and their mixtures similar in composition to the high level PUREX-process liquid waste (noble metals, 0.1 - 0.2 g/dm^3 each, 3 - 3.5 mol/dm^3 HNO_3) were saturated with nitrogen oxides for 40 minutes.

Procedure

For ease of laboratory experiments, all the operations (extraction, scrubbing and stripping) were performed in one stage at an organic-to-water ratio (r) 1:1, except for the silver scrubbing and extraction at r = 0.28 - 0.1 performed in 2 stages in both cycles. The aqueous solutions, organic phases and dissolved residues of silver chloride and palladosoamine were analysed using an atomic-absorption spectrometer Z-8000 Hitachi. Chemically pure reagents (acids, ammonia) were not further purified. Each operation was checked against blank tests.

RESULTS AND DISCUSSION

Palladium separation and purification characteristics.

The entire process consists of two extraction cycles involving the following operations: extraction, scrubbing and stripping (re-extraction), the first cycle re-extract (Pd product) conversion to chloride and the Pd precipitation from the second cycle re-extract.

Extraction.

In the first cycle 98-99% Pd is extracted in a centrifugal contactor at a phase contact time (τ) of 10s and r = 0.1 by a 0.3 mol/dm^3 PS solution in TEB or TEB (~45vol%)-HPP mixtures. PS is essentially similar to DHS and DOS in efficiency (Table 1). With PS in other diluents, the extract retains its phase stability (no third phase or cruds) at about 1g/dm^3 Pd (r = 0.2). Under these conditions the extraction of Pd by DF is equal to 12% due to a low concentration of active sulphide sulphur (0.036 mol/dm^3) and is accompanied with black Pd-free cruds resulted from side reactions of the acid and diesel fuel impurities (resins and admixtures). No specific differences have been noticed for the PS extraction of Pd and impurities either from reagent-pure solutions or from their mixtures.

The separation factor $\alpha = 10^5 - 10^6$ suggests a good separation of Pd from Rh, Ru and Sb. Because of no phase contact time limitations in the second cycle, Pd is slowly extracted from the first cycle re-extract (1 – 2 g/dm^3 Pd) converted to a chloride solution (1 - 4 mol/dm^3 HCl) at τ = 60min, r = 0.03-0.10. A 0.5 - 1.0 mol/dm^3 PS solution in TEB extracts 97-98% Pd in one stage. Following two cycles, the total Pd concentration increases in the extract up to 30 – 60 g/dm^3 (i.e. by 100 - 300 times). The separation of Pd from all other metals is of the same order of magnitude both for the first and second cycles.

Scrubbing and Stripping.

The extract scrubbing in both cycles is unlikely to separate Pd from Rh and Ru due to kinetically inert complexes of these metals with organic sulfides.[7] The lability of silver complexes along with an equilibrium reached within only 10s enables the first cycle extract to be washed free of silver using water. A 0.1 mol/dm^3 Na_2SO_4 solution is more efficient, the silver content being reduced from 2 g/dm^3 to 20 - 40 mg/dm^3 after two extraction stages. In the second cycle, it makes sense to use a 4 mol/dm^3

HCl solution to separate silver further. In both cycles 98-99% Pd is reextracted by 12% aqueous ammonia solution in two stages. Contrary to extraction, the re-extraction is more efficient from PS and DOS than from DHS. Free ammonia (0.1mol/dm^3) in the extract interacts with $[PdL_2A_2]$ (L = an organic sulphide, A = NO_3, Cl) to form organic-insoluble compounds of the $[Pd(NH_3)_4]A_2$ type. Good wettability of these products by the organic phase makes their dissolution in the aqueous ammonia phase kinetically difficult. The actual Pd concentration in the extraction operations in both cycles and the stripping operation in the second cycle is high enough (90 g/dm^3) to provide its quantitative yield into palladosoammine by acidifying the re-extract. Pd sponge can be produced from these palladosoammines by the procedure adopted in natural Pd purification technology.

Extractant	Diluent	D_{Pd}	M	C_M,mg/L	D_M	$\alpha_{Pd,M}$
PS	TEB	970	Pd	176 (178)	970 (764)	
DHS	TEB	4400	Ag	100 (148)	71 (60)	14
DOS	TEB	490	Rh	230 (195)	4.3×10^{-4} ($<3\times10^{-4}$)	2.2×10^{6}
PS	TEB+PIT	360	Ru	161 (165)	3.3×10^{-4} ($<4\times10^{-3}$)	2.9×10^{6}
DF	-	1.2	Sb	115 (208)	2.2×10^{-3} ($<1\times10^{-3}$)	4.4×10^{5}

Table 1 Liquid-liquid extraction (D) and mutual separation (α) of metals in system of 0.3mol/dm^3 petroleum sulphides in tri-ethylbenzene and 3mol/dm^3 HNO_3: r = 0.1 and τ = 10s (in brackets: data for metal mixtures)

Nitrate to Chloride Conversion.

For this purpose NH_3 is evaporated until its volume is halved, regenerated and treated with HCl under heating. The resulted ammonium nitrate and chloride (40g/dm^3) contribute to the Pd extraction in the second cycle. After acidifying (with HCl) the first cycle re-extract can precipitate AgCl, its solubility varying from 36 to 360 mg/dm^3 in a 1 - 4 mol/dm^3 HCl – 1 mol/dm^3 NH_4Cl mixture. For Pd/Ag separation 4 mol/dm^3 HCl is an optimum acidity because of lower D_{Ag} (1.3×10^{-3}) against 1mol/dm^3 HNO_3 (0.013) and the lack of AgCl precipitates or probable base metal (Sb, etc) hydrolysis products as a result of their poor separation during the first cycle.

Noble Metals Distribution.

Basic radiochemical impurities involved in the extractive[3] and sorptive[9] separation of fission Pd are ^{106}Ru, ^{110m}Ag and ^{125}Sb. Table 2 shows the both cycle efficiencies while Table 3 lists the Ag distribution through the second cycle. The Pd separation from simulated solutions with other noble metals present reveals no surprises in the above process.

Silver Distribution.

The first extraction cycle as could be expected does not separate Pd from Ag. The two metals are essentially separated at two scrubbing stages to yield $S_{Pd,Ag}$ = 7 for each stage. The Pd re-extraction contributes slightly to this separation ($S_{Pd,Ag}$ = 1.4). This can be accounted for by the fact the extract contains a non-extractable form Ag different from its routine form $[AgL_2](NO_3)$. As a result of the first cycle re-extract conversion to 1mol/L HCl, about 50% Ag precipitates as AgCl (S=1.6) in accordance with the estimated solubility of AgCl in chloride solutions. The $S_{Pd,Ag}$ is found to be 100 prior to the second cycle. The Ag content of the second cycle extract was identical to that of the blank test. That is, there was no way of evaluating the purification from Ag. To define the separation factor more exactly in the second cycle, Pd solutions in AgCl-saturated 1 and 4mol/L HCl have been tested (Table 3).

Pd is mostly purified by extraction and washing (at the first stage). The Ag content of the extract and further products is independent of initial acidity since the AgCl dissolution is cancelled by its extraction as [AgLCl]. The tests of runs #1 and #8 products demonstrate that the total separation factor is equal to 4×10^3 and 4×10^5 for 1 mol/dm^3 and 4 mol/dm^3 HCl respectively. Table 3 indicates that the Pd concentration can increase four-fold by Pd stripping and extractant regeneration.

$[M]_{org}$, mg/dm^3				$[M]_{aq}$, mg/dm^3				$S_{Pd,M}$		
Pd	Ag	Rh	Ru	Pd	Ag	Rh	Ru	Pd	Ag	Ru
Cycle I										
Extraction										
698	558	0.205	0.19	6.1	10	225	185	1	$4x10^3$	$4x10^3$
Scrubbing (I and II stages)										
692	83	0.19	0.17	6.1	475	<0.01	<0.01	6.8	1	1
688	16	0.19	0.16	4.5	102	<0.05	<0.01	7.2	1	1
Stripping (Re-extraction)										
78	5.6	0.2	0.18	644	11	0.01	0.056	1.4	18	4
Conversion Nitrates to Chlorides										
				550	6	0.01	0.056	1.6		
Cycle II										
Extraction										
514	<0.02	<0.001	<0.005	36.3	6	0.01	0.056	>300	>10	>10
Scrubbing										
	<0.02	<0.001	<0.005	48.4	<0.02	<0.01	<0.005		1	1
Stripping (Re-extraction)										
	<0.02	<0.001	<0.005	372	<0.02	<0.001	<0.005			
Precipitation of Palladosoammine										
				160	<0.02	<0.01	<0.005			

Table 2 Behaviour of Ag, Rh and Ru during extraction of Pd from a modelling solution (C_M, mg/dm^3: Pd 200, Ag 165, Rh 225, Ru 185, Sb 75)

N°	Flow	Stage	[Pd], mg/dm^3		[Ag], mg/dm^3	
			I	II	I	II
1	Feed Solution		2400	2500	9.6	125
2	Aqueous Raffinate		46	215	10.4	129
3	Extract (r = 0.1, τ = 10 s)		23500	22800	<0.19	<0.13
4	Scrub (HCl)	1	<0.5	0.33	0.08	0.1
5	(r = 1, τ = 30 min)	2	<0.5	0.25	<0.004	<0.002
6	Scrub (water)	1	<0.5	0.1	<0.002	<0.001
7	(r = 1, τ = 30 min)	2	<0.5	0.1	<0.001	<0.001
8	Strip (re-extract)	1	94000	91000	0.09	0.01
9	(r = 4, τ = 30 min)	2	200	78	<0.004	<0.002
10	Extractant (recycled)		20	17	<0.005	<0.015

Table 3 Behaviour of Pd and Ag on extractive separation mentioned metals in systems 0.5mol/dm^3 solution of petroleum sulfides in tri-ethylbenzene – 1(I) and 4(II) mol/dm^3 HCl.

Rh and Ru Distribution.

The first cycle behaviour of these metals indicates the Pd separation at the extraction stage ($S_{Pd,M}>10^3$) and the stripping stage ($S_{Pd,M.}>10$) but not at the extract scrubbing stage. In the second cycle the factor $S_{Pd,M.}>10$ is the lower purification limit since the Rh and Ru content of the extract falls outside the limits of the detection (0.001 - 0.005mg/dm^3). That is why the Rh and Ru distribution through other second cycle stages could not be followed. It can be expected that with macroconcentrations of Pd the separation factor from Rh and Ru microconcentrations will not differ in both extraction cycles.

Sb Distribution.

The Sb content of the first cycle extract, wash water, re-extract and regenerated organic phase was similar to that of the blank test (0.02 - 0.10mg/dm^3). The $S_{Pd,Sb}>10^3$ ($D<10^{-3}$) is valid only for the first cycle extraction operation. It follows from[10] that $D_{Sb}<10^{-2}$ for the Sb extraction from HCl. It suggests to $S_{Pd,Sb} > 10^4$ in the second cycle.

Pd Purity

Pd metal reduced from palladosoammine by hydrogen contains about 10^{-4}% Ag (by an order of magnitude lower than American Pd containing 0.005% Ag according to ASTM B 589-2), 10^{-3}% Rh and 10^{-3}% Ru. The impurity level accuracy depends on the metal detection limits of the blank test.

Thus, the extraction process developed to separate and further purify Pd metal shows much promise for further research using actual high-level spent nuclear fuel solutions.

REFERENCES

1. *Feasibility of Separation and Utilization of Ruthenium, Rhodium and Palladium from High Level Wastes. Technical Reports Series. No. 308.* IAEA, Vienna, 40 p, (1989).
2. Shaldayev VS *Recovery of platinum metals during spent nuclear fuel reprocessing. Foreign experience.* Moscow, CNIIAI, 1990, 28 p (in Russian).
3. Arseenkov LV, Lunichkina KP, Renard Ed V et al *Atomnaya Energiya*, **72**(5), 461, (1992) (in Russian).
4. Kirishima K, Shibayama N, Nakahira N et al *Proc. Intern. Conf. on Nuclear Waste Management and Environmental Remediation*, Prague, **1**, 667, (1993).
5. Shmidt VS and Shorokhov NA *Atomnaya Energiya*, **64**(2), 103, (1988). (in Russian).
6. Torgov VG, Andrievsky VN, Gilbert EN et.al. *Proc. Sib. Branch Science Acad. of USSR, Chem. Ser*, **1969**(12/5), 148 (in Russian).
7. Torgov VG *Isotopenpraxis*, **20**(9), 352, (1984).
8. Cowley A, *Platinum 1998*, Johnson Mathey, London, 52 p, (1998).
9. Zaitsev BN, Korolyev VA, Popik VP et. al. *Radiokhimia*, **1988**(3), 411 (in Russian).
10. Gilbert EN, Torgov VG and Veryevkin GV *Proc. Sib. Branch Science Acad. of USSR, Chem. Ser.*, **1978**(7/3), 84 (in Russian).

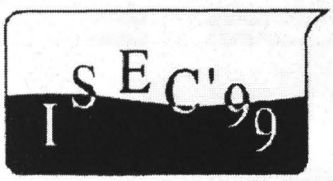

A NEW PROCESS PRODUCING PHOSPHORIC ACID FROM PHOSPHATE ROCK AND HYDROCHLORIC ACID VIA FERRIC PHOSPHATE

Joseph Mizrahi
Consulting Chemical Engineer, Haifa, Israel

ABSTRACT
The paper describes a novel solvent extraction industrial process for the production of commercial grades of phosphoric acid (i.e. liquid-fertilizers), from calcium phosphate rock and hydrochloric acid solutions, improving significantly on the old IMI process.

Keywords: phosphoric acid, ferric phosphate, HCl, D2EHPA

INTRODUCTION

The IMI process, invented in 1956[1] and implemented since the early 60's in a few plants, starts with the dissolution of calcium phosphate rock in an excess of HCl solution. After separation of the insoluble residues, the leach solution containing phosphoric acid, excess HCl, $CaCl_2$ and other minor chlorides and impurities is separated by a very complicated solvent extraction process with pentanol and/or butanol, consisting of 6 batteries with many internal recycle streams. The residual solution has to be stripped from significant amounts of HCl and soluble solvent before its disposal. The mixed solution of H_3PO_4 and HCl resulting from the solvent extraction process, needs to be evaporated and concentrated up to 95% H_3PO_4, to separate the HCl and recover the solvent, in an expensive and energy-consuming multiple-effect system. Additional finishing operations are also needed to assure the quality needed.

The complications in the IMI process derive inherently from the limitations caused by the composition of the leach solution of H_3PO_4 and $CaCl_2$ and by the nature of the pentanol / butanol solvent. Consequently, the IMI process could only find economic justification in the production of the more expensive grades of phosphoric acid, which have limited markets. In view of the available sources of by-product hydrochloric acid and of the large markets for fertilizers, a less expensive process is needed to make liquid-fertilizer-grade phosphoric acid.

DESCRIPTION OF THE NEW PROCESS

The new process (patent applied for) is illustrated in the block diagram in Figure 1 and consists of the following steps :

a) Phosphate concentrate [stream 1] is reacted in mildly acid conditions with a recycled boiling solution of $FeCl_3$ and HCl [stream 2]. Near the boiling point, $FeCl_3$ is hydrolysed and acts as an acid. The $FeCl_3$ content of this solution is adjusted to the phosphate content, to produce and precipitate $FePO_4$, which is very insoluble:

$$Ca_3(PO_4)_2 \text{ (solid)} + 2\,FeCl_3 = 2\,FePO_4 \text{ (solid)} + 3\,CaCl_2$$

Part of the ferric phosphate could be in the form of hydrated crystals, $FePO_4,2H_2O$ (yellowish-white powder with a specific gravity of 2.87), but most of the ferric cations are substituted into the natural phosphate lattice without major size change.

At the same time, HCl in this solution reacts with the other components present in the phosphate (carbonate, hydroxide, silico-fluoride) and other cations (ferrous, aluminum, silicates). Alkali silico-fluorides are also completely precipitated with alkali chlorides present in the rock or added to the system. A small excess of HCl (less than 1%) is maintained at the end of the reaction.

b) The solids are separated and efficiently washed from the solution, by conventional methods and displacement with wash water. Elimination of solubles, essential for the final product quality, is

© 2000 Society of Chemical Industry

easily obtained. The filtrate and wash water [stream 3] containing mainly $CaCl_2$ and solubles/colloids impurities, with a slight excess of HCl , are discarded or treated to recover $CaCl_2$ in a saleable form.

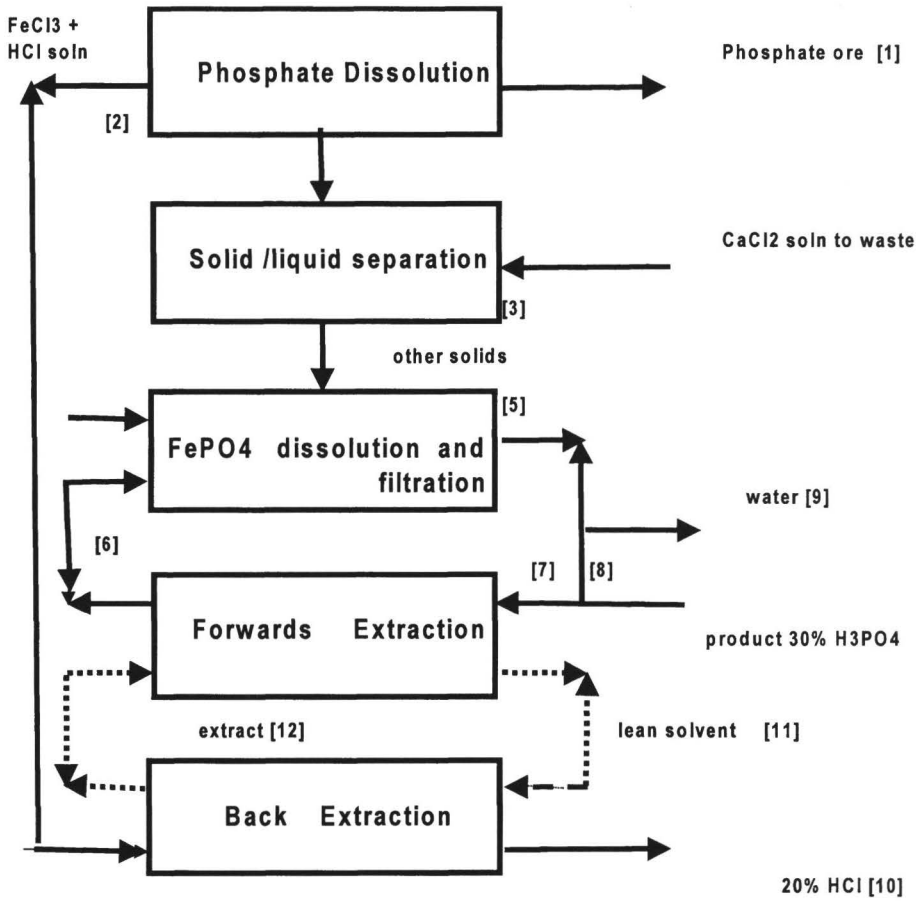

Figure 1 - Schematic Block Diagram of the process

c) The wet solids are dissolved into a recycled phosphoric acid solution in excess [stream 5]. $FePO_4$ is completely dissolved, resulting in a solution of mixed ferric phosphates in solution [stream 6]. Figure 2 shows the maximum saturation solubility of $FePO_4$ in mol/kg, as function of the concentration of H_3PO_4 in mol/kg. at 30C. It can be seen that the solubility is rather high and increases as the H_3PO_4 concentration increases, although the trend is levelling. The mol ratio of Fe/PO_4 in the solutes starts at 0.33, mono $Fe(H_2PO_4)_3$, then as the concentration increases towards 50% by weight total solutes, the molar ratio tends to 0.5, equi-molar mixture of mono- and di-$Fe_2(HPO_4)_3$. From this data, preliminary design ratio and concentrations were chosen to allow sufficient driving forces for continuous dissolution. The stream [5] before dissolution contains 21% H_3PO_4 and after dissolution16-17 % H_3PO_4 and 18% $FePO_4$. The molar ratio Fe/PO_4 of 0.41 corresponds to 60% mono- and 40% di-ferric phosphates .

A small amount of "insolubles"(sand, clays, precipitated alkali silico-fluorides) is separated, washed with the make-up water [stream 9] and discarded.

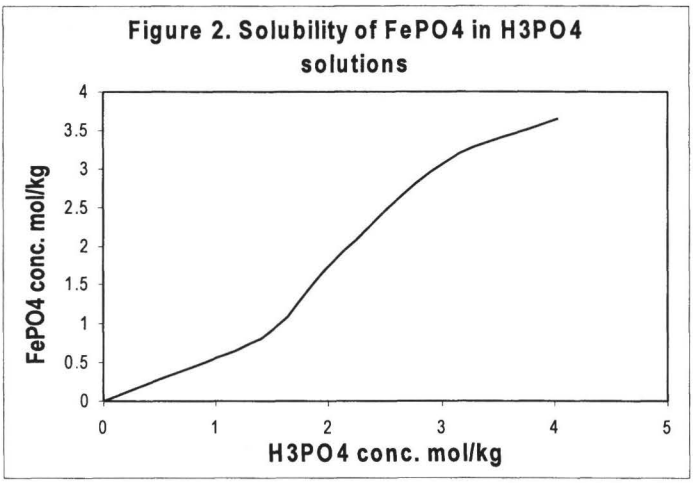

d) The next stage is the virtually complete solvent extraction of ferric iron from stream [6], starting with about 6.7 % of ferric cations at very low pH.with an organic solution of 20-40% w/w (0.62-1.24 mol/kg) D2EHPA (di-(2-ethyl-hexylphosphate) in a low-aromatic paraffinic diluent .

The Forward Extraction equilibrium curve at 40C is shown in Figure 3 for a solvent containing 20% by weight of D2EHPA (technical grade, 95% from Sigma) in a diluent, Isopar-K from Exxon Chemicals.

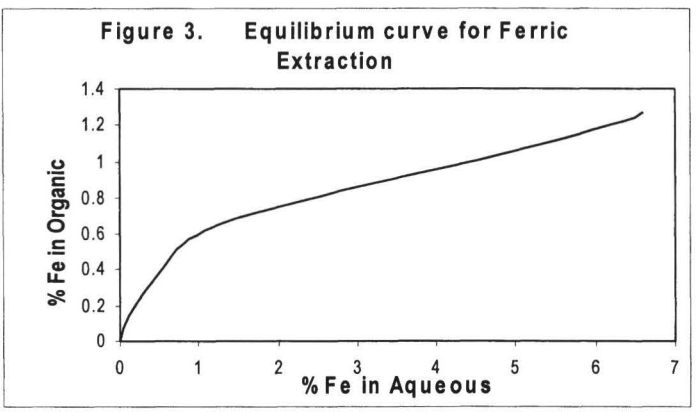

The aqueous "raffinate" from the extraction battery is a 30% phosphoric acid solution with less than 0.05% residual ferric cations. Part of this solution is diluted back to 21% and recycled to the dissolution step [stream 5], while the remaining [stream 7] constitutes the 30% phosphoric acid product, which can be further concentrated and/or converted, according to needs, into DAP (di-ammonium phosphate), MCP (mono-calcium phosphate), as part of high grade NPK mixtures, or into feed-grade DCP (di-calcium phosphate), or eventually purified further to more valuable grades.

d) The ferric-loaded extract [stream 8] may contain 1-2.5 % ferric, depending on D2EHPA concentration, and is back-extracted with the typically 20% HCl feed [stream 10] (lower concentrations of HCl could be used without significant penalty). The resulting aqueous solution of

$FeCl_3$ and HCl [stream 2] is recycled to the phosphate attack The lean solvent goes to the extraction [stream 9].

The Back Extraction equilibrium curve at 40C is shown in Figure 4 for a solvent containing 20% D2EHPA in Isopar. It was found that for efficient back-extraction, the free HCl content in the aqueous phase should not exceed 4-6%. This is a very important and unexpected design data, which controls the way in which the back-extraction battery is operated.

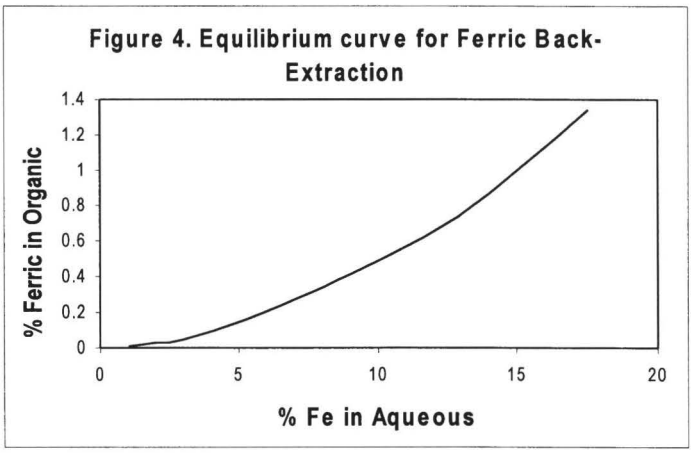

DISCUSSION, NEW FEATURES AND ADVANTAGES

1. All known phosphoric acid processes are quite complicated and expensive, since they involve the separation of phosphoric acid from a more or less soluble calcium salt (sulfate, chloride, nitrate) in aqueous solution with partial mutual solubility. In the new process, the separation is between insoluble ferric phosphate solids and a solution of soluble calcium salts (mainly chloride) calcium and similar cations, i.e. magnesium, potassium, sodium, aluminum, etc.

2. In the new process, the ferric values are mostly kept in an internal closed cycle and most phosphates ores have sufficient iron content to supply to make-up for losses. $FeCl_3$ in a hot, near boiling aqueous solution, has an acid reaction, sufficient to attack and convert calcium phosphate minerals. The terminal conditions of this conversion are mildly acidic (less than 1% HCl). Excess ferric input could create neutral or slightly alkaline pH and precipitate ferric hydroxide .

3. The new process is less sensitive to the HCl feed concentration and can be operated with cheaper by-product 8-15% HCl feed solution, while the IMI process cannot operate practically with a concentration lower than 20% HCl.

4. The solubility of the resulting $FePO_4$ is very low at hot temperatures and in the mild acid conditions prevailing in the reaction. Washing of the $CaCl_2$ and other solubles from the $FePO_4$ precipitate is easy to achieve, as the precipitate separates readily.

5. The novel scheme for the separation of $FePO_4$ into H_3PO_4 and ferric values is based on the chemical potential of the concentrated HCl feed solution. By dissolving $FePO_4$ in a phosphoric acid solution, there is no substantial contamination of the phosphoric acid product with other anions. The solvent extraction system constitutes a barrier and the cations (ferric against H^+) are exchanged between the phosphate side and the chloride side without significant cross-contamination

6. The chemical potential of the HCl feed solution allows the use of strong cations exchangers, effective at a pH lower than 1, and allows the Forward Extraction of relatively concentrated H_3PO_4 and $FePO_4$ solutions, resulting in 30% H_3PO_4 or more in the product solution.

7. The relatively high concentration of streams result in a compact installation with relatively smaller solvent extraction equipment, a simpler flowsheet with fewer contact stages, much lower solvent solubility and volatility and a simple concentration system.

IMPLEMENTATION FACTORS

Although the new process consumes the same amounts of phosphate concentrate and hydrochloric acid, it has the following advantages over the IMI process, as demonstrated by detailed process engineering studies:

- a considerably lower capital investment,
- a much smaller energy consumption and
- the possibility of using more dilute HCl sources with a minimum penalty.

These advantages result from the following process features :

- as the solvent is not volatile, there is no need to strip / recover it from outgoing streams and the losses to ambient are minimal.
- the waste $CaCl_2$ stream does not "see" the solvent,
- a product stream of 31% H_3PO_4 with no HCl is obtained from the solvent extraction and needs to be concentrated only to the merchant 85% H_3PO_4,
- there are much fewer stages (14 in total) in the solvent extraction cycle, all conducted at more or less ambient temperature.

The new process uses only conventional equipment and well-known separation technology and can be demonstrated and optimized with a minimum piloting effort. The engineering is straightforward and there are numerous possibilities of add-on and of backward integration with existing installations.

ACKNOWLEDGEMENT .

The author gladly acknowledges experimental work performed by Dr V Kislik at the Casali Institute, Hebrew University in Jerusalem.

REFERENCE

1. U.S. patent No 2,880,063

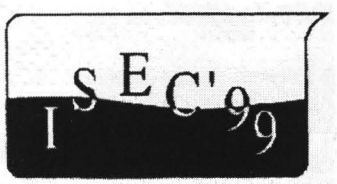

SELECTION OF EXTRACTANTS FOR THE REMOVAL OF CADMIUM FROM INDUSTRIAL GRADE PHOSPHORIC ACID

I Ortiz, S Zamacona, AM Urtiaga
Departamento de Química, ETSII y T. Universidad de Cantabria, Avda. de los Castros, 39005 Santander, Spain

ABSTRACT
The separation of cadmium from phosphoric acid is a subject of interest due to the high toxicity of this heavy metal, which is transferred to phosphate fertilisers in the manufacturing process. Liquid-liquid solvent extraction techniques can offer high removal efficiencies, provided a suitable extraction system could be used. In this work the study concerning the selection of a suitable extractant and back-extractant agents for the removal of cadmium from wet phosphoric acid is presented. The use of a thiophosphinic acid and CYANEX 302, adequate to perform the Cd extraction from a highly acidic media, was tested in previous experiments. However, the simultaneous presence of copper in the industrial grade phosphoric acid causes the oxidation and deactivation of this extractant. The search of an adequate extraction system was performed following two different approaches: i) The total extraction of Cu(II) by a selective extractant in a first step, followed by the extraction of Cd(II) using CYANEX 302. LIX 860 and ACORGA M5640 were tested, and ii) The search of a new extractant for the selective extraction of Cd(II) in the presence of copper. ALAMINE 336 and ALIQUAT 336 were tested. Finally ALIQUAT 336 was selected as a suitable extractant in order to achieve the cadmium removal from phosphoric acid, using water as stripping agent.

Keywords: cadmium, phosphoric acid, Aliquat 336, Cyanex 302, non-dispersive solvent extraction

INTRODUCTION

Almost all heavy metals are found in phosphate rocks, and thus implicitly in fertilisers. The most frequent are Cd, Ni, Pb, Zn, Cu, V, V, Mo and Hg. In the wet phosphoric process, heavy metals contained in the rock get redistributed between phosphoric acid and waste phosphogypsum. Cadmium being one of the most toxic elements, it has been shown that 80% of its initial content in the rock passes to the acid and as a consequence to the phosphate fertilisers when the acid is used as a raw material.

A number of processes have been developed for the removal of Cd and other heavy metals from phosphoric acid, e.g., i) those based on calcination, ii) solubilization with acidic solutions, iii) selective removal of Cd by precipitation or flotation, iv) ion exchange processes and v) liquid-liquid extraction processes. The latter leads to high removal efficiencies provided a suitable extractant could be used, also a second regeneration step is necessary to reuse the extractant and strip the removed cadmium.

As a fundamental part of a general work consisting of the development of a membrane assisted solvent extraction process for the removal of cadmium from wet phosphoric acid has been published,[1] here will be presented the study concerning the selection of suitable extractant and back-extractant agents.

Initially and following the related literature [2,3,4] several experiments were carried out with a thiophosphinic acidic extractant, CYANEX 302, and using high concentrations of hydrochloric acid as stripping agent. When using a synthetic feed solution consisting of laboratory grade H_3PO_4 with added amounts of cadmium, good results were obtained both for extraction and the back-extraction steps.[5] Analysis of the process permitted a mathematical model and design parameters to be obtained for the operation in a non-dispersive solvent extraction process in hollow fibre modules.[6] However, the these results could not be repeated when working with industrial grade phosphoric acid. After several experiments it was concluded that the presence of copper in the industrial acid and the ability of CYANEX 302 to extract this metal gives as a result a copper loaded organic phase where a redox reaction takes place leading to the oxidation of the organic compound and to the simultaneous reduction of copper.[7,8,9] The nature of the Cu(I)-CYANEX 302 complex explains the

© 2000 Society of Chemical Industry

ineffectiveness of the acid stripping, since it is necessary to reoxidize the metal ion for recovery to be effected.

As a consequence it was decided to continue the work with a search of an adequate extraction system. Two different approaches were considered: i) the total extraction of Cu(II) by a selective extractant as an initial step, followed by the extraction of Cd(II) using CYANEX 302 and, ii) the search of a new extractant for the selective extraction of Cd(II) in the presence of copper.

EXPERIMENTAL

Industrial grade wet phosphoric acid kindly supplied by Fertiberia SA (Spanish company) was used as raw feed aqueous phase. The metallic content in the acid is shown in Table 1. The copper selective extraction tests were carried out using two extractants, LIX 860 and ACORGA M5640, supplied by Henkel and Zeneca respectively and used without further purification. For the extraction of Cd in the presence of Cu long chain amines, Alamine 336 and Aliquat 336 (Henkel) and mixtures of Cyanex 302 (Cytec) and Aliquat 336 were tested. Kerosene (Petronor SA) was used as diluent in all cases. Isodecanol (Exxon) was used as a modifier of the organic phase in the experiments with Alamine 336 and Aliquat 336.

Extraction equilibrium experiments were carried out in closed glass tubes in a rotatory SBS stirrer (5-140 rpm). The concentration of cadmium in the aqueous solutions was measured by Inductively Coupled Plasma Emission spectroscopy (ICP) and atomic absorption spectroscopy using standard techniques.

Metal	Concentration (mg/dm^3)	Metal	Concentration (mg/dm^3)
Cadmium	16	Nickel	48
Chromium	292	Lead	8
Copper	34	Zinc	335
Iron	2013		

Table 1. Metallic content in the industrial phosphoric acid

RESULTS

Copper Extraction

LIX 860 and Acorga M5640 extractants

Equal volumes of the organic extractant phase and phosphoric acid were contacted. Figures 1 and 2 show the copper extraction percentage as a function of the content of extractant in the organic phase. Cadmium concentration in the organic phase remained unchanged. Therefore in the experimental conditions under consideration both LIX 860 and Acorga M5640 behave as selective extractants of copper.

Best extraction results were obtained with LIX 870. The stripping behaviour of this extractant was investigated using hydrochloric acid and sulphuric acid as stripping agents. Equal volumes of a previously loaded organic phase (30% of LIX 860 in kerosene with a copper concentration of 0.025 M) and two different acids were contacted. Results are given in table 2.

The stripping efficiency of these two highly concentrated acids is below 50%. This fact and the limited Cu extraction (80% when using 50% v/v of LIX 860 in the organic phase) lead to discard the use of LIX860 and Acorga M5640 as selective Cu extractants.

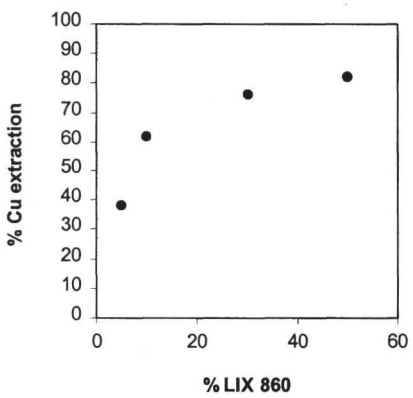

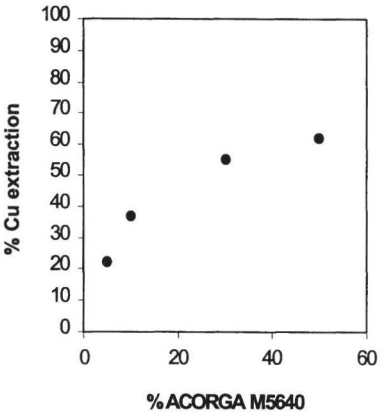

Figures 1 and 2. Percentage copper extraction using LIX 860 and ACORGA M5640 extractants

HCl, 4 mol/dm^3	H_2SO_4, 2 mol/dm^3
48	28

Table 2. Percentage stripping

Binary extractant

Binary extractants formed by mixtures of Cyanex 302 and Aliquat 336 have been proposed in the literature for the recovery of Cu from leaching solutions eluates.[10] Cyanex 302 is an organic acid and consequently it will react with an organic base, such as Aliquat 336, to form an organic salt, a so-called binary extractant.

The binary extractant was prepared by mixing equimolar quantities (0.126 mol/dm^3) of Cyanex 302 and Aliquat 336. Volumes of phosphoric acid and organic phases ranging in proportions 6:1 were used in the extraction experiments. The initial concentrations of Cd and Cu in the acid were raised to 50 mg/dm^3 each

The extraction efficiencies obtained were 66% and 99% for the cadmium and copper respectively. To obtain a loaded organic phase for its use in the stripping test, a second extraction step was carried out, using the organic phase coming from the first extraction and 19% of Cd and 99% of Cu were extracted. Figure 3 shows a flow diagram of the sequence of experiments. Several stripping agents were tested: water, NaCl, NH_4Cl and NH_4OH. NH_4OH (2 mol/dm^3) offered the best results and was selected as stripping agent.

Table 3 shows the results of two successive stripping-extraction cycles. It can be noticed that there is a decrease in the efficiency of cadmium and copper extraction in each consecutive cycle, although copper was efficiently stripped. The deactivation of the organic phase can be explained by the redox reaction between copper and Cyanex 302.

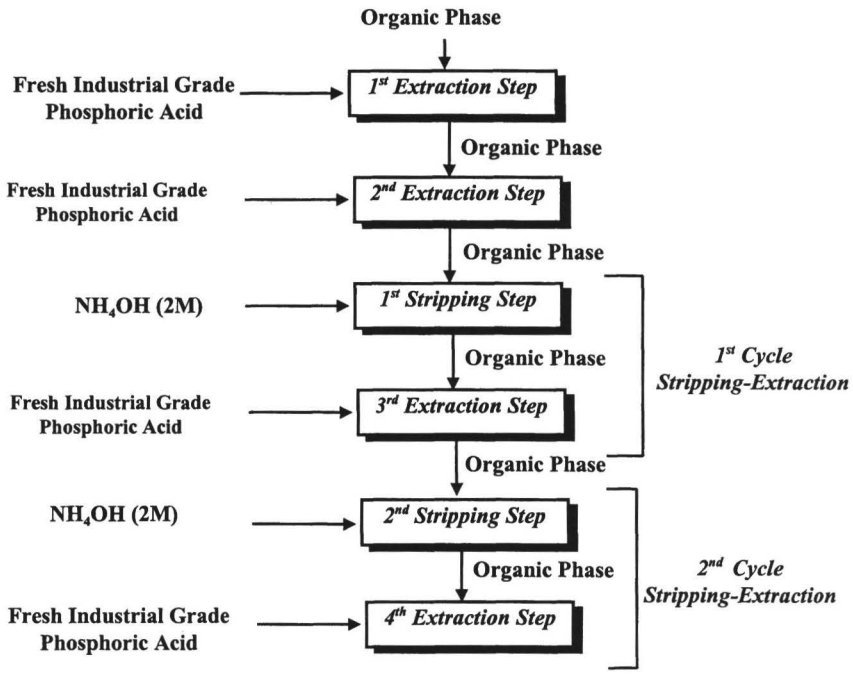

Figure 3. Diagram of the sequence of experiments with binary extractants

	% Stripping		% Extraction	
	Cd	Cu	Cd	Cu
1st Stripping-extraction cycle	6	72	5	88
2nd Stripping-extraction cycle	28	100	2	16

Table 3. Percentage stripping and extraction in two successive experimental cycles

Cadmium Extraction

Two ammonium salts were tested for the selective extraction of cadmium. Alamine 336 is a tertiary ammonium salt, whereas Aliquat 336 is a quaternary ammonium salt. Equal volumes of phosphoric acid and organic phase were contacted. Table 4 shows the results obtained with different percentages of the extractants in the organic phase. It can be noticed that for the same extractant concentration the efficiency of the cadmium extraction is higher using Aliquat 336. It was also checked that there was no extraction of copper.

Composition of the organic extractant (%v/v)	% of Cd extraction
5% Alamine 336	4.2
10% Aalamine 336	36.3
30% Alamine 336	54
30% Aliquat 336	90

Table 4. Cd extraction efficiency of Alamine 336 and Aliquat 336.

Different publications in the literature indicated that water could be used as stripping agent[11,12]. In the present study an organic phase (30% Aliquat 336, 30% isodecanol, 40% kerosene) previously loaded with 0.016 mol/dm^3 of cadmium was put into contact with water, obtaining the stripping of 55% of the cadmium.

Therefore, following these experiments Aliquat 336 was selected as a suitable extractant in order to achieve the cadmium removal from phosphoric acid, using water as stripping agent.

ACKNOWLEDGMENTS

Financial support from the European Commission under the frame of the project AVI*-CT94-0014 is gratefully acknowledged.

REFERENCES

1. Zamacona S, Alonso AI, Galan B, Urtiaga AM, Ortiz I, El-Reefy SA, Daoud JA, Gallego T, Perez de Ortiz ES, Kislik V, Eyal A, Yüksel M, Saglam M, Demircioglu M, and Kabay N, *International Conference Water in the Mediterranean. Istanbul (T)*, November 25-29, (1997).
2. *Spanish Patent N°ES 2020138* ERCROS SA Procedimiento de eliminación de cadmio del ácido fosfórico (1991).
3. Rickelton WA and Robertson AJ, *US Patent N° 5028403*, (1991).
4. Almela A and Elizalde MP, *Hydrometallurgy*, **37**, 47, (1995).
5. Zamacona S, Urtiaga AM, Galan AM, Alonso AI, Irabien A, and Ortiz I, *Chemical Industry and Environment II*. Politecnico di Torino, **2**, 505, (1996).
6. Alonso AI, Urtiaga AM, Zamacona S, Irabien A, and Ortiz I, *J. Membr. Sci.*, **130**, 193, (1997).
7. Cote G and Bauer D, *Rev. Inorg. Chemistry*, **10**, 121, (1989).
8. Sole KC and Hiskey JB, *Hydrometallurgy*, **37**, 129, (1995).
9. Urtiaga AM, Zamacona S, Irabien A and Ortiz I, in *Int. Symp. Liquid-Liquid Two Phase Flow and Transport Phenomena*. Editor: D.M. Maron, Begell House Inc., 291, (1998).
10. Tait B, *Solv. Extr. Ion Exch.*, **10**, 799, (1992).
11. Stenström S and Aly G, *Hydrometallurgy*, **14**, 231, (1985).
12. Stenström S and Aly G, *Hydrometallurgy*, **14**, 257, (1985).

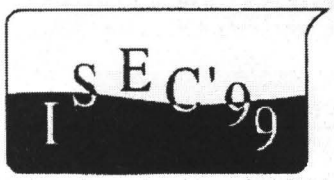

PRODUCTION OF WO_3 FROM SCHEELITE CONCENTRATES BY EXTRACTION TECHNOLOGY

SI Stepanov, VG Giganov, GP Giganov and AM Chekmarev
D.Mendeleev University of Chemical Technology of Russia,
Institute "GINZVETMET", Moscow, Russia.

ABSTRACT
The paper reports the results obtained by the laboratory scale study of WO_3 production from scheelite concentrate using autoclave soda leaching of W and Mo followed by their extraction and separation with methyltrialkylammonium (MTAA) carbonate from carbonate solutions. The extraction raffinates are returned to the leaching stage for reuse. The flowsheet of WO_3 production is presented and discussed.

Keywords: tungsten, molybdenum, carbonates, alkylammonium carbonates

INTRODUCTION

Autoclave soda leaching (ASL) is a traditional method used to process scheelite concentrates. The carbonate solutions obtained in the process contain W, Mo and some other impurities. These solutions are used to produce ammonium para-tungstate and WO_3 and can be processed by different hydrometallurgical methods. One of the most widely used methods[1] includes the following stages: 1) neutralisation of carbonate solutions with sulphuric or hydrochloric acid; 2) precipitation of MoS_3 and some other impurities from weakly acidic solutions; 3) liquid-liquid extraction of tungsten by tertiary amines from purified solutions; 4) stripping of tungsten from the organic phase with ammonium hydroxide; 5) recovery of ammonium para-tungstate by evaporation of the strip solution followed by production of WO_3. However, this process has some disadvantages due to the large quantities of reagents used to neutralise the ASL solutions that results in the formation of large volume of waste water after solvent extraction recovery of tungsten, which contain high concentration of sodium sulphate or chloride. Special processing of solutions is also required due to insufficient selectivity of the extractant. To improve these drawbacks, some alternative methods based on different variants of solvent extraction[2-4] or sorption[5] recovery and separation of W and Mo from carbonate or alkaline-carbonate solutions have been developed.

The present paper reports the results obtained on a laboratory scale technological study of processing Schlitz concentrate. The technology is based on the use of ASL, solvent extraction and separation of W and Mo from the carbonate solutions, recovery of ammonium para-tungstate by evaporation of the stripping solution followed by production of WO_3 as the final product. This technology was developed in the Mendeleev University of Chemical Technology of Russia in collaboration with the Institute "GINZVETMET" and tested at Nalchick's Hydrometallurgical Plant.

EXPERIMENTAL

The intermediate molybdo-scheelite concentrate (Schlitz concentrate) used in this work had the following composition (%): WO_3: 30-35, Mo: 2.0-4.0, Si: <10, P: <0.11, As: 0.2, F: 1.0-1.5. The ASL was carried out in 0.5 dm^3 steel autoclaves at a temperature of 225°C and pressure of 25 atm. The soda equivalent in the leaching solution was varied from 2 to 4. Technical grade soda (without additional purification) was used as sodium carbonate. The content of NaCl in soda was <0.5%. The methyltrialkylammonium carbonate (MTAA: $[(C_7H_{15}\text{-}C_9H_{19})_3CH_3N]_2CO_3$) was prepared from an industrial sample of MTAA methylsulphate and used as the main extractant. The contents of quaternary ammonium sulphate (QAS) and amines (recalculated for the "wet" product) were not less than 96% and not more than 4%, respectively. MTAA carbonate was prepared from MTAA methylsulfate by consecutive treatment with 9.0 mol/dm^3 H_2SO_4 (three contacts with O:W = 1:1) and 5.0% NaOH (up to pH = 10-11 in the final aqueous phase) followed by final processing with 5.0% Na_2CO_3 (three contacts with O:W=1:1).The completeness of conversion was monitored by functional

© 2000 Society of Chemical Industry

chemical analysis of R_4N^+ and CO_3^{2-}. The diluent used for the solvent extraction was kerosene with 15% of iso-octanol. The concentrations of W, Mo and impurities in water solutions were analysed by conventional analytical methods.

RESULTS AND DISCUSSION

The results obtained in six solvent extraction-leaching cycles by using two-stage counter-current leaching of W and Mo from the concentrate with circulation of extraction raffinates are presented in the Table 1. The degree of recovery of W in each cycle was constant and equalled greater than 99.8% in all cases. Molybdenum, present in scheelite as powellite $CaMoO_4$, was also leached with the tungsten, but then remained as molybdenite (MoS_2) in the residual cakes. The content of other impurities in solvent extraction and leaching solutions were negligible and did not accumulated.

Cycle Num.	Second leaching stage										%Re*
	Input					Output					
	Raffinate of n-1 cycle, ΣV=1.28 L, g/dm^3;					Carbonate solution, ΣV=1.40 L, g/dm^3			Residual cake		
	WO_3	Mo	SiO_2	F	Na_2CO_3	WO_3	Mo	Na_2CO_3	WO_3	Mo	WO_3
1	0.75	0.07	0.80	1.60	83	2.1	0.15	109	0.04	0.30	99.92
2	3.75	0.18	0.70	1.35	76	22.5	1.25	95	0.03	0.29	99.94
3	6.50	0.19	0.75	1.10	71	15.5	1.51	85	0.04	0.38	99.92
4	14.5	0.65	0.52	1.45	72	42.0	2.31	91	0.04	0.30	99.97
5	31.3	1.25	0.87	1.85	73	64.3	3.00	85	0.03	0.35	99.95
6	37.5	1.50	0.70	2.15	121	92.5	3.87	89	0.09	0.30	99.83
	First leaching stage					WO_3: 32.35%, Mo: 2.66%					
	Output										
	Feed extraction solution, g/dm^3					1 stage: S:L = 1:4, sample 80g, soda equivalent = 2.2, T=225C, 8 autoclaves, τ = 3 hours.					
1	66.8	4.75	0.95	1.40	44.5						
2	70.5	4.50	1.25	1.10	42.4						
3	75.2	3.80	1.50	1.50	46.6	2 stage: S:L = 1:3, sample cake from two autoclaves from 1 stage, T=225C, 4 autoclaves.					
4	83.3	3.88	0.97	2.0	42.4						
5	103.7	6.75	1.19	1.9	49.8						

* %Re – Recovery degree

Table 1 Two-stage counter-current leaching of W and Mo from scheelite concentrate

As seen in Table 1, the volume of sodium carbonate solutions increases by 40%, after two-stage counter-current leaching due to addition of washing water, for rinsing the leaching cakes and organic extracts, to the main solution. To decrease the water imbalance, the possibility of one-stage leaching of W and Mo has been investigated. The results of this study are shown in Table 2. As seen, the extent of W recovery in this case reached 98.5 - 99.5% which is not dramatically less than in the two-stage leaching, and the content of impurities in the leaching solutions remains at the same level. At the same time, sodium carbonate concentration increases up to 80 g/dm^3 in the leaching solutions and up to 120 g/dm^3 in the extraction raffinates. This leads to a decrease of co-extraction of impurities into organic phase, but the extent of extraction of W and Mo also decreases to 95 - 96%. The results obtained have shown that one-stage leaching is more promising if ASL is carried out at higher temperature.

Cycle Num.	Input					Output							Re %
	Raffinate, (v = 0.96dm³), g/dm³;					Carbonate solution, (V=1.05 dm³), g/dm³					Residual cake, %		
	WO_3	Mo	SiO_2	F	Na_2CO_3	WO_3	Mo	SiO_2	F	Na_2CO_3	WO_3	Mo	WO_3
0	-	-	-	-	146	75.2	5.5	0.9	1.8	82.7	0.33	0.3	99.4
1	3.62	0.18	0.8	1.6	121	78.3	5.5	1.1	2.0	72.0	0.27	0.3	99.5
2	3.00	0.13	1.0	1.8	108	78.7	5.1	1.1	2.0	79.5	0.71	0.3	98.5

Table 2 One-stage leaching of W and Mo from scheelite concentrate (WO_3: 32.35%, Mo: 2.66%)
1 stage: S:L = 1:4, sample 80g, soda equivalent = 3.3, T = 225°C, 3 autoclaves, τ = 3 hours.
Solvent extraction: 50% carbonate MTAA, O:W = 2.5:1, 4 steps.

The recovery of W and Mo by using solvent extraction raffinates for ASL is comparable with that when using water sodium carbonate solutions. The results of solvent extraction of W, Mo and other impurities from ASL solution obtained from two-stage leaching of scheelite concentrate with 50% vol. MTAA carbonate solution at O:W = 2:1 are presented in Table 3. As seen, the main impurities are displaced from the organic phase in the course of loading with W and Mo in the counter-current extraction. The extent of W and Mo recoveries achieved are 95 - 96%. Hence, the use of MTAA carbonate as an extractant gives a possibility of separating all main impurities directly from the leaching solutions without their neutralisation with mineral acid. This allows, in turn, to return the carbonate solutions to the ASL stage for reuse.

Type of solution	Content of elements, g/dm³					
	WO_3	Mo	SiO_2	F	As	Na_2CO_3
Feed solution	77	5.47	1.02	1.1	0.075	51
Raffinate of 4th step	2.8	0.19	0.96	1.08	0.075	89
Extract of 1st step	49.4	3.55	0.04	0.01	-	-

Table 3 Counter-current solvent extraction of W and Mo

One of the important problems of W solvent extraction from sodium carbonate solutions is contamination of the organic phase by sodium and formation of substandard WO_3 due to the mechanical capture of the water dispersion, which reaches 0.5%. Thus the organic phase was washed with water (O:W = 5–10:1, two steps of counter-current extraction) to decrease sodium contamination.

The stripping of W and Mo from organic phase with 300-350 g/dm³ water solutions of NH_4HCO_3 + $(NH_4)_2CO_3$ mixture with mass ratio of 1 : 3-3.5 and O:W = 4:1 was carried out in a four stage counter-current extraction cascade. The stripping solutions obtained contained from 115 - 150 g/dm³ WO_3 and from 9.0 - 13.0 g/dm³ Mo. An average ratio of Mo to W in the stripping solutions varies from 1:10 to 1:15. To obtain WO_3 of standard quality it is necessary to decrease the Mo content in the product by 50-100 times. The highly efficient separation of Mo and W from the carbonate solutions can be achieved by using selective extraction of Mo thiocomplexes with MTAA carbonate as is shown in Table 4.

It has been found that the quantitative formation of stable $MoOS_3^{2-}$ and MoS_4^{2-} in the carbonate media is achieved after 30 - 60 minutes at a temperature of 40 – 50°C. The required purification from Mo is achieved when using $(NH_4)_2S$ input of around 90% or more, recalculated to MoS_4^{2-}. The recovery of Mo from the water solution following three stages counter-current extraction with 20% vol. MTAA carbonate solution and O:W = 1:1 was 98-99%. The residual Mo content in the aqueous phase provides a product WO_3 of standard quality.

Relation of $(NH_4)_2S$:Mo, M:M	Content of phases, g/dm^3				Recovery degree, %		Relation of Mo: WO_3 in raffinate, g/g
	Raffinate		Extract				
	WO_3	Mo	WO_3	Mo	WO_3	Mo	
4.85:1	106	0.022	10	9.23	8.6	99.8	1:4818
4.0:1	111.8	0.06	4.2	9.19	3.6	99.4	1:1863
3.5:1	113.7	0.156	2.3	9.09	1.9	98.3	1:729
2.8:1	114.5	1.82	1.5	7.45	1.3	80.5	1:63
2.5:1	114.9	2.61	1.1	6.65	0.9	71.8	1:44

Table 4 Separation of W and Mo from carbonate solutions.
20% vol. carbonate MTAA, O:W = 1:1, three stages counter-current extraction.
Feed solution, (g/dm^3): WO_3: 116, Mo: 9.25, SiO_2: 0.3, Na: 0.29, NH_4CO_3 + $(NH_4)_2CO_3$: 250.

The 25% $(NH_4)_2CO_3$ aqueous solution with the addition of an oxidising agent was also used for the Mo stripping at O:W = 4:1. Average composition of the stripping solutions obtained was as follows: Mo: 32-34, WO_3: 7-9, $(NH_4)_2SO_4$: 110-130 and $(NH_4)_2CO_3$: 150-200 g/dm^3.

The solutions, purified from Mo carbonate, containing W were concentrated by evaporation to between a third and quarter of their volume to obtain solid ammonium para-tungstate. The yield of W in ammonium para-tungstate was 85-90%. The composition of WO_3 after roasting of ammonium para-tungstate is presented in Table 5.

N	Stripping sln, g/dm^3				ED**, %	Solution after evaporation, g/dm^3				RD***, %
	WO_3	Mo	SiO_2	Na		WO_3	Mo	SiO_2	Na	
1	148	0.068	0.27	0.35	70	62	0.23	0.4	0.63	87.5
2	132	0.07	0.25	0.23	73	57	0.28	0.37	0.6	88.4
3	116	0.05	0.18	0.2	80	63	0.31	0.22	0.78	89.2

N	Content of impurities in WO_3, %					
	Mo	Si	Ca	Fe	Na	Al
1	0.012	0.003	0.003	0.002	0.004	0.002
2	0.014	0.003	0.003	0.003	0.005	0.002
3	0.017	0.003	0.003	0.003	0.0049	0.002

** ED – Extent of Evaporation, %; *** RD – Output of W in ammonium para-tungstate, %.

Table 5 Composition of ammonium carbonate stripping solutions and quality of WO_3.

The general technological flowsheet for the processing of the scheelite concentrates using ASL and solvent extraction for recovery and separation of W and Mo from carbonate solutions with MTAA carbonate is presented in Figure 1.

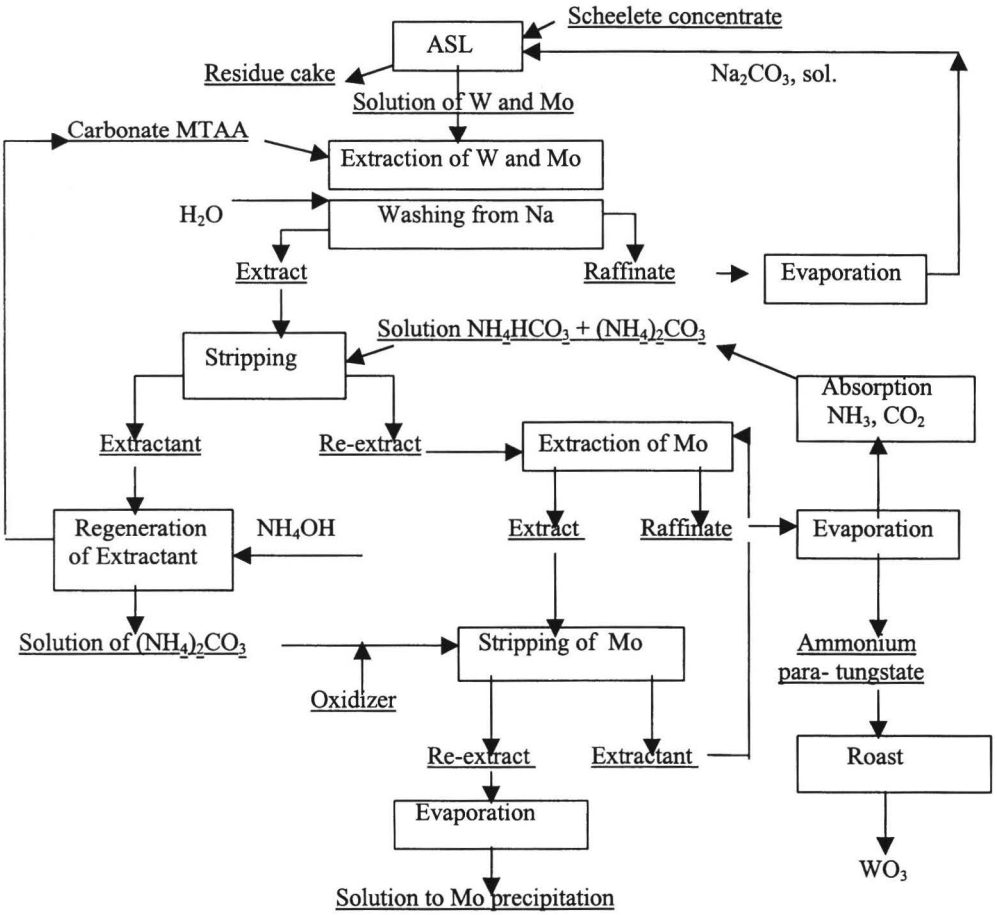

Figure 1. General technological flowsheet for scheelite concentrate processing.

REFERENCES

1 Zelikman AN. *Proceedings of IX Solvent Extraction Conference of Russia*. Adler, 3, (1991), (Russian edit.).
2 Drobnick JL and Lewis CJ. In: *Hydrometallurgy", Moscow*, 232, (1971), (Russian edit.).
3 Kulmukhamedov GV, Zelikman AN, Veriovkin GV, Ivanov IM, Zaitzev VP and Bushmakina VI. *Chem.Technik*, **11**, 498, (1989).
4 Zaitzev VP, Ivanov IM, Kalish NK and Us TV. *Proc. II Int. Conf. Hydrometallurgy*, Changsha, 137, (1992).
5 Vezina JA and Gow VA. *Canad. Min. Met. Bull.*, **656**, 1418, (1966).

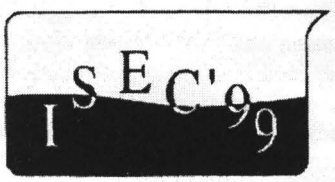

SEPARATION AND CONCENTRATION OF L-PHENYLALANINE IN HOLLOW FIBRE MODULES: DECREASE OF THE EXTRACTION RATE

H Escalante[1] and A Irabien[2]

[1]Escuela de Ingeniería Química. UIS, A.A. 678. Bucaramanga. Colombia

[2]Departamento de Química, Universidad de Cantabria. Avda los Castros s/n, 39005 Santander. Spain

ABSTRACT

The objective of this work is to evaluate the separation/concentration process of L-phenylalanine by means of non-dispersive extraction and back extraction (NDSX) in hollow fibre modules and to describe the separation process. The viability of the NDSX process has been previously reported using the commercial extractant Aliquat 336 and ammonium chloride as the stripping reagent.[1] To obtain a suitable model for the L-phenylalanine mass transfer flux in hollow fibre modules kinetic experiments were performed at a laboratory scale, allowing the evaluation of the mass transfer coefficient and equilibrium parameters.[2] Experiments carried out over a long time of the separation/concentration of L-phenylalanine solutions of 10 g/dm^3, led to the conclusion that a slow but continuous decrease of the mass transfer rate takes place in the process. This can be explained by the formation of a neutral complex of L-phenylalanine bisulfate and Aliquat 336, which is responsible for the aminoacid accumulation in the organic phase and the decrease of the mass transfer rate in the process.

Keywords: *L*-phenylalanine, Alamine 336, hollow fibre module, non-dispersive extraction

INTRODUCTION

During the last few years the market for some L-aminoacids has increased, leading to the development of new manufacture processes. A typical example is the new sweetener aspartame, L-aspartyl-L-phenylalanine methylester (1-methyl-N-aspartyl-L-phenylalanine). Its adoption in foods and especially in soft drinks has given rise to a major increase in the market for L-phenylalanine (L-Phe) increasing from 50 tons in 1981, to over 3000 tons in 1984, and to nearly 6000 tons in 1987.[3,4]

For the separation/concentration of aminoacids new separation processes have been considered by differents authors: emulsion liquid membranes,[4,5,6,7,8] and supported liquid membranes.[9,10] Non-Dispersive Extraction in Hollow Fibre Modules (NDX) combines the advantages of membrane processes with solvent extraction processes.[11]

The viability of the coupled process of extraction and backextraction using an ammonium chloride solution, by means of nondispersive extraction was studied by Escalante et al.[1], due to the accumulation of L-phenylalanine in the organic phase the back-extraction process was studied using sulfuric acid as the stripping reagent.[2] In these studies L-phenylalanine was taken as the target molecule produced in the bioprocess and it was extracted by Aliquat 336 as the anionic form, which can be found at a pH higher than 9 due to its zwitterionic behaviour.[9] Sulfuric acid has also been used as the stripping reagent in the back-extraction process of L-phenylanalanine in emulsion liquid membranes by Hong and Yang.[6]

EXPERIMENTAL

To study the separation/concentration process of L-phenylalanine a set of seven consecutive experiments were carried out under the following experimental conditions: feed solution contains 10 g/dm^3 L-phenylalanine (Aldrich); a 1 : 2 ratio of feed solution volume to organic phase volume and a 1 : 1 ratio of organic phase volume to stripping phase volume were employed; the pH of the feed solution and the stripping solution were kept constant and equal to pH 10.5 and 0.1 respectively. The experimental time cycle was 48 hours, and in each experiment, after this time, the aqueous feed solution was renewed, but the organic and aqueous stripping phases were not changed. Aliquat 336

© 2000 Society of Chemical Industry

(Fluka), a commercial mixture of trialkylmethylammonium chlorides (trialkyl = C_8- C_{10} mainly capryl) was used as extractant with Kerosene (Petronor, S.A.) as diluent. To avoid the segregation of a third (second organic) phase the addition of a modifier (a high molecular weight alcohol) was necessary, so a 30% v/v of isodecanol (Exxon Chemicals) was added to the organic phase. The feed solution, containing 10 g/dm^3 of L-phenylalanine (Aldrich), was adjusted to pH = 11 by addition of NaOH; and sulphuric acid, pH = 0.1, was used as stripping reagent. A feed volume of 0.5 dm^3, an organic extraction volume of 0.25 dm^3 and a stripping solution volume of 0.05 dm^3 were used under a recycling operational mode in the experiments. The experimental set-up is shown in Figure 1.

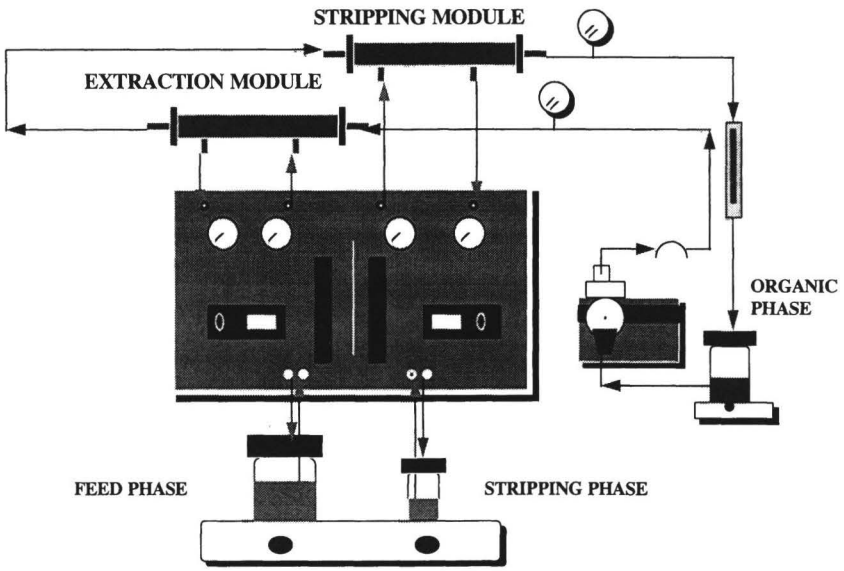

Figure 1. Experimental setup of the coupled hollow fibre EX and BEX processes.

The L-Phe is extracted in the first module by ion exchange with hydrogen sulfate according to Equation 1:

$$\overline{(R_4N)^+(HSO_4)^-} + (L\text{-}Phe)^- + OH^- \text{ Ü } \overline{(R_4N)^+(L\text{-}Phe)^-} + SO_4^{2-} + H_2O \qquad (1)$$

Then the aminoacid is recovered by sulfuric acid in the second module. In these experiments 90% of L-Phe of the feed solution was extracted, while the back-extraction yield reached 98%, therefore the organic phase was regenerated and ready for further use.

RESULTS AND DISCUSSION

The kinetic behaviour of the system has been previously fitted to a mathematical model based on seven differentia equations.[2] The variables of the experimental operation can be taken into account by the following parameters, given in Table 1:

$$a_A = \frac{V_{MA}}{Q_A L} \qquad b_A = \frac{2.n.p.r.}{Q_A} \qquad d_A = \frac{Q_A}{V_{TA}}$$

Phase	VM(dm^3)	VT(dm^3)	Q(dm^3/s)	a($s.m^{-1}$)	b($s.m^{-2}$)	d(s^{-1})	Flow
Feed	0.055	0.400	$5.5x10^{-3}$	$0.625x10^2$	$3.59x10^5$	$1,37x10^{-2}$	outside fibre
Organic	0.024	0.145	$7.5x10^{-4}$	$0.200x10^3$	$2.67x10^6$	$5,17x10^{-3}$	inner fibre
Stripping	0.055	0.160	$2.5x10^{-3}$	$0.137x10^3$	$0.79x10^6$	$1.56x10^{-2}$	outside fibre

Table 1.Experimental conditions.

To explain the experimental decrease in the mass transfer rate, which has been obtained. The accumulation of sulfuric acid and amino acid salt in the stripping phase may be responsible for a new equilibrium leading to a concentration decrease of the $[(R_4N)^+(L\text{-}Phe)^-]$ species in the organic phase:

$$2OH^- + \overline{(R_4N)^+(HSO_4)^-}\ \overline{(L\text{-}Phe.H_2).HSO_4} \ \ddot{U}\ \overline{(R_4N)^+(L\text{-}Phe)^-} + 2SO_4^{=} + 2H_2O \qquad (2)$$

where:

$$K_1 = \frac{\overline{(R_4N)^+(L\text{-}Phe)^-}\ a_{\ddot{o}}^{\ddot{a}}[SO_4^{=}]^2}{\overline{(R_4N)^+(HSO_4)^-\ (L\text{-}Phe.H_2).HSO_4}} \qquad (3)$$

leading to an equilibrium concentration in the organic phase given by:

$$C_O^{mE*} = \frac{K_{Eq} C_{OM} C_A^{mE}}{C_{AE} + \frac{K_{Eq}}{K_1}.(C_{AE})^2 C_A^{mE} + K_{Eq}.C_A^{mE}} \qquad (4)$$

A simulation of the process model introducing this new equilibrium parameter to be optimized leads to the fitting shown in Figures 2 and 3, where KM = 1.12×10^{-8} m/s, KEq = 1.32, K1 = 7.0×10^{-4} and s = 0.264, which is the range of the experimental error.

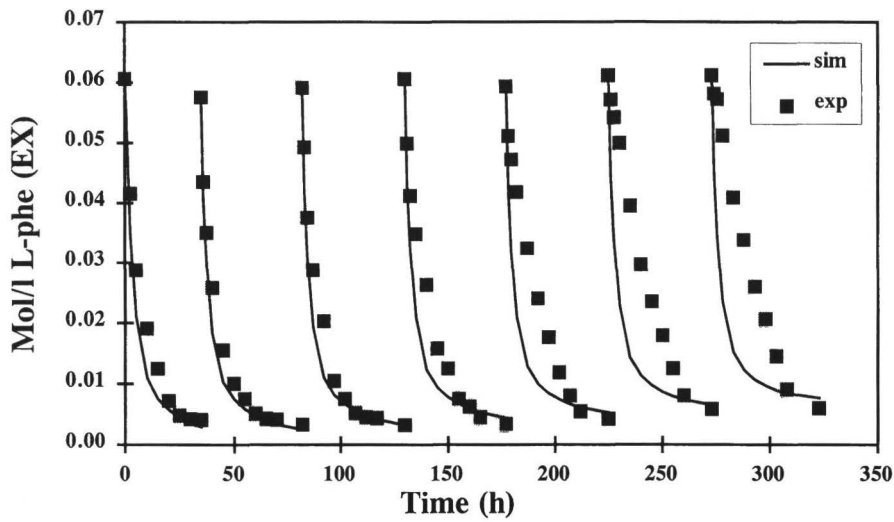

Figure 2. Two equilibria model. Experimental and simulated results of the kinetic behaviour in the L-Phe separation step.

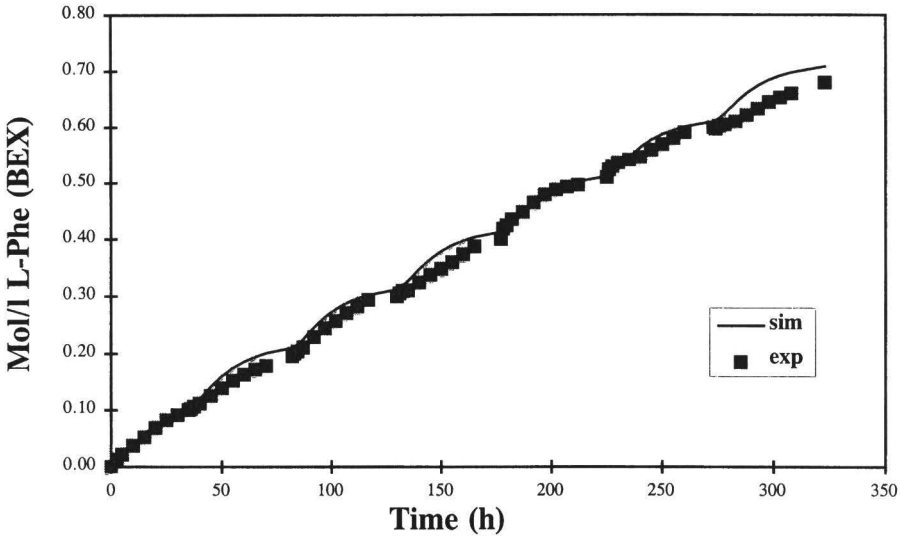

Figure 3. Two equilibria model. Experimental and simulated results of the kinetic behaviour in the L-Phe concentration step.

CONCLUSIONS

An organic phase based on Aliquat 336, 30% (v/v), isodecanol 30% (v/v) and kerosene has been used as the extraction reagent and sulfuric acid, at pH = 0.1 as the stripping agent. Starting with 10g/dm^3 of L-Phe in the feed solution, after seven experiments a high concentration of L-Phe was reached in the back-extraction solution, i.e. 0.7 mol/dm^3 (more than 100 g/dm^3).

The main parameters of the process:equilibrium constants, KEq = 1.32, K1 = 7.0 x10^{-4} and membrane mass transfer coefficient, KM = 1.12x10^{-8} m/s have been evaluated allowing a good description of the experimental results as shown in Figures 2 and 3. These results allow the evaluation of this technology with a model based on the mass transfer rate and two equilibrium parameters.

ACKNOWLEDGMENTS

We acknowledge to COLCIENCIAS (governmental establishment of Colombia) the grant given to H. Escalante.

REFERENCES

1. Escalante H, Ortíz I and Irabien A, *Proc ISEC'96,* University of Melbourne., **2**, 1493, (1996).
2. Escalante H, Alonso AI, Ortíz I and Irabien A, *Sep. Sci. Technol.*, 33 (1), 119, (1998).
3. Bailey JE and Ollis DF, *Biochemical Engineering Fundamentals*, McGraw-Hill. New York. 840, (1986).
4. Thien MP, Hatton TA and Wang DIC, *Biotechnol. Bioeng.*, **32**, 604, (1988).
5. Ha HY and Hong SA, *Proc ISEC'90*, Elsevier, Amsterdam, 1899, (1990).
6. Hong SA and Yang JW, *J. Membrane Sci.*, **86**, 181, (1994).
7. Chan ChCh and Yang JF. *Separ. Sci. Technol.*, **30**, 15, 300, (1995).
8. Pickering PJ and Chaudhouri JB, *Proc. ISEC'96,* University of Melbourne, 1477, (1996).
9. Molinari R, de Bartolo L and Drioli E, *J. Membrane Sci.*, **73**, 203, (1992).
10. Bryjak M, Wieczorek P, Kafarski P and Lejczack B, *J. Membrane Sci.*, **56**, 167, (1991).
11. Prasad R and Sirkar K, *J. Membrane Sci.*, **5**, 153, (1990).

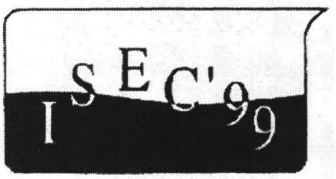

PROCESS DEVELOPMENT, DESIGN AND SCALE-UP USING A LARGE SCHEIBEL EXTRACTION COLUMN

Teh C Lo
T. C. Lo & Associates, 21 Miller Rd, Wayne, N. J. 07470, U.S.A.

ABSTRACT
An extraction process was developed for recovery of an organic intermediate compound from the effluents of the reactors for a fine Chemical Plant. Laboratory studies and pilot plant tests were performed in a Karr reciprocating-plate column, a Scheibel extractor and an Oldshue-Rushton column. From the data obtained in the pilot plants, preliminary designs on these three types of columns were proposed. Economics and advantages of each system were evaluated. It was concluded that a 1.45m (4ft 9inch) diameter Scheibel column with many stages was the choice for the design of the process. The Hoffmann-La Roche Company has long been associated and experienced with Scheibel Columns. The Scale-up and design of the Scheibel extraction column are described. Performance data of the plant extractor and an economic evaluation of the process are presented.

Keywords: Scheibel column, column design, column scale-up

INTRODUCTION

This paper presents a case study of an extraction process development, design and scale-up using a 4ft 9inch diameter Scheibel extraction column. In a fine chemical plant, the effluents from the reactor contain a substantial amount of unreacted organic intermediate process compound, which were recovered by extraction. Pilot plant tests had been performed in a Scheibel column, Karr reciprocating-plate column, and in an Oldshue-Ruston (Mixco) column. Pilot plant runs for Karr reciprocating-plate column have been performed in the Roche Pilot Plant, and for the Scheibel column and Mixco column, at York Co. and the Mixing Equipment Co., respectively. Based on the pilot plant performance data, column designs have been proposed by the York Corp., Chem Flow Corp, and Mixco Co. A summary of the column characteristics for the pilot plants and proposed large scale columns is given in Table 1.

DISCUSSION OF THE SCALE-UP

The scale-up from the pilot plant performance data can be summarized as follows:

A. Scheibel Column

The 3" diameter Scheibel column used in the pilot plant test and the proposed large scale column were the type which incorporated horizontal baffles without wire mesh packing between stages.[2] Figure 1 shows the compartment of the Scheibel column.

Scheibel has stated that:

- The optimal height of the mixing section can be scaled up based on the square root factor of the diameter.
- The HETS varies with the square root of the diameter.

$$(HETS)_2/(HETS)_1 = (D_2/D_1)^{0.5}$$

Total throughput

The 3" pilot columns were operated in a throughput range of 102-120 GPH/ft^2 York proposed to design for 415 GPH/ft^2 in a 4'9" column. The scale-up factor for the specific throughput is 4.

© 2000 Society of Chemical Industry

TABLE 1
Summary of Scale-up and Design of the Extraction Columns

	York-Scheibel Column			Chem-Flow, Karr Column			Mixco Column		
	Pilot Plant Test	Plant Design	Scale-up factor	Pilot Plant Test	Plant Design	Scale-up factor	Pilot plant Test	Plant Design	Scale-up factor
Column Diameter	3"	4'-9'	19	3"	3'-10"	15.3	6"	6'-0"	12
Total Throughput. gph/ft	102	415	4	652	635	1	230	258	1.1
Extraction Section									
No. of Actual Stages	36	33		46	104		20	12	
Height Per Statge	1"	8"	8	2.3"	2.2"	1	3"	3'-0"	12
Total Ht. Ext. Section	3'-0"	22'-0"		8'-0"	18'-10"		5'-0"	36'-0"	
Stage Efficiency	22%	18.2%	0.83	17.5%	5.8%		20%	50%	2.5
HETS	4.6"	44"	9.6	12"	38"	~3	15"	6'-0"	4.8
No. of Theo. Stages	8	6*		8	6*		4	6*	
Wash Section									
No. Actual Stages		11		6	18			3	
Ht. Per Stage		8"		2"	2½"			3'-0"	
Total Ht. of Wash Sect.		7'-0"		1'-0"	3'-7"			9'-0"	
Stage Efficciency		-			-		-		
HETS		-			-		-	1**	
No. of Theo. Stages		1**		~	1**				
Material of Construction	Pyrex	304 s/s		Pyrex	304s/s		Pyrex	304s/s	
Drive, HP		10			30			5	

* Six Theoretical Stages is required for an Extraction Efficiency of 99% Recovey
** One Theoretical Stagte is required for the Washing of Organic Salt form Solvent Extract

Stage efficiency and HETS

The stage efficiency in the 3" column was 22% (HETS = 4.6"). The plant design is based on an efficiency of 18.2% (HETS = 44"). On scale-up, the stage efficiency remains about the same, but the HETS is 10 times greater.

Scheibel columns are marketed by York Process Equipment Company, and sizes up to 2.55 m (8'6") in diameter are in service. A detailed description and design criteria for Scheibel columns are presented by Scheibel.[3] Scale-up procedures for a Scheibel extraction column have also been reported.[4]

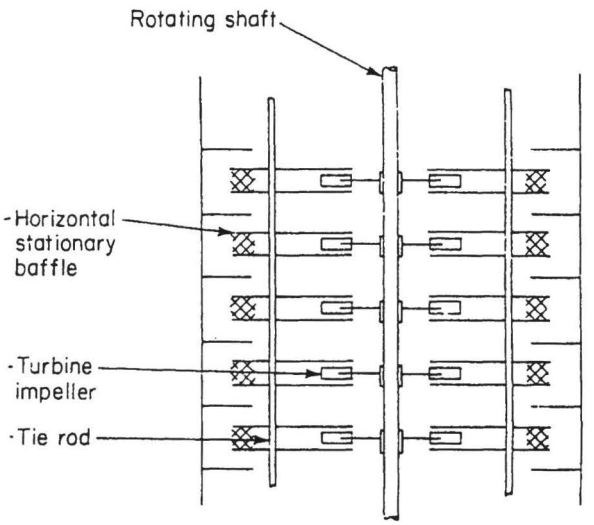

Figure 1. Compartment of Scheibel Column with Horizontal Baffle without wire Mesh Packing Between Stages

Stage efficiency and HETS

The stage efficiency in the 3" column was 22% (HETS = 4.6"). The plant design is based on an efficiency of 18.2% (HETS = 44"). On scale-up, the stage efficiency remains about the same, but the HETS is 10 times greater.

Scheibel columns are marketed by York Process Equipment Company, and sizes up to 2.55 m (8'-6") in diameter are in service. A detailed description and design criteria for Scheibel columns are presented by Scheibel[3]. Scale-up procedures for a Scheibel extraction column have also been reported[4].

B. Mixco Column

Total throughput

The 6"diameter pilot column with 20 stages was used for pilot testing at the Mixing Equipment Co. The total throughput for the pilot column was 230 GPH/ft^2. The 6' diameter column was designed for a throughput of 258 GPH/ft^2. The scale-up factor for the throughput is 1.1. The superficial velocity of fluid for the plant column was designed to be the same as that for the pilot column.

Stage efficiency and HETS

The stage efficiency in the 6" diameter column was found to be 20%. Mixco proposed that for the 6' diameter column, a stage efficiency of 50% can be achieved. The scale-up factor on the stage efficiency is 2.5. The stage height for the pilot column was 3" and that for the plant design was 3'0" which represents a factor of 12. The HETS for 6" diameter pilot column was 15", and the HETS for the large column is 6'0". The scale-up factor for HETS is 4.8.

Oldshue -Rushton columns up to 2.7m (9ft) in diameter have been reported to be in service for extraction. A description and design criteria for the Oldshue-Rushton columns have been reported.[2, 6]

C. Karr Reciprocating-Plate Column

Total throughput

The column has the highest throughput as compared with other columns shown in Table 1. This is consistent with the data, which appears in the literature.

Although a throughput as high as 1,300 GPH/ft.^{2} had been obtained in the 3" diameter column test, a throughput of 650 GPH/ft.^{2} which gave the lowest value of HETS was chosen as the basis for the design. The scale-up of throughput is 1:1.

HETS

The HETS obtained from the 3'-diameter column was about 12". For the 3'-10" diameter column design, a HETS of 38" was proposed by Chem Flow. Thus, the scale-up factor is approximately 3.

At the time when this piloting test was conducted at Hoffmann-La Roche in the early 1970s, the Karr Reciprocating-Plate columns was in the early stages of development. A 18"-diameter column was the largest column installed by Chem-Flow Co. However, the reciprocating-plate columns have gained increasing industrial applications in recent years. Description and design criteria for reciprocating-plate columns have been reported.[2,5]

CHOICE OF THE EXTRACTION COLUMN

Choosing a contactor is still both an art and science. It is largely based on one's experience. The vendor's experience, pilot-testing procedures, scale up methods, costs for capital equipment and maintenance, and reliability of operation should be considered and evaluated at an early stage before the pilot-plant tests are committed. Although equipment cost and installation ought to be a major consideration, in many actual cases previous experience and practice are the deciding factors.

Since the cost for these three types of columns was very close, the choice of the extraction column was mainly dependent upon the degree of confidence in the scale-up and experience with the extraction column. Roche has long been associated with Scheibel extraction columns, and with others, the Scheibel column was the choice for the design.

PERFORMANCE OF THE SCHEIBEL EXTRACTION COLUMN

Figure 2 Shows the process flow diagram for the 4' 9" diameter x 48' 0" overall height Scheibel extraction column. The column was installed and started up in early 1970s. The column has performed smoothly ever since with minimal maintenance required. Production capacity has been met, and extraction efficiency of 99.5% has been achieved. Table 2 shows a comparison of operating data with the design basis for the column.

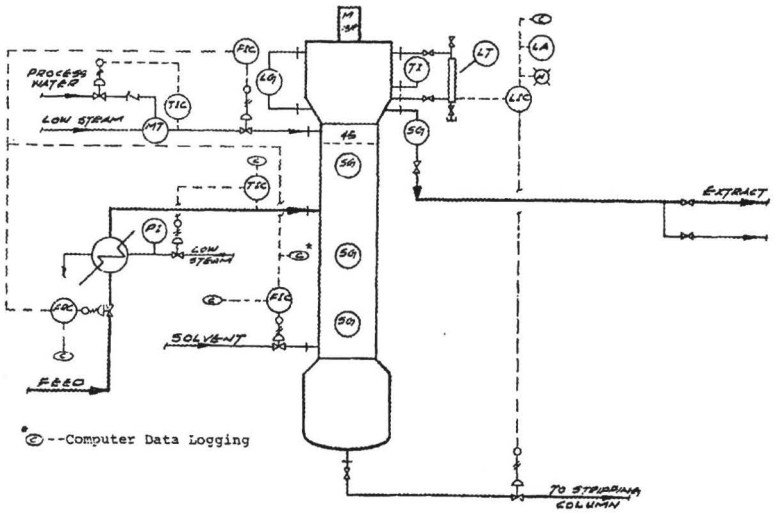

Figure 2 . Flow Diagram of Process Control for a Scheibel Extraction Column.

TABLE 2

Comparison of Operating Data With Design for A 4'-9" Diameter Scheibel Extractor.

Operating Condition	Performance	Design
Temperature, °C	44	45
Throughput		
Total, GPH	6,000	7,200
GPH/FT^2	345	415
Agiator speed, RPM	28	15-50
Efficiency		
Extraction Efficiency, %	99.5	99.0
No. of Theoretical Stages	6.7	6
HETS, Inches	39	44
Stage Efficiency, %	20	18
Volumetric Efficiency, hr^{-1}	14.2	15.2

ACKNOWLEDGMENTS

The author is grateful to his former managers at Hoffmann-La Roche Inc. for their encouragement and support in the years during this project was in development, design and start-up. Thanks also to Ms. N. Kuo for her help in the preparation of this manuscript.

REFERENCES

1. Lo TC, Baird M and Hanson C(eds), *"Handbook" of Solvent Extraction"*, Wiley-Interscience, New York, (1983).
2. Lo TC, in Schweitzer (ed.) *Handbook of Separation Techniques for Chemical Engineers*, Third Edition, McGraw-Hill, Section 1.10. (1997).
3. Sheibel EG *"Scheibel Columns,"* Chapter 13.3 in Ref. 1.
4. U.S. Department of Commerce, National Technical Information Service, NTIS Report No. DE 3013576," Scale-Up Procedure for a Scheibel Extraction Column", (1983).
5. Lo TC and Prochazka J,*" Reciprocating-Plate Extraction Column"* Chapter 13.in Ref. 1.
6. Oldshue JY,*" Oldshue-Rushton Column,"* Chapter 13.4 in Ref. 1.



Simulation and Modelling

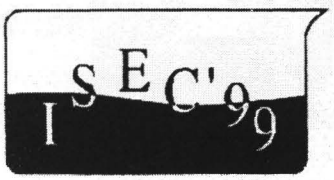

MODELLING OF THE SEPARATION OF CADMIUM FROM PHOSPHORIC ACID USING EMULSION LIQUID MEMBRANES

T Gallego Lizon and ES Pérez de Ortiz
Department of Chemical Engineering and Chemical Technology, Imperial College of Science, Technology and Medicine, London SW7 2BY, UK

ABSTRACT
This work deals with the use of the emulsion liquid membrane for the recovery of cadmium from phosphoric acid. The liquid membrane contained the extractant Cyanex 302 and the surfactant Arlacel C. Results on the extraction rate at different stirring speeds, together with measurements of the continuous phase-emulsion interfacial area using endoscopic photography, indicated that the extraction rate-controlling mechanism was a combination of chemical resistances and the diffusional resistance in the continuous phase diffusional film. A mathematical model was developed for extraction with this type of mass transfer regime and a pseudo-first order interfacial reaction. Experimental results over a wide range of experimental conditions were in good agreement with the model predictions.

Keywords: cadmium, phosphoric acid, Cyanex 302, emulsion liquid membrane, mass transfer, modelling

INTRODUCTION

The presence of cadmium and other metal compounds in the raw phosphoric acid utilised in the manufacture of fertilisers has generated an increasing search for new processes of pollutant recovery.[1,2,3,4] Among liquid-liquid extraction processes, emulsion liquid membrane extraction appears to be a viable process, since it has potential to yield low metal concentrations in the raffinate and high concentrations in the stripping phase whilst using a low organic inventory.

The extraction of cadmium with an emulsion liquid membrane has been reported[5,6,7,8,9] for moderately acidic feeds. At the highly acidic conditions of phosphoric acid (pH ~ 0), only our preliminary results were found in the literature.[10] In this paper we present the extraction results obtained in a stirred tank reactor of standard configuration over a wide range of conditions, and the variation with stirring speed of the interfacial area between the continuous phase and the emulsion globules, measured using endoscopic photography. From these results it was concluded that the extraction rate was under the mixed control of the chemical reaction and mass transfer in the continuous phase diffusional film. A model developed for extraction under this regime and pseudo-first order interfacial reaction is proposed and compared with the experimental results.

EXPERIMENTAL

$3CdSO_4.8H_2O$ (Aldrich Chemical Co.) was added to H_3PO_4 to create a synthetic phosphoric acid continuous phase. Cyanex 302, the membrane carrier, was kindly supplied by Cytec Co. and used without further purification. Surfactant Arlacel C was provided by ICI surfactants. Low odour kerosene was used as the diluent in the membrane phase containing the extractant and the surfactant, and HCl and NaCl (Merck, p.a.) were analytical grade reagents used to form the internal phase of the emulsion. The stripping phase was chosen to be a mixture of NaCl (3mol/dm^3) and HCl (1 mol/dm^3), as previous findings[10] showed the chlorine ion to be responsible for the reaction with the metal/reagent complex.

Cadmium concentrations in the feed phase were modified between 0.0003 and 0.0032 mol/dm^3 and Cyanex 302 concentrations in the membrane phase between 0.05 and 0.91 mol/dm^3. The Arlacel C concentration was held constant at a value of 5% v/v in the organic solution.

© 2000 Society of Chemical Industry

Unless otherwise stated, the effect of the various parameters was individually investigated, so that only one variable was modified at a time whilst the others were being held constant. Standard conditions were selected and are summarised in Table 1.

Initial cadmium concentration in continuous phase	0.00042 mol/dm^3
Phosphoric acid concentration	4.5 mol/dm^3
Surfactant (Arlacel C) concentration	5% v/v
Reagent (Cyanex 302) concentration	0.3 mol/dm^3
Stripping phase composition	NaCl (3mol/dm^3) + HCl (1mol/dm^3)
Treat ratio ($V_{continuous\ phase}/V_{emulsion}$)	20
Phase ratio ($V_{membrane}/V_{stripping\ phase}$)	1
Homogeniser speed	3000 rpm
Stirring speed	300 rpm

Table 1 Standard experimental conditions

The emulsion globules were photographed using an endoscope, with a high powered light source attached to a high speed video camera system (Kodak EcktaPro 1000 Imager), and the interfacial area of the dispersion was then evaluated assuming spherical globule shape.
The geometry of the tank is described in Table 2.

Internal diameter of vessel	0.09 m
Liquid height in vessel	0.125 m
Impeller diameter	0.0365 m
Impeller type	6 flat-blade turbine

Table 2 Tank Dimensions

MODEL

It is assumed that due to the reduced solubility of the reagents in opposite phases, the chemical reactions taking place are interfacial. In view of the relatively large concentration of carrier present in the organic phase, its rate of transfer through the membrane was not expected to affect the overall transfer mechanism. Kinetic data obtained by Maurin[11] for extraction in a two-phase system indicated that the reaction is of pseudo-first order with respect to C_{Cd}, i.e. $(r_{Cd}) = k_E' \cdot C_{Cd}$. It was further assumed that no globule coalescence or break-up took place in the tank, and that the external phase was well mixed. The values of the physical properties were assumed constant.

As discussed in the Results section, experimental results on the rate of extraction at different Cd and extractant concentrations, and over a range of stirring speeds, showed that the rate of extraction was under the mixed control of diffusional resistances in the continuous phase diffusional film and of the rate of reaction. Thus these are the resistances considered in this model. The film theory was applied to flat sheet geometry.

At quasi-steady state, the rate of mass transfer of cadmium from the bulk of the continuous phase to the interface between the continuous and membrane phases, must be equal the rate of reaction at the interface:

$$r = k_c \cdot \left(C_{Cd}^b - C_{Cd}^i\right) \cdot a_s = k_E' \cdot C_{Cd}^i \qquad (1)$$

where,

$$k_E^{'} = k_E \cdot C_{Cyanex302} \tag{2}$$

From experimental results, the variation with time of cadmium concentration in the bulk of the continuous phase was given by:

$$C_{Cd}^{b} = C_{Cd}^{o} \exp(-\beta \cdot t) \tag{3}$$

In these equations a_S is the specific area (m^{-1}), $C_{Cd}{}^{b}$, $C_{Cd}{}^{i}$, $C_{Cd}{}^{o}$ are the bulk, interfacial and feed cadmium concentration ($kmol/m^3$) and $C_{Cyanex\ 302}$ is the concentration of Cyanex 302 in the membrane phase ($kmol/m^3$). k_C is the continuous phase mass transfer coefficient (m/s); k_E and k_E' are the rate of reaction ($m^3/s{\cdot}kmolC302$) constant and first-order reaction rate constant (s^{-1}), and t is the time. β (s^{-1}) is a parameter, which can be regressed from experimental findings.

Rearranging these equations, the following expressions for the interfacial concentration and the rate of reaction were obtained:

$$C_{Cd}^{i} = \frac{C_{Cd}^{o}}{\left(\frac{k_E^{'}}{k_c a_s} + 1\right)} \exp(-\beta \cdot t) \tag{4}$$

$$r = \frac{-\partial C_{Cd}^{b}}{\partial t} = \frac{C_{Cd}^{o}}{\left(\frac{1}{k_c a_s} + \frac{1}{k_E^{'}}\right)} \exp(-\beta \cdot t) \tag{5}$$

and

$$\beta = \frac{k_c a_s}{1 + \frac{k_c a_s}{k_E^{'}}} \equiv \frac{1}{\frac{1}{k_E^{'}} + \frac{1}{k_c a_s}} \tag{6}$$

This model gives the rate of extraction as a function of time, specific interfacial area, the pseudo first order reaction rate constant, and the mass transfer coefficient in the continuous phase. The specific interfacial area at different conditions was calculated from measured Sauter mean diameters, according to:

$$a_s = \frac{6\phi}{d_{32}} \tag{7}$$

where ϕ is the emulsion hold-up and d_{32} is the Sauter mean diameter (m).

The mass transfer coefficients in the continuous phase have been calculated for different stirring speeds and emulsion hold-ups using Skelland and Lee's correlation.[12] Thus, the only parameter that was estimated by regression was the reaction rate constant.

RESULTS AND DISCUSSION

Study of the rate controlling resistances in a stirred tank reactor

Figure 1 shows the variation of the mass transfer rate, rE, and the specific interfacial area, a_S, with the stirring speed N. The dependence of the mass transfer rate with N was to $N^{2.9}$, whilst that of the interfacial area was only to $N^{1.01}$. This means that the increase in extraction rate with stirring speed is substantially larger than the increase in interfacial area. Another operating parameter that increases with N is the mass transfer coefficient in the continuous phase. Skelland and Lee[12] proposed a correlation for dispersion in stirred tanks in which the continuous phase mass transfer coefficient is proportional to $N^{1.8}$. The addition of the powers of N for the effect on interfacial area

and on the mass transfer coefficient gives 2.8, which is approximately the same power as obtained for the variation of rE with N. It was therefore concluded that the mass transfer resistance in the continuous phase was at least part of the rate controlling mechanism.

Effects of Cd and reagent concentrations

Results plotted in Figures 2 and 3 show the effect on extraction rate of the extractant and Cd concentrations, respectively. An analysis of this data is beyond the scope of this paper, but it can be concluded that the rate of the interfacial chemical reaction is well of pseudo-first order with respect to Cd, as described by equations 1 and 2 [13].

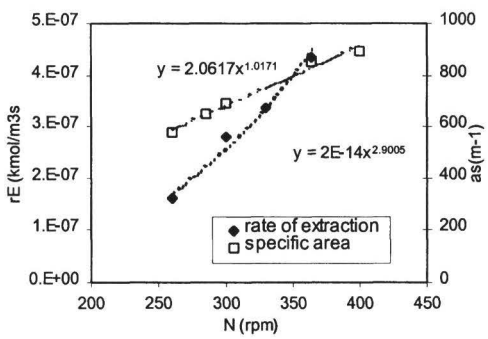

Figure 1. Experimental variation of a_S and r_E predicted with stirring speed at standard conditions defined in Table 1.

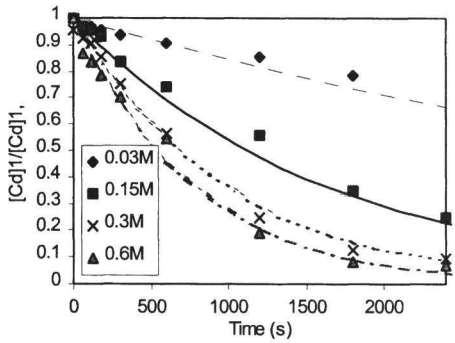

Figure 2. Effect of Cyanex concentration by the quasi-steady state model.

Comparison of predicted and experimental results

Extraction results were calculated with the model using Skelland and Lee[12] correlation for the estimation of k_C, and the a_S measured values. The rate constant of chemical reaction was obtained by regression using the extraction experimental values and equation 6.

Figure 2 displays predicted results obtained with the model and the experimental data at different reagent concentrations. Corresponding values of the β-parameter and of k_E'/a_S are presented in Table 3.

$C_{Cyanex\ 302}$ (mol/dm^3)	β (s^{-1})	a_S (m^{-1})	k_E'/a_S (m/s)
0.03	0.000175	640	$3.09 \cdot 10^{-7}$
0.15	0.00062	655	$1.58 \cdot 10^{-6}$
0.3	0.00105	675	$4.6 \cdot 10^{-6}$
0.6	0.0013	710	$8.29 \cdot 10^{-6}$

Table 3 Reaction rate coefficients for various reagent concentrations

The value of the interfacial extraction reaction constant (k_E/a_S) is independent of the specific area, as expected, and equal to $1.39 \cdot 10^{-5}$ m^4/kmol·s.

Predicted and experimental results of Cd extraction as a function of Cyanex and Cd concentrations, and at different stirring speeds, are shown in Figures 2, 3 and 4, respectively. Lines

indicate predicted results, whilst markers represent experimental data. In general predicted and experimental results are in good agreement. Results predicted by the model were best for cadmium concentrations smaller or equal to $8.4 \cdot 10^{-4}$ mol/dm^3 (Figure 3); above this value diffusional resistances in the internal phase may become important as the concentration of the complex increases. It can be observed in Figure 4 that predicted values are good, except for those at a stirring speed of 264 rpm, for which the predicted extraction rate values are higher than the experimental. This may be due to the fact that at this low stirring speed the emulsion may not be fully dispersed, with the consequent decrease in interfacial area.

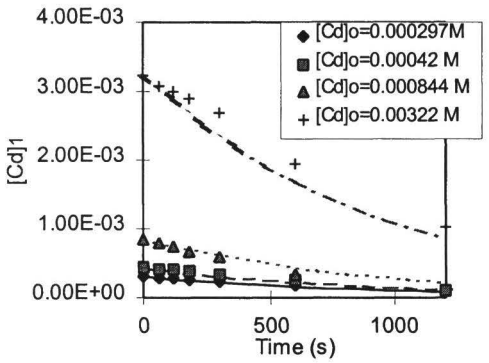

Figure 3. Effect of continuous phase initial concentration on predictions determined with the with the quasi-steady state model. $\beta = 0.00105 s^{-1}$, $k_c = 2.35 \cdot 10^{-6} m/s$, $a_s = 675 m^{-1}$.

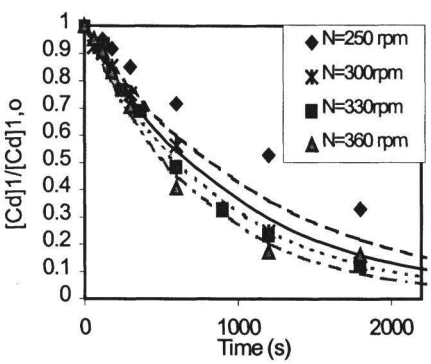

Figure 4 Effect of stirring speeds on Cd^{2+} predictions determined with the quasi-steady state model. $k_E' = 0.003 s^{-1}$.

CONCLUSIONS

Predicted and experimental extraction rates agree well within a wide range of conditions which cover those of industrial operations. However, large deviations were encountered at large initial Cd concentrations in the continuous phase, and at stirring speeds below 300 rpm. The former may be due to mass transfer resistances in the membrane phase caused by the high concentration of complex, and the latter to incomplete emulsion dispersion.

REFERENCES

1 Almela A and Elizalde MP. *Hydrometallurgy*, **37**, 47, (1995).
2 Alonso AI, Urtiaga AM, Zamacona S, Irabien A and Ortiz I, *J. Membr. Sci.*, **130**, 193, (1997).
3 Daoud JA, El Reefy SA, Aly HF. *Sep. Sci. Technol.*, **33**, 537, (1998).
4 Kabay N, Demircioglu M, Ekinci H, Yüksel, Saglam M, Akçay M and Streat, M. *Ind. Eng. Chem. Res.*, **37**, 2541, (1998).
5 Izatt RM, Bruening RL, Geng W, Cho MH and Christensen JJ. *Anal Chem.* **59**, 2405, (1987).
6 Raghuraman BJ, Tirmizi NP, Kim BS and Wiencek JM. *Environ. Sci. Technol.*, **29**, 979, (1995).
7 Ally R, Pareau D, Stambouli M and Durand G. *Proceed., ISEC'96*, 911, (1996).
8 Li QM, Liu Q, Li K and Tong SY. *Talanta*, **44**, 657, (1997).
9 Li QM, Liu Q, Zhang QF, Wei XJ and Guo JZ. *Talanta*, **46**, 927, (1998).
10 Gallego Lizon T and Pérez de Ortiz ES. *Proceedings of the International Symposium on Liquid-Liquid*

Two-Phase Flow and Transport and Phenomena, 301, November, (1997).
11 Maurin M. *M.Sc Thesis*, University of London, (1996).
12 Skelland AHP, Lee JM. *AIChE J.* **27**, 99, (1981).
13 Gallego Lizon T. *Ph.D. Thesis*, University of London, (1998).

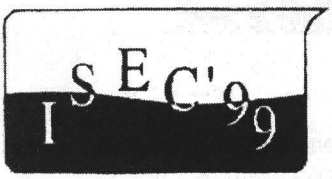

HOLLOW FIBRE MODULES AS NOVEL PHASE CONTACTORS FOR THE SEPARATION OF MULTI-CATION MIXTURES BY CHEMICAL EXTRACTION

Andreas Geist, Jae-Il Kim, Pawel Plucinski[1] and Walter Nitsch[2]
Forschungszentrum Karlsruhe, Institut für Nukleare Entsorgungstechnik, D-76021 Karlsruhe, Germany.
[1]University of Bath, Dept. of Chemical Engineering, Bath BA2 7AY, UK
[2]TU München, Institut für Technische Chemie, D-85748 Garching, Germany

ABSTRACT
The separation of multi-cation mixtures using a hollow fibre module (HFM) is presented. Experimental results on the co-extraction of divalent cations (Cd^{2+}, Cu^{2+}, Ni^{2+}, Zn^{2+}) into bis(2-ethylhexyl) phosphoric acid (D2EHPA) show good agreement with calculated results. Calculations are based on a predictive and descriptive modeling of mass transport and exchange in HFM. The influence of common proton and complexant concentrations on the distribution of individual metallic species is demonstrated. The reliability of the modeling allows calculations on the separation of Am^{3+} from Eu^{3+} with purified Cyanex 301 (bis(2,2,4-trimethylpentyl)dithiophosphinic acid). The results indicate that Am^{3+} can be extracted quantitatively with only minimal co-extraction of Eu^{3+} in a single HFM pass.

Keywords: americium, cadmium, copper, europium, nickel, zinc, Cyanex 301, bis(2-ethylhexyl)phosphoric acid, hollow fibre module, mass transfer, modelling

INTRODUCTION

Hollow fibre modules (HFM) are efficient phase contacting devices in liquid-liquid-extraction.[1] Their field of application is comparable to that of countercurrent column contactors. However, HFMs offer several distinct advantages, promoting the application of liquid-liquid-extraction for the separation of dilute species.

Because the two phases are macroscopically separated by a micro-porous membrane, flow rates of both organic and aqueous phases can independently be adjusted over a wide range. This is crucial for obtaining high volume reduction factors. Mutual contamination of phases with entrainment does not occur. Furthermore, very small diffusion distances in HFM result in compact dimensions (approx. one-tenth the length of conventional columns[2]).

The outstanding potential of non-dispersive chemical extraction has already been demonstrated on the mass transfer system: Zn^{2+}/H_2SO_4 – D2EHPA/kerosene, and a predictive modeling of the chemical mass transfer process in HFM has been established.[2] Mass transfer in this system is limited by diffusion in the range of concentrations of interest.[3]

To our knowledge, predictive modeling of multi-cation co-extraction/separation by chemical extraction in HFM has not yet been established. We therefore investigate co-extraction and separation of two or more metal cations in HFM. The known mass transfer system Me^{2+}/H_2SO_4 – D2EHPA/ kerosene (Me = Cd, Cu, Ni, Zn) is utilized, where mass transfer is limited by diffusion for all species regarding both extraction and back-extraction.[4]

EXPERIMENTAL

D2EHPA (>98%, Bayer AG, Germany) is used as received. It is diluted in WBC-15, a technical grade iso-dodecane fraction (Biesterfeld Chemicals, Germany). Metal salts are analytical grade sulfates.

The HFM setup is described.[2] Both phases pass through the module in counter-current, single-pass mode. The aqueous phase flows in the lumen of the hollow fibres (HF). Modules are Hoechst-Celanese Liqui-Cel 5PCM-105 type modules (9000 HF, membrane material polypropylene, average

© 2000 Society of Chemical Industry

pore size 0.05 µm, HF i.d. = 0.24 mm, HF o.d. = 0.30 mm, active length = 0.55 m, active diameter = 0.05 m). Static pressure in the aqueous phase is kept ca. 0.5 bar higher than in the organic phase in order to maintain proper phase separation.

Inlet and outlet concentrations are measured with ICP-AES (Spectroflame Modula, Germany). Stationary outlet concentrations are plotted vs. aqueous flow rate.

Stirred cell experiments are conducted in a Nitsch stirred cell (see [5,6] for details) with Cyanex-301, purified according to[7], and dissolved in WBC-15 to a concentration of 0.4 kmol/m^3. Aqueous phase is 2 mg/L Eu^{3+} (as $Eu(NO_3)_3$, analytical grade) in acetate buffer (0.01 kmol/m^3) of pH = 5.0. Aqueous concentration in the stirred cell is plotted versus time, and initial fluxes are determined at varying stirring speeds.

CALCULATION OF CO-EXTRACTION IN HFM

Calculation of mass transfer for chemical single species extraction limited by diffusion in HFM is described.[2] Fundamental physical and chemical phenomena (diffusion in aqueous and organic phases, mass exchange according to experimentally determined equilibrium and stoichiometry data, flow of phases, module geometry etc.) are taken into account, and no fitting parameters are used. This modeling is modified for calculating co-extraction and separation of multi-cation mixtures.

In a system limited by diffusion, the following steps of mass transfer have to must be considered:

1. diffusion of metal ions and protons in the lumen of HF
2. diffusion of complexant and metal complexes in the pores of the hydrophobic membrane material
3. diffusion of complexant and metal complexes in the shell-side of the HFM

Due to the fast chemical reaction (as mass transfer is limited by diffusion) of the metals investigated, Me_i^{2+}, with complexant molecules, $(HX)_2$,

$$Me_i^{2+} + m_i \overline{(HX)_2} \rightleftharpoons \overline{Me_i X_2 (HX)_{2m_i-2}} + 2\,H^+ \qquad (1)$$

chemical equilibrium for each metallic species is established at the liquid/liquid interface, with individual equilibrium constants, K_i:

$$K_i = \frac{\left[\overline{Me_i X_2 (HX)_{2m_i-2}}\right]^* \cdot \left([H^+]^*\right)^2}{\left[Me_i^{2+}\right]^* \cdot \left(\left[\overline{(HX)_2}\right]^*\right)^{m_i}} \qquad (2)$$

Interfacial concentrations, $[A]^*$, can be expressed by

$$j_A = k_A \cdot \left([A] - [A]^*\right) \qquad (3)$$

with bulk concentrations $[A]$, individual mass transfer coefficients k_A, and fluxes j_A. Individual fluxes are coupled according to the stoichiometry of the mass exchange equation (equation 1):

$$j_{Me_i X_2 (HX)_{2m_i-2}} = -\,j_{Me_i^{2+}} \qquad (4)$$

$$j_{(HX)_2} = \sum m_i \cdot j_{Me_i^{2+}} \qquad (5)$$

$$j_{H^+} = -2 \cdot \sum j_{Me_i^{2+}} \qquad (6)$$

and individual equilibrium conditions K_i for all Me_i^{2+} involved are rewritten:

$$K_i = \frac{\left(\left[Me_iX_2(HX)_{2m_i-2}\right] + j_{Me_i^{2+}}/\beta_{Me_iX_2(HX)_{2m_i-2}}\right)\cdot\left(\left[H^+\right] + 2\cdot\sum j_{Me_i^{2+}}/\beta_{H^+}\right)^2}{\left(\left[Me_i^{2+}\right] - j_{Me_i^{2+}}/\beta_{Me_i^{2+}}\right)\cdot\left(\left[(HX)_2\right] - \sum m_i\cdot j_{Me_i^{2+}}/\beta_{HX}\right)^{m_i}} \quad (7)$$

All K_i are coupled via both the common proton and complexant concentrations, $[H^+]$ and $[(HX)_2]$, and the sum terms in equation 7, analogous to reference[8].

Hence, with known individual mass transfer coefficients and equilibrium constants, fluxes of the key components can be calculated. Aqueous mass transfer coefficients (in the lumen of HF) can be calculated according to an analytical solution given.[9] Shell-side mass transfer coefficients are calculated according to a correlation given.[10] Equilibrium constants are taken from[2]. By numerical calculation of fluxes and a cell-wise calculation of the module (considering changes in concentration within a cell due to both convection and mass transfer across the liquid/liquid interface), concentration profiles and metal outlet concentrations, $[Me_i^{2+}]_{out}$, are calculated.

SEPARATION OF DIVALENT CATIONS

Figure 1 shows results from zinc/cadmium separation/co-extraction. Extraction efficiency is increased with decreasing aqueous flow rate, Q_{aq}, due to longer residence time. The two figures demonstrate the influence of complexing agent concentration. At a relatively low complexant concentration (0.05 kmol/m^3, figure 1A), zinc is readily extracted (from 100 mg/L to less than 0.1 mg/L, depending on flow rate), whereas cadmium is removed only to a small extent (e.g. from 10 mg/L to ca. 7 mg/L). This effect is caused by proton release due to zinc extraction, which impedes cadmium extraction. Simply by increasing complexant concentration to 0.5 kmol/m^3 (Figure 1B), both zinc and cadmium are extracted to approximately the same extent. In this case, cadmium is extracted, due to higher complexant concentration. Note the good agreement between experimental and calculated results.

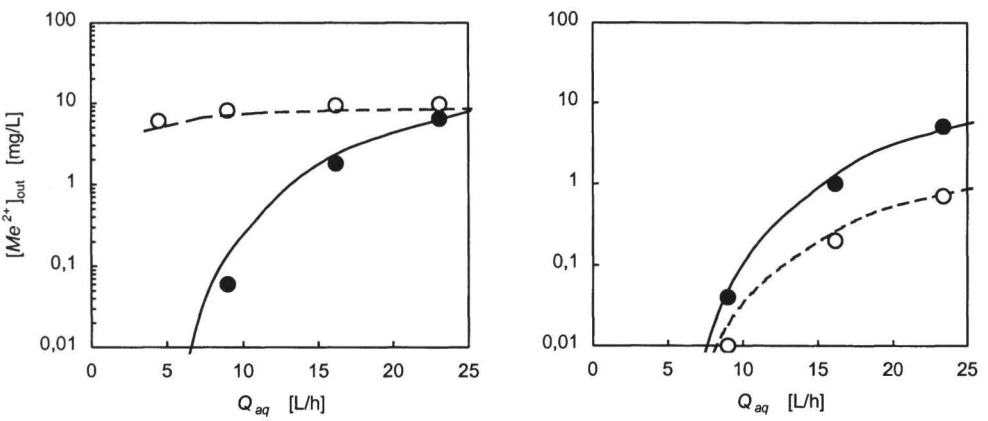

Figure 1 Zinc/cadmium co-extraction in a HFM. $[Zn^{2+}]_{in}$ = 100 mg/L; $[Cd^{2+}]_{in}$ = 10 mg/L; pH_{in} = 5.5; Q_{org} = 1.8 L/h. Symbols: experiments; lines: calculated. ● —— zinc; O - - - cadmium

A: $[(D2EHPA)_2]$ = 0.05 kmol/m^3 B: $[(D2EHPA)_2]$ = 0.5 kmol/m^3

Similar calculations were performed for the separation of a mixture of four cations (Zn^{2+}, Cd^{2+}, Cu^{2+}, Ni^{2+}, see figure 2): Metals are removed according to their extractability with D2EHPA (Zn^{2+} > Cd^{2+} > Cu^{2+}> Ni^{2+}),[2] with nickel remaining practically unaffected.

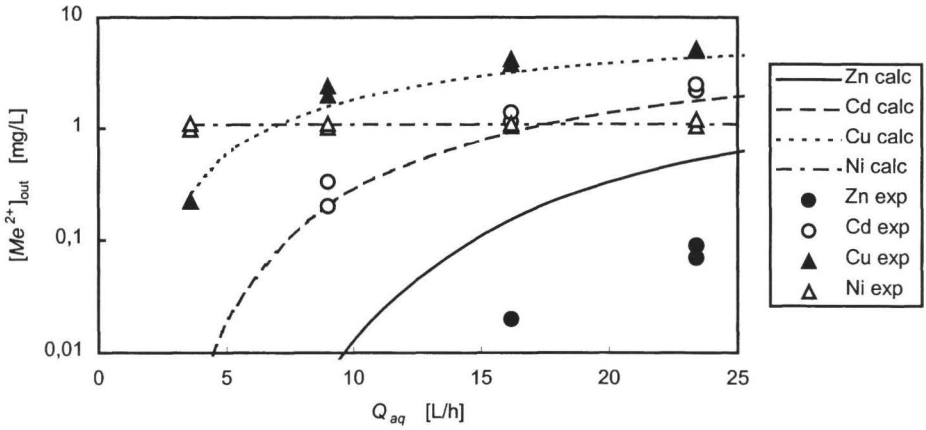

Figure 2: Zinc/cadmium/copper/nickel separation in a HFM. $[Zn^{2+}]_{in} = [Cd^{2+}]_{in} = [Cu^{2+}]_{in} = 11$ mg/L; $[Ni^{2+}]_{in} = 1.1$ mg/L; $pH_{in} = 5.5$; $[(D2EHPA)_2] = 0.05$ kmol/m^3; $Q_{org} = 1.6$ L/h. Symbols: experiments; lines: calculated.

AMERICIUM/EUROPIUM (Am^{3+}/Eu^{3+}) SEPARATION

The fact that calculating mass transfer yields satisfactory results for co-extraction and separation, prompted calculations of Am^{3+}/Eu^{3+} separation. The complexant is Cyanex-301, which, in a purified form, is able to separate Am^{3+} from Eu^{3+} with a high separation factor.[7] Equilibrium and stoichiometric data are taken from[7]. Stirred cell experiments (see Figure 3) indicate that extraction rate is limited by diffusion, as can be seen from the linear increase in flux, $j_{t=0}$, with stirrer speed, n_{aq}.

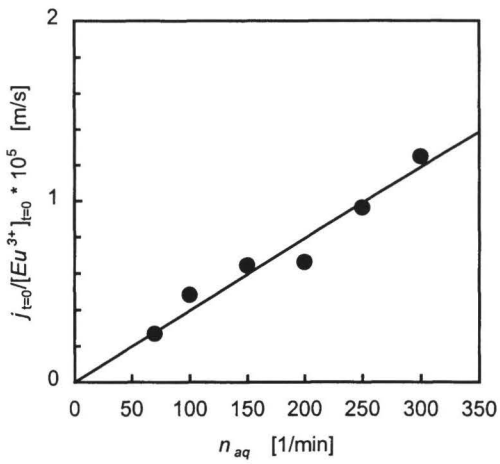

Figure 3. Stirring speed dependency of europium extraction with purified Cyanex-301. $[Eu^{3+}]_{t=0} =$ 2 mg/L, $[Cyanex\text{-}301] = 0.4$ kmol/m^3, $pH_{t=0} = 5.0$ (buffered), $n_{org} = n_{aq}$.

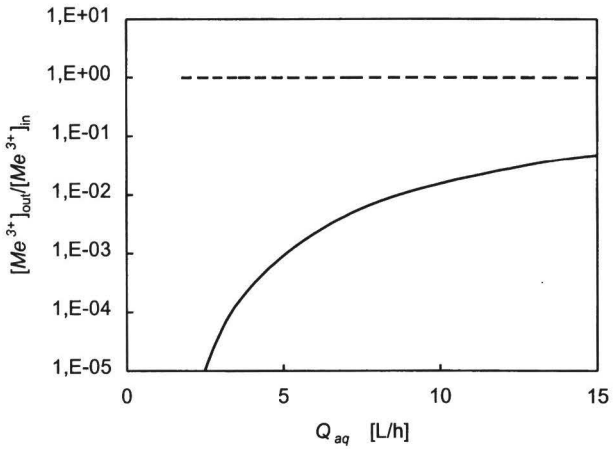

Figure 4: Calculated americium/europium separation with purified Cyanex-301 in a HFM. $[Am^{3+}]_{in}$ = 10 mg/L; $[Eu^{3+}]_{in}$ = 1000 mg/L; pH_{in} = 4.2; [*Cyanex-301*] = 1.0 kmol/m^3; $Q_{org} = Q_{aq}$. —— Am^{3+}; - - - Eu^{3+}

With this data, Am^{3+}/Eu^{3+} separation in a HFM using purified Cyanex-301 is calculated. Figure 4 shows the result of the calculations. At a flow rate of 5 L/h, 99.9% of Am^{3+} is transferred to the organic phase (i.e. a decontamination factor of 1000), whereas only ca. 0.3% of Eu^{3+} (not noticeable in figure 4) is co-extracted.

CONCLUSION

The potential for predictive modelling of the separation of multi-cation mixtures with non-dispersive chemical extraction is demonstrated. Such calculations permit evaluation of HFM separation technology and are very helpful for process scale-up, as no fitting parameters are used. The modeling is easily adapted to other mass transfer systems limited by diffusion (be it physical or chemical extraction), giving preliminary information about the applicability of HFM extraction for a separation task.

NOMENCLATURE

j	flux	kmol/m^{2}s
k	mass transfer coefficient	m/s
K	equilibrium constant	(depending on stoichiometry)
m	stoichiometric factor	–
n	stirring speed	1/min
Q	flow rate	[L/h]
[]	concentration	kmol/m^3 or mg/L

Subscripts, superscripts:

aq	in aqueous phase
in	at inlet
out	at outlet
org	in organic phase
i	regarding component *i*
*	at liquid/liquid interface

REFERENCES

1 Kim BM, *J. Membr. Sci.* **21**, 5-19 (1984)
2 Daiminger U, Geist A, Nitsch W and Plucinski P, *Ind. Eng. Chem. Res.* **35**, 184 (1996)
3 Walter JA, Kneißl F and Nitsch W, in: *Solvent Extraction in the Process Industries (Proc. ISEC 1993)* **2**, 1206. Eds: D. H. Logsdail, M. J. Slater. Elsevier (1993)
4 Geist A, Plucinski P and Nitsch W, *Chem. Ing. Tech.* **69**(7), 946 (1997)
5 Nitsch W, Raab M and Wiedholz R, *Chem. Ing. Tech.* **16**, 1026 (1973)
6 Waubke M, *Doctoral Thesis*, TU München (1988)
7 Zhu Y, Chen J and Jiao R, *Solv. Extr. Ion Exch.* **14**(1), 61-68 (1996)
8 Nitsch W and van Schoor A, *Chem. Eng. Sci.* **38**(12), 1947 (1983)
9 Skelland AHP, *Diffusional Mass Transfer*, John Wiley & Sons, N.Y. (1974)
10 Costello MJ, Fane AG, Hogan PA and Schofield RW, *J. Membr. Sci.* **80**,1 (1993)



MODELLING OF CONTINUOUS REACTIVE EXTRACTION AND STRIPPING OF ZINC IN HOLLOW FIBRE MODULES

P Schöner, W Nitsch, P Plucinski[1] and A Fedorov[2]
Technische Universität München, Institut für Technische Chemie, 85748 Garching, FRG
[1]present address: University of Bath, Department of Chemical Engineering, Bath , UK
[2]present address: National Technical University of Ukraine, Department of Cybernetics of Chemical Technology Processes, Kiev, Ukraine

ABSTRACT
The experimental studies carried out recently by our research group confirm the great potential of hollow fibre modules as extraction devices, especially in environmental engineering. With a continuous working extraction-stripping plant for Zn/DEPA (bis(2-ethylhexyl)phosphate) in iso-dodecane stable operating conditions have been achieved for one week (time was limited by the volume of the storage tank). A maximum concentration ratio (enrichment factor) of 340 was obtained without optimisation of the process. The performance of the continuous process can be calculated, and therefore designed and optimised by using a physico-chemical model developed in our group.

Keywords: zinc, bis(2-ethylhexyl)phosphate, hollow fibre module, reactive extraction, modelling

INTRODUCTION

In the last few years the demand for separation processes in environmental engineering has been constantly growing. So the object of our investigations is to show that liquid/liquid extraction in hollow fibre modules is advantageous for the enrichment of ppm range concentrations in the field of environmental applications. As a model system we use Zn/DEPA in iso-dodecane (see equation 1).

$$Zn^{2+} + 1.5\,\left(\overline{HX}\right)_2 \rightleftharpoons \overline{ZnX_2(HX)} + 2H^+ \qquad (1)$$

In previous studies[1, 2] as a standard procedure, typical industrial throughputs were realised reducing the zinc concentration from 100 mg/l to less than 2 mg/l (limiting value). In the experiments the commercially available Liqui-Cel® cross-flow modules (Hoechst-Celanese) were used. The possibility of the separation of multi-cation matrices has also been demonstrated[3]. However until now studies of extraction and stripping were performed separately. The aim of the present work concerns the operation and modelling of a continuously working extraction-stripping plant.

EXPERIMENTAL

Figure 1 shows the process scheme of the zinc recovery plant. In module I zinc is removed (extracted) from the wastewater into the organic phase as $\left[\overline{ZnX_2(HX)}\right]$. Subsequently in module II zinc is stripped by sulphuric acid with regeneration of the complexing agent ($\overline{HX}$).
Liqui-Cel® cross-flow modules were used with an active length of 15 cm and a diameter of 5 cm. For details of the equipment see Schöner et al.[4].

The aqueous phase contains 100 mg/l zinc (as zinc sulphate - Merck, p.a.). The initial pH value varied between 5.3 and 5.7. The organic (extraction) phase is a solution of bis(2-ethylhexyl)phosphate (DEPA, Bayer AG) in iso-dodecane (WBC15, Biesterfeld, Germany). The regeneration (stripping) of the organic phase was achieved using 1 molar sulphuric acid (Merck p.a.).

© 2000 Society of Chemical Industry

The concentration of zinc was measured using inductive coupled plasma atomic emission spectroscopy (SPECTROFLAME, Spectro, Germany).

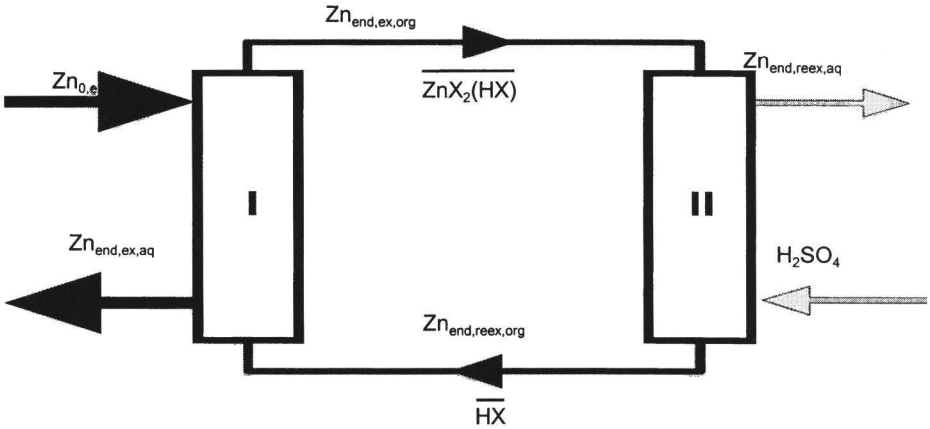

Figure 1: Schematic view of the continuous extraction stripping process

MODELLING

Because of the many parameters influencing the overall process a physico-chemical modelling of the process (fluid dynamics and mass transfer) is advantageous for an efficient optimisation of the plant.

To model the mass transfer, the module was divided into a two dimensional matrix of balance elements (Figure 2), taking into account the fluid dynamics of the cross-flow mode.

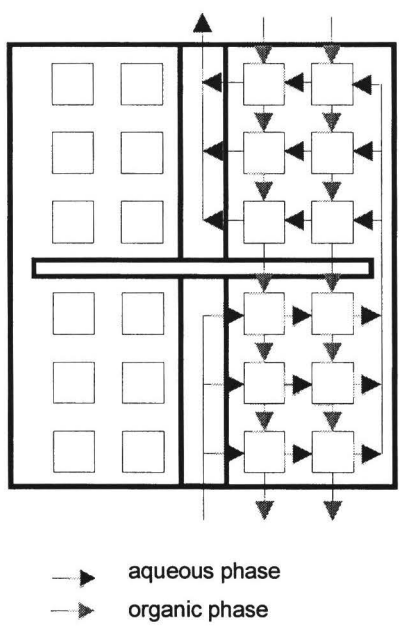

Figure 2: Scheme of cells matrix

The calculation of the mass transfer in a balance element was based on:

- coupling of the fluxes of the individual species (Zn^{2+}, H^+, complexing agent, complex) at the liquid/liquid interface – the site of chemical reaction,
- transport limited mass transfer (i.e. the interfacial chemical reaction is fast and therefore equilibrium can be established).

In the calculations no fitting parameters were used, therefore one can designate it as predictive modelling. The mass transfer coefficients in the shell side were calculated using our experimental correlation[4], those for the lumen-side were calculated according to Skelland's analytical solution[5]. The relevant equilibrium values in equation 2 were measured in our laboratory.

$$K = \frac{\left[\overline{ZnX_2(HX)}\right]\cdot\left[H^+\right]^2}{\left[Zn^{2+}\right]\cdot\left[\overline{(HX)_2}\right]^{1.5}} \qquad (2)$$

RESULTS AND DISCUSSION

For the coupling of extraction and stripping the following three parameters are important:

- the final zinc concentration of the purified wastewater [$Zn_{end,ex,aq}$],
- the final zinc concentration in the stripped solution [$Zn_{end,reex,aq}$] and
- the so called enrichment factor ([$Zn_{end,reex,aq}$]/[$Zn_{0,ex,aq}$]).

Assuming that for technological reasons the initial zinc concentration of the wastewater [$Zn_{0,ex,aq}$] and the volumetric flow rate F_{aq} are fixed, the optimisation of the three response values can be achieved by varying the

- type of module (geometry),
- volumetric flow rate F_{acid} ,
- concentration of the acid and
- volumetric flow rate of the organic phase F_{org}.

For most applications optimisation means achieving the limiting value for the zinc concentration in the purified wastewater [$Zn_{end,ex,aq}$] and the maximum value for the concentration of zinc [$Zn_{end,reex,aq}$] in the acid. A typical example of the calculation according to the proposed model together with experimental results is shown in Figure 3.

If one varies the volumetric flow rate of the acid (the other parameters being kept constant) the performance of the extraction is less effective for values lower than approximately 0.03 l/h (Figure 3a). This is because the mass flow of free complexing agent (F_{org}·[HX]) decreases due to the organic phase being not completely regenerated (initial loading [$Zn_{end,reex,org}$]).

Considering the stripping (Figure 3b), the reduction of the acid flow rate F_{acid} results in a higher concentration of zinc ([$Zn_{end,reex,aq}$]), so the optimal operating range is at an acid flow rate of approximately 0.03 l/h, caused by the decrease of extraction efficiency (Figure 3a).
In our example an increase of zinc concentration in the final stripping solution by an enrichment factor of 340 is achieved without optimising the concentration of the acid or the complexing agent.

Figure 4 shows the optimisation strategy directed to the maximum enrichment factor for the fluxes F_{acid} and F_{org} as variables. The corresponding results are demonstrated in Figure 5.

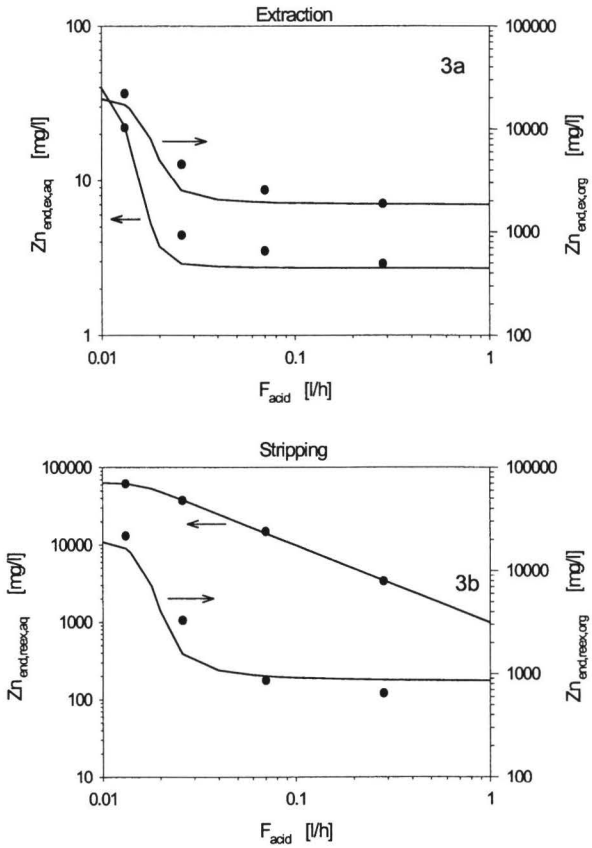

Figure 3: Variation of acid flow rate
15 cm module, $Zn_{0,ex,aq}$=100 mg/l, $[H_2SO_4]$=1 mol/l, $[(DEPA)_2]$=0.5 mol/l, F_{aq}=10 l/h, F_{org}=1 l/h points – experimental data; lines – calculated results

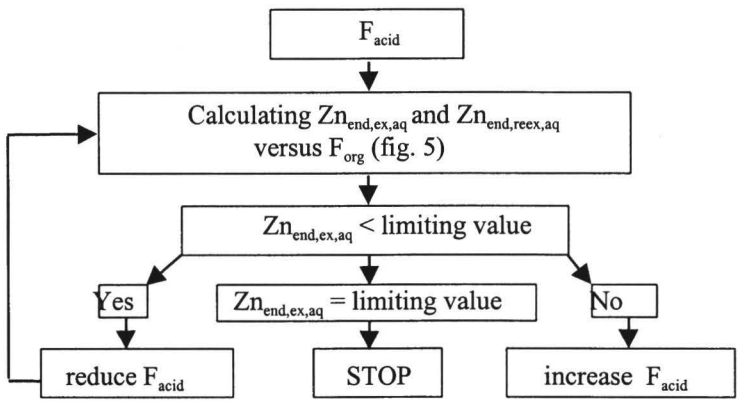

Figure 4: Optimisation strategy

The most important aspect regarding separation efficiency is the high sensitivity of the enrichment factor to the selected acid flow rate F_{acid} (Figure 5b). In this connection however the demand for the maximum enrichment factor means a narrow operating range in the flow rate F_{org} (Figure 5a).

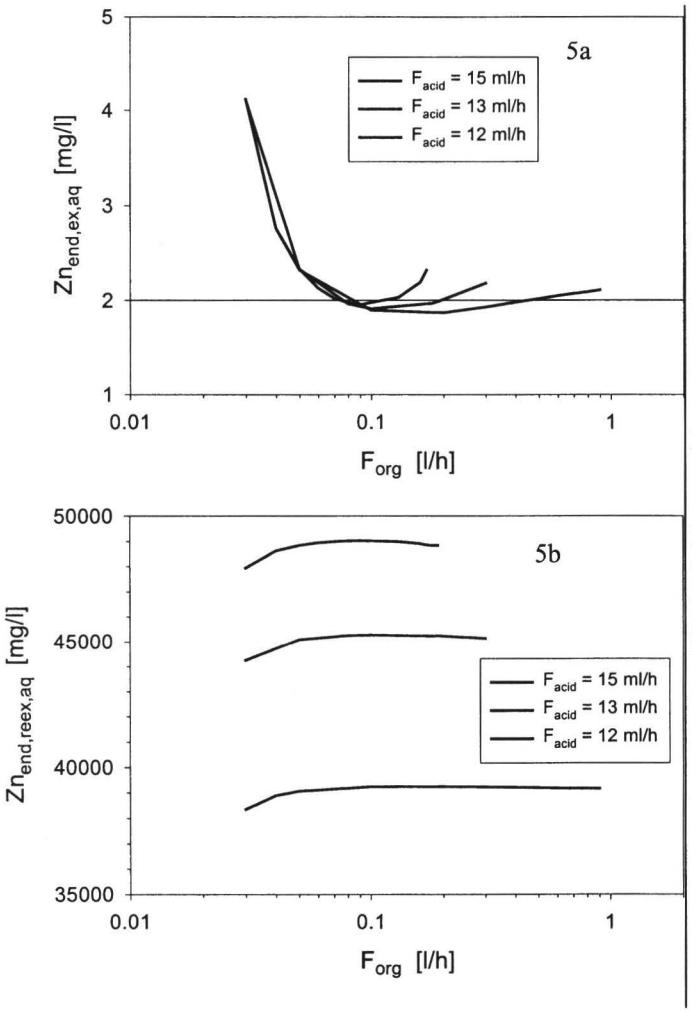

Figure 5: Optimisation

F_{aq} = 6 l/h,
$[(DEPA)_2]$ = 0.5 mol/l,
$[Zn_{0,ex,aq}]$ = 100 mg/l,
$[H_2SO_4]$ = 1.0 mol/l

CONCLUSION

Regarding chemical liquid/liquid extraction in hollow fibre modules, because of the multiplicity of variables (i.e. 11 variables for the extraction/stripping mode) an empirical (black box) optimisation would be extremely ineffective. Therefore the presented very good agreement of the proposed model with the experimental data (Figure 3) is important because it proves the reliability of the above calculation procedure. This means it is possible to concern all the operation variables to achieve a complete treatment of optimisation. Furthermore the model allows dynamic simulation as well as characterisation of sensitivities.

REFERENCES

1. Daiminger UA, Geist AG, Nitsch W and Plucinski PK, *Ind. Eng. Chem. Res*, **35**, 184, (1996)
2. Daiminger U, *Ph. D. thesis*, Technische Universität München, (1996).
3. Geist A, Plucinski P and Nitsch W, *Chem.-Ing.-Techn.*, **69**, 946, (1997).
4. Schöner P, Plucinski P, Nitsch W and Daiminger U, *Chem. Eng. Science*, **53**, 2319, (1998).
5. Skelland AHP, "*Diffusional Mass Transfer*", John Wiley & Sons, New York, (1974).

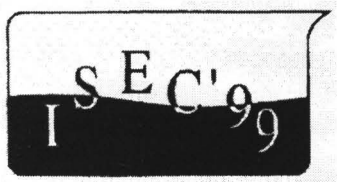

MATHEMATICAL MODELLING OF METAL PERMEATION ACROSS A SUPPORTED LIQUID MEMBRANES CONSIDERING MEMBRANE RATE CONTROLLING PARAMETERS

Graciela Benzal [1], Anil Kumar [1], A Delshams [2] and AM Sastre [1]
[1]Department of Chemical Engineering; [2]Department of Applied Mathematics I, Universitat Politècnica de Catalunya, ETSEIB, E08028 Barcelona, Spain

ABSTRACT
This paper presents general aspects in the field of liquid membrane modelling considering the following steps: a) equilibrium reaction between the solute and the carrier to form the solute-carrier complex at the interface; b) mass transfer by diffusion of the solute-carrier complex in the membrane phase to the membrane-stripping phase interface; c) another equilibrium reaction between the complex and stripping phase reagent to release the solute at the membrane stripping phase interface into the stripping phase. This model presents a description of the systems which include the rate constant as parameters controlling the behaviour of the process.

Keywords: supported liquid membrane, modelling

INTRODUCTION

Liquid membranes continue to command significant attention during the last few years in the field of environment and hydrometallurgy. Before scaling-up any liquid membrane (LM) configuration, a theoretical model of the liquid membrane system is needed to design an efficient recovery process in terms of better stability. In the past few years, we have introduced a comprehensive programme on the kinetic modelling of liquid membranes for metal separation process. An analysis of the modelling of the FSSLM (Flat Sheet Supported Liquid Membrane, further abbreviated as SLM through out the paper) system is presented considering co-transport phenomena taking into account the kinetic reactions and other important chemical parameters. More details of this process are described elsewhere.[1-5] In the SLM system, transport through a liquid membrane takes place via following consecutive steps: partitioning of a species from the aqueous feed phase into the membrane phase, complexation by the carrier inside the membrane phase, and transport of the complex through the membrane. At the receiving side of the membrane, decomplexation and partitioning of the species into the aqueous receiving phase takes place. The three phases in SLM are defined as: (i) Aqueous feed phase containing metal cation; (ii) Membrane phase i.e. a polymeric support, impregnated with organic phase containing extractant (carrier) and diluent and (iii) Receiving phase in which the metal ion is uncomplexed from membrane phase. The present paper deals with the modelling of an SLM system considering a chemical reaction which takes place at feed-membrane interface and enables us to obtain $C_{Mf}(t)$ (concentration of metal in the feed phase) and $C_C(t)$ (concentration of metal complex in membrane) as a function of time, reaction velocity constants and initial conditions. Our model is based on the Fick's second law,[1,2] taking into account the non-steady state of diffusion of the metal complex in the membrane gives the function $u(x,t)$. Considering the function $u(x,t)$, and taking into account the reaction that takes place at the membrane-strip interface, we obtain $C_{MS}(t)$ (concentration of metal in strip phase) as a function of time, initial conditions of system and reaction velocity constant. Interestingly, the reaction velocity constant plays an important role in the modelling of a liquid membrane system. The objective of this paper is to perform the mathematical modelling of a SLM system taking into consideration the initial conditions, characteristics of the membrane and kinetics parameters of the chemical reaction that takes place in the system. The present SLM model illustrates the permeation behaviour of solute transported in very long time and at this time, solute concentrations are not measurable experimentally.

© 2000 Society of Chemical Industry

MODELLING

The supported liquid membrane (SLM) modelling system is divided into three different but inter-related parts. In all these parts, pseudo rate constants of the reaction play an important role. These constants are considered as kinetic parameters, as explained below.

Mathematical model for the behaviour of metal concentration in feed phase and metal-complex concentration in membrane phase.

In the feed-membrane interface, the chemical reaction that takes place is as follows:

$$M_f + P_f + E \underset{k_r}{\overset{k_f}{\rightleftharpoons}} C$$

and the rate of the reaction is presented in the system (1).

(1)
$$\begin{cases} \dfrac{dC_{Mf}}{dt} = -k_1 C_E C_{Mf} C_{Pf} + k_{-1} C_C & t = 0, \quad C_{Mf} = C^o_{Mf} \qquad (1.1) \\ \dfrac{dC_C}{dt} = k_1 C_E C_{Mf} C_{Pf} - k_{-1} C_C & t = 0, \quad C_C = 0 \qquad (1.2) \\ C_{Pf} = \dfrac{K_w}{C_\delta - C_{Mf}} & \qquad (1.3) \end{cases}$$

where

$$k_1 = \frac{k_f}{k_{DE}} \qquad k_{-1} = \frac{k_r}{k_{DC}}$$

$$k_{DE} = \frac{C_E}{C_{Ef}} \qquad k_{DC} = \frac{C_c}{C_{cf}}$$

The system (1) consists of two ordinary differential equations (o.d.e.) (1.1) and (1.2) plus an algebraic equation (1.3), obtained from the charge balance in the feed phase (see chemical equation), which gives the free protons concentration. The solution is:

$$C_{Mf}(t) = M_2 + (C^o_{Mf} - M_2)\exp\left(\frac{-k_{-1}(M_2 - M_1)t}{M_2 - C_\delta}\right) \qquad (1.4)$$

$$C_C(t) = (C^o_{Mf} - M_2)\left[1 - \exp\left(\frac{-k_{-1}(M_2 - M_1)t}{M_2 - C_\delta}\right)\right] \qquad (1.5)$$

where

$$M_2 = \frac{1}{2}\left(K_{ex}C_E K_w + C_\delta + C^o_{Mf}\right) + \frac{1}{2}\sqrt{\left(K_{ex}C_E K_w + C_\delta + C^o_{Mf}\right)^2 - 4C^o_{Mf}C_\delta} \qquad (1.6)$$

$$M_1 = \frac{1}{2}\left(K_{ex}C_E K_w + C_\delta + C^o_{Mf}\right) - \frac{1}{2}\sqrt{\left(K_{ex}C_E K_w + C_\delta + C^o_{Mf}\right)^2 - 4C^o_{Mf}C_\delta}$$

On the basis of the theory of stability of solutions of o.d.e,[1] it turns out that:

$$C_{Mf} \to M_2, \text{ for } t \to \infty, \text{ and hence } \frac{C^o_{Mf} - M_2}{C^o_{Mf}}100 \qquad (1.7)$$

(1.7) is the maximum percentage of the transported metal.

Mathematical model for the diffusion of the metal-complex through the membrane.

In the present system of SLM modelling, co-transport phenomenon of metal-complex is considered. It is also assumed that a) total density, temperature and pressure are constant, and that there exists only diffusion of the metal-complex without overflow; b) constant diffusion coefficient of solute (only dilute solutions are considered); c) one-dimensional diffusion along a spatial variable 'x'. Since the system is heterogeneous (the chemical reaction takes place only in a restricted zone), the source term denotes the complex generation, which can be incorporated as a boundary condition just on the surface where the reaction takes place. Hence, the non-steady-state diffusion of the complex is expressed by the following partial differential equation (p.d.e) with initial and boundary conditions:

$$\frac{\partial u}{\partial t} = D_e \frac{\partial^2 u}{\partial x^2}; \quad \begin{matrix} 0 < x < L \\ t > 0 \end{matrix} \quad (2.1); \quad u(x,0) = 0, \quad 0 \le x \le L \quad (2.2); \quad \begin{cases} u(0,t) = C_C(t) & \forall\, t > 0 \\ \dfrac{\partial u(L,t)}{\partial t} = 0 & \forall\, t > 0 \end{cases} (2.3)$$

where $u(x,t)$ is the function indicating complex concentration in the membrane for any position x and time t, the equation (2.1) is the Fick's second law of diffusion[1] defined for the thickness of the membrane (L), (2.2) indicates that there is no complex in the membrane at t = 0, and (2.3) are the boundary conditions,[1] when x = 0 represent the feed boundary (Dirichlet condition) and when x = L (insulated boundary) indicates that the metal-complex does not flow to the stripping phase (Neumann condition).

The solution of (2.1) - (2.3) can be obtained through the methods of eigenfunction expansions,[1] and is given as:

$$u(x,t) = C_C(t) - \frac{4H}{\pi}\sum_{n=1}^{\infty}\frac{\exp(-Bt)-\exp(-\lambda_n D_e t)}{(2n-1)(\lambda_n D_e - B)}\operatorname{sen}\frac{(2n-1)\pi}{2L}x \qquad (2.4)$$

$$\lambda_n = \frac{(2n-1)^2\pi^2}{4L^2} \qquad B = -k_{-1}\frac{(M_2 - M_1)}{M_2 - C_\delta} \qquad H = (C^o_{Mf} - M_2)B$$

where λ_n, n =1,2,... are the eigenvalues of the problem, and D_E is the diffusion coefficient of the extractant (liquid membrane carrier) in the organic phase. Hence, D_E can be considered as the diffusion coefficient of metal-complex as the size of the metal ion is much smaller than extractant molecule.

Mathematical model for the behaviour of metal concentration in the stripping phase.

A chemical reaction that takes place at membrane-strip interface uncomplex the metal-complex which diffuses to the stripping phase and the chemical reaction is:

$$C + R \underset{k_r^2}{\overset{k_f^2}{\rightleftarrows}} M_S + E$$

The reaction velocity equation in terms of the metal concentration in the stripping phase (C_{MS}) is given by

$$(3)\begin{cases} \dfrac{dC_{Ms}}{dt} = k_2 C_R C_C - k_{-2} C_{Ms} C_E \quad ; t = 0 \quad C_{Mf} = 0 & (3.1) \\ C_C(t) = g(t); \quad t = 0 \quad C_C = 0 & (3.2) \\ C_{Ps} = \dfrac{K_w}{C_{\delta S} - C_{Ms}} & (3.3) \end{cases}$$

where $k_2 = \dfrac{k_f^2}{k'_{DE}}$ $\quad k_{-2} = \dfrac{k_r^2}{k'_{DC}}$

$k'_{DE} = \dfrac{C_E}{C_{Es}}$ $\quad k'_{Dc} = \dfrac{C_c}{C_{cs}}$

Where $g(t) = u(L,t)$ is the function of metal-complex diffused through the membrane and is derived from (2.4) for x = L, by:

$$g(t) = u(L,t) = C_C(t) - \frac{4H}{\pi}\sum_{n=1}^{\infty}\frac{\exp(-Bt)-\exp(-\lambda_n D_e t)}{(2n-1)(\lambda_n D_e - B)}(-1)^{n+1} \qquad (3.4)$$

$g(t)$ is the metal-complex concentration at the membrane-strip interface,

(3.1) is a lineal o.d.e with initial conditions, (3.2) is the previously mentioned metal-complex obtained in the membrane, and (3.3) is given by the charge balance in the stripping phase.

The solution $C_{Ms}(t)$ of (3) is given by:

$$C_{Ms}(t) = k_2 C_R (C^0_{Mf} - M_2)\left\{I_1 + I_2 + \frac{4B}{\pi}\sum_{n=1}^{\infty}\frac{(-1)^{n+1}}{(2n-1)(\lambda_n D_e - B)}[I_3 + I_4]\right\} \qquad (3.5)$$

where,

$$I_1 = \frac{1-\exp(-k_{-2}C_E t)}{k_{-2}C_E}; \qquad I_2 = \frac{\exp(-k_{-2}C_E t)-\exp(-Bt)}{k_{-2}C_E - B};$$

$$I_3 = \frac{\exp(-k_{-2}C_E t)-\exp(-Bt)}{k_{-2}C_E - B}; \qquad I_4 = \frac{\exp(-\lambda_n D\ t)-\exp(-k_{-2}C_E t)}{k_{-2}C_E - \lambda_n D_E};$$

where k_2 and k_{-2} are the pseudo rate constants, which are considered as kinetic parameters in expression (3.5).

For $t \to \infty$, from (3.5), it follows that $C_{MS} \to \dfrac{k_2}{k_{-2}}\dfrac{C_R}{C_E}(C^0_{Mf} - M_2)$ (3.6)

and therefore the ratio between the parameters k_2 and k_{-2} depends on the strippant and extractant concentration.

RESULTS AND DISCUSSION

The modelling of SLM system taking into account the co-transport phenomena followed by mathematical expressions: (1.4) and (1.5), explain the metal behaviour in the feed phase and metal complex in membrane phase respectively. Expression (2.4) represents the non-steady-state of the diffusion phenomena of metal-complex in membrane and (3.6) explains the metal complex concentration at membrane-strip interface for all time "t". Finally, (3.5) represents the metal concentration in the stripping phase.

The validity of this mathematical model has been checked against the experimental data performed in our Laboratory[1] where the SLM system for this modelling was established for the following conditions: (i) the membrane was impregnated with (0.064-0.445 mol/dm^3) of LIX 79 dissolved in cumene; (ii) characteristics of the membrane: L = 1.25 x 10^{-3} dm; $\varepsilon = 0.75$; $\tau = 1.67$; (iii) the feed phase (source phase) contained Au(I) (5.0 x 10^{-5} mol/dm^3) at pH 9.2; (iv) the stripping phase (receiving phase) contained different concentration of NaOH; (v) the equilibrium constant $K'_{ex} = k_f / k_r$ determined for the first reaction in this chemical system is $K'_{ex} = 1.25 \times 10^{11}$. Diffusion coefficient of the metal complex D_E = 1.4 x 10^{-6} dm²/min. By suitably adjusting the parameter k_{-1} (pseudo rate constant), our model agrees well with the experimental data up to 180 minutes. For times greater than 180 min., our model allows to infer the posterior and final behaviour of the fraction of metal ion transported. Figures 1 and 2 [using Matlab software] are obtained from equations (1.4) and (1.5).

[NaOH]	0.1mol/dm^3	0.50mol/dm^3	0.85mol/dm^3	1.0mol/dm^3
t =180 min.	76%	59%	56%	54%
$t \to \infty$	16%	16%	16%	16%
Parameter: k_{-1}	1.5x10^{-2}	3x10^{-2}	3.4x10^{-2}	3.6x10^{-2}

Table 1 Percentage of metal in feed solution for different concentrations of stripping reagent at different time. C_E = 0.254 mol/dm^3 C^o_{Mf} = [Au(I)] = 5 x 10^{-5} mol/dm^3

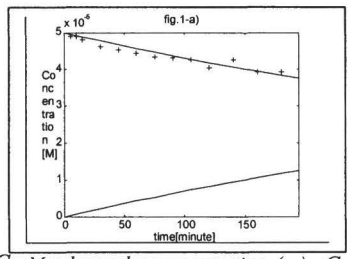

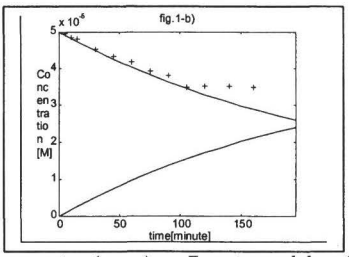

C_C:Metal-complex concentration (-.-), C_{Mf}:Metal feed concentration (___), Experimental data (+)

Fig. 1-a) C_R =[NaOH]=0.1 mol/dm^3 *Fig. 1-b) C_R = [NaOH]=1 mol/dm^3*

Figure 1: Plot C_{Mf} vs t, C_t vs t and experimental data, for different concentrations of stripping reagent and its effect on the transport of metal. C_E =[Lix79] = 0.254 and, C^o_{Mf} = [Au(I)] = 5.1x10^{-4} mol/dm^3

It should be noticed that the final percentage of metal concentration in the feed phase is the same in every case but the time is longer when the concentration of the stripping reagent is lower.

From Figure 2, Table 2 and (1.7) is indicated that for a higher extractant concentration, higher values of metal transport are achieved. From the last two columns in Table 2, it follows that at t = 600 min., using twice the extractant concentration only an increase of 14% in the metal transported is observed.

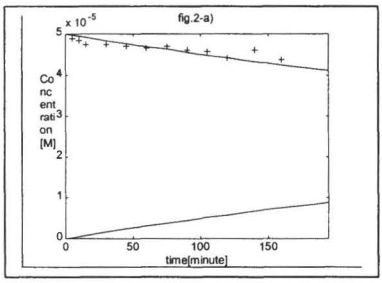

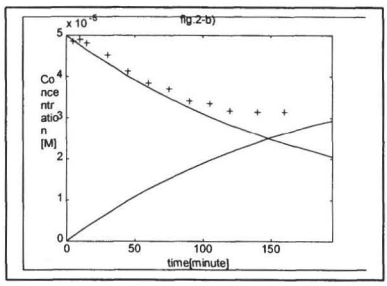

C_C :*Metal-complex concentration (-.-),* C_{Mf} :*Metal feed concentration (____), Experimental data (+)*

Fig. 2-a) C_E = [Lix79] = 0.064 mol/dm^3 Fig. 2-b) C_E = [Lix79] = 0.445 mol/dm^3

Figure 2: Plot C_{Mf} vs t, C_t vs t and experimental data for different extractant concentration and its effect on the transport of the metal. C_R = [NaOH]=1 mol/dm^3 and, C^o_{Mf} = [Au(I)]=5 x 10^{-5} mol/dm^3

[Lix 79]	0.064 mol/dm^3	0.127 mol/dm^3	0.254 mol/dm^3	0.445 mol/dm^3
C_{Ms}/C^o_{Mf} t = 600min	83%	74 %	57%	43%
$t \rightarrow \infty$	38%	26%	16%	10%
Parameter k_{-1}	3x10^{-2}	3x10^{-2}	3x10^{-2}	3x10^{-2}

Table 2 Percentage of metal concentration in the feed phase at different times and extractant concentration. [NaOH] = 1 mol/dm^3, C^o_{Mf} = [Au(I)]=5x 10^{-5} mol/dm^3

No proportional increase of metal transport was found with increase of extractant concentration. This is because the concurrent increase in viscosity results in a steady decrease in the diffusivity of the carrier as well as the metal carrier complex. This phenomena could be explained by D = kT/(6πrη) where k, T, r and η denote the Boltzmann constant, the absolute temperature, the molecular radius of the metal complex and the viscosity of the organic phase respectively. Babcock and Kumar et al.[2,3,4] have also suggested the predominant cause of such behaviour is the concentration gradient of the metal complex, the viscosity of the organic phase and hindered diffusion of the metal complex caused by aggregation of the complex, and the tortuosity of the pores of the membrane.

On the other hand, the proposed model fits the experimental data when varying the metal concentration in the feed phase, and equations (1.7) indicates that at longer times, the metal concentrations in the feed phase is higher when increasing the metal concentration as seen in Table 3. This is probably due to membrane saturation and lower effective membrane area in the SLM. This is also theorised that this is due to a change in the rate determining steep for transport process. At low feed concentrations, diffusion of the metal species across the boundary layer is the rate determining step, while at higher feed cation concentrations, the aqueous feed/ organic membrane interface is "saturated" with the cations, and the diffusion of the complexes across the membrane phase because the rate determining step.[2]

Metal	5.0 x 10^{-5} mol/dm^3	2.5 x 10^{-4} mol/dm^3	5.1 x 10^{-4} mol/dm^3	8.9 x 10^{-4} mol/dm^3
T= 180 min.	59 %	34%	57%	69%
T= 840 min.	19%	11%	10%	20%
$t \rightarrow \infty$	16 %	11 %	8%	6%
Parameter k_{-1}	3 x 10^{-2}	3 x 10^{-2}	8 x 10^{-3}	2 x 10^{-3}

Table 3 Percentage of metal in feed phase for different times and initial metal concentration. [NaOH] = 1 mol/dm^3. C_E = 0.254 mol/dm^3

Figures 3 and 4 [using Matlab]are obtained from equations (2.6) and (2.4) for the different cases.

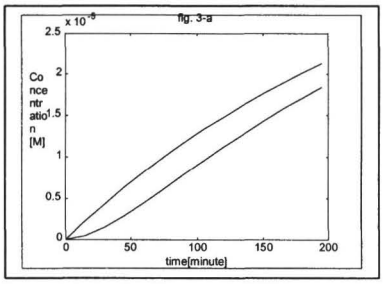

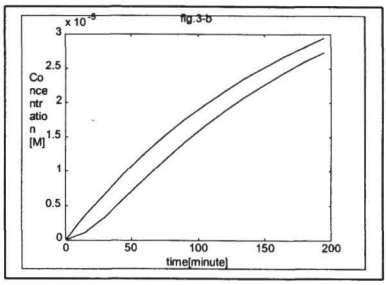

C_C:Metal-complex concentration (-.-), C_{MS} :Metal stripping concentration (__)

Fig. 3-a) C_E = [Lix79] = 0.254 mol/dm^3 Fig.3-b) C_E = [Lix79] = 0.445 mol/dm^3

Figure 3: Plot C_{Ms} vs t, C_t vs t for different extractant concentration. C_R = [NaOH]=1 mol/dm^3 and C^o_{Mf}= [Au(I)]=5 x10^{-5} mol/dm^3

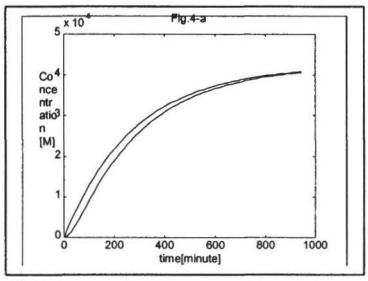

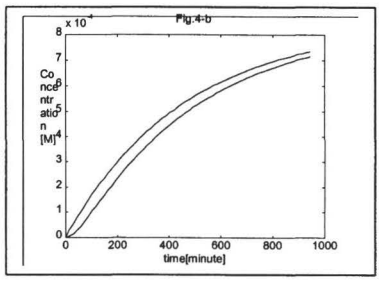

C_C :Metal-complex concentration (-.-), C_{MS} :Metal stripping concentration (__)

Fig. 4-a) C^o_{Mf} = [Au(I)]=5x10^{-5}M Fig.4-b) C^o_{Mf} = [Au(I)]=8.9x10^{-4}M

Figure 4: Plot C_{Ms} vs t, C_t vs t for different metal concentration. C_R = [NaOH]=1 mol/dm^3 and C_E = [Lix79]=0.254 mol/dm^3

The values of parameters corresponding to figures 3 and 4 are presented in table 4

Parameters	Fig. 3-a	Fig. 3-b	Fig. 4-a	Fig. 4-b
k_{-1}	3 x 10^{-2}	3 x 10^{-2}	3 x 10^{-2}	2 x 10^{-3}
$\frac{k_2}{k_{-2}} = \frac{C_E}{C_R}$	0.254	0.445	0.254	0.254

Table 4

As seen in figure 3 and 4, the difference between the complex and stripping concentrations is observed, and this difference decreases with increase in time and totally disappears (at time ∞) in the case of different metal concentration and different extractant concentration.
From the proposed model the concentration of metal complex at any given time, t, can be interpreted in the membrane phase. This difference may be due to membrane diffusional resistance (Δ_0) defined as $\Delta_0 = L\tau^2/(D_{0,b}\varepsilon)$ which is caused by the membrane characteristics and initial metal and extractant concentrations.[2]

NOTATION

C_{Mf}: metal concentration in feed [mol/dm^3] D_e : effective diffusion coefficient [dm^2/min],

C^0_{Mf}:initial metal concentration in feed [mol/dm^3]

C_{Pf}: protons concentration in feed [mol/dm^3]

C^0_{Pf} : initial protons concentration in feed [mol/dm^3]

C_δ : concentration of OH^- in feed phase[mol/dm^3]

t : time variable. [minute]
x : space variable [dm]
M_f : free metal in feed
P_f : protons in feed.
E : extractant in membrane.
C: complex in membrane.

k_f and k_r : forward and reverse rate of extraction.

k^2_f and k^2_r : forward and reverse rate of stripping.

k_{DC} and k_{DE} :Distribution coefficient of metal-complex and extractant respectively. (feed phase)

k'_{DC} k'_{DE} : Distribution coefficient of metal-complex and extractant respectively. (stripping phase)

C_{Cf} and C_{Ef} : metal-complex and extractant concentration in aqueous phase. (feed)

C_{Cs} and C_{Es} : metal-complex and extractant concentration in aqueous phase. (stripping)

$K_{ex} = \dfrac{k_f k_{DC}}{k_r k_{DE}}$: pseudo equilibrium constant for feed-membrane interface.

k_1 *and* k_{-1}, k_2 *and* k_{-2} pseudo rate constants.

$D_e = \dfrac{\varepsilon}{\tau^2} D_E$

$D_{0,b}$: Diffusion coefficient of metal in bulk Organic phase.

C_E : extractant concentration in membrane[mol/dm^3]

C_c : metal-complex concentration in membrane[mol/dm^3].

R: stripping phase (receiving phase).

M_S : metal in stripping phase.

P_S : protons in stripping phase.

E : extractant (carrier) in membrane.

K_w : ionic product of water.

ε: porosity.
τ: tortuosity.
L: membrane thickness [dm]

D_E : diffusion coefficient of extractant in organic phase [dm^2/min].

C_{Ms} : metal concentration in stripping phase[mol/dm^3]

C^0_{Ms} : initial metal concentration in stripping phase [mol/dm^3].

C^0_{Ps} : initial protons concentration in stripping phase[mol/dm^3].

C_{PS} : protons concentration in stripping phase[mol/dm^3]

$C_{\delta S}$: concentration of OH^- in stripping phase[mol/dm^3]

ACKNOWLEDGEMENTS

This work was supported by the CICYT (QUI 96-1025).Benzal G gratefully acknowledges the economical support during the first period of her stay to the Facultad de Química de la Universidad Nacional de Tucumán, Tucumán, Argentina from which she is on leave. Dr. Anil Kumar, on leave from PREFRE, Bhabha Atomic Research Centre, Tarapur, India, gratefully acknowledges the support of Spanish Ministry of Education and Culture (CICYT) for awarding a Visiting Scientist fellowship.

REFERENCES

1 Ho WSW and Sirkar KK, *Membrane Handbook*, Van Nostrand Reinhold, New York (1992).
2 Danesi PR, *Sep. Sci Technol.*, **19**, 857, (1984).
3 Chrisstoffels LAJ and Feike de Jong RD, *ACS Ser. 642*, Amer Chem Soc, Washington DC, chap 3, 18, (1996).
4 Peterson RT and Lamb J, *ACS Ser. 642*, Amer Chem Soc, Washington DC, chap 4, 57, (1996).
5 Misra BM and Gill JS, *ACS Ser. 642*, Amer Chem Soc, Washington DC, chap 25, 361, (1996).
6 Bird RB, Stewart WE and Lightfoot EN, "*Fenómenos de transporte*", Reverté, (1992).
7 Bear J, "*Dynamics of fluid in porous media*",Dover Publications, inc.,(1972).
8 Hirsch MW and Smale S, *"Ecuaciones diferenciales, sistemas dinámicos y álgebra lineal"*, Alianza Editorial Madrid, (1983).
9 Crank J, "*The Mathematics of Diffusion*", Oxford Science Publications, (1975).
10 Haberman R, *"Elementary Applied Partial Differential Equations"*, Prentice Hall, Inc. Third Edition, (1998).
11 Haberman R, *"Elementary Applied Partial Differential Equations"*, Prentice Hall, Inc. Third Edition, (1998).

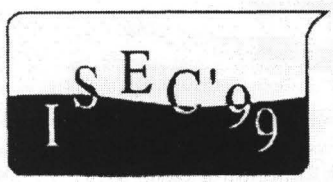

MODELLING PHASE EQUILIBRIA IN INDUSTRIAL CAPROLACTAM RECOVERY FROM AQUEOUS AMMONIUM SULPHATE SOLUTIONS WITH BENZENE

André B de Haan and Simon H Niemann
DSM-Research, P.O. Box 18, 6160 MD Geleen, The Netherlands

ABSTRACT
An Aspen Plus model was developed for the description of phase equilibria in the industrial recovery of caprolactam from aqueous ammonium sulphate solutions with benzene. New experimental data are presented at 20, 40 and 60°C and ammonium sulphate concentrations ranging from 0 to 40 wt.%. It appeared impossible to correlate these data with the Aspen Plus Electrolyte NRTL model. Excellent correlation results were obtained with the orginal NRTL model when ammonium sulphate was treated as an always fully dissociated pseudo component. The experimental and calculated results indicate that, compared to the current isothermal operation, significant increases in the aqueous product stream caprolactam concentration (3-5 times) can be obtained.

Keywords: caprolactam, ammonium sulphate, benzene, modelling,

INTRODUCTION

Caprolactam, the monomer of Nylon 6, is produced in a multistep process in which crude caprolactam is obtained by neutralizing the reaction mixture from the Beckman rearrangement with aqueous ammonia. This results in the formation of a concentrated, 65-70 wt%, crude aqueous caprolactam phase in equilibrium with a nearly saturated aqueous ammonium sulphate solution. After separating the two phases, the caprolactam from both streams is recovered and purified by extraction with benzene. For the ternary benzene-caprolactam-water and caprolactam-water-ammonium sulphate systems, the availability of liquid-liquid equilibrium data is limited to 20°C.[5-8] In industrial practice however, these data are of limited value because the extraction is usually operated at higher temperatures. The effect of temperature and ammonium sulphate on the distribution of caprolactam has been studied by several authors.[9-12] Unfortunately they only report the caprolactam distribution, making the development of a sound thermodynamic model impossible.

The objective of this study was to develop a thermodynamic model in Aspen Plus for the quaternary system caprolactam-water-benzene-ammonium sulphate. Because insufficient phase equilibrium data were available, additional data have been measured at 20, 40 and 60°C and ammonium sulphate concentrations ranging from 0 to 40 wt.%. Initially we tried to perform the data correlation with the Aspen Plus Electrolyte NRTL model.[13-16] However, due to continuous numerical problems we decided to treat ammonium sulphate as an fully dissociated pseudo component and use the original NRTL model. The obtained experimental data are compared with data reported by other authors and the capability of the NRTL model to correlate the experimental data is discussed. Finally the experimental data are used to derive optimal process conditions.

EXPERIMENTAL

Materials

Distilled water and the other materials were used as received. Benzene (>99% purity), caprolactam (>99.5% purity) were supplied by the DSM caprolactam plants. Ammonium sulphate (>99.5% purity) was purchased from Merck.

© 2000 Society of Chemical Industry

Liquid-Liquid Equilibrium Measurements

Three identical experimental setups, consisting of a thermostatted stirred glass equilibrium cell (volume 1000 cm^3, ±0.1 K), were used. For each experiment a feed mixture, consisting of the desired caprolactam, water and ammonium sulphate weight fractions, was prepared. Because considerable volume changes occur when caprolactam is extracted into the benzene phase, the aqueous phase volume had to be restored to its original value to keep the ammonium sulphate concentration as constant as possible. This was done by adding an aqueous caprolactam solution, with the same water/caprolactam ratio as the feed mixture. The resulting error appeared to be considerably less than inaccuracy of the ammonium sulphate analysis. When the desired temperature was reached, stirring was continued for 30 more minutes to ensure equilibrium was attained. After stopping the stirrer, the mixture was allowed the required time, generally two or more hours, to obtain full separation in completely clear liquid phases. Samples were taken from all phases and analyzed for all four components.

Analytical Methods

Liquid chromatography was used to measure the caprolactam concentration, Karl-Fisher titration for the water concentration, ion chromatography for the ammonium sulphate concentration and gas chromatography for the benzene concentration. The concentrations of caprolactam, water, ammonium sulphate and benzene were obtained with a relative accuracy of ±1%, ±1%, ±4% and ±1% respectively. The raw composition data were normalized to obtain a total sample composition of 100%.

DATA CORRELATION

The goal of this study was to develop a thermodynamic model that allows modelling of the caprolactam recovery process with Aspen Plus. Therefore we decided to consider the Electrolyte NRTL model available in Aspen Plus first. Although this model was especially developed for mixed solvent systems, it appeared impossible to continue this approach due to serious numerical problems and extremely long simulation times. Based on this experience we decided to follow the approach of Mock et. al.[14] and introduce the following two simplifications:

the Pitzer-Debye-Hückel and Born contributions were dropped;
ammonium sulphate was considered to be always fully dissociated.

Doing so the Electrolyte NRTL model reduces to the classical NRTL model[15] in which the interaction parameters G_{ji} and τ_{ji} are calculated from:

$$G_{ji} = \exp(-\alpha_{ji}\tau_{ji})$$

$$G_{ji,ki} = \exp(-\alpha_{ji,ki}\tau_{ji,ki})$$

The Aspen Plus data regression system[15] was used to determine the interaction parameters a_{ij}, b_{ij} and non-randomness parameter α_{ij}. The benzene-water interaction parameters were determined from binary solubility data.[17] The data for the caprolactam/water/benzene system were used for the remaining non-electrolyte interaction parameters. Correlation of the experimental data for the ammonium sulphate containing systems provided the interactions with ammonium sulphate. During data correlation it appeared that the values of the solvent-salt non-randomness parameter α_{ij} were critical in obtaining a good representation of the experimentally observed phase behaviour. Table 1 lists the correlated parameters.

System	α_{ij} (-)	a_{ij} (-)	a_{ji} (-)	b_{ij} (K)	b_{ji} (K)
Water - Benzene	0.200	2.280	2.272	1340	359.2
Caprolactam - Benzene	0.300	-6.050	1.139	1242	432.6
Caprolactam - Water	0.300	24.89	-6.166	-6123	1147
Caprolactam - Ammonium Sulphate	-0.057	25.90	23.75	274.2	-14869
Water - Ammonium Sulphate	0.146	3.682	-15.88	1921	2245
Benzene - Ammonium Sulphate	-1.000	-4.369	5.241	1579	-310.0

Table 1. Aspen Plus NRTL Parameters for the Caprolactam/Water/Benzene/Ammonium Sulphate System

RESULTS AND DISCUSSION

Caprolactam/Water/Benzene System

Figure 1a shows a ternary diagram in which the the data obtained in this study are compared with the data reported by Morachevski [5] and Tettamanti [6] at 20°C. The curves and tie lines have been calculated with the NRTL model. It is clear that the experimental data are in good agreement with the literature data and that the two-phase region as well as the tie lines is well represented. The good representation of the tie lines is illustrated more clearly in figure 1b, where the equilibrium caprolactam concentration in the organic phase is plotted against the equilibrium caprolactam concentration in the aqueous phase at 20, 40 and 60°C. For each of the three temperatures good agreement between the experimental points and the calculated curves is obtained.

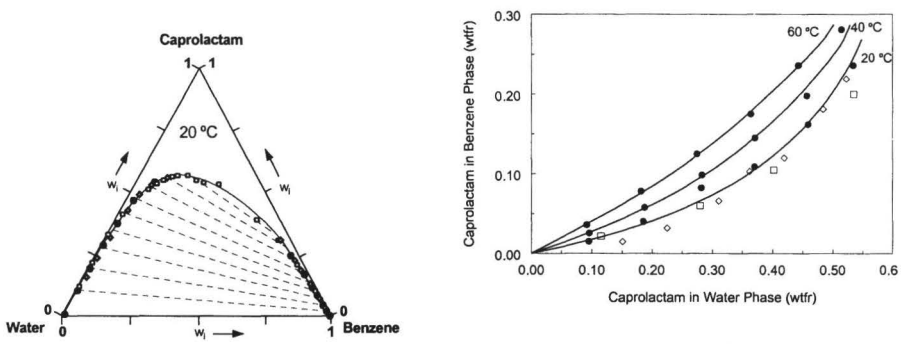

(a) (b)

Figure 1. Experimental (●) and calculated equilibrium compositions in the ternary caprolactam/water/benzene system at 20°C (a) and distribution of caprolactam between the organic and aqueous phase at 20, 40 and 60°C (b) compared with data reported by Morachevski [5] (◊) and Tettamanti [6] (□).

Figure 1b illustrates clearly that at higher temperatures the caprolactam concentration in the organic phase is increased considerably. This result implies that the extraction of caprolactam from the aqueous phase requires considerably less solvent when conducted at the higher temperatures.

Extraction of caprolactam from the organic phase however, yields the highest caprolactam concentrations in the aqueous phase at low temperatures.

Caprolactam/Water/Ammonium Sulphate System

The experimental data obtained at 20°C in this study are compared with data reported by Tettamanti [7] and Shubtsova [8] in figure 2. The curves and tie lines have been calculated with the NRTL model. Interesting to notice is that addition of sufficient ammonium sulphate causes the homogeneous caprolactam/water system to split into two liquid phases. Besides this two liquid phase regional so an S-L_1-L_2, S-L and S_1-S_2-L region [7,8] are present because caprolactam and ammonium sulphate are solids under these conditions. The experimental data obtained in this study agree very well with the data reported in the literature, indicating that the used experimental procedures are valid. For this study the NRTL model was only used to calculate the liquid-liquid equilibrium region. Figure 2 illustrates that good agreement between the experimental and calculated results are obtained.

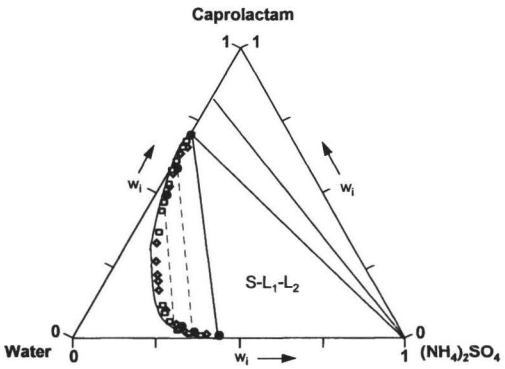

Figure 2. Experimental (●) and calculated (ÄÄÄÄ) equilibrium compositions in the ternary caprolactam/water/ammonium sulphate system at 20 °C compared with data reported by Tettamanti [7] (◊) and Shubtsova [8] (□).

Caprolactam/Water/Benzene/Ammonium Sulphate System

Figure 3 illustrates the experimentally observed and calculated effects of ammonium sulphate on the equilibrium compositions in the caprolactam/water/benzene system at 40°C. Addition of 5 wt% ammonium sulphate to the aqueous phase causes significant salting out effects of caprolactam, resulting in considerable changes of the slope of the tie-lines. The tie-line slope change at 15 wt% ammonium sulphate is even more pronounced and a three liquid phase equilibrium region was observed. This three phase region disappears when going to 40 wt% ammonium sulphate because the salting out effect becomes so strong that hardly any caprolactam can dissolve in the aqueous phase and even the water/caprolactam system becomes immiscible.

The salting out effect of ammonium sulphate on caprolactam is shown more clearly in figure 4a, where the distribution of caprolactam between the organic phase and the aqueous phase is shown. Addition of ammonium sulphate is a powerful tool to increase the caprolactam concentration in the organic phase and thereby reducing the amount of required benzene. At higher temperatures, the caprolactam distribution becomes even more favourable as shown in figure 4b and demonstrated before for the ammonium sulphate free system.

Comparison of the calculated curves and the experimental data in figures 3 and 4 shows that the effects of ammonium sulphate on the phase behaviour in the caprolactam/water/benzene system are very well represented with the NRTL model. Only in case of the three phase equilibrium the calculations break down because Aspen Plus has no facility to perform three liquid phase flash calculations.

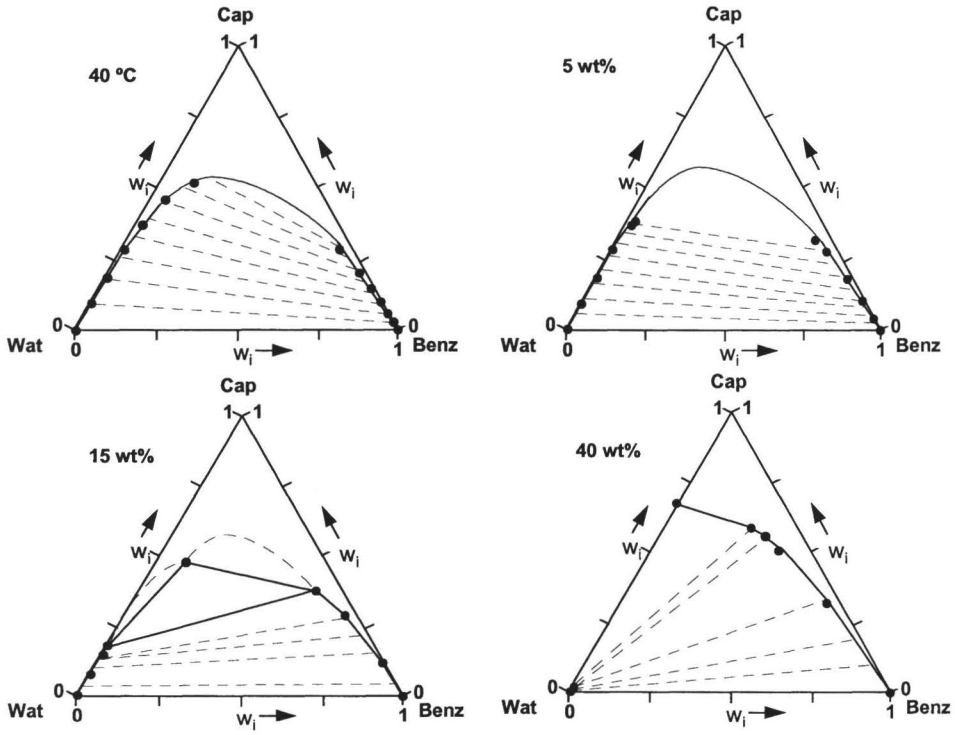

Figure 3. Experimental (●) and calculated (ÄÄÄÄ) effect of ammonium sulphate on the equilibrium compositions in the caprolactam/water/benzene system at 40°C.

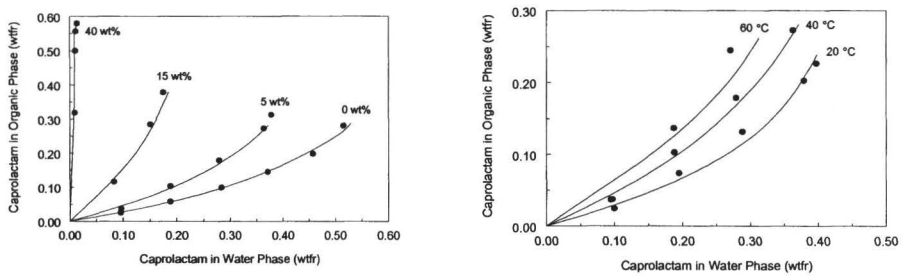

(a) (b)

Figure 4. Experimental (●) and calculated (ÄÄÄÄ) effect of ammonium sulphate (a) and temperature (b) on the distribution of caprolactam between the organic and aqueous phase at 40°C (a) respectively 5 wt% ammonium sulphate (b) on an ammonium sulphate free basis.

CONCLUSIONS

A thermodynamic model was developed within Aspen Plus for the description of phase equilibria in the industrial recovery of caprolactam from aqueous ammonium sulphate solutions with benzene. New experimental data have been reported at 20, 40 and 60°C and ammonium sulphate concentrations ranging from 0 to 40 wt.%. At low ammonium sulphate concentrations (5 wt%) this system exhibits the classical two liquid phase equilibrium. However, due to the strong salting out of caprolactam three liquid phases were observed at intermediate ammonium sulphate concentrations (15 wt%). At high ammonium sulphate concentrations (40 wt%) two liquid phases were found.

It appeared impossible to correlate these data with the Electrolyte NRTL model available in Aspen Plus. Excellent correlation results were obtained with the original NRTL model when ammonium sulphate was treated as an always fully dissociated pseudo component. The experimental and calculated results indicate that, compared to the current isothermal operation, significant increases in the aqueous product stream caprolactam concentration (3-5 times) can be obtained. This can be realized by combining extraction at higher temperatures in the presence of 5-10 wt% ammonium sulphate with back extraction into pure water at low temperatures.

ACKNOWLEDGEMENTS

The authors are very grateful to R. Navis of DSM-Research and J. Bindels of DSM-Chemlab for their assistance with the experimental and analytical work. A.J.F. Simons and L. Groot-Zevert are acknowledged for helpful discussions and continued interest.

REFERENCES

1. Simons AJF and Haasen NF, *"Handbook of Solvent Extraction"*, Edited by Lo TC, Baird MHI and Hanson C, John Wiley & Sons, New York 557, (1983)
2. Ritz J, Fuchs H, Kieczka H and Moran WC, *"Ullmann's Encyclopedia of Industrial Chemistry"*, 5th Ed., **A5,** 31, (1986)
3. Ries HC and Muller RG, *"Caprolactam"*, Part I and II, Process Economics Program, Stanford Research Institute, Stanford, CA (1965)
4. Ries HC and Ushiba AK, *"Caprolactam"*, Supplement A and B, Process Economics Program, Stanford Research Institute, Stanford, CA (1968, 1976)
5. Morachevskii AC and Sabinin VE, *J. Appl. Chem. USSR* **33**(8), 1775, (1960)
6. Tettamanti K, Cogradi M and Sawinsky J, *Polytechnica* **4,** 201, (1960)
7. Tettamanti K and Nogradi M, *Periodica Polytechnica* 5(1), 15, (1960)
8. Shubtsova IG, Nikurashina NI and Rybalov SK, *Russ. J. Phys. Chem.* **49**(1), 35, (1975)
9. Kasatkin AG, Kagan SZ and Trukhanov VG, *Khim. Prom.* 190, (1961)
10. Pandya HP, *Adv. Chem. Eng. Nucl. Process Ind.* 504, (1994)
11. Pandya HP and S.A. Puranik SA, *J. Inst. Eng. (India), Chem. Eng. Div.* **76** (9), 1, (1995)
12. Alessi V, Penzo R, Slater MJ and Tessari R, *Chem. Eng. Technol.* **20**, 445, (1997)
13. Chen CC and Evans LB, *AIChE J.* **32**(3), 444, (1986)
14. Mock B, Evans LB and Chen CC, *AIChE J.* **32**(10), 1655, (1986)
15. Aspen Technology, "Aspen Plus Reference Manual, Vol 2", (1994)
16. Liu Y and Watanasiri S, *Fluid Phase Equil.* **116**(1-2), 193, (1996)
17. Shaw D, *"Solubility Data Series"*, Pergamon Press, Oxford **37**, 63, (1989)

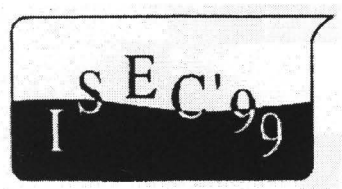

MODELLING AND OPTIMIZATION OF SULFOLANE EXTRACTION, A NEURAL NETWORK APPROACH

Guoqiang Su, Xiaoming Wen, and Weiyang Fei
Department of Chemical Engineering, Tsinghua University, Beijing 100084, China

ABSTRACT
A two-direction operating artificial neural network was proposed for both process modeling and optimization. The network is used for modeling when it operates forward and for optimization when backward. For the backward operation, equations to update the network inputs for desired outputs have been deduced with the gradient descent algorithm. The application of the network to Sulfolane Extraction has been studied.

Keywords: aromatics, sulfolane, modeling, artificial neural networks

INTRODUCTION

The Sulfolane Extraction Process [1] is well known for the production of high purity BTX with high recovery and has been used all over the world. However, due to the complexity of the process flow and the non-ideality of the system treated, the modeling and optimization of the process are still difficult targets. It is costly both in experiments and in programming to develop conventional simulation and optimization software based on first principles. Even though this kind of software is available, it is usually time-consuming to run and is difficult to use for the real time application. While artificial neural networks (ANNs) provide attractive solutions to the problems.

A neural network is basically a parallel distributed processor that employs a massive interconnection of neurons (nodes). With its node characteristics, network topology and learning ability, a neural network is able to approximate any nonlinear continuous function arbitrarily accurately [2] and is computational efficient. It has the ability to evolve good process models from example data and require little or no *a priori* knowledge of the task to be performed.

In this paper, A two-direction operating artificial neural network is proposed and constructed for both process modeling and optimization and has been applied to the Sulfolane Extraction Process.

THE TWO-DIRECTION OPERATING NEURAL NETWORK

Topology

There are many types of neural networks being studied and/or used in applications. The most common one is the feed-forward neural network, which is employed in this study.

The topology of the two-direction operating neural network is shown in Figure 1. The network inputs are arranged in two groups: 1) process inputs, such as the compositions of the feedstock. If different process units are intended to be modeled, equipment parameters can also be included in this group. 2) Operating variables, such as the operating temperatures, the solvent to feed ratio, etc. They are the decision variables in the process optimization. The outputs of the network are the performance of the process unit, i.e. the process outputs, such as product recoveries, product purity, etc.

When the network operates forward as in the usual case, it maps from the inputs to its outputs and process modeling is performed. Can the network work in reverse, i.e. determining the operating variables for desired outputs? In the next section, we will discuss how the network operates both forward and backward for process modeling and optimization.

© 2000 Society of Chemical Industry

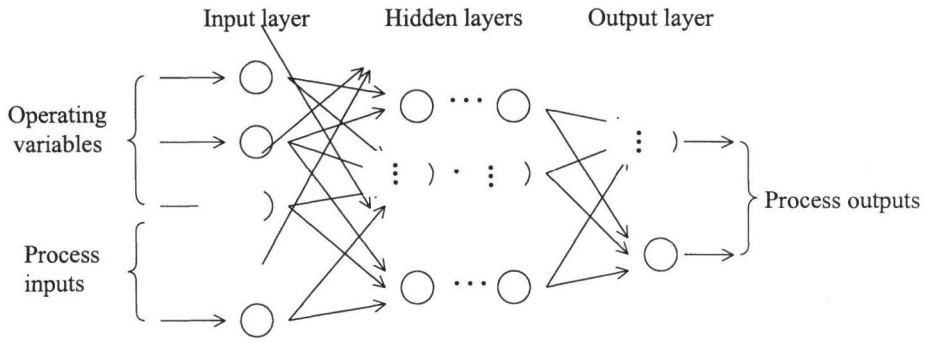

Figure 1. Topology of the two-direction operating neural network

Learning and Operating

Learning is to minimize the prediction errors of the network by adjusting the connection weights. Learning can be considered essentially a nonlinear optimization task. Any nonlinear programming algorithm can be used. In this study, the commonly used Back-propagation algorithm [3] is applied. Training samples consisting of input-output vector pairs is first rectified to remove the random and gross errors and then is used to train the network. During the procedure, an input pattern (including parameters in both the two input groups) is fed to the network and propagated forward through the network to generate an output vector. The differences between the network outputs and the sample values (Y) form error signals, which are then back-propagated through the network to update the connection weights (see Figure 2). This process is repeated for all the input-output patterns and finally trains the network to reproduce the input-output mappings to within an acceptably small error.

As shown in Figure 2, the network operates in two directions. In the forward direction, it is used as a simulator to predict the performance of the process unit with the given process inputs (X) and operating variables (U).

In the backward direction, the network is used to perform process optimization. It works in the following way: keeping the connection weights of the trained network fixed; given the process inputs (X); setting the desired process performance (Y) as the target network outputs; modifying the operating variables in the second network input group until the network converges. Then the appropriate operating parameters ($\tilde{U}$) are obtained. The convergence means that the differences between the calculated outputs and the target outputs fall into the convergence criterion. When the network is trained by selected samples with the optimum operation states, it can find the optimum operating parameters for the desired performance with the given process inputs.

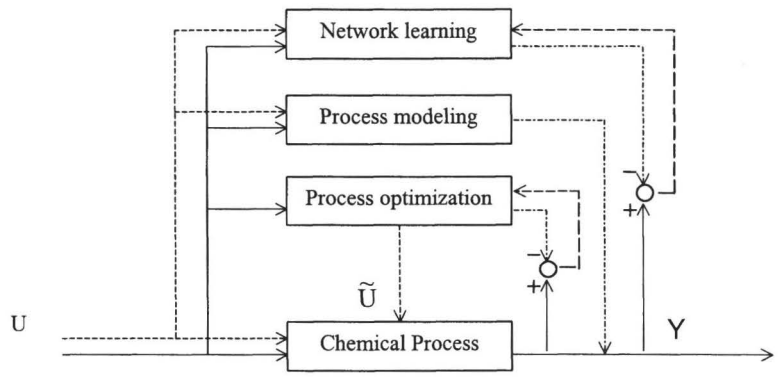

Figure 2. Learning and operating of the two-direction operating neural network

With the usually used error measure or cost function:

$$E = \sum_{i=1}^{n_t} (Y_i - O_i^t)^2 / 2$$

the adjustments of the operating variables in the network inputs can be deduced for a t layer neural network (including the input and output layers), with the use of the gradient descent algorithm:

$$\Delta U_j = -\alpha \frac{\partial E}{\partial U_j}$$

$$\frac{\partial E}{\partial U_j} = -\sum_{i=1}^{n_t} (Y_i - O_i^t) \frac{\partial O_i^t}{\partial U_j}$$

$$\frac{\partial O_i^k}{\partial U_j} = f'(Net_i^k) \sum_{l=1}^{n_{k-1}} W_{li}^{k-1} \frac{\partial O_l^{k-1}}{\partial U_j} \quad (k = 2,3,...,t)$$

$$\frac{\partial O_i^1}{\partial U_j} = \begin{cases} 1 & (i = j) \\ 0 & (i \neq j) \end{cases}$$

where f is the activation function in the neurons.

The two-direction operating neural network is designed auto-adaptive. When better operating parameters are obtained and proved, the corresponding input-output vector pair is added to the training samples and relatively worse data are deleted, then the network is trained again. Therefore, the network can at least lead the process to the best operation level in its history.

MODELING AND OPTIMIZATION OF SULFOLANE EXTRACTION

Sulfolane Extraction Process

The simplified process flow of Sulfolane Extraction is shown in Figure 3. The feedstock, such as hydrotreated pyrolysis gasoline or catalytic reformate, is introduced into the liquid-liquid extraction column and flows counter-currently against the solvent (sulfolane) which flows down from the top of the column. The solvent, usually called primary solvent, extracts aromatics and some non-aromatics into the bottoms, which, called rich solvent, is fed into the top of the extractive stripping column. This stripper strips the non-aromatics from the rich solvent, for recycle to the extractor. If required, some lean solvent, called secondary solvent, is added to the stripper's feed to increase the selectivity. The bottoms from the extractive stripping column contain the aromatics and solvent that are separated in the solvent recovery column. Lean solvent from the solvent recovery column is routed back. The non-aromatics from the top of the extractor contain small amounts of solvent that must be recovered in the raffinate water wash column. The hydrocarbons in the washing water are recovered in the water stripper, and the water is returned to the system in a closed-loop recycle.

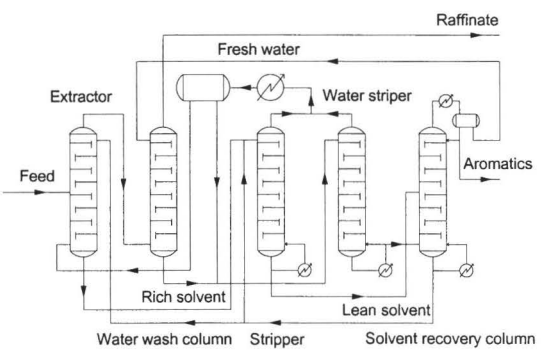

Figure 3. Simplified PFD of Sulfolane Extraction

Establishment of the Network

The selected operating variables, process inputs, and process performance are listed in Table 1 as the network inputs and outputs. Therefor the network is with 8 input nodes and 4 output nodes.

After determining the input and output structure of the network, the effects of the number of hidden layers and the number of nodes in the hidden layers have been tested. Based on the comparison

of the network performances of different structures, the network of one hidden layer with 10 nodes is employed.

Inputs			Outputs	
Operating variables	Sr_1	Primary solvent to feed ratio	R_B	Recovery of benzene
	Sr_2	Secondary solvent to feed ratio	R_T	Recovery of toluene
	T_1	Temperature of the primary solvent	R_X	Recovery of C_8^+aromatics
	T_2	Bottom temperature of the stripper	X_{NA}	Nonaromatic content of the product
	P	Top pressure of the stripper		
Process inputs	X_B	Benzene content of the feedstock		
	X_T	Toluene content of the feedstock		
	X_X	C_8^+ aromatic content of the feedstock		

Table 1 Inputs and Outputs of the Neural Network

The sigmoid function is used as the activation function in each neuron:

$$f(x) = \frac{1}{1+e^{-x}}$$

The network has been trained with the data samples from the industry and the simulation results of AESCAD that is special purpose computer aided process design software for Sulfolane Extraction.[4,5] The optimum operation states were chosen for the samples, to ensure the optimization function of the neural network.

Performance of the Network

When the network learning is finished, an ANN based simulator is obtained. The modeling performance of the trained network has been tested with four sets of industrial data that are not included in the training samples. The comparison is listed in Table 2. It is shown that the network indeed predicts fairly well the aromatic recoveries and the aromatic quality, thus it is feasible to model Sulfolane Extraction by the network.

Outputs		R_B	R_T	R_X	X_{NA}(ppm)
1	Network prediction	0.9973	0.9849	0.9799	312
	Test sample	0.9981	0.9848	0.9814	298
	Relative deviation(%)	0.08	0.01	0.15	4.70
2	Network prediction	0.9947	0.9957	0.9879	205
	Test sample	0.9912	0.9960	0.9883	192
	Relative deviation(%)	0.35	0.03	0.04	6.77
3	Network prediction	0.9969	0.9881	0.9758	2670
	Test sample	0.9980	0.9882	0.9755	2685
	Relative deviation(%)	0.11	0.01	0.03	0.56
4	Network prediction	0.9915	0.9907	0.9937	335
	Test sample	0.9913	0.9907	0.9936	354
	Relative deviation(%)	0.02	0.00	0.01	5.37

Table 2 Modeling Results for Sulfolane Extraction

In the optimization mode, the network operates backward and the optimum operating parameters are obtained. The optimization results are listed in Table 3. It is shown that the optimization results of the network are consistent with those obtained by AESCAD. Since AESCAD has been used successfully in the process design and optimization of several industrial sulfolane extraction units, it is practical to use the two-direction operating neural network for the optimization of Sulfolane Extraction.

Parameters	Sr_1	Sr_2	T_1(°C)	T_2(°C)	P(MPa)
The network	4.99	0.00	90.4	162.8	0.124
AESCAD	5.01	0.00	90.1	164.0	0.125

Table 3 Comparison of the Optimization Results of the Network and AESCAD

CONCLUSIONS

Neural networks are attractive approaches for modeling and optimization of complex processes. This paper discussed the use of one neural network both for the modeling and optimization of Sulfolane Extraction. The simulation and optimization results of the proposed two-direction operating neural network are in good agreement with the industrial data and the results of the first principle based software. Therefor, it is feasible to use the network for the modeling and optimization of Sulfolane Extraction. The proposed approach can also be used for other processes.

NOMENCLATURE

E	cost function of ANN
Net	net input of neurons: $Net_i^k = \sum_{j=0}^{n_{k-1}} W_{ji}^{k-1} O_j^{k-1}$ (k=2, …, t)
n_k	number of nodes of the kth layer
O	output of neurons: $O_i^k = f(Net_i^k)$ (k=2, …, t), $O_i^1 = (U \text{ or } X)_i$
t	total number of layers
U	operating variables
$\tilde{U}$	optimum operating parameters
W^k_{ij}	weights from node i in the kth layer to node j in the $(k+1)^{th}$ layer
X	process inputs
Y	process outputs, target outputs of ANN
α	step size

ACKNOWLEDGEMENT

This work was carried out in the Solvent Extraction Laboratory, State Key Laboratory of Chemical Engineering, China.

REFERENCES

1. Kosters WCG, 'Sulfolane Extraction Process', in Lo TC, et al., Ed., *'Handbook of Solvent Extraction'*, John Wiley & Sons, New York, 541, (1983).
2. Wang Z, Tham MT, and Morris AJ, *Int. J. Control*, **56**, 665, (1992).
3. Rumelhart DE, McClelland JL, *'Parallel Distributed Processing: Explorations in the Microstructure of Cognition'*, MIT Press, Cambridge, (1986).
4. Wen X and Fei W, 'Application of Computer Aided Process Design to Sulfolane Extraction', *AIChE 1998 Spring Meeting*, March, 1998, New Orleans.
5. Wen X, *PhD Thesis*, Tsinghua University, (1996).

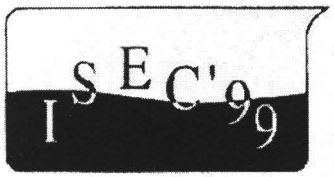

A NEW METHOD FOR THE SIMULATION OF MULTISTAGE METAL EXTRACTION PROCESSES BASED ON THE STEADY-STATE LOCAL LINEARIZATION

M Tanaka[1], K Koyama[1] and J Shibata[2]

[1]Materials Processing Department, National Institute for Resources and Environment, MITI, 16-3 Onogawa, Tsukuba, Ibaraki 305-8569, Japan

[2]Department of Chemical Engineering, Kansai University, 3-3-35 Yamate-cho, Suita, Osaka 564-8680, Japan

ABSTRACT

This paper describes a new method for the computer simulation of the multistage metal solvent extraction processes at the steady state. In this method, the equations obtained by mathematically differentiating the process with respect to the operational parameter capable of independent continuous variation (steady-state local linearization) are numerically solved under appropriate initial conditions. Model calculations considering the extraction equilibrium constant as a variable operational parameter are carried out for the countercurrent multistage extraction process and the countercurrent multistage extraction - stripping process. The validity of this method is demonstrated by the excellent agreement of the solutions with those by the conventional relaxation method. An advantage of this method over the conventional method is that one can quickly draw a detailed diagram showing the effect of one operational parameter on the process efficiency.

Keywords: copper, oxime, countercurrent cascade, modelling, computer simulation, steady-state local linearization,

INTRODUCTION

Multistage processes such as the countercurrent extraction process (EP) and countercurrent extraction - stripping process (ESP) shown in Figs. 1 and 2, respectively, are often used in the plant operation of a metal solvent extraction to enhance the extraction or separation efficiency. Since there are many operational parameters in the multistage solvent extraction processes, computer simulation plays an important role in assessing the process efficiency.

We have been investigating the roles of various operational parameters in the EP and ESP by computer simulation[1,2]. In order to analyze the numerical results of the simulation, we presented a method for mathematically differentiating the multistage process at the steady state with respect to the operational parameters capable of independent continuous variation (steady-state local linearization, SLL)[1,3]. The SLL not only clarifies the symbolic relation underlying the numerical results of the simulation, but also provides a new simulation method for the multistage process. One example of the results from this new method has already been shown for the EP[3].

Until now, some methods have been proposed to simulate the multistage processes[4-6]. These methods need long iterative procedures to obtain a steady-state solution. In contrast, this method can very quickly draw a detailed diagram to represent the effect of one operational parameter capable of independent continuous variation on the process efficiency.

The aim of the present paper is to show the differential equations for the EP and ESP expressing the relationship between the metal molarity in the aqueous phase from each stage and an operational parameter (SLL of the EP and ESP), to explain how these equations are utilized in the present simulation method, and to demonstrate its validity and effectiveness by the

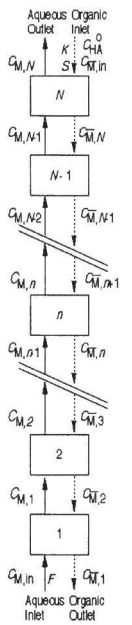

Figure 1 Schematic diagram of EP.

© 2000 Society of Chemical Industry

comparison with the numerical results using the conventional simulation method.

The extraction equilibrium constant, K, is a measure of the extraction ability of the organic phase and thus an important operational parameter. Therefore, as an example, we selected K as the operational parameter.

EQUATIONS

Assumptions.

The assumptions for the subsequent equations are as follows: (i) The temperature and pressure are constant. (ii) Equilibrium is immediately attained in each stage. (iv) The process is at steady state. (v) The volume of each phase does not change during the extraction.

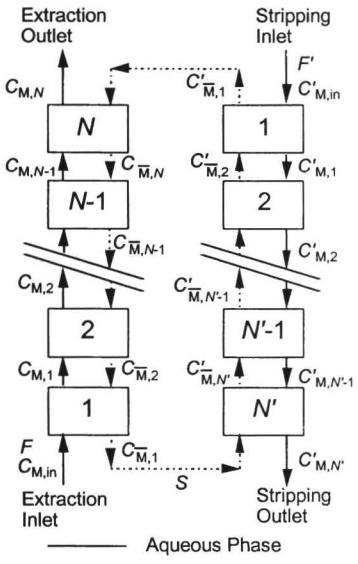

Figure 2 Schematic diagram of ESP.

EP.

In a previous paper[3], a non-homogeneous second-order linear difference equation with variable coefficients with respect to $dC_{M,n}$ was derived on the basis of the material balance of M^{m+} around each stage. By mathematically solving this equation, we derived the equation for EP expressing the relationship between the differentials of $C_{M,n}$ and ln K as

$$dC_{M,n} = B_{\ln K}(n, N)d(\ln K) \tag{1}$$

Here, the coefficient $B_{\ln K}(n, N)$ is written as

$$B_{\ln K}(n,N) = \frac{B_{\ln K}(N,N)[B_{\ln K}(n,n)/B_{\ln K}(N,N) - rB_{\overline{M},\mathrm{in}}(n,n)]}{1 - rB_{\overline{M},\mathrm{in}}(n,n)} \tag{2}$$

where

$$B_{\overline{M},\mathrm{in}}(n,n) = \sum_{i=1}^{n}(\prod_{j=1}^{i-1}\alpha_j)r^{-i} / [1 + \sum_{i=1}^{n}(\prod_{j=1}^{i}\alpha_j)r^{-i}] \tag{3}$$

$$B_{\ln K}(n,n) = -\sum_{i=1}^{n}(\prod_{j=1}^{i-1}\alpha_j)\beta_i r^{-j} / [1 + \sum_{i=1}^{n}(\prod_{j=1}^{i}\alpha_j)r^{-i}] \tag{4}$$

$$r = F/S \tag{5}$$

Here $\prod_{j=1}^{i-1}\alpha_j = 1$ when $i = 1$. The quantities α_n and β_n are the coefficients in the following equation:

$$dC_{\overline{M},n} = \alpha_n dC_{M,n} + \beta_n d(\ln K) \tag{6}$$

Equation 6 expresses the relationship between the differentials of the metal molarities in both phases from each stage along with the differential of ln K and can be called the differential equilibrium

relation. When α_n and β_n are mathematically expressed, the values of $dC_{M,n}$ in the EP are obtained using equation 1.

ESP.

In a previous paper[1], we derived the equation for the ESP expressing the relationship between the differentials of $C_{M,N}$ and $\ln K$ as

$$dC_{M,N} = \frac{\psi' - \psi}{r + \theta + (F/F')\theta'} d(\ln K) \tag{7}$$

Here, θ and ψ are the coefficients in the following equation:

$$dC_{\overline{M},1} = \theta dC_{M,N} + \psi d(\ln K) \tag{8}$$

where

$$\theta = [1 - rB_{\overline{M},in}(N,N)]/B_{\overline{M},in}(N,N) = (\prod_{i=1}^{N}\alpha_i)r^{-N} / \sum_{i=1}^{N}(\prod_{j=1}^{i-1}\alpha_j)r^{-i} \tag{9}$$

$$\psi = -B_{\ln K}(N,N)/B_{\overline{M},in}(N,N) = \sum_{i=1}^{N}(\prod_{j=1}^{i-1}\alpha_j)\beta_i r^{-(i-1)} / \sum_{i=1}^{N}(\prod_{j=1}^{i-1}\alpha_j)r^{-(i-1)} \tag{10}$$

Equation 10 states that ψ is the weighted average of β for each stage in EP, where the relative weight of the nth stage is expressed as $(\prod_{i=1}^{n-1}\alpha_i)r^{-(n-1)} / \sum_{i=1}^{N}(\prod_{j=1}^{i-1}\alpha_j)r^{-(i-1)}$.

From our previous results[3], the following equation holds by regarding the extraction section in the ESP as EP:

$$dC_{M,n} = B_{\overline{M},in}(n,N)dC'_{\overline{M},1} + B_{\ln K}(n,N)d(\ln K) \tag{11}$$

where

$$B_{\overline{M},in}(n,N) = \frac{B_{\overline{M},in}(N,N)[B_{\overline{M},in}(n,n)/B_{\overline{M},in}(N,N) - rB_{\overline{M},in}(n,n)]}{1 - rB_{\overline{M},in}(n,n)} \tag{12}$$

From eqs 7, 9,10, and 11, we obtain the equation expressing the relationship between $dC_{M,n}$ and $d(\ln K)$ as

$$dC_{M,n} = \left\{\frac{[(r+\theta)\psi' + (F/F')\theta'\psi]}{r + \theta + (F/F')\theta'} B_{\overline{M},in}(n,N) + B_{\ln K}(n,N)\right\} d(\ln K) \tag{13}$$

On the basis of the symmetrical nature of the ESP, the equation for $dC'_{M,n'}$ is obtained by interchanging the prime in eq 13 as

$$dC'_{M,n'} = \left\{\frac{[(r'+\theta')\psi + (F'/F)\theta\psi']}{r' + \theta' + (F'/F)\theta} B'_{\overline{M},in}(n',N') + B'_{\ln K}(n',N')\right\} d(\ln K) \tag{14}$$

When the α_n, $\alpha'_{n'}$, β_n, and $\beta'_{n'}$ are mathematically expressed, the values of $dC_{M,n}$ and $dC'_{M,n'}$ in the ESP are calculated by eqs 13 and 14, respectively.

MODEL CALCULATIONS

Assumptions, Procedure, and Conditions.

As a numerical example of the simulation, we dealt with the extraction by a cation-exchange reagent where the stoichiometric relation of the extraction is expressed as

$$M^{m+} + (l/p)\overline{(HA)_p} = \overline{MA_m(HA)_{l-m}} + mH^+ \qquad (15)$$

In addition to the previously mentioned assumptions, we further assume the following points: (i) The aqueous phase consists of H^+, M^{m+}, X^{q-}, and water. (ii) The organic phase consists of $(HA)_p$, the diluent, and the metal-extractant complex, $MA_m(HA)_{l-m}$, where l is constant. (iii) The activity coefficients of H^+, M^{m+}, $(HA)_p$, and $MA_m(HA)_{l-m}$ are unity,
Thus, K is expressed as

$$K = \frac{C_{\overline{M},n} C_{H,n}^m / (\text{kmol m}^{-3})^{m-l/p}}{C_{M,n} C_{\overline{(HA)_p},n}^{l/p}} \qquad (16)$$

The equations for α_n and β_n under these assumptions were previously derived[3].

The calculation was carried out using the conventional relaxation method [6-7] and the method based on eq 1 or eqs 13 and 14.

In the relaxation method, the distribution of M^{m+} within each stage was calculated on the basis of eq 16 and the non-steady state material balance equation for M^{m+} for each stage was simultaneously solved by allowing the initial conditions for a sufficiently long time to reach steady state. The initial conditions (molarities of M^{m+} in the aqueous phase from respective stages when the time is zero) were equal to those of the aqueous feeds, although we confirmed that the initial conditions do not affect the steady-state solutions[2].

In the method based on eq 1 or eqs 13 and 14, the initial conditions (molarities of M^{m+} in the aqueous phase from respective stages when K is a certain value) were first calculated by the relaxation method. Eq 1 for the EP or eqs 13 and 14 for the ESP for each stage was then integrated with respect to ln K along with calculating the distribution of M^{m+} within each stage based on eq 16.

An equation solver, Equatran-G for Windows[8], was used in the actual calculation. The Runge-Kutta-Verner method[9] was used for numerical solution of the differential equations.

The simulation was done under the fixed conditions shown in Table 1. These conditions were set up in reference to the SX-EW process for the copper oxide ores where the hydroxyoximes were used as the extractants[10].

Table 1 Conditions for the simulation.

Common to EP and ESP	
l	2
m	2
p	1
N	4
r	1
C°_{HA}/kmol m^{-3}	0.2
$C_{M,in}$/kmol m^{-3}	0.05
$C_{H,in}$/kmol m^{-3}	0.01
EP	
$C_{\overline{M},in}$/kmol m^{-3}	0
ESP	
N'	3
r'	0.2
$C'_{M,in}$/kmol m^{-3}	0.5
$C'_{H,in}$/kmol m^{-3}	2

Results.

Figures 3 and 4 show the results of the simulation for the EP and ESP, respectively. The solid curves in these figures denote the normalized molarities ($C_{M,n}/C_{M,in}$) for each stage in the EP and the extraction section of the ESP, respectively. The circles and squares denote the solutions by the relaxation method. To calculate the numerical solutions of eq 1 or eqs 13 and 14, the values denoted by the circles and squares at the left ends of the figures were used as the initial values. In these figures, the numerical solutions of eq 1 or eqs 13 and 14 agree with those by the relaxation method in all the regions in the figures. This fact validates the present method based on eq 1 or eqs 13 and 14. As shown in Fig. 3, the rise in K reduces the $C_{M,n}$ values in the EP. This means that the metal recovery by the EP is enhanced with the rise in K. On the other hand, as shown in Fig. 4, with the rise in K, the $C_{M,n}$ values in the ESP first decrease, reach minima in the log K range from 0.6 to 1, and thereafter increase. This means that the metal recovery by the ESP first increases, reaches maximum, and thereafter decreases. The decrease in the metal recovery in the greater log K region indicates that the stripping of the metal becomes very difficult in this region[1].

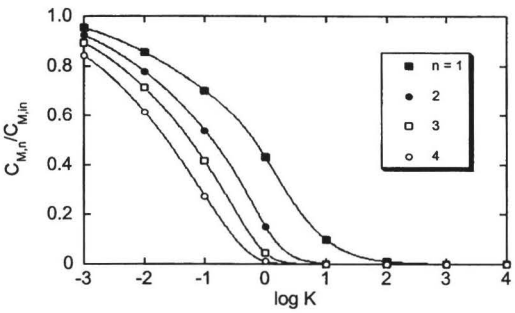

Figure 3 Variation in the aqueous metal molarity from each stage in EP.

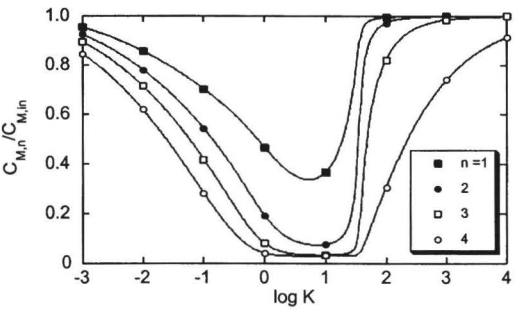

Figure 4 Variation in the aqueous metal molarity from each stage in the extraction section of ESP.

CONCLUSIONS

We have described and validated a method to calculate the variation in the performance of the EP and ESP with K. This method is based on the differential equation expressing the relationship between the metal molarity in the aqueous phase from each stage and K. We can readily derive similar equations with respect to the other operational parameters capable of independent continuous variation and utilize them for the simulation.

The applicability of this method is limited to the cases where the α_n and β_n are mathematically expressed and would diminish when the stage sequence loses the regularities as those in the EP and ESP. The latter is because the coefficients of d(ln K) in the equations corresponding to eq 1 or eqs 13 and 14 becomes very complicated. Nevertheless, a distinct advantage of this method is that we can quickly draw a detailed curves expressing the variation in the process performance with the variation in one operational parameter. In this sense, this method would be useful to find the optimum operational conditions for the relatively simple multistage solvent extraction processes such as the EP and ESP.

NOMENCLATURE

$B_{\ln} K(n, N)$ = coefficient in eq 1 and is defined by eq 2 where n and N denote the nth stage and the total number of the stages, respectively, kmol m^{-3}

$B_{\ln} K(n, n)$ = value defined by eq 4, kmol m^{-3}

$B_{\overline{M},in}(n,N)$ = coefficient in eq 11 and is defined by eq 12 where n and N denote the nth stage and the total number of the stages, respectively, dimensionless

$B_{\overline{M},in}(n,n)$ = value defined by eq 3, dimensionless

C = molarity, kmol m^{-3}

F = flow rate of the aqueous phase, m^3/s

HA = monomeric species of the extractant

K = extraction equilibrium constant, dimensionless

l = number of extractant anions in the metal-extractant complex, dimensionless

M = metal to be extracted

m = valency of the metal cation, dimensionless

N = total number of stages, dimensionless

n = stage number, dimensionless

p = aggregation order of the extractant, dimensionless

r = ratio of flow rates defined by F/S, dimensionless

S = flow rate of the organic phase, $m^3\ s^{-1}$

α_n = coefficient in eq 6, dimensionless

β_n = coefficient in eq 6, kmol m^{-3}

θ = coefficient in eq 8 and is defined by eq 9, dimensionless

ψ = coefficient in eq 8 and is defined by eq 10, kmol m^{-3}

Subscript: in = inlet

Superscripts: o = total molarity, $\overline{\ }$ = organic phase species, ' = stripping section

REFERENCES

1. Tanaka M, Koyama K and Shibata J, *Ind. Eng. Chem. Res.*, **37**, 1943, (1998)
2. Tanaka M, Koyama K, Kobayashi M and Shibata J, *Solv. Extr. Ion Exch.* (submitted).
3. Tanaka M, Koyama K and Shibata J, *Ind. Eng. Chem. Res.*, **36**, 4353, (1997).
4. Goto T, *'Proc. Int. Solv. Extr. Conf. 1971'*, SCI, London, 1011, (1971)
5. Chapman TW, *AIChE Symp. Ser.*, **74,** 120, (1978).
6. Rod V, *Chem. Eng. J.*, **29**, 77, (1984).
7. Rose A, Sweeny AF and Schrodt VN, *Ind. Eng. Chem.*, **50**, 737, (1958).
8. Peterson JN, Chen C-C and Evans LB, *Chem. Eng.*, **1978**(Aug. 28), 107.
9. Verner JH, *SIAM J. Numer. Anal.*, **15,** 772, (1978).
10. Szymanowski J, *'Hydroxyoximes and Copper Hydrometallurgy'*, CRC, Boca Raton, (1993).

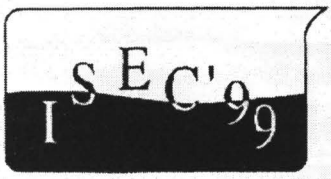

DISTREC: A NEW COMPUTER PROGRAM FOR SOLVENT EXTRACTION EQUILIBRIUM CALCULATIONS, MODELLING AND SIMULATION

M Aguilar[1], JL Beltran[2] and JL Cortina[1]

[1] Department of Chemical Engineering, Universitat Politecnica de Catalunya, Barcelona, Spain

[2] Department of Analytical Chemistry, University of Barcelona, Barcelona, Spain

ABSTRACT

A new program for treating liquid-liquid distribution data (DISTREC) written under MATLAB™ environment for use on personal computers is presented. This program, DISTREC, has been developed trying to allow two basic functions: modelling of experimental distribution data and calculation of the constants of the different reactions involved and simulation of two-phase distribution systems.

Keywords: copper, Cyanex 272, equilibrium modelling, modelling, simulation

INTRODUCTION

During the last decades great effort has been made to study and describe metal extraction reactions in terms of composition of the species and extraction constants.[1-4] The results of many studies, however, seem to indicate that when dealing with macro-amounts of metals, the transfer of these species to the organic diluent is not a unique process. First, because more than one metallic species are usually extracted, and the existence of a series of processes that may occur simultaneously with the main reactions. These side-reactions may include: self association of the extractant in the diluent, acid-base reactions of the extractant in the aqueous phase, complex formation of the metal ions with anionic components of the ionic medium, solvation of metal complexes extracted and polymerisation of metal species in the organic phase. To deal with these problems, in the early 1970's, an approach based on chemical equilibrium for interpretation of liquid-liquid reactions was applied and numerical computer programs as LETAGROP-DISTRB [5-6] developed to calculate the equilibrium constants associated to different reactions proposed in the model. Since this time, very little has been done to improve the computer programs developed although a number of limitations have been detected. Among them, there are limitations in: the number of chemical components (a maximum of 4) and species of the chemical systems (a maximum of 20); in the statistical treatment and in data management for input data preparation. Additionally, a lack of computer programs for simulating liquid-liquid extraction processes have been identified in the Solvent Extraction arena as noted in the last Solvent Extraction Workshops and Meetings. Definition and design of solvent extraction based processes in multi-component systems could simplify research efforts by combining thermodynamic data on metal-extractant reactions with computer programs. In the present paper, a new program for treating liquid-liquid distribution data will be presented. This program DISTREC, written under MATLAB™ [7] software for use on personal computers has been developed as a new tool for liquid-liquid distribution systems with the following functions:

to be used for the calculation of the constants of the different reactions involved;

to be used in simulation of two phase distribution systems.

It can be applied to multi-component systems, overcoming the limitations in either number of components or species compared with other programs found in the literature such as LETAGROP and DISPC. The main features of this new program are: (a) easy use and simplicity of the input data system; (b) improvement of statistical data treatment; (c) display possibilities for evaluating experimental data and calculating data for the proposed chemical models; (d) display possibilities for evaluating equilibrium isotherms.

Evaluation of this new program for studying different metal distribution studies were compared with those obtained using programs such as LETAGROP-DISTRB or DISPC.

© 2000 Society of Chemical Industry

DISTREC program.

This program was developed to be user-friendly and highly interactive in operation taking into account the facilities provided by personal computers and new software network facilities as MATLAB for simplifying visual and graphical displays. In this way, their use is based on menu-driven selections, allowing modification of the chemical model of the system studied. Moreover, the user has direct access to graphics routines for the presentation of data and results. These graphics are presented on the computer screen and are printed directly or easily exported to other programs via the Windows clipboard.

MATLAB^R environment.

MATLAB^R (standing for MATrix LABoratory) is a technical computing environment for high-performance numeric computation and visualisation. MATLAB^R integrates numerical analysis, matrix computation, signal processing, and graphics in an easy-to-use environment where problems and solutions are expressed just as they are written mathematically without traditional programming. MATLAB^R is an interactive system whose basic data element is a matrix that does not require dimensioning. This allows you to solve many numerical problems in a fraction of the time it would take to write a program in a language such as Fortran, Basic, or C. In the present version of MATLAB environment, no limitations in the number of components and species are introduced.

Program components.

The program structure is shown in figure 1, and has been originally designed for dealing with two different options:

1) determination, estimation and calculation of equilibrium constants from experimental data;
2) simulation of liquid-liquid distribution systems.

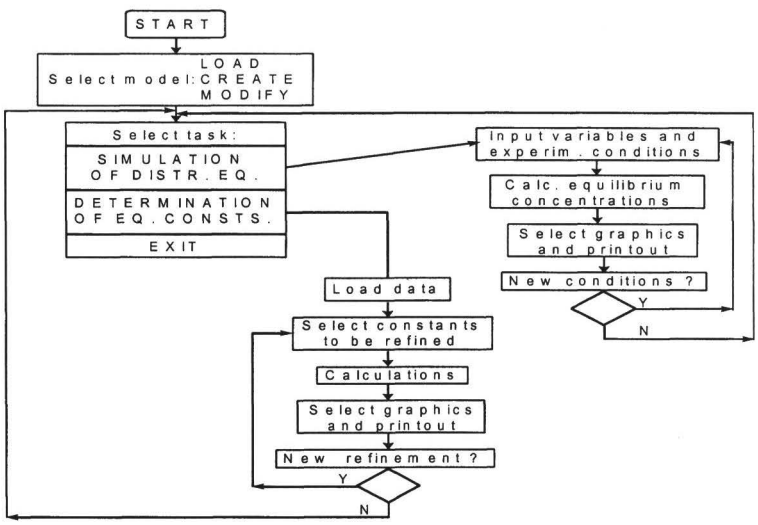

Figure 1. DISTREC program structure

The principal components of the structure are described briefly as follows:

a) Editing Inputs Block.

Two different files could be created by an interactive program: *Model Input File* and *Experimental Input File.*

Input Model File. This option asks for the components of the system, indicating their presence in the aqueous and in the organic phase, and following species are described by formation reactions

from the system components, indicating the stoichiometric coefficients as well as the formation constants (in logarithmic form). An example of the Input Model is shown in Table 1.

Experimental Data File. This part of the input contains the experimental data, including both total concentration of components of the system and some equilibrium concentration data (e.g. aqueous phase pH, etc.) as well as the distribution coefficient and phase ratio (Vaq, Vo) in the following format. In the first position the total millimoles of each component of the system (except for H^+), ordered as in the Model Input, followed by pH of the aqueous phase, organic and aqueous volumes, and finally the log D value. One example for the model example is collected in table 1.

input model as displayed on the computer screen:

THE SPECIES IN THIS SYSTEM ARE:

SPECIES	PHASE	logBeta
1)Cu(1)	Aq.	0.0000
2)SO_4(1)	Aq.	0.0000
3)Cyanex(1)	Aq.	0.0000
4)H(1)	Aq.	0.0000
5)Cu(1)SO_4(1)	Aq.	2.4990
6)Cyanex(1)H(1)	Aq.	3.7200
7)Cyanex(1)H(1)	Org.	8.0200
8)Cyanex(2)H(2)	Org.	19.0090
9)Cu(1)Cyanex(4)H(2)	Org.	33.7740

experimental data input:

105.615 605.615 842 2.974 10 10 -1.187
.....
115.753 615.755 1263 3.151 10 10 -0.627

Table 1. Model and Experimental Data Input example for DISTREC.
Extraction of Cu(II) with Cyanex 272 disolved in toluene from sulphate media

b) Resolution of the mass balances block.

Each experimental point of the chemical system, defined by the given volumes of the aqueous and the organic phases, the total concentrations of the components, proton activity (-pH) and the distribution coefficient, could be considered as an equilibrium system, composed of n_c components in which could be included a total number of n_s species (including both the organic and aqueous phases). The concentration of the j species in the aqueous phase and in the organic phase ($S_{j,A}$) and ($S_{j,o}$) respectively are given by:

$$S_{j,A} = \beta_{j,A} \prod_{k=1}^{n_c} C^{\,cf(j,k)}{}_{k,A}$$

$$S_{j,o} = S_{j,A} K_d j$$

where cf(j,k) denotes the stoichiometric coefficient of the k component in the j species, $\beta_{j,A}$ the formation constant of the species j in the aqueous phase, $C_{k,A}$, the free concentration of the of the k component in the aqueous phase and Kd_j the distribution constant of the species j. From here it is possible to define the mass balance for each component, defining the total mass amount of component "i" of the system (M_i) as:

$$M_i = \sum_{j=1}^{n_S} (V_a \bullet Cf(j,i) \bullet S_{j,a} + V_o \bullet cf(j,i) \bullet S_{j,o}$$

where V_o and V_a denote the organic and aqueous phase volumes, respectively. In this way, n_c-1 equations (providing that mass balance it is not applied to the hydrogen ion), in a system with n_c-1 variables which correspond to the free concentration of the rest of components (in this step the equilibrium constants are considered fixed values) are obtained. Taking into account that the mass balance system will be solved when differences between the total quantity of theoretical and experimental mass is lower than a predetermined (prefixed) value (when the sum of the absolute differences, for each component is lower than 10^{-10} millimoles). To solve this system an algorithm of the program [9] allows the calculation of the equilibrium concentration of components and species in solution. Once the mass balances have been solved the program calculates the theoretical values of the distribution coefficient for each point (D). Taking into account that the value of (D_{calc}) is calculated for the first component described in the definition of the system, this will be equal to:

$$D = \frac{\sum_{i=1}^{n_S} cf(i,1) \bullet S_{i,o}}{\sum_{i=1}^{n_S} cf(i,1) \bullet S_{i,a}}$$

c) Refining of equilibrium constants block.

The refinement of the equilibrium constants is carried out by the REFINE procedure, using the Gauss-Newton non-linear least-squares algorithm[10] by numerical differentiation until a minimum in the sum of square residuals is attained. In this procedure the group of constants to refine is calculated allowing the minimisation of the objective function U, using an iterative process in which the value of the equilibrium constant is successively incremented until it reaches a minimum in the objective function U. This function is defined as the difference between the experimental and calculated values of the logarithm of the distribution coefficient ($\log D_{exp}$ and $\log D_{cal}$, respectively):

$$U = \sum_{i=1}^{n_p} (\log D_{i,\exp} - \log D_{i,cal})^2$$

where n_p is the total number of experimental points. The program uses log D values instead of D due to the fact that the minimisation process is preferentially performed over values with approximately similar orders of magnitude. The minimisation process is repeated until the relative change of U between two iterations is less than 0.01%. In the case of divergence in the refinement procedure, the method is modified to optimise the shifts of the constants by using the method described by Wenworth.[11] If after the application of this correction an effective reduction of the U value is achieved, the program returns to the Gauss-Newton, and otherwise the minimisation process is stopped. In any of the cases, the set of constants which define a minimum value of the objective function are always retained. Once the minimisation process has been finished, the program gives the refined constants together with both the estimated standard deviation ($\sigma(\log K)$), U and the standard deviation of the residuals (σ):

$$\sigma = \sqrt{\frac{U}{(n_p - 1)}}$$

After that, the constants are stored in the file of results. At this point the user could choose between starting as new process of refinement or finishing the execution of the program.

APPLICATIONS

The DISTREC program has been applied to the treatment of experimental data for different solvent systems of metal extraction described in the literature.[1] Selected systems included the

determination of ligand distribution, ligand in the aqueous phase, ligand aggregation on the organic phase, ligand metal complex formation on the organic phase. All the studied systems have been treated by using graphical methods, and numerical methods using LETAGROP. An example of application of the DISTREC program in the extraction of Cu(II) with Cyanex 272 containing the acid 2,4,4(trimethylpentyl)phosphinic acid (HL) from sodium sulphate solutions is shown in Figure 2.

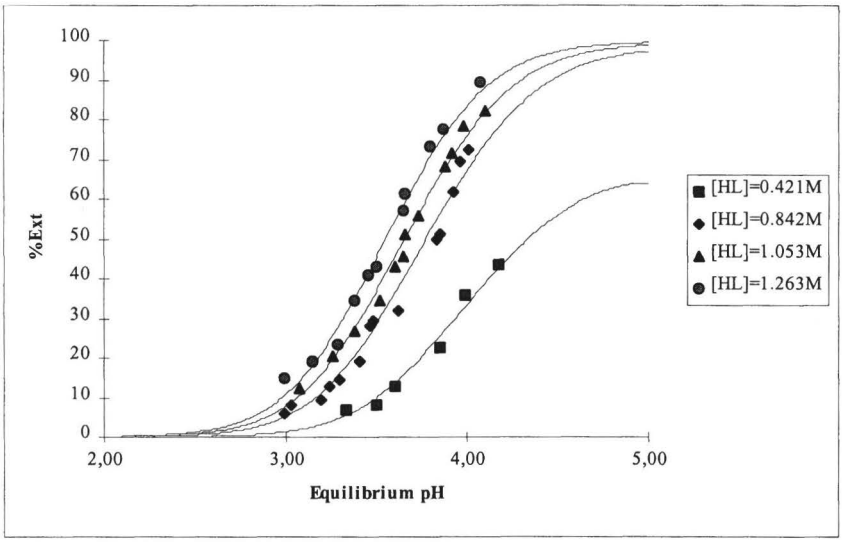

Figure 2. Variation of the extraction percentage of Cu(II) as a function of pH for different total extractant concentrations in 0.5mol/dm^3 Na_2SO_4.
The solid lines have been calculated using the constant given in Table 1.

CONCLUSIONS

The different routines implemented in DISTREC for the calculation of the mass balances, refinement of constants are well known by the users of least-squares based programs for the determination of stability constants in complex equilibria. In this sense, DISTREC is a classical program. However, the aim in their development was not simply the refinement of equilibrium constants from distribution data as a black box, but rather their use is dedicated to taking a closer look at experimental data. The graphical information obtained directly on the screen (experimental and calculated data, together with the distribution of residuals) can be very useful in searching for possible errors in the experimental data and in planning new experimental designs when a system is studied. The possibilities of changing the model (by adding or deleting species) and with a selection of the master variables (pH, ligand concentration, complexing concentrations) range are also very valuable in searching for the best chemical model for a given system. In this way, the statistical tests given by the program are also a help for the user. Moreover, the results obtained by DISTREC are in accordance with those obtained with other programs when they are applied to the same data, but their advantages are the on-line plotting facilities and their interactive use.

REFERENCES

1. Aguilar M, in *Developments in Solvent Extraction*, ed. Alegret S, Ellis Horwood Series in Analytical Chemistry, (1988).
2. Sato T, Maeda T, Mizuno Y and Nakamura T, *Solv. Extr. & Ion Exch.*, **2**(6), 755, (1984).
3. Baes CF Jr, McDowell WJ and Bryan SA, *Solv. Extr. & Ion Exch.*, **5**(1), 1, (1987).
4. Rydberg J and Sullivan JC, *Acta Chem. Scand.*, **13**, 2057, (1959).

5. Liem H and Ekelund R, *Acta Chem. Scand.*, **A33**, 481, (1975).
6. Liem H, *Acta Chem. Scand.*, **25**, 1521, (1971).
7. MATLAB, MathWorks Incorporated.
8. Beltran JL, Compaño R, Granados M, Guiteras J and Prat MD, *Ana. Quim*, 87, 593, (1991).
9. Izquierdo A and Beltran JL, *Journal of Chemometrics*, **3**(A), 209, (1988).
10. Durand E, *Solutions Numeriques des Equations Algébriques, Tome II: Systems de Plusiers Equations,* Mason, Paris (1972).
11. Wentworth WE, *J. Chem. Educ.*, **42**, 96, (1965).

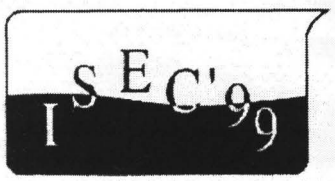

SOFT MODELLING TECHNIQUES: A TOOL FOR STUDYING SOLVENT EXTRACTION PROCESSES

JL Cortina[1], M Aguilar[1], M El Gharbi[1] and R Tauler[2]
[1]Department of Chemical Engineering, Universitat Politecnica de Catalunya, Barcelona, Spain
[2]Department of Analytical Chemistry, University of Barcelona, Barcelona, Spain

ABSTRACT
Solvent extraction of Cu(II) from sulphate solutions by Cyanex 272 was studied by VIS-NIR spectroscopic measurements and both soft modelling multivariate curve resolution procedures and hard modelling techniques to describe the liquid-liquid distribution equilibria were applied.

Keywords: copper, modelling, alternative least squares (ALS), curve resolution

INTRODUCTION

During the last decades, liquid-liquid extraction reactions played an important role in the development of separation processes, mainly in connection with hydrometallurgical processing of minerals or solid wastes, as well in analytical applications.[1,2] During this time the description of the metal extraction processes have been based on experimental procedures directed to the determination of the distribution coefficients by measuring changes of the distributed species, usually metallic species, in the aqueous phase. However, little has been done with regard to the organic phase.[3] The advances in analytical instrumentation based on spectroscopic techniques such as UV, VIS, NIR, IR[4] offer new routes to the study the metal extraction reactions by following the changes in the organic phase spectra as is the case for most of the amines or organophosphorus based reagents. Secondly, several modern chemometric techniques, such as partial least-squares (PLS) and alternating least-squares (ALS) multivariate curve resolution procedures, developed to obtain the most useful information from multivariate data have been applied to the study of chemical speciation in aqueous solutions with excellent results.[5-10] Soft modelling multivariate curve resolution allows the determination of the number of species present in the experiment, the calculation of the distribution profiles of the species and the pure spectra of each chemical species. In this context, the main objectives of this paper are:

a) the development of new experimental procedures based on the use of VIS-NIR spectroscopic measurements to study metal extraction reaction in solvent extraction systems, and

b) the application of soft modelling multivariate curve resolution procedure to describe the liquid-liquid distribution equilibria.

The selected model system was the extraction of Cu(II) from sulphate solutions at 0.5 mol/dm^3 ionic strength at 25°C by Cyanex 272 containing the active component di(2,4,4-trimethylpentyl)phosphinic acid. The extraction of Cu(II) ions with this phosphinic acid derivative was studied by: (a) monitoring the changes in the VIS-NIR spectrum at the organic phase and, (b) by following changes of the metal concentration in the aqueous phase by molecular and atomic absorption spectrophotometry. The second order VIS-NIR absorbance data were analyzed with a soft modelling multivariate curve resolution procedure which allows the determination of the number of different species along the experimental conditions; prediction of the metal loading profiles in the organic phase, and the calculation of the pure spectrum of each chemical species.[5-9] Additionally, the distribution coefficient was determined as a function of both pH and ligand concentration in the organic phase. The data were analyzed using soft and hard modelling techniques, including graphical slope analysis method and a numerical method using the program LETAGROP-DISTR.[11] Analysis of the results showed that the extraction of Cu(II) ions can be explained assuming the formation of metal complexes in the organic phase with a general composition $CuL_2(HL)_{2,0}$.

© 2000 Society of Chemical Industry

EXPERIMENTAL

Reagents and solutions

Cyanex 272 containing di(2,4,4-trimethylpentyl)phosphinic acid (DTMPPA = HL)), kindly supplied by Cytec (Canada), was used as obtained. Purity (89±2%) of the active component was evaluated by NaOH titration. Stock solutions of Cu(II) (1 g/dm^3) were prepared by dissolving the sulfate salt (Merck a.r. grade) in water. Sodium sulfate, sodium hydroxide and sulfuric acid (Merck a.r. grade), were used for the preparation of solutions.

Batch Metal Distribution with Cyanex 272

The extraction of Cu(II) was carried out with batch experiments at 25°C. Volumes of 10 cm^3 of an organic phase of Cyanex 272 dissolved in toluene were mixed mechanically in glass tubes with an aqueous solution (10 cm^3) having composition 0.5 mol/dm^3 (Cu^{2+}, H^+, Na^+)SO_4^{2-} until equilibrium was achieved. To determine the time to reach equilibrium, the distribution of Cu(II), at constant pH, were determined as a function of time, and 10 minutes were enough to reach the equilibrium. After phase separation with a high-speed centrifuge the equilibrium pH was measured. Metal content in both phases was determined by Atomic Absorption Spectrophotometry using a Varian 640 AAS with air-acetylene flame.

Spectrophotometric data acquisition and treatment

Spectrophotometric measurements were performed with a Hewlett Packard HP8453 spectrophotometer. This single beam instrument was equipped with a quartz cuvette 1cm pathlength. The spectra were recorded from 400-1100 nm using a Cyanex 272-toluene solution as blank. The absorbance values of the extracted complexes were stored in the wavelength range from 400 to 1000 nm in steps of 1 nm. The data treatment was carried out with MATLAB for Windows (Math Works, Version 4.2).[12]

Chemometrics methods

The VIS-NIR spectrophotometric data were analyzed with a multivariate curve resolution procedure, alternating least-square (ALS) which is implemented in a small set of MATLAB.[8-10] Essentially the data treatment consists of the following steps:

a) data arrangement: The data from an extraction experiment are collected in a matrix **D** (M x N), whose M rows are the spectra recorded at the different pH values.

b) estimation of the number of chemical species, NS, present in each complexation experiment. This number is estimated by rank analysis, using principal component analysis (PCA) or some related techniques based on factor analysis such as evolving factor analysis (EFA) or fixed-size moving window factor analysis (FSMW).[7-9]

Solving the linear model (generalized Beer law) equation in matrix form iteratively by ALS to obtain the matrix of pure spectra **S** and the matrix of species distribution **C** which best fit the data. In matrix form, this model can be written as:

$$\mathbf{D}=\mathbf{CS}+\mathbf{E}$$

where **E** is the matrix of the residuals not explained by the chemical species in **C** and **S** and should be close to the experimental error. This iterative method starts with an initial estimation of the C data matrix obtained from EFA profiles of the experimental data matrix and considering the presence of NS absorbing species.[7-8]

RESULTS

Soft Modelling

Rank analysis of the individual and combined data matrices of the VIS-NIR spectra obtained suggested that one absorbing species is present for the Cu(II)-SO_4^{2-}—HL-toluene system under the experimental conditions. Analysis of the data matrix using principal component analysis (PCA) and EFA (Figure 1b), shown than one component explained 99.97% of the total data variation and that the inclusion of the second factor produce an improvement of the fitting of the same order as the experimental error. This does not agrees with some of the previous solvent extraction studies published previously where two species where used to explain the experimental results.[17] These results were checked and confirmed in the next steps of the data treatment. The ALS procedure was applied to the column-wise augmented data matrix obtained by grouping the different ligand extraction series ($[HL]_o$= 0.4, 0.8, 1.0 and 1.5 mol/dm^3). The VIS-NIR spectra changes obtained as a function of pH is shown in figure 1a.

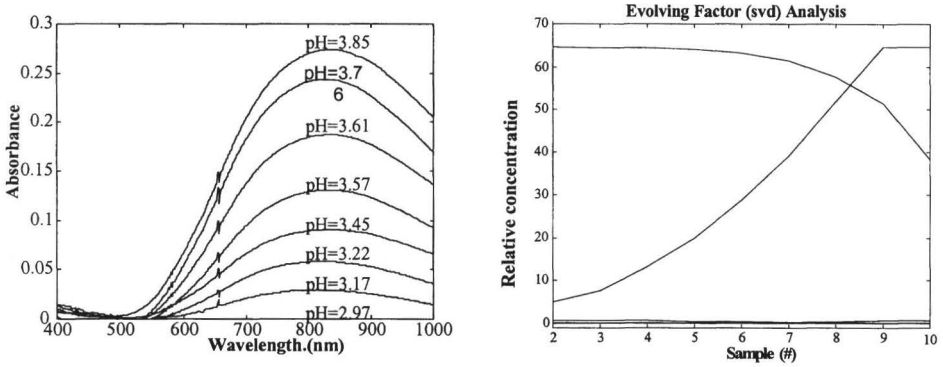

Figure 1a. VIS_NIR spectral changes in the organic phase as a function of pH in the aqueous phase [Cu (II)] = 0.1 mol/dm^3, $[HL]_o$= 1.0 mol/dm^3 (toluene) and for a phase ratio (V_o/V = 1).

Figure 1b. Evolving Factor Analysis plot for the data matrix of the four set of ligand concentrations.

Hard Modelling

Classical methods for studying liquid-liquid distribution reactions were applied. These methodologies allowed the determination of the metal-complex stoichiometry as well as the stability constants of the species formed in the working range. The distribution of Cu(II) between the organic phase containing Cyanex 272 and the aqueous phase can be obtained directly as:

$$D = \frac{[Cu(II)]_o}{[Cu(II)]} \qquad (1)$$

where $[Cu(II)]_o$ denotes the total concentration of Cu^{2+} in the resin phase and [Cu(II)] its total concentration in the aqueous phase in mol/dm^3.

Metal distribution data from aqueous solutions 0.5 mol/dm^3 Na_2SO_4 by Cyanex 272 are plotted as log D versus pH in Figure 2, showing that the distribution functions are straight lines of slope 2.

Accordingly, the extraction of these metal ions with Cyanex 272 can be described by the following general reaction:

$$Cu^{2+} + (2 + q - t)\,HL_o + t\,SO_4^{-} \Leftrightarrow Cu(SO_4)_t\,L_{2-t}(HL)_{q,o} + (2 - t)\,H^{+} \qquad (2)$$

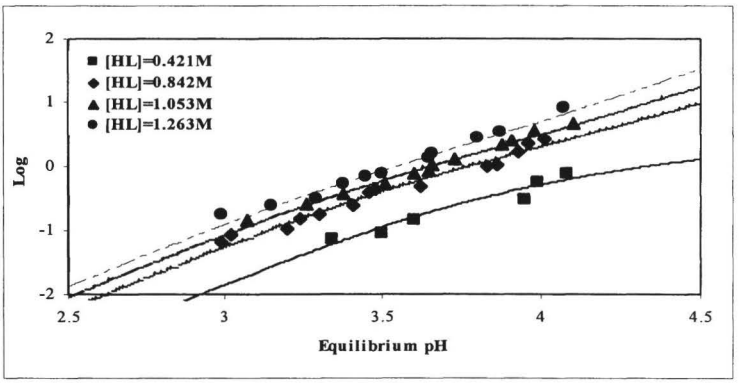

Figure 2. Variation of the distribution coefficient of Cu(II) as a function of pH for different total extractant concentrations in 0.5 mol/dm^3 Na_2SO_4. The solid lines have been calculated using the constants given in table 1 by the program LETAPL.[13]

Polynuclear copper (II) complexes in the resin phase have been excluded because plots log D versus pH are independent of metal concentration and assuming that SO_4^{2-} ions are not co-extracted to the organic phase equation (2) can be expressed as:

$$Cu^{2+} + (2+q)\,HL_o \Leftrightarrow Cu\,L_2(HL)_{q,o} + 2\,H^+ \tag{3}$$

The corresponding equilibrium constant of the extraction process (K) is defined by:

$$K^o = \frac{\{CuL_2(HL)_2\}\{H^+\}^2}{\{Cu^{2+}\}\{HL\}_o^{(2+q)}} = \frac{[CuL_2(HL)_q]_o[H^+]^2\gamma_{CuL_2(HL)_{q,o}}\gamma_{H^+}^2}{[Cu^{2+}][HL]_o^{2+q}\gamma_{Cu^{2+}}\gamma_{HL_o}^{(2+q)}} = K^*\Gamma \tag{4}$$

where {}and γ_i denote the activity of "i" species and K^* is the stoichiometric equilibrium constant for the extraction reaction:

$$K^* = \frac{[CuL_2(HL)_q]_o[H^+]^2}{[Cu^{2+}][HL]_o^{2+q}} \tag{5}$$

and "Γ" is the term containing all the activity coefficients. As a preliminary hypothesis, the term "Γ" can be expected to remain constant.

In order to relate the distribution of the metal with the metal composition in the organic phase, the formation of a simplest species may be assumed. Hence, according to previous results, if only one species of the type $CuL_2(HL)_q$ is formed the distribution coefficient for (M^{2+}) becomes:

$$D = \alpha\,K^*[HL]_o^{(2+q)}[H^+]^{-2} \tag{6}$$

where $\alpha = (1+\beta_{Cu\text{-}SO4}[SO_4^{2-}]$ and $\beta_{Cu\text{-}SO4}$ is the formation constant of the $CuSO_4(aq)$ complex.

The dependence of the distribution coefficient on extractant concentration in the organic phase at constant pH allow us an estimation of the p coefficient (p = 2). Further analysis of the experimental data obtained in the distribution equilibrium studies was evaluated by the computer program LETAGROP-DISTR. In this program, for a given model, the computer searches for the best set of equilibrium constants K^*, that would minimize the sum squared error defined by:

$$U = \Sigma(\log D_{exp} - \log D_{calc})^2 \quad (7)$$

where D_{exp} is the distribution ratio of copper (II) determined experimentally and D_{cal} is the value calculated by the program solving the mass balance equation, assuming a particular set of species and constants. This program also calculates the standard deviation s(log D):

$$\sigma(\log D) = (U / N_p)^{1/2} \quad (8)$$

where N_p is the difference between total number of experimental points and the total number of equilibrium constants calculated.

The initial extraction reaction and its corresponding equilibrium constant are given on the basis of the graphical slope analysis. Combining the soft modelling results where changes in the organic phase is due to the formation of one species with the slope analysis results a species of the type $CuL_2(HL)_q$ is the responsible of the extraction process. A comparison of the different reasonable chemical models that fit the experimental data is performed analyzing the U function. The best model assuming the formation of the species $CuL_2(HL)_2$ was selected due to its minimum value.

Model	σ(logD)	U	LogK*
CuL_2	0.20	1.75	-1.79 ± 0.10
$CuL_2(HL)$	0.14	0.84	-0.06 ± 0.07
$CuL_2(HL)_2$	0.12	0.69	1.69 ± 0.07
$CuL_2(HL)_3$	0.16	1.19	3.46 ± 0.10
$CuL_2(HL)_4$	0.22	2.16	5.26 ± 0.16

Table 1. Analysis of the variation of the error-square function (U), with the solvation number.

CONCLUSIONS

The description of the metal extraction reactions in the solvent extraction of Cu(II) from sulphate solutions with Cyanex 272 dissolved in toluene was accomplished by determination of the number of chemical species present in the organic phase by following the changes in the VIS-NIR spectra and a preliminary step of the graphical and numerical treatment. The extraction process could be explained considering the formation of the species $CuL_2(HL)_2$ while previous studies of this system described the extraction of Cu(II) by the formation of two species: $CuL_2(HL)$ and $CuL_2(HL)_2$.

ACKOWLEDGEMENT

This work was supported by CICYT Project QUI-96-1025-C03 (MEC, España). We are grateful to Cytec for kindly donating Cyanex 272 and to R. Izquierdo for her collaboration in the work.

REFERENCES

1. Ritcey GM and Ashbrook AM, '*Solvent Extraction to Process Metallurgy*, Part 1, Elsevier BV, Toronto, (1984).
2. Menon SK and Agrawal YK, *Reviews in Analytical Chemistry*, **XI**(3-4), 1509, (1992)

3. Tavlarides LL, *Sep. Sci. Tech.*, **22**, 581, (1987).
4. Kowalski BR, *'Process Analytical Chemistry'*, Blackie Academic & Professional, Glasgow, (1996).
5. Tauler R, *Chemom. Intell. Lab. Syst.*, **30**, 133, (1995).
6. Tauler R, Smilde A and Kowalski BR, *J. Chemom.* , **9**, 31, (1995)
7. Tauler R, Fleming S and Kowalski BR, *Anal. Chem.*, **65**, 2040, (1993).
8. Malinowski ER and Howery DE, *'Factor Analysis in Chemistry'*, Wiley, New York, (1991).
9. Tauler R, Smilde A and Kowalski BR, *J. Chemom.*, **9**, 31, (1995).
10. Tauler R, Izquierdo-Ridorsa A and Casassas E, *Chemom. Intell. Lab. Syst*, **18**, 293, (1993).
11. Liem, D.H., *Acta Chem. Scand*, **25**, 1521, (1971)
12. Matlab, Math Works, Natick, MA, (1993).
13. Cortina, J.L., *Ph D Thesis*, Universitat de Barcelona, (1992).
14. Sastre AM, Miralles N and Figuerola E, *Solv. Extr. Ion Exch.*, **8**, 597, (1990).

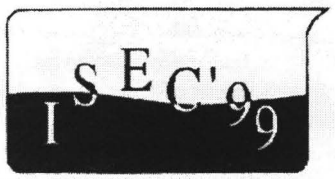

CO-CURRENT EXTRACTION: DESIGN OF INDUSTRIAL EQUIPMENT BY SCALING-UP LABORATORY TESTS

V Alessi, A Franzoni, C Gradella and R Penzo
Enichem, Centro Ricerche, Via Taliercio 14, 46100 Mantova, Italy
MJ Slater
University of Bradford, Bradford, W.Yorks. BD7 1DP, UK

ABSTRACT
The kinetics of co-current liquid-liquid extraction in pipes have been studied by laboratory experiments with streams sampled from a caprolactam and a phenol industrial plant. Whatever the set of experimental conditions a dependency of degree of extraction on energy input has been found. There are constraints on operating conditions imposed by entrainment problems and minimum flow rates for creating a dispersion. Equations given by Calderbank and Newman were used to calculate film mass transfer coefficients which, in addition to contact time, drop size and extraction factor, were used to obtain theoretical values of degree of extraction. Such values are conservative with respect to experimental data. Scale-up is based on drop size estimation to give suitable pipe diameter and velocity, and small-scale threshold energy consumption required to reach equilibrium (at the chosen velocity) to give pipe length.

Keywords: toluene/cyclohexanone oxime/water, aromatics/phenol/water, phenol cleavage stream/ acetone-carboxylic acid salts/water, co-current extraction, mass transfer, scale-up.

INTRODUCTION

Although the industrial application of co-current extraction is in some cases very attractive, the literature on this topic, mainly concerning the scale-up from laboratory tests, is very poor. The performance of co-current extraction is limited by the equilibrium distribution of the solute. Therefore its application in industrial processes is useful in cases of favourable partition equilibria or high solvent/raffinate ratios, the advantage being the possibility of avoiding throughput limitations caused by hydrodynamic problems, of operating with high superficial velocities and small residence times, and of reaching the requested performance in simple equipment of reasonable size. Co-current plant can be used to extend the performance of existing plants by contacting an entering stream with an effluent stream.

Usually the kinetics of the mass transfer process are very fast in systems typical of petrochemical processes and a contact time in the range from a few seconds to a few tens of seconds is sufficient to reach equilibrium so that in several cases mixing the phases in the existing pipes of the plant is practicable.

Different sets of experimental conditions can heavily influence the successive steps of phase settling and solute recovery, and therefore the economics of the process, because of possible problems due to entrainment, emulsion formation, or undesired co-extraction of other solutes present in the system.

It is useful to evaluate by laboratory tests how the parameters influencing the kinetics of mass transfer impact on the degree of extraction and, by comparing different sets of experimental conditions giving similar performance, to be able to scale-up the extraction equipment. Unfortunately little work has been done on this topic and no rule is available in the literature to size industrial co-current extractors from laboratory experimental data.

Recently we have faced the problem of co-current extraction for solute recovery both in caprolactam and phenol processes and have tried to obtain a better understanding of the kinetics of the mass transfer process in these two cases by laboratory experiments to allow sizing of industrial equipment.

© 2000 Society of Chemical Industry

EXPERIMENTAL

Glass tubes were used as in-line mixers in our laboratory rig so that it was easy to vary drop size, contact time and linear velocity by simply changing diameter and length of the tube in addition to variation of flow rates. The tube diameters were 2.5 mm to 11 mm and velocities were 0.20 m/s to 3.9 m/s. In glass pipes drop size evaluation by image recording and processing is possible. The dispersed phase injector was co-axial to the mixing pipe and allowed almost the same linear velocity of the continuous phase to be obtained to avoid chaotic initial contact. The raffinate and the solvent phase were weighed and fed by pumps. At the end of the pipe, the streams were collected in a settler, separated, weighed, and analyzed. The evaluation of the Hausen extraction efficiency [1] is possible by measuring the inlet and outlet solute concentration and knowing the equilibrium distribution. It is important to do some preliminary tests to evaluate the useful range for linear velocity and its correlation with drop size, because too small drops could compromise the separation of phases in the settler.

The system *water/cyclohexanone oxime/toluene* (system A) with the raffinate from the industrial caprolactam plant and the systems *sulphatic aqueous solution/phenol/aromatic hydrocarbons* (system B) and *clevage product/acetone-salts of organic acids/water* with raffinate and solvent from the industrial phenol plant (system C), were studied. Physical properties and main experimental conditions are reported in Table 1.

System	Raffinate	Solute	Solvent	R	$\Delta\rho$ (kg/m^3)	γ (N/m)	U (m/s)	θ (s)
A	water	oxime	toluene	0.08-5.0	127	$19\cdot 10^{-3}$	0.4-2.6	0.2-7.7
B	water	phenol	organic(1)	0.3-5.0	290	$19\cdot 10^{-3}$	0.8-3.9	0.1-1.4
C 1	water	acetone	organic(2)	0.06-0.12	26	$1.5\cdot 10^{-3}$	0.2-1.0	0.5-50
C 2	organic	RCOONa	water	8.3-16.7	26	$1.5\cdot 10^{-3}$	0.2-1.0	0.5-50

(1) Main components: cumene and α-methylstyrene.

(2) Cleavage product of a phenol plant containing mainly acetone, phenol, cumene, α-methyl-styrene.

Table 1 Physical properties of the streams and main experimental conditions

Systems A and B are characterized by a significant difference of density and a high value of the interfacial tension so can tolerate high linear velocities (up tp 4 m/s in the laboratory pipes), and consequently small drop size, with no problem of separation in the settler. In contrast, system C shows entrainment problems when the linear velocity reaches values of about 0.5 m/s. In this system a cross mass-transfer operates because of the presence of two solutes: acetone (solute 1) is transferred from water into the organic phase and Na salts of organic acids (solute 2) from the organic phase into water.

Laboratory tests were performed at room temperature varying pipe diameter, pipe length, flow rates and phase ratio.

RESULTS AND DISCUSSION

As the flow of a fluid through a pipe and fluid dynamic conditions are associated with a pressure difference Δp over the length of the pipe, it is useful to relate the operating parameters (the volumetric flow rate F and the pipe length and diameter, L and D) and the physical properties of the

fluids (density ρ and viscosity μ) using the the power input P required to pump the liquids through the whole pipe divided by the flow rate F, corresponding to the energy consumption per unit volume:

$$|\Delta p| = P/F \tag{1}$$

The pressure drop and the Reynolds number are linked to the Fanning friction factor, hence

$$|\Delta p| = (32 \cdot \rho \cdot U^2/Re) \cdot L/D = 32 \cdot \mu \cdot U \cdot L/D^2 \quad \text{(laminar)} \tag{2}$$

$$|\Delta p| = 0.158 \cdot Re^{-0.25} \cdot \rho \cdot U^2 \cdot L/D \quad \text{(turbulent)} \tag{3}$$

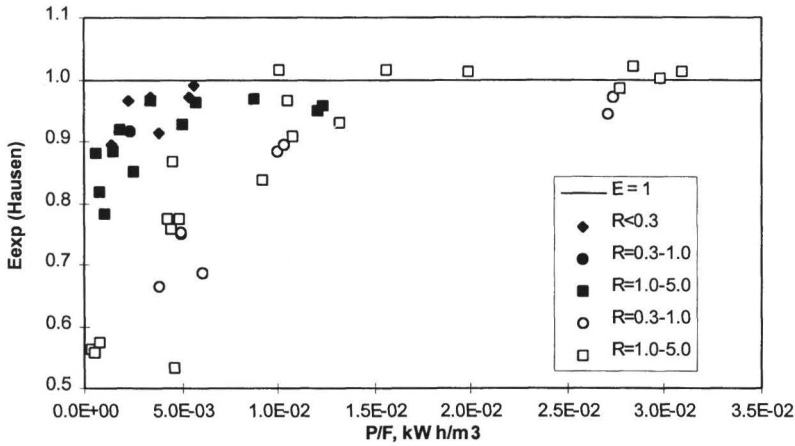

System A = black marks, System B = empty marks

Figure 1. Power input per unit flow rate for System A and B

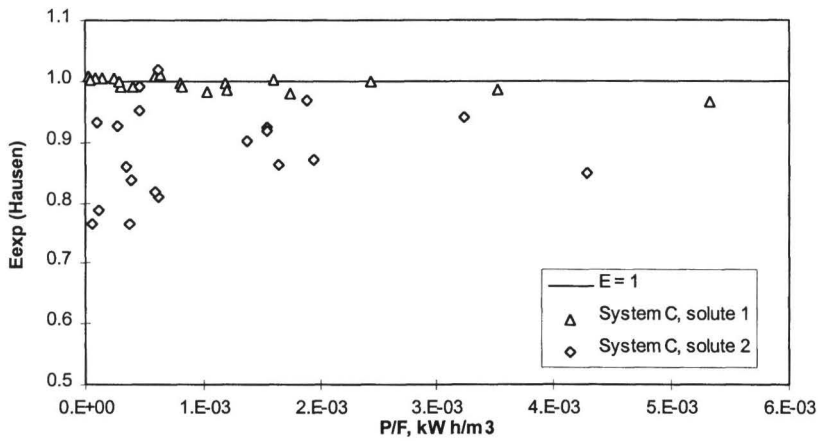

Figure 2. Power input per unit flow rate for System C

RESULTS

Figures 1 and 2 show the variation of the experimental values of degree of extraction for increasing values of the power input per unit flow rate for systems A and B and for system C respectively.

With the exception of acetone extraction in system C, which reaches the equilibrium value so rapidly that it is impossible to detect a trend, the graphs show that the degree of extraction increases as P/F increases to the point of equilibrium, with a noticeable effect of flow ratio, and significant differences in energy consumption for the systems A, B and C.

If we consider that a power per unit volume of about 0.2 to 2 kW/m^3 is typical in stirred tanks (in which large residence time must be considered) it is possible to make comparison between the two mixers in terms of cost of energy used per unit of product.

THEORETICAL APPROACH

We have tried to explain the experimental values of the efficiency obtained with the three systems by using the mass transfer coefficients. Considering a slice of mixer having a volume $dV=\pi \cdot D^2 \cdot dL/4$ characterized by a specific interfacial area a the rate equation becomes

$$\phi \cdot dV \cdot dc_d/dt = K_{od} \cdot a \cdot dV \cdot (c_{de} - c_d) \quad (4)$$

and taking into account the material balance for the in-line mixer (Eq. 5), the equilibrium equation for the solute distribution (Eq. 6), the extraction factor (Eq. 7) and the definition of Hausen efficiency (Eq. 8)

$$F_d \cdot (c_{dIN} - c_d) = F_c \cdot (c_c - c_{cIN}) \quad (5)$$

$$c_{de} = m \cdot c_c \quad (6)$$

$$\lambda = m \cdot F_d/F_c \quad (7)$$

$$E = (c_{dOUT} - c_{dIN})/(c_{de} - c_{dIN}) \quad (8)$$

we obtain the equation (Eq. 9)

$$dc_d/dt = (K_{od} \cdot a/\phi) \cdot (\lambda \cdot c_{dIN} - (1 + \lambda) \cdot c_d + m \cdot c_{dIN}) \quad (9)$$

which when integrated from 0 to the total contact time θ necessary to reach the final concentration c_{dOUT}, assuming K_{od}, K_{oc}, a and ϕ independent of time, allows the efficiency to be obtained as a function of K_{od}

$$E = 1 - \exp[\, -6 \cdot K_{od} \cdot \theta \cdot (1 + \lambda)/d \,] \quad (10)$$

or K_{oc}

$$E = 1 - \exp[\, -6 \cdot K_{oc} \cdot \theta \cdot (1 + \lambda)/(m \cdot d) \,] \quad (11)$$

By evaluating the film mass transfer coefficients and using the two film theory K_{od} and K_{oc} can be determined. For the continuous phase film coefficient the Calderbank and Moo-Young [2] equation was used; for the dispersed phase film coefficient the Newman [3] equation was used, assuming that very small drops behave as rigid spheres. A time-averaged value was used in the integration. To evaluate drop size the Kubie and Gardne [4] equation for empty pipes (Eq. 12) and Streiff [5] equation for pipes with structured packing (Eq. 13) can be used to obtain the maximum drop size d_M (d_{32} is about 0.5 d_M) or d_{32} directly:

$$d_M/D = 1.518 \cdot We^{-0.6} \cdot Re^{0.1} \quad (12)$$

$$d_{32}/d_h = 0.21 \cdot We^{-0.5} \cdot Re^{0.15} \quad (13)$$

DISCUSSION

Figure 3 shows the parity diagram between calculated and experimental Hausen efficiencies. The calculated values are in general lower than obtained experimentally and so are safe predictions. The approximations introduced (d_{32} evaluation, independence of K_{od}, K_{oc}, a, ϕ and m of time in the integration, possible presence of some entrance effect) have therefore to be questioned individually

before better prediction methods can be offered. The possible coalescence and redispersion of drops as experienced in stirred tanks is one possible source of much higher mass transfer coefficients than estimated but this process is not very amenable to modelling. The unsteady-state nature of drop formation and uncertain entry effect on hydrodynamics and mass transfer needs much more study.

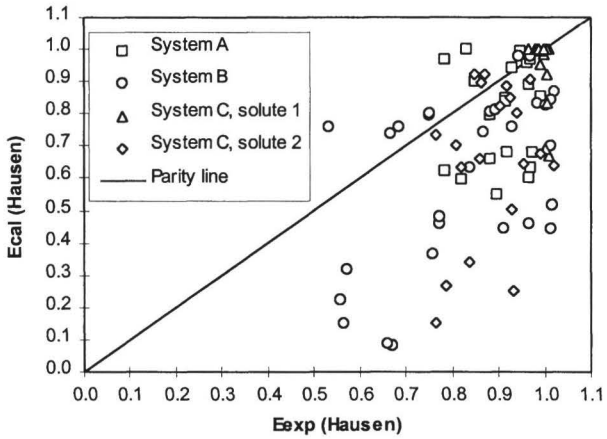

Figure 3. Comparison between experimental and calculated efficiency

With systems A and B turbulent flow was realized in most tests (Re in the range 2200-15000); with system C laminar flow was, in general, obtained (Re < 2400).

By image recording, a good distribution of the dispersed phase on the cross section of the pipe was always found at the velocities used.

By image recording and processing d_{32} values were determined. At the moment, with only very few images processed, the Streiff equation (13) is preferred in spite of the absence of any packing inside the pipes of the laboratory rig. For tests with laminar flow (system C) equation (13) was also used to evaluate d_{32} because no equation for laminar flow in empty pipes was found in the literature.

For all the laboratory experiments a dependence of extent of mass transfer on P/F has been found. Independently of which parameter is varied to increase power, efficiency steadily increases as P/F increases, asymptotically tending to unit value.

The threshold of P/F beyond which degree of extraction is at its maximum value has been evaluated for the four extraction processes (Figures 1 and 2): around 5 $W \cdot h/m^3$ for systems A, 15 $W \cdot h/m^3$ for systems B, and 2.5 $W \cdot h/m^3$ for solute 2 of system C; for solute 1 of system C mass transfer is so fast that no threshold was found.

For the industrial equipment pipe diameter and linear velocity are chosen to obtain an average drop size similar to that used on the small scale, such as to avoid or minimize entrainment/emulsion problems as noted in the laboratory work. The length of the pipe is evaluated on the basis of the minimum length (at a chosen velocity and phase ratio) required to give threshold power input per unit flow rate determined from the laboratory tests. Because of the large diameter of the industrial pipe, a turbulent regime is usually operating. If any problems of distribution of the dispersed phase arise, or if smaller drops are desired to increase interfacial area, a structured packing can be inserted into the pipe and the hydraulic diameter of the packing and Eq. (13) should be used in evaluating Re and drop size. In this case a hydraulic diameter close to that of the laboratory pipe (e.g. d_h = 10 mm) can be chosen that would reduce risks related to scale-up.

Co-current equipment sized in accordance with the rules described above is operating in the EniChem phenol plant in Mantova (Italy). The equipment gives the expected performance both in acetone and salts cross-extraction (system C). A co-current extractor for the recovery of cyclohexanone oxime (system A) has been sized for the EniChem caprolactam process based on

"Amoximation" tecnology.

CONCLUSIONS

Scaling-up a co-current extractor has been carried out using the correlation between the efficiency of the mass transfer process and the power input on flow rate applied to the pipe, and equations for drop size prediction. A threshold of P/F to obtain equilibrium partition is determined. Pipe diameter and linear velocity are chosen to give a suitable drop size and pipe length is chosen using the small-scale threshold power on flow rate data. Industrial equipment sized in accordance with these scale-up rules has given the required performance. A theoretical approach based on the two film coefficients method to correlate degree of extraction to raffinate overall mass transfer coefficient has been tried. The comparison of experimental and calculated efficiencies shows that performance is better than predicted: much more work is needed to develop better fundamental methods of design.

NOMENCLATURE

Standard Nomenclature is used except for the following:

E	efficiency
p	pressure
P	power input
R	raffinate/solvent flow ratio

GREEK

θ	contact time

SUBSCRIPTS

e	equilibrium
h	hydraulic
M	maximum

REFERENCES

1. Lo TC, Baird MHI and Hanson C, Ed ."*Handbook of solvent extraction*", Wiley & Sons,184, (1983).
2. Calderbank FH and Moo-Young M, *Chem. Eng. Sci.*, **16**, 39, (1961).
3. Newman AB, *Trans. Am. Inst. Chem. Engrs.*, **27**, 203, (1931).
4. Kubie J and Gardner GC, *Chem. Eng. Sci.*, **32**, 195, (1977).
5. Streiff F, *Sulzer Technical Review*, **3**, 108, (1977).

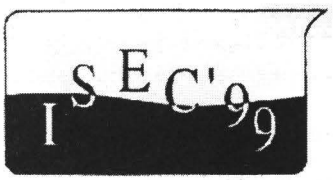

INFLUENCE OF CONTINUOUS PHASE FLOW FIELD AND COMPARTMENT GEOMETRY ON DROPLET BREAKAGE IN ROTATING DISC CONTACTORS

G Modes and H-J Bart
Universität Kaiserslautern, Lehrstuhl für Thermische Verfahrenstechnik, Gottlieb-Daimler-Straße, 67653 Kaiserslautern, Germany

ABSTRACT
This paper presents the investigation of the influence of compartment geometry and continuous phase flow structure on the breakage of droplets in Rotating Disc Contactors (RDC). The observations lead to the result, that the breakage mechanism can be characterised by correlating the ratio of destroying to resistive forces. Additionally, a change in the macroscopic flow structure of continuous phase due to a change in compartment geometry will influence the breakage probability of the dispersed phase markedly. Experimental and simulated column results, using that new correlation in a droplet population balance model (DPBM), will be given.

Keywords: droplet breakage, fluid dynamics, Rotating Disc Contactors

INTRODUCTION

Since the beginning of the sixties, the development of the DPBM constituted a considerable advance in the theoretical analysis of solvent extraction columns.[1,2] If interdroplet coalescence could be neglected, a volume or mass balance for droplets of diameter d ± δd/2 leads to the following population balance equation (PBE):[3]

$$\frac{\partial P(t,z,d)}{\partial t} = v_d \frac{\partial P(t,z,d)}{\partial z} + D_d \frac{\partial^2 P(t,z,d)}{\partial z^2} - g(t,z,d)P(t,z,d) + \int_0^{d_{max}} \beta(d_0,d)\, g(t,z,d)\, P(t,z,d)\, \delta d \qquad (1)$$

The function P(t,z,d)δd is the volume fraction of drops of diameter between d ± δd/2 at column height z at time t. The first term at the right hand side of equation (1) represents the transport of droplets due to drop diameter depended rising velocity v_d, the second part describes the axial dispersion. The third term describes the loss of droplets with size d ± δd/2, whereas the win due to breakage is given by the last integral term. The problem with equation (1) are the droplet size dependent parameters (e.g. the breakage frequency g(d) and the daughter droplet size distribution β(d_0,d)), which have to be determined with high experimental effort.

DROPLET BREAKAGE IN STIRRED COLUMNS

Drops break into several smaller drops due to the turbulent structure of the flow pattern and column internals. This situation has been extensively studied in stirred tanks.[4] Based on this assessment Cruz-Pinto and Korchinsky[5] proposed expressions for the breakage frequency and the daughter droplet distribution in a RDC. Unfortunately they found, that the free parameter in the given equations vary substantially with the working conditions of the column. A more fundamental work on single droplet breakage in a RDC is from Bahmanyar et al.[6] and Cauwenberg et al.[7,8] They studied single droplet breakage and gave empirical correlations for the breakage probability p. It has been proposed that the ratio between the fractions of broken and of non-broken droplets should be correlated as a function of a modified drop Weber number (We_m). According to Cauwenberg[7] this reads for a column with diameter 0.152 m and laminar conditions as to:

$$\frac{p}{1-p} = 0.258 \cdot We_m^{1.16} \qquad (2)$$

© 2000 Society of Chemical Industry

The Weber number represents the ratio of the shearing forces to the resistive surface forces. In addition Bahmanyar[6] proposed the following expression for the daughter droplet probability density:

$$\beta(d_0,d) = 3x_m(x_m-1)\left[1-\left(\frac{d^3}{d_0^3}\right)\right]^{(x_m-2)}\frac{d^5}{d_0^6} \qquad (3)$$

with x_m as the average number of daughter droplets being produced in case of the breakage of a mother droplet with diameter d_0. It depends on number of revolutions, components and geometry.

EXPERIMENTAL

The comparison of simulations based on equation (1) and experimental hold-up and droplet size distributions for a pilot plant RDC lead to the result, that the given correlations are not applicable to an altered geometry under counter-current flow conditions.[9] Due to this, single droplet breakage was investigated with an experimental set up, which allows the change of compartment height, rotor diameter and stator inner diameter for a single RDC-compartment. The diameter of the column is 0.15 m (0.152 m [6,7,8]). The geometry for the presented observations is as follows: the rotor diameter is 0.09 m (0.101 m [6,7,8]), the shaft diameter 0.054 m (0.015 m [6,7,8]), the stator inner diameter 0.105 m (0.11 m [6,7,8]) and the height of the compartment is 0.03 m (0.076 m [6,7,8]). It should be accentuated, that, compared with Cauwenberg[7,8] and Bahmanyar,[6] this geometry has a much smaller free area between shaft and stator and that the ratio of compartment height to column diameter is more than two times smaller. This is important, since the authors pointed out, that the given correlations remain to be tested especially for that geometry.

In each experimental run about 2000 mono-dispersed droplets are produced continuously 0.4 m below the compartment. Within the distance between droplet production and compartment entrance, droplets reach the stationary rising velocity and enter the compartment with a superimposed rotational movement. In the compartment a varying fraction of droplets break. This modified experimental method, compared with Cauwenberg,[8] was used since it represents the real droplet behaviour in the column in a more realistic way. If breakage occurs, it happens always at the edge of the rotor blade, a fact which has been also reported by Cauwenberg.[8] In each case the breakage produced outlet distribution is measured at the top of the equipment by a so-called capillary method.[10] With the assumptions that breakage occurs only once at the edge of the rotor the population balance (1) for one compartment and for stationary conditions may be reduced to the following form :

$$P(d)_{IN} - P(d)_{OUT} = \int_0^{d_{max}} \beta(d_0,d)\cdot p(d)\cdot P(d)\delta d_0 - p(d)\cdot P(d) \qquad (4)$$

The breakage probability and the daughter droplet distribution can be determined with an optimisation procedure, using the experimental compartment outlet distributions to evaluate x_m in equation (3).

The varied values are: the mother droplet diameter, the rotor speed, the rotor diameter and system dependent parameters like density, interfacial tension and viscosity. The two investigated extraction systems are the saturated test systems toluene-water and butyl acetate-water.

RESULTS

Figure 1 depicts the change of breakage probability of different sized toluene droplets with agitation. In the observed range between $2.1\cdot10^{-3}$ and $4\cdot10^{-3}$ m a strong increase of breakage probability appears with increasing droplet size and rotational speed. The dotted lines are the linear fitting curves

for each droplet size. The solid line represents a correlation given by Bahmanyar,[7] which is restricted to revolutions below 4.17 s^{-1} and to a bigger rotor diameter and compartment height. This explains the fact that the correlation results in too small values compared to the experimental ones, but gives the correct trend. In addition to this, the mean number of breakage produced droplets x_m in equation (3) is estimated. The value of this parameter was equal to 2 for the agitation range between 4.17 and 6.67 s^{-1} for all the droplet diameters investigated. Between 6.67 and 8.33 s^{-1} it increased up to 2.4 for the bigger droplets. The comparison with the correlation given by Bahmanyar[7] was again insufficient.

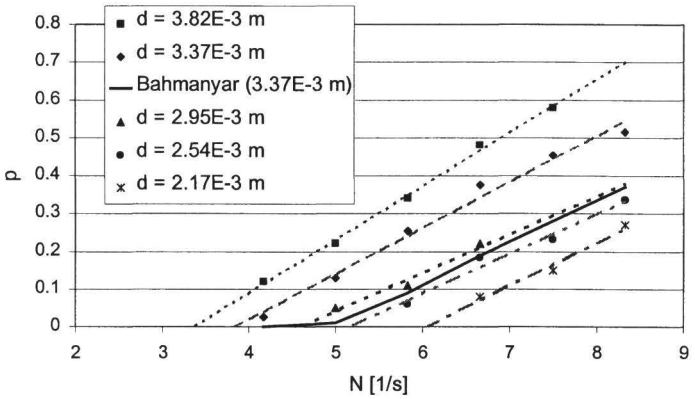

Figure 1: Breakage probability for different droplet diameters vs. rotational speed

The critical rotational speed is the minimum of agitation for which a droplet of given size is stable. The value of this characteristic parameter can be determined in two ways: first from the linear extrapolation of the experimental results to zero breakage probability,[11] and second from the fitting of a equation of type (2) to experimental results[7] with the critical rotor speed, the preconstant and the exponent as the varied parameters. The results of both procedures are depicted in Figure 2.

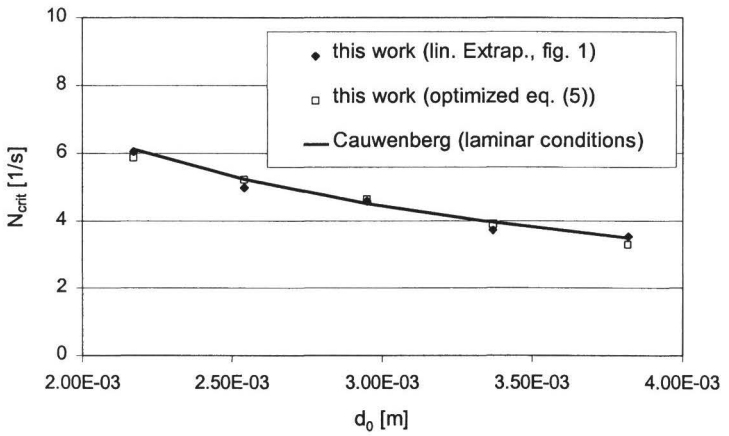

Figure 2: Critical rotor speed vs. mother droplet diameter

It can be seen that the experimental values are in good agreement with the proposed correlation. Considering the deviations in the breakage probability, this result seems to be surprising. This fact must be explained with the macroscopic flow patterns change due to the different compartment geometry. Since the critical parameter depends only on the shearing forces at the edge

of the rotor blade the smaller compartment height and stator free surface have no influence. The strong increase of the breakage probability in this work (see Figure 1) in comparison to literature must then result from a higher probability for the appearance of the drops in the region, where the shear forces are big enough to destroy them. Very encouraging is the fact, that it was possible to fit our experimental results with a correlation of the type of equation (2) with nearly the same exponent as reported by Cauwenberg.[8] Only the preconstant changed due to the different compartment geometry. For all the data points we found the following expression:

$$\frac{p}{1-p} = 9.69 \cdot We_m^{1.2} \qquad (5)$$

The consistency between the critical parameter and between the exponents in equations (2) and (5) supported the assumption, that the breakage mechanism itself can be described with the idea of relating force ratio to the ratio of breaking and non-breaking drops. In addition the influence of geometry and macroscopic flow structure has to be considered, since the real breakage rate of droplets is mainly governed by the probability of presence in the shear region at the edge of the rotor. First single particle fluid dynamics simulations lead to the result, that the probability of appearance in the shear field increases for each droplet with increasing continuous phase flow rate.[13] Due to this it is indispensable to realise also experiments under counter-current conditions.

Figure 3 illustrates the comparison between experiment and DPBM-simulation for a pilot plant RDC with the same geometry as described above. The active height of this column is 1.5 m, the continuous phase flow rate is 60 dm^3/h and the dispersed phase flow rate is 56 dm^3/h. The breakage probability is calculated with equation (5), v_d and D_{ax} in equation (1) are taken from single droplet experiments.[9]

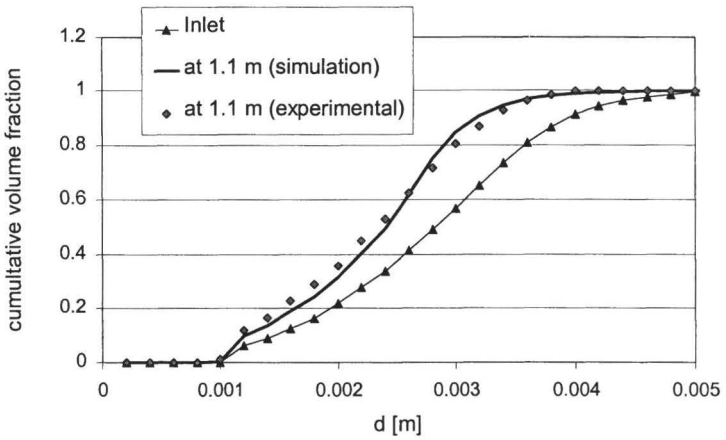

Figure 3 : Cumultative volume distribution in a pilot plant RDC for N = 5 s^{-1}

The numerical treatment of equation (1) is discussed elsewhere.[3] It can be seen, that the evolution of the droplet size distribution along the column axis is predicted very well applying the modified breakage correlation.

CONCLUSIONS

Single droplet observations have been realised to investigate the influence of compartment geometry and continuous phase flow regime on the breakage of droplets in a Rotating Disc Contactor. It has been shown, that the known correlations have to be extended to the influence of compartment height, stator free area and continuous phase flow, since the breakage probability is in strong

dependency of the path of each droplet throughout the compartment. For the changed geometry a modified correlation for the calculation of breakage probability has been proposed. It has been shown that the DPBM based simulation of the mentioned pilot plant RDC with the new correlation is in good agreement with experimental results.

NOMENCLATURE

D_R	rotor diameter [m]
d	droplet diameter [m]
g(d)	droplet breakage frequency [s^{-1}]
N	revolution [s^{-1}]
P(t,z,d)	probability density for droplet with diameter d at height z at time t [m^{-1}]
$P(d)_{IN}$, $P(d)_{OUT}$	compartment inlet- or outlet-distribution [m^{-1}]
p	breakage probability
t	time [s]
We_m	modified Weber number [$We_m = (\rho^{0.5} \mu^{0.5} D_R d (N^{1.5} - N_{cr}^{1.5})/\gamma)$]
x_m	average number of produced daughter droplets
z	column height [m]
$\beta(d_0,d)$	daughter droplet volume probability density [m^{-1}]

REFERENCES

1. Valentas KJ and Amundson NR, *AIChE J.*, **5** , 533, (1966)
2. Casamatta G and Vogelpohl A, *Ger. Chem. Eng.*, **8** , 96103, (1985)
3. Kronberger T, Ortner A, Zulehner W and Bart H-J., *Computers Chem. Engng.*, **19** , 634, (1995)
4. Coulaloglou CA and Tavlarides LL, *Chem. Eng. Sci.*, **32**, 1289, (1977)
5. Cruz-Pinto JJC and Korchinsky WJ, *Chem. Eng. Sci.*, **36**, 687, (1981)
6. Bahmanyar H and Slater MJ, *Chem. Eng. Technol.*, **14**, 79, (1991)
7. Cauwenberg V, Degreve J and Slater MJ, *Can. J. Chem. Eng.*, **75**, 1046, (1996)
8. Cauwenberg V, Van Rompay P, Mao Z-Q and Slater MJ. in *Proc. ISEC'93,York (UK)* Ed Logsdail DH and Slater MJ, Elsevier Science, 421, (1993)
9. Modes.G, Bart H-J, Bröder D and Rodriguez D, *Chem. Eng. Tech.*, (1999) (in prep.)
10. Pilhofer T and Miller H-D, *Chem. Ing. Tech.*, **44**, 295, (1972)
11. Haverland H and Vogelpohl A, *Chem. Ing. Tech.*, **60**, 541, (1988)
12. Modes G and Bart H-J, *Paper at CHISA'98*, Prague (1998)
13. Rodriguez D, *Diploma work*, Universität Kaiserslautern (1998)

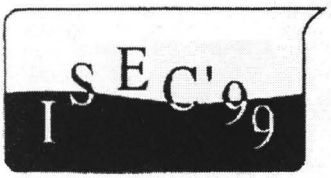

MASS TRANSFER PERFORMANCE IN A PULSED SIEVE PLATE EXTRACTION COLUMN

GS Luo, HB Li, WY Fei and JD Wang
Department of Chemical Engineering, Tsinghua University, Beijing 100084, China

ABSTRACT
Mass transfer experiments were carried out in a pulsed-sieve-plate extraction column (PSEC) of 150mm diameter with a working system of 30%TBP (in kerosene) - nitric acid - water. The mass transfer and axial mixing coefficients were evaluated from the measured solute concentration profiles and by the dynamic stimulus-response process. The experimental data of diffusional height of transfer unit from the two methods were correlated and a semi-empirical correlation was developed for predicting the mass transfer performance in PSEC. In this equation the influence of the column diameter was considered. The values of apparent height of transfer unit predicted by $(HTU)_{ocp} = (HTU)_{oc} + (HTU)_{ocd}$ were compared with the experimental data, which showed they fit very well.

Keywords: TBP/nitric acid/water, sieve-plate column, mass transfer, axial mixing, transfer unit

INTRODUCTION

As mentioned in previous work,[1,2] knowledge of extraction columns is not completely clear and data of the mass transfer coefficient in the pulsed sieve plate extraction column are still lacking. A great deal of experimental effort has been expended principally for the purpose of evaluating column performance. For design and engineering, up to now, it is still necessary to find some simple semi-empirical correlations for the prediction of mass transfer performance in extraction columns, especially the correlations for large diameter columns.

The work described in this paper studies the mass transfer performance in a standard type pulsed sieve plate column of 150 mm diameter with 30%TBP(kerosene)-nitric acid-water as a working system by the concentration profile method and the dynamic process.[1,3]

EXPERIMENTAL

Experiments were carried out in an air pulsed glass column of 150 mm diameter and effective height 2 m equipped with 41 sieve plates of the standard type. A switch valve was located on the feed line for introducing the tracer acid and a sampling port located just below the bottom plate for collecting the raffinate samples while the experiments of dynamic process were performed. Eight sampling ports which were specially designed[4] to guarantee the purity of each phase were situated at equal distances along the height of the column. Samples of two phases were taken simultaneously from each port for concentration profile measurement under every given operation condition. The dispersed phase hold up was estimated by volumetric replacement method. All the materials were purchased from Beijing chemical plant. TBP and nitric acid were chemical grade and deionised water was used.

For the steady state method, the outlet concentration of the two phases can be obtained directly. However, for the dynamic response method it must be calculated from the three evaluated parameters and the dynamic diffusion mass transfer model. Then the apparent and diffusional height of transfer unit can be calculated from the following the equations.

$$(HTU)_{oc} = \frac{U_c}{k_{oc}a} = \frac{H}{(NTU)_{oc}} \tag{1}$$

© 2000 Society of Chemical Industry

$$(HTU)_{ocp} = \frac{H}{(NTU)_{ocp}} = \frac{H}{\int_{x_r}^{x_f} \frac{dx}{x - x^*}} \tag{2}$$

$$(HTU)_{ocd} = (HTU)_{ocp} - (HTU)_{oc} \tag{3}$$

RESULTS AND DISCUSSION

Diffusional height of transfer unit, $(HTU)_{ocd}$

The influence of operation conditions on $(HTU)_{ocd}$ is plotted in figure 1. It can be seen that $(HTU)_{ocd}$ depends on the two phase flow rate and the pulse intensity. With an increase of pulse intensity, the diffusional height of transfer unit is increased slowly. However, $(HTU)_{ocd}$ will decrease quickly when the dispersed phase flow rate is increased. It is very difficult to see the influence of the continuous phase flow rate on $(HTU)_{ocd}$. The reason is when the pulse intensity is increased, the degree of axial mixing is increased, but the dispersed phase hold-up will increase at the same time. These two effects determine that $(HTU)_{ocd}$ will not change seriously as the pulse intensity is increased. When the dispersed phase flow rate is increased, the hold-up will increase quickly, then the axial mixing coefficient will decrease, and $(HTU)_{ocd}$ decreases quickly. From the figure, it may be concluded that the diffusional height of transfer unit in PSEC is influenced by the operation conditions together. It is very difficult to study them separately. Based on this result, a semi-empirical equation in the form of equation (4) for predicting $(HTU)_{ocd}$ in PSEC is correlated from the experimental data.

$$(HTU)_{ocd} = 0.14(Af / u_c)^{0.44}(1-\phi)^{1.5}(u_c / u_d)^{0.57} \tag{4}$$

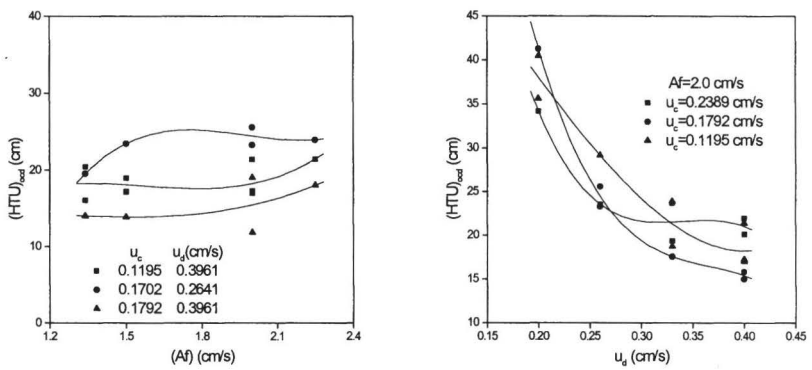

Figure 1. The influence of operation conditions on $(HTU)_{ocd}$

Figure 2 is the comparison of the calculated results by equation (4) with the experimental data. All the data from the dynamic response process and steady state method are plotted in this figure. As shown, the values calculated by equation (4) fit very well with the experimental data. It can also be seen the data from the dynamic response process are reliable. The maximum deviation is less than 30%.

Apparent height of transfer unit in PSEC

The function of the apparent height of transfer unit in PSEC vs. operation conditions are plotted in figures 3 and 4.

As generally known, the apparent height of transfer unit in PSEC is influenced by pulse intensity, physical properties of working systems, column configuration, two phase flow rates, and so on. In figures 3 and 4, it can be seen that the operation conditions influence the mass transfer performance significantly. When the pulse intensity and dispersed phase flow rate are increased, the apparent height of transfer unit is decreased. This is because the hold-up and mass transfer areas increase quickly, and mass transfer coefficients are increased.

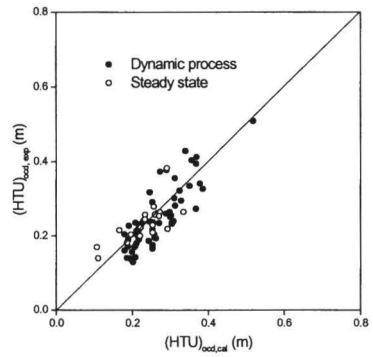

Figure 2. The comparison between experimental and the calculated values of $(HTU)_{ocd}$

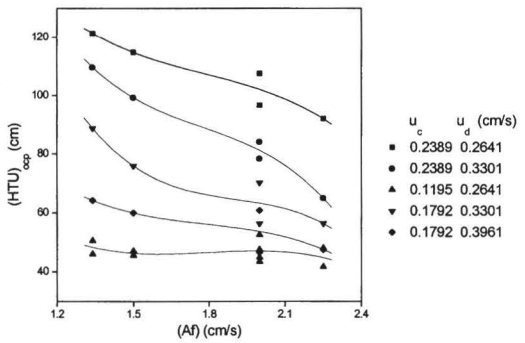

Figure 3. The influence of pulse intensity on $(HTU)_{ocp}$

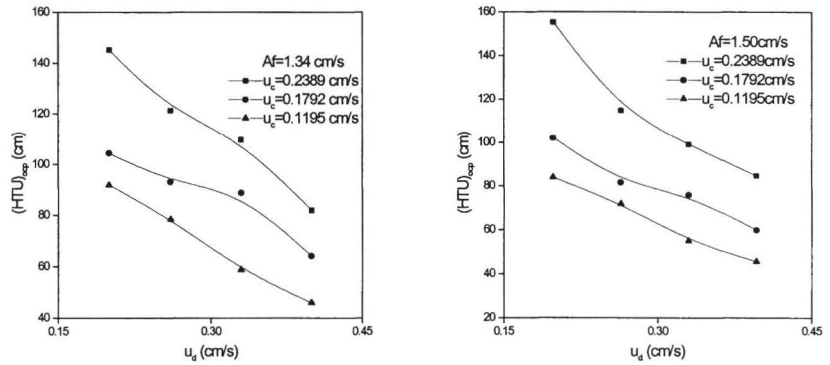

Figure 4. The influence of two phase flow rate on $(HTU)_{ocp}$

While the continuous phase flow rate is raised, the apparent height of transfer unit will increase. The reason is the "true" height of transfer unit is increased quickly according to $(HTU)_{oc} = \dfrac{U_c}{K_{oc}a}$ with the continuous phase flow rate increasing. Therefore, $(HTU)_{ocp}$ is increased with a increase of the continuous phase flow rate.

Equation (6) proposed by Miyauchi et al.[5] was used to predict the apparent height of transfer unit, and equation (5) suggested by Luo et al.[2] was used to calculate the "true" height of transfer unit. The comparison results for 150 mm and 40 mm diameter columns are plotted in figure 5, which shows that the apparent height of a transfer unit in 150 mm and 40 mm diameter column are predicted accurately by these equations. The calculated values of apparent height of transfer unit fit the experimental data well with the standard deviation of 12.4%.

$$(HTU)_{oc} = 25.86\frac{U_c}{\phi(1-\phi)^{1.5}} \tag{5}$$

$$(HTU)_{ocp} = (HTU)_{oc} + (HTU)_{ocd} \tag{6}$$

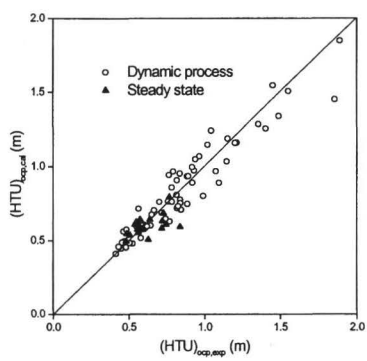

Figure 5. The comparison of experimental data with the calculated values of $(HTU)_{ocp}$

CONCLUSIONS

According to experimental results, we may conclude that it is reliable to use dynamic response to evaluate the mass transfer performance in large diameter column. In our work, the diffusional height of transfer unit and apparent height of transfer unit in PSEC can be calculated by the following semi-empirical equations.

$$(HTU)_{ocd} = 0.14(Af / u_c)^{0.44}(1-\phi)^{1.5}(u_c / u_d)^{0.57}$$

By using the following equations and the equation presented in this paper for calculation of the diffusional height of transfer unit in PSEC, the apparent height of transfer unit may be predicted accurately.

$$(HTU)_{oc} = 25.86\frac{U_c}{\phi(1-\phi)^{1.5}}$$

$$(HTU)_{ocp} = (HTU)_{oc} + (HTU)_{ocd}$$

NOMENCLATURE

A	Pulsed amplitude [m]
a	Interfacial area [m^2/m^3]
f	Pulsed frequency [1/s]
H	Effective height of column [m]
$(HTU)_{oc}$	"True" height of transfer unit [m]
$(HTU)_{ocd}$	Diffusional height of transfer unit [m]
$(HTU)_{ocp}$	Apparent height of transfer unit [m]
k_{oc}	Overall mass transfer coeff based on continuous phase [m/s]
N_{oc}, $(NTU)_{oc}$	Number of " true" transfer unit
$(NTU)_{ocp}$	Number of apparent transfer unit
U	Superficial velocity [m/s]
x	Solute conc. in continuous phase
x*	Equil conc. of solute in cont. phase
x_f	Feed solute concentration
x_r	Raffinate solute concentration
y	Solute concentration in dispersed phase
ϕ	Dispersed phase hold-up [%]

Subscripts

c	Continuous phase
d	Dispersed phase

ACKNOWLEDGMENT

We acknowledge the support of the National Natural Science Foundation of China in this work.

REFERENCES

1 Luo GS, Fei WY and Wang JD, *J. Chem. Ind. and Eng.*, **45**(5), 567, (1994)
2 Luo GS, Fei WY and Wang JD, *Proc. ISEC'96,* Melbourne, Australia, **2**, 1215, (1996)
3 Lei X,Qian Y, Fei WY and Wang JD, *Proc.ISEC'86.* DECHEMA, Munchen. **III**, 215, (1986)
4 Luo G.S., *Ph.D. Thesis*, Tsinghua Univ., Beijing, (1993)
5 Miyaucher T and Vermeulen T, *T & EC Fundam* . **2**,113, (1963)

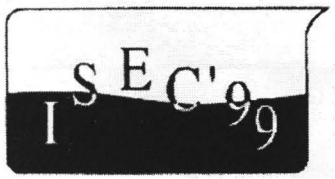

PREDICTION OF FLOODING IN RANDOM AND STRUCTURED PACKED COLUMNS USING A DRIFT FLUX METHODOLOGY

Lintong S Hutahaean, David M Schaefer, Jeffrey S Kanel[1] and Vincent Van Brunt

Chemical Engineering, Department University of South Carolina, Columbia, SC 29208, USA

[1]Technical Center, Union Carbide Corporation, P.O Box 8361 South Charleston WV 25303, USA

ABSTRACT

Two correlations for flooding in packed extraction towers for continuous phase wetting show reduced average errors when compared to others. Both correlations are derivatives of the Wallis form of flooding correlation and consistent with his drift flux theory. The first correlation $J_c^{1/2} + J_d^{1/2} = (0.705 - 0.06315 \ln(a_p/\varepsilon^2(\sigma/(\Delta\rho g))^{1/2})(0.8586 + 0.065\rho_d/\Delta\rho - 0.0064(\rho_d/\Delta\rho)^2)$ where $J_c = V_c^2\rho_c/(g\varepsilon^3/a_p\Delta\rho)^{1/2}$ and $J_d = V_d^2\rho_d/(g\varepsilon^3/ap\Delta\rho)^{1/2}$ only has general packing parameters and dimensionless variables and is suitable for all types of packing. It has an average deviation of 37% for all known flooding data.

Keywords: organic compounds/water, packed column, packings, column flooding, modelling

INTRODUCTION

Flooding in multiphase fluid systems has proceeded along different paths. For flooding in vapor-liquid systems it is assumed that the liquid will wet the solid surfaces or packing and a force balance leads to empirical correlations. In contrast, flooding in liquid-liquid systems is largely devoted to the industrially relevant case of continuous phase wetting the solid or packing surfaces. The literature for flooding in packed liquid extraction towers with continuous phase wetting includes the historical works of Dell and Pratt (1951), Sakiadis and Johnson(1954), and Watson et al.(1973).

Like the previous researchers the review papers by Kumar and Hartland (1994,1997) present previous correlations and proceed to develop their own. The Kumar and Hartland papers discuss the two approaches used to develop flooding criteria. In the first, flooding is predicted by differentiating the slip velocity equation and solving for the maximum velocity. The slip velocity is calculated from the dispersed phase holdup which, in turn, is calculated from the Sauter mean dispersed phase drop size. Empiricism is distributed in each of these steps leaving one uncertain as to how the error is passed successively from step to step. The alternative procedure is to develop a direct correlation in which the empiricism is grouped. The well known Dell and Pratt correlation is of this type. Its foundation is the application of a macroscopic energy balance on the two liquid phases.

In contrast to these processing-based approaches to flooding, the need for understanding and analysis of limiting flow behavior in nuclear reactors has led to an extensive literature to describe limiting flow behavior and flooding under a variety of flow regimes, geometries and flow orientations (see Bancroft and Lee, 1986). The two flooding limit equations are based on different physical phenomena: the first is to empirically modify an equation for wave instability in a film (Kutateladze), and the second is to empirically modify a momentum balance between the two fluid phases (Wallis). While the first is suitable for describing dispersed phase wetted flooding, it is the second Wallis analysis which appeared suitable for modeling the continuous phase wetted case. This paper summarizes the application of Wallis's drift flux theory to modeling flooding for continuous phase wetted systems in packed towers.

A second motivation for this work was that in spite of its ability to predict flooding the Dell and Pratt equation has now become limited in utility due to the small number of published empirical constant for both packing type and packing size needed for its use. Thus, a second goal of this work was to update the Dell & Pratt equation so that it could be used with the newer packings.

© 2000 Society of Chemical Industry

Chemical system			Physical properties	Range
Dispersed	Solute	Continuous	Continuous phase density, g/cm	0.79 - 1.58
Benzene	None	Water	Dispersed phase density, g/cm	0.682 - 13.6
M.I.B.K.	None	Water	Continuous phase viscosity, cP	0.58 - 15
Dibutyl carbitol	None	Water	Dispersed phase viscosity, cP	0.41 - 70
i-Octane	None	Water	Density difference ($\Delta\rho$), g/cm	0.076 - 12.6
Butyl acetate	None	Water	Interfacial tension, dyne/cm	8.6 - 375
Butyl acetate	None	Glycerol soln.		
Chlorex	None	Water		
Carbon tetrachloride	None	Water	Packing type and size	Size (cm)
Mercury	None	Water		
Mercury	None	Glycerin	Raschig rings	0.6 - 3.81
Petroleum ether-CCl_4	None	Water	Berl saddles	0.6 - 2.5
Toluene	None	Water	Lessing rings	0.635 - 1.27
Toluene	None	Glycerol soln	IMTP	2.54 - 3.81
Petroleum ether	None	Water	Solid cylinder	0.635
Gasoline	None	Water	Glass bead	0.8
Gasoline	None	Glycerol soln.	Norton 2T	
Naphtha	None	Water		
Isopar M	None	Water		
Heptane	None	Sulfolane		
Kerosene	None	Water		
Petr. solvent-CCl_4	None	Water		
Petr. solvent-M.E.K.	None	Water		
Mineral oil-petr.	None	Water		
solvent	None	Water		
Petr. solvent	None	Toluene		
Water	None	Petroleum ether		
Water	None	CCl_4		
Water	None	CCl_4		
Glycerol soln	None	Petroleum ether-		
Water	None	CCl_4		
Water	None	M.I.B.K.		
Water	None	Naphtha		
Water	None	Nitrobenzene		
Water	None	Petr. solvent		
Water	None	Petr. solvent-		
Water	None	CCl_4		
Water	None	Petr. solvent-		
Petr. solvent-CCl_4	None	M.E.K.		
Petr. solvent	None	Mineral oil		
Water	Acetone	Sugar solution		
Toluene		Sugar solution		
		Mineral oil-petr.		
		Solvent		
		Water		

Table 1. Systems and range of physical, transport, and geometrical parameters of flooding data used to develop the correlation.

CHARACTERIZATION OF DATA

All available flooding data were used to develop the correlations in this paper. The data are summarized in the following tables 1 and 2.

Table 2 shows the available data and its distribution with respect to continuous or dispersed phase wetting (CPW/DPW), with or without mass transfer (NMT/MT) and whether or not the data meets two flooding criteria. The first is whether the drop size will be sufficiently small as to not get trapped in the packing. If the drops get too large, then they will be retained in the packing and reduce the available flowfields. The second is whether the ratio of tower diameter to packing size is greater than 8, if the packing size is too great then the packing will not have an appreciable effect on the uniformity of the continuous phase flowfield. Lastly the number of datapoints that meet both criteria are shown.

	Total		Critical packing size criterion		Column to packing diameter criterion		Both Criteria	
Wetting	NMT	MT	NMT	MT	NMT	MT	NMT	MT
CPW	802	68	589	63	356	47	190	42
DPW	207	7	173	7	179	6	151	6

Note: NMT= no mass transfer; MT=with mass transfer

Table 2. Summary of all available flooding data

CORRELATION OF DATA USING WALLIS DRIFT FLUX THEORY

Wallis used a dimensionless momentum balance similar to the procedure used by Dell and Pratt to develop his equation for flooding. The general form is in terms of a dimensionless velocities of the continuous phase and dispersed phase. Figure 1 shows the correlation coordinates and all the data. Two different correlations were developed and are shown below. The first correlation only has parameters in it that are physical properties or are general packing parameters. Unlike the Dell and Pratt correlation specific empirical constants are not included for the type or size of packing. The second correlation has specific parameters for both size and shape.

As can be seen from table 3 the correlations have comparable average deviations. Table 4 shows the constants for correlation 2 along with revised Dell and Pratt constants.

Correlation 1. This model is of the general Wallis form $J_c^{1/2} + J_d^{1/2} = C$, where C depends only on the geometry and physical properties of the system. For liquid liquid systems $J_c = V_c^2\rho_c/(g\varepsilon^3/a_p\Delta\rho)^{1/2}$ and $J_d = V_d^2\rho_d/(g\varepsilon^3/ap\Delta\rho)^{1/2}$. The resulting final correlation is

$$J_c^{1/2} + J_d^{1/2} = (0.705 - 0.06315\ \ln(a_p/\varepsilon^2(\sigma/(\Delta\rho g))^{1/2})(0.8586 + 0.065\rho_d/\Delta\rho - 0.0064(\rho_d/\Delta\rho)^2)$$

The above correlation predicts that $(J_c^{1/2} + J_d^{1/2})$ decreases with $(a_p/\varepsilon^2(\sigma/(\Delta\rho g))^{1/2})$. This makes sense since a larger value of this group means a larger value of dropsize to packing size ratio, and thus, the drops will experience more resistance to flow through the packing. The major advantage of this correlation is that it includes the packing characteristics in terms of the specific surface area and void fraction so it can be used for all types of packing. However, the prediction for data of Mackowiak was poor. Most of Mackowiak data have slopes lower than -1 on $J_c^{1/2}$ versus $J_d^{1/2}$ (steeper than the others), for data with stacked bialecki packing the slope is close to -2. Also none of his data meet the column to packing ratio criteria. Large departure of slope from -1 is most probably

because of the geometry of the bialecki packing that has relatively small openings compared to other types of packing. This is particularly true for a tube column with stacked bialecki packing where for small dispersed phase flow the drops tend to move along the wall of the packing where the continuous phase velocity, due to wall effect, is slower. The prediction for stacked bialecki is much improved if the second term in equation 20 ($J_d^{1/2}$) is multiplied by 1.9 so for this case the correlation is:

$$J_c^{1/2} + 1.9J_d^{1/2} = (0.705 - 0.06315 \ln(a_p/\varepsilon^2(\sigma/(\Delta\rho g))^{1/2})(0.8586 + 0.065\rho_d/\Delta\rho - 0.0064(\rho_d/\Delta\rho)^2)$$

Investigator	Type of packing whose constant: a) Given in the original work b) Determined in this work	% of data	Average Deviation, %			
			Dell and Pratt	Kumar and Hartland	Corr. 1	Corr. 2
Dell and Pratt	a) Raschig rings, Berl saddles, Lessing rings	79.2	41.9	35.5	34.6	35.2
	b) Bialecki, Stacked bialecki, Solid cylinder, Fillip, Glass bead, Hiflow, Montz,	20.8	49.6	88.1	47.6	45.1
Kumar and Hartland	IMTP, Norton 2T, Pall rings	97.5	43.7	45.6	37.4	37.4
	a) Raschig rings, Berl saddles, Lessing rings, Bialecki, Stacked bialecki, Glass bead, Montz, IMTP, Norton 2T, Pall rings					
	b) Solid cylinder, Fillip, Hiflow	2.5	28.0	31.1	23.3	26.9
All data	All the above types of packing	100	43.2	45.2	37.0	37.1

Table 3. Comparison of correlations using fractionated data. Average deviation is the average relative error in predicting dispersed phase velocity.

Correlation 2. This model took the Wallis form; however the slope was allowed to deviate from -1. This model also was consistent with that of Dell and Pratt.

$$J_c^{1/2} = C_1 - C_2 J_d^{1/2}$$

C_1 and C_2 were assumed to be function of the dimensionless group developed from the dimensional analysis performed. Thus, a similar method to the previous model was applied to obtain the expression for C_1 and C_2. From the multiple least squares regression it appeared that only the following dimensionless groups were significant for C_1 and C_2. For C_2, however, the inclusion of group ρ_d/ρ_c improved the correlations. The final format of this correlation is

$$J_c^{1/2} = K_1 (a_p/\varepsilon^3(\sigma/(\Delta\rho g))^{1/2})^{-0.101} - K_2 (\rho_d/\rho_c)^{0.03}(a_p/\varepsilon^3(\sigma/(\Delta\rho g))^{1/2})^{0.058} J_d^{1/2}$$

K_1 was adjustable constant that depended on type of packing. The value for K_2 was 0.835. The values for K_1 were given in the table below along with constants for Dell and Pratt correlation. The Dell and Pratt constants were those that listed in their paper except for packing types and size for which no such constants had been given before. This includes solid cylinder, glass bead, Norton 2T, and IMTP packings.

Type of packing		K_1	Dell and Pratt constants
Raschig rings:	0.6 cm	0.74	0.68
	0.635 cm	0.75	0.68
	0.9525 - 1 cm	0.68	0.68
	1.27 - 1.905 cm	0.68	0.77
	2.54 cm	0.68	0.82
	3.8 cm	0.73	0.82
Berl saddles:	0.6 - 0.635 cm	0.77	0.68
	1.27 - 2.54 cm	0.73	0.88
Lessing rings:	0.635 cm	0.75	0.80
	0.9525 cm	0.87	0.80
	1.27 cm	0.81	0.80
Cylinder: 0.635 cm		0.90	0.80*
Glass bead 0.8 cm		0.89	0.80
Norton 2T (structured packing)		0.69	0.77*
No.25 IMTP		0.69	0.87*
No.40 IMTP		0.69	0.80*
Bialecki		0.95	0.80*
Stacked bialecki		0.70	0.55*
BX			
CI			
Filip		0.65	0.77*
Hiflow		0.67	0.80*
Montz BI-300		1.37	0.85*
Pall rings		0.89	0.65*
SMV			

Table 4. Constants for Correlation 2 and Dell and Pratt correlation.

REFERENCES

1. Bailes PJ, Gledhill J, Godfrey JC and Slater MJ, *Chem Eng Res Des*, **64**, 43, (1986)
2. Ballard JH and Piret, EL, *Ind Eng Chem*, **42**, 1088, (1950)
3. Bankoff SG and Lee SC, *A Critical Review of the Flooding Literature* (NRC publication), (1983).
4. Berteti JW, *Trans AIChE*, **38**, 1023, (1942).
5. Blanding FH and Elgin JC, *Trans AIChE*, **38**, 305, (1942).
6. Breckenfeld RR. and Wilke CR, Chem Eng Prog, **46**, 187, (1950).
7. Brunazzi E, Paglianti A, *AIChE J.*, **43**, 317, (1997).
8. Brunner G, *Paper to be published in SENDAI 1997*
9. Bruno TJ and Ely JF (Eds.), *Supercritical Fluid Technology*, CRC Press, Boca Raton, (1991).
10. Crawford JW. and Wilke CR, *Chem Eng Prog*, **47**, 423, (1951).
11. Dell FR and Pratt HRC, *Trans I Chem E*, **29**, 89, (1951).
12. Gallant RW and Yaws CL, *Physical Properties of Hydrocarbon*, Gulf Publishing Co., Houston, (1993).
13. Gayler R, Roberts NW and Pratt HRC, *Trans I Chem E*, **31**, 57, (1953).
14. Gayler R and Pratt HRC, *Trans I Chem E*, **29**,110, (1951).
15. Gayler R and Pratt HRC, Trans I Chem E, **31**, 69, (1953).
16. Godfrey JC and Slater MJ, *Liquid-Liquid Extraction Equipment*, John Wiley & Sons, New York, (1994).
17. Hetsroni G (Editor), *Handbook of Multiphase Systems*, Hemisphere Pub. Corp., McGraw-Hill, New York, (1982).
18. Hoffing EH and Lockhart FJ, *Chem Eng Prog*, **50**, 94, (1954).
19. Houlihan R and Landau J, *Can J. Chem Eng*, **52**, 758, (1974).
20. Jayanti S, Tokarz A and Hewitt GF, *Int. J. Multiphase Flow*, **22**, 307, (1996).
21. Jeong JH and No HC, *Int. J. Multiphase Flow*, **22**, 499, (1996).
22. Kister HZ, *Distillation Design*, McGraw-Hill, New York, (1992).

23. Koizumi Y and Ueda T, *Int. J. Multiphase Flow*, **22**, 31, (1996).
24. Kumar A and Hartland S, *Ins Chem Engrs*, **72**, 89, (1994).
25. Lacy CE and Dukler AE, *Int. J. Multiphase Flow*, **20**, 219, (1994).
26. Lacy CE and Dukler AE, *Int. J. Multiphase Flow*, **20**, 235, (1994).
27. Laddha GS, and Degaleesan TE, *Transport Phenomena in Liquid Extraction*, Tata McGraw-Hill Publishing Co. Ltd., New Delhi, (1978).
28. Leva M., *Tower Packings and Packed Tower Design*, The United States Stoneware Co., Akron, (1951).
29. Lewis JB, Jones, and Pratt HRC, *Trans I Chem E*, **29**, 126, (1951).
30. Lo TC, Baird MHI., and Hanson C, (Editors), *Handbook of Solvent Extraction*, Krieger Publishing Co., Florida, (1991).
31. Mackowiak J., and Billet R, *Ger Chem Eng*, **3**, 234, (1980).
32. Moore RJ, Pratt HRC and Stevens GW, *Solvent Extr Ion Exch*, **7**, 1043, (1989).
33. Nemunaitis RR, Eckert JS, Foote EH, and Rollinson LR, *Chem Eng Prog*, **67**, 60, (1971).
34. Rathkamp PJ, Bravo JL and Fair JR, *Solvent Extraction and Ion Exch.*, **5**, 367, (1987).
35. Rocha JA, Bravo JL, and Fair JR, *Ind Eng Chem Res*, **32**, 641, (1993).
36. Row SB, Koffolt JH, and Withrow JS, *Trans AIChE*, **37**, 559, (1941).
37. Sakiadis BC and Johnson AI, *Ind Eng Chem*, **46**, 1229, (1954).
38. Siebert AF and Fair JR, *Ind Eng Chem Res*, **27**, 470, (1988).
39. Siebert AF and Little CT, Publication No. E-89-2, Separation Research Program, The Univ. of Texas at Austin, Austin, (1988).
40. Siebert AF, Reeves BE and Fair JR, *Ind Chem Res*, **29**, 1901, (1990).
41. Siebert AF and Moosberg DG, *Sep Sci Technol*, **23**, 2049, (1988).
42. Siebert AF, Humphrey JL and Fair JR, *Sep Sci Technol*, **22**, 281, (1987).
43. Stevens GW and Pratt HRC, *AIChE J*, **32**, 2079, (1986).
44. Strigle Jr RF, Random Packings and Packed Towers, Gulf Publishing Co., Houston, Texas, (1987).
45. Thornton JD, *Science and Practice of Liquid-Liquid Extraction,* Oxford University Press, New York, (1992).
46. Thornton JD, *Chem Eng Sci*, **5**, 201, (1956).
47. Toye D, Marchot P, and L'Homme G, *Meas Sci Technol*, **7**, 436, (1996).
48. Venkataraman G and Laddha GS, *AIChE J*, **6**, 355, (1960).
49. Wallis BG, *One-dimensional Two-phase Flow*, McGraw-Hill, New York, (1969).
50. Watson JS and McNeese LE, *AIChE J*, **19**, 230, (1973).
51. Watson JS and McNeese LE, ORNL Report, (1972).
52. Watson JS, McNeese LE, Day J and Carroad PA, *AIChE J*, **21**, 1080, (1975).
53. Zapke A and Kroger DG, *Int. J. Multiphase Flow*, **22**, 461, (1996).
54. Schroeder RR and Kintner RC, *AIChE Journal*, Vol 11, No 1 5-8 (1965).
55. Godfrey JC and Slater MJ, *Trans IChemE*, **69**, 130, (1991).

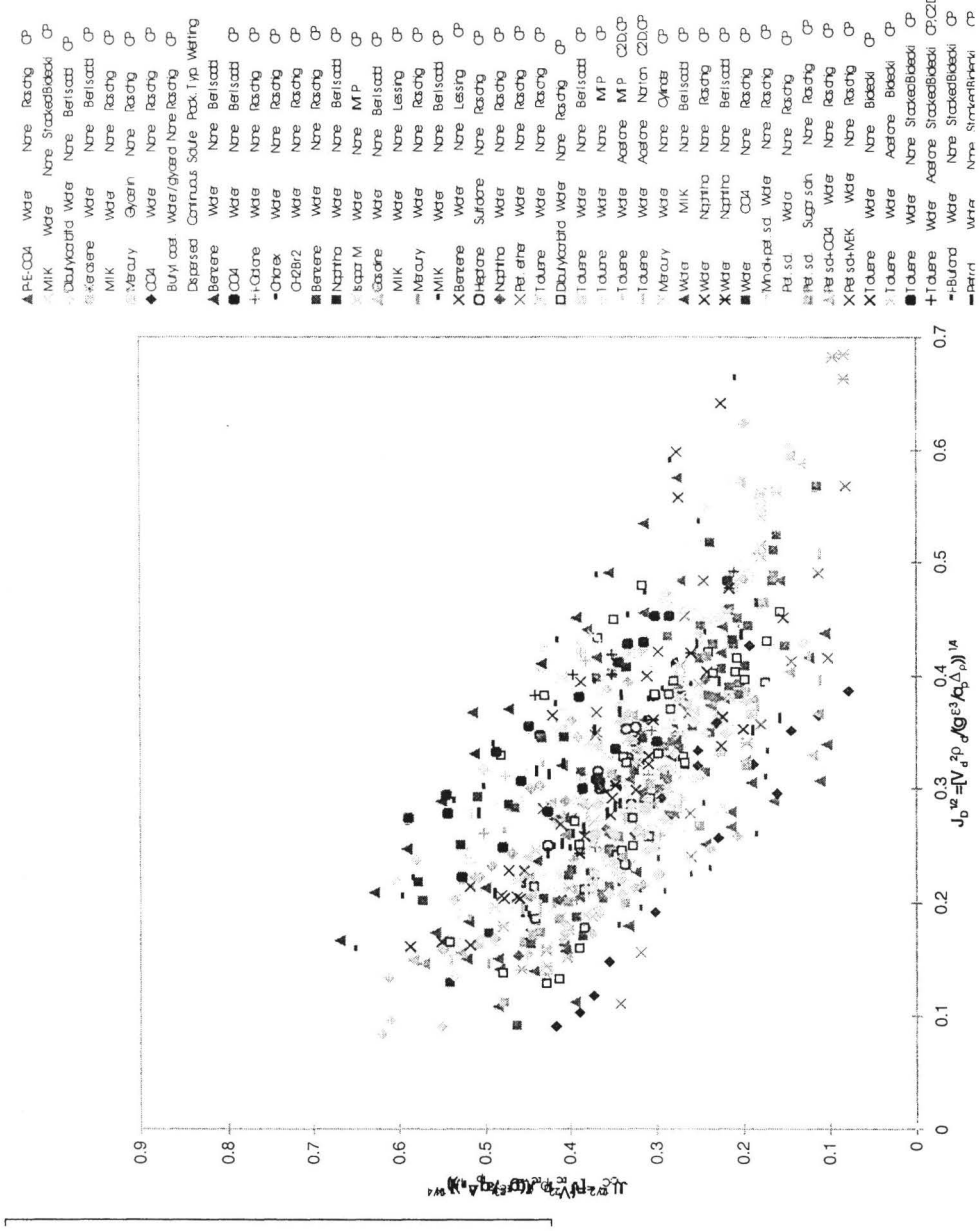



Supercritical Extraction

A MECHANICALLY AGITATED SUPERCRITICAL EXTRACTION COLUMN

Antero Laitinen and Juha Kaunisto
VTT Chemical Technology, P.O.Box 1401, FIN-02044 VTT, Finland

ABSTRACT
A mechanically agitated high-pressure extraction column was tested by extracting ethanol from aqueous solution using supercritical carbon dioxide at 10 MPa and 40°C as a solvent. The measured values of the height equivalent to a theoretical stage (HETS) ranged from 0.37 to 0.8 m depending on the type of the column, solvent-to-feed ratio and rotor speed. The K_{od}·a -values ranged from 0.006 s^{-1} to 0.015 s^{-1}. The measured column capacities were between 80 and 50 $m^3m^{-2}h^{-1}$.

Keywords: ethanol, carbon dioxide, supercritical extraction, mechanical agitated column, Rotating Disc Contactor, Oldshue-Rushton column

INTRODUCTION

Countercurrent extraction operations using supercritical fluids as solvents are of increasing interest particularly in food and pharmaceutical industry. The favorable mass transfer properties, such as liquid-like density, relatively low viscosity and high diffusivity coefficient, of supercritical fluids can be utilized in the process. Because a supercritical solvent, such as carbon dioxide, is typically a gas at NTP, the separation of the solute from the solvent is usually relatively simple and cost-effective. Additionally, carbon dioxide is non-toxic, non-corrosive, non-flammable, and the second least expensive solvent after water.[1]

Up to now almost all countercurrent supercritical fluid extraction studies have been carried out in spray, sieve tray or packed columns.[2-8] In these studies countercurrent supercritical extraction columns, particularly packed columns, have been shown to be very efficient compared to conventional liquid-liquid extraction columns. Although the packing increases the column efficiency compared to spray columns, the capacity of the column is greatly reduced if the column is packed. To maintain the same capacity, the diameter of the packed column must be larger than in the spray column. On the other hand, a large column diameter is not desirable in high pressure vessel design due to pressure vessel cost. One solution combining the high capacity of the spray columns and the high efficiency of the packed columns could be mechanically agitated extraction column.

This paper reports mass transfer efficiencies and hydraulic characteristics of a novel high pressure bench-scale mechanically agitated extraction column operated under high pressure conditions.

EXPERIMENTAL

Equipment

A novel high-pressure extraction column (Chematur Ecoplanning) is 35 mm in diameter and 2 m high. The maximum operating pressure of this column is 30 MPa and the maximum rotating speed is approximately 450 rpm. A special pressure compensating sealing system was developed to lead the electrically driven agitator shaft through the column head. Windows at both ends and in the middle of the column allows observation of phase behaviour. The column is equipped with a heating jacket, through which water is circulated. The maximum extraction temperature is approximately 80°C. A schematic sketch of the column is seen in Figure 1. A commercial high-pressure unit (Nova AG) was applied to pump carbon dioxide into the column and separate the product from the carbon

© 2000 Society of Chemical Industry

dioxide solvent. A piston pump (Lewa AG) was used to pump the liquid feed stream. Carbon dioxide flow-rates in solvent and extract streams were measured by turbine flow meters (EG&G Flow Technology). Needle valves were used to control the flow-rates and phase boundary as well as the pressure inside the column.

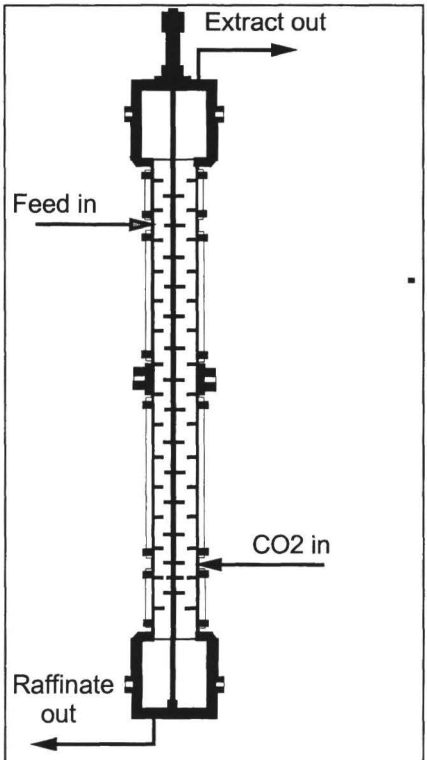

Figure 1. High pressure extraction column.

Procedure

Ethanol was extracted from water initially containing 10 wt% ethanol using dense carbon dioxide solvent at 10 MPa and 40 °C. Carbon dioxide was the dispersed phase in all experiments. Carbon dioxide solvent stream was not recycled to make certain that the solvent stream was ethanol free. Instead, fresh carbon dioxide from the container was used.

Each extraction experiment lasted 4-5 hours. During the run, samples were taken from feed, raffinate and extract streams. The extract was collected and the ethanol content analyzed. The feed and raffinate tanks were continuously weighed during the run to measure the mass flow-rates of the corresponding streams. Both rotating disk (RDC) and Oldshue-Rushton (ORC) types of column were tested. Aqueous ethanol solutions were analyzed by GC.

Carbon dioxide (99.7%) was obtained from AGA, and ethanol (99.5%) was purchased from Primalco.

Calculations.

Recently, Lim et al.[7] have measured the ethanol distribution coefficient between supercritical carbon dioxide and water at 10.1 MPa and 40°C. According to their measurements, the distribution coefficient value is 0.12. The total agitated height h of the column is:

$$h = HTU_{od} NTU_{od} \tag{1}$$

Where (NTU_{od}) is the number of transfer units and (HTU_{od}) is the height of a transfer unit for the dispersed phase. For dilute solutions and immiscible solvent (NTU_{od}) and (HTU_{od}) can be written as:

$$NTU_{od} = \int_{c_2}^{c_1} \frac{dc}{c^* - c} \tag{2}$$

$$HTU_{od} = \frac{V_d}{K_{od}a} \tag{3}$$

Where c is the weight fraction of solute in the dispersed extract phase, c* is the equilibrium value, V_d is superficial velocity of the dispersed phase, K_{od} is the overall mass transfer coefficient based on the dispersed phase, and a is the interfacial area. According to Treybal[9] the following relationship between the height equivalent of a theoretical stage (HETS) and height of a transfer unit (HTU_{od}) can be written:

$$HETS = \frac{\ln l}{l-1} HTU_{od} \tag{4}$$

where l is the extraction coefficient

$$l = m\frac{F_{solv}}{F_{aq}} \tag{5}$$

m is the distribution coefficient, and F_{solv} and F_{aq} are solvent mass flow-rate and feed mass flow-rate, respectively.

RESULTS AND DISCUSSION

Column Efficiency

The values of the height equivalent to a theoretical stage (HETS) and the overall mass-transfer coefficient $K_{od}\cdot a$ are seen in Figures 2 and 3.

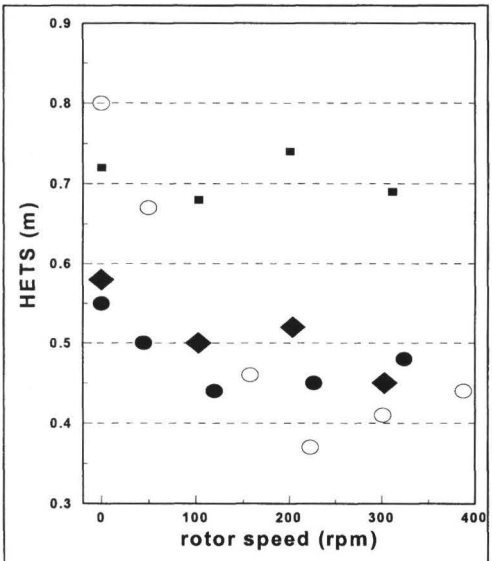

Figure 2. Effect of agitation on HETS.
(O) RDC, S/F=13/1; (♦) RDC, S/F=13/2;
(●) ORC, S/F=14/1;(■) ORC, S/F=14/2.

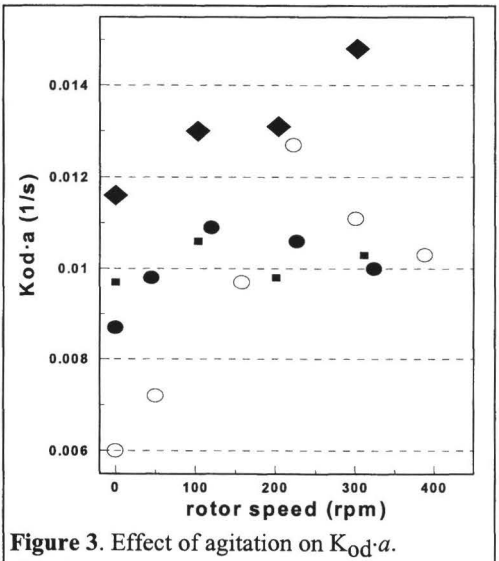

Figure 3. Effect of agitation on $K_{od}\cdot a$.
(O) RDC, S/F=13/1; (♦) RDC, S/F=13/2;
(●) ORC, S/F=14/1;(■) ORC, S/F=14/2.

The measured values of the height equivalent to a theoretical stage (HETS) ranged from 0.37 to 0.8 m. At the high solvent-to-feed ratio (S/F=13/1) agitation did have a significant effect on rotating disk column (RDC) efficiency. HETS-values decreased from 0.8 m to 0.37 m after agitation was introduced. The column seemed to reach optimum efficiency, when the rotor speed was around 200 rpm. The efficiency of Oldshue-Rushton column (ORC) also increased slightly after agitation was introduced at the high solvent-to-feed ratio (S/F= 14/1). Agitation did not have a significant effect on RDC or ORC efficiency at lower solvent-to-feed ratios (S/F=13/1 or S/F=14/2). It is expected, that at lower solvent-to-feed ratios the column approaches equilibrium, and therefore agitation could not any more enhance the column efficiency.

Generally, $K_{od}{\cdot}a$ -values increased when agitation was turned on. The highest value of 0.0148 s^{-1} was measured for the RDC at S/F=13/2 and 303 rpm. $K_{od}{\cdot}a$ -value approximately doubled from 0.006 s^{-1} to 0.013 s^{-1} in rotating disk column (RDC) at S/F=13/1 when the rotor speed was increased from 0 to 200 rpm. This is probably due to the fact that rotating disks significantly reduced the dispersed phase drop size at this solvent-to-feed ratio. In case of Oldshue-Rushton column (ORC) only moderate increase was observed. At high solvent-to-feed ratios an optimum rotor speed was found for each column. In case of rotating disk column the optimum rotor speed was approximately 200 rpm, and in the case of Oldshue-Rushton column the optimum speed was approximately 100 rpm. At lower solvent-to-feed ratios, agitation did not significantly increase the overall mass-transfer coefficient.

Column Capacity

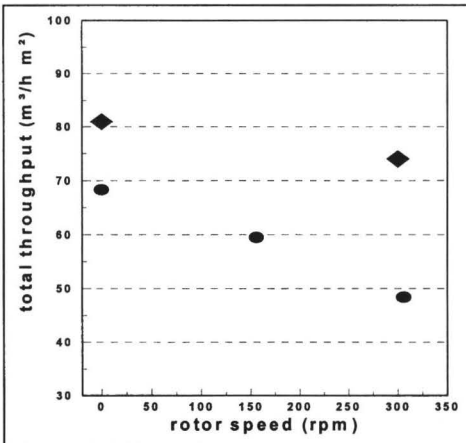

Figure 4. Effect of agitation on column total throughput.(♦) RDC; (●) ORC.

The capacities of the high-pressure rotating disk (RDC) and Oldshue-Rushton columns (ORC) calculated as feed plus solvent rate divided by the smallest cross-sectional area of the column are seen in Figure 4. In both cases agitation decreased the column capacity. Agitation decreases dispersed phase drop size causing decrease in column capacity. Compared to conventional liquid-liquid extraction columns, the capacity of supercritical fluid extraction columns are higher.[3] This is most probably due to the relatively large density difference of the dispersed and continuous phases in supercritical fluid extraction.

CONCLUSIONS

A mechanically agitated high-pressure extraction column seems to successively combine the advantages of other types of column, i.e. high efficiency of packed columns and high capacity of spray columns, in a single unit. This allows the construction of slim high-pressure columns, which is desirable due to cost reasons. The new mechanically agitated column can also be applied on other processes that take place continuously in high pressure and demand effective agitation.

NOMENCLATURE

a = interfacial area, m^2/m^3
c = concentration (weight fraction) of solute in the dispersed phase
F = flow rate, kg/h
h = total agitated height of the column, m
HETS = height equivalent to a theoretical stage, m
HTU_{od} = height of a transfer unit based on the dispersed phase, m
K_{od} = overall mass transfer coefficient based on the dispersed phase, m/s
l = extraction coefficient = mF_{solv}/F_{aq}
m = distribution coefficient = concentration in solvent phase/concentration in feed phase
NTU_{od} = number of transfer units based on the dispersed phase
V = superficial velocity, m/s

SUBSCRIPTS

aq = aqueous phase
d = dispersed phase
solv = solvent phase
1 = at the top of the column
2 = at the bottom of the column

SUPERSCRIPTS

* = equilibrium value

REFERENCES

1. Dixon DJ and Johnston KP, in *Kirk-Othmer Encyclopedia of Chemical Technology, 4th ed.*, Wiley and Sons, New York, **23**, 452, (1997).
2. Peter S and Brunner G, *Angew. Chem. Int. Ed. Engl*, **17**, 746, (1978).
3. Rathkamp PJ, Bravo JL and Fair JR, *Solv. Extr. Ion Exch.*, **5**(3), 376, (1987).
4. Lahiere RJ and Fair JR, *Ind. Eng. Chem. Res.*, **26**(10), 2086, (1987).
5. Seibert AF, Moosberg DG, Bravo JL, and Johnston KP, in *Proc. 1st Int. Symp. Supercritical Fluids*, Nice, France, Société Francaise de Chimie, 561, (1988).
6. Brunner G, Malchow Th, Stürken K, Gottschau Th, *J. Supercrit. Fluids*, **4**, 72, (1991).
7. Lim JS, Lee Y-W, Kim J-D and Lee YY, *J. Supercrit. Fluids*, **8**(2), 127, (1995).
8. Simões PC, Matos HA, Carmelo PJ, de Azevedo EG and Nunes da Ponte M, *Ind. Eng.Chem. Res.*, **34**(2), 613, (1995).
9. Treybal RE,*'Liquid Extraction'*,McGraw-Hill, New York, (1963).

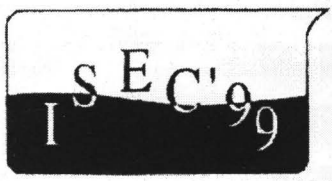

SEPARATION OF ENANTIOMERIC ACIDS AND BASES BY SUPERCRITICAL FLUID EXTRACTION

B Simándi[1], S Keszei[1], E Fogassy[2], E Székely[1], A Prechl[1], V Varga[1], S Kemény[1] and J Sawinsky[1]

[1]Dept. of Chem. Eng., Techn. Univ. of Budapest, H-1521 Budapest, Hungary

[2]Dept. of Org. Chem. Eng., Techn. Univ. of Budapest, H-1521 Budapest, Hungary

ABSTRACT

(±)-*cis* (and *trans*) permetric acids were resolved with *R*-(+)-α-phenylethylamine and *S*-(+)-2-benzylamino-1-butanol, respectively. The resolution of tetramisole with O,O'-dibenzoyl-(2*R*,3*R*)-tartaric acid was also studied in detail. The parameters affecting the extent of the resolution (extraction pressure, temperature, time) have been investigated. The influence of base/acid molar ratio on the quantity and quality of the products have also been examined. For a better understanding of the process the effect of the density of the fluid was investigated as well.

Keywords: permetric acid, tetramisole, enantiomeric separation, supercritical extraction, carbon dioxide

INTRODUCTION

The enantiomers of, for example, pharmaceuticals or agrochemicals can display quite different activity and toxicity profiles (one enantiomer may be inactive, or one may be toxic, or the two enantiomers might have unequal degrees or different kinds of activities), which makes development of enantiomer separation methods necessary. Enantiomer separation methods are usually based on different physical properties of diastereomers formed by reaction of the mixture of enantiomers with an optically active molecule. Resolution through direct crystallisation is still the most important method.[1]

Racemic mixtures can be resolved via chromatographic methods due to a difference in association of the two enantiomers with an optically active stationary phase. In recent years an increasing interest has focussed on supercritical fluid chromatography (SFC). In comparison to other chromatographic methods SFC, using carbon dioxide as solvent, has several advantages: unique selectivity, operation at near room temperature, environmental awareness.[2,3] It is also suitable for separation of the enantiomers via a preparative procedure. However, the small-scale character of this chromatographic method is a severe limitation.[4,5]

For preparative and industrial scale separations of enantiomers supercritical fluid extraction (SFE) seems to be very promising. In a preliminary study we found, that the molecular chiral differentiation in supercritical carbon dioxide is much more efficient for chrysanthemic and permetric acids (*cis*- and *trans* isomers) than that with the known methods.[6,7] There have been no other reports, to our knowledge, of chiral separation using SFE.

The purpose of present study is to demonstrate the applicability of the SFE for the separation of enantiomeric acid and base mixtures.

EXPERIMENTAL

Materials and Methods

Both the racemic mixtures of various acids (1, 2) and base (3), and the resolving agents (4, 5, 6) (see Table 1) were prepared in our laboratory. All the reagents were checked by analytical methods before use and no significant impurities were present.

Other reagents and solvents were obtained from Reanal Ltd., Budapest. The samples were prepared by mixing the racemic acids or base with the corresponding chiral bases or acid in non-

© 2000 Society of Chemical Industry

equivalent molar ratio. A porous supporting material (Perfilt), impregnated with these mixtures, was put into the extractor vessel and extracted with supercritical CO_2.

Optical rotation of extracts and raffinates was measured on a Perkin-Elmer 241 polarimeter. Enantiomeric excess (ee) was determined from optical rotation on the basis of calibration with enantiomeric mixtures of known purity.

Apparatus and Extraction

Figure 1 shows the schematic flow diagram of the laboratory equipment. Initially the extractor is filled with the prepared raw material and pressurised. Once the system has attained the required temperature and pressure, the carbon dioxide is expanded into the separator through a micrometering valve, and the extract is precipitated in the separator. The CO_2 is evaporated and its volume is measured with a gas meter.

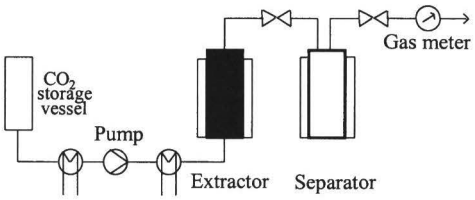

Figure 1. Flow diagram of the laboratory equipment

RESULTS AND DISCUSSION

Solubility in Supercritical CO_2

First the solubility of the raw materials was examined at the circumstances as used in resolution experiments. Pure components were extracted with CO_2 and the extracts were collected as separate samples subsequently in time. The loading concentrations, calculated from the weights of the samples and the CO_2 passing through the system, are given in Table 1 for the most important temperature and pressure setting.

(±)-*trans*-permetric acid (1)	1.90 wt.%
(±)-*cis*-permetric acid (2)	1.56 wt.%
tetramisole (3)	0.18 wt.%
S-(+)-2-benzylaminobutan-1-ol (4)	0.38 wt.%
R-(+)-α-phenylethylamine (5)	0.08 wt.%
(−)-O,O'-dibenzoyl-(2*R*,3*R*)-tartaric acid (6)	0 wt.%

Table 1 Loading concentration of the raw materials in supercritical CO_2 (T = 39C, P = 150 bar)

Table 1 shows that the racemic mixtures (1, 2, 3) are much more soluble in supercritical carbon dioxide than the resolving agents (4, 5, 6). The supporting material does not dissolve in supercritical carbon dioxide.

Resolution by SFE

The mixtures of *S*-(+)-2-benzylaminobutan-1-ol (5) (chiral base) with racemic *trans*-permetric acid (2) in a 0.5:1 molar ratio were prepared and extracted with supercritical carbon dioxide at different extraction conditions. The influence of pressure and temperature on the quantity and quality of the products was investigated. The extracts were collected as separate samples successively

in time. Each of them was examined separately. The extracts contained the free enantiomers and some chiral base whereas the raffinates were the mixtures of diastereomeric salts. Both the enantiomeric excess and the chemical yield (yield = mass of recovered product / mass of initial racemic acid) of the (–)-enantiomer decreased significantly in the subsequent extract samples during the SFE (Figure 2). The enantiomeric excess of the (–)-enantiomer in the total extract was 48%.

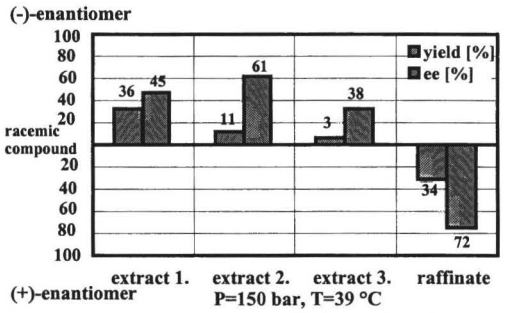

Figure 2. Resolution of racemic *trans*-permetric acid (2) by SFE using *S*-(+)-2-benzylaminobutan-1-ol (5) (extracts 1, 2 and 3 were obtained at 45, 90 and 450 g g^{-1} specific CO_2 consumption, respectively)

The pressure of CO_2 (in the range of 100–200 bar) was found to have direct bearing on the yield and enantiomeric excess. The extraction yield increased at high pressure. The enantiomeric excess of the extracts obtained from single extraction increased from 40% to 49% with a pressure increase from 100 bar to 200 bar (Figure 3).

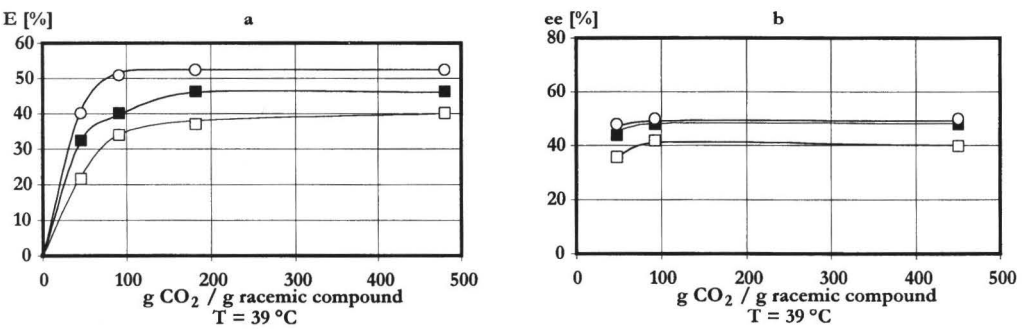

Figure 3. Effect of the pressure a) on the extraction curve and b) on the enantiomeric excess curve (pressure: □ 100 bar ■ 150 bar ❍ 200 bar)

The effect of temperature was investigated only in the supercritical state (33 – 47C) of the solvent. All the extractions were carried out at 100 bar. The enantiomeric excess of the extracts obtained from single extraction were 42% and 28% at temperatures 33C and 47C respectively, but the ee value did not differ significantly at temperatures 33C and 39C (Figure 4).

The effect of the two variables is to be studied by performing designed experiments in more detail.

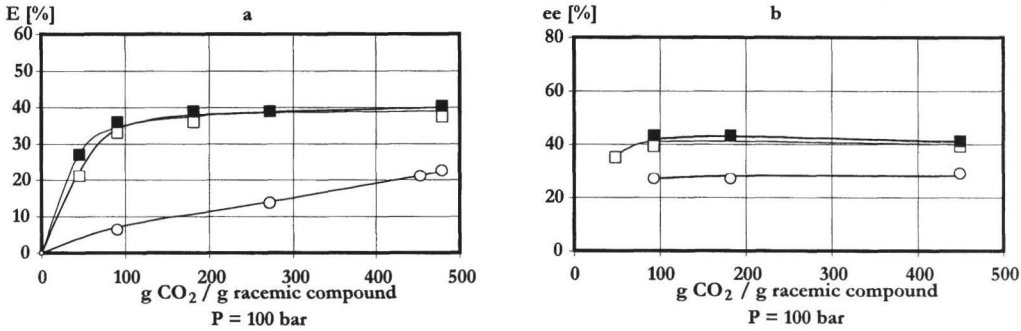

Figure 4. Effect of the temperature a) on the extraction curve and b) on the enantiomeric excess curve (temperature: ■ 33 °C □ 39°C ○ 47 °C)

The novel resolution method can be applied for racemic bases as well. The results of a simple extraction of a mixture of 3 and 6 are given in Figure 5.

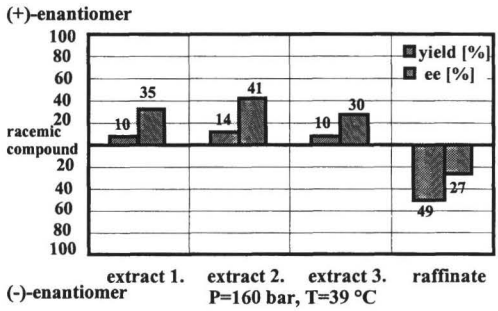

Figure 5. Resolution of tetramisole (**3**) by SFE using O,O'-dibenzoyl-(2*R*,3*R*)-tartaric acid (6) (extracts 1, 2 and 3 were obtained at 200, 400 and 600 g g^{-1} specific CO_2 consumption, respectively)

Effect of molar ratio

The standard separations were carried out by using half equivalent of resolving agent. Variation of the racemic mixture/resolving agent (acid/base) molar ratio resulted an optimum at half quantities of resolving agent for *cis*- and *trans*-permetric acids (Table 2). For characterisation of the enantiomer separation the Fogassy parameter was used. This parameter is the product of the chemical yield and the enantiomeric purity of the products (S = 2 × yield × ee / 10^4). The S value is negative for the (–)-enantiomer. Lower molar ratio 0.25 acid/base was found to be optimal for resolution of the tetramisole (Table 3).

a

acid / base	1 / 0.25	1 / 0.5	1 / 0.75
extract	-0.1080	-0.4752	-0.3264
raffinate	+0.1008	+0.4896	+0.3420

b

acid / base	1 / 0.25	1 / 0.5	1 / 0.75
extract	+0.0660	+0.2660	+0.1675
raffinate	-0.0980	-0.2880	-0.1656

Table 2 Effect of the molar ratio on the Fogassy parameter (S) at the resolution a) of *trans*-permetric acid and b) of *cis*-permetric acid (P=150 bar, T=39C)

base / acid	1 / 0.125	1 / 0.25	1 / 0.5
extract	+0.0352	+0.2448	+0.0860
raffinate	-0.0312	-0.2646	-0.0923

Table 3. Effect of the molar ratio on the Fogassy parameter (S) at the resolution of tetramisole (P=160 bar, T=39C)

Effect of solvent density

It is well known generally, that the dissolving power of a given supercritical fluid depends on its density, which is determined by the pressure and temperature. The influence of the CO_2 density on the ee values of the total extracts of *cis*- and *trans*-permetric acids is shown in Figure 6.

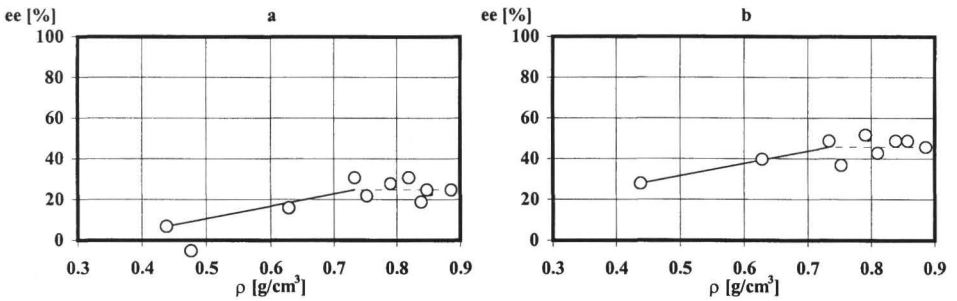

Figure 6. Influence of the CO_2 density on the ee values of the total extracts a) of *cis*-permetric acid and b) of *trans*-permetric acid

It can be seen that the ee value is virtually linearly related to density below 0.7 g/cm^3, and approaches a constant value in the higher density region. However, in the range of 0.7–0.9 g/cm^3 the results are scattering which shows that other parameters then these that are reflected in the density have significant influence.

Since the tetramisole is scarcely soluble in CO_2 at densities below 0.65 g/cm^3, only densities in the range of 0.65–0.9 g/cm^3 were investigated. Figure 7 shows that the ee values decrease with density. However, the effect is complex, and can not be characterised by a single parameter. Further studies are needed to map the effects of temperature and pressure.

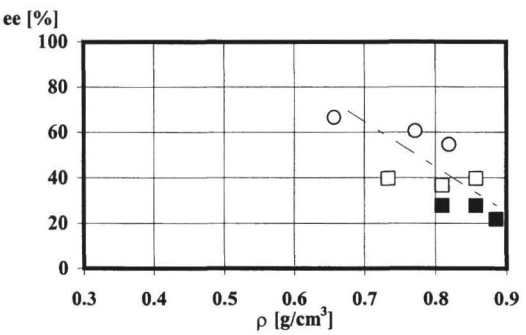

Figure 7. Influence of the CO_2 density on the ee values of the total extracts of tetramisole (temperature: ■ 33C □ 39C ❍ 45C)

CONCLUSIONS

Supercritical fluid extraction is a new and promising technique for the resolution of some racemic acids and base. Some reasons for choosing a supercritical fluid over other solvating systems are:

- the unique solvation and favourable mass transfer properties controlled simply by adjustment of the system pressure and/or temperature;
- carbon dioxide is an ideal solvent because it is non-toxic, non-explosive, readily available and easily removed from the products;
- it is possible to eliminate or to reduce environmental hazard associated with toxic organic solvents;
- the critical temperature of carbon dioxide is 31 °C, which allows operation close to ambient temperature, eliminating decomposition or racemisation of thermally labile substances.

ACKNOWLEDGEMENT

This research was supported by the Hungarian National Science Foundation (OTKA), Grant No. T016880, and by Ministry of Education and Culture (MKM, FKFP 0269/1997).

REFERENCES

1 Sheldon RA, *Chirotechnology: Industrial Synthesis of Optically Active Compounds*, Marcel Dekker Inc., New York, (1993).
2 Juvancz Z and Markides K, *LC-GC Int.* **5**, 44, (1993).
3 Anton K, Eppinger J, Frederiksen L, Francotte E, Berger TA and Wilson WH. *J. Chromatogr.* **666**, 395, (1994).
4 Fuchs G, Doguet L, Barth D and Perrut M. *J. Chromatogr.* **623**, 329, (1992).
5 Kot A, Sandra P and Venema A. *J. Chromatogr. Sci.* **32**, 439, (1994).
6 Simándi B, Keszei S, Fogassy E and Sawinsky J. *J. Org. Chem.* **62**, 4390, (1997).
7 Simándi B, Keszei S, Fogassy E, Kemény S and Sawinsky J. *J. Supercrit. Fluid,* **13**, 331, (1998).

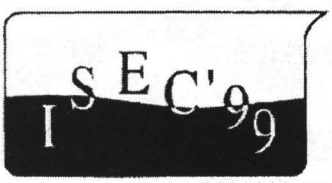

SUPERCRITICAL FLUID EXTRACTION OF TOCOPHEROLS FROM OLIVE TREE LEAVES

A de Lucas[1], E Martínez de la Ossa[2], J Rincón[1], MA Blanco[2] and I Gracia[2]

[1] Dpto. Ingeniería Química. Universidad de Castilla-La Mancha. Facultad de Ciencias Químicas. Avda. Camilo José Cela, 10. 13004 Ciudad Real, Spain

[2] Dpto. Ingeniería Química. Facultad de Ciencias. Universidad de Cádiz. Polígono Río San Pedro, s/n. 11510 Puerto Real (Cádiz), Spain

ABSTRACT

Olive tree leaves, a residue obtained during the harvest of olives for oil production, were treated with supercritical carbon dioxide to examine the possibility of obtaining tocopherol. Tocopherol extraction rates were determined as a function of pressure (250-450 bar), temperature (40-60C) and particle size (0.25-1.5 mm).

Keywords: tocopherol, olive leaves, supercritical extraction, carbon dioxide.

INTRODUCTION

Tocopherols are highly valuable compounds because of their activity as vitamin E and capacity as an anti-oxidant. The isomer with the highest vitamin E activity is α-tocopherol and over the years it has become an important additive to all kind of food products.[1]

For some time an increasing interest in both detection and search for new alternative tocopherol extraction and isolation techniques has been observed. Among them, supercritical fluid technology has been found to be especially promising. It has been applied to extract tocopherols from natural materials such as rice bran,[2] palm oil,[3] or soybean,[4] and enrichment factors up to four with respect to the solvent-obtained extracts have been obtained. Residues and by-products have also been commonly used for tocopherol extraction purposes. Thus, Brunner[5] used deodorizer condensates in a countercurrent column and Shishikura et al.[6] obtained 30% (w/w) tocopherol concentrates from soybean sludge. Finally, it should be noted that additional enrichment of tocopherol species has been realised by using an additive entrainer[6] or coupling this technique to supercritical fluid chromatography.[4, 6]

The main advantages of supercritical fluids over classical extraction agents are that their high diffusivity, low viscosity and low surface tension can speed up mass transfer phenomena, and that it is possible to modify solute solubilities through alteration of pressure and/or temperature. The use of supercritical CO_2 as a solvent in the food industry has advantages over other solvents because CO_2 is non-toxic, non-flammable, non-corrosive, cheap and ready available in large quantities and high purity. Also, CO_2 has a relatively low critical pressure (73 bar) and critical temperature (31.1C), and it is easy to handle as a solvent and easy to remove from any solute without energetic requirements. All these advantages are very important in the extraction of thermo-labile compounds.[7]

In this work we have used supercritical CO_2 for the extraction of olive tree leaves, a residue obtained during the harvest of olives for oil production. The aim of the work is to analyse the effect of pressure, temperature and particle size on the extraction rates of tocopherol from olive tree leaves.

EXPERIMENTAL

Materials

Liquid CO_2 (purity 99.5 %) was supplied by Carburos Metalicos, S.A. (Madrid, Spain). Olive tree leaves were collected in the Ciudad Real area (Spain). The samples were maintained at 55°C for 2 hours to reduce their humidity to 6% by weight in a dry basis. Next, they were allowed to reach ambient

© 2000 Society of Chemical Industry

temperature and, finally, ground and sieved to obtain three size fractions whose average diameter were 1.5 mm, 0.5 mm, and 0.25 mm.

Apparatus and extraction procedure

The flow diagram of the extraction equipment is shown in Figure 1 and it has been described in detail elsewhere.[8] Basically, it works as follows: liquid carbon dioxide is provided from a steel cylinder (SC). After cooling (LC) and filtering (F), the CO_2 is compressed by a positive displacement HPLC type pump (P). The pressure is regulated by a back-pressure-regulator (BPR) and checked by a manometer (M). The compressed fluid is passed through a vertically mounted extractor (EX) from the bottom. The extractor is a 75 cm^3 stainless steel cylinder (17.48 mm i.d. x 304.8 mm length). To keep the extractor temperature at the desired value a digital controller regulates the electric current through a resistor (R) that surrounds the extractor cylinder. The oil-laden gas from the extractor is passed through a heated metering valve (MV) where the supercritical CO_2 is depressurized, and the separated extract is collected in a cooled receiver (RE). The gas flow through the extractor is measured by a turbine flow meter (FM) and totalized by a digital flow computer (FC). In all experiments, the CO_2 flow rate is maintained at 1 NL/min, and the extraction was run on 15g samples of olive tree leaves.

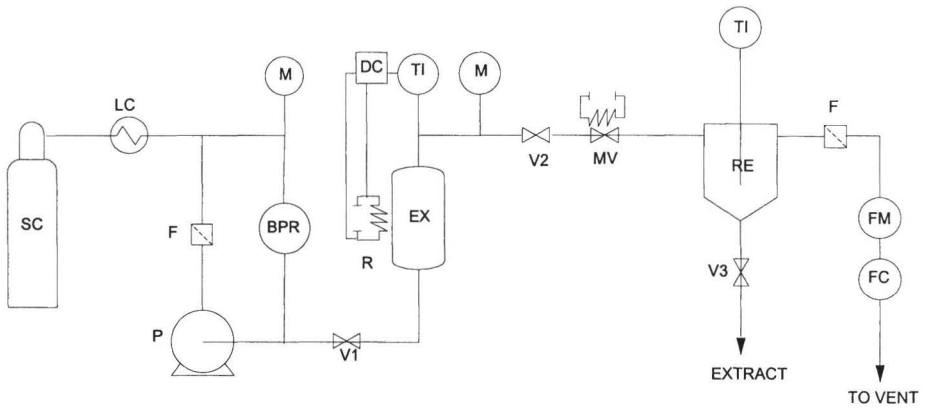

Figure 1. Extraction apparatus

HPLC analysis of tocopherol

The tocopherol analyses were performed by HPLC using a Hewlett Packard 1100 liquid chromatograph. The tocopherol was measured using methanol as a mobile phase and a 5μm RP-18 column 4 x 250 mm (Lichrosphere, Merck) as stationary phase. Solute detection was accomplished by using a UV detector set at 293 nm. Conditions were: temperature: 25°C (isocratic), mobile phase at 1 cm^3/min.

RESULTS AND DISCUSSION

The effect of pressure on the extraction rate of tocopherol from olive tree leaves was investigated at pressures of 250, 350 and 450 bar. The experimental results are presented in Figure 2, where tocopherol yield (expressed as mg of tocopherol/100 g of leaves) is plotted against extraction time. As it can be observed, at all operating conditions most of tocopherol is extracted during the first two hours of operation. It can also be observed that the maximum amount of tocopherol was obtained at 250 bar and that a further increase of pressure up to 350 and 450 bar decreased tocopherol recovery. This result may be explained by considering that the extraction of tocopherol is related to the extraction capabilities of other matrix compounds. Then, a competitive extraction of other diluting materials should occur when rising pressure. Brunner[3] observed a similar behaviour in the supercritical extraction of tocopherols from palm leaves at 70°C and pressures from 30 to 50 MPa.

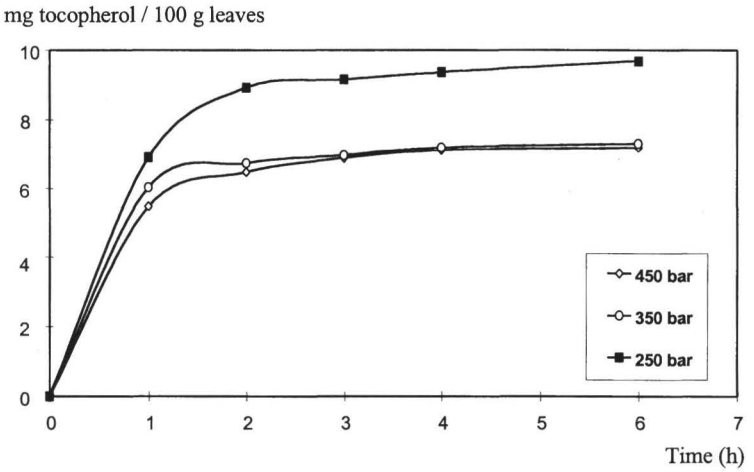

Figure 2. Influence of pressure on tocopherol yield. Experimental conditions: Temperature = 40°C; CO_2 flow rate = 1 NL/min; Particle diameter = 0,5 mm.

The influence of particle size is presented in Figure 3. As was shown before, most of tocopherol is recovered during the first two hours of extraction. Figure 3 also shows that tocopherol recovery increases with increasing particle diameter. To explain this result it should be considered that, in the supercritical extraction of oily extracts from natural products, the oil yield increases with decreasing particle size due to that the higher specific area of small particles results on an increasing proportion of easy-accessible oil.[9] Then, since competitive extraction between tocopherol and other easily extractable materials always exists, those experimental conditions favouring extraction of other compounds than tocopherol (i. e. small particle sizes) will adversely affect its recovery.

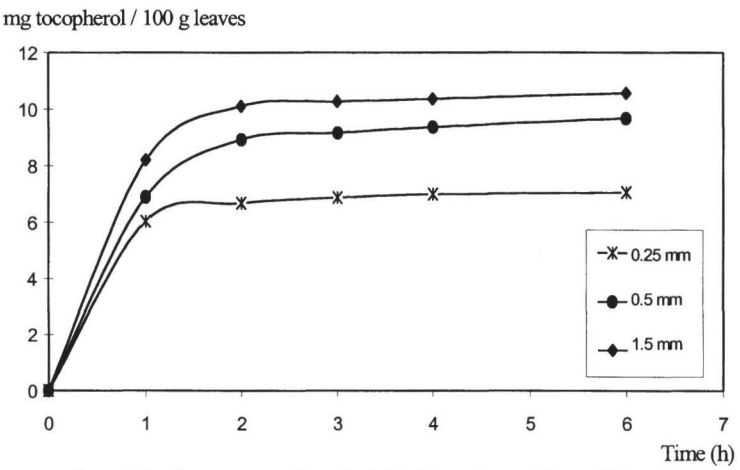

Figure 3. Influence of particle size on tocopherol yield. Experimental conditions: Pressure = 250 bar; Temperature = 40°C; CO_2 flow rate = 1 NL/min.

The effect of temperature on the extraction rate of tocopherol was also investigated. As shown in figure 4, no significative influence of this variable was observed in the experimental range analysed (40-60°C). It should be related to the fact that, by increasing the extraction temperature, there are two opposite effects affecting tocopherol solubility: On the one hand, tocopherol vapour pressure

increases, which favours its solubility, and, on the other hand, supercritical CO_2 density decreases, which negatively affects the solubility of any solute.

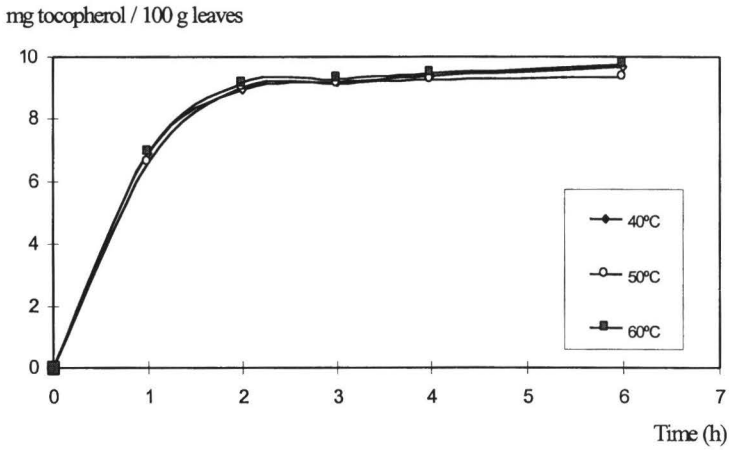

Figure 4. Influence of temperature on tocopherol yield. Experimental conditions: Pressure = 250 bar; CO_2 flow rate = 1 NL/min; Particle diameter = 0,5 mm.

ACKNOWLEDGMENT

We thank to the CICYT for their financial support under Project OLI96-2125.

REFERENCES

1 Kiritsakis AK, *El aceite de oliva*. Capítulo 4. Madrid Vicente ediciones. Madrid, (1992).
2 Fisher RJ. *Food Technol.* **43**, 90, (1991).
3 Brunner G, Birtigh A and Johannsen M. *J. Supercrit. Fluids*, **8**, 46, (1995).
4 King JW, Favati F and Taylor SL. *Sep. Sci & Technol.* **31**, 1843, (1996).
5 Brunner G, Malchow T, Sturken K and Gottschau T. *J. Supercrit. Fluids*, **4**, 72, (1991).
6 Shishikura A, Fujimoto K, Kaneda T, Arai K and Saito S. *J. Jpn. Oil Chem. Soc. (Yukagaku)*, **37**, 8, (1988).
7 King JW and List GR. *Supercritical Fluid Technology in Oil And Lipid Chemistry,* Chapter 3: Supercritical Fluid Extraction of Oil Seeds. Ed. AOCS Press. Champaign, Illinois, (1996).
8 De Lucas A, Rincón J, Álvarez A, Gracia I, García A and García MA, *JAOCS*, **73**, 1127, (1996).
9 Sovova H. *Chem. Eng. Sci,* **49**, 409, (1994).

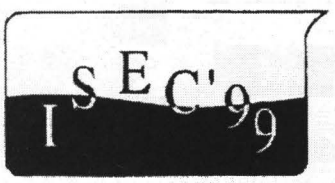

SUPERCRITICAL FLUID EXTRACTION OF BORAGE OIL

A Delgado, A Molero and E Martínez de la Ossa
Department of Chemical Engineering, Food Technology and Environmental Technology, University of Cádiz, Apdo 40, E-11510 Puerto Real (Cádiz), Spain

ABSTRACT
In this study an extraction process by liquid and supercritical carbon dioxide of borage seed oil has been studied. The variables of the process have been optimised, and GLA level of the oils extracted analysed. The best results were obtained by operating the system at 300 bar and 40C with a flow rate of 1.5 dm^3/min. It has been necessary to carry out a pre-treatment of raw material (dehydration and grinding).

Keywords: γ-linolenic acid, borage seed oil, supercritical extraction, carbon dioxide

INTRODUCTION

Gamma-linolenic acid (GLA) is an unsaturated fatty acid that has therapeutic, dietetic, cosmetic and dermatological applications.[3] It is synthesised from linoleic acid incorporated into the diet. However, several factors, including stress, ageing, diabetes, or consumption of alcohol can reduce or inhibit the production of GLA, leading to a variety of ailments. Consequently, the possibility of restoring adequate levels of GLA through dietary supplementation has raised interest in products rich in GLA.[4]

Some of the most important commercial sources of GLA are the oils extracted from the seeds of borage (*Borago officinalis L.*) and evening primrose (*Oenothera officinalis L.*) and from the pips of blackcurrant (*Ribes nigrum L.*), borage oil having the highest amount.[5]

Borage seed oil is conventionally obtained by solvent extraction with hexane. However, this process can lead to some undesirable physicochemical changes of GLA, altering its nutritional properties.

Taking into account this fact, Supercritical Extraction (SCE) appears as a potential alternative to the conventional process. SCE presents a wide range of industrial applications, mainly in the food sector.[8] The most commonly used solvent is carbon dioxide due to its properties: it is cheap, non-toxic, non-corrosive, abundant, non-flammable and it presents moderate critical values.[6]

For these reasons, the object of this study is the process for obtaining borage seed oil, a source of GLA, by using liquid and supercritical carbon dioxide, thus optimising both the operative conditions: pressure, temperature, flow rate, and the suitability of the raw material: size and humidity.

EXPERIMENTAL

Soxhlet system

The oils were extracted in a Soxhlet system for sixteen hours, using hexane as solvent. For 35 g samples, 250 cm^3 of hexane was used.

Supercritical extraction

A schematic diagram of the extraction system is illustrated in Figure 1. Details of the instrumentation have already been described.[1] In the first place, the borage seeds are introduced in the extractor, placing in their edges glass wool to protect the sample from being pulled. Then CO_2 from a storage cylinder is introduced into the extractor at the appropriate pressure with the help of a compressor. Once the desired operating conditions have been achieved, pressure and temperature, the extraction process begins, controlling the flow rate through the micrometic valve.

© 2000 Society of Chemical Industry

GLA methyl ester Analysis

Oils obtained by Soxhlet extraction and SCE with supercritical carbon dioxide were transesterified following the method by AOCS. The fatty acid methyl esters obtained were analysed by CG. The capillary gas chromatographic analysis was performed with on a Hewlett Packard 5890 gas chromatograph. Integration was performed with on a Hewlett-Packard Chemstation - A.02.01 Integrator. The chromatographic conditions were:

- Carbowax 20 M capillary column (25 m x 0,20 μm)
- Oven Temperature: 190°C
- Detector Temperature: 250°C
- Injector Temperature: 250°C
- Mobile Phase: H_2 (40 cm^3/min)
- Split Ratio: 1:100

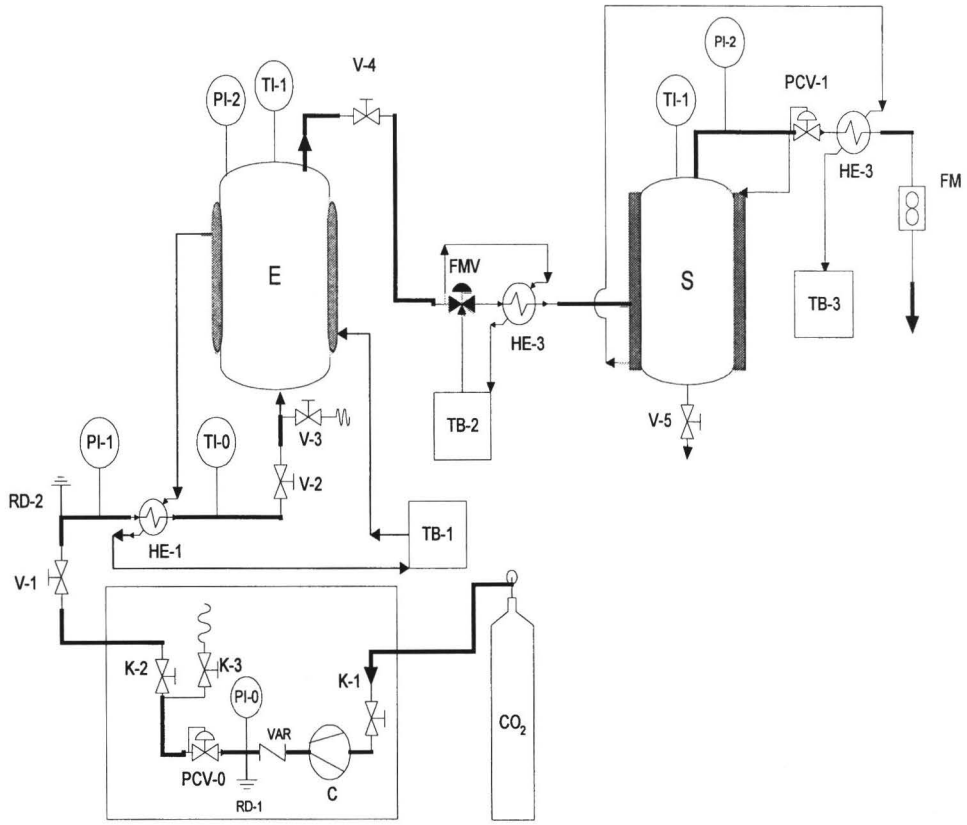

E : Extractor
S : Separator
FM : Flow meter
PCV : Regulator pressure valve
K : On-off valve (compressor)
VAR : O-ring check valve
TB : Thermostatic bath
RD : Rupture Disc
V : On-off valve (extractor)
TI : Temperature indicator

Figure 1 Schematic Diagram of the Supercritical Extraction System

Seed Pre-Treatment Methods:

The seed was crushed using a grinder. The fractions obtained were sieved with the help of a sieving set of CISA with a net between 1.5 and 0.297 mm long. The seeds were dehydrated in a thermostatted heater at 65C for thirty minutes so as not to alter the oil quality.

Variable	Range
Pressure (bar)	50 - 350
Temperature (°C)	10 - 60
Extraction Time (hours)	0 - 5
Flow Rate (L/min)	0.5 - 2
Seed Size (mm)	0.5 – 1.5
Seed Humidity (%)	0 – 7.4

Table 1 Determining Factors in Supercritical Extraction of Borage Seed Oil

RESULTS AND DISCUSSION

Supercritical extraction.

The optimal values of the influential variables in the extraction have been obtained. This selection has been basically based in the economy of the process, showing the results in Table 2. Under these conditions, yields round about 26 % have been obtained.

Variable	Optimal Value
Pressure (bar)	300
Temperature (°C)	40
Flow Rate (L/min)	1.5
Time Extraction (h)	3
Size (mm)	0.75
Humidity (%)	1.8

Table 2 Optimal conditions of extraction by CO_2

Furthermore, the variation of the GLA composition in the extraction with CO_2 has also been studied as a function of time, the results being shown in Table 3. The aim of these experiments was to work on the solubility of the different fatty acids in carbon dioxide, establishing thus the basis for further research on the obtaining of GLA concentrates.

	Fatty acid composition (%)of borage oil extracted by SC-CO_2				
Time (min.)	Palmitic	Stearic	Oleic	Linoleic	GLA
30	11,76	3,68	18,04	40,14	23,81
60	12,95	4,04	18,27	38,22	23,03
120	12,50	4,05	18,37	38,11	22,32
180	10,89	5,00	19,57	36,86	22,06

Table 3 Evolution of the fatty acids from oil extracted by supercritical carbon dioxide at optimal conditions as a function of time

Fatty acid methyl ester analysis indicated that the fatty acid content was practically invariant in relation to extraction time. From the obtained results we cannot see a clear tendency which allows us to consider a fractionated separation from the different fatty acids by controlling only the extraction time. Therefore, it seems that the fatty acids are extracted, generally, in the same way as the oil. The same happens in the extraction of other vegetable oils with supercritical carbon dioxide.[2,7]

Comparison with Soxhlet Extraction

Aiming to establish a comparison between this traditional technique and the extraction with CO_2-SC, different extractions with hexane (Soxhlet system) were performed. The results obtained as well as those found for other vegetable seeds are shown in the following Table 4:

Seed	% CO_2	% Hexane
Borage	26,4	30,1
Grape [7]	6,9	7,5
Sunflower [9]	36,0	38,4
Soybean [9]	16,4	19,9

Table 4 Yields obtained for several seed oils extracted by CO_2-SC and hexane

The efficiency of the extraction with CO_2-SC is highly inferior to that obtained with hexane, in common with the rest of the raw materials. This is due to the highest selectivity of the supercritical carbon dioxide, especially triglycerides.

In regards to the GLA contents, similar performance in both oils have been found, maybe however a slight advantages towards the CO_2-SC extraction, being in any case, higher than those obtained in other oils rich in GLA (Table 5)

Vegetable Oil	% GLA
Borage (CO_2-SC)	21.65
Borage (hexane)	20.02
Primrose (hexane) [10]	8.10
Blackcurrant (hexane) [10]	14.80

Table 5 % GLA of oils rich in GLA

All these reasons can lead to considering supercritical extraction as a viable means to obtaining oil rich in GLA.

REFERENCES

1. Delgado A, *Master Thesis,* University of Cádiz (Spain), (1998).
2. Esquivel M; Bernardo-Gil MG, *Grasas y Aceites*, **44**(1), (1993).
3. Fantozzi P; Montanari L; De Stefano A; Sensidoni A, *Atti del II Congreso: I Fluidi Supercritici e Le Loro Applicazioni*, (1993).
4. Favatti F; King JW; Mazzanti M, *J. Amer.Oil Chem. Soc.*, **68** (6), (1991).
5. Gunstone FD, *Prog Lipid. Res*, **I** (2), 1992.
6. Martínez de la Ossa E; Galán MA, *Ingeniería Química*, (1990).
7. Molero A; Gordillo MD; Martínez de la Ossa E, *Grasas y Aceites*, **48**, (1997).
8. Phelps CL; Smart MG; Wai CM, *J. Chem. Ed*, **73** (12), (1996).
9. Stahl E; Schütz E; Mangold K, *J. Agric. Food Chem*, **28**, (1980).
10. Uzzan A, *Revue Fançaise des Corps Gras*, **33** (10), (1988).

SUPERCRITICAL FLUID EXTRACTION OF ANTHOCYANINS FROM GRAPE POMACE

C Mantell, E Martínez de la Ossa and M Rodríguez
Department of Chemical Engineering, Food Technology and Environmental Technologies. University of Cádiz. Apdo.40. E-11510. Pto. Real (Cádiz). Spain

ABSTRACT
The extraction of food additives from natural sources, has been subject of numerous investigations recently. Traditional solvent extraction, generally requires multiple stages that make the process difficult and the product more expensive. Supercritical extraction is a good technique for this purpose. The objective of this work is to study the applicability of supercritical extraction of anthocyanins from grape pomace to be used as a food colorant. The variables studied are temperature, pressure, solvent flow rate and co-solvent concentration.

Keywords: anthocyanins, grape pomace, supercritical extraction, carbon dioxide, methanol co-solvent

INTRODUCTION

Anthocyanins are responsible of pigmentation of many plants[1] and are, today, used as natural red food dyes. Recently, several works have demonstrated some properties of this substances such as anti-oxidants,[2] anti-convulsants and anti-carcinogens, all of which increases their advantages as food additives. Recent investigations have studied the extraction of anthocyanins from different plants but currently, its principal source is the skin of red grape and in particular, the grape waste from the red vinification.[3]

The use of supercritical CO_2 in the extraction of food additives present great advantages due to its low critical point, 31°C and 73.9 bar, that permits the extraction of thermo-labile substances. Also CO_2 can be separated quickly from the solute extracted at room temperature, so that the solvent recuperation step can be eliminated. The problem of supercritical CO_2 is that the extraction yield decreases when polar substances like the anthocyanins must be extracted. In these cases, the addition of a small amount of some co-solvent, such as methanol, ethanol, etc., leads to an increase in efficiency of the extraction of polar substances as it increases the polarity of CO_2.[4]

The present work studies the application of supercritical CO_2 plus methanol, as co-solvent, for the recovery of anthocyanins from tempranillo grape pomace. An experimental design with 2^4 experiments is developed to study the influence of pressure, temperature, percentage co-solvent and solvent flow rate. The amount of anthocyanins recovery has been determined by HPLC.

EXPERIMENTAL

Samples

Tempranillo grape pomace was supplied from the winery Domecq S.A. (Jerez, Spain). The raw material was stored at –20°C in the dark until the manual separation of the seed.

Supercritical fluid extraction (SFE)

Supercritical fluid extraction was performed using an *Isco* SFX 220 extractor with two chambers with 10 cm^3 volume. The SFE was performed with 1g approx. and two pumps (models 100DX and 260DX) supply both the solvent and co-solvent at the operating pressure. The flow rate of the extraction was controlled with a micrometric valve at the exit of the extractor (Figure 1)

© 2000 Society of Chemical Industry

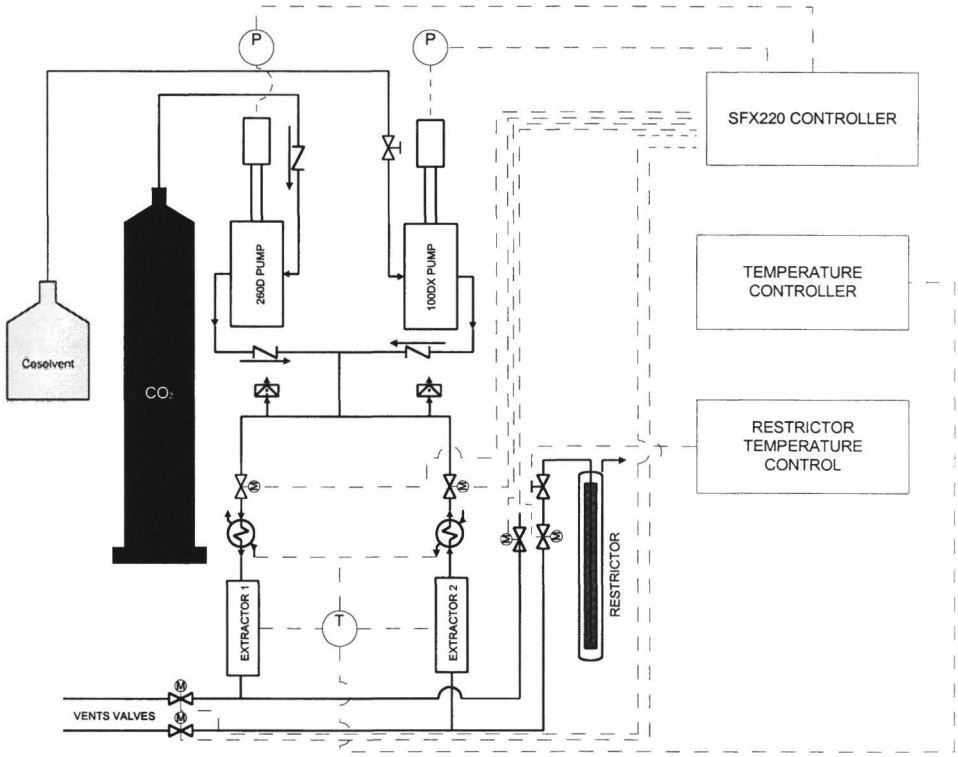

Figure 1. Flow diagram of the experimental equipment.

A factorial design was created to study the effects of four factors: pressure, temperature, percentage co-solvent and solvent flow rate, in 16 runs. The order of the experiments was fully randomized to provide protection against the effects of hidden variables. The values of the factors assessed were as follows: pressures, 100 and 500 bar; temperatures, 40 and 60°C; percentage of co-solvent, 5.04 and 20.15% molar methanol; and solvent flow rates, 0.012 and 0.0226 mol/min.

Extracts were collected over methanol and stored at -4°C in the dark until HPLC analysis.

Preparation of the extracts for the analysis

Extracts in methanol were distilled to remove methanol in an inert atmosphere, diluted to 5 cm^3 with 10% acetonitrile and 90% of a 4.5% formic acid solution in water, and filtered with a 0.45 μm filter.

HPLC

A Hewlett Packard model 1100, HPLC with quaternary pump and UV-VIS detector was used for the identification of the anthocyanins in the extract. A modified Hebrero et al. method[5], solvent flow rate 0.8 cm^3/min, was used for the identification of the main anthocyanins. Anthocyanins quantification was performed from peak areas using a calibration curve from a standard of malvidin-3,5-diglucoside provided by *Symta,* (Figure 2).

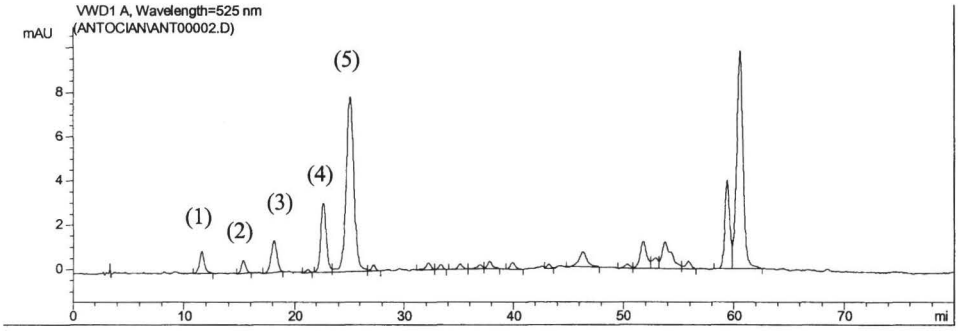

Figure 2. HPLC chromatogram of anthocyanins. (1) Delfinin-3-monoglucoside; (2) Cyanidin-3-monoglucoside; (3) Petunidin-3-monoglucoside; (4) Peonidin-3-monoglucoside; (5) Malvidin-3- monoglucoside

RESULTS AND DISCUSSION

Experimental results from SFE of anthocyanins in Tempranillo grape skins pomace are shown in figures 3 and 4.

Effect of pressure

At all studied conditions, a pressure increase produces a decrease in the extraction yield. The best yields of the extraction of anthocyanins from grape pomace are obtained at low pressure and this effect is more important at low percentages of co-solvent. These results agree with those reported for the SFE of other food colourants, such as carotenoids.[4]

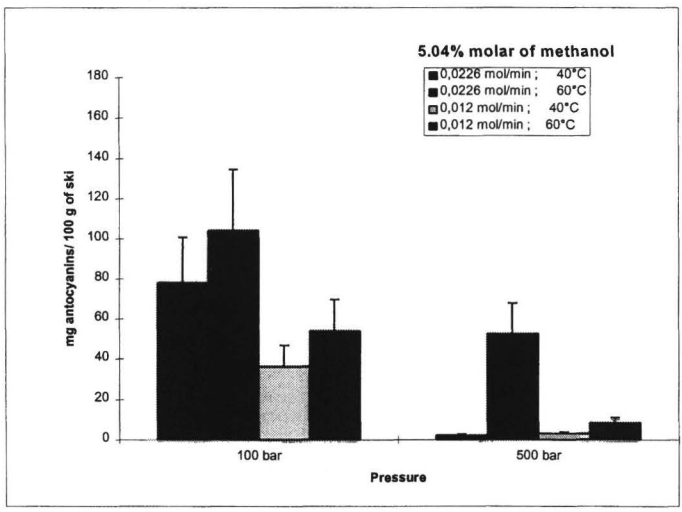

Figure 3. SFE with CO_2 + 5.04% methanol of Anthocyanins at different pressures, temperatures and flow rates.

Effect of temperature

In all cases, the best yield of extraction was obtained at 60°C. This effect is due to the increase of the solubility of anthocyanins with the temperature. For the selection of the optimal temperature it is necessary to study the thermal degradation of the substance.

Effect of percentage co-solvent

The increase of the percentage of methanol in solvent increases the extraction yield. This effect, which is not relevant at 100 bar, at 500 bar improves the yield of the extraction enormously.

Effect of flow rate of solvent

Generally, an increase of the flow rate leads to higher levels of anthocyanins. This effect is due to the presence of higher amount of solvent in the operation that improves the yield of the extraction.

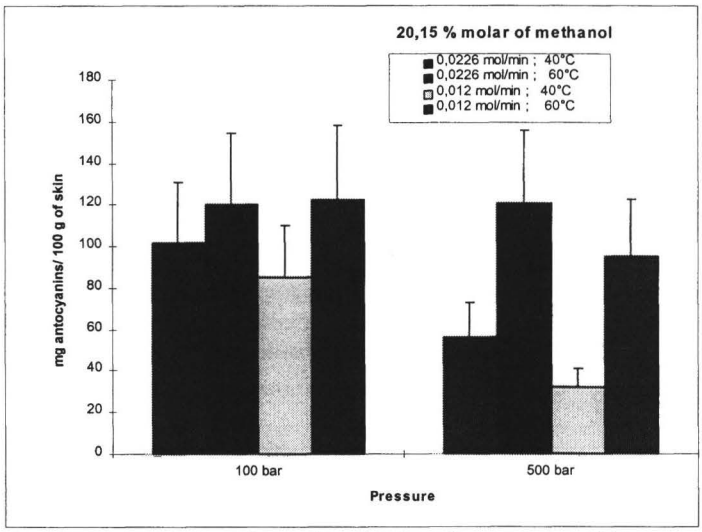

Figure 4. SFE with CO_2 + 20.15% methanol, of Anthocyanins at different pressures, temperatures and flow rates.

CONCLUSIONS

From the above discussion, it can be concluded that: a co-solvent like methanol is necessary to extract anthocyanins by using supercritical CO_2; pressure is the main variable for the optimization of the process and the best pressure is 100 bar; the amount of co-solvent is the second most important variable and the best yield has been obtained at 20.15% molar of methanol; finally, temperature and solvent flow rate are less significant in the process.

REFERENCES

1. Strack D and Wray V, *Methods in Plant Biochemistry* **I**, 325, (1989)
2. Tsuda T, Watanabe M, Ohshima K, Norinobu S, Choi S, Kawakishi S and Osawa T, *J. Agric. Food. Chem.*, **42**, 2407, (1994).
3. Francis FJ, *Trends in Food Sci. and Technol.*, **3**, 27, (1992).
4. Barth MM, Zhou C, Kute KM and Rosenthal GA, *"J. Agric. Food Chem.*, **43**, 2876, (1995).
5. Hebrero E, Santos-Buelga C and Rivas-Gonzalo JC, *Am. J. Enol. Vitic*, **39**(3), 227, (1988).



ACETIC ACID EXTRACTION BY SUPERCRITICAL CARBON DIOXIDE: PRESSURE EFFECT

C Pereyra, G Di Giacomo[1] and E Martínez de la Ossa
Dpto. Ingeniería Química, Tecnología de Alimentos y Tecnologías del Medio Ambiente. Facultad de Ciencias. Universidad de Cádiz. Pol. Río San Pedro, apdo. 40. 11510 Puerto Real, Cádiz. Spain
[1]Dipartimento di Ingegneria Chimica, Università de L'Aquila, 67040 Monteluco di Roio, L'Aquila, Italy

ABSTRACT
In this work the pressure effect on the acetic acid extraction from aqueous solutions, using supercritical carbon dioxide, has been studied. Two parameters that are interesting from the engineering point of view, selectivity and loading, have been determined. A single pass flow apparatus has been used, operating at 313K and 10 and 20 MPa. Experimental results show the selectivity is closely dependent on pressure, while loading is only pressure dependent for acetic acid concentrations up to 40% w/w.

Keywords: acetic acid, carbon dioxide, supercritical extraction

INTRODUCTION

Acetic acid, a raw material for the production of several industrial products,[1] is traditionally obtained from fossil fuels, but due to the continuous increase in their prices new processes are being sought. An alternative could be by microbiological routes, from fermentation broths.[2] However, these routes present a problem, the acetic acid obtained is very dilute, about 5-8 % volume,[3] so that a concentration or removal process is necessary. Distillation is the most widely used process at industrial level, but the acetic acid is the bottom product, requiring distillation of 90% of the fermentation broth.[4] Other techniques which have been studied, such as the combination of solvent extraction with distillation[4] or extractive distillation.[4,5] Any of these are satisfactory for acetic acid removal from aqueous solutions, therefore applicability of supercritical extraction is being studied.[6-11]

In this work, extraction of acetic acid using supercritical carbon dioxide is studied, determining the most interesting two parameters from the engineering point of the view: the solvent selectivity for acetic acid and the acetic acid loading in supercritical carbon dioxide. For this, a single pass flow apparatus has been used operating at 313K and two pressures, 10 and 20 MPa, by determining how the pressure affects these parameters, working in a concentration range of 5 - 50% w/w of acetic acid in aqueous solution, thus complementing literature data.

EXPERIMENTAL

The single pass flow apparatus used is shown in Figure 1. The validity of this apparatus has been tested previously for other systems, the data obtained agreeing perfectly with the literature.[12-14] Full description and operating procedures are given in a previous work.[12]

In the experiments for each run 60 grams of carbon dioxide were passed through the apparatus, at mass flow rate of 0.5 g/min. Into the cryogenic traps an accurately know quantity of propanol was introduced to take the water and the acetic acid. The composition of the extract was determined as follows: amount of carbon dioxide was directly measured, from the flow-meter totalizer; water, by Karl-Fischer titration; and the acetic acid, by titration using sodium hydroxide and phenolphthalein. As the total propanol amount in the sample is known, the amounts of water and acetic acid on the solvent-free extract are calculated from the material balances.

The raffinate composition cannot be determined with this apparatus because it is not possible to measure the carbon dioxide in the liquid phase, but it is possible to determine the composition of the solvent-free raffinate. Water and acetic acid amounts that remain in the equilibrium cell are calculated by difference between the amounts of water and acetic acid in the feed and those that constitute the solvent-free extract.

© 2000 Society of Chemical Industry

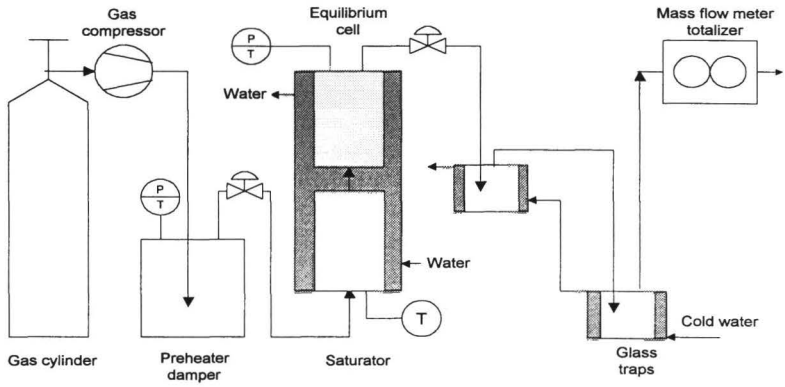

Figure 1. Single pass flow apparatus

The reagents used in the extraction process and in the analysis were:

carbon dioxide, Carburos Metálicos, 99.95%;
glacial acetic acid, Panreac, 99.7%;
distilled water Milli-Ro 6, Millipore;
propanol, Merck, 99.5%;
sodium hydroxide, Panreac, 97.0%;
phenolphthalein, Merck;
Hydranal-Solvent, -Titrant 5, -Standard 5.00, Riedel-de-Haën.

RESULTS AND DISCUSSION

Selectivity and loading data are presented in Figures 2, 3 and 4, 5, respectively. These data have been presented against the weight percent of acetic acid in liquid phase, on a solvent-free basis, together with the data from other authors.[10,11]

The carbon dioxide selectivity of acetic acid between the liquid and the supercritical phase is defined by the ratio of the distribution coefficient of acetic acid and water, while the acetic acid loading is defined by the ratio of acetic acid and carbon dioxide in the supercritical phase:

$$S = \frac{y_{AcH}/x_{AcH}}{y_{H_2O}/x_{H_2O}} = \frac{y_{AcH}/X_{AcH}}{y_{H_2O}/X_{H_2O}} \qquad L = 100 \cdot \left(\frac{M_{AcH}}{M_{CO_2}}\right)\left(\frac{y_{AcH}}{y_{CO_2}}\right) \qquad (see\ nomenclature)$$

As can be seen in Figures 2 and 3, at two pressures the selectivity increases as acetic acid concentration increases in the aqueous phase, reaching a maximum, which is pressure dependent, and then decreases slowly. The pressure effect on the selectivity is dependent on the acetic acid concentration: until 20% w/w of acetic acid in the liquid phase higher values are obtained at 20 MPa, while from 20% to 50% w/w the selectivity is better at 10 MPa. For higher concentrations, the selectivity is not pressure dependent, as found by other authors.[11]

With reference to the loading (Figures 4 and 5), this increases continuously with the weight percent of the acetic acid in the liquid phase, lineally and slowly until 40-50% w/w, but then it increases quickly at higher concentrations. This parameter is not modified by the pressure at low acetic acid concentrations.

The data obtained in this work are in accord with literature data, under all the conditions tested.

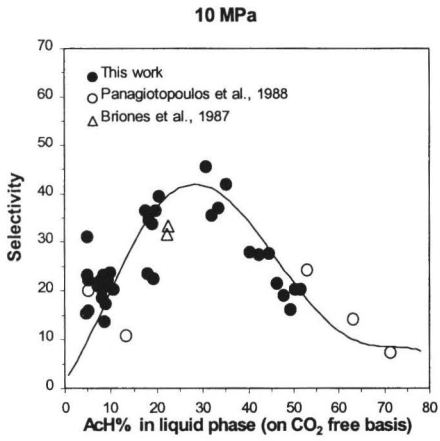

Figure 2. Carbon dioxide selectivity for acetic acid at 313K and 10 MPa

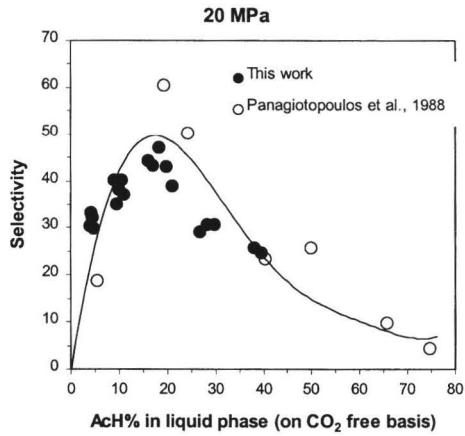

Figure 3. Carbon dioxide selectivity for acetic acid at 313 K and 20 MPa

From the obtained results, at lower concentrations of acetic acid pressure does not affect the loading very much and 20 Mpa, gives a better selectivity than 10 Mpa. Thus it is possible to conclude that at lower concentrations of acetic acid, at 313 K, the pressure of 20 MPa is more effective.

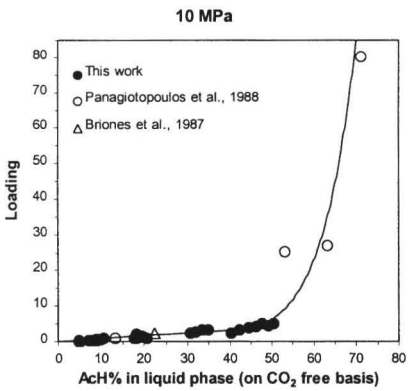

Figure 4. Loading of acetic acid in carbon dioxide at 313K and 10 MPa

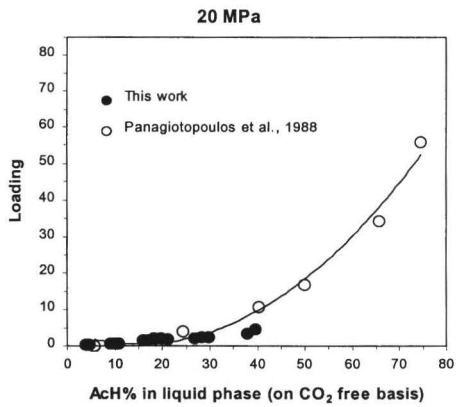

Figure 5. Loading of acetic acid in carbon dioxide at 313K and 20 MPa

NOMENCLATURE

X_i:	Mole fraction of component i in liquid phase, on carbon dioxide-free basis
x_i, y_i:	Mole fraction of component i in liquid and supercritical phases, respectively
M_i:	Molecular weight of the component i
S:	Carbon dioxide selectivity for acetic acid
L:	Acetic acid loading in supercritical carbon dioxide

REFERENCES

1. *Anuario de Ingeniería Química. Ingeniería Química*, 259, (1989).
2. Busche RM, Shimshick EJ and Yates RA *Biotech. and Bioeng. Symp.*, **12**, 249, (1982)
3. Xandri TJM *Cátedra de Industrias Agrícolas. Grupo XII. Universidad Politécnica de Madrid.* (1977).
4. Garwin L and Hutchison KE, *Ind. Eng. Chem.*, **42**, 727, (1950)
5. Pereyra López C, *Tesis de Licenciatura. Universidad de Cádiz.* (1992).
6. Snedecker RA *Thesis Doctoral. Princeton University.* (1955).
7. Elgin JC and Weinstock JJ, *J. Chem. Eng. Data,* **4,** 3, (1959).
8. Yates RA *United State Patent, nº 82986*, (1981).
9. Busche RM, Shimdhick EJ and Yates RA. *Biotech. and Bioeng. Symp.*, **12**, 249, (1982).
10. Briones JA, Mullins JC, Thies MC and Kim BU. *Fluid Phase Equilibria*, **36**, 235, (1987).
11. Panagiotopoulos AZ, Willson RC and Reid RC, *J. Chem. Eng. Data*, **33**, 321, (1988).
12. Di Giacomo G, Brandani V, del Re G and Mucciante V, *Fluid Phase Equilibria*, **52**, 405, (1989).
13. Martínez de la Ossa E, Brandani V, del Re G, Di Giacomo G and Ferri E, *Fluid Phase Equilibria*, **56**, 325, (1990).
14. Di Giacomo G, Brandani V, del Re G and Martínez de la Ossa E, *Quaderni dell'ingegnere chimico italiano. La Chimica & L'Industria*, **2**, 2, (1991).

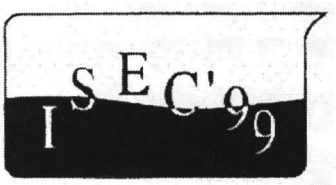

REGENERATION OF ß-CYCLODEXTRIN WITH SUPERCRITICAL CARBON DIOXIDE

G Del Re, G Di Giacomo and M Cinti
Università di L'Aquila, Dipartimento di Chimica, Ingegneria Chimica e Materiali, I 67040 Monteluco di Roio, L'Aquila, Italy

ABSTRACT
Regeneration of ß-cyclodextrin/cholesterol complex resulting from low cholesterol food production was investigated using supercritical carbon dioxide as solvent. From the few available experimental data it appears that this task should be feasible, but quantitative and systematic measurements are required for process design and optimisation. The main purpose of this study was to confirm the feasibility of the supercritical carbon dioxide regeneration process and to evaluate the influence of all the main process parameters like temperature, pressure, solvent flow rate, extraction time along with the influence of different entrainers and their concentration. Several experimental runs were performed at 80 and 100C and for a solvent density range from 500 to 800 kg/m^3, using three different entrainers: methanol, ethanol and 2-propanol at concentrations up to 20 mol %. All the experimental data show that that regeneration is feasible provided that a proper entrainer at proper concentration is used. In addition the effect of temperature is always favourable while the effect of solvent density is less important

Keywords: ß-cyclodextrin, ß-cyclodextrin/cholesterol complex, carbon dioxide, supercritical extraction.

INTRODUCTION

Cyclodextrins are typical host molecules that can include various substances to form complexes. In particular ß-cyclodextrin (ßCD) forms inclusion complex with cholesterol[1] and it is currently used to remove cholesterol from dairy products, egg yolk etc. Claudy et al.[1] have shown that whatever the cholesterol/ßCD ratio used during the preparation of the inclusion complex, the same inclusion complex is always obtained with a molar ratio of 1:3 (cholesterol:ßCD). The inclusion complex is stable, hydrated at room temperature and thermal degradation occurs at about 200°C.

Some processes have been proposed to break the complex and to recover cholesterol and/or ßCD, which can be re-used. One of these processes is based on the hydrolysis of ßCD, that is destroyed,[2] other processes are based on the use of organic solvents, which usually give rise to safety, environmental and energy consumption problems.[3, 4] To overcome these problems the use of supercritical carbon dioxide has been proposed for the regeneration of the inclusion complex cholesterol-ßCD.[5] The use of supercritical fluids for the regeneration of the inclusion complex cholesterol-ßCD is very attractive and it appears to be promising, but systematic data on the effectiveness of supercritical carbon dioxide in breaking the complex are lacking.

In this paper the results of experimental work aimed at evaluating the effectiveness of supercritical carbon dioxide with the addition of different entrainers for the regeneration of ßCD and recovery of cholesterol are reported and discussed. In particular the influence of temperature, pressure and concentration of entrainers, ethanol, methanol and 2-propanol, on cholesterol extraction from the inclusion complex have been evaluated using a HP 7680 FE.

EXPERIMENTAL

The cholesterol-ßCD complex used for the ßCD regeneration tests was prepared according the following procedure: ßCD (10 g) was dissolved in about 600 cm^3 of water, cholesterol (3 g) was dissolved in 350 cm^3 of n-hexane. The solutions were allowed to react for four hours at 30C under vigorous stirring. The ßCD-cholesterol complex was recovered by centrifugation and filtration. It was washed with water and n-hexane to remove ßCD and cholesterol residues, then dried at 40C for 24 hours and stored at 4C. The materials used were: 99% ßCD (Acros), 95% n-hexane (Fluka) and 95-98% cholesterol (Sigma).

The regeneration tests were performed using a HP 7680 T Supercritical Fluid Extractor. The instrument is equipped with a variable restrictor that allows setting both extraction pressure and

© 2000 Society of Chemical Industry

supercritical solvent flow rate. The extracted cholesterol was deposited onto a solid phase trap packed with inert material (HP cat. No.: SS 07680-61350) placed at the variable restrictor exit. To recover the cholesterol the trap is rinsed with 2-propanol (99.5% Aldrich) which is collected in a 2 cm^3 vial. The restrictor and the trap temperature were set at 100C and 90C during the extraction tests and at 65C and 50C during the trap rinse.

The extraction tests were performed by weighting about 0.5 g of ßCD-cholesterol complex, which was transferred to a 7 cm^3 extraction thimble. Pure carbon dioxide (99.9998%, Rivoira) or carbon dioxide with different concentrations of entrainers (ethanol 99.8%, methanol 99.8%, 2-propanol 99.8% all from Aldrich) were used for the extraction.

The extraction procedure consists of repeated 1 minute static extraction followed by 20 minutes dynamic extraction. After each extraction step the extracted cholesterol is recovered by washing the trap with 1 cm^3 of 2-propanol at a flow rate of 2 cm^3/min. The amount of the extracted cholesterol was determined using an enzymatic method (Boehringer Mannheim Cat. No. 139 050).

The extraction tests were performed at 80 and 100°C and at pressures ranging from 167 to 365 bar, corresponding to carbon dioxide density from 500 to 800 kg/m^3.

In table 1 the process conditions for the regeneration tests of ßCD-cholesterol complex are reported along with the total extracted cholesterol. The extracted cholesterol is expressed as the weight % of the total cholesterol found in the complex to be extracted. The ßCD-cholesterol complex used for the extraction tests was the hydrated species with a water content of about 8%.

RESULTS AND DISCUSSION

In figure 1 are reported the experimental data of the regeneration tests using pure carbon dioxide and carbon dioxide with different amounts of ethanol at 80°C and 168 bar (ρ_{CO2} = 500 kg/m^3). There is clear evidence that it is not possible to break the ßCD-cholesterol complex using pure carbon dioxide. For ethanol concentrations lower than 8%, there is only a little improvement in the cholesterol extraction over the use of pure carbon dioxide. When the ethanol concentration in carbon dioxide is equal or greater than 14% a large increase in the cholesterol extraction is observed. A maximum of 43% and 57.8% of cholesterol in the load was extracted using a concentration of ethanol of 14.9 and 19.3% respectively. Nagahama et al.[5] found that it is possible to extract 55% and 80% of cholesterol in the load at 80°C, 176 bar using a concentration of ethanol of 16.1 and 22.3% respectively. The better results of Nagahama et al. are probably due to the different inclusion complex used for the extraction tests. Nagahama et al. used a commercial ßCD-cholesterol complex whose composition (weight fraction, dry basis) was: 0.29 ßCD-cholesterol complex, 0.43 ßCD, 0.28 fat, while in this work pure ßCD-cholesterol complex was used. It is easier for the solvent to come into contact with the cholesterol to be extracted when using ßCD/ßCD-cholesterol complex mixture instead of using pure ßCD-cholesterol complex as in the former case the complex adheres to the surface of ßCD particles. In the latter case, as the cholesterol is extracted, the outer part of the ßCD-cholesterol complex particles is converted to ßCD, so the solvent must diffuse through a layer of ßCD to reach the complex and the extracted cholesterol must diffuse back to the surface of the particles. As extraction takes place it is more and more difficult for the solvent to come in contact with the cholesterol of the complex in the inner part of the particles. This phenomenon also explains the decreasing rate of extraction of cholesterol at long times.

Run No.	T [C]	P [bar]	ρ_{CO2} [g/cm^3]	Entrainer	Entrainer mole %	Q_{CO2} [g/min]	extr. time [min]	tot.extr.CHL [% wt]
1	80	168	0.5	-	-	1.61	80	1.5
2	100	298	0.66	-	-	1.61	60	0.2
3	80	168	0.5	Ethanol	8.2	1.45	160	5.5
4	80	168	0.5	Ethanol	8.2	1.45	60	3.6
5	80	168	0.5	Ethanol	14.9	0.66	160	31.3
6	80	168	0.5	Ethanol	14.9	0.66	200	36.3
7	80	168	0.5	Ethanol	14.9	1.32	180	43.2
8	80	168	0.5	Ethanol	14.9	1.32	180	42.9
9	80	168	0.5	Ethanol	19.3	0.62	200	31.4
10	80	168	0.5	Ethanol	19.3	1.24	220	57.8
11	80	233	0.66	Ethanol	19.3	1.24	180	46.7
12	80	305	0.75	Ethanol	19.3	1.24	220	56.4
13	80	365	0.8	Ethanol	19.3	1.24	160	42.9
14	100	207	0.5	Ethanol	19.3	0.62	200	48.3
15	100	207	0.5	Ethanol	19.3	1.24	120	59.0
16	100	298	0.66	Ethanol	19.3	1.24	140	63.3
17	80	168	0.5	Methanol	14.8	1.4	180	18.2
18	80	168	0.5	2-propanol	14.7	1.26	180	47.3

Table 1 Process conditions and total extracted cholesterol for the regeneration tests of ßCD-cholesterol complex.

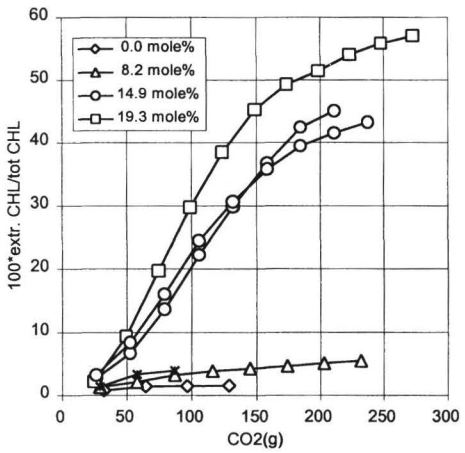

Figure 1. CO_2 extraction of cholesterol from ßCD-cholesterol complex at 80°C, 168 bar (ρ_{CO2}=500 kg/m^3) with ethanol concentration from 0 to 19.3 %.

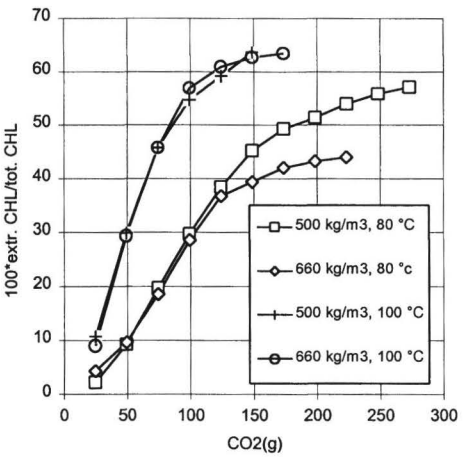

Figure 2. CO_2 extraction of cholesterol from ßCD-cholesterol complex at 80 and 100°C and with ethanol concentration of 19.3 %.

At the beginning of the extraction process the extraction rate of cholesterol is very low when using carbon dioxide with 19.3 mole% of ethanol and even lower when using 14.9%. This is probably due to the presence of hydration water that is quickly removed for the high ethanol concentration in the supercritical solvent.

The results of experimental data for extraction tests at 80 and at 100°C using ethanol concentration of 19.3% reported in figure 2 show that temperature exerts a strong effect on the

cholesterol extraction rate. On the contrary, by comparing the results of test runs nos 1 and 2 of table 1, it can be observed that when pure carbon dioxide is used the cholesterol extraction rate is insensitive to temperature change.

As can be seen from the data reported in figure 3, the cholesterol extraction rate is rather insensitive to carbon dioxide density: a change in density from 500 to 750 kg/m^3 (change of pressure from 168 to 305 bar) does not give any change in cholesterol extraction rate. For further density increase to 750 kg/m^3 (365 bar) a little decrease in cholesterol extraction rate is observed, probably due to the reduced diffusion coefficient of cholesterol in carbon dioxide. The same conclusion can be drawn at 100C from the data reported in figure 2; an increase of carbon dioxide density from 500 to 660 kg/m^3, which means increasing pressure from 207 to 298 bar, has no effect on the cholesterol extraction rate.

The effect of solvent flow rate is shown in figure 4 where experimental data at two flow rates are compared: the cholesterol extraction rate decreases with decreasing solvent flow rate. The experimental data show that it is possible to reach the same ßCD regeneration level by using lower solvent flow rate at expense of a longer but comparable extraction time.

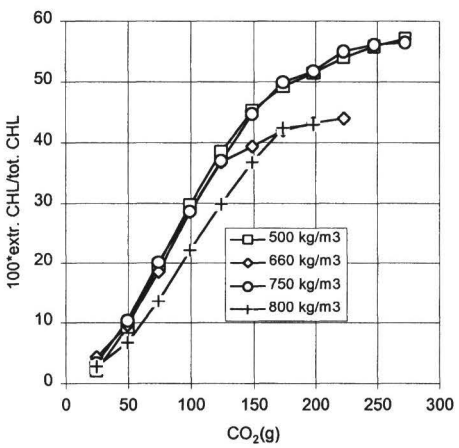

Figure 3. CO_2 extraction of cholesterol from ßCD-cholesterol complex at 80°C, ethanol concentration of 19.3%

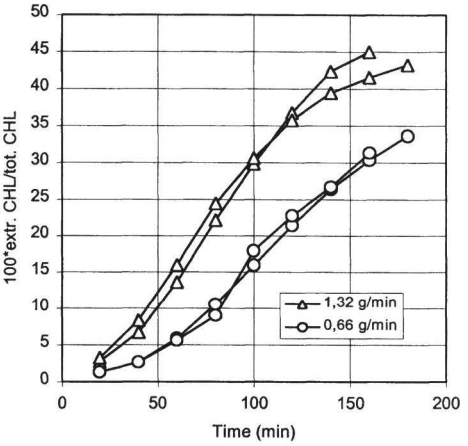

Figure 4. CO_2 extraction of cholesterol from ßCD-cholesterol complex at 80°C, 168 bar (ρ_{CO2}=500 kg/m^3) with different solvent flow rate

Experimental tests using 14.8 mole % of methanol and 2-propanol have been performed to evaluate and compare the effectiveness of different entrainers. The experimental data reported in figure 5 show that methanol is by far less efficient than ethanol for cholesterol extraction, as it has been also found by Nagahama et al.[5] The entrainer effect of 2-propanol is comparable with that of ethanol.

CONCLUSIONS

Cholesterol can be efficiently removed from ßCD-cholesterol complex using supercritical carbon dioxide with the addition of aliphatic alcohols such methanol, ethanol or 2-propanol. The enhancement of cholesterol extraction given by ethanol and 2-propanol is of the same order of magnitude and it is much higher than that one given by methanol.

The effect of ethanol concentration, temperature, pressure and solvent flow-rate on cholesterol extraction from ßCD-cholesterol complex have been evaluated. It has been found that for ethanol concentration below 10 mole % there is no appreciable improvement of cholesterol extraction

over using pure carbon dioxide. Cholesterol extraction increases with increasing temperature, and shows a low decrease with increasing pressure.
The experimental data show that it is possible to carry out the regeneration of ßCD from ßCD-cholesterol complex and recover cholesterol with a safe, environmentally acceptable process.

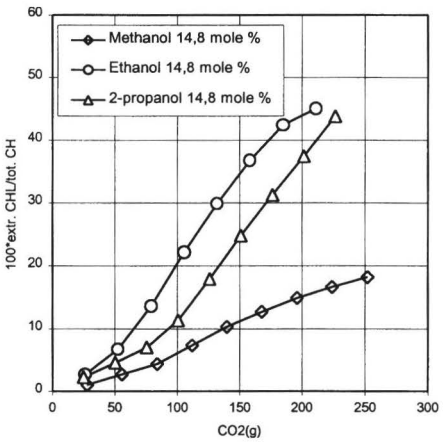

Figure 5. CO_2 extraction of cholesterol from ßCD-cholesterol complex at 80°C, 168 bar (ρ_{CO2}=500 kg/m^3) with different entrainers.

REFERENCES

1 Claudy P, Létoffé JM, Germain P, Bastide JP, Bayol A, Blasquez S, Rao RC and Gonzales B, *J. Thermal Analysis*, **37**, 2497, (1991).
2 Duflot P and Mentink L. *French Pat. Appl.* FR 2 657 623 A1, (1990).
3 Oankenfull D, Sidhu G and Rooney M. *Pat. Appl.* WO 91/16824, (1990).
4 Comini S and Mentink L. *Eur. Pat. Appl.* EP 0 446 600 A1, (1991).
5 Nagahama K, Miyata M and Suzuki T. *Proc. 3rd Int. Symp. on Supercritical Fluids*, 17-19 October, 1994, Strasbourg (France), T3-295.

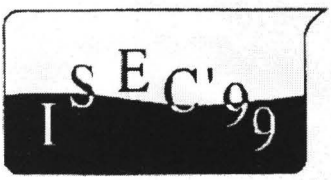

TOCOPHEROL EXTRACTION BY LIQUID AND SUPERCRITICAL CARBON DIOXIDE

MA Blanco, A Molero and E Martínez de la Ossa
Department of Chemical Engineering, Food Tech. and Environmental Technology, University of Cádiz, P.O. Box 40, E-11510. Puerto Real Cádiz, Spain

ABSTRACT
Extraction process of tocopherol from wheat germ by using liquid and supercritical carbon dioxide has been studied. The operational conditions: pressure, temperature, flow rate, were optimised to reach the maximum extraction yield. At the optimal conditions: 200 bar, 40C and 1.5 dm^3/min STP, yields of 25 mg of tocopherol per 100 g of wheat germ were obtained.

Keywords: tocopherol, carbon dioxide, wheat germ, supercritical extraction

INTRODUCTION

Supercritical Fluid Extraction (SFE) is a separation technique that uses the solvent properties of fluids above the critical point. The application of the SFE to the food processing has been developed over the last 20 years, providing a great interest in this industry. At this time SFE in the food industry is carried out using supercritical CO_2 as solvent. Many authors confirm that, for this type of application, CO_2 is a suitable solvent to use since it is non-toxic, non-flammable, non-corrosive, non-polluting, chemically inert, cheap, abundant and, lastly, readily available in large quantities and high purity.[1,2,3,7] On the other hand, in contrast to organic solvents, it is easily removed from any solute without requiring energy by decompression. Since carbon dioxide also has a relatively low critical pressure (73 atm.) and temperature (31.1°C), it is easy and safe to handle and is appropriate for the extraction of volatile and heat sensitive compounds.

Vitamin E or tocopherol (α, β, γ and δ-tocopherol) plays a significant role as an antioxidant in human metabolism. Most of the applications of tocopherol in the food or cosmetic industry[5] are based upon its anti-oxidative and photo-protective properties. It is distributed in plants being especially abundant in vegetable oils. At the moment, vitamin E is obtained from the deodorised oil step in the refining process of vegetable oils.[6]

In this work the recovery of tocopherols from wheat germ is studied by using liquid and supercritical carbon dioxide, optimising the working conditions: pressure, temperature and flow rate of solvent.

MATERIALS AND METHODS

The raw material used for extractions was wheat germ provided by CODEC.S.A, Valladolid (Spain). Carbon dioxide was supplied by "Carburos Metalicos" (purity 99,95%) and methanol by Merck (HPLC grade).

A flow diagram of the supercritical CO_2 plant used, manufactured by NOVA WERKE AG (Effretikon, Switzerland), is shown in Figure 1. The plant and the operating procedure has been described in a previous paper.[1]

The amount of wheat germ oil extracted was gravimetrically determined after the removal of CO_2. The amount of tocopherols in the extracted oil was determined by HPLC, using a "Hewlett Packard 1100" instrument, with an UV-Vis (290 nm.) detector. A Lichrospher RP-18 (Merck) (250 x 4 mm I.D.) column was employed. Methanol, 1 cm^3/min flow rate, was used as mobile phase.

© 2000 Society of Chemical Industry

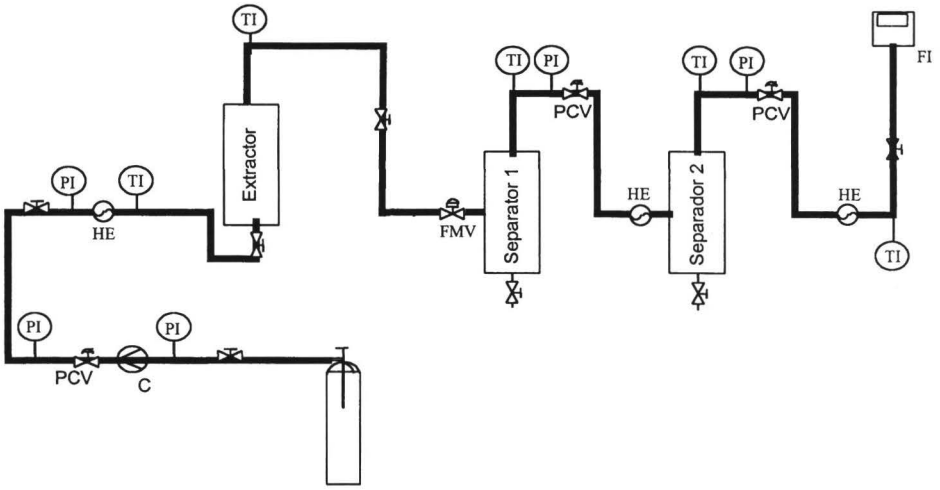

Figure 1.Diagram of the supercritical extraction unit.

RESULTS AND DISCUSSION

Figure 2 shows the pressure and temperature effect on the extraction of tocopherol from wheat germ expressed as percentage recovery of the maximum extraction yield (25 mg of tocopherol per 100 g of wheat germ). As can be seen, extraction yield changes dramatically near the critical pressure of the carbon dioxide, due to variations of the physical properties of the CO_2, such as the density that increases, closely related with its solvent power.

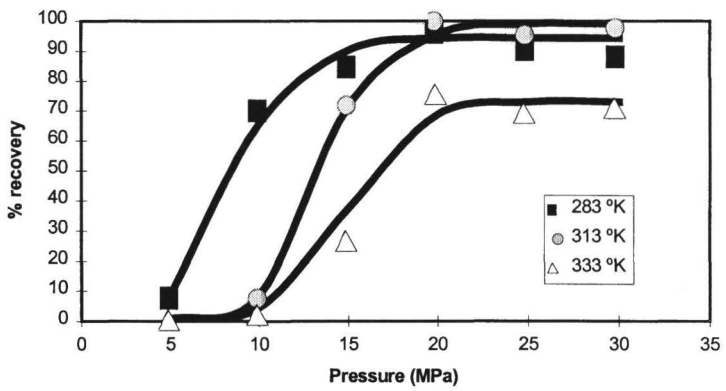

Figure 2. Effect of the pressure on the extraction yield of the tocopherol.

Tocopherols begin to be extracted by liquid CO_2 at lower pressures than supercritical CO_2. At 200 bar, the extraction yield does not depend on the pressure, and the maximum tocopherol recovery is reached, both by liquid and supercritical CO_2. Increasing pressure does not produce

higher extractions yields, so extraction at higher pressure than 200 bar is not justified. On the other hand, controlling temperature is not necessary if the plant is located at an ambient temperature between 10 and 40C as at this pressure the same yields are reached.

Figure 3 shows, the effect of time on the extraction with supercritical CO_2 at 40ºC and 200 bar for different flows rates of CO_2. As expected it can been seen that the yield of extraction increases with increasing time. However, the rate of extraction diminishes with time. Thus for the series of 1.5 and 2.0 dm^3/min a large portion of the tocopherol in wheat germ was extracted (98 %) within 3 hours. A further increase of the extraction time gives a slight increase of the extraction yield, but also increases the expense of solvent. For the smallest flow rate, 1 dm^3/min four hours are needed to reach 92% extraction yield.

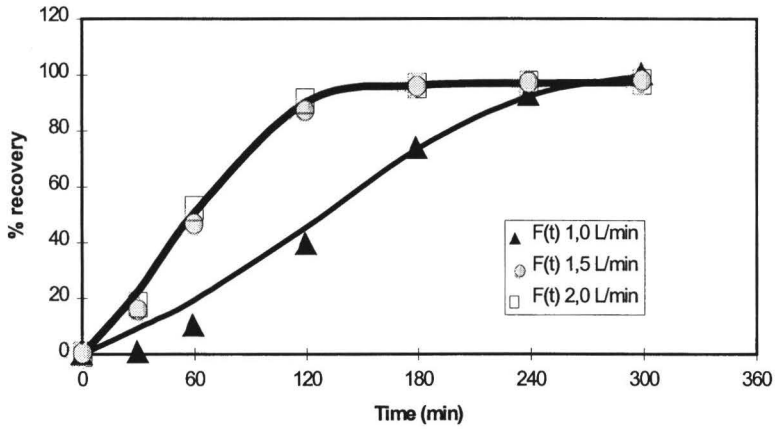

Figure 3. Effect of time at different flow rates on the extraction yield of tocopherol.

As the flow of solvent decreases, the residence time inside the extractor increases. However, although the time of contact between solvent and tocopherol increases, fresh solvent does not get into the extractor and the driving force of extraction, the gradient of concentration, decreases leading to lower yield of extraction.

Therefore it seems reasonable to use a flow rate of 1.5 dm^3/min. in the first steps of extraction, and then use to smaller flows, as has been pointed out by others authors.[1]

Referring to the works of Molero et al.,[4] it can be concluded that the extraction of tocopherol occurs at the same time,or even before, the extraction of wheat germ oil. This way, maximum yields are obtained in both cases for a flow of 1.5 dm^3/min. after 3 hours of extraction.

So, in this work, it has been demonstrated that SFE is a good technique for recovery of tocopherol from wheat germ. Due the similarity of solubility parameters of the different compounds in this matrix, fractionation of a lipid extract by SFE alone is not possible to enrich tocopherol from such a complex mixture. Therefore supercritical fluid chromatography (SFC) could be coupled with SFE for enriching the tocopherol, this being the objective of future work. .

REFERENCES

1. Huber W and Martinez de la Ossa E, *Int. J. of Food Sci. and Tech.* **31**, 143, (1996).
2. Friedrich JP and List GR, *J. Agric. Food Chem.* **30**, 192, (1982).
3. Guerrero L, *Alimentación, Equipos y Tecnología.* **11**(10), 95, (1992).
4. Luque de Castro MD, Valcárcel M and Tena MT, *"Extracción con Fluidos Supercríticos en el Proceso Analítico"*. Ed. Reverté SA, (1993)
5. Molero A, Blanco MA and Martínez de la Ossa E, *Alimentación, Equipos y Tecnología,* Junio, 63, (1997).
6. Shenoy VR, *J. Sci. & Ind. Res.*, **54**, 357, (1995).

7. Stenberg O, *Lipid-Technology*, **8**(5), 105, (1996).
8. Taniguchi M, Kamihira M, Tsuji T and Kobayashi T, *World Congress of Chemical Engineering*. Tokyo (Japan), 1040, (1986).

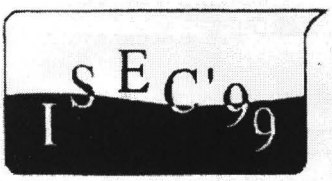

EXTRACTION OF WHEAT GERM OIL BY LIQUID AND SUPERCRITICAL CARBON DIOXIDE

A Molero and E Martínez de la Ossa
Department of Chemical Engineering, Food Technology and Environmental Technology, University of Cádiz, Apdo. 40. E-11510 Puerto Real (Cádiz). Spain

ABSTRACT
This paper describes the extraction of wheat germ oil by liquid and supercritical carbon dioxide, from the point of view of both operative method and pre-treatment of raw material. The yields obtained are very similar to those from the conventional extraction process using hexane as solvent, although higher quality oil is obtained. Furthermore, the fatty acids composition of the wheat germ oil extracted is particularly rich in unsaturated fatty acids.

Keywords: linoleic acid, wheat germ oil, supercritical extraction, carbon dioxide

INTRODUCTION

In recent years, the application of Supercritical Extraction (SCE), and in particular, the use of liquid and supercritical carbon dioxide has been of considerable interest in the food industry. The decaffeination of coffee,[1,2] the preparation of hop extracts for the beer industry[1,2] and the production of spice essences and extracts[3,4] are just three examples.

This separation technique offers extraction yields very similar to those obtained by conventional extraction processes using liquid solvents. Among its advantages, carbon dioxide is non-toxic, non-flammable, non-corrosive; it is cheap and readily available in quantity, with a high degree of purity. Furthermore carbon dioxide has a relatively low critical temperature (31.1°C) and critical pressure (73.8 atm).

For some years, the beneficial effects of vegetable oils in the human diet have been known, this is basically due to their high content of unsaturated fats and their high energy value.[5,6] Linoleic acid is essential for human physiology and must be included in our diet, because it cannot be synthesised by the cell or by cellular tissue from any other fatty acid, nor indeed from any other source.[7,8]

This paper studies the production of wheat germ oil by SCE, using liquid and supercritical carbon dioxide. The working conditions of the process (pressure, temperature and solvent flow rate) and the pre-treatment of the raw material (grain size and humidity) have been optimised. Finally a comparison of the relative qualities of the oils produced by SCE and by organic solvent extraction has been made.

EXPERIMENTAL

The raw material used was wheat germ of 0.75 mm average grain size supplied by CODEC S.A. in Valladolid, Spain. As necessary, the wheat germ was crushed in a "FUTURMAT" model FP mill, of 2 kg capacity and capable of milling to 18 grades of particle size. Milled material used in the study was a fine powder of 0.29 mm average particle diameter. Dehydration of the raw material was carried out by heating to 65°C, for a period of at least 4 hours, until constant weight.

For comparison with conventional extraction process using liquid solvents, a SOXHLET type apparatus with hexane as solvent, was used. Extraction time was 16 hours that guaranteed the full depletion of the grain and allowed the maximum possible extractive yield to be determined. These values are considered very important to establish a basis for comparison with the high-pressure SCE process.

The flow diagram of the equipment used and the operation protocol have been described in a previous paper.[9]

The optimisation of the extraction process covers the following ranges of operating conditions:

© 2000 Society of Chemical Industry

pressure, from 50 to 300 bar; temperature, 10, 40 and 60°C; and solvent flow rate, from 0.5 to 2.0 dm^3/min. For the extractions performed at 10°C, the electric heating jacket was replaced with another brass tube jacket for the circulation of water at that temperature.

The physico-chemical characterisation of the oils obtained was measured by the standard methods of the A.O.A.C.[10] The various indices determined were: acidity (expressed as the % of oleic acid); iodine (by the Hanus method) and saponification. The fatty acid composition of the oil was determined by gas chromatography using a model 5890 Hewlett Packard fitted with a "Carbowax 20M" capillary column and an FID detector.[9]

All the products and chemical reagents used were of analytical quality, the carbon dioxide used was of 99.95% purity (Carburos Metálicos, S. A.).

RESULTS AND DISCUSSION

Figure 1 shows the influence of the pressure at which the extraction process is performed. Near the critical region of carbon dioxide a dramatic change occurs in the amount of oil extracted. This change is due to variations in the physical properties of carbon dioxide, particularly density that is closely related to its solvent capacity.

The extraction yield depends mainly on the pressure and temperature. The use of pressures of around 150 bar makes the extraction of wheat germ oil with liquid and supercritical carbon dioxide equally viable. Beyond these practical limits, it requires a considerable increase in pressure to achieve even a small increase in the separation yield. These results are confirmed by those presented in other studies.[11,12]

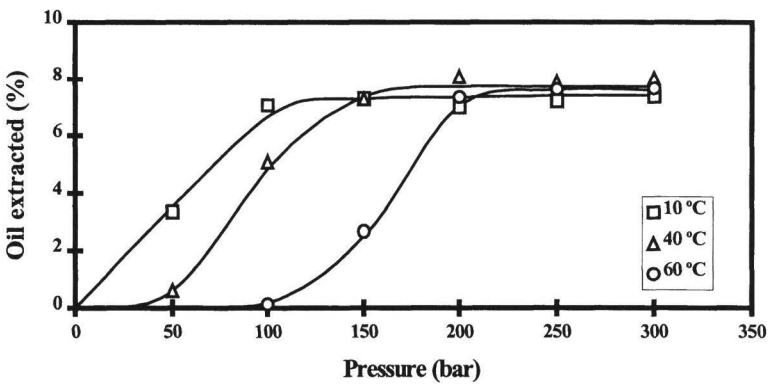

Figure 1 Effect of pressure on the extraction of wheat germ oil in liquid and supercritical carbon dioxide.

Figure 2 shows the effect of CO_2 flow rate on the extraction yield, at operating conditions of 150 bar and 40°C. It can be seen that the maximum oil extraction yield together with the minimum consumption of solvent is achieved at about 1.5 dm^3/min. With these conditions, the optimum extraction time is 3 hours.

Figure 3 shows the extraction yield of oil with supercritical carbon dioxide, comparing partially hydrated wheat germ samples with fully dehydrated samples. As can be observed, no appreciable differences were detected in the yields. Similar results were obtained when the influence of grain size on yield was studied.

Figure 4 shows that no significant difference in extraction yield was obtained when grain was milled to an average particle size of 0.297 mm. It is concluded that wheat germ does not need pre-treatment prior to extraction,[13] in contrast to other seeds.[12]

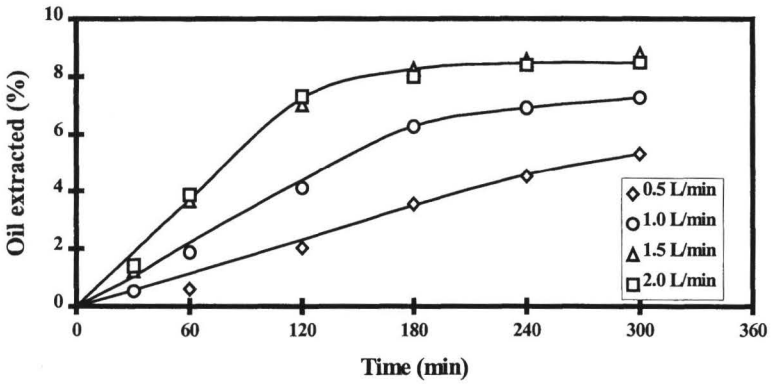

Figure 2. Effect of flow rate of SC-CO_2 on the extraction of wheat germ oil.

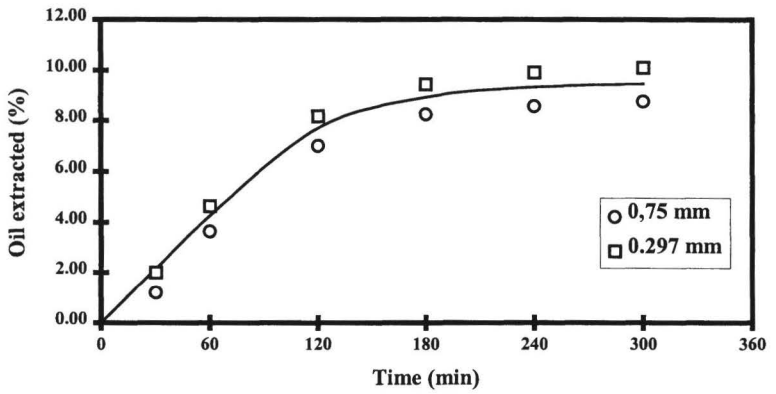

Figure 3. Effect of the wheat germ humidity on the extraction with SC-CO_2.

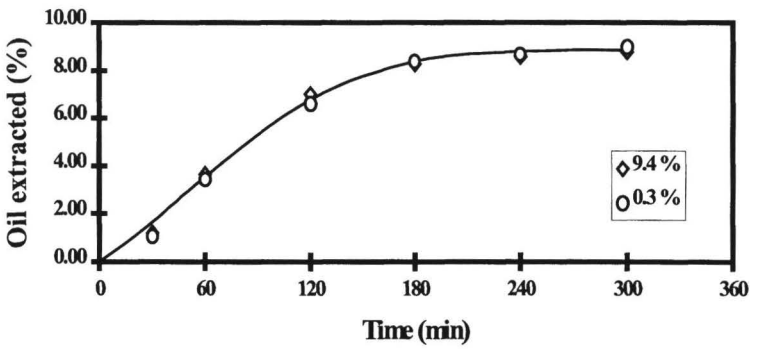

Figure 4. Effect of the size of wheat germ on the extraction of oil in SC-CO_2.

Table 1 gives the experimental yield values for the extraction of wheat germ oil, using both liquid and supercritical carbon dioxide under the optimised operating conditions. For comparison the corresponding data for conventional extraction using hexane also shown.

As can be seen, the apparent yield from the high-pressure extraction of wheat germ oil is lower than extraction with hexane. This difference is due to hexane being much less selective than CO_2.[14,15] Additionally, oil extracted by SCE with carbon dioxide is free from residual solvent, in contrast with oil conventionally extracted.

Operating conditions	Yield (wt. %)
CO_2, 100 bar, 10°C, 3 h	7.3
CO_2, 150 bar, 40°C, 3 h	8.0
CO_2, 200 bar, 60°C, 3 h	7.8
Hexane, Soxhlet, 16 h	8.6

Table 1 Comparison of wheat germ oil extraction yields obtained using hexane and carbon dioxide as solvents

Table 2 presents a comparison of the physico-chemical characterisation of wheat germ oils obtained by the SCE process at the optimum operating conditions for the SCE process, and by the Soxhlet equipment using hexane as solvent.

Physicochemical indices	Solvent			
	carbon dioxide			hexane
	100 bar, 10°C, 3 h	150 bar, 40°C, 3 h	200 bar, 60°C, 3h	Soxhlet, 16 h
Free fatty acid (%)	31.6	12.4	34.4	27.3
Iodine index (g per 100 g)	111	100	115	107
Saponification index	217	185	204	207
Unsaponifiable fraction (%)	1.59	7.28	7.05	2.76

Table 2 Comparison of properties of extracted wheat germ oils obtained using hexane and carbon dioxide as solvents

When the SCE process is carried out at 40°C, the carbon dioxide shows a very high specificity for the triglycerides contained in the wheat germ oil, and consequently extracts lower amounts of the free fatty acids. The values of the iodine and saponification indexes indicate that the quantity of triglycerides present in the oils extracted by the two processes is similar.

Among the purposes of the subsequent oil refining process stage is the reduction of the content of free fatty acids in the oil to acceptable levels. In this way, is clear that supercritical extraction carried out at 150 bar and 40°C would considerably simplify the refining stage given the low content of these undesirable compounds of the oil obtained.

Oil	Fatty acid composition (%)					
	Palmitic C16:0	Palmitoleic C16:1	Stearic C18:0	Oleic C18:1	Linoleic C18:2	Linolenic C18:3
CO_2, 100 bar, 10°C, 3 h	18.91	0.24	0.69	16.41	57.26	6.48
CO_2, 150 bar, 40°C, 3 h	18.15	0.20	0.52	13.94	58.56	8.25
CO_2, 200 bar, 60°C, 3 h	18.48	0.22	0.49	13.81	58.74	8.25
Hexane, Soxhlet, 16 h	18.09	0.22	0.50	13.69	58.99	8.51

Table 3 Fatty acid composition of oil extracted using hexane and liquid and supercritical carbon dioxide

Table 3 gives the fatty acid composition of wheat germ oil obtained by extraction with liquid

and supercritical carbon dioxide, under the different operating conditions tested in comparison with that of oil extracted in the Soxhlet equipment using hexane as solvent. The results show that all the oils contain a high proportion of unsaturated fatty acids - 81% unsaturated against 19% saturated - as occurs with other vegetable oils. Also, in all cases, the main fatty acid is linoleic, representing around 58% of the total.

REFERENCES

1 Stahl E, Quirin KW and Gerard D. *Dense Gases for Extraction and Refining*, Springer, New York, Chap. 2, (1988)
2 Bork M and Körner JP, *Z.F.L.* **42**, 732, (1991).
3 Quirin KW and Gerard D. *Z.F.L.* **41**, 731, (1990).
4 RAPS *Informationsheet, Kulmbach*, (1993).
5 Williams J. *Oléagineux*, **35**, 457, (1980).
6 Connor WE and Connor SL. *Adv. Inter. Med.* **35**, 139, (1990).
7 Cantafora A. *Industrie Alimentari*, **21**, 454, (1982).
8 Carola C. *Riv. Ital. Sostanze Grasse*, **51**, 353, (1974).
9 Molero A. *Tesis de Licenciatura*, 1994, University of Cádiz (Spain).
10 *Standard Methods of Analysis*, Association of Official and Analytical Chemists' Society, Washington, DC, 13th, edn., (1980).
11 Stahl E, Schütz E and Mangold K, *J. Agric. Food Chem.* **28**, 1153, (1980).
12 Molero A, Pereyra C and Martínez de la Ossa E. *Chem. Eng. J.*, **61**, 227, (1996).
13 Taniguchi M, Kamihira M, Tsuji T and Kobayashi T. *World Congress of Chemical Engineering, Tokyo,* , p.1040, (1986)
14 Friedrich JP and List GR. *J. Agric. Food Chem.*, **30**, 192, (1982).
15 Zhao W, Shisshikura A, Fujimoto K, Arai K and Saito S. *Agric. Biol. Chem.*, **51**, 1773, (1987).

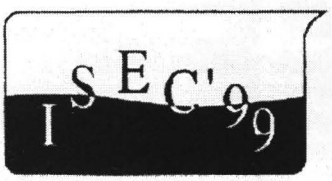

EXTRACTION OF THE ANTIBIOTIC PLEUROMUTILIN FROM FERMENTATION BROTH USING COMPRESSED CARBON DIOXIDE

T Walford, T Lu, R Santos, MB King, AJ Biddlestone and A Stefanska[1]

School of Chemical Engineering, University of Birmingham, Birmingham, B15 2TT, UK

[1]SmithKline Beecham Pharmaceuticals, New Frontiers Science Park, Harlow, Essex, CM19 5AW, UK

ABSTRACT

Compressed CO_2 at temperatures between 30 and 60C and pressures between 50 and 250 bar has been demonstrated to extract the antibiotic pleuromutilin, from pure solid or fermentation broth. Dynamic extractions from fermentation broth has given both yields and extract purities of > 90 %, after 1 hr. In order to obtain an estimate of the maximum solubility that could be achieved from the broth, measurements have been made of the solubility of the pure solid compound in compressed CO_2, using a packed column. Maximum CO_2 solubility within the range of conditions used was found to be 2.4 $mg.g^{-1}$ CO_2. The saturated solubility in a number of organic solvents was also determined and four were used as co-solvents with the CO_2. Using ethanol as co-solvent, at 5 % (v/w) feed, it was possible to increase the solubility of solid pleuromutilin by a factor of 4.6 when compared with pure CO_2. Pleuromutilin solubility into CO_2 from aqueous solution was found to be considerably lower than in packed column extractions. Studies showed that the solids present in the fermentation broth (i.e. cells and insoluble fermentation medium components), decreased the CO_2 solubility and extract purity when compared with culture supernatant. Comparisons have been made between the extraction of fermenter material with CO_2, and with a variety of conventional solvents. CO_2 extracts were of comparable purity to those generated by organic solvent extraction, although yields over a comparable extraction time were lower.

Keywords: pleuromutilin, fermentation broth, supercritical extraction, carbon dioxide, ethanol co-solvent

INTRODUCTION

The use of near critical CO_2 for the extraction of a variety of natural products from complex matrices has been extensively reported.[1] However, the vast majority concern the extraction, fractionation and purification of compounds from plant material. There are relatively few publications covering the processing of fermentation broth, and within this set, even fewer working on the extraction of aqueous rather than lyophilised material.[2,3,4] There are a number of potential advantages with the supercritical extraction of aqueous fermentation material. These include its low-toxicity, rapid removal of solvent at low temperature, and the ability to alter density, resulting in selectivity of the solvent extraction. These advantages are to some degree countered by the need for continuous high volume throughput, and problems encountered handling the aqueous medium, which need to be considered before supercritical extraction can replace conventional technology. However, with continuing environmental legislation regarding solvent use and disposal, and with further process development, supercritical extraction could soon represent a viable alternative to solvent extraction.

Work to date in this area has shown promise. Cocks *et al.*[2] demonstrated that, using lyophilised broth, a variety of solvent extractable metabolites were also extractable with CO_2, with and without co-solvent. They indicated that the range of compounds extracted was more selective than with conventional solvents. Work by te Bokkel [3] and Malik, [4] has illustrated the effect of broth pre-treatment on the extraction rate and yields of cyclosporin and milbemycins respectively.

Pleuromutilin is a diterpenoid antibiotic discovered in 1951.[5] It is produced by a number of fungal species and is found in both the cells and extracellular fluid of the fermentation broth. This gives the opportunity to study extraction from whole broth and supernatant. Pure pleuromutilin has previously been shown to be extractable from an ethanol/water solution using supercritical CO_2.[6]

© 2000 Society of Chemical Industry

EXPERIMENTAL

Crystals of pleuromutilin were obtained by solvent extraction of culture broth at a purity of approximately 85%. These, and all other samples, were analysed by HPLC using a Rainin Microsorb C18 5μm column (0.46 mm i.d. x 250 mm) with guard column (0.46 mm i.d. x 50 mm), with 1 cm^3 min^{-1} flow rate and column oven temperature of 30C. The column was eluted with 40 / 60 (v/v) acetonitrile / distilled water. Detection was by UV absorbance at 205 nm. The crystals were further purified by chromatography using a Rainin Microsorb C18 5μm preparative column (21.4 mm i.d. x 250 mm), eluting at 10 cm^3 min^{-1} with 40/60 (v/v) acetonitrile/deionised water, followed by crystallisation of selected fractions from the eluant. Pleuromutilin with a purity of >99.5% was generated. The solubility of the compound was determined in a range of solvents by generating a saturated solution at 20 ± 0.5C, and analysing this solution after 30 minutes by HPLC. All solvents used were >99 % in purity. CP grade (99.995 % pure) CO_2 was used in all experiments.

Fermentation broth for extraction was generated by shake flask fermentation. Culture supernatant was produced by centrifugation and subsequent filtration through Whatman 541 filter papers. CO_2 solubility measurements of the pleuromutilin crystals were carried out using a packed HPLC column,[7] with co-solvent addition at 5% v/w into a pulse damping vessel prior to the column, with the exception of water, where a saturated stream of CO_2 was used. The other three organic solvents are miscible with CO_2 under the conditions used, whereas water solubility in CO_2 is far less than the 5 % v/w used. The aqueous solutions of pleuromutilin used for model extractions were stored at 5C, leading to a maximum solubility of ≈ 250 $\mu g cm^{-3}$. 200 cm^3 of whole broth and supernatant were extracted using a 500 cm^3 volume temperature controlled pressure vessel. This low volume was used to allow for sufficient head-space for foam build up on charging or depressurisation. Carbon dioxide flow was introduced into the vessel via a HPLC type cup filter, (with a pore size of 10μm), measured using a mass flow meter and controlled using metering valves. Flow rate was maintained at ~ 600 gh^{-1}. After the extraction period, the extract collectors and connecting lines were washed out with solvent. This was evaporated to give an extract weight and analysed by HPLC. Broth was acidified to pH 3 when extracted with organic solvents, to mimic the acidifying affect of CO_2 on aqueous solutions.

RESULTS AND DISCUSSION

The solubility of pure pleuromutilin in CO_2 is seen to be a function of extraction temperature and pressure used (figure 1).

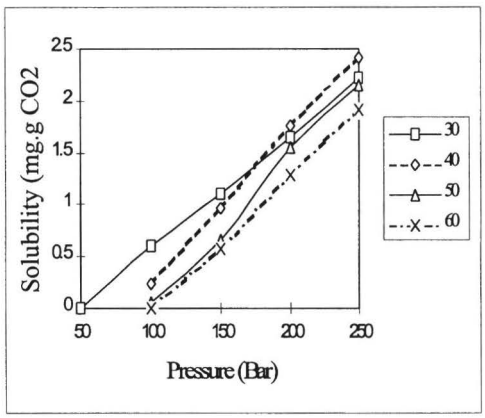

Figure 1. Solubility of pleuromutilin in compressed CO_2

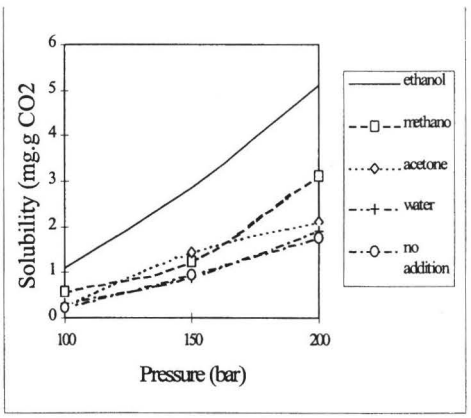

Figure 2. The influence of co-solvent on solubility at 40C

These parameters affect the solvating power by altering the density of the CO_2 used, with maximum solubility observed at higher densities.

Although the pleuromutilin used for these solubility experiments was > 99.5% pure, the remaining impurities were found to be highly soluble in CO_2. Impurity removal was accentuated at higher temperatures, and with the co-solvent additions. This technique may be of use to remove trace impurities from bulk crystals that as pleuromutilin and its impurities, have substantial differences in CO_2 solubility. The use of co-solvents, at 5% v/w, enhanced solubility in all cases with the exception of water addition, which was comparable with pure CO_2 at 40°C (figure 2). The solubility of solid pure pleuromutilin in organic solvents is high compared to that in CO_2 (table 1). The solubility is further decreased when used to extract from dilute aqueous solutions (figure 3), although this is more a function of solvent density and phase contacting.

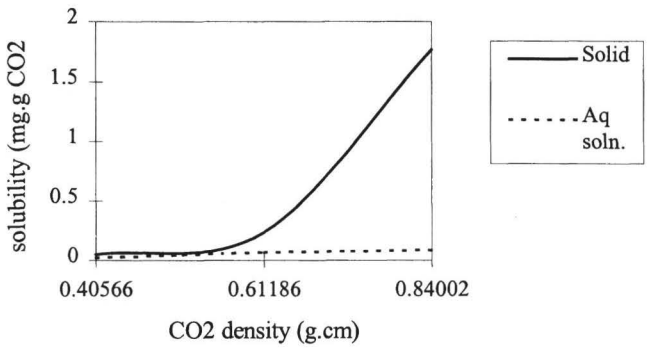

Figure 3. The effect of CO_2 density on pleuromutilin extraction from solid and dilute solution

Solvent	Pleuromutilin Solubility $mg.cm^{-3}$
Methanol	413
Acetone	311
Ethanol	261
Ethyl acetate	185
Chloroform	114
Toluene	22
CO_2 (40C/ 250 Bar)	2.4
Water	0.5
Hexane	0.2

Table 1 Pleuromutilin solubility

The advantages of carbon dioxide extraction are in its ability to selectively extract components and rapidly concentrate the solutes. This removes the requirement for solvent concentration that may be time consuming and generate heat that can accelerate degradation of sensitive metabolites. By selectively solublising compounds of interest, the resultant extract may be substantially purer than with conventional solvent extraction, leading to fewer subsequent process stages and higher overall yields.[4]

Shake flask fermentation broth was used to compare the extraction of whole broth and supernatant using CO_2, and three conventional solvents previously used for the extraction of pleuromutilin and related metabolites.[5,8] This broth had a pleuromutilin titre of 686 $\mu g.cm^{-3}$, with approximately 510 $\mu g.cm^{-3}$ in the supernatant. 200 cm^3 of whole broth and supernatant were extracted with CO_2 for 30 minutes at 40°C/100 bar. Duplicate samples of 50 cm^3 whole broth and supernatant were extracted at pH 3 with an equal volume of solvent (table 2).

Using whole broth at pH 3, the organic solvents extracted between 81 - 86% of the pleuromutilin, compared with 30% for CO_2 (figure 4). The purity of the extracts ranged from 52 - 79%, (CO_2 was 74 %). With supernatant at pH 3, the organic solvents extracted between 42 - 100% of the pleuromutilin, compared with 40% for CO_2 (figure 5). The purity of the extracts ranged from 52 - 88%, (CO_2 was 84%). Emulsification was particularly heavy with the ethyl acetate supernatant extraction, and solvent recovery and removal from the aqueous phase was incomplete for all samples.

Extractant	Extraction material[1]	Total extract (mg)	Purity (%)	Amount Extracted (%)
CO_2 (40°C/ 100 bar)[2]	Supn	60.40	83.75	39.65
	WB	55.60	74.26	30.08
Ethyl acetate[3]	Supn	25.6	53.11	42.61
	WB	54.25	51.55	81.49
Toluene	Supn	34.50	88.20	95.34
	WB	37.30	78.62	85.46
Chloroform	Supn	61.75	52.28	101.17
	WB	48.45	57.55	81.26

[1] (Supn) supernatant, (WB) whole broth;

[2] CO_2 extraction 200 cm^3 of broth compared to 50 cm^3 for solvent extractions

[3] heavy emulsification at pH 3 with the ethyl acetate extraction of the supernatant

Table 2 Comparison of supernatant and whole broth extraction at pH 3 with compressed CO_2 and organic solvents.

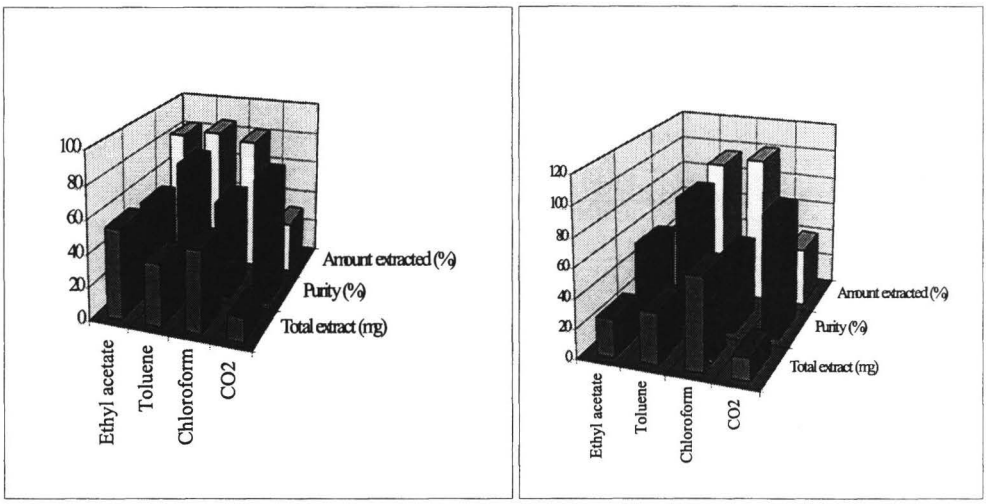

Figures 4 and 5. Comparison between CO_2 and conventional solvent extraction of pleuromutilin from whole broth (left) and supernatant (right) at pH 3

The overall comparison between CO_2 and solvent extraction is encouraging, as the CO_2 extraction process has not yet been fully optimised. Although the yields are lower than those for the organic solvents, the purity is comparable. The best organic solvent was toluene, which as it has a boiling point of 110.5C, requires heat input to remove the solvent and concentrate the extract, even under

vacuum distillation. It should be noted that whereas the solvent extractions were carried out with good phase dispersion, the CO_2 was bubbled through the broth with no additional phase mixing.

Mixing enhancement, particularly with whole broth, is an area than is currently being investigated with a view to carrying out continuous extractions.

	Extraction after 1 hour	Extract purity at end point (%)
Whole broth 100 bar 40°C	31.5	80.3
Supernatant 100 bar 40°C	80.4	92.8
Supernatant 100 bar 30°C	94.3	76.3

Table 2 Comparison of extraction after 1 hour, and final extract purity

The extraction time profile was investigated using whole broth and supernatant at 100 bar, 40C and with supernatant at 100 bar, 30°C. The broth used for these experiments was from a separate batch to that used in solvent extraction experiments. It can be seen that the extraction rate is enhanced from the supernatant using sub-critical CO_2 at 30°C, compared to supercritical CO_2 at 40°C (figure 6). This can be explained in terms of solvent density, as sub-critical CO_2 has a density of 0.7656 $g.cm^{-3}$, compared with 0.6118 $g.cm^{-3}$ for the supercritical CO_2. This would also explain the fact that at a higher density thus solvating power the extract purity is lower, due to the co-extraction of impurities (table3).

The effect of the solids in the whole broth on extraction rates is also shown in this experiment. After rapid initial extraction, the high viscosity of the whole broth limits the mass transfer of pleuromutilin into the CO_2 extracting zone in the central core of the vessel, from the poorly mixed outer regions of the vessel. As the supernatant is of lower viscosity, there is greater mixing as the CO_2 enters the vessel, so enhanced mass transfer is seen.

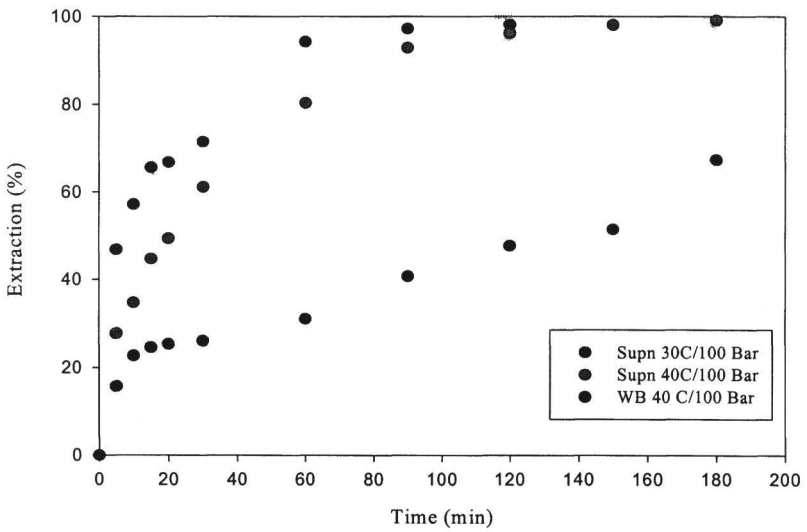

Figure 6. Pleuromutilin extraction time course from supernatant (supn) and whole broth (wb).

This work has shown the capability of compressed CO_2 to extract the antibiotic pleuromutilin from fermentation broth, and generate material that is comparable with conventional solvent extraction. As CO_2 is gaseous at ambient conditions, upon depressurisation it leaves no solvent residues in either the aqueous fermentation broth or the solute extract. This can be an important consideration in disposal of extracted broth. In addition a rapid depressurisation of the spent broth can substantially reduce the number of viable cells by pressure disruption. The potential for CO_2 extraction of microbial metabolites from fermentation broth is well illustrated by the results of these experiments. Further work is being carried out to develop a continuous extraction process for pleuromutilin and other fermentation metabolites.

Shake flask fermentation broth was used to compare the extraction of whole broth and supernatant using CO_2, and three conventional solvents previously used for the extraction of pleuromutilin and related metabolites.[5,8] This broth had a pleuromutilin titre of 686 $\mu g.cm^{-3}$, with approximately 510 $\mu g.cm^{-3}$ in the supernatant. 200 cm^3 of whole broth and supernatant were extracted with CO_2 for 30 minutes at 40°C/100 bar. Duplicate samples of 50 cm^3 whole broth and supernatant were extracted at pH 3 with an equal volume of solvent (table 2).

REFERENCES

1 Beven CD and Marshall PS *Natural Product Reports* **1994** , 451
2 Cocks S, Wrigley SK, Chicarelli-Robinson M and Smith RM. *J.Chrom.A.*, **697**, 115, (1995)
3 te Bokkel DW *Ph.D. thesis,* University of Western Ontario, Canada.(1990)
4 Malik N *Ph.D. thesis*, University of Leeds. UK (1993)
5 Kavanagh F, Hervey A and Robbins WJ *Proc. Nat. Acad. Sci.*, **37**, 570, (1951)
6 Coenen H and Hagen R. *German Patent No.DE3318194* (1984)
7 Walford T, Lu T, Santos R and King MB. *Proceedings of the 5th Meeting on Supercritical Fluids, Materials and Natural Product Processing*, Nice, 489, (1998)
8 Michel KH and Higgens CE *US patent No.4129721* (1978)

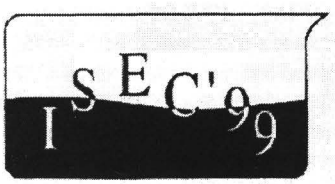

DIRECT SUPERCRITICAL FLUID EXTRACTION OF ORGANIC COMPOUNDS FROM AQUEOUS SOLUTIONS

Yu A Zolotov, IA Revelsky and IN Glazkov
Analytical Chemistry Division, Chemistry Department,
Lomonosov Moscow State University, 119899, Moscow, Russia

ABSTRACT
A solventless off-line SFE method has been developed which excludes the use of organic solvents for trapping and for washing out of analytes. Regularities of direct SFE from aqueous solutions of chlorinated pesticides, polychlorinated biphenyls, phthalates and polynuclear aromatic hydrocarbons have been also investigated. Comparison of direct SFE from water, micro-LLE, and solid phase extraction of ultratraces of chlorinated biphenyls (10^{-12}-10^{-9} g) has been performed.

Keywords: organic pollutants, polyaromatic hydrocarbons, phthalates, chlorinated biphenyls, chlorinated pesticides, supercritical extraction, carbon dioxide, nitrous oxide

INTRODUCTION

Most dangerous organic environment pollutants (polychlorinated biphenyls, polychlorinated dibenzodioxins, polychlorinated dibenzofurans, chlorinated pesticides, polyaromatic hydrocarbons etc.) have usually to be determined in water on ppb or even ppt level. Therefore sample preparation, including pre-concentration is very important. It is based mainly on liquid/liquid extraction (LLE) including usually multi-step procedures and is time consuming. Other methods based on solid phase extraction use different approaches for removing targeted compounds from the sorbent namely organic solvents or thermo-desorption. The main disadvantages of these approaches are the use of organic solvents during isolation of pollutants and extract collection and the use of only a very small part of the final extract for the determination of analytes after the pre-concentration stage. These drawbacks cause dilution of analytes, their contamination with impurities present in the organic solvents, loss of analytes during evaporation or trapping, necessity of using a large water sample, increasing analysis time etc.[1] Modern variants of the above methods: solid phase micro-extraction and micro-LLE only partially eliminate some of the listed drawbacks.

One of alternative approaches for organic ultratrace analysis is direct off-line SFE from aqueous solutions.

The region of supercritical fluid is interesting especially as an extraction medium. Density and solvent power of supercritical fluids are close to the respective values for liquids. However the viscosity of a supercritical fluid is close to viscosity of gas and diffusion coefficients are between gas, and liquid values.

Some possible advantages of supercritical fluids as extraction medium are:

- exclusion of toxic organic solvent use;
- possibility of selective extraction by slight changes of the pressure and temperature;
- much higher degree of extractant purity than of organic solvents because carbon dioxide and nitrous oxide that are commonly used fluids are gases at ambient conditions;
- simplicity of concentrating and removing extractant from the extract.

There are some publications on direct supercritical fluid extraction of a limited number of organic compounds. The concentrations of the organic compounds in water were not lower than ppb level and extraction time was up to 2 hours. In addition, an organic solvent was used in most cases for the collection of the targeted compounds from the flow of supercritical fluid at the outlet of SFE cell when off-line SFE was carried out.[2, 3] In this case contamination of SFE extract with organic solvent impurities takes place. Therefore these works demonstrate only the possibility of direct SFE from aqueous solutions and do not show true features of a direct SFE sample preparation in the case of ultratrace organic analysis.

© 2000 Society of Chemical Industry

Trapping of small quantities of organic compounds from the flow of supercritical fluid is the key point of all SFE methods in the case of their off-line use. There are some approaches to trapping. The most widely used approach is based on the trapping of extracted analytes into a small quantity (1 cm^3 and more) of organic solvent.[5-9] Disadvantages of this approach are the dilution of extracted compounds and their contamination with impurities present in the organic solvent. Degree of recovery greatly depends on the volatility of analytes and it is higher for low volatile compounds.

Another approach is based on the sorption of organic compounds on solid sorbents or in empty glass vials and subsequent recovery of them with an organic solvent.[5-8, 9-11] The main drawback of this approach is the contamination of the extract solution due to impurities from the organic solvent and a higher loss of extracted compounds in the case of empty vials.

The third approach includes use of short capillary columns with bonded stationary phases for trapping of extracted compounds and their recovery with a small quantity (0.1 cm^3) of an organic solvent.[12] This method seems to be superior to other SFE off-line methods. The main limitation of the latter method and also the former ones is the sampling of only small part of the organic solution of analytes (0.001 - 0.01 part) and therefore it is impossible to reach extremely low detection limits.

The aim of our research was the development of direct SFE technique from aqueous solutions of traces of organic pollutants that will allow the complete exclusion of the use of organic solvents. Regularities of direct SFE from aqueous solutions of different organic compounds based on this technique were also investigated.

EXPERIMENTAL

A number of different organic compounds have been used including: n-alkanes (mixture C8-C24); polyaromatic hydrocarbons (acenaphthylene, acenaphthene, fluorene, phenanthrene, anthracene, fluoranthene, pyrene, benzo(a)anthracene, chrysene); chlorinated pesticides (α-HCCH, β-HCCH, δ-HCCH, Heptachlor, Aldrin, heptachlorepoxide, α-endosulfan, dieldrin, 4,4'-DDE, endrin, β-endosulfan, 4,4'-DDD, endrin aldehyde, endosulfan sulfate, 4,4'-DDT) and polychlorinated biphenyls (mixture 2,3,4,4',6-pentachlorobiphenyl, 2,2',3,4,6-pentachlorobiphenyl, 2,2',3,4,4',5-hexachloro-biphenyl, 2,2',3,3',4,4',5,5'-octachlorobiphenyl, 2,2',3,3',5,5'6,6'-octachlorobiphenyl; Arochlor-1260); phthalates (dimethoxyethylphthalate, dicyclohexylphthalate, diphenylphthalate, diphenyl-isophthalate, butylisooctylphthalate, diisooctylphthalate, bis(2-ethylhexyl)isophthalate, di-isononyl-phthalate).

Solventless trapping of extracted compounds after SFE was fulfilled by collecting the extracted analytes on a special sorption cartridge. The cartridge was a glass GC injector liner filled with silica wool and placed after the restrictor. During the collection of analytes the cartridge was cooled by the rapid evaporation of the supercritical fluid at the restrictor outlet.

The SFE 30 extraction unit (CE Instruments, Milan, Italy) with a homemade SFE extraction cell (inner volume 15 cm3) was used. Supercritical CO_2 and N_2O were used as extractants. The water sample volume in all cases was about 10 cm^3. The extraction cell was spiked with the mixture of the investigated compounds and then dynamic SFE was carried out. The extraction was performed at different pressures (from 8 to 25 MPa) using heated metallic restrictor (5 cm long). The flow rate in this case was 0.7-2.6 cm^3/min (for liquid). The outlet of the restrictor was heated (100 - 150C).

Standard equipment for solid phase extraction was used. Model compounds were extracted using C18 and Purasep 200 cartridges and C18 extraction disks. Sorbents conditioning was performed. 5 cm^3 methylene chloride/ethyl acetate (1:1) (in case of Purasep 200 5 cm^3 acetone) and 5 cm^3 methanol were used for this purpose. Investigated compounds were spiked to water sample (10 cm^3) and then the latter was adjusted to pH 2 with 6 mol/dm^3 HCl. The extraction was performed with water sample flow rate of 1 cm^3/min in case of cartridges and 3 - 5 cm^3/min in the case of disk. Elution of organic compounds was carried out by 5 cm^3 ethyl acetate and 5 cm^3 of methylene chloride. Eluates were combined and concentrated under nitrogen to 0.5 cm^3. Then the whole extract volume was injected into the GC.

Extract analysis was carried out using capillary GC model 4160 with split/splitless injector, on-column injector, flame-ionization and electron capture detectors (ECD). Make-up gas (nitrogen) for ECD was purified using oxygen purifier. Thermodesorption and cryofocusing were used for injection of interesting compounds trapped on the cartridge into GC. Cryofocusing was performed using a homemade cooler based on the Peltier effect. The cartridge (injector liner) was put into the GC injector. Separation of the extracted compounds was performed using 25 m × 0.32 mm fused silica capillary column with SE-54 (0.15 micron film thickness). Acquiring and acquisition of chromatographic data were performed using Chrom-Card Data System (CE Instruments, Milan, Italy).

RESULTS AND DISCUSSION

Trapping effect of gaseous CO_2 and N_2O flow rate at the outlet of SFE system on the trapping efficiency of the model compounds using cartridge has been investigated. The model mixtures of n-alkanes, PAHs, CPs and PCBs were spiked into the extraction cell filled with silica wool and then dynamic SFE was performed. The flow rate of gaseous CO_2 at the end of the restrictor was measured (5 - 1500 cm^3/min). It has been shown that for the flow rates higher than 400 cm^3/min collection efficiency greater than 70% could be achieved. In this case the cooling effect of the rapidly expanding supercritical fluid during evaporation on trapping of extracted compounds was used. The range of small supercritical fluid flow rates (2 - 30 cm^3/min for gas or ~ 0.1 cm^3/min for liquid) was not so interesting because in this case the SFE stage is too long and there is the problem of the restrictor plugging. Use of high fluid flow rates (up to 2.5 cm^3/min for liquid) has allowed these problems to be solved.

The effect of the restrictor temperature and extraction cell pressure and temperature on collection efficiency of analytes was also investigated. Heating the restrictor has allowed the elimination of plugging but at temperatures higher than 150C a decrease in the collection efficiency has been observed. Change of extraction cell pressure and temperature in the range from 8 to 25 MPa and from 40 to 100C respectively has not influenced the collection efficiency when the flow rate of gaseous CO_2 or N_2O at the outlet of the SFE system was higher than 400 cm^3/min.

Direct SFE of mixtures of organic compounds from aqueous solutions was performed using the described trapping system.

As a result of the high supercritical fluid flow rate and heating of the restrictor, extraction time was very low (about 2-5 min) and plugging of the restrictor was not observed.

Regularities of direct SFE from aqueous solutions of the chlorinated pesticides, polychlorinated biphenyls, phthalates and polynuclear aromatic hydrocarbons have been also investigated. The influence of extraction conditions, namely pressure, temperature, SF flow rate, nature of the analytes and SF, kinetics of the SFE, etc., on the recovery of the extracted compounds have been studied. Concentrations of the targeted compounds in water were in the range of 0.1 -1 ppb for hydrocarbons and phthalates, 1-100 ppt for CP's and 0.1-10 ppt for PCB's. Thermo-desorption efficiency was about 90% and trapping efficiency about 70-80%. SFE recoveries of studied ecotoxicants from water samples were higher than 90%. On the basis of the obtained results, methods for the determination of PAH's, chlorinated pesticides and PCB's in waters were developed.

A comparison of direct SFE from water, micro-LLE, and solid phase extraction for ultratraces of chlorinated biphenyls (10^{-12}-10^{-9} g) was performed.

In case of micro-LLE and SPE analysis of whole organic extract was performed using a large volume injection system. It included a 'gas curtain' for preventing solvent vapours penetrating into the separating column and detector.

Micro-LLE was performed using a homemade special vessel for micro-LLE. The water sample volume was 10 cm^3. The investigated compounds were spiked into the extraction vessel and extraction with 0.3 cm^3 of hexane was performed over 2 minutes. Then extract was separated and the whole extract volume was injected into the GC.

The influence of the quantity of analyte in the water sample on the recovery by respective methods was investigated. The results are presented in Table 1.

Quantity of PCB in sample, g	Concentration ppt	Recovery[1], %				
		Direct SFE	Micro-LLE	SPE[2]		
				C18 (cartridge)	Purasep 200 (cartridge)	C18 (disk)
10^{-9}	100.0	97±9	92±7	92±7	87±8	89±6
10^{-10}	10.0	91±8	90±6	30±8	9±4	7±3
10^{-11}	1.0	94±8	93±11	5±2	-	-
10^{-12}	0.1	88±11	60±30	-	-	-

[1] Recovery includes sorption and elution degree.
[2] Dash indicates that there were no model compounds registered at the detection limit (10^{-13}g).

Table 1 Comparison of micro-liquid extraction, solid phase extraction and direct supercritical fluid extraction efficiency from water depending on analytes quantity (water sample: 10 cm^3; sample: mixture of 5 PCBs; whole extract analysis by GC (ECD))

As seen from the Table, direct SFE recovery is not influenced by the quantity of extracted compounds but SPE is not suitable when the quantity of analyte is less than 0.1 ng in the sample. It was shown also that only micro-LLE could be compared with direct supercritical fluid extraction at ultratrace concentration level. However in case of micro-LLE the reproducibility was less than that of SFE. The poor results for SPE especially at ultratrace level can be explained by incomplete elution of small quantities of analytes from the sorbents. It was shown that in the case of ultra-low concentration levels 0.1-1 ppt (10^{-12}-10^{-11} g of analytes in the water sample, respectively) direct SFE from water was more accurate and reproducible than micro-LLE and SPE.

CONCLUSION

A true solventless off-line SFE method has been developed which excludes the use of organic solvents for trapping and for recovery of analytes. The trapping system allowed a high collection efficiency for compounds of different volatility as in case of supercritical extraction from solid (and dry) matrix and of direct SFE from water.

Methods for the determination of polynuclear aromatic hydrocarbons, phthalates, chlorinated pesticides and polychlorinated biphenyls in aqueous solutions based on their direct SFE and off-line solventless SFE/GC coupling have been developed. High SFE recovery of targeted compounds from water and high efficiency of their solventless transfer into GC have been achieved. The detection limits of the developed methods at 0.1-10 ppt levels have been achieved.

It is shown that direct SFE of the investigated compounds from aqueous solutions is more preferable. In this case no organic solvent is used and the analysis of the whole extract volume is provided. In the case of ultra-low concentration levels, 0.1-10 ppt, direct SFE from water was more accurate, fast and reproducible than conventional sample preparation methods based on LLE and SPE.

The very small analysis time of the proposed method for ultratrace organic pollutants determination in aqueous matrixes may allow the fast screening of water samples for priority pollutant content.

ACKNOWLEDGMENTS

We are very grateful to Neolab and Baker Companies for supply of analytical equipment to our Analytical Chemistry Chair.

REFERENCES

1 Revelsky IA, Golovko IV, Yashin YuS, Efimov IP, Zirko BI, Glazkov IN, Revelsky AI, Vulikh PP and Zolotov YuA, *Analytical Methods and Instrumentation*, **2**, 163, (1995).
2 Barnabas IJ, Dean JR, Hitchen SM and Owen SP, *J. Chromatogr. A.*, **665**, 307, (1994).
3 Kane M, Dean JR, Hitchen SM, Dowel CJ and Tranter RL, *Analyst.*, **120**, 355, (1995).
4 Reighard TS and Olesik SV, *Critical Reviews in Analytical Chemistry*, **26**, 1, (1996).
5 Barnabas IJ and Dean JR, *Analyst*, **119**, 2381, (1994).
6 Chester L, Pinkston JD and Raynie DE, *Anal. Chem.*, **68**, 487R, (1996).
7 Hüsers N and Kleiböhmer W, *J. Chromatogr. A.*,**697** , 107, (1995).
8 Wenklawiak BW, Heemken OP, Sterzenbach D, Schipke J, Theobald N and Weigelt V, *Anal. Chem.*, **67**, 4577, (1995).
9 Mulcahey LJ and Taylor LT, *Anal. Chem.*, **64**, 2352, (1992).
10 Miller DJ, Hawthorne SB and McNally MP, *Anal. Chem.*, **65**, 1038, (1993)
11 Levy JM, Ravey RM, Houk RK and Ashraf-Khorassani Mehdi, *Fresenius J. Anal. Chem.*, **344**, 517, (1992).
12 Vejrosta J, Ausorgova A, Fanta J and Janda V in: P Sandra (ed), *Proc. 16th Int. Symp. Capillary Chromatography*, Riva del Garda, Hüthig, Heidelberg, May 27–30 (1994).
13 Hedrick JL and Taylor LT, *Anal. Chem.*, **61**, 1986, (1989).

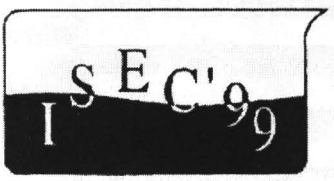

SUPERCRITICAL FLUID EXTRACTION OF PCBS FROM REAL WORLD ST LAWRENCE RIVER SEDIMENTS

Wu Zhou and Lawrence L Tavlarides
Department of Chemical Engineering and Materials Science
Syracuse University, Syracuse, NY 13244, USA

ABSTRACT
A program is underway to determine engineering design information to develop a supercritical fluid extraction (SFE) process to remediate soils contaminated with polychlorinated biphenyls (PCBs). Results of equilibrium partition and laboratory scale desorption experiments are reported here. An apparatus has been developed to study PCB partition equilibrium between soils and supercritical fluids (SCFs). PCB partition equilibrium studies between supercritical CO_2 (SC-CO_2) and three real world St. Lawrence River sediments with similar soil properties and PCB congener distribution patterns but different total PCB concentrations were conducted at 50°C and five different SCF densities. Linear adsorption isotherms describe the equilibrium data over the range of conditions studied. Laboratory scale PCB desorption experiments on a real world St. Lawrence River sediment were conducted to investigate the effects of SCF flow rate and co-solvent on PCB extraction efficiencies. It is found that PCB concentration in the sediment can be reduced from 2200 ppm to less than 10 ppm in 25 minutes of extraction time with the presence of 5% (mole) methanol in supercritical CO_2. The presence of 5% (mole) methanol in supercritical CO_2 increases PCB desorption rates and reduces final PCB residual concentrations in sediments. CO_2 flow rate shows important effects on both PCB desorption rate and final PCB residual concentration when pure CO_2 is used as the SCF. These flow rate effects are not significant after ~7.5 minutes of extraction time for SC-CO2 with 5% (mole) methanol.

Keywords: chlorinated biphenyls, contaminated sediment, supercritical extraction, carbon dioxide, methanol co-solvent

INTRODUCTION

It has been estimated that about 385 million pounds of PCB's exist in landfill and other storage, and another 24 million pounds exist in sediments, soil, vegetation and animals.[1] The potential environmental threat of the large amount of PCB's has called for the development of effective PCB cleanup techniques. Among various efforts, the application of supercritical fluid extraction (SFE) in the removal of toxic organics from environmental samples is receiving much attention due to the unique properties of supercritical fluids such as low viscosity, high diffusivity, and easily tunable solvent power.[3] Pioneering research on the application of SFE in the remediation of environmental pollutants suggests that SFE of toxic organics from soils has promise as a method of remediation. [2, 4-8]

A process concept is advanced at Syracuse University for the treatment of soils contaminated with PCB's and polyaromatic hydrocarbons (PAH's). The program includes solubility data acquisition of PCB's and PAH's in SCF's,[9-12] PCB partitioning equilibrium studies, desorption rate data acquisition for real world samples over a broad range of conditions,[2] desorption rate data analysis, bench-scale data acquisition to confirm laboratory operation conditions and specify extractor configuration, and, eventually, large scale testing with a mobile demonstration unit. PCB partitioning equilibrium data between supercritical CO_2 and real world St. Lawrence River Sediments and PCB desorption results on St. Lawrence River sediments are presented here.

EXPERIMENTAL

Apparatus.

Figure 1 shows the schematic of an apparatus developed to study PCB partitioning equilibrium between soils and SCF's. High pressure CO_2 is delivered through the CO_2 cylinder, compressor, and back-pressure regulator subsystem. The CO_2 vessel and the syringe pump, both thermostatic, are used to prepare the mixture of CO_2 and co-solvent. A thermostatic equilibrium subsystem includes an equilibrium vessel, a circulating pump, and a six-port valve. After PCB

© 2000 Society of Chemical Industry

partitioning equilibrium is achieved, the sample loop is depressurized and then rinsed using hexane. PCB concentration in the sample vial is analyzed using a Hewlett-Packard 5890 Series II GC. PCB concentrations in SCF and sediment are calculated based on the volume of the sample loop, the density and total volume of SCF in the system, total PCBs in the system, and the amount of sediment in the equilibrium vessel.

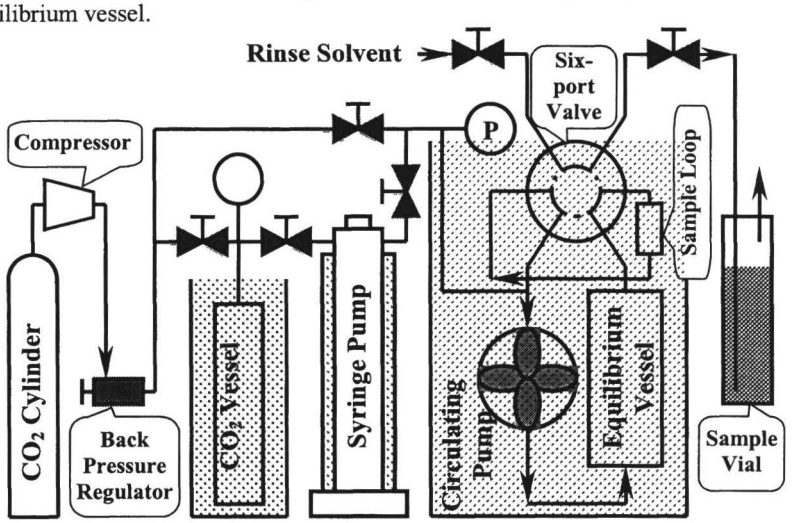

Figure 1. PCB Partitioning Equilibrium Apparatus

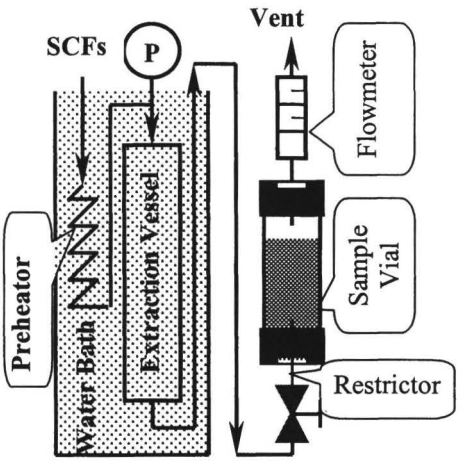

Figure 2. Schematic diagram of the Laboratory Scale SFE Unit

Figure 2 shows the schematic of a laboratory scale SFE unit that uses the same CO_2 delivery system as shown in Figure 1. Restrictors are employed to control CO_2 flow rate. Effluent PCB's are collected in a set of sample vials filled with hexane. PCB concentrations in the sample vials are then analyzed by GC. Residual PCB's in the sediments are analyzed using the method presented of Chen et

al.[2] The PCB concentrations at different extraction time are backward calculated based on the final PCB residual concentration in the treated sediment and the amounts of PCB's in each sample vial.

Materials.

To conduct the equilibrium studies, contaminated soil samples with similar properties and PCB congener distribution patterns but different PCB levels are needed. Three real world St. Lawrence River sediment samples have been obtained from a contaminated site near Massena, New York. All sediments were prepared by air-drying and sieving through a No.30 screen. Mineral properties, total organic carbon (TOC), and initial PCB concentrations of the three sediments are given in Table 1. These data show that the three samples have similar soil properties yet different levels of PCB concentrations.

Sediments	Composition (%)			TOC (%)	PCB Conc. (ppm)
	Sand	Clay	Silt		
St. L. R. Sediment #1	37.67	32.72	29.60	1.34	130
St. L. R. Sediment #2	55.73	23.21	21.06	1.21	710
St. L. R. Sediment #3	58.38	22.1	19.53	1.76	2200

Table 1. Sediment Properties

Figure 3 shows the PCB congener distribution patterns of the three sediments and Aroclor 1248 that is the original PCB contaminant on the site from which the three sediments have been obtained. It is shown that the PCB congener distribution patterns in the three sediments have shifted to the light chlorinated end (left side in Figure 3) from the original pattern of Aroclor 1248. This shift is possibly caused by naturally occurring dechlorination processes. Compared with the PCB congener pattern in Aroclor 1248, the PCB patterns in the three sediment samples are relatively close.

RESULTS AND DISCUSSIONS

PCB partitioning equilibrium studies between St. Lawrence River sediments and SC-CO_2 were conducted at three temperatures (40, 50, and 60°C) and five different SC-CO_2 density levels (5.5, 8.0, 10.5, 13, and 15.5mole/dm^3). Six St. Lawrence River sediment samples with different initial PCB concentrations were prepared from the three sediments and their mixtures. Data were collected for each isotherm from 6 equilibrium experiments on each of the six sediment samples. To reduce moisture effects on equilibrium results, all the air-dried sediment samples are stored in a constant temperature (25°C) and humidity (50%) room for at least 2 weeks prior to the experiments. The isotherms at 50°C and five CO_2 densities are given in Figure 4. The results show a linear relationship between the equilibrium PCB concentrations in the two phases. The laboratory scale PCB desorption studies were conducted for 60 minutes on air-dried St. Lawrence River sediment #3 at a temperature of 50°C and a pressure of 116.3 atm (corresponding to a CO_2 density of 10.5 mole/dm^3). Both pure CO_2 and CO_2 with 5% methanol were used as SCF's. Two 8 cm length silica restrictors, 40μm ID and 50μm ID, were employed to control CO_2 flow rate, 0.76 and 1.35 g/min respectively. Table 2 shows the experimental results and Figure 5 demonstrates the corresponding desorption curves. It is found that PCB concentration in sediment can be reduced from approximately 2200 ppm to less than 10 ppm (more than 99.5% extraction efficiency) in 25 minutes of extraction time with the presence of 5% (mole) methanol.

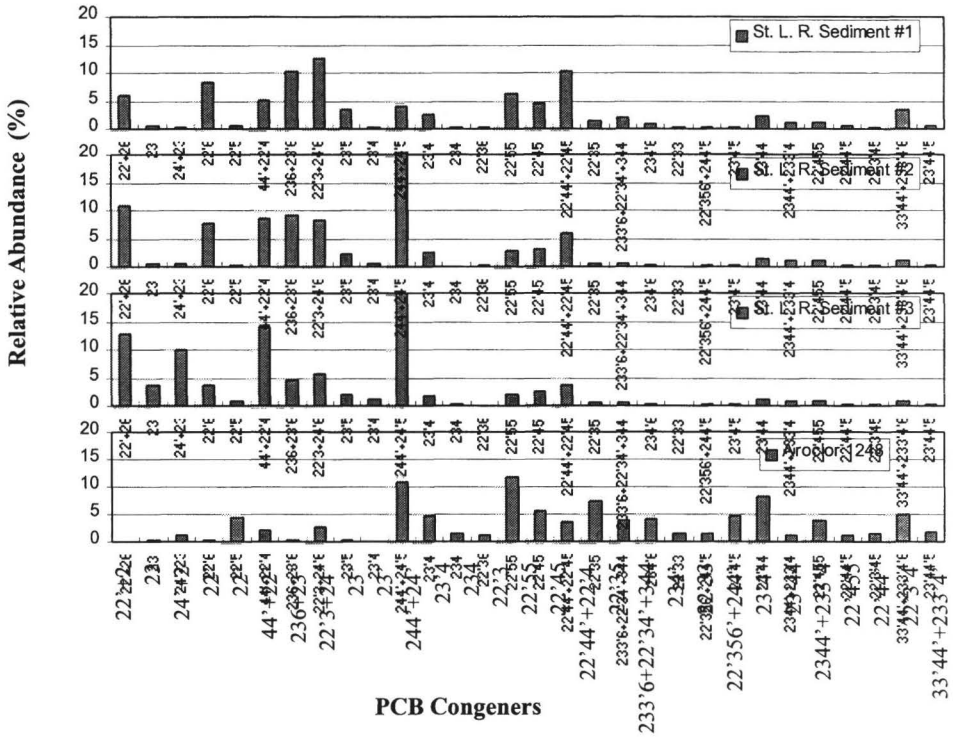

Figure 3. PCB Congener Distribution Patterns (only congeners with no less than 1% relative abundance in at least one sample are shown here)

Time	Experimental conditions and PCB concentrations (ppm) in sediments			
(min)	CO_2 0.76 g/min	CO_2+5% MEOH 0.76 g/min	CO_2 1.35 g/min	CO_2+5% MeOH 1.35 g/min
0	2098	2210	2121	2198
0.5	2076	2136	1976	2004
1.5	1821	1467	1358	1236
3.5	1350	524	470	316
7.5	576	35.9	134	57.8
15	219	13.2	80.4	15.3
25	141	9.41	55.7	8.10
40	103	5.79	41.6	5.32
60	71	4.21	32.0	3.76

Table 2 PCB desorption data for St. Lawrence River sediment #3

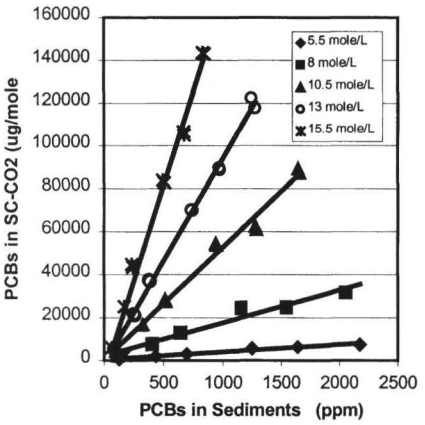

Figure 4. PCB Partition Equil. between SC-CO_2 and St. L. River Sediment at 50°C

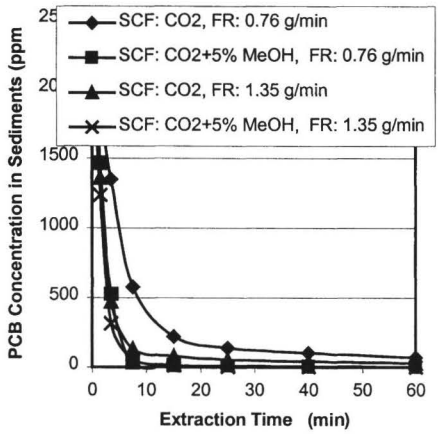

Figure 5. PCB Desorption from St. L. R.Sediment #3 at 50 °C and 116.3 atm (FR: CO_2 flow rate)

Figure 5 shows that, for pure CO_2, larger (1.35 versus 0.76 g/min) CO_2 flow rate increases the desorption rate and reduces final PCB residual concentration. These flow rate effects are not significant after ~7.5 minutes of extraction time in the presence of 5 molar percent methanol in the SCF.

CONCLUSIONS

A new apparatus has been developed and tested to study PCB partitioning equilibrium between soils and supercritical fluids. PCB partition equilibrium studies between supercritical CO_2 (SC-CO_2) and three real world St. Lawrence River sediments were conducted at 50°C and five different SCF densities. Experimental results show linear adsorption isotherms over the range studied. It is found that soil moisture content can significantly affect the PCB equilibrium studies.

PCB desorption experiments on real world St. Lawrence River sediments were conducted in a laboratory scale SFE unit. It is found that PCB concentration in the sediment can be reduced from 2200 ppm to less than 10 ppm (99.5% extraction efficiency) in 25 minutes of extraction time with the presence of 5% (mole) methanol in supercritical CO_2. The presence of 5% (mole) methanol in supercritical CO_2 increases PCB desorption rates and reduces final PCB residual concentrations in sediments. CO_2 flow rate shows important effects on both PCB desorption rate and final PCB residual concentration when pure CO_2 is used as the SCF. These CO_2 flow rate effects are not significant after ~7.5 minutes of extraction time in the presence of 5 molar percent methanol. Based on these results, CO_2 with 5% (mole) methanol and lower CO_2 flow rate are recommended for the extraction of PCBs from contaminated soils/sediments.

FUTURE WORK

PCB partitioning equilibrium between CO_2 with 5% (mole) methanol and St. Lawrence River sediments will be studied. PCB partitioning equilibrium models will be established and used for the analysis of PCB desorption data. A bench scale SFE unit equipped with a 2 liter extractor will be used for the study of PCB desorption rates from the St. Lawrence River sediments. An economic analysis of the SFE process will then be conducted based on the results of bench scale PCB desorption studies.

ACKNOWLEDGMENT

The financial support from the National Institute of Environmental Health Sciences Superfund Basic Research Program, Grant No. NIEHS 2P4E5049/303, is gratefully acknowledged.

REFERENCES

1. Amend LJ and Lederman PB, *Environ. Prog.*, **11**, 173 (1992).
2. Chen P, Zhou W and Tavlarides LL, *Environ. Prog.* **16**, 227, (1997).
3. McHugh M and Krukonis V, *"Supercritical Fluid Extraction"*, Butterworth Publishers: Stoneham, MA, p10, (1986).
4. Brady BO, Kao CP, Dooley KM, Knopf FC and Gambrell RP, *Ind. Eng. Chem. Res.*, **26**, 261, (1987).
5. Dooley KM, Ghonasgi D, Knopf FC and Gambrell RP, *Environ. Prog.*, **9**, 197, (1990).
6. Dooley KM, Kao CP, Gambrell RP and Knopf FC, *Ind. Eng. Chem. Res.*, **26,** 2058, (1987).
7. Erkey C, Madras G, Orejuela M and Akgerman A, *Environ. Sci. Technol.*, **27**, 1225, (1993).
8. Ghonasgi D, Gupta S, Dooley KM and Knopf FC, , *AIChE J.*, **37**, 944, (1991).
9. Yu E, Richter M, Chen P, Wang X, Zhang Z and Tavlarides LL, *Ind. Eng. Chem. Res.*, **34,** 340, (1995).
10. Anitescu G and Tavlarides LL, *J. Supercrit. Fluid*, in press (1998).
11. Anitescu G and Tavlarides LL, *J. Supercrit. Fluid*, **10,** 175, (1997).
12. Anitescu G and Tavlarides LL, *J. Supercrit. Fluid*, **11**, 37, (1997).

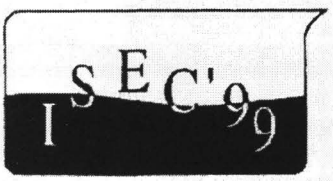

LIGAND-ASSISTED SUPERCRITICAL FLUID EXTRACTION AND ENVIRONMENTAL MANAGEMENT NEEDS FOR REMOVAL OF METALS

RV Fox, RD McMurtrey and JD Navratil
Lockheed Martin Idaho Technologies Inc., Idaho National Engineering and Environmental Laboratory, P. O. Box 1625, Idaho Falls, Idaho, USA 83415-3921

ABSTRACT
A brief historical overview of ligand-assisted supercritical fluid extraction with carbon dioxide is given. Applications for waste processing enhancement and environmental remediation are given for both liquid and solid matrices where metal and radionuclide extraction is involved. Advantages of solvent extraction using carbon dioxide over conventional solvents are discussed along with research needs to apply the technology to the environmental management area.

Keywords: radionuclide, supercritical extraction, carbon dioxide, ligand assisted

INTRODUCTION

Baron Cagniard de la Tour is credited with the discovery, in 1822, of the critical point of a substance.[1] Later, in 1876, Hannay and Hogarth investigated and demonstrated the solvent powers of supercritical carbon dioxide.[1] By the early 1930's, the solvent properties of near critical hydrocarbons were being exploited to effect separations in the petroleum industry.[1] By the 1950's commercial, large-scale production of low-density polyethylene was, and still is today, conducted at 150C to 300C using pressures as high as 200 Mpa.[1] Solvent extraction using near critical and supercritical solvents is a viable and mature technology with several niche applications in the food and beverage, chemical, pharmaceutical, precision cleaning, and petroleum refining industries.

Up to 1990, supercritical (SC) and liquid carbon dioxide (CO_2) had been primarily used for the extraction and separation of organic compounds. It is well known that both liquid CO_2 and SC-CO_2 are poor solvents for ionic species. The use of SC-CO_2 as a solvent for the intentional solvation and extraction of ionic species, primarily metals, is a relatively new phenomena. Although some investigators have demonstrated liquid carbon dioxide extraction of metal-ligand compounds, the first demonstration of ligand-assisted supercritical fluid extraction (SFE) was accomplished by Dr. Chien Wai and K. Laintz in 1991 at the University of Idaho using a fluorinated dithiocarbamate ligand on copper.[2] That work was specifically selected and funded by the U.S. Department of Energy (DOE) Idaho Field Office under the DOE Office of Technology Development, Innovative Technology program. Later in 1991, a collaborative research effort between the Idaho National Engineering and Environmental Laboratory (INEEL) and Dr. Wai explored the complexation and transport of metal sulfides in SC-CO_2.[3] Additional studies of metal-ligand complex formation and solubility in SC-CO_2 were conducted by Wai and researchers at the Pacific Northwest National Laboratory in collaboration with C. Yonker.[4] Wai holds the seminal patent and publications in the area of ligand-assisted supercritical fluid extraction.[2, 4-6] Wai and co-workers have pioneered methods for selective extraction of arsenic, antimony, caesium, copper, lead, mercury, nickel and a host of other metals including selected actinides and lanthanides.[7–15] This research has included study of many common metal complexing agents having O, N, P, and S functional groups and also ligands having fluorine substitutions to enhance their solubility in the SC solvent. Ligand studies have also included macromolecules such as crown ethers and calixarenes.[16]

The advances made by Dr. Wai and others have caused ligand-assisted supercritical carbon dioxide extraction to be proposed as an alternative solvent extraction technique for the selective removal of heavy metals and radionuclides from both liquid and solid waste matrices. Primarily targeted are those situations where SFE could be employed as a separation technique for extraction of key metals and radionuclides, such as the removal of a target metal or radionuclide to below an

© 2000 Society of Chemical Industry

established regulatory level that would result in a waste re-classification (e.g., from a high level radioactive waste to a low level radioactive waste). It has also been proposed that the solvent properties of SC-CO_2 be employed in a sequential extraction process for removal of organic materials followed by ligand-assisted SC-CO_2 extraction of metals. In that manner mixed-waste streams could be effectively processed resulting in significant waste volume minimisation with minimal production of secondary waste. Since the original proposal was funded by the DOE and since the technology is inherently waste minimising, the obvious target for development and deployment of the technology is within the DOE community where 'Treatability Study' opportunities for the given matrices exist in abundance.

This paper will now briefly outline how ligand-assisted SFE can be applied for waste processing and environmental remediation within the DOE system for situations where metal and radionuclide extraction and separation are either required or could be employed to effect significant benefits. The research needs in the environmental management area at the INEEL will also be discussed along with some advantages of this new solvent extraction technique.

WASTE TREATMENT

Applications in the Waste Treatment Area

Compared to conventional aqueous and organic solvent extraction systems known and in use in the radiochemistry world, carbon dioxide has some distinct advantages which are not easily dismissed, especially in light of the fact that baseline and existing High Level Waste (HLW) pre-treatment techniques are expensive and produce large volumes of secondary HLW. Carbon dioxide is non-toxic, non-flammable, commercially available in rail car quantities at a very low price, can easily be recycled, gives rise to only a fraction of the secondary waste which is generated by baseline separation technologies, and only requires half the energy which a distillation process would require yet delivers equivalent or better separation. Disadvantages include the use of a positive pressure system and the weak solvent nature of carbon dioxide.

Recent advances in critical fluid science have led to a better understanding of the properties of materials which enhance their solubility in critical fluids and the solvent-solute interactions occurring in critical fluid solvent systems. A case in point is the recent reporting[17,18] of a supercritical carbon dioxide solvent being loaded with a uranium nitrate/tributylphosphate complex to as high as 0.429 mol/dm^3. This solubility level is equivalent to typical PUREX solvent loading for the same complex (0.13 to 0.47 mol/dm^3). These results provide a small glimpse of the solvent power and waste minimisation potential of critical fluids.

In the waste management area ligand-assisted SFE has the potential to selectively remove metals to the parts-per-billion range or lower from both solid and aqueous waste streams. The solvent also has the capability to be loaded to very high concentrations with organic compounds and metals. Solid materials such as tools, metal, personal protective equipment, cloth, plastic, glass, shielding materials, etc., can easily be surface decontaminated using a ligand-assisted SFE process, thus reducing the total mass of radioactive materials entering the waste stream. One such example is where researchers at the INEEL demonstrated in a 'Treatability Study' the successful ligand-assisted SFE of cobalt-60 from lead shot.[19] The shot, previously employed as shielding material, was contaminated with less than 100 nanoCurie/gram cobalt-60. The contaminated lead was retrieved from the waste stream, where it had been entered as a mixed waste, and cleaned in the following manner: The shot was loaded into an extraction cell and subjected to approximately 20 MPa SC-CO_2 modified with a 2 mole percent alcohol/ligand mixture at 65C for 1 hour and a flow rate of 10 cm^3/minute. The ligand used contained a phosphorous functional group and demonstrated a hundred-fold specificity for cobalt over lead. After 1 hour the surface of the lead shot was cleaned thoroughly enough for recovery and re-use of the lead as shielding material. The lead had been scheduled for disposal via encapsulation and burial. A total of 50 pounds of lead shot was cleaned producing less than a single gram of secondary waste using the ligand-assisted SFE method. The commercial nitric

acid rinse process identified as a potential decontamination technique was far too aggressive chemically and trial cleaning tests resulted in dissolution of lead and the creation of significant volumes of secondary mixed-waste containing lead and radioactive cobalt.

As was demonstrated with the lead shot, a number of porous and non-porous solid materials could also be easily surface decontaminated and either be returned to service, or enter the waste stream far less contaminated. Additionally, due to the penetrating power of supercritical carbon dioxide volumetrically contaminated porous solids can be decontaminated if the conditions permit.

Liquid waste streams having pH extremes, high salts content, high organic content and high solids content can be treated using the ligand-assisted SFE technique without the need for prior chemical neutralisation or solids separation. Wastewater resulting from a ligand-assisted SFE process would be of high enough quality to be returned for use as a solvent; thus, reducing the overall quantity of water needed in a process. In effect, the same water would be cleaned and reused repeatedly. The carbon dioxide solvent would also be repeatedly recycled. In relation to treatment of liquid waste streams ligand-assisted SFE has the potential to function with minimal consumption of energy (compared to distillation) and with minimal production of secondary waste. Critical fluid processing has advantages over filtration processes by not being susceptible to fouling and by having significantly increased throughput. Critical fluid processing has advantages over chemical precipitation and flocculation techniques relative to selectivity, separation and the volume of secondary waste produced. Critical fluid processing has advantages over ion exchange because it does not employ resins susceptible to organic fouling and cannot be fouled by waste streams having high solids content. Critical fluid processing is as efficacious or even more efficacious than ion exchange due to the fact that the same ligand used in an ion-exchange resin is used and made mobile in the solvent as opposed to being fixed on a solid matrix.

SFE Research Needs in the Waste Treatment Area

Early metal-ligand solubility studies in critical carbon dioxide were primarily oriented towards demonstration of the phenomena using many metals and many conventional ligands. Early studies also focused on quantitative measurement of the extent of metal-ligand and free ligand solubility in the solvent. More recently, investigations have concerned themselves with parameters that most affect the solubility of ligand and metal-ligand systems, including the study of the chemical properties of ligands which demonstrate higher carbon dioxide solubility. Currently, critical fluid investigations are of the nature of describing the solute-solvent molecular level physical/chemical interactions that contribute to solubility phenomena as it occurs in critical fluids.

To advance SFE into the DOE Waste Management area further, research is required into the nature of ligand and metal-ligand partitioning between the aqueous and SC phase. Additional and on-going research is required for the study and development of new ligands specific for use in a SCE system. Solubility models that either exist or are currently being developed need to be extended to include the presence of multiple components such as other organics and water. Metal and ligand chemical reaction kinetics and thermodynamic properties should also be studied for a more thorough understanding of the interaction between metal and ligand in the given solvent system. Additionally, the effects of high radiation levels on all components of the system, including carbon dioxide, must be studied. General research trends should move towards lowering the pressure requirements of a SFE system used on radioactive materials. Recovery of the metal-ligand species from the process and recycle of the ligand are also areas requiring further research and development. Finally, the effects that other matrix components (salts, water, etc.) have on metal-ligand binding and phase partitioning need additional study.

'Treatability Studies' are a must. The DOE rarely accepts a technology if a 'Treatability Study' and/or equivalent field trials have not been performed on actual materials. Surrogate testing simply will not suffice. 'Treatability Studies', or their equivalent, need to be performed on solid and liquid waste streams arising from routine activities at various DOE sites. Unfortunately, conducting a 'Treatability Study' often requires adequate facilities and radiologically trained personnel for the task,

items which may only be available at certain DOE facilities. One approach for conducting the needed field trials would be to demonstrate SFE on existing materials already declared a waste. Another strategy would be to obtain solids and fluids from various process streams and perform SFE on those materials prior to their declaration as a waste. A final strategy would be to search for a waste stream for which there is no current treatment option, obtain samples, and conduct a 'Treatability Study' if SFE is deemed applicable to the situation.

ENVIRONMENTAL RESTORATION

Applications in the Environmental Restoration Area

Critical fluid extraction using carbon dioxide is a separation technology which has recently come into focus in the environmental restoration area.[20] Removal of toxic metals and radionuclides from groundwater and soil has been and still does represent a significant technical challenge to the separations science community. Commercially available separation technologies face demands for lower levels of contaminants in the treated product and smaller volumes of secondary wastes produced for applications across both federal and industrial sectors. Current metal separation methods for groundwater include evaporation/distillation, filtration, chemical precipitation, magnetic separation, flocculation, electrowinning, ion exchange and solvent extraction. Each of those methods has technical limitations that become sharply manifest when a separation challenge requires a method that is efficacious, selective and efficient. It is also known that when dealing with hazardous metals and radionuclides in today's regulatory environment the word "efficacious" equates to sub parts-per-million and lower separations for metals and can mean less than 10 nanoCuries per gram radiological activity for DOE clean-up activities. The chemical complexity of both aqueous and soil matrices only adds to the separations challenge. It is evident from several published DOE Technology Needs Statements that significant technical gains must be made in the separation sciences field where metal removal from environmental matrices is concerned.

Critical fluid processing has been demonstrated to have utility for environmental restoration applications and can potentially meet several DOE needs by reducing risk, reducing cost, greatly reducing the volume of secondary waste, and decreasing environmental impact. Ligand-assisted SFE tests conducted on various soils by researchers at the University of Idaho have demonstrated removal of bound metals of interest to below the Environmental Protection Agency (EPA) Toxicity Characteristic Leach Procedure criteria.[21] An interesting note is the inability of even the ligand-assisted SFE technique to be able to totally remove all bound metal from soil. That fact could present a challenge for DOE environmental restoration applications because radionuclide removal is specified as "activity remaining in the treated product" as opposed to EPA criteria for heavy metals that are usually listed as parts-per-million. Other researchers have also demonstrated removal of selected radionuclides, including caesium, uranium and plutonium, from soil matrices with high success.[22]

For liquid matrices both ligand-assisted SFE and simple SFE of pre-existing organometallic complexes has been demonstrated on environmental samples.[23, 24] The most common technical challenge is recovery of the metal-ligand complex, recovery of the carbon dioxide solvent, and subsequent drying of the carbon dioxide to remove water. Carbon dioxide drying usually requires employment of a CO_2 distillation tower.[25]

SFE Research Needs in the Environmental Restoration Area

Even though ligand-assisted SFE has great potential for environmental restoration applications within the DOE community, before the technique can be widely applied within the DOE sector there must be a fundamental understanding of: 1) how radionuclides and other metals interact with the critical fluid solvent; 2) how radionuclides and other metals interact with metal ligands dissolved in the critical fluid solvent; and, 3) the role which the solvent plays in the formation and stabilisation of metal-ligand complexes. Fundamental information arising from those studies will

allow for the safe and predictable operation of a SFE system wherein fissile materials are being extracted and concentrated. Additional areas of study include determining metal speciation in soils. Although much research has been conducted in this area it is still unclear as to how to remove intercalated metals from within the soil matrix just short of total mineral destruction via aggressive acid digestion.[26, 27]

SUMMARY

Critical fluid science as applied to waste treatment and environmental restoration is beginning to mature and the potential role of critical fluid processing within the DOE sector is beginning to clarify. For example, soil and water decontamination processes could certainly benefit from advances in SFE. Technical challenges and knowledge gaps remain; however, it is precisely those technical challenges and knowledge gaps that beckon investigations into the fundamental nature of metal, ligand and solvent interactions. Carbon dioxide used as a solvent is by no means touted as the end-all solution to the myriad of non-trivial scientific challenges facing the DOE. However, selective metal and radionuclide extraction using critical carbon dioxide as a solvent is a novel approach to solvent extraction radiochemistry and with further understanding, can be successfully, safely and efficiently utilised.

REFERENCES

1 McHugh M and Krukonis V. *Supercritical Fluid Extraction: Principles and Practice*, 2nd ed.; Butterworth-Heinemann: Newton, MA, (1994).
2 Laintz KE, Wai CM, Yonker CR and Smith RD. *J. Supercrit. Fluids*, **4**, 194, (1991).
3 Propp WA, Carleson TE, Wai CM and Huang S. *EGG-SCM-9908*, (1991).
4 Laintz KE, Wai CM, Yonker CR and Smith RD. *Anal. Chem.*, **64**, 2875, (1992).
5 U.S. Patent 5,536,538.
6 Laintz KE and Wai CM, *Anal. Chem.*, **64**, 311, (1992).
7 Lin Y, Smart NG and Wai CM. *Environ. Sci. Technol.*, **29**, 2706, (1995).
8 Smart NG, LiN Yand Wai CM. *Am. Environ. Lab.*, **8**, 38, (1996).
9 Wai CM. *Anal. Sci.*, **11**, 165, (1995).
10 Lin Y and Wai CM *Environ. Sci. Technol.*, **28**, 1190, (1994).
11 Lin Y and Wai CM. *Anal. Chem.*, **66**, 1971, (1994).
12 Wood DJ and Wai CM. *Anal. Chem.*, **65**, 1350, (1993).
13 Du HS and Wai CM. *Talanta*, **40**, 173, (1993).
14 Wai CM. *Talanta*, **43**, 2083, (1996).
15 U.S. Patent 5,274,129.
16 Wilson EK. *Chemical and Engineering News*, **April**, 27, (1996).
17 Carrott MJ, Waller BE, Smart NG and Wai CM. *Chem. Commun.*, **1**, (1998).
18 Carrott MJ and Wai CM. *Anal. Chem.*, **70**, 2421, (1998).
19 Fox RV. *FY-1996 INEEL LDRD Report*, (1996).
20 Smart NG, Elashani S, Wai CM, Carleson TE and Fox RV. *SPECTRUM 96*, Seattle, WA, (1996).
21 Personal communication Dr. Chien Wai, University of Idaho, Moscow, ID, (1998).
22 Personal communication Dr. A Shadrin, VG Khlopin Radium Institute, St. Petersburg, Russia, (1998).
23 U.S. Patent 5,087,370.
24 Smart NG, Carleson TE, Elshani S, Wang S and Wai CM. *Ind. Eng. Chem. Res.*, **36**, 1819, (1997).
25 Personal communication J. Moses, CF Technologies, Boston, MA, (1998).
26 Navratil JD, Greenwell RD and Macasek F. *Proceeding of the Sixth International Radioactive Waste Management and Environmental Remediation*, Amer. Soc. Mech. E., New York, (1997).
27 Navratil JD, Todd TA and Van Vliet JA. *J. Radioanal. Nucl. Chem.*, **229**, 99, (1998).

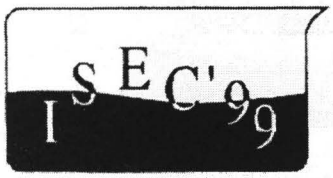

SUPERCRITICAL FLUID EXTRACTION IN GOLD HYDROMETALLURGY

Emmanuel O Otu
Department of Chemistry, Division of Natural Sciences, Indiana University Southeast, New Albany, IN 47150 USA

ABSTRACT
The dicyanoaurate (I) ion-pair, ($Na^+...Au(CN)_2^-$), has limited solubility in supercritical carbon dioxide (sc-CO_2); however, solvation by tributylphosphate (TBP) further enhances the ion pair hydrophobicity, and hence solubility in the non-polar sc-CO_2. sc-CO_2 at about 4,000 psi and 150C, or higher, yields quantitative recovery of gold from the loaded activated carbon in under 2.5h static time, when this time is divided into 15 minutes interval, with dynamic periods in between. Sodium cyanide is the largest waste in the hydrometallurgical recovery of gold. A high concentration is currently used in the desorption stage by existing methods. The use of supercritical CO_2 will drastically reduce the amount of NaCN in the entire gold mining operation. The requisite amount of NaCN to maintain the ion-pair is already available from the wet loaded activated carbon that contacted the ore leachate. This novel method has the potential to eliminate the use of cyanide in gold hydrometallurgy. The method is benevolent to the environment, and the CO_2 can be recycled.

Keywords: gold, cyanide, tri-*n*-butylphosphate, activated carbon, supercritical extraction, carbon dioxide

INTRODUCTION

Supercritical carbon dioxide (sc-CO_2) is an environmentally benign and non-toxic solvent whose application in chemical processes drastically reduces and/or eliminates solvent disposal costs and exposure of personnel to toxic solvent. The extraction of organic compounds has been the focus of many applications due to the non-polar nature of carbon dioxide. To mobilise polar species like metal ions into carbon dioxide, a lowering of electrostatic energy by neutralisation of the ionic charge has to occur,[1, 2] and can be achieved by chelation, ion-pairing and other forms of metal complexes formation. A few reports on the use of sc-CO_2 for the extraction of metal ions and other inorganic complexes have appeared in the literature.[3-8] The sc- CO_2 was either modified with the complexing agent(s) or the sample matrix spiked with the complexing agent(s), and the complexes formed leached with sc-CO_2. Such methods have been used to accomplish the extraction of, for example: some lanthanides, Th, U, Hg, Zn and Cu. The ligands used include, tributylphosphate, β-diketones and crown ethers.

The use of activated carbon (charcoal) for the extraction of gold from cyanide leach solutions dates back to 1894.[9] Carbon-in-pulp, carbon-in-leach and carbon-in-column processes are various modes of gold adsorption on carbon. Zadra and co-workers[10] revolutionised recovery of the adsorbed gold. Their method involves soaking the gold laden carbon in a solution containing approximately 1% w/v NaOH and 0.1%w/v NaCN at 90C for upwards of 24 h., and electrowinning to recover the desorbed gold. Various modifications of this method have also been reported. Reports have also appeared in the literature where gold was eluted from activated carbon using solutions containing organic solvents, for example: ethanol, acetone and acetonitrile, with or without cyanide present.[11-15]

Gold is adsorbed on carbon as the dicyanoaurate (I) complex ion, $Au(CN)_2^-$, from a NaCN solution. The dicyanoaurate (I) ion is not expected to dissolve in the non-polar CO_2. However, charge neutralisation by a cation to form an ion-paired species will facilitate its dissolution. Although the mechanism of gold adsorption on activated charcoal was in contention for sometime, the proposal of ion pairing ($M^{n+}..(Au(CN)_2^-)_n$) seems favoured.[16,17] Solvation liquid-liquid extraction of ($M^{n+}..(Au(CN)_2^-)_n$) ion-pairs with various neutral organophosphates and amines have also been reported.[18,19]

The attendant increase in hydrophobicity of the sodium dicyanoaurate (I) ion-pair as a result of solvation complexation with tributylphosphate (TBP) has been shown to increase the extraction of this species using sc-CO_2. This paper describes a novel method that leads to drastic reduction, perhaps total elimination, of the amount of toxic cyanide waste resulting from the processing of gold ore. Initial work

© 2000 Society of Chemical Industry

from this laboratory appeared in recent literature.[20]

EXPERIMENTAL

Materials.

Activated charcoal (Type GRC-11 12 x 30) was obtained from Calgon Carbon Corporation (Pittsburgh, PA). Gold standard solutions in deionized water were made from $KAu(CN)_2$ obtained from Johnson Matthey (Ward Hill, MA). The solution used to adsorb gold onto the carbon also contained 250 mg/dm^3 NaCN. NaCN of reagent grade quality was obtained from Sigma Chemical Co. (St. Louis, MO).

The activated charcoal was washed to remove fines and dried overnight in an oven at 100C. A weighed amount (40 g) was contacted with 200 cm^3 of 100 mg/dm^3 gold solution for 7 days in a beaker which was opened and stirred at least twice a day. The carbon was separated from the solution by suction filtration (through a Whatman No.4 filter paper) and transferred to a tight-capped plastic bottle. The extent of gold loading of the carbon (0.5 mg/g) was calculated from the difference in the concentration of gold in solution before and after the loading (contact) period. The water content of the loaded carbon was determined from the difference in the weight of samples before and after oven drying to constant weight.

SFE/SFC grade sc-CO_2 (with a helium head pressure of 2,000 psi) was obtained from Air Products and Chemicals, Inc. (Allentown, PA). Extraction pressures were achieved with a Spe-ed SFE pump from Applied Separations (Allentown, PA). The procedure is described fully in the previous work.[20]

RESULTS AND DISCUSSION

Temperature has been shown to be a very important parameter in the desorption of gold from activated carbon.[11-15, 21] Also, the presence of NaCN is crucial in both the Zadra method and other methods that employ caustic/cyanide solution containing an organic solvent.[12, 21] Tables 1 and 2 show the effect of these two parameters on the elution of gold sorbed on activated carbon using sc-CO_2. It is apparent from the results shown that elevated temperature and ionic strength are also of paramount importance to achieve higher recovery of gold with sc-CO_2 elution. When TBP was used, it was spiked on the carbon before desorption. The average water content of the wet loaded carbon was 30.4%; samples used to test effect of ionic strength were air dried in an overnight at 100C. Miller and co-workers[19, 22] showed that organophosphorus esters (like TBP) solvate and quantitatively extract $M^+...Au(CN)_2^-$ ion-pairs to form $NaAu(CN)_2$.pTBP, where p is the number of TBP molecules solvating the ion pair. The ion-pair-TBP solvate adduct is more hydrophobic than the ion-pair itself. Therefore, it is conceivable that the elution of gold from activated carbon by the non-polar sc-CO_2 is favoured by the presence of TBP as shown in Table 1, 27% gold extracted in the absence of TBP but 73% extracted in the presence of TBP.

Temperature (°C)	% Gold Extracted	
50	1.4	
100	6.5	30.9*
150	27.2	73.4*

Conditions: 4,000 psi; 1 g wet gold-loaded activated charcoal; 1.0 cm^3 of 1 mol/dm^3 NaCN, static time = 30 min. and dynamic time = 20 min.
*contained 1 cm^3 TBP and 0.5 cm^3 1 mol/dm^3 NaCN, 6,000 psi.

Table 1 Effect of temperature on the elution of gold from activated carbon using sc-CO_2

Condition	% Gold Extracted
Dry charcoal	0.3
Dry charcoal + 1.5 cm^3 H_2O	2.9
Dry charcoal + 1.5 cm^3 1 mol/dm^3 NaCN	32.1

Conditions: 6,000 psi; Temp. = 150°C; static time = 30 min. and dynamic time = 20 min.

Table 2 Effect of ionic strength on the elution of gold from activated carbon by sc-CO_2.

An enthalpy change (ΔH^o) for the desorption process of 36.5 kJ/mol was calculated from a plot of log D vs I/T, figure 1, when TBP was not present. The distribution ratio, D, is the percent of gold desorbed divided by percentage remaining on the carbon. A ΔH^o value of 47.3 kJ/mol was estimated in the presence of TBP. In addition to the usual assumptions made in applying the van't Hoff equation, it was assumed that allowing similar time periods for the temperatures used would produce distribution ratios consistent with the extent of equilibrium at these temperatures. The dynamics of the system was neglected. Thus, the ΔH^o values are estimates.

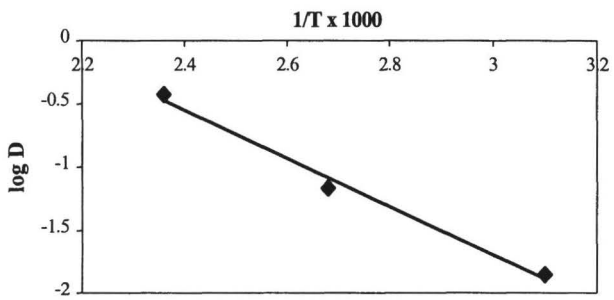

Figure 1. van't Hoff plot for the elution process

To optimise the sc-CO_2 elution, static and dynamic extraction times, pressure, and amounts of NaCN and TBP were examined. Static time regime was found to be more important than the dynamic time segment of the process, and a threshold pressure of about 4,000 psi was needed.[20] There is some sort of trade-off regarding the presence, or otherwise, of TBP and NaCN. Some proponents of the use of organic solvent solutions to desorb gold from activated carbon contend that the presence of NaCN is not necessary.[11, 12, 14] In the present example of using sc-CO_2, if time is not a constraining factor, which undoubtedly it is, addition of TBP may not be necessary. Static time greater than 3 h. could lead to quantitative desorption of gold in the absence of TBP.[20] The results in Table 2 also show a strong influence of the presence of NaCN. On the other hand, the presence of TBP yielded 73% extraction in 0.5 h. compared to 60% in 3 h. when it was absent. Moreover, no extra NaCN, other than that in the wet loaded carbon, is needed when TBP is present.

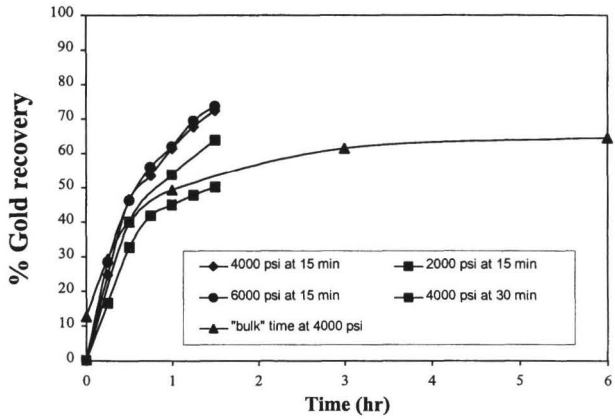

Figure 2. Effect of static time and pressure on the elution process.
Conditions: 0.5 g "loaded" carbon; 0.5 cm^3 TBP; 1cm^3, 1 mol/dm^3 NaCN ; 20 min. dynamic time; 150C

The static time profile shown in Figure 2 indicates a kinetic and equilibrium region, with the latter occurring at around 65% recovery of gold in 6 h. To improve the percentage recovery, it was worthwhile to work within the kinetic region. Instead of bulk static times, short static time duration were performed on a given carbon sample. The elution mixture was replaced between static-dynamic cycles. The total recovery after six-15 minute repeated cycles rose to 82%. Extrapolation of the curves indicates that quantitative recovery would be achieved between 2.5 to 3 h. a time frame that is comparable to the faster elution time of conventional methods.

Figure 2 also shows the effect of pressure, with repeated cycling. Cumulative percent gold recovery at 4,000 psi was about 30% higher than at 2,000 psi. Recoveries at 4,000 psi were statistically the same as that at 6,000 psi, which suggests a threshold pressure for the miscibility of the solvated ion-pair. It seems also, that there is no significant advantage with pressures higher than 4,000 psi.

CONCLUSIONS

Work from this laboratory has reported the few instances where an inorganic anionic species has been mobilised into sc-CO_2. NaCN is the largest waste in the hydrometallurgy of gold. The use of supercritical CO_2 in the desorption step, where a high concentration of NaCN is currently being used, will drastically reduce the amount of NaCN required. In the present sc-CO_2 method, the requisite amount of NaCN to maintain the ion-pair will already be available from the wet loaded activated carbon (which contained 250 mg/dm^3 NaCN and the loaded carbon was 30% wet, i.e., ca 0.001% w/v NaCN).

ACKNOWLEDGEMENT

The author wishes to thank Dr. Frank Schweighardt of Air Products and Chemicals, Inc. for donating supercritical CO_2 and Calgon Carbon Corporation for providing the activated carbon. James Wilson performed some of the extractions.

REFERENCES

1 Fuoss RM, and Kraus CA. *J. Amer. Chem. Soc.* **55,** 1019, 2387, (1933).
2 Born M. *Z. Phyzik*, **1**, 45, (1920).
3 Laintz KE and Tachikawa E. *Anal. Chem.* **66**, 2190, (1994).
4 Liu Y, Lopez-Avila V and Alcaraz M. *Anal. Chem.* **66**, 3788, (1994).
5 Wang J and Marshall WD. *Anal. Chem.* **66**, 3900, (1994).

6 Lin Y, Smart NG and Wai CM. *Environ. Sci. Technol.* **29**, 2706, (1995).
7 Lin Y, Wai CM, Jean FM and Brauer RD. *Environ. Sci. Technol.* **28**, 1190, (1994).
8 Kouletsis RK and Otu EO. *29th Middle Atlantic Regional Meeting-American Chemical Society, May 24-26, Washington, D.C*, (1995).
9 Johnson WD. *US Patent* 522,260, July 3, (1894).
10 Zadra JB, Engel AK and Heinen HJ. *U.S. Bur. Mines, Rep. Invest.* No. 4843, (1952).
11 Vegter NM and Sandenbergh RF. *Hydrometallurgy,* **28**, 205, (1992).
12 Espiell E, Roca A, Creulls M and Nunez C. *Hydrometallurgy*, **19**, 321, (1988).
13 Muir DM, Hinchliffe W and Griffin A. *Hydrometallurgy*, **14**, 151, (1985).
14 Muir DM, Hinchliffe W, Tsuchida N and Ruane M. *Hydrometallurgy*, **14**, 47, (1985).
15. Heinen HJ, Peterson DG and Lindstrom RE. in Weiss A. (ed.); *World Mining and Metals Technology*, AIME, New York; Chapter 33; 551, (1976).
16 McDougall GJ, Hancock, RD, Nicol MJ, Wellington OL and Copperwaite RG. *J. S. Afr. Min. Metall.* **80**, 344, (1980).
17 Adams MD and Fleming CA. *Metall. Trans. B*, **20B**, 315, (1989).
18 McDougall GJ, Adams MD and Hancock RD. *Hydrometallurgy*, **18**, 125, 139; **19**, 95, (1987).
19 Mooiman MB and Miller JD. *Hydrometallurgy*, **27**, 29, (1991).
20 Otu EO. *Sep. Sci. Tech.* **32**, 1107, (1998).
21 Sivakumaran A. *M.Sc. Thesis,* University of Waterloo, Waterloo, Ontario, Canada, (1991).
22 Miller JD, Wan RY, Mooiman MB and Sibrell PL. *Sep. Sci. Tech.* **22**, 487, (1987).

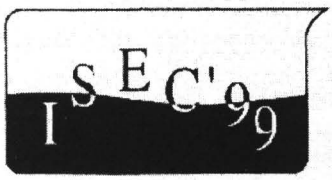

MODELLING OF SUPERCRITICAL FLUID EXTRACTION FROM NATURAL MATERIALS WITH INTERACTION AMONGST SOLUTES AND SOLID

Motonobu Goto, Akio Kodama and Tsutomu Hirose
Department of Applied Chemistry and Biochemistry, Kumamoto University, Kumamoto 860-8555 Japan

ABSTRACT
Extraction or leaching of solutes from natural solid material with supercritical fluid is a process involving mass transfer. Local interaction among solutes and solid matrix within a natural material significantly influences the extraction behaviour. A mass transfer model accounting for the solute-solid interaction and solute-solute interaction was developed. Interaction between solute and solid matrix was modelled by using adsorption isotherm type expression. Experimental data for the extraction of essential oil and cuticular wax from peppermint leaves and the extraction of oil and water from fish meat were analysed.

Keywords: essential oil, supercritical extraction, carbon dioxide, modelling, mass transfer

INTRODUCTION

Extraction process from natural materials may consist of releasing solutes from porous or cellular matrix into solvent and mass transfer process. The solutes fixed or trapped in a matrix by physical or chemical forces must be released and transferred to the supercritical fluid by dissolving or desorption. Then, the dissolved solutes diffuse out in a matrix to the surface of a particle. Finally, they move across a stagnant film around a particle to the bulk fluid phase. The solutes of interest vary from small to large molecules or low to high boiling point molecules. Their content in a feed material also varies significantly. Thus, rate-limiting processes for the extraction of these materials may be different from one material to another.

Several attempts have been devoted to the modelling of the extraction process.[1-3] The extraction of oil from seeds has been most intensively modelled. Since oil content of seeds is relatively high and oil consists of similar compounds, a mass transfer model was often employed. Fick's diffusion model has been applied.[4,5] A simpler model has been also applied where mass transfer was expressed by a linear driving force approximation.[6,7] Desorption models have been developed where the local dissolving process is considered to be desorption phenomena of solutes adsorbed on a matrix.[8,9] Extracts from natural materials such as leaves consist of essential oil and cuticular wax. The extraction rate of essential oil is much lower than the value expected from the solubility of the solute in supercritical fluid.[5,9,10] This behaviour was explained by adsorption mechanism[9] or diffusion mechanism.[5] On the contrary, the extraction rate of cuticular wax is controlled by the solubility where the extracted concentration of solute is close to its solubility.[5]

Therefore, various models have been developed to analyse the extraction behaviour of various kinds of materials. The objective of this paper is to develop versatile model that is applicable to extraction controlled by a mass transport process, solubility in fluid phase, solute-solid interaction, and solute-solute interaction. The model is applied to explain the extraction behaviour of essential oil and cuticular wax from peppermint leaves[10,11] and of oil and water from fish meal.[12]

MODEL DEVELOPMENT

A versatile model has been developed that can explain the extraction behaviour for varieties of materials. Depending on the material and the solute of interest, the extraction behaviour is controlled by either one of the following or some of them; solute-solid interaction (adsorption), solute-fluid interaction (solubility), or mass transfer. For example, the extraction of oil or wax from plant materials is usually controlled by the solubility,[4] whereas the extraction of essential oil is

© 2000 Society of Chemical Industry

controlled by solute-solid interaction.[9,11] There may be some interaction among solutes in fluid phase.[12]

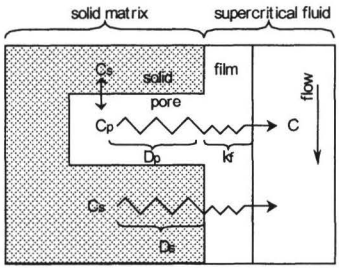

Figure 1. Schematic drawing of extraction process.

Consider a packed bed containing particles of natural materials. Pure solvent enters the bed, void volumes in the bed are initially free of solute, and the process is isothermal. The governing equations are as follows:

$$\alpha\frac{\partial C}{\partial t}+u\frac{\partial C}{\partial z}=D_L\frac{\partial^2 C}{\partial z^2}-(1-\alpha)k_f a_p\left[C-C_p(R)\right] \tag{1}$$

When mass transport process in a particle is expressed as shown in Figure 1, the mass balance for the solute in the pores in porous particle is

$$\beta\frac{\partial C_p}{\partial t}+(1-\beta)\frac{\partial C_s}{\partial t}=D_p\frac{1}{r^2}\frac{\partial}{\partial r}\left(r^2\frac{\partial C_p}{\partial r}\right) \tag{2}$$

If the solute diffuse in solid phase in non-porous particle,

$$\frac{\partial C_s}{\partial t}=D_s\frac{1}{r^2}\frac{\partial}{\partial r}\left(r^2\frac{\partial C_s}{\partial r}\right) \tag{3}$$

Initial and boundary conditions may be given by

$$D_p\left(\partial C_p/\partial r\right)_{r=R}=k_f\left[C-C_p(R)\right] \text{ or } D_s\left(\partial C_s/\partial r\right)_{r=R}=k_f\left[C-C(R)\right] \tag{4}$$

$$\left(\partial C_p/\partial r\right)_{r=0}=\left(\partial C_s/\partial r\right)_{r=0}=0 \tag{5}$$

$$D_L\left(\partial C/\partial z\right)_{z=0}=u\left(C-C_0\right)_{z=0},\ \left(\partial C/\partial z\right)_{z=L}=0 \tag{6}$$

$$C(t=0)=0,\ C_p(t=0)=C_{p0},\ C_s(t=0)=C_{s0} \tag{7}$$

The cumulative fraction of solute extracted up to time t is given by

$$F(t)=\frac{u}{(1-\alpha)LC_0}\int_0^t C dt \tag{8}$$

The curve F versus t corresponds to the integrated form of the extraction curve where F is unity for the complete extraction.

Interaction among solutes, fluid and solid

Local dissolving rate.

During the extraction process, the local dissolving rate of solute into the fluid phase at solid (or liquid) /SCF interface within a porous particle or at the surface of non-porous particle is a function of solute concentration in solid phase or in fluid phase.

$$\Omega=f(C_s,C_p) \tag{9}$$

Assuming that the dissolving rate is expressed by reversible reaction such as adsorption/desorption where the rate is non-linear Langmuir form,

$$\Omega = k_a(1 - C_s / C_m)C_p - k_d C_s \tag{10}$$

When $C_m >> C_s$, the rate equation becomes linear.

$$\Omega = k_a C_p - k_d C_s \tag{11}$$

If dissolving is irreversible, the equation is first order kinetics.

$$\Omega = -k_d C_s \tag{12}$$

Local equilibrium.

The local extraction process must satisfy the following two conditions to account for the phenomena observed for both controlled by the solute-fluid interaction (solubility) and solute-solid interaction (adsorption):

i) The maximum concentration dissolved in fluid phase should be equal or less than the solubility. In the case of solubility controlled, the extraction concentration is close to the solubility.
ii) There is some interaction between solute and solid matrix in order to explain the slow extraction for essential oil.

These situations can be described by a formula of BET adsorption isotherm that is often used in adsorption equilibria:

$$\frac{C_s}{C_m} = \frac{KC_p / C_{sat}}{(1 - C_p / C_{sat})[1 + (K-1)C_p / C_{sat}]} \tag{19}$$

where C_m corresponds to maximum amount of mono-layer adsorption and K corresponds to adsorption equilibrium constant which indicates the strength of interaction between solute and solid. Since C_{sat} is a solute-fluid interaction parameter, two interaction parameters, C_m and K, determine the equilibrium relation of solute at fluid-solid interface.

When equilibrium constant, K is unity or infinity, above equation is simplified to:

$$C_s / C_m = (C_p / C_{sat}) / (1 - C_p / C_{sat}) \quad (K = 1) \tag{20}$$

$$C_s / C_m = 1 / (1 - C_p / C_{sat}) \quad (K = \infty) \tag{21}$$

When the interaction between solute and solid is considerably strong, the equation does not include solubility, C_{sat}. The simplest expression is a linear equilibrium given by

$$C_s = K_L C_p \tag{22}$$

When $K << 1$ or $C_m << 1$, fluid phase concentration approaches the equilibrium solubility independent of solid phase concentration, that is, rectangular form.

$$C_p = C_{sat} \tag{23}$$

Langmuir type equilibrium equation can be obtained, when rate equation becomes equilibrium.

$$C_s / C_m = K_{LM} C_p / (1 + K_{LM} C_p) \tag{24}$$

When concentration in fluid phase and solid phase are interchanged, one obtains reverse Langmuir equation, where solubility controlled extraction can be expressed.

$$C_s = (C_p / C_{sat}) / [K_{LM} / (1 - C_p / C_{sat})] \tag{25}$$

These relations are shown in Figure 2. For BET equation, fluid phase concentration, C_p is larger for smaller value of K. When K is small, that is, interaction between a solute and solid phase is trivial, C_p is close to unity even at small C_s, that is, fluid phase concentration is close to the solubility. This corresponds to a case where extracted concentration is close to the solubility until almost

complete extraction as observed in vegetable oil or wax from plant materials.[10] On the other hand, when K is large, that is, interaction between a solute and solid phase is more influential, C_p is small even for large solid phase concentration or C_s/C_m is close to unity. This is a case where extracted concentration is much smaller than the solubility as observed in essential oil from leaves.[9,10]

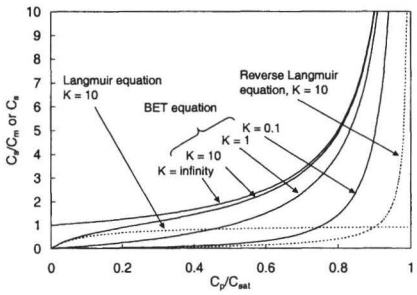

Figure 2. Equilibria of solute between solid and fluid phase.

Interaction among solutes

Since natural materials contain many kinds of extractable components, the extraction process is multi-component system. Solute concentration in pore fluid phase is a function of solid phase concentration and solubility in fluid phase.

$$C_{p,j} = f\left(C_{s,j}, C_{sat,j}(C_{p,k})\right) \tag{25}$$

The solubility is influenced by fluid phase concentration of the other components. The influence is positive or negative depending on the system. Although the interaction could be expressed by multi-component phase equilibria, simpler relationship might be often practical.

RESULT AND DISCUSSION

Experimental data[10] for the extraction of essential oil and cuticular wax from peppermint leaves with SC-CO_2 were analysed by the developed model with BET adsorption equation. A semi-continuous flow extractor with supercritical carbon dioxide measured the extraction behaviour of these components. The extracted concentration of essential oils was less than 5% of the solubility value, whereas that of cuticular waxes was close to the solubility. We have assumed that $C_m = C_s$ and mass transfer parameters were estimated by correlations.[11] Figure 3 shows the comparison between the experimental extraction curves and the model calculation. The model simulated well the extraction behaviour. The adsorption equilibrium constants, K optimised were 1 for cuticular wax and 15 for essential oil. This indicates that the interaction between essential oil and solid matrix of leaf is larger than that between cuticular wax and matrix. Therefore, the solute concentration leaving the extractor is much smaller than the solubility for essential oil, whereas it is close to the solubility for cuticular wax.

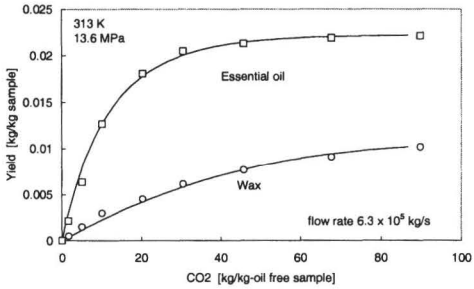

Figure 3. Extraction curve of essential oil and wax from peppermint.

Experimental data for the extraction of oil and water from fish meat with SC-CO_2 were analysed by the model with solute-solute interaction.[12] It was assumed that partially dried fish meat was porous and oil concentration in pore fluid phase was equal to the equilibrium solubility which was a function of water concentration as shown in Figure 4. Since there is interaction between water and protein, water concentration in fluid phase was assumed to be a function of water concentration in solid phase. A mass transfer model that incorporated the negative interaction between oil and water in the supercritical phase simulated the experimental data for oil extraction from fish meal. Interaction of water with solid matrix influenced the extraction of water. The water concentration in SC-CO_2 phase influenced the solubility of oil, resulting in reduction of extraction rate of oil.

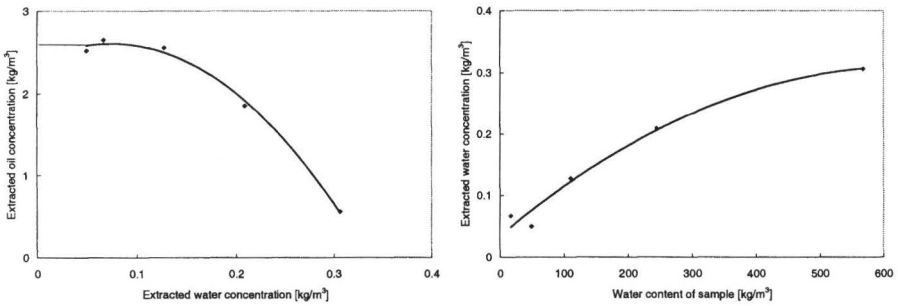

Figure 4. Relationship among extracted oil concentration, extracted water concentration, and water content of feed for fish meal extraction.

CONCLUSIONS

A simple model accounting for mass transfer, equilibrium solubility, and solute-solid interaction was developed. The local extraction phenomena influenced by both solubility of solute in fluid phase and interaction among solutes and solid was incorporated into the model. The extraction behaviours of peppermint and fish meal were analysed by the model with interactions.

NOMENCLATURE

a_p	specific surface area, 1/m
C	solute concentration in CO_2 in the bed void volume, kg/m^3
C_m	parameter in BET isotherm, kg/m^3
C_p	solute concentration in the pore volume of a particle, kg/m^3
C_s	solute concentration in the leaf, kg/m^3 of solid fraction of a particle
C_{sat}	equilibrium solubility, kg/m^3

C_0	total solute concentration, kg/m^3
D_p	pore phase diffusion coefficient, m^2/s
D_s	solid phase diffusion coefficient, m^2/s
F	cumulative fraction of solute extracted
k_f	external mass-transfer coefficient, m/s
K	equilibrium constant
r	radius of spherical particle, m
t	time, s
α	void fraction in bed
β	porosity of a particle

REFERENCES

1 Akgerman A and Madras G. *Supercritical Fluids Fundamentals for Application*, Kluwer Academic Publishers: Dordrecht, 669, (1994).
2 Brunner G. *Gas Extraction*, Springer: New York, 188, (1994).
3 Reverchon E. *J. Supercritical Fluids*, **10**, 1, (1997).
4 Brunner G. *Ber. Bunsenges. Phys. Chem*, **88**, 887, (1984).
5 Reverchon E., Donsi G and Osseo LS. *Ind. Eng. Chem. Research*, **32**, 2721, (1993).
6 Lee AKK, Bulley NR, Fattori M and Meisen A. *J. Am. Oil Chem. Soc.*, **63**, 921, (1986).
7 Schaeffer ST, Zalkow LH and Teja AS. *J. Supercrit. Fluids*, **2**, 15, (1989).
8 Recasens F, McCoy BJ and Smith JM. *AIChE J.*, **35**, 951, (1989).
9 Goto M, Sato M and Hirose T. *J. Chem. Eng. Japan*, **26**, 401, (1993).
10 Roy BC, Goto M, Kodama A and Hirose T. *J. Chem. Tech & Biotech.*, **67**, 21, (1996).
11 Goto M, Roy BC, Kodama A and Hirose T. *J Chem. Eng. Japan*, **31**, 171, (1998).
12 Dunford NT, Goto M and Temelli F. *J. Supercrit. Fluids*, **13**, 303, (1998).

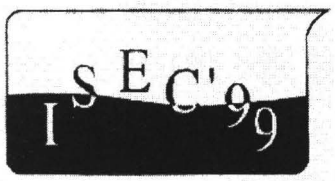

MODELLING OF THE FLUID–SOLID EQUILIBRIA OF THE ANTIBIOTIC PENICILLIN G IN SUPERCRITICAL CARBON DIOXIDE

MD Gordillo, A Molero and E Martínez de la Ossa
Department of Chemical Engineering, Food Technology and Environmental Techn. Faculty of Sciences, University of Cádiz, 11510 Puerto Real (Cádiz), Spain

ABSTRACT
The aim of this work is to evaluate and to compare different group contribution methods to predict the critical properties of Penicillin G, and different equations of state for the correlation of solubility data of this antibiotic in supercritical carbon dioxide. Critical parameters have been estimated using Lydersen, Ambrose and Joback group contribution methods. The experimental data have been correlated using the Reldich-Kwong and Soave-Redlich-Kwong equations of state with Lorent-Berthelot mixing rules.

Keywords: Penicillin G, supercritical extraction, carbon dioxide, equations of state,

INTRODUCTION

The interest in Supercritical Fluid Technology relies on the possibilities offered by this technique, supercritical fluids processes, developed on industrial or research scale, use the unique possibility of continuous change of the solvent power of these fluids. Carbon dioxide (CO_2) is an ideal solvent because it is non-toxic, non-flammable, and non-explosive; available in high purity and at low cost; highly selective for some solutes and separable from the extracted solutes.[1, 2, 3]

The interest of the pharmaceutical industry in this new technology is mainly related to the possibility of processing pharmaceutical compounds without organic solvents. Obviously, the first step to evaluate the possibilities of supercritical extraction as an alternative process to extraction with liquid solvents is to determine the solubility of the antibiotic in supercritical carbon dioxide and its variation with pressure and temperature.

In previous work,[4] we reported the results of an experimental study of the solubility of Penicillin G in supercritical CO_2 at pressure from 100 to 350 bar and temperature from 313.15 to 333.15 K.

There are two common approaches to correlate these data, namely theoretical equations of state and statistical methods.[5] In this work, the first approach has been used. To correlate solubility form equations of state requires tedious computational effort and physical property values that are often difficult to obtain.

MODELLING

The solubility, y_i, of a pure solid in a supercritical fluid, through thermodynamic model, is expressed by [6]

$$y_i = \frac{P_i^{Sat}}{\hat{\phi}_i^F P} \exp \frac{(P - P_i^{Sat}) v_i^S}{RT}$$

where P_i^{Sat} and v_i^S are the vapour pressure and the molar volume of pure solid, and $\hat{\phi}_i^F$ is the fugacity coefficient of solid in the supercritical phase (at pressure P and temperature T). The calculation of the solubility y_i, therefore, requires a knowledge of P_i^{Sat}, v_i^S and an equation of state (with its associated mixing rules) for the calculation of $\hat{\phi}_i^F$.

In this work, the Redlich-Kwong [7] (RK) and Soave-Redlich-Kwong [8] (SRK) equations of state with Lorentz-Berthelot mixing rules have been used to calculate fugacity coefficient. To calculate this

© 2000 Society of Chemical Industry

coefficient, a binary interaction parameter K_{ij} must be obtained by fitting the experimental solubility data.

If a cubic equation of state is used, some properties should be known for the compounds involved in the system under investigation, such as critical temperature (T_c), critical pressure (P_c) and acentric factor (ω) of the compounds. As well, in the Lorentz-Berthelot mixing rules,[6] the critical volume should be also known. In the SRK equation, the acentric factor (ω) of Penicillin G has been calculated from the definition.[6] In this way, an acentric factor of 1.2884 has been obtained.

Clapeyron equation[6] has been chosen for vapour pressure correlation. As regards molar volume calculation, experimental determination of solid density, as well as group contribution methods are available. In this work, the solid density has been determined using a mercury porosimeter. The obtained molar volume is 0.226 dm^3/mol. In the case of carbon dioxide, all these parameters are known.

The problem starts with the availability of the properties of Penicillin G. Critical properties cannot be experimentally determined so that one should evaluate them through the use of predictive methods, like group contribution methods.

A wide variety of physico-chemical properties can be predicted on the assumption that every molecule can be split into a set of groups of atoms, whose contribution to the molecular property is independent of the chemical nature, number, or relative position of the other groups in the molecule.

In the Penicillin G molecule, the following groups of atoms can be considered:

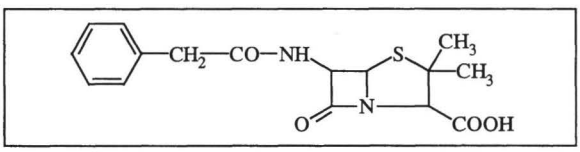

Number of groups	Group	Number of groups	Group
2	$-CH_3$ (nonring)	1	$-\overset{\vert}{C}=O$ (nonring)
1	$-\overset{\vert}{C}H_2$ (nonring)	1	$-\overset{\vert}{C}=O$ (ring)
3	$-\overset{\vert}{C}H-$ (ring)	1	—COOH
1	$-\overset{\vert}{\underset{\vert}{C}}-$ (ring)	1	$-\overset{\vert}{N}H$ (nonring)
5	$=\overset{\vert}{C}H$ (ring)	1	$-\overset{\vert}{N}-$ (ring)
1	$=\overset{\vert}{C}-$ (ring)	1	—S— (ring)

Table 1 Groups of atoms of Penicillin G molecule

In this model, the critical temperature, pressure, and volume of the Penicillin G, needed to use a cubic equation of state, have been estimated using the following group contribution methods:

Lydersen method [9]

This estimation method employs structural contributions to estimate T_c, P_c and V_c. The units employed are Kelvins, atmospheres, and cubic centimetres per gram mole. The Δ quantities are evaluated by summing contributions for atoms or groups of atoms previously described in Table 1. To employ these methods, only the normal boiling point T_b and the molecular weight M are needed. The relations are shown in Table 2.

Joback modification of Lydersen method [10]

One of the first very successful group contribution method to estimate critical properties, previously described, was developed by Lydersen. Since this time, more experimental values have been reported and efficient statistical techniques have been developed to determine the optimum group contributions. Joback re-evaluated Lydersen's scheme and determined the values of the group contributions. His proposed relations are also shown in Table 2. The units employed are Kelvin, bars, and cubic centimetres per gram mole. This method is also used to estimate the normal boiling point (see Table 2).

Ambrose method [10]

As in the case of Lydersen method, the three critical properties T_c, P_c and V_c are estimated by a group contribution technique. However, the relations used are different (see Table 2). As in the Joback method, the units employed are Kelvin, bars, and cubic centimetres per gram mole. In the case of Ambrose method, the benzene molecule is considered like only a group of atoms.

	Lydersen	Joback	Ambrose
T_c	$T_b\left[0{,}567+\sum\Delta_T-\left(\sum\Delta_T\right)^2\right]^{-1}$	$T_b\left[0{,}584+0{,}965\sum\Delta_T-\left(\sum\Delta_T\right)^2\right]^{-1}$	$T_b\left[1+(1{,}242+\sum\Delta_T)^{-1}\right]$
P_c	$M\left[0{,}34+\sum\Delta_P\right]^{-2}$	$\left[0{,}113+0{,}0032\,n_A-\sum\Delta_P\right]^{-2}$	$M\left[0{,}339+\sum\Delta_P\right]^{-2}$
V_c	$40+\sum\Delta_V$	$17{,}5+\sum\Delta_V$	$40+\sum\Delta_V$
T_b		$198+\sum\Delta_b$	

Table 2 Group contribution methods

MODELLING DISCUSSION

The critical temperature, pressure and volume, and the boiling temperature calculated, for Penicillin G by using the Lydersen, Joback and Ambrose group contribution methods, are shown in Table 3.

	T_c	P_c	V_c	T_b
Lydersen	$T_b \cdot 1.2547$ K	22.91 atm	899 mL/mol	
Joback	1224 K	25.20 bar	869 mL/mol	974 K
Ambrose	$T_b \cdot 1.2626$ K	23.55 bar	940 mL/mol	

Table 3 Critical parameters and boiling temperature by using different contribution methods

In the Lydersen and Ambrose methods, all equations depending on normal solid boiling temperature (vapour pressure and critical temperature of pure solid) have been expressed as a function of this parameter. For these methods, two variables, the boiling temperature (T_b) and the interaction parameter (K_{12}) have been estimated by minimising the average absolute relative deviation (AARD) between experimental and predicted solubility data, defined as

$$AARD\ (\%) = \frac{1}{N}\sum_{i=1}^{N}\left|\frac{y_{exp} - y_{cal}}{y_{exp}}\right| \cdot 100$$

where N is the number of experimental points.

The predicted boiling temperature and binary interaction parameter by regressing the experimental data with Redlich-Kwong and Soave-Redlich-Kwong equations of state, by using these three group contribution methods, are shown in Table 4.

LYDERSEN RK				AMBROSE RK				JOBACK RK			
T (K)	T_b (K)	K_{12}	AARD (%)	T (K)	T_b (K)	K_{12}	AARD (%)	T (K)	T_b (K)	K_{12}	AARD (%)
313.15	961	0.057	22.28	313.15	951	0.075	23.21	313.15	974	0.039	27.71
323.15	961	0.045	21.97	323.15	951	0.064	22.19	323.15	974	0.026	28.39
333.15	961	0.035	30.39	333.15	951	0.054	29.13	333.15	974	0.016	41.56
		AARD (%)	24.88			AARD (%)	24.84			AARD (%)	32.55
P ≥ 200 bar (%)		AARD	5.01	P ≥ 200 bar (%)		AARD	4.95	P ≥ 200 bar (%)		AARD	13.84

LYDERSEN SRK				AMBROSE SRK				JOBACK SRK			
T (K)	T_b (K)	K_{12}	AARD (%)	T (K)	T_b (K)	K_{12}	AARD (%)	T (K)	T_b (K)	K_{12}	AARD (%)
313.15	899	0.392	23.87	313.15	964	0.390	22.58	313.15	974	0.373	27.34
323.15	899	0.378	21.75	323.15	964	0.378	21.84	323.15	974	0.361	27.36
333.15	899	0.366	33.32	333.15	964	0.368	29.96	333.15	974	0.350	41.73
		AARD (%)	26.31			AARD (%)	24.79			AARD (%)	32.14
P ≥ 200 bar (%)		AARD	13.84	P ≥ 200 bar (%)		AARD	5.21	P ≥ 200 bar (%)		AARD	13.84

Table 4 Predicted boiling temperature and binary interaction parameter by regressing the experimental data with RK and SRK equations of state

The values of these variables have no physical meaning, they are just fitting parameters. In fact, this approach is quite questionable, since pure component properties are obtained from fitting data related to the carbon dioxide-penicillin system. In this way, different numerical values of these parameters can be obtained if the fitting is performed on solubility data of the same antibiotic but in a different supercritical fluid.

The obtained results in the solubility prediction show that the correlation with RK equation of state gives better results that with the SRK equation in the case of Lydersen group contribution method. On the other hand, the Ambrose and Joback methods, with the SRK equation offer better results that with the RK equation.

The selection of the best group contribution method is based on the results obtained with each one. The Ambrose method yields the smaller error, but it is more complicated in its use than Joback's, since the later allows the estimation of the boiling temperature. In this way, a fitting parameter is eliminated in the proposed model, obtaining, therefore, higher AARD values.

For all group contribution methods and equations of state, the AARD obtained suggest the goodness of the procedure. As can be seen in Figures 1, 2 and 3, at temperatures of 313.15 and 333.15 K, the correlation with the Lydersen and Ambrose methods gives better results. However, at 323.15 K

the fitting is better with the Joback method. In this case, the boiling temperature has been estimated, so that only K_{ij} has been used as fitting parameter. The results obtained in the correlation of all solubility data show a further improvement in AARD when two parameters, K_{ij} and T_b are used for the fitting.

At high pressure, where the supercritical extraction is more important because of the higher solubility data, AARD are quite lower than obtained in all experimental conditions, as can be seen in Table 4. The correlation, discussed above, provide therefore a good prediction for the fluid-solid equilibrium of the Penicillin G and supercritical CO_2 system.

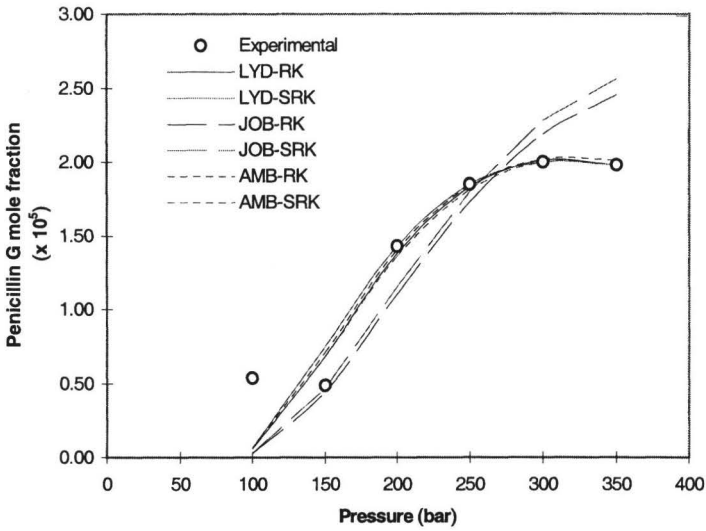

Figure 1. Correlation of Penicillin G solubility data in CO_2 at 313.15 K by using different approach.

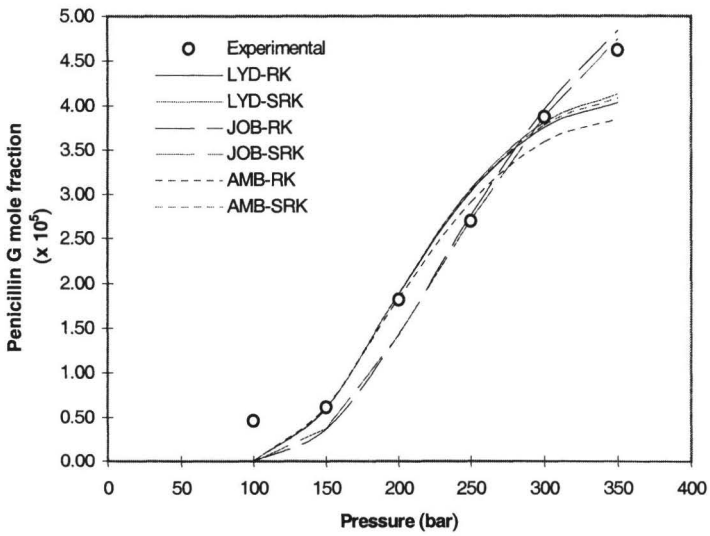

Figure 2. Correlation of Penicillin G solubility data in CO_2 at 323.15 K by using different approach.

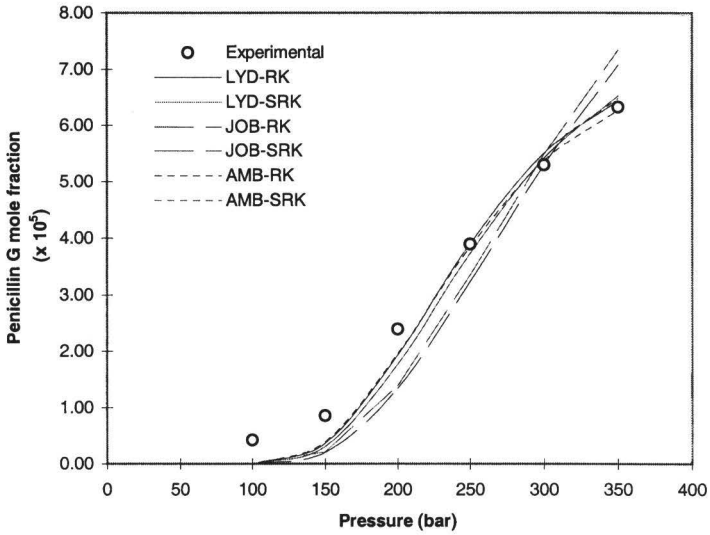

Figure 3. Correlation of Penicillin G solubility data in CO_2 at 333.15 K by using different approach.

REFERENCES

1. Martínez de la Ossa E and Galán Serrano MA *Ingeniería Química*, **7**,169, (1990).
2. Martínez de la Ossa E and Galán Serrano MA *Ingeniería Química,* **1**, 251, (1990).
3. Martínez de la Ossa E and Galán Serrano MA Ingeniería Química, **8**,125, (1990).
4. Gordillo MD *Master Thesis* Cádiz (Spain), (1998).
5. Alessi P, Cortesi A, Kikic I and Foster NR *Chem. Biochem. Eng.*, **11**(1), 19,(1997).
6. Walas SM, *"Phase Equilibria in Chemical Engineering"*, Butterworth Publisher, Boston, (1985).
7. Redlich D and Kwong JNW *Chem. Rev.*, **44**, 223, (1949).
8. Soave G, *Chem. Eng. Sci.,* **27**, 1197, (1972)..
9. Reid RC, Prausnitz JM and Sherwood TK. *"The Properties of Gases and Liquids"*. 3er Ed., McGraw-Hill, New York, (1977).
10. Reid RC, Prausnitz JM and Poling BE. *"The Properties of Gases and Liquids"*. 4th Ed., McGraw-Hill, New York, (1987).

AUTHOR INDEX

Abu-Shady AI 1325
Adachi M 107
Adda M 549
Afonin MA 1371
Aguilar JC 1013
Aguilar M 1127 1267 1555 1561
Ahuis F 239
Akiba K 1103
Akita S 363 387
Al-Mudhaf HF 1325
Alessi V 1567
Alguacil FJ 381 1155
Almela A 703
Alonso E 167
Alonso JJ 167
Aly HF 347 1351 1387
Amer SA 1325
Angelov G 463
Anticó E 1115
Arnaldos J 1285
Asakura T 1469
Asano T 829
Avila-Rodríguez M 1209

Babain VA 1345
Bailador H 161
Bailes PJ 503 609
Bakastova NV 971
Ban T 493
Bandekar SV 71
Bandyopadhyay M 921
Bao B-R 353 1357 1361
Baranov SM 1381
Barron Zambrano JA 1209
Bart H-J 125 835 847 927 939 959 1573
Becker O 475
Belnet F 637
Beltran JL 1555
Belova VV 1139
Benedetto JS 189 711 717
Benjamin I 3
Benzal G 1529
Berrama T 983
Berthon C 1333
Biddlestone AJ 1639
Birkett JE 1463
Blanco MA 1607 1629
Bogacki MB 1193
Böhmer V 1095
Bolton GT 445
Boluda N 161
Bond AH 299
Bonnesen PV 1365
Borowiak-Resterna A 359 1197
Boshoff G 789
Botella A 643
Bothwell P 1463
Boubals N 317
Bourget CC 1187
Bouvier C 871
Brajenovic N 1167
Brewer KN 1345
Brodkorb MJ 513
Buchalier EM 1455
Bukar NV 567
Burgard M 681

Canari R 597
Canselier JP 171
Cara G 1023
Carvalho JMR 915 959 977
Castillo E 47
Cattrall RW 1053
Chang Z 405
Charbonnel MC 1333
Chartroux C 239
Chayama K 675
Chekmarev AM 805 1161 1493
Chen D 469
Chen J 405
Chen M 419
Chen S-J 259
Chen W-J 259
Chiarizia R 53 299
Chimenos JM 759
Chizhevskaya SV 805
Chowdhury DA 393
Chu D 1109
Cichy W 1065
Ciminelli VST 953
Cinti M 1623
Clark P 789
Cocero MJ 167
Cohn-Syzov N 131
Cole PM 1437
Comba P 687
Conner C 1365
Cordier PY 317 323
Correia PFMM 977
Cortina JL 47 771 1127 1267 1285 1555 1561
Costa MC 271
Costic S 1403
Cote G 871 1197
Cox M 805 1187
Cruz-Pinto JJC 487
Cusack RW 427
Czapla C 835

Da Silva CE 189
Da Silva GL 953
Dai YY 177 183 419 625
Daldon M 1333
Dannus P 25
Dantas Neto AA 195 783

Dantas TN de C 195 783
Daoud JA 1351
Datta S 921
Davies BM 1437
de Barros Neto EL 171
de Gyves J 1013 1019
de Haan AB 1543
De Ketelaere RF 947 995
de La Salles WF 783
de Lucas A 1607
Del Re G 1623
Delgado A 1611
Deljouie P 813
Delmas F 729
Delmau LH 1365
Delshams A 1529
Denniss IS 1381 1463
Dhadke PM 71 245
Di Giacomo G 1619 1623
Diaz G 201 1449
Dieleman CB 681
Dietz ML 53 299
Ding S-D 259
Dinh B 655
Dozol JF 1095
Drake A 1417
Dreisinger DB 1443
Drew MGB 281
Druzhinina IA 1475
du Preez AC 305 311
Dunga NTK 249
Dunowicz R 369
Durand G 965 983 1071 1143
Dzygiel P 1035

Eckstein A 615
Eidelman Ch 549
El Gharbi M 1561
El-Afifi S 347
El-Hefny N 1387
Elizalde MP 703 1227
Enachescu F 1403
Enarsson Å 323
Ennassef K 1071
Ernst B 681
Escalante H 1499
Esimantovskiy V 1345
Esparducer A 759
Espiell F 759
Eyal AM 131 369 597 603

Falgueras J 201
Fan Z-P 353
Feather A 789 1443
Fedorov A 1523
Fei W 451 457 469 1543 1579
Fernandes CE 271
Fernández AI 759
Fernández MA 759
Flett DS 1187
Fogassy E 1601
Fontàs C 1029
Fortes MCB 717
Foulon C 1143
Fox RV 1657
François N 317
Franzoni A 1567
Frías C 1449
Fujinaga K 341
Fujine S 1469
Fukunaga S 393
Furusaki S 83 1297

Galán B 543
Gallego Lizon T 1511
García MA 201
García-Carrera A 1095
García Liranza E 735 753
Gautam PK 1001 1375
Gega J 1007
Geist A 1517
Giganov GP 1493
Giganov VG 1493
Glatz DJ 427
Glazkov IN 1645
Gloe K 239 687
Góis LMN 481
Gomes MLACN 487
Gomis V 161
Gonzalo A 1273
Gordillo MD 1675
Goto M 83 865 1297
1469 1669
Gourdon C 171 463
Gracia I 1607
Gradella C 1567
Granados M 47
Grieser F 813
Grinbaum B 509 549 1455
Grishchenko AB 893
Guimarães MML 487

Haddad R 1155
Hall S 1455
Hampe MJ 329
Hano T 219 989 1297
Harada M 107
Hardy R 475
Hatate Y 537
Hatton TA 83
Haverlock TJ 669 1365
Hay BP 299
Hebrant M 207
Hegazi MF 1325
Helal A-A A 213
Hendrawan H 877
Herbst RS 1345
Herlinger AW 299
Herranz J 1285
Hidalgo M 1029 1121

Hill NJ 1339
Hirai T 723 1397
Hirata A 137 143 149
Hirata M 219 989
Hirayama N 585
Hirose T 1669
Ho JMY 231
Hoffmann A 947
Hoffmann S 631
Hokura A 561
Holmes TL 427
Honbu T 95
Honjo T 585 1149
Horwitz EP 53
Hossain KZ 1149
Hotoku S 1469
Hotta M 1173
Huang H 625
Huang Z 259
Huber VJ 299
Hudson MJ 271 281 317 323
Hutahaean LS 1585
Hyodo N 363 387

Ibach S 239
Iberhan L 1261
Iglesias M 1115
Inoue K 255 687 741
Irabien A 1499
Ishibashi H 255
Ishikawa I 1215
Ismael C 915
Itabashi O 741
Ito M 59 1173
Iveson PB 271 281 323

Jääskeläinen E 525
Jakovljevic B 1133
Jakubiak A 1203
Jarudilokkul S 101 113
Jensen MP 1089
Jerabek K 1267
Jiang WB 183
Jidkova TI 1139
Jing Y-D 259

Kafarski P 1035
Källvenius G 323
Kamata S 393
Kamei K 1469
Kaneda M 433
Kanel JS 1585
Kanki T 829
Kanno A 1423
Kaplan P 965
Kato D 859
Kato T 1423
Katoh S 107
Kaunisto J 1595
Kawaizumi F 493
Kawakita H 137
Kawano Y 95 537 1181
Kelly N 1417
Kemény S 1601
Keszei S 1601
Kholkin AI 1139
Khopkar SM 245
Kihara T 1469
Kim H 829
Kim JI 335 1517
Kim V 567
Kimura S 1469
King MB 1639
Kinugasa T 89
Kirschling P 1411
Kirschneck D 531
Kleinberger R 1455
Kobayashi N 363 387
Koch J 439
Kocherginsky NM 893
Kodama A 1669
Kojima D 865
Kojima I 59
Koltunov VS 1381
Komasawa I 95 723 1397
Kokubu S 219
Kolev SD 1053
Komatsu Y 265 1249
Kondo K 899
Korchinsky WJ 445 619
Korda TM 1475
Koroleva MYu 573 971
Kosogorov AV 499
Koyama K 801 1549
Kozlowski C 1007
Krzyanowska E 287 293
Kuboi R 95
Kubota F 1297
Kuipa PK 503
Kumar A 47 1001 1155
1303 1375 1529
Kunogi K 249
Kurihara C 675
Kusakabe S 1309
Kuwata S 255
Kuznetsov GI 499
Kyuchoukov G 1193 1203

Laitinen A 1595
Lam CSW 231
Law JD 1345
Le QTH 663
Le S 911
Lee J-D 65
Lee JGM 609
Lefrancois L 637
Lenhard Z 1177
Leonard RA 1365
Lewis C 475

Li D 795 889 905 911 1081 1109 1233 1239
Li HB 1579
Li SS 277
Li Z 625
Liljenzin JO 281 317 323
Liu H 405
Liu Z-Q 259
Lo J-M 65
Lo TC 1503
Long WK 231
Lu J 795 905
Lu T 1639
Lu YC 183
Ludwig R 249
Lumetta GJ 1365
Luo GS 183 1579

Ma G 905 1109
Ma HL 277
Ma L 353 1357
Macanas J 1047
Mack C 329
McMurtrey RD 1657
Madic C 281 317 323 1333
Maiboroda AB 1161
Maljkovic Da 1177
Maljkovic Du 1177
Malkhede DD 245
Malve SP 77
Mansur MB 953
Mantell C 1615
Marchenko VI 1381
Marcilla A 643
Marques JJ 481
Marr R 531
Marták J 1041
Martín D 201 1449
Martin PD 445
Martínez de la Ossa E 1607 1611 1615 1619 1629 1633 1675
Martins AH 717
Masson IO 1127
Masutani M 1279
Matsumoto M 219 899
Matsumoto S 765
Matsumoto Y 1423
Matsunaga H 1313
Matt D 681
Mattison P 375
May I 1339 1381 146
McMurtrey RD 1657
Mendes-Tatsis MA 155
Menoyo B 703 1227
Mewes D 841
Mezhov EA 1381
Mickler W 225
Miesiac I 1411
Mijangos F 703
Millies M 841
Mineo H 1469
Mingote RM 711
Miralles N 1285
Miranda TLS 953
Mizrahi J 1481
Mizuno T 59
Modes G 1573
Molero A 1611 1629 1633 1675
Moreno Daudinot AM 735 753
Moriya Y 819
Mörters M 847
Motomizu S 591
Moulin C 1333
Moura MCPA 195
Movsowitz RL 1455
Moyer BA 669 1365
Muhammed M 9
Muñoz M 1023 1047
Murakami Y 137 143 149 1423
Murashova NM 579
Muraviev D 1273 1291

Nagao S 865
Nagayoshi K 1181
Nagel VM 1437
Nakahara Y 989
Nakamura K 859
Nakano Y 1469
Nakashio F 865 933 1297
Nanoti A 927
Narita H 693
Nash KL 555 1089
Navarro Mendoza R 1209
Navratil JD 1657
Niemann SH 1537
Nieuwoudt I 1319
Nii S 363 387 493 1059 1279
Nishihama S 723
Nishiki T 859
Nishimura S 765
Nitsch W 631 853 1517 1523
Noda H 433
Noel D 637
Noguchi Y 1245
Nogueira CA 729
Noro J 561
Nucciarone D 1133

Oda T 143
Ogawa N 819
Ohto K 255 687
Okubo T 899
Okumura M 341
Olaya MM 643
Oleinikova M 1047
Olenicheva OO 567
Olszanowski A 287 293

Onoe Y 883
Oprea F 1403
Ortiz I 1487
Osipov AN 893
Otu EO 1663

Paatero E 525
Pagnucco CD 1133
Paimin R 1053
Paiva AP 399
Palet C 1029
Pareau D 965 983 1071
Pareau S 1143
Parsons AR 609
Pastuschak VG 1381
Penzo R 1567
Pereira JAFR 481
Perera JM 813
Pereyra C 1619
Pérez O 1449
Pérez de Ortiz ES 1511
Pietrelli L 747
Phillips C 1431
Plucinski P 335 1517 1523
Poitrenaud C 655
Ponzo G 747
Poppenborg LH 101 113
Poulad-Meyer L 603
Povetkina MV 805
Prat MD 47
Pratt HRC 469
Prechl A 1601
Presson MT 1333
Preston JS 305 311
Pursell MR 155
Pushkov AA 499

Qin W 119

Rambocus S 1417
Rambusch T 239 687
Ranieri L 747
Rat B 655
Regueiras PFR 487
Reich A 225
Reis MTA 959
Reitmeir J 335
Renard EV 1475
Reuben BG 1417
Revelsky IA 1645
Rice NM 1255
Rickelton WA 1133
Rincón J 1607
Ritcey GM 37 519
Rodríguez M 1615
Rodríguez de San Miguel E 1013 1019
Romanovski VV 1371
Romanovskiy VN 1345
Roos M 939
Rosales Bárazaga B 735
Rosinda M 915
Rouquette H 1095
Rovira M 771 1285
Ruiz F 161
Russell ML 323

Sabolová E 1041
Sachleben RA 669 1365
Sakoguchi A 933
Salum A 953
Salvadó V 1029 1115 1121
San Román F 543
Sana T 1181
Sanagi K 89
Sánchez JM 1121
Sano M 765
Sano N 829
Santos R 1639
Sanyal SK 921
Sastre AM 47 381 771 1001 1095 1155 1209 1285 1303 1375 1529
Sato K 1215 1221 1245
Sato T 1173 1215 1221 1245
Saucedo Medina TI 1209
Savilova OA 1381
Sawinsky J 1601
Schaefer DM 1585
Schlosser S 1023 1041 1065
Schmitt H 531
Schöneberger A 927
Schöner P 1523
Segarra M 759
Seibert F 475
Seike Y 341
Sekido E 675
Sekine T 561
Senol A 411
Shafirov VL 805
Shehata FA 347 1387
Shibata J 765 1549
Shimosato T 585
Shioi A 107
Shiomori K 95 537 1181
Shiraishi Y 1397
Shukla JP 1001 1375
Simándi B 1601
Simonin JP 877
Sinegribova OA 567 825
Singh RK 1001 1375
Skachkov VS 499
Slater MJ 513 1567
Smirnov IV 1345
Soares PSM 1127
Soldenhoff K 777
Sole KC 1443
Spjuth L 281 323
Stambouli M 965 983 1143
Stefanska A 1639
Stepanov SI 1493

Stephan H 687
Stevens GW 469 813
Stichlmair J 487
Stuckey DC 101 113 155
Su G 1543
Sun D 911
Suzuki S 697
Suzuki TM 741
Svirdenkova OV 567 825
Szczepaska I 359
Sze YKP 231
Székely E 1601
Szymanowski J 19 1065 1193 1197 1203 1261 1411

Tachimori S 693 697
Tahiani F 1221
Takada T 219
Takahashi K 363 387 493 1059
Takanashi H 219 989
Takayanagi T 591
Takehara A 143
Takeuchi H 89 363 387 1279
Tambourgi EB 189 481 711
Tamhina B 1167
Tamura K 697
Tanaka I 561
Tanaka M 801 1549
Tang J 795
Tani K 493
Tarasov VV 825
Tatarchuk VV 1475
Tauler R 1561
Tavlarides LL 1651
Taylor RJ 1339 1381 1463
Todd TA 1345 1371
Tokarz A 841
Tomita A 829
Tomlinson MA 1255
Tondre C 207 637
Torgov VG 1475
Torrado A 1291
Traving M 125
Troshkina ID 1161
Tseng C-M 65
Tsuchiya M 1423
Tsuji H 675
Tsurubou S 265 1249
Tsuzaki K 1423

Uchiyama G 1469
Uemasu I 651
Ueoka R 933 1423
Uhlemann E 225
Umetani S 265 663 1249
Uribe-Ramírez AR 619
Urtiaga AM 1487
Usui Y 697

Valiente M 1023 1047 1121 1273 1291
Van Brunt V 1585
Van der Linden J 995
Varadarajan A 77
Varga V 1601
Venter DL 1319
Verhaege M 947
Viera Martínez R 735
Virnig M 375
Vogelpohl A 439 615
Vögtle F 239
Vojkovic V 1167

Wada E 591
Wakui Y 741 1103
Walford T 1639
Walkowiak W 1007
Wallwork AL 1463
Wang C 1233 1239
Wang JD 1579
Wang L 1053
Wang T-J 1361
Wang Yujie 889
Wang Yujun 177
Wang Y-D 419 625
Warshawsky A 1267
Watanabe K 89
Watanabe M 1469
Watarai H 819 883
Waterfall RC 445
Wei Z 1233
Weigl M 853
Weill J 877
Wen X 1543
Wieczorek P 1035
Wieser-Jeunesse C 681
Wildberger A 927
Wilkins D 777
Wiœniewski M 359
Wisniewski M 1261
Wood DJ 1345 1371

Xia C 259
Xu L 419

Yaftian MR 681
Yaita T 693
Yamada M 561
Yamada S 537
Yamaguchi M 433 865
Yamashita H 433
Yang ST 119
Yang Y-Z 353
Yano K 899
Yao N 405
Yokosawa R 1059
Yokoyama T 741 1103
Yoshizawa H 537
Yoshizuka K 687 933 1297
Yu J 451 457

Yu S-N 353 1357
Yuan CY 277
Yuan SG 277
Yurtov EV 573 579 971

Zagorodni AA 9
Zaitsev B 1345
Zamacona S 1487
Zamponi G 487
Zeid MM 1351
Zhang P 741
Zheng T 795
Zheng Z 905
Zhou W 1651
Zhu L 259
Zhu S 177
Zhuravleva GI 1381
Zolotov Yu A 1645
Zushi E 933

KEYWORD INDEX

ANALYSIS

analysis 47 65 71 77 83 245
ATR spectroscopy 813
capillary electrophoresis 591
external reflection spectra 819
EXAFS 693
FAB-MS spectra 1233 1239
flame A A S 59
fluorescence tracers 847
FT-Raman spectroscopy 703
ICP-AES 1149
NMR spectroscopy 597 603 1333
optosensor 47
organic pollutants 1651
preconcentration 53
radiochemical-spectrophotometry 83
Time-Resolved Laser-Induced Fluorescence (TRLIF) 1333
UV-Visible spectroscopy 703 1167 1333
voltammetry 65

BIOTECHNOLOGY

antigen-antibody interaction 107
bioaffinity separation 107
enzymatic hydrolysis 149
extractive fermentation 119
fermentation broth 131 155 167
non-aqueous enzymology 137
surfactant-coated enzyme 137

EXTRACTANTS 277 341
- *bite size* 663
- *easily solidifying* 341
- *in situ formation* 341
- *interligand contact* 663
- *molecular recognition* 663
- *substituent effect* 663

Acorga CLX-50 871
alcohols: 1221
- *butanol* 183
- *1-decanol* 155
- *diol derivatives* 219
- *1-dodecanol* 161
- *2-ethylhexanol* 219
- *fatty alcohols* 161
- *glycols* 1319
- *1-octanol* 567

amides:
- *cyclic amide* 697
- *diamide* 259 693
- *glycolamides* 693
- *malonamides* 271 281 637 693 1333
- *nicotinamide derivatives* 359

amines; 95 101 519 597 603 1161 1537
- *Alamine 304-1* 1417
- *Alamine 336* 231 411 519
- *771* 789 1417 1455 1499
- *Amberlite LA-2* 1065
- *di-n-octylamine* 971 1161
- *dodecylamine* 1161
- *Hostarex A327* 977
- *primary amine N1923* 795 889
- *Primene JMT* 915
- *tertiary amines* 1417
- *sec-tridecylamine* 1411
- *tri-dodecylamine* 983
- *tri-n-octylamine* 537 835 971 1007 1041 1065 1161 1245 1279 1411
- *quaternary ions*
- *Aliquat 336* 231 789 905 1001 1029 1053 1143 1375 1417 1487
- *amines* 375 591 1417 1537
- *alkylammonium alkylbenzenesulphonates* 1139
- *alkylammonium carbonates* 1493
- *cetylpyridinium ion* 1167
- *cetyltrimethylammonium ion* 1167
- *tetrabutylammonium chloride* 1417
- *tetrabutylphosphonium chloride* 1417
- *tetraoctylammonium chloride* 1417
- *trioctylmethylammonium chloride* 1155 1245
- *tetraphenylarsonium* 1167
- *tetraphenylphosphonium* 1167
- *benzene* 1543

bis(ethanedithioamido)-2,4-dioxo-3-oxymino pentane 77
- *butyraldehyde* 1469
- ***carboxylic acid:*** 311 317
  - *2-bromodecanoic acid* 323
  - *humic acid* 213 335
  - *oleic acid* 971
  - *sodium oleate* 971
  - *Versatic acid* 525 1437
- *chloroform* 177
- ***β-diketone*** 265 585
  - *acylpyrazolone* 225 663
  - *LIX54* 225 1193
  - *thenoyltrifluoroacetone* 561 1249 1387

dimyristoyl-phosphatidylcholine 1423
diphenylsemicarbazide 47
dithiocarbamic acids: 341
- *pyrrolidinedithiocarbamic acid* 341
- *tetramethylene dithiocarbamate* 65

© 2000 Society of Chemical Industry

dithizone 853
EDTA-DOA 865
guanidine:
LIX79 1303
hydroxamic acid: 347 1339
neo-decanohydroxamic acid 1261
acetohydroxamic acid 1463
8-hydroxyquinoline compounds
5-chloro-8-hydroxy-quinoline 899
Kelex 100 207 813 871 1013 1203 1221
isopropylmyristate 877
macrocyclic compounds 239 265
cage compounds 239
calixarene: 245 249 1095 1365
calixarene (resorcarene) 965
calixarene carboxylate 255 687
phosphorylated calix[4]arene 681
cobalt dicarbollide 1345 1371
crown ether 299 585 669 1149 1365 1371 1387
stereoisomers 299
monoazathiacrown ether 675
cryptand derivatives 265
nitriles: 1319
acetonitrile 1397
nitrogen bases 1319
nitrogen disulphides 399
oximes: 293 1555
degradation 287 293
isomerisation 293
Acorga M5640 995
2-ethylhexanal oxime 765
2-hydroxyoxime 883
2-hydroxy-5-nonylacetophenone 287
2-hydroxy-5-nonylbenzaldehyde 287
2-hydroxy-5-t-octylbenzaldehyde 293
2-hydroxy-5-t-octylbenzophenone 293
2-hydroxy-5-t-octylacetophenone 293
LIX63 1143 1173
LIX84 759 1193 1285
LIX84I 1279
LIX 860 995 1181 1487
M5640 1487
P5100 287
SME529 287
phenolic derivatives 585
4-n-dodecyl-6-(2-thiazolylazo) resorcinol 1313
nonyl phenol 375
phospholenes: 381
1-(dodecyloxy)-3-methyl-oxo-Δ^3-phospholene 1209
1-(2,6-dimethylhept-4-yloxy)-3-methyl-1-oxo-Δ^3-phospholene 1209
phosphorus acids: 225 299 305
phosphinic acids
1,3-benzenedimethylbis(phenyl-phosphinic acid) 1103
bis(2-ethylhexyl)phosphinic acid 723
PIA-8 1187
PIA-226 723
bis(2,4,4-trimethylpentyl) phosphinic acid 1239
Cyanex 272 703 735 741 753 953 1019 1079 1081 1133 1187 1239 1303 1443 1487 1561
bis(2,4,4-trimethylpentyl))dithio-phosphinic acid
Cyanex 301 703 947 1001 1081 1155 1227 1375 1517
bis(2,4,4-trimethylpentyl)mono-thiophosphinic acid 1233
Cyanex 302 703 735 753 1081 1155 1227 1233 1375 1511
di-2-ethylhexylmonothiophosphoric acid 225
di-2-ethylhexyldithiophosphoric acid 1291
DP 8R 735 753
diphosphinic acid 53
P507 735
phosphonic acids
aminomethylenephosphonic acid 729
2-ethylhexylphosphonic acid mono-2-ethylhexyl ester 71 723 899 905 1125 1133 1177
Ionquest 801 1127 1187
PC-88A 71 735 753 1187 1297
mono-octyloctanphosphonate (MOOP) 1177
N-piperidinomethane-1,1-diphosphonic acid 1089
phosphonic acid esters 305 1035
chiral 1035
diphosphonate derivatives 305
bis(dialkylphosphonates) 393
phosphoric acids
bisalkyl hydrogenphosphate 687
di(2-ethylhexyl)phosphoric acid D2EHPA 189 201 225 329 543 567 579 711 717 723 729 741 825 829 847 865 877 915 927 947 971 989 1023 1089 1113 1115 1121 1181 1185 1273

D2EHPA cont 1291 1351 1437 1443 1481 1517 1523
salts 1255
di(2-ethylhexyl)thiophosphoric acid 771 959 1047
phosphoric acid esters 1035
chiral 1035
di(1-methylheptyl)methyl phosphate 911
octylphenyl acid phosphate 1351
tri-n-butylphosphate, TBP 189 265 419 655 723 801 805 921 1161 1209 1585 1669
N-piperidinomethane-1,1-*diphosphonic acid* 1089
phosphorus oxides: 265 381 1133
acetoamidophosphine oxide groups (CMPO) 1095
Cyanex 921 381 1007 1133
Cyanex 923 381 469 777 1065 1081 1109 1261
Cyanex 925 381 777 1155 1261
trioctylphosphine oxide 561 1309 1325 1357 1417
polyethylene oxides 625
polyoxyethylene nonyl phenyl ether 363 387
polyoxyethylene-10-dodecyl ether 1423
poly-siloxane
aminopoly-siloxane 927
pyrazolone derivatives 225
pyrazole-thione 1357 1361
4-benzoyl-2,4-dihydro-5-methyl-2-phenyl-3H-pyrazol-3-thione 1357 1361
pyridine derivatives: 311 1437
pyridine carboxylate ester 1437
pyridine-3,5-dicarboxamides 1197
pyridylazo 883
oligopyridines 323
terpyridine 317
N-8-quinolylsulfonamide 933
saponified coconut oil 195 783
silver nitrate 1059
sulfolane 1549
sulfoxide derivatives: 353
dihexylsulphoxide 1215
sulphide derivatives 1475
3,6-dithiaoctane 59
phosphorus sulphides: Cyanex 471X 777 1071
surfactants: 83 155 335 405 419 573 853
AOT 83 95 101 853 859
dodecyltrimethylammonium bromide 853
ECA 4360 953 977 983 1071
ECA 11522 959
nonionic surfactant 107 171 363 387
Parabar 9220 965
Parabar 9551 947
sodium dodecylbenzene sulfate 419
sodium dodecylsulfate 405
Softanol 30 155
Softanol 120 155
Span 80 947 983 989 1071
Triton X-100 207
Tween 80 419 971
thiourea derivatives 399
toluene 1573
triazines 317 323

EXTRACTION EQUIPMENT

air sparging 503
capacitance imaging 445
capacity 499
centrifugal contactors 499 1345 1365 1381 1463
coalescence 487 503 615 631
co-current mixers 1573
scale-up 1573
columns: 439 445 615
agitated column 427 1601
axial mixing 475 915 1585
column design 427 1503
column dynamics 487
column flooding 433 1591
column hold-up 433
column scale-up 427 1503
column stirred 959
distributor design 439
fluidised bed column design 1285
Karr column 549
Kuhni column 487
mixer-settler column 493
Oldshue-Rushton column 1601
packed column 475 915 1591
packings 1591
Raschig ring 451 469
Super-mini-ring 451 457 469
pulsed column 463 965 1455
packed column 451
perforated plate 469
sieve-plate column 469 1585
Rotating Disc Contactor 1579 1601
Scheibel column 1503
spray column 1403
stirred column 959
transfer units 1585

vibrating perforated plate column 481
dispersion 445
distribution 445
drop behaviour 513 609
drop coalescence 615
drop size 439
droplet breakage 487 1579
droplet swarm 457 615 847
efficiency 493 499
electric field (DC) 503 609
electrical resolution 503
emulsion breaking 503
emulsion formation 101
emulsion swelling 971
entrainment 499 631
extractor comparison 531
flow phenomena 463 509
fluid dynamics 1579
horizontal rotating cell 825
Graesser contactor 101
high viscosity 457 531
hydrodynamics 451 469
in-line mixers 519 525 531
impeller design 433
membrane extraction:
activated composite membranes 1047
bulk liquid membrane 1041 1059 1065
emulsion/surfactant liquid membrane 503 573 631 947 953 959 965 971 977 983 989 1071 1511
hollow fibre membrane 183 889 893 1029
impregnated Langmuir-Blodgett membrane 1313
liposomes 1423
microporous membrane 631
polymer inclusion membranes 1007 1053
porous membrane 1053
rotating membrane cell 877
supported liquid membrane 47 543 995 1001 1007 1013 1019 1023 1029 1035 1155 1297 1529
water diffusion 971
mixer-settler 1455
Morris extractor 195
phase distribution 439
phase equilibria 643
phase separation 631
pilot plant 1443
Reynolds number 531
stirred cell 847 853
tomography 445
turbulent energy 463
Vibro-mix extractor 537
videocamera 503

EXTRACTION TECHNIQUES
aphrons 419
applied voltage 865
aqueous/organic biphasic system 137 155 143
aqueous two-phase system 149
binary extractants 1001 1139 1155 1375
biphasic reactions 369
coalescence 487 503 615 631
colloidal aggregates 567
concentrated solutions 25
counter-current cascade 723 1555
diffusion coefficient 841
diffusivity 619
diluent effect 1121 1387
dispersion model 131
electrolytes 25
electrophoretic mobility 835
extraction
acid base couple extraction 131
aqueous two-phase system 149
cloud point extraction 19 171 363
co-current extraction 1573
coextraction 255
electro-extraction 183
exchange extraction 1255
extraction chromatography 53 125 927 1267
extractive reaction 143
ion-pair extraction 59 131 271 591
mechanism of extraction 95 387 591 899 921 1109 1333
reactive extraction 549 939 1523
foam separation 405
gelation 579
ion-size selective masking reagents 265
impregnated resins 8 771 1115 1267 1273 1285
impregnated polymers 927
Amberlite resins 131
Amberlite XAD-2 771 1115 1273 1285
Amberlite XAD-4 125 927 1273
Amberlite XAD-7 1313 1273
Amberlite XAD-16 125 927
aqua impregnated resins 1291
continuous fluidized bed 1285
encapsulated resins 1279
new supports 1267
inclusion complex 651
interfacial effects:
interfacial adsorption 3 939
interfacial behaviour 579 933
interfacial complexation 883

interfacial contamination 503
interfacial convection 155 579
interfacial covering 835
interfacial cruds 805
interfacial films 825
interfacial kinetics 813 853 893 905 911 1143
new methods of study 883
interfacial reaction 829 847 859
interfacial resistance 893
interfacial tension 829
liquid-liquid interface 819 841
ion exchange:
aminomethylphosphonic acid 747
dihydrogen tetratitanate hydrate 1249
double and triple phase separation (IX-SX) 1249
resins:
carboxylic acid 1291
iminodiacetic acid 1291
phosphoric acid 1291
ion hydration 1309
ion solvation 1309
kinetics 95 101 329 537 579 871 877 883 889 893 899 927 933 1333 1381
Lewis cell 101 155 865 871 905 911 921 1333
mass transfer 433 451 457 469 493 615 825 829 835 841 847 921 1511 1517 1537 1573 1673
multicomponent kinetics 513 619 847
medium effects 871
reaction kinetics 939
salt effects 643 877
solvent effects 329
'test system' 513
two-film theory 893
mechanochemical assisted extraction 805
micellar extraction: 207
micellar enhanced ultrafiltration 19
reversed micellar extraction 859
reverse micelle 83 89 95 101 107 113 119 335 579 625
microemulsion extraction 195 783
non-dispersive solvent extraction 543 1303 1487 1499 1517 1523 1537
hollow fibre module 1041 1297 1411 1499 1517 1523 1537
pertraction 1023 1041 1065
phase equilibria 643
predispersed solvent extraction 419
preneutralisation 525
reactive sorption 125 927
reducing agents:
hydroxylamine derivatives 1381
salting out 643 1325
separation 53
enantiomeric separation 1607
solubility parameters 637
solvation 3 271
stable emulsions 805
stripping
precipitation stripping 9 801
synergism 277 299 305 311 317 323 329 561 585 899 1357 1371 1437
supercritical extraction 167 1601 1607 1613 1617 1621 1625 1629 1635 1639 1645 1651 1657 1663 1669 1673 1679
carbon dioxide 167 1601 1607 1613 1617 1621 1625 1629 1635 1639 1645 1651 1657 1663 1669 1673 1679
nitrous oxide 1651
ethanol co-solvent 1645
methanol co-solvent 1621 1657
ligand-assisted 1663
thermodynamics 555 841 1109 1143
third phase 637 1177
water content of extracted complexes 1187
water solubilisation 625

FEEDS

activated carbon 1669
alkaline high-level nuclear wastes 1365
alkaline solution 375 1221
ammoniacal solution 1193
ammonium carbonate liquors 735
ammoniacal etching solution 759
ARSEP process 1449
bastnasite ore 795
batteries 201
nickel-cadmium 537 747
nickel-metal hydride 741
borage leaves 1617
brine 1255
Caron process 735
C_3-C_4 fraction 1403
cobalt-nickel mixed sulphide 735 753

contaminated sediments 1657
copper anode slimes 777
CUPREX process 1449
β–cyclodextrin-cholesterol complex 1629
dyestuffs 183
electroplating wastewater 231
enzyme condensation reaction 369
Fe-Ni alloy etch solution 765
fermentation broth 125 1645
fission products 1475
geological standard rocks 59
grape pomace 1621
irradiated fuel 1431
Kakanda tailings 1443
landfill leachate 225
light oil 1397
desulfurisation 1397
MERCUREX process 1449
neutral oils 1319
nickel laterite 753
nuclear reprocessing 697 1469
olive leaves 1613
olive mill waste-water 977
PARC process 1469
phosphate rock 1481
phosphoric acid 1227 1351 1487
1511
pickling liquor 189 197
Purex process 1339 1381 1431
1463 1469 1475
silvered copper wires 1071
spent fuel reprocessing 697
TALSPEAK 1089
tannery effluent 195
Thorp process 1431
tri-n-butyl phosphate (TBP) 409
waste-water 195 219 225
231
wheat germ 1635
ZINCEX process 201 1449
ZINCLOR process 1449
zinc residues 711

MEDIA/ANIONS
ammonium sulphate 1543
anion effect 669
boric acid 795
carbonate 1493
chloride: 359 381 399
783 1197 1203
1245 1255
hydrochloric acid 271 387 393
1173 1215 1481
cyanide 375 1669
fluoride 789
hydrogen phthalate 1417
hydrogen sulphide removal 1403
hydroxide 1221 1403
nitrate 669 681 1387
nitric acid 259 637 703
1585
nitroxide radicals 893
perchlorate 669 1309
phosphoric acid 1227 1481
silicic acid: 805
silicates 989
sodium nitrate 669
sodium perchlorate 669
sulphate 1233 1239
sulphuric acid 741 747 915
thiocyanate 1167

METALS
acid 189 1209
actinides: 249 317 555
1089 1095 1333
1339 1345
americium 259 281 323
1371 1517
neptunium 1381 1469
rejection 1463
plutonium 697 1381 1431
alkali metals: 265 585 1249
1309
caesium 965 1345 1365
1371
potassium 1255
sodium 255 1255 1371
alkaline earth metals: 265 299 567
825 1249 1309
calcium 305 989 1047
1255 1437
magnesium 1047 1255
aluminium 561 1047
anion extraction (cyanides) 375
antimony 71
arsenic 65 1261
bismuth 71 245
boron 219
cadmium 543 747 1013
1053 1215 1303
1487 1511 1517
cerium(IV) 795 889
chromium: 47 195
chromium (III) 245 329 1007
chromium (VI) 231 1007
cobalt 311 347 735
741 753 933
953 1177 1313
1443
copper:
copper(I) 59 675
copper (II) 759 813 871
933 995 1047
1053 1071 1193
1197 1203 1273
1285 1279 1291
1303 1313 1487

copper (cont.) 1517 1555 1567
gallium 363 387 561
723 899
germanium 871
gold 381 393 777
783 1155 1303
1669
indium 561 711 717
723 1019 1047
iron: 271 711 717
729 829 915
1019 1173 1481
reduction 711
reductive stripping 729
***lanthanoid** (rare earth):* 249 317 335
555 567 681
687 693 741
801 825 865
889 911 1023
1081 1089 1095
1103 1109 1309
1333
stripping 1133
erbium (III) 905 1127
europium 259 323 1371
1387 1517
gadolinium 1297
holmium 1023
lanthanum 1103
lutetium 1103
neodymium 1023 1121
samarium 801 1297
thulium 1387
yttrium 1109 1115
lead 245 1013 1221
1227
manganese 245 1047 1443
molybdenum 1493
nickel 207 311 525
543 735 741
753 747 765
877 883 947
953 1177 1181
1187 1313 1437
1517
niobium 789
platinum group metals: 771 1139
osmium 1161
palladium 71 359 537
771 883 1143
1475
platinum 71 771 1143
rhodium 71 771 1029
ruthenium 1167
radionuclide 53 1663
selenium(IV) 77 921
scandium 1233 1239
silver 239 399 675
1001 1071 1375
strontium 1345 1371
tantalum 789
technetium 1365 1431 1469
tellurium (IV) 921
thallium 71
thorium(IV) 213 245 353
795 1357 1361
tin 71 1047 1245
transition metals 1309
tungsten 1493
uranium 347 353 519
697 1351 1357
1361 1431 1455
yttrium 1109 1115
zinc 201 847 853
877 927 933
959 1047 1203
1209 1215 1221
1273 1279 1291
1303 1517 1523
zirconium 567 825

MODELLING

3 25 411
655 921 1127
1511 1517 1523
1529 1537 1543
1549 1555 1561
1591 1673 1679
ab initio calculations 281
alternative least squares 1567
articial neural networks 1549
bite size 663
computational chemistry 277
computer simulation 933 1555 1561
concentrated solutions 25
curve resolution 1567
dispersion model 125
electrolytes 25
equations of state 1679
equilibrium modeling 669 1561
factorial design 717
Flory-Huggins theory 637
HSAB principle 277
interligand contact 663
molecular dynamics 3
molecular modeling 239
molecular dynamics simulations 883 933
molecular mechanics calculation 277 687
molecular recognition 663
numerical simulation 959
277
quantitative structure property relationship, QSPR 687
semi-empirical molecular orbital method 933
simultaneous mass transfer 939
steady-state local linearisation 1555
Stefan-Maxwell principles 503 619

UNIFAC model 619 655
Chem-UNIFAC 655
UNIQUAC 655

ORGANIC COMPOUNDS

ACE inhibitory peptides 149
acetone 1573
amine 1035
aromatics: 1549
aromatics/phenol/water 1573
polyaromatic hydrocarbons 1651
acids: 1041
acetic acid 835 877 1325 1625
amino acid: 131 1035 1537
glycylphenylalanine 143
phenylalanine 859 1499
carboxylic acid 119 1041 1537
chiral separation 1035
citric acid 125 1411
dicarboxylic acid 597
lactic acid 983
linoleic acid 1639
γ–linolenic acid 1617
nicotinic acid 411
permetric acid 1607
phthalic acid 1417
phthalates 1651
propionic acid 1325
tartaric acid 125
unsaturated fatty acid 1059
anthocyanin 1621
biologically active peptides 149
chlorinated biphenyls 1651 1657
chlorinated pesticides 1651
caprolactam 427 1543 1573
β–cyclodextrin 1629
cyclodextrin 651
desulfurization 1397
enzyme 89
erythromycin 155
essential oil 1673
ethanol 161 1601
organic compounds/water 1591
pancreatin 107
phenol: 171 419 1065 1319 1573
phenol cleavage stream/ acetone-carboxylic acid salts/water 1573
hydroxybenzoic acid 977
β–phenylethylamine 1035
pleuromutilin 1645
porphyrin 819
protein extraction 83 89 95 119
selectivity 101 113
TBP-kerosene/acetic acid/water 451
TBP-diluent/H_2O/LiCl 655
tetramisole 1607
tocophenol 1613 1635
toluene/acetone/water 427 433
toluene/acetone/phenol/water 503
toluene/cyclohexanone oxime/water 1573
trypsin 107
volatile organic compound (VOC) 177
wheat germ oil 1639
xylene 651
zein 149
zwitterion 131

PRODUCTS

alkylglucoside 369
antitumour effect 1423
apoptosis 1423
dioxalane 549
enzymatic hydrolysis 149
enzymatic peptide synthesis 137 143
kyotorphin synthesis 143
thermolysin catalysed hydrolysis 149
thermolysin catalysed synthesis 143
silicate microballoons 989
synthesis of materials 8
templating 8



ISBN 0 901001 84 8 (volume two)
available as a two volume set only
ISBN 0 901001 83 X (volume one)